British Journal of Pharmacology

February 1994

Volume 111 Number 2 pages 389–648

Br. J. Pharmacol. (1994), **111**, 389–390

SPECIAL REPORT

Separation and characterization of a novel isoenzyme of cyclic nucleotide phosphodiesterase from rat cerebrum

Jun Mukai, Tomoko Asai, Michiko Naka & [1]Toshio Tanaka

Department of Molecular and Cellular Pharmacology, Mie University School of Medicine, 2-174 Edobashi, Tsu, Mie 514, Japan

Anion-exchange chromatography on a Mono-Q column of the supernatant fraction, after ultracentrifugation, from a homogenate of rat cerebrum, prepared under isotonic conditions in the presence of protease inhibitors, yielded a novel isoenzyme of cyclic nucleotide phosphodiesterase (PDE) with properties unlike those of known PDEs. The isoenzyme was insensitive to stimulation by Ca^{2+}/calmodulin and cyclic GMP, and it hydrolyzed both cyclic AMP and cyclic GMP with K_M values of 0.109 ± 0.008 μM and 1.78 ± 0.04 μM, respectively. The ratio of V_{max} of hydrolysis of cyclic GMP to that of cyclic AMP was 1.90 ± 0.07. Nicardipine (PDE I inhibitor), SK&F 94120 (PDE III inhibitor), rolipram (PDE IV inhibitor) and zaprinast (PDE V inhibitor) had very weak inhibitory effects on the PDE activity of the isoenzyme. These results suggest that the isoenzyme is a novel and previously unreported species of PDE, which we tentatively designate PDE VIII.

Keywords: Cyclic AMP phosphodiesterase; phosphodiesterase inhibitors; rat cerebrum; PDE VIII

Introduction Recent information obtained from cloning, primary-sequence, and drug-selectivity studies suggests that there exists a large superfamily of phosphodiesterases (PDEs), which consists of seven distinct families of PDE isoenzymes (Beavo *et al.*, 1990; Michaeli *et al.*, 1993). Many studies have illustrated clear differences among tissues in terms of the distribution of PDE isoenzymes. In a previous paper, the rat cerebrum was shown to be the source of three activities, designated PDE I, PDE II and PDE IV (Nicholson *et al.*, 1989). However, the low resolution of the ion-exchange chromatographic techniques employed in the earlier study failed adequately to fractionate the various isoforms in this tissue. In the present study we separated the PDE isoenzymes in the rat cerebrum by anion-exchange chromatography on a Mono-Q column, and characterized the various PDE activities by both pharmacological and biochemical techniques.

Methods *Isolation of PDE isoenzymes from the rat cerebrum* The study was performed on tissue obtained from adult male rats that had been killed by cervical dislocation. All preparative procedures were performed at 4°C.

Five grams of cerebral cortex were excised from rats and rinsed several times in ice-cold homogenization buffer [Buffer A: Tris-HCl 50 mM (pH 7.5), sucrose 0.25 M, EGTA 0.1 mM, dithiothreitol 0.1 mM, leupeptin 20 μM, soybean trypsin inhibitor 10 μg ml^{-1}, pepstatin 10 μg ml^{-1}, chymostatin 10 μg ml^{-1} and (*p*-amidinophenyl)methanesulphonyl fluoride hydrochloride 1 μM]. The tissue was gently homogenized, with a Potter S homogenizer, in 8–10 volumes of Buffer A. The homogenate was then centrifuged at 100,000 *g* for 60 min. The resultant supernatant, containing cytosolic PDEs, was filtered through glass wool and then through a cellulose acetate 0.20 μm filter unit (ADVANTEC Toyo Roshi Kaisha, Ltd., Tokyo, Japan). The filtered supernatant was applied to a Mono-Q HR 5/5 (Pharmacia LKB Biotechnology, Uppsala, Sweden) anion-exchange column (0.5 × 5 cm) at a flow rate of 0.5 ml min^{-1}, after the column had been equilibrated with Buffer B [Tris-HCl 50 mM (pH 7.5), EGTA 0.1 mM, dithiothreitol 0.1 mM and (*p*-amidinophenyl)-methanesulphonyl fluoride hydrochloride 1 μM]. The loaded column was washed with 30 ml of Buffer B. The cytosolic PDE isoenzymes were then eluted with a 100-ml linear gradient of NaCl (0–0.12 M) in Buffer B, at a flow rate of 0.5 ml min^{-1}. Fractions of 1 ml each were collected.

Analytical procedures PDE activity was measured by a two-step assay (Masuoka *et al.*, 1990). The molecular mass of the novel isoenzyme was determined by gel filtration on Superose 12 HR 10/30 (Pharmacia LKB Biotechnology).

Materials Papaverine hydrochloride and 3-isobutyl-1-methylxanthine (IBMX) were purchased from Wako Pure Chemical Industries, Ltd. (Osaka, Japan). Ro 20-1724 (4-(3-butoxy-4-methoxybenzyl)-2-imidaziolidine) was purchased from BIOMOL Res. Lab. Inc. (PA, U.S.A.). Nicardipine was purchased from Sigma Chemical Co. (St Louis, MO, U.S.A.). SK&F 94120 (5-(4-acetamido-phenyl)pyrazin-2-[1H]-one), rolipram, cilostazol and zaprinast were gifts from SmithKline Beecham Pharmaceuticals (King of Prussia, PA, U.S.A.), Meiji Seika Kaisha, Ltd. (Tokyo, Japan), Otsuka Pharmaceuticals (Osaka, Japan) and Taisho Pharmaceutical Co., Ltd. (Tokyo, Japan), respectively.

Results Chromatography on a Mono-Q column of the cytosolic supernatant fraction from rat cerebrum yielded three peaks of PDE activity (Figure 1). The enzymatic activity responsible for the second (Peak II) and third (Peak III) peaks was stimulated several fold by the addition of Ca^{2+}/calmodulin (data not shown), suggesting that it was equivalent to PDE I. PDE II and PDE IV, observed in a previous study (Nicholson *et al.*, 1989), were eluted between 0.2 M and 0.6 M NaCl (data not shown).

The first peak (Peak I) of PDE activity, eluted at 0.06 M NaCl, had very high affinity for adenosine 3′:5′-cyclic monophosphate (cyclic AMP) [$K_M = 0.109 \pm 0.008$ μM ($n = 3$)] and relatively high affinity for guanosine 3′:5′-cyclic monophosphate (cyclic GMP) [$K_M = 1.78 \pm 0.04$ μM ($n = 3$)], as shown in Table 1. The ratio of the V_{max} for hydrolysis of cyclic GMP to that for cyclic AMP was greater than one [1.90 ± 0.07 ($n = 3$)]. The hydrolysis of both substrates showed simple Michaelis-Menten kinetics. Ca^{2+}-calmodulin failed to increase the hydrolysis of either cyclic AMP or cyclic GMP. Similarly, cyclic GMP failed to increase the hydrolysis of cyclic AMP.

The effects of various inhibitors of PDEs on the activity in Peak I are shown in Table 1. Nicardipine, a PDE I inhibitor, had a weakly inhibitory effect on the hydrolysis of cyclic AMP [$IC_{50} > 300$ μM) ($n = 3$)]. Rolipram and Ro 20-1724, selective inhibitors of PDE IV, had weakly inhibitory

[1] Author for correspondence.

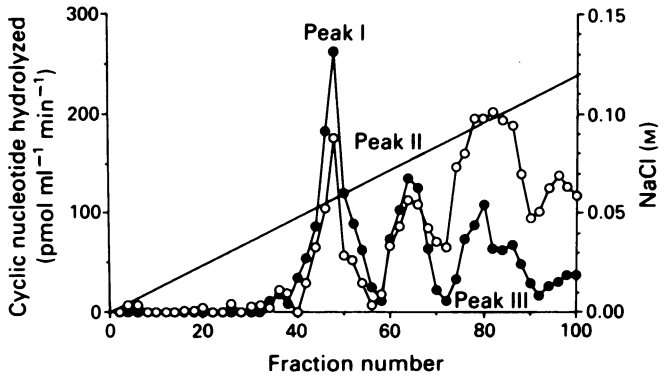

Figure 1 Representative profile after chromatography on a Mono-Q anion-exchange column of cytosolic phosphodiesterase activity from the rat cerebrum. The supernatant from a homogenate of rat cerebrum that had been centrifuged at 100,000 *g* was chromatographed on a Mono-Q column as described in Methods and 1 ml fractions were collected. The concentration of substrate was 1 μM for both cyclic AMP (●) and cyclic GMP (○). The gradient of 0–0.12 M NaCl is shown by a solid line. These data are representative of data obtained in four separate experiments.

effects on the hydrolysis of cyclic AMP [$IC_{50} > 300$ μM ($n = 3$)].Similarly, SK&F 94120 and cilostazol, selective PDE III inhibitors, had weakly inhibitory effects on the hydrolysis of cyclic AMP [$IC_{50} > 300$ μM ($n = 3$)]. Zaprinast, a selective PDE V inhibitor, also had a weakly inhibitory effect on the hydrolysis of cyclic GMP [$IC_{50} = 23.5 \pm 3.1$ μM ($n = 3$)]. IBMX had an inhibitory effect on the activity in Peak I, with an IC_{50} value of 26.5 ± 2.5 μM ($n = 3$). Cyclic AMP acted as a potent competitive inhibitor of the hydrolysis of cyclic GMP with a K_i value of 0.120 ± 0.026 μM ($n = 3$). Cyclic GMP also inhibited the hydrolysis of cyclic AMP in a competitive manner with a K_i value of 2.58 ± 0.08 μM ($n = 3$).

Gel filtration indicated that the isoenzyme in Peak I had a molecular mass of 298 ± 8 kDa ($n = 3$).

Discussion This study revealed the presence of a novel isoenzyme of cyclic nucleotide phosphodiesterase in the rat cerebrum. The activity designated Peak I was a cyclic nucleotide PDE with a low K_M that was insensitive to stimulation by Ca^{2+}/calmodulin and cyclic GMP. By contrast to PDE III, this activity had a V_{max} for cyclic GMP that was greater than that for cyclic AMP. With respect to its pharmacological properties, the activity in Peak I was resistant to inhibition by selective inhibitors of PDE III and of PDE IV. These data suggest that the activity designated Peak I represents a novel isoenzyme, which does not easily fit the criteria used in the present classification of PDE isoenzymes (Beavo *et al.*, 1990).

Nicardipine, a potent inhibitor of both intact PDE I and trypsin-treated PDE I (Matsushima *et al.*, 1987), had no effect on the activity of the novel isoenzyme. This result suggests that the material in Peak I is not a proteolytic byproduct of PDE I.

The IC_{50} for zaprinast was 30 to 200 fold higher than the values reported for PDE V from the bovine photoreceptor (Beavo *et al.*, 1990) and the canine trachea (Torphy *et al.*, 1989). The hydrolysis of both cyclic AMP and cyclic GMP as substrates showed simple Michaelis-Menten kinetics in each case. Cyclic AMP was a potent competitive inhibitor of the hydrolysis of cyclic GMP by this isoenzyme, having a K_i of the same order of magnitude as its K_M. Cyclic GMP also inhibited the hydrolysis of cyclic AMP in a competitive manner with a K_i of the same order of magnitude as its K_M. These results suggest that the material in Peak I is not a mixture of PDE V and another activity.

In summary, it appears that we have identified an eighth isoenzyme of PDE, which we tentatively designate PDE VIII, from the rat cerebrum.

Table 1 Properties of the novel enzymatic activity from the rat cerebrum

Property	*Peak I*
Molecular mass (kDa)	298 ± 8
Kinetic data	
K_M cyclic AMP (μM)	0.109 ± 0.008
K_M cyclic GMP (μM)	1.78 ± 0.04
$\frac{V_{max}\text{ cyclic GMP}}{V_{max}\text{ cyclic AMP}}$	1.90 ± 0.07
Sensitivity to inhibitors	
IC_{50} (μM)[a]	
SK&F 94120	>300
Cilostazol	>300
Rolipram	>300
Ro 20-1724	>300
Nicardipine	>300
IBMX	26.5 ± 2.5
Zaprinast[b]	23.5 ± 3.1
K_i (μM)	
Cyclic AMP (on hydrolysis of cyclic GMP)	0.120 ± 0.026
Cyclic GMP (on hydrolysis of cyclic AMP)	2.58 ± 0.08
Activators	
Ca^{2+}-calmodulin	Not activated
Cyclic GMP	Not activated

Data represent means ± s.e.mean of results from three separate experiments, each of which was performed in triplicate. For determinations of values of K_M and V_{max}, concentrations of substrate between 0.06 μM and 100 μM were used.
[a]Cyclic AMP at 1 μM. [b]Cyclic GMP at 1 μM.

References

BEAVO, J.A. & REIFSNYDER, D.H. (1990). Primary sequence of cyclic nucleotide phosphodiesterase isoenzyme and the design of selective inhibitors. *Trends Pharmacol. Sci.*, **11**, 150–155.

MASUOKA, H., ITO, M., NAKANO, T., NAKA, M. & TANAKA, T. (1990). Effects of ruthenium red on activation of Ca^{2+}-dependent cyclic nucleotide phosphodiesterase. *Biochem. Biophys. Res. Commun.*, **169**, 315–322.

MATSUSHIMA, S., TANAKA, T., SAITOH, M., WATANABE, M. & HIDAKA, H. (1987). Different sensitivities of Ca^{2+}, calmodulin-dependent cyclic nucleotide phosphodiesterases from rabbit aorta and brain to dihydropyridine calcium channel blockers. *Biochem. Biophys. Res. Commun.*, **148**, 1468–1474.

MICHAELI, T., BLOOM, T.J., MARTINS, T., LOUGHNEY, K., FERGUSON, K., RIGGS, M., RODGERS, L., BEABO, J.A. & WIGLER, M. (1993). Isolation and characterization of a previously undetected human cAMP phosphodiesterase by complementation of cAMP phosphodiesterase-deficient saccharomyces cerevisiae. *J. Biol. Chem.*, **268**, 12925–12932.

NICHOLSON, C.D. & WILKE, R. (1989). The ability of denbufylline to inhibit cyclic nucleotide phosphodiesterase and its affinity for adenosine receptors and the adenosine re-uptake site. *Br. J. Pharmacol.*, **97**, 889–897.

TORPHY, T.J. & CIESLISKI, L.B. (1989). Characterization and selective inhibition of cyclic nucleotide phosphodiesterase isoenzymes in canine tracheal smooth muscle. *Mol. Pharmacol.*, **37**, 206–214.

(Received September 23, 1993
Accepted October 6, 1993)

Br. J. Pharmacol. (1994), **111**, 391–393

SPECIAL REPORT

Functional expression of human D_3 dopamine receptors in differentiated neuroblastoma × glioma NG108-15 cells

[1]Guy R. Seabrook, John A. Kemp, Stephen B. Freedman, Shil Patel, Heather A. Sinclair & George McAllister

Merck Sharp and Dohme Research Laboratories, Neuroscience Research Centre, Terlings Park, Eastwick Road, Harlow, Essex, CM20 2QR

This study describes the depression of calcium currents caused by activation of human D_3 dopamine receptors which have been stably expressed in the neuroblastoma × glioma NG108-15 cell line. Transfected cells, which had been differentiated with prostaglandin E_1 and isobutylmethylxanthine, exclusively expressed D_3 receptor mRNA, which was demonstrated by reverse transcription polymerase chain reaction techniques. Transfected cells had high affinity binding sites for iodosulpiride, with a K_d of 0.8 nM and receptor density of 240 fmol mg^{-1} protein. Calcium currents were recorded using nystatin-perforated patch clamp techniques. In contrast to untransfected cells that had been differentiated, high-threshold calcium currents in differentiated hD_3-NG108-15 cells were depressed by application of dopamine and quinpirole. These responses were abolished by the dopamine receptor antagonist S-(−)-sulpiride (1 μM), demonstrating that they were caused by the activation of the transfected dopamine receptors. Coupling of human D_3 receptors to calcium currents was sensitive to the action of pertussis toxin, suggesting the involvement of G-proteins of the G_i and/or G_o subtype. These results demonstrate that human D_3 receptors represent a functional class of dopamine receptor.

Keywords: D_3 dopamine receptor; sulpiride; quinpirole; calcium currents; NG108-15 cells

Introduction Antipsychotic drugs bind to several classes of dopamine receptors, three of which have recently been cloned from human tissue; these include the D_2, D_3 and D_4 receptors (e.g. Sokoloff *et al.*, 1990). D_3 receptors are highly homologous to D_2 receptors, consequently these receptors may also have inhibitory effects upon neuronal excitability (Sokoloff *et al.*, 1990). Although D_3 receptors, and their mRNA, are localized mainly in limbic areas of the brain which are associated with emotional behaviour (Bouthenet *et al.*, 1991), the lack of selective ligands with defined agonist and antagonist activity has impeded attempts to determine its functional importance. Thus it is clearly necessary to determine whether or not human D_3 cDNA encodes a functional class of dopamine receptor at the cellular level.

Endogenous D_2-like dopamine receptors in neurones and neuroblastoma cell lines can couple to several effector mechanisms that include the inhibition of adenylate cyclase, activation of potassium currents and depression of calcium currents (Kebabian & Calne, 1979; Berry-Kravis *et al.*, 1984; Lledo *et al.*, 1992). These actions are predominantly sensitive to pertussis toxin and are presumed to be mediated by G-proteins of the G_i and/or G_o types. In contrast, the coupling mechanism(s) of human D_3 receptors has proved elusive. It is clear from numerous transfection studies that D_3 receptors do not couple efficiently via pathways associated with D_2 receptors in either Chinese hamster ovary cells, rat 1 fibroblasts, GH_4C_1 pituitary cells, or non-differentiated NG108-15 cells, despite their ability to couple weakly to G-proteins in some of these cell lines (Sokoloff *et al.*, 1990; Seabrook *et al.*, 1992; Castro & Strange, 1993; Freedman *et al.*, 1993). To investigate further the coupling mechanism(s) of the D_3 receptor, whole cell calcium currents were recorded from differentiated NG108-15 cells, a cell type which has a diversity of G-proteins by which several inhibitory neurotransmitters systems may couple (McFadzean *et al.*, 1989; Caulfield & Brown, 1991).

Methods The methods for cell culture, stable transfection with human D_3 receptor cDNA, and radioligand binding were as previously described (Seabrook *et al.*, 1992; McAllister *et al.*, 1993; Freedman *et al.*, 1993). Cells were differentiated for 3 to 5 days using prostaglandin E_1 (10 μM) and isobutylmethylxanthine (50 μM), and whole cell calcium currents were recorded by the nystatin perforated patch clamp technique (e.g. Caulfield & Brown, 1991). The pipette solution contained (in mM): CH_3O_3SCs 100, CsCl 25, $MgCl_2$, HEPES 40, adjusted to pH 7.3 with CsOH. Cells were perfused at a rate of 1 to 2 ml min^{-1} with an extracellular solution that contained (in mM): NaCl 155, glucose 10, HEPES 10, KCl 5, $CaCl_2$ 5 and tetrodotoxin 0.5 μM, pH 7.4, at 22°C. Drugs were applied directly to the superfusion solution. Cells were voltage-clamped at −80 mV, and calcium currents were elicited by 100 ms depolarizing pulses to 0 mV (0.033 Hz). Calcium currents were amplified with an Axopatch 200 patch clamp amplifier (Axon Instruments), and captured on line via a CED1401 interface (Cambridge Electronic Design) which was connected to a Compaq 386 microcomputer. Leak currents were subtracted with the amplifier, and by the CED voltage-clamp analysis software. Data are expressed as the mean ± s.e.mean and where stated the mean was determined from the subpopulation of cells that responded to agonist application with >5% depression in the peak current amplitude. Drugs were obtained from the following sources: quinpirole, dopamine, S-(−)-sulpiride (Research Biochemicals Inc.); ω-conotoxin GVIA (Sigma); nisoldipine (Miles Pharmaceuticals).

Results Fifty-four neomycin resistant clones were identified of which three had detectable levels of iodosulpiride binding. The dissociation constant for [^{125}I]-iodosulpiride in the cell line used for functional assays was 0.8 nM with a B_{max} of 240 fmol mg^{-1} protein. The profile of ligand binding to hD_3 receptor in NG108-15 cells was consistent with that of hD_3 receptors expressed in Chinese hamster ovary cells (Freeman *et al.*, 1993). Using PCR primers able to detect D_2 mRNA in human and rat tissues, and human D_3 receptor mRNA (McAllister *et al.*, 1993), only hD_3 receptor mRNA was found in the differentiated hD_3-NG108-15 cell line. No effects of exogenously applied dopamine (10 μM; $n = 7$), quinpirole (100 nM; $n = 4$), or (−)-noradrenaline (10 μM; $n = 4$) were seen on whole cell calcium currents in the non-transfected, differentiated NG108-15 cells.

[1] Author for correspondence.

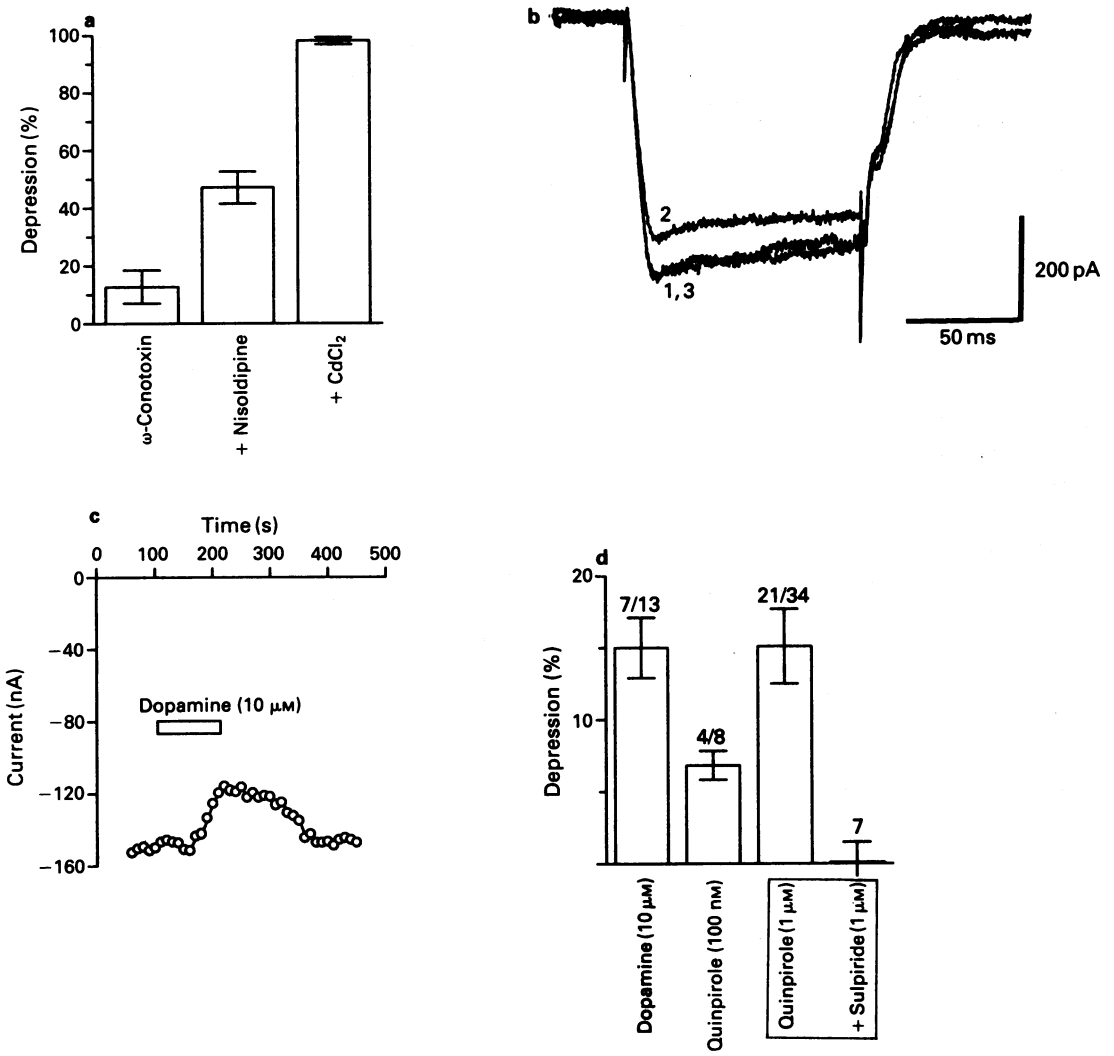

Figure 1 Whole cell patch clamp recordings of calcium currents in differentiated NG108-15 cells. Calcium currents were elicited by 100 ms depolarizations from −80 to 0 mV. (a) Depression of high threshold calcium currents by ω-conotoxin GVIA (100 nM), plus nisoldipine (1 μM) and with cadmium (30 μM). $n \geqslant 5$ cells. (b) Superimposed calcium currents recorded in control conditions (1), 1 μM quinpirole (2) and after recovery (3). (c) Time course of the depression in the peak calcium current with dopamine in an individual cell. (d) Antagonism of the depression of calcium currents caused by hD_3 receptor activation with S-(−)-sulpiride (1 μM). Numbers represent number of cells responding in each sample (see Methods).

High-threshold calcium currents in differentiated hD_3-NG108-15 cells were attenuated by both ω-conotoxin GVIA, nisoldipine, and almost completely blocked by $CdCl_2$ (Figure 1). In differentiated hD_3-NG108-15 cells, in contrast to undifferentiated cells (Freedman *et al.*, 1993), both dopamine and quinpirole caused a reversible depression of these calcium currents in the majority of cells studied (Figure 1). The magnitude of the depression seen with quinpirole was the same with either whole cell (16 ± 3% in 13/20 cells) or nystatin perforated patch clamp recording (12 ± 3% in 8/14 cells). These responses were selectively inhibited by S-(−)-sulpiride (1 μM; Figure 1), as well as by pretreatment of cells with pertussis toxin (1 μg ml^{-1} for 18–24 h, $n = 9$ cells). In cells exhibiting just the low threshold transient calcium currents, or under conditions which preferentially elicit the low threshold current (e.g. steps from −80 or −100 mV to −20 mV), 5/6 of these cells did not respond to the application of dopamine (10 μM).

Discussion This study describes the depression of calcium currents in a neuroblastoma-×-glioma cell line by activation of heterologously expressed human D_3 dopamine receptors. High-threshold calcium currents in differentiated NG108-15 cells are regulated following activation of several other types of neurotransmitter receptors, including α-adrenoceptors and muscarinic receptors (McFadzean *et al.*, 1989; Caulfield & Brown, 1991). In the present study, dopamine did not affect calcium currents in the untransfected, differentiated NG108-15 cell line used for transfection studies, consistent with the absence of endogenous catecholamine receptors that regulate calcium currents in this parent cell line. Furthermore, no dopamine receptor mRNA or specific binding of iodosulpiride was detected in untransfected and differentiated cells. The depression of calcium currents by dopamine (10–20% at 10 μM) in hD_3-NG108-15 cells was mimicked by the D_3 receptor ligand quinpirole. These responses were also abolished by the dopamine receptor antagonist S-(−)-sulpride (1 μM), and by pertussis toxin. Thus, human D_3 receptors can couple to the depression of calcium currents via pertussis toxin sensitive G-proteins, presumably of the G_o or G_i type(s).

In conclusion, this study demonstrates that human D_3 cDNA encodes a functional dopamine receptor. Coupling of D_3 receptors to the depression of calcium currents, and their presence within the ventral tegmental area and substantia

nigra, suggests that these receptors may regulate transmitter release within the basal ganglia. Identification of agonists and antagonists that selectively act upon D_3 receptors will not only enable a better understanding of the functional role that these receptors have within the CNS, but may also provide the basis of novel therapies for conditions that disrupt central dopaminergic pathways in the brain.

The authors would like to thank J. Gillard for initial screening of cell lines and tissue culture, as well as Professor J.-C. Schwartz and Dr P. Sokoloff for the supply of human D_3 receptor cDNA and the rat D_2 CHO cell line.

References

BERRY-KRAVIS, E., FREEDMAN, S.B. & DAWSON, G. (1984). Specific receptor-mediated inhibition of cyclic AMP synthesis of dopamine in neuroblastoma × brain hybrid cell line NCB-20. *J. Neurochem.*, **43**, 413–420.

BOUTHENET, M.-L., SOIUL, E., MARTRES, M.-P., SOKOLOFF, P., GIROS, B. & SCHWARTZ, J.-C. (1991). Localisation of dopamine D_3 receptor mRNA in the rat brain using *in situ* hybridization histochemistry: comparison with dopamine D_2 receptor mRNA. *Brain Res.*, **504**, 203–219.

CASTRO, S.W. & STRANGE, P.G. (1993). Coupling of D_2 and D_3 dopamine receptors to G-proteins. *FEBS Lett*, **315**, 223–216.

CAULFIELD, M.P. & BROWN, D.A. (1991). Pharmacology of the putative M_4 muscarinic receptor mediating Ca-current inhibition in neuroblastoma × glioma hybrid (NG108-15) cells. *Br. J. Pharmacol.*, **104**, 39–44.

FREEDMAN, S.B., PATEL, S., MARWOOD, R., EMMS, F., SEABROOK, G.R., KNOWLES, M.R. & MCALLISTER, G. (1993). Expression and pharmacological characterisation of the human D_3 receptor. *J. Pharmacol. Expt. Ther.* (in press).

KEBABIAN, J.W. & CALNE, D.B. (1979). Multiple receptors for dopamine. *Nature*, **277**, 93–96.

LLEDO, P.M., HOMBURGER, V., BOCKAERT, J. & VINCENT, J.-D. (1992). Differential G protein-mediated coupling of D_2 dopamine receptors to K^+ and Ca^{2+} currents in rat anterior pituitary cells. *Neuron*, **8**, 455–463.

MCALLISTER, G., KNOWLES, M.R., PATEL, S., MARWOOD, R., EMMS, F., SEABROOK, G.R., GRAZIANO, M., BORKOWSKI, D., HEY, P.J. & FREEDMAN, S.B. (1993). Characterisation of a chimeric hD3/hD2 dopamine receptor expressed in CHO cells. *FEBS Lett.*, **324**, 81–86.

MCFADZEAN, I., MULLANEY, I., BROWN, D.A. & MILLIGAN, G. (1989). Antibodies to the GTP binding protein, G_o, antagonize noradrenaline-induced calcium current inhibition in NG108-15 hybrid cells. *Neuron*, **3**, 177–182.

SEABROOK, G.R., PATEL, S., MARWOOD, R., EMMS, F., KNOWLES, M.R., FREEDMAN, S.B. & MCALLISTER, G. (1992). Stable expression of human D_3 dopamine receptors in GH_4C_1 pituitary cells. *FEBS Lett*, **312**, 123–126.

SOKOLOFF, P., GIROS, B., MARTRES, M.-P., BOUTHENET, M.-L. & SCHWARTZ, J.-C. (1990). Molecular cloning and characterisation of a novel dopamine receptor (D_3) as a target for neuroleptics. *Nature*, **347**, 146–151.

(Received October 14, 1993
Accepted November 8, 1993)

Br. J. Pharmacol. (1994), **111**, 394–396

SPECIAL REPORT

Pharmacokinetics, plasma protein binding and urinary excretion of N^{ω}-nitro-L-arginine in rats

Mohammad A. Tabrizi-Fard & [1]Ho-Leung Fung

Department of Pharmaceutics, School of Pharmacy, State University of New York at Buffalo, Buffalo, NY 14260, U.S.A.

The *in vivo* disposition of N^{ω}-nitro-L-arginine (L-NOARG) has been examined in rats. Plasma concentrations of L-NOARG following an intravenous dose of 10 mg kg^{-1} were determined by high-performance liquid chromatography. Plasma L-NOARG concentrations declined biexponentially, with average half-lives of 11 min and 20 h. L-NOARG clearance did not appear to exhibit concentration-dependency below a plasma concentration of 4.56×10^{-4} M (100 mg l^{-1}). Ultrafiltration studies revealed insignificant binding of L-NOARG to rat plasma proteins. Urinary excretion of unchanged L-NOARG was minimal. These pharmacokinetic information may be useful in the design of *in vivo* experiments involving L-NOARG, as well as in the interpretation of the pharmacodynamics of this important nitric oxide synthase inhibitor.

Keywords: Nitric Oxide (NO); N^{ω}-nitro-L-arginine (L-NOARG); pharmacokinetics, protein binding; high-performance liquid chromatography (h.p.l.c.)

Introduction Nitric oxide synthase inhibitors such as N^{ω}-nitro-L-arginine (L-NOARG) have been used extensively to determine the degree of nitric oxide (NO) involvement in many biological systems (Moncada *et al.*, 1991). Recently, these compounds have also been considered as possible therapeutic agents in their own right, e.g., in the treatment of endotoxaemia and in preventing the development of disabling hypotension that is associated with interleukin and other related cytokine therapy (Kilbourn & Griffith, 1992). The *in vivo* disposition of these compounds is not known and design of dosage regimens for investigation of the effects of these compounds had been largely empirical. We have developed a sensitive and reproducible analytical method for the determination of L-NOARG in biological fluids and have obtained some basic information about the pharmacokinetics of L-NOARG in conscious rats.

Methods Male Sprague-Dawley rats (323 ± 24 g) underwent surgery under ether anaesthesia for implantation of an indwelling cannula in the right jugular vein. The cannula was threaded to exit at the back of the neck of the animal. One day later, an intravenous bolus dose of 10 mg kg^{-1} L-NOARG (in saline) was given through the jugular cannula, followed by flushing with normal saline. Blood samples (400 µl) were taken through the (heparinized) cannula and the haematocrit was measured. The blood was immediately centrifuged for 2 min at 13,000 *g* and the plasma was stored at −20°C until analysis. For infusion studies, both the jugular and the femoral veins were implanted in indwelling cannulas, and were threaded to exit through the back of the neck. L-NOARG, at 70 mg kg^{-1} in 10 ml normal saline, was infused over 26 min at a rate of 2.69 mg kg^{-1} min^{-1} into the femoral vein cannula and blood samples were collected through the jugular vein cannula.

The plasma concentration of L-NOARG was analysed by a reverse-phase high-performance liquid chromatography (h.p.l.c.) method that we developed. Briefly, the internal standard (theophylline, 1 mM) was added and plasma proteins were precipitated with 70–72% perchloric acid. The resultant supernatant was neutralized with NaOH. A 50 µl aliquot was then injected into a C-8 reverse-phase column Ultrasphere (250 × 4.6 (i.d.) mm, 5 µm) which was preceded by a 45 × 4.6 (i.d.) mm guard column (both from Beckman, San Ramon, CA, USA). The mobile phase used was 18.5 mM heptane sulphonic acid/10% methanol (pH = 2.7) at 1.5 ml min^{-1}, and UV detection was accomplished at 280 nm. The calibration curves of L-NOARG in plasma were linear between 2.4×10^{-6} to 2.4×10^{-4} M (0.52 to 52 µg ml^{-1}), and recovery from plasma was complete. L-NOARG in urine was assayed similarly.

Plasma protein binding of L-NOARG was determined by an ultrafiltration method (Oellerich *et al.*, 1984). Aliquots of rat plasma (600 µl) were first equilibrated for 20 min at 37°C, and five different concentrations of L-NOARG (between 2.4×10^{-6} to $2.4 \times 10^{-4} \times 10^{-4}$ M, each in triplicate) were examined. Samples were equilibrated for another 30 min and then each sample was divided into two portions, one of which was subjected to ultrafiltration (30 min at 37°C, 500 *g*, DYNAC, Becton Dickinson and Company), while the other served as control. The ultrafiltrate and the control sample were analysed by h.p.l.c. as described.

Materials L-NOARG, theophylline (anhydrous crystals), heptane sulphonic acid (sodium salt) were purchased from Sigma Chemical Company (St. Louis, MO, U.S.A.). Ultrafiltration tubes (Centrifree) were obtained from Amicon (Beverly, MA, USA). All solvents used were of HPLC grade (Fisher Scientific, Pittsburgh, PA, U.S.A.).

Data analysis The PCNONLIN computer programme (Statistical Consultants Inc., Lexington, KY, U.S.A.) was used to fit the experimental data to a two-compartment pharmacokinetic model. The Lagrange polynomial method (Rocci & Jusko, 1983) was used to calculate the area under the plasma concentrations vs. time curve (AUC), and the distribution volume at steady state (V_{ss}). Clearance (Cl) was calculated as dose/AUC. Statistical analyses were performed using Student's *t* test. Statistical significance was concluded when $P < 0.05$. Data were expressed as mean ± s.d.

Results Following intravenous administration of a bolus dose of 10 mg kg^{-1} in rats, plasma L-NOARG declined in a biexponential manner (Figure 1). The average half-lives of the rapidly (α) and slowly (β) declining phases of the drug were 11.0 ± 3.1 min, and 20.0 ± 4.9 h, respectively. Parameters value obtained through noncompartmental analysis, viz: V_{ss}, Cl, and mean residence time (MRT) were

[1] Author for correspondence.

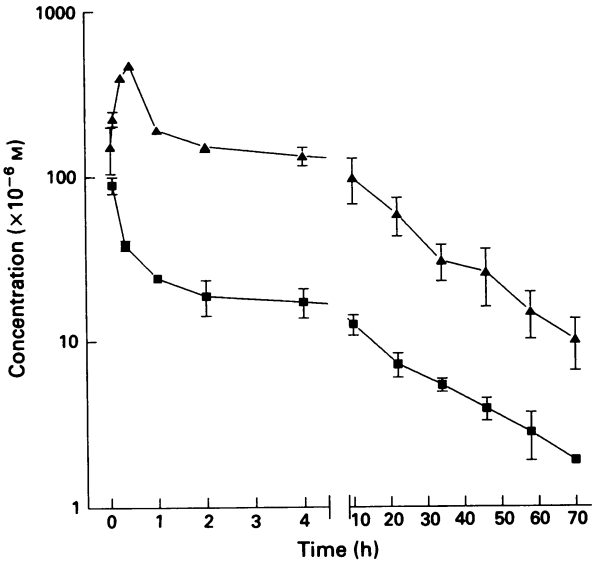

Figure 1 Semilogarithmic plot of plasma N^{ω}-nitro-L-arginine (L-NOARG) concentration vs. time after i.v. bolus (■, $n = 5$) and short infusion (▲, $n = 3$) of L-NOARG in rats at 10 mg kg^{-1} and 70 mg kg^{-1} (2.69 mg kg^{-1} min^{-1}), respectively. The last plasma concentration (at 70 h) after bolus dose was the mean value from two rats only.

2.47 ± 0.40 l kg^{-1}, 84.6 ± 12.4 ml h^{-1} kg^{-1}, and 29.8 ± 6.7 h, respectively. In another study involving a continuous infusion of L-NOARG (70 mg kg^{-1}) at a rate of 2.69 mg kg^{-1} min^{-1}, maximum plasma concentrations close to 4.56×10^{-4} M (100 mg l^{-1}) were reached (Figure 1). The V_{ss} (2.03 ± 0.33 l kg^{-1}) and Cl (87.0 ± 23.6 ml h^{-1} kg^{-1}) values obtained from these animals were similar to those found after the intravenous bolus dose ($P > 0.05$). Ultrafiltration studies revealed insignificant binding of L-NOARG to rat plasma proteins *in vitro* over the concentration-range of 2.4×10^{-6} M to 2.4×10^{-4} M. Within this range, ultrafiltrate concentrations were 101 ± 2.1% of total plasma concentrations ($n = 15$, $P > 0.05$ when compared to controls). Following bolus administration of 10 mg kg^{-1} ($n = 5$), L-NOARG was not detectable (< 1 μg ml^{-1}) in the urine collected, the volume of urine excreted over the length of the study ranged between 10 to 40 ml.

Discussion It is now well established that NO synthase inhibitors such as L-NOARG inhibit the physiological production of NO. Attempts have been made to exploit this inhibitory effect for potential therapeutic gains, e.g., in the management of cytokine-mediated and septic shock (Kilbourn & Griffith, 1992). Currently, *in vivo* dosage regimens for NO synthase inhibitors were largely formulated on an empirical basis since little pharmacokinetic information on the clearance, biodistribution, and excretion of these compounds is available.

Huber *et al.* (1992) measured plasma L-NOARG concent rations from dogs after an oral dose of 30 mg kg^{-1}, and found that they decline only 27% from 3 to 24 h after dosing. This finding suggested that L-NOARG may be slowly cleared from the body, but slow absorption of the enzyme inhibitor may have confounded this interpretation. Schwarzbacher & Raberger (1992) measured L-NOARG concentrations for 30 min after intravenous administration of L-NOARG methyl ester, and found the L-NOARG concentration to be constant over this sampling period. Neither study provided fundamental pharmacokinetic information on L-NOARG.

In the first examination of the pharmacokinetics of L-NOARG, we showed that this inhibitor has a mean residence time of about 30 h, at which time – according to the definition of this parameter (Gibaldi & Perrier, 1982) – 50% of the drug still remained in the body. The apparent elimination half-life was 20 h. This slow elimination was consistent with the prolonged duration of action of L-NOARG seen in some *in vivo* systems. For example, Kolesnikov *et al.* (1993) found that single bolus injection of a low dose of L-NOARG retarded the development of morphine tolerance in mice for several days. Persson *et al.* (1992) also reported a single bolus dose of L-NOARG provided sustained hypertension and bradycardia (up to 24 h) in dogs.

The apparent volume of distribution of L-NOARG was about 2.5 l kg^{-1}, vastly exceeding normal plasma volume in the rat (about 40 ml kg^{-1}, Creskoff *et al.*, 1963). Preliminary studies in our lab (unpublished data) indicated that blood L-NOARG concentration is approximately equivalent to plasma concentration. Thus, L-NOARG is likely to be extensively distributed to extravascular tissues, although little binding to plasma proteins could be detected.

Little unchanged L-NOARG can be detected in the urine. Therefore, the clearance of L-NOARG may arise primarily from metabolism or biliary excretion. The nature of the metabolites is at present unknown.

In summary, we have characterized some of the fundamental pharmacokinetic characteristics of L-NOARG in conscious rats. These results, plus those to be obtained in other animals, should aid in the rational design of dosage regimens for the examination of the *in vivo* effects of L-NOARG.

Footnote

While this paper was undergoing the review process, a similar study was published (Piotrovskij *et al.* (1993), *Drug Metabolism and Disposition*, **21**, 962–963) which confirmed the pharmacokinetic parameters obtained in this study.

This work was supported in part by grant HL22273 from the National Institutes of Health. The excellent technical assistance of Zhuang-Wu Li was acknowledged.

References

CRESKOFF, A.J., FITZ-HUGH, T. & FARRIS, E.J. (1963). Hematology of the rat- methods and standards. In *The Rat in Laboratory Investigation*. ed. Farris E.J. & Griffin J.Q. pp. 406–413. New York: Hafner Publishing Co.

GIBALDI, M. & PERRIER, D. (1982). Noncompartmental analysis based on statistical moment theory. In *Pharmacokinetics*. pp. 409–417. New York: Marcel Dekker.

HUBER, S., GROHS, J.G., SCHWARZACHER, S. & RABERGER, G. (1992). Oral N^G-nitro-L-arginine in conscious dogs: 24 hour hypertensive response in relation to plasma levels. *Amino Acids*, **2**, 225–232.

KILBOURN, R.G. & GRIFFITH, O.W. (1992). Overproduction of nitric oxide in cytokine-mediated and septic shock. *J. Natl. Cancer Inst.*, **84**, 827–831.

KOLESNIKOV, Y.A., PICK, C.G., CISZEWSKA, G. & PASTERNAK, G.W. (1993). Blockade of tolerance to morphine but not to *k* opioids by a nitric oxide synthase inhibitor. *Proc. Natl. Acad. Sci. USA*, **90**, 5162–5166.

MONCADA, S., PALMER, R.M.J. & HIGGS, E.A. (1991). Nitric oxide: physiology, pathophysiology, and pharmacology. *Pharmacol. Rev.*, **43**, 109–141.

OELLERICH, M. & MULLER-VAHL, H. (1984). The EMIT free level ultrafiltration technique compared with equilibrium dialysis and ultracentrifugation to determine protein binding of phenytoin. *Clin. Pharmacokinet.*, **9** (Suppl 1), 61–70.

PERSSON, P.B., BAUMANN, J.E., EHMKE, H., NAFZ, B., WITTMANN, U. & KIRCHHEIM, H.R. (1992). Phasic and 24 h blood pressure control by endothelium-derived relaxing factor in conscious dogs. *Am. J. Physiol.*, **262**, H1395–H1400.

ROCCI Jr, M.L., & JUSKO, W.J. (1983). Lagran program for area and moments in pharmacokinetic analysis. *Com. Pro. Biom.*, **16**, 203–216.

SCHWARZACHER, S. & RABERGER, G. (1992). L-N^G-nitro-arginine methyl ester in the anesthesized rabbit: venous vasomotion and plasma levels. *J. Vasc. Res.*, **29**, 290–292.

(Received October 5, 1993
Accepted November 9, 1993)

Br. J. Pharmacol. (1994), **111**, 397–405

The pharmacology of the nicotinic antagonist, chlorisondamine, investigated in rat brain and autonomic ganglion

[1]P.B.S. Clarke, *I. Chaudieu, H. El-Bizri, *P. Boksa, M. Quik, B.A. Esplin & R. Čapek

Department of Pharmacology and Therapeutics, McGill University, 3655 Drummond St, Montreal, Canada H3G 1Y6 and *Department of Psychiatry, McGill University, 6875 LaSalle Blvd., Verdun, Canada H4H 1R3

1 A single administration of the ganglion blocker, chlorisondamine (10 mg kg^{-1}, s.c.) is known to produce a quasi-irreversible blockade of the central actions of nicotine in the rat. The mechanism of this persistent action is not known. It is also unclear whether chlorisondamine can block neuronal responses to excitatory amino acids and whether chronic blockade of nicotinic responses also occurs in the periphery.

2 Acute administration of chlorisondamine (10 mg kg^{-1}, s.c.) to rats resulted in a blockade of central nicotinic effects (ataxia and prostration) when tested 1 to 14 days later, but caused no detectable cell death in tissue sections sampled throughout the rostrocaudal extent of the brain which were stained in order to reveal neuronal degeneration.

3 Long-term blockade of central nicotinic effects by chlorisondamine was not associated with significant alterations in the density (B_{max}) of high-affinity [^{3}H]-nicotine binding to forebrain cryostat-cut sections.

4 In cultured dissociated mesencephalic cells of the foetal rat, chlorisondamine and mecamylamine inhibited [^{3}H]-dopamine release evoked by N-methyl-D-aspartate (NMDA, 10^{-4} M), but only at high concentrations (IC_{50} approx. 600 and 70 μM, respectively). A high concentration of chlorisondamine (10^{-3} M) had no effect on responses to quisqualate (10^{-5} M) and only slightly reduced responses to kainate (10^{-4} M). Mecamylamine (10^{-3} M) was ineffective against both agonists.

5 In adult rat hippocampal slices, chlorisondamine depressed NMDA receptor-mediated synaptically-evoked field potentials, but again only at high concentrations (10^{-4}–10^{-3} M). Synaptic responses that were mediated by non-NMDA excitatory amino acid receptors were less affected.

6 In rat isolated superior cervical ganglion, electrically-evoked synaptic transmission was reduced 1 h after acute *in vivo* administration of chlorisondamine (0.1 mg kg^{-1}, s.c.). However, *in vivo* administration of a higher dose (10 mg kg^{-1}, s.c.) did not significantly affect ganglionic transmission when tested two weeks later, despite the continued presence of central nicotinic blockade.

7 These results indicate that the persistent CNS nicotinic blockade by chlorisondamine is not accompanied by changes in nicotinic [^{3}H]-nicotine binding site density or by neuronal degeneration in the brain; that at doses sufficient to produce nicotinic receptor blockade, chlorisondamine acts in a pharmacologically selective manner; and that chronic central blockade is not accompanied by long-term peripheral ganglionic blockade.

Keywords: Chlorisondamine; nicotinic receptors; nicotine; mecamylamine; ganglion blockers; NMDA receptors; dopamine release

Introduction

Chlorisondamine (CHL) is a nicotinic antagonist of the ganglion blocking class and exerts negligible effects at nicotinic cholinoceptors of the skeletal muscle endplate (Plummer *et al.*, 1955; Grimson *et al.*, 1955). Consistent with its bisquaternary structure, chlorisondamine does not appear to penetrate the CNS readily. However, behavioural studies in rats have shown that chlorisondamine, when administered centrally, exerts an extremely long-lasting blockade of the central actions of nicotine (Clarke & Kumar, 1983; Clarke, 1984, Reavill *et al.*, 1986; Fudala & Iwamoto, 1987; Kumar *et al.*, 1987; Mundy & Iwamoto, 1988; Clarke & Fibiger, 1990; Corrigall *et al.*, 1992). For example, a single administration of chlorisondamine (0.2–5.0 μg, i.c.v.) produced a dose-dependent blockade of the locomotor stimulant effect of nicotine (Clarke, 1984) which appears to reflect a site of action in the brain rather than the spinal cord (Clarke *et al.*, 1988). The central blockade resulting from chlorisondamine administration showed little sign of waning even at 5 weeks after a single administration. A similarly persistent blockade occurred after systemic administration of a high dose (10 mg kg^{-1}, s.c.) (Clarke, 1984; El-Bizri & Clarke, 1994b). Although there is *in vitro* evidence that chlorisondamine blocks CNS nicotinic receptors acutely (Izenwasser *et al.*, 1991; Marks *et al.*, 1993; El-Bizri & Clarke, 1994a), the mechanism underlying its long-term blocking action is not understood.

The extreme persistence of the blocking effect raises the possibility that chlorisondamine destroys certain neurones, perhaps targeting those neurones which express nicotinic receptors. From a light microscopic examination of Nissl-stained sections from rat brain, Kumar *et al.* (1987) tentatively suggested that chlorisondamine is unlikely to act as a neurotoxin. In order to re-evaluate this possibility, we have now employed a more sensitive method which selectively reveals degenerating neurones. Since chlorisondamine administration produces insensitivity to nicotine, we have also tested whether persistent blockade by chlorisondamine is accompanied by a reduced density of brain nicotinic receptors and whether systemic administration of a high dose of chlorisondamine, sufficient to induce long-term central blockade, is accompanied by persistent ganglion block in the periphery.

[1] Author for correspondence.

Methods

Male adult Sprague-Dawley rats (Charles River, Quebec) were maintained on food and water *ad libitum*. They were housed in groups of two or three subjects per cage, randomly allocated with respect to drug treatment, in a room illuminated from 07 h 00 min to 19 h 00 min. Behavioural testing was carried out between 09 h 00 min and 16 h 00 min. All rats were initially drug-naive.

Evaluation of possible neuronal degeneration following chlorisondamine treatment

Fifteen rats (220 to 330 g) were randomly allocated to five groups ($n = 3$). Four groups received chlorisondamine (10 mg kg^{-1}, s.c.) and were tested behaviourally for central nicotinic blockade 1, 3, 7, or 14 days later. The fifth group received saline s.c. and was tested after 3 days. Following behavioural testing, each animal was killed for histological assessment of neuronal degeneration.

Production of excitotoxic lesions At each survival time, one or two additional rats were infused intracerebrally with the excitotoxin, N-methyl-D-aspartate (NMDA) in order to provide positive controls for nicotinic behavioural effects and for neuronal degeneration. Briefly, animals were anaesthetized with sodium pentobarbitone (55 mg kg^{-1}, i.p.) and mounted in a stereotaxic device (David Kopf, Tujunga, CA), with the tooth bar positioned 3.3 mm below the interaural line. NMDA (0.1 M in 0.1 M sodium phosphate buffer, pH 7.4) was infused into the dentate gyrus (0.25 µl over 5 min) and into ventral thalamus (0.5 µl over 5 min), via 30 gauge stainless steel cannulae attached by polyethylene tubing to a syringe pump (Sage Instruments, Cambridge, MA, U.S.A.). The cannula was withdrawn after a further 3 min, and the wound sutured. Seizure activity was observed a few hours after surgery and was abolished by administration of 8 mg kg^{-1}, i.p. of diazepam. Animals were killed one day later.

Behavioural testing Behavioural tests served to confirm central nicotinic blockade by CHL. Rats were scored individually for prostration and ataxia induced by nicotine (0.8 mg kg^{-1}, s.c.); both effects are due to central actions of nicotine (Clarke, 1984). A plexiglass cage was employed, measuring 35 cm by 30 cm by 16 cm high, with a wire grill lid and a thin layer of sawdust underfoot. Rats were tested individually. At 2, 4, 6, 8, and 10 min after injection, the presence or absence of prostration and ataxia were separately noted within a 15 s observation period.

Detection of neuronal degeneration Animals were deeply anaesthetized with sodium pentobarbitone (65 mg kg^{-1}, i.p.) and were perfused intracardially with ice-cold saline (1 min) followed by fixative (4% paraformaldehyde in 0.1 M phosphate buffer, pH 7.4, 20 min). Brains were removed, post-fixed in the same fixative for 3–8 days at 4°C, divided into three blocks, and cut on a freezing microtome. Serial 40 µm sections were taken at 0.5 mm intervals, through the entire rostrocaudal extent of the brain. Brain sections were stored for 3–4 days at 4°C in multiwell plates modified with polypropylene mesh bottoms to allow incubation in fixative. The silver staining procedure of Gallyas *et al.* (1980) was used, as modified by Nadler & Evenson (1983). Processed sections were mounted on microscope slides, coverslipped with Permount mounting medium (Fisher Scientific Co., Fair Lawn, New Jersey), and examined by light microscopy at 100 × –400 × magnification. Neuronal degeneration was detected by the presence of argyrophilic material.

[^{3}H]-nicotine binding following chlorisondamine treatment

Twenty-two rats (300 to 375 g) were randomly allocated and received CHL (10 mg kg^{-1}) or saline ($n = 11$ per group). Fourteen days later, four rats in each group were tested for nicotine-induced ataxia and prostration (see above). The remaining seven rats in each group did not receive nicotine and were killed at this time for radioligand binding analysis.

Brain nicotinic receptors were quantified by [^{3}H]-nicotine binding, as previously described (Clarke *et al.*, 1984). Slide-mounted coronal brain sections were used, since the ultimate intention was to map CHL-induced changes by autoradiography. However, initial results were essentially negative (see Results), and autoradiography was not performed. Cryostat sections were taken at two levels of the brain (10.6 and 4.2 mm anterior to interaural zero (Paxinos & Watson, 1986), corresponding to mid-striatal and posterior thalamic levels, respectively) and stored at −40°C until use. Thawed sections were labelled with [^{3}H]-(−)-nicotine in buffer, rinsed, dried, and scraped into vials for liquid scintillation counting. Non-specific binding was defined by the addition of 10^{-5} M (−)-nicotine ditartrate to the incubation.

Radiochemical purity was tested by thin layer chromatography, since impure samples of [^{3}H]-nicotine can produce a second (non-specific) component of binding (Romm *et al.*, 1990). In addition, saturation experiments were performed in brains from control rats ($n = 2$), and CHL-treated animals ($n = 2$).

These experiments were performed on anterior brain sections (IA 10.6) and employed ten [^{3}H]-nicotine concentrations (0.1–32 nM). Since weighted-nonlinear curve fitting analysis of binding isotherms (LIGAND, Elsevier Biosoft; Munson & Rodbard, 1980) revealed only a single population of sites in each of these subjects, two-point Scatchard analysis (Dunn *et al.*, 1988) was performed on the remaining anterior brain sections, at 1 and 16 nM [^{3}H]-nicotine. Posterior brain sections (IA 4.2) were processed in this way several weeks later.

Responses to excitatory amino acids in cultured cells

Mesencephalic cell cultures were prepared as previously described (Mount *et al.*, 1989). Briefly, anteroventral mesencephalic tissue was dissected from the brains of Sprague-Dawley rat embryos (Charles River, Quebec, Canada) on day 15 of gestation. The tissue was mechanically dissociated and diluted to approximately 10^6 cells ml^{-1} in Dulbecco's modified Eagle's medium (DMEM; Gibco Canada, Burlington, Ont., Canada) containing nystatin (24 u ml^{-1}), KCl (20 mM), and 10% v/v heat-inactivated foetal calf serum (Gibco, Canada). Cells were grown on 24-well Multiwell plates coated wtih poly-D-lysine (20 µg ml^{-1}). Cultures were maintained at 37°C in humid air containing 10% CO_2.

Release experiments followed a protocol previously described in detail (Mount *et al.*, 1990). Briefly, cells were rinsed with Krebs-Ringer-HEPES buffer (KRH), pH 7.4, with the following composition (mM): NaCl 125, KCl 4.8, HEPES 25, NaOH 5, $MgSO_4$ 1.2, KH_2PO_4 1.2, D-glucose 5.6, $CaCl_2$ 2.2, pargyline 0.1 and ascorbate 1.0. Cells were then loaded with [^{3}H]-dopamine (50 nM) for 20–30 min at 37°C, in the presence of 50 µM desipramine (Mount *et al.*, 1989). After [^{3}H]-dopamine loading, each well was rinsed four times with KRH at 23°C, until spontaneous release was stable (4–6% total [^{3}H]-dopamine content per 5 min).

When the effect of a single drug was tested on [^{3}H]-dopamine release, KRH buffer (500 µl per well) was collected after a 5 min ('basal release') period, followed immediately by a 5 min ('stimulation') incubation in the presence of drug. When two drugs were tested, cells were exposed to the first drug (antagonist) during the first 5 min ('basal release') period, and then exposed to both drugs (antagonist and agonist) for the second 5 min ('stimulation') period. Radioactivity remaining in the cells was counted after extraction in

acidified ethanol; previous experiments have shown that 90% of both released and cellular radioactivity elutes with standards (Mount *et al.*, 1989). For data presentation, basal [^{3}H]-dopamine release was subtracted from drug-stimulated release, and the resulting value was expressed as a percentage of the total [^{3}H] content present in the cells during the relevant measurement period.

The effects of mecamylamine 10^{-4} M and CHL 10^{-3} M in the absence of agonist were examined by comparison with control tissue wells treated with KRH (Ringer-HEPES buffer) during the 'stimulation' period. Subsequently, the effects of the same concentrations of antagonist were studied on responses to quisqualate (Quis, 10^{-5} M), kainate (KA, 10^{-4} M), and NMDA (10^{-4} M). These concentrations of agonist have been found to produce half-maximal to maximal effects (Mount *et al.*, 1990). Finally, responses to NMDA (10^{-4} M) were examined in the presence of a range of concentrations of mecamylamine (10^{-5}–10^{-3} M) or CHL (10^{-6}–10^{-3} M). The number of wells per condition was 9–21.

Synaptic responses in hippocampal slice

Hippocampal slices (425 μm thick) were prepared from adult male Sprague-Dawley rats and maintained at 30°C in a recording chamber. The upper surface of the slice was exposed to a flow of moist 95% O_2 and 5% CO_2, and the lower surface rested on a nylon mesh exposed to oxygenated artificial cerebrospinal fluid (ACSF) of the following composition (mM): NaCl 124, KCl 5.0, $NaHCO_3$ 25.6, $CaCl_2$ 2.0, NaH_2PO_4 1.2, $MgSO_4$ 1.0 or 0.0 and D-glucose 10. The ACSF was perfused through the chamber at 1 ml min^{-1}. Field potentials were recorded in the pyramidal (CA1) cell body layer by a micropipette (10–20 MOhm) filled with 4 mM NaCl. Stimulating pulses (0.1 ms) were delivered by a bipolar electrode in the stratum radiatum to activate the cells orthodromically. Unless stated otherwise, the intensity of stimulus was adjusted to produce a population spike with an amplitude corresponding to 70% to 90% of maximum. Chlorisondamine and DL-2-amino-5-pentanoic acid (APV) were dissolved in ACSF and perfused through the recording chamber. A microcomputer-based system was used for data acquisition and analysis, as previously described (Theoret *et al.*, 1984).

In a typical experiment, magnesium-free medium was used. During a 5 min baseline period, electrical stimulation was applied every 10 s, consisting of single pulses of 0.1 ms duration. Evoked responses to the same stimulus were recorded 20–28 min and again 45–53 min after the start of perfusion with the drug dissolved in ACSF. In some experiments, a second, higher concentration of drug was tested in the same fashion, with no intervening wash-out period. Three distinct population spikes were identified and quantified, by expressing the peak voltage of each as a percentage of its individual pre-drug baseline.

Twenty-three rats were used, weighing 150 to 200 g. The temporal stability of the preparation was tested in three control experiments in which a slice was perfused with Mg-free medium for between 4 and 6 h.

Transmission in superior cervical ganglion

Twenty-three rats, weighing 195 to 270 g, were used. To examine the chronic effects of CHL, 20 rats were randomly allocated to two groups and received CHL (10 mg kg^{-1}) or saline (n = 10 per group). Twelve days later, four rats in each group were tested for nicotine-induced ataxia and prostration (as described previously). The remaining six rats in each group did not receive nicotine and were killed at this time for electrophysiological studies. The acute effect of CHL on ganglionic transmission was examined in an additional three rats that received a lower dose of CHL (0.1 mg kg^{-1}, s.c.) only 1 h before they were killed.

Superior cervical ganglia were dissected under ether anaesthesia and transferred to a bath containing 5 ml Krebs solution (composition (mM): NaCl 120, KCl 4.6, $CaCl_2$ 2.4, $MgSO_4$ 1.2, $NaHCO_3$ 25, KH_2PO_4 1.2 and D-glucose 9.9) bubbled with 95% O_2/5% CO_2 at pH 7.4. The preganglionic and internal carotid (postganglionic) nerves were aspirated into glass suction electrodes fitted with Ag/AgCl electrodes for stimulation and recording, respectively (Dunant, 1967; Quik & Lamarca, 1982). Supramaximal square wave pulses of 1.0 ms duration were applied at 0.2 Hz to the stimulating electrode from a stimulator via an isolation unit (Grass Instrument Co., Quincy, MA). The evoked potentials recorded from the internal carotid nerve were displayed on an oscilloscope (Tektronix, Portland, OR, U.S.A.) and permanent records were made on polaroid film. Data were analysed as peak postganglionic population action potentials.

Drugs

(−)-Nicotine di-(+)-tartrate (Sigma) was dissolved in 0.9% w/v NaCl solution (saline) and neutralized to pH 7.2 ± 0.1 with NaOH. Chlorisondamine Cl (gift of CIBA-Geigy, Summit, New Jersey) was dissolved in saline. All systemic injections were subcutaneous (s.c.), given in the flank in a volume of 1 ml kg^{-1}. Doses of nicotine and CHL refer to the base; doses of other drugs are of the salt. [^{3}H]-dopamine and [^{3}H]-(−)-nicotine (specific activity 20 and 68.8 Ci mmol^{-1}, respectively) were purchased from New England Nuclear (Boston, MA, U.S.A.). N-methyl-D-aspartic acid (NMDA), kainic acid (KA), quisqualic acid (Quis) and DL-2-amino-5-pentanoic acid (APV) were obtained from Sigma Chemical Co. (St Louis, MO, U.S.A.). Diazepam was obtained from Sabex Pharmaceuticals (Boucherville, Canada). Other chemicals were reagent grade and were obtained commercially.

Analysis of data

Data were analysed by ANOVA or by t tests. For comparisons with a single control group, Dunnett's test was used (Dunnett, 1955). Probability values are for 2-tailed tests.

Results

Evaluation of possible neuronal degeneration following chlorisondamine treatment

Administration of nicotine resulted in prostration and ataxia in all 10 rats that had not received chlorisondamine. All ten subjects became prostrate in the first 2 min after injection. From 2 to 4 min post injection, three subjects were still prostrated, and all subjects were ataxic. Ataxia persisted throughout all subsequent 2 min periods, except for one rat which recovered in the final period (8–10 min). In contrast, none of the 15 rats that had received chlorisondamine manifested these behavioural effects of nicotine; three of these rats had received chlorisondamine 24 h before.

Processed brain sections from control (saline-treated) and CHL-treated rats were indistinguishable. Consistent with previous reports (Gallyas *et al.*, 1980; Nadler & Evenson, 1983), sections possessed a general golden-brown appearance (Figure 1), with three types of silver grain distribution: (1) some sections from all levels of the brain were overlaid with a sparse and even distribution of silver grains, which was anatomically nonspecific and inconsistently observed across adjacent sections, and hence was probably the result of random silver precipitation; (2) within some magnocellular neurones in the vestibular nuclei of the brain stem, and (3) a characteristic pattern of grains was seen running along blood vessels. None of these silver grain distributions suggested neuronal degeneration.

Clear signs of neuronal degeneration were, however, observed in rats lesioned with NMDA (Figure 1a,b,c and d). Degenerating cell bodies and processes containing grey or

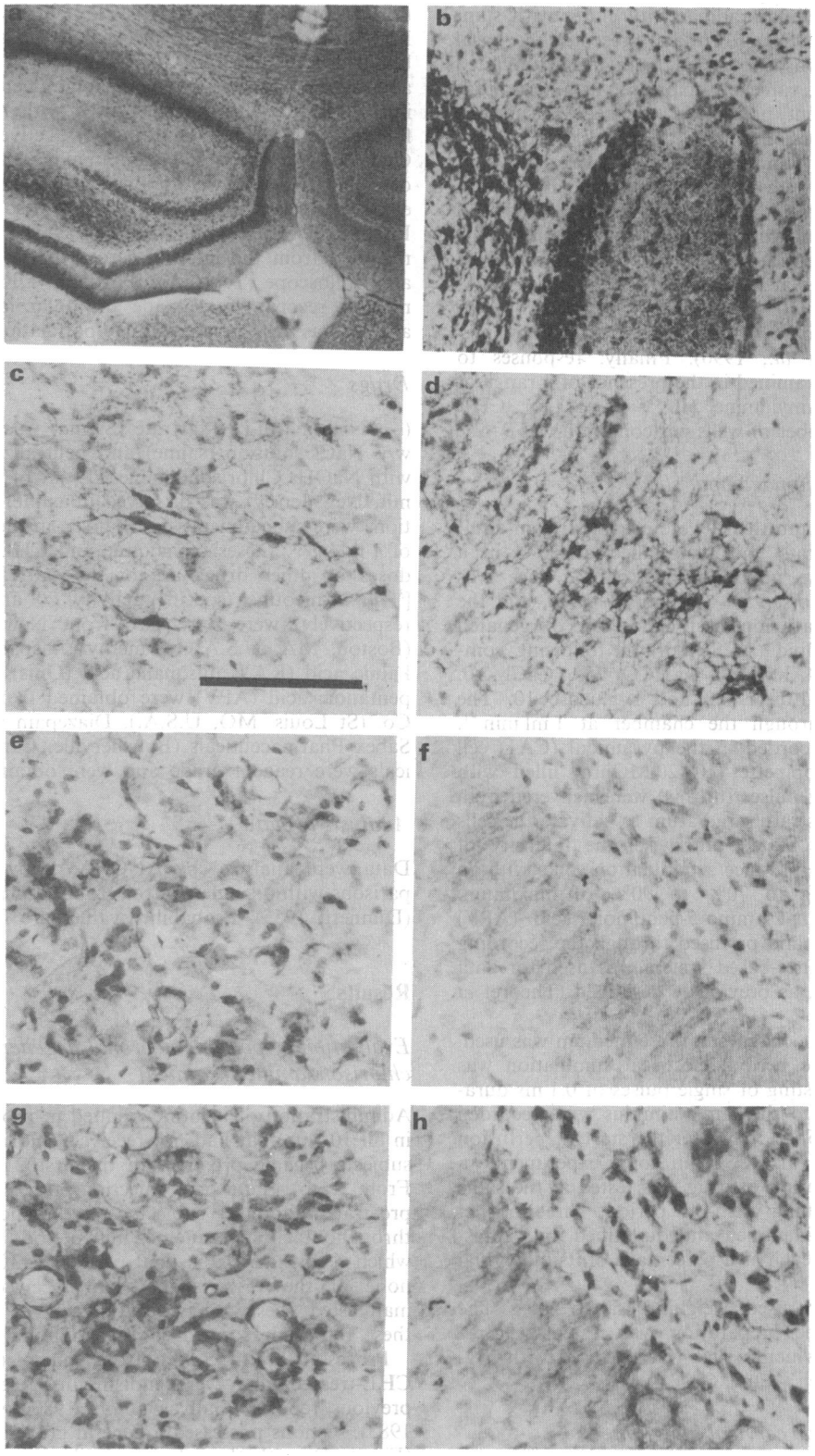

Figure 1 Coronal sections (40 μm thick) of rat brain stained by the method of Gallyas *et al.* (1980) in order to reveal degenerating neurones. Panel (a) (× 100 magnification) shows the hippocampus and dentate gyrus of a rat which had received a unilateral (left side) infusion of the excitotoxin NMDA. The pyramidal and dentate granule cell layers are stained black on the lesioned side. The dorsomedial hippocampal area in panel (a) is shown at higher magnification (× 200) in panel (b) where black-stained pyramidal and granule cell bodies and some processes are visible. Panels (c–h) are at × 400 magnification; the calibration bar in (c) indicates 100 μm. Panel (c) shows several stained neurones in the ventral thalamus of a rat that had sustained an NMDA lesion in this area; degenerating cell bodies and processes are visible. Panels (e) and (g) show corresponding images from rats which had received systemic saline or chlorisondamine, respectively, three days before they were killed; only golden-brown staining of cells and neurophil is seen. Panels (d), (f) and (h) show neurones in the hippocampal pyramidal cell layer from NMDA-lesioned, saline- and chlorisondamine-treated rats, respectively; again, no degeneration is observed except in the lesioned animal. A colour photograph is available from the authors upon request.

black granular deposits were readily identified in both dentate gyrus and ventral thalamus. Degenerating axons were also clearly visible (Figure 1c and d).

Tritiated nicotine binding following chlorisondamine treatment

Behavioural tests confirmed blockade of the central nicotinic actions that were observed in control animals. Thus, none of the four CHL-treated rats displayed ataxia or prostration, whereas all four of the control rats did.

Non-linear regression analysis of specific binding revealed a single population of sites in each of the four rats tested. The two saline-treated control animals yielded apparent K_D and B_{max} values of 5.9 and 4.7 nM and 15.4 and 14.0 fmol/section, respectively. The corresponding values in CHL-treated rats were 4.7 and 3.7 nM, and 14.3 and 12.3 fmol/section. Scatchard plots illustrating these data are shown in Figure 2. For all four rats, Hill coefficients were near unity (range 0.99–1.06).

Subsequent analyses included data from all subjects. B_{max} values extrapolated from 2-point Scatchard analyses did not differ significantly between saline- and CHL-treated groups, either at the anterior brain level (mean ± s.e.mean, respectively: 16.7 ± 0.8 and 14.9 ± 1.1; t = 1.33, d.f. 12, $P > 0.1$), or at the posterior level (respectively: 13.9 ± 1.0 and 15.1 ± 1.2; t = 0.77, d.f. 12, $P > 0.1$). Values of the apparent K_D differed significantly between saline- and CHL-treated groups at the anterior brain level (respectively: 6.13 ± 0.36 and 4.71 ± 0.36; $P < 0.02$). However, at the posterior level, no significant difference was found (respectively: 3.71 ± 0.31 and 4.10 ± 0.43; $P > 0.1$).

Responses to excitatory amino acids in cultured cells

When given alone, high concentrations of CHL (10^{-3} M) and mecamylamine (10^{-4} M) had no effect on [^{3}H]-dopamine release ($P > 0.4$). The mean (± s.e.mean) release (in excess of basal) for KRH-treated, mecamylamine-treated, and CHL-treated samples was − 0.07% ± 0.12%, 0.19% ± 0.17%, and 0.03% ± 0.13%, of total cellular [^{3}H]-dopamine stores, respectively.

Release of [^{3}H]-dopamine in response to Quis 10^{-5} M was not significantly affected by these high concentrations of mecamylamine and CHL ($P > 0.2$). Quis-evoked release was 4.25% ± 0.27% (no antagonist), 3.90% ± 1.21% (CHL) and 3.53% ± 0.82% (mecamylamine). KA-evoked release was 13.3 ± 0.6% (no antagonist), 11.0 ± 0.7% (CHL) and 11.7 ± 0.6% (mecamylamine). The small effect of CHL on the KA response was statistically significant ($P < 0.05$). Both mecamylamine and CHL reduced NMDA-(10^{-4} M)-induced [^{3}H]-dopamine release in a concentration-related manner (mecamylamine: $P < 0.001$; CHL: $P < 0.001$; Figure 3). Mecamylamine produced a significant attenuation at 10^{-4} M and complete blockade at 10^{-3} M. CHL produced a significant, albeit incomplete, attenuation of the NMDA response only at 10^{-3} M ($P < 0.01$). IC_{50} values of approximately 70 μM for mecamylamine and 600 μM for CHL were obtained (mean of three experiments).

Synaptic responses in hippocampal slice

In magnesium-free medium, baseline evoked responses were multiphasic (Figure 4). Addition of magnesium (1.0 mM) or APV (100 μM) to the superfusion medium abolished secondary spikes (Figure 4). These findings confirm previous observations suggesting that the primary and secondary spikes are mediated by non-NMDA and NMDA excitatory amino acid receptors, respectively (Coan & Collinridge, 1987).

Control experiments indicated that the slice preparation was stable throughout the observation period. The mean values of the primary spike at the three measurement times

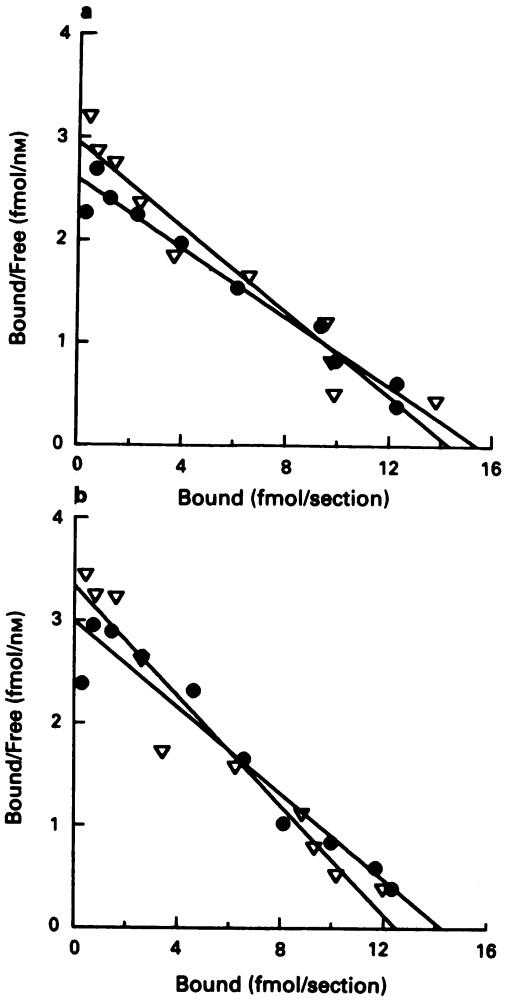

Figure 2 Scatchard plots of [^{3}H]-nicotine binding to cryostat-cut forebrain sections. Concentrations of radioligand were 0.1–32 nM. Two animals (a) had received an injection of saline 2 weeks before they were killed; two animals (b) had received a systemic dose of chlorisondamine (10 mg kg^{-1}, s.c.), sufficient to produce persistent central nicotinic blockade.

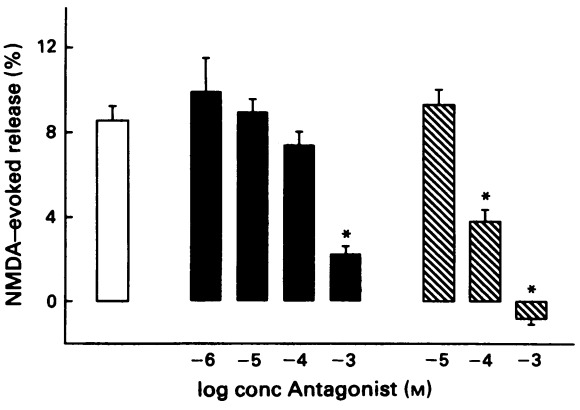

Figure 3 Effects of chlorisondamine and mecamylamine on the release of [^{3}H]-dopamine evoked by N-methyl-D-aspartate (NMDA: 10^{-4} M) in rat cultured mesencephalic cells. The vertical axis show mean (± s.e.mean, $n = 9–21$) agonist-stimulated release, expressed as a percentage of residual cellular ^{3}H content (see text). Compared to controls (no antagonist: open columns), both chlorisondamine (solid columns) and mecamylamine (hatched columns) reduced or blocked responses to NMDA, but only at high concentrations.

were, respectively, 103, 123 and 93% of baseline. Corresponding values for secondary spikes were 120, 126 and 90%. Tertiary spikes appeared less stable (85, 117 and 66%, respectively).

Chlorisondamine had no effect on the magnitude of primary (non-NMDA) responses (Figure 5). In contrast, secondary spikes were reduced ($P<0.001$); they were unaffected by lower concentrations (10^{-6} and 10^{-5} M), but were somewhat decreased at 10^{-4} M and abolished at 10^{-3} M (Figure 5). Tertiary spikes were similarly affected (Figure 5). The blockade produced by the highest concentration was followed during a wash-out period of 45 to 60 min duration; recovery from blockade was observed in 4 out of 5 experiments, and partial recovery occurred in the remaining experiment.

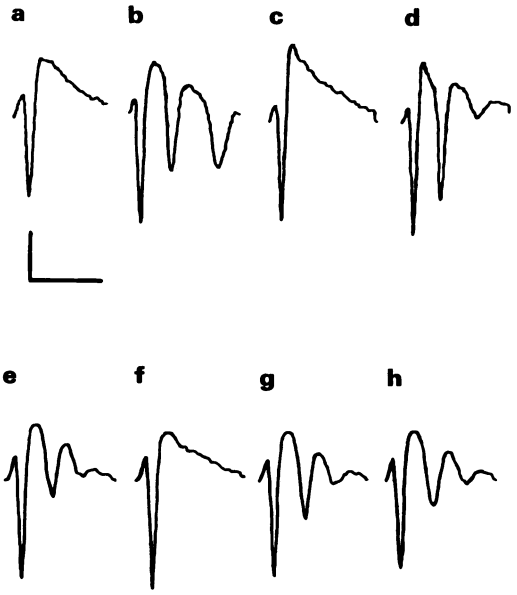

Figure 4 Representative CA1 hippocampal population spikes in response to electrical stimulation of the stratum radiatum. In normal artificial cerebrospinal fluid (ACSF), only one population spike was seen (a); after a period of superfusion in Mg^{2+}-free medium, two later spikes appeared (b) which could then be abolished by a high concentration of chlorisondamine (10^{-3} M; c); recovery occurred after withdrawal of drug (d). In a second experiment, the later negative components occurring in Mg^{2+}-free medium (e) were abolished by superfusion with D,L-2-amino-5-pentanoic acid (10^{-4} M; f). Recovery occurred upon wash-out (g). Subsequently, a lower concentration of chlorisondamine (10^{-4} M) had little or no effect (h). Calibration scale: 5 mV (vertical), 10 ms (horizontal).

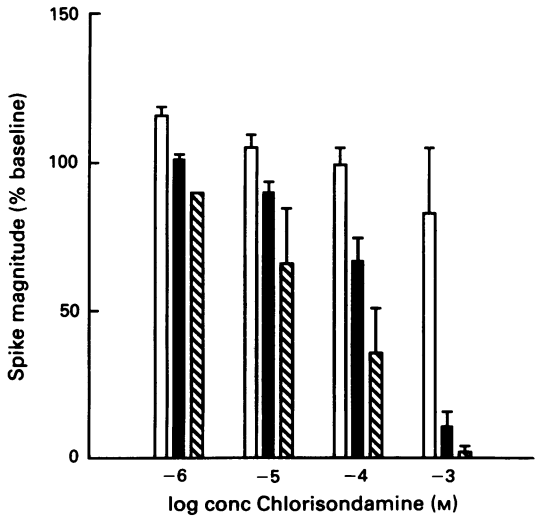

Figure 5 Effects of chlorisondamine on CA1 population spikes in hippocampal slices. The vertical axis shows the mean (± s.e.mean, $n = 3-7$) magnitude of electrically-evoked primary (open columns), secondary (solid columns) and tertiary (hatched columns) population spikes as a percentage of pre-drug baseline. Chlorisondamine reduced secondary and tertiary spikes in a concentration-dependent manner, but had little or no effect on the magnitude of primary spikes.

Table 1 Effect of chlorisondamine on nicotinic receptor-mediated transmission in rat superior cervical ganglion

Treatment	*Survival*	n	*Action potential amplitude* (mV)
Saline	1 h	3	0.57 ± 0.13
Chlorisondamine	1 h	5	0.19 ± 0.08*
Saline	12 days	9	0.47 ± 0.09
Chlorisondamine	12 days	10	0.57 ± 0.07

Chlorisondamine was given s.c. (0.1 mg kg^{-1} with 1 h survival: 10 mg kg^{-1} with 12 days survival). Values represent mean ± s.e.mean. Significance of difference from control ganglia: *$P<0.05$.

Transmission in superior cervical ganglion

In behavioural tests, nicotine induced prostration and ataxia in the four control (saline-treated) rats, but not in four rats treated 14 days before with CHL. Ptosis, which occurred within minutes of injection of CHL, was absent in all animals 24 h later.

Acute administration of CHL (0.1 mg kg^{-1}) 1 h prior to the animal's death significantly reduced the magnitude of postganglionic potentials ($P<0.05$; Table 1). In contrast, administration of the much higher dose of CHL (10 mg kg^{-1}) two weeks beforehand had no significant effect on postganglionic potentials ($P>0.3$ compared to saline-treated controls).

Discussion

A single administration of chlorisondamine, in a sufficient dose, produces an extremely long-term blockade of all the centrally-mediated behavioural effects of nicotine that have been examined to date. Such effects include locomotor stimulation and locomotor depression (Clarke, 1984), depression of operant behaviour and the nicotine cue (Kumar *et al.*, 1987), conditioned taste aversion (Reavill *et al.*, 1986), conditioned place aversion (Fudala & Iwamoto, 1987), nicotine-induced impairment of autoshaping response (Mundy & Iwamoto, 1988), and nicotine intravenous self-administration (Corrigall *et al.*, 1992). The present observations add nicotine-induced ataxia and prostration to this list, and additionally show that central nicotinic blockade was complete within 24 h of chlorisondamine administration.

Does chlorisondamine cause neuronal degeneration?

Little or no neuronal degeneration was detected in chlorisondamine-treated rats, despite evidence of central nicotinic blockade in the same animals tested just before death. The absence of observable pathology does not appear to reflect an insensitive method, since clear signs of axonal and somatodendritic degeneration were seen in the brains of subjects lesioned with NMDA.

Could chlorisondamine have destroyed a population of neurones which, though small, may be crucial for the mediation of the behavioural effects of nicotine? The extensive nature of our survey, in which one thousand brain sections

were processed and examined, makes this possibility unlikely. Furthermore, strong evidence exists that the locomotor stimulant effect of nicotine is mediated through a direct action on mesolimbic dopaminergic neurones (Clarke, 1990); since this behavioural effect is blocked persistently by chlorisondamine (Clarke, 1984), it is noteworthy that no signs of degeneration were observed in dopamine-containing systems in the present study.

Does chlorisondamine alter nicotinic receptor number?

Persistent central nicotinic blockade resulting from chlorisondamine administration was not associated with a decreased density of nicotinic receptors, as assessed by high-affinity [^{3}H]-nicotine binding at two rostrocaudal levels of the brain. There was an indication that binding affinity was slightly altered by chlorisondamine, but this finding must be viewed with caution since it was only obtained at one of the two brain levels examined. High affinity [^{3}H]-nicotine binding sites represent a prevalent subtype of nicotinic receptors in rat brain (Lindstrom *et al.*, 1987) which are believed to be a major target for subconvulsive doses of nicotine (Clarke, 1987; London *et al.*, 1988). It would thus appear unlikely that chlorisondamine produces its persistent blockade by regulating the number of central nicotinic receptors. However, this possibility cannot be ruled out completely, since other populations of central nicotinic receptors exist that are not labelled with high affinity by [^{3}H]-nicotine (Clarke *et al.*, 1985; Couturier *et al.*, 1990; Schulz *et al.*, 1991).

Two weeks of chronic nicotine treatment *in vivo* results in an upregulation of high affinity agonist binding sites in rodent brain (Wonnacott, 1990). This paradoxical effect has been attributed to the development of a form of functional antagonism mediated by receptor desensitization (Marks *et al.*, 1983; Schwartz & Kellar, 1983). In contrast, in the present study, no such upregulation was observed after an equivalent period of demonstrable and complete nicotinic blockade, a blockade furthermore that is insurmountable (El-Bizri & Clarke, 1994b). Our observations therefore suggest that nicotine-induced functional blockade may not be the mechanism by which nicotine upregulates its own receptors.

Is chronic central blockade by chlorisondamine unrelated to nicotinic receptors?

Although there is evidence that chlorisondamine can block central nicotinic receptors acutely (Izenwasser *et al.*, 1991; El-Bizri & Clarke, 1994a), the possibility must be considered that chlorisondamine may be exerting its long-term block independently of nicotinic receptors. This appears unlikely for three reasons. Firstly, chlorisondamine persistently blocks diverse behavioural effects of nicotine that are probably not all mediated by the same neuronal systems with the CNS. Secondly, the long-term blocking action of chlorisondamine does not, as far as is known, extend to behavioural effects of non-nicotinic agents (Clarke, 1984; Reavill *et al.*, 1986; Kumar *et al.*, 1987). Thirdly, *in vivo* administration of CHL results in a block of nicotinic responses tested *in vitro*, yet fails to alter responses to hypertonic K^+ or to (+)-amphetamine (El-Bizri & Clarke, 1994b).

Are mecamylamine and chlorisondamine selective nicotinic antagonists?

Mecamylamine has been very widely used as an antagonist of the central effects of nicotine. Surprisingly, its pharmacological selectivity has not been well established. Indeed, mecamylamine has been shown to reduce responses mediated by glutamate receptors in several species and tissues (MacLeod *et al.*, 1984; Olney *et al.*, 1987; O'Dell & Christensen, 1988; Snell & Johnson, 1989). In most cases, high concentrations of mecamylamine have been used.

In the present experiments, mecamylamine antagonized NDMA receptor-mediated responses, but concentrations greater than 10 μM were required. Consistent with electrophysiological findings (Bijak *et al.*, 1991), mecamylamine did not affect responses to quisqualate. The central concentrations of mecamylamine that are achieved following systemic administration are not known. However, a dose of 1 mg kg^{-1}, which is usually sufficient to block central actions of systemically administered nicotine (Clarke, 1987), would attain a concentration of around 10 μM if evenly distributed. This estimate is consistent with *in vitro* tests showing that such a concentration produces a near-total blockade of nicotinic responses (El-Bizri & Clarke, 1994a). Thus, mecamylamine, at the doses usually encountered in behavioural studies (i.e. not exceeding 1 mg kg^{-1}), can probably be regarded as a moderately selective nicotinic antagonist.

We also found that chlorisondamine exerted only minimal effects on responses mediated by kainate or quisqualate receptors, but reduced NMDA receptor-mediated responses. Complete blockade of NMDA receptor-mediated actions required millimolar concentrations in both preparations. In the hippocampal slice, partial attenuation was evident at a concentration of 10^{-4} M chlorisondamine, but in the cultured cells, no clear effect was observed at 10^{-4} M or below. The basis for this apparent difference in potency is not known, but possibly reflects a difference in the receptor subtypes present, the effective concentrations of the agonist at the receptors, or the temporal characteristics of synaptically released *versus* exogenously applied agonist.

As with mecamylamine, the concentrations of chlorisondamine required to block the central actions of systemically applied nicotine are not known. A dose of 5 μg (14 nmol) given intracerebroventricularly is sufficient to produce a central blockade (Clarke, 1984), and assuming that this dose were entirely retained in the CNS and uniformly distributed, the resulting concentration would certainly be no more than 3 μM. This estimate is consistent with *in vitro* tests in which near-total block occurred at 1 μM chlorisondamine in the presence of concurrent nicotinic stimulation (El-Bizri & Clarke, 1994a). Under these conditions, mecamylamine and chlorisondamine were approximately equipotent, whereas mecamylamine was some ten fold more potent than chlorisondamine in antagonizing NMDA responses. These observations suggest that chlorisondamine may well be a more selective nicotinic antagonist than the more widely-used mecamylamine.

Selective central block by chlorisondamine

Clinically, chlorisondamine is considered to have a somewhat longer duration of action than other common ganglion blockers (Grimson *et al.*, 1955). Nevertheless, we have shown that the ganglion blocking action is shorter-lived than the central blockade exerted by this drug. Indeed, the absence of ptosis noted on the day after drug administration suggests that ganglion blockade may have dissipated within a matter of hours.

Although the mechanism by which chlorisondamine produces its long-term central blockade is not fully understood (see El-Bizri & Clarke, 1994b), several differences may be noted between central and peripheral responses examined to date. Firstly, the prevalent subtypes of nicotinic receptor located on peripheral neurones appear to differ from those that are prevalent in the CNS (Deneris *et al.*, 1991). Secondly, in the periphery, block of nicotinic cholinergic transmission has been measured, whereas in brain tissue, only block of responses to endogenous agonists has been examined. Thirdly, the possibility exists that chlorisondamine is trapped within the CNS by the blood-brain barrier; this issue is investigated in a companion paper (El-Bizri & Clarke, 1994b).

It appears that systemic administration of a high dose of chlorisondamine provides a means of achieving long-term

antagonism of the central actions of nicotine in the absence of lasting ganglionic blockade, at least in rats. There is some reason to hope that a CNS-selective nicotinic receptor blocker would help people give up tobacco smoking and maintain abstinence (Clarke, 1991). Chlorisondamine may provide a starting point in the search for such a drug.

We thank Ms Annie Constantin for excellent technical assistance; Dr Allan Collins for advice on [^{3}H]-nicotine purification; and CIBA-Geigy for a gift of chlorisondamine. This work was supported by funding from NIDA (to P.B.S.C.) and MRC Canada (to M.Q., P.B., R.C. and P.B.S.C.). P.B.S.C. is a Chercheur Boursier of the FRSQ.

References

BIJAK, M., JAROLIMEK, W. & MISGELD, U. (1991). Effects of antagonists on quisqualate and nicotinic receptor-mediated currents of midbrain neurones in culture. *Br. J. Pharmacol.*, **102**, 699–705.

CLARKE, P.B.S. (1984). Chronic central nicotinic blockade after a single administration of the bisquaternary ganglion-blocking drug chlorisondamine. *Br. J. Pharmacol.*, **83**, 527–535.

CLARKE, P.B.S. (1987). Nicotine and smoking: a perspective from animal studies. *Psychopharmacol. (Berlin)*, **92**, 135–143.

CLARKE, P.B.S. (1990). Dopaminergic mechanisms in the locomotor stimulant effects of nicotine. *Biochem. Pharmacol.*, **40**, 1427–1432.

CLARKE, P.B.S. (1991). Nicotinic receptor blockade therapy and smoking cessation. *Br. J. Addict.*, **86**, 501–505.

CLARKE, P.B.S. & FIBIGER, H.C. (1990). Reinforced alternation performance is impaired by muscarinic but not by nicotinic receptor blockade in rats. *Behav. Brain Res.*, **36**, 203–207.

CLARKE, P.B.S., FU, D.S., JAKUBOVIC, A. & FIBIGER, H.C. (1988). Evidence that mesolimbic dopaminergic activation underlies the locomotor stimulant action of nicotine in rats. *J. Pharmacol. Exp. Ther.*, **246**, 701–708.

CLARKE, P.B.S. & KUMAR, R. (1983). Characterization of the locomotor stimulant action of nicotine in tolerant rats. *Br. J. Pharmacol.*, **80**, 587–594.

CLARKE, P.B.S., PERT, C.B. & PERT, A. (1984). Autoradiographic distribution of nicotine receptors in rat brain. *Brain Res.*, **323**, 390–395.

CLARKE, P.B.S., SCHWARTZ, R.D., PAUL, S.M., PERT, C.B. & PERT, A. (1985). Nicotinic binding in rat brain: autoradiographic comparison of ^{3}H-acetylcholine, ^{3}H-nicotine, and ^{125}I-alpha-bungarotoxin. *J. Neurosci.*, **5**, 1307–1315.

COAN, E.J. & COLLINRIDGE, G.L. (1987). Characterization of a N-methyl-D-aspartate receptor component of synaptic transmission in rat hippocampal slices. *Neuroscience*, **22**, 1–8.

CORRIGALL, W.A., COEN, K.M., FRANKLIN, K.B.J. & CLARKE, P.B.S. (1992). The mesolimbic dopamine system is implicated in the reinforcing effects of nicotine. *Psychopharmacol.*, **107**, 285–289.

COUTURIER, S., BERTRAND, D., MATTER, J.M., HERNANDEZ, M.C., BERTRAND, S., MILLAR, N., VALERA, S., BARKAS, T. & BALLIVET, M. (1990). A neuronal nicotinic acetylcholine receptor subunit (alpha 7) is developmentally regulated and forms a homo-oligomeric channel blocked by alpha-BTX. *Neuron*, **5**, 847–856.

DENERIS, E.S., CONNOLLY, J., ROGERS, S.W. & DUVOISIN, R. (1991). Pharmacological and functional diversity of neuronal nicotinic acetylcholine receptors. *Trends Pharmacol. Sci.*, **12**, 34–40.

DUNANT, Y. (1967). Organisation topographique et fonctionelle du ganglion cervical superieur chez le rat. *J. Physiol. (Paris)*, **59**, 17–38.

DUNN, G., KOSHIKAWA, N., DURCAN, M.J. & CAMPBELL, I.C. (1988). An examination of experimental design in relation to receptor binding assays. *Br. J. Pharmacol.*, **94**, 693–698.

DUNNETT, C.W. (1955). A multiple comparison procedure for comparing several treatments with a control. *J. Am. Statist. Assoc.*, **50**, 1096–1121.

EL-BIZRI, H. & CLARKE, P.B.S. (1994a). Blockade of nicotinic receptor-mediated release of dopamine from striatal synaptosomes by chlorisondamine and other nicotinic antagonists administered *in vitro*. *Br. J. Pharmacol.*, **111**, 406–413.

EL-BIZRI, H. & CLARKE, P.B.S. (1994b). Blockade of nicotinic receptor-mediated release of dopamine from striatal synaptosomes by chlorisondamine administered *in vivo*. *Br. J. Pharmacol.*, **111**, 414–418.

FUDALA, P.J. & IWAMOTO, E.T. (1987). Conditioned aversion after delay place conditioning with nicotine. *Psychopharmacol.*, **92**, 376–381.

GALLYAS, F., WOLFF, J.R., BOTTCHER, H. & ZABORSKY, L. (1980). A reliable and sensitive method to localize terminal degeneration and lysosomes in the central nervous system. *Stain Technol.*, **55**, 299–306.

GRIMSON, K.S., TARAZI, A.K. & FRAZER, J.W. (1955). A new orally active quaternary ammonium, ganglion blocking drug capable of reducing blood presure, SU-3088. *Circulation*, **11**, 733–741.

IZENWASSER, S., JACOCKS, H.M., ROSENBERGER, J.G. & COX, B.M. (1991). Nicotine indirectly inhibits [3H]dopamine uptake at concentrations that do not directly promote [3H]dopamine release in rat striatum. *J. Neurochem.*, **56**, 603–610.

KUMAR, R., REAVILL, C. & STOLERMAN, I.P. (1987). Nicotine cue in rats: effects of central administration of ganglion-blocking drugs. *Br. J. Pharmacol.*, **90**, 239–246.

LINDSTROM, J., SCHOEPFER, R. & WHITING, P. (1987). Molecular studies of the neuronal nicotinic acetylcholine receptor family. *Mol. Neurobiol.*, **1**, 281–337.

LONDON, E.D., CONNOLLY, R.J., SZIKZAY, M., WAMSLEY, J.K. & DAM, M. (1988). Effects of nicotine on local cerebral glucose utilization in the rat. *J. Neurosci.*, **8**, 3920–3928.

MACLEOD, N.K., JAMES, T.A. & STARR, M.S. (1984). Muscarinic action of acetylcholine in the rat ventromedial thalamic nucleus. *Exp. Brain Res.*, **55**, 553–561.

MARKS, M.J., BURCH, J.B. & COLLINS, A.C. (1983). Effects of chronic nicotine infusion on tolerance development and nicotinic receptors. *J. Pharmacol. Exp. Ther.*, **226**, 817–825.

MARKS, M.J., FARNHAM, D.A., GRADY, S.R. & COLLINS, A.C. (1993). Nicotinic receptor function determined by stimulation of rubidium efflux from mouse brain synaptosomes. *J. Pharmacol. Exp. Ther.*, **264**, 542–552.

MOUNT, H., QUIRION, R., KOHN-ALEXANDER, J. & BOKSA, P. (1990). Subtypes of excitatory amino acid receptors involved in the stimulation of [^{3}H]dopamine release from cell cultures of rat ventral mesencephalon. *Synapse*, **5**, 271–280.

MOUNT, H., WELNER, S., QUIRION, R. & BOKSA, P. (1989). Glutamate stimulation of [^{3}H]dopamine release from dissociated cell cultures of rat ventral mesencephalon, *J. Neurochem.*, **52**, 1300–1310.

MUNDY, W.R. & IWAMOTO, E.T. (1988). Actions of nicotine on the acquisition of an autoshaped lever-touch response in rats. *Psychopharmacol.*, **94**, 267–274.

MUNSON, P.J. & RODBARD, D. (1980). LIGAND: a versatile computerized approach for characterization of ligand-binding systems. *Anal. Biochem.*, **107**, 220–239.

NADLER, V.J. & EVENSON, D.A. (1983). Use of excitatory amino acids to make axon-sparing lesions of the hypothalamus. *Methods in Enzymology (Part H)*, **103**, 393–400.

O'DELL, T.J. & CHRISTENSEN, B.N. (1988). Mecamylamine is a selective non-competitive antagonist of N-methyl-D-aspartate-induced currents in horizontal cells dissociated from the catfish retina. *Neurosci. Lett.*, **94**, 93–98.

OLNEY, J.W., PRICE, M.T., LABYUYERE, J., SHAHID SALLES, K., FRIEDRICH, G., MULLER, M. & SILVERMAN, E. (1987). Anti-parkinsonian agents are phencyclidine agonists and N-methyl-aspartate antagonists. *Eur. J. Pharmacol.*, **142**, 319–320.

PAXINOS, G. & WATSON, C. (1986). *The Rat Brain in Stereotaxic Coordinates*. 2nd edn. Orlando, Florida: Academic Press.

PLUMMER, A.J., TRAPOLD, J.H., SCHNEIDER, J.A., MAXWELL, R.A. & EARL, A.E. (1955). Ganglionic blockade by a new bisquaternary series, including chlorisondamine dimethochloride. *J. Pharmacol. Exp. Ther.*, **115**, 172–184.

QUIK, M. & LAMARCA, M.V. (1982). Blockade of transmission in rat sympathetic ganglia by a toxin which co-purifies with alpha-bungarotoxin. *Brain Res.*, **238**, 385–399.

REAVILL, C., STOLERMAN, I.P., KUMAR, R. & GARCHA, H.S. (1986). Chlorisondamine blocks acquisition of the conditioned taste aversion produced by (−)-nicotine. *Neuropharmacol.*, **25**, 1067–1069.

ROMM, E., LIPPIELLO, P.M., MARKS, M.J. & COLLINS, A.C. (1990). Purification of L-[^{3}H]nicotine eliminates low affinity binding. *Life Sci.*, **46**, 935–943.

SCHULTZ, D.W., LORING, R.H., AIZENMAN, E. & ZIGMOND, R.E. (1991). Autoradiographic localization of putative nicotinic receptors in the rat brain using 125I-neuronal bungarotoxin. *J. Neurosci.*, **11**, 287–297.

SCHWARTZ, R.D. & KELLAR, K.J. (1983). Nicotinic cholinergic receptor binding sites in the brain: regulation in vivo. *Science*, **220**, 214–216.

SNELL, L.D. & JOHNSON, K.M. (1989). Effects of nicotinic agonists and antagonists on N-methyl-D-aspartate-induced 3H-norepinephrine release and 3H-(1-1-(2-thienyl)cylcohexyl-piperidine) binding in rat hippocampus. *Synapse*, **3**, 129–135.

THEORET, Y., BROWN, A., FLEMING, S.P. & ČAPEK, R. (1984). Hippocampal field potential: a microcomputer-aided comparison of amplitude and integral. *Brain Res. Bull.*, **12**, 589–595.

WONNACOTT, S. (1990). The paradox of nicotinic acetylcholine receptor upregulation by nicotine. *Trends Pharmacol. Sci.*, **11**, 216–219.

(Received May 4, 1993
Revised September 21, 1993
Accepted September 23, 1993)

Br. J. Pharmacol. (1994), **111**, 406–413

Blockade of nicotinic receptor-mediated release of dopamine from striatal synaptosomes by chlorisondamine and other nicotinic antagonists administered *in vitro*

H. El-Bizri & [1]P.B.S. Clarke

Department of Pharmacology and Therapeutics, McGill University, 3655 Drummond Street, Montreal, Canada H3G 1Y6

1 Central nicotinic receptor function examined *in vitro*, by measuring nicotine-induced [^{3}H]-dopamine release from rat striatal synaptosomes.

2 The agonists (−)-nicotine, acetylcholine, 1,1-dimethyl-4-phenylpiperazinium (DMPP) and cytisine (10^{-7}–10^{-4} M) all increased [^{3}H]-dopamine release in a concentration-dependent manner. Cytisine did not produce a full agonist response, compared to the other agonists.

3 The actions of nicotine, acetylcholine and cytisine were largely dependent on external Ca^{2+}. In contrast, DMPP (10^{-5} and 10^{-4} M) evoked a marked release of [^{3}H]-dopamine even in the absence of Ca^{2+}. Nevertheless, in the presence of external Ca^{2+}, responses to DMPP were completely blocked by the nicotinic antagonists chlorisondamine and mecamylamine (5×10^{-5} M); in the absence of external Ca^{2+}, blockade was only partial.

4 Chlorisondamine, mecamylamine and dihydro-β-erythroidine (10^{-8}–10^{-4} M) produced a concentration-dependent block of responses to nicotine (10^{-6} M). Approximate IC_{50} values were 1.6, 0.3 and 0.2×10^{-6}, respectively. Chlorisondamine and mecamylamine blocked responses to nicotine (10^{-7}–10^{-4} M) insurmountably, whereas dihydro-β-erythroidine behaved in a surmountable fashion.

5 The occurrence of use-dependent block was tested by briefly pre-exposing the synaptosomes to nicotine during superfusion with antagonist, and determining the response to a subsequent nicotine application. Consistent with a possible channel blocking action, brief pre-exposure to agonist increased the antagonist potency of chlorisondamine (approximately 25 fold). No significant use-dependent block was detected with dihydro-β-erythroidine.

Keywords: Nicotine; acetylcholine; cytisine; DMPP; chlorisondamine; mecamylamine; dihydro-β-erythroidine; nicotinic receptors; calcium dependence; surmountable antagonism

Introduction

Chlorisondamine (CHL) is a nicotinic receptor antagonist possessing a ganglionic profile of action (Grimson *et al.*, 1955; Plummer *et al.*, 1955; Schneider & Moore, 1955). The bisquaternary structure of CHL appears to impede passage across the blood brain barrier, but a single administration of the drug, given either directly into the cerebral ventricles or in a sufficiently high dose systemically, results in a pharmacologically selective and remarkably persistent (several weeks) blockade of central actions of nicotine (Clarke & Kumar, 1983; Clarke, 1984; Reavill *et al.*, 1986; Fudala & Iwamoto, 1987; Kumar *et al.*, 1987; Mundy & Iwamoto, 1988; Clarke & Fibiger, 1990; Corrigall *et al.*, 1992; El-Bizri & Clarke, 1994; Clarke *et al.*, 1994). In contrast, ganglionic blockade induced by CHL is transient (Grimson *et al.*, 1955; Plummer *et al.*, 1955; Schneider & Moore, 1955; Clarke *et al.*, 1994).

The mechanisms underlying the central nicotinic blockade associated with CHL administration have not been elucidated. Reports of central blockade by CHL have relied almost exclusively on behavioural measures that reflect central actions of nicotine. However, two recent *in vitro* studies reported that CHL abolished nicotine-induced inhibition of dopamine uptake in striatal tissue slices (Izenwasser *et al.*, 1991) and nicotine-induced rubidium efflux from mouse striatal synaptosomes (Marks *et al.*, 1993).

The additional observation that CHL does not inhibit high-affinity binding of [^{3}H]-acetylcholine or [^{3}H]-nicotine to rat brain membranes (Schwartz *et al.*, 1982; Clarke *et al.*, 1984) suggests that this antagonist does not act at the agonist recognition site(s) situated on the nicotinic receptor macromolecule. Indeed, at autonomic ganglia, CHL appears to act as a nicotinic receptor channel blocker, producing a block, the onset of which is both voltage- and use-dependent (Traber *et al.*, 1967; Alkadhi & McIsaac, 1974). A channel blocking mechanism has also been proposed for CHL at non-mammalian nicotinic receptors (Lingle, 1983a,b; Neely & Lingle, 1986).

Nicotine has been shown to induce the release of several neurotransmitters in the CNS via a direct action on nerve terminals (Balfour, 1982; Wonnacott *et al.*, 1989). This phenomenon has been repeatedly described in the nigrostriatal dopaminergic system, where micromolar concentrations of nicotine stimulate the release of dopamine in a receptor-mediated manner, both *in vitro* (Giorguieff *et al.*, 1976; 1977; Giorguieff Chesselet *et al.*, 1979; Westfall *et al.*, 1987; Rapier *et al.*, 1988; 1990; Rowell & Wonnacott, 1990; Izenwasser *et al.*, 1991; Grady *et al.*, 1992) and *in vivo* (Giorguieff *et al.*, 1976; Imperato *et al.*, 1986). Thus, the ability of nicotine to promote dopamine release from striatal synaptosomes provides a reliable *in vitro* assay for CNS nicotinic receptor function. We have used this assay to examine the mechanism by which acute *in vitro* administration of CHL produces blockade of CNS nicotinic responses.

Methods

Male Sprague-Dawley rats (Charles River, St Constant, Quebec), weighing 200–250 g, were maintained on a 12/12 h light-dark cycle. Rats were house four per cage, and food and water were available *ad libitum*. Subjects were allowed to accommodate to the housing conditions for 4 days after arrival, and were drug-naive at the start of each experiment.

[1] Author for correspondence.

Dopamine release from superfused synaptosomes

Rats were decapitated, and both striata (total wet weight 160–200 mg) were immediately dissected in ice-cold 0.32 M sucrose/5 mM HEPES adjusted to pH 7.5 with NaOH. Striata were homogenized in 20 vol of the sucrose/HEPES solution (12 up and down strokes, at 850 RPM, in a 0.25 mm clearance glass/Teflon homogenizer). The homogenate was centrifuged at 1000 *g* for 10 min at 4°C. Supernatant was recentrifuged at 12000 *g* for 20 min at 4°C. The final pellet, consisting of the crude synaptosomal (P2) fraction, was resuspended in the superfusion buffer (5 ml g^{-1} of wet tissue weight). The superfusion buffer (SB) was composed of the following (mM): NaCl 128, KCl 2.4, $CaCl_2$ 3.2, KH_2PO_4 1.2, $MgSO_4$ 0.6, HEPES 25, D-glucose 10, L-ascorbic acid 1 and pargyline 0.1 adjusted with NaOH to pH 7.5. The synaptosomal preparation was incubated with [^{3}H]-dopamine (0.12×10^{-6} M) for 10 min at 37°C. The synaptosomes were then centrifuged at 1000 *g* for 5 min at RT and the pellet was gently resuspended in an equal volume of SB.

Superfusion

The apparatus comprised 16 identical channels. Each channel consisted of a length of Tygon or silicone tubing (0.8 mm i.d.) leading to and from a retention chamber comprising a polypropylene filter unit (Millipore Corp., Bedford, MA, U.S.A.), fitted with a 13 mm diameter A/E glass fibre filter (1 μm pore size, Gelman Sciences Inc., Ann Arbor, MI, U.S.A.). The superfusate was continuously pumped downward through the chamber, at a rate of 0.4 ml min^{-1}, via a peristaltic pump (Masterflex, Cole-Parmer, Chicago, IL, U.S.A.) positioned downstream to the chamber. Upstream to the chamber two 1 ml syringes (Becton Dickinson, NJ, U.S.A.) were connected to the superfusion tubing via 25 gauge needles. The first syringe was used in order to introduce the drug (or SB for control channels), and the second to introduce buffer containing 20 mM KCl. In order to reduce the possibility of contaminants, all syringes used in these experiments were washed with bleach, followed by thorough rinsing with distilled water.

Each experiment comprised several assays. At the start of each assay, channels were thoroughly rinsed by superfusion with distilled water followed with SB. Next, 100 μl of the synaptosomal suspension was injected into the tubing immediately upstream to the superfusion chamber; synaptosomes were retained within the chamber on the filter. Following a superfusion period of 25 min, 28 samples per channel were collected in consecutive 1 min intervals into polypropylene minivials (Sarstedt, Montreal, Canada) containing 2 ml of scintillation fluid (Hi-Safe III, Fisher Scientific, Montreal, Canada). Following an initial collection period of 10 min, a 1 min (0.4 ml) pulse of drug or SB (control channels) was injected. In some experiments, this was followed 10 min later by a 1 min (0.4 ml) pulse of buffer containing high KCl (20 mM) given to all channels. Superfusate samples were collected for a further 8 min. Finally, the filters holding the synaptosomes were removed in order to measure residual radioactivity. Samples were measured in a liquid scintillation counter (Wallac 1410, LKB, Sweden).

In each assay, data were collected simultaneously from all 16 channels. Two rats provided striatal tissue for each assay. Care was taken to include control (SB only) channels in all assays, and to counterbalance treatment conditions across channels and across individual assays. In experiments using Ca^{2+}-free medium, an equivalent molar concentration of Mg^{2+} and EGTA (2.25 mM) was substituted. In experiments with antagonists, these were present throughout each assay, including the 25 min washout period prior to the sample collection.

Throughout the paper we shall refer to the tritium released as dopamine release, since it has been established that in similar synaptosomal preparations preloaded with [^{3}H]-dopamine, tritium released by nicotinic agonists or by depolarization largely corresponds to dopamine itself (Rapier *et al.*, 1988).

Data analysis

Basal release was defined as the mean radioactivity released (d.p.m./min) over the six 1 min samples collected immediately prior to drug or SB administration. Basal [^{3}H]-dopamine release corresponded to 3×10^{-15} mol mg^{-1} of original wet tissue. For each channel, the release occurring in each 1 min collection period was calculated as a percentage of basal release; evoked release was taken as the peak value that occurred in the first three periods after a drug challenge. EC_{50} and IC_{50} values were determined by linear interpolation of points either side of 50% of maximal effect. Drug effects were examined by analysis of variance, using commercial software (Systat, Evanston, IL, U.S.A.). Multiple comparisons with a control group were made with Dunnett's test (Dunnett, 1955); other multiple comparisons were made by Student's *t* test with Bonferroni's correction (Glantz, 1992).

Drugs

Chemicals and supplies were as follows: [8-^{3}H]-dopamine (specific activity 20–40 Ci $mmol^{-1}$; New England Nuclear, Boston, MA, U.S.A.). (−)-nicotine hydrogen tartrate, cytisine, 1,1-dimethyl-4-phenylpiperazinium iodide (DMPP), diisopropylfluorophosphate (DFP) (Sigma Chemical Corp., St. Louis, MO, U.S.A.), acetylcholine hydrochloride, pargyline hydrochloride, atropine sulphate (Research Biochemicals Inc., Natick, MA, U.S.A.), mecamylamine hydrochloride (Mec) and dihydro-β-erythroidine (DHBE) (gifts of Merck and Co, Rahway, NJ, U.S.A.), chlorisondamine chloride (CHL) (gift of Ciba-Geigy, Summit, NJ, U.S.A.). Other chemicals and reagents were purchased from commerical sources. For *in vitro* administration, drugs were dissolved in superfusion buffer (SB). Stock solutions of drugs were prepared twice a week, and stored at −40°C. Dilutions were freshly made prior to use for each assay.

Results

Concentration-dependent effects of nicotine on striatal [^{3}H]-dopamine release

(−)-Nicotine ($3.2 \times 10^{-8} - 10^{-4}$ M) increased [^{3}H]-dopamine release in a concentration-dependent manner (Figure 1), with an estimated EC_{50} of 1.6×10^{-7} M. Significant effects occurred at 10^{-7} M and above (Dunnett's test: $P < 0.02$), and a maximal effect was achieved at 10^{-6} M.

Effects of nicotinic agonists and high K^+ buffer on striatal [^{3}H]-dopamine release

In the first set of assays, four nicotinic agonists (nicotine, ACh, cytisine and DMPP) were tested at 10^{-7}–10^{-4} M. The superfusion medium contained DFP (10^{-4} M) and atropine sulphate (10^{-6} M) in order to inhibit hydrolysis of ACh and to prevent activation of muscarinic cholinoceptors, respectively. All four agonists increased [^{3}H]-dopamine release in a concentration-dependent manner (Figure 2). Cytisine did not behave as a full agonist (Figure 2b). Neither ACh nor DMPP appeared to produce maximal effects within the range of concentrations tested (Figure 2c and 2d). With the exception of DMPP (Figure 2d), removal of external Ca^{2+} from SB abolished agonist-induced [^{3}H]-dopamine release. Thus, in the absence of external Ca^{2+}, DMPP significantly evoked release ($P < 0.001$), but the other agonists did not ($P > 0.6$ for each agonist). Omission of external Ca^{2+} reduced basal [^{3}H]-dopamine release by 63%.

High K^+ (20 mM) buffer increased [^{3}H]-dopamine release to a peak value of 378 ± 19.5% ($n = 8$) of baseline. Removal of external Ca^{2+} from SB resulted in K^+-evoked release of 173 ± 14.6% ($n = 8$), corresponding to a 74% decrease. In this experiment, omission of external Ca^{2+} reduced basal [^{3}H]-dopamine release by 57%.

Nicotinic blockade by in vitro *chlorisondamine, mecamylamine and dihydro-β-erythroidine*

The effects of CHL, Mec and DHBE on responses to nicotine (10^{-6} M) and to hypertonic K^+ (20 mM) were examined. Each antagonist was tested in a different set of assays. All three antagonists (10^{-8}–10^{-4} M) produced a concentration-dependent blockade of [^{3}H]-dopamine release evoked by 10^{-6} M nicotine (Figure 3). Approximate IC_{50} values were: CHL (1.6×10^{-6} M), Mec (0.3×10^{-6} M) and DHBE (0.2×10^{-6} M). CHL pretreatment also significantly increased basal release ($P < 0.025$), but differences from the control group were small (<20%), and did not reach significance at any concentration of CHL ($P > 0.05$). Neither Mec nor DHBE significantly altered basal release ($P > 0.5$ for each).

Surmountable vs insurmountable blockade by in vitro *chlorisondamine, mecamylamine and dihydro-β-erythroidine*

CHL, Mec and DHBE at concentrations = IC_{50} (see above) were tested against graded concentrations of nicotine (10^{-7}–10^{-4} M). The partial blockade that was produced by CHL was not overcome by increasing concentrations of nicotine (10^{-7}–10^{-4} M) (Figure 4a). Similar results were obtained with Mec (Figure 4b). In contrast, blockade by DHBE was completely reversed by increasing concentrations of nicotine (Figure 4c). None of the antagonists altered dopamine release induced by high K^+ buffer; [^{3}H]-dopamine release (mean ± s.e.mean) after administration of high K^+ buffer in control channels compared to those perfused with CHL, Mec and DHBE were, respectively: 195 ± 6%, 195 ± 7%, 206 ± 5% and 180 ± 6% ($n = 30$).

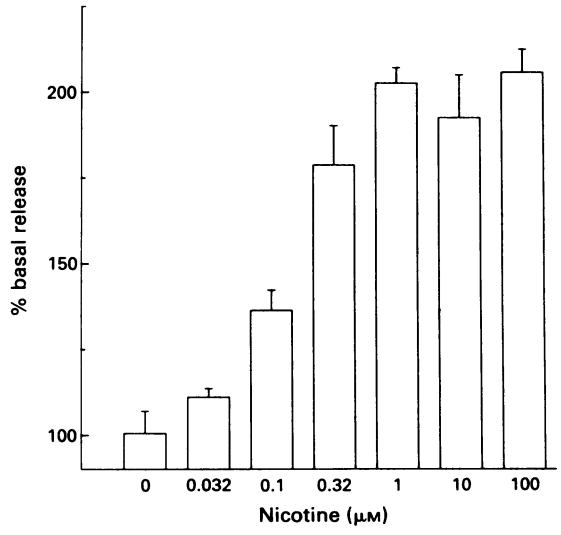

Figure 1 Effects of (−)-nicotine (3.2×10^{-8}–10^{-4} M) on [^{3}H]-dopamine release from striatal synaptosomes. Synaptosomes were superfused with SB for 35 min prior to administration of a 1 min pulse of (−)-nicotine or SB (control). The vertical axis represents the mean peak (±s.e.mean) release, calculated as a percentage of basal release ($n = 6$–9).

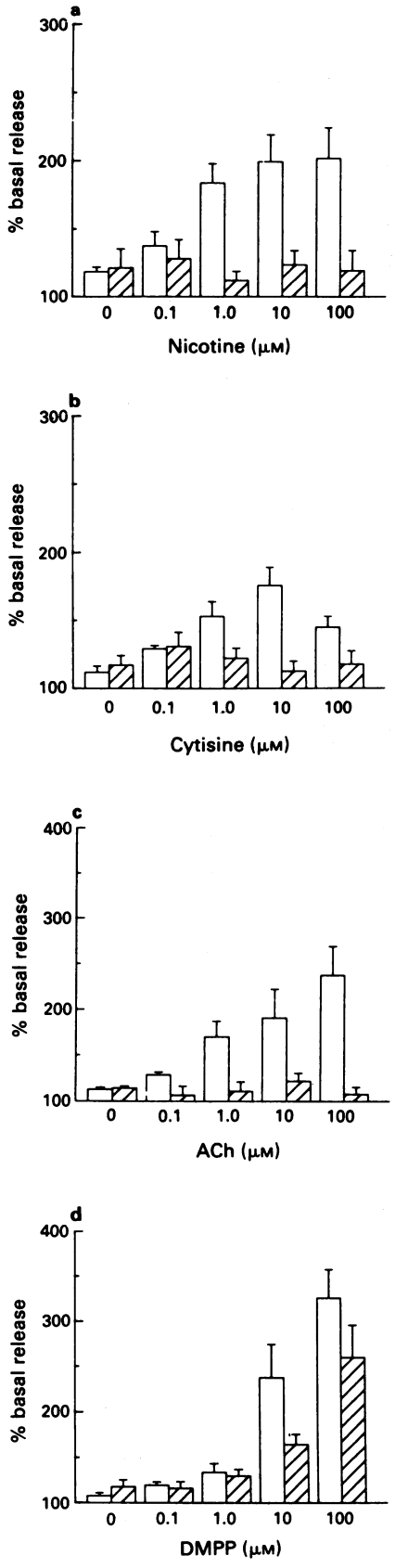

Figure 2 Effects of nicotinic agonists (10^{-7}–10^{-4} M) on [^{3}H]-dopamine release from striatal synaptosomes, in presence of external Ca^{2+} (open columns) and absence of external Ca^{2+} (hatched columns). Synaptosomes were superfused with SB for 35 min prior to administration of a 1 min pulse of the agonist or SB (controls). (a) (−)-Nicotine; (b) cytisine; (c) acetylcholine (ACh); (d) 1,1-dimethyl-4-phenylpiperazzinium (DMPP). The vertical axis represents the mean (±s.e.mean) peak release, calculated as a percentage of basal release ($n = 6$).

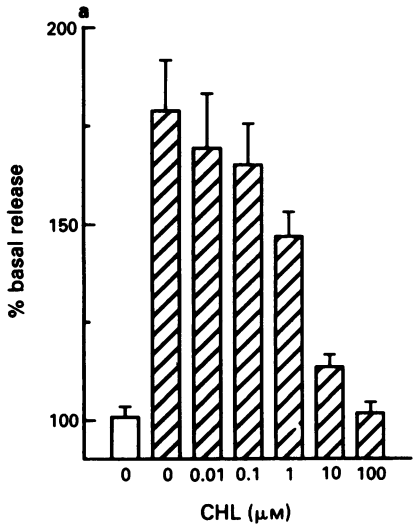

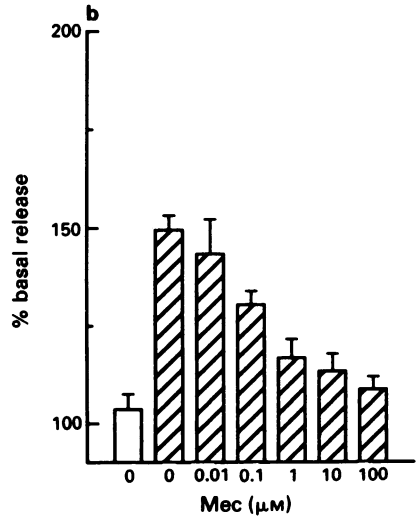

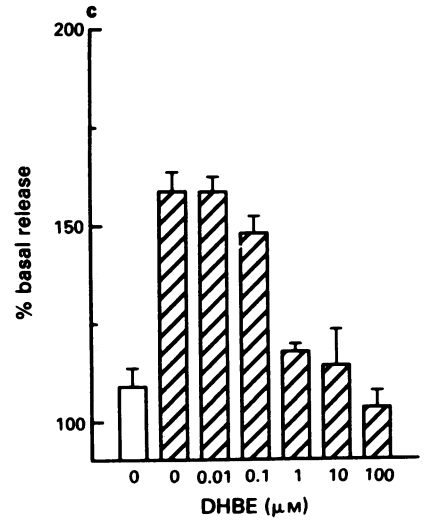

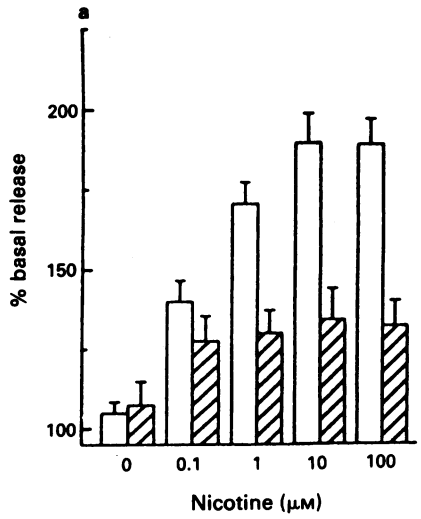

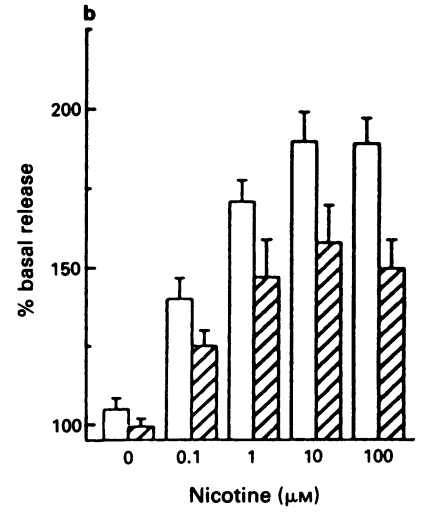

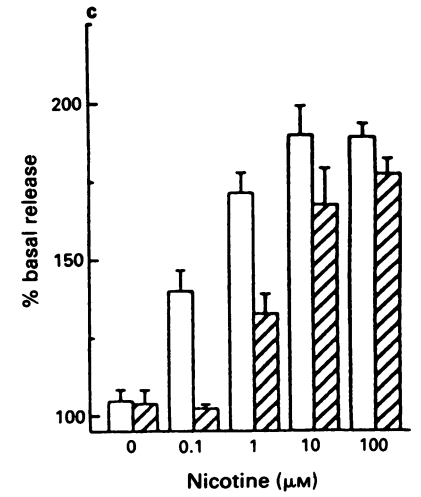

Figure 3 Effects of antagonists (10^{-8}–10^{-4} M) on [^{3}H]-dopamine release, from striatal synaptosomes, induced by a 1 min pulse of (−)-nicotine (10^{-6} M). Antagonists were present in the SB throughout the superfusion period prior to the challenge with (−)-nicotine (hatched columns). Control channels (open columns) were superfused and challenged with SB only. (a) CHL; (b) mecamylamine (Mec); (c) dihydro-β-erythroidine (DHBE). The vertical axis represents the mean (±s.e.mean) peak release, calculated as a percentage of basal release ($n = 12$).

Figure 4 Tests of surmountable vs insurmountable antagonism. Synaptosomes were superfused with a 1 min pulse of (−)-nicotine (10^{-7}–10^{-4} M) or SB, following a 35 min period of superfusion with antagonist (hatched columns) or SB (open columns). Antagonists were present at approximate IC_{50} concentrations determined against (−)-nicotine 10^{-6} M: (a) chlorisondamine (CHL, 1.2×10^{-6} M); (b) mecamylamine (Mec, 0.3×10^{-6} M); (c) dihydro-β-erythroidine (DHBE, 0.22×10^{-6} M). The vertical axis represents the mean (±s.e. mean) peak release, calculated as a percentage of basal release ($n = 6$).

Use-dependent vs non use-dependent blockade by in vitro *chlorisondamine, mecamylamine and dihydro-β-erythroidine*

The effects of pre-exposure to nicotine on the potency of CHL, Mec and DHBE were tested. Each antagonist was tested in a different set of assays. Channels were perfused with SB or with SB containing antagonist (10^{-8}–10^{-5} M), throughout the experiment. Half of the perfusion channels received an initial 0.4 ml pulse of nicotine (10^{-6} M) whilst the remainder received an equivalent pulse of SB. Thirty-five minutes later, channels were randomly allocated to receive a 0.4 ml challenge with nicotine (10^{-6} M) or SB.

In channels that did not receive antagonist, pre-exposure to a brief pulse of nicotine reduced the effect of a subsequent nicotine dose. The reduction was similar in each set of assays: 32.3% for CHL, 45.4% for Mec, and 35.7% for DHBE. In order to control for this reduction in the response to nicotine, values of peak release were normalized within each set of assays, and were thus expressed in relation to SB alone or nicotine (0% and 100%, respectively).

Pre-exposure of the synaptosomes to nicotine altered the effect of CHL ($P<0.025$), resulting in a leftward shift of the CHL dose-response curve (Figure 5a). The estimated IC_{50} value of CHL was reduced from 1.8×10^{-6} M to 6.8×10^{-8} M, a 26-fold difference.

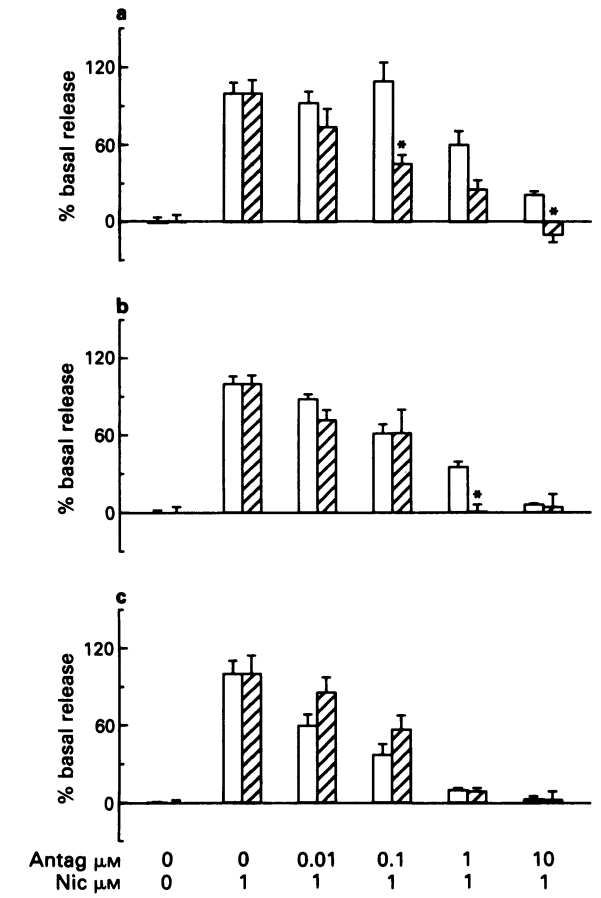

Figure 5 Tests for use-dependent blockage. Synaptosomes were superfused throughout each assay with SB or SB containing antagonist (10^{-8}–10^{-5} M): (a) chlorisondamine (CHL); (b) mecamylamine (Mec); (c) dihydro-β-erythroidine (DHBE). Half of the superfusion channels received an initial 1 min pulse of (−)-nicotine (10^{-6} M) (hatched columns), the remaining channels receiving a pulse of SB (open columns). Thirty min later, channels were randomly allocated to receive a 1 min pulse of nicotine (10^{-6} M) or SB. The vertical axis represents the mean (± s.e.mean) peak release evoked by the challenge dose, calculated as a percentage of basal release (a, $n = 12$; b, $n = 5$; c, $n = 5$). *Different from channels not prestimulated with nicotine at same concentration of antagonist ($P<0.01$).

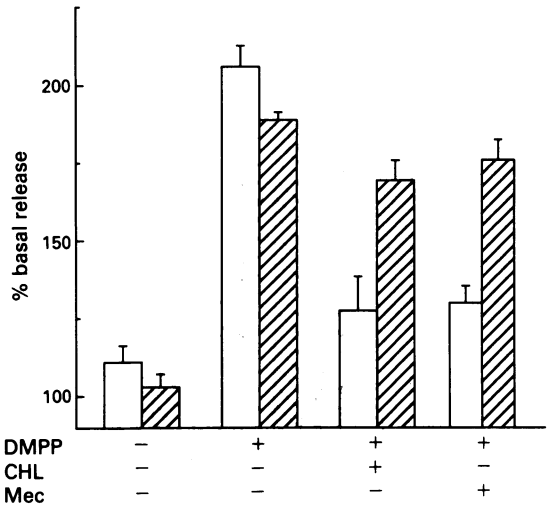

Figure 6 Effects of nicotinic antagonists chlorisondamine (CHL, 5×10^{-5} M) and mecamylamine (Mec, 5×10^{-5} M) on responses to 1,1-dimethyl-4-phenylpiperazinium (DMPP, 10^{-5} M), in presence of Ca^{2+} (open columns) and in absence of Ca^{2+} (hatched columns). Antagonists were superfused for 35 min prior to the administration of a 1 min pulse of DMPP or SB. The vertical axis represents the mean (± s.e.mean) peak release, calculated as a percentage of basal release ($n = 4$).

Nicotine pre-exposure did not significantly alter the effects of Mec as assessed by ANOVA ($P>0.2$), but a significant effect was observed at one concentration of antagonist (Figure 5b). No such effect was evident with DHBE ($P>0.2$; Figure 5c). Estimated IC_{50} values for Mec, with and without pre-exposure to nicotine, were 1.6×10^{-7} and 2.1×10^{-7} M, respectively. Corresponding values for DHBE were 1.4×10^{-7} and 2.6×10^{-8} M.

Basal release prior to test pulse was significantly altered by CHL ($P<0.025$), but not by nicotine pre-exposure ($P>0.2$). However, as in Experiment 3, the effect of CHL was small; a marginally significant change (23% increase over control) occurred at only one concentration (10^{-5} M; $P<0.05$). Neither Mec nor DHBE significantly altered basal release ($P>0.1$ for each).

Effects of mecamylamine and chlorisondamine on DMPP-induced release in Ca^{2+}-free medium

Channels were randomly allocated to three groups which were perfused, with either PB alone. PB containing Mec (5×10^{-5} M), or CHL (5×10^{-5} M). Within each group, half the channels were perfused in the presence of external Ca^{2+}, and half in its absence. After 35 min, a 0.4 ml pulse of DMPP (10^{-5} M) or PB (control channels) was given.

DMPP (10^{-5} M) induced [^{3}H]-dopamine release even in the absence of external Ca^{2+} (Figure 6; see also Figure 2d). In the presence of Ca^{2+}, both Mec (5×10^{-5} M) and CHL (5×10^{-5} M) greatly attenuated the DMPP response (Figure 6). In contrast, these antagonists only slightly reduced the effect of DMPP in the absence of external Ca^{2+} (Figure 6). This difference was confirmed by ANOVA, which revealed a significant interaction between antagonist treatment (control vs Mec vs CHL) and external Ca^{2+} ($P<0.001$).

Discussion

Nicotine-induced dopamine release has been well documented in striatal synaptosome-enriched preparations (Rapier *et al.*, 1988; 1990; Rowell & Wonnacott, 1990; Grady *et al.*, 1992) and slices (Giorguieff *et al.*, 1976; 1977; Giorguieff-

Chesselet *et al.*, 1979; Westfall *et al.*, 1987; Izenwasser *et al.*, 1991). Two mechanisms of action have been identified. At very high concentrations of nicotine (10^{-3} M or higher) dopamine release is evoked in a Ca^{2+}-independent manner (Marien *et al.*, 1983; Westfall *et al.*, 1987; Grady *et al.*, 1992), by a mechanism that is not blocked by classical nicotinic antagonists such as (+)-tubocurarine and Mec (Westfall *et al.*, 1987; Grady *et al.*, 1992); it has been suggested that a tyramine-like depleting action may be involved (Westfall *et al.*, 1987). In contrast, dopamine release evoked by lower concentrations of nicotine (10^{-4} M or lower) is largely Ca^{2+}-dependent and is reduced or blocked by classical nicotinic receptor antagonists (Giorguieff *et al.*, 1977; Giorguieff-Chesselet *et al.*, 1979; Westfall *et al.*, 1987; Rapier *et al.*, 1990; Grady *et al.*, 1992). These characteristics have been confirmed in the present study.

We have also shown that cytisine produced only moderate dopamine release. The counterbalanced experimental design permits direct comparison with the other agonists, and the results suggest that cytisine may act as a partial agonist. Such a conclusion is consistent with the results of behavioural and pharmacokinetic studies (Stolerman *et al.*, 1983; Reavill *et al.*, 1990), but would not have been predicted from previous electro-physiological and *in situ* hybridization studies. In oocytes expressing pairwise combinations of nicotinic receptor subunits, cytisine appears to require the presence of one or more beta4 subunits per receptor in order to exert appreciable agonist activity; substitution of beta4 subunits with beta2 subunits leads to a complete loss of agonist activity (Luetje & Patrick, 1991). Curiously, nigrostriatal dopamine neurones do not appear to express beta4 subunits, at least as indicated by mRNA levels detected by *in situ* hybridization (Dineley-Miller & Patrick, 1992), whereas they do appear to express beta2 subunits (Wada *et al.*, 1989). Lesion studies have identified a population of nicotinic receptors associated with nigrostriatal dopaminergic terminals (Schwartz *et al.*, 1984; Clarke & Pert, 1985), that appear to comprise combinations of alpha4 and beta2 subunits (Flores *et al.*, 1992). Several explanations could possibly account for the low efficacy of cytisine: for example, beta4 subunits may be prevalent in dopaminergic cells despite low mRNA abundance; nicotine-induced dopamine release may be mediated by a mixed population of receptor subtypes; native receptors may consist of more than pairwise combinations of alpha and beta subunits (Conroy *et al.*, 1992); and oocyte-expressed receptors may differ from native receptors in other respects. In the mouse, Marks and colleagues have recently reported evidence suggesting that cytisine acts as a full agonist in evoking [^{3}H]-dopamine release from striatal synaptosomes (Grady *et al.*, 1992), but as a partial agonist in inducing rubidium efflux from midbrain synaptosomes (Marks *et al.*, 1993).

The classical nicotinic agonist DMPP (Van Rossum, 1962a) appears to differ significantly from ACh, nicotine and cytisine in its mode of action. A significant releasing action of DMPP was demonstrated in the absence of external Ca^{2+}. This occurred at a concentration of DMPP as low as 10^{-5} M, whereas a calcium-independent action of DMPP has previously been reported only at a higher concentration of 5×10^{-4} M (Westfall *et al.*, 1987). Also, the antagonists CHL and Mec almost completely blocked responses to DMPP in the presence of external Ca^{2+}; whereas only partial blockade occurred in the absence of Ca^{2+}. This result suggests that DMPP evoked transmitter release via separate mechanisms in these two conditions. These results also demonstrate that a 'calcium-independent' drug effect may occur by a mechanism that may to a large extent be suppressed in the presence of external calcium. In adrenal chromaffin cells, DMPP is reported to evoke transmitter release in the absence of external Ca^{2+} by mobilizing calcium from internal stores (Sasakawa *et al.*, 1986). Possibly, a similar action can occur in striatal tissue.

CHL displayed an insurmountable mode of action in our CNS preparation as previously described in an autonomic ganglion (van Rossum, 1962b). We also found that brief concurrent exposure to nicotine resulted in a marked increase in the potency of CHL. To our knowledge, a 'use-dependent' action has not previously been reported in CNS tissue for any nicotinic antagonist. The use-dependent block observed with CHL is consistent with a possible channel blocking mechanism of action, and indeed, a nicotinic channel blocking action has been proposed for CHL in mammalian ganglia (Traber *et al.*, 1967; Alkadhi & McIsaac, 1974) and in non-mammalian muscle (Lingle, 1983a,b; Neely & Lingle, 1986). Nevertheless, the superfusion method used in our experiments does not permit us to rule out alternative explanations, such as the possibility that CHL enhanced nicotine-induced receptor desensitization.

Mecamylamine, which is probably the most widely used centrally-active nicotinic antagonist, acted insurmountably but did not exhibit use-dependent block. In the periphery, there are reports of either insurmountable or surmountable antagonism by Mec, and even of both components occurring together (van Rossum, 1962b). The nature of blockade by Mec has not been studied before in isolated CNS tissue. However, behavioural experiments have provided evidence for both surmountable and insurmountable actions of Mec in the CNS (Stolerman *et al.*, 1983). Thus, the mechanism of action of Mec appears complex (for review see, Martin *et al.*, 1989).

Less is known about the mode of action of DHBE. Although DHBE is active at nicotinic receptors at autonomic ganglia and skeletal muscle, it has been used principally for CNS electrophysiological studies (Krnjevic, 1975). In the present study, nicotinic blockade by DHBE was found to be surmountable and not use-dependent. These observations are both novel, in the context of the CNS.

The pattern of results obtained in our functional assay is reminiscent of previous findings from radioligand binding studies. Nicotinic receptors labelled with high affinity by [^{3}H]-nicotine and [^{3}H]-ACh represent a prevalent subtype in the brain, thought to be important for mediating the actions of low doses of nicotine (Clarke, 1987; Benwell *et al.*, 1988; for review, see Wonnacott, 1987). Most centrally-active nicotinic antagonists that have been tested do not inhibit [^{3}H]-nicotine or [^{3}H]-ACh binding, suggesting that they do not compete for agonist recognition sites (Marks & Collins, 1982; Schwartz *et al.*, 1982; Clarke *et al.*, 1984; Schwartz & Kellar, 1985). The antagonists CHL and Mec, which we have shown to act insurmountably, are two such examples. In contrast, the antagonist DHBE, which acted in a surmountable fashion, is one of the few nicotinic antagonists known that inhibit high affinity nicotinic [^{3}H]-ACh and [^{3}H]-nicotine binding (Marks & Collins, 1982; Schwartz & Kellar, 1985; Clarke *et al.*, 1984; Marks *et al.*, 1993). Whether any significance can be attached to this correlation is as yet unclear.

We wish to thank Drs Sharon Grady, Michael Marks and Allan Collins for generously sharing their expertise, which was indispensable in setting up the release assay. We thank Dr Brian Collier for his valuable comments. We also thank Miss Melanie Reuben for excellent technical assistance. The following companies generously donated drugs: Ciba-Geigy (chlorisondamine), and Merck, Sharp and Dohme (mecamylamine and dihydro-β-erythroidine). Supported by the Medical Research Council of Canada. H.E.-B. was a Hydro-Quebec Fellow and is an MRC (Canada) Student. P.B.S.C. holds a Senior I Career Award from the FRSQ.

References

ALKADHI, K.A. & McISAAC, R.J. (1974). Effect of preganglionic nerve stimulation on sensitivity of the superior cervical ganglion to nicotinic blocking agents. *Br. J. Pharmacol.*, **51**, 533–539.

BALFOUR, D.J. (1982). The effects of nicotine on brain neurotransmitter systems. *Pharmacol. Ther.*, **16**, 269–282.

BENWELL, M.E., BALFOUR, D.J. & ANDERSON, J.M. (1988). Evidence that tobacco smoking increases the density of (−)-[^{3}H]-nicotine binding sites in human brain. *J. Neurochem.*, **50**, 1243–1247.

CLARKE, P.B.S. (1984). Chronic central nicotinic blockade after a single administration of the bisquaternary ganglion-blocking drug chlorisondamine. *Br. J. Pharmacol.*, **83**, 527–535.

CLARKE, P.B.S. (1987). Recent progress in identifying nicotinic cholinoceptors in mammalian brain. *Trends Pharmacol. Sci.*, **8**, 32–35.

CLARKE, P.B.S., CHAUDIEU, I., EL-BIZRI, H., BOKSA, P., QUIK, M., ESPLIN, B.A. & CAPEK, R. (1994). The pharmacology of the nicotinic antagonist, chlorisondamine, investigated in rat brain and autonomic ganglion. *Br. J. Pharmacol.*, **111**, 397–405.

CLARKE, P.B.S. & FIBIGER, H.C. (1990). Reinforced alternation performance is impaired by muscarinic but not by nicotinic receptor blockade in rats. *Behav. Brain Res.*, **36**, 203–207.

CLARKE, P.B.S. & KUMAR, R. (1983). Characterization of the locomotor stimulant action of nicotine in tolerant rats. *Br. J. Pharmacol.*, **80**, 587–594.

CLARKE, P.B.S. & PERT, A. (1985). Autoradiographic evidence for nicotine receptors on nigrostriatal and mesolimbic dopaminergic neurons. *Brain Res.*, **348**, 355–358.

CLARKE, P.B.S., PERT, C.B. & PERT, A. (1984). Autoradiographic distribution of nicotine receptors in rat brain. *Brain Res.*, **323**, 390–395.

CONROY, W.G., VERNALLIS, A.B. & BERG, D.K. (1992). The α5 gene product assembles with multiple acetylcholine receptor subunits to form distinctive receptor subtypes in brain. *Neuron*, **9**, 679–691.

CORRIGALL, W.A., FRANKLIN, K.B.J., COEN, K.M. & CLARKE, P.B.S. (1992). The mesolimbic dopaminergic system is implicated in the reinforcing effects of nicotine. *Psychopharmacology (Berl)*, **107**, 285–289.

DINELEY-MILLER, K. & PATRICK, J. (1992). Gene transcripts for the nicotinic acetylcholine receptor subunit. Beta4, are distributed in multiple areas of the rat central nervous system. *Brain Res. Mol. Brain Res.*, **16**, 339–344.

DUNNETT, C.W. (1955). A multiple comparison procedure for comparing several treatments with a control. *J. Am. Statist. Assoc.*, **50**, 1096–1121.

EL-BIZRI, H. & CLARKE, P.B.S. (1994). Characterization of central nicotinic blockade by chlorisondamine administered *in vivo*. *Br. J. Pharmacol.*, **111**, 414–418.

FLORES, C.M., ROGERS, S.W., PABREZA, L.A., WOLFE, B.B. & KELLAR, K.J. (1992). A subtype of nicotinic cholinergic receptor in rat brain is composed of α4 and β2 subunits and is up-regulated by chronic nicotine treatment. *Mol. Pharmacol.*, **41**, 31–37.

FUDALA, P.J. & IWAMOTO, E.T. (1987). Conditioned aversion after delay place conditioning with nicotine. *Psychopharmacology*, **92**, 376–381.

GIORGUIEFF, M.-F., LE FLOC'H, M.L., GLOWINSKI, J. & BESSON, M.J. (1977). Involvement of cholinergic presynaptic receptors of nicotinic and muscarinic types in the control of the spontaneous release of dopamine from striatal dopaminergic terminals in the rat. *J. Pharmacol. Exp. Ther.*, **200**, 535–544.

GIORGUIEFF, M.F., LE FLOC'H, M.L., WESTFALL, T.C., GLOWINSKI, J. & BESSON, M.J. (1976). Nicotinic effect of acetylcholine on the release of newly synthesized [^{3}H]dopamine in rat striatal slices and cat caudate nucleus. *Brain Res.*, **106**, 117–131.

GIORGUIEFF-CHESSELET, M.F., KEMEL, M.L., WANDSCHEER, D. & GLOWINSKI, J. (1979). Regulation of dopamine release by presynaptic nicotinic receptors in rat striatal slices: effect of nicotine in a low concentration. *Life Sci.*, **25**, 1257–1262.

GLANTZ, S.A. (1992). *Primer of Biostatistics*, 3rd edn., New York: McGraw Hill.

GRADY, S., MARKS, M.J., WONNACOTT, S. & COLLINS, A.C. (1992). Characterization of nicotinic receptor-mediated [^{3}H]dopamine release from synaptosomes prepared from mouse striatum. *J. Neurochem.*, **59**, 848–856.

GIMSON, K.S., TARAZI, A.K. & FRAZER, J.W. (1955). A new orally active quaternary ammonium, ganglion blocking drug capable of reducing blood pressure, SU-3088. *Circulation*, **11**, 733–741.

IMPERATO, A., MULAS, A. & DI CHIARA, G. (1986). Nicotine preferentially stimulates dopamine release in the limbic system of freely moving rats. *Eur. J. Pharmacol.*, **132**, 337–338.

IZENWASSER, S., JACOCKS, H.M., ROSENBERGER, J.G. & COX, B.M. (1991). Nicotine indirectly inhibits [^{3}H]dopamine uptake at concentrations that do not directly promote [^{3}H]dopamine release in rat striatum. *J. Neurochem.*, **56**, 603–610.

KRNJEVIC, K. (1975). Acetylcholine receptors in vertebrate CNS. In *Handbook of Psychopharmacology*, vol. 6. ed. Iversen, L.L., Iversen, S.D. & Snyder, S.H. pp. 97–126. New York: Plenum.

KUMAR, R., REAVILL, C. & STOLERMAN, I.P. (1987). Nicotine cue in rats: effects of central administration of ganglion-blocking drugs. *Br. J. Pharmacol.*, **90**, 239–246.

LINGLE, C. (1983a). Different types of blockade of crustacean acetylcholine-induced currents. *J. Physiol.*, **339**, 419–437.

LINGLE, C. (1983b). Blockade of cholinergic channels by chlorisondamine on a crustacean muscle. *J. Physiol.*, **339**, 395–417.

LUETJE, C.W. & PATRICK, J. (1991). Both alpha- and beta-subunits contribute to the agonist sensitivity of neuronal nicotinic acetylcholine receptors. *J. Neurosci.*, **11**, 837–845.

MARIEN, M., BRIEN, J. & JHAMANDAS, K. (1983). Regional release of ^{3}H-dopamine from rat brain in vitro: effects of opioids on release induced by potassium, nicotine, and L-glutamic acid. *Can. J. Physiol. Pharmacol.*, **61**, 43–60.

MARKS, M.J. & COLLINS, A.C. (1982). Characterization of nicotine binding in mouse brain and comparison with the binding of alpha-bungarotoxin and quinuclidinyl benzilate. *Mol. Pharmacol.*, **22**, 554–564.

MARKS, M.J., FARNHAM, D.A., GRADY, S.R. & COLLINS, A.C. (1993). Nicotinic receptor function determined by stimulation of rubidium efflux from mouse brain synaptosomes. *J. Pharmacol. Exp. Ther.*, **264**, 542–552.

MARTIN, B.R., ONAIVI, E.S. & MARTIN, T.J. (1989). What is the nature of mecamylamine's antagonism of the central effects of nicotine? *Biochem. Pharmacol.*, **38**, 3391–3397.

MUNDY, W.R. & IWAMOTO, E.T. (1988). Actions of nicotine on the acquisition of an autoshaped lever-touch response in rats. *Psychopharmacology (Berlin)*, **94**, 267–274.

NEELY, A. & LINGLE, C.J. (1986). Trapping of an open-channel blocker at the frog neuromuscular acetylcholine channel. *Biophys. J.*, **50**, 981–986.

PLUMMER, A.J., TRAPOLD, J.H., SCHNEIDER, J.A., MAXWELL, R.A. & EARL, A.E. (1955). Ganglionic blockade by a new bisquarternary series, including chlorisondamine dimethochloride. *J. Pharmacol. Exp. Ther.*, **115**, 172–184.

RAPIER, C., LUNT, G.G. & WONNACOTT, S. (1988). Stereoselective nicotine-induced release of dopamine from striatal synaptosomes: concentration dependence and repetitive stimulation. *J. Neurochem.*, **50**, 1123–1130.

RAPIER, C., LUNT, G.G. & WONNACOTT, S. (1990). Nicotinic modulation of ^{3}H-dopamine release from striatal synaptosomes: pharmacological characterisation. *J. Neurochem.*, **54**, 937–945.

REAVILL, C., STOLERMAN, I.P., KUMAR, R. & GARCHA, H.S. (1986). Chlorisondamine blocks acquisition of the conditioned taste aversion produced by (−)-nicotine. *Neuropharmacology*, **25**, 1067–1069.

REAVILL, C., WALTHER, B., STOLERMAN, I.P. & TESTA, B. (1990). Behavioural and pharmacokinetic studies on nicotine, cytisine and lobeline. *Neuropharmacology*, **29**, 619–624.

ROWELL, P.P. & WONNACOTT, S. (1990). Evidence for functional activity of up-regulated nicotine binding sites in rat striatal synaptosomes. *J. Neurochem.*, **55**, 2105–2110.

SASAKAWA, N., ISHII, K. & KATO, R. (1986). Nicotinic receptor-mediated intracellular calcium release in cultured bovine adrenal chromaffin cells. *Neurosci. Lett.*, **63**, 275–279.

SCHNEIDER, J.A. & MOORE, R.F. (1955). Electrophysiological investigation of chlorisondamine dimethochloride (EcolidTM). A new ganglionic blocking agent. *Proc. Soc. Exp. Biol. Med.*, **89**, 450–453.

SCHWARTZ, R.D. & KELLAR, K.J. (1985). In vivo regulation of ^{3}H-acetylcholine recognition sites in brain by nicotinic cholinergic drugs. *J. Neurochem.*, **45**, 427–433.

SCHWARTZ, R.D., LEHMAN, J. & KELLAR, K.J. (1984). Presynaptic nicotinic cholinergic receptors labelled by ^{3}H-acetylcholine on catecholamine and serotonin axons in brain. *J. Neurochem.*, **42**, 1495–1498.

SCHWARTZ, R.D., MCGEE, R. JR & KELLAR, K.J. (1982). Nicotinic cholinergic receptors labeled by ^{3}H-acetylcholine in rat brain. *Mol. Pharmacol.*, **22**, 56–62.

STOLERMAN, I.P., PRATT, J.A., GARCHA, H.S., GIARDINI, V. & KUMAR, R. (1983). Nicotine cue in rats analysed with drugs acting on cholinergic and 5-hydroxytryptamine mechanisms. *Neuropharmacology*, **22**, 1029–1037.

TRABER, D.L., CARTER, V.L. JR & GARDIER, R.W. (1967). Regarding a necessary condition for ganglionic blockage with competitive agents. *Arch. Int. Pharmacodyn. Ther.*, **168**, 339–343.

VAN ROSSUM, J.M. (1962a). Classification and molecular pharmacology of ganglionic blocking agents Part I: Mechanisms of ganglionic synaptic transmission and mode of action of ganglionic stimulants. *Int. J. Neuropharmacol.*, **1**, 97–110.

VAN ROSSUM, J.M. (1962b). Classification and molecular pharmacology of ganglionic blocking agents Part II: Mode of action of competitive and noncompetitive ganglionic blocking agents. *Int. J. Neuropharmacol.*, **1**, 403–421.

WADA, E., WADA, K., BOULTER, J., DENERIS, E., HEINEMANN, S., PATRICK, J. & SWANSON, L.W. (1989). Distribution of alpha 2, alpha 3, alpha 4, and beta 2 neuronal nicotinic receptor subunit mRNAs in the central nervous system: a hybridization histochemical study in the rat. *J. Comp. Neurol.*, **284**, 314–335.

WESTFALL, T.C., PERRY, H. & VICKERY, L. (1987). Mechanisms of nicotine regulation of dopamine. In *Tobacco Smoking and Nicotine*. ed. Martin, W.R., Van Loon, G.R., Iwamoto, E.T. & Davis, L. pp. 209–224. New York: Plenum Press.

WONNACOTT, S. (1987). Brain nicotine binding sites. *Hum. Toxicol.*, **6**, 343–353.

WONNACOTT, S., IRONS, J., RAPIER, C., THORNE, B. & LUNT, G.G. (1989). Presynaptic modulation of transmitter release by nicotinic receptors. *Prog. Brain Res.*, **79**, 157–163.

(Received May 4, 1993
Revised September 21, 1993
Accepted September 23, 1993)

Br. J. Pharmacol. (1994), **111**, 414–418

Blockade of nicotinic receptor-mediated release of dopamine from striatal synaptosomes by chlorisondamine administered *in vivo*

H. El-Bizri & [1]P.B.S. Clarke

Department of Pharmacology and Therapeutics, McGill University, 3655 Drummond St, Montreal, Canada H3G 1Y6

1 The chronic nicotinic blockade produced following *in vivo* administration of chlorisondamine was investigated *in vitro*. Nicotine-induced [^{3}H]-dopamine release from striatal synaptosomes was used as a measure of central nicotinic receptor function.

2 In synaptosomal preparations from rats pretreated with a single administration of chlorisondamine (10 mg kg^{-1}, s.c.), 1, 7, 21, 42, 63 or 84 days before they were killed, responses to (−)-nicotine (10^{-6} M) were blocked.

3 *In vivo* administration of chlorisondamine (10 mg kg^{-1}, s.c.), 7 days before rats were killed, produced a nicotinic blockade *in vitro* that was insurmountable even with a high concentration of (−)-nicotine (10^{-4} M).

4 Both *in vitro* and *in vivo* administration of chlorisondamine blocked nicotinic responses to acetylcholine (10^{-4} M). In contrast, neither *in vitro* nor *in vivo* administration of chlorisondamine reduced [^{3}H]-dopamine release induced by high K^+ (20×10^{-3} M) or (+)-amphetamine (10^{-6} M).

5 Nicotinic blockade resulting from *in vitro* administration of chlorisondamine (10^{-5} M) recovered partially after 60 min wash-out, and completely by 90 min. In contrast, no recovery was seen in synaptosomes prepared from rats pretreated with chlorisondamine (10 mg kg^{-1}, s.c.) *in vivo*.

6 Thus, *in vivo* treatment with chlorisondamine results in a quasi-irreversible, insurmountable block of CNS nicotinic receptors. The persistence of this block *ex vivo* indicates that physical trapping by the blood brain barrier is not solely responsible for the persisent blockade seen *in vivo*. The resistance of this blockade to prolonged *in vitro* wash-out suggests that the underlying mechanism differs from that associated with *in vitro* administration.

Keywords: Chlorisondamine; nicotine; acetylcholine; dopamine; nicotinic receptors; nicotinic; transmitter release

Introduction

Chlorisondamine (CHL) is a ganglionic nicotinic receptor antagonist (Plummer *et al.*, 1955) which has been used clinically as an antihypertensive (Boura & Green, 1984). Studies in rats have shown that central administration of CHL (5 or 10 μg kg^{-1} i.c.v.) results in a blockade of a variety of behavioural effects of nicotine that are mediated via CNS nicotinic receptors (Clarke & Kumar, 1983; Clarke, 1984; Reavill *et al.*, 1986; Fudala & Iwamoto, 1987; Kumar *et al.*, 1987; Mundy & Iwamoto, 1988; Corrigall *et al.*, 1992). This blockade is remarkably persistent, lasting at least 5 weeks after a single administration of CHL (Clarke, 1984). Although CHL is a bisquaternary amine and appears to penetrate the CNS poorly, administration of a sufficiently large systemic dose (10 mg kg^{-1}, s.c.) also results in a long-lasting central nicotinic blockade (Clarke, 1984; Clarke *et al.*, 1994), whereas ganglion blockade is only transient (Clarke *et al.*, 1994).

The mechanism underlying this persistent central antagonism is not known. The blockade is selective, insofar as administration of CHL did not reduce the behavioural effects of non-nicotinic agents such as apomorphine, midazolam, morphine, cocaine or amphetamine (Reavill *et al.*, 1986; Kumar *et al.*, 1987; Corrigall *et al.*, 1992). The apparent absence of recovery from central nicotinic blockade (Clarke, 1984) suggested the possibility of a neurotoxic mechanism, but in a companion paper (Clarke *et al.*, 1994), we present evidence that CHL does not cause neuronal degeneration. In addition, the persistent central blockade produced by CHL was not accompanied by a change in the density of [^{3}H]-nicotine binding sites in rat forebrain (Clarke *et al.*, 1994).

In the preceding paper (El-Bizri & Clarke, 1994), we characterized the nicotinic blockade produced by acute, *in vitro* administration of CHL. Nicotinic receptor function was assayed by measuring nicotine-induced release of [^{3}H]-dopamine from rat striatal synaptosomes. In the present study, we use the same assay in order to examine the mechanisms underlying the persistent block of central nicotinic responses that follows *in vivo* administration of CHL. By testing nicotinic responses in synaptosomes prepared from rats that had received CHL *in vivo*, it was possible to test whether this persistent central blockade is due solely to physical trapping of the drug (or, possibly, a metabolite) by the blood brain barrier. The chronic blockade produced by *in vivo* administration of CHL was compared to the acute blockade produced by *in vitro* administration of the drug.

Methods

Full details of the procedures for synaptosomal preparation and superfusion are given in an accompanying paper (El-Bizri & Clarke, 1994).

Data analysis

Basal and drug-induced dopamine release were calculated as in the preceding paper (El-Bizri & Clarke, 1994). Statistical results refer to tests of analysis of variance, made using commercial software (Systat, Evanston, IL, U.S.A.).

[1] Author for correspondence.

Drugs

Drugs were as described in the preceding paper (El-Bizri & Clarke, 1994), except as follows. (+)-Amphetamine sulphate was supplied by Smith, Kline and French (Canada). For *in vivo* administration, chlorisondamine chloride (CHL) was dissolved in 0.9% w/v NaCl solution (saline). Injections were given s.c. in a volume of 1 ml kg^{-1}, and the dose refers to the base. For *in vitro* administration, drugs were dissolved in superfusion buffer (SB).

Procedures

Persistence of CHL blockade ex vivo: *effect of survival duration* Animals in each of six groups were randomly allocated for pretreatment with CHL (10 mg kg^{-1}, s.c., $n = 4$ per survival time) or saline (s.c., $n = 4$ per survival time), and were killed 1, 7, 21, 42, 63 or 84 days later, depending on the group. Synaptosomes from each pretreated animal were tested with nicotine (10^{-6} M; 2 or 3 channels per rat) and SB (1 or 2 channels per rat). Ten minutes later all channels received a 1 min pulse of SB containing high KCl (20×10^{-3} M).

Surmountable vs insurmountable blockade by CHL ex vivo As above, rats were randomly allocated for pretreatment with CHL (10 mg kg^{-1} s.c., $n = 4$) or saline (Sal, $n = 4$). They were killed one week later. Synaptomes prepared from these animals were superfused with a range of nicotine concentrations (10^{-7}–10^{-4} M) (1 or 2 channels per condition per rat).

Selectivity of blockade by CHL: investigated after in vitro *or* in vivo *administration* Six rats were used: four received saline and two received CHL (10 mg kg^{-1}, s.c.) one week before they were killed. In order to test blockade following *in vitro* administration of CHL, synaptosomes from the saline-pretreated rats were allocated to two groups of channels. One group was superfused for 25 min with SB, and the other group received SB containing CHL (10^{-5} M) before administration of test drugs. In order to test blockade following *in vivo* administration of CHL, synaptosomes from rats treated with CHL *in vivo* were perfused for 25 min with SB prior to challenge. Thus there were three *in vivo/in vitro* pretreatment conditions: Sal/SB, Sal/CHL, and CHL/SB. Synaptosomal preparations were then challenged acutely with SB, acetylcholine (ACh; 10^{-4} M), (+)-amphetamine (10^{-6} M) or high K^+ buffer (20×10^{-3} M), in a counterbalanced set of 4 assays. Thus, there were 12 combinations of pretreatment and treatment (4–5 channels per condition). In order to inhibit hydrolysis and possible muscarinic actions of ACh, diisopropylfluorophosphate (DFP; 10^{-4} M) and atropine (10^{-6} M) were added to the superfusion buffer, and these compounds were present throughout all conditions.

Recovery from blockade by CHL after in vitro *and* in vivo *administration* First, recovery from blockade was tested following *in vitro* administration of CHL. Nicotinic responses were examined after a 30 min period of wash-out, as follows: in a set of 3 assays using 6 rats, synaptosomes were allocated to two groups of channels, receiving either SB or SB containing CHL (10^{-5} M) for a period of 35 min. Next, equal numbers of channels in each group were perfused with either SB or nicotine (10^{-6} M). A washout period of 30 min followed, during which all channels contained SB. A second dose of SB or nicotine (10^{-6} M) was then given, allocated randomly but in equal number to channels that had previously received SB or nicotine. The procedure was repeated in a second set of 3 assays, except that the wash-out time was extended to 60 min.

Subsequently, the extent of recovery from blockade was compared following *in vivo* vs *in vitro* administration of CHL. In three counterbalanced assays, using 6 rats, synaptosomes were allocated to three groups of channels, corresponding to combinations of *in vivo* and *in vitro* pretreatment, as above: Sal/SB, Sal/CHL and CHL/SB. Following the 35 min *in vitro* pretreatment period, equal numbers of channels in each group received SB or nicotine (10^{-6} M). After a wash-out period of 90 min, a second nicotine or SB superfusion was made. Channels that had previously received a SB challenge now received nicotine (10^{-6} M), and *vice-versa*. The experiment was repeated in another set of 6 assays, using a higher *in vitro* dose of CHL (10^{-4} M), which resulted in a complete nicotinic blockade.

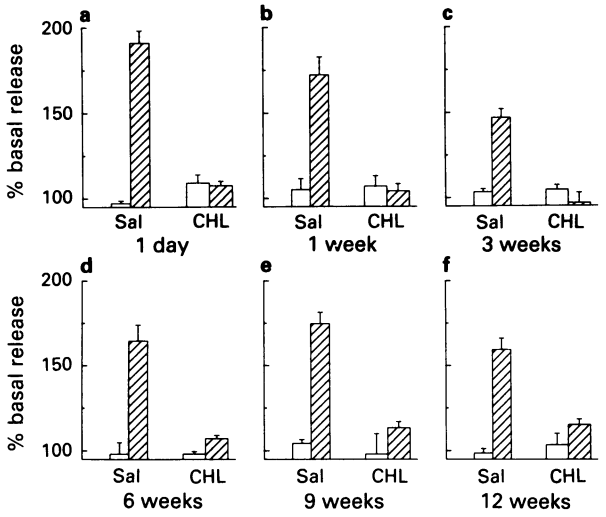

Figure 1 Effects of *in vivo* chlorisondamine (CHL) pretreatment on (−)-nicotine-induced [^{3}H]-dopamine release from rat striatal synaptosomes. Rats received a single pretreatment with CHL (10 mg kg^{-1}, s.c.) or saline and were permitted to survive for different periods before they were killed: (a) 1; (b) 7; (c) 21; (d) 42; (e) 63 or (f) 84 days. Synaptosomes were superfused with superfusion buffer (SB) for 35 min prior to administration of a 1 min pulse of (−)-nicotine (10^{-6} M) (hatched columns) or SB (open columns). The vertical axis represents the mean (± s.e.mean) peak release, calculated as a percentage of basal release ($n = 4$ rats).

Results

Persistence of CHL blockade ex vivo: *effect of survival duration*

A complete block of nicotinic responses was observed *ex vivo*, even several weeks after single administration of CHL (10 mg kg^{-1} s.c.). Thus, striatal synaptosomes prepared from rats that had been pretreated with CHL and permitted to survive for between one day and 12 weeks, failed to release [^{3}H]-dopamine when stimulated by 10^{-6} M nicotine (Figure 1). CHL pretreatment had little if any effect on K^+-induced

Table 1 High K^+-induced [^{3}H]-dopamine release* from saline (Sal) or chlorisondamine (CHL) pretreated rats

Survival time (days)	*Sal pretreatment*	*CHL† pretreatment*
1	180 ± 11	193 ± 6
7	186 ± 18	213 ± 19
21	187 ± 15	178 ± 9
42	200 ± 19	203 ± 22
63	219 ± 9	209 ± 20
84	190 ± 10	199 ± 14

*Mean (± s.e.mean) peak release, calculated as a percentage of basal release ($n = 4$), in response to K^+ 20 mM. †Dose (10 mg kg^{-1}, s.c.).

[^{3}H]-dopamine release at any of the time points tested (Table 1). CHL pretreatment did not alter the basal release ($P > 0.2$), irrespective of survival time ($P > 0.5$).

Surmountable vs insurmountable blockade by CHL ex vivo

As shown in Figure 2, blockade produced by *in vivo* CHL pretreatment was complete, and was insurmountable, even when tested with a high concentration (10^{-4} M) of nicotine.

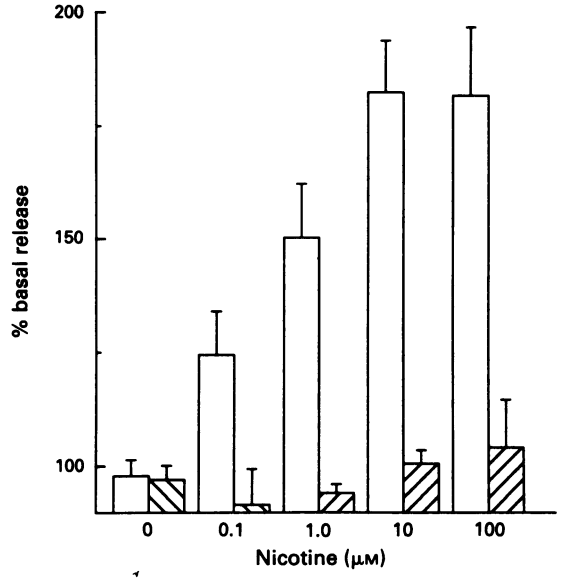

Figure 2 Effects of *in vivo* chlorisondamine (CHL) pretreatment (hatched columns) on (−)-nicotine-induced [^{3}H]-dopamine release from rat striatal synaptosomes. Rats received a single pretreatment with CHL (10 mg kg^{-1}, s.c.) (hatched columns) or saline (open columns) one week before they were killed. Synaptosomes were superfused for 35 min prior to a 1 min pulse of (−)-nicotine or superfusion buffer. The values represents the mean (± s.e.mean) peak release, calculated as a percentage of basal release ($n = 4$ rats).

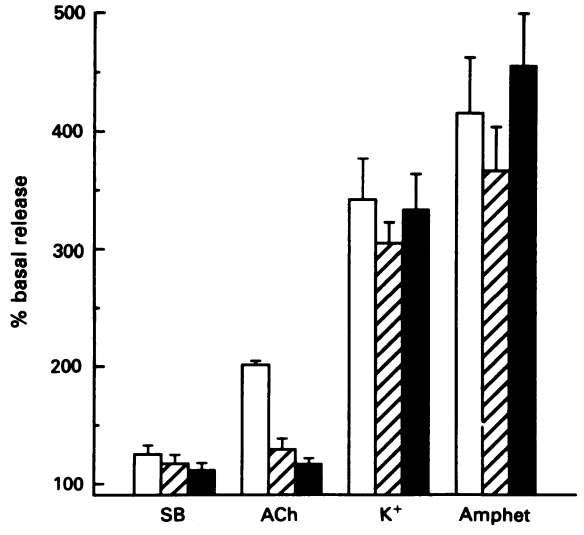

Figure 3 Effects of *in vivo* or *in vitro* chlorisondamine (CHL) pretreatment on [^{3}H]-dopamine release induced by nicotinic and non-nicotinic agents, from rat striatal synaptosomes. Rats received a single pretreatment with CHL (10 mg kg^{-1}, s.c.) or saline one week before they were killed. Synaptosomes from the saline-pretreated rats were superfused with superfusion buffer (SB) (Sal/SB, open columns) or SB containing CHL (10^{-5} M) (Sal/CHL, hatched columns). Synaptosomes from CHL-pretreated rats were superfused with SB (CHL/SB, solid columns). Synaptosomes were superfused in this way for 35 min prior to a 1 min pulse of SB alone, acetylcholine (ACh, 10^{-4} M), (+)-amphetamine (Amphet, 10^{-6} M) or high K$^+$ buffer (20×10^{-3} M). The vertical axis represents the mean (± s.e.mean) peak release, calculated as a percentage of basal release ($n = 6$–12).

Blockade by CHL after in vitro *or* in vivo *administration*

In control synaptosomes that had not been exposed to CHL, the three stimuli (ACh, (+)-amphetamine, high K$^+$) produced different peak amounts of [^{3}H]-dopamine release (Figure 3). Prior exposure to CHL, either *in vivo* or *in vitro*, did not reduce responses to high K$^+$ or (+)-amphetamine. However, prior exposure to CHL resulted in a complete blockade of responses to ACh, and this was the case whether CHL had been given *in vivo* or *in vitro* (Figure 3).

Recovery from blockade following *in vitro* administration of CHL occurred slowly. The extent of recovery did not differ between channels that had received a pre-wash pulse of nicotine and those that had not. After 30 min wash-out no recovery was seen (Figure 4a), but after 60 min wash-out partial recovery was observed (Figure 4b). This is confirmed statistically, as follows. After a 30 min wash-out, CHL-pretreated channels failed to show a nicotinic effect (Tukey's test: $P > 0.9$). After a 60 min wash-out, CHL-pretreated channels were now stimulated by nicotine (Tukey's test: $P < 0.01$) but this nicotinic effect was less than in channels that had not received CHL (ANOVA $P < 0.05$).

When *in vivo* and *in vitro* CHL treatments were subse-

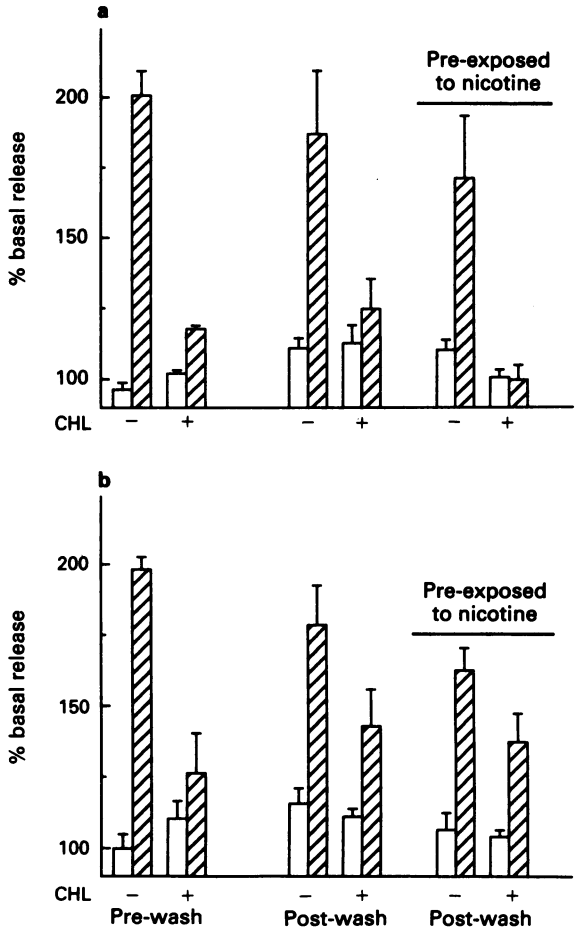

Figure 4 Effects of wash-out with superfusion buffer (SB) on nicotinic blockade produced by *in vitro* chlorisondamine (CHL) administration. Synaptosomes were either superfused with SB or SB containing CHL (10^{-5} M) for 35 min, followed by the first challenge (a 1 min pulse of (−)-nicotine 10^{-6} M or SB). All channels were then washed with SB alone for 30 min (a) or 60 min (b), followed by a second challenge with (−)-nicotine (10^{-6} M) (hatched columns) or SB (open columns), in a counterbalanced manner. Pre-exposed to nicotine, denotes the channels that were initially challenged with nicotine rather than SB. The vertical axis represents mean (± s.e.mean) peak release, calculated as a percentage of basal release ($n = 6$–12).

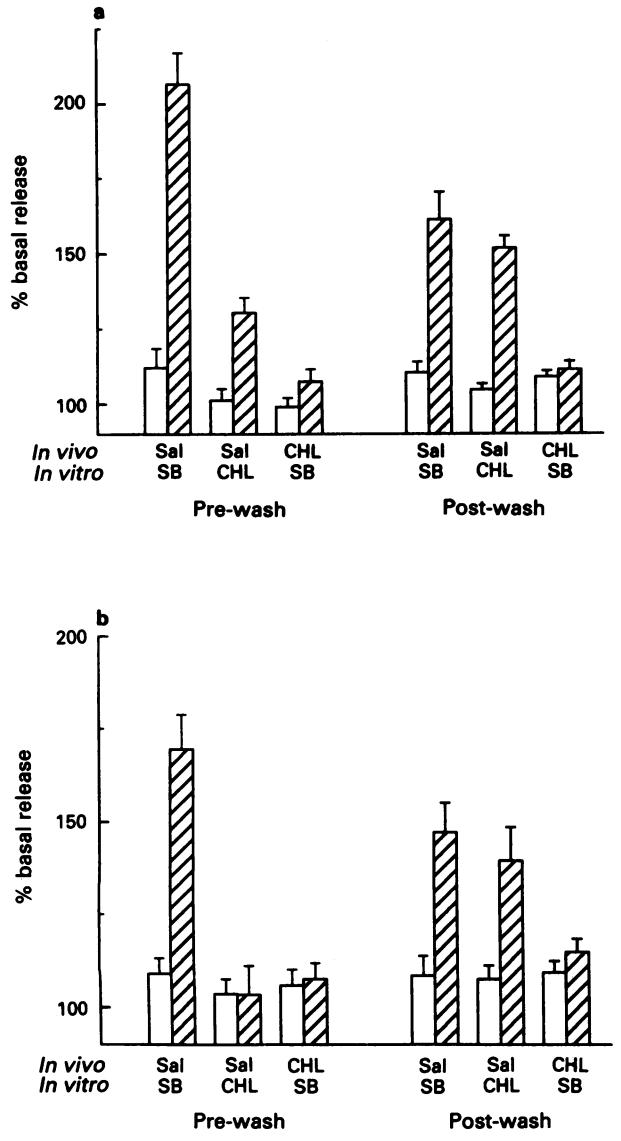

Figure 5 Effects of 90 min wash-out with superfusion buffer (SB) on nicotonic blockade, produced by *in vitro* or *in vivo* chlorisondamine (CHL) administration. Rats received a single pretreatment with CHL (10 mg kg^{-1}, s.c.) or saline one week before they were killed. Synaptosomes from the saline-pretreated rats were superfused with SB or SB containing CHL: (a) 10^{-5} M; (b) 10^{-4} M. Synaptosomes from CHL-pretreated rats were superfused with SB. After a 35 min superfusion period, all synaptosomes received 2 pulses, separated by a 90 min wash period with SB alone, one pulse with (−)-nicotine (10^{-6} M) (hatched columns) and the other with SB (open columns). The order of the pulses was counterbalanced within each pretreatment group. The vertical axis represents mean (± s.e.mean) peak release, calculated as a percentage of basal release (a: $n = 5-6$; b: $n = 8-10$).

quently compared, both treatments resulted in nicotinic blockade prior to the wash-out period, as expected. The nicotinic blockade following *in vitro* administration of CHL was complete at 10^{-4} M but not at 10^{-5} M (Figure 5). Following the 90 min wash-out period, synaptosomes that had been exposed *in vitro* to either of the CHL concentrations showed complete recovery of the nicotinic response (Figure 5). Thus, the effect of the post-wash nicotine challenge was not significantly reduced by pretreatment with either the low ($P > 0.1$) or high ($P > 0.2$) concentration of CHL. In marked contrast, synaptosomes prepared from rats that had received CHL *in vivo* showed no signs of recovery from nicotinic blockade (Figure 5).

Discussion

The long-lasting central blockade by CHL is well documented in *in vivo* studies using behavioural testing (Clarke & Kumar, 1983; Clarke, 1984; Reavill *et al.*, 1986; Fudala & Iwamoto, 1987; Kumar *et al.*, 1987; Mundy & Iwamoto, 1988; Corrigall *et al.*, 1992; Clarke *et al.*, 1994). Here, we demonstrate for the first time that *in vivo* administration of CHL results in *ex vivo* blockade, using an *in vitro* assay of brain nicotinic receptor function. Remarkably, this blockade persisted even 12 weeks after *in vivo* pretreatment with CHL, and resisted extensive washing *in vitro*. We further demonstrate that CHL exerts a selective action, in so far as neither *in vivo* nor *in vitro* administration of CHL altered the responses to high K^+ buffer or (+)-amphetamine. We are not aware of any other selective nicotinic antagonist that produces such a persistent central blockade.

Is the long-lasting block in vivo *due to persistence of chlorisondamine in the CNS?*

At physiological pH, CHL is positively charged and does not readily cross the blood brain barrier (Clarke, 1984). Presumably, therefore, any CHL that reaches the CNS following systemic administration of a high dose may be retained for some time. Physical trapping of this sort suggested itself as a possible cause for the long-lasting blockade by CHL. However, the blood brain barrier clearly cannot contribute in synaptosomal experiments, where CHL block was persistent.

What mechanism(s) would underlie the persistent central nicotinic block following in vivo *administration of CHL?*

In the present study, we have demonstrated that extended washing did not effect recovery in synaptosomes prepared from rats pretreated with CHL *in vivo*. In contrast, a 60 min wash-out period produced a partial recovery from blockade following *in vitro* administration of CHL, and this recovery became complete by 90 min wash.

This final experiment therefore demonstrates that the mechanism underlying the acute blockade following *in vitro* administration of CHL differs from that associated with the chronic blockade occurring after *in vivo* administration of the drug. The basis for this difference is not clear. Possibly, CHL is transformed *in vivo* but not *in vitro*, forming an active metabolite which is more slowly reversible than CHL itself. It is also conceivable that *in vivo*, the receptors undergo a conformational change, assuming a stable state in which CHL (or a metabolite) is captured. In non-mammalian tissue, Lingle and Neely (Lingle, 1983a,b; Neely & Lingle, 1986) proposed that, following use-dependent block by CHL, the receptor assumes a stable-blocked state in which CHL would be trapped within the closed ion channel. Whether this proposal, derived from acute *in vitro* studies, relates to the chronic *in vivo* blockade produced by CHL is not clear. Moreover, whereas in the experiments of Lingle and colleagues (Lingle, 1983a,b; Neely & Lingle, 1986), recovery from blockade by CHL required re-exposure to agonist, such a requirement was not observed in the present study (Figure 4).

Is the chronic blocking action of CHL reversible?

The turnover rate of CNS nicotinic receptors is unknown. However, nicotinic receptor turnover, where studied in other tissues, has typically been found to occur over a period of hours to a few days at most (Kemp & Edge, 1987; Higgins & Berg, 1988; Avila *et al.*, 1989; Fumagalli *et al.*, 1990). A possible effect of CHL on nicotinic receptor synthesis or on the assembly of the receptor subunits is unlikely, since high affinity [^{3}H]-nicotine binding appears to be unaltered during persistent blockade by CHL (Clarke *et al.*, 1994). Thus, it is

likely that over the course of this extended period of blockade, several generations of nicotinic receptors are produced and then degraded. This suggests that an extremely slow dissociation of the active compound from its binding sites cannot by itself explain the persistent central blockade; even if CHL were to bind irreversibly to CNS nicotinic receptors, persistent *in vivo* blockade would require either efficient recycling of the antagonist, or a reserve of antagonist retained in the brain. Possibly, the long-lasting *in vivo* blockade by CHL results from a combination of a slow dissociation of the active compound, with some form of physical trapping provided either by the synaptic environment or by the blood brain barrier.

The nicotinic blockade obtained after a single *in vivo* administration of CHL was not overcome by a high concentration of acetylcholine (10^{-4} M) or even by concentrations of nicotine that would be acutely toxic or lethal *in vivo* (10^{-4} M). Circulating concentrations of nicotine in habitual cigarette smokers are typically in the range of $0.1-0.5 \times 10^{-6}$ M, and during active cigarette smoking, transient concentrations several-fold higher may be achieved in the brain (Benowitz *et al.*, 1990; Russell, 1990). In this concentration-range, nicotine can induce receptor-mediated dopamine release (Giorguieff *et al.*, 1977; Giorguieff Chesselet *et al.*, 1979; Westfall *et al.*, 1987; Rapier *et al.*, 1988; Grady *et al.*, 1992; El-Bizri & Clarke, 1994). Thus, it is likely that the receptor subtype(s) that were blocked by CHL in our experiments would mediate some of the central effects of nicotine encountered during smoking. The persisent and insurmountable antagonism seen following administration of CHL may be of relevance in the context of developing a pharmacological treatment for nicotine dependence.

We wish to thank Drs Sharon Grady, Michael Marks and Allan Collins for generously sharing their expertise, which was indispensable in setting up the release assay. We thank Dr Brian Collier for his valuable comments. We also thank Miss Melanie Reuben for excellent technical assistance. Ciba-Geigy generously donated samples of chlorisondamine. Supported by the Medical Research Council of Canada. H.E.-B. was a Hydro-Quebec Fellow and is an MRC (Canada) Student. P.B.S.C. holds a Senior I Career Award from the FRSQ.

References

AVILA, O.L., DRACHMAN, D.B. & PESTRONK, A. (1989). Neurotransmission regulates stability of acetylcholine receptors at the neuromuscular junction. *J. Neurosci.*, **9**, 2902–2906.

BENOWITZ, N.L., PORCHET, H.C. & JACOB, P. (1990). Pharmacokinetics, metabolism, and pharmacodynamics of nicotine. In *Nicotine Psychopharmacology: Molecular, Cellular, and Behavioural Aspects*. ed. Wonnacott, S., Russell, M.A.H. & Stolerman, I.P. pp. 112–157. Oxford: Oxford University Press.

BOURA, A.L.A. & GREEN, A.F. (1984). Peripheral anti-hypertensives: ganglion and adrenergic neurone blocking agents. In *Discoveries in Pharmacology Vol. 2*. ed. Parnham, M.J. & Bruinvels, J. pp. 73–104. Amsterdam: Elsevier.

CLARKE, P.B.S. (1984). Chronic central nicotinic blockade after a single administration of the bisquaternary ganglion-blocking drug chlorisondamine. *Br. J. Pharmacol.*, **83**, 527–535.

CLARKE, P.B.S., CHAUDIEU, I., EL-BIZRI, H., BOKSA, P., QUIK, M., ESPLIN, B.A. & CAPEK, R. (1994). The pharmacology of the nicotinic antagonist, chlorisondamine, investigated in rat brain and autonomic ganglion. *Br. J. Pharmacol.*, **111**, 397–405.

CLARKE, P.B.S. & KUMAR, R. (1983). Characterization of the locomotor stimulant action of nicotine in tolerant rats. *Br. J. Pharmacol.*, **80**, 587–594.

CORRIGALL, W.A., FRANKLIN, K.B.J., COEN, K.M. & CLARKE, P.B.S. (1992). The mesolimbic dopaminergic system is implicated in the reinforcing effects of nicotine. *Psychopharmacology* (Berlin), **107**, 285–289.

EL-BIZRI, H. & CLARKE, P.B.S. (1994). Blockade of nicotinic receptor mediated release of dopamine from striatal terminals by chlorisondamine and other nicotinic antagonists administered *in vitro*. *Br. J. Pharmacol.*, **111**, 406–413.

FUDALA, P.J. & IWAMOTO, E.T. (1987). Conditioned aversion after delay place conditioning with nicotine. *Psychopharmacology*, **92**, 376–381.

FUMAGALLI, G., BALBI, S., CANGIANO, A. & LMO, T. (1990). Regulation of turnover and number of acetylcholine receptors at neuromuscular junctions. *Neuron*, **4**, 563–569.

GIORGUIEFF CHESSELET, M.F., KEMEL, M.L., WANDSCHEER, D. & GLOWINSKI, J. (1979). Regulation of dopamine release by presynaptic nicotinic receptors in rat striatal slices: effect of nicotine in a low concentration. *Life Sci.*, **25**, 1257–1262.

GIORGUIEFF, M.-F., LE FLOC'H, M.L., GLOWINSKI, J. & BESSON, M.J. (1977). Involvement of cholinergic presynaptic receptors of nicotinic and muscarinic types in the control of the spontaneous release of dopamine from striatal dopaminergic terminals in the rat. *J. Pharmacol. Exp. Ther.*, **200**, 535–544.

GRADY, S., MARKS, M.J., WONNACOTT, S. & COLLINS, A.C. (1992). Characterization of nicotinic receptor-mediated [^{3}H]dopamine release from synaptosomes prepared from mouse striatum. *J. Neurochem.*, **59**, 848–856.

HIGGINS, L.S. & BERG, D.K. (1988). Metabolic stability and antigenic modulation of nicotinic acetylcholine receptors on bovine adrenal chromaffin cells. *J. Cell Biol.*, **107**, 1147–1156.

KEMP, G. & EDGE, M. (1987). Cholinergic function and alpha-bungarotoxin binding in PC12 cells. *Mol. Pharmacol.*, **32**, 356–363.

KUMAR, R., REAVILL, C. & STOLERMAN, I.P. (1987). Nicotine cue in rats: effects of central administration of ganglion-blocking drugs. *Br. J. Pharmacol.*, **90**, 239–246.

LINGLE, C. (1983a). Blockade of cholinergic channels by chlorisondamine on a crustacean muscle. *J. Physiol.*, **339**, 395–417.

LINGLE, C. (1983b). Different types of blockade of crustacean acetylcholine-induced currents. *J. Physiol.*, **339**, 419–437.

MUNDY, W.R. & IWAMOTO, E.T. (1988). Actions of nicotine on the acquisition of an autoshaped lever-touch response in rats. *Psychopharmacology* (Berlin)., **94**, 267–274.

NEELY, A. & LINGLE, C.J. (1986). Trapping of an open-channel blocker at the frog neuromuscular acetylcholine channel. *Biophys. J.*, **50**, 981–986.

PLUMMER, A.J., TRAPOLD, J.H., SCHNEIDER, J.A., MAXWELL, R.A. & EARL, A.E. (1955). Ganglionic blockade by a new bisquaternary series, including chlorisondamine dimethochloride. *J. Pharmacol. Exp. Ther.*, **115**, 172–184.

RAPIER, C., LUNT, G.G. & WONNACOTT, S. (1988). Stereoselective nicotine-induced release of dopamine from striatal synaptosomes: concentration dependence and repetitive stimulation. *J. Neurochem.*, **50**, 1123–1130.

REAVILL, C., STOLERMAN, I.P., KUMAR, R. & GARCHA, H.S. (1986). Chlorisondamine blocks acquisition of the conditioned taste aversion produced by (−)-nicotine. *Neuropharmacology*, **25**, 1067–1069.

RUSSELL, M.A.H. (1990). Nicotine intake and its control over smoking. In *Nicotine Psychopharmacology: Molecular, Cellular, and Behavioural Aspects*. ed. Wonnacott, S., Russell, M.A.H. & Stolerman, I.P. pp. 374–418. Oxford: Oxford University Press.

WESTFALL, T.C., PERRY, H. & VICKERY, L. (1987). Mechanisms of nicotine regulation of dopamine. In *Tobacco Smoking and Nicotine*. ed. Martin, W.R., Van Loon, G.R., Iwamoto, E.T. & Davis, L. pp. 209–224. New York: Plenum Press.

(Received May 4, 1993
Revised September 21, 1993
Accepted September 29, 1993)

Br. J. Pharmacol. (1994), **111**, 419–424

Involvement of neurokinins in the non-cholinergic response to activation of 5-HT_3 and 5-HT_4 receptors in guinea-pig ileum

*M.J. Ramírez, *E. Cenarruzabeitia, [1]†J. Del Río & *B. Lasheras

Department of Pharmacology, Schools of *Pharmacy and †Medicine, University of Navarra, 31080 Pamplona, Spain

1 The involvement of neurokinins in the non-cholinergically-mediated contractile response induced by stimulation of 5-HT_3 and 5-HT_4 receptors has been examined in the longitudinal muscle-myenteric plexus preparation of the guinea-pig ileum.

2 The 5-HT_3 receptor agonist, 2-methyl-5-hydroxytryptamine (2-methyl-5-HT), showed a lower potency in this preparation than the more selective 5-HT_4 receptor agonist 5-methoxytryptamine. The effect of both drugs was markedly reduced by atropine.

3 Substance P (SP) and neurokinin B (NKB) produced biphasic concentration-response curves in the preparation. Neurokinin A (NKA), the NK_1 receptor agonist, [Sar^9,$Met(O_2)^{11}$]SP and the NK_3 receptor agonist, senktide yielded monophasic concentration-response curves.

4 After desensitization of the NK_1 receptor with SP or [Sar^9,$met(O_2)^{11}$]SP, in the presence of atropine, the contractile response to 2-methyl-5-HT was entirely blocked. Desensitization of NK_3 receptors with NKB, also in the presence of atropine, fully suppressed the 5-HT_4 receptor-mediated contraction evoked by 5-methoxytryptamine.

5 In preparations prelabelled with [^{3}H]-choline, SP produced a concentration-dependent increase in tritium overflow, an index of [^{3}H]-acetylcholine release, while an inverse relationship was found with NKB. At low neurokinin concentrations, the releasing effect of NKB was much more marked.

6 It is suggested that in the response to 5-HT_3 receptor stimulation, there is a role for SP and acetylcholine. NKB appears to be preferentially involved in the release of acetylcholine elicited by stimulation of 5-HT_4 receptors.

Keywords: 5-HT; 5-HT_3 receptor; 5-HT_4 receptor; neurokinins; substance P; guinea-pig ileum

Introduction

The contractile effect of 5-hydroxytryptamine (5-HT) in the guinea-pig isolated ileum involves both myogenic and neural mechanisms (Gaddum & Picarelli, 1957). The activation of neuronally-located receptors by 5-HT gives rise to a biphasic concentration-response curve (Buchheit *et al.*, 1985; Butler *et al.*, 1988; Fozard, 1990). The first, high potency phase of the curve, seems to be mediated by the 5-HT_4 receptor (Clarke *et al.*, 1989; Craig & Clarke, 1990), while the second phase, obtained with higher concentrations of 5-HT, would correspond to the activation of the 5-HT_3 receptor (Buchheit *et al.*, 1985; Sanger & Nelson, 1989).

It has been reported that the neuronal actions of 5-HT are mediated by both acetylcholine and substance P release (Buchheit *et al.*, 1985). Substance P (SP) and the structurally related peptides, neurokinin A (NKA) and neurokinin B (NKB), belong to a family of biologically active peptides known as tachykinins. The mammalian members of the tachykinin family are called neurokinins and their actions are mediated through three different types of receptors, NK_1, NK_2 and NK_3 (Henry, 1987; Quirion & Dam, 1988; Guard & Watson, 1991) which are preferentially activated by SP, NKA and NKB respectively (Laufer *et al.*, 1985; Buck & Burcher, 1986; Guard & Watson, 1991), although each peptide can activate all three receptor subtypes to a certain extent.

By using the longitudinal muscle-myenteric plexus (LMMP) preparation we have studied the involvement of the different neurokinins in the contractile response elicited by activation of either 5-HT_3 or 5-HT_4 receptors. The 5-HT_3 receptor agonist 2-methyl-5-hydroxytryptamine (2-Me-5-HT) (Richardson *et al.*, 1985; Bradley *et al.*, 1986) as well as 5-methoxytryptamine (5-MeOT), a more selective agonist for 5-HT_4 than for 5-HT_3 receptors (Eglen *et al.*, 1990; Hill *et al.*, 1990; Fozard, 1990) were used in this study. Neurokinin receptor desensitization by the endogenous peptides or by some more selective synthetic analogues was used as a means of studying the role of the different neurokinins in the contractile response to 5-HT. The ability of the neurokinins to increase tritium overflow from preparations prelabelled with [^{3}H]-choline, an index of [^{3}H]-acetylcholine release (e.g. Wikberg, 1977), was also studied.

The results suggest the participation of SP and acetylcholine in the response to 5-HT_3 receptor stimulation, as well as a conspicuous role for NKB in the response elicited by activation of the 5-HT_4 receptor.

Methods

Guinea-pigs of either sex weighing 300–400 g were stunned by a blow to the head and bled. The ileum was excised approximately 10 cm from the ileo-caecal junction and longitudinal muscle strips with the myenteric plexus attached (LMMP) were prepared as described by Paton & Vizi (1969).

Contractility studies

LMMP strips were suspended in a 10 ml organ bath containing Tyrode solution (composition in mM: NaCl 136, KCl 2.7, $CaCl_2$ 1.8, $MgCl_2$ 1.05, NaH_2PO_4 0.42, $NaHCO_3$ 11.9, glucose 5.5) aerated with 95% O_2/5% CO_2 and maintained at 37°C. Contractile responses were recorded isometrically with a resting tension of 0.5 g. Before the experiments were started, tissues were equilibrated for 30 min.

Concentration-response curves were constructed in a non-cumulative fashion with an agonist exposure period of 30 s on a 10 min dose-cycle. In studies with antagonists, each strip

[1] Author for correspondence.

was used to record two concentration-response curves: the first for the agonist alone and the second for the agonist in the presence of the antagonist, each strip serving as its own control. Antagonists were allowed to pre-equilibrate for 15 min prior to the addition of the agonists.

Characterization of the concentration-response curves

Responses were measured as an increase in the isometric tension and expressed as a percentage of the maximum response. In the presence of an antagonist, results were expressed as a percentage of the maximal response obtained with the agonist alone. Monophasic curves were characterized by the agonist concentration yielding a half-maximal effect, EC_{50}. Biphasic curves were described as follows: for each part, the fractional response contributing to the total response was calculated and the maximum indicated as E_{max1} and E_{max2}. The agonist concentrations which produced half maximal effects were denoted by EC_{50}^1 and EC_{50}^2 respectively.

Desensitizing studies

For desensitization studies, the LMMP preparation was treated repeatedly with high concentrations (0.5 μM) of the neurokinin until the response faded to baseline level. The preparation was then washed and the response to the 5-HT receptor agonist was recorded. Results are expressed as a percentage of the response obtained prior to desensitization.

Release experiments

The method employed to measure the release of acetylcholine was a modification of that described by Kilbinger & Wessler (1980). Briefly, LMMP strips weighing approximately 30 mg were suspended isometrically under a tension of 0.5 g in a 5 ml organ bath and superfused with Tyrode solution containing 1 μM choline. After 30 min incubation with [methyl- ^{3}H]-choline (8 μCi ml^{-1}) and continuous stimulation during this time through platinum electrodes with square wave pulses (0.2 Hz, 1 ms, 13.5 V), the strips were superfused with Tyrode solution containing 10 μM hemicholinium-3 to prevent reuptake of choline. After a washout period of 60 min, aliquots were collected in 3 min fractions. Strips were stimulated twice (S_1, S_2) by field stimulation (1 Hz, 1 ms, 13.5 V), the two pulses being spaced 21 min apart (Torocsik & Vizi, 1991). Drugs were added to the superfusion fluid 21 min after S_2. The spontaneous outflow was calculated by fitting a linear regression line based on the samples taken before and during S_1 stimulation.

Tritium content of the superfused samples was measured by liquid scintillation spectrometry. Under the present experimental conditions, the validity of assuming total tritium as a measure of [^{3}H]-acetylcholine released has been extensively documented (Szerb, 1976; Wikberg, 1977; Yau *et al.*, 1991).

The effect of the drugs studied (D) on the outflow of ^{3}H-label was expressed as a percentage of the increase in the output of ^{3}H-label evoked by the second electrical stimulation (S_2). The increase in the output of ^{3}H-label in response to either the drug or the second electrical stimulation was calculated by subtracting the output during the preceding resting period of 3 min from the output during the stimulation.

Data analysis

The significance between groups was assessed by Student's *t* test (two groups) or ANOVA followed by Scheffe test (several groups). To characterize the concentration-response curves, log EC_{50} was calculated with GraphPAD, ISI Software.

Drugs used

The following drugs were purchased from the suppliers indicated: 5-hydroxytryptamine creatinine sulphate, substance P acetate, atropine sulphate, choline bromide, hemicholinium-3 bromide (Sigma, U.S.A.); 2-methylserotonin maleate (2-methyl-5-HT), 5-methoxytryptamine hydrochloride (Heterocyclic Research, U.S.A.); neurokinin A, neurokinin B (Bachem, Switzerland); [Sar^9, Met(O$_2$)^{11}]SP, senktide (RBI, U.S.A.); choline chloride[methyl-^{3}H] (NEN-Du Pont, Boston, MA, U.S.A.). Methysergide maleate was a gift from Sandoz, Switzerland. Peptides were made up in a stock 0.1 mM concentration in 0.1 N acetic acid; aliquots were stored frozen and diluted before use. All other drugs were dissolved in distilled water.

Results

Contractility studies

The concentration-response curves to 5-MeOT and to 2-Me-5-HT were monophasic. The agonist potencies (− log EC_{50}) were 6.0 ± 0.1 and 5.0 ± 0.2 respectively. Atropine, 0.1 μM, blocked by more than 50% the maximum effect of both 5-HT receptor agonists (Figure 1). The blockade was substantially identical when atropine 1 μM was used.

The concentration-response curve to the neurokinin NKB was biphasic, the initial phase occurred between concentrations of 0.5 nM and 5 nM, and the second phase between

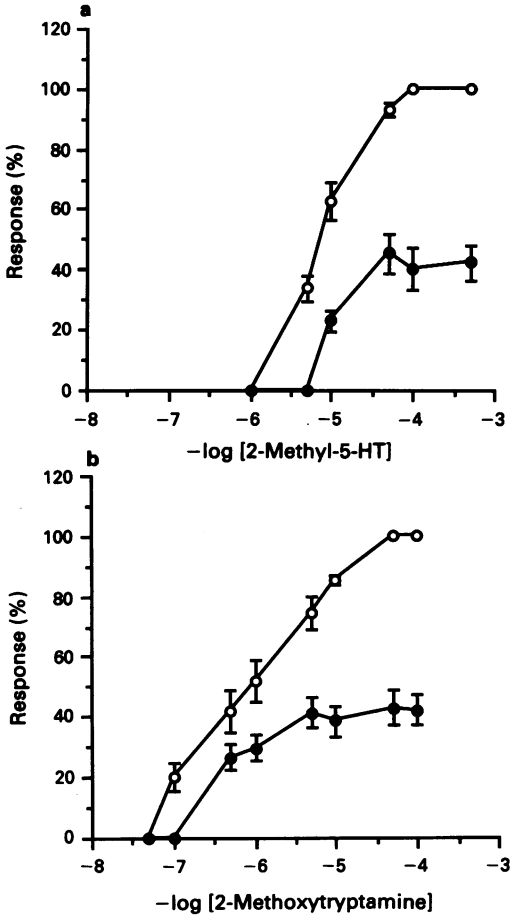

Figure 1 Concentration-response curve to 2-methyl-5-HT (a) and 5-methoxytryptamine (b) in the LMMP preparation of the guinea-pig ileum in absence (○) or in the presence (●) of 0.1 μM atropine. Values are means ± s.e. from eight preparations and are expressed as a percentage of the maximum control response.

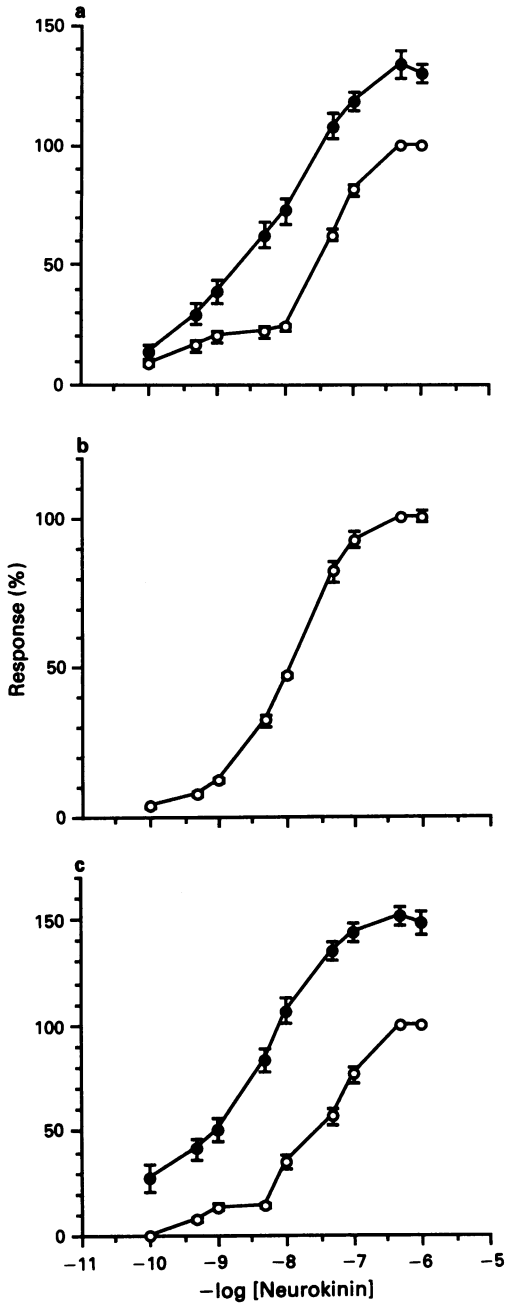

Figure 2 Concentration-response curves to neurokinins in the LMMP preparation of guinea-pig ileum. (a) (○) Substance P (SP) and (●) [Sar^9,met(O$_2$)^{11}]SP; (b) (○) neurokinin A (NKA); (c) (○) NKB and (●) senktide. Values are means ± s.e. from 10–12 preparations and were expressed as percentage of the maximum response obtained with SP (a), NKA (b) or NKB (c).

5 nM and 1 μM ($-\log EC_{50}^1 = 9.3 \pm 0.1$; $-\log EC_{50}^2 = 7.1 \pm 0.01$). The concentration-response curve to SP was also biphasic ($-\log EC_{50}^1 = 8.6 \pm 0.1$; $-\log EC_{50}^2 = 7.3 \pm 0.1$) (Figure 2). NKA gave rise to a monophasic concentration-response curve ($-\log EC_{50} = 7.9 \pm 0.1$). The selective neurokinin receptor agonists, [Sar^9, Met(O$_2$)^{11}]SP and senktide, also yielded monophasic concentration-response curves, with $-\log EC_{50}$ values of 8.2 ± 0.1 and 8.3 ± 0.1 respectively (Figure 2).

Desensitization studies

The application to the LMMP preparation of a high concentration of any neurokinin (0.1–0.5 μM) produced a contraction that faded to baseline after a contact time of 6–12 min. When a desensitization to a particular neurokinin was produced, the tissue became insensitive to further doses of the same neuropeptide, although other neurokinins were still active in the preparation (Table 1). For example, after desensitization to NKB, approximately 40% of the response to SP remained and *vice versa*. The response to any of the three neurokinins was completely abolished in tissues preincubated with NKA, 0.5 μM (not shown).

Desensitization with the selective NK$_1$ agonist, [Sar^9, Met(O$_2$)^{11}]SP, abolished the response to low concentrations of SP, corresponding to the first phase of the biphasic concentration-response curve, while the response to higher SP concentrations was only partially inhibited. Responses to different concentrations of NKB were not modified by NK$_1$ receptor desensitization (Table 1).

Inactivation of the neurokinin receptors did not affect the muscarinic receptors of the preparation, since the response to carbachol, 1 μM, was not modified after desensitization with the neurokinins (not shown).

As described above, a contractile response to either 5-MeOT or 2-Me-5-HT was still present after atropine (Figure 1). A fixed concentration of both 5-HT receptor agonists, approximately the EC_{50} was used for the subsequent experiments. In the presence of atropine 0.1 μM, the remaining response to 5-MeOT, 1 μM, was blocked after preincubation of the preparation with NKB, whereas the remaining effect of 2-Me-5-HT, 10 μM, was blocked after preincubation with either SP or NKB. The contractile response to both 5-HT receptor agonists was entirely (2-Me-5-HT) or almost entirely (5-MeOT) suppressed in tissues desensitized with NKA (0.5 μM) in the presence of atropine (Table 2).

By use of selective neurokinin receptor agonists, the non-cholinergic contraction elicited by 2-Me-5-HT was abolished after desensitization of the preparation with [Sar^9, Met(O$_2$)^{11}] SP. The same desensitization procedure also reduced significantly the atropine-resistant response to 5-MeOT (Table 2). Desensitization with the NK$_3$ agonist, senktide, did not modify the non-cholinergic response induced by stimulation of either 5-HT$_3$ or 5-HT$_4$ receptors (Table 2).

Another experiment was carried out in which the contractile response to 5-MeOT was recorded, in the absence of

Table 1 Effect of desensitization of NK$_1$ and NK$_3$ receptors on the response to endogenous neurokinins in the LMMP preparation of the guinea-pig ileum.

		Desensitization of NK$_1$ receptors		*Desensitization of NK$_3$ receptors*	
Neurokinin		*SP*	*[Sar^9,Met(O$_2$)^{11}]SP*	*NKB*	*Senktide*
SP	100 nM	0	39.1 ± 6.0	41.8 ± 4.4	100
	10 nM	0	0	–	100
	1 nM	0	0	–	100
NKB	100 nM	36.5 ± 3.9	44.8 ± 3.8	0	64.2 ± 18.0
	10 nM	–	74.4 ± 8.4	0	0
	1 nM	–	100	0	0

Desensitization was obtained by the repeated addition of the neurokinin or synthetic analogue (0.5 μM) until the response faded to baseline level. Results are expressed as percentage of the values obtained before desensitization (mean ± s.e. of 6–8 determinations).

Table 2 Effect of desensitization to neurokinins on the response to 2-methyl-5-HT and 5-methoxytryptamine in the presence of atropine (0.1 μM) in the LMMP preparation of the guinea-pig ileum.

Desensitization procedure	2-Methyl-5-HT (10 μM) Before desensitization	2-Methyl-5-HT (10 μM) After desensitization	5-Methoxytryptamine (1 μM) Before desensitization	5-Methoxytryptamine (1 μM) After desensitization
NK_1 receptors:				
SP	61.0 ± 5.0	0	75.3 ± 5.3	67.8 ± 7.9
[Sar^9,Met(O$_2$)^{11}]SP	53.6 ± 4.0	0	71.3 ± 6.1	25.4 ± 1.8
NK_2 receptors:				
NKA	61.0 ± 5.0	0	76.7 ± 5.9	16.7 ± 3.9
NK_3 receptors:				
NKB	61.0 ± 5.0	0	77.5 ± 6.2	0
Senktide	54.2 ± 4.5	50.9 ± 4.5	71.0 ± 6.0	67.4 ± 7.8

Desensitization was obtained by the repeated addition of the neurokinin or synthetic analogue (0.5 μM) until the response faded to baseline level. Results are expressed as percentage of the contraction obtained with the 5-HT receptor agonist in the absence of atropine (mean ± s.e. of 6–8 determinations).

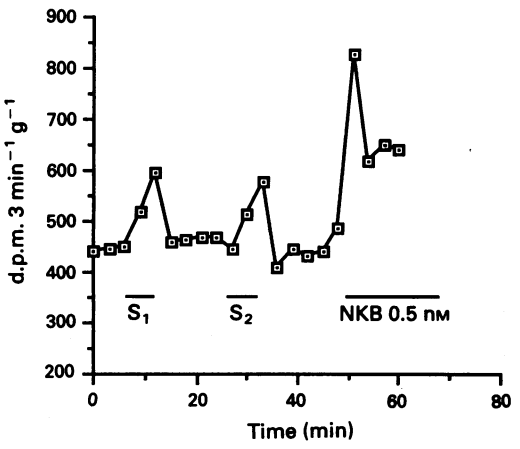

Figure 3 Representative experiment showing the effect of neurokinin B (NKB 0.5 nM) on tritium release used as an index of [^{3}H]-acetylcholine release from the LMMP preparation of guinea-pig ileum. Strips preincubated with [methyl-^{3}H]-choline were subsequently superfused with Tyrode solution containing 10 μM hemicholinium-3. Electrical stimulation (1 Hz, 1 ms, 13.5 V) was performed 6 min (S_1) and 27 min (S_2) after the end of the 60 min washout period. Superfusion with NKB started 21 min after S_2.

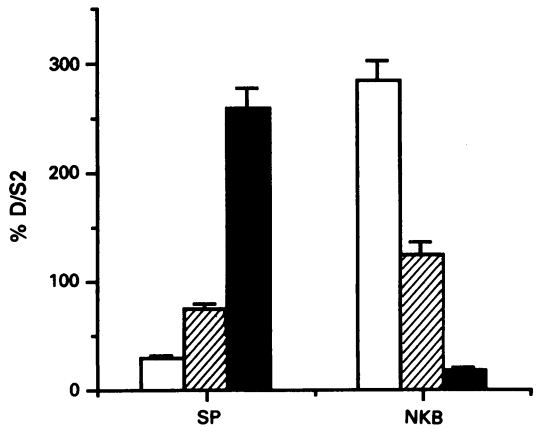

Figure 4 Effect of different concentrations of substance P (SP) and neurokinin B (NKB) on ^{3}H-overflow from LMMP preparations of guinea-pig ileum preloaded with [^{3}H]-choline (□) 0.5 nM, (▨) 5 nM, and (■) 0.1 μM. The effect of the neurokinins (D) on the outflow of ^{3}H-label is expressed as a percentage of the increase in the output of ^{3}H-label evoked by the second electrical stimulation (S_2). Values are mean ± s.e. from 6–8 preparations.

atropine, after the usual desensitization procedure with senktide. The response to 5-MeOT was then 68.4 ± 5.9% (mean ± s.e. of eight experiments) of the control response to the 5-HT$_4$ receptor agonist.

Effect of SP and NKB on tritium overflow from preparations prelabelled with [^{3}H]-choline

Both SP and NKB were able to promote ^{3}H-overflow from the LMMP preparation preloaded with [^{3}H]-choline. A representative experiment is shown in Figure 3. The neurokinins were tested at three different concentrations (0.5, 5 and 100 nM), corresponding to the high- or low-affinity phase of the concentration-response curve. SP produced a concentration-dependent increase in [^{3}H]-overflow, while an inverse relationship was found with NKB, i.e. lower concentrations produced a much higher ^{3}H-overflow (Figure 4).

Discussion

The results of the present study suggest the involvement of two different neurokinins, SP and NKB, in the non-cholinergic response to activation of 5-HT$_3$ and 5-HT$_4$ receptors in guinea-pig ileum. Apparently, only NKB seems to be involved in the response induced by 5-HT$_4$ receptor stimulation.

It is known that the response mediated by the 5-HT$_4$ receptor subtype is atropine-sensitive (Clarke *et al.*, 1989). Accordingly, the monophasic concentration-response curve to 5-MeOT, an agonist more selective for 5-HT$_4$ than for 5-HT$_3$ receptors (Fozard, 1990), was partially antagonized by atropine 0.1 μM. The role of acetylcholine in the response to 5-HT$_3$ receptor activation has not been clearly established (Buchheit *et al.*, 1985; Fox & Morton, 1990), but in the present study, the concentration-response curve to the selective 5-HT$_3$ receptor agonist 2-Me-5-HT (Richardson *et al.*, 1985) was markedly attenuated by atropine, 0.1 μM, suggesting that acetylcholine is also implicated in the response mediated by activation of this 5-HT receptor subtype.

The nature of the atropine-resistant component in the contractile response to both 2-Me-5-HT and 5-MeOT was next considered in the present study. It has been proposed that the contractile effect of 5-HT in the LMMP preparation is mediated, at least in part, by SP (Buchheit *et al.*, 1985), although this point has been controversial (Sanger & Nelson, 1989; Craig *et al.*, 1990; Fox & Norton, 1990). It is known that this preparation contains not only NK_1 receptors for SP, but also NK_3 receptors for NKB (Yau & Youther, 1982; Laufer *et al.*, 1985). Biphasic concentration-response curves were obtained with both neurokinins; the first phase of the curve probably corresponding to the activation of the receptor for which the neurokinin is more specific (SP for NK_1

and NKB for NK_3 receptors) while the second phase, with higher concentrations of the neurokinin, should originate from the activation of both neurokinin receptor subtypes.

To study the implication of the neurokinins in the contractile response evoked by activation of either 5-HT_3 or 5-HT_4 receptors, agonist-induced desensitization was used to block the neurokinin effect. Even though potent competitive antagonists of NK_1 receptors were recently described (e.g. Watling & Krause, 1993), there is not enough evidence on the selectivity of antagonists for other neurokinin receptor subtypes. Agonist-induced desensitization may consequently represent a valid alternative to receptor blockade. In fact, desensitizing studies provided the first indication of neurokinin receptor heterogeneity (Lee *et al.*, 1982; Laufer *et al.*, 1985). After desensitization of the preparation with NKB, a significant percentage of the response to SP remained and *vice versa*. When the desensitization was produced with the selective agonist senktide (Wormser *et al.*, 1986; Guard *et al.*, 1990), the contractile response to low concentrations of NKB was suppressed, as expected, while the response to SP was not affected. The remaining response to high concentrations of NKB after NK_3 receptor desensitization would correspond to stimulation of the myogenic NK_1 receptor also present in the preparation.

The contractile response to 2-Me-5-HT was abolished after desensitization with either SP or NKB in the presence of atropine. To assess which neurokinin was preferentially involved in this response the desensitization procedure was repeated with the selective NK_1 receptor agonist [Sar^9, $Met(O_2)^{11}$]SP (Drapeau *et al.*, 1987). The response to 2-Me-5-HT was fully suppressed, while desensitization with the NK_3 agonist senktide had no effect on the atropine-resistant response. These results suggest the specific involvement of SP in the response to 5-HT_3 receptor activation. Coexistence of acetycholine with neurokinins has been repeatedly described in excitatory enteric neurones (see review by Furness *et al.*, 1992) and it is possible that 5-HT_3 receptor activation releases both of these neurotransmitters which contribute to the contractile response.

At variance with the above data, the atropine-resistant response to the 5-HT_4 receptor agonist, 5-Me-OT, was only abolished after desensitization with NKB. Neither SP nor the NK_3 agonist, senktide, modified the response. Interestingly, the contractile response to 5-MeOT was essentially the same after adding atropine to the preparation or desensitizing with senktide in the absence of the muscarinic receptor antagonist. This may be indicative of a direct coupling between NKB-containing neurones and cholinergic neurones in the myenteric plexus. The ability of senktide to release acetylcholine in this preparation has been described (Guard & Watson, 1991; Fox & Morton, 1991; see also below). Surprisingly, a high percentage of the atropine-resistant response to 5-MeOT was eliminated when desensitizing with the NK_1 receptor agonist [Sar^9, $Met(O_2)^{11}$]SP. As shown in Figure 2, the concentration-response curve to NKB is biphasic. The first phase is likely to correspond to the specific activation of NK_3 receptors whereas the second part would represent the activation not only of NK_3 receptors, but also of a muscular NK_1 receptor (Kilbinger *et al.*, 1986) with a presumably higher contribution to the contractile response. Another possible explanation for the remaining effect of 5-MeOT after desensitization with senktide could be the activation of NK_2 receptors, since desensitization of the preparation to NKA markedly blocks the response to 5-MeOT 1 μM. Some authors have suggested the mediation of this neurokinin receptor subtype in the contractile response of the preparation (Jacoby *et al.*, 1986; Dion *et al.*, 1987), while this possibility has been excluded by others (Laufer *et al.*, 1988).

When SP and NKB were compared in preparations preloaded with [^{3}H]-choline for their ability to induce ^{3}H-overflow, an index of [^{3}H]-acetylcholine release (Szerb, 1976; Wikberg, 1977), NKB produced at a low concentration a much more marked ^{3}H-overflow than SP. This result argues in favour of the physiological significance of NKB as an acetylcholine releaser in this preparation. Other studies in different tissues (e.g. Arenas *et al.*, 1991) are also indicative of the potency of NKB in inducing acetylcholine release. As shown in Figure 4, a very high SP concentration was necessary to induce a marked acetylcholine release. This would explain the biphasic concentration-response curve to SP: the first phase of the curve would correspond to stimulation of muscular NK_1 receptors, while the second phase would be the result of both NK_1 receptor stimulation and acetylcholine release after NK_3 receptor activation. The decreased acetylcholine release when increasing the NKB concentrations would in turn originate from the activation of NK_1 receptors at higher concentrations of NKB.

An alternative interpretation of the present results could be an unpredictable direct desensitizing effect of the neurokinins on 5-HT receptors. For example, electrophysiological (Clapham & Neher, 1984), biochemical (Role *et al.*, 1981) and functional (Molinero & Del Río, 1987) experiments indicate that SP reduces the action of acetylcholine at nicotinic receptors and it has been suggested that SP may enhance nicotinic receptor desensitization (Akasu *et al.*, 1984; Clapham & Neher, 1984). While a direct regulatory action of the neurokinins on 5-HT receptors cannot be discounted, it was verified that the muscarinic receptors of the LMMP preparation were not affected by the desensitization procedures used in this study since the contractile response to carbachol was not modified.

In summary, acetylcholine and the neurokinins SP and NKB appear to be involved in the contractile response to either 5-HT_3 or 5-HT_4 receptor activation in the LMMP preparation of the guinea-pig ileum. Whilst SP seems to be more specifically involved in the response to 5-HT_3 receptor activation, it is of particular interest to note the possible involvement of NKB-containing neurones in the cholinergic response elicited by 5-HT_4 receptor stimulation. This possibility should be taken into consideration when analysing the mechanism of action of compounds such as cisapride or metoclopramide, which stimulate 5-HT_4 receptors (Linnik *et al.*, 1991; Meulemans & Schuurkes, 1992), and are widely used for the treatment of different gastrointestinal disorders.

We thank S. Lizaso for technical help. M.J.R. is a fellow from Gobierno de Navarra (Spain).

References

AKASU, T., OHTA, Y. & KOKETSU, K. (1984). Neuropeptides facilitate the desensitization of nicotinic acetylcholine-receptor in frog skeletal muscle endplate. *Brain Res.*, **290**, 342–347.

ARENAS, E., ALBERCH, J., LOPEZ-NAVARRO, E., SOLSONA, C. & MARSAL, J. (1991). Neurokinin receptors differentially mediate endogenous acetylcholine release evoked by tachykinins in the neostriatum. *J. Neurosci.*, **11**, 2332–2338.

BRADLEY, P.B., ENGEL, G., FENIUK, W., FOZARD, J.R., HUMPHREY, P.P.A., MIDDLEMISS, D.N., MYLECHARANE, E.J., RICHARDSON, B.P. & SAXENA, P.R. (1986). Proposals for the classification and nomenclature of functional receptors for 5-hydroxytryptamine. *Neuropharmacology*, **25**, 563–576.

BUCK, S.H. & BURCHER, E. (1986). The tachykinins: a family of peptides with a brood of receptors. *Trends Neurosci.*, **9**, 65–68.

BUCHHEIT, K.H., ENGEL, G., MUTSCHLER, E. & RICHARDSON, B. (1985). Study of the contractile effect of 5-hydroxytryptamine in the isolated longitudinal muscle strip from guinea-pig ileum. *Naunyn Schmied. Arch. Pharmacol.*, **329**, 36–41.

BUTLER, A., HILL, J.M., IRELAND, S.J., JORDAN, C.C. & TYERS, M.B. (1988). Pharmacological properties of GR 38032F, a novel antagonist of 5-HT_3 receptors. *Br. J. Pharmacol.*, **94**, 387–412.

CLAPHAM, D.E. & NEHER, E. (1984). Substance P reduces acetylcholine-induced currents in isolated bovine chromaffin cells. *J. Physiol.*, **347**, 255–277.

CLARKE, D.E., CRAIG, D.A. & FOZARD, J.R. (1989). The 5-HT_4 receptor: naughty, but nice. *Trends Pharmacol. Sci.*, **10**, 385–386.

CRAIG, D.A. & CLARKE, D.E. (1990). Pharmacological characterization of a neuronal receptor to serotonin in guinea-pig ileum with properties similar to the 5-HT_4 receptor. *J. Pharmacol. Exp. Ther.*, **252**, 1378–1386.

CRAIG, D.A., EGLEN, R.M., WALSH, L.K.M., PERKINS, L.A., WHITING, R.L. & CLARKE, D.E. (1990). 5-Methoxytryptamine and 2-methyl-5-hydroxytryptamine-induced desensitization as a descriminative tool for the 5-HT_3 and putative 5-HT_4 receptors in the guinea-pig ileum. *Naunyn Schmied. Arch. Pharmacol.*, **342**, 9–16.

DION, S., D'ORLEANS-JUSTE, P., DRAPEAU, G., RHALEB, N.E., ROUISSI, N., TOUSIGNANT, C. & REGOLI, D. (1987). Characterization of neurokinin receptors in various isolated organs by the use of selective agonists. *Life Sci.*, **41**, 2269–2278.

DRAPEAU, G., D'ORLÉANS-JUSTE, P., DION, S., RHALEB, N.E. & REGOLI, D. (1987). Selective agonist for substance P and neurokinin receptors. *Neuropeptides*, **10**, 43–54.

EGLEN, R.M., SWANK, S.R., DUBUQUE, L.K. & WHITING, R.L. (1990). Characterization of serotonin receptors mediating contractions of guinea-pig ileum *in vitro*. *Br. J. Pharmacol.*, **99**, 216P.

FOX, A.J. & MORTON, I.K.M. (1990). An examination of the 5-HT_3 receptor mediating contraction and evoked [^{3}H]-acetylcholine release in the guinea-pig ileum. *Br. J. Pharmacol.*, **101**, 553–556.

FOZARD, J.R. (1990). Agonists and antagonists of 5-HT_3 receptors. In *Cardiovascular Pharmacology of 5-Hydroxytryptamine*. ed. Saxena, P.R., Wallis, D.I., Wouters, W. & Bevan, P. pp. 101–115. Dordrecht: Kluwer Academic.

FURNESS, J.B., BORNSTEIN, J.C., MURPHY, R. & POMPOLO, S. (1992). Roles of peptides in transmission in the enteric nervous system. *Trends Neurosci.*, **15**, 66–71.

GADDUM, J.H. & PICARELLI, Z.P. (1957). Two types of tryptamine receptor. *Br. J. Pharmacol. Chemother.*, **12**, 323–328.

GUARD, S., WATSON, S.P., MAGGIO, J.E., TOO, H.-P. & WATLING, K.J. (1990). Pharmacological analysis of [^{3}H]-senktide binding to NK_3 tachykinin receptors in guinea-pig ileum longitudinal muscle-myenteric plexus and cerebral cortex membranes. *Br. J. Pharmacol.*, **99**, 767–773.

GUARD, S. & WATSON, S.P. (1991). Tachykinin receptor types: classification of membrane signalling mechanism. *Neurochem. Int.*, **18**, 149–165.

HENRY, J.L. (1987). Discussion of nomenclature for tachykinins and tachykinins receptors. In *Substance P and Neurokinins*. ed. Henry, J.L., Couture, R., Cuello, A.C., Pelletier, G., Quirion, R. & Regoli, D. p. xvii. New York: Springer-Verlag.

HILL, J.M., BUNCE, K.T. & HUMPHREY, P.P.A. (1990). Investigation of the neuronal non-5-HT_3 receptor mediating contractions of guinea-pig ileum. *Br. J. Pharmacol.*, **99**, 182P.

JACOBY, H.I., LOPEZ, I., WRIGHT, D. & VAUGHT, J.L. (1986). Differentiation of multiple neurokinin receptors in the guinea-pig ileum. *Life Sci.*, **39**, 1995–2003.

KILBINGER, H., STAUB, P., ERLHOF, I. & HOLZER, P. (1986). Antagonist discrimination between subtypes of tachykinin receptors in the guinea-pig ileum. *Naunyn Schmied. Arch. Pharmacol.*, **334**, 181–187.

KILBINGER, H. & WESSLER, I. (1980). Inhibition by acetylcholine of the stimulation-evoked release of [^{3}H]-acetylcholine from guinea-pig myenteric plexus. *Neuroscience*, **5**, 1331–1340.

LAUFER, R., GILON, C., CHOREV, M. & SELINGER, Z. (1988). Desensitization with a selective agonist discriminates between multiple tachykinin receptors. *J. Pharmacol. Exp. Ther.*, **245**, 639–643.

LAUFER, R., WORMSER, V., FRIEDMAN, Z.Y., GILON, C., CHOREV, M. & SELINGER, Z. (1985). Neurokinin B is a preferred agonist for a neuronal substance P receptor and its action is antagonized by enkephalin. *Proc. Natl. Acad. Sci. U.S.A.*, **82**, 7444–7448.

LEE, C.M., IVERSEN, L.L., HANLEY, M.R. & SANDBERG, B.E.B. (1982). The possible existence of multiple receptors for substance P. *Naunyn Schmied. Arch. Pharmacol.*, **318**, 281–287.

LINNIK, M.D., BUTLER, B.T., GADDIS, R.R. & AHMED, N.K. (1991). Analysis of serotonergic mechanism underlying benzamide-induced gastroprokinesis. *J. Pharmacol. Exp. Ther.*, **259**, 501–507.

MEULEMANS, A.L. & SCHUURKES, J.A.J. (1992). Is the action of cisapride on the guinea-pig ileum mediated via 5-HT_4 receptors? *Eur. J. Pharmacol.*, **212**, 51–59.

MOLINERO, M.T. & DEL RIO, J. (1987). Substance P, nicotinic acetylcholine receptors and antinociception in the rat. *Neuropharmacology*, **26**, 1715–1720.

PATON, V.D. & VIZI, E.S. (1969). The inhibitory action of noradrenaline and adrenaline on acetylcholine output by guinea-pig ileum longitudinal muscle strip. *Br. J. Pharmacol.*, **35**, 10–28.

QUIRION, D.R. & DAM, T.V. (1988). Multiple neurokinin receptors: recent developments. *Regul. Pept.*, **22**, 18–25.

RICHARDSON, B.P., ENGEL, G., DONATSCH, P. & STADLER, P.A. (1985). Identification of serotonin M-receptor subtypes and their specific blockade by a new class of drugs. *Nature*, **316**, 126–131.

ROLE, L.W., LEEMAN, S.E. & PERLMAN, R.L. (1981). Somatostatin and substance P inhibit cathecolamine secretion from isolated cells of guinea-pig adrenal medulla. *Neuroscience*, **6**, 1813–1821.

SANGER, G.J. & NELSON,D.R. (1989). Selective and functional 5-hydroxytryptamine$_3$ receptor antagonism by BRL 43694 (granisetron). *Eur. J. Pharmacol.*, **159**, 113–124.

SZERB, J.C. (1976). Storage and release of labelled acetylcholine in the myenteric plexus of guinea-pig ileum. *Can. J. Physiol. Pharmacol.*, **54**, 12–22.

TOROCSIK, A. & VIZI, E.S. (1991). Presynaptic effects of methoctramine on release of acetylcholine. *Neuropharmacology*, **30**, 293–298.

WATLING, K.J. & KRAUSE, J.E. (1993). The rising sun shines on substance P and related peptides. *Trends Pharmacol. Sci.*, **14**, 81–84.

WIKBERG, J. (1977). Release of [^{3}H]-acetylcholine from isolated guinea-pig ileum. A radiochemical method for studying the release of the cholinergic neurotransmitter in the intestine. *Acta Physiol. Scand.*, **101**, 302–317.

WORMSER, U., LAUFER, R., HART, Y., CHOREV, M., GILON, C. & SELINGER, Z. (1986). Highly selective agonist for substance P receptor subtypes. *EMBO J.*, **5**, 2805–2808.

YAU, W.M., BOWEN, D.J. & YOUTHER, M.L. (1991). Evidence for an involvement of eicosanoids in neurokinin$_3$-receptor mediated acetylcholine release from myenteric neurons. *Neurosci. Lett.*, **129**, 259–261.

YAU, W.M. & YOUTHER, M.L. (1982). Direct evidence for a release of acetylcholine from the myenteric plexus of guinea-pig small intestine by substance P. *Eur. J. Pharmacol.*, **81**, 665–668.

(Received May 17, 1993
Revised September 1, 1993
Accepted October 5, 1993)

Br. J. Pharmacol. (1994), **111**, 425–430

Nitric oxide-dependent release of vasodilator quantities of calcitonin gene-related peptide from capsaicin-sensitive nerves in rabbit skin

S.R. Hughes & [1]S.D. Brain

Pharmacology Group, Division of Biomedical Sciences, King's College, Manresa Road, London SW3 6LX

1 Calcitonin gene-related peptide (CGRP) is a potent and long lasting vasodilator in the cutaneous microvasculature of many species including the rabbit. In this study we have investigated the role of nitric oxide in the release of endogenous CGRP, in response to capsaicin, in rabbit skin.

2 Cutaneous blood flow was measured in response to intradermally-injected agents by a multiple site ^{133}Xenon clearance technique.

3 The increased blood flow induced by capsaicin (100 nmol/site) and CGRP (3 pmol/site) was totally inhibited by the CGRP antagonist $CGRP_{(8-37)}$ (1 nmol/site), whilst the increased blood flow induced by sodium nitroprusside (0.3, 1 and 3 nmol/site) was unaffected by $CGRP_{(8-37)}$.

4 The nitric oxide synthase inhibitor N^G-nitro-L-arginine methyl ester (L-NAME, 30 nmol/site) had no effect on the vasodilator response induced by CGRP, but significantly inhibited capsaicin-induced blood flow. The inhibitory effect of L-NAME on capsaicin-induced blood flow was reversed by intradermal L-arginine (300 nmol/site), whilst the inactive enantiomer D-NAME (30 nmol/site) and the α-adrenoceptor agonist phenylephrine (10 pmol/site), at a dose which had a similar effect to L-NAME on basal blood flow, had no effect on capsaicin-induced blood flow.

5 These results suggest that CGRP is the important vasodilator which is released from capsaicin-sensitive sensory nerves in rabbit skin and that the release of CGRP, but not its mechanism of vasodilator action, is nitric oxide-dependent in the rabbit cutaneous microvasculature.

Keywords: CGRP; nitric oxide; capsaicin; N^G-nitro-L-arginine methyl ester (L-NAME); sensory nerves; skin blood flow

Introduction

The 37 amino acid peptide, calcitonin gene-related (CGRP) is a potent mediator of increased blood flow in the cutaneous microvasculature of man and and other species (Brain *et al.*, 1985). The C-terminal fragment of human αCGRP has recently been identified as the CGRP receptor antagonist, $CGRP_{(8-37)}$ (Chiba *et al.*, 1989). $CGRP_{(8-37)}$ has been shown to displace [^{125}I]-[Tyr^O]CGRP from binding sites and inhibit adenosine 3':5'-cyclic monophosphate (cyclic AMP) accumulation in rat liver plasma membrane (Chiba *et al.*, 1989). In other *in vitro* preparations it has been demonstrated that $CGRP_{(8-37)}$ is a competitive antagonist of vascular CGRP receptors. $CGRP_{(8-37)}$ reversibly antagonizes CGRP-induced vasodilatation in tissues that include the rat mesenteric arterial bed (Han *et al.*, 1990) and porcine coronary arteries (Franco-Cereceda, 1992). In *in vivo* studies, $CGRP_{(8-37)}$ has been shown to possess selective antagonistic activity in the rat (Donoso *et al.*, 1990; Gardiner *et al.*, 1990) and in rabbit skin (Hughes & Brain, 1991).

Capsaicin (8-methyl-*N*-vanillyl-6-noneamide) selectively activates sensory nerves by binding to specific neuronal sites to stimulate the activation of cationic channels (Docherty *et al.*, 1991; Marsh *et al.*, 1992). In the rabbit, intradermal injection of capsaicin induces a vasodilator response which is inhibited by the CGRP antagonist $CGRP_{(8-37)}$ (Hughes *et al.*, 1992). This suggests that CGRP is the important vasodilator neuropeptide which is released from capsaicin-sensitive nerves in skin. Substance P is often co-localized with CGRP in capsaicin-sensitive nerves. However, substance P, despite well established potent vasoactive effects in rat skin (Lembeck & Holzer, 1979), is extremely weak when injected intradermally in the rabbit (Brain *et al.*, 1985; Brain & Williams, 1985) and a selective neurokinin-1 antagonist (Beresford *et al.*, 1991) has no effect on capsaicin-induced blood flow in rabbit skin (Hughes *et al.*, 1992).

The vasodilator action of CGRP is of interest in that at least two distinct mechanisms exist, depending on tissue type. CGRP can act via a selective rise in levels of cyclic AMP to induce vascular relaxation (Kubota *et al.*, 1985; Grace *et al.*, 1987); or, in the rat aorta where N^G-L-arginine methyl ester (L-NAME) inibits CGRP-induced relaxation (Gray & Marshall, 1992), CGRP can act via an endothelial, nitric oxide-dependent mechanism to cause vascular relaxation (Brain *et al.*, 1985; Grace *et al.*, 1987; Gray & Marshall, 1992). The dual mechanism of vasodilator action of CGRP is in keeping with the finding that the hypotensive response to intravenous CGRP in the rat can be partially attenuated by nitric oxide synthase inhibitors (Gardiner *et al.*, 1991; Abdelrahman *et al.*, 1992).

Evidence exists to suggest that nitric oxide, in addition to having relaxant effects on vascular smooth muscle, may also have a role as a neurotransmitter; possibly in mediating the efferent function of non-adrenergic non-cholinergic (NANC), vasoactive intestinal peptide (VIP)-containing nerves in tissues such as the trachea, fundus and anococcygeus. Evidence is based upon studies where nitric oxide synthase has been localized in nerves (Bredt *et al.*, 1990) and where inhibitors of nitric oxide-synthase attenuate nerve-stimulated relaxation. In some tissues, it is suggested that VIP and nitric oxide function as co-transmitters (Li & Rand, 1990; Tucker *et al.*, 1990; Burnett *et al.*, 1992) whilst in other studies it is suggested that nitric oxide alone may be the functionally important mediator (Gillespie *et al.*, 1989; Gibson *et al.*, 1990; Desai *et al.*, 1991; Belvisi *et al.*, 1992).

Little is known about the role of nitric oxide in the efferent function of sensory nerves. In this study we have investigated the effect of a nitric oxide synthase inhibitor on the sensory nerve-mediated vasodilator response induced by capsaicin in rabbit skin.

[1] Author for correspondence.

Preliminary findings of this study have been published in the proceedings of the European Workshop on Inflammation Meeting, London, 1992 (Brain *et al.*, 1993).

Methods

Preparation of animals

Experiments were carried out on the dorsal skin of male New Zealand White rabbits (1.5–2.5 kg). Rabbits were anaesthetized with sodium pentobarbitone (30 mg kg^{-1}, i.v., via the marginal ear vein, plus further maintenance doses given as necessary). The dorsal hair was shaved and the skin marked out for multiple intradermal injections as follows: a line was drawn along the spine from neck to tail. Each side of the dorsal skin was then divided into three equal segments, making six segments in total. Three lines of three injection sites were marked in each segment so that there were nine injection sites in each segment. This enabled nine agents to be injected in each experiment, with six replicates of each. The injection sites were allocated with each test agent in each segment, according to a balanced site pattern.

Measurement of blood flow

Blood flow changes were assessed at the multiple sites in the dorsal skin through the use of a ^{133}Xenon (^{133}Xe) clearance technique (Williams, 1976; 1979; Brain *et al.*, 1985; Hughes & Brain, 1991). Alterations in microvascular blood flow induced by intradermal injection of vasoactive agents have been expressed as the percentage change in ^{133}Xe clearance which occurs at test sites as compared to control (saline-injected) sites in each experiment.

The following protocol was followed. Agents were made up in saline (1 ml of each test combination) so that the doses required for injection were in 0.1 ml. Test agents were made up just before use and stored on ice. Equal quantities of ^{133}Xe (0.74 MBq from a stock solution with a specific activity of ± 1665 MBq mg^{-1}) were mixed with each 1 ml sample of test agent. The solutions were then transferred to 1 ml syringes fitted with 27 gauge needles and rapidly injected intradermally according to the previously-determined balanced site pattern, with six injections for each test agent. Two samples of each test agent were injected into tubes and stored under liquid paraffin until the experiment was completed. The rabbit was then left for a 15 min period (timed from midway through the injection procedure), to allow clearance of ^{133}Xe from the injected sites. The rabbit was then killed by anaesthetic overdose.

The dorsal skin was removed and injection sites punched out with a 20 mm diameter steel punch. The injection sites were placed in tubes and covered with 2 ml paraffin oil to reduce the escape of ^{133}Xe. The skin sites and the injection fluid samples were then counted in an automatic gamma-counter (LKB 1282 commpugamma CF) for radioactivity.

Results were calculated using the following equation where

Xe_S = count/min saline-injected skin

Xe_A = count/min test-agent-injected skin

Xe_I = count/min in 0.1 ml volume of injection fluid

$$\frac{[\ln Xe_S - \ln Xe_A] \times 100}{[\ln Xe_I - \ln Xe_S]} = \%$$ change in ^{133}Xe clearance at test sites as compared to control, saline-injected sites.

A similar clearance of ^{133}Xenon (22 ± 1%) was observed at the control, saline-injected sites of all experiments (mean ± s.e.mean % change values for $n = 28$ animals).

The inhibitory effect of $CGRP_{(8-37)}$ has been tested on the dose-related increases in microvascular blood flow induced by intradermal human α CGRP, capsaicin and sodium nitroprusside. $CGRP_{(8-37)}$ was injected at 1 nmol, a dose previously shown to induce complete inhibition of the increase in microvascular blood flow induced by intradermal capsaicin in rabbit skin (Hughes *et al.*, 1992). The inhibitory effect of L-NAME has been tested on equivalent, dose-related increases in microvascular blood flow induced by intradermal human α CGRP and capsaicin. The effect of the inactive enantiomer D-NAME on human α CGRP and capsaicin-induced blood flow and the reversal effect of L-arginine on L-NAME-induced inhibition of capsaicin-induced blood flow has also been investigated. L-NAME was injected intradermally at 30 nmol. This is the highest dose of L-NAME which lacks non-specific inhibitory effects on basal blood flow, as shown by the lack of effect of D-NAME. L-Arginine was injected at a dose of 300 nmol which lacks effect on basal blood flow. The possible inhibitory effect of phenylephrine on the increase in microvascular blood flow induced by intradermal capsaicin has also been investigated.

Materials and preparation of drugs

Human α CGRP was a gift from Dr U. Ney, Celltech, Slough, Bucks. $CGRP_{(8-37)}$ was obtained from Bachem (UK) Ltd., Saffron Waldron, Essex. These peptides were all stored at 10 μM in saline, in 0.1 ml aliquots, at − 30°C until just before use. Sodium nitroprusside (Nipride) was purchased from Roche Ltd., Welwyn Garden City, Herts. L-NAME, the enantiomer D-NAME and L-arginine were all purchased from Sigma Chemical Company Ltd., Poole, Dorset and made up just before use. Capsaicin (pelargonic acid vanillyl amide) was obtained from Fluka Chemicals Ltd., Glossop, Derbyshire and was made up as follows: 100 mg ml^{-1} in a mixture (2:1:7) of absolute ethanol: Tween 80 (Sigma): saline and then diluted in saline immediately prior to use. Solvent controls were used as necessary. ^{133}Xe was obtained already dissolved in saline from Amersham International plc, Aylesbury, Bucks and stored at 4°C. Sodium pentobarbitone (Sagatal) was obtained from May and Baker, Dagenham, Essex.

Statistics

The significance of differences between treatments was assessed by Bonferroni's modified t test where the s.e. estimate for the analysis of variance is used to account for multiple comparisons ($^*P < 0.05$; $^{**}P < 0.01$).

Results

The dose-related ability of CGRP, capsaicin and sodium nitroprusside to increase cutaneous blood flow in rabbit skin is shown in Figure 1. It is clearly shown that the CGRP antagonist, $CGRP_{(8-37)}$, when injected intradermally with the vasodilators, totally inhibits blood flow induced by CGRP and capsaicin, with little effect on that induced by sodium nitroprusside. In previous studies, conducted in rabbit skin using a similar protocol, we have also shown that $CGRP_{(8-37)}$ has no effect on the increase in cutaneous blood flow induced by vasoactive intestinal peptide (VIP) and prostaglandin E_1 (Hughes & Brain, 1991). The inhibitory effect of $CGRP_{(8-37)}$ on basal blood flow suggests that endogenously released CGRP may, like NO, have a modulatory role in the control of basal tone in the cutaneous microvasculature of the rabbit.

Intradermal L-NAME inhibits basal blood flow in rabbit skin. In Figure 2, L-NAME is shown to inhibit significantly dose-related increases in cutaneous blood flow induced by intradermal capsaicin, while having no inhibitory effect on equivalent vasodilator responses induced by increasing doses of CGRP. Figure 3a shows that D-NAME, the inactive enantiomer of L-NAME has no effect on basal levels of blood flow or the increased blood flow induced by intradermal capsaicin (100 nmol/site) and CGRP (3 pmol/site). The

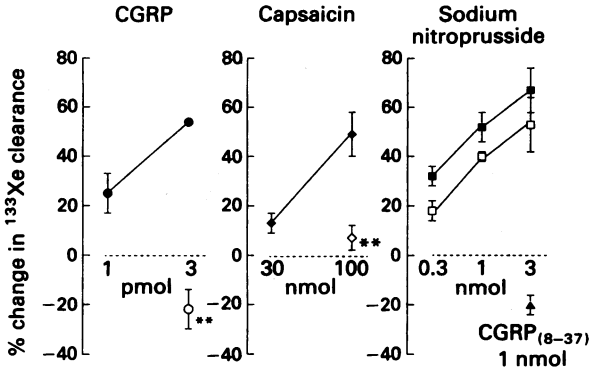

Figure 1 The effect of CGRP$_{(8-37)}$ on increased blood flow induced in rabbit skin by intradermal calcitonin gene-related peptide (CGRP), capsaicin and sodium nitroprusside. The dose-related increases in blood flow induced by (●) CGRP; (◆) capsaicin and (■) sodium nitroprusside; the effect of CGRP$_{(8-37)}$ (1 nmol/site) on the increased blood flow induced by the higher dose of CGRP (3 pmol/site) and capsaicin (100 nmol/site) and each dose of sodium nitroprusside (0.3, 1 and 3 nmol/site) is shown by the same open symbols. The effect of CGRP$_{(8-37)}$ (1 nmol/site) on basal blood flow is indicated by (▲) and the dashed line represents the response to saline. Results are expressed as mean ± s.e.mean values for $n = 4$ rabbits and the significnt inhibitory effect of CGRP$_{(8-37)}$ is shown as $^{**}P<0.01$.

significant inhibitory effect of L-NAME on capsaicin-induced blood flow is also shown.

L-Arginine, the substrate for nitric oxide, reverses the inhibitory effect of L-NAME on capsaicin-induced blood flow at a dose which has no effect on basal blood flow, as shown in Figure 3b. The possibility that the reversal effect of L-arginine is due only to the potentiation of capsaicin-induced blood flow is ruled out by control experiments showing that the co-injection of L-arginine has no effect on the capsaicin-induced response. Results are expressed as mean ± s.e.mean % change in ^{133}Xe clearance in $n = 4$ rabbits, as follows: capsaicin (100 nmol/site) 46 ± 6%; capsaicin + L-arginine 43 ± 5%; L-arginine alone (300 nmol/site) − 6 ± 4%.

The inhibition of basal blood flow induced by L-NAME could be partially responsible for its inhibition of capsaicin-induced blood flow. For this reason, experiments were conducted to investigate the effect of the α_1-adrenoceptor agonist, phenylephrine, on capsaicin-induced blood flow, as shown in Figure 3c. A dose of phenylephrine which reduced basal blood flow to a similar extent to that which was observed with L-NAME was chosen, and its inhibitory effect on capsaicin induced blood flow was compared to that of L-NAME. Phenylephrine had no effect on capsaicin-induced blood flow, whilst in the same animals, L-NAME inhibited capsaicin-induced blood flow to a significant level.

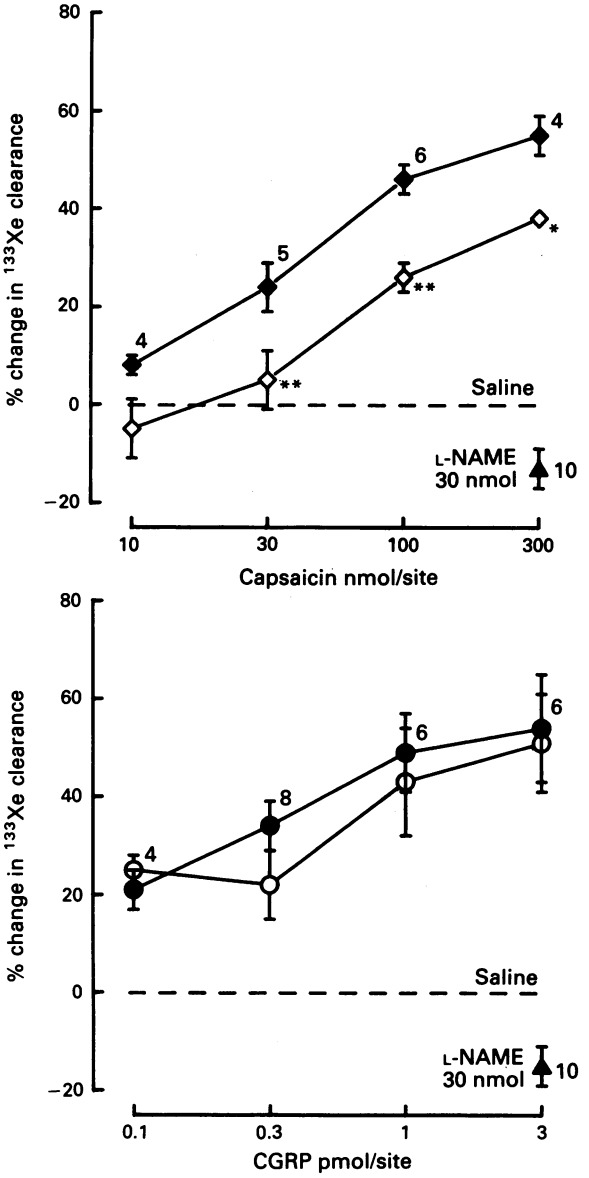

Figure 2 The effect of N^G-nitro-L-arginine methyl ester (L-NAME) on dose-related increases in cutaneous blood flow induced by (a) intradermal capsaicin and (b) calcitonin gene-related peptide (CGRP). Responses induced by increasing doses of capsaicin (10–300 nmol/site) (◆) and CGRP (0.1–3 pmol/site) (●); the effect of L-NAME (30 nmol/site) on these responses is represented by the same open symbols. Significant inhibition of capsaicin induced blood flow by L-NAME: $^{*}P<0.05$; $^{**}P<0.01$. The inhibition of basal blood flow induced by L-NAME alone is shown as (▲) and the response to intradermal saline injection is represented by the dashed line. Results are expressed as mean ± s.e.mean values for $n = 4$–10 rabbits, as labelled.

Discussion

The results confirm that CGRP is the important, potent vasodilator which is released from capsaicin-sensitive sensory nerves in skin, as the CGRP antagonist CGRP$_{(8-37)}$ acts selectively to inhibit substantially the increased blood flow induced by capsaicin. This finding is in agreement with a previous study in which CGRP$_{(8-37)}$ was shown to inhibit completely the increase in cutaneous blood flow induced, not only by capsaicin, but by the analogue olvanil, which was found to be more potent than capsaicin in activating the efferent function of cutaneous sensory nerves (Hughes *et al.*, 1992). In separate studies, we have also demonstrated that an antibody to human α CGRP causes a partial inhibition of capsaicin-induced responses (Buckley *et al.*, 1992).

In contrast to studies in the rat aorta and feline cerebral arterioles (Gray & Marshall, 1992; Wei *et al.*, 1992), we suggest that it is unlikely that CGRP increases blood flow in the cutaneous microcirculation via a nitric oxide-dependent mechanism since, in the present study, the nitric oxide synthase inhibitor L-NAME had little effect on CGRP-induced blood flow. However, our results clearly show that capsaicin-induced vasodilator responses are inhibited by L-NAME and therefore suggest that nitric oxide may play a central modulatory role in the efferent function of sensory nerves.

Interestingly, CGRP$_{(8-37)}$ did not inhibit sodium nitroprusside-induced increased blood flow in the rabbit skin in this study. This is in contrast to studies carried out in an *in vivo* study of feline cerebral arterioles where CGRP$_{(8-37)}$ inhibited the vasodilator response to nitroglycerin and sodium nitro-

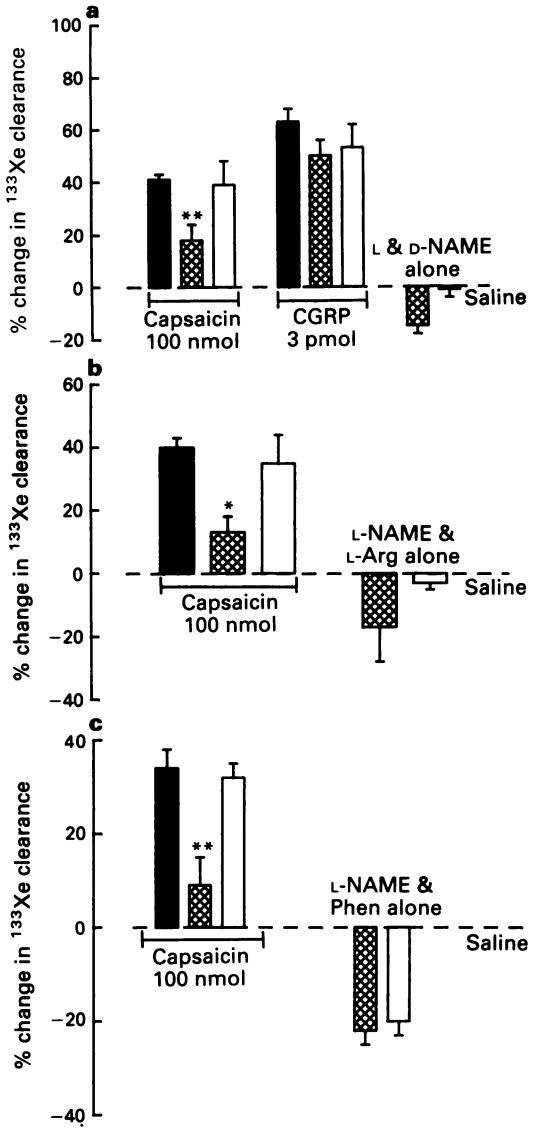

Figure 3 The effect of N^G-nitro-L-argiine methyl ester (L-NAME) and D-NAME on blood flow induced by a high dose of capsaicin and calcitonin gene-related peptide (CGRP) in rabbit skin (a), the reversal effect of L-arginine on capsaicin-induced blood flow which has been inhibited by L-NAME (b) and the effect of phenylephrine (Phen) on capsaicin-induced blood flow (c) in rabbit skin. The increased blood flow induced by capsaicin (100 nmol/site) and CGRP (3 pmol/site) is shown by the closed columns and the effect of addition of L-NAME (30 nmol/site) by the cross hatched columns. (a) Shows the effect of D-NAME (30 nmol/site) on both capsaicin and CGRP-induced blood flow (open columns, as labelled) and (b) shows the effect of L-arginine (300 nmol/site) on the response to capsaicin + L-NAME (open column). The effect of phenylephrine (10 pmol/site) on blood flow induced by capsaicin (open columns) is shown in (c). The responses induced when the agents are injected alone are also shown. The response to saline is shown as the dashed line and results are expressed as mean ± s.e.mean for (a) $n = 5$, for (b) $n = 3$ rabbits and (c) $n = 6$ rabbits. A significant inhibitory effect is shown by: $^*P < 0.05$; $^{**}P < 0.01$.

prusside (Wei *et al.*, 1992). The results led Wei and co-authors to suggest that nitrovasodilators activate sensory nerves to release vasodilator amounts of CGRP in the cephalic circulation. It is of interest that a similar mechanism of action is not suggested by our present experiments in skin. It is more probable that, in our experiments, sodium nitroprusside stimulates vascular relaxation in the cutaneous microcirculation as a consequence of its direct conversion to nitric oxide, a well established mechanism of action (Ignarro, 1990).

The obvious suggestion from our observation that L-NAME inhibited capsaicin, but not CGRP-induced blood flow, is that endogenous nitric oxide plays a central role in the release, but not the action of CGRP. The results are supported by the finding that the enantiomer of L-NAME, D-NAME, had no effect on capsaicin-induced blood flow and that the inhibitory effect of L-NAME was reversed by addition of L-arginine, the substrate for nitric oxide synthesis. We have previously examined the role of endogenous nitric oxide in detail in rat skin (Lawrence & Brain, 1992). Intradermal L-NAME acts locally in the cutaneous microvasculature to cause an inhibition of basal blood flow. We consider this to be due to an inhibition of the basal production of nitric oxide by the constitutive enzyme of microvascular endothelial cells, which normally acts to effect a dilator tone in the microvasculature (Hughes *et al.*, 1990; Lawrence & Brain, 1992). NO has been shown to have an important role in the maintenance of both vascular tone and resting blood pressure (Rees *et al.*, 1989). The inhibition of basal blood flow observed in this study after intradermal injection of L-NAME, has been controlled for by investigating the possible inhibitory effect of phenylephrine, at a dose that reduces basal blood flow to the same extent as L-NAME. Phenylephrine was without effect on capsaicin-induced blood flow, a finding which further supports our suggestion that L-NAME inhibits capsaicin-induced blood flow by acting to inhibit the release of the vasodilator CGRP.

If nitric oxide plays an important modulatory role in the release of CGRP from capsaicin-sensitive nerves it would be most probable that nitric oxide synthase is situated on, in, or near the capsaicin-sensitive nerve ending. Immunocytochemical studies have led to evidence which suggests the existence of nitric oxide synthases in nerves both peripherally and centrally (Bredt *et al.*, 1990). Most of the studies investigating the functional effect of nitric oxide in neurotransmission have concentrated on VIP containing NANC nerves; e.g. the trachea (Tucker *et al.*, 1990; Belvisi *et al.*, 1992), the anococcygeus (Gillespie *et al.*, 1989; Gibson *et al.*, 1990) and the stomach (Li & Rand, 1990; Desai *et al.*, 1991). It is suggested that nitric oxide is the physiologically important mediator of the bronchodilator response in the human trachea (Belvisi *et al.*, 1992) and in the reflex relaxation of the stomach (Desai *et al.*, 1991), although the possibility that VIP and nitric oxide might function as co-transmitters cannot be totally excluded in other species and tissues (Li & Rand, 1990; Tucker *et al.*, 1990; Burnett *et al.*, 1992).

Evidence for the localization of nitric oxide to sensory nerves has recently been demonstrated in dorsal root ganglion cells (Morris *et al.*, 1992). The results suggest that nitric oxide could act to increase selectively cyclic GMP in satellite cells, thus raising the possibility that nitric oxide may have a signalling function within the sensory nervous system. A role for nitric oxide in the afferent function of sensory nerves is suggested by the finding that nitric oxide synthase inhibitors are antinociceptive in the mouse (Moore *et al.*, 1991); although this effect is most probably due to a mechanism of action within the central nervous system. Capsaicin and bradykinin have been shown to increase cyclic GMP levels in cultured dorsal root ganglion cells (Burgess *et al.*, 1989; Wood *et al.*, 1989). This raises the possibility that nitric oxide plays an important role in capsaicin-induced activation of sensory nerves by increasing cyclic GMP levels, which would in turn, lead to neuropeptide release in the periphery.

A modulatory effect of nitric oxide on the release of neuropeptides from sensory nerves has not previously been demonstrated. A recent study by Whittle and coworkers gives evidence to suggest that nitric oxide mediates rat mucosal vasodilatation induced by intragastric capsaicin, but not by CGRP (Whittle *et al.*, 1992). The CGRP antagonist $CGRP_{(8-37)}$ was not used in this study, therefore it was not possible to determine whether capsaicin responses can also be

inhibited by the CGRP antagonist in their model. The authors cannot, as a result, be certain of the site of action of nitric oxide and suggest that nitric oxide mediates rat mucosal vasodilatation induced by intragastric capsaicin. This highlights the problems in determining the site of action of nitric oxide in affecting sensory nerve responses. The major vasoactive neuropeptides released from sensory nerves; substance P and CGRP, can both act via nitric oxide-dependent mechanisms. It is well established that substance P can act to stimulate vascular relaxation and hypotension via nitric oxide-dependent mechanisms (Whittle *et al.*, 1989) and oedema formation induced by substance P in the rat is inhibited by L-NAME (Hughes *et al.*, 1990), whilst CGRP can also act via a nitric oxide-dependent mechanism to relax vascular smooth muscle in certain tissues, as previously discussed. However, our experiments clearly show that the increase in microvascular blood flow induced by exogenously administered CGRP in the rabbit skin is not inhibited by L-NAME and is thus nitric oxide-independent. The nitric oxide-independent response to CGRP in rabbit skin is supported by studies in rat skin (Ralevic *et al.*, 1992). In contrast, capsaicin-induced blood flow, due to the release of CGRP, is inhibited by the CGRP antagonist $CGRP_{(8-37)}$ and also by L-NAME. We consider this is good evidence that nitric oxide plays an essential role in the release of but not the action of CGRP from capsaicin-sensitive nerves in the cutaneous microvasculature.

The potency of CGRP as a peripheral vasodilator is well established, but its release and action as a mediator in physiological and pathological conditions is poorly understood. It has been suggested that it is the mediator released to cause the axon-reflex flare (Brain *et al.*, 1985) and studies suggest it could have a pro-inflammatory role if released at sites of inflammation (Brain & Williams, 1985; Buckley *et al.*, 1991a,b). Thus, nitric oxide could play an important modulatory role in the efferent function of sensory nerves and this could be especially important in the microcirculation where CGRP is an extremely potent vasodilator.

This study was supported by a grant from the British Heart Foundation.

References

ABDELRAHMAN, A., WANG, Y.-X., CHANG, S.D. & PANG, C.C.Y. (1992). Mechanism of the vasodilator action of calcitonin gene-related peptide in conscious rats. *Br. J. Pharmacol.*, **106**, 45–48.

BELVISI, M.G., STRETTON, C.D., YACOUB, M. & BARNES, P.J. (1992). Nitric oxide in the endogenous neurotransmitter of bronchodilator nerves in humans. *Eur. J. Pharmacol.*, **210**, 221–222.

BERESFORD, I.J.M., BIRCH, P.J., BALSAT, M.C., ROGERS, H., FERNANDEZ, L. & HAGAN, R.M. (1991). Effect of the spirolactam NK-1 receptor antagonist, GR82334, on neurokinin- and electrical stimulation-induced oedema in the rat. *Br. J. Pharmacol.*, **102**, 360P.

BRAIN, S.D., HUGHES, S.R., CAMBRIDGE, H. & O'DRISCOLL, G. (1993). The contribution of calcitonin gene-related peptide (CGRP) in neurogenic vasodilator responses. *Agents Actions*, **38**, C19–C21.

BRAIN, S.D. & WILLIAMS, T.J. (1985). Inflammatory oedema induced by synergism between calcitonin gene-related peptide (CGRP) and mediators of increased vascular permeability. *Br. J. Pharmacol.*, **86**, 855–860.

BRAIN, S.D., WILLIAMS, T.J., TIPPINS, J.R., MORRIS, H.R. & MACINTYRE, I. (1985). Calcitonin gene-related peptide is a potent vasodilator. *Nature*, **313**, 54–56.

BREDT, D.S., HWANG, P.M. & SNYDER, S.H. (1990). Localization of nitric oxide synthase indicating a neural role for nitric oxide. *Nature*, **347**, 768–770.

BUCKLEY, T.L., BRAIN, S.D., COLLINS, P.D. & WILLIAMS, T.J. (1991a). Inflammatory edema induced by interactions between IL-1 and the neuropeptide calcitonin-gene-related peptide. *J. Immunol.*, **146**, 3424–3430.

BUCKLEY, T.L., BRAIN, S.D., JOSE, P.J. & WILLIAMS, T.J. (1992). The partial inhibition of the inflammatory response induced by capsaicin using the Fab fragment of a selective calcitonin gene-related peptide antiserum in rabbit skin. *Neuroscience*, **48**, 963–968.

BUCKLEY, T.L., BRAIN, S.D., RAMPART, M. & WILLIAMS, T.J. (1991b). Time-dependent synergistic interactions between the vasodilator neuropeptide, calcitonin gene-related peptide (CGRP) and mediators of inflammation. *Br. J. Pharmacol.*, **103**, 1515–1519.

BURGESS, G.M., MULLANEY, I., MCNEILL, M., COOTE, P.R., MINHAS, A. & WOOD, J.N. (1989). Activation of guanylate cyclase by bradykinin in rat sensory neurones is mediated by calcium influx: possible role of the increase in cyclic GMP. *J. Neurochem.*, **53**, 1212–1218.

BURNETT, A.L., LOWENSTEIN, C.J., BREDT, D.S., CHANG, T.S.K. & SNYDER, S.H. (1992). Nitric oxide: a physiologic mediator of penile erection. *Science*, **257**, 401–403.

CHIBA, T., YAMAGUCHI, A., YAMATANI, T., NAKAMURA, A., MORISHITA, T., INUI, T., FUKASE, M., NODA, T. & FUJITA, T. (1989). Calcitonin gene-related peptide receptor antagonist human CGRP(8–37). *Am. J. Physiol.*, **256**, E331–E335.

DESAI, K.M., SESSA, W.C. & VANE, J.R. (1991). Involvement of nitric oxide in the reflex relaxation of the stomach to accommodate food or fluid. *Nature*, **351**, 477–479.

DOCHERTY, R.J., ROBERTSON, B. & BEVAN, S. (1991). Capsaicin causes prolonged inhibition of voltage-ativated calcium currents in adult rat dorsal root ganglion neurons in culture. *Neuroscience*, **40**, 513–521.

DONOSO, V.S., FOURNIER, A., ST-PIERRE, S. & HUIDOBRO-TORO, P.J. (1990). Pharmacological characterization of CGRP1 receptor subtype in the vascular system of the rat: studies with hCGRP fragments and analogs. *Peptides*, **11**, 885–889.

FRANCO-CERECEDA, A. (1992). Resiniferatoxin-, capsaicin- and CGRP-evoked porcine coronary vasodilatation is independent of EDRF mechanisms but antagonized by CGRP(8–37). *Acta Physiol. Scand.*, **141**, 331–337.

GARDINER, S.M., COMPTOM, A.M., KEMP, P.A., BENNETT, T., BOSE, C., FOULKES, R. & HUGHES, B. (1990). Antagonistic effect of human αCGRP[8–37] on the *in vivo* regional haemodynamic actions of human αCGRP. *Biochem. Biophys. Res. Commun.*, **171**, 938–943.

GARDINER, S.M., COMPTON, A.M., KEMP, P.A., BENNETT, T., FOULKES, R. & HUGHES, B. (1991). Haemodynamic effects of human αcalcitonin gene-related peptide following administration of endothelin-1 or N^G-nitro-L-arginine methyl ester in conscious rats. *Br. J. Pharmacol.*, **103**, 1256–1262.

GIBSON, A., MIRZAZADEH, S., HOBBS, A.J. & MOORE, P.K. (1990). L-N^G-monomethyl arginine and L-N^G-nitro arginine inhibit non-adrenergic, non-cholinergic relaxation of the mouse anococcygeus muscle. *Br. J. Pharmacol.*, **99**, 602–606.

GILLESPIE, J.S., LIU, X. & MARTIN, W. (1989). The effect of L-arginine and N^G monomethyl L-arginine on the response of the rat anococcygeus muscle to NANC nerve stimulation. *Br. J. Pharmacol.*, **98**, 1080–1082.

GRACE, G.C., DUSTING, G.J., KEMP, B.E. & MARTIN, T.J. (1987). Endothelium and the vasodilator action of rat calcitonin gene-related peptide (CGRP). *Br. J. Pharmacol.*, **91**, 729–733.

GRAY, D.W. & MARSHALL, I. (1992). Nitric oxide synthesis inhibitors attenuate calcitonin gene-related peptide endothelium-dependent vasorelaxation in rat aorta. *Eur. J. Pharmacol.*, **212**, 37–42.

HAN, S.P., NAES, L. & WESTFALL, T.C. (1990). Inhibition of periarterial nerve stimulation-induced vasodilatation of the mesenteric arterial bed by CGRP(8–37) and CGRP receptor desensitization. *Biochem. Biophys. Res. Commun.*, **168**, 786–791.

HUGHES, S.R. & BRAIN, S.D. (1991). A calcitonin gene-related antagonist ($CGRP_{8-37}$) inhibits microvascular responses induced by CGRP and capsaicin in skin. *Br. J. Pharmacol.*, **104**, 738–742.

HUGHES, S.R., BUCKLEY, T.L. & BRAIN, S.D. (1992). Olvanil: more potent than capsaicin at stimulating the efferent function of sensory nerves. *Eur. J. Pharmacol.*, **219**, 481–484.

HUGHES, S.R., WILLIAMS, T.J. & BRAIN, S.D. (1990). Evidence that endogenous nitric oxide modulates oedema formation induced by substance P. *Eur. J. Pharmacol.*, **191**, 481–484.

IGNARRO, L.J. (1990). Biosynthesis and metabolism of endothelium-derived nitric oxide. *Annu. Rev. Pharmacol. Toxicol.*, **30**, 535–560.

KUBOTA, M., MOSELEY, J.M., BUTERA, L., DUSTING, G.J., MACDONALD, P.S. & MARTIN, T.J. (1985). Calcitonin gene-related peptide stimulates cyclic AMP formation in rat aortic smooth muscle cells. *Biochem. Biophys. Res. Commun.*, **132**, 88–94.

LAWRENCE, E. & BRAIN, S.D. (1992). Responses to endothelins in the rat cutaneous microvasculature: a modulatory role of locally-produced nitric oxide. *Br. J. Pharmacol.*, **106**, 733–738.

LEMBECK, F. & HOLZER, P. (1979). Substance P as neurogenic mediator of antidromic vasodilation and neurogenic plasma extravasation. *Naunyn Schmied. Arch. Pharmacol.*, **310**, 175–183.

LI, C.G. & RAND, M.J. (1990). Nitric oxide and vasoactive intestinal polypeptide mediate non-adrenergic, non-cholinergic inhibitory transmission to smooth muscle of the rat gastric fundus. *Eur. J. Pharmacol.*, **191**, 303–309.

MARSH, S.J., STANSFELD, C.E., BROWN, D.A., DAVEY, R. & MCCARTHY, D. (1992). The mechanism of action of capsaicin on sensory C-type neurons and their axons in vitro. *Neuroscience*, **23**, 275–289.

MOORE, P.K., OLUYOMI, A.O., BABBEDGE, R.C., WALLACE, P. & HART, S.L. (1991). L-N^G-nitro arginine methyl ester exhibits antinociceptive activity in the mouse. *Br. J. Pharmacol.*, **102**, 198–202.

MORRIS, R., SOUTHAM, E., BRAID, D.J. & GARTHWAITE, J. (1992). Nitric oxide may act as a messenger between dorsal root ganglion neurones and their satellite cells. *Neurosci. Letts.*, **137**, 29–32.

RALEVIC, V., KHALIL, Z., DUSTING, G.J. & HELME, R.D. (1992). Nitric oxide and sensory nerves are involved in the vasodilator response to acetylcholine but not calcitonin gene-related peptide in rat skin microvasculature. *Br. J. Pharmacol.*, **106**, 650–655.

REES, D.D., PALMER, R.M.J. & MONCADA, S. (1989). Role of endothelium-derived nitric oxide in the regulation of blood pressure. *Proc. Natl. Acad. Sci. U.S.A.*, **86**, 3375–3378.

TUCKER, J.F., BRAVE, S.R., CHARALAMBOUS, L., HOBBS, A.J. & GIBSON, A. (1990). L-N^G-nitro arginine inhibits non-adrenergic, non-cholinergic relaxations of guinea-pig isolated tracheal smooth muscle. *Br. J. Pharmacol.*, **100**, 663–664.

WEI, E.P., MOSKOWITZ, M.A., BOCCALINI, P. & KONTOS, H.A. (1992). Calcitonin gene-related peptide mediates nitroglycerin and sodium nitroprusside-induced vasodilation in feline cerebral arterioles. *Circ. Res.*, **70**, 1313–1319.

WHITTLE, B.J.R., LOPEZ-BELMONTE, J. & MONCADA, S. (1992). Nitric oxide mediates rat mucosal vasodilatation induced by intragastric capsaicin. *Eur. J. Pharmacol.*, **218**, 339–341.

WHITTLE, B.J.R., LOPEZ-BELMONTE, J. & REES, D.D. (1989). Modulation of the vasodepressor actions of acetylcholine, bradykinin, substance P and endothelin in the rat by a specific inhibitor of nitric oxide formation. *Br. J. Pharmacol.*, **98**, 646–652.

WILLIAMS, T.J. (1976). Simultaneous measurement of local plasma exudation and blood flow changes induced by intradermal injection of vasoactive substance, using ^{131}I albumin and ^{133}Xe. *J. Physiol.*, **254**, 4–5P.

WILLIAMS, T.J. (1979). Prostaglandin E_2, prostaglandin I_2 and the vascular changes of inflammation. *Br. J. Pharmacol.*, **65**, 517–524.

WOOD, J.N., COOTE, P.R., MINHAS, A., MULLANEY, I., MCNEILL, M. & BURGESS, G.M. (1989). Capsaicin-induced ion fluxes increase cyclic GMP but not cyclic AMP levels in rat sensory neurones in culture. *J. Neurochem.*, **53**, 1203–1211.

(Received May 17, 1993
Revised September 23, 1993
Accepted October 5, 1993)

Br. J. Pharmacol. (1994), **111**, 431–434

Induction of emesis in *Suncus murinus* by pyrogallol, a generator of free radicals

Yoshifumi Torii, Hiroshi Saito & [1]Norio Matsuki

Department of Chemical Pharmacology, Faculty of Pharmaceutical Sciences, The University of Tokyo, Tokyo 113, Japan

1 We investigated whether or not pyrogallol, a generator of free radicals, is emetogenic in *Suncus murinus*, the house musk shrew. Pyrogallol (i.p.) caused dose-dependent emesis in suncus with an ED_{50} value of 77.3 mg kg^{-1}. At a dose of 128 mg kg^{-1}, all suncus vomited with mean latency of 18.8 ± 5.2 min and the number of vomiting episodes was 8.6 ± 2.9.

2 The prophylactic effects of N-(2-mercaptopropionyl)-glycine (MPG), an antioxidant, and tropisetron, a 5-hydroxytryptamine$_3$ (5-HT_3) receptor antagonist, were studied. Pyrogallol (128 mg kg^{-1}, i.p.)-induced emesis was prevented by treatment with MPG (i.p.) or tropisetron (s.c.) with ID_{50} values of 149 mg kg^{-1} and 117 μg kg^{-1}, respectively.

3 Pyrogallol-induced emesis was completely prevented by surgical abdominal vagotomy.

4 The present results indicate that pyrogallol-induced emesis is characteristically very similar to that caused by cisplatin and support the idea that generation of free radicals causes the release of peripheral 5-HT, which stimulates vagal afferent sensory nerves to cause emesis.

Keywords: Emesis; radical; pyrogallol; cisplatin; 5-hydroxytryptamine; suncus

Introduction

Recently, many cancer chemotherapeutic agents have been developed, but the concomitant side effects, including bone marrow suppression, nephrotoxicity, nausea, vomiting and hair loss remain major problems in cancer chemotherapy. In particular, nausea and vomiting cause serious discomfort to patients. Considering the quality of life of the cancer patients, it is very important to overcome such side effects. Among cancer chemotherapeutic agents, cisplatin is known to have potent anticancer effects and also known to cause severe vomiting.

Recently, it has been shown that 5-hydroxytryptamine$_3$ (5-HT_3) receptor antagonists have prophylactic effects on the emesis, and many 5-HT_3 receptor antagonists have been developed (Andrews *et al.*, 1988; Matsuki *et al.*, 1992). It is recognized that cisplatin is converted to an active metabolite(s) (Mutoh *et al.*, 1992), which it is proposed releases 5-HT from the enterochromaffin cells, and that the released 5-HT stimulates the abdominal visceral afferent nerves which transmit impulses to the 'vomiting centre' to cause emesis. 5-HT_3 receptor antagonists are less effective against delayed emesis (Aapro, 1992); therefore, drugs that can prevent the release of 5-HT may be more useful in cisplatin-induced emesis than 5-HT_3 receptor antagonists.

However, little is known about the mechanism of cisplatin-induced release of 5-HT. Cisplatin is known to cause lipid peroxidation of various tissues (Hannemann & Baumann, 1988; Torii *et al.*, 1993a). We have already reported that cisplatin-induced emesis was completely prevented by preadministration of N-(2-mercaptopropionyl)-glycine (MPG), an antioxidant (Torii *et al.*, 1993a). Moreover, cisplatin-induced emesis was exaggerated by ferric chloride, which is known to catalyze the production of cytotoxic oxygen radicals, and ameliorated by deferoxamine, an iron chelator (Matsuki *et al.*, 1994). These results suggest that oxygen radicals are involved in cisplatin-induced emesis. In the present study, we found that pyrogallol, a generator of free radicals, caused emesis in *Suncus murinus*.

[1] Author for correspondence.

Methods

Animals

Experiments were performed on healthy adult female *Suncus murinus* (the house musk shrew) weighing 35–50 g. All animals were housed under a 12 h light/dark cycle with free access to food and water.

Experimental procedures

Drug treatment Pyrogallol (1,2,3-trihydroxybenzen) was used as a generator of free radicals. The agent was administered intraperitoneally in suncus and behavioural changes including vomiting were observed for 90 min. The number of vomiting episodes and the latency to the first vomit were recorded. Initially vomiting is always accompanied by an expulsion of gastric contents. The dose of pyrogallol was increased from 32 mg kg^{-1}, in two fold steps. The ED_{50} value of the emetic effect was calculated by Brownlee's up-and-down method (Brownlee *et al.*, 1953).

The antiemetic effects of tropisetron (s.c.), a 5-HT_3 receptor antagonist, and MPG (i.p.) on pyrogallol (128 mg kg^{-1}, i.p.)-induced emesis were investigated. These agents were administered 30 min prior to the injection of pyrogallol. The ID_{50} values for pyrogallol-induced emesis were also calculated by the up-and-down method.

Vagotomy In five animals, an abdominal vagotomy was performed. Details of the method of surgical vagotomy have been described elsewhere (Torii *et al.*, 1991b). In brief, the animals were anaesthetized with pentobarbitone, 35 mg kg^{-1} i.p., after which the bilateral vagus attached to the oesophagus just below the diaphragm was isolated and sectioned. These animals were allowed to recover for at least 1 week before being tested.

Drugs

The drugs used in the experiments were as follows: pyrogallol (Tokyo Kasei Kogyo Co., Ltd., Tokyo, Japan) and MPG (Sigma Chemical Co.). Tropisetron was provided by Sandoz.

These drugs were dissolved in saline. The volume of drug solutions injected was adjusted to 0.1 ml 50 g^{-1} body weight.

Table 1 The emetic effect of pyrogallol in *Suncus murinus*

Dose (mg kg^{-1})	*No. of suncus vomiting/tested*	*No. of vomiting episodes*	*Latency* (min)	*ED_{50} value* (mg kg^{-1})
128	5/5	8.6 ± 2.9	18.8 ± 5.2	77.3
64	1/5	3	23	
32	0/1	–	–	

Values for the number of vomiting episodes and the latency per vomiting suncus are mean ± s.e.mean, but actual values are indicated when the number of vomiting suncus was less than three.
– No suncus vomited at the dose.

Table 2 Prophylactic effects of N-(2-mercaptopropionyl)-glycine (MPG) and tropisetron on pyrogallol-induced emesis in *Suncus murinus*

Treatment	*Dose*	*No. of suncus vomiting/tested*	*No. of vomiting episodes*	*Latency* (min)	*ID_{50} value*
MPG (i.p.)	320 (mg kg^{-1})	0/2	–	–	149 (mg kg^{-1})
	160	2/5	3,3	14,16	
	80	3/3	7.0 ± 2.1	16.3 ± 3.4	
	Control	1/1	7	12	
Tropisetron (s.c.)	1000 (μg kg^{-1})	0/1	–	–	117 (μg kg^{-1})
	500	0/1	–	–	
	250	0/3	–	–	
	126	2/5	2,1	4,12	
	63	3/3	3.7 ± 1.8	5.0	
	Control	1/1	12	13	

Values for the number of vomiting episodes and the latency per vomiting animal are means ± s.e.mean.
MPG and tropisetron were injected 30 min before the administration of pyrogallol (128 mg kg^{-1}, i.p.).

Table 3 The effects of the surgical vagotomy on pyrogallol-induced emesis in *Suncus murinus*

Treatment	*No. of suncus vomiting/tested*	*No. of vomiting episodes*	*Latency* (min)
Sham operation	4/4	8.3 ± 0.9	20.8 ± 1.1
Vagotomy	0/5	–	–

The operated animals were used for experiments after 1 week.
Pyrogallol (128 mg kg^{-1}) was intraperitoneally injected.
Values for the number of vomiting episodes and latency are mean ± s.e.mean.

Results

Intraperitoneal injection of pyrogallol induced dose-dependent emesis in suncus (Table 1). The calculated ED_{50} value was 77.3 mg kg^{-1}. At the dose of 128 mg kg^{-1}, all five suncus vomited with a latency of 18.8 ± 5.2 min and the number of vomiting episodes was 8.6 ± 2.9 times ($n = 5$). The duration of pyrogallol (128 mg kg^{-1})-induced emesis, time between the first and the last episode, was 15.0 ± 6.5 min. The duration was significantly shorter than emesis caused by cisplatin (20 mg kg^{-1}, i.p.), reported by Mutoh *et al.* (1992) (57.6 ± 12.7 min, $P < 0.05$ by Student's t test). Injection of pyrogallol caused salivation, grooming and transient immobilization before the start of emesis. Such behavioural effects were observed after administration of cancer chemotherapeutic agents, nicotine, veratrine, copper sulphate and X-irradiation. Pyrogallol was not fatal at any of the doses studied, all the animals being alive 1 week after the injection of pyrogallol. Pyrogallol also did not affect the body weights significantly.

Table 2 shows the prophylactic effects of MPG and tropisetron on pyrogallol (128 mg kg^{-1}, i.p.)-induced emesis. Both MPG and tropisetron prevented pyrogallol-induced emesis with the respective ID_{50} values of 149 mg kg^{-1} and 117 μg kg^{-1}. As reported previously, neither MPG nor tropisetron itself caused apparent behavioural change of animals (Torii *et al.*, 1991a; 1993a).

The effect of surgical vagotomy on pyrogallol-induced emesis was investigated (Table 3). In a sham operated group, pyragollol-induced emesis was not influenced ($n = 4$). However, the pyrogallol-induced emesis was completely prevented by surgical vagotomy ($n = 5$). In a separate experiment we confirmed that vagotomized suncus did not vomit after receiving copper sulphate (40 mg kg^{-1}, p.o.). This indicates that the nervous connections involved in the vomiting reflex were retained in the vagotomized suncus.

Discussion

Cisplatin is a very effective antineoplastic agent against various types of solid tumours (Rozencweig *et al.*, 1977). However, clinical use of cisplatin is limited because of bone marrow suppression, nephrotoxicity, nausea and vomiting. For bone marrow toxicity, haematopoietic cytokines, such as granulocyte-colony stimulating factor (G-CSF) and granulocyte-macrophage-colony stimulating factor (GM-CSF), have been introduced to treat granulocytopenia developed by cancer chemotherapy (Hollingshead & Goa, 1991). As to nephrotoxicity, it was reported that cisplatin elevated blood urea nitrogen and creatinine concentration and that antioxidants and radical scavengers attenuated cisplatin-induced nephrotoxicity (McGinness *et al.*, 1978; Dobyan *et al.*, 1986; Sugihara & Gemba, 1986). Sangeetha *et al.* (1990) reported that generation of free radicals following chemotherapy was increased in cancer patients. We propose that cisplatin-induced emesis is also mediated by oxygen free-radicals for the following reasons (Torii *et al.*, 1993a): (1) MPG blocks cisplatin-induced emesis; (2) cisplatin causes lipid peroxidation in the various tissues of suncus and (3) X-irradiation, which is known to release OH· from the water molecule, also causes emesis (Torii *et al.*, 1993b).

In the present study, we showed that pyrogallol, a potent

Table 4 Comparison of cisplatin-, pyrogallol- and 5-hydroxytryptamine (5-HT)-induced emesis in *Suncus murinus*

	Emetic stimuli			
	Cisplatin (20 mg kg^{-1}, i.p.)	*X-irradiation* (800 cGy)	*Pyrogallol* (128 mg kg^{-1}, i.p.)	*5-HT* (10 mg kg^{-1}, i.p.)
Tropisetron (s.c.)	Effective[a]	Effective[b]	Effective	Effective[c]
(ID_{50} value)	(25 μg kg^{-1})	(29 μg kg^{-1})	(117 μg kg^{-1})	(7.8 μg kg^{-1})
Surgical vagotomy	Effective[e]	Effective[b]	Effective	Effective[c]
MPG (i.p.)	Effective[d]	NT	Effective	Not effective[d]
(ID_{50} value)	(130 mg kg^{-1})		(149 mg kg^{-1})	

NT: not tested.
[a]Torii *et al.*, 1991a; [b]Torii *et al.*, 1993b; [c]Torii *et al.*, 1991b; [d]Torii *et al.*, 1993a; [e]Mutoh *et al.*, 1992.

generator of superoxide anion (O_2^-) (Marklund & Marklund, 1974), induced emesis in suncus. Pyrogallol is known to be both competitive and non-competitive inhibitor of catechol *O*-methyl-transferase (COMT) (Crout, 1961; Baldessarini & Greiner, 1973). The latter noncompetitive inhibitory activity increases with pre-incubation of pyrogallol (Crout, 1961). The pyrogallol is rapidly autoxidized and generates O_2, hydrogen peroxide (H_2O_2), and hydroxyradical (OH·) by the Haber-Weiss reaction [$O_2 + H_2O_2 \rightarrow OH\cdot + OH^- + O_2$]. These reactive species are thought to contribute significantly to the noncompetitive effects of pyrogallol on COMT, which contains an essential sulphydryl group (Axelrod & Tomchick, 1958). 5-HT is present in high concentrations in the gastrointestinal tract, predominantly in the enterochromaffin cells (ECs) (Erspamer, 1966). Because 5-HT is emetogenic in *Suncus* (Torii *et al.*, 1991b), inhibition of enzymes which break down 5-HT may promote emetic response. However, 5-HT is not metabolized by COMT because 5-HT has no catechol structure. The great majority of 5-HT is metabolized to 5-hydroxyindoleacetaldehyde by monoamine oxidase (MAO), and then to 5-hydroxyindoleacetic acid (5-HIAA) by aldehyde dehydrogenase. The release of 5-HT from the intestinal mucosa is regulated by a complex pattern of neuronal and humoral inputs to the ECs (Racké & Schwörer, 1991). Noradrenaline (NA) is shown to be present in abdominal vagal fibres (Lundberg *et al.*, 1976). There is a possibility that inhibition of COMT increases the concentration of NA that may affect the release of 5-HT. However, stimulation of α_2-adrenoceptor on ECs is thought to inhibit the release of 5-HT (Racké & Schwörer, 1991). Therefore, it is likely that the emetogenic activity of pyrogallol is not due to the inhibition of COMT, but to the production of oxygen radicals.

Pyrogallol-induced emesis was blocked by injection of MPG. In rabbit aortic rings, pyrogallol elicits endothelium-dependent contractions and the contractions are attenuated by MPG (Goldschmidt & Tallarida, 1991). They reported that endothelium-dependent vasodilatation depends on the presence of a sulphydryl group that scavenges O_2^-, produced from pyrogallol. Therefore, we think that MPG blocks pyrogallol-induced emesis by scavenging O_2^-, generated by pyrogallol.

Pyrogallol-induced emesis was prevented by tropisetron. The surgical abdominal vagotomy at the lower part of the oesophagus also prevented pyrogallol-induced emesis completely. These results suggest that pyrogallol shows its emetogenic effect peripherally, probably indirectly via the release of 5-HT and the stimulation of 5-HT_3 receptors on the vagal afferents.

Table 4 summarizes the overall data of our recent studies including the present data. There are marked similarities among cisplatin-, X-irradiation- and pyrogallol-induced emesis. X-irradiation to the abdomen but not to the head causes emesis in suncus (Torii *et al.*, 1993b). All three types of emesis were blocked by surgical vagotomy and tropisetron. However, MPG has no inhibitory effect on 5-HT-induced emesis. These results suggest that the generation of free radicals occurs before the release of 5-HT from ECs. The ID_{50} value for tropisetron vs pyrogallol was a little higher than against other emetogens. We selected the dose of each stimulus so that 100% animals vomit in control conditions. But, it is still possible that 128 mg kg^{-1} pyrogallol was stronger than other stimuli. However, this is not likely since MPG blocked both cisplatin- and pyrogallol-induced emesis with similar efficacies. NA is known to cause emesis by stimulating α_2-adrenoceptors in the area postrema (Beleslin & Strbac, 1987). It is possible that the lower effectiveness of tropisetron is due to increase of NA by pyrogallol in the central nervous system. Both the central effect is probably not essential, because pyrogallol-induced emesis was completely blocked by vagotomy. Therefore, we do not have an explanation for the different efficacies of tropisetron.

The latency of pyrogallol-induced emesis (18.8 min) was also similar to that of X-irradiation (20.0 min: Torii *et al.*, 1993b) and *cis*-diaqodiammineplatinum (II) (a metabolite of cisplatin) (17.8 min: Mutoh *et al.*, 1992). Moreover, the latency of 5-HT (i.p.) was very short (less than 1 min) (Torii *et al.*, 1991b). Taken together, these results suggest that generation of free radicals at the peripheral site is an important step for the release of 5-HT, and that the release of 5-HT occurs or the concentration of 5-HT reaches the critical level about 20 min after the generation of free radicals.

The duration of pyrogallol-induced emesis was significantly shorter than that caused by cisplatin. Cisplatin is known to be accumulated in the cells and remains there in the long term (Oku *et al.*, 1988). On the other hand, pyrogallol is converted into several pyrogallol sulphate esters *in vivo* (Eccleston & Ritchie, 1973), and may be excreted by the kidney. Therefore, the short duration of pyrogallol-induced emesis is probably due to its fast turnover.

In summary, pyrogallol induced emesis in suncus, and the emesis was prevented by MPG, tropisetron and surgical vagotomy. MPG had no significant effect on antitumour activity of cisplatin *in vitro* (Torii *et al.*, 1993a). Therefore, antioxidants and radical scavengers may become new types of prophylactic drugs against cancer chemotherapeutic agent-induced emesis.

The authors are grateful to Dr P.L.R. Andrews for critical comments on the manuscript.

References

AAPRO, M.S. (1992). Pharmacological treatment of delayed emesis. In *Mechanisms and Control of Emesis*. ed. Bianchi, A.L., Grelot, L., Miller, A.D. & King, G.L. pp. 141–146. Colloque INSERM: John Libbey Eurotext Ltd.

ANDREWS, P.L.R., RAPEPORT, W.G. & SANGER, G.J. (1988). Neuropharmacology of emesis induced by anti-cancer therapy. *Trends Pharmacol. Sci.*, **9**, 334–341.

AXELROD, J. & TOMCHICK, R. (1958). Enzymatic O-methylation of epinephrine and other catechols. *J. Biol. Chem.*, **233**, 702–705.

BALDESSARINI, R.J. & GREINER, E. (1973). Inhibition of catechol-O-methyl transferase by catechols and polyphenols. *Biochem. Pharmacol.*, **22**, 247–256.

BELESLIN, D.B. & STRBAC, M. (1987). Noradrenalin-induced emesis: alpha-2 adrenoceptor mediation in the area postrena. *Neuropharmacol.*, **26**, 1157–1165.

BROWNLEE, K.A., HODGES, J.R.Jr. & ROSENGLATT, M. (1953). The up-and-down method with small samples. *J. Am. Stall. Assoc.*, **48**, 262–277.

CROUT, J.R. (1961). Inhibition of catechol-O-methyl transferase by pyrogallol in the rats. *Biochem. Pharmacol.*, **6**, 47–50.

DOBYAN, D.C., BULL, J.M., STREBEL, F.R., SUNDERLAND, B.A. & BULGER, R.E. (1986). Protective effects of o-(beta-hydroxyethyl)-rutoside on cis-platinum-induced acute renal failure in the rat. *Lab. Invest.*, **55**, 557–563.

ECCLESTON, D. & RITCHIE, I.M. (1973). Sulfate ester formation from catecholamine metabolites and pyrogallol in rat brain *in vivo*. *J. Neurochem.*, **21**, 635–646.

ERSPAMER, V. (1966). Occurrence of indolealkyl amines in nature. In *Handbuch der Experimentellen Pharmakologie*. ed. Eichler, O. & Farag, A. Vol. 19, pp. 132–181. Berlin: Springer.

GOLDSCHMIDT, J.E. & TALLARIDA, R.J. (1991). Pharmacological evidence that captopril possesses an endothelium-mediated component of vasodilation: effect of sulfhydryl groups on endothelium-derived relaxing factor. *J. Pharmacol. Exp. Ther.*, **257**, 1136–1145.

HANNEMANN, J. & BAUMANN, K. (1988). Cisplatin-induced lipid peroxidation and decrease of gluconeogenesis in rat kidney cortex: different effects of antioxidants and radical scavengers. *Toxicol.*, **51**, 119–132.

HOLLINGSHEAD, L.M. & GOA, K.L. (1991). Recombinant granulocyte colony-stimulating factor (rG-CSF): a review of its pharmacological properties and prospective role in neutropenic conditions. *Drugs*, **42**, 300–330.

LUNDBERG, J.M., AHLMAN, H., DAHLSTRÖM, A. & KEWENTER, J. (1976). Catecholamine-containing nerve fibres in the human abdominal vagus. *Gastroenterol.*, **70**, 472–474.

MARKLUND, S. & MARKLUND, G. (1974). Involvement of the superoxide anion radical in the autoxidation of pyrogallol and a convenient assay for superoxide dismutase. *Eur. J. Biochem.*, **47**, 469–474.

MATSUKI, N., TORII, Y. & SAITO, H. (1994). Effects of iron and deferoxamine on cisplatin-induced emesis: further evidence for the role of free radicals. *Eur. J. Pharmacol.*, (in press).

MATSUKI, N., TORII, Y., UENO, S. & SAITO, H. (1992). *Suncus murinus* as an experimental animal model for emesis and motion sickness. In *Mechanisms and Control of Emesis*. ed. Bianchi, A.L., Grelot, L., Miller, A.D. & King, G.L. pp. 323–329. Colloque INSERM: John Libbey Eurotext Ltd.

McGINNESS, J.E., PROCTOR, P.H., DEMOPOULOS, H.B., HOKANSON, J.A. & KIRKPATRICK, D.S. (1978). Amelioration of cisplatinum nephrotoxicity by orgotein (superoxide dismutase). *Physiol. Chem. Phys.*, **10**, 267–277.

MUTOH, M., IMANISHI, H., TORII, Y., TAMURA, M., SAITO, H. & MATSUKI, N. (1992). Cisplatin-induced emesis in *Suncus murinus*. *Jpn. J. Pharmacol.*, **58**, 321–324.

OKU, M., NODA, T., KIYOZUKA, Y., NINOMIYA, Y., HINO, K., OKAMURA, Y., MARUYAMA, M. & ICHIJO, M. (1988). Pharmacokinetic analysis of intraperitoneal cisplatinum administration. *J. Jpn. Soc. Cancer Ther.*, **23**, 657–664.

RACKÉ, K. & SCHWÖRER, H. (1991). Regulation of serotonin release from the intestinal mucosa. *Pharmacol. Res.*, **23**, 13–25.

ROZENCWEIG, M., VON HOFF, D.D., SLAVIK, M. & MUGGIA, F.M. (1977). *Cis*-diamminedichloroplatinum (II). A new anticancer drug. *Ann. Intern. Med.*, **86**, 803–812.

SANGEETHA, P., DAS, U.N., KORATKAR, R. & SURYAPRABHA, P. (1990). Increase in free radical generation and lipid peroxidation following chemotherapy in patients with cancer. *Free Radical Biol. Med.*, **8**, 15–19.

SUGIHARA, K. & GEMBA, M. (1986). Modification of cisplatin toxicity by antioxidants. *Jpn. J. Pharmacol.*, **40**, 353–355.

TORII, Y., SAITO, H. & MATSUKI, N. (1991a). Selective blockade of cytotoxic drug-induced emesis by 5-HT_3 receptor antagonist in *Suncus murinus*. *Jpn. J. Pharmacol.*, **55**, 107–113.

TORII, Y., SAITO, H. & MATSUKI, N. (1991b). 5-Hydroxytryptamine is emetogenic in the house musk shrew, *Suncus murinus*. *Naunyn-Schmied. Arch. Pharmacol.*, **344**, 564–567.

TORII, Y., MUTOH, M., SAITO, H. & MATSUKI, N. (1993a). Involvement of free radicals in cisplatin-induced emesis in *Suncus murinus*. *Eur. J. Pharmacol.*, **248**, 131–135.

TORII, Y., SHIKITA, M., SAITO, H. & MATSUKI, N. (1993b). X irradiation-induced emesis in the house musk shrew. *Suncus murinus*. *J. Radiat. Res.*, **34**, 164–170.

(Received May 25, 1993
Revised August 15, 1993
Accepted October 6, 1993)

Br. J. Pharmacol. (1994), **111**, 435–438

An endothelium-dependent contraction in canine mesenteric artery caused by caffeine

Hiroshi Jino, Hachiro Usui, Shinji Temma, Hiroaki Shirahase & [1]Kazuyoshi Kurahashi

Pharmacology Division, Radioisotope Research Center, Kyoto University, Kyoto, 606, Japan

1 We examined whether or not caffeine caused an endothelium-dependent contraction (EDC) in canine mesenteric artery and whether the endothelium-dependent contracting factors (EDCF) were arachidonic acid metabolites.

2 Caffeine (1, 3 and 10 mM) caused a transient contraction in endothelium-intact arterial strips. Removal of the endothelium significantly attenuated the caffeine (1 and 3 mM)-induced contraction.

3 Caffeine (1 mM)-induced EDC was not affected by quinacrine and manoalide (phospholipase A_2 inhibitors), indomethacin and aspirin (cyclo-oxygenase inhibitors), ONO-3078 and S-1452 (thromboxane A_2 antagonists) or AA-861 and TMK-777 (lipoxygenase inhibitors).

4 Caffeine (1 mM)-induced EDC was also unaffected by 50-235 (an endothelin A receptor antagonist). In addition, catalase combined treatment with superoxide dismutase, or allopurinol (antioxidant) did not affect the EDC.

5 Gro-PIP and NCDC (phospholipase C inhibitors) did not affect the caffeine-induced EDC. However, wortmannin (a phospholipase D inhibitor) and staurosporine (a protein kinase C inhibitor) attenuated the caffeine-induced EDC.

6 The present experiments demonstrate that caffeine causes an EDC in canine mesenteric artery and suggest that the EDCF mediating this response is probably not arachidonic acid metabolites, endothelin or superoxide. Instead, caffeine-induced EDC may be due to activation of the phospholipase D pathway.

Keywords: Canine mesenteric artery; caffeine-induced endothelium-dependent contraction; endothelium-derived contracting factor

Introduction

Furchgott & Zawadzki (1980) have reported that acetylcholine (ACh) produces an endothelium-dependent relaxation in rabbit thoracic aorta. Nitric oxide is considered to be one of the endothelium-derived relaxing factors (Palmer *et al.*, 1987). In contrast, we have reported that various vasoactive substances (ACh, Usui *et al.*, 1983; 1986; noradrenaline, Usui *et al.*, 1987; arachidonic acid, Shirahase *et al.*, 1987; ATP, Shirahase *et al.*, 1988b; nicotine, Shirahase *et al.*, 1988a; A-23187, Shirahase *et al.*, 1988c) produce an endothelium-dependent contraction (EDC) in canine basilar artery. Since such EDC is attenuated by phospholipase A_2 (PLA_2) inhibitors, cyclo-oxygenase inhibitors, thromboxane A_2 (TXA_2) synthetase inhibitors and TXA_2 antagonists, we have proposed that the endothelium-derived contracting factor (EDCF) is probably TXA_2 (Usui *et al.*, 1986; 1987; Shirahase *et al.*, 1987; 1988a,b,c).

Caffeine causes a transient contraction by releasing Ca^{2+} from the endoplasmic reticulum in skeletal and smooth muscle cells (Endo, 1977; Karaki & Weiss, 1988), but few authors have investigated whether caffeine causes an endothelium-dependent contraction.

We recently observed an EDC produced by caffeine in canine mesenteric, coronary and renal arteries, but not in the basilar artery (Jino *et al.*, 1992). The present experiments were undertaken to elucidate the pharmacological nature of caffeine-induced EDC and to determine whether the EDCF for caffeine-induced EDC in canine mesenteric artery is arachidonic acid metabolites, endothelin or superoxide.

Methods

Mongrel dogs of either sex (8–15 kg) were supplied by the Institute of Laboratory Animals at the Faculty of Medicine of Kyoto University (Kyoto, Japan). The animals were housed in steel cages at ambient temperature with a 12-h light/dark cycle and a humidity of about 60%. They were allowed free access to dog food and water. Mesenteric and basilar arteries were isolated from dogs after anaesthesia with ketamine (50 mg kg^{-1}, i.m.) and exsanguination from the common carotid artery. The isolated arteries were removed and cleaned of excess fat and connective tissue. Then the vessels were prepared as helically cut arterial strips (3 mm in width and 15 mm in length for mesenteric artery and 2 mm in width and 15 mm in length for basilar artery) with ligatures placed at both ends. One end of each strip was attached to a holder and the other to a strain gauge force-displacement transducer (Nihonkoden FD) which was connected to a polygraph (San-ei Instrument, 8S) on which isometric tension was recorded.

Each strip was then placed in a 10 ml tissue organ bath containing a physiological salt solution of the following composition (mM): NaCl 120, KCl 4.7, $MgSO_4$ 1.2, KH_2PO_4 1.2, $CaCl_2$ 2.5, $NaHCO_3$ 25 and glucose 10. The bathing solution was maintained at 37 ± 0.5°C and was bubbled with 95% O_2 and 5% CO_2 (pH 7.4) throughout the experiments. An initial 1.5 g tension was applied to each strip and an equilibration period of 120 min was allowed before starting the experiments. The resting tension was readjusted periodically until equilibration was achieved. The endothelium was removed by rubbing the intimal surface. The presence of endothelium was initially confirmed by the ability of ACh (10^{-6} M) to cause relaxation during contraction induced by noradrenaline (NA) (10^{-6} M). Any strips that did not relax in response to ACh were discarded. After it was observed that the KCl (60 mM)-induced contraction was no different between endothelium-intact and endothelium-removed strips (so as to detect smooth muscle damage), caffeine was added to the organ bath. The experiments were carried out in parallel using both endothelium-intact and endothelium-denuded strips at the same time. Caffeine was added to the organ bath 3–4 times

[1] Author for correspondence.

with a washout interval of 30 min between additions. After the contractile response reached a steady level, various agents were added to the organ bath 20 min before the addition of caffeine.

Measurement of inositol-1,4,5-triphosphate

After arterial strips had been equilibrated for 120 min in normal Krebs-Henseleit solution, they were stimulated with caffeine (1, 3 and 10 mM) for 15 s and immediately frozen in liquid nitrogen. Frozen tissue samples were then weighed and homogenized in 6% trichloroacetic acid. After centrifugation of homogenate, the supernatant was extracted with diethyl ether to remove the trichloroacetic acid. The content of inositol-1,4,5-triphosphate (IP_3) was determined by a protein binding assay (TRK 1000; Amersham, Tokyo, Japan) according to the method of Langland & Diamond (1990) and was expressed as pmol mg^{-1} wet weight.

Drugs

Caffeine and indomethacin were purchased from Nacalai Tesque, Kyoto, Japan, manoalide from Wako Pure Chemical Industries Ltd., Kyoto, Japan, aspirin, 2-nitro-4-carboxyphenyl-*N*,*N*-diphenylcarbamate (NCDC), quinacrine, allopurinol, superoxide dismutase (SOD), catalase, L-α-glycerophospho-D-*myo*-inositol 4-monophosphate (Gro-PIP) and staurosporine from Sigma Chemical Co., St. Louis, MO, U.S.A. [9,11-Dimethyl-methane-11,12-methano-13,14-dihydro-13-aza-14-oxo-15 (β) cyclophenyl-ω-pentenor-TXA_2 L-arginine salt] (ONO-3708) was kindly provided by Ono Pharmaceutical Co. Ltd., Osaka, Japan, calcium (5Z)-1**R**,2S,-3S,4S-7 [3-phenylsulphonyl-aminobicyclo[2.2.1]hept-2yl]-5-heptenoate hydrate (S-1452) and myriceron caffeoyl ester (50-235) by Shionogi & Co., Osaka, Japan, 2,3,5-trimethyl-6-(12-hydroxy-5,10-dodecadiynyl)-1,4-benzoquinone (AA-861) by Takeda Chemical Industries Ltd., Osaka, Japan, 1-[{5'-(3''-methoxy-4''-ethoxycarbonyloxyphenyl)-2',4'-pentadienoyl} aminoethyl]-4-diphenylmethoxypiperidine (TMK-777) by Terumo Corp., Tokyo, Japan, and wortmannin by Sandoz, Basle, Switzerland.

Statistics

All results are expressed as means ± s.e.mean. Statistical analysis was performed using Student's paired *t* test, and the criterion of significance was a *P* value less than 0.05.

Results

Contractile responses to caffeine in endothelium-intact or endothelium-denuded strips in canine mesenteric artery

The endothelium-dependence of the contractile response to caffeine was examined in canine mesenteric artery. Caffeine (1, 3 and 10 mM) caused a transient contraction of endothelium-intact strips in a concentration-dependent manner (Figure 1). Repeated application of caffeine with a 30 min washout period caused reproducible transient contractions. Caffeine-induced contractions reached a stable level after 3–4 applications of caffeine over 2 h. The contraction produced by caffeine at 1, 3 and 10 mM resulted in a tension of 0.22 ± 0.02 g ($n = 12$), 0.50 ± 0.02 g ($n = 12$) and 0.76 ± 0.07 g ($n = 8$), respectively. As shown in Figure 2, removal of the endothelium significantly ($P < 0.05$) decreased the response to caffeine (1 and 3 mM), but did not affect contraction induced by caffeine (10 mM). Thus, part of contraction induced by caffeine (1 and 3 mM) was EDC and the caffeine (10 mM)-induced contraction was endothelium-independent (Figure 2). The EDC induced by caffeine (1 mM) was subsequently analysed in more detail.

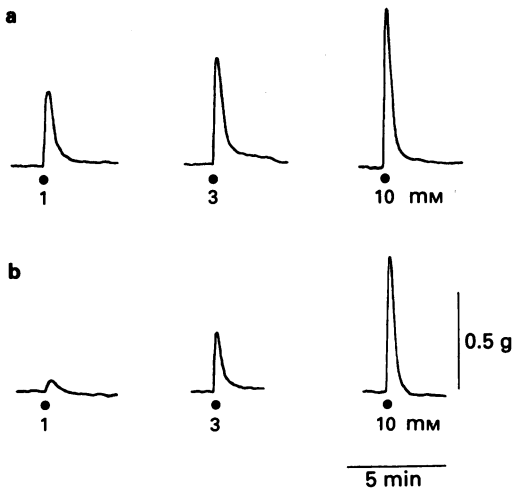

Figure 1 Representative tracings shown caffeine-induced contraction in canine mesenteric artery with (a) and without (b) endothelium.

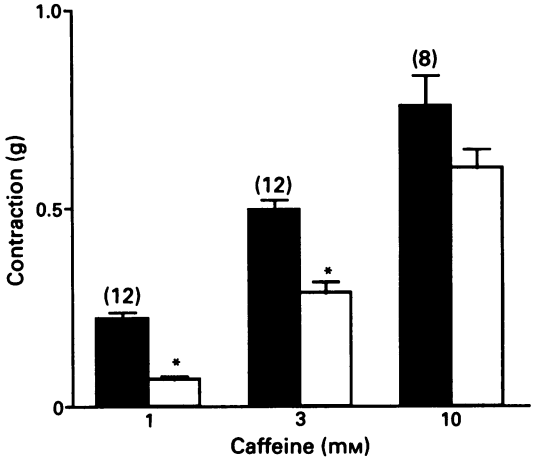

Figure 2 Contractile responses to caffeine (1, 3 and 10 mM) in endothelium-intact (solid columns) or endothelium-denuded (open columns) preparations in canine mesenteric artery. *Indicates a significant difference from the value in endothelium-intact preparations ($P < 0.05$). The number of experiments is shown in parentheses.

Effects of blocking agents on caffeine-induced endothelium-dependent contraction in canine mesenteric artery

We have previously reported that an EDC in canine basilar artery induced by vasoactive substances was attenuated by PLA_2 inhibitors, cyclo-oxygenase inhibitors, TXA_2 synthetase inhibitors, or TXA_2 antagonists (Usui *et al.*, 1986; Shirahase *et al.*, 1987). The effects of these inhibitors or antagonists on the caffeine-induced EDC were examined in the present study. Quinacrine (10^{-6} M) or manoalide (10^{-6} M) (PLA_2 inhibitors), aspirin (2×10^{-4} M) or indomethacin (10^{-6} M) (cyclo-oxygenase inhibitors) and ONO-3708 (10^{-8} M) or S-1452 (10^{-8} M) (TXA_2 antagonists) did not significantly attenuate the caffeine-induced EDC (Table 1). The same concentrations of aspirin and indomethacin augmented the caffeine-induced EDC and prolonged its duration. AA-861 (10^{-5} M) and TMK-777 (10^{-6} M) (5-lipoxygenase inhibitors) had no effect on the EDC. In contrast, ACh-induced EDC in the canine basilar artery was attenuated by quinacrine, manoalide, aspirin, indomethacin, ONO-3708 and S-1452 at the concentration indicated above (Table 1).

It has been reported that endothelin (Yanagisawa *et al.*, 1988) and superoxide (Katusic & Vanhoutte, 1989) are

Table 1 Effects of blocking agents on caffeine (1 mM)-induced EDC in canine mesenteric artery and acetylcholine (ACh, 10^{-7} M)-induced EDC in canine basilar artery

Agents	Concentration (M)	Contraction (%) Caffeine-EDC	ACh-EDC
Phospholipase A_2 inhibitors			
Manoalide	10^{-6}	99 ± 9 (4)	33 ± 8 (4)
	3×10^{-6}	76 ± 9 (5)	23 ± 5 (3)
Quinacrine	10^{-6}	86 ± 5 (3)	35 ± 5 (3)
Cyclo-oxygenase inhibitors			
Aspirin	2×10^{-4}	101 ± 8 (8)	22 ± 3 (3)
Indomethacin	10^{-6}	114 ± 11 (6)	20 ± 5 (3)
Thromboxane A_2 antagonists			
ONO-3708	10^{-8}	82 ± 5 (3)	10 ± 2 (3)
S-1452	10^{-8}	87 ± 8 (3)	15 ± 3 (3)
Lipoxygenase inhibitors			
AA 861	10^{-5}	82 ± 8 (3)	
TMK-777	10^{-6}	72 ± 6 (3)	
Endothelin antagonist			
50-235	10^{-5}	87 ± 8 (4)	
Antioxidants			
SOD (150 u ml^{-1}) + catalase (1000 u ml^{-1})		118 ± 9 (3)	
Allopurinol	10^{-5}	127 ± 7 (3)	

EDC in the absence of any agents was taken as 100%. The numbers in parentheses indicate the number of experiments. Abbreviations in text.

EDCFs. Therefore, we examined whether the caffeine-induced EDC was caused by the release of endothelin or superoxide. Caffeine-induced EDC was not affected by an endothelin A receptor antagonist, 50-235 (10^{-5} M), although the same concentration of this agent antagonized 80% of the endothelin-1 (10^{-8} M)-induced contraction. SOD (150 u ml^{-1}) treatment combined with catalase (1000 u ml^{-1}) or allopurinol (10^{-5} M) had no effect on the caffeine-induced EDC (Table 1).

Effects of phospholipase C inhibitors and a phospholipase D pathway inhibitor on caffeine-induced endothelium-dependent contraction in canine mesenteric artery

We examined whether caffeine-induced EDC was due to the activation of PLC and/or PLD. Gro-PIP (3×10^{-6} and 10^{-5} M) and NCDC (10^{-6} and 3×10^{-6} M) (PLC inhibitors) did not affect caffeine-induced EDC (Figure 3). In addition, caffeine (1, 3 and 10 mM) did not affect the content of IP_3 in endothelium-intact canine mesenteric arterial strips. The IP_3 content in the absence of caffeine was 4.8 ± 0.5 pmol mg^{-1} wet weight ($n = 5$). The content of IP_3 was not significantly altered by the presence of caffeine (1, 3 and 10 mM) and the respective IP_3 levels were 4.4 ± 0.5 pmol mg^{-1} wet weight ($n = 3$), 5.0 ± 1.0 pmol mg^{-1} wet weight ($n = 4$) and 3.0 ± 1.3 pmol mg^{-1} wet weight ($n = 4$). In contrast, wortmannin (3×10^{-7}, 10^{-6} and 3×10^{-6} M) (PLD pathway inhibitor) attenuated the caffeine-induced EDC with decreases of 12 ± 8% ($n = 5$), 41 ± 7% ($n = 5$) and 78 ± 7% ($n = 4$), respectively. However, wortmannin (3×10^{-7} M) did not affect the contraction induced by KCl (70 mM) or by NA (10^{-5} M). The inhibitory effect of wortmannin (10^{-6} M) on the caffeine-induced EDC was significantly ($P<0.05$) more potent than the effect on the contraction induced by KCl (70 mM) with a decrease of 19 ± 3% ($n = 3$) or NA (10^{-5} M) with a decrease of 11.2 ± 5% ($n = 3$). Staurosporine (10^{-8}, 3×10^{-8} and 10^{-7} M) (protein kinase C inhibitor) attenuated the caffeine-induced EDC, and the decreases were 16 ± 4% ($n = 5$), 33 ± 3% ($n = 7$) and 62 ± 4% ($n = 9$), respectively. However, staurosporine (10^{-8} M) did not affect the contraction induced by KCl (70 mM) or by NA (10^{-5} M). Staurosporine (3×10^{-8} M) attenuated the caffeine-induced EDC significantly ($P<0.05$) more potently than the contraction induced by KCl (70 mM) with a decrease of 15 ± 5% ($n = 3$) or NA (10^{-5} M) with a decrease of 2 ± 0.5% ($n = 3$).

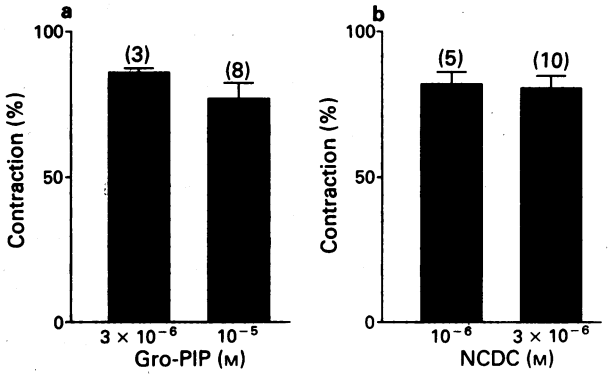

Figure 3 Effects of L-α-glycerophospho-D-*myo*-inositol 4-monophosphate (Gro-PIP, a) and 2-nitro-4-carboxyphenyl-*N*,*N*-diphenylcarbamate (NCDC, b) on caffeine (1 mM)-induced EDC in canine mesenteric artery. EDC in the absence of any agent was taken as 100%. The number of experiments is shown in parentheses.

Discussion

We have previously reported that vasoactive substances (ACh, NA, arachidonic acid, ATP, nicotine and A-23187) cause an EDC in canine basilar artery (Usui *et al.*, 1983; 1986; 1987; Shirahase *et al.*, 1987; 1988a,b,c). There have been few reports on EDC in peripheral arteries. The present study demonstrates that caffeine caused a transient contraction in endothelium-intact strips in canine mesenteric artery, while removal of the endothelium definitely decreased this caffeine-induced contraction. These results clearly indicate that caffeine caused an EDC, as has previously been reported in canine basilar artery. We examined whether the pharmacological nature of the caffeine-induced EDC in canine mesenteric artery was similar to ACh-induced EDC in canine basilar artery.

In canine basilar artery, EDCs induced by various vasoactive substances are attenuated by PLA_2 inhibitors, cyclo-oxygenase inhibitors, TXA_2 synthetase inhibitors and TXA_2 antagonists (Usui *et al.*, 1983; 1986; 1987; Shirahase *et al.*, 1987; 1988a,b,c). In addition, since the TXA_2 content of endothelium-intact preparation is higher than that of endothelium-denuded strips of the canine basilar artery, we have proposed that the EDCF for ACh-induced EDC is probably TXA_2 (Usui *et al.*, 1986; Shirahase *et al.*, 1987). In this study, caffeine-induced EDC was not affected by quinacrine and manoalide (PLA_2 inhibitors), aspirin and indomethacin (cyclo-oxygenase inhibitors), ONO-3708 and S-1452 (TXA_2 antagonists) and AA 861 and TMK-777 (lipoxygenase inhibitors). These results indicate that the EDCF for caffeine-induced EDC is probably not TXA_2 or any of the leukotrienes.

Subsequent to endothelin being identified by Yanagisawa *et al.* (1988), many investigators have reported that it is released from the endothelium of various arteries (Miller *et al.*, 1993) and have proposed that it is one of EDCFs. In addition, it has been reported that superoxide is an EDCF, since A-23187 causes an EDC which is blocked by combined treatment with SOD and catalase in the canine basilar artery (Katusic & Vanhoutte, 1989). However, the caffeine-induced EDC was not affected by 50-235 (an endothelin A receptor antagonist) (Fujimoto *et al.*, 1992) or by allopurinol (antioxidant) and SOD combined treatment with catalase. These results suggest that the caffeine-induced EDC is not due to the release of endothelin and/or the production of superoxide.

It has been reported that bradykinin increases the IP_3 and

cytosolic Ca^{2+} concentration in porcine endothelial cells through a mechanism involving bradykinin-induced hydrolysis of phosphatidylinositol 4,5-diphosphate via PLC activation (Lambert *et al.*, 1986). Therefore, we examined whether the caffeine-induced EDC involved PLC activation in the canine mesenteric artery. Gro-PIP (Cruz-Rivera *et al.*, 1990) and NCDC (Walenga *et al.*, 1980) are PLC inhibitors, and neither agent affected the caffeine-induced EDC. These results indicate that the caffeine-induced EDC is not due to the activation of PLC, and this view is further supported by the finding that caffeine did not increase IP_3 production. Recently, there has been increasing evidence suggesting that PLD plays an important role in intracellular signal transduction in bovine pulmonary artery and aortic endothelial cells (Martin, 1988; Pirotton *et al.*, 1990), primary cultured human abdominal aortic smooth muscle cells and rat aortic smooth muscle cells (Welsh *et al.*, 1990). Wortmannin inhibits the activation of PLD by a chemotactic peptide (formyl-Met-Leu-Phe) in human neutrophils (Reinhold *et al.*, 1990; Bonser *et al.*, 1991). Caffeine-induced EDC was attenuated by wortmannin in a concentration-dependent manner, suggesting that this EDC may involve the activation of the PLD pathway. This view is supported by the findings that staurosporine, a potent protein kinase C inhibitor (Tamaoki *et al.*, 1986), also attenuated the caffeine-induced EDC in a concentration-dependent manner. These results suggest that caffeine activates the PLD pathway to cause the EDC.

Thus, the present experiments suggest that caffeine causes an EDC by the activation of the PLD pathway in endothelial cells and/or smooth muscle cells. The EDCF for this caffeine-induced EDC is probably not arachidonic acid metabolites, endothelin or superoxide, although it may be diacylglycerol. In man, caffeine increases blood pressure by elevating vascular resistance rather than by enhancing cardiac output (Pincomb *et al.*, 1988), and the caffeine-induced EDC may play an important role in this enhancement of vascular resistance.

Supported by a grant from the Smoking Research Foundation, Japan.

References

BONSER, R.W., THOMPSON, N.T., RANDALL, R.W., TATESON, J.E., SPACEY, G.D., HADOSON, H.F. & GARLAND, L.G. (1991). Demethoxyviridin and wortmannin block phospholipase C and D activation in human neutrophil. *Br. J. Pharmacol.*, **103**, 1237–1241.

CRUZ-RIVERA, M., BENNETT, C.F. & CROOKE, S.T. (1990). Glycerol-3-phospho-D-*myo*-inositol 4-phosphate (Gro-PIP) is an inhibitor of phosphoinositide-specific phospholipase C. *Biochim. Biophys. Acta*, **1042**, 113–118.

ENDO, M. (1977). Calcium release from the sarcoplasmic reticulum. *Physiol. Rev.*, **57**, 71–108.

FUJIMOTO, M., MIHARA, S., NAKAJIMA, S., UEDA, M., NAKAMURA, M. & SAKURAI, K. (1992). A novel non-peptide endothelin antagonist isolated from bayberry, Myrica cerifera. *FEBS Letts.*, **305**, 41–44.

FURCHGOTT, R.F. & ZAWADZKI, J.V. (1980). The obligatory role of endothelial cells in the relaxation of arterial smooth muscle by acetylcholine. *Nature*, **288**, 373–376.

JINO, H., USUI, H., SHIRAHASE, H. & KURAHASHI, K. (1992). Caffeine causes an endothelium-dependent contraction in canine artery. *Med. Sci. Res.*, **20**, 169–170.

KARAKI, H. & WEISS, G.B. (1988). Calcium release in smooth muscle. *Life Sci.*, **42**, 111–121.

KATUSIC, Z.S. & VANHOUTTE, P.M. (1989). Superoxide anion is an endothelium-derived contracting factor. *Am. J. Physiol.*, **257**, H33–37.

LAMBERT, T.L., KENT, R.S. & WHORTON, A.R. (1986). Bradykinin stimulation of inositol polyphosphate production in porcine aortic endothelial cells. *J. Biol. Chem.*, **261**, 15288–15293.

LANGLAND, J.M. & DIAMOND, J. (1990). The effect of phenylephrine on inositol 1, 4, 5-trisphosphate levels in vascular smooth muscle measured using a protein binding assay system. *Biochem. Biophys. Res. Commun.*, **173**, 1258–1265.

MARTIN, T. (1988). Formation of diacylglycerol by a phospholipase D-phosphatidate phosphatase pathway specific for phosphatidylcholine in endothelial cells. *Biochim. Biophys. Acta*, **962**, 282–296.

MILLER, R.C., PELTON, J.T. & HUGGINS, J.P. (1993). Endothelins – from receptors to medicine. *Trends Pharmacol. Sci.*, **14**, 54–60.

PALMER, R.M.J., FERRIGE, A.G. & MONCADA, S. (1987). Nitric oxide release accounts for the biological activity of endothelium-derived relaxing factor. *Nature*, **327**, 524–526.

PINCOMB, G.A., LOVALLO, W.R., PASSEY, R.B. & WILSON, M.F. (1988). Effect of behavior state on caffeine's ability to alter blood pressure. *Am. J. Cardiol.*, **61**, 798–802.

PIROTTON, S., ROBAYE, B., LAGNEAU, C. & BOEYNAEMS, J.M. (1990). Adenine nucleotides modulate phosphatidylcholine metabolism in aortic endothelial cells. *J. Cell. Physiol.*, **142**, 449–457.

REINHOLD, S.L., PRESCOTT, S.M., ZIMMERMAN, G.A. & MCINTYRE, T.M. (1990). Activation of human neutrophil phospholipase D by three separable mechanisms. *FASEB J.*, **4**, 208–214.

SHIRAHASE, H., USUI, H., KURAHASHI, K., FUJIWARA, M. & FUKUI, K. (1987). Possible role of endothelial thromboxane A_2 in the resting tone and contractile response to acetylcholine and arachidonic acid in canine cerebral arteries. *J. Cardiovasc. Pharmacol.*, **10**, 517–522.

SHIRAHASE, H., USUI, H., KURAHASHI, K., FUJIWARA, M. & FUKUI, K. (1988a). Endothelium-dependent contraction induced by nicotine in isolated canine basilar artery – possible involvement of a thromboxane A_2 (TXA_2) like substance. *Life Sci.*, **42**, 437–445.

SHIRAHASE, H., USUI, H., MANABE, K., KURAHASHI, K. & FUJIWARA, M. (1988b). Endothelium-dependent contraction and -independent relaxation induced by adenine nucleotides and nucleoside in the canine basilar artery. *J. Pharmacol. Exp. Ther.*, **247**, 1152–1157.

SHIRAHASE, H., USUI, H., MANABE, K., KURAHASHI, K. & FUJIWARA, M. (1988c). An endothelium-dependent contraction induced by A-23187, a Ca^{++} ionophore in canine basilar artery. *J. Pharmacol. Exp. Ther.*, **247**, 701–705.

TAMAOKI, T., NOMOTO, H., TAKAHASHI, I., KATO, Y., MORIMOTO, M. & TOMITA, F. (1986). Staurosporine, a potent inhibitor of phospholipid/Ca^{++} dependent protein kinase. *Biochem. Biophys. Res. Commun.*, **135**, 397–402.

USUI, H., FUJIWARA, M., TSUBOMURA, T., KURAHASHI, K., NOMURA, S. & MIZUNO, N. (1986). Possible involvement of prostanoids in cholinergic contractile response of canine cerebral artery. In *Neural Regulation of Brain Circulation*. ed. Owman, C. & Hardebo, J.E. pp. 261–272. Amsterdam: Elsevier.

USUI, H., KURAHASHI, K., ASHIDA, K. & FUJIWARA, M. (1983). Acetylcholine-induced contractile response in canine basilar artery with activation of thromboxane A_2 synthesis sequence. *Med. Sci. Res.*, **11**, 418–419.

USUI, H., KURAHASHI, K., SHIRAHASE, H., FUKUI, K. & FUJIWARA, M. (1987). Endothelium-dependent vasocontraction in response to noradrenaline in the canine cerebral artery. *Jpn. J. Pharmacol.*, **44**, 228–231.

WALENGA, R., VANDERHOEK, J.Y. & FEINSTEIN, M.B. (1980). Serine esterase inhibitors block stimulus-induced mobilization of arachidonic acid and phosphatidyl-inositide-specific phospholipase C activity in platelets. *J. Biol. Chem.*, **255**, 6024–6027.

WELSH, C.J., SCHMEICHEL, K., CAO, H. & CHABBOTT, H. (1990). Vasopressin stimulates phospholipase D activity against phosphatidylcholine in vascular smooth muscle cells. *Lipids*, **25**, 675–684.

YANAGISAWA, M., KURIHARA, H., KIMURA, S., TOMOBE, Y., KOBAYASHI, M., MITSUI, Y., YAZAKI, Y., GOTO, K. & MASAKI, T. (1988). A novel potent vasoconstrictor peptide produced by vascular endothelial cells. *Nature*, **332**, 411–415.

(Received May 24, 1993
Revised September 24, 1993
Accepted October 6, 1993)

Br. J. Pharmacol. (1994), **111**, 439–444

Study on the vascular reactivity and α_1-adrenoceptors of portal hypertensive rats

Jyh-Fei Liao, *Pi-Chin Yu, **Han-Chieh Lin, **Fa-Yauh Lee, †Jon Son Kuo & [1]*May Chuen-May Yang

Department and Institute of Pharmacology, National Yang-Ming Medical College, *Department of Medical Research and **Division of Gastroenterology, Department of Medicine, Veterans General Hospital-Taipei, Taipei and †Department of Medical Research, Taichung Veterans General Hospital, Taichung, Taiwan

1 Vascular hyporesponsiveness in portal hypertension has been demonstrated to various vasoconstrictors including noradrenaline (NA). The present study aimed to determine whether the attenuated vascular responsiveness to NA is due to a change in the affinity or the number of α_1-adrenoceptors.

2 Partial portal vein ligation (PVL) was performed in Sprague-Dawley rats to produce portal hypertension. Vascular responsiveness to NA was assayed in portal vein, mesenteric artery or tail artery. The affinity and number of α_1-adrenoceptors were determined by specific binding of [^{125}I]-HEAT (2-β-4-hydroxy-3-iodophenyethyl-aminomethyltetralone).

3 In the presence of yohimbine (10^{-7} M, an α_2-adrenoceptor antagonist), propranolol (10^{-6} M, a β-adrenoceptor antagonist), and two catecholamine uptake inhibitors, desipramine (10^{-7} M) and normetanephrine (10^{-6} M), the maximum responses to NA were decreased in all three blood vessels of PVL rats: 45% decrease in portal vein, 25% in mesenteric artery and 18% in tail artery.

4 The EC_{50} values of NA and the pA_2 values of prazosin, an α_1-adrenoceptor antagonist, in all three blood vessels were not significantly different between sham-operated and PVL rats.

5 The K_D and B_{max} values for specific binding of [^{125}I]-HEAT or the K_i values for NA in the crude membrane preparations of either mesenteric artery or tail artery were also not significantly different between the two groups.

6 It is concluded that the vascular hyporesponsiveness to NA in the mesenteric artery or tail artery of PVL rats is not due to changes in the affinity or number of α_1-adrenoceptors.

Keywords: Portal hypertension; portal vein; mesenteric artery; tail artery; α_1-adrenoceptor; noradrenaline

Introduction

It is known that chronic portal hypertension is associated with increased cardiac ouptut and splanchnic blood flow and decreased total peripheral and splanchnic vascular resistances (Vorobioff *et al.*, 1983). The decreased vascular resistance may, in part, result from the attenuated vascular reactivity to endogenous vasoconstrictors, such as noradrenaline (NA) (Kiel *et al.*, 1985), arginine vasopressin (Murray & Paller, 1986), and angiotensin II (Finberg *et al.*, 1981). The nature of the attenuation of vascular reactivity is not clear at present. Accumulated evidence has suggested that functional antagonism by elevation of vasodilator substances and a defect in the cellular contractile apparatus in the vascular smooth muscle may be involved in the hyporesponsiveness of portal hypertension. Benoit *et al.* (1984) and Pizcueta *et al.* (1990) hypothesized that hyperglucagonism plays a key role in the decreased vascular sensitivity to various vasoconstrictors. Recently, in studying the role of endothelium in regulation of vascular tone, investigators have revealed that nitric oxide (Vallance & Moncada, 1991; Pizcueta *et al.*, 1992; Lee *et al.*, 1993) and endothelin (Yu *et al.*, 1992) may be responsive for the hyporesponsiveness of portal hypertension. However, the hyporesponsiveness was not only to vasoconstrictors but also to vasodilators (Kaumann & Groszmann, 1989; Chao *et al.*, 1992). In addition, there are also studies indicating that the hyporesponsiveness in portal hypertension may be attributed to impairment of intracellular mechanisms (Murray & Paller, 1985; Chao *et al.*, 1992).

Despite the well documented attenuated vascular response to NA it is generally accepted that, in patients with decompensated liver cirrhosis, sympathetic nervous activity is increased (Bichet *et al.*, 1982; Arroyo *et al.*, 1983; Tage-Jensen *et al.*, 1988). Although many reports have described the decreased responsiveness to NA or a related α-adrenoceptor agonist (MacGilchrist *et al.*, 1991; Lee *et al.*, 1992), the vascular receptor number and affinity of NA in portal hypertension have not been studied. It is possible that elevated plasma concentrations of NA may affect the receptor number or the affinity and so affect vascular reactivity (Villamediana *et al.*, 1988). Using platelets and lymphocytes, MacGilchrist *et al.* (1990) did not find an adrenoceptor down-regulation in cirrhotic patients. However, platelet and lymphocyte receptors may not be representative of vascular receptors. The purpose of this study was to clarify whether the hyporesponsiveness to NA occurs at the receptor level. Therefore, we investigated whether there were alterations in the number and affinity of vascular α-adrenoceptor in portal hypertensive rats.

Methods

Portal hypertensive (PVL) rats

Partial portal vein ligation was performed according to the method described by Chojkier & Groszmann (1981). Briefly, male Sprague-Dawley rats (200–250 g) were anaesthetized with ether. A midline incision was made and the portal vein proximal to the bifurcation was exposed. A 3–0 silk ligature was made around the portal vein and a piece of PE50 tubing (Clay Adams). The PE tubing was then removed and the abdomen closed. On sham-operated rats, no ligature was applied, the abdomen was closed after exposure of the portal vein.

[1] Author for correspondence.

Pressure measurement

Two weeks after surgery, rat was anaesthetized with ketamine (150 mg kg^{-1}). The ileocolic vein was cannulated with PE50 tubing for measuring portal venous pressure. Portal venous pressures in ligated rats were between 12–17 mmHg, whereas in sham-operated rats were between 5–10 mmHg. Immediately after the portal pressure was confirmed, tail artery, mesenteric artery and portal vein were removed into aerated Krebs-Henseleit solution and cleaned. The composition of Krebs-Henseleit solution was (mM): NaCl 115, $CaCl_2$ 2.1, $MgSO_4$ 1.2, NaH_2PO_4 1.2, $NaHCO_3$ 25, KCl 5.0 and glucose 11.

Tension experiments

The blood vessels were cut into segments and prepared as previously described (Yang *et al.*, 1990; 1991; Chao *et al.*, 1992). The tension generated was recorded on a Grass polygraph (7D) via force displacement transducer (FT03). The tissue chamber was maintained at 37°C and bubbled with a gas mixture of 95% O_2 and 5% CO_2. Tissues were equilibrated under resting tension for 1 h. Preliminary experiments showed that the optimal tension for the portal vein was 0.7 g, mesenteric artery 1.2 g, and tail artery 1 g. Tissue responsiveness was indicated by the consistent responses of two consecutive tests with KCl (60 mM). After equilibration, cumulative dose-response curves to NA (10^{-8}–3×10^{-5} M) were first obtained. The tissues were then rinsed and allowed to recover for about 30 min. The dose-response curves to NA were repeated in the presence of 10^{-8} M prazosin (an α_1-adrenoceptor antagonist). Effects of 10^{-7} M and 10^{-6} M prazosin were tested in the similar manner after a recovery period of 45 min. All of the dose-response curves to NA were performed in the presence of 10^{-7} M yohimbine (an α_2-adrenoceptor antagonist), 10^{-6} M propranolol (a β-adrenoceptor antagonist), and two catecholamine uptake inhibitors, desipramine (10^{-7} M) and normetanephrine (10^{-6} M) (Han *et al.*, 1990).

Receptor binding assay

The technique for receptor binding assays follows that of Han *et al.* (1987) with some modifications. In brief, the tail artery from two rats and the mesenteric artery from four rats were pooled and homogenized in a glass homogenizer in 1 ml homogenizing buffer (50 mM Tris, 5 mM EDTA, pH 7.4). The homogenate was further diluted with 1 ml of 2 × binding buffer (318 mM NaCl, 2 mM Tris, 10 mM $MgCl_2$, pH 7.4) and 4 ml of binding buffer (154 mM NaCl, 20 mM Tris, 5 mM $MgCl_2$, pH 7.4) for binding assay. Aliquots of the homogenate preparation (200 µl, 30–60 µg protein per assay) were incubated with [^{125}I]-HEAT (2-β-4-hydroxy-3-iodophenyethylaminomethyltetralone, 2200 Ci $mmol^{-1}$, NEN, Du Pont) at 5–6 concentrations or with 270 pM [^{125}I]-HEAT and seven concentrations of NA (10^{-9}–10^{-3} M) in a final volume of 250 µl for 30 min at 30°C. Nonspecific binding was assessed by adding prazosin (10^{-5} M). At the end of the incubation, 10 ml of ice-cold wash buffer (150 mM NaCl, 20 mM HEPES, pH 7.4) was added and filtered through a 24 mm glass fibre filter (Whatman GF/C). The filter was then rinsed with additional 10 ml of ice-cold wash buffer and counted in a gamma counter (1277 Gammamaster, Pharmacia, Wallac Oy). All of the determinations were performed in duplicate. The portal vein was not used in this assay since binding was too low (specific bound = 29 c.p.m. with 210 pM [^{125}I]-HEAT added to 30 µg homogenate protein per assay) in a sample pooled from four rats.

Calculations

Tension was expressed as mN mm^{-2} (Murphy, 1980). EC_{50} was calculated from the plot of the percentage response against log dose. pA_2 was calculated according to Arunlakshana & Schild (1959). The density of receptor sites (B_{max}) and the dissociation constant (K_D) were determined by Scatchard analysis (Scatchard, 1949). The inhibition constant K_i was calculated according to Munson & Rodbard (1980). Data are expressed as mean ± s.e.mean. Significance was determined by the Student's *t* test or one way analysis of variance (ANOVA) followed by Newman-Keuls test at $P < 0.05$.

Results

Tension experiments

As shown in Figure 1, the maximum contractile response of the tail artery to NA was the greatest among the three blood

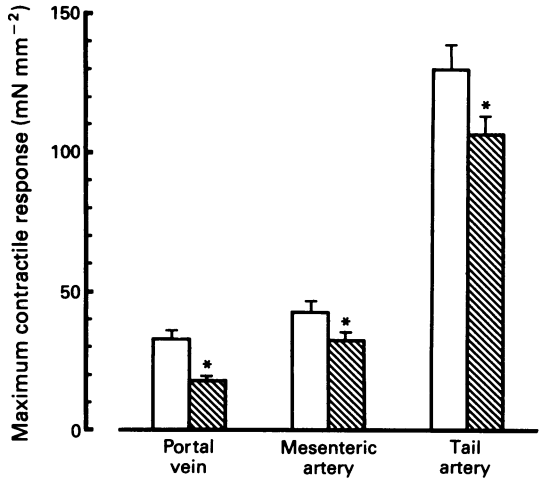

Figure 1 Maximum contractile response to noradrenaline in blood vessels from portal hypertensive (PVL) and sham-operated (Sham) rats. The data are shown as mean ± s.e.mean of 6–8 experiments. *$P < 0.05$, significantly different between Sham (open column) and PVL (hatched column) rats by Student's *t* test.

Table 1 The EC_{50} values for noradrenaline on blood vessels of portal hypertensive (PVL) and sham-operated (Sham) rats

		EC_{50} (10^{-7} M)		
Blood vessel	n	*Sham*	n	*PVL*
Portal vein	16	3.5 ± 0.4*	18	3.0 ± 0.4**
Mesenteric artery	17	11.5 ± 3.1	15	12.9 ± 3.2
Tail artery	19	1.3 ± 0.2**	18	1.5 ± 0.2***

The data are shown as mean ± s.e.mean. *$P < 0.05$, **$P < 0.01$ and ***$P < 0.001$, significantly different from the corresponding mesenteric artery of sham-operated or PVL rats by Student's *t* test.

Table 2 The pA_2 values for prazosin on blood vessels of portal hypertensive (PVL) and sham-operated (Sham) rats

Blood vessel	n	*Sham*	n	*PVL*
Portal vein	5	8.9 ± 0.1*	7	9.0 ± 0.1**
Mesenteric artery	5	9.6 ± 0.2	5	9.9 ± 0.2
Tail artery	6	8.7 ± 0.1**	6	8.9 ± 0.1**

The data are shown as mean ± s.e.mean. *$P < 0.05$ and **$P < 0.01$, significantly different from the corresponding mesenteric artery of sham-operated or PVL rats by Student's *t* test.

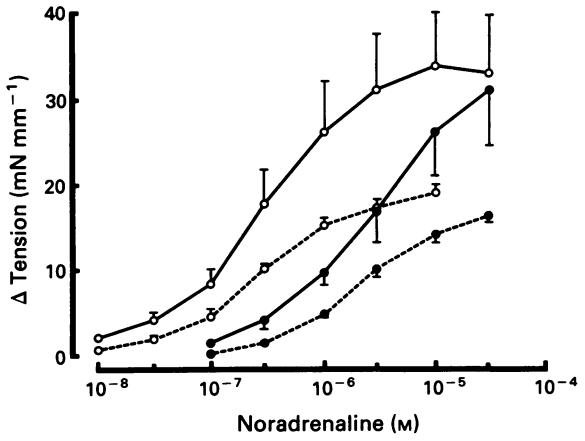

Figure 2 Cumulative concentration-response curves to noradrenaline in the absence and presence of prazosin (10^{-8} M) of portal vein of portal hypertensive (PVL) and sham-operated (Sham) rats. The data are shown as mean ± s.e.mean of 5–7 experiments: Sham (O—O), Sham + prazosin (●—●), PVL (O——O), PVL + prazosin (●——●).

vessels tested. When comparing the vascular reactivity to NA between PVL and sham-operated rats, the maximum responses were decreased in all three blood vessels of PVL rats: a 45% decrease in portal vein, 25% in mesenteric artery and 18% in tail artery (Figure 1). However, the EC_{50} values of NA were not changed between the two groups (Table 1). It was noted that the EC_{50} value of NA in the mesenteric artery was much higher than that in the portal vein or tail artery. As shown in Figure 2, the α_1-adrenoceptor antagonist, prazosin, was able to shift the dose-response curves to NA to the right. In contrast to the affinity of NA, the affinity of prazosin in the mesenteric artery was higher than that in the portal vein or tail artery (Table 2). However, the pA_2 values of prazosin in the three blood vessels were not different between the PVL and sham-operated rats.

Receptor binding assay

As shown in Figure 3a (the representative of five similar experiments), the binding of [^{125}I]-HEAT to the tail artery homogenate of sham-operated rats appeared to be saturable. Scatchard analysis of such binding data indicated that [^{125}I]-HEAT bound to a single population with an apparent K_D of

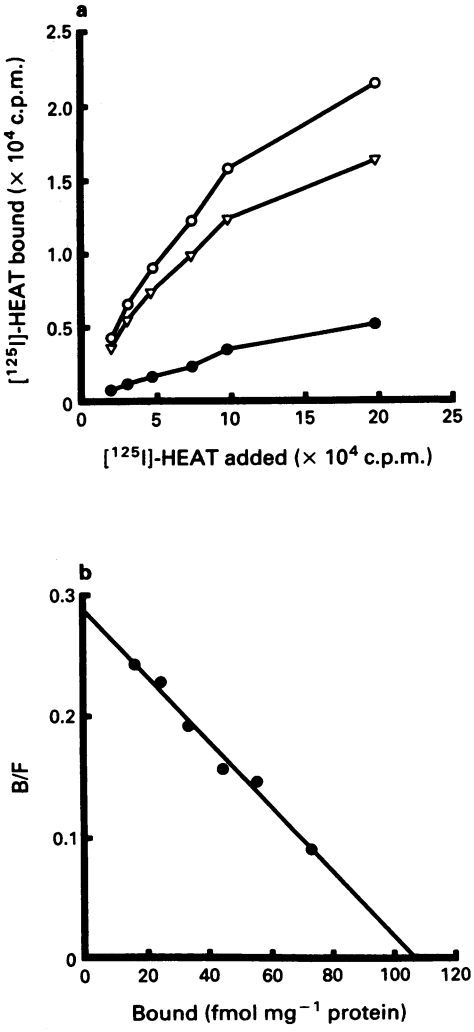

Figure 3 Binding of [^{125}I]-HEAT to tail artery homogenates of sham-operated rats. The data are shown as the average of duplicate determinations from one experiment. This figure is representative of five similar experiments with duplicate determinations. (a) Saturation binding; total bound (O), nonspecific bound (●), specific bound (▽); (b) Scatchard plot.

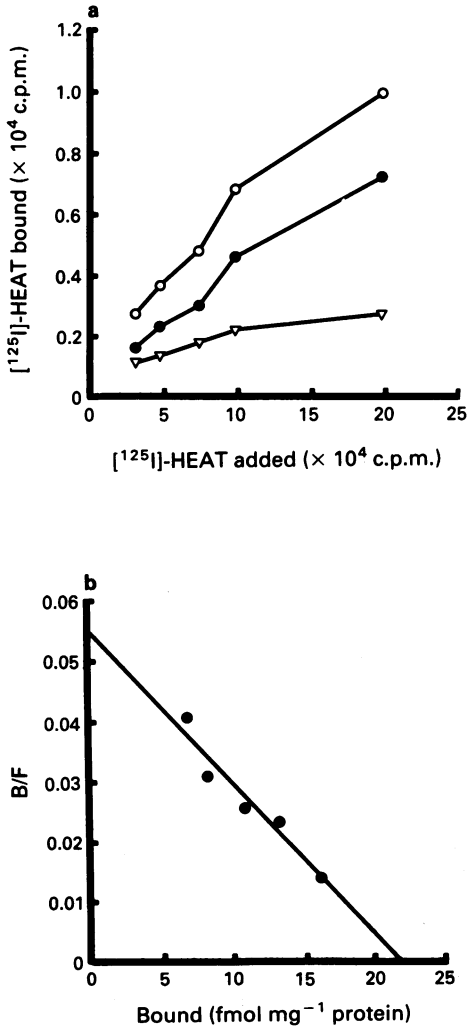

Figure 4 Binding of [^{125}I]-HEAT to mesenteric artery homogenate of portal hypertensive (PVL) rats. The data are shown as the average of duplicate determinations from one experiment. This figure is representative of three similar experiments with duplicate determinations. (a) Saturation binding; total bound (O), nonspecific bound (●), specific bound (▽); (b) Scatchard plot.

Table 3 The K_D and B_{max} values of [^{125}I]-HEAT on blood vessels of portal hypertensive (PVL) and sham-operated (Sham) rats

	Mesenteric artery			*Tail artery*		
	n	K_D (pM)	B_{max} (fmol mg^{-1} protein)	n	K_D (pM)	B_{max} (fmol mg^{-1} protein)
Sham	3	80 ± 4	20 ± 4	5	133 ± 35	82 ± 9**
PVL	3	78 ± 19	19 ± 4	5	139 ± 27	87 ± 17*

The data are shown as mean ± s.e.mean. *$P<0.05$ and **$P<0.01$, significantly different between mesenteric artery and tail artery of Sham-operated or PVL rats.

Table 4 The K_i values for noradrenaline on blood vessels of portal hypertensive (PVL) and sham-operated (Sham) rats

	Mesenteric artery		*Tail artery*	
	n	K_i (μM)	n	K_i (μM)
Sham	3	17.9 ± 9.7	5	9.7 ± 1.0
PVL	3	7.0 ± 3.5	5	30.4 ± 9.3

The data are shown as mean ± s.e.mean.

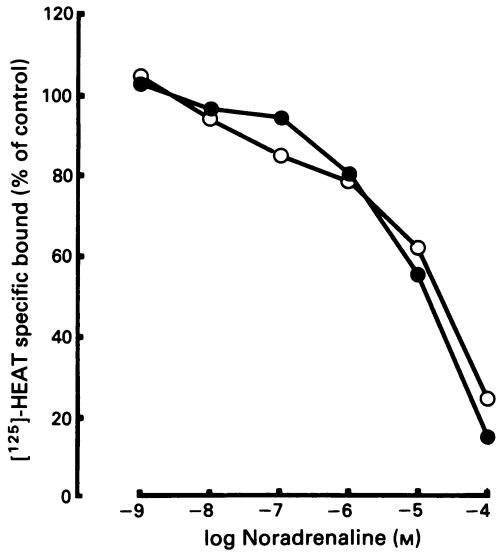

Figure 5 Competition of noradrenaline with [^{125}I]-HEAT for specific binding to mesenteric artery or tail artery homogenates of sham-operated rats. The data are shown as the average of duplicate determinations from one experiment as (○) for mesenteric artery and (●) for tail artery. This figure is representative of 3–5 similar experiments with duplicate determinations. [^{125}I]-HEAT = 270 pM.

122 pM and density of binding sites (B_{max}) of 107 fmol mg^{-1} protein (Figure 3b). Similarly, a single population of [^{125}I]-HEAT binding sites was observed in the mesenteric artery. Figure 4 (representative of three similar experiments) illustrates that the K_D and B_{max} were 96 pM and 22 fmol mg^{-1} protein, respectively, in the mesenteric artery homogenate of PVL rats. It appeared that the receptor number in the tail artery was about 4 fold greater than that in the mesenteric artery (Table 3). When sham-operated and PVL rats were compared, the K_D and B_{max} values for [^{125}I]-HEAT in either the mesenteric artery or tail artery were not significantly different. Figure 5 shows the competition of NA for [^{125}I]-HEAT binding to mesenteric and tail artery homogenates of sham-operated rats. The data were well fitted to a simple, one-site model but not multi-site models. The K_i for NA in either mesenteric artery or tail artery was not significantly different between sham-operated and PVL rats (Table 4).

Discussion

The present study is the first to demonstrate that the α_1-adrenoceptor number and the affinity of NA are not altered in the vascular smooth muscle of PVL rats. Tension experiments *in vitro* demonstrated that the maximum response, but not the ED_{50} value of NA, was decreased in portal vein, mesenteric artery, tail artery in PVL rats. The results suggest a decrease in efficacy but not the sensitivity to NA. Receptor binding experiments showed that B_{max} and K_D for [^{125}I]-HEAT and K_i for NA were not significantly changed in either the mesenteric artery or tail artery of PVL rats, suggesting the changes in vascular reactivity were not due to changes in receptor density or affinity. Therefore, the present results suggest that the vascular hyporesponsiveness to NA in PVL rats may be due to a defect at the post-receptor level.

Villamediana *et al.* (1988) reported that there was no difference in response to NA in the femoral artery of cirrhotic rats compared with control *in vitro*, whereas Kiel *et al.* (1985) reported an increase in the ED_{50} value of NA in perfused intestinal vasculature of portal hypertensive rats. The differences may relate to the nature of the experimental preparations. *In vivo* experiments will be affected more profoundly by the circulating substances. The present study showed that the attenuated maximum response to NA was most prominent in the portal vein and mesenteric artery, indicating the splanchnic circulation was more affected by portal hypertension.

In tension experiments, the present study also showed that the affinity for NA (as indicated by ED_{50} value) was lower, but the affinity for prazosin (as indicated by the pA_2 value) was higher in the mesenteric artery than in either the tail artery or portal vein. The tension studies were complicated by differences in maximal responses to the same agonist between different blood vessels. However, De Mey & Vanhoutte (1981) reported that the ED_{50} values of NA differed significantly between canine isolated blood vessels: it was the lowest in the femoral artery, followed by the saphenous and femoral vein, and was highest in the splenic artery. They also speculated that the presence of mainly α_1-adrenoceptors in arteries, and of both α_1- and α_2-adrenoceptors in veins, demonstrates the heterogeneous pharmacological behaviour of vascular smooth muscle. Since yohimbine was added to block the activation of α_2-adrenoceptors by NA in our tension experiments, it is unlikely that α_2-adrenoceptors are involved in the lower affinity for prazosin in the portal vein or tail artery. Medgett & Langer (1984) suggested that the wide range in prazosin affinity is a result of its ability to differentiate between two subtypes of α_1-adrenoceptors. They proposed a directly innervated α_1-adrenoceptor subtype with a high affinity for prazosin (the affinity constant K_B <0.4 nM) and that the remaining α_1-adrenoceptors are located farther away from the nerve terminals and have a lower sensitivity to prazosin (K_B >1.6 nM). The higher affinity for prazosin in the densely innervated mesenteric artery in the present study seems consistent with this proposal. Molecular cloning studies have identified at least three distinct subtypes (α_{1A}, α_{1B} and α_{1C}) of α_1-adrenoceptors; however, the K_i values for prazosin for these three α_1-adrenoceptor subtypes are similar (Schwinn & Lomasney,

1992). Therefore, the nature of the different potency of prazosin against the α_1-adrenoceptor response in isolated blood vessels remains to be determined.

MacGilchrist *et al.* (1990) reported that the binding characteristics of α-adrenoceptors in platelet and lymphocyte were not different between cirrhotic patients and healthy subjects. By comparing the pressor reactivity to sympathetic and non-sympathetic agonists, they further concluded that the impaired responses were not caused by sympathetic desensitization. In addition, Murray & Paller (1985) found that the decreased pressor response to angiotension II in cirrhotic rats was the result of a post-receptor defect. The present study also provides evidence to suggest that the vascular hyporesponsiveness to NA may be due to a post-receptor mechanism. Our previous paper (Chao *et al.*, 1992) demonstrated that vascular hyporesponsiveness also occurred in response to potassium chloride, a depolarizing agent that induces vasoconstriction by receptor-independent mechanisms. In studying the actions of synthetic parathyroid hormone, this paper (Chao *et al.*, 1992) showed that the utilization of calcium may be involved in the vascular hyporesponsiveness of PVL rats. At the present time, it is not known whether there are changes in the contractile apparatus in vascular smooth muscle cells of PVL rats.

Recently, evidence has accumulated that the vascular endothelium plays an important role in regulation of vascular tone (Furchgott, 1983). Vallance & Moncada (1991) proposed that the overproduction of nitric oxide may contribute to the hyperdynamic circulation in cirrhosis. By using nitric oxide synthase inhibitor Claria *et al.* (1992), Lee *et al.* (1992) and Pizcueta *et al.* (1992) have confirmed this hypothesis. Furthermore, the preliminary data from our laboratory also demonstrated an elevation in both cyclic AMP and cyclic GMP contents in blood vessels of PVL rats. It is also possible that overproduction of nitric oxide functionally antagonizes the constrictor response to vasoconstrictors in portal hypertension. However, this explanation is not suitable for the elevation of cyclic AMP, since the *in vitro* experiment is devoid of circulating vasodilators. The role of cyclic nucleotides is currently under investigation.

References

ARROYO, V., PLANAS, R., GAYA, J., DEULOFEU, R., RIMOLA, A., PEREZ-AYUSO, R.M., RIVERA, F. & RODES, J. (1983). Sympathetic nervous activity, renin-angiotensin system and renal excretion of prostaglandin E_2 in cirrhosis. Relationship to functional renal failure and sodium and water excretion. *Eur. J. Clin. Invest.*, **13**, 271–278.

ARUNLAKSHANA, O. & SCHILD, H.O. (1959). Some quantitative uses of drug antagonists. *Br. J. Pharmacol. Chemother.*, **14**, 48–59.

BENOIT, J.N., BARROWMAN, J.A., HARPER, S.L., KVIETYS, P.R. & GRANGER, D.N. (1984). Role of humoral factors in the intestinal hyperemia associated with chronic portal hypertension. *Am. J. Physiol.*, **240**, G486–G493.

BICHET, D.G., VAN PUTTEN, V.J. & SCHRIER, R.W. (1982). Potential role of increased sympathetic activity in impaired sodium and water excretion in cirrhosis. *N. Engl. J. Med.*, **307**, 1552–1557.

CHAO, T.W., YU, P.C., KUO, J.S., PANG, P.K.T. & YANG, M.C.M. (1992). Responsiveness to synthetic parathyroid hormone in the portal vein of portal hypertensive rats. *J. Hepatol.*, **16**, 326–331.

CHOJKIER, M. & GROSZMANN, R.J. (1981). Measurement of portal-systemic shunting in the rat by using γ-labelled microspheres. *Am. J. Physiol.*, **140**, G371–G375.

CLARIA, J., JIMENEZ, W., ROS, J. & ASBERT, M. (1992). Pathogenesis of arterial hypotension in cirrhotic rats with ascites: role of endogenous nitric oxide. *Hepatology*, **15**, 343–349.

DE MEY, J. & VANHOUTTE, P.M. (1981). Uneven distribution of postjunctional alpha$_1$- and alpha$_2$-like adrenoceptors in canine arterial and venous smooth muscle. *Circ. Res.*, **48**, 875–884.

FINBERG, J.P.M., SYROP, H.A. & BETTER, O.S. (1981). Blunted pressor response to angiotension and sympathomimetic amines in the bile duct ligated dog. *Clin. Sci.*, **61**, 535–539.

FURCHGOTT, R.F. (1983). Role of endothelium in responses of vascular smooth muscle. *Circ. Res.*, **53**, 557–573.

HAN, C., ABEL, P.W. & MINNEMAN, K.P. (1987). Heterogeneity of α-adrenergic receptors revealed by chlorethylclonidine. *Mol. Pharmacol.*, **32**, 505–510.

HAN, C., LI, J. & MINNEMAN, K.P. (1990). Subtype of α-adrenoceptors in rat blood vessels. *Eur. J. Pharmacol.*, **190**, 97–104.

KAUMANN, A.J. & GROSZMANN, R.J. (1989). Catecholamines relax portal and mesenteric veins from normal and portal hypertensive rats. *Am. J. Physiol.*, **257**, G977–G981.

KIEL, J.W., PITTS, V., BENOIT, J.N., GRANGER, D.N. & SHEPHERD, A.P. (1985). Reduced vascular sensitivity to norepinephrine in portal-hypertensive rats. *Am. J. Physiol,*. **248**, G192–G195.

LEE, F.Y., ALBILLOS, A., COLOMBATO, L.A. & GROSZMANN, R.J. (1992). The role of nitric oxide in the vascular hyporesponsiveness to methoxamine in portal hypertensive rats. *Hepatology*, **16**, 1043–1048.

LEE, F.Y., COLOMBATO, L.A., ALBILLOS, A. & GROSZMANN, R.J. (1993). N^{ω}-Nitro-L-arginine administration corrects peripheral vasodilation and systemic capillary hypotension and ameliorates plasma volume expansion and sodium retention in portal hypertensive rats. *Hepatology*, **7**, 84–90.

MACGILCHRIST, A.J., DEIGHTON, N.M., HAMILTON, C.A. & REID, J.L. (1990). Binding studies of platelet and lymphocyte α-adrenoceptors in patients with cirrhosis. *Br. J. Clin. Pharmacol.*, **30**, 644–647.

MACGILCHRIST, A.J., SUMNER, D. & REID, J.L. (1991). Impaired pressor reactivity in cirrhosis: evidence for a peripheral vascular defect. *Hepatology*, **13**, 689–694.

MEDGETT, I.C. & LANGER, S.Z. (1984). Heterogeneity of smooth muscle α-adrenoceptors in rat tail artery *in vitro*. *J. Pharmacol. Exp. Ther.*, **229**, 823–830.

MUNSON, P.J. & RODBARD, D. (1980). Ligand: a versatile computerized approach for characterization of ligand-binding systems. *Anal. Biochem.*, **107**, 220–239.

MURPHY, R.A. (1980). Mechanics of vascular smooth muscle. In *Handbook of Physiology*, Section 2. ed. Bohr, D.F., Somlyo, A.P. & Sparks, H.V. The cardiovascular system, Vol II. pp. 325–351. Bethesda: American Physiology Society.

MURRAY, B.M. & PALLER, M.S. (1985). Decreased pressor reactivity to angiotensin II in cirrhotic rats. Evidence for a post-receptor defect in angiotension action. *Circ. Res.*, **57**, 424–431.

MURRAY, B.M. & PALLER, M.S. (1986). Pressor resistance to vasopression in sodium depletion, potassium depletion, and cirrhosis. *Am. J. Physiol.*, **251**, R525–R530.

PIZCUETA, M.P., CASAMITJANA, R., BOSCH, J. & RODES, J. (1990). Decrease systemic vascular sensitivity to norepinephrine in portal hypertensive rats: role of hyperglucagonism. *Am. J. Physiol.*, **258**, G191–G195.

PIZCUETA, M.P., PIQUE, J.M., BOSCH, J., WHITTLE, B.J.R. & MONCADA, S. (1992). Effect of inhibiting nitric oxide biosynthesis on the systemic and splanchnic circulation of rats with portal hypertension. *Br. J. Pharmacol.*, **105**, 184–190.

SCATCHARD, G. (1949). The attractions of proteins for small molecules and ions. *Ann. N.Y. Acad. Sci.*, **51**, 660–672.

SCHWINN, D.A. & LOMASNEY, J.W. (1992). Pharmacologic characterization of cloned α_1-adrenoceptor subtypes: selective antagonists suggest the existence of a fourth subtype. *Eur. J. Pharmacol.*, **227**, 433–436.

TAGE-JENSEN, U., HENRIKSEN, J.H., CHRISTENSEN, E., WIDDING, A., RING-LARSEN, H. & CHRISTENSEN, N.J. (1988). Plasma catecholamine level and portal venous pressure as guides to prognosis in patients with cirrhosis. *J. Hepatol.*, **6**, 350–358.

VALLANCE, P. & MONCADA, S. (1991). Hyperdynamic circulation in cirrhosis: a role for nitric oxide? *Lancet*, **337**, 776–778.

VILLAMEDIANA, L.M., DIEGUEZ, G., SANTOS, J.C., GARCIA-VILLALON, A.L., CARAMELO, C. & LOPEZ-NOVOA, J.M. (1988). Vascular reactivity to norepinephrine in rats with cirrhosis of the liver. *Can. J. Physiol. Pharmacol.*, **66**, 567–572.

VOROBIOFF, J., BREDFELDT, J.E. & GROSZMANN, R.J. (1983). Hyperdynamic circulation in portal-hypertensive rat model: a primary factor for maintenance of chronic portal hypertension. *Am. J. Physiol.*, **244**, G52–G57.

YANG, M.C.M., KUO, J.S. & PANG, P.K.T. (1990). Mechanisms of the vascular action of parathyroid hormone. *J. Pharmacol. Exp. Ther.*, **252,** 840–844.

YANG, M.C.M., TU, M.S., CHEN, C.F., HONG, C.Y. & KUO, J.S. (1991). cAMP and vascular action of endothelin. *Pharmacology*, **42,** 252–256.

YU, P.-C., KUO, J.-S., LIN, H.-C. & YANG, M.C.M. (1992). Effects of endothelin in portal hypertension rats. *Clin. Sci.*, **83,** 165–170.

(Received July 5, 1993
Revised September 14, 1993
Accepted October 7, 1993)

Br. J. Pharmacol. (1994), **111**, 445–454

Characterization of the histamine receptors in the guinea-pig lung: evidence for relaxant histamine H_3 receptors in the trachea

[1]Lars Olaf Cardell & *Lars Edvinsson

Department of Otorhinolaryngology, Malmö General Hospital, Malmö, and *Department of Internal Medicine, University of Lund, Lund, Sweden

1 The histamine receptors were characterized on isolated circular segments of trachea and pulmonary arteries from the guinea-pig. The motor responses to histamine H_1-, H_2- and H_3-receptor agonists and antagonists were tested and the responses obtained were analysed in relation to the respiratory epithelium and the vascular endothelium.

2 Histamine induced a biphasic response in trachea and in pulmonary arteries. In low concentrations, histamine acted as a potent relaxant agent of precontracted segments and in moderate concentrations it constricted both precontracted and resting segments. When arterial segments from different parts of the pulmonary vascular tree were compared, only small interregional differences in the vasomotor response were seen.

3 Mepyramine caused a parallel shift to the right of the histamine-induced concentration-response curves for both the trachea and the pulmonary artery, indicating a contractile H_1-receptor. Cimetidine did not affect the histamine-induced contraction of the trachea, but a shift to the left was evident for low concentrations of histamine in the pulmonary artery. This is consistent with a dilator H_2-receptor in the pulmonary artery. The pA_2-value for mepyramine in the pulmonary artery, 8.75, was not affected by the presence of cimetidine. Thioperamide, a selective H_3 antagonist, shifted the concentration-response for the trachea to the left. Schild analysis for histamine and mepyramine yielded a line with a slope of 0.61, whereas the same analysis in the presence of thioperamide yielded a line with a slope of 1.05 and an approximated pA_2-value of 9.57. These results indicate the presence of a relaxant H_3 receptor in the trachea. In precontracted tracheal segments, application of mepyramine and cimetidine did not affect the low dose histamine relaxation. Thioperamide caused a parallel shift of the histamine concentration-response curve to the right, supporting the suggestion of a dilator H_3-receptor in the trachea. The pA_2-value for thioperamide, in the presence of mepyramine, was 7.79. In precontracted pulmonary arteries the histamine-induced dilatation was small. In the presence of mepyramine a rather strong histamine-induced dilatation became evident and this concentration-response curve could be shifted to the right by cimetidine, with a pA_2-value of 6.49. This is compatible with a dilator H_2-receptor.

4 The H_1-receptor agonists, thiazolylethylamine, 2-methylhistamine and pyridylethylamine and the rather unselective H_2-agonist, 4-methylhistamine, induced contraction of resting tracheal and pulmonary arterial segments. In precontracted segments of trachea, all H_1 and H_2 agonists studied induced a dilator response. The two rather unselective histamine receptor agonists 2-methylhistamine and 4-methylhistamine were about 100 times more potent than other H_1 and H_2 agonists tested. In the pulmonary artery, the H_2 agonists, impromidine, dimaprit and 4-methylhistamine induced a concentration-dependent relaxation. The relaxation of the pulmonary artery, elicited by the H_1 agonists, thiazolylethylamine and pyridylethylamine, was smaller, but more potent than the response induced by the H_2 agonists. This may reflect the presence of a separate dilator H_1-receptor.

5 **R**-α-methylhistamine induced a three phased response in precontracted tracheal segments. In low concentrations, a concentration-dependent dilator response appeared. At moderate concentrations, a stage with a plateau or a small contraction was seen, followed at high concentrations by a new concentration-dependent relaxation. The first dilator phase was similar to that obtained for histamine in the same preparation.

6 Removal of the epithelium or endothelium enhanced the contractile histamine response in both the trachea and the pulmonary artery as well as the dilator response in the trachea. These results support the hypothesis that the endothelial layer may serve as a barrier against the penetration of certain mediators. In the precontracted pulmonary artery, the small initial dilatation was abolished whereas the second dilatation seen in the presence of mepyramine was slightly reduced. This may reflect the influence of two separate histamine receptors, one of which is associated with the release of an endothelium-dependent dilator factor or factors.

7 In the guinea-pig trachea, histamine-induced contraction is mediated through H_1-receptors whereas dilatation probably involves an H_3-receptor on the smooth muscle. The guinea-pig pulmonary artery appears to be endowed with a contractile H_1 receptor on the smooth muscle cells and a dilator H_1 receptor located on the endothelium. A dilator H_2 receptor on the smooth muscle cells seems, at least *in vitro*, to be the most potent mediator of histamine-mediated pulmonary arterial dilatation.

Keywords: Histamine; histamine receptors; **R**-α-methylhistamine; H_3-receptors; pulmonary blood vessels; trachea

[1] Author for correspondence.

Introduction

Histamine has long been recognized as an important chemical messenger (Hill, 1990; Schwartz *et al.*, 1990). It is distributed within mast cells in almost all mammalian tissues and has an established role as a mediator of inflammation and allergy (Bevan, 1982). Histamine can probably also function as a neurotransmitter or neuromodulator (Hill, 1990; Schwartz *et al.*, 1990; Ishikawa & Sperelakis, 1987). In the lung, histamine is one among several autacoids that possesses potent physiological properties. Immunological reactions can stimulate histamine release within the lung from mast cells and basophils (Riley & West, 1953; Lichtenstein, 1975), inducing bronchoconstriction, contraction of vascular smooth muscle and increased vascular permeability (Adams & Lichtenstein, 1979; Valentovic *et al.*, 1992).

Three classes of histamine receptors, H_1, H_2 and H_3, have been identified in vertebrates (Ash & Schild, 1966; Black *et al.*, 1972; Arrang *et al.*, 1983). H_1 receptors are coupled to inositol phosphate hydrolysis and mediate a variety of responses, including smooth muscle contraction, increased vascular permeability and hormone release (Hill, 1990). H_2-receptors are coupled to adenylate cyclase via a G_s-protein and the functional H_2-responses include smooth muscle relaxation and inhibition of the immune system (Foreman *et al.*, 1985). H_3-receptors were originally recognized in rat brain where they appeared to be involved in the feedback control of both histamine synthesis and release (Arrang *et al.*, 1987). Binding studies suggested that H_3-receptors also existed in guinea-pig lung (Arrang *et al.*, 1987).

Histamine causes bronchoconstriction through stimulation of H_1-receptors. Although H_2- and H_3-receptors have been demonstrated in lung parenchyma and airways, their role is unclear (Barnes & Ichinose, 1989). In isolated blood vessels, vasoconstriction is usually mediated through H_1-receptors located on the vascular smooth muscle, whereas vasodilatation can involve the action of H_1 and/or H_2-receptors (Edvinsson & Owman, 1975; Ottosson *et al.*, 1989; Krstic *et al.*, 1991). In certain smooth muscle preparations, one and the same concentration of exogenously applied histamine, may activate both constrictor and dilator mechanisms through different histamine receptors at separate locations. A histamine H_1-induced contraction could therefore theoretically mask a dilator H_1-, H_2- or H_3-receptor-mediated response (Mikkelson *et al.*, 1984). These technical obstacles together with the lack of highly selective H_1 agonists (Hill, 1990) have probably contributed to the difficulties in obtaining a clearcut picture of the histamine receptor-mediated dilator responses.

H_3-receptors seem to modulate cholinergic neurotransmission in guinea-pig trachea acting at both parasympathetic ganglia and at postganglionic nerve fibres (Ichinose *et al.*, 1989). Furthermore, these receptors also inhibit non-adrenergic, non-cholinergic bronchoconstriction (Ichinose & Barnes, 1989) and plasma extravasation (Ichinose *et al.*, 1990). In cerebral arteries, exogenous histamine has also been reported to activate H_3-receptors causing relaxation (Ea Kim & Oudart, 1988; Ea Kim *et al.*, 1992).

The present study was designed to characterize the H_1-, H_2- and H_3-receptors in guinea-pig trachea and pulmonary arteries and to study the involvement of the respiratory epithelium and vascular endothelium, respectively, in the motor responses elicited.

Methods

Young male guinea-pigs (200–300 g) were killed by a blow on the neck. The lungs, including the heart and trachea, were quickly removed and immersed in a cold (+4°C) buffer solution (for composition, see below). An arterial branch system was isolated from either side of the lung. Circular segments were dissected at four different levels; main pulmonary artery (MPA, located next to the heart), large lobar arteries (second to third branches), small lobar arteries (SLA, fourth to fifth branches) and intrasegmental arteries (ISA, ninth to tenth branches). In addition, the distal portion of the trachea was dissected free of surrounding tissue. The vessels and the trachea were used in the experiments either immediately or, occasionally, following overnight storage in a cold buffer solution. Circular segments were mounted on two L-shaped metal prongs. One prong was connected to a force displacement transducer attached to a computer for continuous registration of isometric tension and the other to a displacement device. The mounted segments were immersed in small (2.5 ml) temperature-controlled (37°C) tissue baths containing the buffer solution. The solution was equilibrated with 5% CO_2 in O_2, giving a pH of 7.4.

Initially, a tension of 0.2–3 mN (depending on the dissecting level/diameter) was applied to the arterial segments and 2–3mN was applied to the tracheal segments (Cardell *et al.*, 1990). The segments were subsequently allowed to stabilize at this level of tension for 90 min. The contractile ability of each segment was then examined by exposure to a potassium rich (60 mM) buffer solution (for composition, see below). Only when two reproducible contractions had been elicited was the individual segment used in further studies. The integrity of the vascular endothelium was assessed at the end of the experiments by obtaining a dilator response to acetylcholine (10^{-6} M) (Furchgott, 1984). The presence of tracheal epithelium was confirmed by staining with a 5% silver nitrate solution followed by light microscopy (Abrol *et al.*, 1984). There were no differences in the response to the histamine agonists when concentration-response curves obtained by cumulative application were compared to those obtained by a single dose procedure (Cardell *et al.*, 1990).

In a separate study, the vascular endothelium was removed by rubbing the intimal surface with a small wooden stick inserted via one cut end of the pulmonary artery. The tracheal epithelium was removed according to the same procedure (Goldie *et al.*, 1986). Verification of the absence of endothelium or epithelium was always checked by the use of silver nitrate and acetylcholine (see above). The responses to potassium and to the maximally effective concentration of histamine were completely reversible. Studies of responses in the absence and presence of antagonists could consequently be carried out by successive cycles of agonist exposures in each segment. The rubbing experiments were carried out in matched pairs of segments, with one segment in each series having an intact endothelium or epithelium. The log concentration-response relationship was approximated by linear regression analysis of the data within the 20% to 80% interval (Cardell *et al.*, 1993). The pD_2 value (i.e. the negative logarithm of the concentration eliciting half the maximum response, EC_{50}/IC_{50}) and $E_{max}\%/I_{max}\%$ (the maximal contraction/dilatation elicited by an agonist expressed as a percentage of the contraction induced by 60 mM K^+/agonist precontraction) was calculated for each experiment. The concentration ratios (CR) were defined as the ratio of the EC_{50} value in the presence and absence of a given concentration of agonist (B). The pA_2 was calculated as described by Arunlakshana & Schild (1959) and modified by Tallarida *et al.* (1979); log (CR-1)/B.

Solutions and drugs

The following solutions were used: (a) standard buffer solution (mM): NaCl 119, KCl 4.6, $CaCl_2$ 1.5, $MgCl_2$ 1.2, $NaHCO_3$ 15, NaH_2PO_4 1.2 and glucose 11; (b) 60 mM K^+ buffer solution: as above, but substituting equimolar amounts of NaCl with KCl. Analytical-grade chemicals and twice-distilled water were used for preparing all solutions.

The following drugs were used: **R**-α-methylhistamine (kindly donated by Dr J.C. Schwarz, Unité de Neurobiologie

et Pharmacologie de l'INSERM, Centre Paul Broca, Paris, France), 2-pyridylethylamine, 2-methylhistamine, 2-thiazolylethylamine, dimaprit, 4-methylhistamine, impromidine (kind gifts from the Smith, Kline & French Laboratories, Welwyn Garden City, U.K.), acetylcholine chloride (Sigma, U.S.A.), atropine sulphate (Sigma, U.S.A.), cimetidine hydrochloride (S.K.F., U.K.), 5-hydroxytryptamine creatinine sulphate (Serva, Germany), ketanserin hydrochloride (Janssen, Belgium), mepyramine (ACO, Sweden), noradrenaline hydrochloride (Sigma, U.S.A.), prazosin hydrochloride (Pfizer, U.S.A.), propranolol (ICI, U.K.), prostaglandin $F_{2\alpha}$ (Astra, Sweden), spantide (Ferring AB, Sweden), thioperamide (Sigma, U.S.A.), vasoactive intestinal peptide (Peninsula, U.S.A.), yohimbine (Serva, Germany). All agents were dissolved in, and further diluted in, saline containing 1% bovine serum albumin (Behringwerke, Marburg, Germany) and used in the experiments within 30 min to avoid any possible degradation. The concentrations of the agents are expressed as the final molar concentration in the tissue bath.

Statistics

Statistical differences between means were tested by analysis of variance (ANOVA) followed by Scheffe's method (Wallenstein *et al.*, 1980). Statistical significance was assumed when $P<0.05$.

Results

Histamine responses and regional differences

Histamine elicited a strong concentration-dependent contraction of tracheal segments (E_{max}%, 116 ± 31%; pD_2, 5.03 ± 0.44; $n = 24$) and of pulmonary arteries (E_{max}%, 116 ± 31%; pD_2, 5.31 ± 0.28; $n = 22$) (Figure 1a,b). The relaxant effects of histamine were studied after precontraction with either prostaglandin $F_{2\alpha}$, 5-hydroxytryptamine or acetylcholine (trachea). Low concentrations of histamine induced a concentration-dependent dilatation of the precontracted trachea (I_{max}%, 27 ± 17; pD_2, 7.20 ± 0.61; $n = 25$) followed by a contraction at higher concentrations (Figure 2). In the precontracted pulmonary artery only a small histamine-induced dilatation was seen (I_{max}%, 9 ± 3; $n = 6$). The presence of mepyramine (10^{-6} M), unmasked a strong concentration-dependent histamine-induced arterial dilatation (I_{max}%, 69 ± 13; pD_2; 6.02 ± 0.16; $n = 5$) (Figure 3) and increased the tracheal dilatation (I_{max}%, 56 ± 11; pD_2, 7.23 ± 0.25; $n = 6$). No differences in the histamine-induced dilator responses were seen between the different precontracting agents.

In order to investigate regional variations in the histamine responses of the pulmonary vascular tree, arteries from four different levels (MPA, LLA, SLA, ISA) were compared. Only

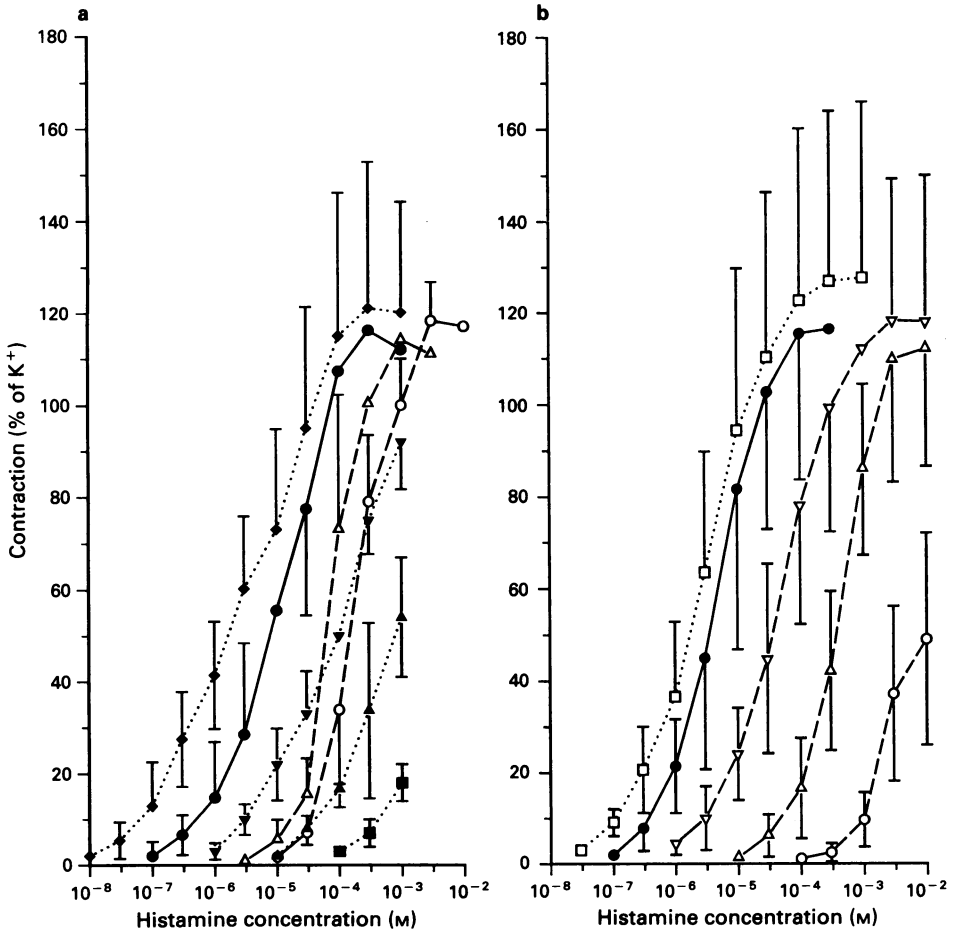

Figure 1 Concentration-response of histamine in guinea-pig trachea (a) and pulmonary artery (LLA) (b). Contractile effects of histamine are indicated by (●). Mepyramine 1×10^{-8} M, (pD_2; LLA, 4.26 ± 0.29; ▽), 1×10^{-7} M (pD_2; trachea, 4.02 ± 0.23; LLA, 3.42 ± 0.22; △) and 1×10^{-6} M (pD_2; trachea, 3.78 ± 0.09; ○) induced a parallel shift to the right of the histamine-induced concentration-response curves for both the trachea and the pulmonary artery. Cimetidine 1×10^{-5} M (□) caused a slight shift to the left of the histamine curve in the LLA (pD_2, 5.46 ± 0.37; $n = 11$). Thioperamide 1×10^{-6} M (◆) shifted the histamine curve for the trachea to the left and the rightward shift induced by mepyramine was more pronounced in the presence of thioperamide (mepyramine; 1×10^{-8} M (▼), 1×10^{-7} M (▲) and 1×10^{-6} M(■). Responses are expressed as a percentage of potassium (60 mM)-induced contraction (K^+) and each point is the mean with s.d. Trachea, control; $K^+ = 3.37 \pm 2.89$ mN; $n = 24$: antagonist experiments $n = 5-6$. Pulmonary artery, control; $K^+ = 3.61 \pm 2.22$ mN; $n = 22$: antagonist experiments $n = 8-12$.

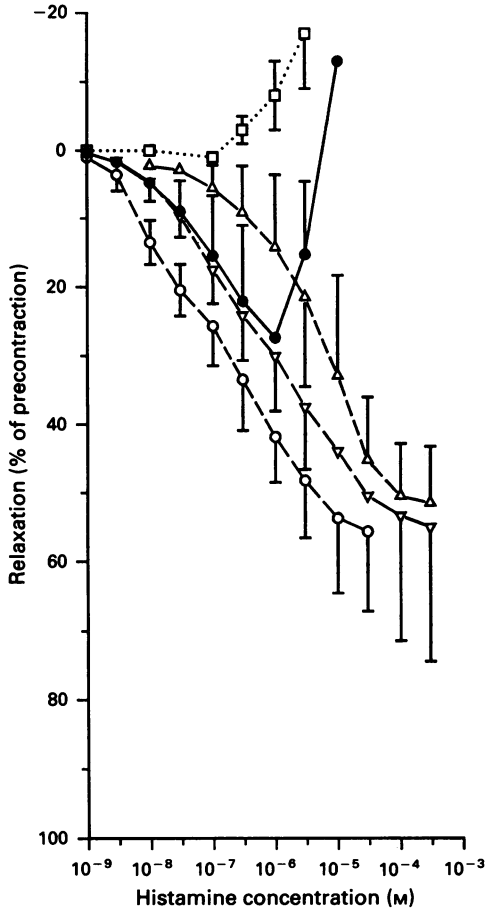

Figure 2 Biphasic response of histamine in tracheal segments precontracted with acetylcholine 1×10^{-6} M (●). In the presence of mepyramine 1×10^{-6} M the contraction seen at high histamine concentrations (3×10^{-6} M and 1×10^{-5} M) was abolished whereas the relaxation remained (○). The dilator concentration-response curve of histamine in the presence of mepyramine (1×10^{-6} M) was shifted to the right in parallel by the H_3 antagonist thioperamide 1×10^{-7} M (pD_2, 6.54 ± 0.50; ▽) and 1×10^{-6} M (pD_2, 5.50 ± 0.50; △). Thioperamide 1×10^{-5} M abolished the histamine-induced dilator response (□). Responses are expressed as a percentage of acetylcholine-induced contraction and each point is the mean with s.d. Control $n = 25$, antagonist experiments $n = 5-9$.

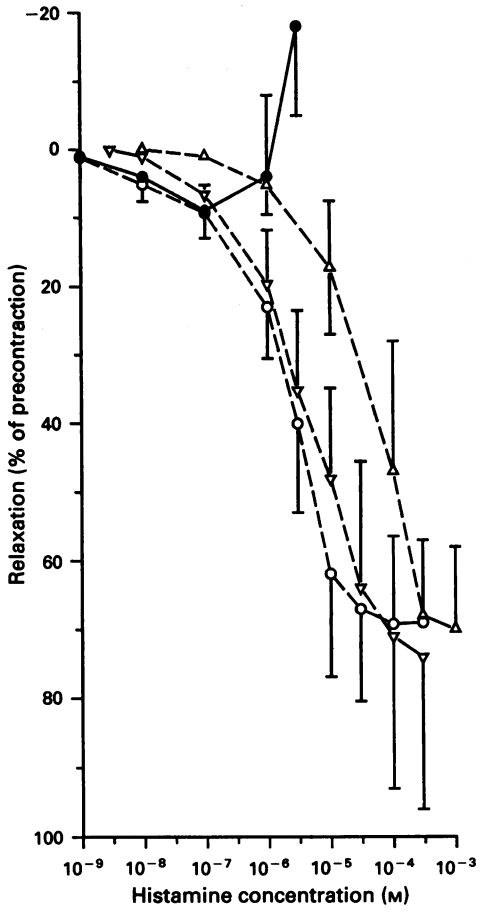

Figure 3 Response of histamine in pulmonary arterial segments precontracted with prostaglandin $F_{2\alpha}$ 3×10^{-6} M (●). In the presence of mepyramine 1×10^{-6} M a strong histamine-induced relaxation became evident (pD_2, 6.02 ± 0.16; ○). Cimetidine 1×10^{-7} M (pD_2, 5.93 ± 0.19; ▽) and 1×10^{-5} M (pD_2, 4.58 ± 0.29; △) in the presence of mepyramine (1×10^{-6} M) shifted the concentration-response curve in parallel to the right. Responses are expressed as a percentage of prostaglandin $F_{2\alpha}$- induced contraction and each point is the mean with s.d. Control, $n = 6$, antagonist experiments $n = 6-9$.

relatively small differences in sensitivity (pD_2) and maximally contractile response (E_{max}%) were seen. The large arteries, MPA and LLA, exhibited slightly higher histamine sensitivity (pD_2, 5.19 ± 0.39; $n = 16$ and 5.31 ± 0.28; $n = 22$, respectively) than the small arteries SLA and ISA (pD_2, 4.88 ± 0.37; $n = 8$ and 4.80 ± 0.17; $n = 4$, respectively). In the smallest arteries, ISA (ninth to tenth branches), the relative maximal contraction was also smaller (E_{max}%; 103 ± 11) than in the larger arteries (E_{max}%: MPA, 127 ± 33%; LLA, 116 ± 31%; SLA, 121 ± 37%) (Figure 4). Dilator experiments revealed no significant differences between these arterial regions (not illustrated).

Antagonist experiments

Mepyramine caused a parallel shift to the right of the histamine-induced concentration-response curves for both the trachea and the pulmonary arteries (Figure 1a,b). The dextral displacement of the concentration-response curves was used in a Schild analysis. The concentration-ratios for mepyramine yielded a line with the slope of 0.61 ($r = 0.98$, $y = 5.03-0.61x$) without and 1.05 ($r = 0.99$; $y = 10.05 - 1.05x$) with the presence of thioperamide. In the presence of thioperamide mepyramine caused a concentration-dependent shift of the histamine responses, showing a pA_2-value for mepyramine in the trachea of 9.57. In the pulmonary artery mepyramine yielded a line with a slope of 1.12 ($r = 0.99$, $y = 9.76 - 1.12x$), suggesting a simple competitive antagonism at one receptor site. The resulting pA_2 values were 8.25 in trachea and 8.75 in the pulmonary artery, respectively. Cimetidine did not affect the histamine-induced concentration-response curve for the trachea (e.g. cimetidine 10^{-7} M; E_{max}%, 110 ± 23; pD_2 4.93 ± 0.29; $n = 5$: cimetidine 10^{-5} M; E_{max}%, 103 ± 29; pD_2 5.41 ± 0.39; $n = 4$). A small shift to the left was seen in the pulmonary artery, but this leftward shift was only significant for low concentrations of histamine (10^{-7} M, 3×10^{-7} M and 10^{-6} M) (Figure 1b). Thioperamide did not affect the histamine-induced concentration-response curve for the pulmonary artery, but a leftward shift was seen in the trachea (E_{max}%, 121 ± 31.7; pD_2 5.55 ± 0.27; $n = 7$). In the precontracted trachea, application of mepyramine (10^{-7} M or 10^{-6} M) abolished the contraction seen at high histamine concentrations (Figure 2) and consequently the maximal dilator response (I_{max}%) increased, without significantly changing the pD_2-values (mepyramine 10^{-6} M; I_{max}%, 56 ± 11; pD_2, 7.23 ± 0.25; $n = 6$). Addition of cimetidine (10^{-5} M) did not further change the dilator response (I_{max}%, 54 ± 18; pD_2, 7.17 ± 0.03; $n = 5$) nor did mepyramine in higher concentrations (10^{-5} M). The H_3-antagonist, thioperamide, in the presence of mepyramine (10^{-6} M), caused a parallel shift to the right of the histamine-induced dilatation

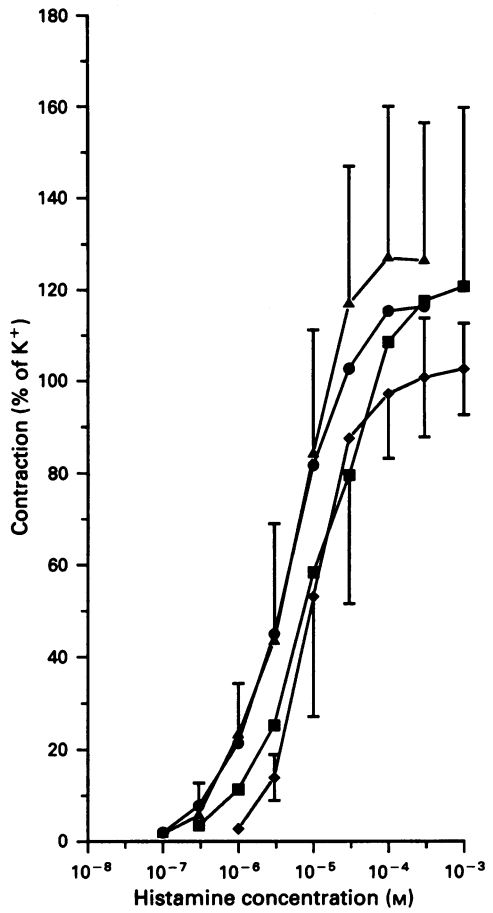

Figure 4 Regional variations in the histamine-induced contractile response of the pulmonary vascular tree. Circular segments from four different levels were tested. Main pulmonary artery (MPA, located next to the heart, ▲), large lobar arteries (LLA, second to third branches, ●), small lobar arteries (SLA, fourth to fifth branches, ■) and intrasegmental arteries (ISA, ninth to tenth branches, ◆). Responses are expressed as a percentage of potassium (60 mM)-induced contraction (K^+) and each point is the mean with s.d. (MPA, $K^+ = 3.11 \pm 2.05$ mN, $n = 16$; LLA, $K^+ = 3.61 \pm 2.22$ mN, $n = 22$; SLA, $K^+ = 2.37 \pm 1.25$ mN, $n = 8$ and ISA, $K^+ = 1.03 \pm 0.49$ mN, $n = 4$).

(Figure 2). Schild analysis yielded a line with the slope of 0.77 ($y = 5.98\text{-}0.77x$) with a corresponding pA_2-value of 7.79. When thioperamide was added in the absence of mepyramine, the histamine-induced dilatation became gradually inhibited and at a thioperamide concentration of 10^{-5} M the dilator response was totally abolished. The contractile response to thioperamide at higher concentration remained unaffected (Figure 2).

In the precontracted pulmonary artery, low concentrations of histamine induced only small dilator responses, roughly 10% of the precontraction level, followed by a strong contraction at high concentrations. In the presence of mepyramine, the contraction was abolished and a concentration-dependent dilatation was unmasked (Figure 3). A change of the mepyramine concentration from 10^{-7} M to 10^{-6} M did not affect the I_{max}% and pD_2-values for the dilatation. However, if the experiments were performed with both cimetidine and mepyramine in the bath, cimetidine in rising concentrations caused a parallel shift of the concentration-response curve to the right, without any further change in I_{max}% (Figure 3). A Schild plot yielded a line with the slope of 1.10 ($y = 7.14\text{-}1.10x$) and a pA_2-value of 6.49. Thioperamide did not affect the histamine-induced arterial dilator response.

In tracheal and pulmonary arterial segments precontracted by histamine (10^{-5} M), mepyramine induced a total relaxation with a pD_2 value of 6.42 ± 0.18 for the trachea ($n = 6$) and 7.61 ± 0.25 for the arteries ($n = 6$). No significant differences were seen in this mepyramine-induced dilatation when cimetidine (10^{-5} M) was present in the bath (pD_2, 6.30 ± 0.20 in trachea and 7.75 ± 0.30 in arteries, $n = 4$). Furthermore, addition of cimetidine to histamine precontracted arteries did not induce any dilator response ($n = 6$).

H_1 and H_2 agonist experiments

H_1-receptor agonists (thiazolylethylamine, 2-methylhistamine, and pyridylethylamine) induced contractions of tracheal and pulmonary arterial segments at rest. The order of potency was the same for both types of tissues; 2-methylhistamine > pyridylethylamine > thiazolylethylamine. H_2-agonists (impromidine and dimaprit) induced no or very small contractions, whereas 4-methylhistamine induced a moderate contraction.

In precontracted segments of trachea the histamine agonists induced a dilator response, followed by a constriction for H_1-agonists at higher concentrations. The contractile response was abolished with mepyramine 10^{-6} M. Scrutinizing the dilator response, the two rather unselective H_1 and H_2 receptor antagonists, 2-methylhistamine and 4-methylhistamine, induced a potent concentration-dependent relaxation. These relaxations were not affected by the presence of mepyramine (10^{-6} M) and cimetidine (10^{-6} M). Other H_1 and H_2 agonists were less potent. In the pulmonary artery, H_2-receptor agonists (impromidine, dimaprit and 4-methylhistamine) induced a more uniform concentration-dependent relaxation with the following potency order; impromidine > 4-methylhistamine > dimaprit. These relaxations were abolished with cimetidine (10^{-5} M). H_1 agonists (thiazolylethylamine and pyridylethylamine) induced a small relaxation (about 5–10% of the arterial precontraction level) starting at 10^{-7} M. At 10^{-6} M, the small dilator responses reversed to strong contraction. Even though the dilator responses of the two tested H_1-receptor agonists were much smaller than the responses induced by the three H_2-receptor agonists, they induced their dilator responses in low concentrations. The potency and effectiveness of the histamine agonists, on resting and precontracted trachea and pulmonary artery segments are summarized in Table 1.

H_3 agonist experiments

R-α-methylhistamine, an H_3 receptor agonist, induced a three-phased motor response of precontracted tracheal segments. At low concentrations, a concentration-dependent dilator response was seen and at moderate concentrations an intermediate stage with a plateau or a small contraction appeared. This was followed at high concentrations by a new concentration-dependent relaxation (Figure 5). The first dilator effect of **R**-α-methylhistamine in the trachea was similar to that obtained for histamine. The maximal dilator response as well as the corresponding pD_2-values were calculated separately for the two relaxing phases (First dilation: acetylcholine precontraction; E_{max}%, 25 ± 11; pD_2 7.58 ± 0.47; $n = 10$. 5-Hydroxytryptamine precontraction; E_{max}%, 26 ± 12; pD_2 7.47 ± 0.15; $n = 6$. Second dilatation: 5-hydroxytryptamine precontraction; E_{max}%, 111 ± 43; pD_2 4.44 ± 0.31; $n = 6$). The onset of **R**-α-methylhistamine-induced dilator responses in the trachea occurred less than 20 s after its addition to the bath. No difference was found between the relaxation induced by **R**-α-methylhistamine on tracheal segments precontracted by ACh, prostaglandin $F_{2\alpha}$ ($PGF_{2\alpha}$) or 5-HT. However, in tracheal segments precontracted by histamine, only one dilator phase was seen (E_{max}%, 124 ± 25; pD_2 4.38 ± 0.23; $n = 16$), corresponding to the second dilatation seen in the ACh, $PGF_{2\alpha}$ or 5-HT precontracted segments (Figure 5). The presence of mepyramine (10^{-8} M, 10^{-5} M) and cimetidine (10^{-8} M, 10^{-5} M) in the bath did not affect the dilator effects of **R**-α-methylhistamine (nor did it affect the first and second dilatation of ACh, $PGF_{2\alpha}$ or

Table 1 Motor responses of histamine H_1- and H_2-receptor agonists in guinea-pig trachea and pulmonary large lobar artery

		Trachea			*Pulmonary artery*	
Contraction	*n*	E_{max}%	pD_2	*n*	E_{max}%	pD_2
Thiazolylethylamine	4	49 ± 18	4.29 ± 0.29	12	127 ± 29	5.11 ± 0.75
Pyridylethylamine	8	83 ± 27	4.73 ± 0.23	9	130 ± 55	4.82 ± 0.41
2-Methylhistamine	6	98 ± 18	5.14 ± 0.18	10	131 ± 62	5.47 ± 0.43
4-Methylhistamine	4	32 ± 8	4.39 ± 0.38	6	62 ± 13	3.97 ± 0.13
Impromidine	4	0	–	4	14 ± 8	3.90 ± 0.33
Dimaprit	4	0	–	4	0	–
Dilatation	*n*	I_{max}%	pD_2	*n*	I_{max}%	pD_2
Thiozolylethylamine	7	76 ± 20	5.26 ± 0.63	5	15 ± 8	7.77 ± 0.32
Pyridylethylamine	3	63 ± 9	6.11 ± 0.15	6	12 ± 7	7.50 ± 0.47
2-Methylhistamine	5	58 ± 21	7.61 ± 0.26	NP		
4-Methylhistamine	5	46 ± 14	7.12 ± 0.25	5	35 ± 19	6.48 ± 0.56
Impromidine	4	48 ± 13	5.46 ± 0.21	7	48 ± 16	7.54 ± 0.34
Dimaprit	6	41 ± 25	5.50 ± 0.52	5	60 ± 4	5.73 ± 0.33

Maximal contractile response (E_{max}%), expressed as a percentage of the contraction induced by 60 mM potassium; maximal dilator response (I_{max}%), expressed as a percentage of precontraction and sensitivity (pD_2) expressed as the negative logarithm of the concentration eliciting half the maximal response.
NP, not performed. The values represent the mean ± s.d.

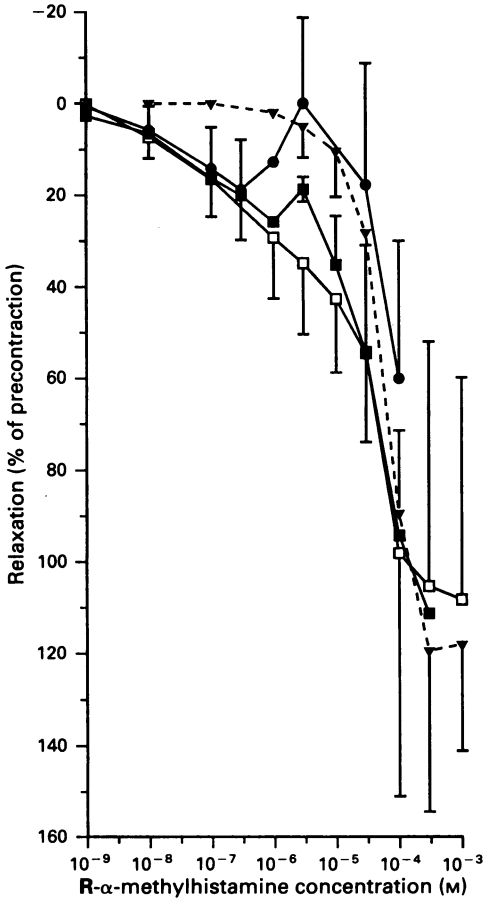

Figure 5 The three phased motor response induced by the H_3-receptor agonist **R**-α-methylhistamine on guinea-pig tracheal segments precontracted with acetylcholine 1×10^{-6} M (●), prostaglandin $F_{2\alpha}$ 1×10^{-6} M (■) and simple one phased dilator response induced by the same H_3 agonist in tracheal segments precontracted by histamine 3×10^{-5} M (▼). The symbols (□) indicate that the concentration-dependent dilator response of **R**-α-methylhistamine on segments precontracted by prostaglandin $F_{2\alpha}$ 1×10^{-6} M is not affected by the presence of mepyramine 1×10^{-6} M. Responses are expressed as a percentage of precontraction and each point is the mean with s.d. $n = 5-9$.

Table 2 **R**-α-methylhistamine induced motor response of guinea-pig pulmonary large lobar arterial segments

		R*-α-*methylhistamine* *contraction	
Pulmonary artery	*n*	I_{max}%	pD_2
RαMeHA control	18	68 ± 36	3.82 ± 0.18
RαMeHA + Mep 10^{-9} M	6	70 ± 26	3.93 ± 0.22
RαMeHA + Mep 10^{-8} M	3	11 ± 6	3.54 ± 0.17[a]
RαMeHA + Mep 10^{-7} M	3	0	–
RαMeHA + Cim 10^{-7} M	5	89 ± 28	4.11 ± 0.29
RαMeHA + Mep 10^{-5} M	5	74 ± 41	3.74 ± 0.15
		R*-α-*methylhistamine* *dilatation	
Pulmonary artery	*n*	I_{max}%	pD_2
RαMeHA control[b]	6	0	–

Maximal contractile response (E_{max}%), expressed as a percentage of the contraction induced by 60 mM potassium; maximal dilator response (I_{max}%), expressed as a percentage of precontraction and sensitivity (pD_2) expressed as the negative logarithm of the concentration eliciting half the maximal response. RαMeHA, **R**-α-methylhistamine; Mep, mepyramine; Cim, cimetidine; [a]complete concentration-response curve could not be obtained; [b]prostaglandin $F_{2\alpha}$ precontraction. The values represent the mean ± s.d.

5-HT precontracted segments nor the segments precontracted by histamine). This dilator response was not affected by the muscarinic receptor antagonist, atropine (10^{-6} M), the α_1-, α_2- and β-adrenoceptor antagonists prazosin (10^{-6} M), yohimbine (10^{-6} M) and propranolol (10^{-6} M), respectively, or the tachykinin antagonist, spantide (10^{-6} M). There were no contractile effects of **R**-α-methylhistamine ($10^{-10}-3 \times 10^{-5}$ M) on the tracheal segments.

High concentrations of **R**-α-methylhistamine induced a concentration-dependent contraction of pulmonary arteries at rest. This contraction was competitively blocked by mepyramine whereas cimetidine was without effect (Table 2). In the precontracted artery dilator responses were not seen after application of **R**-α-methylhistamine ($10^{-10}-3 \times 10^{-5}$ M). Addition of mepyramine (10^{-6} M) or cimetidine (10^{-6} M) did not reveal any masked dilator response.

Removal of the tracheal epithelium and vascular endothelium

Removal of the epithelium in the trachea shifted the concentration-response curve for the histamine-induced contraction to the left and increased the maximal contractile response (pD_2 5.74 ± 0.23, $P<0.01$; E_{max}%, 162 ± 29; $P<0.01$; $n=9$). The potency of the dilator response to histamine was also increased (pD_2, 8.51 ± 0.36, $P<0.05$; I_{max}%, 25 ± 11; $n=6$) (Figure 6a).

In the pulmonary arterial segments, removal of the endothelium affected the histamine-induced contractile response in the same way as the epithelium displacement in the trachea, and thus led to a slightly higher sensitivity and an enlargement of the maximum contraction (not significant) (pD_2, 5.54 ± 0.15; E_{max}%, 133 ± 41; $n=6$) (Figure 6b). In the precontracted pulmonary artery, the small initial dilatation was abolished (Figure 6c) whereas the larger dilatation seen in the presence of mepyramine was only slightly reduced (pD_2, 5.91 ± 0.24; I_{max}%, 66 ± 23; $n=6$). The contractile responses seen at higher histamine concentrations were potentiated (Figure 6c).

Discussion

Histamine in low concentrations acts as a relaxant agent of precontracted guinea-pig isolated pulmonary arterial and tracheal segments, whereas in high concentrations it induces contraction of both precontracted and resting segments. This discussion will mainly focus on the histamine-induced dilator response, since the concept of histamine H_1 receptor-mediated contraction of isolated tracheal and pulmonary arteries is already well established (Ash & Schild, 1966; Timmerman, 1991).

The responses to histamine in isolated vascular preparations vary considerably depending upon the species (Toda, 1986), the type of vessels (Van de Voorde & Leusen, 1984) and the region within the vascular bed from which the tissue has been derived (Shirai *et al.*, 1987; Tsuru *et al.*, 1987). In the present study, arteries from various parts of the pulmonary vascular tree were examined, but only small intraregional differences in the histamine-induced contractile response were seen. Histamine contraction was slightly more potent in large, proximal arteries than in small, more distally located arteries. When studying relaxations, no significant differences were seen.

The concept of H_1-receptor-mediated contraction of the trachea and the guinea-pig pulmonary artery is supported by the mepyramine-induced rightward shift of the concentration-response curves obtained. The slope of 0.61 in the trachea implicates involvement also of another site, possibly a H_3 receptor. The finding of a slope 1.05 in the presence of thioperamide supports this idea. The slope did not differ from unity for the pulmonary artery which suggests a simple competitive antagonism at one receptor site. Dissociation constant (pA_2) values of 8.0–9.3 for mepyramine and 6.1–7.0 for cimetidine have been reported in different test preparations (Ottosson *et al.*, 1988). Thus, the pA_2 values found in the present study, 9.57 and 8.75 for mepyramine

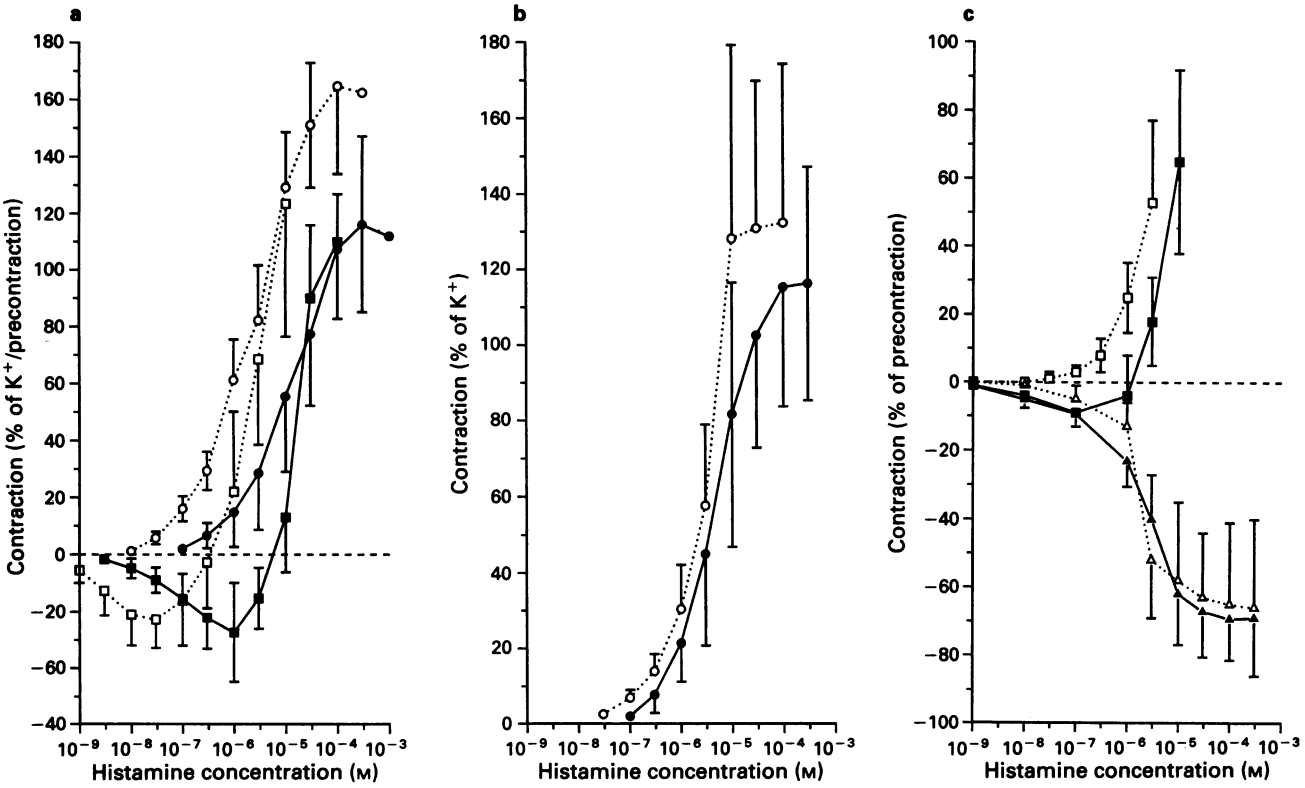

Figure 6 Enhancement of the histamine response in tracheal segments. Filled symbols represent the control and open symbols represent segments where the epithelium and endothelium, respectively, have been removed by rubbing the luminal side of the specimens. (a) Histamine-induced contraction of resting (●, ○, $n=9$) and acetylcholine precontracted (■, □, $n=9$) tracheal segments. Responses are expressed as a percentage of potassium (60 mM)-induced contraction (●, ○) and acetylcholine-induced precontraction (■, □). Since in these experiments, the contraction induced by potassium (60 mM) corresponded to the contraction induced by acetylcholine 1×10^{-6} M both types of curves could be compared in the same diagram. (b) Histamine-induced contractions of control (●) and rubbed (○, $n=6$) resting pulmonary arterial segments. Responses are expressed as a percentage of potassium (60 mM)-induced contraction. (c) The histamine-induced biphasic response of pulmonary arterial segments precontracted by prostaglandin $F_{2\alpha}$ 1×10^{-6} M (■) is exchanged for an enhanced contractile response by rubbing (□, $n=7$) and an endothelium independent relaxation by adding of mepyramine 10^{-6} M, (Δ and ▲, $n=6$). Responses are expressed as a percentage of acetylcholine 1×10^{-6} M-induced precontraction. Each point is the mean with s.d.

and 6.49 for cimetidine, are in accordance with those found in histamine receptor subtype characterizations carried out previously.

In some species, bronchodilatation is mediated via H_2-receptors (Okpako *et al.*, 1978; Chand & De Roth, 1979). In contrast, Chand & Eyre (1978) and Vincec *et al.* (1984) have described a histamine-induced tracheal relaxation not affected by H_2-antagonists and have suggested the existence of H_1-receptor subtypes or a third histamine receptor in the trachea. In the present study, histamine (10^{-9} M–10^{-6} M) induced a relaxation of precontracted tracheal segments followed by a contraction at higher concentrations. In the presence of mepyramine, the contractile component was abolished, and the maximal dilatation increased without any change in the pD_2-value. Since there was no difference in the dilator responses between mepyramine at concentrations of 10^{-6} M and 10^{-5} M, the involvement of a 'traditional' dilator H_1-receptor is less likely. Cimetidine did not affect the dilator response, which speaks against the involvement of H_2 receptors. Consequently, an H_3 receptor must be considered. The selective H_3 receptor antagonist, thioperamide (10^{-5} M), totally inhibited the dilator response of histamine in precontracted tracheal segments. The contractile responses seen at higher histamine concentrations were not affected. In the presence of mepyramine, thioperamide induced a parallel shift to the right of the dilator histamine response. The slope was 0.77 and the pA_2-value 7.79, supporting the involvement of an H_3 receptor. Unexpectedly, all the tested H_1 and H_2 agonists induced a concentration-dependent relaxation of the precontracted tracheal segments. Two of them, the H_1 agonist, 2-methylhistamine, and the H_2 agonist, 4-methylhistamine, were about 100 times more potent than the rest, and their pD_2-values corresponded with the value obtained for histamine during the same conditions. Both agonists are known to be potent but rather unselective. **R**-α-methylhistamine is about 15 times more potent than histamine as an H_3 agonist, but possesses only 1% of the activity of histamine on H_1 and H_2 receptors (Arrang *et al.*, 1987). This rather selective H_3 agonist induced a three phased response on precontracted tracheal segments, two dilator parts with a plateau or slight contraction in between. The slight contraction was eliminated by treatment with mepyramine, leaving the two dilator parts unaffected. Cimetidine did not affect this biphasic dilator response. The first dilatation, induced by low concentrations of **R**-α-methylhistamine, was slightly more potent than the dilatation induced by histamine in the same preparation. The second dilatation was elicited only at very high concentrations of **R**-α-methylhistamine. In tracheal segments precontracted by histamine, only the late second dilatation was seen. These data imply that the first 'low dose' dilatation induced by **R**-α-methylhistamine could be the result of an involvement of an H_3-receptor, whereas the second 'high dose' dilatation may be the result of a more unspecific action.

The respiratory epithelium modifies the reactivity of the tracheal smooth muscle in response to several drugs, including histamine (Barnes *et al.*, 1985). In the present study, removal of the respiratory epithelium increased the potency of the histamine-induced contractions about 6 times and the relaxation about 10 times. The fact that removal of epithelium increases the sensitivity of tracheal segments not only to several contracting stimuli, but also to dilator agents (isoprenaline and adenosine), has also been reported by Holroyde (1986). These results suggest that the epithelium represents a permeability barrier the removal of which facilitates the access of exogenous substances (both contractile and relaxant) (Munakata *et al.*, 1989; Iriarte *et al.*, 1991). However, the possibility of a simultaneously existing mechanism for release of an epithelium-dependent relaxing factor(s) in response to histamine cannot be ruled out (Farmer *et al.*, 1986; Fedan *et al.*, 1988; VanHoutte, 1988). Recent reports have established that at least part of the inhibitory response in the trachea is mediated by nitric oxide (Belvisi *et al.*, 1992), but the question as to whether nitric oxide is released directly from nerves in the airways, from airway epithelial cells and/or from endothelial cells of the bronchial vessels is open.

Histamine-induced relaxation can generally be mediated through H_2-receptors located on the muscle cells (Toda, 1986; Stepanovic *et al.*, 1988) but in many isolated vascular preparations, relaxation elicited by histamine is dependent upon the presence of an intact endothelium (VanHoutte *et al.*, 1986; Chen & Suzuki, 1989). Further, depending on the species and the vessels, this endothelium-dependent relaxation occurs through activation of H_2-receptors (Van de Voorde & Leusen, 1984; Sercombe *et al.*, 1986) and/or H_1-receptors (Satoh & Inui, 1984; Abacioglu *et al.*, 1987; Szarek *et al.*, 1992) located on the endothelial cells resulting in a subsequent release of inhibitory substances. In the present experiments, precontracted pulmonary arteries exhibited a biphasic response to histamine. In the presence of mepyramine, histamine caused a concentration-dependent relaxation at all concentrations tested. Addition of cimetidine caused a parallel shift of this curve to the right. Schild analysis revealed a pA_2-value of 6.49 for cimetidine, indicating an H_2-receptor. The presence of a dilator H_2-receptor is further supported by the studies of contractile responses, where cimetidine enhanced the response to low concentrations of histamine. Hence, this could reflect the elimination of the influence from a dilator cimetidine-sensitive receptor (Boe *et al.*, 1980). When the endothelium was mechanically removed, the small histamine-induced dilatation seen prior to the following contraction disappeared and the remaining contraction was slightly enhanced. With mepyramine present in endothelium denuded preparations, histamine still induced a strong dilator response. The relaxation was slightly reduced from 69% in unrubbed to 51% in the rubbed segments without any significant change of the potency. These results show that histamine has a strong direct relaxant effect on precontracted pulmonary arteries. Furthermore, according to the presented results, the presence of an intact endothelium seems to contribute to the relaxant effect of histamine. The endothelium-dependent part of the relaxation could be mediated through a H_1 receptor triggered release of an endothelium derived relaxing factor (nitric oxide) and/or a cyclo-oxygenase product (Abacioglu *et al.*, 1987; Ortiz *et al.*, 1992). The importance of this endothelium-dependent component cannot be evaluated from the present results since the contractile H_1 receptor on the vasculature will tend to mask such a response. Investigations with the use of substances interfering with the formation of nitric oxide and cyclo-oxygenase products will be needed to solve this question.

The finding that the H_1 receptor agonists, 2-pyridylethylamine and 2-thiazolylethylamine induce dilatation (10–15%) of precontracted pulmonary arteries supports the notion of dilator H_1 receptors on the endothelium. The tested H_2 receptor agonists had the following order of potency: impromidine > 4-methylhistamine > dimaprit, and induced relaxations between 35–60%. According to Abacioglu *et al.* (1987), the dose-related relaxant effect of impromidine is independent of vascular endothelium which supports the assumption of a dilator H_2-receptor on the vascular smooth muscle. **R**-α-methylhistamine did not induce any dilator responses in precontracted pulmonary arteries, but in high concentration this H_3 agonist induced a concentration-dependent contraction in segments at rest. The concentrations needed to induce this contraction were about 100 times higher than the concentration of histamine producing the same effect. The **R**-α-methylhistamine elicited contraction could be gradually blocked by mepyramine in rising concentrations, indicating that **R**-α-methylhistamine in high concentrations probably could also activate H_1-receptors.

In conclusion, histamine induced a biphasic effect of guinea-pig trachea and pulmonary arteries. At low concentrations a relaxation was seen in precontracted segments

followed by contraction at higher concentrations. The contraction of either specimen was mediated through histamine H_1-receptors. In the pulmonary artery, the main part of the relaxant response seems to be mediated via H_2 receptors on the smooth muscle. However, the involvement of an endothelium-dependent relaxing factor or factors cannot be excluded. In the trachea, histamine-induced relaxation may involve H_3 receptors on the airway smooth muscle. Furthermore, the results support the suggestion that exogenous histamine could activate H_3 receptors and consequently this third class of receptors might exist in tissues other than nerve terminals.

This work was supported by grants from Swedish Medical Research Council (projects number 5958 and 6859), the Swedish Society of Medicine, the Swedish Society of Medicine Research, Swedish Association for Allergology and the University of Lund.

References

ABACIOGLU, N., ERCAN, Z.S., KANZIK, H., ZENGIL, H., DEMIRYUREK, T. & TURKER, R.K. (1987). Endothelium-dependent relaxing effect of histamine on the isolated guinea-pig main pulmonary artery strips. *Agents Actions*, **22**, 30–35.

ABROL, R.P., HUGHES, W.M., KRUEGER, G.A. & COOK, D.A. (1984). Detection of endothelium in cerebral blood vessels. *J. Pharmacol. Methods*, **12**, 213–219.

ADAMS, G.K. & LICHTENSTEIN, L. (1979). *In vitro* studies of antigen-induced bronchospasm: effect of antihistamine and SRS-A antagonist on response of sensitized guinea pig and human airways to antigen. *J. Immunol.*, **122**, 555–562.

ARRANG, J.-M., GARBARG, M., LANCELOT, J.-C., LECOMTE, J.-M., POLLARD, H., ROBBA, M., SCHUNACK, W. & SCHWARTZ, J.-C. (1987). Highly potent and selective ligands for histamine H_3-receptors. *Nature*, **327**, 117–123.

ARRANG, J.-M., GARBARG, M. & SCHWARTZ, J.-C. (1983). Autoinhibition of brain histamine release mediated by a novel class (H_3) of histamine receptor. *Nature*, **302**, 832–837.

ARUNLAKSHANA, O. & SCHILD, H.O. (1959). Some quantitative uses of drug antagonists. *Br. J. Pharmacol. Chemother.*, **14**, 48–58.

ASH, A.S.F. & SCHILD, H.O. (1966). Receptors mediating some actions of histamine. *Br. J. Pharmacol.*, **27**, 427–439.

BARNES, P.J., CUSS, F.M. & PALMER, J.B. (1985). The effect of airway epithelium on smooth muscle contractility in bovine trachea. *Br. J. Pharmacol.*, **86**, 685–692.

BARNES, P.J. & ICHINOSE, M. (1989). H_3 receptors in airways. *Trends Pharmacol. Sci.*, **10**, 264.

BELVISI, M.G., STRETTON, C.D., YACOUB, M. & BARNES, P.J. (1992). Nitric oxide is the endogenous neurotransmitter of bronchodilator nerves in humans. *Eur. J. Pharmacol.*, **210**, 221–222.

BEVAN, M.A. (1982). *Pharmacology of Histamine Receptors*. ed. Ganellin, G.R. & Parsons, M.E. pp. 103–145. Bristol: Wright.

BLACK, J.W., DUNCAN, W.A.M., DURANT, C.J., GANELLIN, C.R. & PARSONS, E.M. (1972). Definition and antagonism of histamine H_2-receptors. *Nature*, **236**, 385–390.

BOE, J., BOE, M.-A. & SIMONSSON, B.G. (1980). A dual action of histamine on isolated human pulmonary arteries. *Respiration*, **40**, 117–122.

CARDELL, L.O., UDDMAN, R. & EDVINSSON, L. (1993). A novel ET_A-receptor antagonist, FR 139317, inhibits endothelium-induced contractions of guinea-pig pulmonary arteries, but not trachea. *Br. J. Pharmacol.*, **108**, 448–452.

CARDELL, L.O., UDDMAN, R. & EDVINSSON, L. (1990). Analysis of endothelin 1-induced contractions of guinea-pig trachea, pulmonary veins and different types of pulmonary arteries. *Acta Physiol. Scand.*, **139**, 103–111.

CHAND, N. & DE ROTH, L. (1979). Dual histamine receptor mechanism in guinea-pig lung. *Pharmacology*, **19**, 185–190.

CHAND, N. & EYRE, P. (1978). Spasmolytic action of histamine in airway smooth muscle of horse. *Agents Actions*, **8**, 191–198.

CHEN, G. & SUZUKI, H. (1989). Direct and indirect actions of acetylcholine and histamine on intrapulmonary artery and vein muscles of the rat. *Jpn. J. Physiol.*, **39**, 51–65.

EA KIM, L., JAVELLAUD, J. & OUDART, N. (1992). Endothelium-dependent relaxation of rabbit middle cerebral artery to histamine H_3-agonist is reduced by inhibitors of nitric oxide and prostacyclin synthesis. *Br. J. Pharmacol.*, **105**, 103–106.

EA KIM, L. & OUDART, N. (1988). A highly potent and selective H_3 agonist relaxes rabbit middle cerebral artery, in vitro. *Eur. J. Pharmacol.*, **150**, 393–396.

EDVINSSON, L. & OWMAN, C. (1975). A pharmacologic comparison of histamine receptors in isolated extracranial and intracranial arteries in vitro. *Neurology*, **25**, 217–276.

FARMER, S.G., FEDAN, J.S., HAY, D.W.P. & RAEBURN, D. (1986). The effects of epithelium removal on the sensitivity of guinea-pig isolated trachealis to bronchodilator drugs. *Br. J. Pharmacol.*, **89**, 407–414.

FEDAN, J.S., HAY, D.W.P., FARMER, S.G. & RAEBURN, D. (1988). Epithelial cells: modulation of airway smooth muscle reactivity. In *Asthma: Basic Mechanisms and Clinical Management*. ed. Barnes, P.J., Rodger, I.W. & Thomson, N.C. pp. 143–162. London: Academic Press.

FOREMAN, J.C., RISING, T.J. & WEBBER, S.E. (1985). A study of the histamine H2-receptor mediating relaxation of the parenchymal lung strip preparation of the guinea-pig. *Br. J. Pharmacol.*, **86**, 465–473.

FURCHGOTT, R.F. (1984). The role of endothelium in the responses of vascular smooth muscle to drugs. *Annu. Rev. Pharmacol. Toxicol.*, **24**, 175–197.

GOLDIE, R.G., PAPADIMITRIOU, J.M., PATERSON, J.W., RIGBY, P.J., SELF, H.S. & SPINA, D. (1986). Influence of the epithelium on responsiveness of guinea-pig isolated trachea to contractile and relaxant agonists. *Br. J. Pharmacol.*, **87**, 5–14.

HILL, S.J. (1990). Distribution, properties, and functional characteristics of three classes of histamine receptor. *Pharmacol. Rev.*, **42**, 45–83.

HOLROYDE, M.C. (1986). The influence of epithelium on the responsiveness of guinea-pig isolated trachea. *Br. J. Pharmacol.*, **87**, 501–507.

ICHINOSE, M. & BARNES, P.J. (1989). Inhibitory histamine H_3-receptors on cholinergic nerves in human airways. *Eur. J. Pharmacol.*, **163**, 383–386.

ICHINOSE, M., BELVISI, M.G. & BARNES, P.J. (1990). Histamine H_3-receptors inhibit neurogenic microvascular leakage in airways. *J. Appl. Physiol.*, **68**, 21–25.

ICHINOSE, M., STRETTON, C.D., SCHWARTZ, J.C. & BARNES, P.J. (1989). Histamine H_3-receptors inhibit cholinergic bronchoconstriction in guinea pig airways. *Br. J. Pharmacol.*, **97**, 13–15.

IRIARTE, C.F., PASCUAL, R., VILLANUEVA, M.M., ROMAN, M., ORTIZ, J.L., CORTIJO, J. & MORCILLO, E. (1991). Epithelium modulates the reactivity of sensitized guinea pig trachea: influence of the surface of drug entry. *J. Pharm. Pharmacol.*, **43**, 392–395.

ISHIKAWA, S. & SPERELAKIS, N. (1987). A novel class (H_3) of histamine receptors on perivascular nerve terminals. *Nature*, **327**, 158–160.

KRSTIC, M.K., STEPANOVIC, R.M., VUCKOVIC, S.M. & KRSTIC, S.K. (1991). Endothelium-independent relaxation of the rat femoral artery caused by activation of histamine H_2-receptors. *Arch. Int. Pharmacodyn.*, **313**, 15–22.

LICHTENSTEIN, L.M. (1975). The mechanism of basophil histamine release induced by antigen and calcium ionophore. *J. Immunol.*, **114**, 1692–1699.

MIKKELSEN, E., SAKR, A.M. & JESPERSEN, L.T. (1984). Studies of the effect of histamine in isolated human pulmonary arteries and veins. *Acta Pharmacol. Toxicol.*, **54**, 86–93.

MUNAKATA, M., HUANG, I., MITZNER, W. & MENKES, H. (1989). Protective role of epithelium in the guinea pig artery. *J. Appl. Physiol.*, **66**, 1547–1552.

OKPAKO, D.T., CHAND, N. & EYRE, P. (1978). The presence of inhibitory histamine H2-receptors in guinea-pig tracheobronchial muscle. *J. Pharm. Pharmacol.*, **30**, 181–186.

ORTIZ, J.L., LABAT, C., NOREL, X., GORENNE, I., VERLEY, J. & BRINK, C. (1992). Histamine receptors on human isolated pulmonary arterial muscle preparations: effects of endothelial cell removal and nitric oxide inhibitors. *J. Pharmacol. Exp. Ther.*, **260**, 762–767.

OTTOSSON, A., JANSEN, I. & EDVINSSON, L. (1988). Characterization of histamine receptors in isolated human cerebral arteries. *Br. J. Pharmacol.*, **94**, 901–907.

OTTOSSON, A., JANSEN, I. & EDVINSSON, L. (1989). Pharmacological characterization of histamine receptors in the human temporal artery. *Br. J. Clin. Pharmacol.*, **27**, 139–145.

RILEY, J.F. & WEST, G.B. (1953). The presence of histamine in tissue mast cells. *J. Physiol.*, **120**, 528–537.

SATOH, H. & INUI, J. (1984). Endothelial cell-dependent relaxation and contraction induced by histamine in the isolated guinea-pig pulmonary artery. *Eur. J. Pharmacol.*, **97**, 321–324.

SCHWARTZ, J.C., ARRANG, J.-M. & POLLARD, H. (1990). A third histamine receptor type. Characterization, localisation and functions of the H_3-receptor. *Agents Actions*, **30**, 13–23.

SERCOMBE, R., VERRECHIA, C., PHILIPSON, V., OUDART, N., DIMITRIADOU, V., BOUCHAUD, C. & SEYLAZ, J. (1986). Histamine-induced contractions and dilatation of rabbit middle cerebral arteries in vitro: role of endothelium. *Blood Vessels*, **23**, 137–153.

SHIRAI, M., SADA, K. & NINOMIYA, I. (1987). Nonuniform effects of histamine on small pulmonary vessels in cats. *J. Appl. Physiol.*, **62**, 451–458.

STEPANOVIC, R.M., KUTUSIC, Z.S., KRSTIC, S.K. & KRISTIC, M.K. (1988). Analysis of the response of the guinea-pig common carotid artery to histamine. *Period. Biol.*, **90**, 305–307.

SZAREK, J.L., BAILLY, D.A., STEWART, N.L. & GRUETTER, C.A. (1992). Histamine H_1-receptors mediate endothelium-dependent relaxation of rat isolated pulmonary arteries. *Pulm. Pharmacol.*, **5**, 67–74.

TALLARIDA, R.J., COWAN, A. & ADLER, M.W. (1979). pA_2 and receptor differentiation: a statistical analysis of competitive antagonism. *Life Sci.*, **25**, 637–654.

TIMMERMAN, H. (1991). Histamine agonists and antagonists. *Acta Otolaryngol.*, **479**, 5–11.

TODA, N. (1986). Mechanism of histamine-induced relaxations in isolated monkey and dog coronary arteries. *J. Pharmacol. Exp. Ther.*, **239**, 529–535.

TSURU, H., KOHNO, S., IWATA, M. & SHIGEI, T. (1987). Characterization of histamine receptors in isolated rabbit veins. *J. Pharmacol. Exp. Ther.*, **243**, 696–702.

VALENTOVIC, M.A., BALL, J.G., MORENAS, M., SZAREK, J.L. & GRUETTER, C.A. (1992). Influence of nitrovasodilators on bovine pulmonary histamine release. *Pulm. Pharmacol.*, **5**, 97–102.

VAN DE VOORDE, J. & LEUSEN, I. (1984). Effect of histamine on aorta preparations of different species. *Arch. Int. Pharmacodyn. Ther.*, **268**, 95–105.

VANHOUTTE, P.M. (1988). Editorial. Epithelium derived relaxing factor: myth or reality? *Thorax*, **43**, 665–668.

VANHOUTTE, P.M., RUBANYI, G.M., MILLER, V. & HOUSTON, D.S. (1986). Modulation of vascular smooth muscle contraction by the endothelium. *Annu. Rev. Physiol.*, **48**, 307–320.

VINCEC, K., BLACK, J. & SHAW, J. (1984). Relaxation and contraction responses to histamine in the human lung parenchymal strip. *Eur. J. Pharmacol.*, **98**, 201–210.

WALLENSTEIN, S., ZUCKER, C.L. & FLEISS, J. (1980). Some statistical methods useful in circulation research. *Circ. Res.*, **47**, 1–9.

(Received May 20, 1993
Revised July 23, 1993
Accepted October 7, 1993)

Br. J. Pharmacol. (1994), **111**, 455–458

Comparison of the effects of caffeine and other methylxanthines on $[Ca^{2+}]_i$ in rat ventricular myocytes

*P. Donoso, S.C. O'Neill, K.W. Dilly, N. Negretti & [1]D.A. Eisner

Department of Veterinary Preclinical Sciences, University of Liverpool, Liverpool L69 3BX and *Facultad de Medicina, Departmento Fisiologia y Biofisica, Casilla 70055, Santiago 7, Chile

1 The effects of caffeine and other methylxanthines were investigated on intracellular calcium concentration ($[Ca^{2+}]_i$) and contraction in rat isolated ventricular myocytes. The use of the fluorescent indicator, Indo-1, allowed simultaneous measurement of $[Ca^{2+}]_i$ and the intracellular concentration of the methylxanthines.

2 Rapid application of caffeine (10 mM) produced a transient rise of $[Ca^{2+}]_i$ which decayed to resting levels. This was accompanied by a transient contraction which decayed to a level above baseline. The addition of theophylline also produced a transient increase of $[Ca^{2+}]_i$. However, following the initial transient, contraction decayed before redeveloping to a maintained level.

3 Direct measurements showed that $[caffeine]_i$ rose more quickly than did $[theophylline]_i$. The slower rise of $[theophylline]_i$ was associated with a delay in the increase of $[Ca^{2+}]_i$. At lower concentrations of the methylxanthines, theophylline was less effective than caffeine at initiating Ca release. The rate of entry of theobromine was similar to that of theophylline.

4 Isocaffeine did not produce a rise of $[Ca^{2+}]_i$. The rate of rise of $[isocaffeine]_i$ was much slower than that of either caffeine or theophylline.

5 Measurements of the oil:water partition coefficient showed that the order of relative partitioning into oil was: caffeine > theophylline > theobromine > isocaffeine. This is similar to the order of rate of entry into the cell.

6 We conclude that many of the differences in the effects of these methylxanthines can be attributed to differences in membrane permeability due to differences in oil:water partition.

Keywords: $[Ca^{2+}]_i$; cardiac muscle; contraction; caffeine; methylxanthine

Introduction

Caffeine and other methylxanthines have a variety of effects in cardiac muscle (see O'Neill *et al.*, 1993). These include: (i) the release of Ca^{2+} ions from the sarcoplasmic reticulum (SR); (ii) a shift of the relationship between $[Ca^{2+}]_i$ and tension such that a lower $[Ca^{2+}]_i$ is required to activate contraction; and finally (iii) caffeine also has actions as a phosphodiesterase inhibitor. The first two of these effects have been studied recently in isolated cardiac myocytes. The fluorescent Ca-indicator Indo-1 (Grynkiewicz *et al.*, 1985) is particularly useful in this context as it allows measurement of both $[Ca^{2+}]_i$ and the intracellular caffeine concentration ($[caffeine]_i$). Therefore it is possible to correlate the effects of caffeine directly with its intracellular concentration (O'Neill *et al.*, 1990; O'Neill & Eisner, 1990; Baro *et al.*, 1993).

Caffeine has been used in many studies of excitation-contraction coupling. The other methylxanthines have also been examined at both cellular (Chapman & Miller, 1974) and subcellular (Rousseau *et al.*, 1988) sites of action. One aim of this kind of study is that the use of different analogues may provide a substance which has only one of the effects of caffeine mentioned above and may therefore be of use for studying the control of contraction. In the present paper we have studied the effects of various methylxanthines on rat isolated ventricular myocytes. The results show that many of the differences between the actions of these compounds can be attributed to differences in the rate of entry into the cell and correlate with differences in the oil-water partition coefficient.

[1] Author for correspondence.

Methods

Ventricular myocyte experiments

The experiments were performed on single ventricular myocytes. Rats were killed by cervical dislocation. The methods for isolating cells and for measuring $[Ca^{2+}]_i$ and $[caffeine]_i$ from the fluorescence of Indo-1 have been published previously (O'Neill *et al.*, 1990; Eisner *et al.*, 1989). Briefly, the estimation of $[caffeine]_i$ depends on the fact that caffeine quenches the fluorescence of Indo-1 (O'Neill *et al.*, 1990). Therefore, when caffeine is applied, there are two effects on Indo-1 fluorescence: (i) The change of $[Ca^{2+}]_i$ will produce opposite effects at the two emission wavelengths (400 and 500 nm). (ii) Caffeine will produce a concentration-dependent (but wavelength and $[Ca^{2+}]_i$-independent) decrease of the fluorescence at both wavelengths. Separation of these two effects allows $[Ca^{2+}]_i$ and $[caffeine]_i$ to be calculated. In order to do this, the relationship between the 400:500 nm emission ratio and the fluorescence at 400 nm (F_{400}) is first determined in the absence of caffeine. Then in the presence of caffeine, the value of F_{400} associated with a given ratio is compared with that in the absence of caffeine. This comparison gives a measure of the caffeine-induced quench from which $[caffeine]_i$ can be calculated. The method depends on the fact that the quench of Indo-1 fluorescence produced by caffeine is independent of both emission wavelength and $[Ca^{2+}]$ (O'Neill *et al.*, 1990). We find that this is also the case for the quench produced by theophylline. In the case of theobromine, however, the quench is not independent of wavelength. Under these conditions it is impossible to separate $[Ca^{2+}]_i$- and quench-induced changes of fluorescence. In order to be able to measure the rate of entry of theobromine into the cell we have performed the experiments in a Ca-free solution after previously having discharged the SR Ca content with caffeine. Under these conditions there are no $[Ca^{2+}]_i$-induced changes of fluorescence and the rate of entry

of theobromine can be estimated from the quench at any wavelength. Finally, isocaffeine fluoresces when excited at the wavelengths used to excite Indo-1. This fluorescence is greater at an emission wavelength of 400 than 500 nm. This produces a step artefact in the 400:500 nm ratio trace (e.g. Figure 5). It does not, however, appreciably perturb the estimate of the quench which develops much more slowly.

Indo-1 was loaded into the cells as the acetyoxymethyl (AM) ester. The results are presented as the ratio of the fluorescence emitted at 400 nm to that at 500 nm because of the problems of quantifying $[Ca^{2+}]_i$ when the dye is loaded in this way (Highsmith *et al.*, 1986).

The experimental solution contained (mM): NaCl 134, KCl 4, $MgCl_2$ 1, HEPES 10, glucose 11, $CaCl_2$ 1; titrated to pH 7.4 with NaOH. The solution was equilibrated with air. The various methylxanthines were added at concentrations of up to 10 mM without osmotic compensation. All experiments were carried out at 26°C.

Determination of oil-water partition coefficients

The oil-water partition coefficients were measured from the distribution between the experimental solution (above) and either olive oil or hexadecane. In the initial experiments hexadecane was used as this is reported to be a good model for biological membranes (Stein, 1986). However we found that the hexadecane:water partition coefficient was of the order of 10^{-5} for isocaffeine. It was difficult to measure such small values and therefore we changed to the somewhat more polar olive oil. The concentrations of the methylxanthines in the aqueous phases were determined by measurements of the ultra-violet absorption spectrum. In the case of caffeine (which has the highest oil:water solubility ratio) 1 ml of a 0.1 mM aqueous solution was mixed with 1 ml of olive oil. The amount of caffeine in the olive oil was measured from the reduction in the concentration in the aqueous phase. For isocaffeine the oil:water partition coefficient was too low for this method to be used without having to employ impracticably large volumes of olive oil. In these cases the following indirect procedure was adopted: 2 ml of a 10 mM aqueous solution of isocaffeine was mixed with 20 ml of olive oil. The amount of isocaffeine in the oil phase was determined by removing the oil and re-extracting the isocaffeine into fresh (isocaffeine-free) aqueous phase. For theophylline and theobromine either method could be used. One concern with these determinations was that the presence of impurities in the original compounds might interfere with the estimates. For example any caffeine contamination would give an artificially high oil:water ratio. This problem was excluded by measuring the absorption spectrum of the second aqueous phase which was found to have the spectral characteristics of the compound under investigation and did not include a component with the spectral properties of caffeine. Partition coefficients were measured at 21°C.

Nomenclature

In this paper we have tested the following compounds: caffeine (1,3,7-trimethylxanthine): isocaffeine (1,3,9-trimethylxanthine); theophylline (1,3-dimethylxanthine); theobromine (3,7-dimethylxanthine). These methylxanthines were obtained from Sigma.

Results

Figure 1 shows a comparison of the effects of caffeine and theophylline at a concentration of 10 mM. Both agents produce a transient increase of $[Ca^{2+}]_i$ presumably due to the release of Ca^{2+} ions from the SR. There are, however, differences in the contraction. In the case of caffeine the peak contraction relaxes monotonically to a plateau level. In contrast, in theophylline, the contraction relaxes to a minimum

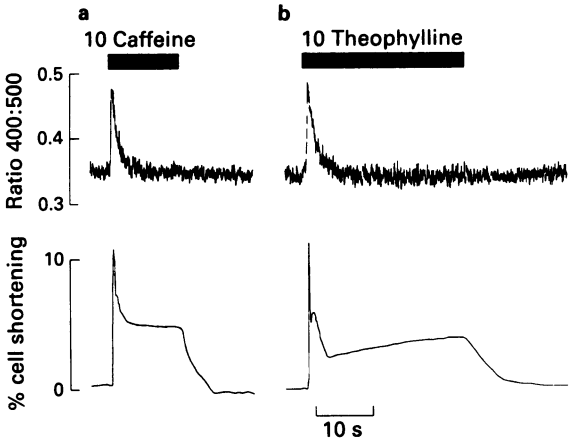

Figure 1 Comparison of the effects of caffeine and theophylline on $[Ca^{2+}]_i$ and contraction in the same cell. In both panels traces show: top, $[Ca^{2+}]_i$ (measured from the 400:500 nm Indo-1 ratio); bottom, contraction. Caffeine (a) or theophylline (b) were added at a concentration of 10 mM as shown above the records.

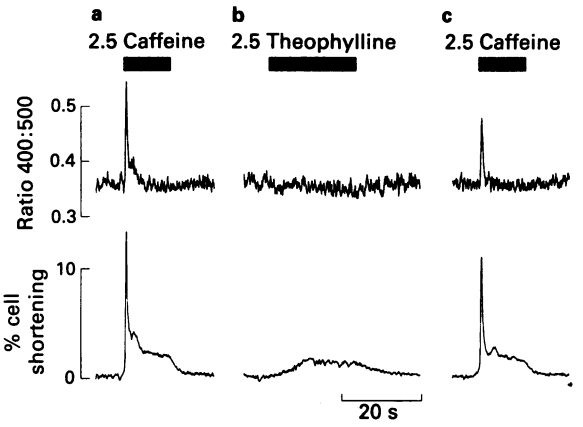

Figure 2 Comparison of the effects of a low (2.5 mM) concentration of caffeine or theophylline on $[Ca^{2+}]_i$ and contraction in the same cell. In each panel caffeine or theophylline was added for the period shown by the solid bars. Panels show: (a) caffeine; (b) theophylline; (c) caffeine.

level before redeveloping again. The effects of lower concentrations of these agents are shown in Figure 2. The application of 2.5 mM caffeine (Figure 2a) produces a transient increase of $[Ca^{2+}]_i$ which is accompanied by a contractile response which, although mainly transient, does have a small sustained phase. In contrast when the same concentration of theophylline is applied (Figure 2b) there is no release of calcium or transient contraction. The contraction record shows only a small, slowly developing, maintained component. Finally Figure 2c shows that a subsequent exposure to caffeine produces a similar response to the initial one.

The effects of theophylline are reminiscent of those found previously for slow application of caffeine which results in a slowly developing contraction (O'Neill *et al.*, 1990). For this reason we have investigated the rate at which theophylline enters the cell. The experiment illustrated in Figure 3 shows measurements of $[Ca^{2+}]_i$ and [methylxanthine]$_i$ on the same cell during the application of 10 mM of either caffeine or theophylline. It is clear that [caffeine]$_i$ (Figure 3a) increases considerably more quickly than does [theophylline]$_i$ (Figure 3b) despite being applied at the same rate. The superimposed records (Figure 3c) show that the increase of $[Ca^{2+}]_i$ with respect to the time after addition of the methylxanthine is correspondingly delayed in theophylline compared to caffeine.

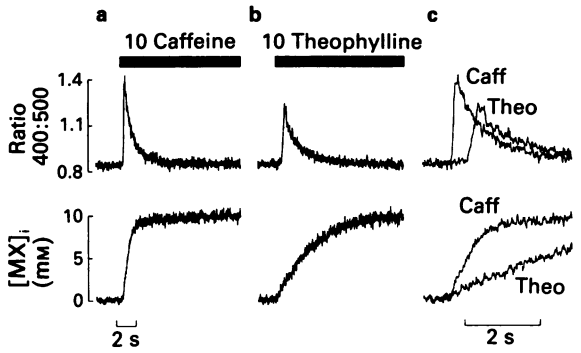

Figure 3 Comparison of the effects of caffeine and theophylline on $[Ca^{2+}]_i$ with their rate of entry into the cell. In all panels traces show: above, $[Ca^{2+}]_i$; below, methylxanthine concentration ($[MX]_i$). Panels (a) and (b) show the effects of adding caffeine or theophylline on the same cell; (c) shows the initial part of the records of (a) and (b) superimposed on an expanded timescale.

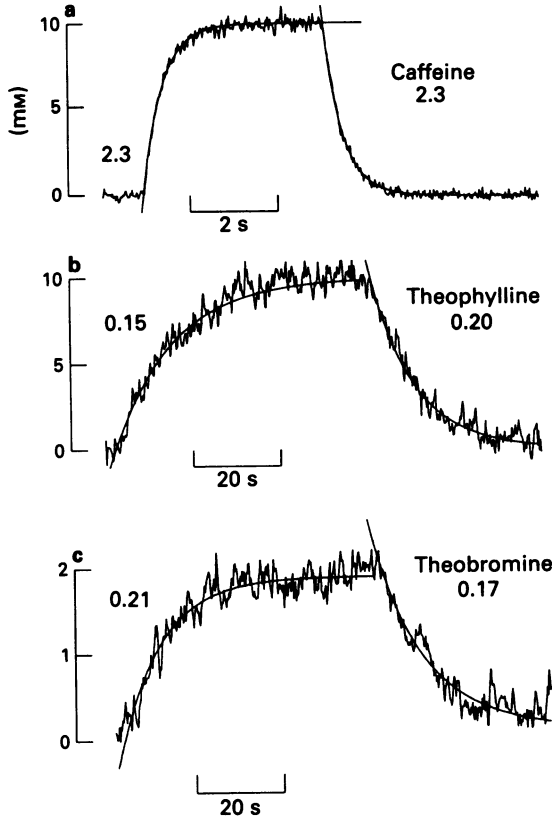

Figure 4 A comparison of the rate of entry of caffeine, theophylline and theobromine on the same cell. In all panels the traces show the calculated concentrations of the methylxanthines: (a) 10 mM caffeine; (b) 10 mM theophylline; (c) 2 mM theobromine. The smooth curves drawn through the data are best-fit single exponentials with the rate constants (s^{-1}) indicated. Note that the timescale for (a) is different from that for (b) and (c). This experiment was performed in a Ca-free solution (see Methods).

Theobromine had a similar rate of entry into the cell to theophylline. This is illustrated in Figure 4 which shows (on the same cell) the changes of intracellular concentration for caffeine, theophylline and theobromine. In this experiment, because of the problem of dissolving higher concentrations, theobromine was used at a lower concentration (2 mM) than the other methylxanthines. This experiment was performed in a Ca-free solution. In Ca-containing solutions, theobromine produced a release of calcium from the SR as judged by a transient rise of $[Ca^{2+}]_i$ of similar magnitude to that produced by theophylline. Because the quench produced by theobromine is different at the two emission wavelengths (see Methods), it is not possible to quantify the exact magnitude of the release produced by theobromine.

The experiment illustrated in Figure 5 compares the actions of caffeine with those of isocaffeine. The trace labelled 'quench' shows the percentage quenching of the fluorescence. This develops much more slowly for isocaffeine than for caffeine, indicating that isocaffeine enters the cell much more slowly than does caffeine. The Indo-1 ratio trace shows an increase when isocaffeine is added. This effect, which occurs long before isocaffeine has entered the cell is due to the fact that isocaffeine, unlike caffeine, fluoresces. The fluorescence emission of isocaffeine is greater at 400 than 500 nm and therefore increases the ratio. It should be noted that, as the increase of fluorescence is much less than the quench (particularly at 500 nm) and develops much more quickly, this effect does not interfere with the calculation of the quench. Figure 5 also shows the effects of adding caffeine at the same time as removing isocaffeine. The transient additional quench indicates that caffeine enters the cell much faster than isocaffeine leaves. This addition of caffeine produces a transient rise of $[Ca^{2+}]_i$ which is much smaller than the control one, suggesting that isocaffeine has released some (but not all) of the SR calcium. This is supported by the observation (not shown) that the application of isocaffeine produces a slow decrease in the magnitude of the systolic Ca transient.

The data for the rate constants of entry of the various methylxanthines are summarized in Table 1. Caffeine has the highest rate of entry, followed by theophylline and theobromine. Isocaffeine is considerably slower than any of the others. It should be noted that the solution changing system used in the present experiments was no quicker than the rate

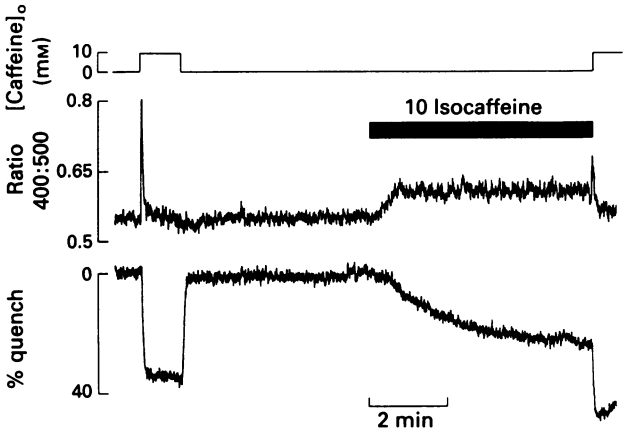

Figure 5 A comparison of the effects of caffeine and isocaffeine. Traces show: top, $[Ca^{2+}]_i$; bottom, the % quench of the Indo-1 signal. Caffeine (10 mM) was first added and removed; then isocaffeine (10 mM) was added. Finally isocaffeine was removed while simultaneously adding caffeine (10 mM).

Table 1 Summary of the rate constant of entry into the cell (column 2) and the oil-water partition coefficient (column 3) for the various methylxanthines

Methylxanthine	*Rate constant of entry* (s^{-1})		*Oil:water partition coefficient*	
Caffeine	2.3 ± 0.12	(5)	0.077 ± 0.007	(4)
Theophylline	0.20 ± 0.02	(6)	0.0216 ± 0.002	(5)
Theobromine	0.23 ± 0.03	(4)	0.0066 ± 0.0009	(8)
Isocaffeine	0.0045 ± 0.0009	(4)	0.0011 ± 0.0001	(5)

The data show mean ± s.e.mean (number of measurements).

constant of changes of $[caffeine]_i$. It is therefore likely that the rate constant for caffeine entry is an underestimate as higher values have been reported previously (O'Neill *et al.*, 1990). Table 1 also shows the values for the relative oil:water partition coefficients for the various methylxanthines. It is clear that caffeine is the most oil soluble and isocaffeine the least.

Discussion

The results presented here characterize the rate of entry of various methylxanthines into ventricular myocytes and allow these to be compared to the effects on $[Ca^{2+}]_i$ and contraction. We find that theophylline enters the cell more slowly than caffeine. The effects of theophylline on $[Ca^{2+}]_i$ and contraction are exactly those to be expected from a low rate of entry. A consistent observation was that, when the caffeine-evoked contraction had a transient component which decayed to a steady-level, that produced by theophylline would initially decline further before a secondary increase followed. As explained previously (O'Neill *et al.*, 1990) the transient phase is due to a transient increase of $[Ca^{2+}]_i$. The maintained phase is due to a direct effect of the methylxanthine on the contractile machinery. Caffeine enters the cell quickly so the maintained phase develops while $[Ca^{2+}]_i$ is declining and the result is a smooth fall to the steady level. In contrast the lower rate of entry of theophylline means that $[Ca^{2+}]_i$ has declined (and contraction relaxed more fully) before the second phase begins. This lower rate of entry of theophylline compared to caffeine can explain why, although theophylline is more potent than caffeine in releasing calcium from the isolated SR (Rousseau *et al.*, 1988), it is less effective in releasing calcium in intact cells (Figure 2). Previous work has shown that if caffeine is applied slowly the rise of $[Ca^{2+}]_i$ is less than if it is applied quickly (O'Neill & Eisner, 1990).

We have also found that isocaffeine enters the cell much less quickly than theophylline (or caffeine). This difference is particularly striking for two isomers. It has, however, been shown by use of u.v. and n.m.r. spectroscopy that isocaffeine is much more polarizable than is caffeine (Yanuka & Bergmann, 1986). This may account for its relative lack of solubility in the membrane. As indicated in Table 1 there is a good correlation between the rates of entry and the oil:water partition coefficient. This is not unexpected. For a given membrane the permeability to substances which simply move through the lipid phase depends on the molecular size and the partition coefficient between the membrane and the aqueous phases. It is clear that, the higher the oil:water partition coefficient, the faster the rate of entry. It should, however, be noted that the relative differences in the rate of entry are considerably greater than those of the partition coefficient. Furthermore, although theobromine and theophylline enter the cell at similar rates, their partition coefficients are different. There are two explanations for the lack of complete correlation between the partition coefficients and the rate of entry. (i) The various methylxanthines may differ in properties other than partition coefficient. Previous work has shown that permeability across a lipid membrane can be accounted for by the combination of partition coefficient and molecular size (Stein, 1986). It is therefore possible that the molecular size of the methylxanthines, when in the membrane, contributes. (ii) Another possibility is that the lipid phase of the membrane behaves in a different way as regards the relative solubilities of the methylxanthines from olive-oil. Despite these quantitative discrepancies, the major conclusion is that the rates of entry and therefore some of the effects of the methylxanthines correlate with the oil:water partition coefficients.

The work described in this paper was supported by grants from the Wellcome Trust and British Heart Foundation. P.D. was supported by The British Council and the Royal Society.

References

BARO, I., O'NEILL, S.C. & EISNER, D.A. (1993). Changes of $[Ca^{2+}]_i$ during refilling of the sarcoplasmic reticulum in rat ventricular and vascular smooth muscle. *J. Physiol.*, **465**, 21–41.

CHAPMAN, R.A. & MILLER, D.J. (1974). Structure-activity relations for caffeine: a comparative study of the inotropic effects of methylxanthines, imidazoles and related compounds on the frog's heart. *J. Physiol.*, **242**, 615–634.

EISNER, D.A., NICHOLS, C.G., O'NEILL, S.C., SMITH, G.L. & VALDEOLMILLOS, M. (1989). The effects of metabolic inhibition on intracellular calcium and pH in isolated rat ventricular cells. *J. Physiol.*, **411**, 393–418.

GRYNKIEWICZ, G., POENIE, M. & TSIEN, R.Y. (1985). A new generation of Ca^{2+} indicators with greatly improved fluorescence properties. *J. Biol. Chem.*, **260**, 3440–3450.

HIGHSMITH, S., BLOEBAUM, P. & SNOWDOWNE, K.W. (1986). Sarcoplasmic reticulum interacts with the Ca(2+) indicator precursor fura-2 AM. *Biochem. Biophys. Res. Commun.*, **138**, 1153–1162.

O'NEILL, S.C., DONOSO, P. & EISNER, D.A. (1990). The role of $[Ca^{2+}]_i$ and $[Ca^{2+}]_i$-sensitization in the caffeine contracture of rat myocytes: measurement of $[Ca^{2+}]_i$ and $[caffeine]_i$. *J. Physiol.*, **425**, 55–70.

O'NEILL, S.C., DONOSO, P. & EISNER, D.A. (1990). The role of $[Ca^{2+}]_i$ and $[Ca^{2+}]_i$-sensitization in the caffeine contracture of rat myocytes: measurement of $[Ca^{2+}]_i$ and $[caffeine]_i$. *J. Physiol.*, **425**, 55–70.

O'NEILL, S.C., DONOSO, P., LAMONT, C. & EISNER, D.A. (1993). The effects of caffeine on cardiac muscle. In *Modulation of Cardiac Calcium Sensitivity*. ed. Lee, J.A. & Allen, D.G. Oxford: Oxford University Press.

O'NEILL, S.C. & EISNER, D.A. (1990). A mechanism for the effects of caffeine on Ca release during diastole and systole in isolated rat ventricular myocytes. *J. Physiol.*, **430**, 519–536.

ROUSSEAU, E., LADINE, J., LIU, Q.-Y. & MEISSNER, G. (1988). Activation of the Ca^{2+} release channel of skeletal muscle sarcoplasmic reticulum by caffeine and related compounds. *Arch. Biochem. Biophys.*, **267**, 75–86.

STEIN, W.D. (1986). *Transport and Diffusion across Cell Membranes*. New York: Academic Press.

YANUKA, Y. & BERGMANN, F. (1986). Spectroscopic studies on caffeine and isocaffeine. *Tetrahaedron*, **42**, 5991–6002.

(Received August 17, 1993
Revised October 1, 1993
Accepted October 8, 1993)

Br. J. Pharmacol. (1994), **111**, 459–464

Induction of Na^+/K^+-ATPase activity by long-term stimulation of nicotinic acetylcholine receptors in C2C12 myotubes

[1]R.H. Henning, S.A. Nelemans, J. van den Akker & A. den Hertog

Department of Pharmacology/Clinical Pharmacology, University of Groningen, Bloemsingel 1, 9713 BZ Groningen, The Netherlands

1 To investigate the role of long-term stimulation of nicotinic acetylcholine receptors (AChRs) on the regulation of membrane potential, non-contracting C2C12 myotubes were stimulated for 1–4 days with carbachol (10 μM) and membrane potentials were measured by the intracellular microelectrode technique after washing out of the drug.

2 The membrane potential (− 45.7 mV) gradually increased by 10.1 mV to − 55.8 mV during 4 days treatment, which was caused by enhanced electrogenic Na^+/K^+-pumping.

3 The concentration-dependent enhancement of Na^+/K^+-ATPase activity in long-term carbachol-treated myotubes (4 days, EC_{50} = 5.3 μM) was prevented by co-treatment with the competitive nicotinic AChR antagonist, pancuronium but not by the muscarinic antagonist, atropine.

4 Enhanced Na^+/K^+-ATPase activity still developed in carbachol-stimulated myotubes during co-treatment (4 days) with the nicotinic AChR-channel blocker, chlorpromazine (1 μM). Membrane depolarization as such, obtained by incubation in high K^+ medium (40 mM, 4 days) did not enhance Na^+/K^+-ATPase activity.

5 Non-treated myotubes possessed a high-affinity ouabain binding site (K_d = 119 nM) in association with the low Na^+/K^+-pumping activity. Long-term stimulation of myotubes (4 days) with carbachol or with a combination of carbachol and chlorpromazine was accompanied by the development of an additional low-affinity ouabain binding site (K_d = 13 μM).

6 Binding of monoclonal antibodies directed against either α_1- or α_2-subunit of Na^+/K^+-ATPase were both increased in myotubes treated with carbachol (4 days).

7 These results support the concept that nicotinic AChRs regulate Na^+/K^+-ATPase activity, independent of the functionality of the receptor-operated ion-channel.

Keywords: Na,K transporting ATPase; nicotinic acetylcholine receptor; C2C12 myotubes

Introduction

Long-term interruption of neuromuscular transmission by drugs or toxins induces denervation-like changes in skeletal muscle (Chang *et al.*, 1975; Simpson, 1977). Thus, long-term administration of competitive blockers of the nicotinic acetylcholine receptor (AChR) is associated with the development of extrajunctional nicotinic AChRs and a decrease in membrane potential (Berg & Hall, 1975; Pestronk *et al.*, 1980). The development of these properties is thought to be related to the cessation of muscle contraction, for they are almost completely counteracted by direct stimulation (Drachman & Witzke, 1972). However, the disruption of stimulation of nicotinic AChRs might also contribute to the effects observed on long-term administration of competitive blockers. Indeed, some studies suggest a trophic role for ACh. For instance, it has been found that drugs interfering only with nerve impulse-dependent ACh release induce less extrajunctional nicotinic AChRs than agents that block spontaneous ACh release as well (Pestronk *et al.*, 1976; Mathers & Thesleff, 1978). Moreover, a possible role for nicotinic AChRs is strongly supported by a study demonstrating denervation-like changes in the skeletal muscle of animals that had been chronically treated with low concentrations of the nicotinic AChR antagonist (+)-tubocurarine not interfering with muscular contraction (Hogue *et al.*, 1992). To examine the role of nicotinic AChRs in the regulation of skeletal muscle properties, we studied the effect of long-term stimulation of nicotinic AChRs on the membrane potential of non-innervated, non-contracting C2C12 myotubes.

[1] Author for correspondence.

Methods

Cell culture

C2C12 cells, a murine myoblast cell line (Yaffee & Saxel, 1977) were obtained from the American Tissue Type Collection, Rockville, U.S.A. Cells were cultured, for most experiments on glass cover slips, in 9.6 cm^2 plastic wells at 37°C in Dulbecco's modified essential medium, 7 mM $NaHCO_3$ and 10 mM HEPES (DMEM) supplemented with 10% foetal calf serum. When cells reached 80% confluence, medium was changed to DMEM supplemented with 5% horse serum (HS). Low Na^+ (23 mM) medium was obtained by diluting DMEM with medium of the following composition (mM): glucaminechloride 125, KCl 6, $CaCl_2$ 1.2, $MgCl_2$ 2.5, NaH_2PO_4 1.2, glucose 11, HEPES 10, HS 5% (pH 7.4). High K^+ (60 mM) medium was obtained by mixing DMEM with medium of the following composition (mM): KCl 131, $CaCl_2$ 1.2, $MgCl_2$ 2.5, NaH_2PO_4 1.2, glucose 11, HEPES 10, HS 5% (pH 7.4). Control medium was obtained by appropriately diluting DMEM with medium of the following composition (mM): NaCl 125, KCl 6, $CaCl_2$ 1.2, $MgCl_2$ 2.5, NaH_2PO_4 1.2, glucose 11, HEPES 10 (pH 7.4). Myotubes were used 7 days after initiating myoblast fusion. Spontaneous contractions of the myotubes were not observed.

Electrophysiology

Membrane potential was measured by microelectrodes filled with 1 M KCl as described previously (Henning *et al.*, 1992). Experiments were performed following a 15 min wash at 25°C in a 1 ml bath superfused at a rate of 1.5 ml min^{-1} with the following solution (mM): NaCl 125, KCl 6, $CaCl_2$ 1.2,

$MgCl_2$ 2.5, NaH_2PO_4 1.2, glucose 11, HEPES 10 (pH 7.4). In the low Na^+ solution (23 mM), NaCl (102 mM) was replaced with glucaminechloride. Drugs used were applied by changing the superfusing fluid with buffer containing the required drug concentration.

[^{3}H]-ouabain binding

The number of [^{3}H]-ouabain binding sites was determined by measuring the specific binding of [^{3}H]-ouabain at several ouabain concentrations (20 nM–1 μM). Total binding at 20°C was assessed in buffer of the following composition (mM): NaCl 150, $MgCl_2$ 4, HEPES 10 (pH 7.4). Non-specific binding was determined in a buffer of the following composition (mM): KCl 150, $MgCl_2$ 4, HEPES 10 (pH 7.4). Cells were successively washed three times in the buffer, incubated for 30 min in 1 ml buffer containing the final ouabain concentration including [^{3}H]-ouabain (0.5–3.0 μCi.ml^{-1}) and washed four times with ice-cold buffer. A final wash was performed with additional 2% ethanol. Thereupon, cells were solubilized in 1 ml NaOH (1 M) and radioactivity was measured by liquid scintillation counting. Data were subjected to kinetic modelling (Munson & Rodbard, 1980). A two-site binding model was preferred over a one-site binding model if a significant reduction in the residual sum of squares of the fitted curve was obtained (F test, $P<0.05$).

Analysis of Na^+/K^+-ATPase antibody binding

Two monoclonal antibodies were used (courtesy of Dr K.J. Sweadner). McK1 is a mouse IgG_1 antibody raised against rat kidney Na^+/K^+-ATPase, which cross-reacts with the α_1-subunit of both native and denatured mouse Na^+/K^+-ATPase (Felsenfeld & Sweadner, 1988). McB2 is a mouse IgG_1 antibody raised against rat axolemma Na^+/K^+-ATPase and recognizes the α_2 subunit of the native and denatured enzyme (Urayama *et al.*, 1989). Staining procedure consisted of an initial wash (30 min) of cells grown on monolayers on glass coverslips, followed by fixation for 30 min in periodate-lysine-paraformaldehyde, an overnight wash in 0.02 M potassium phosphate buffered saline (KPBS, pH 7.4) and treatment with Triton X-100 (0.3%) and H_2O_2 (10%) in KPBS for three periods of 10 min. After washing with KPBS containing 0.3% Triton X-100 (KPBS-T), the monolayers were incubated with McK1 (dilution 1:24) or McB2 (1:10) for 60 h. Secondary antibodies (RAM/IgG (H + L), 1:400, Nordic Immunological Lab, Tilburg, the Netherlands) were introduced for 2 h after washing in KPBS-T. After washing, cells were subsequently incubated with rabbit peroxidase-anti-peroxidase (1:800, Nordic) in a solution containing 0.05% 3,3-diaminobenzidine (DAB), 2.5% nickel ammonium sulphate (NAS), 0.04% ammonium chloride and 0.004% H_2O_2. Staining intensity was determined after washing in KPBS-T by scanning the absorbance of the cells at 497 nm (100 pixels at 10 μm distance in an area of 200 × 200 μm) using a Leitz orthoplan microscope with 10 × objective and equipped with a Leitz MPV compact photometer with scanning stage control unit as described by Wolters *et al.* (1984). Coverslips were scanned at 20 randomly chosen areas. Data were corrected for non-specific absorbance of the cells and are presented as mean ± s.e.mean of the absorbance. Control coverslips with treated and non-treated myotubes that were processed without incubation with the primary or secondary antibody did not stain.

Results

Membrane potential: acute effects of carbachol

In acute experiments, the non-hydrolysable AChR agonist, carbachol (1–30 μM) evoked a sustained and reproducible depolarization of the cells (Figure 1a). The amplitude of the depolarization was dependent on the agonist concentration, reaching a maximum at 30 μM (43.4 ± 2.2 mV; $n = 6$). This action of carbachol was inhibited by the competitive nicotinic AChR antagonist, pancuronium (Figures 1b,d), but not by the muscarinic receptor antagonist, atropine (1 μM; not shown). Under low Na^+ conditions (23 mM), the depolarization evoked by carbachol (30 μM) was greatly reduced, being 9.2 ± 1.0 mV ($n = 6$). Chlorpromazine is known to block the nicotinic AChR-coupled ion-channel use-dependently (Changeux, 1990). In fact, carbachol (10 μM) evoked only an initial depolarization in the presence of chlorpromazine (1 μM; Figure 1c).

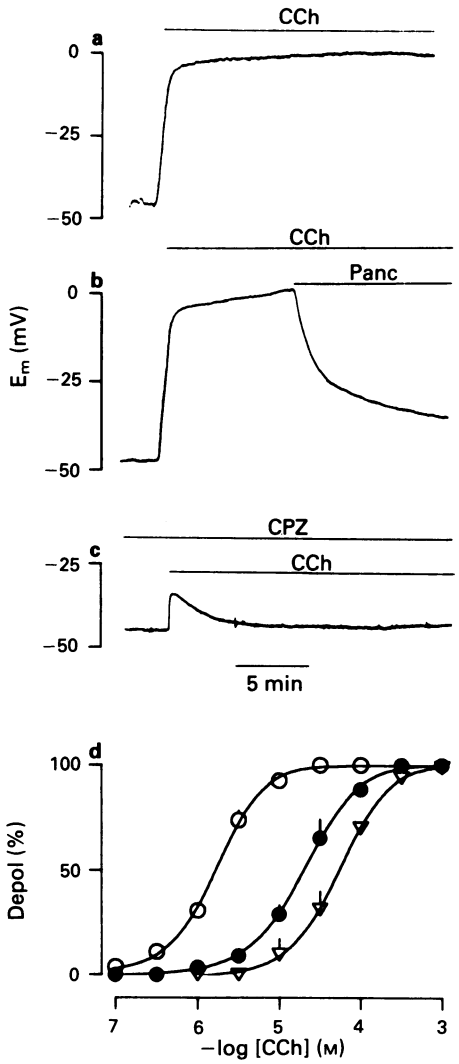

Figure 1 The acute effect of carbachol (CCh) on membrane potential (E_m) of C2C12 myotubes under different experimental conditions. (a) Recording of the sustained depolarization evoked by carbachol (10 μM; horizontal bar); (b) the antagonistic effect of pancuronium (Panc, 1 μM; horizontal bar); (c) use-dependent block by chlorpromazine (CPZ, 1 μM); (d) concentration-effect curve of carbachol (○; $n = 6$) and in the presence of pancuronium (0.3 μM, ●; $n = 4$) and (1 μM, ▽; $n = 4$). Data (± s.e.mean) are expressed as the percentage of the maximal depolarization (43.4 ± 2.2 mV; $n = 6$).

Membrane potential: long-term effects of carbachol

The effect of chronic stimulation of the nicotinic AChRs was studied by treatment of the C2C12 myotubes for several days with carbachol and assessed by measuring their membrane potential in the absence of the agonist (≥ 15 min). Non-treated myotubes possessed a relative small membrane potential of about −46 mV and inhibition of Na^+/K^+-pumping by ouabain (200 μM) resulted in a minor reduction of their

Table 1 The effect of long-term stimulation of nicotinic acetylcholine receptors (AChRs) on membrane potential of C2C12 myotubes

	Incubation	*After washing*			
Treatment	E_m† (mV)	E_m (mV)	E_m (Ouab) (mV)	V_{el} (mV)	n
None	− 46.2 ± 1.5	− 45.7 ± 0.6	− 43.5 ± 0.8	− 1.2 ± 1.0	30
Carbachol	− 8.4 ± 2.2	− 55.8 ± 1.3*	− 45.4 ± 1.4	− 10.4 ± 1.9*	12
Carbachol/CPZ	− 54.6 ± 2.9	− 52.9 ± 1.3*	− 44.1 ± 1.3	− 8.8 ± 1.8*	12
High K^+	− 13.7 ± 3.3	− 42.6 ± 1.3	− 44.6 ± 0.5	− 2.0 ± 1.4	12

Cells had been incubated for 4 days in the presence of carbachol (10 μM), the combination of carbachol (10 μM) and chlorpromazine (CPZ; 1 μM) or high K^+ (40 mM) medium; membrane potential was measured by the intracellular microelectrode technique. E_m† represents the membrane potential still in the presence of drugs or high K^+ ($n = 4$). After washing, the membrane potential was determined in the absence (E_m) and in the presence of ouabain (200 μM; E_m (Ouab)) to calculate electrogenic Na^+/K^+-pumping (V_{el}). Values are expressed as mean ± s.e.mean of n experiments.
*Significantly different from non-treated cells, $P < 0.01$.

membrane potential (1.2 mV; Table 1; Figure 2a). Myotubes incubated for 4 days with carbachol (10 μM) maintained their depolarization in the presence of the agonist (Table 1). However, after removing carbachol (10 μM), the myotubes showed a pronounced increase in membrane potential of about − 10 mV compared to non-treated cells (Table 1; Figure 2a,b). Inhibition of Na^+/K^+-ATPase in carbachol-treated myotubes by ouabain (200 μM) caused a significantly higher reduction in membrane potential than in non-treated cells (Figure 2a,b; Table 1). The membrane potential of non-treated and carbachol-treated cells reached comparable values in the presence of ouabain (Figure 2a,b; Table 1). The enhanced Na^+/K^+-ATPase activity induced by carbachol (10 μM) developed gradually during the 4 days treatment and declined slowly after withdrawal of the nicotinic AChR agonist (Figure 2c,d). Carbachol treatment for 4 days produced a concentration-dependent increase in electrogenic Na^+/K^+-pumping ($EC_{50} = 5.3$ μM; Figure 2e), at similar concentrations to those observed in acute experiments (Figure 1d).

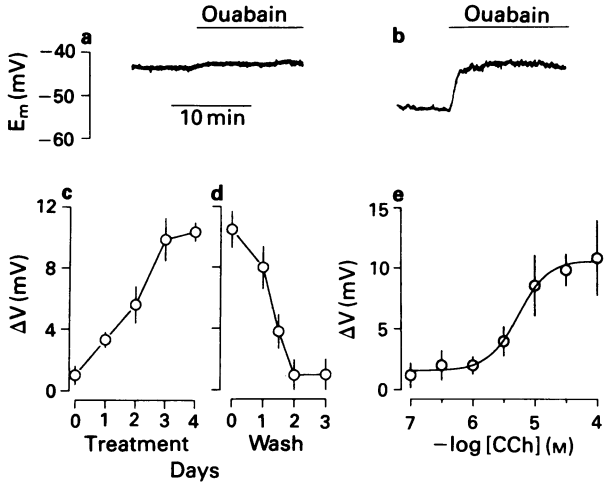

Figure 2 The effect of 4 days treatment of the cells with carbachol (10 μM) on membrane potential and electrogenic Na^+/K^+-pumping in C2C12 myotubes, measured in the absence of carbachol. (a) The membrane potential of non-treated cells showed a small reduction upon inhibition of electrogenic pumping with ouabain (200 μM; horizontal bar); (b) treated cells showed a pronounced decrease in membrane potential in the presence of ouabain (200 μM); (c) the development of electrogenic pumping in time during carbachol treatment; (d) the decline of electrogenic pumping in time after washing 4 days carbachol treated cells; (e) concentration-effect curve of the amount of electrogenic pumping after 4 days of treatment with various concentrations of carbachol (0.1–100 μM). Values (± s.e. mean) are expressed as the difference between membrane potential in the absence and presence of ouabain (200 μM; $n \geq 12$).

To assure that the development of enhanced Na^+/K^+-ATPase activity was mediated by nicotinic AChRs, myotubes were treated with carbachol (4 days) in the presence of identical concentrations of selective antagonists. Myotubes simultaneously treated with carbachol (10 μM) and the nicotinic AChR antagonist, pancuronium (1 μM) possessed the same membrane potential (− 46.8 ± 1.7 mV; $n = 10$) as non-treated or pancuronium-treated myotubes. Pancuronium-treated myotubes showed the same membrane potential as non-treated cells (− 45.0 ± 2.9; $n = 6$). In contrast, the muscarinic antagonist, atropine (1 μM) did not prevent the increase in Na^+/K^+-pumping of myotubes as observed in cells treated for 4 days with carbachol (10 μM). A similar increase in membrane potential (10.1 ± 2.0 mV; $n = 12$) as in carbachol-treated myotubes was observed in the presence of ouabain (200 μM).

The development of enhanced Na^+/K^+-ATPase activity in long-term carbachol-stimulated myotubes might be due to the Na^+-influx passing the receptor coupled ion-channel. This was investigated in myotubes treated for 4 days with carbachol and chlorpromazine, inhibiting the nicotinic AChR coupled Na^+-influx (Figure 1c). In the presence of chlorpromazine, the carbachol-stimulated nicotinic AChR-channel was completely blocked, as demonstrated by the observation that the membrane potential of cells, treated for 4 days with carbachol (10 μM) and chlorpromazine (1 μM), still in the presence of both drugs (− 54.6 mV; Table 1), did not change after withdrawal of carbachol (− 51.6 ± 1.2 mV; $n = 8$). After removing both drugs, myotubes treated with a combination of carbachol (10 μM) and chlorpromazine (1 μM) showed an increase in membrane potential comparable to that of long-term carbachol-treated cells (Table 1). Long-term treatment of the myotubes with chlorpromazine alone did not change the membrane potential (− 44.0 ± 2.4 mV; $n = 10$) compared to non-treated cells. Inhibition of the Na^+/K^+-ATPase by ouabain (200 μM) of cells treated with carbachol (10 μM) and chlorpromazine (1 μM), caused a pronounced increase in membrane potential, as found in myotubes treated with carbachol alone (Table 1).

To investigate whether the development of Na^+/K^+-ATPase activity was related to the maintained depolarization of carbachol-treated myotubes, the effect of high K^+ medium (40 mM; 4 days) was investigated. At the end of the incubation period, myotubes showed a depolarization of 32.5 mV still in the presence of high K^+ (40 mM) (Table 1). Changing to normal conditions after the high K^+ treatment produced a normal membrane potential as observed in non-treated cells, not significantly affected by ouabain (200 μM; Table 1).

Na^+/K^+-ATPase up-regulation

Ouabain binding The nature of the development of enhanced Na^+/K^+-ATPase activity in carbachol-treated myotubes was investigated by determination of [^{3}H]-ouabain binding in the myotubes. Non-treated myotubes possessed a high-affinity site (Figure 3a, Table 2). In myotubes treated with carbachol (10 μM) or a combination of carbachol and chlorpromazine

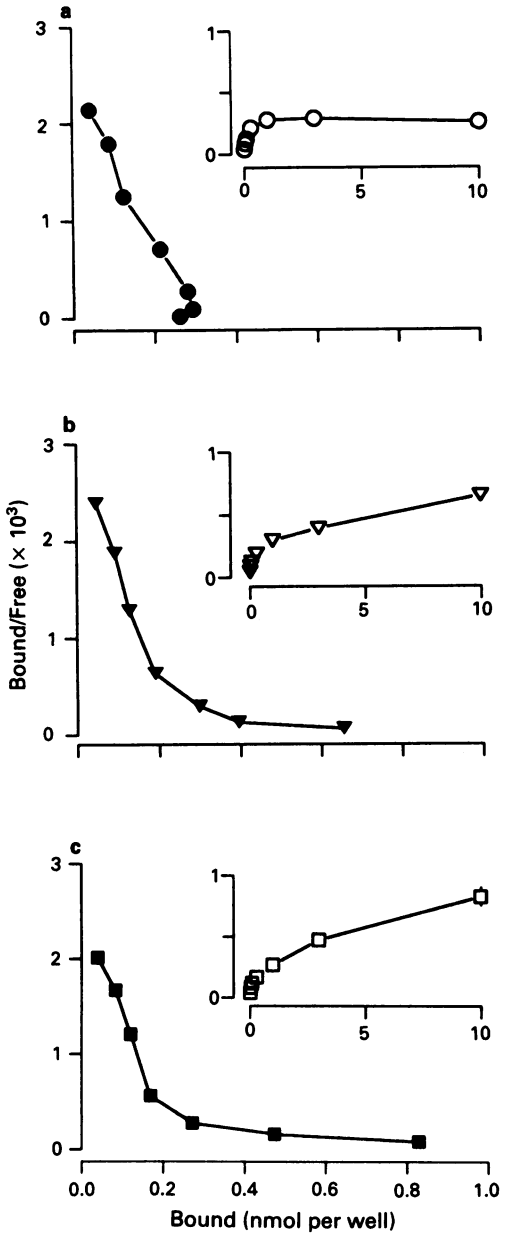

Figure 3 The effect of carbachol treatment of cells on ouabain binding represented by Scatchard plots and saturation binding curves (inserts). (a) A single high-affinity binding site was found in non-treated cells; (b) an additional low-affinity binding site was analysed after 4 days treatment with carbachol (10 μM); (c) a high-affinity as well as a low-affinity binding site was also observed after 4 days treatment with carbachol (10 μM) and chlorpromazine (1 μM). Inserts: abscissae represent ouabain concentration (μM), ordinates represent specific binding (nM); data are expressed as mean ± s.e.mean. Binding parameters are provided in Table 2.

Table 3 The effect of treatment (4 days) with carbachol (10 μM) on Na^+/K^+-ATPase-antibody binding in C2C12 myotubes

	Absorbance (× 100)	
	Control	*Carbachol*
McK1	22.1 ± 1.5	32.2 ± 1.1*
McB2	22.9 ± 1.7	32.2 ± 1.4*

Values are expressed as mean ± s.e.mean of the absorbance of 497 nm in areas of 0.04 mm^2. Data are pooled across 20 series of 100 measurements each.
*$P < 0.01$.

(1 μM), both possessing increased electrogenic Na^+/K^+-pumping, the ouabain binding was characterized by two sites ($P < 0.005$). Besides the high-affinity site (nM range) also found in non-treated myotubes, an additional low-affinity site (μM range) was present (Figure 3b,c; Table 2). The appearance of the low-affinity site accounted for a 4–5 fold increase in the total number of ouabain binding sites in myotubes treated with carbachol (10 μM) or a combination of carbachol and chlorpromazine (1 μM)-treated myotubes (Table 2).

Antibody binding To obtain a more specific characterization of the increase in Na^+/K^+-ATPase activity of carbachol-treated myotubes, binding of two monoclonal antibodies was studied, i.e. McK1 (Felsenfeld & Sweadner, 1988) and McB2 (Urayama *et al.*, 1989) directed against α_1- or α_2-subunits of Na^+/K^+-ATPase, respectively. Both antibodies stained the myotubes intracellularly and at the plasma membrane (not shown). Incubation of the myotubes for 4 days with carbachol (10 μM) caused an increase in staining intensity of about 45% for both antibodies compared to non-treated myotubes (Table 3).

Discussion

The results presented here show that long-term treatment of C2C12 myotubes with carbachol, measured in the absence of the agonist, induced a concentration-dependent increase in membrane potential of C2C12 myotubes, caused by an increased Na^+/K^+-ATPase activity, accompanied by an increased binding of ouabain and Na^+/K^+-ATPase directed antibodies. The carbachol-induced increase in Na^+/K^+-ATPase activity was abolished in the presence of pancuronium, but not by atropine at an equal concentration. Therefore, pancuronium showed a greater potency in antagonizing the carbachol-induced response than atropine, demonstrating that the carbachol-induced increase in Na^+/K^+-ATPase activity was mediated by nicotinic rather than muscarinic AChRs (Buckett *et al.*, 1968). It is unlikely that nicotinic AChR-mediated enhancement of Na^+/K^+-ATPase activity is caused by the depolarization of the myotubes, as long-term incubation in high K^+ medium failed to induce an excess Na^+/K^+-ATPase activity. Intracellular Na^+ might represent the mechanism responsible for the induction of

Table 2 The effect of long-term stimulation of nicotinic acetylcholine receptors (AChRs) on ouabain binding in C2C12 myotubes

Treatment	n	K_{d1} (nM)	K_{d2} (μM)	B_{max1} (fmol per well)	B_{max2} (fmol per well)
None	5	119 ± 11	–	296 ± 10	–
Carbachol	5	79 ± 14	13 ± 5*	227 ± 27	983 ± 35
Carbachol/CPZ	3	56 ± 8	10 ± 2*	160 ± 14	1330 ± 125

Cells had been incubated for 4 days in the presence of carbachol (10 μM) or the combination of carbachol (10 μM) and chlorpromazine (CPZ; 1 μM). [^{3}H]-ouabain binding was measured after extensive washing of the drugs and is represented by the affinity (K_{d1}, K_{d2}) and the number of associated binding sites (B_{max1}, B_{max2}). Values are expressed as mean ± s.e.mean of n experiments.
*Represents the preference of a two-site binding model over a one-site model (F-test, $P < 0.001$).

Na^+/K^+-ATPase activity in carbachol-stimulated C2C12 myotubes. In chick myotubes, long-term treatment with veratridine to activate voltage-operated Na^+-channels, up-regulated Na^+/K^+-ATPase by increasing synthesis of the β-subunit of the enzyme for 24 h (Taormino & Fambrough, 1990), followed by a decrease of the Na^+/K^+-ATPase degradation rate (Wolitzky & Fambrough, 1986). However, it seems unlikely that an increase in nicotinic AChR-mediated intracellular Na^+ is responsible for the increase in Na^+/K^+-ATPase activity of carbachol-stimulated C2C12 myotubes, as carbachol-stimulated myotubes still developed enhanced Na^+/K^+-ATPase activity and increased ouabain binding in the presence of the nicotinic AChR ion-channel blocking agent, chlorpromazine. That different mechanisms are involved in the carbachol and veratridine induction of Na^+/K^+-ATPase activity is supported by the time-course of the action of carbachol, being 3–4 fold longer than in veratridine-stimulated myotubes. These results show that the nicotinic AChR is not only a classical ligand-operated ion-channel (Changeux, 1990), but also regulates long-term cellular processes.

The development of enhanced Na^+/K^+-ATPase activity in carbachol-stimulated myotubes was accompanied by an increase of ouabain binding and an enhanced binding of monoclonal antibodies directed against the α_1- and the α_2-subunit of the Na^+/K^+-ATPase. These results suggest that the increase in Na^+/K^+-ATPase activity of nicotinic AChR-stimulated myotubes is due to an increase in the number of Na^+/K^+-ATPase sites. An attempt to study involvement of *de novo* synthesis of Na^+/K^+-ATPase by incubating the carbachol-treated myotubes in the presence of chlorheximide (1 $\mu g\ ml^{-1}$) was obstructed because of detachment of the cells within 48 h. The development of the low-affinity binding site accounted for the increase in total ouabain binding. The existence of multiple ouabain binding sites has been attributed to the expression of different isozymes of the Na^+/K^+-ATPase α-subunit at the plasma membrane (Sweadner, 1989). In contrast, the development of a specific ouabain binding site in carbachol-treated myotubes was accompanied by an equal increase in binding of antibodies directed against the α_1- or α_2-subunit of the Na^+/K^+-ATPase. This contradiction might be explained by the ability of the antibodies to bind to plasma membrane as well as to intracellular Na^+/K^+-ATPase, thus being unable to detect α-subunit specific Na^+/K^+-ATPase at the plasma membrane. Moreover, development of the low-affinity ouabain binding site might be dependent on mechanisms other than regulation of α-subunit incorporation, such as e.g. phosphorylation of Na^+/K^+-ATPase subunits (Vasilets *et al.*, 1990; Chibalin *et al.*, 1992). Nevertheless, although the precise molecular mechanism increasing the Na^+/K^+-ATPase binding in C2C12 cells is poorly understood, our study clearly demonstrates that long-term stimulation of nicotinic AChRs results in an up-regulation of Na^+/K^+-ATPase binding sites.

In view of the observation that the increased Na^+/K^+-ATPase activity in carbachol-treated C2C12 myotubes is independent of ion-transport, nicotinic AChR-mediated activation of a second messenger system should be considered. So far, stimulation of nicotinic AChRs has been shown to activate the phospholipase C (PLC) route, inducing formation of inositol(1,4,5)trisphosphate and mobilization of Ca^{2+} from internal stores in C2C12 myotubes (Grassi *et al.*, 1993). The regulation of *Xenopus* oocyte Na^+/K^+-ATPase by protein kinase C (Vasilets *et al.*, 1990), which is activated by the PLC route, suggests that the contribution of the PLC route in the induction of Na^+/K^+-ATPase activity in long-term nicotinic AChR-stimulated myotubes needs further attention.

Thus, long-term stimulation of nicotinic AChRs induced an adaptive response in C2C12 myotubes, represented by an increase in Na^+/K^+-ATPase activity and a concomitant increase in membrane potential. In this respect, long-term stimulation of nicotinic AChRs of non-contracting C2C12 myotubes serves as a model of innervation of skeletal muscle (Berg & Hall, 1975; Chang *et al.*, 1975; Mathers & Thesleff, 1978; Pestronk *et al.*, 1980). Further studies examining the involvement of nicotinic AChRs in the regulation of other innervation-related properties of skeletal muscle (Pestronk *et al.*, 1980; Rogart & Regan, 1985) are in progress.

In summary, we have shown that long-term activation of nicotinic AChRs in C2C12 myotubes increases the membrane potential by augmentation of electrogenic Na^+/K^+-pumping. This increase in Na^+/K^+-ATPase activity is associated with the appearance of an additional low-affinity [^{3}H]-ouabain binding site and an increase in binding of antibodies specific for α_1- and α_2-subunits of the enzyme. Consequently, this study exposes the apparent ability of ligand-operated nicotinic AChRs to mediate adaptive responses of the cell upon chronic receptor activation.

Monoclonal antibodies McK1 and McB2 were a generous gift of Dr K.J. Sweadner. The assistance of A. Pasma and Dr G.J. ter Horst with the antibody staining is gratefully acknowledged. This study was partly sponsored by grant 900-549-133 from The Netherlands Organisation for Scientific Research (NWO).

References

BERG, D.K. & HALL, Z.W. (1975). Increased extrajunctional acetylcholine sensitivity produced by chronic post-synaptic neuromuscular blockade. *J. Physiol.*, **244**, 659–676.

BUCKETT, W.R., MAJORIBANKS, C.E.B., MARWICK, F.A. & MORTON, M.B. (1968). The pharmacology of pancuronium bromide (Org. Na 97), a new potent steroidal neuromuscular blocking agent. *Br. J. Pharmacol. Chemother.*, **32**, 671–679.

CHANG, C.C., CHUANG, S.T. & HUANG, M.C. (1975). Effects of chronic treatment with various neuromuscular blocking agents on the number and distribution of acetylcholine receptors in the rat diaphragm. *J. Physiol.*, **250**, 161–173.

CHANGEUX, J.P. (1990). The nicotinic acetylcholine receptor: an allosteric protein prototype of ligand-gated ion channel. *Trends Pharmacol. Sci.*, **11**, 485–492.

CHIBALIN, A.V., VASILETS, L.A., HENNEKES, H., PRALONG, D. & GEERING, K. (1992). Phosphorylation of Na,K-ATPase α-subunits in microsomes and in homogenates of *Xenopus* oocytes resulting from the stimulation of protein kinase A and protein kinase C. *J. Biol. Chem.*, **267**, 22378–22384.

DRACHMAN, D.B. & WITZKE, F. (1972). Trophic regulation of acetylcholine sensitivity of muscle: effect of electrical stimulation. *Science*, **176**, 514–516.

FELSENFELD, D.P. & SWEADNER, K.J. (1988). Fine specificity mapping and topography of an isozyme-specific epitope of the Na,K-ATPase catalytic subunit. *J. Biol. Chem.*, **263**, 10932–10942.

GRASSI, F., GIOVANNELLI, A., FUCILE, S. & EUSEBI, F. (1993). Activation of the nicotinic acetylcholine receptor mobilizes calcium from caffeine-insensitive stores in C2C12 mouse myotubes. *Pflügers Arch.*, **422**, 591–598.

HENNING, R.H., NELEMANS, S.A., VAN DEN AKKER, J. & DEN HERTOG, A. (1992). The nucleotide receptors on mouse C2C12 myotubes. *Br. J. Pharmacol.*, **106**, 853–858.

HOGUE, C.W., WARD, J.M., ITANI, M.S. & MARTYN, J.A.J. (1992). Tolerance and upregulation of acetylcholine receptors follow chronic infusion of *d*-tubocurarine. *J. Appl. Physiol.*, **72**, 1326–1331.

MATHERS, D.A. & THESLEFF, S. (1978). Studies on neurotrophic regulation of murine skeletal muscle. *J. Physiol.*, **282**, 105–114.

MUNSON, P.J. & RODBARD, D. (1980). LIGAND: a versatile computerized approach for characterization of ligand-binding systems. *Annal. Biochem.*, **107**, 220–225.

PESTRONK, A., DRACHMAN, D.B. & GRIFFIN, J.W. (1976). Effect of botulinum toxin on trophic regulation of acetylcholine receptors. *Nature*, **264**, 787–789.

PESTRONK, A., DRACHMAN, D.B., STANLEY, E.F., PRICE, D.L. & GRIFFIN, J.W. (1980). Cholinergic transmission regulates extrajunctional acetylcholine receptors. *Exp. Neurol.*, **70**, 690–696.

ROGART, R.B. & REGAN, L.J. (1985). Two subtypes of sodium channel with tetrodotoxin sensitivity and insensitivity detected in denervated mammalian skeletal muscle. *Brain Res.*, **329**, 314–318.

SIMPSON, L.L. (1977). The effects of acute and chronic botulinum toxin treatment on receptor number, receptor distribution and tissue sensitivity in rat diaphragm. *J. Pharmacol. Exp. Ther.*, **200**, 343–351.

SWEADNER, K.J. (1989). Isozymes of Na^+/K^+-ATPase. *Biochim. Biophys. Acta*, **988**, 185–220.

TAORMINO, J.P. & FAMBROUGH, D.M. (1990). Pre-translational regulation of the (Na^+/K^+)-ATPase in response to demand for ion transport in cultured chicken skeletal muscle. *J. Biol. Chem.*, **265**, 4116–4123.

URAYAMA, O., SHUTT, H. & SWEADNER, K.J. (1989). Identification of three isozyme proteins of catalytic subunit of the Na,K-ATPase in rat brain. *J. Biol. Chem.*, **264**, 8271–8280.

VASILETS, L.A., SCHMALZING, G., MÄDEFESSEL, K., HAASE, W. & SCHWARTZ, W. (1990). Activation of protein kinase C by phorbol ester induces downregulation of the Na^+/K^+-ATPase in oocytes of Xenopus laevis. *J. Membr. Biol.*, **118**, 131–142.

WOLITZKY, B.A. & FAMBROUGH, D.M. (1986). Regulation of the (Na^+/K^+)-ATPase in cultured chick skeletal muscle. *J. Biol. Chem.*, **261**, 9990–9999.

WOLTERS, G.H.J., PASMA, A., WIEGMAN, J.B. & KONIJNENDIJK, W. (1984). Glucose-induced changes in histochemically determined Ca^{2+} in B-cell granules, ^{45}Ca uptake, and total Ca^{2+} of rat pancreatic islets. *Diabetes*, **33**, 409–414.

YAFFEE, D. & SAXEL, O. (1977). Serial passage and differentiation of myogenic cells isolated from dystrophic mouse muscle. *Nature*, **270**, 725–727.

(Received July 30, 1993
Revised October 5, 1993
Accepted October 12, 1993)

Br. J. Pharmacol. (1994), **111**, 465–468

α_1-Adrenoceptors in the conduction system of rat hearts

[1]Kazuto Saito, *Tetsuro Suetsugu, *Yoshiya Oku, *Atsushi Kuroda & *Hiromitsu Tanaka

Health Service Center, National Institute of Fitness and Sports, 1-Shiromizu, Kanoya City, Kagoshima 891-23, Japan and *First Department of Internal Medicine, Faculty of Medicine Kagoshima University, 8-35-1 Sakuragaoka, Kagoshima City, Kagoshima 890, Japan

1 We have characterized α_1-adrenoceptor in the conduction systems of the rat heart by quantitative autoradiography.

2 Consecutive 20 μm thick sections from a single rat heart containing the sinoatrial (SA) node and atrioventricular (AV) node were incubated with increasing concentrations of [^{3}H]-prazosin with or without 10 μM phentolamine. After exposure to ^{3}H-Ultrofilm, optical densities corresponding to the SA node and AV node were determined by computerized densitometry after comparison with ^{3}H standards.

3 The SA node and AV node were stained heavily for cholinesterase and they contained a higher concentration of α_1-adrenoceptors than the adjacent myocardium without a significant change in the affinity.

4 These results support the hypothesis that α_1-adrenoceptors may play an important role not only in inotropism but also in chronotropism of rat hearts.

Keywords: α_1-Adrenoceptors; sinoatrial node; atrioventricular node; autoradiography; rat heart

Introduction

The question of whether α_1-adrenoceptors can mediate a chronotropic response is still not clearly resolved. Several studies have demonstrated a negative chronotropic action of catecholamines mediated through α-adrenoceptor stimulation in canine cardiac Purkinje fibres (Posner *et al.*, 1976), in human right atrial specialized fibres (Rabine *et al.*, 1978), and in the right atria of rabbits (Dukes *et al.*, 1984). However, Wagner & Brodde (1978) and Brown & Carpentier (1988) have failed to show such an action in guinea-pigs. On the contrary, several authors have reported that α-adrenoceptor stimulation results in a positive chronotropic action in rat hearts (Flavahan & McGrath, 1981; Tung *et al.*, 1985).

The concentration of β-adrenoceptors is high in the specialized cardiac conduction system in comparison with the working myocardium (Saito *et al.*, 1988; 1989; Molenaar *et al.*, 1990). In this study, we attempted to determine whether α_1-adrenoceptors were present in the specialized cardiac conduction system of rat hearts.

The sinoatrial (SA) node and atrioventricular (AV) node of rats are not easily isolated by dissection, and sufficient amounts of materials for membrane ligand studies are difficult to obtain. For these reasons, we used quantitative autoradiographic techniques with [^{3}H]-prazosin.

Methods

Male Wistar rats, 8-weeks old, were kept under normal laboratory conditions with light on from 06 h 00 min to 18 h 00 min and access to water and rat chow *ad libitum*. After overnight fasting, animals were anaesthetized with ethyl ether and the heart were removed immediately and placed in 3 mM HEPES buffer, pH 7.4, containing (mM): NaCl 140, KCl 5, $MgCl_2$ 1, $CaCl_2$ 1.5 and glucose 11 at 4°C. The areas containing the SA node and AV node were dissected as previously described (Saito *et al.*, 1988; 1989).

Holding up the right atrial appendage with a small forceps, the right atrium including the junctional area to the superior vena cava was cut out, frozen by immersion in isopentane at −30°C. The wall of right ventricle was cut open to expose the area containing the attachment of the tricuspid valve and interatrial and interventricular septa. The area corresponding to both septa, between the coronary sinus and the aorta, was removed under a dissecting microscope. The tissue was frozen immediately by immersion in isopentane and was then stored at −70°C for no longer than 7 days.

Frozen tissues were cut into 20 μm-thick sections in a cryostat at −20°C. Using light microscopy, we identified the SA and AV node in tissue sections stained with sodium hydrogen maleate buffer (65 mM) containing acetylcholine iodide (2 mM), sodium citrate (5 mM), copper sulphate (3 mM) and potassium ferricyanide (0.5 mM) to detect cholinesterase activity (Karnovsky, 1964). Adjacent unstained sections containing the SA and AV node were thaw-mounted onto gelatin-coated glass slides and placed under vacuum at 4°C for no longer than 24 h before incubation.

Unstained sections were incubated for 15 min at room temperature in Tris-buffer (50 mM), pH 7.4 containing $MgCl_2$ (10 mM) and phenylmethylsulphonylfluoride (10 μM). To determine the number of α_1-adrenoceptors from 5 rats, we labelled tissue sections *in vitro* by incubation for 120 min at room temperature in fresh buffer containing [^{3}H]-prazosin (Amersham, specific activity 76.2 Ci mmol^{-1}) in concentrations ranging from 0.03 to 2 nM. Non-specific binding was measured by incubating alternate sections under the same conditions with addition of 10 μM phentolamine (Sigma).

Autoradiography

After incubation, the sections were rinsed in 50 mM Tris-buffer, pH 7.4, followed by two washes of 10 min each in the same buffer and a 30 s rinse in cold distilled water. The sections were then dried under a stream of cold air, placed in X ray cassettes together with ^{3}H-standards, and exposed to Ultrofilm (LKB Industries, Rockville, MD, U.S.A.) for two months. The films were then processed as previously described (Saito *et al.*, 1988). Sets of ^{3}H-standards were prepared as described by Unnerstall *et al.* (1982). Known amounts of increasing concentrations of [^{3}H]-prazosin were thoroughly mixed with heart paste, placed as blocks of tissue on microtome specimen holders, and frozen on dry ice. Tissue sections, 20 μm thick, were cut in a cryostat at −20°C and thaw-mounted onto gelatin-coated glass slides. Parallel sets of standards obtained from consecutive sections were used

[1] Author for correspondence.

for determination of protein concentrations (Lowry et al., 1951) and radioactivity.

Data analysis

Using a computer mouse to outline the area, we measured the optical densities by computerized microdensitometry (MCID, Imagining Research Inc., Canada) in the area corresponding to the conduction system stained heavily for cholinesterase. The computer automatically averaged the values, and then converted the value of the optical densities to the concentration of radioactivity, based on a comparison with the standard curve (Unnerstall et al., 1982).

Scatchard plots of [^{3}H]-prazosin binding at 7 concentrations (0.03–2 nM) were analysed using the LIGAND computer programme to determine the density of binding sites and the affinity of the receptor for the radioligand (Munson & Rodbard, 1980).

All data are expressed as mean ± s.e.mean. Differences were evaluated by Student's t test, and $P<0.05$ was considered statistically significant.

Results

The SA node was localized in the sections containing SA node artery and stained heavily for cholinesterase (Figure 1a). We measured the optical density that corresponded to α_1-adrenoceptor binding in the area surrounding the SA node artery and detected a high concentration of [^{3}H]-prazosin binding sites (Figure 1b) with lower concentrations in the right atrium.

Our results demonstrated a single population of saturable high affinity binding sites with averaged maximum binding capacities (B_{max}) of 61.6 ± 1.6 fmol mg^{-1} protein and 116.7 ± 6.6 fmol mg^{-1} protein for right atrium and SA node, respectively ($P<0.01$) without significant changes in the dissociation constants (K_d). A typical example is shown in Figure 2.

We also found the area stained heavily for cholinesterase localized to the border between the interatrial and interventricular septa (Figure 3a). Unfortunately we could not differentiate between the atrioventricular node and the His bundle; we, therefore, measured the density corresponding to α_1-adrenoceptor binding in that area as the A-V conduction system. We detected a high concentration of [^{3}H]-prazosin binding sites in the A-V conduction system with low concentrations in the interventricular septa (Figure 3b). The left and right bundle branch also contained a high concentration of [^{3}H]-prazosin binding sites in comparison with the interventricular septum (Figure 3b). Scatchard analysis of [^{3}H]-prazosin binding to the A-V conduction system also showed a single population of saturable high affinity binding sites. The mean value of K_d and B_{max} in the interventricular septa, A-V conduction system, right atrium and SA node are shown in Table 1. The value of B_{max} both in the SA node and the A-V conduction system was significantly higher than in the

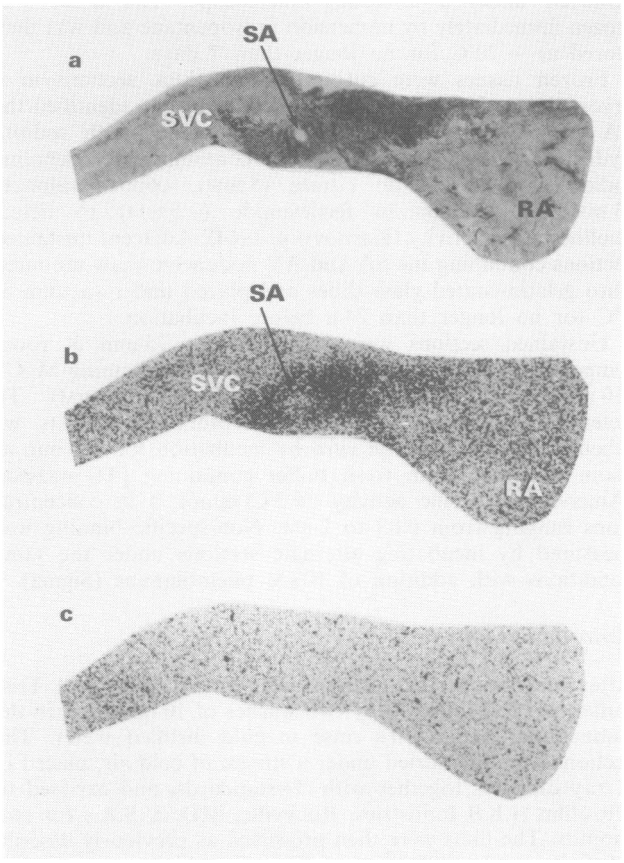

Figure 1 Autoradiographic localization of α_1-adrenoceptors in the rat sinoatrial node. (a) Cholinesterase staining of the sinoatrial node and right atrium of the rat heart. (b) total [^{3}H]-prazosin binding. The section was incubated in the presence of 1 nM [^{3}H]-prazosin as described in Methods. (c) Nonspecific binding. The section was incubated as in (b) with addition of 10 μM phentolamine. SA: sinoatrial node; SVC: superior vena cava; RA: right atrium.

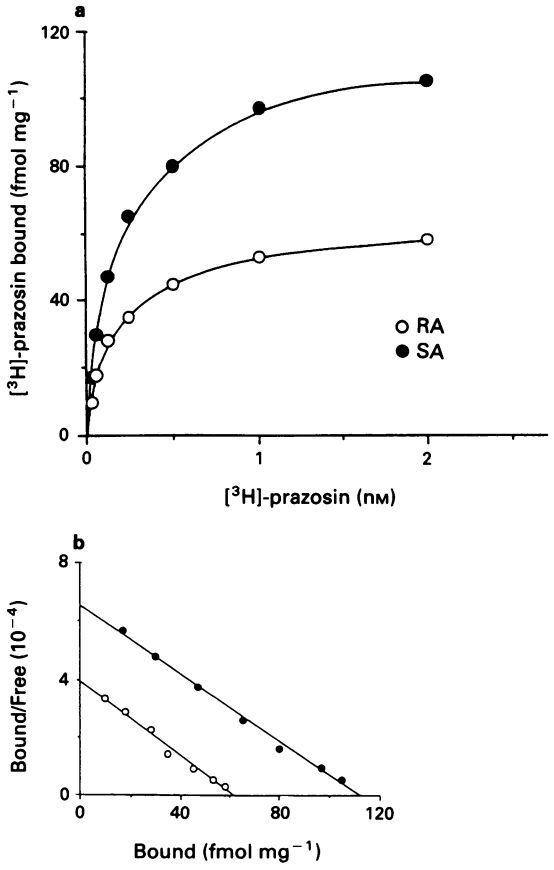

Figure 2 Specific [^{3}H]-prazosin binding to sinoatrial node sections from a rat heart. Saturation curve (a) and Scatchard analysis (b). Sections were incubated with increasing concentrations of [^{3}H]-prazosin with and without 10 μM phentolamine, as described in Methods. The figure represents a typical example. In this example, B_{max} was 111.5 and 60.4 fmol mg^{-1} protein and K_d was 170 and 152 pM for sinoatrial node (●) and right atrium (○), respectively.

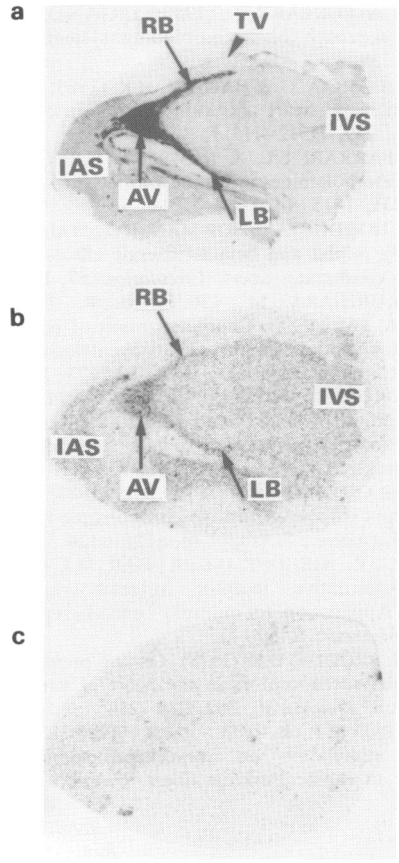

Figure 3 Autoradiographic localization of α_1-adrenoceptors in the rat atrioventricular conduction system. (a) Cholinesterase staining of the atrioventricular conduction system and interseptal area of a rat heart. (b) Total [^{3}H]-prazosin binding. The section was incubated in the presence of 0.25 nM [^{3}H]-prazosin as described in Methods. (c) Nonspecific binding. The section was incubated as in (b) with the addition of 10 μM phentolamine. AV: atrioventricular conduction system; IAS: interatrial septum; IVS: interventricular septum; LB: left bundle branch; RB: right bundle branch.

interventricular septum and the right atrium ($P<0.01$), but there was no significant difference in the K_d value among these areas.

Discussion

In this study, we demonstrated specific [^{3}H]-prazosin binding sites in the specialized conduction system of rat hearts. Both the SA node and AV node had a higher concentration of [^{3}H]-prazosin binding sites than that of the surrounding myocytes.

Tissue quenching of radioisotope energy in quantitative receptor autoradiography with tritiated ligands is one factor linked to the failure to attain precise quantitation of receptors in myelin-rich areas such as brain white matter (Herkenham & Sokoloff, 1984). However, cardiac tissues are innervated by un-myelinated nerve fibres (Chiba & Yamauchi, 1970; Levy & Martin, 1979), therefore, quenching was not taken into consideration in the present study. Our results do not allow us to determine the specific cellular localization of

Table 1 Characterization of α_1-adrenoceptors in specific areas of rat hearts

Area	B_{max} (fmol mg^{-1})	K_d (pM)
Right atrium	61.6 ± 1.6	177 ± 16
Sinotrial node	116.7 ± 6.6	182 ± 15
Interventricular septum	50.4 ± 2.7	116 ± 20
Atrioventricular conduction system	114.5 ± 3.9	175 ± 17

Values are means ± s.e.mean for 5 hearts.

all the α_1-adrenoceptors in the conduction system. Some α_1-adrenoceptors could be localized in blood vessels or connective tissue within the area. However, a significant increase in α_1-adrenoceptor in the conduction system may be predominantly due to specific conduction cells, because nerve terminals within this area contain almost exclusively α_2-adrenoceptors (Langer, 1980) and the arteriole wall contains less α_1-adrenoceptors than do myocytes (Muntz *et al.*, 1985).

The effect of α_1-adrenoceptor stimulation on heart rate is different in various experimental animal species. Posner *et al.* (1976) have demonstrated a negative chronotropic action of low concentration of adrenaline (10^{-11} through 10^{-7} M) in the presence of β-adrenoceptor blockade in canine cardiac Purkinje fibres. Rabine *et al.* (1978) have also shown the same results in human specialized atrial fibres. In both instances, the negative chronotropic effects were blocked by phentolamine. However, Brown & Carpentier (1988) have reported that noradrenaline did not have an α-mediated action on automaticity of the guinea-pig sinus node preparations, but it did prolong the action potential duration through α_1-adrenoceptor stimulation, and they suggested that the conflicting results regarding the effects of α-adrenoceptor stimulation in the heart appear to be due to differences in the number and/or affinity of receptors in different species. Conflicting with these results, it has also been reported that α-adrenoceptor stimulation results in positive chronotropic action in rat hearts (Tung *et al.*, 1985).

This different effect of α_1-adrenoceptor stimulation on heart rate in various experimental animal species may be due to a difference in the coupling process subsequent to agonist binding to the myocardial α_1-adrenoceptor and/or the presence of α_1-adrenoceptors in the conduction cells.

Zaza *et al.* (1990) have studied the negative chronotropic action of α_1-adrenoceptor stimulation in adult canine Purkinje fibres using sodium selective microelectrodes and reported that α_1-adrenoceptors are coupled to the activation of the Na-K pump; therefore, this could cause a fall in intracellular sodium ion which could reduce intracellular calcium ion via Na^+-Ca^{2+} exchange. This action is closely related to its negative chronotropic action. However, Endo *et al.* (1991) have demonstrated that an acceleration of phosphatidylinositol metabolism and positive inotropic action in response to the activation of α_1-adrenoceptor stimulation occurred in rat hearts. The same mechanism could be involved in the rat cardiac conduction system, because Tung *et al.* (1985) have shown a positive chronotropic response induced by α_1-adrenoceptor stimulation in rat isolated atria.

Further studies need to characterize the α_1-adrenoceptor in the conduction system of several animal species.

In conclusion, our findings support the evidence that α_1-adrenoceptors may play an important role in the regulation of cardiac chronotropic activity in rat hearts.

References

BROWN, R.A. & CARPENTIER, R.G. (1988). Alpha-adrenoceptor-mediated effects of norepinephrine on the guinea pig sinus node. *J. Electrocardiol.*, **21**, 213–217.

CHIBA, T. & YAMAUCHI, A. (1970). On the fine structure of the nerve terminals in the human myocardium. *Z. Zellforsch.*, **108**, 324–338.

DUKES, I.D. & VAUGHAN WILLIAMS, E.M. (1984). Effects of selective alpha-1-, alpha-2-, beta-1- and beta-2-adrenoceptor stimulation on potentials and contractions in the rabbit heart. *J. Physiol.*, **355**, 523–546.

ENDO, M., HIRAMOTO, T., ISHIHATA, A., TAKANASHI, M. & INUI, J. (1991). Myocardial alpha-1-adrenoceptors mediate positive inotropic effect and changes in phosphatidylinositol metabolism: Species differences in receptor distribution and the intracellular coupling process in mammalian ventricular myocardium. *Circ. Res.*, **68**, 1179–1190.

FLAVAHAN, N.A. & MCGRATH, J.C. (1981). α_1-adrenoceptors can mediate chronotropic responses in the rat heart. *Br. J. Pharmacol.*, **73**, 586–588.

HERKENHAM, M. & SOKOLOFF, L. (1984). Quantitative receptor autoradiography: tissue defatting eliminates differential self-absorption of tritium radiation in gray and white matter of brain. *Brain Res.*, **321**, 363–368.

KARNOVSKY, M.J. (1964). The localization of cholinesterase activity in rat cardiac muscle by electron microscopy. *J. Cell. Biol.*, **23**, 217–232.

LANGER, S.E. (1980). Presynaptic regulation of the release of catecholamines. *Pharmacol. Rev.*, **32**, 337–362.

LEVY, M.N. & MARTIN, P.J. (1979). Neural control of the heart. In: *Handbook of Physiology*, Section 2: The Cardiovascular System Volume I. ed. Berne, R.T. pp. 581–620. Baltimore: Waverley Press.

LOWRY, O.H., ROSEBROUGH, N.J., FARR, A.L. & RANDALL, R.J. (1951). Protein measurement with the Folin phenol reagent. *J. Biol. Chem.*, **193**, 265–275.

MOLENAAR, P., RUSSELL, F.D., SHIMADA, T. & SUMMER, R.J. (1990). Densitometric analysis of beta-1- and beta-2-adrenoceptors in guinea-pig atrioventricular conduction system. *J. Mol. Cell. Cardiol.*, **22**, 483–495.

MUNSON, P.J. & RODBARD, D. (1980). LIGAND: A versatile computerized approach of ligand-binding system. *Anal. Biochem.*, **107**, 220–239.

MUNTZ, K.H., GARCIA, C. & HAGLER, H.K. (1985). Alpha-1-receptor localization in rat heart and kidney using autoradiography. *Am. J. Physiol.*, **249**, H512–H519.

POSNER, P., FARRAR, E.L. & LAMBERT, C.R. (1976). Inhibitory effects of catecholamines in canine cardiac Purkinje fibers. *Am. J. Physiol.*, **231**, 1415–1420.

RABINE, L.M. HORDOF, A.J., BOWMAN, F.O., MALM, J.R. & ROSEN, M.R. (1978). Alpha and beta adrenergic effects on human atrial specialized conducting fibers. *Circulation*, **57**, 84–90.

SAITO, K., KURIHARA. M., CRUCIANI, R., POTTER, W.Z. & SAAVEDRA, J.M. (1988). Characterization of beta-1- and beta-2-adrenoceptor subtypes in the rat atrioventricular node by quantitative autoradiography. *Circ. Res.*, **62**, 173–177.

SAITO, K., TORDA, T., POTTER, W.Z. & SAAVEDRA, J.M. (1989). Characterization of beta-1- and beta-2-adrenoceptor subtypes in the rat sinoatrial node and stellate ganglia by quantitative autoradiography. *Neurosci. Lett.*, **96**, 35–41.

TUNG, L.H., RAND, M.J. & LOUIS, W.J. (1985). Cardiac alpha-adrenoceptors involving positive chronotropic responses. *J. Cardiovasc. Pharmacol.*, **7**, (suppl 6), s121–s126.

UNNERSTALL, J.R., NIEHOFF, D.L., KUHAR, M.J. & PALACIOS, J.M. (1982). Quantitative receptor autoradiography using [^{3}H] Ultrofilm: Application to multiple benzodiazepine receptors. *J. Neurosci. Methods*, **6**, 59–73.

WAGNER, J. & BRODDE, O.E. (1978). On the presence and distribution of alpha-adrenoceptors in the heart of various mammalian species. *Arch. Pharmacol.*, **302**, 239–254.

ZAZA, A., KLINE, R.P. & ROSEN, M.R. (1990). Effects of alpha-adrenergic stimulation on intracellular sodium activity and automacity in canine Purkinje fibers. *Circ. Res.*, **66**, 416–426.

(Received July 20, 1993
Revised October 5, 1993
Accepted October 11, 1993)

Br. J. Pharmacol. (1994), **111**, 469–472

Inhibition of olfactory cyclic nucleotide-activated current by calmodulin antagonists

Steven J. Kleene

Department of Anatomy and Cell Biology, University of Cincinnati, 231 Bethesda Avenue, ML 521, Cincinnati, OH 45267-0521, U.S.A.

1 In amphibian olfactory receptor neurones, much of the depolarizing current in response to odours is carried by cationic channels that are directly gated by cyclic AMP. The effects of four calmodulin antagonists on the cyclic AMP-activated receptor current were studied in single olfactory cilia of the frog.

2 Two antagonists, W-7 and trifluoperazine, were potent and reversible inhibitors of the cyclic AMP-activated current. IC_{50} values were 5 μM for W-7 and 13 μM for trifluoperazine. A third antagonist, calmidazolium, irreversibly blocked the current. The fourth, mastoparan, had little effect.

3 Calmodulin was unable to reverse the effects of W-7 and trifluoperazine, suggesting that these inhibitors act directly on the cyclic AMP-gated channels.

4 Neither W-7 nor trifluoperazine inhibited a Ca^{2+}-activated Cl^- current which also contributes to the odorant response. These compounds thus allow the two components of the olfactory receptor current to be discriminated.

Keywords: Olfaction; transduction; receptor neurone; cilia; cyclic nucleotide-gated channel; calmodulin antagonists; W-7; trifluoperazine

Introduction

In amphibians, an adenosine 3′:5′-cyclic monophosphate (cyclic AMP)-mediated cascade initiates olfactory transduction. This occurs in the cilia of the olfactory receptor neurones (Kurahashi, 1989; Firestein *et al.*, 1990; Lowe & Gold, 1991). Many odorants increase the activity of adenylate cyclase in the cilia (Pace *et al.*, 1985; Sklar *et al.*, 1986; Shirley *et al.*, 1986; Boekhoff *et al.*, 1990; Bruch & Teeter, 1990). The cyclic AMP formed directly gates channels in the ciliary membrane (Nakamura & Gold, 1987), leading to a depolarizing inward current carried by cations. The cilia contain a high density of cyclic AMP-gated channels (Lowe & Gold, 1993; Kurahashi & Kaneko, 1993), and it has been confirmed in intact neurones that these channels conduct much of the receptor current in response to odours (Kurahashi, 1990; Firestein *et al.*, 1991; Lowe & Gold, 1993). If external Ca^{2+} is present, Ca^{2+} enters through the cyclic AMP-gated channels, activates Cl^- channels, and gives rise to a secondary receptor current carried by Cl^- (Kurahashi & Yau, 1993; Kleene, 1993).

It is useful to have pharmacological agents that can distinguish between the cationic and Cl^- components of the olfactory receptor current. I now report that W-7 and trifluoperazine are potent and reversible inhibitors of the cationic current that flows through the cyclic AMP-gated channels. These compounds have almost no effect on the Ca^{2+}-activated Cl^- portion of the receptor current. W-7 and trifluoperazine are often used as calmodulin antagonists. In this case, however, evidence suggests that they act on the cyclic nucleotide-gated channels directly rather than through calmodulin.

Methods

Ciliary patch procedure

Single olfactory receptor neurones were isolated from the dorsal olfactory epithelium of the northern grass frog (*Rana pipiens*). A recording micropipette was brought near one of the cilia and suction applied until the end of the cilium entered the pipette. Suction was continued until the olfactory vesicle touched the tip of the pipette and a high-resistance seal formed. Then the pipette was raised briefly into the air, causing excision of the cilium from the cell. The cilium remained sealed inside the recording micropipette with the cytoplasmic face of the membrane exposed to the bath. The pipette containing the cilium could be quickly transferred through the air to various pseudointracellular baths without rupturing the seal. Additional details have been presented elsewhere (Kleene & Gesteland, 1991a).

Solutions

Extracellular solutions were used to bathe intact cells and to fill the recording pipettes. The cell suspension was stored in standard extracellular solution, which contained (mM): NaCl 115, KCl 3, HEPES 5, $MgCl_2$ 2, $CaCl_2$ 1 and NaOH 2 (pH 7.2). Recording pipettes contained extracellular solution made without $MgCl_2$ and $CaCl_2$. This omission prevented open-channel block of the cyclic AMP-gated channels by external Ca^{2+} and Mg^{2+} (Nakamura & Gold, 1987; Dhallan *et al.*, 1990; Zufall & Firestein, 1993). In addition, it prevented the secondary Cl^- current that depends on external Ca^{2+} (Kurahashi & Yau, 1993; Kleene, 1993). Patch formation was accomplished in standard extracellular solution, since it was nearly impossible to form high-resistance seals without divalent cations in the bath. The small amount of Ca^{2+} and Mg^{2+} sucked into the pipette during the patch procedure quickly diffused back into the pipette. After seal formation, this was detectable as a gradual increase in cyclic AMP-activated current at negative potentials, as the blocking effect of the external divalent cations was relieved. This process was complete within 1–3 min.

After a cilium was excised from a neurone, the pipette containing the cilium was transferred through a series of pseudointracellular solutions which bathed the cytoplasmic face of the ciliary membrane. The standard pseudointracellular solution contained (mM): KCl 110, NaCl 5, HEPES 5, $CaCl_2$ 0.8, BAPTA 2 and KOH 9 (pH 7.2). Free Ca^{2+} was determined to be 0.1 μM as described elsewhere (Kleene &

Gesteland, 1991b). When calmodulin was used, 1 μM calmodulin was added to a solution containing 0.9 μM free Ca^{2+}. Inhibitors were added to the pseudointracellular bath as indicated.

Electrical recording

Both the recording pipette and chamber were coupled to a List L/M-EPC7 patch-clamp amplifier by Ag/AgCl electrodes, each bathed in extracellular solution. All recordings were done under voltage clamp at room temperature (25°C). Current was adjusted to zero with the open pipette in the well in which the patching procedure was done. Both the bath and the pipette contained extracellular solution at this stage. After excision of a cilium, the pipette was transferred through a series of pseudointracellular baths. Each bath was connected by a salt bridge to a common reference bath. The salt bridge contained extracellular solution plus 5% (w/v) agarose (Sigma Type I). A correction was applied for the liquid junction potential between each pseudointracellular bath and its salt bridge (Hagiwara & Ohmori, 1982).

Voltage ramps (−100 to +100 mV, 0.2 mV ms^{-1}) were generated by pCLAMP software (Axon Instruments, Foster City, CA, U.S.A.). Current-voltage (*I-V*) records were acquired at a sampling rate of 500 Hz. In all records, an upward deflection represents increasing positive current from the bath into the pipette. Potentials are reported as bath (cytoplasmic) potential relative to pipette potential. Results of repeated experiments are reported as mean ± s.e.mean.

Materials

W-7 (N-(6-aminohexyl)-5-chloro-1-naphthalenesulphonamide) hydrochloride, trifluoperazine dihydrochloride, and calmidazolium (compound R24571) were purchased from Sigma Chemical Co. (St. Louis, MO, U.S.A.), as were all other reagents. W-7 and calmidazolium were diluted from 10 mM stock solutions in ethanol. Dilutions of these inhibitors were sonicated to ensure solution. Mastoparan was synthetic (Sigma catalogue No. M5280), and calmodulin was from bovine brain (Sigma No. P2277).

Results

Recordings were made from single cilia excised from frog olfactory receptor neurones (Kleene & Gesteland, 1991a). One cilium of a cell was sucked inside a patch pipette. A high-resistance seal was made between the base of a cilium and the tip of the pipette, and the pipette containing the cilium was detached from the cell. The cilium remained inside the pipette with the cytoplasmic face of its membrane exposed to the bath (Kleene & Gesteland, 1991a).

Addition of 100 μM cytoplasmic cyclic AMP activated a large ciliary membrane conductance (Figure 1, top, curve '0'). This was due to cationic channels directly gated by cyclic AMP (Nakamura & Gold, 1987). Addition of a calmodulin antagonist, W-7, to the cytoplasmic bath caused a decrease in conductance that depended on the concentration of W-7 (Figure 1) and became stable within 1 min. Inhibition was nearly complete with 100 μM W-7 and was largely reversible. Within 3–5 min after removal of 100 μM W-7, 80 ± 5% (range 70 to 92%, $n = 4$) of the cyclic AMP-activated current returned. Another calmodulin antagonist, trifluoperazine, also produced nearly complete inhibition at 100 μM, although the IC_{50} was higher than that of W-7 (Figure 1). Inhibition took 1–2 min and was mostly reversible. Within 6–8 min after removal of 100 μM trifluoperazine, 83 ± 5% (range 65–103%, $n = 6$) of the cyclic AMP-activated current returned. Both W-7 and trifluoperazine were somewhat more effective at positive potentials, as reported for other inhibitors of cyclic nucleotide-gated channels (Frings *et al.*, 1992; Haynes, 1992; Kleene, 1993).

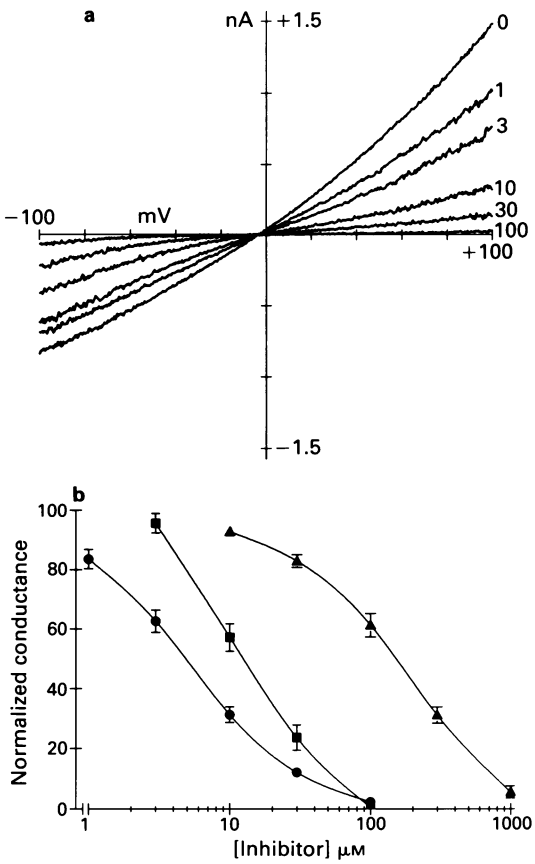

Figure 1 Inhibitors of the cyclic AMP-activated ciliary current. (a) A pipette containing a cilium was moved through baths containing a pseudointracellular solution plus 100 μM cyclic AMP and W-7 as shown (in μM). In each bath, the *I-V* relation was measured. The *I-V* curve in the absence of cyclic AMP and inhibitor (not shown) was subtracted from each record so that only the cyclic AMP-activated current is plotted. (b) The slope of the *I-V* plot, measured between −50 and +50 mV, is plotted against the concentration of inhibitor added. Inhibitors are W-7 (●), trifluoperazine (■), and amiloride (▲). All points are means of determinations in 7–9 cilia. For each experiment, conductance in the absence of inhibitor was defined as 100 and the other values were normalized to this. The maximum cyclic AMP-activated conductance (slope of the '0' curve between −50 and +50 mV) averaged 8.7 ± 4.3 nS ($n = 9$, range 4.3 to 15.0 nS) for the W-7 experiments, 8.1 ± 0.9 nS ($n = 8$, range 4.7 to 12.3 nS) for the trifluoperazine experiments, and 11.6 ± 1.2 nS ($n = 8$, range 8.1 to 17.9 nS) for the amiloride experiments. Where error bars are not shown, the s.e.mean was less than 3. Interpolation from the dose-response curves shown gave estimated IC_{50} values of 5 μM for W-7, 13 μM for trifluoperazine, and 150 μM for amiloride.

A third calmodulin antagonist, calmidazolium, caused a very slow and irreversible inhibition of the cyclic AMP-activated conductance. In the five cilia tested, effects of calmidazolium were first seen at 3–10 μM. Inhibition progressed for periods exceeding 10 min and continued even after transfer to a bath lacking the inhibitor. One calmodulin antagonist, the peptide mastoparan, had little effect on the ciliary cyclic AMP-activated conductance. At 10 μM, mastoparan inhibited the conductance by just 9 ± 2% (range 4 to 13%, $n = 5$). Inhibition by amiloride, which is not considered a calmodulin antagonist, is shown in Figure 1 for comparison. Amiloride has been shown to inhibit both the odour-induced receptor current (Persaud *et al.*, 1987; Frings & Lindemann, 1988) and the cyclic AMP-gated channels (Suzuki, 1990; Frings *et al.*, 1992).

Calmodulin was unable to reverse inhibition of the cyclic AMP-activated current by W-7 or trifluoperazine. In the presence of 5 μM W-7, this current was reduced by about

Table 1 Inhibitors of the cyclic nucleotide-activated current in olfactory receptor neurones

Inhibitor	IC_{50} (μM)	*Species*	*Reference*
Amiloride	–	Bullfrog	Suzuki, 1990
	17	Frog	Frings *et al.*, 1992
	70	Rat	Frings *et al.*, 1992
	150	Frog	This paper
Calmidazolium	–	Frog	This paper
D600	12	Frog	Frings *et al.*, 1992
3′,4′-Dichlorobenzamil (DCB, DCPA)	3.7	Frog	Kolesnikov *et al.*, 1990
	15	Frog	Kleene, 1993
	~4	Carp	Kolesnikov & Kosolapov, 1993
(+)-*cis*-Diltiazem	120	Frog	Frings *et al.*, 1992
(−)-*cis*-Diltiazem	47	Frog	Kolesnikov *et al.*, 1990
	70	Frog	Frings *et al.*, 1992
	128	Frog	Kleene, 1993
Nifedipine	–	Tiger salamander	Zufall & Firestein, 1993
Trifluoperazine	13	Frog	This paper
W-7	5	Frog	This paper

In all cases the inhibitor was applied to the cytoplasmic face of the membrane and little free Ca^{2+} or Mg^{2+} was present. Saturating concentrations of cyclic AMP were used in all but two cases (Suzuki, 1990; Kolesnikov & Kosolapov, 1993). In three cases (Suzuki, 1990; Zufall & Firestein, 1993; Kolesnikov & Kosolapov, 1993) single cyclic AMP-gated channels were studied. In the others, a macroscopic cyclic AMP-activated current was measured. Intact single cilia were studied in this paper and in Kleene (1993). The other studies used membrane patches excised from the soma or dendrite. A channel cloned from rat olfactory cDNA was inhibited by (−)-*cis*-diltiazem with an IC_{50} of 0.5–1 mM (Dhallan *et al.*, 1990). IC_{50} values were determined at different voltages as described in the individual references.

50% (Figure 1). Addition of 1 μM cytoplasmic calmodulin in the continued presence of the inhibitor had no significant effect ($n = 4$). In the presence of 10 μM trifluoperazine, 1 μM calmodulin caused a small additional decrease in the cyclic AMP-activated current ($n = 4$).

In amphibians, the olfactory receptor current includes both the cyclic AMP-activated cationic current and a Ca^{2+}-activated Cl^- current (Kurahashi & Yau, 1993; Kleene, 1993). It is thus useful to know whether the calmodulin antagonists allow the two currents to be distinguished. Neither W-7 or trifluoperazine substantially inhibited the ciliary Cl^- current activated by 300 μM cytoplasmic free Ca^{2+}. W-7 (100 μM) reduced this current by 5 ± 4% (range −11 to 19%, $n = 9$) and trifluoperazine (100 μM) by 5 ± 2% (range −1 to 10%, $n = 5$). Amiloride also reduced the Cl^- current by just 5 ± 3% (range −4 to 15%, $n = 5$).

Discussion

Two calmodulin antagonists, W-7 and trifluoperazine, have been found to be potent and reversible inhibitors of the cyclic AMP-activated cationic current that underlies olfactory transduction in amphibians. It seems likely that the compounds inhibit the cyclic AMP-gated channels directly rather than via calmodulin. Calmodulin was unable to reverse any of the partial inhibition caused by moderate doses of W-7 or trifluoperazine. Ca^{2+}-calmodulin does reduce the ligand affinity of the cyclic nucleotide-gated channels from rod photoreceptors (Hsu & Molday, 1993) and olfactory receptor neurones (Chen & Yau, 1993). However, this should only slightly reduce the current at the saturating concentrations of cyclic AMP used in this study.

W-7 and trifluoperazine must not be regarded as specific inhibitors. W-7 has been reported to block various Ca^{2+} channels and currents (Greenberg *et al.*, 1987; Ehrlich *et al.*, 1988; Nakazawa *et al.*, 1993), voltage-dependent Na^+ current (Ichikawa *et al.*, 1991), and Ca^{2+}-activated K^+ channels (Kihira *et al.*, 1990). Trifluoperazine inhibits Ca^{2+} currents (Greenberg *et al.*, 1987; Nakazawa *et al.*, 1993), voltage-dependent Na^+ current (Ichikawa *et al.*, 1991), Ca^{2+}-activated (McCann & Welsh, 1987; Kihira *et al.*, 1990; Ikemoto *et al.*, 1992) and ATP-sensitive (Müller *et al.*, 1991) K^+ channels, and GABA-activated Cl^- current (Yang & Zorumski, 1989). In ventricular and vascular myocytes, trifluoperazine depressed I_{Ca}, I_{Na}, and I_K (Klöckner & Isenberg, 1987). Many of these studies (Greenberg *et al.*, 1987; Klöckner & Isenberg, 1987; McCann & Welsh, 1987; Ehrlich *et al.*, 1988; Kihira *et al.*, 1990; Nakazawa *et al.*, 1993) included evidence suggesting that inhibition of channel activity was not mediated by calmodulin.

A number of compounds inhibit current through the olfactory cyclic nucleotide-gated channel (Table 1), but none can be considered specific inhibitors. W-7 and trifluoperazine inhibit at lower concentrations than most and are readily available from commercial suppliers. They allow discrimination between the two components of the olfactory receptor current present in amphibians. W-7 and trifluoperazine inhibit the cyclic nucleotide-activated cationic current but not the Ca^{2+}-activated Cl^- current. The same is true of DCB and (−)-*cis*-diltiazem (Kleene, 1993) and also amiloride. W-7 (Ichikawa *et al.*, 1991) and to a lesser extent trifluoperazine (Ikemoto *et al.*, 1992) are membrane-permeant, so they should be effective from either side of the neuronal membrane. For these reasons, W-7 and trifluoperazine are useful inhibitors of the cyclic nucleotide-activated channels that initiate olfactory transduction.

I am grateful to Robert Gesteland for critical reviews of the manuscript and to Barbara Cincush for technical assistance. This work was supported by National Institutes of Health grants R01 DC00926, P01 DC00347, and R01 DC00352.

References

BOEKHOFF, I., TAREILUS, E., STROTMANN, J. & BREER, H. (1990). Rapid activation of alternative second messenger pathways in olfactory cilia from rats by different odorants. *EMBO J.*, **9**, 2453–2458.

BRUCH, R.C. & TEETER, J.H. (1990). Cyclic AMP links amino acid chemoreceptors to ion channels in olfactory cilia. *Chem. Senses*, **15**, 419–430.

CHEN, T.-Y. & YAU, K.-W. (1993). Modulation by Ca^{2+}-calmodulin of cyclic nucleotide-gated cation channel of rat olfactory receptor neurons. *Soc. Neurosci. Abstr.*, **19,** 13.

DHALLAN, R.S., YAU, K.-W., SCHRADER, K.A. & REED, R.R. (1990). Primary structure and functional expression of a cyclic nucleotide-activated channel from olfactory neurons. *Nature*, **347,** 184–187.

EHRLICH, B.E., JACOBSON, A.R., HINRICHSEN, R., SAYRE, L.M. & FORTE, M.A. (1988). *Paramecium* calcium channels are blocked by a family of calmodulin antagonists. *Proc. Natl. Acad. Sci. U.S.A.*, **85,** 5718–5722.

FIRESTEIN, S., SHEPHERD, G.M. & WERBLIN, F.S. (1990). Time course of the membrane current underlying sensory transduction in salamander olfactory receptor neurons. *J. Physiol.*, **430,** 135–158.

FIRESTEIN, S., ZUFALL, F. & SHEPHERD, G.M. (1991). Single odor-sensitive channels in olfactory receptor neurons are also gated by cyclic nucleotides. *J. Neurosci.*, **11,** 3565–3572.

FRINGS, S. & LINDEMANN, B. (1988). Odorant response of isolated olfactory receptor cells is blocked by amiloride. *J. Membr. Biol.*, **105,** 233–243.

FRINGS, S., LYNCH, J.W. & LINDEMANN, B. (1992). Properties of the cyclic nucleotide-gated channels mediating olfactory transduction. *J. Gen. Physiol.*, **100,** 45–67.

GREENBERG, D.A., CARPENTER, C.L. & MESSING, R.O. (1987). Interaction of calmodulin inhibitors and protein kinase C inhibitors with voltage-dependent calcium channels. *Brain Res.*, **404,** 401–404.

HAGIWARA, S. & OHMORI, H. (1982). Studies of calcium channels in rat clonal pituitary cells with patch electrode voltage clamp. *J. Physiol.*, **331,** 231–252.

HAYNES, L.W. (1992). Block of the cyclic GMP-gated channel of vertebrate rod and cone photoreceptors by *l-cis*-diltiazem. *J. Gen. Physiol.*, **100,** 783–801.

HSU, Y.-T. & MOLDAY, R.S. (1993). Modulation of the cGMP-gated channel of rod photoreceptor cells by calmodulin. *Nature*, **361,** 76–79.

ICHIKAWA, M., URAYAMA, M. & MATSUMOTO, G. (1991). Anticalmodulin drugs block the sodium gating current of squid giant axons. *J. Membr. Biol.*, **120,** 211–222.

IKEMOTO, Y., YOSHIDA, A. & ODA, M. (1992). Blockade by trifluoperazine of a Ca^{2+}-activated K^+ channel in rat hippocampal pyramidal neurons. *Eur. J. Pharmacol.*, **216,** 191–198.

KIHIRA, M., MATSUZAWA, K., TOKUNO, H. & TOMITA, T. (1990). Effects of calmodulin antagonists on calcium-activated potassium channels in pregnant rat myometrium. *Br. J. Pharmacol.*, **100,** 353–359.

KLEENE, S.J. (1993). Origin of the chloride current in olfactory transduction. *Neuron*, **11,** 123–132.

KLEENE, S.J. & GESTELAND, R.C. (1991a). Transmembrane currents in frog olfactory cilia. *J. Membr. Biol.*, **120,** 75–81.

KLEENE, S.J. & GESTELAND, R.C. (1991b). Calcium-activated chloride conductance in frog olfactory cilia. *J. Neurosci.*, **11,** 3624–3629.

KLÖCKNER, U. & ISENBERG, G. (1987). Calmodulin antagonists depress calcium and potassium currents in ventricular and vascular myocytes. *Am. J. Physiol.*, **253,** H1601–H1611.

KOLESNIKOV, S.S. & KOSOLAPOV, A.V. (1993). Cyclic nucleotide-activated channels in carp olfactory receptor cells. *Biochim. Biophys. Acta*, **1150,** 63–72.

KOLESNIKOV, S.S., ZHAINAZAROV, A.B. & KOSOLAPOV, A.V. (1990). Cyclic nucleotide-activated channels in the frog olfactory receptor plasma membrane. *FEBS Lett.*, **266,** 96–98.

KURAHASHI, T. (1989). Activation by odorants of cation-selective conductance in the olfactory receptor cell isolated from the newt. *J. Physiol.*, **419,** 177–192.

KURAHASHI, T. (1990). The response induced by intracellular cyclic AMP in isolated olfactory receptor cells of the newt. *J. Physiol.*, **430,** 355–371.

KURAHASHI, T. & KANEKO, A. (1993). Gating properties of the cAMP-gated channel in toad olfactory receptor cells. *J. Physiol.*, **466,** 287–302.

KURAHASHI, T. & YAU, K.-W. (1993). Co-existence of cationic and chloride components in odorant-induced current of vertebrate olfactory receptor cells. *Nature*, **363,** 71–74.

LOWE, G. & GOLD, G.H. (1991). The spatial distributions of odorant sensitivity and odorant-induced currents in salamander olfactory receptor cells. *J. Physiol.*, **442,** 147–168.

LOWE, G. & GOLD, G.H. (1993). Contribution of the ciliary cyclic nucleotide-gated conductance to olfactory transduction in the salamander. *J. Physiol.*, **462,** 175–196.

MCCANN, J.D. & WELSH, M.J. (1987). Neuroleptics antagonize a calcium-activated potassium channel in airway smooth muscle. *J. Gen. Physiol.*, **89,** 339–352.

MÜLLER, M., DEWEILLE, J.R. & LAZDUNSKI, M. (1991). Chlorpromazine and related phenothiazines inhibit the ATP-sensitive K^+ channel. *Eur. J. Pharmacol.*, **198,** 101–104.

NAKAMURA, T. & GOLD, G.H. (1987). A cyclic nucleotide-gated conductance in olfactory receptor cilia. *Nature*, **325,** 442–444.

NAKAZAWA, K., HIGO, K., ABE, K., TANAKA, Y., SAITO, H. & MATSUKI, N. (1993). Blockade by calmodulin inhibitors of Ca^{2+} channels in smooth muscle from rat vas deferens. *Br. J. Pharmacol.*, **109,** 137–141.

PACE, U., HANSKI, E., SALOMON, Y. & LANCET, D. (1985). Odorant-sensitive adenylate cyclase may mediate olfactory reception. *Nature*, **316,** 255–258.

PERSAUD, K.C., DESIMONE, J.A., GETCHELL, M.L., HECK, G.L. & GETCHELL, T.V. (1987). Ion transport across the frog olfactory mucosa: the basal and odorant-stimulated states. *Biochim. Biophys. Acta*, **902,** 65–79.

SHIRLEY, S.G., ROBINSON, C.J., DICKINSON, K., AUJLA, R. & DODD, G.H. (1986). Olfactory adenylate cyclase of the rat. *Biochem. J.*, **240,** 605–607.

SKLAR, P.B., ANHOLT, R.R.H. & SNYDER, S.H. (1986). The odorant-sensitive adenylate cyclase of olfactory receptor cells. *J. Biol. Chem.*, **261,** 15538–15543.

SUZUKI, N. (1990). Single cyclic nucleotide-activated ion channel activity in olfactory receptor cell soma membrane. *Neurosci. Res.*, Suppl. **12,** S113–S126.

YANG, J. & ZORUMSKI, C.F. (1989). Trifluoperazine blocks GABA-gated chloride currents in cultured chick spinal cord neurons. *J. Neurophysiol.*, **61,** 363–373.

ZUFALL, F. & FIRESTEIN, S. (1993). Divalent cations block the cyclic nucleotide-gated channel of olfactory receptor neurons. *J. Neurophysiol.*, **69,** 1758–1768.

(Received September 13, 1993
Accepted October 13, 1993)

Br. J. Pharmacol. (1994), **111**, 473–482

Involvement of ET_A receptors in the facilitation by endothelin-1 of non-adrenergic non-cholinergic transmission in the rat urinary bladder

M.V. Donoso, C. Salas, G. Sepúlveda, J. Lewin, *A. Fournier & [1]J.P. Huidobro-Toro

Unidad de Regulación Neurohumoral, Departmento de Fisiología, Facultad de Ciencias Biológicas, Pontificia Universidad Católica de Chile, Casilla 114-D, Santiago-1, Chile and *INRS-Santé, Université du Québec, 245 Boulevard Hymus, Pointe-Claire, Québec H9R 1G6, Canada

1 Endothelin-1 (ET-1; 3–10 nM) raised the tone of rat bladders bathed in buffer containing atropine (1 μM) plus guanethidine (3.4 μM). In addition, ET-1 potentiated, in a concentration-dependent fashion (1–10 nM), the contractions evoked by both transmural nerve stimulation and applications of exogenous adenosine 5'-triphosphate (ATP).

2 The threshold concentration of ET-1 required to facilitate non-adrenergic non-cholinergic (NANC) transmission and potentiate ATP-induced contractions, was about 10 fold lower than that required to increase the bladder tone (3 nM).

3 The ET-1-induced increase in basal tension reached its maximal effect within 60–90 s. In contrast, the 7.8 μM ATP-induced contractions increased by 50% within the first minute following incubation with 10 nM ET-1 but required about 5 min to develop the maximal effect.

4 The ET-1-induced potentiation of NANC or ATP responses was long-lasting and persisted in spite of extensive washing. The recovery of the bladder excitability depended on the concentration of ET-1. Following the application of 3 nM ET-1, recovery required 30 min; applications of 10 nM ET-1 required at least 60 min for full recovery.

5 The ET-1-induced potentiation of responses was selective for ATP and related structural analogues. ET-1 did not modify the contractions induced by acetylcholine, 5-hydroxytryptamine, prostaglandin $F_{2\alpha}$ or bradykinin.

6 The potency of ET-2 was similar to that of ET-1. ET-3 and ET-C-terminal hexapeptide were inactive up to 100 M. Sarafotoxin S6b was 2 to 3 fold less potent than ET-1 whereas sarafotoxin S6c (100 nM) was inactive. AGETB-9 and AGETB-89, two ET_B receptor agonists, were also inactive (up to 100 nM).

7 Removal of one or both disulphide bonds in ET-1 and tryptophan-21 formylation of ET-1, resulted in inactive peptides (up to 100 nM).

8 The ET-1 receptor antagonists, BE-18257B and FR 139317, blocked both the ET-1-induced rise in tone and the potentiation of ATP responses in a concentration-dependent fashion. FR 139317 was at least 30 fold more potent than BE-18257B. Both antagonists blocked at lower concentrations the ET-1 increase in bladder tone as compared to the ATP potentiation. The antagonism was slowly reversible.

9 Results are consistent with the presence of ET_A receptors in the rat bladder, which mediate both actions of ET-1. The interaction of ET-1 with purinergic mechanisms is discussed.

Keywords: Endothelin-1; bladder neurotransmission; purinergic mechanisms; urinary bladder; ATP potentiation; NANC transmission; ET-A antagonists

Introduction

Adenosine 5'-triphosphate (ATP) has long been proposed as a non-adrenergic non-cholinergic (NANC) neurotransmitter (Burnstock *et al.*, 1978b). Recent evidence suggests that ATP may participate in synaptic physiology as a neurotransmitter and/or as a co-transmitter of central and peripheral neurones (Burnstock, 1990a,b; Evans *et al.*, 1992; Evans & Surprenant, 1992). ATP activates membrane bound receptors different from those of adenosine; the ATP receptors are classified into two main types, P_{2x} and P_{2y} (Burnstock & Kennedy, 1985). The P_{2x}-purinoceptor is thought to mediate rapid-onset excitatory responses and is characterized by a fast rate of desensitization following prolonged exposure to ATP or α,β-methyleneadenosine 5'-triphosphate. In addition, the P_{2x}-purinoceptor is selectively blocked in a competitive manner by suramin (Dunn & Blakeley, 1988). Recent solubilization of the ATP receptor suggests that it is an ionophore, sharing features with other channel-operating receptors (Bo *et al.*, 1992).

The role of ATP in neurotransmission has been investigated in the peripheral nervous system (Burnstock *et al.*, 1978a; Brown *et al.*, 1979; Hoyle & Burnstock, 1985). The most solid evidence supporting ATP as a neurotransmitter is derived from investigations in the vas deferens (Fedan *et al.*, 1981; Meldrum & Burnstock, 1983; Sneddon & Burnstock, 1984; Sneddon & Westfall, 1984; Stjärne & Astrand, 1984), the mesenteric artery (Ramme *et al.*, 1987), and the rat bladder (Burnstock *et al.*, 1978b; Kasakov & Burnstock, 1983; Hoyle & Burnstock, 1985; Acevedo & Contreras 1985).

Previous studies from our laboratory demonstrated that while bradykinin facilitated purinergic mechanisms operating in the bladder, ET-1 potentiated the vas deferens neurotransmission (Acevedo *et al.*, 1990; Donoso *et al.*, 1992). The recent discovery that the novel 21 amino acid peptide endothelin-1 (ET-1) is synthesized in the bladder epithelia, as well as in non-vascular bladder smooth muscle (Saenz de Tejada *et al.*, 1992), raised the possibility of studying the putative role of this peptide in the bladder NANC transmission. Although ET-1 was linked originally only to the control of blood flow (Yanagisawa & Masaki, 1989; Lerman *et al.*,

[1] Author for correspondence.

1990), it was soon recognized that ET-1 is synthesized in various organs. ET exerts effects on smooth muscles in the respiratory, intestinal and urogenital tracts, as well as neurones and epithelial cells (for recent reviews see Simonson & Dunn, 1990; Highsmith et al., 1992; Filep, 1992). In addition, human ET-1 plasma levels average 1 to 2 pg ml^{-1} (Hartter & Woloszczuk, 1989; Stewart et al., 1992), supporting a possible hormonal role. Receptors for ET-1 are probably membrane-bound proteins belonging to the GTP-coupled superfamily of receptors (Arai et al., 1990; Sakurai et al., 1990). Based on pharmacological principles, receptors for ET have been tentatively characterized into 2 main types: ET_A and ET_B (Masaki, 1991).

In this paper, we characterize pharmacologically the ET receptors in the bladder, examine the influence of ET on NANC transmission and compare the facilitation of the NANC responses with the potentiation of the direct muscular action of exogenous ATP and its analogues.

Methods

Bioassay

Adult male Sprague Dawley rats (250–300 g), raised in our Animal Reproduction Laboratories, were killed by cervical dislocation; the abdominal cavity was opened, the bladder was mechanically voided, excised from surrounding tissues, and mounted in a bath for the recording of isometric contractions as detailed by Acevedo & Contreras (1985). Unless otherwise specified, the composition of the incubation buffer was (mM): NaCl 118, KCl 5.4, $CaCl_2$ 2.5, KH_2PO_4 1.2, $MgSO_4$ 1.2, $NaHCO_3$ 23.8, glucose 11.1, atropine 0.001 and guanethidine 0.0034. To maintain pH close to 7.4, the buffer was bubbled wtih 95% O_2/5% CO_2. Only when specified, the bladder was everted; i.e., the mucosal side faced the superfusion media.

Tissues were initially adjusted to 1 g of basal tension which was maintained throughout the experimental procedure. Nerve-evoked contractions were elicited by transmural stimulation with electrical square pulses of 70 V, 1 ms duration, 0.15, 0.5, 1.5, 5, 15 Hz during 30 s, delivered by a Grass S44 stimulator. Such contractions were secondary to nerve activation as they were abolished by 200 nM tetrodotoxin.

Isometric contractions were recorded with force displacement transducers (FT 03C) connected to a Grass oscillograph. The incubation buffer was changed every 15 min during 1 h before the experiment.

Experimental protocols

Bladder tone Increasing concentrations of ET-1 ranging from 0.1 to 10 nM were applied in a non-cumulative manner at regular 15 min intervals. The peptides were incubated with the tissues for 5 min, unless otherwise stated and rinsed from the tissues when the maximal response had been achieved. At the end of each concentration-response experiment, four applications of 10 nM ET-1 were made. The increase in bladder tone was quantified as the grams (g) of tension generated by each peptide concentration. Similar protocols were performed with ET-2, ET-3, ET-C-terminal hexapeptide, the sarafotoxins, and a variety of ET-1 structural analogues. A separate preparation was used to examine the effect of each peptide; in all cases, the preparations were challenged, at the end of the experiment, with 10 nM ET-1 to assess tissue viability. Results are expressed either as the peptide concentration-response curves or as the peptide concentration required to increase bladder basal tension by 0.5 g ($C_{0.5\,g}$).

In a separate series of experiments, bladders were first incubated in normal buffer and challenged with 7.8 μM ATP and 1.5 Hz for 30 s. Thereafter, the preparations were incubated in Ca^{2+}-free buffer containing 0.1 mM EGTA for 30 min before challenge with 7.8 μM ATP, nerve stimulation and 10 nM ET-1.

To ascertain whether the ET-1-induced motor activity was mediated in part by neuronal mechanisms, additional experiments were performed in separate preparations pretreated with 200 nM tetrodotoxin for 2 min prior to ET-1 applications.

Nerve-evoked contractions The effect of 0.01–30 nM ET-1, applied for 5 min prior to electrical stimulation, was examined on the nerve-evoked contractions caused by 30 s trains of pulses (0.15–15 Hz). Separate tissues were used to evaluate the effect of each ET-1 concentration on the frequency-response curve. A resting period of 15 min was allowed between the trains of pulses during which the preparations were washed. As a control, a frequency-contraction experiment was performed immediately before initiating tissue incubation with ET-1. The mean tension of the phasic and tonic components generated by the nerve-evoked contractions was assessed.

To examine the potency of ET-2, ET-3 and the ET-C-terminal hexapeptide, sarafotoxin S6b and S6c, the ET-1 structural analogues, as well as AGETB-9 and AGETB-89, concentration-response curves were performed in tissues stimulated with trains of electrical pulses of 5 Hz during 30 s. Each analogue was investigated on a separate preparation; however, all tissues were challenged with 10 nM ET-1 to confirm tissue viability. Results express the concentration of each peptide required to cause a 1 g increase in the tension of the phasic component of the 5 Hz stimuli.

Exogenous ATP To ascertain the effect of ET-1 on the contractile activity induced by exogenous ATP, non-cumulative ATP concentration-response experiments were performed before and after incubation with 1, 3 or 10 nM ET-1. A separate preparation was used to examine the influence of each ET-1 concentration; each preparation was used as its own control. Tissues were incubated with ET-1 for 5 min and challenged with ATP at 15 min intervals; each ATP application was followed by extensive tissue washing. As a further control for this experimental series, in a separate set of tissues, two successive ATP concentration-response experiments, spaced an hour apart, were performed in the same tissues; in the second, saline was added before ATP to test whether the tissues became supersensitive to ATP after 3 h of tissue incubation.

To ascertain the possible influence of neuronal connections on the ET-1-induced potentiation of the ATP responses, a control ATP concentration-response experiment was carried out before and after incubation with 200 nM tetrodotoxin 2 min before applications of 10 nM ET-1.

To assess the influence of the rise in basal tension caused by ET-1, an experiment was performed to compare the potency of ATP under basal tone and after the tone was mechanically increased by 1.3 g to mimic the increase in basal tension caused by 10 nM ET-1. In an additional series of experiments, tone was raised by application of 7.2 μM acetylcholine 30 s before ATP additions.

To evaluate the requirement of external Ca^{2+} on the ET-1-induced potentiation of the ATP motor responses, bladder were initially equilibrated in buffer containing 2.5 mM Ca^{2+}, and challenged with 7.8 μM ATP and with 30 s trains of 1.5 Hz pulses to assess viability. Next, the preparations were incubated in Ca^{2+}-free buffer plus 0.1 mM EGTA for 30 min prior to performing ATP and AMP-PNP concentration-response experiments. Immediately thereafter, tissues were incubated for 5 min with 10 nM ET-1 and the concentration-response protocols were repeated. Each tissue was used to test the effect of only one nucleotide. In some cases, at the end of the experiment, tissues were bathed in buffer containing 2.5 mM Ca^{2+} and challenged with 7.8 μM ATP and electrical pulses.

To examine the potency of ET analogues, including the

C-terminal hexapeptide, the sarafotoxins and ET_B receptor agonists, series of experiments were performed in tissues challenged with 7.8 μM ATP prior to and following a 5 min exposure to 0.01–100 nM of the peptides. Results show either the concentration-response curves for each peptide or the peptide concentration required to increase by 1 g the ATP-induced contractile response (C_{1g}). For these protocols, each peptide was assayed in a separate tissue. In all cases, tissues were tested with 10 nM ET-1 to ensure tissue viability.

Characterization of the ET-1-induced potentiation of the exogenous ATP motor responses

Incubation time To investigate the duration of the incubation with ET-1 necessary to potentiate the exogenous ATP-induced motor responses, tissues were challenged with 7.8 μM ATP before and during incubation with 10 nM ET-1 for 15 and 30 s or 1, 2, 3, 5 and 10 min. A separate preparation was used to study the effect of ET-1 on each incubation period. Upon completion of this protocol, preparations were discarded.

Time-course of tissue recovery from ET-1 effects To assess the duration of the potentiation caused by ET-1, separate tissues were incubated for 5 min with either 3 or 10 nM ET-1. The preparations were extensively washed and 15, 30 and 60 min thereafter, challenged with either 7.8 μM ATP or a 30 s train of 1.5 Hz pulses. The tissues were extensively washed between stimuli. Each preparation was used to study one concentration of ET-1 in the presence of either ATP or electrical pulses.

Specificity of action In separate protocols, concentration-response experiments were performed with adenosine 5'-diphosphate (ADP), 2-methylthioadenosine triphosphate, and the slowly hydrolyzable nucleotides: 5'-adenylylimidodiphosphate (AMP-PNP), α,β-methyleneadenosine 5'-triphosphate (AMP-CPP), and β,δ-methyleneadenosine 5'-triphosphate (AMP-PCP) before and after a 5 min incubation with 10 nM ET-1. Furthermore, non-purine compounds such as acetylcholine, 5-hydroxytryptamine (5-HT), bradykinin, and prostaglandin $F_{2\alpha}$ were examined following an identical protocol. (In the case of acetylcholine, no atropine was added to the incubation buffer). At the initiation of each of these protocols, tissues were challenged with 7.8 μM ATP; at the end, ATP was tested in the presence of 10 nM ET-1 to ensure that the tissues were able to respond with the characteristic ET-1-induced potentiation. Each preparation was used to examine the effect of only one agonist. The concentrations of purine or non-purine agonists required to generate either 0.5 g of tension (ADP) or 2 g of tension (other agonists) was calculated by interpolation from each concentration-response curve.

Pharmacological characterization of the endothelin receptor: studies with BE-18257B and FR 139317

BE-18257B To assess whether the ET-1-induced tone was antagonized by BE-18257B, tissues were incubated with either 0.3, 1, 3, or 7.5 μM of this cyclic peptide for 20 min prior to the application of 10 nM ET-1. ATP concentration-response experiments were also performed, pretreating tissues for 5 min with 10 nM ET-1 plus the solvent and either 3 or 7.5 μM BE-18257B plus 10 nM ET-1. A separate preparation was used to investigate each concentration of antagonist. Reversibility of blockade was tested 60 min after extensive tissue rinsing, challenging with 10 nM ET-1. Since the antagonist was dissolved in dimethylsulphoxide (DMSO), control experiments were performed to assess whether DMSO modified the potency of ATP and ET-1. For this purpose, ATP concentration-response curves were performed in untreated tissues, and bladders exposed to 100 μl (46.9 μM) DMSO. In addition, ATP determinations were performed in the presence of 3 or 7.5 μM of the antagonist.

FR 139317 Similar protocols to those outlined for BE-18257B were performed; the antagonist concentrations were 0.01, 0.1, 1 and 10 μM, and the linear tetrapeptide was dissolved in 50% DMSO and incubated with the tissues for 25 min. Control ATP concentration-response curves were performed in the absence and in the presence of either 50% DMSO, or 1 μM FR 139317.

Statistical analysis

Computerized linear regression analysis of the concentration-response curves was used to interpolate the concentrations of ATP or ADP required to increase the muscular tension by 0.5 g ($C_{0.5g}$) as previously detailed by Donoso *et al.* (1992), or the concentration of the other agonists required to increase the bladder tension by 1 g (C_{1g}) or 2 g (C_{2g}). Likewise, regression analysis was used to derive other values interpolated from concentration-response curves. Since in the majority of the cases each tissue served as it own control, Student's paired *t* test was used to establish the significance of the peptide effect. For multiple comparisons with a single control, Dunnett's *t* tables were used. To study the statistical significance of the shifts in the concentration-response curves, co-variance analysis was used. Significance was set at a *P* value less than 0.05.

Table 1 Endothelin-1 (ET-1)-induced facilitation of NANC neurotransmission

	Phasic contractile component (g)			
Hz	*Control*	*+ 1 nM ET-1*	*+ 3 nM ET-1*	*+ 10 nM ET-1*
0.15	0.7 ± 0.2 (21)	1.4 ± 0.2 (6)	1.9 ± 0.4* (6)	2.0 ± 0.2** (9)
0.5	0.8 ± 0.1 (21)	1.3 ± 0.2* (6)	2.1 ± 0.4** (5)	2.6 ± 0.1** (9)
1.5	1.5 ± 0.2 (15)	2.0 ± 0.2 (9)	2.2 ± 0.2* (9)	2.9 ± 0.3** (9)
5.0	2.9 ± 0.3 (18)	3.8 ± 0.3 (6)	3.8 ± 0.3 (6)	4.2 ± 0.2* (6)
15.0	3.8 ± 0.3 (16)	ND	ND	5.3 ± 0.6 (9)
	Tonic contractile component (g)			
Hz	*Control*	*+ 1 nM ET-1*	*+ 3 nM ET-1*	*+ 10 nM ET-1*
0.5	0.7 ± 0.1 (16)	1.1 ± 0.2 (6)	1.7 ± 0.3* (5)	1.8 ± 0.3** (6)
1.5	0.8 ± 0.1 (15)	1.3 ± 0.1* (6)	3.8 ± 0.2** (9)	3.4 ± 0.3** (9)
5.0	0.8 ± 0.1 (18)	1.3 ± 0.2 (6)	1.3 ± 0.2 (6)	1.5 ± 0.2 (6)
15.0	0.8 ± 0.1 (16)	ND	ND	1.5 ± 0.1** (9)

Values are given ± s.e.mean.
*$P < 0.05$, **$P < 0.01$, Dunnett's *t* tables for multiple comparisons with a single control.
ND, not determined.

Peptides and drug sources

Human endothelin-1 (ET-1), [Trp(For)^{21}]-hET-1, [Met(O)^{7},Trp(For)^{21}]-hET-1, [Cys(ACM)^{1,15}]-hET-1, [Cys(ACM)^{1,15},Trp(For)^{21}]-hET-1, [Cys(ACM)^{1,15},Cys(SH)^{3,11}, Trp(For)^{21}]-hET-1, AGETB-9 (Succ^{8}-[Glu^{9},Ala^{11,15}]-ET-1(8–21)) and AGETB-89 (Succ^{7}-[Asp^{8},Glu^{9},Ala^{11,15}]-ET-1(7–21)) were all synthesized at INRS-Santé, Québec, Canada. Endothelin-2 (ET-2), endothelin-3 (ET-3), sarafotoxin S6b, sarafotoxin S6c, ET-C-terminal hexapeptide and the endothelin receptor antagonist, BE-18257B (cyclo(-D-Glu-L-Ala-allo-D-Ile-L-Leu-D-Trp) were purchased from Peninsula Laboratories (Belmont, CA, U.S.A.). Adenosine 5'-triphosphate (ATP, disodium salt), adenosine 5'-diphosphate (ADP), 5'-adenylylimidodiphosphate (AMP-PNP), α,β-methyleneadenosine 5'-triphosphate (AMP-CPP), β,δ-methyleneadenosine 5'-triphosphate (AMP-PCP), acetylcholine, 5-HT(serotonin), prostaglandin $F_{2\alpha}$, bradykinin, dimethylsulphoxide (DMSO), and tetrodotoxin were purchased from Sigma Chemical Co., MO, U.S.A. 2-Methylthioadenosine triphosphate tetrasodium salt (2-Me-S-ATP) was purchased from RBI (Natick, Mass, U.S.A.). FR 139317 ((R)2-[(R)-2-[[1-(hexahydro-1H-azepinyl] carbonyl]amino-4-methyl-pentanoyl]amino-3-[3-(1-methyl-1H-indolyl)]propionyl]amino-3-(2-pyridyl)propionic acid) was kindly provided by Prof. L. Edvinsson, Lund University, Sweden.

Results

Effects of ET-1

Basal tension ET-1 increased bladder tone with a minimal effective concentration of 3 nM (Figure 1). The peak tension was generated within 60–90 s; tension declined slowly thereafter reaching basal tone within 10 min. Repeated applications of 10 nM ET-1, developed less tension; the fourth application was inactive (Figure 1). The duration of the contractions was likewise shortened. In the absence of external Ca^{2+}, the 10 nM ET-1-induced increase in basal tension was abolished ($n = 6$, $P < 0.001$). Eversion of the bladder, abolished the 10 nM ET-1-induced contractions ($n = 6$, $P < 0.01$).

The contractile response to 10 nM ET-1 was not significantly modified by tetrodotoxin (1.56 ± 0.33 g ($n = 3$) as compared to 1.1 ± 0.08 g ($n = 26$) in untreated preparations). The toxin did not alter the rate of ET-1 desensitization following repeated ET-1 applications.

Facilitation of contractile responses evoked by both nerve stimulation and exogenous ATP ET-1 potentiated, in a concentration-dependent fashion, the motor activity induced either by transmural stimulation or by exogenous ATP (Table 1 and Figure 2). The potentiation of ATP contractions was not decreased by tetrodotoxin. The control ATP $C_{0.5\,g}$ in one particular series of experiments was 0.76 ± 0.39 μM, which decreased to 0.022 ± 0.004 μM ($n = 3$) in the presence of 10 nM ET-1 plus the toxin, reflecting a 34.5 fold potentiation. Eversion of the bladder resulted in a total loss of the ATP-induced motor activity.

Repeated applications of ATP did not sensitize the tissues to the nucleotides; the ATP $C_{0.5\,g}$ calculated from the first concentration-response curve was 2.33 ± 0.7 μM, and that from a second successive curve was 2.19 ± 0.6 μM, ($n = 6$, $F(1,81) = 0.49$, $P > 0.05$).

Mechanically increasing the bladder tone did not modify significantly the potency of ATP. The $C_{0.5\,g}$ was 3.6 ± 1.7 μM versus 2.1 ± 0.9 μM ($n = 3$) obtained when, in the same tissues, the tone was artificially increased. Likewise, precontraction of the bladder with acetylcholine, did not significantly modify the potency of ATP ($F(1,57) = 0.072$, $P > 0.05$).

Characterization of ET-1-induced activity

Concentration-dependency

Potentiation of nerve-evoked contractions ET-1 potentiated the phasic and tonic components of the contractions evoked by 0.15–15 Hz nerve stimulation. Applications of 1 nM ET-1 increased, between 20–80%, the tension generated by both components independently of the frequency of stimulation; larger concentrations of ET-1 produced proportional incre-

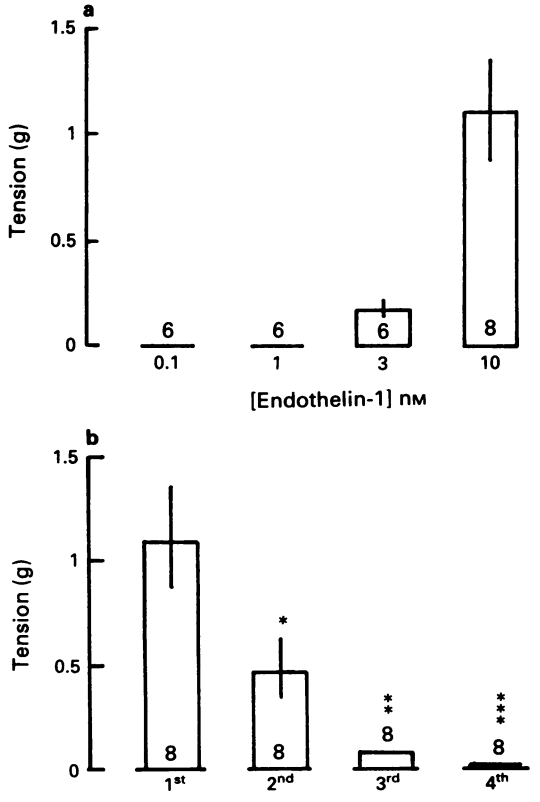

Figure 1 Endothelin-1 (ET-1)-induced increase in bladder tone. (a) Concentration-dependence; (b) tension developed by 4 successive applications of 10 nM ET-1 spaced 15 min apart followed by extensive rinsing between additions. Columns indicate mean values with s.e.mean. Numbers indicate the preparations examined (n). $^{*}P < 0.05$; $^{**}P < 0.01$; $^{***}P < 0.001$.

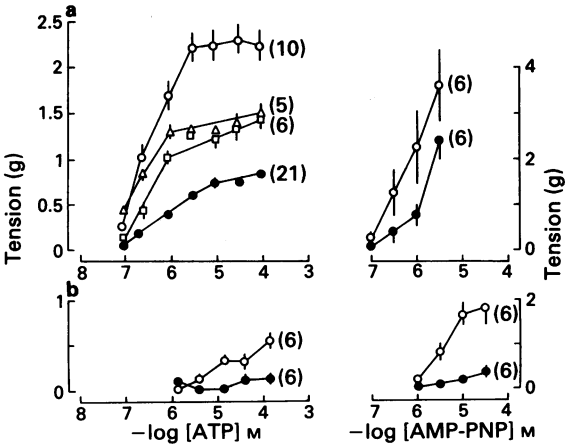

Figure 2 Effect of endothelin-1 (ET-1) on the concentration-response curves to ATP and 5'adenylylimidodiphosphate (AMP-PNP): influence of external Ca^{2+}. ATP and AMP-PNP concentration-response experiments were performed in buffer containing 2.5 mM Ca^{2+} (a) and in Ca^{2+}-free media with 0.1 mM EGTA (b) in the absence (●) and in the presence of either 1 (□), 3 (△) or 10 nM ET-1 (○). Symbols indicate mean values ± s.e.mean. The number of separate tissues used in the determination of each concentration-response curve is indicated in parentheses.

Table 2 Specificity of the 10 nM endothelin-1 (ET-1)-induced potentiation of purinoceptor responses

Purinoceptor agonists		C_{2g} *tension*[a] (μM) *Without ET-1*	*Plus 10 nM ET-1*	*Ratio*
ATP[b]	(10)	2.13 ± 0.4	0.1 ± 0.04**	21.3
ADP[b]	(3)	12.05 ± 1.95	2.73 ± 0.12**	4.4
2-Me-S-ATP	(3)	7.63 ± 2.59	1.96 ± 0.98*	3.8
AMP-CPP	(5)	0.36 ± 0.06	0.11 ± 0.02**	3.3
AMP-PCP	(3)	3.86 ± 1.06	1.33 ± 0.59*	2.9
AMP-PNP	(5)	2.37 ± 0.54	0.73 ± 0.32*	3.2
Non-purinoceptor agonists		C_{2g} *tension*[a] (μM) *Without ET-1*	*Plus 10 nM ET-1*	*Ratio*
Acetylcholine	(6)	0.48 ± 0.23	0.53 ± 0.14	0.9
5-HT	(5)	3.73 ± 1.4	3.16 ± 1.7	1.2
$PGF_{2\alpha}$	(5)	7.1 ± 2.3	3.1 ± 1.8	2.3
Bradykinin	(4)	0.41 ± 0.27	0.28 ± 0.18	1.46

Values are given ± s.e.mean.
[a]Refers to the concentration of agonists required to increase the bladder tension by 2 g; [b]in the particular case of ATP and ADP it refers to the concentration required to increase the bladder tension by 0.5 g.
*$P < 0.05$; **$P < 0.01$. Student's t test.
For abbreviations, see text.

ments in the phasic component while the tonic phase was maximal at 3 nM (Table 1).

Potentiation of exogenous ATP and AMP-PNP-evoked contractions; influence of extracellular Ca^{2+} Incubations with 1, 3 or 10 nM ET-1 caused a non-parallel, leftward displacement of the ATP concentration-response curves, increasing proportionally the maximal ATP contractile response (Figure 2). The F values when comparing these curves with their respective controls were $(1,192) = 68.8$, $P < 0.005$; $(1,185) = 157.8$, $P < 0.005$; and $(1,220) = 249.6$, $P < 0.005$ respectively. In contrast to the rather shallow ATP concentration-response curve, AMP-PNP, produced a significantly steeper curve ($F(1,174) = 39.2$, $P < 0.005$). In the presence of 10 nM ET-1, the AMP-PNP concentration-response curve was shifted 3 fold to the left, in a parallel fashion ($F(1,45) = 8.2$, $P < 0.025$, Figure 2, Table 2). In everted bladders, the con-

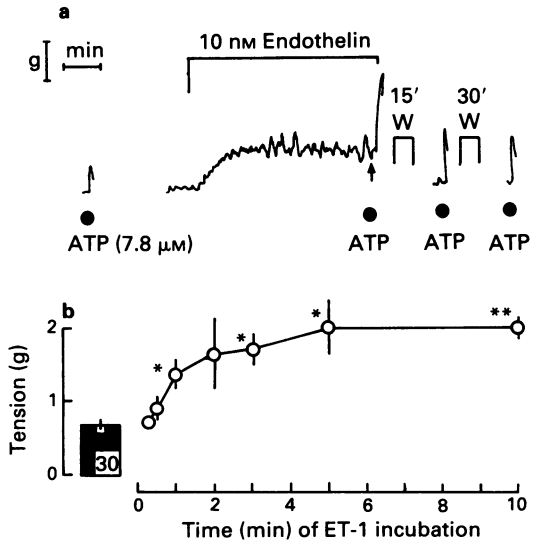

Figure 3 Time-course of the endothelin-1 (ET-1)-induced ATP potentiation. (a) ET-1 (10 nM)-induced potentiation of the 7.8 μM ATP contractions after 5 min of tissue incubation. (W = washout); (b) time-course of the facilitation following incubation with 10 nM ET-1. Solid column: tension generated by a set of 30 applications of 7.8 μM ATP. Symbols indicate mean tension ± s.e.mean generated by 7.8 μM ATP following various incubations with ET-1. AT least 4 separate experiments were performed at each incubation time. *$P < 0.05$; **$P < 0.01$.

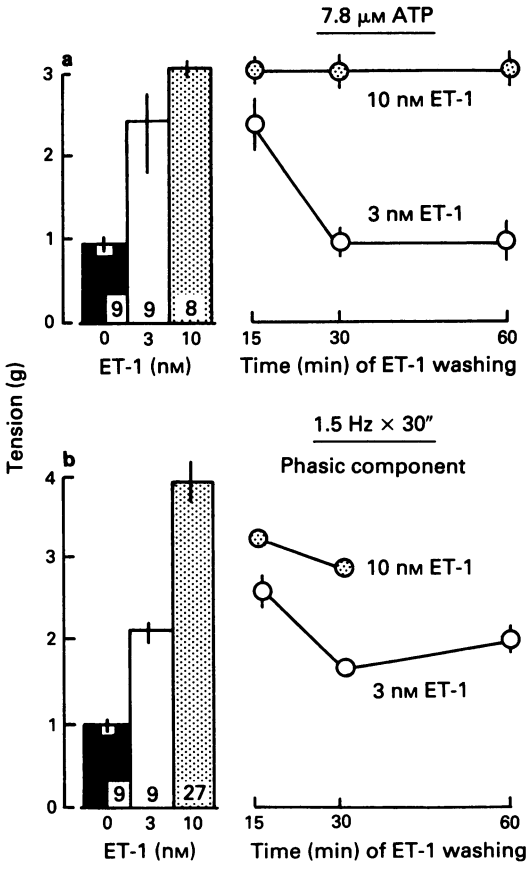

Figure 4 Recovery of endothelin-1 (ET-1)-induced potentiation of the contractions caused by ATP or nerve stimulation. (a) Contractions caused by 7.8 μM ATP alone (solid column), or following a 5 min incubation with either 3 (open column) or 10 nM ET-1 (stippled column) were rinsed and re-challenged with 7.8 μM ATP, 15, 30 and 60 min later ($n = 3$ in each case). (b) Phasic component of the contractions evoked by trains of 1.5 Hz for 30 s in the absence (solid column) and in the presence of a 5 min incubation with either 3 (open column) or 10 nM ET-1 (stippled column). Following incubations, preparations were rinsed and electrically stimulated 15, 30 and 60 min later ($n = 3$ per condition). Symbols indicate the mean tension ± s.e.mean. Numbers inside columns refer to the experiments performed in separate preparations.

tractile activity of AMP-PNP was abolished; priming with 10 nM ET-1 did not potentiate its motor action ($n = 3$).

The motor activity of both ATP and AMP-PNP was significantly reduced ($P < 0.005$) following bladder incubations in Ca^{2+}-free medium. However, 10 nM ET-1 significantly potentiated the contractile action of ATP ($F(1,63) = 25.2$, $P < 0.005$) and AMP-PNP ($F(1,45) = 38.4$, $P < 0.005$) (see Figure 2). Upon addition of Ca^{2+} to the incubation buffer, a partial restoration of the ATP, nerve and ET-1-induced motor activity was observed.

Time-course Within the first minute of 10 nM ET-1 addition, the contractile effect of 7.8 μM ATP increased by 50%. However, the maximal potentiation required about 5 min (Figure 3). In contrast to the ET-1-induced increase in basal tone, this effect of ET-1 was long-lasting and resistant to washing. The duration of the potentiation was dependent on the ET-1 concentration; tissues pretreated with 3 nM ET-1 required about 30 min of tissue washing to restore control levels of contraction to 7.8 μM ATP or nerve stimulation. With 10 nM ET-1 the potentiation to both stimuli was maintained for at least 60 min, in spite of extensive washing (Figures 3 and 4).

Specificity

Purinoceptor agonists ET-1 selectively potentiated the motor activity evoked by purinoceptor agonists, without altering the potency of acetylcholine, 5-HT, prostaglandin $F_{2\alpha}$ or bradykinin (Table 2). While 10 nM ET-1 displaced the ATP concentration-response curve 21 fold to the left, only a 3–4 fold shift was seen with ADP, 2-Me-S-ATP and the slowly hydrolyzable ATP analogues (Table 2). In the case of the latter nucleotides, the ET-1-induced shift was parallel. In the presence of ET-1, the maximal response of ADP was increased.

Characterization of the ET receptor

ET-1 structural analogues ET-2, but not ET-3, mimicked the actions of ET-1. The potency of ET-2 as a contractile agent was 10 fold greater than ET-1, whereas as a potentiator of either ATP or electrical stimulation it was 4 and 1.5 fold more effective than ET-1 respectively. ET-3 and the ET-C-terminal hexapeptide were inactive up to 100 nM. Sarafotoxin S6b was 2–5 times less potent than ET-1; sarafotoxin S6c was inactive (up to 100 nM). The ET_B receptor agonists, AGETB-9 and AGETB-89 were inactive. These results are summarized in Table 3 and Figure 5.

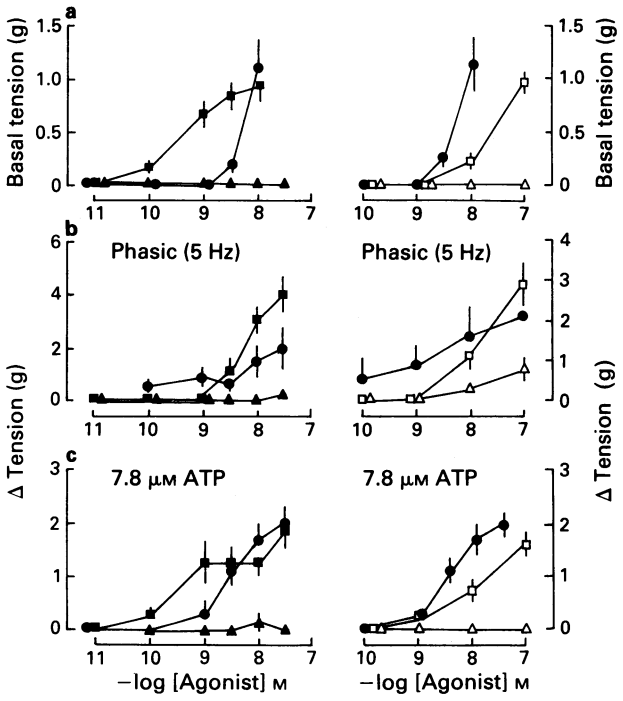

Figure 5 Potency of endothelin-1 (ET-1), ET-2, ET-3, and the sarafotoxins S6b and S6c. Increase in bladder tension (a), and difference in tension caused by the phasic component of the contraction elicited by trains of 5 Hz for 30 s (b), and in the tension generated by 7.8 μM ATP (c) prior to and after a 5 min incubation with varying concentrations of ET-1 (●), ET-2 (■), ET-3 (▲), sarafotoxin S6b (□), and sarafotoxin S6c (△). Symbols represent mean values ± s.e.mean. ($n = 6$, except for sarafotoxin S6c, $n = 3$).

Table 3 Potency of endothelin-1 (ET-1) (nM) and its natural and synthetic derivatives (nM), in contracting the rat bladder detrusor and potentiating NANC nerve evoked contractions and exogenous ATP motor activity

	Basal tension ($C_{0.5\,g}$)		*5 Hz (phasic)* ($C_{1\,g}$)		*ATP (7.8 μM)* ($C_{1\,g}$)	
ET-1	6.2 ± 1.0	(6)	4.1 ± 0.9	(6)	2.9 ± 1.2	(6)
ET-2	0.6 ± 0.2	(6)	2.7 ± 0.5	(6)	0.7 ± 0.3	(6)
ET-3	>100[c]	(6)	>100[c]	(6)	>100[c]	(6)
C-Ter	>100[c]	(3)	>100[c]	(3)	>100[c]	(3)
S6b	29.8 ± 6.9	(6)	7.7 ± 2.6	(6)	10.8 ± 2.2	(6)
S6c	>100[c]	(3)	>100[c]	(3)	>100[c]	(3)
1	15.1 ± 4.5	(6)	23.1 ± 8.0	(6)	9.0 ± 2.4	(6)
2	5.9 ± 2.0	(3)	7.4 ± 1.2	(3)	1.0 ± 0.2	(3)
3	>100[c]	(6)	>100[c]	(6)	>100[c]	(6)
4	>100[c]	(6)	>100[c]	(6)	>100[c]	(6)
5	>100[c]	(6)	>100[c]	(6)	>100[c]	(6)
6	>100[c]	(3)	>100[c]	(3)	>100[c]	(3)
7	>100[c]	(3)	>100[c]	(3)	>100[c]	(3)

Values are given ± s.e.mean.
$C_{0.5\,g}$ refers to the concentration of peptide required to increase tension by 0.5 g; $C_{1\,g}$ refers to the concentration of peptide required to increase tension by 1 g.
[c]Inactive in concentrations up to 100 nM.
S6b = Sarafotoxin S6b.
S6c = Sarafotoxin S6c.
1 = [Trp(For)^{21}]-ET-1.
2 = [Met (O)^{7},Trp(For)^{21}]-hET-1.
3 = [Cys(ACM)^{1,15}]-hET-1.
4 = [Cys(ACM)^{1,15},Trp(For)^{21}]-hET-1.
5 = [Cys(ACM)^{1,15},Cys(SH)^{3,11},Trp(For)^{21}]-hET-1.
6 = AGETB-9.
7 = AGETB-89.

Formyl tryptophan-21 ET-1, was 2 to 6 fold less potent than ET-1; oxidation of methionine-7, together with formylation of tryptophan-21, resulted in a peptide with about equal potency to ET-1 on bladder tone, 3 fold greater potency on the ATP contractions, and 2 fold less potency on nerve-evoked contractions (Table 3). Cleavage of one or both ET-1 disulphide bonds (1,15 or 1,15 and 3,11), resulted in a loss of activity up to 100 nM (Table 3).

Studies with ET_A antagonists BE-18257B: this cyclic peptide was devoid of ET-like activity but reduced, in a concentration-dependent fashion, both the ET-1-induced increase in basal tension and the potentiation of the ATP-induced contractions. The antagonist was apparently more potent against the ET-1-induced increase in basal tension than the potentiation of the ATP contractions (Figure 6a). Whereas 0.3 μM BE-18257B caused a significant reduction in the increase in basal tension, 7.5 μM was required to reduce the potentiation of ATP ($F(1,21) = 3.8$, $P < 0.1$; Figure 6a). The antagonism was slowly reversible; at least 30 min of washout was required to recover either the increase in basal tension or the ATP potentiation induced by ET-1. Neither DMSO nor BE-18257B *per se* modified the potency of ATP (data not shown).

FR 139317: as with BE-18257B, this linear tetrapeptide was devoid of ET-like activity but antagonized in a concentration-dependent fashion, both actions of ET-1. This compound was at least 10 fold more potent than BE-18257B as an ET_A antagonist; its potency against the ET-1-induced increase in bladder basal tension was larger than that required to antagonize the ATP potentiation. In fact, whereas 0.1 μM almost abolished the 10 nM ET-1-induced increase in basal tension, a 10 fold larger concentration was required to cause a significant ($F(1,24) = 6.17$, $P < 0.025$) reduction in the potentiation of ATP, while 10 μM completely antagonized the potentiation ($F(1,49) = 16.8$, $P < 0.005$; Figure 6b). Neither DMSO nor 1 μM FR 139317 modified *per se* the potency of ATP.

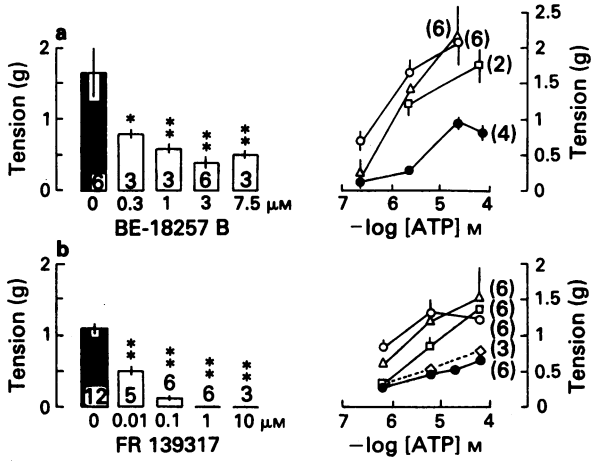

Figure 6 Antagonism of endothelin-1 (ET-1) activity by BE-18257B and FR 139317. (a) BE 18257B blockade of the increase in basal tension caused by 10 nM ET-1 (left panel), and the ATP potentiation (right panel). ATP concentration-response curves were performed either alone (●); in the presence of 10 nM ET-1 (○), or 10 nM ET-1 plus either 3 (△) or 7.5 (□) μM BE-18257B. (b) FR 139317 antagonism of the 10 nM ET-1-induce increase in bladder tension (left panel), and ATP potentiation (right panel). ATP concentration-response curves were performed either alone (●); in the presence of 10 nM ET-1 (○), or 10 nM ET-1 plus 0.1 μM FR (△); 10 nM ET-1 plus 1 μM FR (□), and 10 nM ET-1 plus 10 μM FR (◇). Columns show mean values ± s.e.mean. Numbers indicate the separate preparations examined. $*P < 0.05$; $**P < 0.01$. Symbols indicate mean values ± s.e.mean.

Discussion

The most interesting finding of this investigation is the selectivity of the ET-1-induced potentiation of the contractions induced by exogenous ATP and related analogues, an effect paralleled by the facilitation of the NANC nerve-evoked responses. In the vas deferens, ET-1 also facilitates neurotransmission, potentiating ATP, but not the noradrenaline-induced contractions (Donoso *et al.*, 1992). The ATP receptors in the bladder are P_{2x} in nature, as indicated by the order of potency of several nucleotides: AMP-CPP > AMP-PCP > AMP-PNP > ATP > 2-Me-S-ATP > ADP (Acevedo & Contreras, 1985; Donoso *et al.*, unpublished observations). The similarity between the facilitation of the nerve-evoked contractions and that elicited by exogenous ATP suggests that the ET-1-induced effect involves, at least in part, the participation of endogenous ATP as a bladder transmitter. Furthermore, the facilitation was unaltered by tetrodotoxin, which may imply that intra bladder neurones do not participate in this effect, therefore suggesting a postjunctional site of action for ET-1.

Although the interaction involves essentially P_{2x}-purinoceptors, not all of the ATP analogues were potentiated to the same degree by ET-1. Part of this difference could be due to the finding of Acevedo *et al.* (1992) that adenosine blocks ATP responses. It is possible that adenosine-derived from ATP metabolism may limit the magnitude of the ATP or ADP contractions, flattening their concentration-response curves. In addition, this discrepancy may only be apparent, since the curves of the non-hydrolyzable ATP analogues did not reach the maximal response and the magnitude of the contraction used to quantify the potentiation induced by ET-1 is markedly larger than used in the case of ATP. Furthermore, ET-1 may also inhibit ecto ATPases explaining the lesser potentiation of the non-hydrolyzable ATP analogues.

It is well documented that almost all ET-1 contractions, independent of the smooth muscle, are sluggish and relatively persistent. In the human, rabbit or rat bladder detrusor muscle, the ET-1-induced contractions are slow in developing maximal effect (Maggi *et al.*, 1989a; 1990; Lecci *et al.*, 1991) and are sustained. The present results show that both the ET-1-induced rise in bladder tension and the potentiation of the ATP responses, develop maximally within minutes; however, the potentiation of ATP is extraordinarily persistent, much more so than the ET-1-induced contractions. In addition, our findings demonstrate that the duration of the ATP potentiation is concentration-dependent; the lower the concentration of ET-1, the faster the tissue recovers its original excitability. It is plausible that within physiological concentrations, ET does not produce persistent effects and that the persistence of the effects obtained in pharmacological assays is of doubtful physiological relevance. The persistence of ET-1 activity imposes a serious restriction in evaluating experiments where multiple exposures to ET-1 are required. With regard to the mechanisms advanced to explain the persistence of ET, some investigators invoke a slow rate of dissociation from the ET receptors (Hemsén *et al.*, 1990; Traish *et al.*, 1992), while others propose that ET-1 triggers a late, post-receptor signalling event (Marsault *et al.*, 1991) and a complex process of receptor internalization followed by externalization (Marsault *et al.*, 1993).

The increase in basal tone is not obligatory for the potentiation of the ATP responses. Furthermore, the ET-1-induced rise in tone appears to involve mechanisms different from those underlying the potentiation of NANC transmission or exogenous ATP responses. Several findings support this contention: (1) the concentration of ET-1 required to potentiate either the ATP or the nerve elicited contractions is 3 to 10 fold lower than that required to increase significantly the bladder tone; (2) the time required to achieve the maximal increase in basal tension caused by 10 nM ET-1 is less than that required to cause the maximal ATP facilitation; (3) while

the mechanism leading to the rise in bladder tone rapidly desensitizes, that of the ATP potentiation does not; (4) the motor action of ET-1 is dependent on extracellular Ca^{2+}, while the facilitation of the ATP contractions is attained even in the absence of external Ca^{2+}, suggesting it requires an intracellular pool of Ca^{2+} (Salas *et al.*, 1992); (5) the different rank order of potency of some ET-1 derivatives in raising the bladder tone and potentiating ATP or nerve responses; (6) both ET_A receptor antagonists are more potent against the ET-1-induced rise in tone than the potentiation of ATP.

Several arguments substantiate our hypothesis that ET_A receptor(s) are involved in both the increase in basal tension and the facilitation of purinoceptor mechanisms. First, the order of potency of the natural ETs: ET-2 > ET-1 >> ET-3; the C-terminal hexapeptide, which has an apparent selectivity for the ET_B receptor (Maggi *et al.*, 1989b,c), was inactive. Secondly, whereas sarafotoxin S6b is less potent than ET-1, sarafotoxin S6c is completely inactive within the range of concentrations examined. Similar findings were reported by Maggi *et al.* (1990) with regard to the incease in bladder tension caused by ET-1. Thirdly, ET-1 analogues with one or no disulphide bonds were inactive. In contrast, these peptides have intrinsic activity for the ET_B receptor and were used as pharmacological tools by Germain *et al.* (1993) to describe an ET_B receptor population in the rat trachea. Fourthly, both ET-1 actions were antagonized by compounds with apparent selectivity for ET_A receptors. In agreement with Ihara *et al.* (1991a), the present results also indicate that BE-18257B is a weak and slowly reversible antagonist. Furthermore, FR 139317, a selective ET_A receptor antagonist (Aramori *et al.*, 1993), blocked both ET-1 effects albeit showing marked differences in potency. As in the case of BE-18257B, a considerably lower concentration of antagonist was required to block the ET-1-induced increase in basal tension. The finding that 10 μM completely blocked the potentiation of ATP, suggests that this action is ET_A receptor mediated. In support of the interpretation of ET_A receptors in the bladder, Garcia-Pascual *et al.* (1990) and Traish *et al.* (1992) demonstrated ET binding sites in the rabbit bladder smooth muscle. One of the ET binding sites described by Traish *et al.* (1992) has a pharmacological profile with all the characteristics of an ET_A receptor.

It remains to be established whether the same ET_A receptor underlies the increase in bladder tension and the potentiation of the ATP contractions. It is possible that either the bladder contains subtypes of an ET_A receptor or that this receptor might be coupled to different intracellular transduction mechanisms. Traish *et al.* (1992) demonstrated two ET binding sites in the rabbit bladder, only one of which was properly characterized pharmacologically. A more detailed classification of these sites, using various pharmacological and molecular biology markers will help to elucidate this problem. It is clear however, that the Ca^{2+} requirement for each effect as well as the sensitivity of the two ET_A receptor antagonists used to block these effects are different (Salas *et al.*, 1992). The implication(s) of these latter findings is being further investigated.

Several hypothetical models may account for the ET-induced potentiation of ATP (Figure 7). An ET_A receptor may sensitize the bladder smooth muscle to ATP, acting distal to the receptor. For example, ET facilitates the release of intracellular Ca^{2+} with a slow equilibrium with the extracellular cation in contrast to the Ca^{2+} pool mobilized by ATP (Figure 7a). In this connection, Chau *et al.* (1993) recently suggested that both ET and ATP hydrolyze a separate pool of polyphosphoinositides in neuroblastoma-glioma hybrid cells resulting in additive responses due to the release of separate pools of Ca^{2+}. Alternatively, an ET_A membrane receptor may 'cross-talk' with a P_{2x}-purinoceptor increasing its affinity and/or modifying its ionophore function (Figure 7b). It is possible that these two mechanisms might operate simultaneously. Although less likely, ET may interact directly at an allosteric regulatory site on the P_{2x}-purinoceptor, increasing its affinity or altering the kinetics of its ionophore function (Figure 7c). With regard to the increase in bladder tension caused by the ETs, the ET_A receptor involved could be coupled to a calcium channel mainly dependent on the influx of extracellular Ca^{2+} (Figure 7).

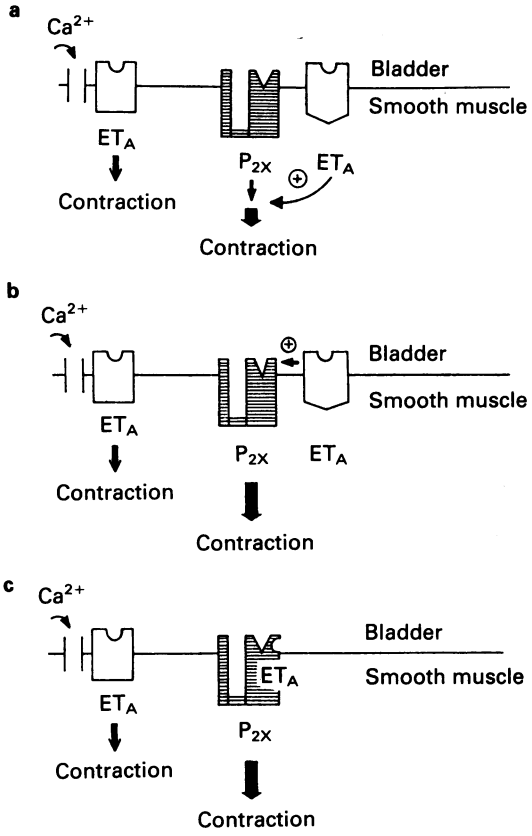

Figure 7 Hypothetical model diagrams: the bladder is endowed with ET_A receptor responsible for the rise in tone. This site is linked, directly or indirectly to Ca^{2+} channels. The bladder contains, in addition, another ET_A binding site that sensitizes the detrusor to actions triggered by ATP acting on P_{2x}-purinoceptors. Three models are proposed to explain the mechanism of the ET-1-induced selective ATP potentiation, an effect which is independent of the rise in basal tone. (a) ET_A receptor activation sensitizes the muscle to ATP, via a mechanism distal to the P_{2x}-purinoceptor. This mechanism entails the release of independent second messengers which as an end result amplifies the motor action of ATP. (b) The ET_A receptor 'cross-talks' with P_{2x}-purinoceptor, favouring purinergic responses. (c) The ET_A receptor is allosterically localized in the P_{2x}-purinoceptor.

These ET_A receptors could be localized in the same or in different bladder smooth muscle cell populations. Ihara *et al.* (1991b) demonstrated that vascular smooth muscle cells express both ET_A and ET_B receptors, while Donoso *et al.* (1992) demonstrated marked differences in the ET-1 responses between the epididymal and prostatic segments of the rat vas deferens. Obviously, neither the available techniques nor current knowledge on ET-1 and ATP pharmacodynamics are sufficient to allow resolution of this question (Van Renterghem *et al.*, 1988; Marsden *et al.*, 1989; Highsmith *et al.*, 1992).

The possible physiological implications of ET-1 in the bladder, given that the epithelial and non vascular smooth muscle cells of this organ synthesize ET-1 (Saenz de Tejada *et al.*, 1992), are of paramount interest. The present results support the hypothesis that ET-1 may participate in the control of bladder tone by acting as an autocrine hormone. Furthermore, we propose that the autocrine role of ET may include the facilitation of NANC transmission.

Since ET-1 is also known to enhance the purinergic motor component of sympathetic neurotransmission in the rat vas

deferens (Donoso *et al.*, 1992), our working hypothesis suggests that ET-1 plays a role as a local modulator of the purinergic component of neurotransmission. The mechanism involved in this interaction warrants further experimentation.

Funded in part by FONDECYT Grant 658-92, Fundación Andes C-11626 and the Quebéc Heart Foundation. M.V.D. is a Research Associate Pharmacologist supported in part by a fellowship from Dirección de Investigaciones, Pontificia Universidad Católica de Chile. A.F. is a scientist from Fonds de la Recherche en Santé du Quebéc. We appreciate the technical and artistic contributions of R. Miranda.

References

ACEVEDO, C.G. & CONTRERAS, E. (1985). Possible involvement of adenine nucleotides in the neurotransmissions of the mouse urinary bladder. *Comp. Biochem. Physiol.*, **82c**, 357–361.

ACEVEDO, C.G., CONTRERAS, E., ESCALONA, J., LEWIN, J. & HUIDOBRO-TORO, J.P. (1992). Pharmacological characterization of adenosine A1 and A2 receptors in the bladder: evidence for a modulatory adenosine tone regulating non-adrenergic non-cholinergic neurotransmission. *Br. J. Pharmacol.*, **107**, 120–126.

ACEVEDO, C.G., LEWIN, J., CONTRERAS, E. & HUIDOBRO-TORO, J.P. (1990). Bradykinin facilitates the purinergic motor component of the rat bladder neurotransmission. *Neurosci. Lett.*, **113**, 227–232.

ARAI, H., HORI, S., ARAMORI, I., OHKUBO, H. & NAKANISHI, S. (1990). Cloning and expression of a cDNA encoding an endothelin receptor. *Nature*, **348**, 730–732.

ARAMORI, I., NIREI, H., SHOUBO, M., SOGABE, K., NAKAMURA, K., KOJO, H., NOTSU, Y., ONO, T. & NAKANISHI, S. (1993). Subtype selectivity of a novel endothelin antagonist, FR 139317, for the two endothelin receptors in transfected Chinese hamster ovary cells. *Mol. Pharmacol.*, **43**, 127–131.

BO, X.N., SIMON, J., BURNSTOCK, G. & BARNARD, E.A. (1992). Solubilization and molecular size determination of the P(2x) purinoceptor from rat vas deferens. *J. Biol. Chem.*, **267**, 17581–17587.

BROWN, C., BURNSTOCK, G. & COCKS, T. (1979). Effects of adenosine 5'-triphosphate (ATP) and α,β-methylene ATP on the rat urinary bladder. *Br. J. Pharmacol.*, **65**, 97–102.

BURNSTOCK, G. (1990a). Noradrenaline and ATP as cotransmitters in sympathetic nerves. *Neurochem. Int.*, **17**, 357–368.

BURNSTOCK, G. (1990b). Co-transmission. *Arch. Int. Pharmacodyn. Ther.*, **304**, 7–33.

BURNSTOCK, G., COCKS, T., CROWE, R. & KASAKOV, L. (1978a). Purinergic innervation of the guinea-pig urinary bladder. *Br. J. Pharmacol.*, **63**, 125–138.

BURNSTOCK, G., COCKS, KASAKOV, L. & WONG, H.K. (1978b). Direct evidence for ATP release from non-adrenergic, non-cholinergic ('purinergic') nerves in the guinea-pig taenia coli and bladder. *Eur. J. Pharmacol.*, **49**, 145–149.

BURNSTOCK, G. & KENNEDY, C. (1985). Is there a basis for distinguishing two types of P2-purinoceptors? *Gen. Pharmacol.*, **16**, 433–440.

CHAU, L.Y., LIN, T.A., CHANG, W.T., CHEN, C.H., SHUE, M.J., HSU, Y.S., HU, C.Y., TSAI, W.H. & SUN, G.Y. (1993). Endothelin-mediated calcium response and inositol 1,4,5-trisphosphate release in neuroblastoma-glioma hybrid cells (NG108-15): cross talk with ATP and bradykinin. *J. Neurochem.*, **60**, 454–460.

DONOSO, M.V.,, MONTES, C.G., LEWIN, J., FOURNIER, A., CALIXTO, J.B. & HUIDOBRO-TORO, J.P. (1992). Endothelin-1 (ET-1)-induces mobilization of intracellular Ca^{2+} stores from the smooth muscle facilitates sympathetic cotransmission by potentiation of adenosine 5'-triphosphate (ATP) motor activity: studies in the rat vas deferens. *Peptides*, **13**, 831–840.

DUNN, P.M. & BLAKELEY, A.G.H. (1988). Suramin: a reversible P_2-purinoceptor antagonist in the mouse vas deferens. *Br. J. Pharmacol.*, **93**, 243–245.

EVANS, R.J., DERKACH, V. & SURPRENANT, A. (1992). ATP mediates fast synaptic transmission in mammalian neurons. *Nature*, **357**, 503–505.

EVANS, R.J. & SURPRENANT, A. (1992). Vasoconstriction of guinea-pig submucosal arterioles following sympathetic nerve stimulation is mediated by the release of ATP. *Br. J. Pharmacol.*, **106**, 242–249.

FEDAN, J.S., HOGABOOM, G.J., O'DONNELL, J.P., COLBY, J. & WESTFALL, D.P. (1981). Contributions by purines to the neurogenic responses of the vas deferens of the guinea-pig. *Eur. J. Pharmacol.*, **69**, 41–53.

FILEP, J.G. (1992). Endothelin peptides: biological actions and pathophysiological significance in the lung. *Life Sci.*, **52**, 119–133.

GARCIA-PASCUAL, A., LARSSON, B. & ANDERSSON, K.E. (1990). Contractile effects of endothelin-1 and localizaton of endothelin binding sites in rabbit lower urinary tract smooth muscle. *Acta Physiol. Scand.*, **140**, 545–555.

GERMAIN, M., BATTISTINI, B., FILEP, J.G., SIROIS, P. & FOURNIER, A. (1993). Endothelin derivatives showing potent effects in the guinea pig trachea. *Peptides*, **14**, 613–619.

HARTTER, E. & WOLOSZCZUK, W. (1989). Radioimmunoassay of endothelin. *Lancet*, **i**, 909.

HEMSÉN, A., FRANCO-CERECEDA, A., MATRAN, R., RUDEHILL, A. & LUNDBERG, J.M. (1990). Occurrence, specific binding sites and functional effects of endothelin in human cardiopulmonary tissue. *Eur. J. Pharmacol.*, **191**, 319–328.

HIGHSMITH, R.F., BLACKBURN, K. & SCHMIDT, D.J. (1992). Endothelin and calcium dynamics in vascular smooth muscle. *Annu. Rev. Physiol.*, **54**, 257–277.

HOYLE, C.H.V. & BURNSTOCK, G. (1985). Atropine-resistant excitatory junction potentials on rabbit bladder are blocked by α,β-methylene ATP. *Eur. J. Pharmacol.*, **114**, 239–240.

IHARA, M., FUKURODA, T., SAEKI, T., NISHIKIBE, M., KOJIRI, K., SUDA, H. & YANO, M. (1991a). An endothelin receptor (ETA) antagonist isolated from streptomyces misakiensis. *Biochem. Biophys. Res. Commun.*, **178**, 132–137.

IHARA, M., SAEKI, T., FUNUBASHI, K., NAKAMICHI, K., YANO, M., FUKURODA, T., MIYAJI, M., MISHIKIBE, M. & IKEMOTO, F. (1991b). Two endothelin receptor subtypes in porcine arteries. *J. Cardiovasc. Pharmacol.*, **17**, S119–S121.

KASAKOV, L. & BURNSTOCK, G. (1983). The use of the slowly degradable analog, α,β methylene ATP, to produce desensitation of the P2-purinoceptor: effect on non-adrenergic, non-cholinergic responses of the guinea-pig urinary bladder. *Eur. J. Pharmacol.*, **86**, 291–294.

LECCI, A., GIULIANI, S., SANTICIOLI, P., ROVERO, P., MAGGI, C.A. & GIACHETTI, A. (1991). Intracerebroventricular administration of endothelins: effects on the supraspinal micturition reflex and blood pressure in the anesthetized rat. *Eur. J. Pharmacol.*, **199**, 201–207.

LERMAN, A., HILDEBRAND, F.L. Jr, MARGULIES, K.B., O'MURCHU, B., PERRELLA, M.A., HEUBLEIN, D.M., SCHWAB, T.R. & BURNETT, J.C. (1990). Endothelin: a new cardiovascular regulatory peptide. *Mayo Clin. Proc.*, **65**, 1441–1455.

MAGGI, C.A., GIULIANI, S., PATACCHINI, R., SANTICIOLI, P., TURINI, D., BARBANTI, G. & MELI, A. (1989a). A potent contractile activity of endothelin on the human isolated urinary bladder. *Br. J. Pharmacol.*, **96**, 755–757.

MAGGI, C.A., GIULIANI, S., PATACCHINI, R., BARBANTI, G., TURINI, D. & MELI, A. (1990). Contractile responses of the human urinary bladder, renal pelvis and renal artery to endothelins and sarafotoxin S6b. *Gen. Pharmacol.*, **21**, 247–250.

MAGGI, C.A., GIULIANI, S., PATACCHINI, R., SANTICIOLI, P., ROVERO, P., GIACHETTI, A. & MELI, A. (1989c). The C-terminal hexapeptide, endothelin-(16-21), discriminates between different endothelin receptors. *Eur. J. Pharmacol.*, **166**, 121–122.

MAGGI, C.A., PATACCHINI, R., GIULIANI, S. & MELI, A. (1989b). Potent contractile effect of endothelin in isolated guinea-pig airways. *Eur. J. Pharmacol.*, **160**, 179–182.

MARSAULT, R., FEOLDE, E. & FRELIN, C. (1993). Receptor externalization determines sustained contractile responses to endothelin-1 in the rat aorta. *Am. J. Physiol.*, **264**, C687–693.

MARSAULT, R., VIGNE, P. & FRELIN, C. (1991). The irreversibility of endothelin action is a property of a late intracellular signalling event. *Biochem. Biophys. Res. Commun.*, **179**, 1408–1413.

MARSDEN, P.A., DANTHULURI, N.R., BRENNER, B.M., BALLERMANN, B.J. & BROCK, T.A. (1989). Endothelin action on vascular smooth muscle involves inositol trisphosphate and calcium mobilization. *Biochem. Biophys. Res. Commun.*, **158**, 86–93.

MASAKI, T. (1991). Tissue specificity of the endothelin-induced responses. *J. Cardiovasc. Pharmacol.*, **17**, S1–S4.

MELDRUM, L.A. & BURNSTOCK, G. (1983). Evidence that ATP acts as a cotransmitter with noradrenaline in sympathetic nerves supplying the guinea-pig vas deferens. *Eur. J. Pharmacol.*, **92**, 161–163.

RAMME, D., REGENOLD, J.T., STARKE, K., BUSSE, R. & ILLES, P. (1987). Identification of neuroeffector transmitter in jejunal branches of the rabbit mesenteric artery. *Naunyn Schmied. Arch. Pharmacol.*, **336**, 267–273.

SAENZ DE TEJADA, I., MUELLER, J.D., DE LAS MORENAS, A., MACHADO, M., MORELAND, R.B., KRANE, R.J., WOLFE, H.J. & TRAISH, A.M. (1992). Endothelin in the urinary bladder. I. synthesis of endothelin-1 by epithelia, smooth muscle and fibroblasts suggests autocrine and paracrine cellular regulation. *J. Urology*, **148**, 1290–1298.

SAKURAI, T., YANAGISAWA, M., TAKUWA, Y., MIYAZAKI, H., KIMURA, S., GOTO, K. & MASAKI, T. (1990). Cloning of a cDNA encoding a non-isopeptide-selective subtype of the endothelin receptor. *Nature*, **348**, 732–735.

SALAS, C., DONOSO, M.V. & LEWIN, J. (1992). Is endothelin-1 (E) a modulator of non-adrenergic non-cholinergic neurotransmission (NANC)? *XIV Annual Meeting Society of Pharmacology of Chile*, p. 28.

SIMONSON, M.S. & DUNN, M.J. (1990). Cellular signalling by peptides of the endothelin gene family. *FASEB J.*, **4**, 2989–3000.

SNEDDON, P. & BURNSTOCK, G. (1984). Inhibition of excitatory junction potentials in guinea-pig vas deferens by α,β methylene-ATP: further evidence for ATP and noradrenaline as co-transmitters. *Eur. J. Pharmacol.*, **100**, 85–90.

SNEDDON, P. & WESTFALL, D.P. (1984). Pharmacological evidence that adenosine triphosphate and noradrenaline are co-transmitters in the guinea-pig vas deferens. *J. Physiol.*, **347**, 561–580.

STEWART, D.J., LEY, R.D., CERNACEK, P. & LANGLEBEN, D. (1992). Increased plasma endothelin-1 in pulmonary hypertension: marker or mediated of disease? *Ann. Int. Med.*, **114**, 464–469.

STJÄRNE, L. & ASTRAND, P. (1984). Discrete event measure single quanta of adenosine 5η-triphosphate secreted from sympathetic nerves of guinea-pig and mouse vas deferens. *Neuroscience*, **14**, 929–946.

TRAISH, A., MORAN, E., KRANE, R.J. & SAENZ DE TEJADA, I. (1992). Endothelin in the urinary bladder. II. Characterization of endothelin receptor subtypes. *J. Urology*, **148**, 1299–1306.

VAN RENTERGHEM, C., VIGNE, P., BARHANIN, J., SCHMID-ALLIANA, A., FRELIN. C. & LAZDUNSKI, M. (1988). Molecular mechanism of action of the vasoconstrictor peptide endothelin. *Biochem. Biophys. Res. Commun.*, **157**, 977–985.

YANAGISAWA, M. & MASAKI, T. (1989). Molecular biology and biochemistry of the endothelins. *Trends Pharmacol. Sci.*, **10**, 374–378.

(Received July 22, 1993
Revised October 5, 1993
Accepted October 14, 1993)

Br. J. Pharmacol. (1994), **111**, 483–488

Fluspirilene block of N-type calcium current in NGF-differentiated PC12 cells

[1,*]C.J. Grantham, M.J. Main & M.B. Cannell

Department of Pharmacology, St. George's Hospital Medical School, Cranmer Terrace, London SW17 0RE and *Lilly Research Centre Ltd., Erl Wood Manor, Windlesham, Surrey GU20 6PH

1 High voltage-activated calcium currents were recorded in nerve growth factor (NGF)-differentiated PC12 cells with the whole-cell patch clamp technique. After exposure to NGF for 3–10 days the PC12 cells developed neurone-like processes and calcium currents which were pharmacologically separable into L- and N-types (defined by sensitivity to nifedipine and ω-conotoxin GVIA respectively).

2 After blocking the L-type calcium channels with nifedipine (10 μM), ω-conotoxin GVIA blocked approximately 85% of the remaining calcium current with an IC_{50} of 3 nM and a Hill coefficient of 1. The block by conotoxin GVIA was irreversible on the time scale of these experiments. These results suggested that the majority of the nifedipine-insensitive calcium current was N-type.

3 Fluspirilene, a substituted diphenylbutylpiperidine with potent neuroleptic properties, reversibly inhibited the N-type component in a dose-dependent manner with an IC_{50} of 30 nM. The Hill coefficient of the block was 0.25. The fraction of current blocked was the same at all test potentials examined (−30 to +40 mV).

4 These data indicate that the neuroleptic properties of fluspirilene may be due, at least in part, to an inhibition of neuronal N-type calcium channels. This finding raises the possibility that modulation of N-type calcium channel activity by drugs derived from substituted diphenylbutylpiperidines may provide a novel way of altering neurotransmitter release and hence brain function.

Keywords: Diphenylbutylpiperidine; calcium channels; calcium channel antagonists; neuroleptic agents; N-type calcium channels; PC12 cells

Introduction

Fluspirilene, a member of the diphenylbutylpiperidine (DPBP) class of neuroleptic drugs (which also includes pimozide, clopimozide and penfluridol), has been shown to have anti-schizophrenic actions (Hassel, 1985). The first evidence for the mechanism of action of DPBPs was the observation that fluspirilene and other DPBPs inhibit [^{3}H]-nitrendipine binding to rat cortical membrane vesicles (Gould *et al.*, 1983). Subsequent binding studies on skeletal muscle (Galizzi *et al.*, 1986), cardiac muscle (Quirion *et al.*, 1985; Qar *et al.*, 1987; King *et al.*, 1989), smooth muscle (Qar *et al.*, 1987) and brain (Quirion *et al.*, 1985; Qar *et al.*, 1987; Kenny *et al.*, 1990) showed that DPBPs bind to receptors for calcium channel antagonists in a variety of tissues. However, the binding site for DPBPs appears to be a discrete site, separate from the dihydropyridine, arylalkylamine and benzothiazepine binding sites of the calcium channel (King *et al.*, 1989).

Fluspirilene, the DPBP with the highest affinity in binding assays, has been shown to block calcium channels in functional studies. Inhibition of calcium movements has been demonstrated in both smooth muscle (Gould *et al.*, 1983; Fraser *et al.*, 1988; Kenny *et al.*, 1990) and neuronal (Galizzi *et al.*, 1986; Qar *et al.*, 1987; King *et al.*, 1989; Enyeart *et al.*, 1990) preparations. Whole-cell patch clamp data have shown that fluspirilene blocks both low voltage-activated (T-type) and high voltage-activated calcium channels in GH3 and GH4C1 cell lines (Enyeart *et al.*, 1990).

Nowycky *et al.* (1985), working with chick dorsal root ganglion cells, introduced a classification for high-voltage-activated (HVA) calcium channels, dividing them into L- and N-type channels. N-type channels are found predominantly in neurones and differ from L-type channels in both their electrophysiological and pharmacological properties (Fox *et al.*, 1987). The CNS distribution of these N-type channels is widespread and is distinct from that of L-type channels (Sher & Clementi, 1991). At the cellular level, N-type channels are clustered at 'active zones' on presynaptic nerve terminals (Smith & Augustine, 1988) and have been implicated in the control of neurotransmitter release from these structures (Hirning *et al.*, 1988).

Previous mechanistic studies did not differentiate between N-type and L-type calcium channels, so it is possible that the anti-schizophrenic action of fluspirilene may be due, at least in part, to modulation of neurotransmitter release via an effect on central N-type channels. To examine this possibility, we used a nerve growth factor (NGF)-differentiated PC12 cell line as a source of N-type calcium channels. PC12 cells are derived from a rat phaeochromocytoma cell line and respond to NGF by acquiring neuronal characteristics, such as extension of neurite-like processes, and by expression of voltage-sensitive sodium and calcium channels (Streit & Lux, 1987; Rudy *et al.*, 1987; Furukawa *et al.*, 1993). A number of studies have demonstrated that the calcium channels in NGF-differentiated PC12 cells can be sub-divided into the types described by Nowycky *et al.* (1985), namely, L-, N- and T-type channels (Garber *et al.*, 1989; Usowicz *et al.*, 1990; Plummer *et al.*, 1989). In this study, we have shown that our line of NGF-differentiated PC12 cells expresses N-type calcium channels and that fluspirilene blocks calcium fluxes through these channels. We conclude, therefore, that a part of the central action of fluspirilene may be the result of an effect on central neurotransmitter release through its antagonism of N-type calcium channel fluxes.

Methods

Growth and preparation of differentiated PC12 cells

PC12 cells, adherent to tissue culture flasks, were isolated by agitation without enzymes, from maintenance cultures which

[1] Author for correspondence.

were routinely passaged once weekly. This procedure produced large clumps of cells which could be dispersed by gentle trituration through a 21-gauge needle up to 5 times to generate a largely unicellular suspension. Induction of neuronal phenotype was achieved by transferring the dispersed cells to poly-L-lysine/collagen-coated glass coverslips and exposing them to NGF in defined culture medium at 37°C in a humidified 95% air/5% CO_2 atmosphere (Doherty *et al.*, 1988). Under this differentiating protocol the PC12 cells' appearance changed from relatively indistinct, masses of dividing cells to one of single, non-dividing, refractile, spherical cells, each developing one or more processes after 1 to 2 days exposure to NGF.

Recording of N-type calcium currents by whole-cell patch clamp technique

Coverslip fragments bearing adherent, differentiated PC12 cells were transferred to a recording chamber, mounted on the stage of a Nikon Diaphot microscope (Nikon Instruments, Japan). The chamber (volume 200 µl) was continuously perfused with either Ca/Na EBS or Ca/TEA EBS flowing at a rate of 2 ml min^{-1}. Drugs were added to the Ca/TEA EBS as required. Low resistance patch electrodes (2–4 MOhm) were pulled from fibre-filled borosilicate glass (Sutter Instruments, U.S.A.) and were filled with a cesium containing solution (see below) to suppress potassium currents.

The whole-cell patch-clamp technique (Hamill *et al.*, 1981) was used to examine voltage-sensitive calcium channels (VSCCs) in NGF-treated PC12 cells. Cells, bathed in Ca/Na EBS, were voltage-clamped with an Axopatch 1B patch clamp amplifier (Axon Instruments Inc., U.S.A.). After achieving whole-cell configuration, the bathing solution was switched to Ca/TEA EBS, to suppress potassium and sodium currents. The PC12 cell VSCCs were examined using stimulation protocols generated by pCLAMP version 5 driving a TL-1 analogue-to-digital converter (Axon Instruments Inc., U.S.A.) in a 486/25 MHz microcomputer (Gateway, U.S.A.). Data were filtered at 5 kHz and digitized by a VR-4-100A digital recorder (Instrutech, U.S.A.) for recording by a VCR. Data were analysed off-line with pCLAMP software.

A ramp protocol was used to obtain a rapid confirmation of the presence of calcium currents in individual cells. The cells were then stepped to the potential which evoked a peak current in order to characterize the whole-cell PC12 current in terms of nifedipine and ω-conotoxin GVIA (CgTX) sensitive components.

Solutions (composition in mM)

Ca/Na EBS $CaCl_2$ 2, KCl 5.4, NaCl 135, $MgCl_2$ 1, (N-[2-hydroxyethyl]piperizine-*N'*-[2-ethanesulphonic acid]) (HEPES) 10, glucose 10, pH 7.4 (adjusted with NaOH).

Ca/TEA EBS $CaCl_2$ 10, KCl 5.4, NaCl 135, $MgCl_2$ 1, TEA Cl 20, HEPES 10, glucose 10, tetrodotoxin 300 nM, pH 7.4.

Pipette solution CsCl 10, CsOH 100, aspartic acid 80, TEA Cl 20, HEPES 30, EGTA 5, MgATP 3, pH 7.2 (adjusted with CsOH).

Culture medium Growth medium for PC12 cells was Dulbecco's Modified Eagle's Medium (Imperial Laboratories, Andover, U.K.) supplemented with 2% foetal calf serum (Sera Lab, U.K.), glutamine 2 mM, penicillin 50 u ml^{-1}, streptomycin 50 µg ml^{-1} (Life Technologies Ltd., Paisley, U.K.), bovine insulin 0.6 iu ml^{-1}, human apo-transferrin 0.125 µg ml^{-1} (Sigma Chemical Co., Poole, U.K.) and SATO's ingredient's (sodium selenite 0.3 µM, progesterone 0.25 µM, L-thyroxine 0.6 µM, triiodothyronine 0.6 µM, putrescine 125 µM, Path-O-cyte-4 1%; Sigma and ICN Biomedicals Ltd., High Wycombe, U.K.) as described by Doherty *et al.* (1988).

Differentiating medium was culture medium without the addition of calf serum and included 100 ng ml^{-1} 7S-nerve growth factor (Calbiochem Novabiochem, Nottingham, U.K.).

Chemicals and materials

All tissue culture-ware was obtained from BD U.K. (Oxford, U.K.), coverslips (No. 0, Chance Proper, Warley, U.K.) were first coated with aqueous poly-L-lysine (Sigma) 50 µg ml^{-1} followed by collagen 25 µg cm^{-2} in 30/20 (v/v) ethanol/water mixture (rat-tail type-VII, Sigma) and air dried before use. Cadmium chloride (Sigma) and CgTX (Bachem, California, U.S.A.) stocks were made up in aqueous solution, while dimethylsulphoxide (DMSO) (Sigma) was the vehicle for nifedipine (Sigma) and fluspirilene (synthesized at Lilly Research Centre Ltd., by J. Fairhurst) stocks. All other chemicals were of reagent grade (Sigma; Fisons, Loughborough, U.K.; Aldrich, Gillingham, U.K.) and all solutions were made up in purified water (>18 MOhm cm^{-1}).

Results

Undifferentiated cells and cells exposed to NGF for less than 3 days had little or no high voltage-activated (HVA) calcium currents. Exposure of cells to NGF for between 3 and 10 days resulted in the growth of neurites and concomitant appearance of HVA calcium current. Cells with only one or two short neurites were selected for experiments as it was found impossible to obtain adequate voltage control in cells with long multiple neurites. Longer term exposure to NGF resulted in a reduction in the number of cells in which it was possible to obtain adequate voltage control (not shown). In chosen cells, the whole-cell calcium current ranged from 200 pA to 1 nA.

Kinetics and cadmium-sensitivity of PC12 calcium current

As illustrated in Figure 1, the bathing and pipette filling solutions allowed measurement of calcium currents without serious contamination from other conductances. Figure 1a shows whole-cell currents generated in response to a depolarizing voltage ramp from −100 mV to +100 mV over 500 ms (holding potential = −40 mV). At very negative potentials the current voltage relationship is linear with a slope conductance of 0.4 pS. This low conductance probably reflects the integrity of the seal between the membrane and pipette (as well as any residual membrane conductance). As the membrane potential became more positive than about −10 mV, a large inward current was observed which reached a peak of 275 pA at +20 mV before decreasing and reversing near to +60 mV. The addition of 0.1 mM Cd^{2+} blocked the inward current, suggesting that the recorded current was due to the activation of HVA calcium currents.

Characterization of nifedipine-resistant calcium current in NGF-treated PC12 cells

Since there are at least three types of HVA calcium channel in neuronal preparations (Nowycky *et al.*, 1985), pharmacological criteria were used to distinguish between the types of calcium channel present. As illustrated in Figure 1b, depolarization beyond −20 mV elicited a rapidly activating inward current which slowly inactivated during the pulse. Addition of 10 µM nifedipine (a dose that produces maximal block of L-type calcium channels: Nowycky *et al.*, 1985) reduced the current elicited in response to depolarizing steps by about 50% at all potentials examined. Subsequent exposure of the cell to 100 nM CgTX resulted in a further

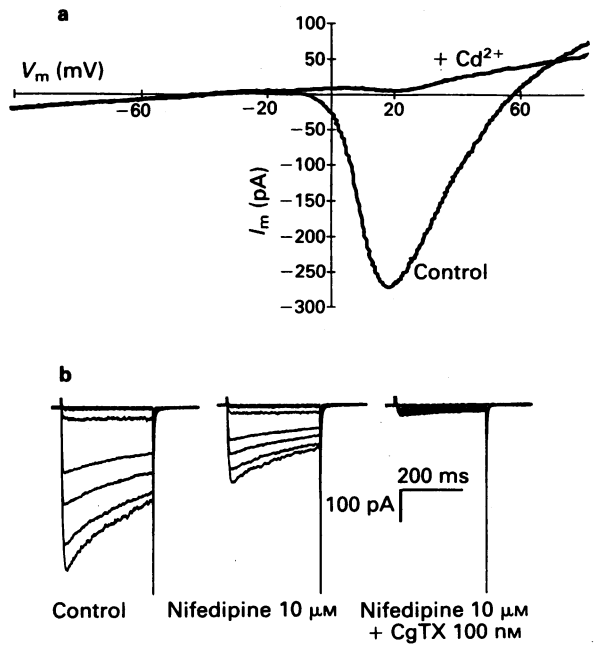

Figure 1 Characterization of PC12 cell calcium current and its sensitivity to inorganic and organic agent(s). (a) Whole-cell recording from a nerve growth factor (NGF)-treated PC12 cell showing the current-voltage relationship before and after cadmium chloride (0.1 mM). The calcium current activated at −10 mV, peaked at +20 mV and reversed at about 60 mV, which was the reversal potential for Ca^{2+} under the conditions used in this series of experiments. Cadmium almost completely blocked the current within 30 s of application and could be washed off with similar rapidity (not shown). (b) Typical PC12 calcium currents evoked by steps from the holding potential (−40 mV) to various potentials between −20 mV and 60 mV in 10 mV increments. The step duration was 300 ms and steps were applied at 5 s intervals. The current present in control and nifedipine-treated traces contained a large component of time-dependent inactivation which largely disappeared after treatment with ω-conotoxin GVIA (CgTX). Application of 10 μM nifedipine resulted in approximately a 50% reduction in current at all voltages without affecting the kinetics of current activation. Application of 100 nM CgTX caused a further reduction of current at all voltages to about 10% of the control current. Note the residual current remaining after combined application of both nifedipine and CgTX.

reduction in the amplitude of the calcium current to 12% of the control. It is possible that this residual current reflects the presence of P-type calcium channels (Llinas *et al.*, 1989; Mintz *et al.*, 1992), but this idea was not explored further. Experiments of the type shown in Figure 1 showed that NGF exposure resulted in the expression of a HVA-calcium current which consisted predominantly of L- and N-type current in approximately equal proportions.

The time course of the block of nifedipine-insensitive current is illustrated in Figure 2a. The cell had been exposed to nifedipine (10 μM) until the current reached a steady level before CgTX was added. CgTX exposure caused the current to decrease with a half time of about 60 s to a new steady level. The dose-response relationship for the inhibition of the nifedipine-insensitive current by CgTX is shown in Figure 2b. Regression analysis suggested that the block of the nifedipine-insensitive current by CgTX was dose-dependent with half maximal block occurring at 3 nM and a Hill coefficient of 1. It is possible that channel run-down contributed to the observed block at 1 nM CgTX since the development of block at this CgTX concentration was very slow ($T_{1/2} > 5$ min). The block by CgTX was not reversible on the time scale of these experiments (not shown). As noted earlier, a component of PC12 calcium current was not blocked by the combination of nifedipine and CgTX, and in these experiments this resistant component comprised about 25% of the nifedipine-resistant current. The inset to Figure 2a shows sample records from an experiment performed to illustrate the graded block of current by CgTX. Three doses (1, 30 and 100 nM) of CgTX were applied sequentially to a single cell. The currents were elicited by steps from a V_{hold} of −40 mV to +20 mV for 200 ms every 5 s.

Effect of fluspirilene on the nifedipine-resistant calcium current in PC12 cells

The above data show that after NGF exposure, the PC12 cells expressed both N- and L-type calcium channels. Since fluspirilene blocks L-type channels (Qar *et al.*, 1987; King *et al.*, 1989; Enyeart *et al.*, 1990), the contribution of L-type channels to the whole-cell current was removed by applying 10 μM nifedipine. As the majority of the residual current in these conditions (about 80%) was due to N-type calcium channels (as shown by its sensitivity to CgTX), it was possible to examine the block of N-type calcium current by fluspirilene. Figure 3a shows that application of 10 μM nifedipine blocked about 50% of the whole-cell current in about 1 min. After the block by nifedipine had stabilized, 10 μM fluspirilene was added to the bathing solution resulting in a further decrease in the amplitude of the calcium current.

Figure 3b shows the dose-dependence of the block by fluspirilene. Fluspirilene reduced the nifedipine-resistant cur-

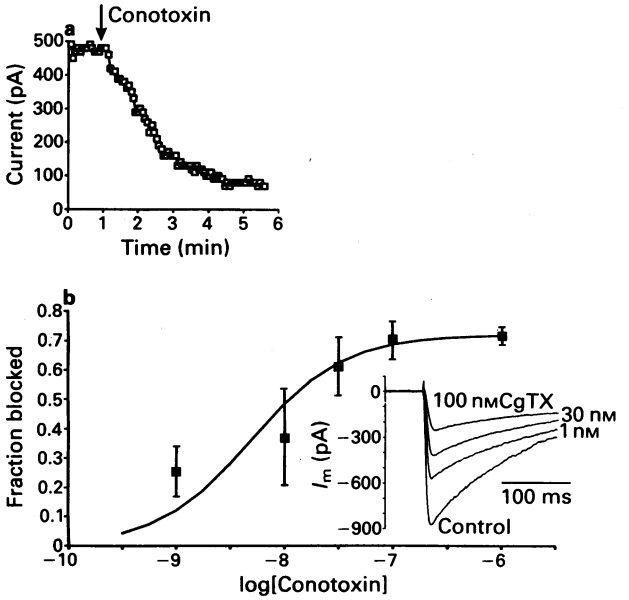

Figure 2 Time course and sensitivity of PC12 cell calcium current to ω-conotoxin GVIA (CgTX) in the presence of nifedipine (10 μM). (a) The time course of inhibition of calcium current after exposure to 100 nM CgTX illustrates a relatively stable current before and after CgTX, with 50% inhibition occurring about 150 s after CgTX application began. Note that a residual current remained after CgTX application amounting to about 20% of the nifedipine-resistant current. A ten fold increase in the dose of CgTX (to 1 μM) did not affect this residual current (data not shown) suggesting that 100 nM CgTX exerted a maximal effect in this preparation. (b) The main panel shows the dose-response to CgTX in the presence of nifedipine (10 μM). Each point shows the mean and standard deviation of pooled data from separate experiments on different cells ($n = 2-5$). The solid line shows a least squares fit to the Hill equation giving an IC_{50} of 3 nM and a Hill coefficient of 1, suggesting that the stoichiometry of inhibition was one CgTX molecule per calcium channel. However, the mean ± s.d. for 1 nM CgTX fell above this curve, possibly due to channel run-down during the long period of time required to attain steady-state at this concentration. The inset shows sample records from an experiment in which three doses (1, 30 and 100 nM) of CgTX were applied sequentially to a single cell. The currents were elicited by steps from a V_{hold} of −40 mV to +20 mV for 200 ms every 5 s.

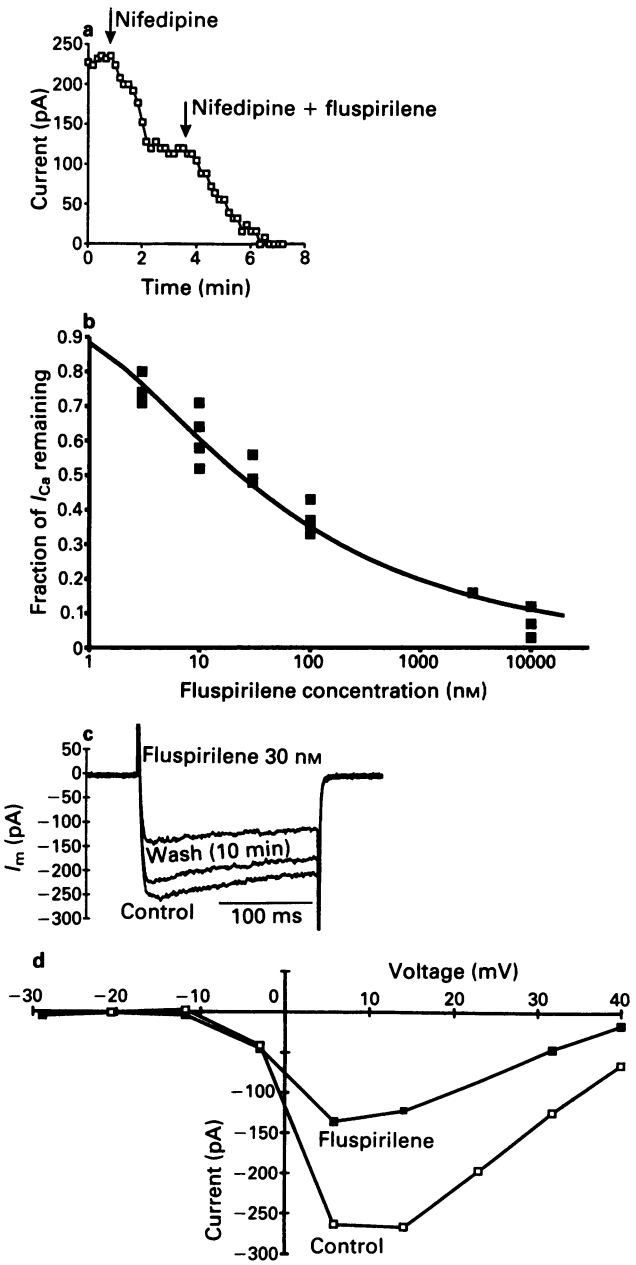

Figure 3 Sensitivity and current-voltage relationship of ω-conotoxin GVIA (CgTX)-sensitive PC12 calcium current to fluspirilene. (a) The time course of current inhibition shows that about 50% of the whole-cell current remained after application of nifedipine (10 μM) and that the $t_{1/2}$ of nifedipine action was about 30 s. After a steady state was reached, fluspirilene (10 μM) was added to the bathing solution and in this cell caused complete abolition of current within 2.5 min. (b) The dose-response curve for fluspirilene was constructed from peak currents measured in the presence of nifedipine (10 μM) in different cells at various doses of fluspirilene using a similar protocol to the one used to generate the dose-response to CgTX. The curve, which shows the individual data points, is shallow with half maximal inhibition of calcium current at about 30 nM fluspirilene. The data were fitted by a Hill equation which gave a Hill coefficient of 0.25, suggesting that the block induced by fluspirilene is more complicated than that produced by CgTX. Note that at 10 μM fluspirilene there was some residual current (about 10% of the nifedipine-resistant current). (c) The reversibility of fluspirilene was investigated with a single step pulse of 200 ms duration to 15 mV from a V_{hold} of −40 mV. A peak current of 260 pA was evoked under this protocol in the presence of nifedipine (10 μM). As shown, fluspirilene (30 nM) reduced the nifedipine-resistant current by about 50%. After washing for 10 min the current recovered to about 85% of its pre-fluspirilene value, indicating that fluspirilene-induced blockade was reversible. The 15% difference between pre- and post-fluspirilene current may be ascribed to current run-down during the 10 min wash period. (d) This panel shows the voltage-dependence of the calcium current in the presence of nifedipine (10 μM) and after the addition of fluspirilene (30 nM). The holding potential was −40 mV and the step duration was 200 ms. The nifedipine-insensitive current activated at about −10 mV and peaked at about 10 mV. The addition of 30 nM fluspirilene reduced the current by approximately 50% at all potentials without any shift in the *I-V* relationship.

rent in a dose-dependent manner with half maximal block occurring at 30 nM. However, the block of the nifedipine-insensitive current by fluspirilene was more complex than that due to CgTX, since the Hill coefficient of the curve fitted to the data was only 0.25. It is notable that Hill coefficients of less than unity have also been reported in binding studies investigating displacement of PN-200-110 by fluspirilene (Kenny *et al.*, 1990) as well as fluspirilene displacement by nitrendipine in rat cardiac sarcolemmal membrane vesicles (King *et al.*, 1989). The fraction of current blocked by fluspirilene did not increase during the test pulse. In four experiments 1 μM fluspirilene blocked 67 ± 8% of the peak and 74 ± 11% of the steady state nifedipine-insensitive current.

Figure 3c shows that the block of nifedipine-insensitive current by fluspirilene was reversible. As shown earlier, application of 30 nM fluspirilene blocked approximately 50% of the nifedipine-resistant current; 10 min after washing out the fluspirilene, the evoked calcium current returned to 85% of its control value. Although recovery from fluspirilene block was incomplete in these experiments, it is likely that calcium current run down could account for the deficit.

Current-voltage relationship of fluspirilene action on the PC12 nifedipine-resistant calcium current

To examine whether the observed block of N-type current by fluspirilene was due to an alteration of channel gating, the current-voltage relationship was measured by applying pulses to different potentials. As shown in Figure 3d, the current activated at about −10 mV and reached a peak at about +10 mV and then decreased again as the reversal potential of the calcium current was approached. The addition of 30 nM fluspirilene decreased the amplitude of the current by about 50% at all potentials examined, suggesting that the block by fluspirilene was not due to a shift in the voltage-dependence of calcium current gating.

Discussion

It is clear that multiple subtypes of voltage-sensitive calcium channels (VSCC) are present in neuronal tissues (Nowycky *et al.*, 1985). In addition, at the level of the single neurone, co-expression of different subtypes of VSCC may occur (Miller, 1987). A number of groups have used the NGF-differentiated PC12 cell-line as a model for examining neuronal calcium channel properties (Plummer *et al.*, 1989; Streit & Lux, 1989; 1990; Usowicz *et al.*, 1990). In all studies, a HVA calcium current was expressed but was not generally subdivided into L- and N-type components. Both electrophysiological and pharmacological criteria have been used to characterize HVA VSCCs (Fox *et al.*, 1987). Dihydropyridine antagonists such as nifedipine and nitrendipine have been shown to block selectively L-type calcium channels (e.g. Nowycky *et al.*, 1985). In our experiments, nifedipine blocked a substantial proportion of the whole-cell calcium current suggesting that there is an L-type component to the HVA current exhibited by PC12 cells. This result is in agreement with the results of Usowicz *et al.* (1990) and Plummer *et al.* (1989).

CgTX, a toxin originally isolated from the venom of the piscivorous cone snail, *Conus geographcus* (Olivera *et al.*, 1984), has been widely used in the identification of N-type

HVA channels (Sher & Clementi, 1991). Usowicz *et al.* (1990) and Plummer *et al.* (1989) demonstrated that in the NGF-differentiated PC12 cell line, CgTX is selective for the N-type channel. In our experiments CgTX blocked a large proportion of the DHP-insensitive current suggesting that L-type and N-type calcium channels are the major channel types expressed in the NGF-treated cells.

As mentioned previously, a small component of the whole-cell current was found to be resistant to blockade by high concentrations of nifedipine and CgTX in combination. Several other types of HVA VSCC, showing resistance to CgTX and nifedipine have been identified recently (P-type – Llinas *et al.*, 1989; Rabbit brain B1 - Mori *et al.*, 1991). The P-type channel, first identified in rat Purkinje neurones and described by Llinas *et al.* (1989), is blocked by AgaIVA, a funnel web spider toxin but not by CgTX (Mintz *et al.*, 1992). It is possible that our residual calcium current represents such a P-type channel. However, further experiments with AgaIVA would be necessary to examine this point.

Fluspirilene is known to interact with HVA calcium channels in skeletal muscle (Galizzi *et al.*, 1986), brain, cardiac and smooth muscle (Quirion *et al.*, 1985; Qar *et al.*, 1987; King *et al.*, 1989; Kenny *et al.*, 1990). In previous studies, the receptor protein was only probed with classical L-type calcium channel antagonists (such as dihydropyridines and phenylaklylamines). Thus, the inhibition of N-type calcium channels by fluspirilene observed here is a novel result.

As noted previously, fluspirilene exhibits a low Hill coefficient for dihydropyridine displacement in binding studies (Kenny *et al.*, 1990). It is notable that we observed a similar low Hill coefficient for the block of N-type (CgTX-sensitive, nifedipine-insensitive) current. However, the low Hill coefficient for fluspirilene inhibition is not easily explainable on the basis of a displacement of nifedipine (and hence a relief of nifedipine block) by fluspirilene as fluspirilene blocks and binds to L-type channels with an affinity of about 22 nM (Gould *et al.*, 1983) which is very close to that observed for N-type channels in these experiments.

An alternative explanation might be that the affinity of the N-type channel for fluspirilene depends on membrane potential (as reported for L-type channels by Enyeart *et al.*, 1990) so that complete blockade of channels examined with a pulse protocol would not occur until the low affinity state was completely occupied by fluspirilene. This model could give a more shallow dose-response than would be seen if there were no change in affinity with depolarization. However, the fraction of current blocked was not sensitive to test pulse potential in the range examined (Figure 3d) so that the low Hill coefficient is not easily explained by the production of a higher affinity state during the test pulse. Furthermore, the fraction of current blocked did not increase during the pulse (see also Figure 3c) so that we have no evidence for the affinity of the channel changing during depolarization. A related explanation for the low Hill coefficient could be that there is more than one binding site for fluspirilene, and each site produces partial blockade with different affinities. Such a model will produce inflexions in the binding curve, that may only be detected if the affinities of the binding sites are sufficiently different.

As a neuroleptic drug, fluspirilene has been used clinically to treat schizophrenic symptoms for many years. Fluspirilene and a few other DPBPs like pimozide and penfluridol are unique among neuroleptic drugs in that they alleviate both the 'positive' and 'negative' symptoms of schizophrenia (Lapierre, 1978; Haas & Beckmann, 1982). Neuroleptic effects against the 'positive' manifestations such as hallucinations and delusions have commonly been ascribed to dopamine antagonism at the D_2 receptor (Seeman, 1980). Yet, in contrast to classical non-DPBP neuroleptics such as haloperidol, fluspirilene also relieves emotional withdrawal symptoms (a 'negative' characteristic of schizophrenia) and additionally instils increased self-confidence together with relaxation (Hassel, 1985), which are features of an anxiolytic agent. These additional properties may be the result of an action of fluspirilene on synaptic transmission not shared by other classical neuroleptic agents. The finding that fluspirilene also blocks N-type calcium channels may therefore provide an explanation for the additional anxiolytic effects of fluspirilene. In support of this idea is the clinical observation that the anxiolytic property of fluspirilene occurs at very low dose levels (Hassel, 1985), a finding which parallels the high potency of this drug on N-type calcium channels reported here. Since N-type channels are believed to be concentrated at sites of synaptic transmission, a N-type channel antagonist which crosses the blood-brain barrier would be expected to be a potent modifier of brain function.

Although not selective for N-type calcium channels, fluspirilene may potentially have a clinical role as a potent, brain penetrable calcium antagonist which could be used to treat disorders resulting from abnormal neuronal cell depolarization. In connection with this point, it is notable that Gandolfo *et al.* (1989), using a rat model of epilepsy, found that fluspirilene potently blocks epileptiform activity via a suppression of neuronal hyperexcitability. The fact that fluspirilene blocks both N- and L-type calcium channels may indicate that there is a region of structural homology between these channel types. It is also possible that chemical modification of the fluspirilene molecule may confer differential selectivity between HVA calcium channel subtypes. Should this be the case, derivatives of fluspirilene could provide novel therapeutic agents for treating disorders of the central nervous system.

We thank Dr P. Doherty for the kind gift of PC12 cells.

References

DOHERTY, P., MANN, D.A. & WALSH, F.S. (1988). Comparison of the effects of NGF activators of protein kinase C and a calcium ionophore on the expression of Thy-1 and N-CAM in PC12 cell line. *J. Cell Biol.*, **107**, 333–340.

ENYEART, J.J., BIAGI, B.A., DAY, R.N., SHEU, S.-S. & MAURER, R.A. (1990). Blockade of low and high threshold calcium channels by diphenylbutylpiperidine antipsychotics linked to inhibition of prolactin gene expression. *J. Biol. Chem.*, **265**, 16373–16379.

FOX, A.P., NOWYCKY, M.C. & TSIEN, R.W. (1987). Kinetic and pharmacological properties distinguishing three types of calcium currents in chick sensory neurones. *J. Physiol.*, **394**, 149–172.

FRASER, S., KENNY, B.A., KILPATRICK, A.T. & SPEDDING, M. (1988). Is fluspirilene a potential ligand for the site of action of class III calcium antagonists? *Br. J. Pharmacol.*, **94**, 463P.

FURUKAWA, K., ONODERA, H., KOGURE, K. & AKAIKE, N. (1993). Time dependent expression of sodium and calcium channels in PC12 cells by nerve growth factor and cAMP. *Neurosci. Res.*, **16**, 143–147.

GALIZZI, J.-P., FOSSET, M., ROMEY, G., LADURON, P. & LAZDUNSKI, M. (1986). Neuroleptics of the diphenylbutylpiperidine series are potent calcium channel inhibitors. *Proc. Natl. Acad. Sci. U.S.A.*, **83**, 7513–7517.

GANDOLFO, G., GOTTESMANN, C., BIDARD, J.-N. & LADZUNSKI, M. (1989). Ca^{2+} channel blockers prevent seizures induced by a class of K+ channel blockers. *Eur. J. Pharmacol.*, **160**, 173–177.

GARBER, S.S., HOSHI, T. & ALDRICH, R.W. (1989). Regulation of ionic currents in phaeochromocytoma cells by nerve growth factor and dexamethasone. *J. Neurosci.*, **9**, 3976–3987.

GOULD, R.J., MURPHY, K.M.M., REYNOLDS, I.J. & SNYDER, S.H. (1983). Antischizophrenic drugs of the diphenylbutylpiperidine type act as calcium channel antagonists. *Proc. Natl. Acad. Sci. U.S.A.*, **80**, 5122–5125.

HAAS, S. & BECKMANN, H. (1982). Pimozide vs. haloperidol in acute schizophrenia. A double-blind control study. *Pharmacopsychiatry*, **15**, 70–74.

HAMILL, O.P., MARTY, A., NEHER, E., SAKMANN, B. & SIGWORTH, F.J. (1981). Improved patch clamp techniques for high resolution current recording from cells and cell-free membrane patches. *Pflügers Arch.*, **391**, 85–100.

HASSEL, P. (1985). Experimental comparison of low doses of 1.5 mg fluspirilene and bromazepam in out-patients with psychovegative disturbances. *Pharmacopsychiatry*, **18**, 297.

HIRNING, L.D., FOX, A.P., MCCLESKEY, E.W., OLIVERA, B.M., THAYER, S.A., MILLER, R.J. & TSIEN, R.W. (1988). Dominant role of N-type calcium channels in evoked release of norepinephrine from sympathetic neurons. *Science*, **239**, 57–60.

KENNY, B.A., FRASER, S., KILPATRICK, A.T. & SPEDDING, M. (1990). Selective antagonism of calcium channel activators by fluspirilene. *Br. J. Pharmacol.*, **100**, 211–216.

KING, V.F., GARCIA, M.L., SHEVELL, J.L., SLAUGHTER, R.S. & KACZOROWISKI, G.J. (1989). Substituted diphenylbutylpiperidines bind to a uniquely high affinity site on the L-type calcium channel. *J. Biol. Chem.*, **264**, 5633–5641.

LAPIERRE, Y.D. (1978). A controlled study of Penfluridol in the treatment of chronic schizophrenia. *Am. J. Psychiatry*, **135**, 956–959.

LLINAS, R., SUGIMORI, M., LIN, J.-W. & CHERKSEY, B. (1989). Blocking and isolation of a calcium channel from neurons in mammals and cephalopods utilizing a toxin fraction (FTX) from funnel-web spider poison. *Proc. Natl. Acad. Sci. U.S.A.*, **86**, 1689–1693.

MILLER, R.J. (1987). Multiple calcium channels and neuronal function. *Science*, **235**, 46–52.

MINTZ, I.M., VEMENA, V.J., SWIDEREK, K.M., LEE, T.D., BEAN, B.P. & ADAMS, M.E. (1992). P-type calcium channels blocked by spider toxin ω-Aga-IVA. *Nature*, **35**, 827–829.

MORI, Y., FREIDRICH, T., KIM, M.-S., MIKAMI, A., NAKAI, J., RUTH, P., BOSSE, E., HOFMANN, F., FLOCKERZI, V., FURUICHI, T., MIKOSHIBA, K., IMOTO, K., TANABE, T. & NUMA, S. (1991). Primary structure and functional expression from complementary DNA of a brain calcium channel. *Nature*, **350**, 398–402.

NOWYCKY, M.C., FOX, A.P. & TSIEN, R.W. (1985). Three types of neuronal calcium channel with different calcium agonist sensitivity. *Nature*, **316**, 440–443.

OLIVERA, B.M., MCINTOSH, J.M., CRUZ, L.J., LUQUE, F.A. & GRAY, W.R. (1984). Purification and sequence of a presynaptic peptide toxin from *Conus geographus* venom. *Biochemistry*, **23**, 5087–5090.

PLUMMER, M.R., LOGOTHETIS, D.E. & HESS, P. (1989). Elementary properties and pharmacological sensitivities of calcium channels in mammalian peripheral neurons. *Neuron*, **2**, 1453–1463.

QAR, J., GALIZZI, J.P., FOSSET, M. & LAZDUNSKI, M. (1987). Receptors for diphenylbutylpiperidine neuroleptics in brain, cardiac and smooth muscle membranes. Relationship with receptors for 1,4-dihydropyridines and phenylalkylamines and with calcium channel blockade. *Eur. J. Pharmacol.*, **141**, 261–268.

QUIRION, R., LAFAILLE, F. & NAIR, N.P.V. (1985). Comparative potencies of calcium channel antagonists and antischizophrenic drugs on central and peripheral calcium channel binding sites. *J. Pharm. Pharmacol.*, **37**, 437–440.

RUDY, B., KIRSCHENBAUM, B., RUKENSTEIN, A. & GREENE, L.A. (1987). Nerve growth factor increases the number of functional sodium channels and induces TTX-resistant sodium channel in PC12 phaeochromocytoma cells. *J. Neuroscience*, **7**, 1613–1625.

SEEMAN, P. (1980). Brain dopamine receptors. *Pharmacol. Rev.*, **32**, 229–313.

SHER, E. & CLEMENTI, F. (1991). ω-Conotoxin-sensitive voltage-operated calcium channels in vertebrate cells. *Neuroscience*, **42**, 301–307.

SMITH, S.J. & AUGUSTINE, G.J. (1988). Calcium ions, active zones and synaptic transmitter release. *Trends Neurol. Sci.*, **11**, 458–464.

STREIT, J. & LUX, H.D. (1987). Voltage dependent calcium currents in PC12 growth cones and cells during NGF-induced cell growth. *Pflügers Arch.*, **408**, 634–641.

STREIT, J. & LUX, H.D. (1989). Distribution of calcium currents in sprouting PC12 cells. *J. Neuroscience*, **9**, 4190–4199.

STREIT, J. & LUX, H.D. (1990). Calcium current inactivation during nerve growth factor induced differentiation of PC12 cells. *Pflügers Arch.*, **416**, 368–374.

USOWICZ, M.M., PORZIG, H., BECKER, C. & REUTER, H. (1990). Differential expression by nerve growth factor of two types of calcium channels in rat phaeochromocytoma cell lines. *J. Physiol.*, **426**, 95–116.

(Received August 19, 1993
Revised October 8, 1993
Accepted October 14, 1993)

Br. J. Pharmacol. (1994), **111**, 489–496

Relationship between cytosolic calcium concentration and force in the papaverine-induced relaxation of medial strips of pig coronary artery

Hiroki Aoki, Junji Nishimura, Sei Kobayashi & [1]Hideo Kanaide

Division of Molecular Cardiology, Research Institute of Angiocardiology, Faculty of Medicine, Kyushu University, Fukuoka 812, Japan

1 The mechanisms of vasorelaxation induced by papaverine were investigated using front-surface fluorometry and fura-2-loaded medial strips of the pig coronary artery.

2 In the presence of extracellular Ca^{2+} (1.25×10^{-3} M), histamine (10^{-4} M) induced abrupt elevations of cytosolic calcium concentration, $[Ca^{2+}]_i$ reaching a peak within 12 s (the first phase); after making a slight shoulder, $[Ca^{2+}]_i$ declined gradually to reach sustained levels (the second phase). Force rapidly rose to reach maximum levels in 3 min, then gradually declined. Papaverine (10^{-7}–10^{-5} M) inhibited both the first and the second phases of $[Ca^{2+}]_i$ elevation and the development of force induced by histamine, in a concentration-dependent manner.

3 In the absence of extracellular Ca^{2+}, histamine (10^{-4} M) induced a transient increase in $[Ca^{2+}]_i$ and force, both of which were inhibited in a concentration-dependent manner by papaverine (10^{-7}–10^{-5} M). When papaverine was washed out, a second application of 10^{-4} M histamine also induced transient increases in $[Ca^{2+}]_i$ and force. The smaller the first response, the greater was the second response. The total amount of $[Ca^{2+}]_i$ released from intracellular stores by the first and second application of histamine in the presence of papaverine was smaller than in its absence, thereby indicating a reduction of Ca^{2+} in the histamine-sensitive store. However, while papaverine (10^{-5} M) did not affect the transient increase in $[Ca^{2+}]_i$ induced by 2×10^{-2} M caffeine, contractions were inhibited.

4 For a given level of $[Ca^{2+}]_i$, the force developed with the cumulative application of histamine (10^{-7} M–10^{-4} M) was greater than that observed with the cumulative application of extracellular Ca^{2+} (0–7.5×10^{-3} M) during high K^+ depolarization. Papaverine (10^{-7} M–10^{-5} M) suppressed, in a concentration-dependent manner, the increase in $[Ca^{2+}]_i$ and the force induced by cumulative applications of both histamine and extracellular Ca^{2+} during high K^+ depolarization. The $[Ca^{2+}]_i$-force curve obtained by depolarization with K^+, but not that obtained during histamine application, was shifted to the right by papaverine. Diltiazem, 10^{-7} M, a concentration causing a similar degree of relaxation to 10^{-5} M papaverine, did not shift the $[Ca^{2+}]_i$-force curve obtained with high K^+. Nitroglycerin (10^{-6} M) and isoprenaline (10^{-6} M) shifted the $[Ca^{2+}]_i$-force curve to the right to a greater extent than did 10^{-5} M papaverine.

5 These findings suggest that papaverine relaxes medial strips of the porcine coronary artery by two mechanisms. The first is mainly due to a decrease in $[Ca^{2+}]_i$, not only through inhibiting Ca^{2+} influx through either voltage-dependent or receptor-operated Ca^{2+} channels, but also by inhibiting agonist-induced intracellular Ca^{2+} release. This occurs presumably by interference with the signal transduction pathway for histamine and by a depletion of Ca^{2+} in histamine-sensitive stores. Secondly, the $[Ca^{2+}]_i$-sensitivity of certain contractile mechanisms may be minimally decreased.

Keywords: Cytosolic calcium; papaverine; fura-2; coronary artery; vasorelaxation; histamine; vascular smooth muscle

Introduction

Changes in cytosolic Ca^{2+} concentration ($[Ca^{2+}]_i$) play a central role in regulating excitation-contraction coupling in smooth muscle cells (Sommerville & Hartshorne, 1986). $[Ca^{2+}]_i$ can be elevated in smooth muscle cells, as in other cells, by the influx of extracellular Ca^{2+} through voltage-dependent (Putney *et al.*, 1989) or ligand-gated (Benham & Tsien, 1987) Ca^{2+} channels of the surface membrane or by the release of intracellular Ca^{2+} due to the activation of the phospholipase C/inositol trisphosphate ($InsP_3$) cascade, coupled to receptors by guanosine 5'-triphosphate (GTP)-binding proteins, or both. It is generally accepted that phosphorylation of the 20 kDa myosin light chain (MLC) by a Ca^{2+}- and calmodulin-dependent enzyme, MLC kinase (MLCK), leads to activation of myosin ATPase by actin and, consequently, smooth muscle contraction (Kamm & Stull, 1985). The Ca^{2+} sensitivity of the contractile regulatory apparatus (i.e. the $[Ca^{2+}]_i$-force relationship) is modulated by agonists (Morgan & Morgan, 1984; Hirano *et al.*, 1990), coupled to G-proteins (Nishimura *et al.*, 1988).

Papaverine is a potent vasorelaxant and reduces the contractile responses to excitatory agonists (Tashiro & Tomita, 1970; Ferrari, 1974). It has been well demonstrated that papaverine inhibits the activity of cyclic nucleotide phosphodiesterases (Ferrari, 1974) and, therefore, that it induces the accumulation of cytosolic cyclic nucleotides (Miyamoto *et al.*, 1976; Kramer & Wells, 1979). Adenosine 3':5'-cyclic monophosphate (cyclic AMP) and guanosine 3':5'-cyclic monophosphate (cyclic GMP) are identified as intracellular messengers for smooth muscle relaxation and are produced by the activation of adenylate and guanylate cyclases, respectively (Adelstein *et al.*, 1978; Ignarro & Kadowitz, 1987).

It has been reported the isoprenaline, and hence, cyclic AMP might decrease $[Ca^{2+}]_i$ of vascular smooth muscle in porcine coronary arterial strips, regardless of whether they

[1] Author for correspondence.

were at rest, under high-K^+ or histamine stimulation (Ushio-Fukai *et al.*, 1993). It was also reported that cyclic AMP hyperpolarizes the cell membrane (Somlyo *et al.*, 1970), probably by opening Ca^{2+}-activated K^+-channels (Sadoshima *et al.*, 1988), inhibits Ca^{2+} influx into cells (Bülbring & Tomita, 1987), and stimulates both Ca^{2+} extrusion from cells (Bülbring & den Hertog, 1980) and Ca^{2+} uptake into intracellular storage sites (Casteels & Raeymaekers, 1979). The findings that cyclic AMP-dependent protein kinase (A-kinase) phosphorylates purified MLCK to reduce its activity (Adelstein *et al.*, 1978) and relaxes skinned smooth muscle contracted with a constant Ca^{2+} concentration (Kerrick & Hoar, 1981), suggest that there might be modulation of the Ca^{2+} sensitivity of the contractile apparatus by A-kinase. Nitroglycerin (Kobayashi *et al.*, 1985), which elevates cytosolic cyclic GMP, and 8-bromo-cyclic GMP (Kai *et al.*, 1987), a membrane-permeable cycle GMP analogue, reduce the $[Ca^{2+}]_i$ of vascular smooth muscle cells. Nitroglycerin reduces the Ca^{2+} sensitivity of the contractile apparatus and inhibits agonist-induced release of intracellular Ca^{2+} (Abe *et al.*, 1990).

In the present study, using front-surface fluorometry (Abe *et al.*, 1990; Hirano *et al.*, 1990) and fura-2-loaded porcine coronary arterial strips, we monitored simultaneously the $[Ca^{2+}]_i$ and force in intact coronary arterial strips, the objective being to characterize the multiple effects of papaverine on $[Ca^{2+}]_i$ and force, at rest and as stimulated either by high K^+ or histamine in the presence and absence of extracellular Ca^{2+}. The relative importance of these effects in the mechanism of relaxation induced by papaverine was examined.

Methods

Tissue preparation

Hearts from adult pigs of either sex were obtained from a local abattoir immediately after the animals had been killed. These hearts were placed in ice-cold physiological salt solution (PSS) and brought to the laboratory. The left circumflex coronary arteries were isolated, and segments 2–3 cm from the origin were excised. The segments were cut open longitudinally and the luminal surface was rubbed with a cotton swab to remove the endothelium. After removal of the adventitia, medial preparations were cut into approximately 1 mm × 5 mm (0.1 mm thick) strips of circular muscle.

Fura-2 loading

The strips were loaded with the Ca^{2+} indicator dye, fura-2 by incubating in oxygenated (a mixture of 95% O_2 and 5% CO_2) Dulbecco's modified Eagle's medium containing 2.5×10^{-5} M fura-2/AM (an acetoxymethyl ester form of fura-2) and 5% foetal bovine serum for 3–4 h at 37°C. The fura-2-loaded strips were washed with normal PSS to remove the extracellular dye, and further incubated in normal PSS for 1 h before the start of measurements. Loading the strips with fura-2 in itself did not affect contractility, as has been described previously (Abe *et al.*, 1990; Hirano *et al.*, 1990).

Simultaneous measurement of force and $[Ca^{2+}]_i$

Isometric force of the strips, mounted vertically in a quartz organ bath, was measured by a force transducer (TB-612T, Nihon Kohden, Japan), simultaneously with $[Ca^{2+}]_i$. During the 1 h fura-2 equilibration period, the strips were stimulated with 1.18×10^{-1} M K^+ every 15 min, and the resting force was adjusted to 250 mg. Consistent responses to 1.18×10^{-1} M K^+-depolarization were obtained before the experimental protocol was started. The developed force was expressed as a percentage with the values in normal (5.9×10^{-3} M K^+) and 1.18×10^{-1} M K^+ PSS being 0% and 100%, respectively. The developed force induced by 1.18×10^{-1} M K^+ was 0.91 ± 0.06 g ($n = 20$). Where indicated, papaverine, diltiazem, isoprenaline or nitroglycerin was applied for 10 min prior to stimulation by high K^+, histamine or caffeine. This incubation was for the purpose of equilibration (Hirano *et al.*, 1990; Abe *et al.*, 1990; Ushio-Fukai *et al.*, 1993).

$[Ca^{2+}]_i$ was assessed by changes in the fluorescence intensity of the fura-2-Ca^{2+} complex, which were monitored with a specifically designed front-surface fura-2 fluorometer (model CAM-OF-1) developed by us in collaboration with the Japanese Spectroscopic Co. (Tokyo, Japan), as previously described (Abe *et al.*, 1990; Hirano *et al.*, 1990). In brief, excitation light (340 nm and 380 nm) was obtained spectroscopically from a xenon light source. Strips were illuminated by guiding the alternating (400 Hz) excitation light through quartz optic fibres arranged in a circle (diameter = 3 mm). Surface fluorescence of strips was collected by optic glass fibres arranged around those conducting the excitation light (diameter = 7 mm) and introduced through a 500 nm bandpass filter into a photomultiplier. The ratio of the fluorescence intensities (collected at 500 nm) at 340 nm excitation to those at 380 nm excitation was monitored and expressed as a percentage; the maintained values in normal (5.9×10^{-3} M K^+) and 1.18×10^{-1} M K^+ PSS were designated 0% and 100%, respectively (Figure 1). The apparent dissociation constant (K_d) of the fura-2:Ca^{2+} complex was considered to be 2.24×10^{-7} M and the absolute value of $[Ca^{2+}]_i$ was calculated according to the method of Gryn-

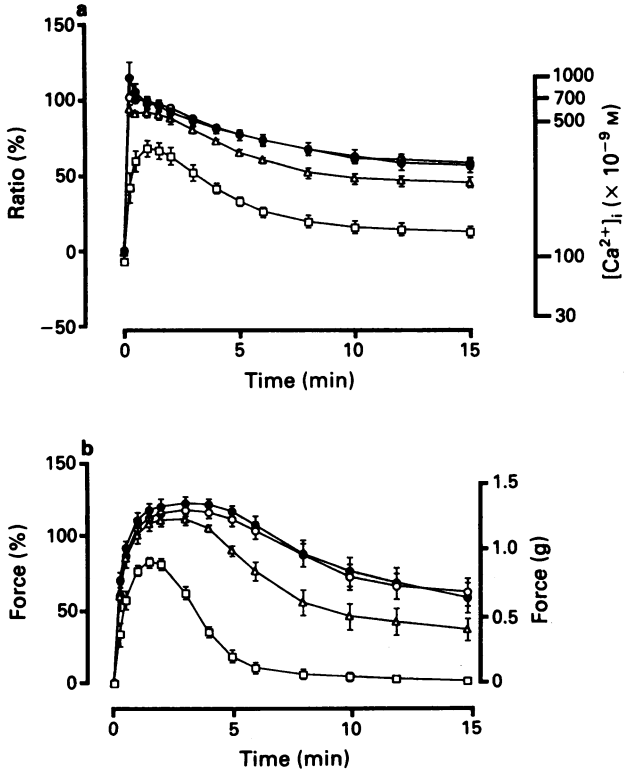

Figure 1 Effects of various concentrations of papaverine on changes in fluorescence ratio (a) and force (b) induced by 10^{-4} M histamine in normal PSS. Strips were pretreated with 0 (●; control), 10^{-7} (○), 10^{-6} (△), 10^{-5} (□) M papaverine. Papaverine was applied for 10 min before and was present during the application of histamine. The abscissa scale in (a) and (b) shows the time (in min) after the application of histamine. Mean values with s.e.mean are shown ($n = 4$).

kiewicz *et al.* (1985). The mean values of 10 different preparations of $[Ca^{2+}]_i$ at rest (0%) and during 1.18×10^{-1} M K^+-depolarization (100%) were 1.08 ± 0.27 ($\times 10^{-7}$ M) and 7.15 ± 1.03 ($\times 10^{-7}$ M), respectively.

Drugs and solutions

Normal PSS was of the following composition (mM): NaCl 123, KCl 4.7, $NaHCO_3$ 15.5, KH_2PO_4 1.2, $MgCl_2$ 1.2, $CaCl_2$ 1.25, and D-glucose 11.5. The Ca^{2+}-free version of PSS (Ca^{2+}-free PSS) contained 2×10^{-3} M ethyleneglycol-*bis*(β-aminoethylether)-*N*,*N*,*N*',*N*'-tetraacetic acid (EGTA) instead of 1.25×10^{-3} M $CaCl_2$. High potassium PSS was made by an equimolar substitution of KCl for NaCl. All solutions were gassed with a mixture of 5% CO_2 and 95% O_2 (pH 7.4 at 37°C). Papaverine hydrochloride, histamine dihydrochloride, and fura-2/AM were purchased from Katayama (Osaka, Japan), Wako (Osaka, Japan), and Dojindo (Kumamoto, Japan), respectively. Nitroglycerin was obtained from Nihon-Kayaku (Tokyo, Japan). (−)-Isoprenaline hydrochloride was purchased from Nikken-Kagaku (Tokyo, Japan). Diltiazem hydrochloride was kindly donated by Tanabe Seiyaku Co. (Osaka, Japan). Fura-2/AM was dissolved in 100% dimethyl sulphoxide (DMSO) and diluted in the medium just before loading the dye. The final concentration of DMSO was 5%.

Statistical analysis

The measured values were expressed as mean ± standard error with the number of observations in different tissues ($= n$) from at least 3 different animals. Student's t test was used to determine the statistical significance. Analysis of variance was used to determine the concentration-dependency of effects of drugs. Analysis of covariance was used to determine the non-overlapping (or shift) of the $[Ca^{2+}]_i$-force relationship. P values < 0.05 were considered to be significant.

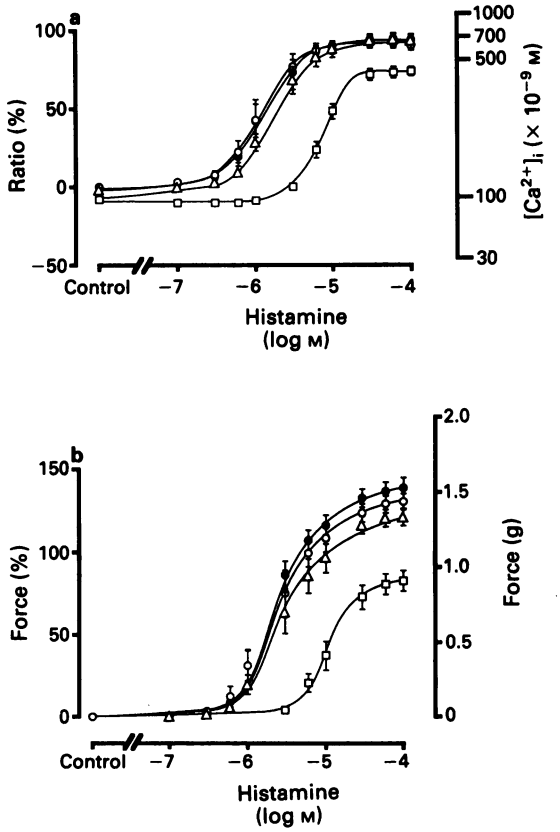

Figure 2 Effects of papaverine on contractions induced by cumulative application of histamine (10^{-7} M–10^{-4} M). Changes in fluorescence ratio (a) and force (b) induced by cumulative application of histamine to strips treated with 0 (●; Control), 10^{-7} (○), 10^{-6} (△) or 10^{-5} (□) M papaverine. Papaverine was applied for 10 min before, and was present during, the cumulative applications of histamine. Values are mean with s.e.mean ($n = 4$).

Results

Effect of papaverine on the increase in $[Ca^{2+}]_i$ and force induced by histamine in the presence of extracellular Ca^{2+}

When histamine (10^{-4} M) was applied in normal PSS, the $[Ca^{2+}]_i$ abruptly increased and reached a first peak at 12 s (the first phase). After a slight shoulder, the $[Ca^{2+}]_i$ declined gradually, but remained at higher than the prestimulation levels (the second phase) (Figure 1a). Force also developed rapidly and reached a maximum about 3 min after exposure to histamine, then declined gradually (Figure 1b). The forces developed at the maximum and after 15 min were 123% (1.12 g) and 44% (0.40 g) of the contraction induced by high K^+, respectively ($n = 4$).

When 10^{-5} M papaverine was applied for 10 min before and during the applications of 10^{-4} M histamine, it reduced both the first and the second phases of the increase in $[Ca^{2+}]_i$. Papaverine also inhibited the development of force induced by 10^{-4} M histamine. Figure 1a and b shows that inhibition of the increases in $[Ca^{2+}]_i$ and force was concentration-dependent (10^{-7}–10^{-5} M). Higher concentrations of papaverine interfered with the fluorimetry and were not examined. These results, together with our previous findings that the first and the second phases of the increase in $[Ca^{2+}]_i$ are mainly due to the release of intracellular Ca^{2+} and the influx of extracellular Ca^{2+} into the cells, respectively (Hirano *et al.*, 1990), suggest that papaverine inhibits both the Ca^{2+} release and Ca^{2+} influx stimulated by histamine.

Effects of papaverine on increases in $[Ca^{2+}]_i$ and force induced by cumulative application of histamine in the presence of extracellular Ca^{2+}

In normal PSS, cumulative application of histamine (10^{-7}–10^{-4} M) led to step-wise, concentration-dependent ($P < 0.001$ by analysis of variance, $n = 4$), increases in $[Ca^{2+}]_i$ and force. Treatment with papaverine (10^{-7}–10^{-5} M) for 10 min before and during the cumulative application of histamine (10^{-7}–10^{-4} M) led to a concentration-dependent inhibition of the increases in $[Ca^{2+}]_i$ ($P < 0.001$ for papaverine, by two way analysis of variance, $n = 4$; Figure 2a). The elevation of $[Ca^{2+}]_i$ by 10^{-4} M histamine was reduced by 10^{-5} M papaverine from $94.4 \pm 2.8\%$ (6.17×10^{-7} M) to $74.1 \pm 3.0\%$ (4.09×10^{-7} M). Papaverine also inhibited the development of force in response to histamine, in a concentration-dependent manner ($P < 0.001$ for papaverine, by two way analysis of variance, $n = 4$; Figure 2b). The force developed in the presence of 10^{-4} M histamine was reduced by 10^{-5} M papaverine from $138.8 \pm 6.5\%$ (1.26 g) to $82.4 \pm 6.3\%$ (0.75 g) ($n = 4$).

Effects of papaverine on histamine- or caffeine-induced release of intracellular Ca^{2+}

When vascular strips were exposed to Ca^{2+}-free PSS containing 2×10^{-3} M EGTA, $[Ca^{2+}]_i$ gradually declined to reach a steady state while the force remained unchanged (Figure 3a and b). As shown in Figure 3a, a first application of 10^{-4} M histamine after 15 min incubation in Ca^{2+}-free PSS caused

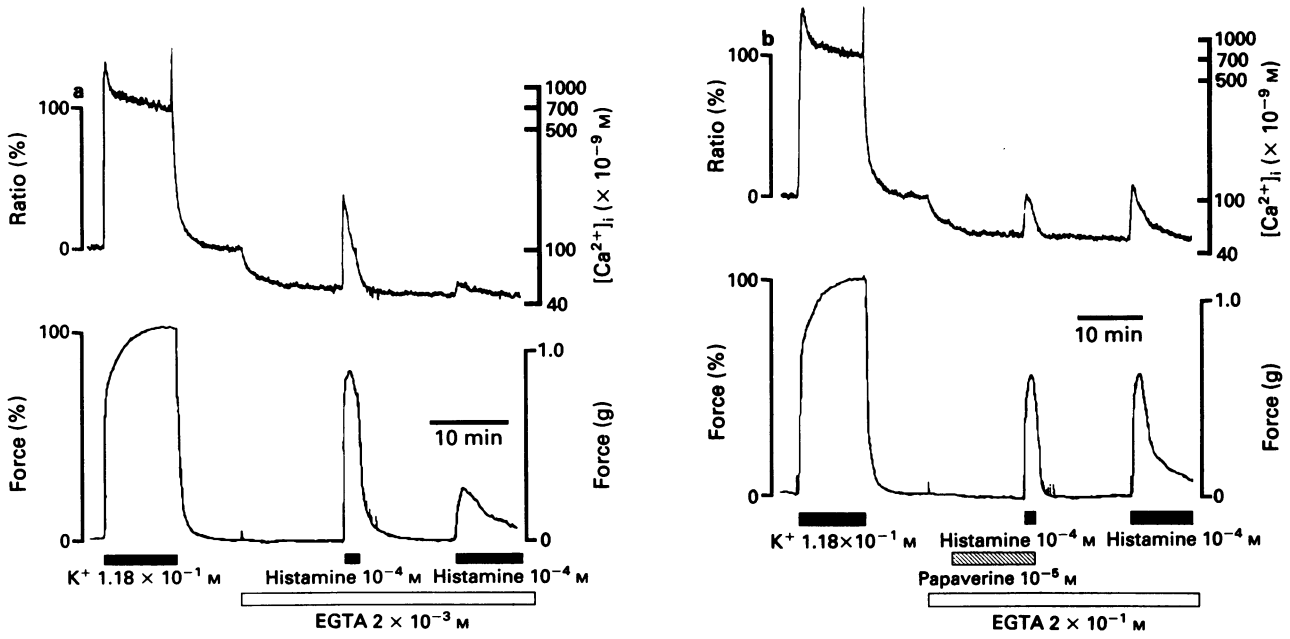

Figure 3 Effects of papaverine on histamine-induced contraction in Ca^{2+}-free PSS containing EGTA, 2×10^{-3} M. Representative recordings of changes in fluorescence ratio and force in the absence (a) and presence (b) of 10^{-5} M papaverine. Strips were incubated in Ca^{2+}-free PSS containing 2×10^{-3} M EGTA for 15 min before and during the first application of histamine, with or without papaverine. Two min after the first application of 10^{-4} M histamine, strips were washed with Ca^{2+}-free PSS and after a further 15 min, a second application of 10^{-4} M histamine was given.

rapid and transient elevations in $[Ca^{2+}]_i$ and force, which began to decline within 1.5 min. After 2 min, histamine was washed out with Ca^{2+}-free PSS. A second application of 10^{-4} M histamine caused only a slight elevation of $[Ca^{2+}]_i$ and force. As shown in Figure 3b, preincubation with 10^{-5}M papaverine inhibited the increases in $[Ca^{2+}]_i$ and force caused by the first application of 10^{-4} M histamine. However, after washing out papaverine and histamine with Ca^{2+}-free PSS after 2 min exposure to histamine, a second application of 10^{-4} M histamine induced transient increases in $[Ca^{2+}]_i$ and force, and these responses were greater than those observed during the second application of histamine without papaverine treatment (compare traces in Figure 3a, b; Figure 4a, b, solid columns, control vs. 10^{-5} M papaverine). Figure 4 shows the mean effects of preincubation with various concentrations of papaverine only during a first exposure to histamine on changes in $[Ca^{2+}]_i$ and the force induced by the first and second (no exposure to papaverine) applications of 10^{-4} M histamine in the absence of extracellular Ca^{2+}. In the presence of papaverine, there was a concentration-dependent inhibition of the increases in $[Ca^{2+}]_i$ and force induced by the first application of histamine ($P<0.05$ by analysis of variance, $n=6$). When responses to the first application of histamine were inhibited more markedly by a higher concentration of papaverine, the responses to the second application of histamine became larger ($P<0.05$ by analysis of variance, $n=6$). In addition, the total amount of released Ca^{2+}, estimated from the elevation of $[Ca^{2+}]_i$ and its duration (Matsumoto *et al.*, 1990), by two applications of histamine combined with exposure to 10^{-5} M papaverine during one application of histamine was smaller than that without papaverine ($P<0.05$ by Student's t test, $n=6$). Therefore, it is likely that inhibition of the histamine-induced Ca^{2+} release by papaverine may be due to interference with the histamine-stimulated signal transduction pathway, to the depletion of Ca^{2+} present in intracellular stores sites, or to a combination of these effects.

Effects of papaverine on caffeine-induced release of intracellular Ca^{2+} were determined with an experimental protocol similar to that used for histamine-induced release. After incubating strips in Ca^{2+}-free PSS containing 2×10^{-3} M EGTA for 15 min, 2×10^{-2} M caffeine induced transient increases in $[Ca^{2+}]_i$ and force (controls in Figure 5a and b). Treatment with 10^{-5} M papaverine 10 min before and during the application of 2×10^{-2} M caffeine had no effect on the increases in $[Ca^{2+}]_i$ (Figure 5a), hence papaverine probably did not affect the Ca^{2+}-release induced by caffeine nor did it deplete the Ca^{2+} present in the caffeine-sensitive storage sites. On the other hand, contractions induced by 2×10^{-2} M caffeine were inhibited by about 50% ($P<0.01$ by Student's t test, $n=4$) by 10^{-5} M papaverine (Figure 5b), thereby suggesting that papaverine slightly inhibited the caffeine-induced contraction, without affecting $[Ca^{2+}]_i$.

Effects of papaverine on increases in $[Ca^{2+}]_i$ and force induced by cumulative applications of extracellular Ca^{2+} during high K^+-depolarization

Effects of papaverine on K^+-depolarization-induced contraction were examined, using the following protocol. After incubation in Ca^{2+}-free PSS containing 2×10^{-3} M EGTA for 10 min and subsequently in Ca^{2+}-free PSS without EGTA for 5 min, the vascular strips were depolarized with 1.18×10^{-1} M K^+- and Ca^{2+}-free PSS. Cumulative applications of extracellular Ca^{2+} ($0-7.5 \times 10^{-3}$ M) during high K^+-depolarization induced step-wise increases in $[Ca^{2+}]_i$ and force, both of which were inhibited by papaverine ($10^{-7}-10^{-5}$ M), in a concentration-dependent manner ($P<0.001$ for both $[Ca^{2+}]_i$ and the concentrations of papaverine, by two way analysis of variance, $n=4$; Figure 6a and b).

Effects of papaverine on the $[Ca^{2+}]_i$-force relationship

Effects of papaverine on the $[Ca^{2+}]_i$-force relationship of the contractions induced by histamine and by 1.18 ± 10^{-1} M K^+-depolarization are shown in Figure 7. This figure was made by plotting the mean values of %ratio and force of Figures 2 and 6. The $[Ca^{2+}]_i$-force relationship determined by cumulative applications of extracellular Ca^{2+} during

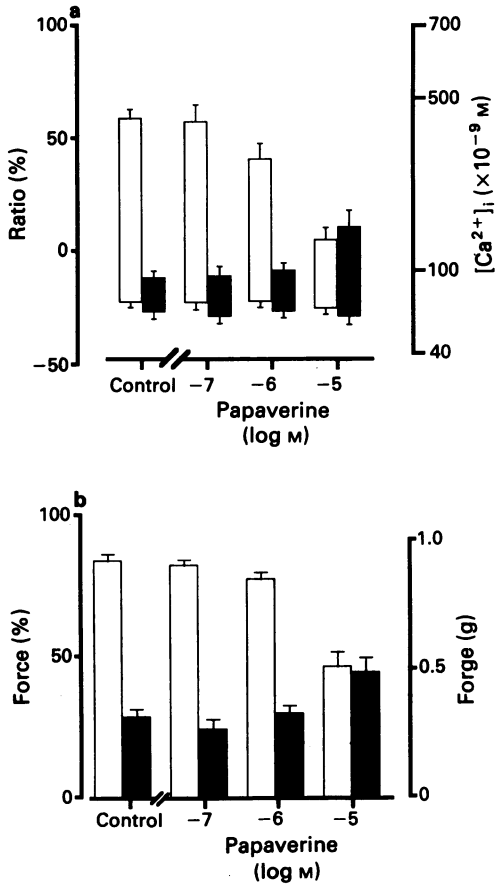

Figure 4 Effects of various concentrations of papaverine on the increases in fluorescence ratio (a) and force (b) induced by 10^{-4} M histamine in the absence of extracellular Ca^{2+}. Open and solid columns show the responses induced by the first and second applications of 10^{-4} M histamine, respectively. The bottom and the top of the column indicate levels before the stimulation and peak response after the stimulation by histamine, respectively. Data are means of 6 different measurements obtained from experimental procedures described in the legend for Figure 3. Values are mean with s.e.mean.

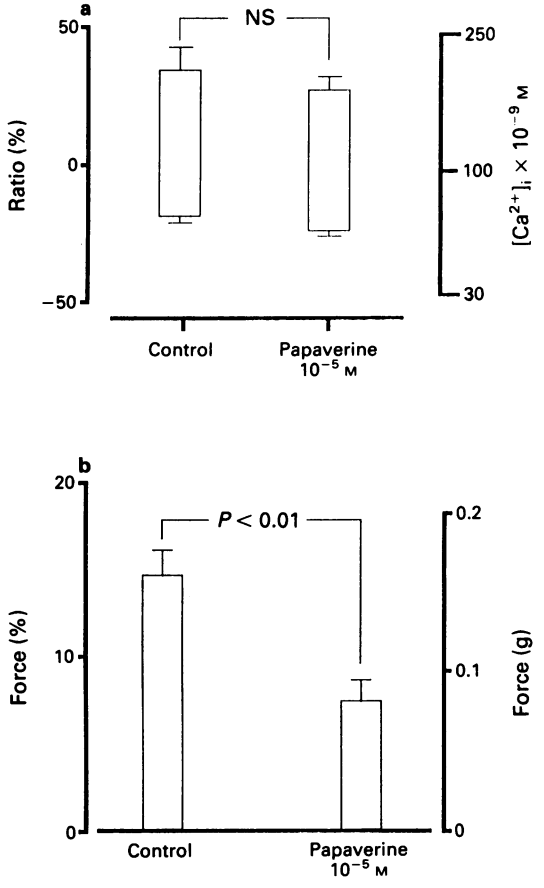

Figure 5 Effects of 10^{-5} M papaverine on the 2×10^{-2} M caffeine-induced increase in fluorescence ratio (a) and force (b) in the absence of extracellular Ca^{2+}. The bottom and top of columns indicate levels before, and peak response after, the stimulation by caffeine, respectively. Data are means of 4 different measurements. Values are mean with s.e.mean. (NS: not significant).

1.18×10^{-1} M K^+-depolarization in the presence of 10^{-5} M papaverine shifted slightly, but significantly ($P<0.05$ by analysis of covariance, $n=4$), to the right from that determined in the absence of papaverine. On the other hand, the $[Ca^{2+}]_i$-force relationship obtained during cumulative applications of histamine in normal PSS in the presence of 10^{-5} M papaverine did not differ from that determined in the absence of papaverine. In addition, in the absence of papaverine, the developed force for given levels of $[Ca^{2+}]_i$ in histamine-induced contractions was greater ($P<0.05$ by analysis of covariance, $n=4$) than that in 1.18×10^{-1} M K^+-depolarization-induced contractions (that is, the control $[Ca^{2+}]_i$-force relationship), thereby suggesting that histamine increases the Ca^{2+} sensitivity of the myofilaments.

Effects of various vasodilators on $[Ca^{2+}]_i$-force relationship during 1.18×10^{-1} M K^+-depolarization

The effects of vasodilators (diltiazem 10^{-7} M, papaverine 10^{-5} M, nitroglycerin 10^{-6} M and isoprenaline 10^{-6} M) on the $[Ca^{2+}]_i$-force relationship during 1.18×10^{-1} M K^+-depolarization were investigated. In the presence of these vasodilators, the force developed by 1.18×10^{-1} M K^+-depolarization in the presence of 1.25×10^{-3} M extracellular Ca^{2+} was reduced by about 30%. $[Ca^{2+}]_i$-force relationships were determined by plotting the ratio and the force during cumulative applications of extracellular Ca^{2+} ($0-7.5 \times 10^{-3}$ M) during high K^+-depolarization in the presence and absence of 10^{-7} M diltiazem, 10^{-5} M papaverine, 10^{-6} M nitroglycerin or 10^{-6} M isoprenaline. Each vasodilator was applied 10 min before starting cumulative applications of extracellular Ca^{2+}. As shown in Figure 8, in the presence of diltiazem, the $[Ca^{2+}]_i$-force relationship did not change, while in the presence of papaverine, nitroglycerin or isoprenaline, the $[Ca^{2+}]_i$-force relationship was shifted to the right ($P<0.05$ for papaverine and $P<0.01$ for nitroglycerin and isoprenaline, by analysis of covariance, $n=4$). In addition, in the presence of nitroglycerin and isoprenaline, the $[Ca^{2+}]_i$-force relationship shifted to the right more prominently than seen in the presence of papaverine ($P<0.05$ by analysis of covariance, $n=4$). Thus, at a given $[Ca^{2+}]_i$ level, development of force in the presence of papaverine was higher than in the presence of nitroglycerin or isoprenaline but lower than in the presence of diltiazem or in the control.

Discussion

Using front-surface fluorometry and fura-2 we have examined the various effects of papaverine on $[Ca^{2+}]_i$ and force in pig coronary arterial strips. Both the first and second phases of the elevation of $[Ca^{2+}]_i$ induced by histamine were inhibited by 10^{-7} to 10^{-5} M papaverine (Figure 1) a concentration-range over which papaverine is known to

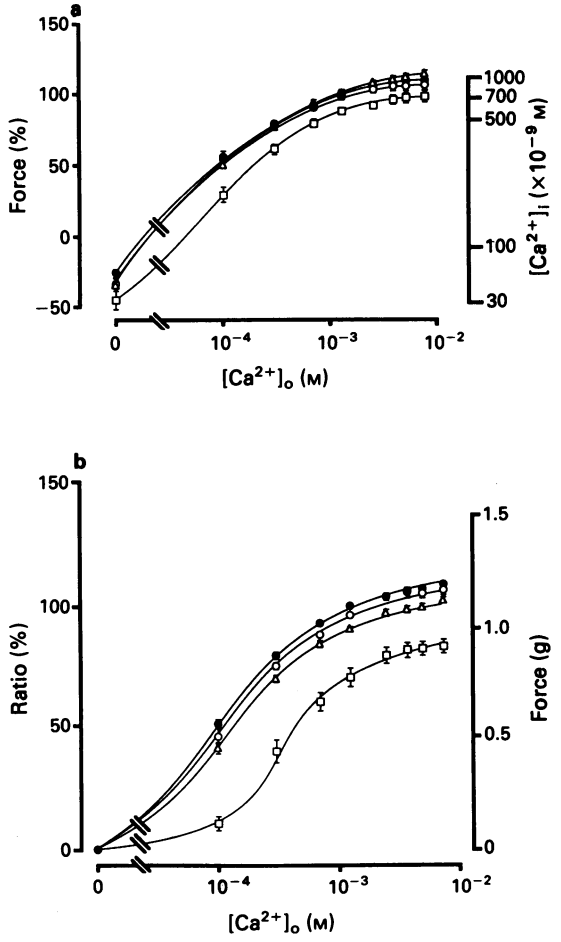

Figure 6 Effects of papaverine on increases in $[Ca^{2+}]_i$ and force induced by cumulative applications of extracellular Ca^{2+} during 1.18×10^{-1} M K^+-induced depolarization: (a) and (b) show effects of various concentrations of papaverine on the changes in fluoresence ratio and force, respectively, in the strips pretreated with 0 (●, control), 10^{-7} (○), 10^{-6} (△) or 10^{-5} (□) M papaverine. Values are mean ± s.e.mean ($n = 4$).

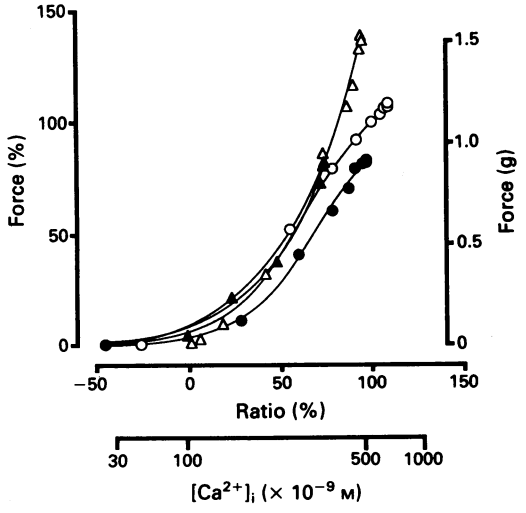

Figure 7 Effects of papaverine on the $[Ca^{2+}]_i$-force relationship, determined by cumulative applications of Ca^{2+} during 1.18×10^{-1} M K^+-induced depolarization (○, ●) and cumulative applications of histamine (△, ▲) in normal PSS. Open and closed symbols show the responses in the absence and presence of 10^{-5} M papaverine, respectively. Data are means of 4 different measurements. The abscissa scales indicate fluorescence ratio and calculated $[Ca^{2+}]_i$ and the ordinate scales indicate force.

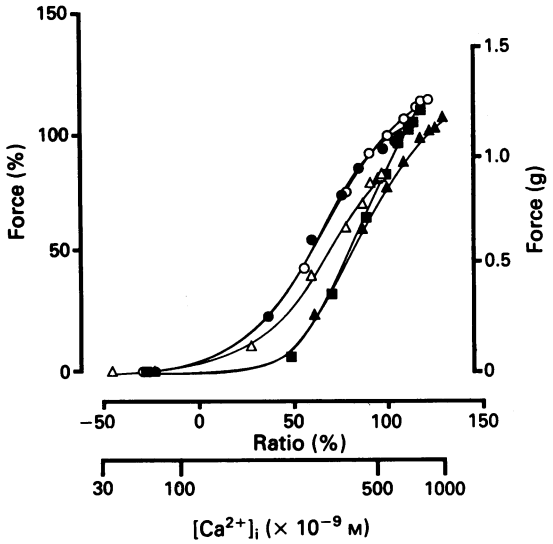

Figure 8 Effects of various vasodilators on the $[Ca^{2+}]_i$-force relationship determined by cumulative applications of Ca^{2+} during 1.18×10^{-1} M K^+-induced depolarization in the strips pretreated with 10^{-5} M papaverine (△), 10^{-7} M diltiazem (●), 10^{-6} M nitroglycerin (▲), 10^{-6} M isoprenaline (■) or the control (○). Data are means of 4 different measurements. The abscissa scale indicates fluorescence ratio and calculated $[Ca^{2+}]_i$, and the ordinate scales the force. The s.e. is omitted for purposes of clarity.

inhibit cyclic nucleotide phosphodiesterases (IC_{50} 10^{-5} M; Kramer & Wells, 1979). This, together with our previous finding that the first and the second phases of histamine-induced responses are mainly due to Ca^{2+} released from store sites and Ca^{2+} influx through the cell membrane, respectively (Hirano *et al.*, 1990), suggests that papaverine inhibits, with a similar potency, not only Ca^{2+} influx but also the Ca^{2+} release stimulated by histamine. Inhibition of intracellular Ca^{2+} release was also observed in experiments carried out in the absence of extracellular Ca^{2+} (Figure 3). Over the same range of concentrations, papaverine also inhibited the Ca^{2+} changes induced by high K^+-depolarization (Figure 6). Compared with these main effects of papaverine on $[Ca^{2+}]_i$ transients, the slight shift of the $[Ca^{2+}]_i$-force curve during high K^+-depolarization to the right in the presence of papaverine appears to indicate a slight reduction in the sensitivity of the contractile apparatus to Ca^{2+} (Figures 7 and 8). These results suggest that the main mechanism for the relaxation induced by papaverine is to decrease $[Ca^{2+}]_i$, through various mechanisms. The processes affected include inhibition of the release of intracellularly stored Ca^{2+} and inhibition of Ca^{2+} influx stimulated by either high K^+-depolarization or by histamine.

Inhibition of the release of stored Ca^{2+}

We found that papaverine inhibits intracellular Ca^{2+} release induced by histamine (Figures 3 and 4), but not by caffeine (Figure 5). Moreover the inhibition by papaverine of the histamine-induced elevation of $[Ca^{2+}]_i$ in Ca^{2+}-free PSS was reversed after washing out papaverine, thereby indicating that papaverine interferes with histamine-activated Ca^{2+}-release mechanisms without affecting those related to caffeine-activated release. Another interpretation is that papaverine might deplete intracellular Ca^{2+} storage sites (Figure 4a). We reported that histamine-sensitive Ca^{2+}-storage sites and caffeine-sensitive Ca^{2+}-storage sites may differ (Matsumoto *et al.*, 1990) in rat aortic smooth muscle cells in primary culture. Papaverine may deplete histamine-sensitive storage sites, without affecting caffeine-sensitive storage sites. Wang & Large (1991) reported that papaverine

inhibited the Ca^{2+}-activated chloride and potassium currents, and thus might induce relaxation in rabbit vascular smooth muscle cells by depleting intracellular Ca^{2+} stores; however it was caffeine-sensitive. The difference in the tissues studied (rabbit ear artery and portal vein vs. porcine coronary artery) or concentration of papaverine ($>10^{-5}$ M vs. $<10^{-5}$ M) may explain the difference in characteristics of papaverine-sensitive intracellular Ca^{2+} stores in these studies.

In vascular smooth muscle, the major physiological pathway for Ca^{2+} release from storage sites seems to be the phospholipase C-mediated phosphatidylinositol cascade coupled to receptors. Papaverine inhibits cyclic nucleotide phosphodiesterases so that both cyclic AMP and cyclic GMP accumulate (Ferrari, 1974; Miyamoto *et al.*, 1976; Kramer & Wells, 1979). These cyclic nucleotides are probably cellular messengers related to the relaxation of smooth muscle induced by papaverine. Cyclic AMP, through cyclic AMP-dependent protein kinase, relaxes smooth muscle by reducing $[Ca^{2+}]_i$ (Suematsu *et al.*, 1984), by inhibiting the formation of inositol 1,4,5-trisphosphate ($InsP_3$: Madison & Brown, 1988; Hall *et al.*, 1989) or by inhibiting the response of the $InsP_3$ receptor (Supattapone *et al.*, 1988). We reported that 8-bromo cyclic GMP, a membrane-permeable cyclic GMP analogue, (Kai *et al.*, 1987), and nitroglycerin (Kobayashi *et al.*, 1985), which elevates cytosolic cyclic GMP, both reduce $[Ca^{2+}]_i$ and cause relaxation (Abe *et al.*, 1990). Nishizuka (1983) found that cyclic GMP inhibits the formation of $InsP_3$ in platelets. Thus, agents which elevate cytosolic levels of cyclic AMP or cyclic GMP, or both, might be expected to inhibit agonist-induced Ca^{2+} release which is probably mediated by $InsP_3$.

Inhibition of Ca^{2+} influx

Papaverine concentration-dependently (10^{-7} M–10^{-5} M) inhibited the histamine-induced, extracellular Ca^{2+}-dependent elevation of $[Ca^{2+}]_i$. In addition, papaverine inhibited increases in the level of $[Ca^{2+}]_i$ and force induced by high K^+-depolarization. Thus, papaverine presumably acts directly or indirectly (via a cyclic nucleotide-dependent protein kinase) on voltage-operated Ca^{2+} channels (VOCs). It was also reported that papaverine inhibited VOCs in tracheal smooth muscle, in a manner independent of intracellular cyclic AMP (Iguchi *et al.*, 1992). Casteels & Suzuki (1980) showed that histamine, through the H_1-receptor, depolarizes vascular smooth muscle, therefore, histamine can increase the Ca^{2+} current flowing through VOCs by depolarizing the membrane or by activating other receptor-mediated pathways on which papaverine may act, or both.

On the other hand, Fujioka (1984) reported that papaverine was more potent than isoprenaline in relaxing K^+-depolarization- or 5-hydroxytryptamine-induced contractions of the dog basilar artery, at a concentration which induces comparable accumulations of cyclic AMP. Thus, the relaxant effects of papaverine may not be due to cyclic AMP alone. Electrophysiological studies showed that papaverine, irrespective of the level of cyclic AMP, inhibits VOCs to cause relaxation of the dog basilar artery. In other electrophysiological studies (Itoh *et al.*, 1981; Brading *et al.*, 1983) and $^{45}Ca^{2+}$ studies (Huddart *et al.*, 1984), papaverine seemed to inhibit Ca^{2+} influx as a means of causing relaxation of smooth muscle.

Reduction of Ca^{2+} sensitivity of the contractile apparatus

It was reported that increases in cyclic AMP reduced the Ca^{2+} sensitivity of the contractile apparatus by activation of A-kinase which phosphorylated MLCK (Adelstein *et al.*, 1978). We have found that nitroglycerin, and hence, cyclic GMP, reduced the Ca^{2+} sensitivity of the contractile apparatus (Abe *et al.*, 1990), while diltiazem had no such effect (Hirano *et al.*, 1990). In the present study, we examined the effect of papaverine on Ca^{2+} sensitivity by comparing its effect in the presence of isoprenaline, nitroglycerin and diltiazem at concentrations causing similar relaxations in vascular strips contracted by high K^+. Isoprenaline and nitroglycerin shifted the Ca^{2+}-force relationship to the right, thus indicating a reduction in Ca^{2+} sensitivity, while diltiazem had no such effect. The Ca^{2+}-force relationship in the presence of papaverine fell between the control or that in the presence of diltiazem (which were identical) and those in the presence of isoprenaline or nitroglycerin. This means that the effect of papaverine in reducing the Ca^{2+} sensitivity of the contractile apparatus is relatively smaller, while its effect in reducing $[Ca^{2+}]_i$ is larger, than those of isoprenaline or nitroglycerin.

In summary, papaverine has various effects on $[Ca^{2+}]_i$ and the development of force in the pig coronary artery. Its main action is to decrease change in $[Ca^{2+}]_i$, while the $[Ca^{2+}]_i$-force relationship is slightly shifted to the right (i.e. there was a decrease in Ca^{2+} sensitivity). At least two mechanisms are involved in the inhibitory effect of papaverine on $[Ca^{2+}]_i$ and it appears to have equal potency on each: firstly, inhibition of Ca^{2+} influx through Ca^{2+} channels opened by either high K^+-depolarization or histamine and, secondly, inhibition of the histamine-induced release of intracellular Ca^{2+} probably due to the inhibition of intracellular signal transduction, presumably the phospholipase C/$InsP_3$ cascade, and to the depletion of stored Ca^{2+}.

We thank M. Ohara and the referees for helpful comments. The present study was supported in part by Grants-in-Aid for Scientific Research on Priority Area (No. 03253208), for General Scientific Research (No. 01480250), and for Developmental Scientific Research (No. 03557043) from the Ministry of Education, Science and Culture, Japan and Grants from Yokoyama Rinshouyakuri, from the Japan Foundation of Cardiovascular Research, from the Ichiro Kanehara Foundation, from the Research Foundation for Cancer and Cardiovascular Disease from the Japan Research Foundation for Clinical Pharmacology, from The Naito Foundation, from the CIBA-GEIGY Foundation (Japan) for the promotion of Science, from the Casio Science Promotion Foundation and from the Uehara Memorial Foundation.

References

ABE, S., KANAIDE, H. & NAKAMURA, M. (1990). Front-surface fluorometry with fura-2 and effects of nitroglycerin on cytosolic calcium concentrations and on tension in the coronary artery of the pig. *Br. J. Pharmacol.*, **101**, 545–552.

ADELSTEIN, R.S., CONTI, M.A. & HATHAWAY, D.R. (1978). Phosphorylation of smooth muscle myosin light chain kinase by the catalytic subunit of adenosine 3':5'-monophosphate-dependent protein kinase. *J. Biol. Chem.*, **253**, 8347–8350.

BENHAM, C.D. & TSIEN, R.W. (1987). A novel receptor-operated Ca^{2+}-permeable channel activated by ATP in smooth muscle. *Nature*, **328**, 275–278.

BRADING, A.F., BURDYGA, T.V. & SCRIPNYUK, Z.D. (1983). The effects of papaverine on the electrical and mechanical activity of the guinea-pig ureter. *J. Physiol.*, **334**, 79–89.

BÜLBRING, G.E. & DEN HERTOG, A. (1980). The action of isoprenaline on the smooth muscle of the guinea-pig taenia coli. *J. Physiol.*, **304**, 277–296.

BÜLBRING, G.E. & TOMITA, T. (1987). Catecholamine action in smooth muscle. *Pharmacol. Rev.*, **39**, 49–96.

CASTEELS, R. & RAEYMAEKERS, L. (1979). The action of acetylcholine and catecholamines on an intracellular calcium store in the smooth muscle cells of the guinea-pig taenia coli. *J. Physiol.*, **294**, 51–68.

CASTEELS, R. & SUZUKI, H. (1980). The effects of histamine on the smooth muscle cells of the ear artery of the rabbit. *Pflügers Arch.*, **387**, 17–25.

FERRARI, M. (1974). Effects of papaverine on smooth muscle and their mechanisms. *Pharmacol. Res. Commun.*, **6**, 97–115.

FUJIOKA, M. (1984). Lack of causal relationship between the vasodilator effect of papaverine and cyclic AMP production in the dog basilar artery. *Br. J. Pharmacol.*, **83**, 113–124.

GRYNKIEWICZ, G., POENIE, M. & TSIEN, R.Y. (1985). A new generation of Ca^{2+} indicators with greatly improved fluorescence properties. *J. Biol. Chem.*, **260**, 3440–3450.

HALL, I.P., DONALDSON, J. & HILL, S.J. (1989). Inhibition of histamine-stimulated inositol phospholipid hydrolysis by agents which increase cyclic AMP levels in bovine tracheal smooth muscle. *Br. J. Pharmacol.*, **97**, 603–613.

HIRANO, K., KANAIDE, H., ABE, S. & NAKAMURA, M. (1990). Effects of diltiazem on calcium concentrations in the cytosol and on force of contractions in porcine coronary arterial strips. *Br. J. Pharmacol.*, **101**, 273–280.

HUDDART, H., LANGTON, P.D. & SAAD, K.H.M. (1984). Inhibition by papaverine of calcium movements and tension in the smooth muscles of rat vas deferens and urinary bladder. *J. Physiol.*, **349**, 183–194.

IGNARRO, L.J. & KADOWITZ, P.J. (1987). The pharmacological and physiological role of cyclic GMP in vascular smooth muscle relaxation. *Annu. Rev. Pharmacol. Toxicol.*, **25**, 171–191.

IGUCHI, M., NAKAJIMA, T., HISADA, T., SUGIMOTO, T. & KURACHI, Y. (1992). On the mechanism of papaverine inhibition of the voltage-dependent Ca^{2+} current in isolated smooth muscle cells from the guinea pig trachea. *J. Pharmacol. Exp. Ther.*, **263**, 194–200.

ITOH, T., KAJIWARA, M., KITAMURA, K. & KURIYAMA, H. (1981). Effects of vasodilator agents on smooth muscle cells of the coronary artery of the pig. *Br. J. Pharmacol.*, **74**, 455–468.

KAI, H., KANAIDE, H., MATSUMOTO, T. & NAKAMURA, M. (1987). 8-Bromoguanosine 3′:5′-cyclic monophosphate decreases intracellular free calcium concentrations in cultured vascular smooth muscle cells from rat aorta. *FEBS Lett.*, **221**, 248–288.

KAMM, K.E. & STULL, J.T. (1985). The function of myosin and myosin light chain phosphorylation in smooth muscle. *Annu. Rev. Pharmacol. Toxicol.*, **25**, 593–620.

KERRICK, W.G.L. & HOAR, P.E. (1981). Inhibition of smooth muscle tension by cyclic AMP-dependent protein kinase. *Nature*, **292**, 253–255.

KOBAYASHI, S., KANAIDE, H. & NAKAMURA, M. (1985). Cytosolic-free calcium transients in cultured vascular smooth muscle cells: microfluorometric measurements. *Science*, **229**, 553–556.

KRAMER, G.L. & WELLS, J.N. (1979). Effects of phosphodiesterase inhibitors on cyclic nucleotide levels and relaxation of pig coronary arteries. *Mol. Pharmacol.*, **16**, 813–822.

MADISON, J.M. & BROWN, J.K. (1988). Differential inhibitory effects of forskolin, isoproterenol, and dibutyryl cyclic adenosine monophosphate on phosphoinositide hydrolysis in canine tracheal smooth muscle. *J. Clin. Invest.*, **82**, 1462–1465.

MATSUMOTO, T., KANAIDE, H., SHOGAKIUCHI, Y. & NAKAMURA, M. (1990). Characteristics of the histamine-sensitive calcium store in vascular smooth muscle. Comparison with norepinephrine- or caffeine-sensitive stores. *J. Biol. Chem.*, **265**, 5610–5616.

MIYAMOTO, M., TAKAYANAGI, I., OHKUBO, H. & TAKAGI, K. (1976). Actions of papaverine on intestinal smooth muscle and its inhibition of cyclic AMP and cyclic GMP phosphodiesterases. *Jpn. J. Pharmacol.*, **26**, 114–117.

MORGAN, J.P. & MORGAN, K.G. (1984). Stimulation-specific patterns of intracellular calcium levels in smooth muscle of ferret portal vein. *J. Physiol.*, **351**, 155–167.

NISHIMURA, J., KOLBER, M. & VAN BREEMEN, C. (1988). Norepinephrine and GTP-γ-S increase myofilament Ca^{2+} sensitivity in α-toxin permeabilized arterial smooth muscle. *Biochem. Biophys. Res. Commun.*, **157**, 677–683.

NISHIZUKA, Y. (1983). Calcium, phospholipid turnover and transmembrane signaling. *Phil. Trans. R. Soc.*, **B302**, 101–112.

PUTNEY, J.W., TAKEMURA, H., HUGHERS, A.R., HORSTMAN, D.A. & THASTRUP, O. (1989). How does inositol phosphate regulate calcium signaling? *FASEB J.*, **3**, 1899–1905.

SADOSHIMA, J., AKAIKE, N., KANAIDE, H. & NAKAMURA, M. (1988). Cyclic AMP modulates Ca^{2+}-activated K^+ channel in cultured smooth muscle cells of rat aortas. *Am. J. Physiol.*, **255**, H754–H759.

SOMLYO, A.V., HAEUSLER, G. & SOMLYO, A.P. (1970). Cyclic adenosine monophosphate: potassium-dependent action on vascular smooth muscle membrane potential. *Science*, **169**, 490–491.

SOMMERVILLE, L.E. & HARTSHORNE, D.J. (1986). Intracellular calcium and smooth muscle contraction. *Cell Calcium*, **7**, 353–364.

SUEMATSU, E., HIRATA, M. & KURIYAMA, H. (1984). Effects of cAMP and cGMP-dependent protein kinases, and calmodulin on Ca^{2+} uptake by highly purified sarcolemmal vesicles of vascular smooth muscle. *Biochem. Biophys. Acta*, **773**, 83–90.

SUPATTAPONE, S., DANOFF, S.K., THEIBERT, A., JOSEPH, S.K., STEINER, J. & SNYDER, S.H. (1988). Cyclic AMP-dependent phosphorylation of a brain inositol trisphosphate receptor decreases its release of calcium. *Proc. Natl. Acad. Sci. U.S.A.*, **85**, 8747–8750.

TASHIRO, N. & TOMITA, A. (1970). The effects of papaverine on the electrical and mechanical activity of the guinea-pig taenia coli. *Br. J. Pharmacol.*, **39**, 608–618.

USHIO-FUKAI, M., ABE, S., KOBAYASHI, S., NISHIMURA, J. & KANAIDE, H. (1993). Effect of isoprenaline on cytosolic calcium concentrations and on tension in the porcine coronary artery. *J. Physiol.*, **462**, 676–696.

WANG, Q. & LARGE, W.A. (1991). Modulation of noradrenaline-induced membrane currents by papaverine in rabbit vascular smooth muscle cells. *J. Physiol.*, **439**, 501–512.

(Received July 7, 1992
Revised August 9, 1993
Accepted October 14, 1993)

Br. J. Pharmacol. (1994), **111**, 497–502

The effects of central myorelaxants on synaptically-evoked primary afferent depolarization in the immature rat spinal cord *in vitro*

[1]R J Siarey, S.K. Long, M.T.H. Tulp & [2]R.H. Evans

Department of CNS-Pharmacology, SOLVAY DUPHAR B V, P O Box 900, 1380 DA Weesp, The Netherlands and *The Department of Pharmacology, University of Bristol, School of Medical Sciences, University Walk, Bristol BS8 1TD

1 In the immature rat *in vitro* hemisected spinal cord preparation the dorsal root-evoked depolarizing potential recorded from an adjacent dorsal root DR-DRP had a mean peak amplitude (± s.e.mean, $n = 27$) of 2.9 ± 0.2 mV and a mean latency to peak amplitude of 106 ± 3 ms. The DR-DRP amplitude was maximal with a stimulus intensity of four times the threshold intensity required to activate the lowest threshold fibres. The peak amplitude and/or integral over a time-source of 0.5 s were used to assess the effects of applied drugs.

2 The DR-DRP was abolished by baclofen (mean IC_{50} 190 ± 46 nM, $n = 7$). The depressant effect of baclofen was reversed by CGP35348 (1 mM). The mean apparent K_d value calculated from dose-ratios was 16.7 ± 6.4 μM ($n = 3$).

3 At a maximally effective concentration, tizanidine (1 μM) produced at the most only a 14% depression of the DR-DRP ($n = 4$). Clonidine (0.3 μM) had an effect similar to that of tizanidine. These depressant effects were reversed by idazoxan (1 μM).

4 The DR-DRP was potentiated by diazepam in a flumazenil (1 μM)-reversible manner. A maximal potentiation of 23.2 ± 2.7% ($n = 5$) was produced by 1 μM diazepam.

5 Diazepam (1 μM) induced a mean bicuculline- (10 μM, $n = 2$) and flumazenil- (1 μM, $n = 8$) sensitive depolarization in the dorsal root of 0.25 ± 0.03 mV ($n = 8$). However, diazepam failed to depolarize dorsal roots ($n = 3$) which had been excised from the spinal cord.

6 Comparison of the above effects with previously reported depressant effects of these drugs on the synaptic output from ventral roots suggests that actions on presynaptic inhibition, as reflected in the DR-DRP, are of subsidiary importance in explaining the muscle relaxant actions of tizanidine or diazepam.

Keywords: Baclofen; diazepam; tizanidine; spinal cord; primary afferent depolarization

Introduction

In a previous study (Siarey *et al.*, 1992b) it was found that the myorelaxant drugs diazepam and tizanidine produced similar levels of depression of N-methyl-D-aspartate (NMDA) receptor-mediated synaptic excitation of motoneurones, as reflected in recordings from ventral roots of *in vitro* spinal cord preparations. These depressant actions were mediated respectively via flumazenil- and idazoxan-sensitive receptors. In the same study baclofen abolished the synaptic excitation of motoneurones and the effect of baclofen was reversed by the $GABA_B$ receptor antagonist, CGP35348 (3-aminopropyl (diethoxymethyl)phosphinic acid) (Bittiger *et al.*, 1990).

The myorelaxant action of diazepam, unlike that of tizanidine or baclofen, is considered to be associated with the potentiation of presynaptic inhibition mediated at $GABA_A$ receptors (Polc *et al.*, 1974). Presynaptic inhibition is reflected in the picrotoxin- or bicuculline-sensitive synaptic depolarization of dorsal root fibres (DR-DRP) evoked from electrical stimulation of an adjacent dorsal root (Eccles *et al.*, 1963). Thus, effects of drugs on this form of presynaptic inhibition can be monitored from their actions on the DR-DRP.

The present paper is an extension of the previous study (Siarey *et al.*, 1992b). In the present study the effects of the three myorelaxant drugs and the NMDA receptor antagonist 2-amino-5-phosphonopentanoate (AP5) have been compared on the DR-DRP.

The results suggest that the previously reported depression of output from motoneurones by tizanidine or diazepam (Siarey *et al.*, 1992b) is independent of their actions on the DR-DRP.

Some of these results have been reported in preliminary form (Siarey *et al.*, 1992a).

Methods

The methods of superfusion, stimulation and recording were as described by Evans *et al.* (1982). Hemisected spinal cord preparations from rats of 2 to 5 days *post partum* age were superfused with medium containing (mM): $MgSO_4$ 1.25, $CaCl_2$ 1.5, NaCl 118, KCl 3, $NaHCO_3$ 24 and dextrose 12. Supramaximal electrical stimulation (0.5 ms square pulses at 10 to 20 times threshold) of a dorsal root (L4 or 5) at a rate of 0.0111 Hz was used to evoke synaptic potentials in the adjacent dorsal root (DR-DRP).

Effects of drugs on the electrically evoked responses were measured as the change in peak amplitude or area after integration over a time course of 0.5 s. In several preparations, for technical reasons, the size of synaptic responses decreased consistently over the period of the experiment. This is illustrated in Figure 1c. The effects of drugs were superimposed on such time-dependent changes.

Unless stated otherwise mean values are presented ± s.e.mean.

Results

The peak of the DR-DRP measured in 27 preparations had a mean latency to peak amplitude of 106 ± 3 ms, a mean amp-

[1] Present address: Institute of Physiology, University of Aarhus, Ole Worms Alle 160, Universitatsparken DK-8000, Aarhus C, Denmark.
[2]Author for correspondence.

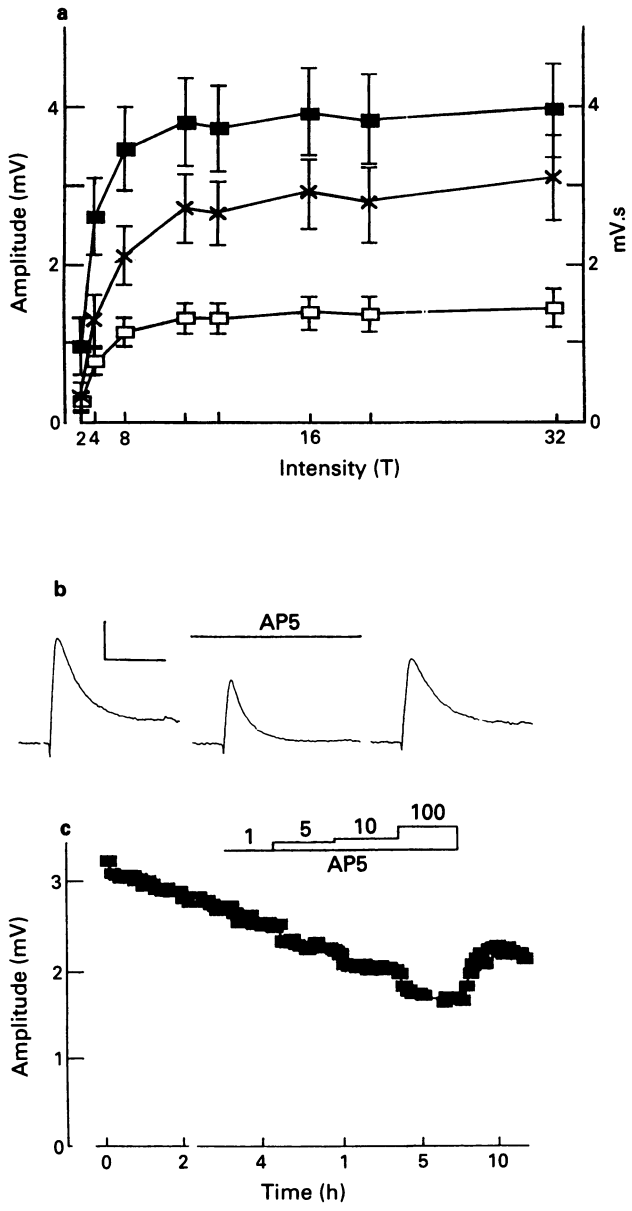

Figure 1 (a) Plot of mean peak amplitude (■), integral over 0.5 s (□) and integral over 2 s (X) of DR-DRP against stimulus intensity in terms of threshold (T) for activation of the lowest threshold fibres. Values are mean ± s.e.mean of at least three observations. It can be seen that the peak amplitude is near maximal at 4T. (b) Effect of 2-amino-5-phosphonopentanoate (AP5, 100 μM) on the DR-DRP. Time course of the effect, on individual values for peak amplitude from the preparation in (b), is plotted in (c). It can be seen that cumulative application of AP5 (μM) preferentially abolished the later component of the potential. Calibration in (b), vertical 1 mV; horizontal 1 s.

litude of 2.9 ± 0.2 mV and a mean time to half decay of 274 ± 14 ms. The peak amplitude of the DR-DRP was near maximal at stimulus intensities of four times the threshold for the lowest threshold fibres (filled squares Figure 1). Stimulus intensities higher than four times threshold increased the amplitude and duration of the long latency (> 0.4 s) component of the DR-DRP (Figure 1). This profile of the DR-DRP is similar to that from a smaller sample described in a previous paper (Siarey *et al.*, 1991).

The depressant effect of the non-NMDA receptor antagonist, 6-cyano-7-nitroquinoxaline-2,3-dione (CNOX) on the DR-DRP has been reported previously (Evans & Long 1990; Siarey *et al.*, 1991). The NMDA receptor antagonist AP5 produced a preferential depression of the long duration component of the DR-DRP (Figure 1b,c) as indicated by respective mean EC_{25} values (μM) of 23.7 ± 5.1 and 2.4 ± 0.4 ($n = 5$) for depression of peak amplitude and area of the DR-DRP.

Effect of baclofen

Figure 2a and b illustrate the depressant effect of baclofen on the DR-DRP. The potential was abolished at concentrations between 1 and 5 μM. The mean ($n = 7$) EC_{50} for depression of the peak amplitude was 275 ± 62 nM. There was no significant difference, in the depressant effect of baclofen, between the peak amplitude and the integrated area of the DR-DRP. As illustrated in Figure 2c, CGP35348 (1 mM) produced a parallel rightward displacement of the concentration-effect plot for baclofen. The mean apparent K_d value calculated from this rightward displacement in three preparations was 16.7 ± 6.4 μM.

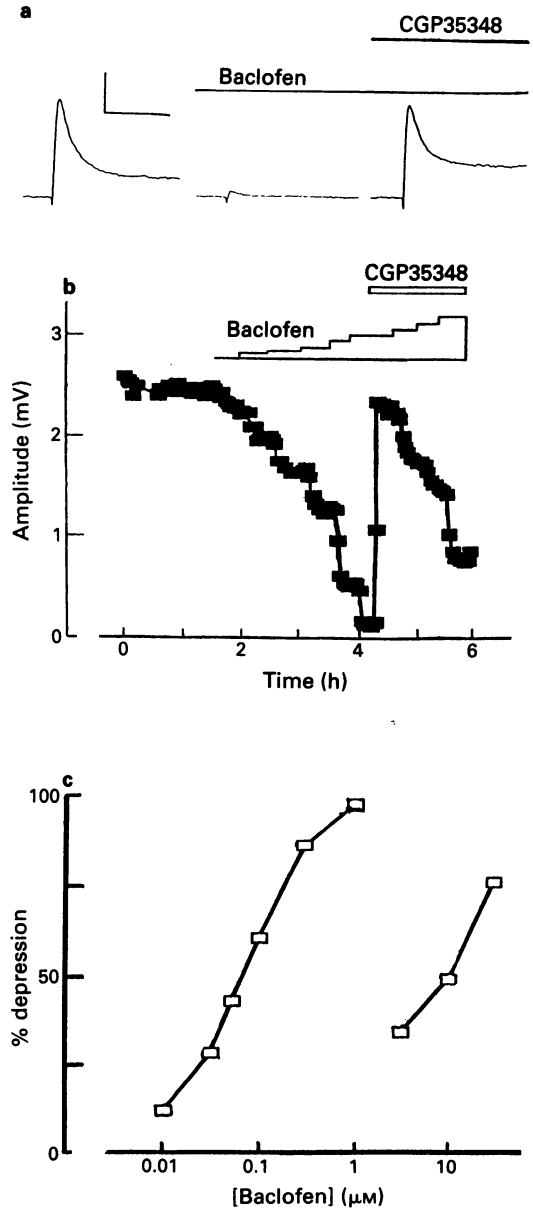

Figure 2 Depressant effect of baclofen on the DR-DRP. It can be seen in (a) that baclofen (1 μM) depressed all components of the DR-DRP; (b) shows the time course of the effect of cumulative (0.01, 0.03, 0.05, 0.1, 0.3, 1, 3, 10 and 30 μM) concentrations of baclofen, as indicated above the plot, on the peak amplitude of the DR-DRP. The $GABA_B$ antagonist, CGP35348 (1 mM) was introduced also as indicated above the plot. (c) Shows the concentration-effect plot of the percentage depressant action of baclofen with the rightward shift induced by CGP35348. Other details as for Figure 1.

Effect of α_2-adrenoceptor agonist

Clonidine (EC_{50} 26 nM) and tizanidine (EC_{50} 135 nM) have been shown to be potent depressants of the synpatic output from motoneurones as recorded from ventral roots (Siarey *et al.*, 1992b). In the present study these two drugs were tested on the DR-DRP at concentrations higher than were required for the above actions. Figure 3 illustrates the weak depression of the DR-DRP produced by clonidine and tizanidine. Thus clonidine (0.3 μM) and tizanidine (1 μM) depressed the peak amplitude of the DR-DRP to mean levels of 92 ± 2% ($n = 3$) and 90 ± 4% ($n = 4$) of respective control values.

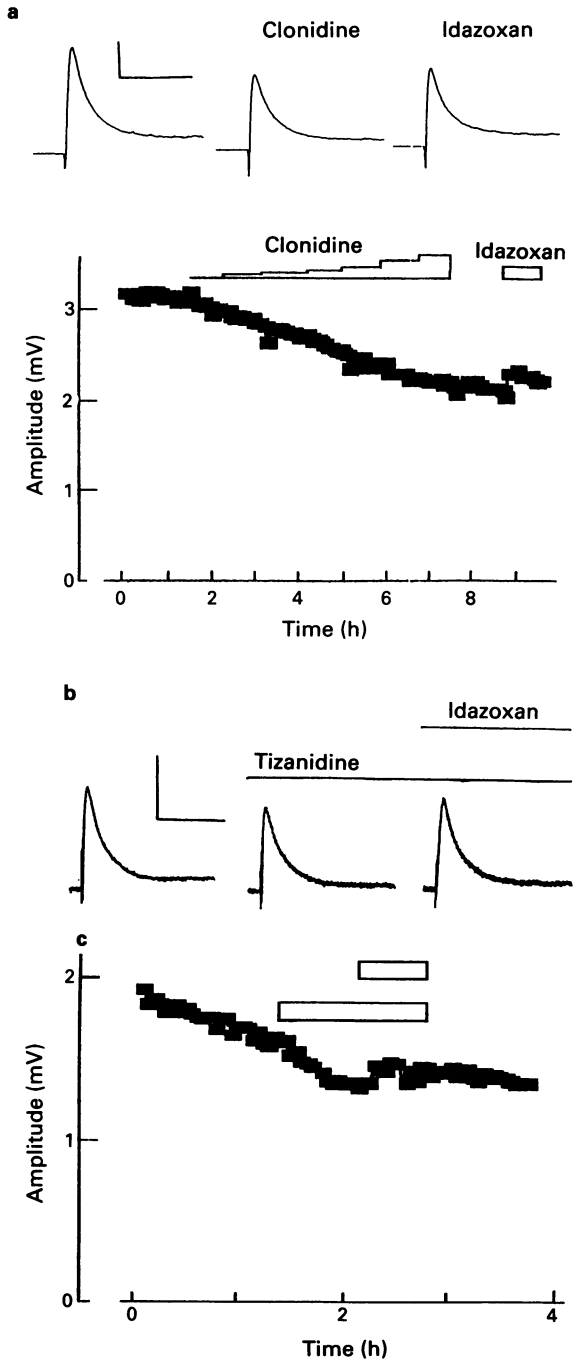

Figure 3 Effect of clonidine (1 μM) (a) and tizanidine (1 μM) (b) on the DR-DRP with the time-courses of the effect on peak amplitude plotted below. Clonidine (0.01, 0.02, 0.03, 0.05, 0.1, 0.3 and 1 μM) was applied cumulatively as indicated on the plot. A small idazoxan (1 μM)-reversible depressant action of both drugs can be seen. Other details as for Figure 1.

There was no significant difference between the effects of peak amplitude and integrated area. As previously observed with the depression of ventral root potentials (Siarey *et al.*, 1992b), the effect of clonidine was very slowly reversible (Figure 3a) but the depressant effects of clonidine and tizanidine were reversed quickly in the presence of idazoxan (1 μM) (Figure 3).

Effect of diazepam

In the previous study from this laboratory, diazepam (1 μM) depressed the integrated polysynaptic output from motoneurones by 50% (Siarey *et al.*, 1992b). In the present study application of diazepam (1 μM) caused depolarization of the dorsal root (see Figure 4a). In eight preparations the mean level of the diazepam-induced depolarization was 0.25 ± 0.03 mV. As illustrated in Figure 4a the diazepam-induced depolarization was reversed in the presence of flumazenil (1 μM) ($n = 6$) or bicuculline (10 μM) ($n = 2$). Dorsal root fibres of the immature rat are very sensitive to depolarization by $GABA_A$ receptor agonists (Allan *et al.*, 1980). However, in the present study diazepam failed to produced measurable depolarization of dorsal roots which had been excised from the spinal cord and to which the application of GABA (2 μM) for 2 min produced depolarization of at least 0.1 mV.

In a series of five preparations from the present study the mean peak amplitude and integrated area of the DR-DRP were increased to levels of 112 ± 2% and 123 ± 3%, respectively, in the presence of diazepam (1 μM). In order to assess the effect of diazepam on the DR-DRP, the peak amplitudes and integrals recorded in the presence of diazepam were measured relative to the control baseline potential before diazepam was introduced. This eliminated the occluding effect of the diazepam-induced depolarization of the dorsal root on the synaptic potentials. In all the preparations the diazepam-induced potentiation of the DR-DRP was reversed to the control levels (100%) in the presence of flumazenil (1 μM) (Figure 4b). Because of the small extent, slow induction and even slower reversal on washout of these diazepam-induced effects the application of flumazenil was particularly important in demonstrating that these effects were significant. This is illustrated in Figure 4b where the reduction in DR-DRP produced by the application of flumazenil is more apparent than the increase which followed the introduction of diazepam. Under similar conditions in this laboratory, potentiation of the DR-DRP to at least 120% was produced by pentobarbitone (50 μM) (Wesselman *et al.*, 1991).

It was shown previously (Siarey *et al.*, 1992b) that diazepam is a potent and selective depressant of the NMDA receptor-mediated component of the long duration segmental excitatory reflex as recorded from a ventral root (DR-LVRP). It might be expected that this depressant effect of diazepam would be explained by potentiation of primary afferent depolarization (Polc *et al.*, 1974). Tizanidine has a selective depressant effect on the segmental reflex which is similar to that of diazepam (Siarey *et al.*, 1992b). However, as shown above, tizanidine depressed primary afferent depolarization. Therefore it was of interest to investigate the relationship between primary afferent depolarization and the DR-LVRP. In three hemisected spinal cord preparations, paired pulses were applied to a dorsal root. The first pulse of each pair was at an intensity sufficient to evoke a DR-DRP but insufficient to evoke a DR-LVRP from the corresponding ventral root. The second pulse of each pair was at higher intensity so that a DR-LVRP was evoked. The second pulse was timed to occur near the peak of the DR-DRP caused by the first pulse. The relative integrated areas of the DR-DRP caused by each pulse alone and in combination are shown in the first column of Table 1 as are the corresponding values for the DR-LVRP. It can be seen (as illustrated in Figure 5) that, despite the increased primary afferent depolarization of

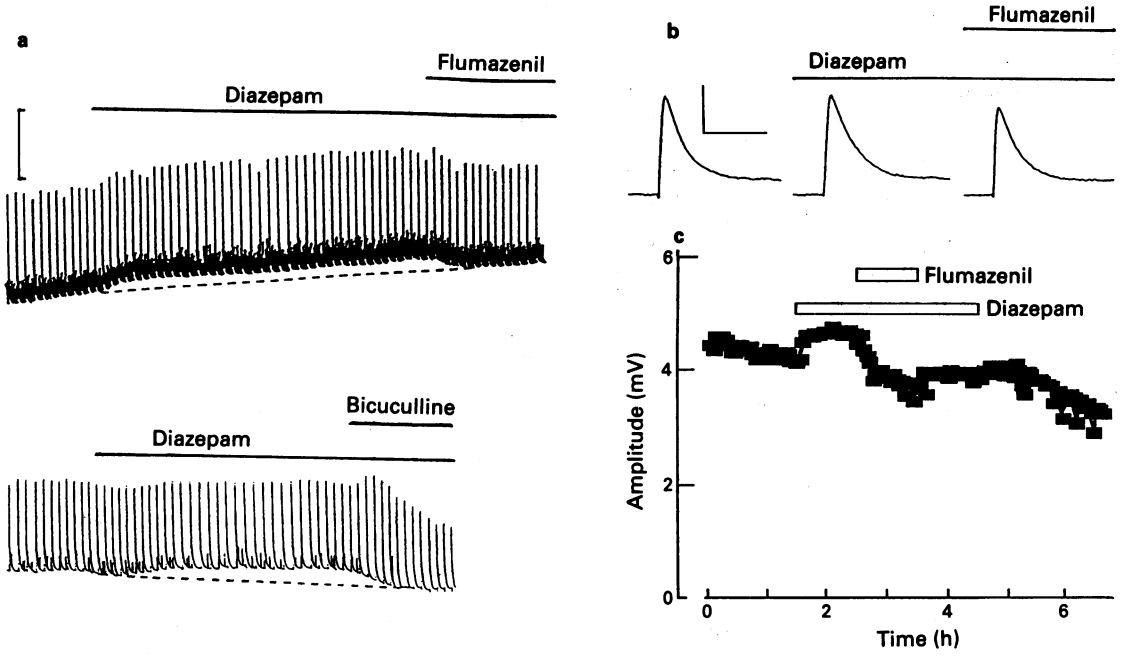

Figure 4 (a) shows the depolarizing action of diazepam (1 μM) on the dorsal root baseline potential of two separate preparations. The dashed line is the projection of the control base line recorded in the absence of diazepam. The diazepam-induced shift was reversed by flumazenil (1 μM) applied to the upper preparation and bicuculline (10 μM) applied to the lower preparation as indicated above the traces. Vertical calibration 2.0 mV in the upper trace, 1.2 mV in the lower trace. The regular vertical deflections are the DR-DRPs evoked following stimulation of an adjacent dorsal root at 90 s intervals. (b) Shows the effect of diazepam (1 μM) on the DR-DRP with the time-course of the effect on peak amplitude plotted in (c). Peak amplitudes were measured from the projected baseline d.c. level as depicted in (a). A small diazepam-induced potentiation can be seen which was reversed on introduction of flumazenil (1 μM) as indicated above the plot. Calibration in (b), 2 mV and 1 s.

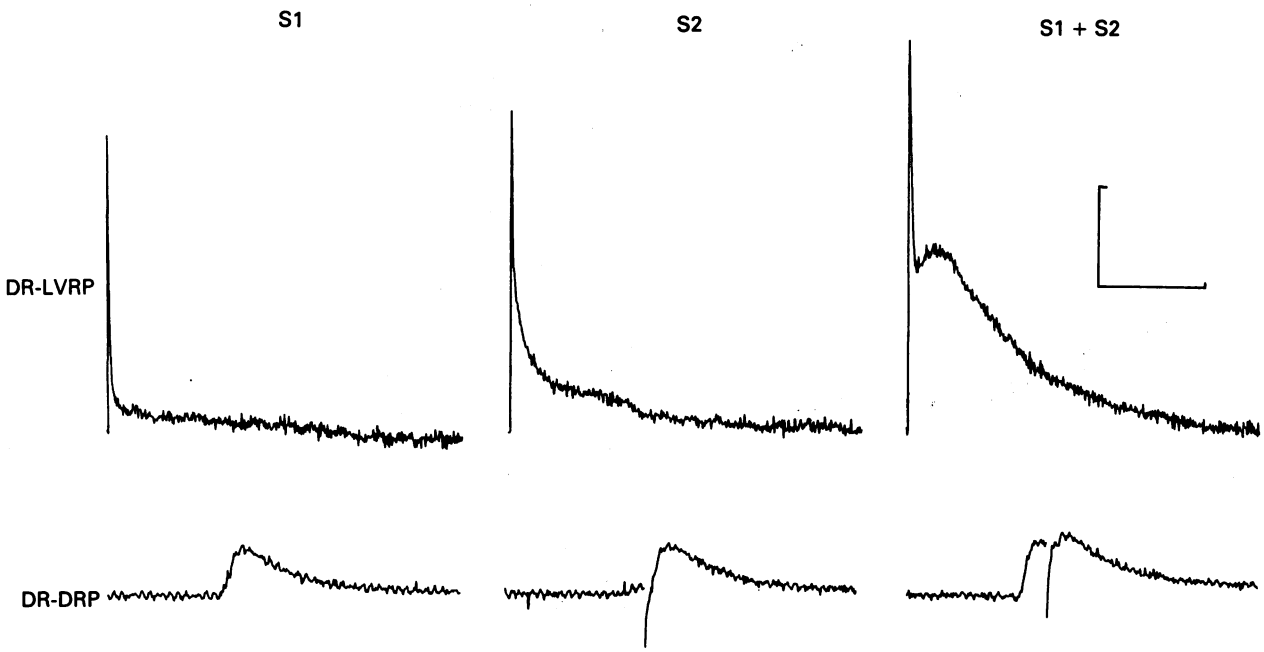

Figure 5 Effect of a low intensity conditioning stimulus (S1) on the DR-LVRP evoked by a high intensity stimulus (S2). Both stimuli were applied to the same dorsal root. The lower traces show the DR-DRP evoked by the combination of stimuli used to evoke the DR-LVRP in the trace above. The DR-DRP was recorded from a dorsal root adjacent to the stimulated one. The lefthand traces are with S1 alone. The centre traces are with S2 alone and the righthand traces are with S1 + S2. It can be seen that S1 and S2 produced similar DR-DRPs. However, the increase in primary afferent depolarization caused by S1, in combination with S2 (at an interval of 70 ms), failed to inhibit the DR-LVRP evoked by S2. On the contrary the combination of stimuli produced a big enhancement of the DR-LVRP. Each trace is an average of six evoked potentials. The vertical scale is 0.2 mV in the upper and 0.27 mV in the lower traces. The corresponding horizontal scales are 10 s and 300 ms.

Table 1 Integrated areas of the evoked potentials expressed as a percentage (100 × (S1 + S2)/S2) of the potential evoked by a high intensity stimulus S2

	DR-DRP		DR-LVRP
Stimulus	*Separate*	*Combined*	*Combined*
	181	140	241
	140	90	125
	188	186	253

The first column is the sum of the areas of the two DR-DRPs when the low intensity stimulus (S1) was applied on a separate occasion from S2. The second column is the area of the DR-DRP when S1 and S2 were applied in combination with an interval of 50 to 90 ms between them. It is seen that the integrated area of the long duration DR-VRP (DR-LVRP) evoked by S2 was increased by S1 from 25 to 153% in each of the three preparations represented in each row. Each value is a mean of at least four responses obtained from each tissue at intervals of 90 s. S1 evoked no significant DR-LVRP.

up to 88%, the DR-LVRP was potentiated by as much as 150% by the first pulse in the pair.

Discussion

The primary afferent depolarization evoked following electrical stimulation of sensory nerves has a central latency of 2 to 3 ms in the anaesthetized cat and is considered therefore to be relayed through at least two interneurones (Eccles *et al.*, 1962). The present EC_{50} value for the depressant action of baclofen on the DR-DRP is not significantly different from the value of 237 nM reported for depression of the dorsal root-evoked monosynaptic population spike of motoneurones by baclofen (Siarey *et al.*, 1992b). We reported a value five fold lower for the depression of polysynaptic excitation. Thus the depressant action of baclofen on the DR-DRP appears to be dominated by depression of transmitter release from primary afferent terminals (Edwards *et al.*, 1989). A significantly lower EC_{50} value would have been expected if depression of the release of GABA and/or depression of polysynaptic excitatory pathways were involved. The apparent K_d value derived from the dose ratios produced by the $GABA_B$ antagonist CGP35348 is not significantly different from previously reported values (Seabrook *et al.*, 1990; Siarey *et al.*, 1992b) which is again consistent with depression of the DR-DRP being mediated at the level of the primary afferent synapse.

The actions of the α_2-adrenoceptor agonists and of diazepam contrast with their depressant actions on the output of the motoneurone (Siarey *et al.*, 1992b). The former agents produced only a small depression and the latter a small potentiation. Our previous study showed that the α_2-adrenoceptor agonists and diazepam had no significant depressant action at primary afferent synapses. Thus the small effects observed in the present study are likely to have been mediated either at excitatory synapses between interneurones or at the axo-axonic synapses between GABAergic interneurones and primary afferents.

The maximal depression of the polysynaptic output of motoneurones produced by clonidine, tizanidine and diazepam, in the previous study, amounted to approximately 50% (Siarey *et al.*, 1992b). In the present experiments the maximal depressant effect of clonidine and tizanidine on the DR-DRP was approximately 10% and diazepam produced a maximal potentiation of approximately 20%. It is impossible to dissociate the primary afferent depolarizing action of afferent volleys in dorsal roots from their excitatory action. However, the experiments illustrated by Figure 5, show that the excitatory effect of dorsal root volleys on the DR-LVRP dominates any possible inhibitory action that might be associated with the DR-DRP. This is probably to be expected because the DR-LVRP outlasts the DR-DRP by several seconds. Therefore it would seem unlikely that potentiation of presynaptic inhibition (Polc *et al.*, 1974) plays a major role in depression of the DR-LVRP by diazepam (Akagi & Yanagisawa, 1987). Incidentally, Figure 5 illustrates also that the DR-LVRP is not exclusively caused by C fibre primary afferents.

The bicuculline-sensitive depolarization of dorsal roots induced by diazepam is unlikely to have been due to a direct GABAmimetic action as occurs with pentobarbitone (Evans, 1979) because the effect was absent from excised dorsal roots which are highly sensitive to GABA. The most likely cause of this effect is potentiation of the action of GABA which is released tonically from GABAergic terminals.

R.H.E. was supported by The Medical Research Council, The Taberner Trust and The Wellcome Trust. R.J.S. was supported by a Solvay Duphar Research Scholarship.

References

AKAGI, H. & YANAGISAWA, M. (1987). GABAergic modulation of a substance P-mediated reflex of slow time course in the isolated rat spinal cord. *Br. J. Pharmacol.*, **91,** 189–197.

ALLAN, R.D., EVANS, R.H. & JOHNSON, G.A.R. (1980). GABA agonists: an *in vitro* comparison between depression of spinal synaptic activity and depolarization of spinal root fibres in the rat. *Br. J. Pharmacol.*, **70,** 609–615.

BITTIGER, H., FROESTL, W., HALL, R., KARLSSON, G., KLEBS, K., OLPE, H.-R., POZZA, M.F., STEINMANN, M.W. & VAN REIZEN, H. (1990). Biochemistry, electrophysiology and pharmacology of a new $GABA_B$ antagonist: CGP35348. In *$GABA_B$ Receptors in Mammalian Function.* ed. Bowery, N.G., Bittiger, H. & Olpe, H.-R. pp. 47–60. Chichester: John Wiley.

ECCLES, J.C., KOSTYUK, P.G. & SCHMIDT, R.F. (1962). Presynaptic inhibition of the central actions of flexor reflex afferents. *J. Physiol.*, **161,** 258–281.

ECCLES, J.C., SCHMIDT, T. & WILLIS, W.D. (1963). Pharmacological studies on presynaptic inhibition. *J. Physiol.*, **168,** 500–530.

EDWARDS, F.R., HARRISON, P.J., JACK, J.J.B. & KULLMAN, D.M. (1989). Reduction by baclofen of monosynaptic EPSPs in lumbosacral motoneurones of the anaesthetised cat. *J. Physiol.*, **416,** 539–556.

EVANS, R.H. (1979). Potentiation of the effects of GABA by pentobarbitone. *Brain Res.*, **171,** 113–120.

EVANS, R.H., FRANCIS, A.A., JONES, A.W., SMITH, D.A.S. & WATKINS, J.C. (1982). The effects of a series of ω-phosphonic α-carboxylic amino acids on electrically evoked and excitant amino acid induced responses in isolated spinal cord preparations. *Br. J. Pharmacol.*, **75,** 65–75.

EVANS, R.H. & LONG, S.K. (1990). Primary afferent depolarization in the rat spinal cord is mediated by pathways utilising NMDA and non-NMDA receptors. *Neurosci. Lett.*, **100,** 231–236.

POLC, P., MOHLER, H. & HAEFELY, W. (1974). The effect of diazepam on spinal cord activities: possible sites and mechanisms of action. *Naunyn. Schmied. Arch. Pharmacol.*, **284,** 319–337.

SEABROOK, G.R., HOWSON, W. & LACEY, M.G. (1990). Electrophysiological characterization of potent agonists and antagonists at pre- and postsynaptic $GABA_B$ receptors on neurones in rat brain slices. *Br. J. Pharmacol.*, **101,** 949–957.

SIAREY, R.J., LONG, S.K. & EVANS, R.H. (1991). Potentiation of synpatic reflexes by D-serine in the rat spinal cord *in vitro*. *Eur. J. Pharmacol.*, **195,** 241–244.

SIAREY, R.J., LONG, S.K. & EVANS, R.H. (1992a). A comparison of the effect of diazepam and tizanidine on synaptically-evoked primary afferent depolarization in the rat spinal cord *in vitro*. *J. Physiol.*, **452**, 200P.

SIAREY, R.J., LONG, S.K. & EVANS, R.H. (1992b). The effect of centrally acting myorelaxants on NMDA receptor-mediated synaptic transmission in the immature rat spinal cord *in vitro*. *Br. J. Pharmacol.*, **107**, 628–633.

WESSELMAN, J.P.M., VAN WILGENBURG, H. & LONG, S.K. (1991). The effects of pentobarbital and benzodiazepines on GABA-responses in the periphery and spinal cord *in vitro*. *Neurosci. Lett.*, **128**, 261–264.

(Received June 16, 1993
Revised September 8, 1993
Accepted October 15, 1993)

Br. J. Pharmacol. (1994), **111**, 503–508

The noradrenaline precursor L-*threo*-3,4-dihydroxyphenylserine exhibits antinociceptive activity via central α-adrenoceptors in the mouse

Atsufumi Kawabata, Kazuyo Kasamatsu, Nahoko Umeda & [1]Hiroshi Takagi

Department of Pharmacology, Faculty of Pharmaceutical Sciences, Kinki University, 3-4-1 Kowakae, Higashi-Osaka 577, Japan

1 Systemic (s.c. or p.o.) administration of L-*threo*-3,4-dihydroxyphenylserine (droxidopa, L-*threo*-DOPS; L-DOPS), a noradrenaline precursor, at a dose-range of 100–800 mg kg^{-1}, produced naloxone-resistant antinociception in a dose-dependent manner in the mouse, as assessed by the tail flick test, kaolin-induced writhing test and formalin-induced nociception test.

2 Antinociception elicited by L-DOPS (400 mg kg^{-1}, s.c.) was not affected by s.c. injection of benserazide, a peripherally preferential L-aromatic amino acid decarboxylase inhibitor, but was suppressed by its intracerebroventricular (i.c.v.) injection.

3 I.c.v. or intrathecal (i.t.) administration of the non-selective α-blocker, phentolamine, significantly reduced L-DOPS-induced antinociception.

4 I.c.v. administration of the α_1-blocker, prazosin, but not the α_2-blocker, yohimbine, abolished the antinociceptive effects of L-DOPS. In contrast, both blockers, when administered i.t., exhibited significant inhibitory effects.

5 These results suggest that systemic L-DOPS produces opioid-independent antinociception, mediated by supraspinal α_1-adrenoceptors and by spinal α_1- and α_2-adrenoceptors and may predict additional therapeutic applications of L-DOPS as an analgesic.

Keywords: L-*threo*-3,4-dihydroxyphenylserine (droxidopa, L-*threo*-DOPS, L-DOPS); noradrenaline precursor; antinociception; analgesia; α-adrenoceptors; L-aromatic amino acid decarboxylase

Introduction

There are multiple descending pain-modulating systems within the CNS. The brainstem-spinal monoaminergic systems function to suppress the transmission of nociceptive information from primary afferent neurones in the spinal dorsal horn, thereby playing a modulatory role in pain processing (for review, see Takagi, 1982; Basbaum & Fields, 1984). In the course of our studies on the sites of action of morphine and opioid peptides, we found that the ventrolateral region of the reticular formation of the medulla oblongata, particularly the nucleus reticularis paragigantocellularis (NRPG) and the nucleus reticularis gigantocellularis (NRGC), play important roles in the generation of opiate-induced analgesia (Takagi, 1980; 1982). Moreover, electrical stimulation of the NRPG and NRGC neurones induces inhibition of spinal dorsal horn neurones that respond to noxious stimuli and induce behavioural antinociception (Akaike *et al.*, 1978; Takagi, 1982). The pathways from these nuclei to the spinal cord are partly noradrenergic; they send excitatory fibres to the pontine A1 or A7 noradrenergic neurones from where the descending noradrenergic fibres reach the spinal dorsal horn (Takagi, 1980; 1982; Kuraishi *et al.*, 1987; Wigder & Wilcox, 1987; Clark & Proudfit, 1991; Yeomans *et al.*, 1992) and noradrenaline released from the descending fibres can inhibit the dorsal horn neurones that respond to noxious inputs (Belcher *et al.*, 1978; Headley *et al.*, 1978; Satoh *et al.*, 1979). Thus, there is considerable evidence that the descending noradrenergic fibres are involved in analgesic mechanisms at the spinal dorsal horn. In contrast, the role of supraspinal noradrenergic systems in nociceptive processing still remains unclear because of its complexity and the inconsistency of available data (Behbehani *et al.*, 1981; Hammond *et al.*, 1980; Sagen & Proudfit, 1985; Heinricher *et al.*, 1988; Millar & Williams, 1989; Fields *et al.*, 1991).

Systemic administration of noradrenaline does not produce analgesia in mammals, because it cannot penetrate the brain through the blood-brain barrier. Recently, a synthetic amino acid, L-*threo*-3,4-dihydroxyphenylserine (L-*threo*-DOPS, L-DOPS), has been clinically introduced as a noradrenaline precursor and antiparkinsonism drug. L-DOPS is converted directly into L-noradrenaline by L-aromatic amino acid decarboxylase, thereby acting as a noradrenaline precursor *in vivo* (Inagaki & Tanaka, 1978). L-DOPS, when administered systemically, selectively increases noradrenaline and its metabolite levels without affecting dopamine levels in mammalian peripheral and CNS tissues (Semba & Takahashi, 1985; Karai *et al.*, 1987; Kato *et al.*, 1987).

In this paper, we show that L-DOPS administered systemically (s.c. and p.o.) exhibits antinociceptive activity in the mouse, mediated by spinal and supraspinal α-adrenoceptors, predicting possible clinical usefulness of L-DOPS as a novel type of analgesic.

Methods

Animals

Male ddY mice weighing 20–30 g (Japan SLC. Inc.) were maintained on a 12 h light-dark cycle on a standard laboratory diet and tap water *ad libitum* before experiments.

Nociceptive assay

Tail flick test Using a tail-flick analgesia meter (MK-330, Muromachi Kikai Co. Ltd., Japan), the tail of each mouse was exposed to a focused light beam, the intensity of which was adjusted to obtain basal latencies of 2–2.5 s. The cut-off time was defined as 8 s to avoid damage to the tail. Results were expressed as latencies, or as Δ latencies obtained by subtracting the basal latency from the test latency. In an experiment, the antinociceptive potency of the drug as per-

[1] Author for correspondence.

centage of maximal possible effect (%MPE) was also calculated by use of the following formula: 100 × (postdrug latency − predrug latency)/(8 − predrug latency).

Kaolin-induced writhing test The kaolin-induced writhing (stretching) test was developed as a model for endogenous bradykinin-induced nociception with clear reproducibility by Fujiyoshi *et al.* (1989, 1990). The mechanism responsible for the induction of writhing reactions is that i.p. injection of kaolin increases bradykinin release through activation of coagulation factor XII, resulting in nociception. In the present study, this test was used with minor modifications. Each mouse was injected i.p. with kaolin suspended in 0.2% Tween 80 solution (5 mg ml^{-1}) in a volume of 0.25 ml per 10 g body weight, and the number of writhing responses was measured for 20 min, immediately after injection.

Formalin-induced nociception test According to the method of Shibata (1985), each mouse received an intraplantar (i.pl.) injection of 25 µl of 0.5% formalin solution in the right hindpaw. The duration of paw-licking (an index of nociception) was measured every 5 min for 30 min, immediately after i.pl. injection. Results were expressed as licking time in the first (0–5 min) and second (10–30 min) phases.

Experimental protocol

Antinociceptive activity of systemically administered L-DOPS In the tail-flick test, L-DOPS at 100–800 mg kg^{-1} was administered s.c. or p.o., and the latency was repeatedly measured 20, 40, 60, 90 and 120 min later. In the writhing assay, kaolin was injected i.p. 30, 60 or 120 min after s.c. administration of L-DOPS (100–400 mg kg^{-1}), followed by observation of writhing responses for 20 min. To assess the effect of L-DOPS on formalin-induced nociception, mice were injected i.pl. with formalin 50 min after L-DOPS (100–200 mg kg^{-1}), and licking responses were observed for a subsequent 30 min.

Naloxone-reversibility of antinociception produced by L-DOPS Naloxone at 1 mg kg^{-1} was administered s.c. 40 min after s.c. treatment with L-DOPS at 400 mg kg^{-1}.

Effects of systemically or centrally administered benserazide on L-DOPS-induced antinociception Benserazide, a peripherally preferential L-aromatic amino acid decarboxylase inhibitor, was administered i.p. at a dose of 1 mg kg^{-1}, 1 h before L-DOPS (400 mg kg^{-1}, s.c.). At this dose, benserazide has been reported to reduce considerably serum but not brain noradrenaline metabolite levels increased by L-DOPS in mouse (Karai *et al.*, 1987). To determine the involvement of enzymatic decarboxylation of L-DOPS into (−)-noradrenaline within the brain in the induction of this effect, benserazide at 25 µg per mouse was also administered i.c.v. (Haley & McCormick, 1957) 30 min before L-DOPS (400 mg kg^{-1}, s.c.).

Effects of i.c.v. and i.t. administration of α-blockers on the antinociceptive activity of L-DOPS Phentolamine, a non-selective α-blocker, at 1 µg per mouse, prazosin, an α_1-blocker, at 1 µg per mouse, and yohimbine, an α_2-blocker, at 1–5 µg per mouse, were administered i.c.v. or i.t. (Hylden & Wilcox, 1980) 40 min after L-DOPS (400 mg kg^{-1}, s.c.).

Drugs employed

The following were used: L-*threo*-3,4-dihydroxyphenylserine (droxidopa; L-DOPS), N-seryl-*N*-(2,3,4-trihydroxybenzyl)-hydrazine (benserazide) (gifts from Sumitomo Pharmaceuticals, Japan), naloxone hydrochloride, prazosin hydrochloride, yohimbine hydrochloride (Sigma, U.S.A.), phentolamine mesylate (Regitin Inj.; Ciba-Geigy, Switzerland). L-DOPS was suspended in 0.2% Tween 80 solution, and other drugs with the exception of prazosin were dissolved in saline. Prazosin was dissolved in a mixture of dimethylsulphoxide (DMSO) and distilled water (1:1 and 1:8 for i.c.v. and i.t. injections, respectively).

Statistical analysis

Results are expressed as means and s.e.means, and statistical analysis was performed by Student's unpaired *t* test for two-group data, or by Newman-Keuls' test for multiple comparison. The difference between groups was considered statistically significant when $P<0.05$.

Results

Antinociceptive effects of s.c. administration of L-DOPS

L-DOPS, administered s.c. at 400 mg kg^{-1}, significantly prolonged tail-flick latency in mice from 40 min after administration, peaking at 60 min followed by gradual recovery (Figure 1a). The antinociceptive effects of L-DOPS at peak time were dose-dependent at 100–400 mg kg^{-1} (Figure 1b). The %MPE in groups treated with vehicle only and L-DOPS at 100, 200, 400 mg kg^{-1} was:- 0.2 ± 2.1, 6.8 ± 2.7, 21.7 ± 2.5 and 28.8 ± 9.2, respectively.

In the kaolin-induced writhing test, L-DOPS (s.c.) at 200 mg kg^{-1} gradually reduced the number of writhing responses, antinociception reaching a maximum at 60 min and disappearing at 120 min (Figure 1c). L-DOPS, at a dose-

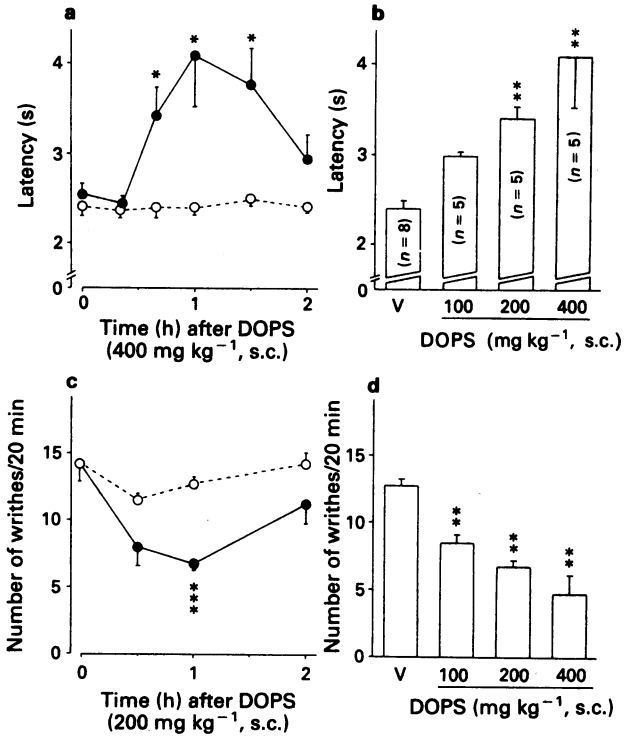

Figure 1 (a) Time-related antinociceptive effects of s.c. administration of L-DOPS (DOPS) in the tail-flick test in mice. (○) Vehicle ($n=8$); (●) DOPS (400 mg kg^{-1}; $n=5$). $^{*}P<0.05$ vs. vehicle. (b) Dose-related effects of s.c. DOPS in the tail-flick test. Data indicate latencies 60 min after s.c. injection. $^{**}P<0.01$ vs. vehicle (V). (c) Time-related antinociceptive effects of s.c. DOPS on the kaolin-induced writhing responses (writhes) in mice. (○) Vehicle; (●) DOPS (200 mg kg^{-1}). $^{***}P<0.001$ vs. vehicle. $n=4$. (d) Dose-related effects of s.c. DOPS in the kaolin-induced writhing test. Data indicate the number of writhing responses (writhes) induced by kaolin injected i.p. 60 min after DOPS (s.c.). $^{**}P<0.01$ vs. vehicle (V). $n=4$. Values in all panels are mean with s.e.mean.

range of 100–400 mg kg^{-1}, significantly suppressed writhing responses in a dose-dependent manner at 60 min after administration (Figure 1d).

In the formalin-induced nociceptive test, L-DOPS, administered s.c. at 100–200 mg kg^{-1}, also exhibited significant antinociceptive activity in the second, but not in the first phase, although an additional dose of L-DOPS (400 mg kg^{-1}) did not elicit further effects. The duration (s) of licking responses in the second phase was 178.1 ± 23.2 ($n = 9$), 125.6 ± 15.1 ($P < 0.05$; $n = 10$) and 103.5 ± 12.6 ($P < 0.05$; $n = 11$) in groups treated with vehicle only and L-DOPS at 100 and 200 mg kg^{-1}, respectively.

Antinociceptive activity of orally administered L-DOPS

As the ultimate aim is for clinical application, oral availability of L-DOPS as an antinociceptive was tested. L-DOPS, administered orally at 800 mg kg^{-1}, prolonged tail-flick latency, following a time pattern similar to that observed with s.c. administration (data not shown). At the peak time of 60 min, L-DOPS at 200–800 mg kg^{-1} exhibited significant antinociceptive activity in a dose-dependent manner (Figure 2).

Lack of naloxone-reversibility of L-DOPS-induced antinociception

In the tail flick test, naloxone, when administered s.c. at 1 mg kg^{-1}, failed to block the antinociception elicited by L-DOPS (400 mg kg^{-1}, s.c.). Δ Latencies (s) in groups treated with vehicle plus vehicle, vehicle plus naloxone, L-DOPS plus vehicle, and L-DOPS plus naloxone were 0.28 ± 0.09, 0.30 ± 0.07, 1.49 ± 0.19 ($P < 0.01$ vs. vehicle plus vehicle) and 1.21 ± 0.17, respectively (not significantly different from L-DOPS plus vehicle) ($n = 11$).

Effects of systemically and centrally administered benserazide on antinociception produced by L-DOPS

Tail-flick latency, prolonged by L-DOPS (400 mg kg^{-1}, s.c.) was not altered by benserazide preadministered i.p. at 1 mg kg^{-1} (1 h before L-DOPS) (Figure 3a). In contrast, benserazide, when preadministered i.c.v. at 25 μg per mouse (30 min before L-DOPS), markedly inhibited the antinociceptive effects of L-DOPS (Figure 3b).

Inhibition of L-DOPS-induced antinociception by i.c.v. and i.t. administration of the α-blocker, phentolamine

Phentolamine, injected i.c.v. at 1 μg per mouse, significantly suppressed antinociception elicited by L-DOPS (400 mg kg^{-1}, s.c.), although it did not modify the tail-flick latency when administered alone (Figure 4a). Similarly, i.t. injection of phentolamine at the same dose significantly reduced L-DOPS-induced antinociception, producing no effect by itself (Figure 4b).

Effects of the α_1-blocker prazosin and the α_2-blocker yohimbine (i.c.v. and i.t.) on the antinociceptive activity of L-DOPS

I.c.v. administration of prazosin at 1 μg per mouse abolished the antinociceptive activity elicited by L-DOPS (400 mg kg^{-1}, s.c.), while producing no effect when administered alone

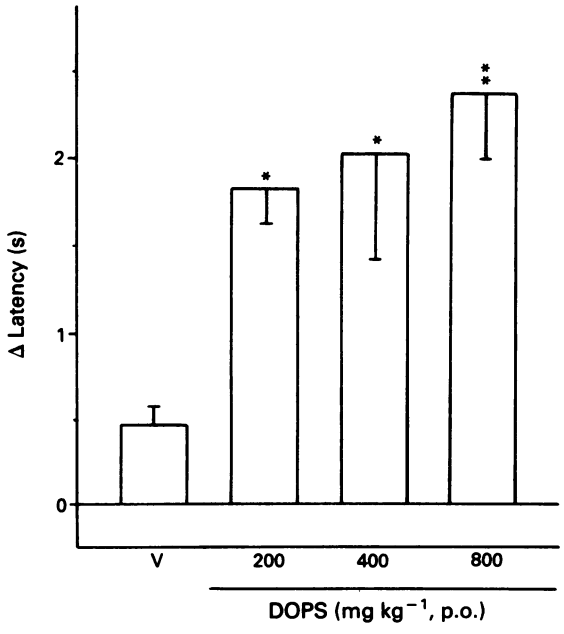

Figure 2 Antinociceptive activity of oral administration of L-DOPS (DOPS) in the tail-flick test in mice. Data indicate Δ latencies 60 min after oral administration of DOPS (200–800 mg kg^{-1}); values are mean with s.e.mean. *$P < 0.05$, **$P < 0.01$ vs. vehicle (V). $n = 6$.

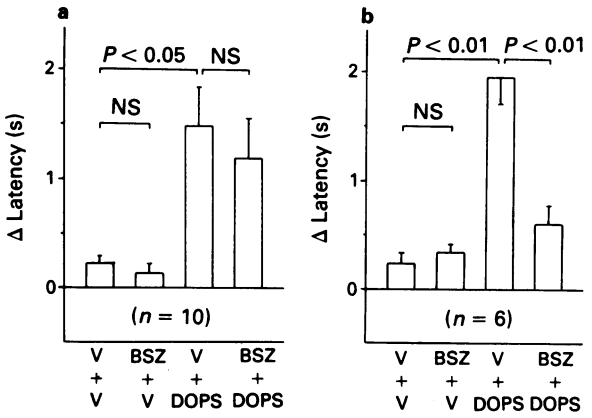

Figure 3 Effects of systemic (a) and central (i.c.v.) (b) administration of benserazide (BSZ) on antinociception produced by L-DOPS (DOPS) in the tail-flick test in mice. BSZ at 1 mg kg^{-1} and at 25 μg per mouse was administered s.c. 60 min before, and i.c.v. 30 min before DOPS (400 mg kg^{-1}, s.c.), respectively. Data indicate Δ latencies 60 min after DOPS; values are mean with s.e.mean. V, vehicle; NS, not significant.

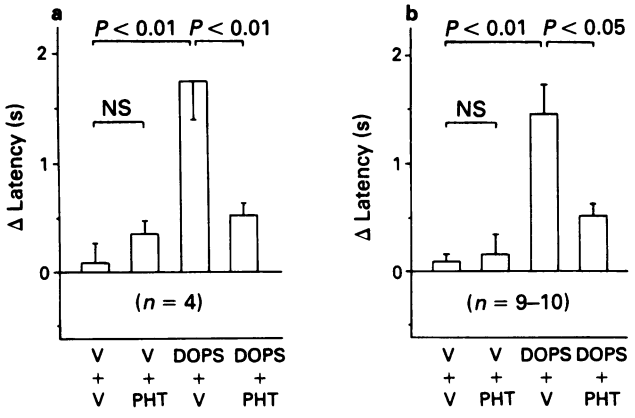

Figure 4 Inhibition by i.c.v. (a) and i.t. (b) phentolamine (PHT) of L-DOPS (DOPS)-induced antinociceptive activity in the tail-flick test in mice. PHT at 1 μg per mouse was administered i.c.v. or i.t. 40 min after s.c. administration of DOPS at 400 mg kg^{-1}. Data indicate Δ latencies 60 min after DOPS; values are mean with s.e.mean. v, vehicle; NS, not significant.

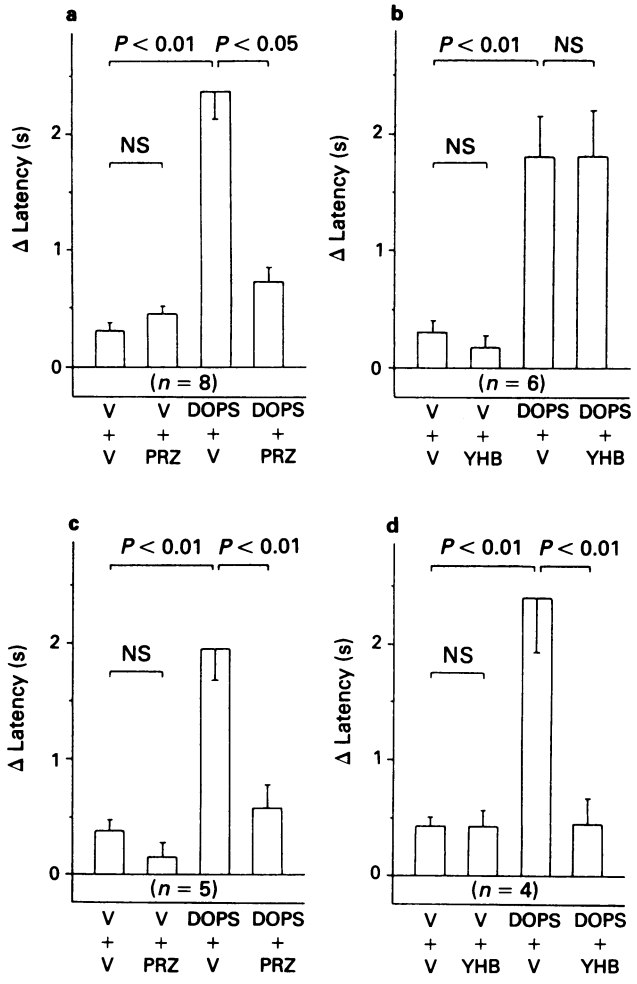

Figure 5 (a) and (b) Effects of i.c.v. prazosin (PRZ) (a) and i.c.v. yohimbine (YHB) (b) on antinociception produced by s.c. L-DOPS (DOPS) in the tail-flick test in mice. PRZ at 1 μg per mouse and YHB at 5 μg per mouse were administered i.c.v. 40 min after DOPS (400 mg kg^{-1}, s.c.). Data indicate Δ latencies 60 min after DOPS. V, vehicle; NS, not significant. (c) and (d) Inhibition of DOPS-induced antinociception by i.t. PRZ (c) and by i.t. YHB (d) in the tail-flick test in mice. PRZ and YHB at 1 μg per mouse were administered i.t. 40 min after DOPS (400 mg kg^{-1}, s.c.). Data indicate Δ latencies 60 min after DOPS. V, vehicle; NS, not significant. Values are mean with s.e.mean.

(Figure 5a). In contrast, i.c.v. administration of yohimbine, even at 5 μg per mouse, failed to block the antinociceptive effects of L-DOPS (Figure 5b).

Prazosin as well as yohimbine, when administered i.t. at 1 μg per mouse, effectively suppressed L-DOPS-induced antinociception, although both drugs by themselves were without effect (Figure 5c,d).

Discussion

The present study indicates that L-DOPS administered systemically produces opioid-independent antinociception in mouse via supraspinal α_1-adrenoceptors, and via spinal α_1- and α_2-adrenoceptors.

L-DOPS-induced antinociception was not blocked by systemically injected benserazide (1 mg kg^{-1}), a peripherally preferential L-aromatic amino acid decarboxylase inhibitor, but was suppressed by its i.c.v. injection (25 μg per mouse). This implies that this antinociceptive effect results from enzymatic conversion of L-DOPS into (−)-noradrenaline in the brain. In support of this finding, Karai *et al.* (1987) have reported that systemic benserazide at the same dose (1 mg kg^{-1}) inhibits L-DOPS-induced increase in levels of 3-methoxy-4-hydroxyphenylethyleneglycol (MHPG), a major metabolite of noradrenaline, in serum but not in brain, and that benserazide, when administered i.c.v. at the same dose (25 μg per mouse), effectively blocks the L-DOPS-induced increased brain MHPG level. Therefore, systemic administration of L-DOPS in combination with benserazide appears able to exhibit a centrally selective action by excluding its peripheral effects.

Both α_1- and α_2-adrenoceptors in the spinal cord are considered to be involved in the production of antinociception by systemic L-DOPS, since i.t. prazosin as well as i.t. yohimbine exhibited significant inhibitory effects. In general, major spinal adrenoceptors mediating antinociception are believed to be of the α_2-subtype, on the basis of reports that i.t. α_2-agonists have powerful antinociceptive properties and that i.t. α_2-antagonists antagonize antinociception produced by i.t. administered noradrenaline and by activation of the bulbospinal noradrenergic pathway (Yaksh & Reddy, 1981; Fleetwood-Walker *et al.*, 1985; Wigder & Wilcox, 1987; Wilcox *et al.*, 1987). However, Kuraishi *et al.* (1985) have found that i.t. prazosin in addition to i.t. yohimbine enhance substance P release in the spinal dorsal horn in response to peripheral mechano-nociceptive stimuli and inhibit the noradrenaline-mediated decrease in substance P release, suggesting a role for both α_1- and α_2-subtypes of adrenoceptors in spinal nociceptive modulation, in agreement with our present results. The discovery of more selective water-soluble α_1-and α_2-blockers, which are easily available, may dramatically clarify this discrepancy.

The finding that i.c.v. prazosin, but not i.c.v. yohimbine, inhibited antinociceptive activity revealed by systemic L-DOPS suggests involvement of supraspinal α_1-adrenoceptors. At present, the detailed mechanisms of nociceptive modulation by supraspinal noradrenergic systems are not well understood, both positive and negative properties of these systems having been reported (Hammond *et al.*, 1980; Behbehani *et al.*, 1981; Sagen & Proudfit, 1985; Heinricher *et al.*, 1988; Miller & Williams, 1989; Fields *et al.*, 1991). Both the α_1-antagonist, prazosin and the α_2-agonist, clonidine, when microinjected into the nucleus raphe magnus (NRM), produce antinociception in the tail-flick test in the rat, while both the α_1-agonist, phenylephrine, and the α_2-antagonist, yohimbine, administered into the same region, promote nociception, implying opposing roles of α_1- and α_2-adrenoceptors within the region of NRM (Sagen & Proudfit, 1985). At the single neurone level, opposing actions of noradrenaline and clonidine, applied iontophoretically into the rostral ventromedial medulla including NRM, have also been observed in anaesthetized rats (Heinricher *et al.*, 1988). In our preliminary experiments, however, phenylephrine, administered i.c.v. at 1–10 μg per mouse, produced dose-dependent antinociception, reversed by prazosin (1 μg per mouse; i.c.v.), and clonidine, administered i.c.v. at 1–3 μg per mouse, produced dose-dependent antinociception, reversed by yohimbine (1 μg per mouse; i.c.v.) (data not shown), thereby suggesting an antinociceptive role for both α_1- and α_2-receptors in the brain. Therefore, α_1-receptors existing in regions other than the NRM in the brain may contribute to the production of antinociception by systemically administered L-DOPS.

Noradrenaline precursors other than L-DOPS have also been demonstrated to exhibit antinociceptive activity. L-Tyrosine, a source of noradrenaline, when administered systemically or centrally, produces potent antinociception in the tail-flick test both in rats and in mice but this effect is mediated by central opioidergic systems and not by its conversion to noradrenaline (Ramarao & Bhargava, 1988; Kawabata *et al.*, 1993). Levodopa (L-DOPA) induces multiphasic opposing effects on nociception, i.e., it produces antinociception following an initial facilitation of nociception. The

antinociceptive effect of L-DOPA is mediated through postsynaptic D_2-receptors, although its hyperalgesic property appears to be related to activation of presynaptic inihibitory autoreceptors on dopamine neurones (Paalzow, 1992). Thus, the mechanism responsible for the antinociceptive effects of L-tyrosine and L-DOPA is clearly different from that for the effects of L-DOPS.

Hoel & Tjølsen (1993) have pointed out changes in skin temperature as a confounding factor in the tail-flick test and in the formalin test in rodents. Compounds exerting their effects via the monoaminergic systems have a profound influence on the cardiovascular system, which may decrease the temperature of the body. L-DOPS actually produces pressor responses and hypothermia in rats, although it does not significantly affect the body temperature in mice (Araki *et al.*, 1981; Nakamura *et al.*, 1987). Both the effects in rats are almost completely inhibited by systemic benserazide, thereby suggesting exclusive participation of peripheral mechanisms (Araki *et al.*, 1981; Nakamura *et al.*, 1987). That the antinociceptive effect of L-DOPS was not reduced by systemic benserazide in the present study, appears to deny the contribution of peripheral vasoconstrictor effects to the production of antinociception, if any, in the mouse. The antinociceptive activity of L-DOPS in the kaolin-induced writhing test may be additional evidence for specificity of the effect. It has been already demonstrated that L-DOPS does not produce side effects on motor functions and behaviour (Nakamura *et al.*, 1987).

That the maximal possible effect was not obtained for any doses of L-DOPS tested, does not necessarily annul the possibility of clinical application of L-DOPS. For instance, L-arginine, the antinociceptive effect of which is not so potent in animal experiments, produces dramatic analgesia in patients with chronic pain (Takagi *et al.*, 1990; Harima *et al.*, 1991; Kawabata *et al.*, 1992). In our preliminary clinical study in collaboration with Dr A Harima (Kyoto Nansei Hospital, Japan), L-DOPS actually elicited potent analgesia in patients with cluster headache and with various somatic pains, without producing any notable side effects (unpublished data). Additionally, that oral availability of L-DOPS was also demonstrated in this study, predicts its possible clinical usefulness as a novel type of analgesic.

We thank Sumitomo Pharmaceuticals Co. Ltd. for financial support. This paper is the fifth on 'Pain modulation by neuroactive amino acids.'

References

AKAIKE, A., SHIBATA, T., SATOH, M. & TAKAGI, H. (1978). Analgesia induced by microinjection of morphine into and electrical stimulation of the nucleus reticularis paragigantocellularis of rat medulla oblongata. *Neuropharmacology*, **17**, 775–778.

ARAKI, H., TANAKA, C., FUJIWARA, H., NAKAMURA, M. & OHMURA, I. (1981). Pressor effect of L-*threo*-3,4-dihydroxyphenylserine in rats. *J. Pharm. Pharmacol.*, **33**, 772–777.

BASBAUM, A.I. & FIELDS, H.L. (1984). Endogenous pain control systems: brainstem spinal pathways and endorphin circuitry. *Annu. Rev. Neurosci.*, **7**, 309–338.

BELCHER, G., RYALL, R.W. & SCHAFFNER, R. (1978). The differential effects of 5-hydroxytryptamine, noradrenaline and raphe stimulation on nociceptive and non-nociceptive dorsal horn interneurone in the cat. *Brain Res.*, **151**, 307–321.

BEHBEHANI, M.M., POMEROY, S.L. & MACK, C.E. (1981). Interaction between central gray and nucleus raphe magnus: role of norepinephrine. *Brain Res. Bull.*, **6**, 361–364.

CLARK, F.M. & PROUDFIT, H.K. (1991). The projection of noradrenergic neurons in the A7 catecholamine cell group to the spinal cord in the rat demonstrated by anterograde tracing combined with immunocytochemistry. *Brain Res.*, **547**, 279–288.

FIELDS, H.L., HEINRICHER, M.M. & MASON, P. (1991). Neurotransmitters in nociceptive circuits. *Annu. Rev. Neurosci.*, **14**, 219–245.

FLEETWOOD-WALKER, S.M., MITCHELL, R., HOPE, P.J., MOLONY, V. & IGGO, A. (1985). An alpha$_2$ receptor mediates the selective inhibition of noradrenaline of nociceptive responses of identified dorsal horn neurones. *Brain Res.*, **247** (Suppl.), 37–84.

FUJIYOSHI, T., DOZEN, M., IIDA, H., IKEDA, K., HAYASHI, I. & OH-ISHI, S. (1990). Demonstration of kinin-release in the peritoneal exudate of kaolin-induced writhing in mice. *Jpn. J. Pharmacol.*, **53**, 255–258.

FUJIYOSHI, T., HAYASHI, I., OH-ISHI, S., KUWASHIMA, M., IIDA, H., DOZEN, M., TANIGUCHI, N., IKEDA, K. & OHNISHI, H. (1989). Kaolin-induced writhing in mice, a new model of possible bradykinin-induced pain for assessment of analgesic agents. *Agents Actions*, **27**, 332–334.

HALEY, T.J. & MCCORMICK, W.G. (1957). Pharmacological effects produced by intracerebral injection of drugs in the conscious mouse. *Br. J. Pharmacol. Chemother.*, **12**, 12–15.

HAMMOND, D.L., LEVY, R.A. & PROUDFIT, H.K. (1980). Hypoalgesia following microinjection of noradrenergic antagonists in the nucleus raphe magnus. *Pain*, **9**, 85–101.

HARIMA, A., SHIMIZU, H. & TAKAGI, H. (1991). Analgesic effect of L-arginine in patients with persistent pain. *Eur. Neuropsychopharmacol.*, **1**, 529–533.

HEADLEY, P.M., DUGGAN, A.W. & GRIERSMITH, B.T. (1978). Selective reduction by noradrenaline and 5-hydroxytryptamine of nociceptive responses of cat dorsal neurons. *Brain Res.*, **145**, 185–189.

HEINRICHER, M.M., HAWS, C.M. & FIELDS, H.L. (1988). Opposing actions of norepinephrine and clonidine on single pain-modulating neurons in rostral ventromedial medulla. In *Proc. 5th World Congr. on Pain*, ed. Dubner, R. & Gebhart, G.F., pp. 509–594. Amsterdam: Elsevier.

HOLE, K. & TJØLSEN, A. (1993). The tail-flick and formalin tests in rodents: changes in skin temperature as a confounding factor. *Pain*, **53**, 247–254.

HYLDEN, J.K. & WILCOX, G.L. (1980). Intrathecal morphine in mice: a new technique. *Eur. J. Pharmacol.*, **67**, 313–316.

INAGAKI, C. & TANAKA, C. (1978). Characteristics of enzymic decarboxylation of L-threo-3,4-dihydroxyphenylserine using hog renal L-aromatic amino acid decarboxylase. *Biochem. Pharmacol.*, **27**, 1081–1086.

KARAI, N., KATO, T,. KATSUYAMA, M. & NAKAMURA, M. (1987). Effect of L-threo-3,4-dihydroxyphenylserine (L-threo-DOPS) on brain and serum MHPG levels in mice: evidence for NE formation in CNS. *Life Sci.*, **40**, 2261–2268.

KATO, T., KARAI, N., KATSUYAMA, M., NAKAMURA, M. & KATSUBE, J. (1987). Studies on the activity of L-threo-3,4-dihydroxyphenylserine (L-DOPS) as a catecholamine precursor in the brain. *Biochem. Pharmacol.*, **36**, 3051–3057.

KAWABATA, A., FUKUZUMI, Y., FUKUSHIMA, Y. & TAKAGI, H. (1992). Antinociceptive effect of L-arginine on the carrageenin-induced hyperalgesia of the rat: possible involvement of central opioidergic systems. *Eur. J. Pharmacol.*, **218**, 153–158.

KAWABATA, A., KASAMATSU, K. & TAKAGI, H. (1993). L-Tyrosine-induced antinociception in the mouse: involvement of central δ-opioid receptors and bulbo-spinal noradrenergic system. *Eur. J. Pharmacol.*, **233**, 255–260.

KURAISHI, Y., HIROTA, N., SATO, Y., KANEKO, S., SATOH, M. & TAKAGI, H. (1985). Noradrenergic inhibition of the release of substance P from the primary afferents in the rabbit spinal dorsal horn. *Brain Res.*, **359**, 177–182.

KURAISHI, Y., SATOH, M. & TAKAGI, H. (1987). The descending noradrenergic system and analgesia. In *Pain and Headache. Neurotransmitters and Pain Control.* Vol. 9, ed. Akil, H. & Lewis, J.W., pp. 101–128. Basel: Karger.

MILLAR, J. & WILLIAMS, G.V. (1989). Effects of iontophoresis of noradrenaline and stimulation of the periaqueductal gray on single-unit activity in the rat superficial dorsal horn. *J. Comp. Neurol.*, **287**, 119–133.

NAKAMURA, M., MIYAGISHI, A,. KOGA, Y., IRIE, T,. SAKURAMA, T,. KATO, T,. BABA, K., KUMASAKA, Y. & HARA, Y. (1987). General pharmacology of (−)-(2*S*,3*R*)-2-amino-3-hydroxy-3-(3,4-dihydroxyphenyl)propionic acid (L-threo-DOPS). *Pharmacometrics*, **33**, 243–261.

PAALZOW, G.H.M. (1992). L-Dopa induces opposing effects on pain in intact rats: (−)-sulpiride, SCH 23390 or α-methyl-DL-*p*-tyrosine methylester hydrochloride reveals profound hyperalgesia in large antinociceptive doses. *J. Pharmacol. Exp. Ther.*, **263**, 470–479.

RAMARAO, P. & BHARGAVA, H.N. (1988). Evidence for the involvement of central opioidergic systems in L-tyrosine methyl ester-induced analgesia in the rat. *Pharmacology*, **37**, 1–7.

SAGEN, J. & PROUDFIT, H.K. (1985). Evidence for pain modulation by pre- and postsynaptic noradrenergic receptors in the medulla oblongata. *Brain Res.*, **331**, 285–293.

SATOH, M., KAWAJIRI, S., UKAI, Y. & YAMAMOTO, M. (1979). Selective and non-selective inhibition by enkephalins and noradrenaline of nociceptive responses of lamina V type neurons in the spinal dorsal horn of the rabbit. *Brain Res.*, **177**, 384–387.

SEMBA, J. & TAKAHASHI, R. (1985). The effects of L-threo-dihydroxyphenylserine on norepinephrine metabolism in rat brain. *Psychiat. Res.*, **15**, 319–326.

SHIBATA, M. (1985). Pharmacological study of formalin-induced inflammatory pain response. *Jpn. J. Oral. Biol.*, **27**, 890–901.

TAKAGI, H. (1980). The nucleus reticularis paragigantocellularis as a site of analgesic action of morphine and enkephalin. *Trends Pharmacol. Sci.*, **1**, 182–184.

TAKAGI, H. (1982). Critical review of pain relieving procedures including acupuncture. In *Advances in Pharmacology and Therapeutics II.* Vol. 1, ed. Yoshida, H., Hagihara, Y. & Ebashi, S. pp. 79–92. New York: Pergamon Press.

TAKAGI, H., HARIMA, A. & SHIMIZU, H. (1990). A novel clinical treatment of persistent pain with L-arginine. *Eur. J. Pharmacol.*, **183**, 1443.

WIGDER, S. & WILCOX, G.L. (1987). Central and systemic morphine-induced antinociception in mice: contribution of descending serotonergic and noradrenergic pathways. *J. Pharmacol. Exp. Ther.*, **242**, 90–95.

WILCOX, G.L., CARLSSON, K.H., JOCHIM, A. & JURNA, I. (1987). Mutual potentiation of antinociceptive effects of morphine and clonidine on motor and sensory responses in rat spinal cord. *Brain Res.*, **405**, 84–93.

YAKSH, R.P. & REDDY, S.V. (1981). Studies in the primate on the analgesic effects associated with intrathecal actions of opiates, α-adrenergic agonists and baclofen. *Anesthesiology*, **54**, 451–467.

YEOMANS, D.C., CLARK, F.M., PAICE, J.A. & PROUDFIT, H.K. (1992). Antinociception induced by electrical stimulation of spinally projecting noradrenergic neurons in the A7 catecholamine cell group of the rat. *Pain*, **48**, 449–461.

(Received July 5, 1993
Revised October 8, 1993
Accepted October 18, 1993)

Br. J. Pharmacol. (1994), **111**, 509–514

Inhibition by fatty acids of cyclic AMP-dependent protein kinase activity in brush border membranes isolated from human placental vesicles

C.M. Doolan & [1]A.K. Keenan

Department of Pharmacology, University College Dublin, Belfield, Dublin 4, Ireland

1 The inhibitory effects of arachidonic acid (AA) and a number of structurally related fatty acids on cyclic AMP-dependent protein kinase activity have been investigated in brush border membranes (BBM) prepared from human placental vesicles.

2 BBM vesicles were characterized by electron microscopy and displayed enrichment of the appropriate marker enzymes, alkaline phosphatase and γ-glutamyltranspeptidase; BBM were prepared by vesicle lysis in hypotonic medium.

3 Cyclic AMP-dependent protein kinase (PKA) activity was measured in BBM. At 1 μM, cyclic AMP stimulated a 4.2 ± 0.06 fold increase over basal levels of [^{32}P]-phosphate incorporation into the synthetic substrate kemptide and this effect was abolished by a selective PKA inhibitor. By use of synergistic pairs of site-selective cyclic AMP analogues, the kinase was identified as the type II enzyme.

4 Cyclic AMP-stimulated PKA activity was inhibited by 10 μM AA and this effect was significantly enhanced by nordihydroguaiaretic acid (NDGA) + indomethacin (Indo), inhibitors of the lipoxygenase and cyclo-oxygenase pathways of AA metabolism respectively.

5 Oleic acid, elaidic acid, but not caprylic or palmitic acids, also significantly inhibited PKA activity and this effect was again enhanced by NDGA + Indo. While arachidonyl alcohol alone was not inhibitory, in the presence of the metabolic inhibitors a significant reduction in stimulated activity was observed.

6 The commercially available PKA type II holoenzyme (activated by cyclic AMP), but not the free catalytic subunit, was inhibitable by AA, oleic or elaidic acids.

7 These results suggest that PKA localized to the brush border membrane of human placental vesicles is inhibited by fatty acids which may compete with cyclic AMP for binding to the kinase regulatory subunit. The reported inhibition by fatty acids of cyclic AMP-dependent Cl^- secretion in epithelial cells may therefore be due in part to negative regulation of a Cl^- channel-associated PKA.

Keywords: Fatty acids; arachidonic acid; cyclic AMP-dependent protein kinase; human placenta; brush border membranes

Introduction

The regulation of chloride (Cl^-) secretion by epithelial cells is an important process in fluid and electrolyte homeostasis. Transepithelial Cl^- movement in secretory epithelia involves entry via the $Na^+/K^+/Cl^-$ cotransporter at the basolateral membrane and exit through Cl^- channels in the apical (brush border) membrane. These channels are regulated *inter alia* by adenosine 3':5'-cyclic monophosphate (cyclic AMP)-dependent protein kinase (PKA), protein kinase C, and calcium/calmodulin-dependent protein kinase (Welsh, 1990; Wagner *et al.*, 1991). Arachidonic acid (AA) and other unsaturated fatty acids have also been shown to regulate Cl^- channels and to inhibit the outwardly rectifying Cl^- channel in airway epithelia (Hwang *et al.*, 1990). The nature of this inhibition is unclear and it has been proposed that fatty acids interact with the channel or an associated protein to alter its function (Anderson & Welsh, 1990). In this study we provide evidence that PKA, localized to the brush border membrane of human placental vesicles, may constitute a target for the negative regulation of Cl^- channels by unsaturated fatty acids. We used brush border membranes prepared from placental vesicles, as opposed to whole cells, in our studies since we wished as far as possible to investigate direct effects of fatty acids on membrane PKA activity, free of regulation by intracellular second messenger systems, or by events occurring at the basolateral membrane. Human placental brush border membrane vesicles have previously been shown to exhibit a Cl^- conductance (Dechecchi & Cabrini, 1988; Illsley *et al.*, 1988) which is inhibitable by AA (Faller & Ryan, 1992).

[1] Author for correspondence.

Methods

Preparation of brush border membrane vesicles

Term human placental tissue was obtained within 30 min of delivery and transported to the laboratory in a solution comprising equal volumes of Dulbecco's Modified Eagle's Medium (DMEM) and phosphate buffered saline (PBS, pH 7.4) at 4°C. Brush border membrane vesicles (BBMV) were prepared as described by Faller & Ryan (1992): the central portion between the maternal and foetal surfaces of the placenta was used, following removal of the maternal decidua. The maternal villous tissue was chopped into small pieces, washed in Buffer A (300 mM mannitol, 10 mM HEPES/Tris HCl, pH 7.0), further finely chopped and agitated in 300 ml Buffer A with a magnetic stirrer for 1 h at 4°C. Following removal of solid tissue by filtration through gauze, the filtrate was centrifuged at 1,000 *g* for 10 min, and the resulting supernatant recentrifuged at 86,000 *g* for 35 min. The pellet obtained was homogenized in 50 ml ice-cold Buffer A in a Dounce homogenizer and the resulting homogenate made 10 mM with respect to $MgCl_2$, stirred for 15 min at 4°C and allowed to stand for a further 15 min. The homogenate was then centrifuged at 5,000 *g* for 15 min and

the resulting supernatant recentrifuged at 86,000 *g* for 35 min. Pellets were resuspended in Buffer A and aliquots snap frozen before storage in liquid nitrogen until required.

Characterization of BBMV

Electron microscopy of BBMV was carried out on samples fixed in phosphate buffer (pH 7.4) containing 2.5% glutaraldehyde, and post fixed in osmium tetroxide. Transmission electron micrographs were produced with a Philips 201 electron microscope. Scanning electron micrographs were produced with a JEOL JEM-200FX electron microscope.

Alkaline phosphatase (EC 3.1.3.1) activity was compared in placental homogenate and BBMV by the methods of Lansing *et al.* (1967). The enzyme substrate used was *p*-nitrophenylphosphate. The amount of *p*-nitrophenol produced was quantified by its absorption at 420 nm and was taken as an index of alkaline phosphatase activity, expressed as μmol *p*-nitrophenol formed mg^{-1} protein min^{-1}.

γ-Glutamyltranspeptidase (EC 2.3.2.2) activity was also measured in homogenate and BBMV, according to Szasz (1969). The enzyme substrate was γ-glutamyl *p*-nitroanilide. The amount of *p*-nitroaniline produced by hydrolysis was quantified by its absorption at 405 nm and was taken as an index of γGT activity, expressed as international units of enzyme activity mg^{-1} protein min^{-1}.

Manipulation of BBMV for measurement of kinase activity

To ensure access of impermeant molecules to their intracellular targets, vesicles were resuspended in 75 mM phosphate buffer, pH 7.0, a procedure calculated to lyse the vesicles osmotically (Placchi *et al.*, 1991). The altered morphology of the resulting brush border membranes (BBM) was confirmed in a number of preparations by transmission electron microscopy.

Measurement of cyclic AMP-dependent protein kinase (PKA) activity

PKA (EC 2.7.1.37) activity was measured by an assay based on the transfer of the terminal phosphate of γ[^{32}P]-ATP to the synthetic substrate kemptide (Giembycz & Diamond, 1990). Assays were carried out at 30°C in a final volume of 100 μl incubation mixture containing 60 μg protein, 'assay cocktail' (0.1 mM EGTA, 40 mM NaF, 1 mM dithiothreitol, 1 mM theophylline, 5 mM sodium arsenate), 10 μg kemptide, stimulators/inhibitors as appropriate, in 75 mM phosphate, pH 7.0. Following a 10 min preincubation period, the reaction was initiated by addition of 2 mM magnesium acetate + 1 mM γ[^{32}P]-ATP ($1-2 \times 10^7$ c.p.m. $mmol^{-1}$). Assays were stopped after 20 min and processed by a modification of the method of Witt & Roskoski (1975): assay mixture was spotted onto P81 phosphocellulose ion exchange chromatography filter papers which were allowed to dry for 30 s and placed in a 75 mM phosphoric acid solution (10 ml/filter). Filters were then washed 3 × 10 min in acid, 1 × 5 min in methanol and ether. Incorporated radioactivity was determined by scintillation counting. Activities were expressed as pmol phosphate transferred mg^{-1} protein min^{-1}.

Use of synergistic pairs of site selective cyclic AMP analogues

The two major isozymes of cyclic AMP-dependent protein kinase (PKA), type I and type II, are distinguished in terms of their regulatory subunits which provide the basis for isozyme classification (Lohmann & Walter, 1984). Each regulatory subunit in turn contains two different intrasubunit cyclic AMP binding sites, sites 1 and 2, which selectively bind certain cyclic AMP analogues (Beebe *et al.*, 1988). Binding of a cyclic nucleotide at one site stimulates binding at the other site. When two cyclic AMP analogues, each selective for a different binding site, are added in combination to PKA, the enzyme is activated in a synergistic fashion. Since the cyclic AMP analogue specificity of site 1 is different for the two isozymes, the synergistic activation of type I and II isozymes may be distinguished. We used the method of Beebe *et al.* (1988) to identify the subtype of PKA present in BBM. Assay mixtures contained 60 μg BBM protein. The type I synergistic pair comprised 1.2 μM (8-(6-aminohexyl)aminoadenosine 3':5'-cyclic monophosphate (8AHA) and 10 nM N6 benzoyladenosine 3':5'-cyclic monophosphate (N6BZL). The type II pair comprised 7 nM 8-thiomethyladenosine 3':5'-cyclic monophosphate (8-S-CH3) and 10 nM N6 benzoyladenosine 3':5'-cyclic monophosphate. The assay conditions were identical to those described above for measurement of PKA activity.

Calculations: the basal activity ratio (activity in the absence, divided by activity in the presence of 1 μM cyclic AMP) was determined and this value was subtracted from the analogue-stimulated activity ratio. Results were expressed as the increment in activity ratio produced by the analogue.

Protein determination

This was carried out according to Lowry *et al.* (1951).

Statistical analysis

Measurements of PKA activities are presented as mean values ± s.e.mean of *n* experiments each performed in triplicate. Statistically significant differences where appropriate were determined by an unpaired Student's *t* test and differences were deemed significant if $P<0.05$.

Materials

γ[^{32}P]-ATP (> 10 Ci $mmol^{-1}$) was purchased from Amersham (U.K.). Kemptide, PKA type II inhibitor from bovine heart, 3':5'-cyclic AMP-dependent protein kinase from bovine heart, protein kinase catalytic subunit from bovine heart, 8-(6-aminohexyl)aminoadenosine 3':5'-cyclic monophosphate, N6-benzoyladenosine 3':5'-cyclic monophosphate, 8-thiomethyladenosine 3':5'-cyclic monophosphate, arachidonic, oleic, elaidic, palmitic and caprylic acids, and arachidonyl alcohol were all obtained from Sigma. P81 filter paper was obtained from Whatman. All other chemicals were of the highest purity commercially available.

Fatty acids and arachidonyl alcohol were dissolved in ethanol and stored in the dark in aliquots, under an atmosphere of nitrogen at − 20°C until required. The final concentration of ethanol in all assays was less than or equal to 0.1% at which concentration ethanol was without effect on PKA activity.

Results

Characterization of brush border membrane vesicles

Alkaline phosphatase and γ-glutamyl transpeptidase are two enzymes localized to the brush border membranes of epithelial cells. When activities of these enzymes were compared in placental homogenates and in BBMV, alkaline phosphatase and γ-glutamyl transpeptidase were enriched in BBMV by factors of 25 ± 4.6 and 30.5 ± 7.8 respectively ($n = 4$ in each case). Transmission and scanning electron micrographs showed the vesicles to be spherical, intact and to have the brush border directed outwards. When vesicles were subjected to hypotonic lysis, the characteristic spherical shape was lost and open fragmented structures indicative of membranes became apparent.

Identification of the type of kinase present in BBM

The presence of PKA activity in BBM was first established. Basal activity was stimulated 4.2 ± 0.06 fold ($n = 4$) by 1 μM cyclic AMP. This stimulation was abolished by the cyclic AMP-dependent protein kinase inhibitor (Walsh inhibitor) PKI (5 μg ml^{-1}) as shown in Figure 1. PKI (a 75 amino acid protein isolated from rabbit skeletal muscle) inactivates the catalytic subunit of the kinase by binding to its protein-substrate site and has been reported to exhibit an extremely high degree of specificity for PKA (Walsh & Glass, 1991). An additional characteristic of PKA is its susceptibility to inhibition by Ca^{2+} and in BBM, stimulated PKA activity was reduced in the presence of 2 mM $CaCl_2$ (Figure 1). We next examined the effects of synergistic pairs of site-selective cyclic AMP analogues on PKA activity and the results obtained are summarized in Figure 2 for the type II directed analogue pair (N6BZL + 8-S-CH3). As can be seen, the increments in activity ratio for N6ZBL and 8-S-CH3 were 0.03 and 0.13 respectively. An additive effect of these analogues would therefore have yielded a ratio of 0.16. However the change in activity ratio observed was 0.58, yielding a synergism quotient (ratio between observed and expected responses) of 3.6. No synergism was observed with the type I-directed pair (N6BZL + 8AHA, data not shown). Thus since the enzyme was synergistically activated by the type II-directed analogue pair only, it is likely to be type II.

Effect of arachidonic acid on cyclic AMP-dependent protein kinase activity

Cyclic AMP-stimulated PKA activity was inhibited by 10 μM arachidonic acid (AA; 20:4, *cis*-5,8,11,14) and this inhibition was significantly enhanced in the presence of a combination of nordihydroguaiaretic acid (NDGA) and indomethacin (Indo) (both 5 μM), which are inhibitors of the lipoxygenase and cyclo-oxygenase pathways of AA metabolism respectively. NDGA + Indo alone did not inhibit cyclic AMP-stimulated PKA activity (results summarized in Figure 3). The enhanced effect in the presence of these inhibitors would suggest that the relevant enzymes are present in BBM (particulate fractions isolated from human placental villous tissue have recently been shown to possess lipoxygenase activity, see Joseph *et al.*, 1993). In separate experiments, no reduction of cyclic AMP stimulated activity was seen with the AA metabolites prostaglandin E_2 (PGE_2), $PGF_{2\alpha}$, 5-HPETE (each at 10 μM) or leukotriene C_4 (24 μM) (data not shown).

Effects of analogues on stimulated PKA activity

Both oleic acid (18:1, *cis*-9) and its *trans* isomer, elaidic acid (18:1, *trans*-9), each at a concentration of 10 μM, significantly inhibited PKA activity in BBM and as with AA, the inhibitory effects of these analogues were enhanced in the presence of NDGA + Indo (see Figure 4). In contrast however, the saturated fatty acids palmitic acid (16:0) and caprylic acid (8:0), did not affect cyclic AMP-stimulated PKA activity at this concentration in the presence or absence of inhibitors and while arachidonyl alcohol alone (10 μM)

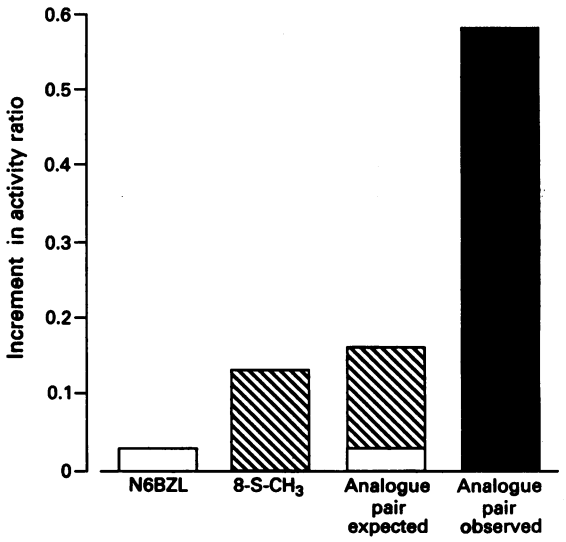

Figure 2 Synergism of cyclic AMP-dependent protein kinase activation in brush border membranes using a type II directed analogue pair. Membranes were incubated with 10 nM N^6-benzoyl-cyclic AMP (N6BZL, open columns), 7 nM 8-thiomethyl-cyclic AMP (8-S-CH3, hatched columns) or a combination of both (solid columns). The basal activity ratio determined in the absence and presence of 1 μM cyclic AMP was 0.08 and was subtracted from all other values. Results are expressed as the increment in activity ratio.

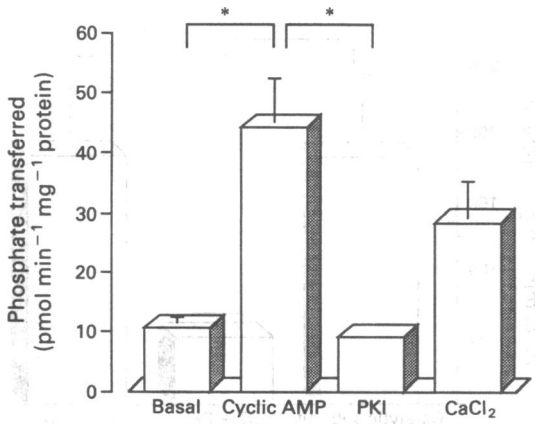

Figure 1 PKA activity in brush border membranes and its stimulation by cyclic AMP (1 μM) alone and in the presence of PKI (5 μg ml^{-1}) or $CaCl_2$ (2 mM). Data represent the mean ± s.e.mean of 4 experiments performed in triplicate. Results are expressed as phosphate transferred (pmol min^{-1} mg^{-1} protein). Asterisks indicate significant differences between values linked by horizontal bars. *$P < 0.05$.

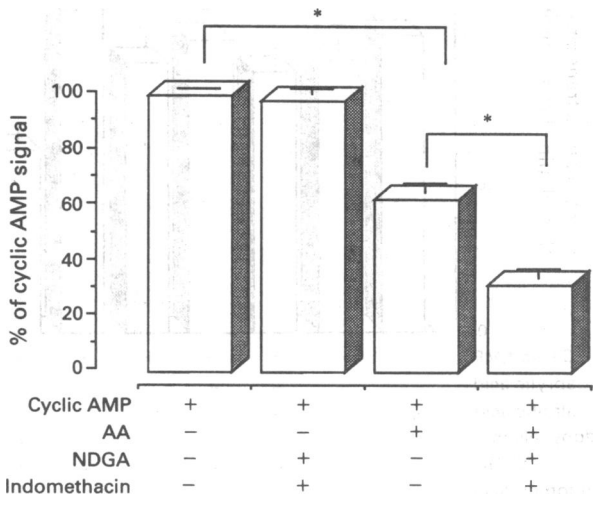

Figure 3 Effects of arachidonic acid (AA, 10 μM) on cyclic AMP stimulated PKA activity in brush border membranes in the absence and presence of inhibitors of AA metabolism (NDGA, indomethacin, 5 μM). Data represent the mean ± s.e.mean of 3 experiments each performed in triplicate. Results are expressed as % of cyclic AMP signal. Asterisks indicate significant differences between values linked by horizontal bars: *$P < 0.005$.

was also without effect, in the presence of NDGA + Indo significant reduction of stimulated activity was observed (Figure 5).

Effects of fatty acids on cyclic AMP-stimulated holoenzyme

With the objective of identifying the site(s) at which AA-mediated inhibition of PKA had occurred, inhibitory effects on stimulated activity of the commercially available type II holoenzyme were investigated. As can be seen in Figure 6, AA, oleic and elaidic acids again significantly lowered the cyclic AMP signal, while the saturated fatty acids palmitic and caprylic acid were again without effect. In these experiments 'basal' activity of the holoenzyme was rather high and PKI reduced the cyclic AMP signal to below 'basal' levels. This probably reflected some contamination of the holoenzyme by free catalytic subunit (CS), the activity of which would be independent of cyclic AMP, yet inhibitable by PKI.

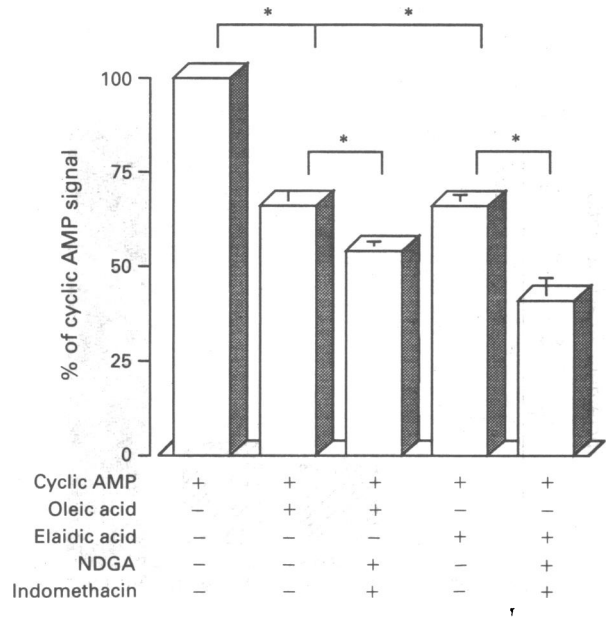

Figure 4 Effects of oleic and elaidic acids (10 μM) on cyclic AMP stimulated PKA activity in brush border membranes in the absence and presence of inhibitors of fatty acid metabolism (NDGA, indomethacin, 5 μM). Data are expressed as the mean ± s.e.mean of 3 experiments performed in triplicate. Results are expressed as % of cyclic AMP signal. Asterisks indicate significant differences between values linked by horizontal bars: $*P<0.05$.

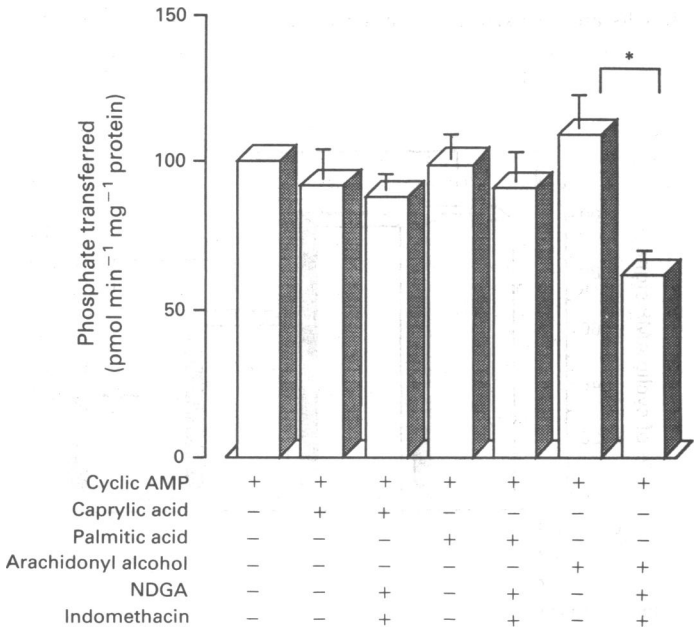

Figure 5 Effects of caprylic and palmitic acids and arachidonyl alcohol (10 μM) both in the presence and absence of inhibitors of fatty acid metabolism (NDGA, indomethacin, 5 μM). Data represent the mean ± s.e.mean of 3 experiments performed in triplicate. Results are expressed as phosphate transferred (pmol min^{-1} mg^{-1} protein). Asterisks indicate significant differences between values linked by horizontal bars: $*P<0.025$.

Effect of AA on activity of the PKA catalytic subunit

Activity of the free catalytic subunit was significantly reduced by PKI, whereas AA at a concentration of 10 μM was without effect (Figure 7).

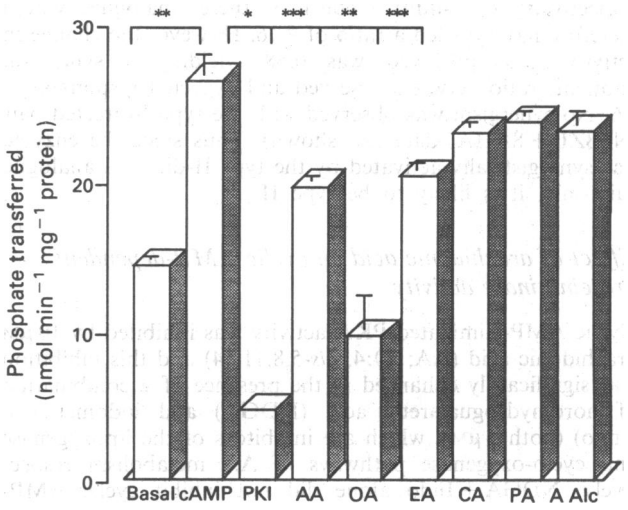

Figure 6 Effects of various fatty acids (10 μM) on cyclic AMP-stimulated activity of the PKA holoenzyme. Cyclic AMP (cAMP, 1 μM) was present in all cases except where basal activity was measured. Abbreviations: arachidonic acid (AA), oleic acid (OA), elaidic acid (EA), palmitic acid (PA), caprylic acid (CA) and arachidonyl alcohol (A Alc). Data represent the mean ± s.e.mean of 3 experiments performed in triplicate. Results are expressed as phosphate transferred (nmol min^{-1} mg^{-1} protein). Asterisks indicate significant differences between values linked by horizontal bars: $*P<0.0005$; $**P<0.005$ and $***P<0.01$.

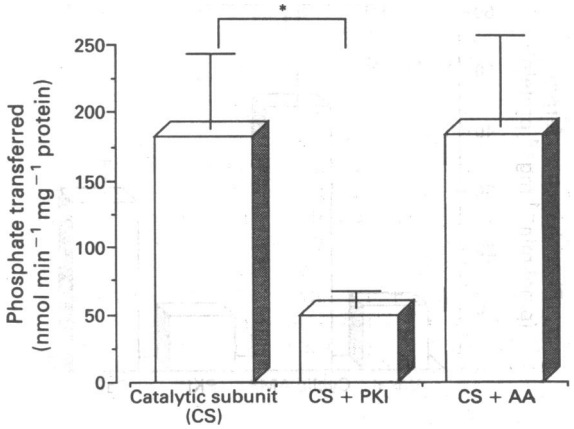

Figure 7 Effects of PKI (5 μg ml^{-1}) and arachidonic acid (AA, 10 μM) on the activity of the PKA catalytic subunit type II from bovine heart. Data represent the mean ± s.e.mean of 3 experiments performed in triplicate. Results are expressed as phosphate transferred (nmol min^{-1} mg^{-1} protein). Asterisks indicate significant differences between values linked by horizontal bars: $*P<0.05$.

Discussion

This study demonstrates for the first time, the inhibition of cyclic AMP-dependent protein kinase activity in human placental brush border membranes by unsaturated fatty acids. Though PKA-regulated Cl^- channel activity has been investigated in a number of such membrane systems there is not general agreement on whether the enzyme is membrane-associated in the vesicle preparation. Thus, while PKA was found to be associated with rabbit and canine cortical renal brush-border vesicles (Hammerman & Hruska, 1982; Weinmann *et al.*, 1987), it was necessary to add exogenous PKA to mouse renal medullary membranes (Reeves *et al.*, 1989) and to a human placental vesicle preparation used to investigate regulation of Cl^- transport (Placchi *et al.*, 1991). While the variability in expression of a membrane-associated kinase may simply reflect differences in the methods of vesicle preparation, it may also be due to the presence of different PKA isozymes in the various tissues. It has been proposed that types I and II are predominantly cytosolic and membrane-bound respectively (Lohmann & Walter, 1984) and therefore if a particular cell type expressed only the soluble type I enzyme, this would not be retained in the vesicle preparation unless activation/translocation had occurred during vesicle isolation. Since the kinase identified in the present study (using synergistic pairs of site-selective cyclic AMP analogues) appears to be type II, its membrane localization is to be expected. We would further propose that the enzyme is localized to the cytosolic surface of BBMV prior to lysis since there is evidence for the existence of proteinases on the outer surface of BBMV, which selectively degrade cyclic AMP-stimulated ectokinases in the course of vesicle isolation (De Jonge *et al.*, 1987).

AA inhibited PKA activity in our system at a concentration (10 μM) previously shown to inhibit Cl^- channel activity in airway epithelial cells (Anderson & Welsh, 1990; Hwang *et al.*, 1990; Faller & Ryan, 1992). A direct role for AA in PKA inhibition is supported by (i) the enhanced effect observed in the presence of inhibitors of metabolism by the lipoxygenase and cyclo-oxygenase pathways (Indo + NDGA) and (ii) by the lack of inhibition in the presence of the AA metabolites PGE_2, $PGF_{2\alpha}$, leukotriene C_4 or 5-HPETE. Indeed AA has been reported to have stimulatory effects on Cl^- secretion via the production of metabolites capable of increasing cyclic AMP levels (Eling *et al.*, 1986). Furthermore in a study using dog tracheal epithelium, an AA-mediated increase in Cl^- secretion was converted to a reduction of secretion by the addition of inhibitors of AA metabolism (Mochizuki *et al.*, 1992). Direct stimulation by AA of epithelial Cl^- secretion has however also been reported recently in the T84 colonic epithelial cell line (Barrett & Bigby, 1993). These authors have suggested that AA may be stimulating Cl^- secretion via channels with conducting properties particular to intestinal epithelia.

To determine whether the inhibition of PKA activity in BBM was specific to AA, the effects of a number of structurally related analogues were examined. The lack of effect of caprylic and palmitic acids observed would agree with the specificity of Cl^- channel inhibition by fatty acids previously documented (Anderson & Welsh, 1990; Hwang *et al.*, 1990; Faller & Ryan, 1992), as would the inhibition obtained with oleic acid. However, in contrast to the findings of Faller & Ryan (1992), we obtained significant inhibition in our system with elaidic acid and with arachidonyl alcohol in the presence of NDGA + Indo. (The latter effect may be due to conversion of the alcohol to a substrate otherwise rapidly metabolized by cyclo-oxygenase or lipoxygenase.)

From our overall results it could be argued that the inhibition of PKA activity by fatty acids in this system is relatively non-specific and that the minimum structural requirement is a monounsaturated 18-carbon chain compound. We would propose an alternative model, namely one whereby all of the 'active' analogues may be converted to AA or a similar polyunsaturated acid by a series of metabolic transformations involving desaturases. These enzymes are known to catalyse the production of polyunsaturated fatty acids from oleic acid (Gurr & James, 1980). Additional evidence for a common fatty acid mediator of PKA inhibition is suggested by the enhanced effect of all unsaturated compounds tested in the presence of NDGA + Indo, despite the fact that oleic and elaidic acids are not substrates for cyclo-oxygenase or lipoxygenase enzymes. In this model therefore, inhibitory activity would not be dependent on an all *cis*-unsaturated structure (elaidic acid was inhibitory) and so a general membrane lipid-altering effect characteristic of *cis*-unsaturated fatty acids (Klausner *et al.*, 1980) would be unlikely to account for the inhibition of PKA.

Fatty acid inhibition of PKA activity may involve binding to the regulatory subunit of the enzyme, since the commercially available PKA type II holoenzyme, but not the free catalytic unit, was inhibitable by unsaturated fatty acids under our assay conditions. It may be therefore that fatty acids act as negative regulators of cyclic AMP binding to the regulatory subunit of PKA.

The ability of unsaturated fatty acids to inhibit specifically a protein kinase has recently been reported in a prokaryotic system (Strauch *et al.*, 1992). These authors demonstrated an inhibition of the prokaryotic kinase Kin A *in vitro* by the *cis*-unsaturated linoleic, arachidonic and oleic acids. No inhibition of kinase activity by the saturated caprylic and palmitic acids was observed. However in contrast to our results, Strauch *et al.* (1992) reported that the *trans*-unsaturated fatty acid elaidic acid did not inhibit kinase activity.

The possibility of a physiological or pathophysiological role for AA or a related substance, in modulation of epithelial Cl^- secretion, has long been a matter for speculation. It has recently been demonstrated that cytosolic extracts purified from Cl^- secreting epithelial cells block outwardly rectifying Cl^- channels and although the exact nature of the inhibitor is unknown, the presence of fatty acids in these extracts has been suggested (Kunzelmann *et al.*, 1991). These authors have also speculated that in cystic fibrosis (CF), where epithelial cyclic AMP-regulated Cl^- transport is defective, elevated concentrations of this inhibitor may be present. Elevations in bradykinin-stimulated AA release have recently been reported in a CF epithelial cell line expressing the major deltaF508 mutation (Levistre *et al.*, 1993), though in this case it is not thought that the increases in AA produced are responsible for impaired regulation of Cl^- transport. Firm evidence has yet to be produced therefore, for a pathophysiological role for altered AA production in modulation of epithelial Cl^- transport.

In summary, this study has shown that a cyclic AMP-dependent protein kinase localized to the brush border membrane of human placental vesicles is subject to negative regulation by fatty acids with a selectivity comparable to that for Cl^- channel inhibition. We propose that the latter inhibition is mediated at least in part indirectly, via binding of fatty acids to the regulatory subunit of PKA which could then interact with a Cl^- channel.

This work was supported by the Cystic Fibrosis Association of Ireland and EOLAS, the Irish Science and Technology Agency. We also wish to thank Ms Colette O'Beirne for secretarial assistance and Mr C. O'Connell for technical assistance in preparation of the electron micrographs.

References

ANDERSON, M.P. & WELSH, M.J. (1990). Fatty acids inhibit apical membrane chloride channels in airway epithelia. *Proc. Natl. Acad. Sci. U.S.A.*, **87**, 7334–7338.

BARRETT, K.E. & BIGBY, T.D. (1993). Involvement of arachidonic acid in the chloride secretory response of intestinal epithelial cells. *Am. J. Physiol.*, **264**, C446–C452.

BEEBE, S.J., BLACKMORE, P.F., CHRISMAN, T.D. & CORBIN, J.D. (1988). Use of synergistic pairs of site-selective cAMP analogs in intact cells. *Methods Enzymol.*, **159**, 118–139.

DECHECCHI, M.C. & CABRINI, G. (1988). Chloride conductance in membrane vesicles from human placenta using a fluorescent probe. Implications for cystic fibrosis. *Biochim. Biophys. Acta*, **945**, 113–120.

DE JONGE, H., SCHMEEDA, H. & SHALTIEL, S. (1987). Orientation of the brush-border membranal protease which specifically splits the catalytic subunit of cAMP-dependent protein kinase. *Eur. J. Biochem.*, **169**, 503–509.

ELING, T.E., DANILOWICZ, R.M., HENKE, D.C., SIVARAJAH, K., YANKASKAS, J.R. & BOUCHER, R.C. (1986). Arachidonic acid metabolism by canine tracheal epithelial cells. Product formation and relationship to chloride secretion. *J. Biol. Chem.*, **261**, 12841–12849.

FALLER, D. & RYAN, M.P. (1992). Factors affecting chloride conductance in apical membrane vesicles from human placenta. *J. Memb. Biol.*, **130**, 227–239.

GIEMBYCZ, M.A. & DIAMOND, J. (1990). Evaluation of kemptide, a synthetic serine-containing heptapeptide, as a phosphate acceptor for the estimation of cyclic AMP-dependent protein kinase activity in respiratory tissues. *Biochem. Pharmacol.*, **39**, 271–283.

GURR, M.I. & JAMES, A.T. (1980). Fatty acids. In *Lipid Biochemistry: an Introduction*. ed. Gurr, M.I. & James, A.T. pp. 18–89. London: Chapman & Hall.

HAMMERMAN, M.R. & HRUSKA, K.A. (1982). Cyclic AMP-dependent protein phosphorylation in canine renal brush-border membrane vesicles is associated with decreased phosphate transport. *J. Biol. Chem.*, **257**, 992–999.

HWANG, T.-C., GUGGINO, S.E. & GUGGINO, W.B. (1990). Direct modulation of secretory chloride channels by arachidonic and other cis unsaturated fatty acids. *Proc. Natl. Acad. Sci. U.S.A.*, **87**, 5706–5709.

ILLSLEY, N.P., GLAUBENSKLEE, C., DAVIS, B. & VERKMAN, A.S. (1988). Chloride transport across placental microvillous membranes measured by fluorescence. *Am. J. Physiol.*, **255**, C789–C797.

JOSEPH, P., SRINIVASAN, N. & KULKARNI, A.P. (1993). Purification and partial characterisation of lipoxygenase with dual catalytic activities from human term placenta. *Biochem. J.*, **293**, 83–91.

KLAUSNER, R.D., KLEINFELD, A.M., HOOVER, R.L. & KARNOVSKY, M.J. (1980). Lipid domains in membranes: evidence derived from structural perturbations induced by free fatty acids and lifetime heterogeneity analysis. *J. Biol. Chem.*, **255**, 1286–1295.

KUNZELMANN, K., TILMANN, M., HANSEN, CH.P. & GREGER, R. (1991). Inhibition of epithelial chloride channels by cytosol. *Pflügers Arch.*, **418**, 479–490.

LANSING, A.I., BELKHOSE, A.I., LYNCH, M.L. & LIEBERMAN, I. (1967). Enzymes of plasma membrane of liver. *J. Biol. Chem.*, **242**, 1722–1776.

LEVISTRE, R., LEMNAOUAR, M., RYBKINE, T., BEREZIAT, G. & MASLIAH, J. (1993). Increase of bradykinin-stimulated arachidonic acid release in a deltaF508 cystic fibrosis epithelial cell line. *Biochim. Biophys. Acta*, **1181**, 233–239.

LOHMANN, S. & WALTER, U. (1984). Regulation of the cellular and subcellular concentrations and distribution of cyclic nucleotide-dependent protein kinases. *Adv. Cyclic Nucleotide Protein Phosphorylation Res.*, **18**, 63–117.

LOWRY, O.H., ROSEBROUGH, N.J., FARR, A.L. & RANDALL, R.J. (1951). Protein measurement with Folin phenol reagent. *J. Biol. Chem.*, **193**, 265–275.

MOCHIZUKI, H., CHAO, A.C. & WIDDICOMBE, J.H. (1992). Arachidonic acid inhibits Cl secretion in cultures of dog tracheal epithelium. *Life Sci.*, **50**, 1129–1135.

PLACCHI, P., LOMBARDO, R., TAMANINI, A., BRUSA, P., BERTON, G. & CABRINI, G. (1991). cAMP-dependent protein kinase inhibits the chloride conductance in apical membrane vesicles of human placenta. *J. Memb. Biol.*, **119**, 25–32.

REEVES, W.B., MCDONALD, G.A., MEHTA, P. & ANDREOLI, T.E. (1989). Activation of K^+ channels in renal medullary vesicles by cAMP-dependent protein kinase. *J. Memb. Biol.*, **109**, 65–72.

STRAUCH, M.A., DE MENDOZA, D. & HOCH, J.A. (1992). cis-Unsaturated fatty acids specifically inhibit a signal-transducing protein kinase required for initiation of sporulation in *Bacillus subtilis*. *Mol. Microbiol.*, **6**, 2909–2917.

SZASZ, G. (1969). A kinetic photometric mode for serum gamma-glutamyltranspeptidase. *Clin. Chem.*, **15**, 124–136.

WAGNER, J.A., COZENS, A.L., SCHULMAN, H., GRUENERT, D.C., STRYER, L. & GARDNER, P. (1991). Activation of chloride channels in normal and cystic fibrosis airway epithelial cells by multifunctional calcium/calmodulin-dependent protein kinase. *Nature*, **349**, 793–796.

WALSH, D.A. & GLASS, D.B. (1991). Utilization of the inhibitor of adenosine cyclic monophosphate-dependent protein kinase and peptides derived from it as tools to study adenosine cyclic monophosphate-mediated processes. *Methods Enzymol.*, **201**, Part B, 304–316.

WEINMANN, E.J., SHENOLIKAR, S. & KAHN, A.M. (1987). cAMP-associated inhibition of Na^+/H^+ exchanger in rabbit kidney brush border membranes. *Am. J. Physiol.*, **252**, F19–F25.

WELSH, M.J. (1990). Abnormal regulation of ion channels in cystic fibrosis epithelia. *FASEB J.*, **4**, 2718–2725.

WITT, J.J. & ROSKOSKI, R. (1975). Rapid protein kinase assay using phosphocellulose-paper absorption. *Anal. Biochem.*, **66**, 253–258.

(Received September 6, 1993
Revised October 14, 1993
Accepted October 20, 1993)

Br. J. Pharmacol. (1994), **111**, 515–520

Evidence from receptor antagonists of an important role for ET_B receptor-mediated vasoconstrictor effects of endothelin-1 in the rat kidney

Robert P. Wellings, [1]Roger Corder, Timothy D. Warner, Jean-Paul Cristol, Christoph Thiemermann & John R. Vane

The William Harvey Research Institute, The Medical College of St. Bartholomew's Hospital, Charterhouse Square, London EC1M 6BQ

1 To characterize the receptor subtype(s) mediating the renal vasoconstrictor effects of the endothelin (ET) and sarafotoxin (SX) peptides in the isolated perfused kidney of the rat, we have examined the effects of endothelin-1 (ET-1), sarafotoxin 6b (SX6b) and sarafotoxin 6c (SX6c) as agonists, BQ-123 and FR 139317 as selective ET_A receptor antagonists, and PD 145065 as a non-selective (ET_A and ET_B) receptor antagonist. We have also compared in the anaesthetized rat the systemic pressor and renal vasoconstrictor effects of ET-1 and SX6c alone or after pretreatment with PD 145065.

2 In the isolated perfused kidney, ET-1, SX6b and SX6c all gave similar concentration-dependent increases in perfusion pressure. The ET_A receptor selective antagonists, BQ-123 and FR 139317, both partially blocked the increase in perfusion pressure induced by ET-1. In contrast, PD 145065 completely blocked the increase in perfusion pressure caused by ET-1.

3 Indomethacin (10 μM) had no effect on the ET-1-induced increases in perfusion pressure but significantly reduced the vasoconstriction induced by low concentrations of SX6c, without affecting responses to high concentrations. In the anaesthetized rat, indomethacin (5 mg kg^{-1}) did not modify the systemic pressor or renal vasoconstrictor effects of ET-1 or SX6c.

4 In anaesthetized rats, bolus intravenous injections of ET-1 or SX6c (0.1, 0.25, 0.5 or 1.0 nmol kg^{-1}) produced initial transient depressor responses followed by sustained and dose-dependent increases in mean arterial pressure (MAP). Both peptides caused an equipotent fall in renal blood flow (RBF). PD 145065 (5 mg kg^{-1}) partially antagonized the systemic pressor effects of ET-1 and SX6c but completely blocked the fall in RBF and rise in renal vascular resistance (RVR) induced by ET-1 and SX6c. PD 145065 also antagonized the transient depressor effect following the bolus administration of either ET-1 or SX6c.

5 These results indicate that ET/SX induced renal vasoconstriction is mediated via ET_A and ET_B-like receptors with ET_B receptors having a predominant role *in vivo*. This may be of therapeutic relevance for an ET_A receptor-selective antagonist may offer only limited protection against the deleterious renal effects of endogenous ETs.

Keywords: Endothelin-1; sarafotoxins; renal vasoconstriction; ET_A antagonists; selective and non-selective ET-antagonists

Introduction

Endothelin-1 (ET-1) causes an increase in renal vascular resistance (RVR) and a decrease in renal blood flow (RBF) (Firth *et al.*, 1988; Badr *et al.*, 1989; King *et al.*, 1989; Miller *et al.*, 1989; Kon & Badr, 1991). Circulating levels of ET-1 are increased both clinically and in animal models of renal failure or damage, and expression of ET-1 mRNA in the kidney of the rat is increased after ischaemia-reperfusion injury (Tomita *et al.*, 1989; Watschinger *et al.*, 1991; Yamakado *et al.*, 1991; Firth & Ratcliffe, 1992). Indeed, under these conditions ET-1 may have a pathophysiological role in the kidney for infusion of selective antibodies for ET-1 or selective antagonists protects the kidney against ischaemia-reperfusion injury and the nephrotoxic effects of cyclosporin (Kon *et al.*, 1990; Kon & Badr, 1991; Fogo *et al.*, 1992).

To date, two endothelin receptor subtypes, ET_A and ET_B have been cloned and characterized (Arai *et al.*, 1990; Sakurai *et al.*, 1990). Initially it was thought that the ET_A receptor was located on vascular smooth muscle to mediate vasoconstriction and the ET_B receptor was located on the endothelium where it mediated vasodilatation through release of prostacyclin and nitric oxide (De Nucci *et al.*, 1988; Warner *et al.*, 1989). It is now apparent that ET_A and ET_B receptors may mediate vasoconstriction (Ihara *et al.*, 1991; Fukuroda *et al.*, 1992; Warner *et al.*, 1993). We (Cristol *et al.*, 1993) and others (Bigaud & Pelton, 1992; Pollock & Opgenorth, 1993) have shown that the renal vasoconstriction in the rat is largely independent of ET_A receptor activation. Here we have assessed further the receptor subtypes mediating the response *in vivo* and *in vitro* in the rat kidney using ET-1 and sarafotoxin (SX) 6b and SX6c as agonists, BQ-123 and FR139317 as ET_A receptor-selective antagonists (Ihara *et al.*, 1992; Sogabe *et al.*, 1993), and the novel non-selective endothelin receptor antagonist, PD145065 (Cody *et al.*, 1993; Doherty *et al.*, 1993). Some of these findings have been presented to the British Pharmacological Society (Wellings *et al.*, 1993).

Methods

Isolated perfused kidney

Wistar rats (Male, 200–400 g) were anaesthetized with sodium pentobarbitone (60 mg kg^{-1}, i.p.). After a mid-line laporotomy, the superior mesenteric and the right renal arteries were isolated. Heparinized saline (200 units) was given i.v. via the femoral vein and a cannula passed retrogradely into

[1] Author for correspondence.

the superior mesenteric artery and then into the right renal artery. The kidney was rapidly removed and perfused at a constant flow of 10 ml min^{-1} with Krebs solution containing (in mM); NaCl 118, KCl 4.7, $NaHCO_3$ 25, KH_2PO_4 1.17, $MgSO_4$ 25, $CaCl_2$ 2.5 and glucose 5.6, pH 7.4, which was heated to 37°C and constantly bubbled with 95% O_2/5% CO_2. In experiments to study the role of prostanoids, indomethacin (10 μM) was added directly to the Krebs solution. Changes in perfusion pressure were monitored with a pressure transducer (Transamerica type 4-422-001) and recorded continuously on a Graphtec chart recorder. After an equilibration period of 30 min, 0.1% (w/v) bovine serum albumin (BSA) was infused for 3 min prior to infusions of either SX6b, SX6c or ET-1 to prevent adhesion of the lowest doses of ET-1 to the glassware. Concentration-response curves were obtained for each of these peptides by infusion for consecutive 3 min periods in a stepwise manner from 10^{-12} to 6×10^{-10} M. Each kidney was used to obtain only one concentration-response curve. In experiments with antagonists, BQ-123, FR 139317 or PD 145065 were infused for 3 min to give a concentration of 10 μM prior to the lowest concentration of peptide and for the duration of the experiment.

Kidney blood flow in vivo

Wistar rats (male, 250–440 g) were anaesthetized with sodium thiopentone (120 mg kg^{-1}, i.p.). The trachea was cannulated to facilitate respiration and body temperature was maintained at 37°C by means of a rectal probe connected to a homeothermic blanket (Biosciences, Sheerness, Kent). The right carotid artery was cannulated and connected to a pressure transducer (Transamerica type 4-422-001) for the measurement of arterial blood pressure which was recorded on a polygraph (Grass 7D, Grass Instruments, Quincy, MA, U.S.A.). Mean arterial pressure (MAP) was calculated as the diastolic pressure plus one third the pulse pressure. A midline laparotomy was performed and the left renal artery was carefully exposed. An ultrasonic flow probe (model 1RB, internal diameter = 1 mm), embedded in a silicone cuff to provide optical alignment, was placed around the left renal artery for measurement of total renal blood flow (RBF) using a Transonic T206 Small Animal Flowmeter (Transonic Systems Inc., New York, U.S.A.). A small amount of acoustical couplant (100 mg Nalco 1181, mixed with 10 ml distilled water; Nalco Chemical Co., Il., U.S.A.) was deposited in the acoustic window of the probe adjacent to the artery, in order to displace all air. Renal vascular resistance (RVR, mmHg ml^{-1} min) was calculated as MAP/RBF. After an equilibration period of 30 min, either vehicle (0.9% saline containing 0.1% BSA) or antagonist (PD 145065, 5 mg kg^{-1}) were injected 3 min prior to a bolus injection of either ET-1 or SX6c at doses of 0.1, 0.25, 0.5 and 1.0 nmol kg^{-1}, always in increasing dose. The time between each injection of ET/SX peptide was 1 h. In the indomethacin study, indomethacin was given as a 5 mg kg^{-1} bolus 30 min prior to the lower dose of ET-1 or SX6c, and a further 2 mg kg^{-1} was given 30 min after the lower dose. Changes in RBF and MAP were recorded 3 min after the injection of the peptide, at which time the initial depressor effect was ended but the renal vasoconstriction was still maintained.

Materials

Sodium pentobarbitone (Sagatal) was obtained from May and Baker Ltd., Dagenham, Essex and Trapanal (sodium thiopentone) was obtained from Byk Gulden (Konstanz, Germany). ET-1, SX6b and SX6c were purchased from the Peptide Institute (Osaka, Japan). The peptides were reconstituted in 0.1% v/v acetic acid and then diluted in 0.9% w/v saline containing 1% w/v bovine serum albumin and 10 mM sodium bicarbonate. The trifluoroacetic acid salts of BQ-123 (*cyclo*-(D-Trp-D-Asp-Pro-D-Val-Leu) and FR 139317 ((**R**)-2-[s]-2-[(1-hexahydro-1H-azepinyl)] carbonyl] amino-4-methyl-pantanoyl] amino-3- [3-(1-methyl-1H-indolyl)] propionyl] amino-3-(2-pyridyl) propionoic acid) and the disodium salt of PD 145065 (Ac-D-Bhg-L-Leu-L-Asp-L-Ile-L-Ile-L-Trp; Bhg = 5H-dibenzyl[a,d]cyclohepten-10-11-dihydroglycine) were dissolved in dimethyl sulphoxide (DMSO) and diluted with 0.9% NaCl for the *in vitro* studies. After further dilution in the perfusion apparatus, this resulted in a final concentration of 0.06% DMSO. For the *in vivo* studies, PD 145065 was dissolved in 0.9% w/v sodium chloride.

Statistics

Statistical differences between points were determined by Student's unpaired two tail t test and $P < 0.05$ was taken to reflect significant difference.

Results

Isolated perfused kidney

The mean basal perfusion pressure for the control isolated kidneys was 87 ± 4 mmHg ($n = 48$) and was unaffected by treatment with indomethacin (85 ± 4 mmHg for the indomethacin treated kidneys, $n = 12$). No significant differences were observed between the respective study groups. Infusion of ET-1, SX6b and SX6c induced concentration-dependent

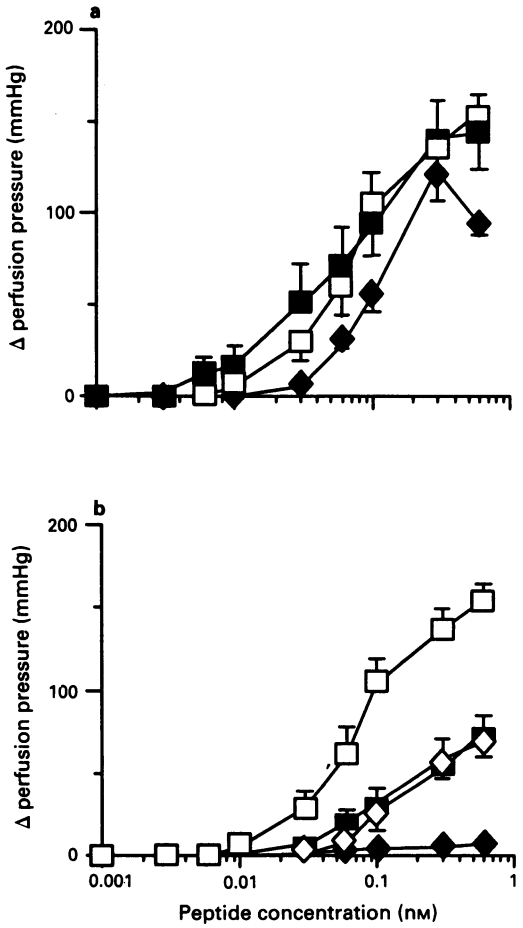

Figure 1 The effect of endothelin-1 (ET-1), sarafotoxin 6b (SX6b) and SX6c on perfusion pressure changes of the isolated perfused kidney of the rat. (a) ET-1, SX6b and SX6c elicit concentration-dependent increases in perfusion pressure; (□) ET-1; (■) SX6b; (◆) SX6c. (b) Responses to ET-1 with co-infusion of either BQ-123, FR 139317 or PD 145065 (all at 10 μM); (□), ET-1; (■), ET-1 with BQ-123; (◇), ET-1 with FR 139317; (◆), ET-1 with PD 145065. Each point represents the mean ± s.e.mean from six observations. Standard errors are shown unless smaller than the symbol size.

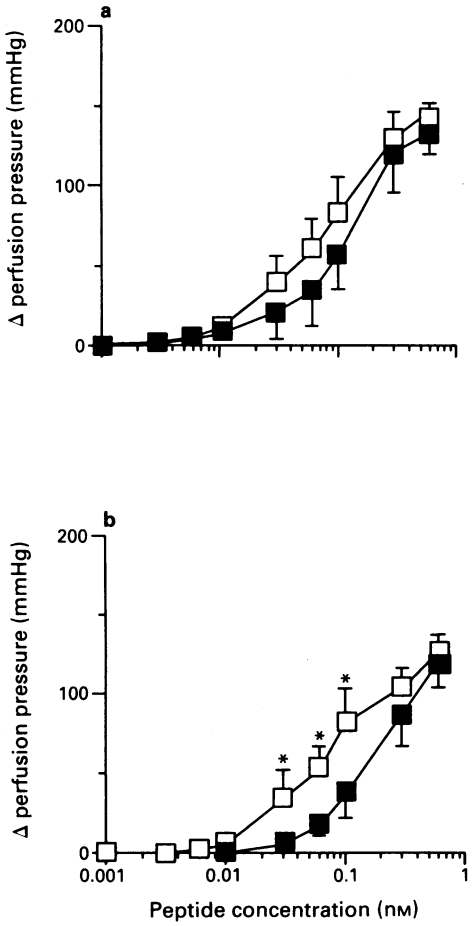

Figure 2 The effect of indomethacin (10 μM) on the responses in the isolated perfused kidney of the rat to either endothelin-1 (ET-1) or sarafotoxin 6c (SX6c). (a) ET-1-induced concentration-dependent increases in perfusion pressure in the presence or absence of 10 μM indomethacin. ET-1 control, (□); ET-1 in the presence of 10 μM indomethacin, (■). (b) SX6c-induced concentration-dependent increases in perfusion pressure in the presence or absence of 10 μM indomethacin. SX6c control, (□); SX6c in the presence of 10 μM indomethacin, (■). Each point represents the mean ± s.e.mean from six observations. Standard errors are shown unless smaller than the symbol size. $*P<0.05$, compared to the corresponding SX6c concentration with indomethacin.

(threshold 10^{-11} M) increases in perfusion pressure (Figure 1a). BQ-123 or FR 139317 significantly reduced the increase in perfusion pressure induced by ET-1 at all concentrations (Figure 1b). PD 145065 completely blocked the rise in perfusion pressure induced by ET-1 at all the concentrations used.

Indomethacin did not affect the increases in perfusion pressure induced by ET-1 (Figure 2a), but significantly reduced those to SX6c at lower concentrations (3×10^{-11} to

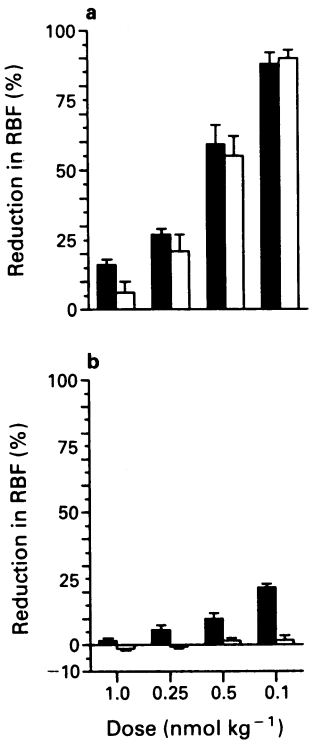

Figure 3 The effect of PD 145065 on the reduction in renal blood flow (RBF) induced by endothelin-1 (ET-1) or sarafotoxin 6c (SX6c) in the anaesthetized rat. (a) ET-1 and SX6c (0.1–1.0 nmol kg^{-1}) produced dose-dependent reductions in renal blood flow. Values are from 3 min after i.v. administration of ET-1 or SX6c. (b) Responses to the same doses of ET-1 or SX6c in animals pretreated with PD 145065 (i.v., 5 mg kg^{-1}) 3 min prior to injection of the peptide. Closed columns, ET-1; open columns, SX6c. Each column with a vertical bar represents the mean ± s.e.mean from six observations.

Table 1 The maximum increase in mean arterial pressure (MAP, mmHg) in response to endothelin-1 (ET-1) or sarafotoxin 6c (SX6c) in the presence or absence of 5 mg kg^{-1} PD 145065

	0.1 nmol kg^{-1}	0.25 nmol kg^{-1}	0.5 nmol kg^{-1}	1.0 nmol kg^{-1}
ET-1 control	7 ± 1 (2.8 ± 0.6)	9 ± 1 (3.6 ± 0.6)	30 ± 8 (3.1 ± 0.3)	41 ± 6 (1.6 ± 0.1)
ET-1/PD 145065	3 ± 2* (0.5 ± 0.2)	6 ± 2* (1.0 ± 0.4)	10 ± 2* (1.4 ± 0.2)	16 ± 2* (1.5 ± 0.2)
SX6c control	12 ± 2 (5.2 ± 1.9)	15 ± 2 (6.2 ± 0.9)	18 ± 4 (9.8 ± 0.9)	19 ± 1 (9.5 ± 0.4)
SX6c/PD 145065	3 ± 2* (1.9 ± 1.5)	4 ± 2* (1.5 ± 0.5)	3 ± 2* (2.0 ± 0.4)	9 ± 2* (0.9 ± 0.2)

Numbers in parentheses are the time delay (min) to the maximal pressor response after peptide administration, $n = 6$ for each group. *Indicates significant differences ($P<0.05$) in MAP for control versus PD 145065 pretreated (5 mg kg^{-1}, 3 min prior to peptide) animals.

Table 2 The change in renal vascular resistance (mmHg ml^{-1} min) calculated 3 min after bolus intravenous injections of endothelin-1 (ET-1) or sarafotoxin 6c (SX6c) (0.1, 0.25 or 0.5 nmol kg^{-1})

	0.1 nmol kg^{-1}		0.25 nmol kg^{-1}		0.5 nmol kg^{-1}	
	Control	*+ PD 145065*	*Control*	*+ PD 145065*	*Control*	*+ PD 145065*
ET-1	4.0 ± 0.6	0.6 ± 0.2*	6.8 ± 0.7	1.3 ± 0.4*	46 ± 19	3.0 ± 0.6*
SX6c	2.1 ± 0.9	0.0 ± 0.1*	6.0 ± 0.2	0.4 ± 0.2*	28 ± 11	0.4 ± 0.2*

$n = 6$ for each group.
*Indicates significant differences in RVR for control versus PD 145065-pretreated (5 mg kg^{-1}, 3 min prior to peptide) animals.

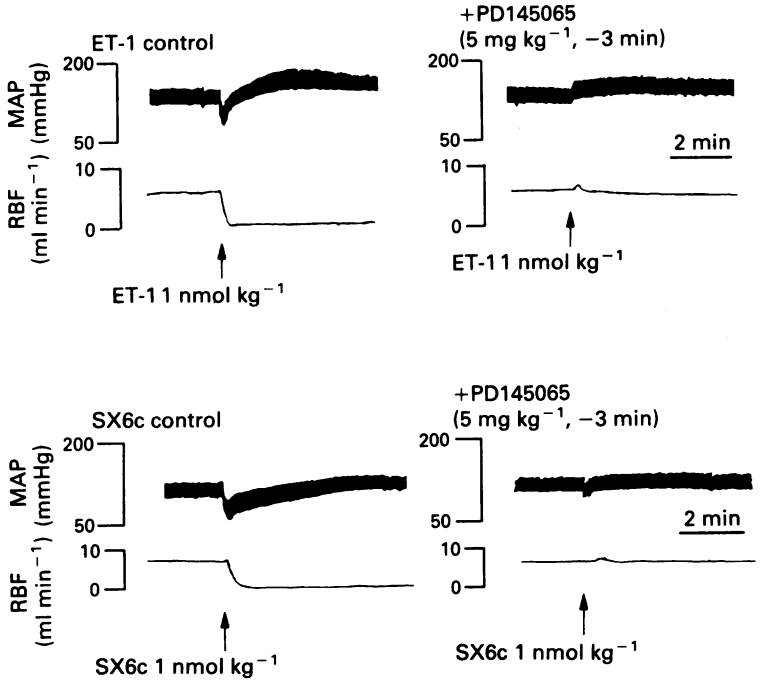

Figure 4 Representative trace of the effects of PD 145065 on the mean arterial pressure and renal blood flow responses to endothelin-1 (ET-1) or sarafotoxin 6c (SX6c). ET-1 or SX6c were administered as i.v. bolus injections (1.0 nmol kg^{-1}). Vehicle or PD 145065 (5 mg kg^{-1}) was administered as an i.v. bolus 3 min prior to the peptide injection. MAP, mean arterial pressure; RBF, renal blood flow.

3×10^{-10} M, Figure 2b). The threshold value for SX6c was also shifted from 10^{-11} to 3×10^{-11} M. The responses to higher concentrations were unaffected.

Systemic and renal effects of ET-1 and SX6c in the anaesthetized rat

Basal values for MAP were 115 ± 3 mmHg, for RBF 7.9 ± 0.2 ml min^{-1} and 14.6 ± 0.4 mmHg ml^{-1} min for RVR ($n = 24$ for each). These values were unaffected by vehicle or PD 145065 (5 mg kg^{-1}). Injection of ET-1 or SX6c produced similar initial and transient falls in MAP (Figure 4). In the case of ET-1 this depressor effect was followed by a sustained, dose-dependent increase in MAP which was maximal within 5 min of injection (Table 1). In contrast, the pressor effect to SX6c was less marked and slower in onset, reaching a maximum within 10 min of injection (Table 1). ET-1 and SX6c produced similar falls in RBF (Figures 3 and 4). Dose-related increases in RVR were observed with both peptides (Table 2). Indomethacin (5 mg kg^{-1}) had no significant effect on the rise in RVR, fall in RBF or increase in MAP induced by ET-1 or SX6c administered at doses of 0.25 or 0.5 nmol kg^{-1} (data not illustrated).

Effect of PD 145065 on blood pressure and renal vasoconstrictor responses

The initial fall in MAP which is observed after ET-1 or SX6c administration was completely blocked by PD 145065 (Figure 4). PD 145065 (5 mg kg^{-1}) significantly reduced the systemic pressor effects of ET-1 and SX6c (Table 1). The time to maximum pressor response was decreased after PD 145065 (Table 1). PD 145065 blocked the fall in RBF and elevation in RVR induced by ET-1 or SX6c at all doses. (Figures 3 and 4, Table 2).

Discussion

Our results suggest that the renal vasoconstrictor effects of the ET/SX peptides are mediated by both ET_A and ET_B receptors, with the ET_B receptor mediating a major part of the effect at higher peptide concentrations. In the isolated perfused kidney, SX6c, which has little or no activity on ET_A receptors (Williams *et al.*, 1991; Warner *et al.*, 1993), was approximately equipotent to the mixed (ET_A and ET_B) receptor agonists ET-1 and SX6b. In addition, the ET_A receptor-selective antagonists, BQ-123 and FR 139317, only partially attenuated the rise in perfusion pressure induced by ET-1, whereas the non-selective (ET_A and ET_B) antagonist, PD 145065, completely blocked it.

A number of studies have demonstrated that the endothelins release a variety of prostanoids (de Nucci *et al.*, 1988; Stier *et al.*, 1992) and in the rat isolated kidney, prostanoid release causes vasoconstriction (Malik & McGiff, 1975). The involvement of secondary mediators in the renal vasoconstriction induced by ET-1 is unclear. Earlier studies in the perfused kidney of the rat show conflicting results; whereas Trybulec *et al.* (1991) showed that indomethacin attenuated ET-1- and ET-3-induced vasoconstriction after bolus administration, Stier *et al.* (1992) showed that indomethacin did not alter the renal vasoconstrictor effects of infused ET-3. The results described here indicate that cyclo-oxygenase products may partly mediate the vasoconstriction, particularly those resulting from ET_B receptor activation since indomethacin reduced the vasoconstriction induced by low concentrations of SX6c. However, indomethacin was ineffective against higher concentrations of SX6c and did not significantly alter the response to ET-1. Consistent with an earlier report (Wright & Fozard, 1990), indomethacin had no effect on haemodynamic and renal responses to ET-1 or SX6c *in vivo*.

We have previously shown that in the anaesthetized rat, BQ-123 has no effect on the reductions in RBF induced by either ET-1, SX6b, SX6c or ET-3 (Cristol *et al.*, 1993), although at the lowest doses of ET-1 or SX6b used, BQ-123 did significantly reduce the increases in RVR. Furthermore,

the reductions in RBF showed no isopeptide selectivity, suggesting that these events were mediated by the ET_B receptor. The systemic pressor effects of ET/SX peptides were blocked partially, but not completely by BQ-123, suggesting a predominant role for the ET_A receptor in mediating the systemic pressor effects of the endothelins (Cristol *et al.*, 1993). Using infusions of ET-1 and BQ-123, Pollock & Opgenorth (1993) have reached similar conclusions concerning the ET receptors mediating systemic and renal vasoconstriction. Here, PD 145065 blocked the reductions in RBF induced by ET-1 or SX6c, at all the doses studied, and attenuated the associated rise in RVR. PD 145065 reduced the rise in MAP induced by ET-1, but did not completely block it. However, because PD 145065 completely prevented any depressor effect this may have resulted in a relatively larger residual pressor effect due to removal of the functional antagonism caused by the dilator response.

The suggestion that non-ET_A receptors mediate vasoconstrictions first came from *in vitro* studies in which selective antagonists of the ET_A receptor failed to inhibit completely endothelin-induced contractions (Ihara *et al.*, 1991; Fukuroda *et al.*, 1992). In addition, we have also shown that BQ-123 was unable to block completely the pressor effects of ET/SX peptides in the anaesthetized, ganglion-blocked rat (McMurdo *et al.*, 1993). This non-ET_A-mediated vasoconstriction may be due to ET_B receptor activation (Ihara *et al.*, 1991; Fukuroda *et al.*, 1992; Clozel *et al.*, 1993) or to a yet to be characterised novel ET receptor (Pollock & Opgenorth, 1993; Warner *et al.*, 1993).

In conclusion, we have previously demonstrated in the anaesthetized rat that the receptor subtype mediating ET-1-induced vasoconstrictions is predominantly non-ET_A. Here we have shown that both ET_A and ET_B receptors are involved in mediating renal vasoconstriction. However, because of the overriding effects of the ET_B-mediated response, only the non-selective antagonist was able to prevent fully the vasoconstriction induced by ET-1 and the ET_B-selective agonist, SX6c. If endothelin is shown to have importance in disease models of renal failure, then receptor antagonism of the ET_A and ET_B subtype is likely to be important for full protection against the pathophysiological effects of endogenously produced endothelin.

This work was supported by the Parke-Davis Pharmaceutical Research, Division of Warner-Lambert Co. We thank Drs A. Doherty and W. Cody of the Medicinal Chemistry Department at Parke-Davis for providing BQ-123, FR 139317 and PD 145065. We also thank Dr J. Firth of the Dept. Molecular Medicine, John Radcliffe Infirmary, Oxford, for demonstrating the technique for isolating and perfusing the rat kidney.

References

ARAI, H., HORI, S., ARAMORI, I., OHKUBO, H. & NAKANISHI, S. (1990). Cloning and expression of a cDNA encoding an endothelin receptor. *Nature*, **348**, 730–732.

BADR, K.F., MURRAY, J.J., BREYER, M.D., TAKAHASHI, K., INAGAMI, T. & HARRIS, R.C. (1989). Mesangial cell, glomerular and renal vascular responses to endothelin in the rat kidney. *J. Clin. Invest.*, **83**, 336–342.

BIGAUD, M. & PELTON, J.T. (1992). Discrimination between ET_A- and ET_B-receptor-mediated effects of endothelin-1 and [$Ala^{1,3,11,15}$] endothelin-1 by BQ-123 in the anaesthetised rat. *Br. J. Pharmacol.*, **107**, 912–918.

CLOZEL, M., GRAY, G.A., BREU, V., LOFFLER, B.M. & OSTERWALDER, R. (1993). The endothelin ET_B receptor mediates both vasodilatation and vasoconstriction in vivo. *Biochem. Biophys. Res. Commun.*, **186**, 867–873.

CODY, W.L., DOHERTY, A.M., HE, J.X., TOPLISS, J., HALEEN, S., LADOUCEUR, D., HILL, K.E., FLYNN, M.A. & REYNOLDS, E.E. (1993). Structure-activity relationships in the C-terminus of endothelin-1 (ET-1); the discovery of potent antagonists. *Proceedings of the 22nd European Peptide Symposium*. ed. Scheider, C.H. & Eberle, A.N. pp. 687–688. Leiden, The Netherlands, ESCOM Science.

CRISTOL, J.P., WARNER, T.D., THIEMERMANN, C. & VANE, J.R. (1993). Mediation via different receptors of the vasoconstrictor effects of endothelins and sarafotoxins in the systemic circulation and renal vasculature of the anaesthetized rat. *Br. J. Pharmacol.*, **108**, 776–779.

DE NUCCI, G., THOMAS, G.R., D'ORLEANS JUSTE, P., ANTUNES, E., WALDER, C.E., WARNER, T.D. & VANE, J.R. (1988). The pressor effects of circulating endothelin are limited by its removal in the pulmonary circulation and by release of prostacyclin and endothelium-derived relaxing factor. *Proc. Natl. Acad. Sci. U.S.A.*, **85**, 9797–9800.

DOHERTY, A.M., CODY, W.L., HE, J.X., DEPUE, P.L., CHENG, X.M., WELCH, K.M., FLYNN, M.A., REYNOLDS, E.E., LADOUCEUR, D.M., DAVIS, L.S., KEISER, J.A. & HALEEN, S.J. (1993). *In vitro* and *in vivo* studies with a series of hexapeptide endothelin antagonists. *J. Cardiovasc. Pharmacol.*, **22**, suppl 8, S98–S102.

FIRTH, J.D. & RATCLIFFE, P.J. (1992). Organ distribution of the three rat endothelin messenger RNAs and the effects of ischemia on renal gene expression. *J. Clin Invest.*, **90**, 1023–1031.

FIRTH, J.D., RATCLIFFE, P.J., RAINE, A.E.G. & LEDINGHAM, J.G.G. (1988). Endothelin: an important factor in renal failure? *Lancet*, **ii**, 1179–1181.

FOGO, A., HELLINGS, S.E., INAGAMI, T. & KON, V. (1992). Endothelin receptor antagonism is protective in in vivo acute cyclosporine toxicity. *Kidney Int.*, **42**, 770–774.

FUKURODA, T., NISHIKIBE, M., OHTA, Y., IHARA, M., YANO, M., ISHIKAWA, K., FUKAMI, T. & IKEMOTO, F. (1992). Analysis of responses to endothelins in isolated porcine blood vessels by using a novel endothelin antagonist, BQ-123. *Life Sci.*, **50**, Pl-107–Pl-112.

IHARA, M., NOGUCHI, K., SAEKI, T., FUKURODA, T., TSUCHIDA, S., KIMURA, S., FUKAMI, T., ISHIKAWA, K., NISHIKIBE, M. & YANO, M. (1992). Biological profiles of highly potent novel endothelin antagonists selective for the ET_A receptor. *Life Sci.*, **50**, 247–255.

IHARA, M., SAEKI, T., FUNABISHI, K., NAKAMICHI, K., YANO, M., FUKURODA, T., MIYAJI, M., NISHIKIBE, M. & IKEMOTO, F. (1991). Two endothelin receptor subtypes in porcine arteries. *J. Cardiovasc. Pharmacol.*, **17**, suppl 7, S119–S121.

KING, A.J., BRENNER, B.M. & ANDERSON, S. (1989). Endothelin: a potent renal and systemic vasoconstrictor peptide. *Am. J. Physiol.*, **256**, F1051–F1058.

KON, V. & BADR, K.F. (1991). Biological actions and pathophysiological significance of endothelin in the kidney. *Kidney Int.*, **40**, 1–12.

KON, V., SUGIARA, M., INAGAMI, T., HARVIE, B.R., ICHIKAWA, I. & HOOVER, R.L. (1990). Role of endothelin in cyclosporine-induced glomerular dysfunction. *Kidney Int.*, **37**, 1487–1491.

MCMURDO, L., CORDER, R., THIEMERMANN, C. & VANE, J.R. (1993). Incomplete inhibition of the pressor effects of ET-1 and related peptides in the anaesthetized rat with BQ-123 provides evidence for a further vasoconstrictor receptor. *Br. J. Pharmacol.*, **108**, 557–561.

MALIK, K.U. & MCGIFF, J.C. (1975). Modulation by prostaglandins of adrenergic transmission in the isolated perfused rabbit and rat kidney. *Circ Res.*, **36**, 599–609.

MILLER, W.L., REDFIELD, M.M. & BURNETT, J.C. (1989). Integrated cardiac, renal and endocrine actions of endothelin. *J. Clin. Invest.*, **83**, 317–320.

POLLOCK, D.M. & OPGENORTH, T.J. (1993). Evidence for endothelin-induced renal vasoconstriction independent of ET_A receptor activation. *Am. J. Physiol.*, **264**, R222–R226.

SAKURAI, T., YANAGISAWA, M., TAKUWA, Y., MIYAZAKI, H., KIMURA, S., GOTO, K. & MASAKI, T. (1990). Cloning of a cDNA encoding a non-isopeptide selective subtype of the endothelin receptor. *Nature*, **348**, 732–735.

SOGABE, K., NIREI, H., SHOUBO, M., NOMOTO, A., AO, S., NOTSU, Y. & ONO, T. (1993). Pharmacological profile of FR139317, a novel, potent endothelin ET_A receptor antagonist. *J. Pharmacol. Exp. Ther.*, **264**, 1040–1046.

STIER, C.T., QUILLEY, C.P. & MCGIFF, J.C. (1992). Endothelin-3 effects on renal function and prostanoid release in the rat isolated kidney. *J. Pharmacol. Exp. Ther.*, **262**, 252–256.

TOMITA, K., UJJIE, K., NAKASHIMI, T., TOMURA, S., MATSUDA, D. & ANDO, K. (1989). Plasma endothelin levels in patients with acute renal failure. *New Engl. J. Med.*, **321**, 1127.

TRYBULEC, M., DUDEK, R.R. & GRYGLEWSKI, R.J. (1991). Effects of endothelin-1 and endothelin-3 on the release of prostanoids from isolated perfused rat kidney. *J. Cardiovasc. Pharmacol.*, **17** (Suppl. 7), S229–S232.

WARNER, T.D., ALLCOCK, G.H., CORDER, R. & VANE, J.R. (1993). Use of the endothelin antagonists BQ-123 and PD 142893 to reveal three endothelin receptors mediating smooth muscle contraction and the release of EDRF. *Br. J. Pharmacol.*, **110**, 777–782.

WARNER, T.D., MITCHELL, J.A., DE NUCCI, G. & VANE, J.R. (1989). Endothelin-1 and endothelin-3 release EDRF from isolated perfused arterial vessels of the rat and the rabbit. *J. Cardiovasc. Pharmacol.*, **13** (suppl. 5), S85–S88.

WATSCHINGER, B., VYCHYTIL, A., SCHULLER, M., HARTTER, E., TRAINDL, O. & POHANKA, K. (1991). The pathophysiological role of ET in acute vascular rejection after renal transplantation. *Transplantation*, **52**, 743–746.

WELLINGS, R.P., WARNER, T.D., CORDER, R., THIEMERMANN, C., CRISTOL, J.P. & VANE, J.R. (1993). A new non-selective endothelin antagonist blocks the vasoconstriction induced by endothelin-1 in the rat kidney, both *in vivo* and *in vitro*. *Br. J. Pharmacol.*, **108**, 110P.

WILLIAMS, D.L. Jr., JONES, K.L., PETTIBONE, D.J., LIS, E.V. & CLINESCHMIDT, B.V. (1991). Sarafotoxin S6c: an agonist which distinguishes between endothelin receptor subtypes. *Biochem. Biophys. Res. Commun.*, **175**, 556–561.

WRIGHT, C.E. & FOZARD, J.R. (1990). Differences in regional vascular sensitivity to endothelin-1 between spontaneously hypertensive and normotensive Wistar-Kyoto rats. *Br. J. Pharmacol.*, **100**, 107–113.

YAMAKADO, M., HIRATA, Y., MATSUOKA, H. & SUGIMOTO, T. (1991). Pathophysiological role of ET in renal transplantation. *J. Cardiovasc. Pharmacol.*, **17**, S477–S479.

(Received August 4, 1993
Revised October 6, 1993
Accepted October 20, 1993)

Br. J. Pharmacol. (1994), **111**, 521–524

Effect of nitric oxide synthase inhibition on long-term potentiation at associational-commissural and mossy fibre synapses on CA3 pyramidal neurones

P.J. Nicolarakis, Y.-Q. Lin & [1]M.R. Bennett

The Neurobiology Laboratory, Department of Physiology, University of Sydney, N.S.W. 2006, Australia

1 The sensitivity of long-term potentiation (LTP) to nitric oxide synthase (NOS) inhibition was determined for two synaptic input systems onto CA3 pyramidal neurones the LTP of which display differential sensitivity to N-methyl-D-aspartate (NMDA) receptor antagonists: the fimbrial input which activates the associational-commissural synapses on the distal apical dendrites and the mossy fibre input which synapses on the proximal apical dendrites of CA3 pyramidal neurones.

2 Following high-frequency stimulation (HFS) of the fimbrial input, average e.p.s.p. amplitude increased by 92.4 ± 22.0% (mean ± s.e.mean; $n = 6$ cells) when compared to the pre-HFS average. In the presence of 100 μM N^{ω}-nitro-L-arginine methyl ester (L-NAME), the enhancement was reduced significantly to 32.2 ± 11.6% ($n = 5$ cells; $P < 0.05$). In the presence of 300 μM L-NAME, the inhibition was more complete, with post-HFS e.p.s.p. amplitude increasing an average 6.2 ± 9.3% ($n = 7$ cells, $P < 0.05$).

3 Following high frequency stimulation of the mossy fibre input, average e.p.s.p. amplitude increased by 57.9 ± 13.0% ($n = 6$ cells) when compared to the pre-HFS average. The presence of 100 μM L-NAME had no significant effect on the enhancement, averaging 63.6 ± 5.9% ($n = 4$ cells; $P > 0.05$). Similarly, increasing the concentration of L-NAME to 300 μM had no significant effect on the potentiation, with the post-HFS amplitude increasing by an average 55.6 ± 9.5% ($n = 5$ cells, $P > 0.05$).

4 These results suggest that LTP at associational-commissural synapses (fimbrial input) is significantly depressed in the presence of the NOS inhibitor L-NAME, while mossy fibre LTP is unchanged.

Keywords: Long-term potentiation; CA3 pyramids; nitric oxide; mossy fibres; fimbria

Introduction

The induction of long-term potentiation (LTP) by high-frequency stimulation of the mossy fibre tract to a CA3 pyramidal neurone is insensitive to blockers of N-methyl-D-aspartate (NMDA) receptors (Harris & Cotman, 1986; Jaffe & Johnston, 1990; Zalutsky & Nicoll, 1990; Katsuki *et al.*, 1991). This contrasts with the LTP described at other excitatory synapses in the hippocampus (including the perforant path to granule cells, associational-commissural to CA3 pyramidal neurones and the Schaeffer collateral to CA1 pyramidal neurones), which have all been shown to be blocked by such treatment (Harris & Cotman, 1986; Errington *et al.*, 1987; Zalutsky & Nicoll, 1990; Katsuki *et al.*, 1991). The high NMDA receptor density in the distal regions of the CA3 apical dendrites, where the fimbrial (associational-commissural) inputs terminate, but low receptor density in the more proximal regions of the dendrites, where the mossy fibres synapse, is consistent with these observations (Monaghan & Cotman, 1985). A number of postsynaptic pharmacological alterations (e.g. postsynaptic injection of calcium chelators, G-protein inhibitors) have also been shown to inhibit selectively the NMDA receptor-dependent form of LTP while having no effect on the non-NMDA receptor mediated mossy fibre LTP (Zalutsky & Nicoll, 1990; Katsuki *et al.*, 1991; 1992; but see Jaffe & Johnston, 1990; Johnston *et al.*, 1992).

NMDA receptor activation can elevate levels of guanosine 3':5'-cyclic monophosphate (cyclic GMP) in rat hippocampi by activating the conversion of L-arginine to nitric oxide (NO) via nitric oxide synthase (NOS; East & Garthwaite, 1991). The pharmacological inhibition of NOS by the L-arginine analogue, N^{ω}-nitro-L-arginine-methyl ester (L-NAME) inhibits the induction of the NMDA receptor-mediated LTP at the Schaeffer-collateral to CA1 synapse (Bon *et al.*, 1992; Haley *et al.*, 1992). These results suggest that NO may be a retrograde messenger the postsynaptic productions of which is stimulated by the activation of NMDA receptors (Gally *et al.*, 1990; Böhme *et al.*, 1991; O'Dell *et al.*, 1991; Schuman & Madison, 1991; Bon *et al.*, 1992; Haley *et al.*, 1992; but see Bliss & Collingridge, 1993).

Fimbria-evoked LTP in CA3 pyramidal neurones exhibits all the characteristics commonly used to describe a Hebbian synapse (associativity, cooperativity and specificity; Katsuki *et al.*, 1991; Zalutsky & Nicoll, 1990; 1992; but see Jaffe & Johnston, 1990) while mossy fibre LTP only displays specificity (Zalutsky & Nicoll, 1992). The fimbria-evoked LTP engages the associational-commissural fibres of the CA3 neurones and so involves transmission at synapses with NMDA receptors (Katsuki *et al.*, 1991). The question arises as to whether these synapses on the distal apical dendrites of CA3 pyramidal neurones utilize NO as a retrograde messenger in the generation of LTP and whether the mossy fibre synapses on the proximal apical dendrites do not. The present work shows that this may be the case.

Methods

Hippocampal slices (400 μm thick) were prepared from 3–5 week old male Wistar rats by conventional techniques (Dingledine *et al.*, 1980). The slices were maintained in a submersion chamber at room temperature, approximately 21°C and continuously perfused with artificial cerebro-spinal fluid (ACSF) containing the $GABA_A$ antagonist, picrotoxinin (20 μM) at a rate of 2–3 ml min^{-1}. The ACSF had the following composition (mM): NaCl 123.8, $NaHCO_3$ 26.2, KCl 2.0, $MgSO_4$ 1.0, KH_2PO_4 1.3, $CaCl_2$ 2 and glucose 10.0. This solution was constantly bubbled with 5% CO_2 and 95% O_2

[1] Author for correspondence.

in order to maintain a pH of approximately 7.3. Microelectrodes of resistances between 80 MΩ and 120 MΩ (filled with 4 M potassium acetate) were positioned in the CA3 region of the hippocampal slices and CA3 pyramidal neurone impalements obtained by making short punctate movements into *stratum pyramidal*. The quality of impalement was determined by the presence of stable resting membrane potentials more negative than −65 mV, stable input resistance and an action potential greater than 80 mV in amplitude. Rectangular stimulating pulses (40–100 μs in duration) were delivered at 0.5 Hz through a bipolar tungsten electrode (tip spacing ≈75 μm) positioned either on the mossy fibre tract well inside the dentate gyrus (to activate mossy fibre synapses) or straddled across the fimbria (to activate associational-commissural synapses). The intensity of the stimulation was set to evoke excitatory postsynaptic potentials (e.p.s.ps) which were sufficiently below the action potential threshold (usually <5 mV) as to prevent non-linear summation of enhanced responses following tetanic stimulation. Evoked e.p.s.ps from these neurones were recorded with an Axoclamp 2A amplifier (Axon Instruments), digitally stored (on line) and later analysed with pCLAMP software (Axon Instruments) on an IBM compatible computer.

The high frequency stimulation (HFS) paradigm delivered to the mossy fibre and fimbrial pathways differed. HFS delivered to the mossy fibre tract consisted of a single 100 Hz train lasting for 1 s (100 impulses) at an intensity just below the action potential threshold. The paradigm for fimbrial stimulation consisted of 5 trains of 10 impulses at 100 Hz, separated by 1 s (a total of 50 impulses) at an intensity just below the action potential threshold. E.p.s.p. amplitude was measured as the difference (mV) between the baseline and peak of a response. The mean amplitude of between 60 and 150 consecutive evoked (0.5 Hz) e.p.s.ps recorded before and 15 to 20 min after the tetanic stimulation were used to assess the degree of potentiation for a given cell. The increase in efficacy of synaptic transmission following tetanic stimulation was calculated as the percentage increase in mean e.p.s.p. amplitude 15 to 20 min after high frequency stimulation.

Both the $GABA_A$ antagonist, picrotoxinin and the nitric oxide synthase inhibitor, N^{ω}-nitro-L-arginine methyl ester (L-NAME) were obtained from Sigma.

Data are expressed as mean percentage increase (± standard error of the mean, s.e.mean) in e.p.s.p. amplitude 15 to 20 min after HFS. The significance of the difference between drug treatments and bath controls was calculated by Student's two-tailed unpaired *t* test, with *P* values of less than 0.05 considered to represent a significant difference.

Results

High frequency stimulation (HFS) of the mossy fibre or fimbrial pathways resulted in the sustained enhancement of excitatory postsynaptic responses. Changes in the amplitude of the e.p.s.p. determined between 15 and 20 min after HFS were used to measure the extent of mossy fibre and fimbrial LTP. The mean amplitudes of the e.p.s.ps were significantly increased for mossy fibre LTP (57.9 ± 13.0%; $n = 6$ cells; $P < 0.05$; Figure 1b) and fimbrial LTP (92.4 ± 22.0%; $n = 6$ cells; $P < 0.05$; Figure 2b) using a single sample Student's *t* test. This potentiation of synaptic efficacy was observed for the duration of the impalements following HFS. To test whether nitric oxide synthase participated in the formation of mossy fibre and fimbrial LTP, hippocampal slices were perfused with normal ACSF containing 100 μM or 300 μM L-NAME, and then subjected to the appropriate tetanic stimulation. The mean e.p.s.p. amplitude after HFS of the mossy fibres rose by an average 63.6 ± 5.9% ($n = 4$ cells) in the presence of 100 μM L-NAME. This enhancement was not significantly different from the control rise in e.p.s.p. amplitude ($P > 0.05$; Figure 1b), thereby suggesting that

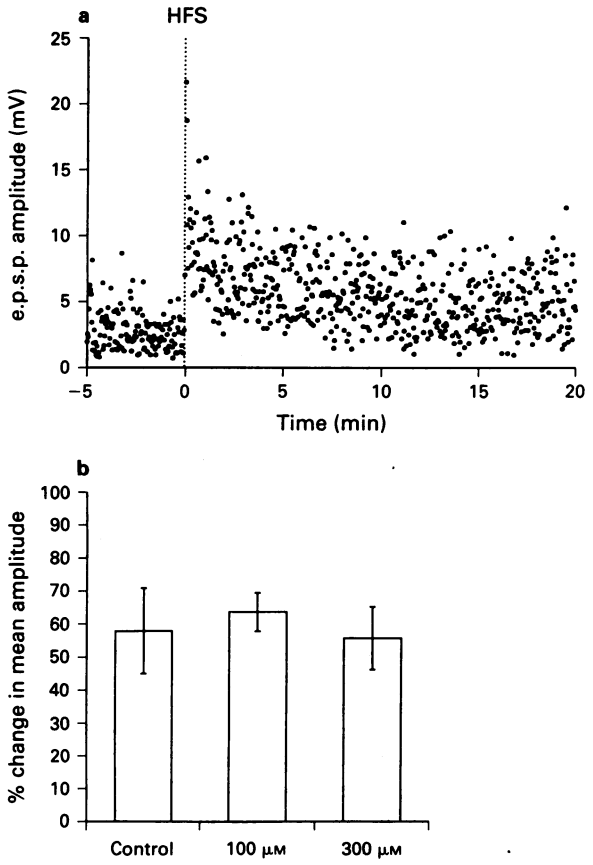

Figure 1 (a) Effect of high frequency stimulation (HFS) of the mossy fibre tract on the amplitude of evoked e.p.s.ps in the presence of 300 μM N^{ω}-nitro-L-arginine methyl ester (L-NAME). (b) The percentage increase in the mean mossy fibre evoked e.p.s.p. amplitude measured following a high frequency stimulation ($n = 6$ cells) was unaffected by the presence of 100 μM ($n = 4$ cells; $P > 0.05$) or 300 μM L-NAME ($n = 5$; $P > 0.05$).

mossy fibre LTP was not sensitive to the inhibition of NOS with L-NAME. A further increase in the L-NAME concentration to 300 μM did not produce any significant change in the magnitude of LTP (55.6 ± 21.3%; $n = 5$ cells; $P > 0.05$; Figure 1a and b).

In the presence of 100 μM L-NAME, the mean e.p.s.p. amplitude rose by an average of 32.2 ± 11.6% ($n = 5$ cells) following HFS of the fimbrial pathway. This was significantly different when compared to the bath control ($P < 0.05$; Figure 2b). In the presence of 300 μM L-NAME, mean e.p.s.p. amplitude rose by an average 6.2 ± 9.3% ($n = 7$ cells) following HFS (Figure 2a). This higher concentration of L-NAME had a significant effect on the magnitude of LTP when compared to the control rise in e.p.s.p. amplitude in the bath control ($P < 0.05$; Figure 2b). These results suggest that fimbrial LTP, but not mossy fibre LTP, can be modulated by the inhibition of NOS.

Discussion

The induction of NMDA-receptor dependent LTP at the associational-commissural synapses with CA3 pyramidal neurones appears to involve the synthesis of NO in much the same way as the induction of NMDA-receptor dependent LTP at the Schaeffer collateral to CA1 synapses (Gally *et al.*, 1990; Böhme *et al.*, 1991; O'Dell *et al.*, 1991; Schuman & Madison, 1991; Bon *et al.*, 1992; Haley *et al.*, 1992; but see Gribkoff & Lum-Ragan, 1992; Field *et al.*, 1992). The sug-

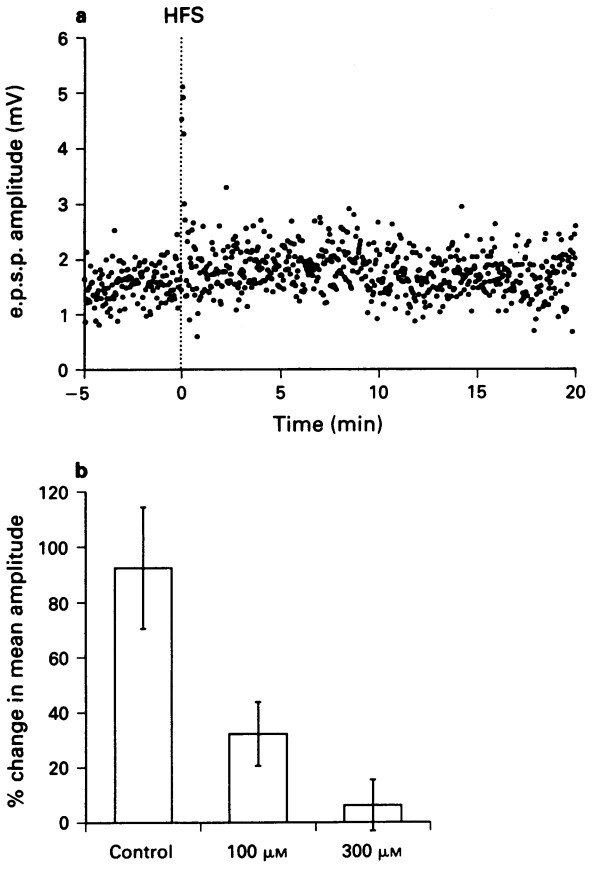

Figure 2 (a) Effect of high frequency stimulation (HFS) of the fimbria on the amplitude of evoked e.p.s.ps in the presence of 300 μM N^{ω}-nitro-L-arginine methyl ester (L-NAME). (b) The percentage increase in the mean fimbrially evoked e.p.s.p. amplitude measured following a high frequency stimulation ($n = 6$ cells) is significantly decreased in the presence of 100 μM L-NAME ($n = 5$ cells; $P < 0.05$) and 300 μM L-NAME ($n = 7$ cells; $P < 0.05$).

gested role for NO in LTP has been that of a putative retrograde messenger, released from a postsynaptic neurone following coincident pre- and postsynaptic activity (Gally *et al.*, 1990). The failure of NOS inhibition to block LTP at the mossy fibre to CA3 pyramidal neurone synapses, at which neither associative nor NMDA-receptor dependent LTP occur, is consistent with the putative link between NMDA receptors, NOS and associative LTP (Gally *et al.*, 1990; East & Garthwaite, 1991).

NOS has been found in hippocampal neurones by use of both the NADPH diaphorase reaction as well as antibodies to NOS-I obtained from the cerebellum. The most intense staining is present in the *stratum radiatum* and subgranular zone of the dentate gyrus, outside the pyramidal cell layer in the *corpus ammonis* as well as in some of the pyramidal cells and their apical dendrites in the CA3 and CA1 regions (Valtschanoff *et al.*, 1992; Vincent & Hope, 1992; Vincent & Kimura, 1992; Schmidt *et al.*, 1992). The nitric oxide-sensitive soluble guanylate cyclase is found in all the CA3 and CA1 pyramidal neurones (Schmidt *et al.*, 1992). Neurones located outside the pyramidal cell layer in the *corpus ammonis* stain both for NOS as well as GABA and are thought to be inhibitory interneurones.

It seems likely that NOS is present in only a proportion of the CA1 and CA3 pyramidal neurones. The presence of guanylate cyclase in all pyramidal neurones suggests that NO released from pyramidal neurones that do contain NOS may act to produce cyclic GMP in other pyramidal neurones that do not contain NOS. The presence of NOS within inhibitory interneurones may indicate that NO could be acting as a paracrine factor, being released from these interneurones to act on neighbouring pyramidal neurones during intense synaptic activity, thereby modulating synaptic transmission in these neurones (Valtschanoff *et al.*, 1992; Vincent & Hope, 1992; Vincent & Kimura, 1992).

The question arises as to how a rapidly diffusing molecule like NO, with a radius of action of around 100 μm (Garthwaite, 1991) may selectively influence the fimbrial but not mossy fibre terminals; if NOS is localized only in the more distal postsynaptic spines of CA3 pyramidal neurones where fimbrial inputs terminate, it may only act on synapses local (within 100 μm) to these sites. Another possibility is that the nitric oxide-sensitive soluble guanylate cyclase occurs only in the associational-commissural but not mossy fibre terminals and NOS is located non-specifically along the CA3 apical dendrite or in some extrasynaptic site. We are at present using antibodies to NOS-I and guanylate cyclase to determine the ultrastructural localization of this enzyme in the apical dendrites of CA3 pyramidal neurones.

Previous work has shown a number of differences in the subcellular mechanisms responsible for the expression of a LTP at the mossy fibre and associational-commissural synapses. In addition, this study suggests the differential presence of a NOS-dependent LTP at these two synaptic pathways which share the same postsynaptic neurone.

References

BLISS, T.V.P. & COLLINGRIDGE, G.L. (1993). A synaptic model of memory – long-term potentiation in the hippocampus. *Nature*, **361**, 31–39.

BÖHME, G.A., BON, C., STUTZMANN, J.-M., DOBLE, A. & BLANCHARD, J.-C. (1991). Possible involvement of nitric oxide in long-term potentiation. *Eur. J. Pharmacol.*, **199**, 379–381.

BON, C., BÖHME, G.A., DOBLE, A., STUTZMANN, J.-M. & BLANCHARD, J.-C. (1992). A role for nitric oxide in long-term potentiation. *Eur. J. Neurosci.*, **4**, 420–424.

DINGLEDINE, R.Y., DODD, Y. & KELLY, J.S. (1980). The *in vitro* brain slice technique as a useful neurophysiological preparation for intracellular recording. *J. Neurosci. Methods*, **2**, 323–362.

EAST, S.J. & GARTHWAITE, J. (1991). NMDA receptor activation in rat hippocampus induces cyclic GMP formation through the L-arginine-nitric oxide pathway. *Neurosci. Lett.*, **123**, 17–19.

ERRINGTON, M.L., LYNCH, M.A. & BLISS, T.V.P. (1987). Long-term potentiation in the dentate gyrus: induction and increased glutamate release blocked by D(−)aminophosphonovalerate. *Neuroscience*, **20**, 279–284.

FIELD, A.C., REDMAN, S.J. & STRICKER, C. (1992). NMDA receptor activation at synapses on CA1 neurons is not necessary for the induction of LTP. *Soc. Neurosci. Abstr.*, **18**, 1347.

GALLY, J.A., READ-MONTAGUE, P., REEKE Jr., G.N. & EDELMAN, G.M. (1990). The NO hypothesis: possible effects of a short lived, rapidly diffusible signal in the development and function of the nervous system. *Proc. Natl. Acad. Sci. U.S.A.*, **87**, 3547–3551.

GARTHWAITE, J. (1991). Glutamate, nitric oxide and cell-cell signalling in the nervous system. *Trends Neurosci.*, **14**, 60–67.

GRIBKOFF, V.K. & LUM-RAGAN, J.T. (1992). Evidence for nitric oxide synthase inhibitor-sensitive and insensitive hippocampal synaptic potentiation. *J. Neurophysiol.*, **68**, 639–642.

HALEY, J.E., WILCOX, G.L. & CHAPMAN, P.F. (1992). The role of nitric oxide in hippocampal long-term potentiation. *Neuron*, **8**, 211–216.

HARRIS, E.W. & COTMAN, C.W. (1986). Long-term potentiation of guinea pig mossy fibre responses is not blocked by N-methyl D-aspartate antagonists. *Neurosci. Lett.*, **70**, 132–137.

JAFFE, D. & JOHNSTON, D. (1990). Induction of long-term potentiation at hippocampal mossy-fiber synapses follows a hebbian rule. *J. Neurophysiol.*, **64**, 948–960.

JOHNSTON, D., WILLIAMS, S., JAFFE, D. & GRAY, R. (1992). NMDA-receptor-independent long-term potentiation. *Annu. Rev. Physiol.*, **54**, 489–505.

KATSUKI, H., KANEKO, S. & SATOH, M. (1992). Involvement of postsynaptic G proteins in hippocampal long-term potentiation. *Brain Res.*, **581**, 108–114.

KATSUKI, H., KANEKO, S., TAJIMA, A. & SATOH, M. (1991). Separate mechanisms of long-term potentiation in two input systems to CA3 pyramidal neurons of rat hippocampal slices as revealed by the whole-cell patch-clamp technique. *Neurosci. Res.*, **12**, 393–402.

MONAGHAN, D.T. & COTMAN, C.W. (1985). Distribution of N-methyl-D-aspartate sensitive L-[3H]glutamate-binding sites in the rat brain. *J. Neurosci.*, **5**, 2909–2919.

O'DELL, T.J., HAWKINS, R.D., KANDEL, E.R. & ARANCIO, O. (1991). Tests of the roles of 2 diffusible substances in long-term potentiation – evidence for nitric oxide as a possible early retrograde messenger. *Proc. Natl. Acad. Sci. U.S.A.*, **88**, 11285–11289.

SCHMIDT, H.H.H.W., GAGNE, G.D., NAKANE, M., POLLOCK, J.S., MILLER, M.F. & MURAD, F. (1992). Mapping of neural nitric oxide synthase in the rat suggests frequent co-localization with NADPH diaphorase but not with soluble guanylyl cyclase, and novel paraneural functions for nitrinergic signal transduction. *J. Histochem. Cytochem.*, **40**, 1439–1456.

SCHUMAN, E.M. & MADISON, D.V. (1991). A requirement for the intercellular messenger nitric oxide in long-term potentiation. *Science*, **254**, 1503–1506.

VALTSCHANOFF, J.G., KHARAZIA, V.N. & WEINBERG, R.J. (1992). Neurons containing nitric oxide synthase in rat hippocampus. *Soc. Neurosci. Abstr.*, **18**, 639.

VINCENT, S.R. & HOPE, B.T. (1992). Neurons that say NO. *Trends Neurosci.*, **15**, 108–113.

VINCENT, S.R. & KIMURA, H. (1992). Histochemical mapping of nitric oxide synthase in the rat brain. *Neuroscience*, **46**, 755–784.

ZALUTSKY, R.A. & NICOLL, R.A. (1990). Comparison of two forms of long-term potentiation in single hippocampal neurones. *Science*, **248**, 1619–1624.

ZALUTSKY, R.A. & NICOLL, R.A. (1992). Mossy fiber long-term potentiation shows specificity but no apparent cooperativity. *Neurosci. Lett.*, **138**, 193–197.

(Received April 23, 1993
Revised October 8, 1993
Accepted October 20, 1993)

Br. J. Pharmacol. (1994), **111**, 525–532

Importance of inositol (1,4,5)-trisphosphate, intracellular Ca^{2+} release and myofilament Ca^{2+} sensitization in 5-hydroxytryptamine-evoked contraction of rabbit mesenteric artery

Joanna M. Seager, [1]Timothy V. Murphy & [2]Christopher J. Garland

Department of Physiology and Pharmacology, University of Southampton, Bassett Crescent East, Southampton SO9 3TU

1 Small strips from third-order branches of rabbit mesenteric artery (approximately 150–200 μM wide) contracted in response to noradrenaline (10 μM) or 5-hydroxytryptamine (5-HT; 10 μM) in oxygenated Krebs solution containing 2.5 mM Ca^{2+}. In a Ca^{2+}-free mock intracellular solution (0 Ca^{2+} plus 0.2 mM EGTA), noradrenaline (10 μM) and caffeine (10 mM) induced only a single, transient contraction in artery strips, while 5-HT (10 μM) failed to induce any response.

2 In strips of mesenteric artery which had been permeabilized with *Staphylococcus* α-toxin and bathed in Ca^{2+}-free mock intracellular solution, noradrenaline (10 μM), caffeine (10 mM) and D-*myo*-inositol (1,4,5)-trisphosphate (IP_3, 100 μM), but not 5-HT (10 or 100 μM) induced a transient contraction. In contrast to the non-permeabilized strips, contractions to noradrenaline, caffeine and IP_3 were restored by prior incubation (10 min) in solution containing 0.08 μM Ca^{2+}. The contractions to noradrenaline and IP_3 in permeabilized muscle strips required the presence of 100 μM guanosine 5′-triphosphate (GTP), although in the absence of Ca^{2+}, GTP alone did not induce contraction.

3 Exposure of permeabilized mesenteric artery strips to IP_3 significantly reduced the subsequent contractile responses to caffeine. Contractile responses to caffeine and IP_3 were abolished by the Ca^{2+}-ATPase inhibitor, thapsigargin (1 μM).

4 Ca^{2+} (0.1–10 μM) induced concentration-dependent contraction in permeabilized artery strips. In strips which were submaximally contracted with 0.5 μM Ca^{2+}/100 μM GTP, the subsequent addition of 5-HT (10 μM) stimulated further contraction. The protein kinase C inhibitor, H-7 (1 μM) abolished the 5-HT/GTP-induced contraction, but did not alter the contraction to Ca^{2+}.

5 In non-permeabilized, endothelium-denuded segments of rabbit mesenteric artery bathed in Ca^{2+}-replete Krebs solution, noradrenaline (10 μM) stimulated a rapid, transient accumulation of IP_3. 5-HT (100 μM) failed to stimulate IP_3 accumulation during exposure periods of up to 5 min. 5-HT (100 μM) did stimulate IP_3 accumulation if the external K^+ concentration was raised (to around 25 mM). This concentration of K^+ alone did not stimulate IP_3 production and the 5-HT-stimulated IP_3 accumulation in the presence of elevated extracellular [K^+] was abolished by the α_1-adrenoceptor antagonist, prazosin (0.1 μM).

6 These results suggest that intracellular Ca^{2+} release does not play an important role in 5-HT-induced smooth muscle contraction in the rabbit mesenteric artery. This is despite the fact that a significant intracellular Ca^{2+} pool is present in these cells, which can be discharged by either noradrenaline or IP_3. However, 5-HT did stimulate smooth muscle contraction in the presence of raised intracellular calcium, suggesting that a component of the contraction to 5-HT will reflect an increase in myofilament Ca^{2+} sensitivity, possibly due to the activation of protein kinase C.

Keywords: 5-Hydroxytryptamine; vascular smooth muscle; permeabilization; *Staphylococcus aureus* α-toxin; inositol (1,4,5)-trisphosphate; myofilament Ca^{2+} sensitization; protein kinase C

Introduction

5-Hydroxytryptamine (5-HT) is a potent vasoconstrictor in a range of different blood vessels, and has been implicated in vascular disorders such as stroke, cerebral vasospasm and angina pectoris (Vanhoutte, 1990; Saxena & Villalón, 1990). The intracellular mechanisms involved in 5-HT-induced contraction of vascular smooth muscle are not clear (see Feniuk & Humphrey, 1989). 5-HT is capable of stimulating smooth muscle contraction in some blood vessels in the absence of extracellular Ca^{2+}, such as the rabbit aorta and bovine coronary artery (Ratz & Flaim, 1984), and the rabbit ear artery (McCalden & Bevan, 1981). 5-HT has also been shown to stimulate phosphatidylinositide hydrolysis, D-*myo*-inositol (1,4,5)-trisphosphate (IP_3) production and intracellular Ca^{2+} release in smooth muscle cells from large arteries, including the rat aorta (Nakaki *et al.*, 1985; Roth *et al.*, 1986; Cohen & Wittenauer, 1987) and aortic myocytes (Cory *et al.*, 1986; Doyle *et al.*, 1986), the rat tail artery (Berta *et al.*, 1986) and the rabbit aorta (Murphy & Garland, 1993). These data suggest that 5-HT-induced contraction of vascular smooth muscle cells involves, at least in part, IP_3-mediated release of intracellular Ca^{2+}.

However, contraction to 5-HT in other vascular preparations appears to be less dependent on intracellular Ca^{2+} release. 5-HT-induced contractions of rabbit saphenous (Towart, 1981) and basilar arteries (Towart, 1981; Cain & Nicholson, 1989; Clark & Garland, 1993), pig coronary artery (Cain & Nicholson, 1989) and dog saphenous vein (Sumner *et al.*, 1992) were almost completely abolished by the removal of extracellular Ca^{2+}, or by Ca^{2+}-channel antagonists. Although 5-HT stimulated phosphoinositide hydrolysis in the rat tail artery (Berta *et al.*, 1986), 5-HT-induced

[1] Present address and address for correspondence(2): Department of Pharmacology, University of Bristol, University Walk, Bristol BS8 1TD

contractions in this vessel were also abolished by the removal of extracellular Ca^{2+}. Furthermore, 5-HT-evoked contraction in the rabbit basilar artery occurred in the absence of phosphatidylinositide hydrolysis (Clark & Garland, 1991).

The main aim of the present study was to examine the importance of intracellular Ca^{2+} release in the 5-HT-induced contraction of smooth muscle cells in third-order branches of the rabbit mesenteric artery. These observations were correlated with experiments studying the ability of 5-HT to stimulate IP_3 production. The ability of 5-HT to release intracellular Ca^{2+} was investigated in small strips of mesenteric artery in which the smooth muscle cells had been permeabilized with *Staphylococcus aureus* α-toxin. The α-toxin forms small pores in the plasma membrane of cells (diam. 2–3 nm), allowing free entry of inorganic ions and low molecular weight molecules (<1,000) across the cell membrane, while leaving plasma-membrane receptors functionally coupled to their cellular effector mechanisms (Nishimura *et al.*, 1988; Kitazawa *et al.*, 1989). This technique has the further advantage that the free intracellular calcium concentration can be precisely controlled. The potential ability of 5-HT to stimulate IP_3 accumulation was measured directly by a competition binding assay first described by Challiss *et al.* (1988). Some of these observations have been presented in a preliminary form (Seager & Garland, 1992ab).

Methods

Preparation of arterial strips

New Zealand white rabbits of either sex (1.8–2.5 kg) were anaesthetized with sodium pentobarbitone (60 mg kg^{-1}, i.v.) and killed by rapid exsanguination. A segment of lower ileum plus attached mesentery was removed and a third-order branch of the mesenteric artery dissected free and placed in Krebs solution bubbled with 95% O_2/5% CO_2. Arteries were cleaned of adhering tissue and cut into segments approximately 2 mm long. The intimal surface of the vessel was gently rubbed with tungsten wire to facilitate removal of the endothelium. Helical strips of mesenteric artery approximately 150–200 μM wide and 1–2 mm in length were cut and snared at each end by gold-plated tungsten wire and held between two stainless steel tubes. One tube was attached to a micrometer, the other to a force transducer (Harvard Instruments, U.S.A.). The tissue was bathed in 1 ml of either Krebs solution or a mock intracellular solution (see below for composition), bubbled with 95% O_2/5% CO_2 at room temperature (20–25°C), to maintain the preparation in a viable form for periods of up to 3 h.

Permeabilization experiments

The viability of individual strips was tested by inducing contraction to either noradrenaline (10 μM) or 5-HT (10 μM) in Krebs solution. The strip was then placed in mock intracellular solution (composition mM: $MgCl_2$ 7, Na_2ATP 5, potassium proprionate 120, phosphocreatinine 5 and HEPES buffer 5) and permeabilized by incubation with *Staphylococcus aureus* α-toxin (2500 haemolytic units ml^{-1}) for 15–20 min. Permeabilization was assessed by the ability of Ca^{2+} to stimulate contraction in concentrations (0.01–10 μM) which had no effect before permeabilization. The free [Ca^{2+}] of the intracellular solution was controlled by either mixing appropriate quantities of solutions containing 10 mM EGTA and 10 mM CaEGTA, or by adding $CaCl_2$ directly to a 0.2 mM EGTA solution. A computer programme adapted from Fabiato & Fabiato (1979) by Dr G.D. Smith (Univ. Glasgow) was used to calculate the equilibrium concentrations of metal ions and affinity constants relating to ionic strength and pH. Affinity constants for H^+, Ca^{2+} and Mg^{2+} binding to EGTA were taken from Smith & Miller (1984). The pH of the intracellular solution was maintained at 7.00; adjustments were made with KOH.

D-myo-Inositol (1,4,5)-trisphosphate (IP_3) measurements

The accumulation of IP_3 was measured by the radioreceptor assay described by Challiss *et al.* (1988). Rabbit mesenteric arteries were dissected as described above and incubated in microfuge tubes containing 125 μl Krebs solution which was maintained at 37°C and regularly bubbled with 95% O_2/5% CO_2. Drugs were added in 25 μl volumes and the reaction stopped after periods of 5, 15, 30, 60 or 300 s by the addition of 150 μl 1 M ice-cold trichloroacetic acid. Prazosin and/or high [K^+] solution, where present, were added 20 min before the addition of an agonist. The tubes were immediately placed on ice and left for approximately 20 min. An aliquot of 250 μl was taken, and the arteries dissolved in 1 M NaOH for subsequent protein determination by the method of Lowry *et al.* (1951). The aliquots were washed with 5 × 2 volumes water-saturated diethylether. Further aliquots (100 μl) were then taken, to which were added 35 μl 60 mM $NaHCO_3$ and 25 μl 30 mM Na_2EDTA. The samples were frozen for later IP_3 assay.

Triplicate 30 μl samples of either the aliquots or standard samples (0.03–9 pmol IP_3) were added to a microfuge tube together with 30 μl D-*myo*-[^{3}H]-inositol (1,4,5)-trisphosphate (approx. 8,000 d.p.m.), 30 μl incubation buffer (100 mM Tris HCl, 4 mM Na_2EDTA, pH = 8) and 30 μl of a binding protein derived from bovine adrenal cortex (approx. 20 mg protein ml^{-1}; see Challiss *et al.*, 1988). The assay mixture was left for 30 min on ice with occasional vortexing. The protein was separated by vacuum filtration using Whatman GF/B filter paper, and washed with 3 × 3 ml 25 mM Tris/HCl/1 mM Na_2EDTA (pH = 8). Scintillant was added to the filter paper samples (Optiphase Hisafe; LKB Wallac, Loughborough, Leics.), which were stored overnight and then subjected to liquid scintillation counting.

Statistics

The contractile force developed by arterial strips is expressed in mN. IP_3 mass accumulation was calculated as pmol IP_3 mg^{-1} protein. Results are expressed as mean ± s.e.mean. Data were analysed by Student's unpaired *t* test (C-Stat, Cherwell Scientific, Oxford, Ox.). Values of $P<0.05$ were taken to indicate a significant difference between groups of data.

Drugs and materials

The composition of the Krebs solution was (mM): NaCl 121.8, $NaHCO_3$ 25.5, KCl 5.2, $MgSO_4$ 1.2, $CaCl_2$ 2.5, disodium EDTA 0.027, ascorbate 0.114 and D-glucose 9.4. Drugs used were: D-*myo*-[^{3}H]-inositol (1,4,5)-triphosphate (specific activity 44 Ci $mmol^{-1}$, radioactive concentration 10 μCi ml^{-1}; Amersham, Aylesbury, Bucks.); D-*myo*-inositol (1,4,5)-trisphosphate (potassium salt; Semat, U.K.); crude *Staphylococcus aureus* α-toxin (Calbiochem, U.S.A.); prazosin hydrochloride (Pfizer, U.S.A.); potassium propionate (BDH, Poole, Dorset); (−)-arterenol bitartrate (noradrenaline); 5-hydroxytryptamine creatinine sulphate; caffeine; thapsigargin; guanosine 5′-triphosphate, tris salt (GTP); disodium adenosine 5′-triphosphate (ATP); creatinine phosphate (sodium salt); N-[2-hydroxyethyl]piperazine-*N*′-[2-ethanesulphonic acid] (HEPES); ethyleneglycol-*bis*-(β-aminoethyl ether) *N,N,N*′,-tetraacetic acid (EGTA); tris[hydroxymethyl]aminomethane (TRIZMA base), 1-(5-isoquinolinesulphonyl)-2-methyl piperazine (H7); all from Sigma, Poole, Dorset. Stock solutions of drugs were made in either Krebs or mock intracellular solution, except for prazosin which was initially dissolved in a solution comprising 2% glycerol, 33%

D-glucose solution (5% w/v) and 65% deionized water, and H-7 and thapsigargin, which were initially dissolved in dimethylsulphoxide (DMSO).

Results

Contractile responses to 5-HT, noradrenaline and caffeine in non-permeabilized strips of rabbit mesenteric artery

The ability of either 5-HT or noradrenaline to stimulate contraction was assessed in strips of mesenteric artery bathed in Krebs solution containing 2.5 mM Ca^{2+}. 5-HT (10 μM) induced a contraction of 0.26 ± 0.02 mN in 20 of 25 preparations. Noradrenaline (10 μM) induced a contraction of 0.27 ± 0.04 mN ($n = 8$). Artery strips which did not contract in Krebs solution in response to either noradrenaline or 5-HT were not used in subsequent experiments.

In Ca^{2+}-free mock intracellular solution, 5-HT (10 or 100 μM) failed to induce any contraction ($n = 4$; data not shown). In contrast, noradrenaline induced a transient contraction under these Ca^{2+}-free conditions (Figure 1a; Table 1). After incubation with 0.08 μM Ca^{2+}, the subsequent application of noradrenaline did not stimulate any response (Figure 1a). Caffeine also induced a transient contraction in Ca^{2+}-free solution (Figure 2a; Table 1). Subsequent application of caffeine, after incubation in a 0.08 μM Ca^{2+}-containing solution, evoked either a small contraction or had no measurable effect. However, in all cases a third application of caffeine failed to induce a contraction in any of the strips (Figure 2a). Contractions to caffeine could be repeated if the artery strip was incubated in intracellular solution containing 1 mM Ca^{2+} for 10 min between each exposure ($n = 4$; data not shown).

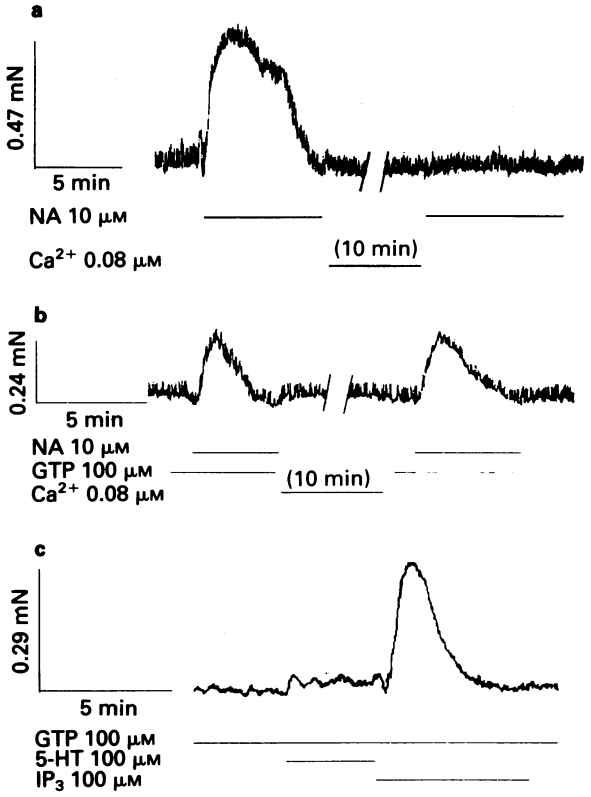

Figure 1 Representative traces of responses of rabbit mesenteric artery smooth muscle to noradrenaline (NA), 5-hydroxytryptamine (5-HT) and inositol (1,4,5)-trisphosphate (IP_3) in a Ca^{2+}-free solution (0 added and Ca^{2+} plus 0.2 mM EGTA). (a) Contraction in non-permeabilized tissue ($n = 6$); (b) and (c), responses in smooth muscle permeabilized with *Staphylococcus aureus* α-toxin- ($n = 6$, $n = 8$, respectively). GTP is guanosine 5'-triphosphate. Lines under the traces indicate the addition of the compounds.

Contractile responses to caffeine, IP_3, noradrenaline and 5-HT in strips of rabbit mesenteric artery permeabilized with Staphylococcus α-*toxin*

After incubation with *Staphylococcus* α-toxin, artery strips contracted when exposed to Ca^{2+} in concentrations above 0.1 μM, with 10 μM Ca^{2+} stimulating a maximum contraction (Figure 3, Table 1). In strips not incubated with α-toxin, the preparation did not contract in the presence of 10 μM Ca^{2+}. Caffeine (10 mM) induced a single, transient contraction in permeabilized artery strips in Ca^{2+}-free intracellular solution (0 added Ca^{2+} plus 0.2 mM EGTA: Figure 2b, Table 1). These contractions could be repeated only if the tissue was incubated in intracellular solution containing 0.08 μM Ca^{2+} for 10 min between each subsequent application of caffeine (Figure 2b).

IP_3 (100 μM), in the presence of GTP (100 μM), also caused a transient contraction in α-toxin-permeabilized mesenteric artery strips bathed in Ca^{2+}-free intracellular solution (Figure 2c, Table 1). Contraction could be restored if the tissue was incubated with intracellular solution containing 0.08 μM Ca^{2+} for 10 min before each subsequent application of IP_3 (Figure 2c). GTP was applied 3 min before the addition of IP_3 and did not by itself induce contraction (Figure 2c). IP_3 failed to stimulate smooth muscle contraction in the absence of GTP (data not shown).

In some experiments, permeabilized strips contracted by caffeine were then incubated with 0.08 μM Ca^{2+} for 10 min, and exposed to 100 μM IP_3/100 μM GTP. Immediately following the removal of IP_3/GTP, without any re-exposure to Ca^{2+}, caffeine was re-applied. The second caffeine-induced contraction was now significantly reduced when compared to the initial contraction to caffeine (following the same protocol but without the addition of IP_3; 43.1 ± 17.2%, $P < 0.05$, Student's unpaired t test, $n = 4$; Figure 2d). In two further experiments, this protocol was reversed. Contraction to 100 μM IP_3 was followed by incubation with Ca^{2+} and then stimulation with caffeine. Without additional incubation in a Ca^{2+} containing solution, the subsequent addition of 100 μM

Table 1 Contractile effects of Ca^{2+}, caffeine, inositol (1,4,5)-trisphosphate (IP_3) and noradrenaline in non-permeabilized artery strips and strips permeabilized with *Staphylococcus aureus* α-toxin

Agent	*Force* (mN)	*Force* (mN)	*Force* (% Ca^{2+})	n
	Non-perm.	Perm.		
Ca^{2+} (10 μM)	0	0.54 ± 0.03	100	10
Caffeine (10 mM)	0.42 ± 0.03	0.43 ± 0.02	64 ± 3	8
IP_3 (100 μM)	–	0.34 ± 0.05	39 ± 18	6
Noradrenaline (10 μM)	0.31 ± 0.06	0.34 ± 0.05	56 ± 8	6

Artery strips were bathed in mock intracellular solution containing 0 Ca^{2+} plus 0.2 mM EGTA. Values represent the mean ± s.e.mean. Contraction is expressed in either mN, or % of the contractile force evoked by 10 μM Ca^{2+}.

IP_3 failed to induce a measurable response. Incubation of permeabilized artery strips with the endoplasmic reticulum Ca^{2+}-ATPase inhibitor, thapsigargin (1 μM) for 30 min prior to incubation with Ca^{2+} abolished any subsequent contractile responses to either caffeine (Figure 2b) or IP_3 (Figure 2c).

Before exposure of permeabilized strips to either noradrenaline or 5-HT, 10 mM caffeine was applied to deplete the Ca^{2+} stored in any remaining cells which may not have been permeabilized. The strips were then incubated with 0.08 μM Ca^{2+}-intracellular solution, a concentration which did not reload Ca^{2+} stores of non-permeabilized cells to any significant extent in this study, but was sufficient to reload the caffeine and IP_3-sensitive intracellular Ca^{2+} stores of permeabilized cells (see above). This procedure ensured that subsequent contractile responses represented those of permeabilized cells only. Following this manipulation, noradrenaline (10 μM), in the presence of GTP (100 μM), caused a transient contraction of α-toxin-permeabilized mesenteric artery strips in Ca^{2+}-free intracellular solution (Figure 1b; Table 1). These contractions were consistently reproducible providing the tissue was incubated with an in-

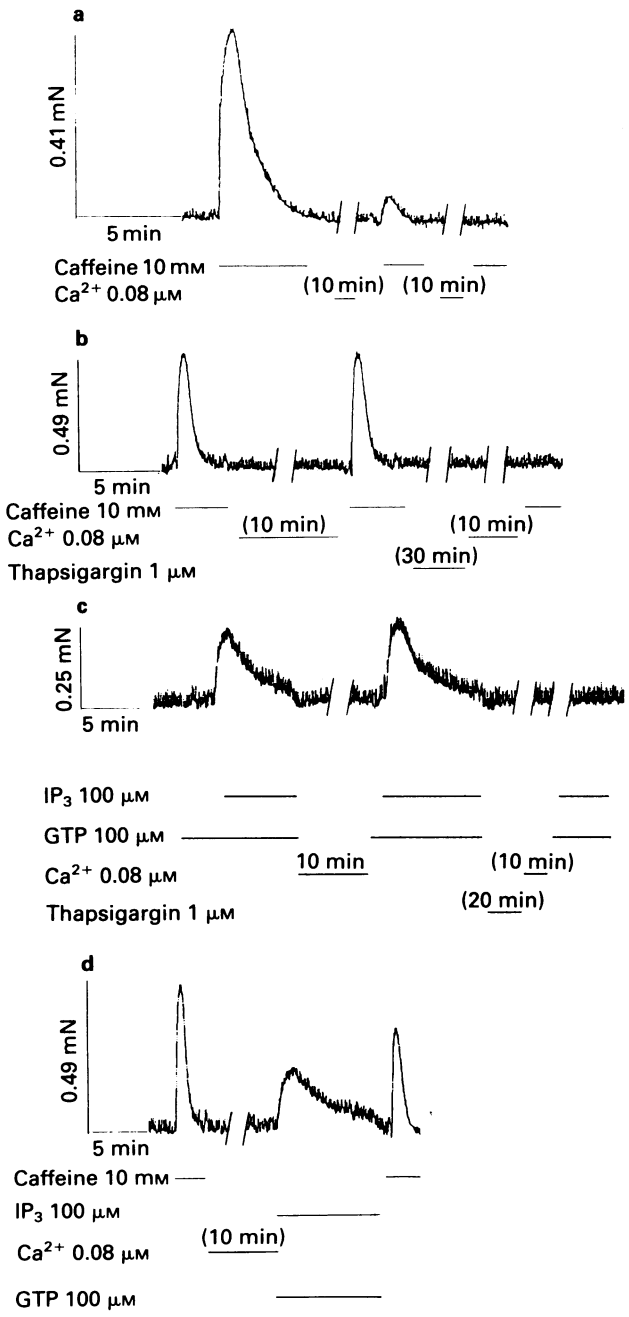

Figure 2 Representative traces of responses of rabbit mesenteric artery smooth muscle to caffeine and inositol (1,4,5)-trisphosphate (IP_3) in a Ca^{2+}-free solution (0 added Ca^{2+} plus 0.2 mM EGTA). (a) Contraction in non-permeabilized tissue ($n = 5$); (b) (c) and (d), responses in smooth muscle permeabilized with *Staphylococcus aureus* α-toxin ($n = 8$, $n = 6$, $n = 4$ respectively). GTP is guanosine 5'-triphosphate. Lines under the traces indicate the addition of the compounds.

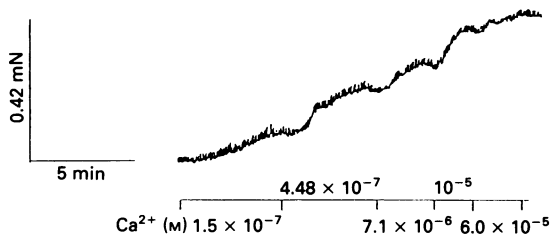

Figure 3 Representative trace of responses of rabbit mesenteric artery smooth muscle permeabilized with *Staphylococcus aureus* α-toxin to cumulative addition of increasing concentrations of Ca^{2+}. The highest concentration of Ca^{2+} applied in this experiment was followed by a contraction of 0.54 ± 0.03 mN ($n = 10$).

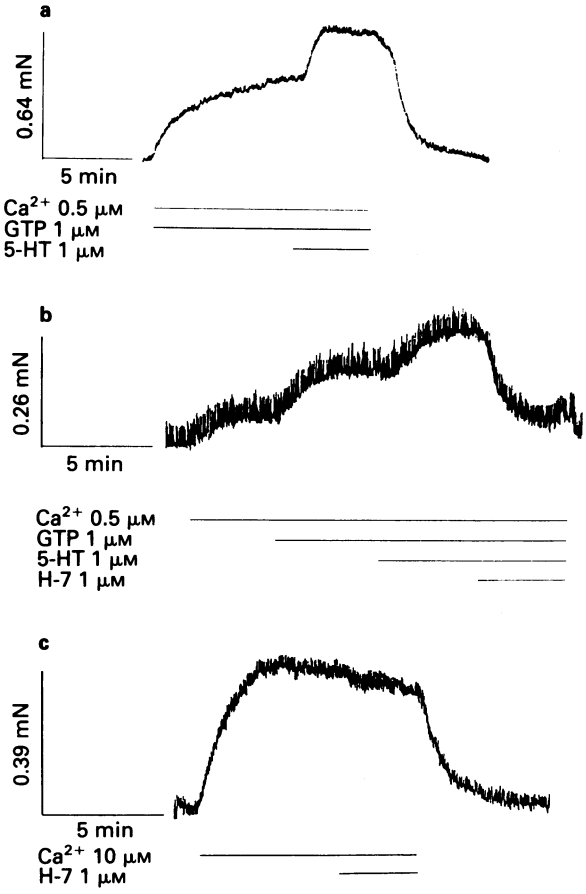

Figure 4 Representative traces of responses of rabbit mesenteric artery smooth muscle permeabilized with *Staphylococcus aureus* α-toxin to Ca^{2+}, guanosine 5' trisphosphate (GTP) and 5-hydroxytryptamine (5-HT), in the presence of thapsigargin (1 μM) and 10 mM EGTA. (a) Effect of 5-HT on preparations sub-maximally contracted with Ca^{2+}/GTP ($n = 4$); (b) effect of the protein kinase C inhibitor, H-7, on Ca^{2+}/GTP/5-HT contractions ($n = 4$); (c) effect of H-7 on contractions induced by Ca^{2+} alone ($n = 4$). Lines under the traces indicate the addition of compounds.

tracellular solution containing 0.08 μM Ca^{2+} for 10 min between each application of noradrenaline (Figure 1b). In the absence of GTP, the contractile response to noradrenaline was either greatly reduced or abolished (data not shown).

Artery strips which had previously responded to 5-HT before permeabilization were incubated in intracellular solution containing 0.08–10 μM Ca^{2+}, for periods of up to 30 min. Following the removal of the Ca^{2+}-containing solution the subsequent addition of 5-HT (100 μM), in the presence of GTP (100 μM), failed to induce any measurable contraction ($n = 8$; Figure 1c). However, 100 μM IP_3 applied immediately after the washout of 5-HT in these experiments, was able to evoke a transient contraction, showing that viable IP_3-releasable Ca^{2+} stores were present in these cells (Figure 1c).

Effect of 5-HT on α-toxin-permeabilized strips of rabbit mesenteric artery sub-maximally contracted with Ca^{2+}

Permeabilized strips of mesenteric artery were submaximally contracted by 0.5 μM Ca^{2+}/100 μM GTP (0.42 ± 0.003 mN, $n = 13$). Subsequent application of 5-HT (1 μM) induced a further increase in tension (25.4% ± 1.5% of Ca^{2+}/GTP contraction, Figure 4a). The increase induced by 5-HT was not significantly different if the release of internal Ca^{2+} stores was prevented by incubation with thapsigargin and 10 mM EGTA (21.0 ± 2.7% of Ca^{2+}/GTP induced contraction, $P > 0.05$). The average amplitude of the contraction induced in response to 0.5 μM Ca^{2+}/100 μM GTP was 0.42 ± 0.05 mN ($n = 4$) in these latter experiments. The protein kinase C inhibitor, H-7 (1 μM) markedly reduced Ca^{2+}/GTP/5-HT-induced contractions (22.6 ± 7.89% of contraction in absence of H-7; $P < 0.05$, Student's unpaired t test, $n = 4$; Figure 4b), but did not significantly reduce similar-sized contraction induced by 10 μM Ca^{2+} alone (Ca^{2+} alone, 0.46 ± 0.06 mN; Ca^{2+} plus H-7, 0.46 ± 0.06 mN, $P > 0.05$, Student's unpaired t test, $n = 4$ for each; Figure 4c).

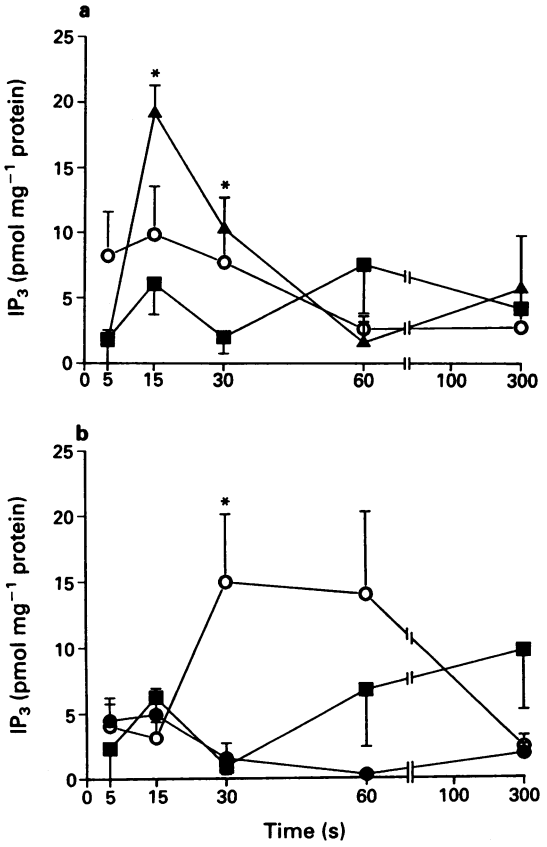

Figure 5 Effect of noradrenaline and 5-hydroxytryptamine (5-HT) on inositol (1,4,5)-trisphosphate (IP_3) mass accumulation in endothelium-denuded segments of rabbit mesenteric artery. Artery segments were bathed in normal Krebs solution (a; see Methods) or Krebs solution containing 25.7 mM K^+ (b). Points represent the mean ± s.e. mean. *Represents a significant increase in IP_3 accumulation compared with the corresponding basal level at the same time point ($P < 0.05$, Student's unpaired t test). (■) Basal levels (a, $n = 5$; b, $n = 6$); (▲) noradrenaline (10 μM, $n = 5$); (○) 5-HT (100 μM, a, $n = 10$; b, $n = 7$); (●) 5-HT (10 μM, $n = 6$).

Effect of 5-HT and noradrenaline on IP_3 accumulation in rabbit mesenteric artery

In endothelium-denuded segments of rabbit mesenteric artery, incubated in a Ca^{2+}-containing Krebs solution, 5-HT (100 μM) failed to stimulate a significant increase in IP_3 accumulation above basal levels, at any time during the 5 min following initial exposure to the agonist (Figure 5a). In contrast, noradrenaline (10 μM) induced a rapid and transient accumulation of IP_3, which peaked 15 s after the addition of noradrenaline and then declined to basal levels over a period of 1 min from the initial application (Figure 5a). In mesenteric arteries bathed in Krebs solution containing 25.7 mM KCl, 5-HT (100 μM) did stimulate a significant increase in IP_3 accumulation within 30 s of initial exposure (Figure 5b). The high K^+ solution alone did not stimulate IP_3 accumulation (Figure 5b). The 5-HT-induced increase was abolished by the α_1-adrenoceptor antagonist prazosin (0.1 μM). In 25.7 mM K^+ Krebs solution, basal IP_3, 0.92 ± 0.52 pmol mg^{-1} protein ($n = 6$): in the presence of 5-HT, 14.96 ± 5.15 pmol mg^{-1} protein ($n = 7$; significant, $P < 0.05$, Student's unpaired t test). In the presence of prazosin, basal IP_3 was 1.90 ± 1.19 pmol mg^{-1} protein ($n = 7$), and prazosin together with 5-HT, 4.85 ± 2.81 pmol mg^{-1} protein ($n = 6$; NS, $P > 0.05$, Student's unpaired t test). In a lower concentration, 5-HT (10 μM) failed to stimulate IP_3 accumulation even during incubation with high [K^+] Krebs solution (Figure 5b).

Discussion

The present study utilized *Staphylococcus* α-toxin-permeabilized smooth muscle cells in the rabbit mesenteric artery to investigate the role of intracelluar Ca^{2+} release in 5-HT-induced contraction. Following incubation with α-toxin, the artery strips contracted when exposed to Ca^{2+} concentrations equivalent to those normally encountered in the cytoplasm of activated, intact cells (see Walsh, 1991). Incubation in physiological solutions containing a low concentration of Ca^{2+}, below the threshold for contraction, allowed repeatable contractions to be evoked to noradrenaline, caffeine or exogenous IP_3. These concentrations of Ca^{2+} did not enable repetitive agonist-induced contractions in non-permeabilized smooth muscle cells. These data indicate that the α-toxin had successfully permeabilized the majority of smooth muscle cells in the artery strips used in this study.

5-HT caused contraction of strips of mesenteric artery in the presence of Ca^{2+}, but did not contract either non-permeabilized or permeabilized artery strips under Ca^{2+}-free conditions. These results suggest that the 5-HT-induced contraction of smooth muscle cells in this artery does not involve intracellular Ca^{2+} release to any significant extent. The inability of 5-HT to contract artery strips in the absence of extracellular Ca^{2+} was not due to a depletion of the intracellular Ca^{2+} store as caffeine, which stimulates intracellular Ca^{2+} release (Itoh *et al.*, 1981), evoked a similar-sized contraction in both intact and permeabilized strips. In addition, the endogenous Ca^{2+} releasing agent IP_3 (Berridge, 1987) caused contraction in permeabilized artery strips, including strips which failed to respond to 5-HT. Caffeine and IP_3 evoked only a single, transient contraction under Ca^{2+}-free conditions, however contraction could be repeated if the strips were incubated in Ca^{2+} containing solution before a

further application of either caffeine or IP_3. Furthermore, contractions to caffeine or IP_3 were abolished by thapsigargin, a selective inhibitor of endoplasmic reticulum Ca^{2+}-ATPase, the enzyme responsible for Ca^{2+}-uptake into this organelle (Thastrup, 1990). These results strongly indicate that caffeine- and IP_3-induced contractions were due to Ca^{2+} release from the endoplasmic reticulum.

The magnitude of the contraction induced by caffeine applied immediately after an IP_3-induced contraction was less than half that of the control contraction to caffeine alone, and IP_3 failed to induce contraction when applied immediately after caffeine. This indicates that IP_3 and caffeine can release Ca^{2+} from the same intracellular pool. Previous studies have attempted to establish the relationship between caffeine and IP_3-sensitive Ca^{2+}-pools in vascular smooth muscle (Saida & van Breemen, 1984; Kanaide *et al.*, 1987; van Breemen & Saida, 1989; Iino, 1990) and other smooth muscle preparations (Iino, 1990). However, as saturating concentrations of IP_3 and caffeine were not used in the present study, the relative size of each pool in the mesenteric artery smooth muscle cells cannot be inferred from these data.

The possibility that exposure to α-toxin disrupted the 5-HT receptor-effector coupling mechanism is also unlikely, as noradrenaline was still able to induce contraction in the absence of extracellular Ca^{2+}, in both permeabilized and non-permeabilized strips. Studies in permeabilized vascular smooth muscle of the rabbit mesenteric artery (Hashimoto *et al.*, 1986; Nishimura *et al.*, 1988; Itoh *et al.*, 1992) and other smooth muscle cells (Kitazawa *et al.*, 1989; Nishimura *et al.*, 1989; Crichton & Smith, 1990) have shown that noradrenaline stimulates contraction through α_1-adrenoceptors, which stimulate IP_3 accumulation and intracellular Ca^{2+} release.

In the absence of GTP, the contraction to noradrenaline in permeabilized preparations of the mesenteric artery was either greatly reduced or abolished, and IP_3 failed to induce any contraction. Receptor-effector coupling in most cells is mediated by a family of GTP-binding proteins, or G-proteins (Gilman, 1987). Under normal conditions the intracellular concentration of GTP (0.1–0.3 mM; Gill *et al.*, 1988) is not a limiting factor in the receptor-mediated response; however, the membrane pores formed by α-toxin are large enough to allow GTP to escape from the cytoplasm. Contractions to noradrenaline in earlier studies in the rabbit mesenteric artery also required GTP, and were attenuated by an inhibitor of G-protein activation, GDP-β-S (Nishimura *et al.*, 1989; 1990). Contractions to IP_3 also required the presence of exogenous GTP, or the non-hydrolyzable GTP analogue GppNHp (Saida *et al.*, 1988), although other studies have been able to demonstrate IP_3-evoked contractions in the absence of exogenous GTP (Hashimoto *et al.*, 1986; Iino 1987; 1990; Crichton & Smith, 1990). It is possible that sufficient endogenous GTP was present in these studies to maintain IP_3-induced Ca^{2+} release. As all experiments in the current study involving 5-HT were performed in the presence of added GTP, it is very unlikely that a loss of G-protein coupling explains the inability of 5-HT to stimulate contraction in the permeabilized strips.

The idea that 5-HT-induced contraction in the rabbit mesenteric artery does not involve intracellular Ca^{2+} release is further supported by the inability of 5-HT to stimulate IP_3 accumulation in this tissue. Failure to stimulate the synthesis of IP_3 was not due to an absence of receptor-coupled phospholipase C in this preparation, as noradrenaline was able to stimulate a rapid, transient increase in IP_3, which correlated well with the rapid, transient contractions evoked by this agonist. In isolated segments of rabbit ophthalmic, renal and mesenteric arteries (Zschauer *et al.*, 1991; Choppin *et al.*, 1993; Seager & Garland, unpublished observations) 5-HT-induced contractions were greatly enhanced by raising the extracellular potassium concentration ($[K^+]_o$). Several previous studies with neuronal tissue have demonstrated that high $[K^+]_o$ enhances receptor-mediated phosphoinositide hydrolysis and IP_3 synthesis (Court *et al.*, 1986; Eva & Costa, 1986; Challiss & Nahorski, 1991), possibly due to increased $[Ca^{2+}]_i$ following depolarization-induced opening of voltage-sensitive Ca^{2+} channels in the plasma membrane (Eberhard & Holz, 1988). This raises the possibility that the increased contraction observed in the presence of raised $[K^+]_o$ may in part reflect an enhanced generation of IP_3. The presence of high $[K^+]_o$ did reveal a 5-HT-stimulated IP_3 accumulation, but only with a supramaximal concentration of 5-HT (100 μM). This effect was probably mediated by α_1-adrenoceptor activation, as it was abolished by the α_1-adrenoceptor antagonist, prazosin. This idea is supported by the finding that contraction of rabbit mesenteric artery to 100 μM 5-HT was also attenuated by prazosin (Cain & Nicholson, 1989).

The predominant 5-HT receptor type present in the mesenteric artery appears to be 5-HT_1, as both 5-carboxamidotryptamine (5-CT) and sumatriptan evoked contraction. In addition, large contractions to 5-CT and 5-HT were obtained in the presence of 1 μM of the 5-HT_2 antagonist, ketanserin (Seager & Garland, unpublished observations). 5-HT_1 receptors do not link to phospholipase C (Humphrey *et al.*, 1993), which is consistent with the results obtained in the present study.

5-HT did stimulate additional contraction in permeabilized mesenteric artery strips sub-maximally contracted with Ca^{2+} and GTP. As similar contractions were obtained in the combined presence of thapsigargin and 10 mM EGTA, changes in $[Ca^{2+}]_i$ did not underlie this additional contraction. These results suggest that the contraction to 5-HT resulted from an increased sensitivity of the contractile filaments to Ca^{2+}. Bradley & Morgan (1987) showed that 5-HT and other agonists can stimulate a high level of contractile force without maintained increases in $[Ca^{2+}]_i$. In the present study, 5-HT failed to enhance Ca^{2+}-induced contractions in the absence of GTP, and GTP alone enhanced Ca^{2+}-induced contractions, implicating G-proteins in the increased myofilament Ca^{2+}-sensitivity. These observations are in general agreement with findings reported in other preparations with other agonists, and the G-protein activator GTP-γ-S (Nishimura *et al.*, 1988; 1991; Kitazawa *et al.*, 1989; Himpens *et al.*, 1990).

The agonist-G-protein mediated increase in Ca^{2+}-sensitivity appears to reflect an increase in myosin light-chain phosphorylation (Kitazawa *et al.*, 1991; Nishimura *et al.*, 1991). In the present study, the protein kinase C inhibitor, H-7, attenuated the 5-HT-induced increase in myofilament sensitivity to Ca^{2+}, implying a role for protein kinase C. The GTP-induced component of the Ca^{2+}-GTP induced contraction was also inhibited by H-7. H-7 can inhibit cyclic nucleotide-dependent protein kinases in addition to protein kinase C (Hidaka *et al.*, 1984), although the possible role of these enzymes in responses to 5-HT will require further study (see Sumner *et al.*, 1992). It has also been suggested that H-7 directly inhibits myosin light chain kinase (Suzuki & Itoh, 1993), but the concentration of H-7 used in the present study did not inhibit contraction to Ca^{2+}, so that the 5-HT-induced increase in Ca^{2+} sensitivity may well involve protein kinase C. Previous studies on the rabbit mesenteric artery have also shown that H-7 and another protein kinase C inhibitor, staurosporine can inhibit noradrenaline, endothelin and GTP-γ-S-induced contractions at fixed $[Ca^{2+}]_i$, and that the protein kinase C activator phorbol 12,13-dibutyrate increased the Ca^{2+}-sensitivity of the contractile filaments (Nishimura *et al.*, 1991).

Protein kinase C activation follows the generation of membrane-bound diacylglycerol following the hydrolysis of phosphotidylinositides (Berridge, 1987). Alternatively, diacylglycerol can be synthesized from other membrane phospholipids. Several recent studies have shown that diacylglycerol can be liberated from phosphatidylcholine by phospholipases C or D (Billah & Anthes, 1990). Noradrenaline (Rapoport & Campbell, 1991; Gu *et al.*, 1992) has been shown to stimulate phosphatidylcholine hydrolysis in

isolated blood vessels; however the ability of 5-HT to do so has yet to be investigated. Studies with 5-HT have indicated that some receptors, namely the 5-HT_2 sub-family, are coupled to IP_3 synthesis (Roth *et al.*, 1985; Nakaki *et al.*, 1985; Doyle *et al.*, 1986). However, in the rabbit basilar artery 5-HT, acting on a '5-HT_1-like' receptor (Parsons & Whalley, 1989), has been shown to elevate diacylglycerol levels and activate contraction in part through protein kinase C, without generating IP_3 (Clark & Garland, 1991; Murphy & Garland, unpublished).

In summary, noradrenaline can contract smooth muscle cells in the mesenteric artery by releasing intracellular stores of Ca^{2+}, an action probably mediated by IP_3. In contrast, 5-HT cannot release intracellular Ca^{2+} and does not stimulate IP_3 synthesis. However, in the presence of raised $[Ca^{2+}]_i$, 5-HT can stimulate contraction through a mechanism involving the sensitization of the myofilaments to Ca^{2+}, possibly by activating protein kinase C. This effect may reflect diacylglycerol release from a membrane phospholipid other than phosphatidylinositide. Under normal conditions, in intact smooth muscle cells, this mechanism will probably be reinforced by Ca^{2+} entry from the extracellular space.

This work was supported by the Wellcome Trust. J.M.S. was supported by an SERC Studentship. T.V.M. is a Wellcome Trust Postdoctoral Fellow. We are extremely grateful to Drs Catherine Crichton and Godfrey Smith of the University of Glasgow for advice on the permeabilization technique.

References

BERRIDGE, M.J. (1987). Inositol trisphosphate and diacylglycerol: two interacting second messengers. *Annu. Rev. Biochem.*, **56**, 159–193.

BERTA, P., SEGUIN, J., VIDAL, N., HAIECH, J., MATHIEU, M.-N. & CHEVILLARD, C. (1986). Influence of Ca^{2+}_e on 5-HT_2- and α_1-induced arterial contraction and phosphoinositide. *Eur. J. Pharmacol.*, **132**, 253–257.

BILLAH, M.M. & ANTHES, J.C. (1990). The regulation and cellular functions of phosphatidylcholine hydrolysis. *Biochem. J.*, **269**, 281–291.

BRADLEY, A.B. & MORGAN, K.G. (1987). Alterations in cytoplasmic calcium sensitivity during porcine coronary artery contractions as detected by aequorin. *J. Physiol.*, **385**, 437–448.

CAIN, D.R. & NICHOLSON, C.D. (1989). Comparison of the effects of cromakalim, a potassium conductance enhancer, and nimodipine, a calcium antagonist, on 5-hydroxytryptamine responses in a variety of vascular smooth muscle preparations. *Naunyn-Schmied. Arch. Pharmacol.*, **340**, 293–299.

CHALLISS, R.A.J., BATTY, I.H. & NAHORSKI, S.R. (1988). Mass measurements of inositol (1,4,5) trisphosphate in rat cerebral cortex slices using a radioreceptor assay: effects of neurotransmitters and depolarization. *Biochem. Biophys. Res. Commun.*, **157**, 684–691.

CHALLISS, R.A.J. & NAHORSKI, S.R. (1991). Depolarization and agonist-stimulated changes in inositol 1,4,5-trisphosphate and inositol 1,3,4,5-tetrakisphosphate mass accumulation in rat cerebral cortex. *J. Neurochem.*, **57**, 1042–1051.

CHOPPIN, A. & O'CONNOR, S.E. (1993). Characterization of the 5-HT receptor which mediates contraction of rabbit partially-depolarized renal arteries. *Br. J. Pharmacol.* Proceedings Supplement (in press).

CLARK, A.H. & GARLAND, C.J. (1991). 5-Hydroxytryptamine-stimulated accumulation of 1,2-diacylglycerol in the rabbit basilar artery: a role for protein kinase C in smooth muscle contraction. *Br. J. Pharmacol.*, **102**, 415–421.

CLARK, A.H. & GARLAND, C.J. (1993). Ca^{2+} channel antagonists and inhibition of protein kinase C each block contraction but not depolarization to 5-hydroxytryptamine in the rabbit basilar artery. *Eur. J. Pharmacol.*, **235**, 113–116.

COHEN, M.L. & WITTENAUER, L.A. (1987). Serotonin receptor activation of phosphoinositide turnover in uterine, fundal, vascular, and tracheal smooth muscle. *J. Cardiovasc. Pharmacol.*, **10**, 176–181.

CORY, R.N., BERTA, P., HAIECH, J. & BOCKAERT, J. (1986). 5-HT_2 receptor-stimulated inositol phosphate formation in rat aortic myoctyes. *Eur. J. Pharmacol.*, **131**, 153–157.

COURT, J.A., FOWLER, C.J., CANDY, J.M., HOBAN, P.R. & SMITH, C.J. (1986). Raising the ambient potassium ion concentration enhances carbachol stimulated phosphoinositide hydrolysis in rat brain hippocampal and cerebral cortical miniprisms. *Naunyn-Schmied. Arch. Pharmacol.*, **334**, 10–16.

CRICHTON, C.A. & SMITH, G.L. (1990). GTP and noradrenaline-induced force in isolated toxin-permeabilized rat anococcygeus and guinea-pig portal vein. *J. Physiol.*, **437**, 543–561.

DOYLE, V.M., CREBA, J.A., RÜEGG, U.T. & HOYER, D. (1986). Serotonin increases the production of inositol phosphates and mobilizes calcium via the 5-HT_2 receptor in A_7r_5 smooth muscle cells. *Naunyn-Schmied. Arch. Pharmacol.*, **333**, 98–103.

EBERHARD, D.A. & HOLZ, R.W. (1988). Intracellular Ca^{2+} activates phospholipase C. *Trends Neurosci.*, **12**, 517–520.

EVA, C. & COSTA, E. (1986). Potassium ion facilitation of phosphoinositide turnover activation by muscarinic receptor agonists in rat brain. *J. Neurochem.*, **46**, 1429–1435.

FABIATO, A. & FABIATO, F. (1979). Calculator programs for computing the composition of solutions containing multiple metals and ligands used for experiments on skinned muscle cells. *J. Physiologie*, **75**, 463–505.

FENIUK, W. & HUMPHREY, P.P.A. (1989). Mechanisms of 5-hydroxytryptamine-induced vasoconstriction. In *The Peripheral Actions of 5-Hydroxytryptamine*. ed. Fozard, J.R. pp. 100–122. Oxford: Oxford University Press.

GILL, D.L., UEDA, T., CHUEH, S.-H. & NOEL, M.W. (1988). Ca^{2+} release from endoplasmic reticulum is mediated by a guanine nucleotide regulatory mechanism. *Nature*, **320**, 461–464.

GILMAN, A.G. (1987). G-proteins: transducers of receptor-generated signals. *Annu. Rev. Biochem.*, **56**, 615–649.

GU, H., TRAJKOVIC, S. & LABELLE, E.F. (1992). Norepinephrine-induced phosphatidylcholine hydrolysis by phospholipases D and C in rat tail artery. *Am. J. Physiol.*, **262**, C1376–C1383.

HASHIMOTO, T., HIRATA, M., ITOH, T., KANMURA, Y. & KURIYAMA, H. (1986). Inositol 1,4,5-trisphosphate activates pharmacomechanical coupling in smooth muscle of the rabbit mesenteric artery. *J. Physiol.*, **370**, 605–618.

HIDAKA, H., INAGAKI, M., KAWAMOTO, S. & SASAKI, Y. (1984). Isoquinolinesulfonamides, novel and potent inhibitors of cyclic nucleotide dependent protein kinase and protein kinase C. *Biochem.*, **23**, 5036–5041.

HIMPENS, B., KITAZAWA, T. & SOMLYO, A.P. (1990). Agonist-dependent modulation of Ca^{2+} sensitivity in rabbit pulmonary artery smooth muscle. *Pflügers Arch.*, **417**, 21–28.

HUMPHREY, P.P.A., HARTIG, P. & HOYER, D. (1993). A proposed new nomenclature for 5-HT receptors. *Trends Pharmacol. Sci.*, **14**, 233–236.

IINO, M. (1987). Calcium dependent inositol trisphosphate-induced calcium release in the guinea-pig taenia caeci. *Biochem. Biophys. Res. Commun.*, **142**, 47–52.

IINO, M. (1990). Calcium release mechanisms in smooth muscle. *Jpn. J. Pharmacol.*, **54**, 345–354.

ITOH, T., KURIYAMA, H. & SUZUKI, H. (1981). Excitation-contraction coupling in smooth muscle cells of the guinea-pig mesenteric artery. *J. Physiol.*, **321**, 513–535.

ITOH, T., SEKI, N., SUZUKI, S., ITO, S., KAJIKURI, J. & KURIYAMA, H. (1992). Membrane hyperpolarization inhibits agonist-induced synthesis of inositol 1,4,5-trisphosphate in rabbit mesenteric artery. *J. Physiol.*, **451**, 307–328.

KANAIDE, H., SHOGAKIUCHI, Y. & NAKAMURA, M. (1987). The norepinephrine-sensitive Ca^{2+}-storage site differs from the caffeine-sensitive site in vascular smooth muscle of the rat aorta. *FEBS Lett.*, **214**, 130–134.

KITAZAWA, T., GAYLINN, B., DENNEY, G.H. & SOMLYO, A.P. (1991). G-protein-mediated Ca^{2+} sensitization of smooth muscle contraction through myosin light chain phosphorylation. *J. Biol. Chem.*, **266**, 1708–1715.

KITAZAWA, T., KOBAYASHI, S., HORIUTI, K., SOMLYO, A.V. & SOMLYO, A.P. (1989). Receptor-coupled, permeabilized smooth muscle. *J. Biol. Chem.*, **264**, 5339–5342.

LOWRY, O.H., ROSEBROUGH, H.T., FARR, A.C. & RANDALL, R.J. (1951). Protein measurements with the Folin phenol reagent. *J. Biol. Chem.*, **193**, 265–275.

McCALDEN, T.A. & BEVAN, J.A. (1981). Sources of activator calcium in rabbit basilar artery. *Am. J. Physiol.*, **241**, H129–H133.

MURPHY, T.V. & GARLAND, C.J. (1993). Noradrenaline and 5-hydroxytryptamine-induced increases in inositol (1,4,5)-trisphosphate accumulation in rabbit aorta: role of extracellular Ca^{2+}. *Br. J. Pharmacol.*, **109**, 33P.

NAKAKI, T., ROTH, B.L., CHUANG, D.-M. & COSTA, E. (1985). Phasic and tonic components in 5-HT_2 receptor-mediated rat aorta contraction: participation of Ca^{++} channels and phospholipase C. *J. Pharmacol. Exp. Ther.*, **234**, 442–446.

NISHIMURA, J., KHALIL, R.A. & VAN BREEMEN, C. (1989). Agonist-induced vascular tone. *Hypertension*, **13**, 835–844.

NISHIMURA, J., KHALIL, R.A., DRENTH, J.P. & VAN BREEMEN, C. (1990). Evidence for increased myofilament Ca^{2+} sensitivity in norepinephrine-activated vascular smooth muscle. *Am. J. Physiol.*, **259**, H2–H8.

NISHIMURA, J., KOLBER, M. & VAN BREEMEN, C. (1988). Norepinephrine and GTP-γ-S increase myofilament Ca^{2+} sensitivity in α-toxin permeabilized arterial smooth muscle. *Biochem. Biophys. Res. Commun.*, **157**, 677–683.

NISHIMURA, J., MORELAND, S., MORELAND, R.S. & VAN BREEMEN, C. (1991). Regulation of the Ca^{2+}-force relationship in permeabilized arterial smooth muscle. In *Regulation of Smooth Muscle Contraction*. ed. Moreland, R.S. pp. 111–128. New York: Plenum Press.

PARSONS, A.A. & WHALLEY, E.T. (1989). Evidence for the presence of 5-HT_1-like receptors in rabbit isolated basilar arteries. *Eur. J. Pharmacol.*, **174**, 189–196.

RAPOPORT, R.M. & CAMPBELL, A.K. (1991). Norepinephrine-induced phosphatidylcholine hydrolysis in intact rat aorta. *Eur. J. Pharmacol. – Mol. Pharmacol.*, **208**, 89–92.

RATZ, P.H. & FLAIM, S.F. (1984). Mechanism of 5-HT contraction in isolated bovine ventricular coronary arteries. *Circ. Res.*, **54**, 135–143.

ROTH, B.L., NAKAKI, T., CHUANG, D.-M. & COSTA, E. (1986). 5-Hydroxytryptamine$_2$ receptors coupled to phospholipase C in rat aorta: modulation of phosphoinositide turnover by phorbol ester. *J. Pharmacol. Exp. Ther.*, **238**, 480–485.

SAIDA, K., TWORT, C. & VAN BREEMEN, C. (1988). The specific GTP requirement for inositol 1,4,5-trisphosphate-induced Ca^{2+} release from skinned vascular smooth muscle. *J. Cardiovasc. Pharmacol.*, **12**, 528–535.

SAIDA, K. & VAN BREEMEN, C. (1984). Characteristics of norepinephrine-sensitive Ca^{2+} store in vascular smooth muscle. *Blood Vessels*, **21**, 43–52.

SAXENA, P.R. & VILLALÓN, C.M. (1990). Cardiovascular effects of serotonin agonists and antagonists. *J. Cardiovasc. Pharmacol.*, **15 (Suppl. 7)**, S17–S34.

SEAGER, J.M. & GARLAND, C.J. (1992a). Intracellular Ca^{2+} release with 5-HT and norepinephrine in the rabbit mesenteric artery. *FASEB J.*, **6**, Abs. 410.

SEAGER, J.M. & GARLAND, C.J. (1992b). Responses to 5-HT in strips of rabbit mesenteric artery permeabilized with staphylococcus α-toxin. *Br. J. Pharmacol.*, **107**, 311P.

SMITH, G.L. & MILLER, D.J. (1984). Potentiometric measurements of stoichiometric and apparent affinity constants of EGTA for protons and divalent ions including calcium. *Biochem. Biophys. Acta*, **893**, 287–299.

SUMNER, M.J., FENIUK, W., McCORMICK, J.D. & HUMPHREY, P.P.A. (1992). Studies on the mechanism of 5-HT_1 receptor-induced smooth muscle contraction in dog saphenous vein. *Br. J. Pharmacol.*, **105**, 603–608.

SUZUKI, A. & ITOH, T. (1993). Effects of calyculin A on tension and myosin phosphorylation in skinned smooth muscle of the rabbit mesenteric artery. *Br. J. Pharmacol.*, **109**, 703–712.

THASTRUP, O. (1990). Role of Ca^{2+}-ATPase in regulation of cellular Ca^{2+} signalling, as studied with the selective microsomal Ca^{2+}-ATPase inhibitor, thapsigargin. *Agents Actions*, **29**, 8–15.

TOWART, R. (1981). The selective inhibition of serotonin-induced contractions of rabbit cerebral vascular smooth muscle by calcium-antagonistic dihydropyridines. *Circ. Res.*, **48**, 650–657.

VAN BREEMEN, C. & SAIDA, K. (1989). Cellular mechanisms regulating $[Ca^{2+}]_i$ smooth muscle. *Annu. Rev. Physiol.*, **51**, 315–329.

VANHOUTTE, P.M. (1990). The endothelium and the role of 5-hydroxytryptamine in vascular disease. In *Cardiovascular Pharmacology of 5-Hydroxytryptamine, Prospective Therapeutic Applications*. ed. Saxena, P.R., Wallis, D.I., Wouters, W. & Bevan, P. pp. 379–390. Dordrecht: Kluwer Academic Publishers.

WALSH, M.P. (1991). Calcium-dependent mechanisms of regulation of smooth muscle contraction. *Biochem. Cell. Biol.*, **69**, 711–800.

ZSCHAUER, A., VAN BREEMEN, C. & UUSITALO, H. (1991). Serotonergic responses in rabbit ophthalmic artery: a pharmacological characterization. *Am. J. Physiol.*, **261**, H1819–H1827.

(Received July 14, 1993
Revised October 15, 1993
Accepted October 26, 1993)

Br. J. Pharmacol. (1994), **111**, 533–538

Radioligand binding studies of α_1-adrenoceptor subtypes in rat heart

[1]Martin C. Michel, *Gertraud Hanft & *,[2]Gerhard Groß

Department of Medicine and *Department of Pharmacology, University of Essen, Essen, Germany

1 In order to characterize the α_1-adrenoceptor subtypes mediating positive inotropic effects of adrenaline (in the presence of propranolol) in rat right ventricular strips and the Ca^{2+} sources used to elicit them, we have used radioligand binding to identify the α_1-adrenoceptor subtypes present in rat heart and the α_1-adrenoceptor affinity and subtype-selectivity of various pharmacological tools.

2 Amitryptiline, mianserin, trimipramine, oxaprotiline, clonidine, chloroethylclonidine, phenoxybenzamine, BE 2254 and 8-OH-DPAT competed for [^{3}H]-prazosin binding in rat heart, vas deferens, liver, spleen, cerebral cortex and hippocampus but none of them displayed detectable α_1-adrenoceptor subtype-selectivity; nitrendipine did not compete for [^{3}H]-prazosin binding in concentrations up to 5 μmol l^{-1}.

3 The α_{1A}-adrenoceptor-selective, 5-methyl-urapidil, (+)-niguldipine, and to a lesser extent (−)-niguldipine competed for [^{3}H]-prazosin binding in rat heart, vas deferens, cerebral cortex and hippocampus with shallow and biphasic curves; analysis of these curves demonstrated that rat heart contains α_{1A}- and α_{1B}-adrenoceptors in a 20:80 ratio.

4 Treatment of rat right ventricular strips with 100 μmol l^{-1} chloroethylclonidine for 30 min at 30°C followed by 60 min washout reduced the number of α_1-adrenoceptors, as assessed by [^{3}H]-prazosin saturation experiments, by 74%. Treatment with 100 μmol l^{-1} $CdCl_2$ did not affect number or affinity of cardiac α_1-adrenoceptors and combined treatment with chloroethylclonidine and $CdCl_2$ reduced α_1-adrenoceptor number by 90%.

5 Treatment of rat right ventricular strips with chloroethylclonidine steepened 5-methyl-urapidil competition curves and increased the relative contribution of α_{1A}-adrenoceptors from 26 to 89%. Treatment with $CdCl_2$ did not affect 5-methyl-urapidil competition curves and combined treatment with chloroethylclonidine and $CdCl_2$ increased the relative contribution of α_{1A}-adrenoceptors to 66%.

6 We conclude that rat heart contains α_{1A}- and α_{1B}-adrenoceptors in a 20:80% ratio. Treatment with chloroethylclonidine reduces α_{1B}-adrenoceptor number by 96% but has only minor effects on α_{1A}-adrenoceptor density. Treatment with $CdCl_2$ does not affect the number of either α_1-adrenoceptor subtype.

Keywords: α_{1A}-Adrenoceptor; α_{1B}-adrenoceptor; 5-methyl-urapidil; (+)-niguldipine; (−)-niguldipine; chlorethylclonidine; rat heart

Introduction

Pharmacological and receptor cloning studies have demonstrated the existence of at least three α_1-adrenoceptor subtypes (Lomasney *et al.*, 1991; Bylund, 1992; Michel *et al.*, 1992). Whereas expression of the cloned α_{1C}-adrenoceptor has not been detected in any peripheral rat tissue (Schwinn *et al.*, 1991), α_{1A}- and α_{1B}-adrenoceptors are found in various rat tissues by radioligand binding (Minneman *et al.*, 1988; Hanft & Gross, 1989; Han & Minneman, 1991) or Northern blotting techniques (Lomasney *et al.*, 1991). Some tissues, including cerebral cortex, kidney and heart, co-express α_{1A}- and α_{1B}-adrenoceptors (Minneman *et al.*, 1988; Hanft & Gross, 1989; Han & Minneman, 1991). The physiological role of the simultaneous presence of multiple α_1-adrenoceptor subtypes within a tissue remains unclear, but mediation of different functions, activation under different conditions, or differential regulation can be envisioned. However, only a few studies have investigated these possibilities.

Rat heart contains considerably more α_1- than β-adrenoceptors (Parini *et al.*, 1988; Michel *et al.*, 1989) which mediate multiple functions including inotropic and electrophysiological effects and (at least in cultured neonatal cardiomyocytes) the development of hypertrophy (Benfey, 1990; Endoh, 1991). We have previously demonstrated that adult rat heart contains α_{1A}- and α_{1B}-adrenoceptors in an approximately 20:80 ratio, respectively (Hanft & Gross, 1989; Hanft *et al.*, 1989), whereas neonatal rat heart contains them in an approximately 35:65 ratio, respectively (Knowlton *et al.*, 1993). In addition we have found that induction of hypertrophy in cultured neonatal cardiomyocytes by the α_1-adrenoceptor agonist, phenylephrine, is mediated solely by the α_{1A}-adrenoceptor, although this subtype represents less than 50% of all cardiac α_1-adrenoceptors (Knowlton *et al.*, 1993). The present two-part study was designed to characterize further rat cardiac α_1-adrenoceptors and to permit the determination of the α_1-adrenoceptor subtype mediating the positive inotropic effects of adrenaline in rat right ventricle and the sources of Ca^{2+} used to elicit these inotropic effects (Michel *et al.*, 1994). The first part of our study uses radioligand binding to determine the affinity and subtype-selectivity for various pharmacological tools to be used in the functional studies (Michel *et al.*, 1994).

Methods

Radioligand binding experiments

Male adult Wistar rats weighing 250–400 g were obtained from Lippische Versuchstierzucht (Extertal, Germany). Immediately following removal, organs were macroscopically freed from connective tissue, blotted, weighed and homogen-

[1] Author for correspondence at: Nephrol. Lab IG1, Klinikum, Hufelandstr. 55, D-45122 Essen, Germany.
[2] Present address: Knoll Pharmaceutical Co., Ludwigshafen, Germany.

ized twice for 15 s with an Ultra Turrax (Janke & Kunkel, Staufen, Germany) in 10 ml of ice-cold buffer (Tris HCl 50 mmol l^{-1}, NaCl 100 mmol l^{-1}, EDTA 2 mmol l^{-1}, pH 7.4). The homogenates were filtered through four layers of gauze and centrifuged at 80,000 g for 20 min at 4°C. The pellets were resuspended in 8 ml of fresh buffer (Tris HCl 50 mmol l^{-1}, EDTA 1 mmol l^{-1}, pH 7.4), incubated for 10 min at 37°C, centrifuged again as described above and washed once more with 8 ml buffer.

[^{3}H]-prazosin binding experiments were performed as previously described (Gross & Lues, 1985; Hanft & Gross, 1989). Briefly, membranes (100–160 μg of membrane protein) were incubated with eight concentrations of [^{3}H]-prazosin ranging from 10 to 600 pmol l^{-1} in saturation binding experiments and ≈200 pmol l^{-1} [^{3}H]-prazosin in competition binding experiments; the assay volume was 2 ml in saturation and 1 ml in competition binding experiments except for studies with niguldipine isomers which were performed in a volume of 2 ml in order to dilute the niguldipine solvent, dimethylsulphoxide. Incubations were carried out at 30°C for 45 min and terminated by rapid filtration over Whatman GF/C filters using a Brandel M24R cell harvester. The filters were washed with 15 ml ice-cold buffer (Tris HCl 50 mmol l^{-1}, pH 7.4) and subsequently dried at 100°C. Membrane-bound radioactivity retained on the filters was measured by liquid scintillation counting in a toluene/Triton-100 mixture with an efficiency of 49%. Non-specific binding was defined by use of 10 μmol l^{-1} phentolamine and was usually 15% at 0.3 nmol l^{-1} [^{3}H]-prazosin. Each data point was measured in duplicate in each experiment. The protein content of the membrane suspensions was determined by the method of Lowry et al. (1951).

In some experiments right ventricular strips were treated with vehicle, 100 μmol l^{-1} of chloroethylclonidine, 100 μmol l^{-1} $CdCl_2$ or both for 30 min followed by 60 min of washout. These treatments were performed in an organ bath containing 20 ml modified Krebs-Henseleit solution of the following composition (mmol l^{-1}): NaCl 118, KCl 4.8, $CaCl_2$ 2.5, $MgSO_4$ 1.2, $NaHCO_3$ 25, KH_2PO_4 1.2, glucose 10 saturated with carbogen at 30°C. Additionally propranolol (10 μmol l^{-1}) oxaprotiline (0.3 μmol l^{-1}) and corticosterone (40 μmol l^{-1}) were present to block β-adrenoceptors, neuronal and extraneuronal catecholamine uptake, respectively. Thereafter the strips were homogenized, the homogenates washed by centrifugation and the resulting pellets used for [^{3}H]-prazosin saturation and 5-methyl-urapidil competition experiments as described above.

Data analysis

Saturation binding experiments were analysed according to Scatchard (1949). Competition binding experiments were analysed by non-linear iterative fitting of the experimental data to monophasic or biphasic sigmoid curves using the InPlot programme (GraphPAD Software, San Diego, CA, U.S.A.); a two-site fit was accepted only when it resulted in a significant improvement of the fit in an F-test with $P<0.05$. Since chloroethylclonidine-treatment markedly reduced specific [^{3}H]-prazosin binding and thus caused considerable data scatter due to the worsened signal/noise ratio, we calculated % inhibition for each 5-methyl-urapidil concentration, averaged these percentages for all experiments and fitted the averaged data. This did not allow the calculation of standard errors for the fitting parameters but yielded more reliable fits than fitting data from individual experiments.

Chemicals

The compounds used in this study were obtained from the following sources: clonidine hydrochloride, amitryptiline hydrochloride, mianserin hydrochloride, trimipramine maleate and $CdCl_2$ from Sigma (Munich, Germany), (+)-oxaprotiline hydrochloride and phentolamine hydrochloride from Ciba Geigy (Basel, Switzerland), 8-OH-DPAT ((±)-2-dipropylamino-8-hydroxy-1,2,3,4-tetrahydro-naphthalene hydrobromide), nitrendipine, phenoxybenzamine hydrochloride, and chloroethylclonidine dihydrochloride from Research Biochemicals (Natick, MA, U.S.A.), 5-methyl-urapidil, (−)- and (+)-niguldipine from Byk Gulden (Konstanz, Germany).

Results

α_1-Adrenoceptor affinities

Among the organic Ca^{2+} entry blockers tested, nitrendipine did not compete for [^{3}H]-prazosin binding in concentrations up to 5 μmol l^{-1} (Table 1). In contrast, (−)- and (+)-niguldipine had very high affinity for α_1-adrenoceptors in various tissues. (+)-Niguldipine competition curves in rat liver and spleen were steep and monophasic, whereas those in heart, vas deferens, cerebral cortex and hippocampus were shallow and biphasic (Table 1), allowing assessment of the ratio of α_{1A}- and α_{1B}-adrenoceptors in these tissues (Table 2). Similar data were obtained with (−)-niguldipine but its α_1-

Table 1 Drug affinities at α_1-adrenoceptors in various rat tissues

	Liver	*Spleen*	*Vas deferens*		*Cerebral cortex*		*Hippocampus*		*Heart*	
	pK_i	pK_i	$pK_{i\ high}$	$pK_{i\ low}$	$pK_{i\ high}$	$pK_{i\ low}$	$pK_{i\ high}$	$pK_{i\ low}$	$pK_{i\ high}$	$pK_{i\ low}$
(+)-Niguldipine	8.06	7.93	10.71	7.51	10.46	7.74	10.04	7.41	10.69	7.84
(−)-Niguldipine	7.84	7.67	9.51	7.74	9.40	7.74	8.69	7.36	7.80	
Nitrendipine	<5	<5	<5		<5		<5		<5	
Amitryptiline	7.82	7.65	7.71		7.79		7.73		7.72	
Mianserin	7.49	7.39	7.44		7.33		7.22		7.33	
Trimipramine	7.83	7.74	7.39		7.57		7.26		7.60	
Oxaprotiline	6.41	6.25	6.14		6.19		6.00		6.26	
Clonidine	6.41	6.49	6.81		6.55		6.64		6.39	
CEC	6.83	6.75	6.39		6.62		6.49		6.62	
PBZ	9.81	9.73	9.01		9.34		9.09		9.35	
BE 2254	9.44	9.42	9.07		9.34		9.16		9.40	
8-OH-DPAT	4.90	4.85	4.90		4.95		4.93		4.90	
5-MU	7.63	7.56	9.16	7.68	9.27	7.31	8.99	7.06	9.23	7.35

5-Methyl-urapidil data are mean of 19 (liver), 6 (spleen), 11 (vas deferens), 26 (cerebral cortex), 10 (hippocampus) and 33 experiments (heart); data are mean of 6 experiments for (−)-niguldipine in the heart, of 4 experiments for (−)-niguldipine in the other tissues, (+)-niguldipine, and BE 2254, of 3 experiments for trimipramine, chloroethylclonidine, phenoxybenzamine, and 8-OH-DPAT, of 2 experiments for nitrendipine, and are from a single experiment for amitryptiline, mianserin, oxaprotilin, and clonidine. In each experiment data were determined in duplicate. Whenever only $pK_{i\ high}$ is given, competition curves were steep and monophasic and, thus, could not be resolved into multiple phases: all competition curves were steep and monophasic in liver and spleen. CEC: chloroethylclonidine, PBZ: phenoxybenzamine, 5-MU: 5-methyl-urapidil.

Table 2 Relative contribution of high affinity sites (α_{1A}-adrenoceptors) in rat vas deferens, cerebral cortex, hippocampus and heart as assessed by (+)- and (−)-niguldipine and 5-methyl-urapidil

	Vas deferens	*Cerebral cortex*	*Hippocampus*	*Heart*
(+)-Niguldipine	57 (4)	40 (4)	63 (4)	17 (4)
(−)-Niguldipine	29 (4)	23 (4)	60 (4)	- (6)
5-Methyl-urapidil	65 (11)	44 (26)	71 (10)	21 (33)

Data are mean of % high affinity sites of the number of experiments given in parentheses. Standard errors are not given since data are derived from analysis of the pooled data.

adrenoceptor subtype-discriminating power was lower than that of (+)-niguldipine (Table 1) and it detected fewer high affinity sites in most tissues (Table 2). Addition of the inorganic Ca^{2+} entry blocker, $CdCl_2$ (in concentrations up to 30 μmol l^{-1}) to the radioligand binding assay did not affect the affinity or B_{max} for [^{3}H]-prazosin in saturation experiments or the position or shape of 5-methyl-urapidil competition curves (data not shown).

Among the neuronal catecholamine uptake blockers amitryptiline, mianserin and trimipramine had high affinity for α_1-adrenoceptors (<60 nmol l^{-1}) but did not exhibit relevant selectivity for α_1-adrenoceptor subtypes (Table 1). Oxaprotiline also failed to discriminate α_1-adrenoceptor subtypes but had an at least ten fold lower α_1-adrenoceptor affinity (0.4–1 μmol l^{-1}; Table 1).

Chloroethylclonidine which irreversibly inactivates α_{1B}-adrenoceptors and its parent compound, clonidine, competed for [^{3}H]-prazosin binding with moderate affinity but in competition studies had similar affinities for all α_1-adrenoceptor subtypes tested (Table 1). Phenoxybenzamine competed for [^{3}H]-prazosin binding in all tissues tested with high affinity but did not discriminate among α_1-adrenoceptor subtypes in competition studies.

BE 2254 had high affinity for α_1-adrenoceptors but did not discriminate α_1-adrenoceptor subtypes (Table 1). 5-Methyl-urapidil competed for [^{3}H]-prazosin binding in rat liver and spleen with steep and monophasic curves but exhibited shallow and biphasic curves in heart, vas deferens, cerebral cortex and hippocampus (Table 1). The relative contributions of α_{1A}- and α_{1B}-adrenoceptors as determined from the 5-methyl-urapidil competition curves are given in Table 2. The 5-hydroxytryptamine (5-HT) 5-HT_{1A} receptor agonist, 8-OH-DPAT, had low affinity for α_1-adrenoceptors and did not discriminate among subtypes (Table 1). The protein synthesis inhibitor, cycloheximide, in concentrations up to 1 mmol l^{-1}, did not affect [^{3}H]-prazosin binding (data not shown).

Effects of chloroethylclonidine and $CdCl_2$ treatment on right ventricular α_1-adrenoceptor number and subtype distribution

Treatment with 100 μmol l^{-1} chloroethylclonidine, 100 μmol l^{-1} $CdCl_2$ or both did not significantly affect the affinity of right ventricular α_1-adrenoceptors for [^{3}H]-prazosin (Figure 1, Table 3). Treatment with $CdCl_2$ did not significantly alter the number of cardiac α_1-adrenoceptors, whereas treatment with chloroethylclonidine or with chloroethylclonidine plus $CdCl_2$ reduced α_1-adrenoceptor number by 74% and 90%, respectively (Figure 1, Table 3).

To determine how the reduction in right ventricular α_1-adrenoceptors involved α_{1A}- and α_{1B}-adrenoceptors, we performed competition studies with the α_{1A}-selective, 5-methyl-urapidil. In membranes from control, chloroethylclonidine-, $CdCl_2$- or chloroethylclonidine plus $CdCl_2$-treated right ventricular strips, 5-methyl-urapidil competed for [^{3}H]-prazosin binding with shallow competition curves which could be resolved into two components (Figure 2, Table 4). The affinity constants of 5-methyl-urapidil at its high and low affinity sites (0.5 nmol l^{-1} and 35.5 nmol l^{-1}, respectively, in membranes from control strips) were similar in all treatment groups. The percentage of high affinity sites (α_{1A}-adrenoceptors), however, was much smaller in control or $CdCl_2$-treated strips than in those treated with chloroethylclonidine (89%). Thus, chloroethylclonidine treatment did not cause a major

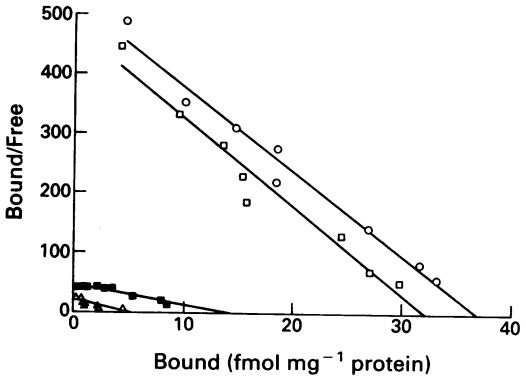

Figure 1 Effects of treatment with chloroethylclonidine and/or $CdCl_2$ on rat cardiac α_1-adrenoceptor density. Tissue strips were treated for 30 min at 30°C in the organ bath with vehicle (○), 100 μmol l^{-1} chloroethylclonidine (■) or 100 μmol l^{-1} $CdCl_2$ (□) or their combination (△). Following 60 min of washout, membranes were prepared on which [^{3}H]-prazosin binding was performed. Data are of a representative saturation binding experiment and have been transformed according to Scatchard (1949). Mean ± s.e.mean of several such experiments are shown in Table 2.

Table 3 Effects of chloroethylclonidine and $CdCl_2$ treatment on number and affinity of rat right ventricular α_1-adrenoceptors

	n	$-log\ K_d$ (mol l^{-1})	B_{max} (fmol mg^{-1} protein)
Control	14	10.25 ± 0.03	35.0 ± 1.7
Chloroethylclonidine	13	9.98 ± 0.06	9.4 ± 1.0***
$CdCl_2$	6	10.20 ± 0.03	36.7 ± 2.5
Chloroethylclonidine + $CdCl_2$	4	10.47 ± 0.50	3.5 ± 1.1***

Rat right ventricular strips were treated in the organ bath with 100 μmol l^{-1} chloroethylclonidine for 30 min followed by 60 min washout, with 100 μmol l^{-1} $CdCl_2$, simultaneously with both, or with neither (control). Thereafter, one concentration-response curve to adrenaline was performed on each preparation in the organ bath before tissues were homogenized and centrifuged for the radioligand binding studies. Data are mean ± s.e.mean of the indicated number of experiments (n).
***$P<0.001$ vs. control or $CdCl_2$-treated strips. Differences in affinity ($-\log K_d$) were not statistically significant. A graphic representation of a representative experiment is given in Figure 1.

Table 4 Effects of chloroethylclonidine and $CdCl_2$ treatment on the subtype distribution of rat right ventricular α_1-adrenoceptors

	Hill-slope	*% high affinity sites*	$pK_{i\ high}$ (mol l^{-1})	$pK_{i\ low}$ (mol l^{-1})
Control	0.66	26	9.33	7.45
Chloroethylclonidine	0.84	89	9.40	6.75
$CdCl_2$	0.65	26	9.34	7.39
Chloroethylclonidine + $CdCl_2$	0.46	66	9.46	6.62

Rat right ventricular strips were treated in the organ bath with 100 μmol l^{-1} chloroethylclonidine for 30 min followed by 60 min washout, with 100 μmol l^{-1} $CdCl_2$, simultaneously with both, or with neither (control). Thereafter, one concentration-response curve to adrenaline was performed on each preparation in the organ bath before tissues were homogenized and centrifuged for the radioligand binding studies. Data are derived from competition binding experiments with 5-methyl-urapidil and 0.2 nmol l^{-1} [^{3}H]-prazosin. Averaged percentage inhibition data from 3–5 experiments were fitted to a two-site model. A graphic representation of the data is given in Figure 2.

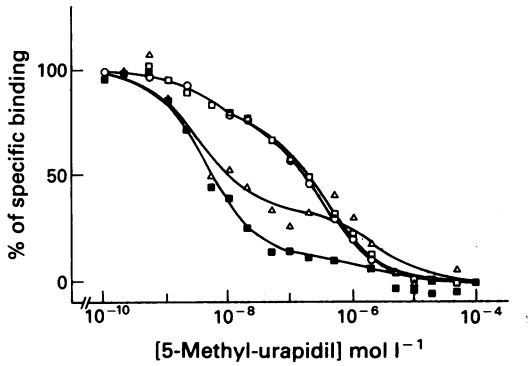

Figure 2 Effects of treatment with chloroethylclonidine and/or $CdCl_2$ on rat cardiac α_1-adrenoceptor subtype distribution. Tissue strips were treated for 30 min at 30°C in the organ bath with vehicle (○), 100 μmol l^{-1} chloroethylclonidine (■) or 100 μmol l^{-1} $CdCl_2$ (□) or their combination (△). Following 60 min of washout, membranes were prepared on which [^{3}H]-prazosin binding was performed. Data are mean of 3–5 experiments; s.e.means were omitted for the sake of clarity. A quantitative analysis of these data is given in Table 3.

change in α_{1A}-adrenoceptor density (from 9.1 to 8.4 fmol mg^{-1} protein) but decreased α_{1B}-adrenoceptors by 96% (from 25.9 to 1.0 fmol mg^{-1} protein). $CdCl_2$-treatment did not cause significant alterations in the density of either subtype.

Discussion

Analysis of the differential effects mediated by cardiac α_1-adrenoceptor subtypes and their possibly complex interaction requires precise characterization of the pharmacological tools used. Thus, in this study we have determined the affinity and possible subtype-selectivity of various pharmacological tools for subsequent functional studies (Michel *et al.*, 1994). In addition the effects of pretreatment with chloroethylclonidine, $CdCl_2$ or both on the number and subtype distribution of α_1-adrenoceptors in rat right ventricular strips was determined.

α_1-Adrenoceptor subtype selectivity of pharmacological tools

We have used six rat tissues to determine the affinity at and possible selectivity for α_1-adrenoceptor subtypes: liver and spleen were used as model systems containing homogeneous populations of α_{1B}-adrenoceptors, whereas vas deferens, cerebral cortex, hippocampus and heart were used as model systems containing α_{1A}- and α_{1B}-adrenoceptors in different ratios (Minneman *et al.*, 1988; Hanft & Gross, 1989; Han & Minneman, 1991). The competition curves of the known α_{1A}-selective (+)- and (−)-niguldipine (Boer *et al.*, 1989) and 5-methyl-urapidil (Hanft & Gross, 1989) for [^{3}H]-prazosin binding were steep and monophasic in liver and spleen which contain only α_{1B}-adrenoceptors but were shallow and biphasic in heart (except for (−)-niguldipine), vas deferens, cerebral cortex and hippocampus which contain both α_{1A}- and α_{1B}-adrenoceptors. (+)-Niguldipine and 5-methyl-urapidil detected similar ratios of α_{1A}/α_{1B}-adrenoceptors in vas deferens, cerebral cortex, hippocampus and heart which are in good agreement with previously published data (Minneman *et al.*, 1988; Hanft & Gross, 1989; Han & Minneman, 1991). Thus, the six tissues used here could represent a useful set to screen for α_1-adrenoceptor affinity and potential subtype selectivity.

We have first used these tissues to identify an organic Ca^{2+} entry blocker suitable for studies on α_1-adrenoceptor-mediated functional effects (Michel *et al.*, 1994). We have previously shown that verapamil is unsuitable to study the involvement of Ca^{2+} channels in α_1-adrenoceptor action since it has high affinity (0.3–1 μmol l^{-1}) for various α_1-adrenoceptor subtypes although it lacks subtype selectivity (Hanft *et al.*, 1989). As shown previously (Boer *et al.*, 1989) and confirmed in the present study (see above) isomers of niguldipine are also unsuitable since they have high affinity for α_1-adrenoceptors and distinguish their subtypes. In contrast the dihydropyridine, nitrendipine, had very low affinity for α_1-adrenoceptors (> 10 μmol l^{-1}) and therefore 100 nmol l^{-1} nitrendipine appears to be useful for studying the involvement of voltage-operated Ca^{2+} channels in α_1-adrenoceptor function.

Since functional studies using adrenaline in densely sympathetically innervated tissues require neuronal catecholamine uptake blockade to avoid disequilibrium, we have also tested various uptake blockers for their α_1-adrenoceptor affinities and potential subtype selectivity. Among the tested agents amitryptiline, mianserin, trimipramine and oxaprotiline, the latter had the lowest affinity for α_1-adrenoceptors and did not selectively recognize one of their subtypes. Thus, oxaprotiline (300 nmol l^{-1}) can be used to block neuronal catecholamine uptake in the organ bath experiments.

Among other compounds tested, BE 2254 had a slightly lower affinity for α_1-adrenoceptors than its iodinated derivative I-BE 2254 (Hanft *et al.*, 1989), which is frequently used as a ligand for the detection of α_1-adrenoceptors in its radioactively labelled form (Johnson & Minneman, 1987), but similarily did not differentiate among α_1-adrenoceptor subtypes. The irreversible antagonist, phenoxybenzamine, also had very high affinity for α_1-adrenoceptors but did not differentiate among subtypes in competition binding studies.

Based on their selectivity in the binding studies, (+)- and (−)-niguldipine might be useful to discriminate α_1-adrenoceptor subtypes in functional studies. On the other hand, several pieces of data argue against the use of niguldipine isomers in functional studies. Firstly, niguldipine is a Ca^{2+} entry blocker in the same concentration-range at which it binds to α_{1A}-adrenoceptors (Boer *et al.*, 1989). Secondly, its antagonism may sometimes be pseudoirreversible (Clarke *et al.*, 1990). Thirdly, niguldipine is highly lipophilic (Boer *et al.*, 1989), and the resulting partitioning into biological membranes results in various experimental problems. This inclu-

des different apparent affinities depending on the amount of membranes used (Boer *et al.*, 1989) and the observation that α_1-adrenoceptor subtypes identified by niguldipine do not always correspond to those identified by other pharmacological tools (Han & Minneman, 1991). This may also explain why niguldipine isomers, especially (−)-niguldipine in the present study detected fewer α_{1A}-adrenoceptors in some tissues than 5-methyl-urapidil. 5-Methyl-urapidil lacks these complicating effects but bears the potential problem of being an agonist at 5-HT_{1A} receptors (Gross *et al.*, 1987). Although this problem is unlikely to be relevant in rat heart which lacks 5-HT_{1A} receptors, our data show that 8-OH-DPAT, another agonist at 5-HT_{1A} receptors, can be used as a control for such effects since it has only low affinity at α_1-adrenoceptors and does not discriminate their subtypes. With regard to other competitive antagonists at α_1-adrenoceptor subtypes, (±)-tamsulosin is approximately 50–100 fold α_{1A}-selective (Hanft *et al.*, 1989). WB 4101 and phentolamine are α_{1A}-selective competitive antagonists although somewhat less so than 5-methyl-urapidil (Minneman *et al.*, 1988; Hanft & Gross, 1989), whereas prazosin (Hanft & Gross, 1989), I-BE 2254 (Hanft *et al.*, 1989) and BE 2254 (present study) do not discriminate α_1-adrenoceptor subtypes. Amidephrine, methoxamine and oxymetazoline are agonists with selectivity for α_{1A}-adrenoceptors in radioligand binding studies (Hanft *et al.*, 1989; Tsujimoto *et al.*, 1989; Knowlton *et al.*, 1993).

Effects of chloroethylclonidine and $CdCl_2$ treatments

Treatment with chloroethylclonidine can inactivate α_{1B}-adrenoceptors (Han *et al.*, 1987; Minneman *et al.*, 1988). This is mostly done at 37°C whereas our organ bath experiments are usually performed at 30°C (Michel *et al.*, 1994). Since alkylating reactions are temperature-dependent, we used a somewhat higher chloroethylclonidine concentration and determined its effectiveness and selectivity in inactivating α_{1B}-adrenoceptors under our experimental conditions. For this purpose we determined the number of α_1-adrenoceptors in [^{3}H]-prazosin saturation experiments and the α_1-adrenoceptor subtype ratio in 5-methyl-urapidil competition experiments in ventricular muscle strips which had been treated in the organ bath for 30 min with 100 μM chloroethylclonidine. In parallel we investigated the effect of treatment with 100 μmol l^{-1} $CdCl_2$ and the combination of chloroethylclonidine and $CdCl_2$. $CdCl_2$ treatment did not affect number, antagonist affinity or subtype distribution of cardiac α_1-adrenoceptors. Chloroethylclonidine treatment reduced the α_1-adrenoceptor number by approximately 73% and simultaneously steepened the 5-methyl-urapidil competition curves. Combined analysis of the saturation and competition experiments demonstrated that chloroethylclonidine effectively inactivated α_{1B}-adrenoceptors since it reduced their number by approximately 96% but remained selective under our conditions since it did not significantly affect α_{1A}-adrenoceptor number. Moreover, our competition studies with chloroethylclonidine show that any chloroethylclonidine which might have been washed out incompletely would not affect functional studies on α_1-adrenoceptors in a subtype-selective manner since chloroethylclonidine like its parent compound clonidine had similar affinity for α_1-adrenoceptor subtypes in various tissues co-expressing α_{1A}- and α_{1B}-adrenoceptors. Similar data were recently obtained in another study from our laboratory, and the non-selective binding of chloroethylclonidine to both α_{1A}- and α_{1B}-adrenoceptors is discussed in detail in that context (Michel *et al.*, 1993).

The reduction in α_{1B}-adrenoceptors with chloroethylclonidine indicated a similar quantitative ratio of α_{1A}/α_{1B}-adrenoceptors as the experiments with 5-methyl-urapidil and (+)-niguldipine (present study) or previous experiments with amidephrine, oxymetazoline, phentolamine, (±)-tamsulosin, or WB 4101 (Minneman *et al.*, 1988; Hanft & Gross, 1989; 1990; Hanft *et al.*, 1989; Han & Minneman, 1991). Thus, α_{1A}- and α_{1B}-adrenoceptors appear to exist in rat heart in an approximately 20:80 ratio. This is in contrast to the α_1-adrenoceptor subtypes present in adult rabbit myocardium. Whereas inactivation studies with chloroethylclonidine have indicated the presence of 37% chloroethylclonidine-resistant sites (Takanashi *et al.*, 1991), competition binding studies with the α_{1A}-adrenoceptor-selective WB 4101 and 5-methyl-urapidil have detected 91% and 100% high affinity sites, respectively (Endoh *et al.*, 1992). Thus, rabbit myocardium may contain a mixture of α_{1A}- and α_{1C}-adrenoceptors but few if any α_{1B}-adrenoceptors. Cardiac α_1-adrenoceptor subtypes in other species have not yet been characterized to our knowledge, but a recent ribonuclease protection study indicated that the α_{1C}-adrenoceptor may be the dominating subtype in the human heart, at least at the level of mRNA (Price *et al.*, 1993).

Taken together our data demonstrate that nitrendipine and oxaprotiline are appropriate compounds to block voltage-operated Ca^{2+} channels and catecholamine uptake, respectively, in functional studies on α_1-adrenoceptor subtypes. To discriminate such subtypes in functional studies, 5-methyl-urapidil appears to be the most useful antagonist, at least in tissues which lack functional 5-HT_{1A} receptors. Treatment with 100 μmol l^{-1} chloroethylclonidine for 30 min at 30°C effectively and selectively inactivates α_{1B}-adrenoceptors without affecting α_{1A}-adrenoceptors. Blockade of Ca^{2+} channels by $CdCl_2$ treatment does not affect α_1-adrenoceptor number of subtype distribution. We believe that this set of drugs and conditions represent a useful set of tools to study the functional role of α_1-adrenoceptor subtypes and the Ca^{2+} sources used by them (Michel *et al.*, 1994).

We thank the respective companies for their gifts of drugs and Mrs Sprungmann and Mrs Jansen for their skilful technical assistance. This work was supported by the Deutsche Forschungsgemeinschaft.

References

BENFEY, B.G. (1990). Function of myocardial α-adrenoceptors. *Life Sci.*, **46**, 743–757.

BOER, R., GRASSEGGER, A., SCHUDT, C. & GLOSSMANN, H. (1989). (+)-Niguldipine binds with very high affinity to Ca^{2+} channels and to a subtype of α_1-adrenoceptors. *Eur. J. Pharmacol.*, **172**, 131–145.

BYLUND, D.B. (1992). Subtypes of α_1- and α_2-adrenergic receptors. *FASEB J.*, **6**, 832–839.

CLARKE, D.E., VIMONT, R.L. & BLUE, D.R.Jr. (1990). Vascular alpha$_1$-adrenoceptors in rat kidney: agonist and antagonist [prazosin, idazoxan, WB4101, (+)-niguldipine] characterization. *Eur. J. Pharmacol.*, **183**, 733.

ENDOH, M. (1991). Myocardial α-adrenoceptors: multiplicity of subcellular coupling processes. *Asia Pac. J. Pharmacol.*, **6**, 171–186.

ENDOH, M., TAKANASHI, M. & NOROTA, I. (1992). Role of alpha$_{1A}$ adrenoceptor subtype in production of the positive inotropic effect mediated via myocardial alpha$_1$ adrenoceptors in the rabbit papillary muscle: influence of selective alpha$_{1A}$ subtype antagonists WB 4101 and 5-methylurapidil. *Naunyn-Schmied Arch. Pharmacol.*, **345**, 578–585.

GROSS, G., HANFT, G. & KOLASSA, N. (1987). Urapidil and some analogues with hypotensive properties show high affinities for 5-hydroxytryptamine (5-HT) binding sites of the 5-HT_{1A} subtype and for α_1-adrenoceptor binding sites. *Naunyn-Schmied. Arch. Pharmacol.*, **336**, 597–601.

GROSS, G. & LUES, I. (1985). Thyroid-dependent alterations of myocardial adrenoceptors and adrenoceptor-mediated responses in the rat. *Naunyn-Schmied. Arch. Pharmacol.*, **329**, 427–439.

HAN, C., ABEL, P.W. & MINNEMAN, K.P. (1987). Heterogeneity of α_1-adrenergic receptors revealed by chloroethylclonidine. *Mol. Pharmacol.*, **32**, 505–510.

HAN, C. & MINNEMAN, K.P. (1992). Interaction of subtype-selective antagonists with α_1-adrenergic receptor binding sites in rat tissues. *Mol. Pharmacol.*, **40**, 531–538.

HANFT, G. & GROSS, G. (1989). Subclassification of α_1-adrenoceptor recognition sites by urapidil derivatives and other selective antagonists. *Br. J. Pharmacol.*, **97**, 691–700.

HANFT, G. & GROSS, G. (1990). The effect of reserpine, desipramine and thyroid hormone on α_{1a}- and α_{1b}-adrenoceptor binding sites: evidence for a subtype-specific regulation. *Br. J. Clin. Pharmacol.*, **30**, 125S–127S.

HANFT, G., GROSS, G., BECKERINGH, J.J. & KORSTANJE, C. (1989). α_1-Adrenoceptors: the ability of various agonists and antagonists to discriminate between two distinct [^{3}H]-prazosin binding sites. *J. Pharm. Pharmacol.*, **41**, 714–716.

JOHNSON, R.D. & MINNEMAN, K.P. (1987). Differentiation of α_1-adrenergic receptors linked to phosphatidylinositol turnover and cyclic AMP accumulation in rat brain. *Mol. Pharmacol.*, **31**, 239–246.

KNOWLTON, K.U., MICHEL, M.C., ITANI, M., SHUBEITA, H.E., ISHIHARA, K., BROWN, J.H. & CHIEN, K.R. (1993). The α_{1A}-adrenergic receptor subtype mediates biochemical, molecular, and morphologic features of cultured myocardial cell hypertrophy. *J. Biol. Chem.*, **268**, 15374–15380.

LOMASNEY, J.W., COTECCHIA, S., LEFKOWITZ, R.J. & CARON, M.G. (1991). Molecular biology of α-adrenergic receptors: implications for receptor classification and for structure-function relationships. *Biochem. Biophys. Acta*, **1095**, 127–139.

LOWRY, O.H., ROSEBROUGH, N.J., FARR, A.L. & RANDALL, R.J. (1951). Protein measurements with the folin phenol reagent. *J. Biol. Chem.*, **193**, 265–275.

MICHEL, M.C., HANFT, G. & GROß, G. (1994). Functional studies on α_1-adrenoceptor subtypes mediating inotropic effects in rat right ventricle. *Br. J. Pharmacol.*, **111**, 539–546.

MICHEL, M.C., KANCZIK, R., KHAMSSI, M., KNORR, A., SIEGL, H., BECKERINGH, J.J. & BRODDE, O.-E. (1989). α- and β-adrenoceptors in hypertension. I. Cardiac and renal α_1-, β_1, and β_2-adrenoceptors in rat models of acquired hypertension. *J. Cardiovasc. Pharmacol.*, **13**, 421–431.

MICHEL, M.C., KANCZIK, R., KHAMSSI, M., KNORR, A., SIEGL, H., BECKERINGH, J.J. & BRODDE, O.-E. (1989). α- and β-adrenoceptors in hypertension. I. Cardiac and renal α_1-, β_1, and β_2-adrenoceptors in rat models of acquired hypertension. *J. Cardiovasc. Pharmacol.*, **13**, 421–431.

MICHEL, M.C., KERKER, J., BRANCHEK, T.A. & FORRAY, C. (1993). Selective irreversible binding of chloroethylclonidine at α_1- and α_2-adrenoceptor subtypes. *Mol. Pharmacol.*, (in press).

MICHEL, M.C., PHILIPP, T. & BRODDE, O.-E. (1992). α- and β-adrenoceptors in hypertension: molecular biology and pharmacological studies. *Pharmacol. Toxicol.*, **70** (Suppl. II), S1–S10.

MINNEMAN, K.P., HAN, C. & ABEL, P.W. (1988). Comparison of α_1-adrenergic receptor subtypes distinguished by chloroethylclonidine and WB 4101. *Mol. Pharmacol.*, **33**, 509–514.

PARINI, A., COUPRY, I., LAUDE, D., DIOP, L., VINCENT, M., SASSARD, J. & DAUSSE, J.-P. (1988). Noradrenaline content and adrenergic receptors in kidney and heart of the prehypertensive and hypertensive Lyon rat strain. *Am. J. Hypertens.*, **1**, 140–145.

PRICE, D.T., SCHWINN, D.A., CARON, M.G. & LEFKOWITZ, R.J. (1993). Tissue specific expression of α_1-adrenergic receptor subtype mRNAs: therapeutic implications for targeted receptor blockade. *Clin. Res.*, **41**, 188A.

SCATCHARD, G. (1949). The attraction of proteins for small molecules and ions. *Ann. NY Acad. Sci.*, **51**, 660–672.

SCHWINN, D.A., PAGE, S.O., MIDDLETON, J.P., LORENZ, W., LIGGETT, S.B., YAMAMOTO, K., LAPTETINA, E.G., CARON, M.G., LEFKOWITZ, R.J. & COTECCHIA, S. (1991). The α_{1C}-adrenergic receptor: characterization of signal transduction pathways and mammalian tissue heterogeneity. *Mol. Pharmacol.*, **40**, 619–626.

TAKANASHI, M., NOROTA, I. & ENDOH, M. (1991). Potent inhibitory action of chloroethylclonidine on the positive inotropic effect and phosphoinositide hydrolysis mediated via myocardial alpha$_1$-adrenoceptors in the rabbit ventricular myocardium. *Naunyn-Schmied. Arch. Pharmacol.*, **343**, 669–673.

TSUJIMOTO, G., TSUJIMOTO, A., SUZUKI, E. & HASHIMOTO, K. (1989). Glycogen phosphorylase activation by two different α_1-adrenergic receptor subtypes: methoxamine selectively stimulates a putative α_1-adrenergic receptor subtype (α_{1a}) that couples with Ca^{2+} influx. *Mol. Pharmacol.*, **36**, 166–176.

(Received June 14, 1993
Revised October 19, 1993
Accepted October 27, 1993)

Br. J. Pharmacol. (1994), 111, 539–546

Functional studies on α_1-adrenoceptor subtypes mediating inotropic effects in rat right ventricle

[1]Martin C. Michel, *Gertraud Hanft & [2,]*Gerhard Groß

Department of Medicine and *Department of Pharmacology, University of Essen, Essen, Germany

1 We have studied the α_1-adrenoceptor subtypes mediating inotropic effects of adrenaline in rat right ventricle and the Ca^{2+} sources used to elicit these effects. α_{1A}-Adrenoceptor-mediated contractile effects in rat vas deferens were studied for comparison in some cases.

2 Treatment with chloroethylclonidine did not affect the maximal β-adrenoceptor-mediated inotropic effects in rat right ventricle or the maximal α_{1A}-adrenoceptor-mediated contractile effects in rat vas deferens; it did not alter the potency of isoprenaline in the ventricle and reduced the potency of the α-adrenoceptor antagonists in vas deferens only slightly. Treatment of right ventricular strips with $CdCl_2$ markedly reduced resting tension and enhanced maximal inotropic effects of isoprenaline but did not affect its potency.

3 Inactivation of cardiac α_{1B}-adrenoceptors by treatment with chloroethylclonidine slightly enhanced the maximal inotropic effects of the full agonist, adrenaline and of several partial agonists.

4 Schild analysis of inhibition experiments with the α_{1A}-adrenoceptor-selective antagonists, 5-methylurapidil and (±)-tamsulosin, demonstrated that adrenaline causes its inotropic effects mainly via the α_{1B}-adrenoceptor subtype. Schild analysis of 5-methyl-urapidil inhibition experiments in chloroethylclonidine-treated ventricles indicated that only α_{1A}-adrenoceptors mediate the inotropic effects of adrenaline following inactivation of the α_{1B}-adrenoceptors.

5 In control ventricles the organic Ca^{2+} entry blocker, nitrendipine and treatment with the inorganic Ca^{2+} entry blocker, $CdCl_2$ did not reduce inotropic effects of adrenaline whereas ryanodine treatment inhibited them. In contrast, nitrendipine and $CdCl_2$ treatment had major inhibitory effects in chloroethylclonidine-treated but lacked inhibitory effects in phenoxybenzamine-treated ventricular strips.

6 We conclude that inotropic effects of adrenaline in rat heart are mediated mainly by α_{1B}-adrenoceptors via release of Ca^{2+} from an intracellular pool. Following inactivation of α_{1B}-adrenoceptors by chloroethylclonidine treatment, α_{1A}-adrenoceptors can fully compensate and mediate inotropic effects by promoting influx of extracellular Ca^{2+} at least partly via voltage-operated channels. Therefore, we speculate that α_{1B}-adrenoceptors exert a tonic inhibitory effect on α_{1A}-adrenoceptors.

Keywords: α_{1A}-Adrenoceptors; α_{1B}-adrenoceptors; rat heart; inotropy; Ca^{2+}

Introduction

Multiple α_1-adrenoceptor subtypes can be distinguished by use of pharmacological and receptor cloning techniques but the physiological relevance of this heterogeneity is not fully understood (Lomasney *et al.*, 1991; Bylund, 1992; Michel *et al.*, 1992). In rat heart, α_{1A}- and α_{1B}-adrenoceptors have been detected by radioligand binding (Minneman *et al.*, 1988; Hanft & Gross, 1989; Hanft *et al.*, 1989; Wang *et al.*, 1991; Knowlton *et al.*, 1993; Michel *et al.*, 1994). Known functions of cardiac α_1-adrenoceptors include inotropic and electrophysiological effects and (at least in cultured neonatal cardiomyocytes) the development of hypertrophy (Benfey, 1990; Endoh, 1991). Whereas the reduction in transient outward currents in rat ventricular cardiomyocytes is mediated by α_{1A}- and α_{1B}-adrenoceptors (Wang *et al.*, 1991), only α_{1A}-adrenoceptors appear to mediate the development of hypertrophy in cultured neonatal rat cardiomyocytes (Knowlton *et al.*, 1993). Therefore, the present study has investigated the α_1-adrenoceptor subtypes mediating the inotropic effects in rat heart and the Ca^{2+} sources used to elicit them. We have previously carried out a pharmacological analysis of the α_1-adrenoceptor subtypes present in rat heart and of the specificity and efficacy of the pharmacological tools used in the present study (preceding paper, Michel *et al.*, 1994).

[1] Author for correspondence at: Nephrol. Lab IG1, Klinikum, Hufelandstr. 55, D-45122 Essen, Germany.
[2] Present address: Knoll Pharmaceutical Co., Ludwigshafen, Germany.

Methods

Inotropic experiments in rat right ventricle and vas deferens

Male adult Wistar rats weighing 250–400 g were obtained from Lippische Versuchstierzucht (Extertal, Germany). α_1-Adrenoceptor-mediated positive inotropic effects were determined in right ventricles of rat heart as previously described (Gross *et al.*, 1988; Hanft & Gross, 1989). Briefly, experiments were performed at 30°C in organ baths containing 20 ml modified carbogen-saturated Krebs-Henseleit solution of the following composition (mmol l^{-1}): NaCl 118, KCl 4.8, $CaCl_2$ 2.5, $MgSO_4$ 1.2, $NaHCO_3$ 25, KH_2PO_4 1.2 and glucose 10. Additionally propranolol (10 μmol l^{-1}), oxaprotiline (0.3 μmol l^{-1}) and corticosterone (40 μmol l^{-1}) were added unless otherwise indicated, to block β-adrenoceptor-mediated responses and neuronal and extraneuronal uptake, respectively. The preparations were stimulated electrically at 1 Hz (3 ms, amplitude 20% above threshold voltage) under isometric conditions (preload 9.8 mN). Prior to each experiment endogenous catecholamine stores were depleted by treatment with tyramine (three times with 100 μmol l^{-1}). In some experiments, right ventricular strips were treated with vehicle, 100 μmol l^{-1} of chloroethylclonidine, 100 μmol l^{-1} $CdCl_2$ or both for 30 min followed by 60 min of washout.

Contractions of rat vas deferens were measured under the same conditions except that the contractions were recorded without electrical stimulation; the resting tension in vas deferens experiments was 4.9 mN.

Chemicals

The compounds used in this study were obtained from the following sources: (−)-adrenaline bitartrate, (−)-phenylephrine hydrochloride, (−)-isoprenaline hydrochloride, oxymetazoline hydrochloride, (±)-propranolol hydrochloride, yohimbine hydrochloride, corticosterone, and $CdCl_2$ from Sigma (Munich, Germany), (+)-oxaprotiline hydrochloride from Ciba Geigy (Basel, Switzerland), nitrendipine, phenoxybenzamine hydrochloride, and chloroethylclonidine dihydrochloride from Research Biochemicals (Natick, MA, U.S.A.), (±)-tamsulosin hydrochloride (formerly known as (±)-YM 12617 or (±)-YM 617) from Yamanouchi Pharmaceutical Co. (Tokyo, Japan), 5-methyl-urapidil from Byk Gulden (Konstanz, Germany), indanidine (formerly known as Sgd 101/75) from Siegfried (Zofingen, Switzerland), cirazoline hydrochloride from Synthelabo (Paris, France), and (−)-amidephrine mesylate from Bristol Myers (Evansville, IN, U.S.A).

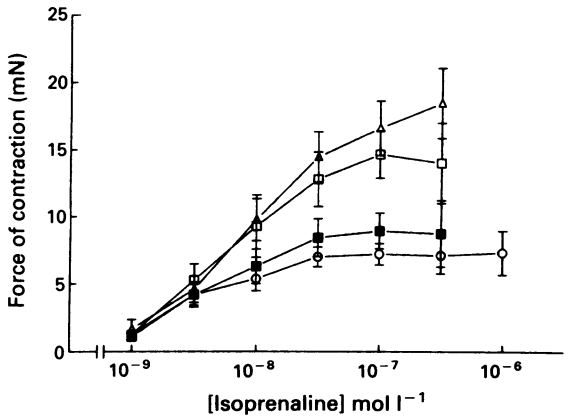

Figure 1 Effects of treatment with chloroethylclonidine and/or $CdCl_2$ on isoprenaline-induced positive inotropic effects. Tissue strips were treated for 30 min at 30°C in the organ bath with vehicle (○), 100 μmol l^{-1} chloroethylclonidine (■), 100 μmol l^{-1} $CdCl_2$ (□) or 100 μmol l^{-1} $CdCl_2$ or their combination (△). Following 60 min of washout, cumulative concentration-response curves for isoprenaline were constructed. Data are mean ± s.e.mean of 7–8 experiments.

Results

Effects of chloroethylclonidine and $CdCl_2$ treatment on β-adrenoceptor-mediated positive inotropic effects in right ventricle

Treatment with chloroethylclonidine, $CdCl_2$ or both did not affect the potency of isoprenaline in eliciting inotropic effects in rat right ventricle (Figure 1); propranolol was omitted from the organ bath in these experiments. Thus, the pD_2 values for isoprenaline were similar under control conditions (8.27 ± 0.18; $n = 8$), in chloroethylclonidine-treated strips (8.28 ± 0.16; $n = 8$), in $CdCl_2$-treated strips (8.13 ± 0.17; $n = 7$), and in strips treated with the combination of chloroethylclonidine plus $CdCl_2$ (8.19 ± 0.15; $n = 8$). The maximal inotropic effects of isoprenaline were also not significantly affected by chloroethylclonidine treatment (9.8 ± 1.3 mN in treated

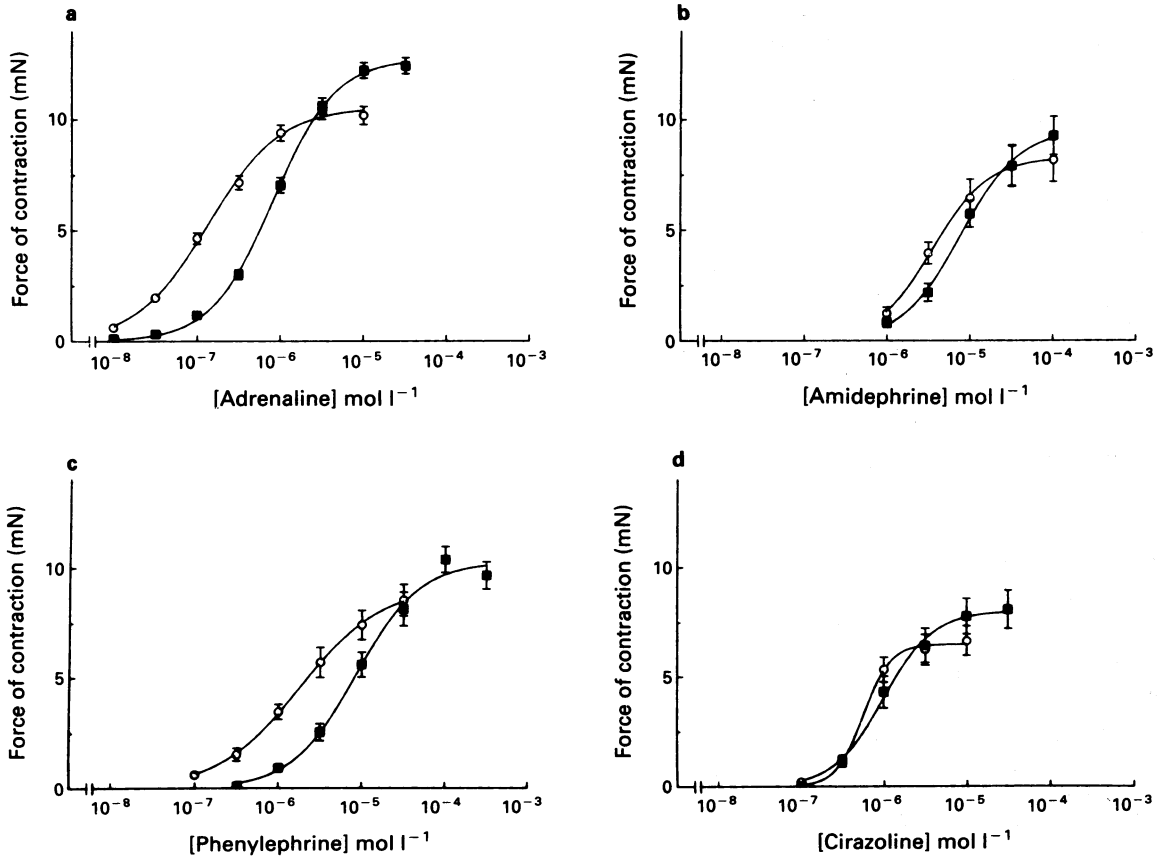

Figure 2 Effects of treatment with chloroethylclonidine on α_1-adrenoceptor-mediated positive inotropic effects. Tissue strips were treated for 30 min at 30°C in the organ bath with vehicle (○) or 100 μmol l^{-1} chloroethylclonidine (■). Following 60 min of washout, cumulative concentration-response curves for the indicated agonists were constructed. Data are mean ± s.e.mean of (a) 49 (control adrenaline), 37–42 (chloroethylclonidine-treated adrenaline), (b) 6 (amidephrine), (c) 8 (phenylephrine) and (d) 9 experiments (cirazoline).

Table 1 Effect of chloroethylclonidine-treatment on α-adrenoceptor agonist-stimulated positive inotropic effects in rat vas deferens

	Control		*Chloroethylclonidine-treated*	
	Developed tension (mN)	pD_2	*Developed tension* (mN)	pD_2
Amidephrine	13.8 ± 1.4	5.35 ± 0.08	13.9 ± 1.8	5.14 ± 0.06
Cirazoline	13.6 ± 1.0	6.57 ± 0.03	13.8 ± 1.0	6.32 ± 0.04***
Phenylephrine	21.1 ± 1.5	5.53 ± 0.03	21.4 ± 1.9	5.22 ± 0.03***

Contractile effects were determined in rat vas deferens following a 30 min treatment with 100 μmol l^{-1} chloroethylclonidine and subsequent 60 min washout or under time-matched control conditions. Data are mean ± s.e.mean of 6 (amidephrine), 8 (cirazoline), and 8 (phenylephrine) experiments. ***$P<0.001$ vs. control.

Table 2 Effect of chloroethylclonidine-treatment on α-adrenoceptor agonist-stimulated positive inotropic effects in rat right ventricle

	Control		*Chloroethylclonidine-treated*	
	Developed tension (mN)	pD_2	*Developed tension* (mN)	pD_2
Adrenaline	10.6 ± 0.4	6.88 ± 0.17	12.5 ± 0.4***	6.10 ± 0.17***
Amidephrine	8.3 ± 1.0†	5.47 ± 0.06	9.3 ± 0.9†	5.17 ± 0.03**
Cirazoline	6.6 ± 0.7†††	6.23 ± 0.02	8.1 ± 0.9†††	5.97 ± 0.07**
Phenylephrine	8.6 ± 0.7†	5.85 ± 0.02	10.5 ± 0.6†	5.03 ± 0.07***

Positive inotropic effects were determined in rat right ventricular strips following a 30 min treatment with 100 μmol l^{-1} chloroethylclonidine and subsequent 60 min washout or under time-matched control conditions. Data are mean ± s.e.mean of 49 (adrenaline control), 42 (adrenaline-treated), 6 (amidephrine), 9 (cirazoline), and 8 (phenylephrine) experiments. **$P<0.01$ and ***$P<0.001$, vs. control; †$P<0.05$ and ††$P<0.001$, vs. adrenaline. A graphic representation of these data is given in Figure 1.

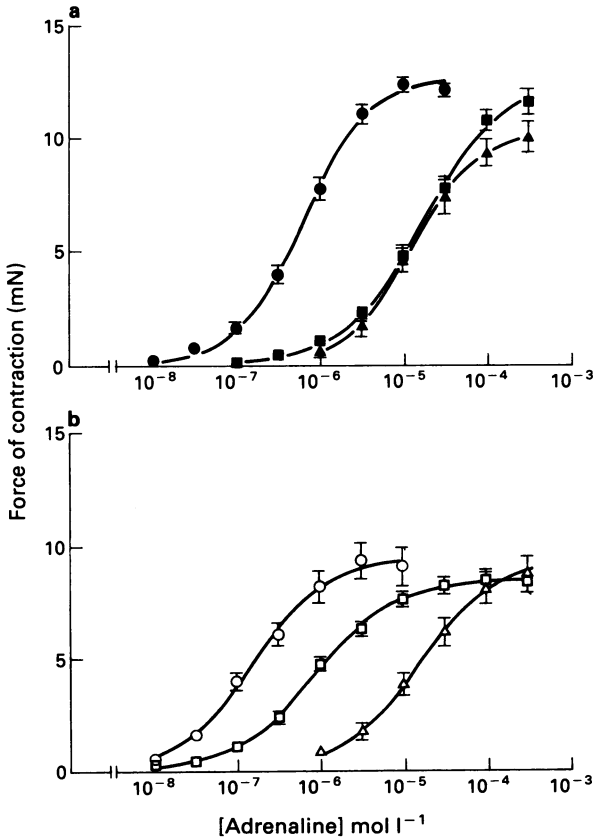

Figure 3 Effects of chloroethylclonidine treatment on α_1-adrenoceptor subtypes mediating the positive inotropic effects of adrenaline. Tissue strips were treated for 30 min at 30°C in the organ bath with vehicle (b, open symbols) or 100 μmol l^{-1} chloroethylclonidine (a, filled symbols). Following 60 min of washout, cumulative concentration-response curves for adrenaline were constructed in the absence (●, ○) and presence of 100 nmol l^{-1} 5-methyl-urapidil (■, □) or prazosin (▲, △). Data are mean ± s.e.mean of 11–14 and 6–19 experiments under control conditions (b) and after chloroethylclonidine treatment (a) respectively.

vs. 8.1 ± 0.8 mN in control strips; Figure 1), but treatment with $CdCl_2$ almost doubled the inotropic effects of isoprenaline to 16.1 ± 2.3 mN in $CdCl_2$-treated and 17.2 ± 2.2 in $CdCl_2$ plus chloroethylclonidine-treated strips. The enhanced inotropic effects of isoprenaline were mainly due to reduced basal force of contraction since basal force was similar in control (27.4 ± 1.3 mN) and chloroethylclonidine-treated strips (23.3 ± 0.6 mN) but significantly reduced in $CdCl_2$-treated (13.2 ± 1.2 mN, $P<0.001$ vs. control) or $CdCl_2$ plus chloroethylclonidine-treated strips (15.8 ± 1.7 mN, $P<0.001$ vs. chloroethylclonidine-treated strips).

Effects of chloroethylclonidine treatment on α_{1A}-adrenoceptor-mediated contractile effects in vas deferens

In rat vas deferens, α_1-adrenoceptor agonists elicited contractile effects with the order of potency: cirazoline > phenylephrine ⩾ amidephrine; maximal contractile effects for amidephrine and cirazoline were approximately 35% smaller than those for phenylephrine (Table 1). Chloroethylclonidine treatment did not alter maximal contractile effects of the partial agonists amidephrine and cirazoline or the more efficacious agonist phenylephrine (Table 1). The potency of the agonists was slightly reduced in chloroethylclonidine-treated strips but this reached statistical significance only for cirazoline and phenylephrine (Table 1).

Effects of chloroethylclonidine treatment on α_1-adrenoceptor-mediated positive inotropic effects in right ventricle

α-Adrenoceptor agonists increased force of contraction with a rank order of potency of adrenaline > cirazoline > phenylephrine > amidephrine (Figure 2, Table 2). Relative to adrenaline (increase in force of contraction 10.6 ± 2.6 mN, $n = 49$) the other compounds were only partial agonists with efficacies of 62% (cirazoline, $n = 9$), 81% (phenylephrine, $n = 8$) and 78% (amidephrine, $n = 6$); indanidine was a very weak partial agonist (~7% of the adrenaline effect at

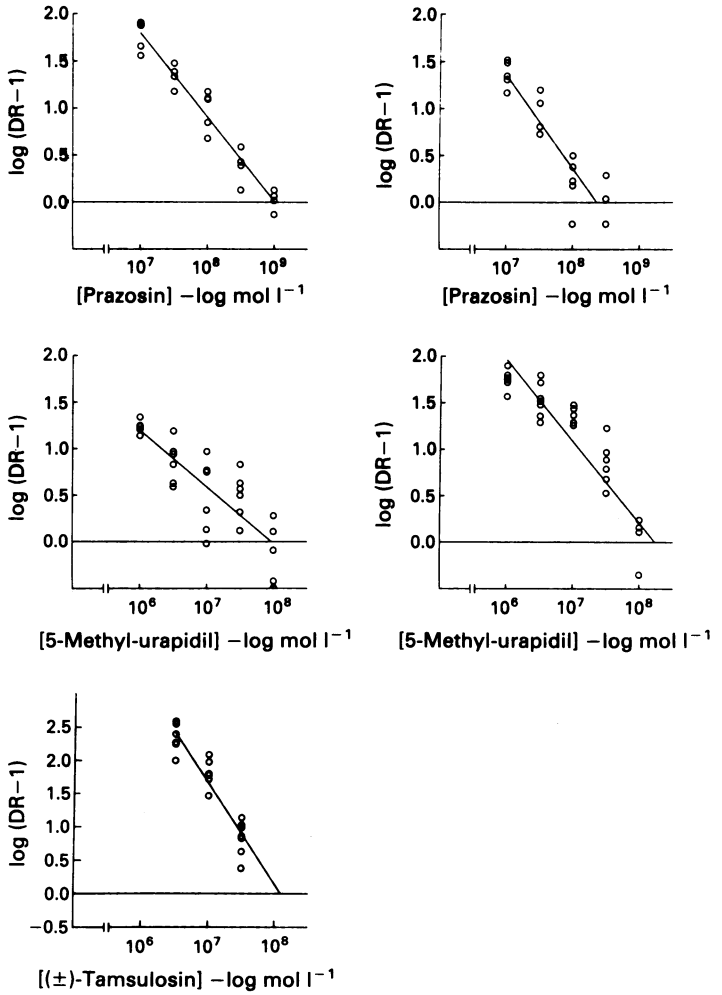

Figure 4 Effects of chloroethylclonidine treatment on α_1-adrenoceptor subtypes mediating the positive inotropic effects of adrenaline. Tissue strips were treated for 30 min at 30°C in the organ bath with vehicle (left panels) or 100 μmol l^{-1} chloroethylclonidine (right panels) with subsequent 60 min of washout. The panels show a Schild analysis of data similar to and including those shown in Figure 3. Each data point represents the shift of the dose-ratio (DR) obtained in the presence of the indicated antagonist concentration in a single experiment; DR was determined as the ratio of the concentration of adrenaline required for half-maximal stimulatory effects in the presence and absence of the antagonist concentration.

300 μmol l^{-1}), and oxymetazoline did not cause consistent positive inotropic effects but rather caused negative inotropic effects in concentrations exceeding 100 μmol l^{-1} which were not affected by addition of 1 μmol l^{-1} prazosin, i.e. apparently unrelated to α_1-adrenoceptors.

Inactivation of α_{1B}-adrenoceptors by treatment with chloroethylclonidine did not alter basal force of contraction (see above) and reduced the potency of the α-adrenoceptor agonists by factors of less than 10 (Figure 2, Table 2). The maximal inotropic effects of adrenaline were significantly enhanced following chloroethylclonidine treatment by approximately 20% ($n = 42$, $P < 0.0001$, Figure 2, Table 2). Maximal inotropic effects of the partial α-adrenoceptor agonists were increased to a similar extent but this did not reach statistically significant levels with the given number of experiments (Figure 2, Table 2).

Effects of chloroethylclonidine treatment on the subtype mediating positive inotropic effects of adrenaline in right ventricle

Prazosin (1–100 nmol l^{-1}), 5-methyl-urapidil (10–1000 nmol l^{-1}), and (±)-tamsulosin (30–300 nmol l^{-1}) concentration-dependently shifted the adrenaline concentration-response curve to the right towards higher concentrations without significantly affecting the maximal inotropic effect (Figures 3 and 4). Whereas 100 nmol l^{-1} 5-methyl-urapidil caused a much smaller right shift in control than in chloroethylclonidine-treated ventricular strips, 100 nmol l^{-1} prazosin shifted the adrenaline concentration-response curve to a similar extent under both conditions (Figure 3); thus, the α_{1A}-selective 5-methyl-urapidil caused a much smaller shift than non-selective prazosin under control conditions, whereas both drugs caused similar shifts following chloroethylclonidine treatment. We quantitatively analyzed these antagonistic effects with Schild plots (Arunlakshana & Schild, 1959). The regression line of the Schild plots for prazosin had a slope which did not significantly differ from unity in control (0.89 ± 0.05) and chloroethylclonidine-treated strips (0.99 ± 0.10) and yielded pA_2 values of 9.01 and 8.36, respectively (Figure 4). The α_2-adrenoceptor selective antagonist, yohimbine (50 nmol l^{-1}) failed to shift the adrenaline concentration-response curve in chloroethylclonidine-treated strips. Schild analysis of the 5-methyl-urapidil shifts revealed a slope which was less than unity in control strips (0.61 ± 0.08; Figure 4). Therefore a pA_2 value could not be calculated; pK_b values calculated for the individual 5-methyl-urapidil concentrations ranged from 8.12 to 7.25. Following chloroethylclonidine treatment the slope of the Schild regression for 5-

methyl-urapidil was steepened and no longer significantly differed from unity (0.88 ± 0.09); the pA_2 value calculated from data obtained with chloroethylclonidine-treated strips was 8.24 (Figure 4). Schild analysis of antagonism by (±)-tamsulosin yielded a slope which was somewhat steeper than unity (1.52 ± 0.14) and the x-axis intercept was 8.09 (Figure 4); in contrast (±)-tamsulosin yielded a pA_2 value of 9.32 for the α_{1A}-adrenoceptor-mediated contraction of rat vas deferens (slope 1.16 ± 0.08).

Effects of chloroethylclonidine treatment on Ca^{2+} sources used by adrenaline for its positive inotropic effects in right ventricle

The organic Ca^{2+} entry blocker, nitrendipine (100 nmol l^{-1}) did not significantly affect resting tension in control (22.4 ± 1.7 mN in the absence and 20.6 ± 0.9 mN in the presence, $n = 8$ and 7, respectively) or chloroethylclonidine-treated rat right ventricle (19.5 ± 1.9 mN in the absence and 17.8 ± 1.4 mN in the presence, $n = 8$ and 12, respectively). Addition of nitrendipine slightly but significantly enhanced the inotropic effects of adrenaline in control strips (pD_2 value from 6.74 ± 0.05 to 7.00 ± 0.05, $n = 8$ and 9, respectively, $P = 0.0023$) but did not alter the maximal response to adrenaline under control conditions (10.0 ± 0.7 and 10.5 ± 0.5 mN in the absence and presence of nitrendipine, respectively; Figure 5). In chloroethylclonidine-treated strips, however, nitrendipine did not enhance the inotropic response to adrenaline (pD_2 value 6.10 ± 0.07 in the absence and 6.11 ± 0.03 the presence of nitrendipine, $n = 8$ and 12, respectively) but significantly reduced the maximal inotropic response to adrenaline from 14.0 ± 0.8 to 11.1 ± 0.8 ($P = 0.0218$; Figure 5).

Treatment with the inorganic Ca^{2+} entry blocker, $CdCl_2$ (100 μmol l^{-1} for 30 min followed by 60 min washout) had little effect on the sensitivity towards the inotropic effects of adrenaline (pD_2 value 6.95 in control and 6.72 in treated strips with $n = 22$ and 18, respectively; Figure 6) and simul-

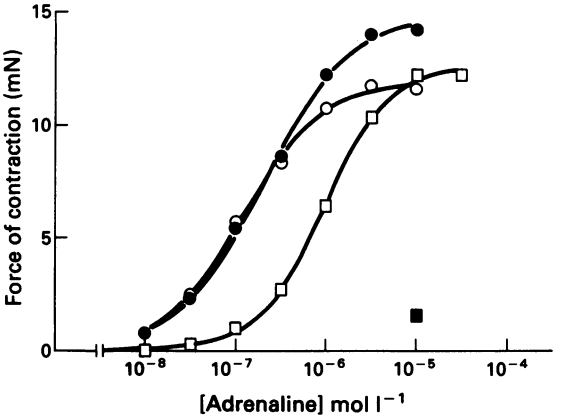

Figure 6 Effects of chloroethylclonidine- and $CdCl_2$-treatment on α_1-adrenoceptor-mediated positive inotropic effects. Tissue strips were treated for 30 min at 30°C in the organ bath with vehicle (○), 100 μmol l^{-1} chloroethylclonidine (□), 100 μmol l^{-1} $CdCl_2$ (●) or the combination of both (■) with subsequent 60 min of washout. Concentration-response curves for adrenaline were constructed in control and chloroethylclonidine- and $CdCl_2$-treated strips but could not be obtained in strips treated concomitantly with both. Data are mean of 18–22 experiments; error bars were omitted for clarity.

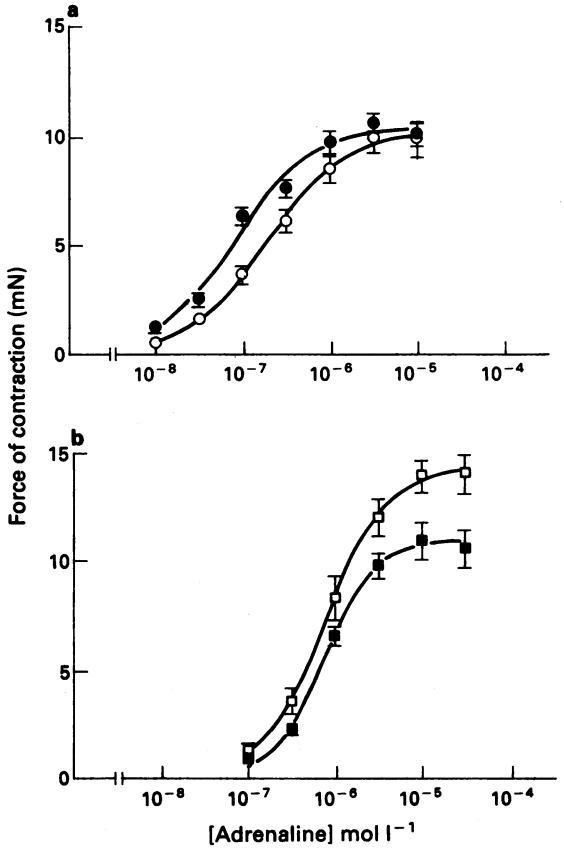

Figure 5 Effects of chloroethylclonidine-treatment and nitrendipine on α_1-adrenoceptor-mediated positive inotropic effects. Tissue strips were treated for 30 min at 30°C in the organ bath with vehicle (a) or 100 μmol l^{-1} chloroethylclonidine (b) with subsequent 60 min of washout. Concentration-response curves for adrenaline were constructed in the absence (open symbols) and presence of 100 nmol l^{-1} nitrendipine (solid symbols). Data are mean ± s.e.mean of 8–12 experiments.

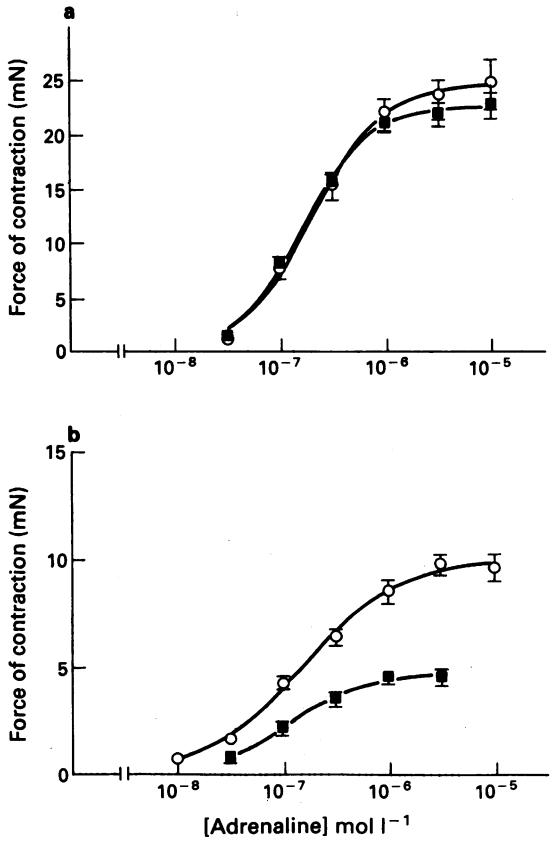

Figure 7 Effects of ryanodine on α_1-adrenoceptor-mediated contractile effects in heart and vas deferens. Concentration-response curves for adrenaline were constructed in the absence (○) and presence of 300 nmol l^{-1} ryanodine (■) in right atrial (b) and vas deferens strips (a). Data are mean ± s.e.mean of 8 experiments.

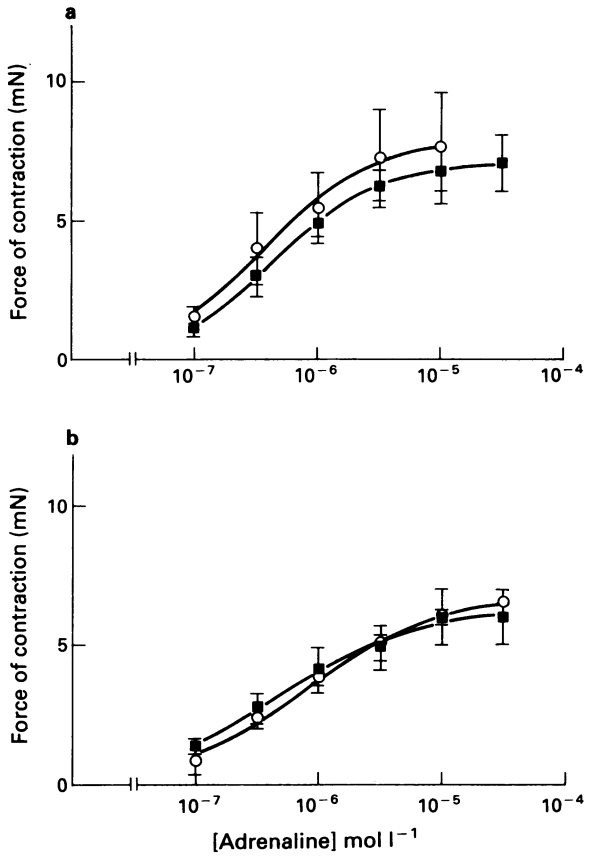

Figure 8 Effects of nitrendipine on α_1-adrenoceptor-mediated inotropic effects in cardiac strips pretreated with phenoxybenzamine. Right ventricular strips were treated with 100 nmol l^{-1} phenoxybenzamine for 5 (a) and 10 min (b) followed by 60 min washout. Adrenaline concentration-response curves were constructed in the absence (○) and presence of 100 nmol l^{-1} nitrendipine (■). Data are mean ± s.e.mean of 3 experiments.

taneously slightly enhanced the maximal responses towards adrenaline. In contrast, treatment with $CdCl_2$ reduced the inotropic response to 10 μmol l^{-1} adrenaline by almost 90% in chloroethylclonidine-treated strips (Figure 6), and the reduction in force of contraction was so pronounced that concentration-response curves could not be analyzed.

Addition of 300 nmol l^{-1} ryanodine to the organ bath 1 h prior to adrenaline reduced basal force of contraction from 23.5 ± 0.8 to 5.3 ± 0.5 mN ($n = 8$ each, $P < 0.0001$). Ryanodine also reduced the (presumably α_{1B}-adrenoceptor-mediated) maximal inotropic responses of adrenaline by ~50% but the sensitivity of the remaining responses of adrenaline (pD_2 value 6.90 ± 0.09) was similar to that in paired control strips (pD_2 value 6.85 ± 0.03; Figure 7). In contrast, ryanodine did not alter the α_{1A}-adrenoceptor-mediated contractile response towards adrenaline in vas deferens with regard to maximal effects or sensitivity (Figure 7).

Non-selective alkylation of α_{1A}- and α_{1B}-adrenoceptors in rat right ventricle by phenoxybenzamine (100 nmol l^{-1} for 5 or 10 min) reduced the maximal inotropic effects of adrenaline (Figure 8) and also slightly decreased its potency (pD_2 values 6.57 ± 0.06 and 6.22 ± 0.15, respectively, $n = 3$ each). In phenoxybenzamine-treated strips, however, addition of 100 nmol l^{-1} nitrendipine did not cause any further reduction of the inotropic effects of adrenaline (Figure 8).

Discussion

Previous studies have investigated the role of cardiac α_1-adrenoceptor subtypes in signalling and growth regulation; α_1-adrenoceptor stimulation reduces a voltage-activated transient outward current in adult cardiomyocytes; while either α_{1A}- or α_{1B}-adrenoceptor inhibition was sufficient to block the late component of this current, only combined α_{1A}- and α_{1B}-adrenoceptor inhibition could antagonize its peak component (Wang *et al.*, 1991). The α_1-adrenoceptor-mediated formation of inositol phosphates and induction of a hypertrophic phenotype in rat cultured neonatal cardiomyocytes involves only the α_{1A}-adrenoceptor subtype (Del Balzo *et al.*, 1990; Knowlton *et al.*, 1993). The present study has investigated the role of α_1-adrenoceptor subtypes in the enhancement of contractility.

The specificity of the tools, 5-methyl-urapidil, (±)-tamsulosin, oxaprotiline, nitrendipine and of the treatments with chloroethylclonidine and/or $CdCl_2$ has been evaluated in our previous studies (Hanft & Gross, 1989; Hanft *et al.*, 1989; Michel *et al.*, 1994). Moreover, our conditions of chloroethylclonidine-treatment do not non-specifically interfere with contractility of cardiac or vas deferens smooth muscle and do not inhibit inotropic effects mediated by β-adrenoceptor stimulation or contractile effects in vas deferens which are mediated by α_{1A}-adrenoceptors (Han *et al.*, 1987; Hanft & Gross, 1989). Thus, functional effects of our chloroethylclonidine treatments are unlikely to result from anything but α_{1B}-adrenoceptor inactivation.

Competitively binding drugs and the irreversible antagonist, chloroethylclonidine, detect similar proportions of α_{1A}- and α_{1B}-adrenoceptors in rat heart in radioligand binding studies (Minneman *et al.*, 1988; Hanft & Gross, 1989; Hanft *et al.*, 1989; Han & Minneman, 1991). However, the two approaches did not yield compatible results with regard to the α_1-adrenoceptor subtype mediating positive inotropic effects in the present study. Based on Schild analysis of the antagonism by the α_{1A}-adrenoceptor-selective WB 4101 and 5-methyl-urapidil, we have previously suggested that adrenaline causes inotropic effects in rat right ventricle via α_{1B}-adrenoceptors (Hanft & Gross, 1989). Our present results with the α_{1A}-adrenoceptor-selective (±)-tamsulosin (Hanft *et al.*, 1989; Michel *et al.*, 1993) support this conclusion. The use of a wider range of 5-methyl-urapidil concentrations than in our previous study (Hanft & Gross, 1989) reduces the slope of the Schild regression to values of less than unity indicating the possible involvement of more than one site and thus not allowing the calculation of pA_2 values. However, pK_b values calculated for the antagonism by the individual 5-methyl-urapidil concentrations were all much closer to its α_{1B}- than its α_{1A}-adrenoceptor affinity. Thus, our previous (Hanft & Gross, 1989) and present data with competitive antagonists suggest that adrenaline causes its positive inotropic effects in rat heart mainly if not exclusively via α_{1B}-adrenoceptors when β-adrenoceptors are blocked. However, a minor contribution of α_{1A}-adrenoceptors, which is not recognized by WB 4101 or (±)-tamsulosin, cannot be ruled out.

On the other hand, effective inactivation of α_{1B}-adrenoceptors by chloroethylclonidine treatment (Michel *et al.*, 1994) yielded apparently opposite results. Thus, chloroethylclonidine treatment did not reduce but rather enhanced the maximal inotropic effects of the full agonist adrenaline or the partial agonists amidephrine, cirazoline or phenylephrine (for which by definition no receptor reserve exists). Chloroethylclonidine treatment steepened the slope of the Schild-regression for the antagonistic effects of 5-methyl-urapidil and resulted in a pA_2 value which is closer to its α_{1A}-adrenoceptor affinity. Rat heart contains much fewer α_{1A}- than α_{1B}-adrenoceptors (Minneman *et al.*, 1988; Hanft & Gross, 1989; Han & Minneman, 1991; Michel *et al.*, 1994) and appears to lack α_{1C}-adrenoceptors in radioligand binding (Minneman *et al.*, 1988; Hanft & Gross, 1989; Han & Minneman, 1991) and Northern blot analysis (Lomasney *et al.*, 1991). Thus, either α_{1A}-adrenoceptors couple much more efficiently to inotropy than α_{1B}-adrenoceptors, or α_{1B}-adrenoceptors exert a tonic inhibitory effect on α_{1A}-adrenoceptors under control conditions which makes the contribution of the latter hard to detect. Although

we lack definitive proof of either hypothesis, we favour the latter for the following reasons. Firstly, lack of reduction of maximal effects by α_{1B}-adrenoceptor inactivation is compatible with the idea of more efficient α_{1A}-adrenoceptor coupling only if this subtype completely dominates the inotropic response. The low antagonistic potencies of the α_{1A}-selective antagonists, WB 4101, (±)-tamsulosin and 5-methyl-urapidil rule out this possibility. Secondly, enhanced inotropic effects of adrenaline following chloroethylclonidine treatment are completely implausible unless a tonic inhibitory effect of α_{1B}-adrenoceptors is postulated. In another study neither WB 4101 nor chloroethylclonidine had affected basal contractility of adult rat cardiomyocytes, but WB 4101 inhibited and chloroethylclonidine enhanced the contractile effects of the α_1-adrenoceptor agonist phenylephrine (Gambassi *et al.*, 1991). Therefore, we speculate that α_{1A}- and α_{1B}-adrenoceptors cross-talk in rat heart. As a result a fully-fledged α_{1A}-adrenoceptor-mediated inotropic response becomes detectable only following α_{1B}-adrenoceptor inactivation. Since the cellular localization of the various adrenoceptor subtypes within the myocardium is unclear, a more detailed understanding of this interaction will probably require the use of a cell line co-expressing the subtypes. On the other hand such α_{1A}/α_{1B}-adrenoceptor cross-talk may not occur in all species since chloroethylclonidine treatment almost completely abolishes the α_1-adrenoceptor-mediated inotropic effects in rabbit myocardium (Takanashi *et al.*, 1991).

Elevations of intracellular Ca^{2+} are crucial for the development of inotropy (Langer, 1992; Stern & Lakatta, 1992), but Ca^{2+} sensitization of the myofilaments may also play an important role in α_1-adrenoceptor-mediated inotropy (Puceat *et al.*, 1992). Since α_{1A}- and α_{1B}-adrenoceptors increase intracellular Ca^{2+} by different mechanisms in extra-cardiac tissues (Minneman, 1988; Wilson & Minneman, 1990), we investigated the sources of Ca^{2+} used by adrenaline in control (mainly α_{1B}-adrenoceptors) and chloroethylclonidine-treated right ventricular strips (mainly α_{1A}-adrenoceptors) to elicit positive inotropic effects; in some cases α_{1A}-adrenoceptor-mediated contractions of rat vas deferens (Han *et al.*, 1987; Hanft & Gross, 1989) were used as an additional model system. In control strips nitrendipine and $CdCl_2$ treatment did not inhibit the inotropic effects of adrenaline but rather slightly enhanced its potency and increased its maximal effects, respectively. Thus, influx of extracellular Ca^{2+} does not appear to be required for the α_{1B}-adrenoceptor-mediated positive inotropic effects. Similarly, α_{1B}-adrenoceptor-mediated vasoconstriction elicited by full agonist in rat aorta (Beckeringh *et al.*, 1984) and generation of inositol phosphates in rat hepatocytes (Wilson & Minneman, 1990) are insensitive to blockade of Ca^{2+} influx. In contrast, ryanodine which modulates Ca^{2+} release from the sarcoplasmic reticulum (Stern & Lakatta, 1992) decreased maximal inotropic effects of adrenaline without altering its potency, indicating the importance of Ca^{2+} release from the sarcoplasmic reticulum. This Ca^{2+} release is unlikely to involve inositol phosphate formation since (a) inositol phosphate formation is too slow to participate in control of the heart beat (Stern & Lakatta, 1992), (b) (at least in neonatal rat cardiomyocytes) inositol phosphate formation occurs via α_{1A}- but not via α_{1B}-adrenoceptors (Del Balzo *et al.*, 1990; Knowlton *et al.*, 1993), and (c) because the ryanodine receptor is distinct from the inositol phosphate receptor (Otsu *et al.*, 1990). Thus, cardiac α_{1B}-adrenoceptors are similar to those in other tissues since they rely on mobilization of Ca^{2+} from intracellular pools rather than on influx of extracellular Ca^{2+} to elicit inotropic effects but are distinct since they are unlikely to do so via generation of inositol phosphates.

A different picture was obtained in the α_{1A}-adrenoceptor models, i.e. in chloroethylclonidine-treated heart and in vas deferens. In chloroethylclonidine-treated heart, $CdCl_2$ treatment and nitrendipine reduced the maximal inotropic effects of adrenaline by 88% and 21%, respectively. The weaker inhibition by nitrendipine compared to $CdCl_2$ treatment could indicate incomplete blockade of voltage-operated Ca^{2+} channels or the concomitant involvement of such channels and other pathways of transmembrane Ca^{2+} fluxes such as the Na^+/Ca^{2+} exchange which can operate bidirectionally (Hilton, 1985). We cannot completely answer this question since higher concentrations of nitrendipine interfered with α_1-adrenoceptor binding but favour the latter possibility since 100 nmol l^{-1} nitrendipine is considerable in excess of its affinity at voltage-operated Ca^{2+} channels (Goa & Sorkin, 1987). In vas deferens, ryanodine failed to alter the α_{1A}-adrenoceptor-mediated contractile response to adrenaline.

In some model systems of α_{1B}-adrenoceptors such as rat aorta, full agonists can rely on mobilization of intracellular Ca^{2+} only whereas partial agonists require influx of extracellular Ca^{2+} (Beckeringh *et al.*, 1984); following partial inactivation of α_{1B}-adrenoceptors by treatment with the alkylating agent, phenoxybenzamine, full agonists may also require influx of extracellular Ca^{2+} to elicit vasoconstriction (Ruffolo *et al.*, 1991). In the present study treatment with phenoxybenzamine failed to cause nitrendipine-sensitivity in rat right ventricle although it reduced the potency of adrenaline to a similar extent to chloroethylclonidine treatment and, in contrast to chloroethylclonidine, even reduced the maximal inotropic response. Thus, α_{1B}-adrenoceptor-mediated inotropic effects do not require influx of extracellular Ca^{2+} but may involve Ca^{2+} release from the sarcoplasmic reticulum via a ryanodine receptor as well as Ca^{2+} sensitization of the myofilaments (Puceat *et al.*, 1992). In contrast α_{1A}-adrenoceptor-mediated contractile effects in rat heart and vas deferens require influx of extracellular Ca^{2+} which occurs at least partly via a voltage-operated Ca^{2+} channel (see also, Han *et al.*, 1987); Ca^{2+} mobilization from ryanodine-sensitive stores may not be involved.

In summary, we have demonstrated that adrenaline (in the presence of propranolol) causes positive inotropic effects via α_{1B}-adrenoceptors independently of influx of extracellular Ca^{2+} in control myocardium. Following inactivation of α_{1B}-adrenoceptors by chloroethylclonidine treatment, α_{1A}-adrenoceptors more than compensate by mediating even greater positive inotropic effects by stimulation of the influx of extracellular Ca^{2+}. Together with previously published data (Del Balzo *et al.*, 1990; Anyukhovsky & Rosen, 1991; Wang *et al.*, 1991; Knowlton *et al.*, 1993) we conclude that α_{1A}- and α_{1B}-adrenoceptors may be coexpressed in rat myocardium to activate distinct physiological responses.

The apparent cross-talk between α_{1A}- and α_{1B}-adrenoceptors may be important under pathophysiological conditions. Thus, in hearts from spontaneously hypertensive rats, α_1-adrenoceptor-mediated iontropic effects appear to be enhanced although the number of α_1-adrenoceptors and their G-protein G_q are unchanged (Brodde & Michel, 1992). Moreover, preliminary data from our laboratory indicate that the ratio of α_{1A}/α_{1B}-adrenoceptors is similar in normotensive WKY ($28 \pm 3/72 \pm 3$) and spontaneously hypertensive rats ($26 \pm 2/74 \pm 2$, $n = 6$ each, unpublished observations). Since β-adrenoceptor-mediated inotropy is reduced rather than enhanced in hypertensive hearts (Brodde & Michel, 1992) and, thus, alterations of the contractile apparatus cannot explain enhanced inotropy, the intriguing possibility exists that enhanced α_1-adrenoceptor function may be related to an altered cross-talk between α_{1A}- and α_{1B}-adrenoceptors.

We thank the respective companies for their gifts of drugs and Mr Hagelskamp for his skilful technical assistance. This work was supported by the Deutsche Forschungsgemeinschaft.

References

ANYUKHOVSKY, E.P. & ROSEN, M.R. (1991). Abnormal automatic rhythms in ischemic purkinje fibers are modulated by a specific α_1-adrenergic receptor subtype. *Circulation*, **83**, 2076–2082.

ARUNLAKSHANA, O. & SCHILD, H.O. (1959). Some quantitative uses of drug antagonists. *Br. J. Pharmacol. Chemother.*, **14**, 48–58.

BECKERINGH, J.J., THOOLEN, M.J.M.C., DE JONGE, A., WILFFERT, B., TIMMERMANS, P.B.M.W.M. & VAN ZWIETEN, P.A. (1984). Differential effects of the calcium entry blocker D 600 on contractions of rat and guinea-pig aortas, elicited by various alpha-1 adrenoceptor agonists. *J. Pharmacol. Exp. Ther.*, **229**, 515–521.

BENFEY, B.G. (1990). Function of myocardial α-adrenoceptors. *Life Sci.*, **46**, 743–757.

BRODDE, O.-E. & MICHEL, M.C. (1992). Adrenergic receptors and their signal transduction mechanisms in hypertension. *J. Hypertension*, **10** Suppl. 7, S133–S145.

BYLUND, D.B. (1992). Subtypes of α_1- and α_2-adrenergic receptors. *FASEB J.*, **6**, 832–839.

DEL BALZO, U., ROSEN, M.R., MALFATTO, G., KAPLAN, L.M. & STEINBERG, S.F. (1990). Specific α_1- adrenergic receptor subtypes modulate catecholamine-induced increases and decreases in ventricular automaticity. *Circ. Res.*, **67**, 1535–1551.

ENDOH, M. (1991). Myocardial α-adrenoceptors: multiplicity of subcellular coupling processes. *Asia Pac. J. Pharmacol.*, **6**, 171–186.

GAMBASSI, G., BERENHOLTZ, S., ZIMAN, B., LAKATTA, E.G. & CAPOGROSSI, M.C. (1991). Opposing effects of α_{1A}- and α_{1B} receptors on the inotropic response to α_1-adrenergic stimulation in adult rat myocytes. *Circulation*, **84** Suppl. II, II–403.

GOA, K.L. & SORKIN, E.M. (1987). Nitrendipine. An updated review. *Drugs*, **33**, 123–155.

GROSS, G., HANFT, G. & RUGEVICS, C.-U. (1988). α_1-Adrenoceptors in rat myocardium: comparison of agonist binding and positive inotropic response. *Naunyn-Schmied. Arch. Pharmacol.*, **338**, 582–588.

HAN, C., ABEL, P.W. & MINNEMAN, K.P. (1987). α_1-Adrenoceptor subtypes linked to different mechanisms for increasing intracellular Ca^{2+} in smooth muscle. *Nature*, **329**, 333–335.

HAN, C. & MINNEMAN, K.P. (1991). Interaction of subtype-selective antagonists with α_1-adrenergic receptor binding sites in rat tissues. *Mol. Pharmacol.*, **40**, 531–538.

HANFT, G. & GROSS, G. (1989). Subclassification of α_1-adrenoceptor recognition sites by urapidil derivatives and other selective antagonists. *Br. J. Pharmacol.*, **97**, 691–700.

HANFT, G., GROSS, G., BECKERINGH, J.J. & KORSTANJE, C. (1989). α_1-Adrenoceptors: the ability of various agonists and antagonists to discriminate between two distinct [^{3}H]-prazosin binding sites. *J. Pharm. Pharmacol.*, **41**, 714–716.

HILTON, P.J. (1986). Cellular sodium transport in essential hypertension. *New Engl. J. Med.*, **314**, 222–229.

KNOWLTON, K.U., MICHEL, M.C., ITANI, M., SHUBEITA, H.E., ISHIHARA, K., BROWN, J.H. & CHIEN, K.R. (1993). The α_{1A}-adrenergic receptor subtype mediates biochemical, molecular, and morphologic features of cultured myocardial cell hypertrophy. *J. Biol. Chem.*, **268**, 15374–15380.

LANGER, G.A. (1992). Calcium and the heart: exchange at the tissue, cell, and organelle levels. *FASEB J.*, **6**, 893–902.

LOMASNEY, J.W., COTECCHIA, S., LEFKOWITZ, R.J. & CARON, M.G. (1991). Molecular biology of α-adrenergic receptors: implications for receptor classification and for structure-function relationships. *Biochem. Biophys. Acta*, **1095**, 127–139.

MICHEL, M.C., BÜSCHER, R., KERKER, J., KRANEIS, H., ERDBRÜGGER, W. & BRODDE, O.-E. (1993). α_1-Adrenoceptor subtype affinities of drugs for the treatment of prostatic hypertrophy. Evidence for heterogeneity of chloroethylclonidine-resistant rat renal α_1-adrenoceptors. *Naunyn-Schmied. Arch. Pharmacol.*, **348**, 385–395.

MICHEL, M.C., HÄNFT, G. & GROß, G. (1994). Radioligand binding studies of α_1-adrenoceptor subtypes in rat heart. *Br. J. Pharmacol.*, **111**, 533–538.

MICHEL, M.C., PHILIPP, T. & BRODDE, O.-E. (1992). α- and β-adrenoceptors in hypertension: molecular biology and pharmacological studies. *Pharmacol. Toxicol.*, **70**, (Suppl. II), S1–S10.

MINNEMAN, K.P. (1988). α_1-Adrenergic receptor subtypes, inositol phosphates, and sources of cell Ca^{2+}. *Pharmacol. Rev.*, **40**, 87–119.

MINNEMAN, K.P., HAN, C. & ABEL, P.W. (1988). Comparison of α_1-adrenergic receptor subtypes distinguished by chlorethylclonidine and WB 4101. *Mol. Pharmacol.*, **33**, 509–514.

OTSU, K., WILLARD, H.F., KHANNA, V.K., ZORZATO, F., GREEN, N.M. & MACLENNAN, D.H. (1990). Molecular cloning of cDNA encoding the Ca^{2+} release channel (ryanodine receptor) of rabbit cardiac muscle sarcoplasmic reticulum. *J. Biol. Chem.*, **265**, 13472–13483.

PUCEAT, M., TERZIC, A., CLEMENT, O., SCAMPS, F., VOGEL, S.M. & VASSORT, G. (1992). Cardiac α_1-adrenoceptors mediate positive inotropy via myofibrillar sensitization. *Trends Pharmacol. Sci.*, **13**, 263–265.

RUFFOLO, R.R.Jr., NICHOLS, A.J., STADEL, J.M. & HIEBLE, J.P. (1991). Structure and function of α-adrenoceptors. *Pharmacol. Rev.*, **43**, 475–505.

STERN, M.D. & LAKATTA, E.G. (1992). Excitation-contraction coupling in the heart: the state of the question. *FASEB J.*, **6**, 3092–3100.

TAKANASHI, M., NOROTA, I. & ENDOH, M. (1991). Potent inhibitory action of chlorethylclonidine on the positive inotropic effect and phosphoinositide hydrolysis mediated via myocardial alpha$_1$-adrenoceptors in the rabbit ventricular myocardium. *Naunyn-Schmied. Arch. Pharmacol.*, **343**, 669–673.

WANG, X.-L., WETTWER, E., GROSS, G. & RAVENS, U. (1991). Reduction of cardiac outward currents by alpha-1 adrenoceptor stimulation: a subtype-specific effect? *J. Pharmacol. Exp. Ther.*, **259**, 783–788.

WILSON, K.M. & MINNEMAN, K.P. (1990). Differential pathways of [^{3}H]-inositol phosphate formation mediated by α_{1A}- and α_{1B}-adrenergic receptors. *J. Biol. Chem.*, **265**, 17601–17606.

(Received June 14, 1993
Revised October 19, 1993
Accepted October 27, 1993)

Br. J. Pharmacol. (1994), **111**, 547–554

Blood pressure reflexes following activation of capsaicin-sensitive afferent neurones in the biliopancreatic duct of rats

Thomas Griesbacher

Department of Experimental and Clinical Pharmacology, University of Graz, Universitätsplatz 4, A-8010 Graz, Austria

1 Inflammatory diseases of the pancreas or diseases which cause obstruction within the biliary or pancreatic duct system are associated with severe pain. Although neuropeptides such as substance P are present in the biliary tree, only few capsaicin-sensitive, substance P-positive nerve fibres have been found in the ducts. In order to obtain functional evidence whether capsaicin-sensitive afferent neurones transmit nociceptive information arising from the biliopancreatic duct, blood pressure reflexes following electrical stimulation of the duct or increases in intraductal pressure were determined in barbiturate-anaesthetized rats.

2 Electrical stimulation of neurones in the biliopancreatic duct was carried out at 30 V, 3 ms, 50 Hz for 20 s. In untreated animals the electrical stimulation resulted in rises in blood pressure by up to 25 mmHg, but in about a quarter of all animals tested this response was absent. Following the administration of phentolamine (7 μmol kg^{-1}, i.p.) the blood pressure responses were changed to pronounced and reproducible depressor reflexes of -5 to -30 mmHg. Retrograde injections into the biliopancreatic duct of 300 μl of a 154 mM sodium chloride solution produced increases in intraductal pressure of approximately 10 mmHg. This elicited shortlasting falls in blood pressure of 3–15 mmHg. Phentolamine significantly augmented the fall in blood pressure to 8–30 mmHg.

3 The depressor reflexes observed in both models after the administration of phentolamine were abolished by morphine (1 μmol kg^{-1}, i.v.). The inhibition by morphine was reversed by naloxone (3 μmol kg^{-1}, i.v.). Naloxone given before morphine did not affect the depressor reflex but prevented the inhibitory action of subsequently injected morphine.

4 Acute s.c. injection of capsaicin (30 mg kg^{-1}) abolished the depressor reflexes in response to both types of nociceptive stimulation in phentolamine-treated rats. The initial pressor effects of electrical stimulation were only partly inhibited by capsaicin whereas the basal depressor reflexes in response to elevation of intraductal pressure were abolished. In rats which had received capsaicin on the day before the experiment or had been treated with capsaicin as neonates, only minor rises in blood pressure were induced by electrical stimulation at the beginning of the experiment and no changes in blood pressure occurred after the administration of phentolamine. After adult or neonatal pretreatment with capsaicin the depressor reflexes in response to increased intraductal pressure were only small and were unchanged by phentolamine.

5 The depressor reflexes following either electrical stimulation or increases in intraductal pressure were abolished by the unselective β-blocker, (−)-propranolol (3 μmol kg^{-1}, i.p.), and greatly reduced by the β_1-blocker, metoprolol (6 μmol kg^{-1}, i.p.). The β_2-preferring adrenoceptor antagonist, butoxamine (3 μmol kg^{-1}, i.p.), had no effect on the depressor responses. The reflex falls in blood pressure were also abolished by hexamethonium (10 μmol kg^{-1}, i.p.) but not by atropine (3 μmol kg^{-1}, i.p.).

6 Both models of stimulation of nociceptive afferents caused identical patterns of blood pressure responses following adrenalectomy or chemical sympathectomy. In adrenalectomized rats, the initial responses consisted of depressor reflexes which were not augmented but significantly reduced by phentolamine and further inhibited by metoprolol. In rats that had been pretreated with 6-hydroxydopamine (total dose 0.6 mmol kg^{-1}) to accomplish chemical sympathectomy, nociceptive stimulation caused rises in blood pressure. Phentolamine treatment abolished these pressor effects but revealed only minor, if any, depressor responses that were unaffected by metoprolol.

7 In summary, the hypotensive effects in both models constitute nociceptive reflexes since they are abolished by morphine and restored by naloxone. The afferent part of the reflex is mediated by nerve fibres sensitive to capsaicin. Both experimental procedures seem to elicit two, presumably separate, reflex mechanisms. Firstly, catecholamines released from the adrenal medulla elevate blood pressure or limit hypotensive responses via activation of vascular α receptors. Secondly, the reflex inhibition of the sympathetic nerve activity in the heart and the vasculature causes the nociceptive depressor reflexes.

Keywords: Pain (biliary); pain reflexes; capsaicin; afferent neurones

Introduction

Obstructive diseases of the biliary and pancreatic duct system associated with elevation of intraductal pressure are frequently accompanied by severe pain (Geenen *et al.*, 1989; Moody *et al.*, 1990; Prinz & Greenlee, 1990). Similar symptoms of pain can be observed in certain patients undergoing diagnostic or therapeutic procedures which cause an elevation of intraductal pressure such as injection of contrast media into the common bile duct during endoscopic retrograde cholangiopancreaticography (Lasson *et al.*, 1988) or balloon dilatation (Jaschke *et al.*, 1992).

Experimental elevation of intraductal pressure also is painful in man (McGowan *et al.*, 1936; Chapman *et al.*, 1949)

and elicits pain-related pseudoaffective reflexes in anaesthetized animals (Woodsworth & Sherrington, 1904; Cervero, 1982a,b). Since the administration of capsaicin onto the surface of the pancreas of cats leads to cardiovascular responses similar to those commonly observed after painful stimuli (Ordway *et al.*, 1983) it might be inferred that nociceptive information arising from the biliopancreatic duct system is conveyed by capsaicin-sensitive afferent nerve fibres. Using immunological techniques, neuropeptides like substance P, calcitonin gene-related peptide or vasoactive intestinal peptide have been found in the biliary tract of several species including rat (Holzer *et al.*, 1982; Inoue *et al.*, 1992), and man (Ueno *et al.*, 1991). However, these peptides can also be contained in nerve fibres which have local effector functions and are not sensitive to capsaicin (Costa *et al.*, 1980; Holzer *et al.*, 1980; Furness *et al.*, 1982). Although the substance P content of the hepatic ducts of rats was found to be greatly reduced by capsaicin pretreatment (Holzer *et al.*, 1982) which indicates that afferent C-fibres are present in the biliary system, Sharkey *et al.* (1984) found only few or no substance P-containing capsaicin-sensitive fibres in the pancreatic duct. Thus, in the present study a functional demonstration for the role of capsaicin-sensitive afferents in the mediation of nociceptive information arising from elevations in pressure in the biliopancreatic duct system was attempted.

A preliminary account of the results has been presented to the British and Italian Pharmacological Societies (Griesbacher *et al.*, 1993).

Methods

Surgical procedures

Female Sprague-Dawley rats (200–280 g) were anaesthetized with pentobarbitone sodium (40 mg kg^{-1}, i.p.) and phenobarbitone sodium (40 mg kg^{-1}, i.p.). The trachea was cannulated to ensure unhindered respiration. One carotid artery was cannulated and connected to a Statham pressure transducer to monitor arterial blood pressure. A jugular vein was cannulated for the i.v. injection of drugs. The abdomen was opened through a midline incision.

Electrical stimulation of the biliopancreatic duct The biliopancreatic duct was carefully dissected from the surrounding pancreatic tissue and placed on a pair of bipolar platinum electrodes. Electrical stimulation was carried out at 30 V, 3 ms, 50 Hz for a period of 20 s. This stimulation was repeated three times at intervals of 5 min. The stimulation protocol was resumed 15 min after the i.p., s.c. or i.v. administration of drugs.

Elevation of intraluminal pressure in the biliopancreatic duct The biliopancreatic duct was cannulated in a retrograde direction with a piece of polyethylene tubing (0.61 mm o.d., 0.28 mm i.d. Intramedic PE-10; Becton Dickinson, Parsippany, NJ, U.S.A.). In order to increase intraluminal pressure, 300 µl of saline was injected into the duct within 15 s and the cannula was then kept closed for further 20 s. The magnitude of the ensuing increase in intraductal pressure was determined with a Statham pressure transducer connected to the cannula via a T-piece. The time intervals for the saline injections and for the administration of drugs were the same as described above for electrical stimulation of neurones in the biliopancreatic duct.

Adrenalectomy Adrenalectomy was performed 15 min before the beginning of the experiments. The adrenal stalk was ligated and the glands were removed. In sham-operated animals, only the inferior pole of the kidney was cleared of the surrounding adipose tissue.

Chemical sympathectomy The rats were pretreated with 6-hydroxydopamine (100 µmol kg^{-1}, s.c.) in the afternoons of the 6 days prior to the experiments. In order to determine the extent of the chemical sympathectomy, noradrenaline levels were determined in the right atrium, the left ventricle, and in the spleen. As control tissues, one adrenal gland and the parietal cerebral cortex were used. At the end of the experiments, the rats were killed by exsanguination. The tissues were removed, weighed, frozen immediately on dry ice, and stored at −70°C until the catecholamine content of the tissues was determined with the aluminium oxide adsorption method and h.p.l.c. analysis (Donnerer, 1988). The tissues were homogenized in 1.5 ml 0.4 M perchloric acid containing 0.5 mM sodium EDTA and 0.5 mM sodium metabisulphate. The homogenates were centrifuged for 10 min at 2×10^4 m s^{-2}. The supernatant and 1.8 ml of 1.0 M Tris buffer (pH 8.6) were added to 100 mg of heat-activated aluminium oxide. As internal standard 10 ng dihydroxybenzylamine was added. The resulting samples were thoroughly shaken for 5 min. After centrifugation the supernatant was discarded and the aluminium oxide pellet was washed with 2 ml of 0.01 M Tris buffer. Catecholamines were eluted from the pellet with 500 µl of 0.2 M perchloric acid. The eluates from adrenal gland were diluted 10 fold with 0.2 M perchloric acid, the eluates from the other tissue samples were used undiluted. Samples of 100 µl were injected onto a reverse phase h.p.l.c. column (Merck 5 µm LiChrospher 100 RP-18, eluent: phosphate buffer pH 5.0 containing 4 mM heptanesulphonic acid and 4% v/v methanol). Noradrenaline and adrenaline was measured by electrochemical detection. The recovery, calculated from the values measured for dihydroxybenzylamine, was 50–90%.

Substances used

Pentobarbitone sodium (Nembutal) was from Sanofi (Libourne, France), phenobarbitone sodium (Apoka, Vienna, Austria) was dissolved in a 154 mM solution of NaCl (saline). Capsaicin (Fluka, Buchs, Switzerland) was dissolved in dimethylsulphoxide at a concentration of 10 mg ml^{-1}. For the neonatal pretreatment of rats, capsaicin was dissolved in 10% (v/v) Tween 80 and 10% (v/v) ethanol in saline. 6-Hydroxydopamine hydrobromide (Sigma, St. Louis, MO, U.S.A.) was dissolved in a solution of 1% (w/v) ascorbic acid in saline at a concentration of 40 mM immediately prior to use. Phentolamine hydrochloride, metoprolol tartrate (Ciba, Basle, Switzerland), morphine hydrochloride (Diosynth, Apeldoorn, Netherlands), naloxone hydrochloride (DuPont, Geneva, Switzerland), (−)-propranolol hydrochloride (ICI, Macclesfield, U.K.), (+)-propranolol hydrochloride, butoxamine hydrochloride, hexamethonium chloride (Sigma, St. Louis, MO, U.S.A.), and atropine sulphate (Merck, Darmstadt, Germany) were dissolved in saline.

Statistical analysis

All values presented are arithmetical means ± s.e.mean. Nonparametric analysis of variance and multiple comparisons among the blood pressure responses before and after the drug administrations during the course of the experiments were made by the Quade test (Conover, 1980). The catecholamine concentrations in tissues from 6-hydroxydopamine-treated rats were compared with those determined in control animals using the Mann-Whitney U test.

Results

Blood pressure reflexes and effects of phentolamine

Electrical stimulation (30 V, 3 ms, 50 Hz, 20 s) of the biliopancreatic duct led to changes in mean arterial pressure lasting for the duration of the stimulation. Out of 43 animals

subjected to electrical stimulation of the biliopancreatic duct before and after the i.p. administration of phentolamine, 31 (72%) responded with an increase in blood pressure by 3–25 mmHg under basal conditions, whereas a smaller number of animals showed either no response (8/43, 19%) or a minute (less than 3 mmHg) fall in blood pressure (4/43, 9%). In all animals, the blood pressure response was transformed into a consistent depressor effect of 5–30 mmHg 15 min after the i.p. administration of phentolamine (7 μmol kg^{-1}, $P<0.001$; Figures 1a–b, 2a, 3a–c, 4a–b, 5a). Phentolamine also reduced basal blood pressure itself from 131 ± 8 mmHg to 105 ± 2 mmHg ($P<0.01$). The stimulation procedure was carried out three times at intervals of 5 min followed by a rest period of 20 min. The time course of the initial pressor responses was slightly different from that of the depressor responses following phentolamine; the pressor effects, when present, started immediately after the beginning of the electrical stimulation, whereas the depressor responses following phentolamine typically set in after a lag period of about 5 s. The depressor response remained stable for at least 90 min.

The retrograde injection of 300 μl saline into the biliopancreatic duct caused reproducible increases in intraductal pressure of about 10 mmHg. This resulted in a fall in mean arterial pressure by 3–15 mmHg which was reversed within about 1 min. Phentolamine (7 μmol kg^{-1}, i.p.) augmented the depressor response to 8–30 mmHg ($P<0.01$; Figures 1c–d, 2e, 3d–f, 4c–d, 5e) while reducing basal blood pressure from 119 ± 4 mmHg to 91 ± 4 mmHg ($P<0.01$). The intraductal injections of saline were carried out at the same time intervals as described above for the electrical stimulations. The ensuing blood pressure responses remained stable for at least 90 min. In order to provide experimental conditions comparable to those in the experiments using electrical stimulation of the biliopancreatic duct, phentolamine was applied in all further experiments. The depressor responses before or after phentolamine exhibited similar time courses including a certain lag period of several seconds between the beginning of the elevation in intraductal pressure and the onset of the fall in blood pressure.

Effects of morphine and naloxone

Following treatment with phentolamine, the hypotensive responses both after electrical stimulation and after increasing intraductal pressure were completely abolished by the i.v. injection of morphine (1 μmol kg^{-1}, Figure 1a and c). The inhibition caused by morphine was reversed 15–25 min after naloxone (3 μmol kg^{-1}, i.v.). In both experimental models, the hypotensive responses after the naloxone seemed to be slightly smaller than those observed before the administration of morphine; however, the difference did not achieve statistical significance. Basal blood pressure in phentolamine-treated rats (80–110 mmHg) was not significantly affected by morphine (70–100 mmHg).

In both experimental models, naloxone administered before morphine did not have any effect on the depressor reflexes in phentolamine-treated rats, but it prevented the inhibitory effect of subsequently applied morphine (Figure 1b and d).

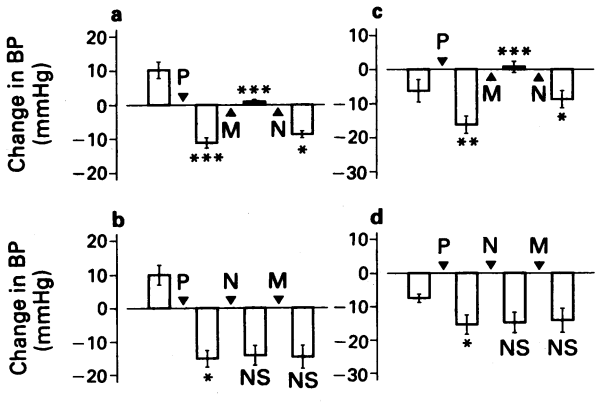

Figure 1 Effects of morphine and naloxone on reflex changes in rat blood pressure (in mmHg) induced by electrical stimulation (30 V, 3 ms, 50 Hz, 20 s) of nerve fibres in the biliopancreatic duct (a and b) and by shortlasting (35 s) increases in intraductal pressure (c and d). During the course of the experiments, phentolamine (P, 7 μmol kg^{-1}, i.p.), morphine (M, 1 μmol kg^{-1}, i.v.) and naloxone (N, 3 μmol kg^{-1}, i.v.) were administered (indicated by the arrows). Significance of difference to the effect before the previous drug administration: $*P<0.05$, $**P<0.01$, $***P<0.001$; NS, not significant. Means ± s.e.mean; $n = 4–6$.

Effects of capsaicin

The depressor reflexes in response to electrical stimulation in phentolamine-treated rats were completely abolished 15 min after acute administration of capsaicin (30 mg kg^{-1}, s.c.) (Figure 2a). The basal pressor response was only partly reduced by capsaicin, but after a subsequent i.p. administration of phentolamine the stimulation procedure failed to produce changes in blood pressure (Figure 2b). When rats were pretreated with capsaicin (30 mg kg^{-1}, s.c.) on the day before the experiment, the pressor response following electrical stimulation was absent in three out of six animals tested. In all animals, the i.p. administration of phentolamine

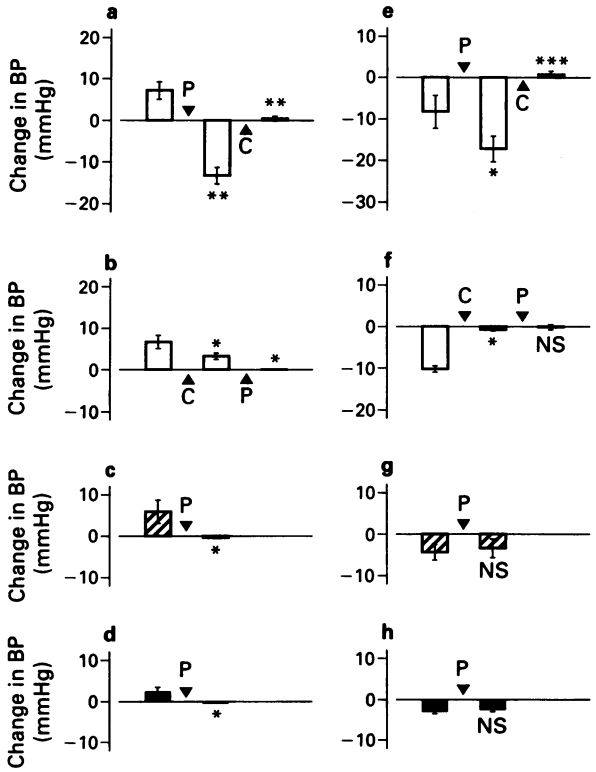

Figure 2 Effects of capsaicin on blood pressure reflexes (in mmHg) elicited by electrical stimulation of nerve fibres in the biliopancreatic duct (a–d) or by shortlasting increases in intraductal pressure (e–h): Phentolamine (P, 7 μmol kg^{-1}) was administered i.p. Acute treatment with capsaicin (C, 30 mg kg^{-1}) during the experiment was made by s.c. injection (a, b, e, f). Pretreatment with capsaicin was made either in adult rats on the day before the experiment (30 mg kg^{-1}, s.c.; hatched columns, c and g) or in neonatal rats on the 2nd day of life (50 mg kg^{-1}, s.c.; solid columns, d and h). Drug administrations are indicated by the arrows. Significance of differences from the effect before the previous drug administration: $*P<0.05$, $**P<0.01$; $***P<0.001$; NS, not significant. Means ± s.e.mean, $n = 4–6$.

abolished the effect of the electrical stimulation on blood pressure (Figure 2c). Rats that had been treated with capsaicin (50 mg kg^{-1}, s.c.) as neonates also responded with only small rises in blood pressure that were abolished by the subsequent administration of phentolamine (Figure 2d).

The depressor responses following elevation of intraductal pressure both before and after the i.p. administration of phentolamine were abolished by capsaicin (Figure 2e and f). When capsaicin was given before phentolamine, the α-blocker was unable to reveal any hypotensive effect (Figure 2f). The initial depressor effects induced by the elevation of intraluminal pressure in the biliopancreatic duct seemed to be smaller in rats that had been pretreated with capsaicin on the day before the experiment (Figure 2g) although the difference did not achieve statistical difference. Similarly, only small hypotensive effects were observed when the animals had been treated with capsaicin on the second day of life (Figure 2h). In both cases, these small hypotensive effects remained unchanged by phentolamine.

Acute administration of capsaicin during the course of the experiment lowered basal blood pressure by about 15 mmHg ($P<0.05$) only when injected prior to treatment with phentolamine; in phentolamine-treated rats, it did not affect blood pressure. Blood pressure in rats treated with capsaicin on the day before the experiment (95–115 mmHg) was not significantly different from blood pressure in untreated animals (100–130 mmHg). However, rats that had received treatment with capsaicin as neonates, showed a significant ($P<0.01$) lower blood pressure as adults (80–95 mmHg).

To ensure that the effects of the capsaicin injections were not unspecific effects of the solvent, DMSO was injected in the appropriate volume (3 ml kg^{-1}, s.c.). This had no effect on blood pressure itself or on any of the reflex responses following either electrical stimulation of the biliopancreatic duct or elevation of intraductal pressure (data not shown, $n=3$).

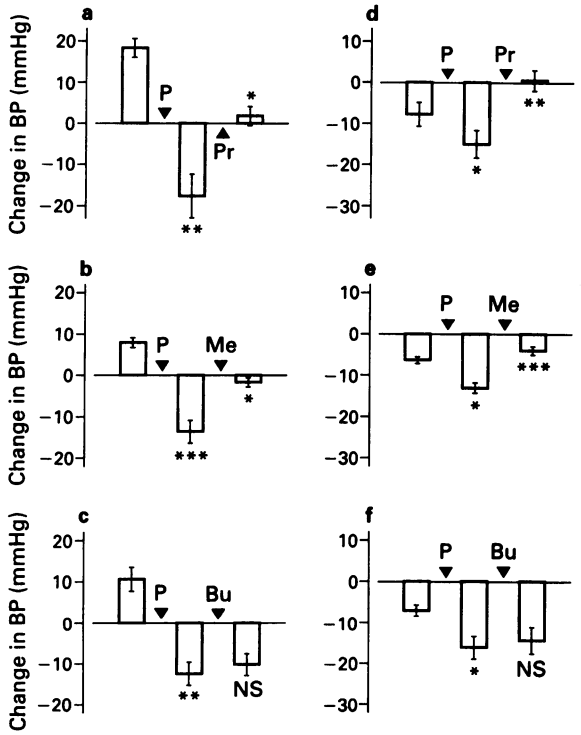

Figure 3 Effects of β-adrenoceptor antagonists on blood pressure reflexes (in mmHg) induced by electrical stimulation of the biliopancreatic duct (a–c) or by shortlasing increases in intraductal pressure (d–f) in anaesthetized rats: Phentolamine (P, 7 μmol kg^{-1}) as well as (−)-propranolol (Pr, 3 μmol kg^{-1}), metoprolol (Me, 6 μmol kg^{-1}) or butoxamine (Bu, 3 μmol kg^{-1}) were administered i.p. (indicated by the arrows). Significance of difference from the effect before the previous drug administration: $*P<0.05$; $**P<0.01$; $***P<0.001$; NS, not significant. Means ± s.e.mean; $n=4-5$.

Effects of β-blockers, hexamethonium, and atropine

The reflex fall in arterial pressure following electrical stimulation of the biliopancreatic duct after the administration of phentolamine was completely blocked by the unselective β-blocker, (−)-propranolol (3 μmol kg^{-1}, i.p.), (Figure 3a). It has been reported that propranolol can also have unspecific local anaesthetic actions which, unlike the adrenoceptor blocking action, are not constrained to the active (−)-enantiomer (Barrett & Cullum, 1968). However, the depressor response (− 8 ± 2 mmHg) was completely unaltered (− 8 ± 2 mmHg, $n=4$) by (+)-propranolol confirming that the inhibitory effect of (−)-propranolol was a specific action on β-adrenoceptors. The β_1 receptor antagonist, metroprolol (6 μmol kg^{-1}, i.p.), also inhibited the depressor reflex (Figure 3b) whereas the β_2-adrenoceptor blocker, butoxamine (3 μmol kg^{-1}, i.p.), had no effect (Figure 3c).

Hexamethonium (10 μmol kg^{-1}, i.p.) abolished the response (Figure 4a). Atropine (3 μmol kg^{-1}, i.p.) seemed to reduce the response slightly (Figure 4b); however, the difference did not achieve statistical difference. The initial pressor responses before phentolamine were not affected by (−)-propranolol or atropine, but were blocked by hexamethonium (Table 1).

The depressor responses following elevation of intraductal pressure in phentolamine-treated rats were blocked by (−)-propranolol (Figure 3d), but were unchanged by (+)-propranolol (− 16 ± 4 mmHg both before and after the i.p. administration). Metoprolol greatly reduced the depressor reflexes (Figure 3e) while butoxamine had no significant effect (Figure 3f). The hypotensive responses were strongly inhibited by hexamethonium, but were not significantly affected by atropine (Figure 4c and d, respectively). The reflex falls in blood pressure observed under basal conditions, i.e. before the administration of phentolamine, were abolished by (−)-propranolol and hexamethonium, but were unaffected by atropine (Table 1).

In both experimental models, neither (−)-propranolol nor metroprolol or butoxamine, in these experiments applied following treatment with phentolamine, had any effect on basal blood pressure (80–110 mmHg) on their own. Hexamethonium and atropine both reduced blood pressure by 5–15 mmHg ($P<0.05$).

Effects of adrenalectomy and chemical sympathectomy

Blood pressure responses to either electrical stimulation of the biliopancreatic duct or to elevation of intraductal pressure were monitored under basal conditions, following the i.p. administration of phentolamine (7 μmol kg^{-1}) and after the subsequent treatment with metoprolol (6 μmol kg^{-1}, i.p.). In sham-operated rats, both procedures elicited blood pressure responses that were comparable to those obtained in animals that had not undergone surgery in the retroperitoneal space (Figure 5a and d; compare Figure 3b and f, respectively).

In adrenalectomized rats, the initial blood pressure responses to electrical stimulation of the biliopancreatic duct consisted of depressor, rather than pressor, effects. Phentolamine significantly ($P<0.05$) reduced these falls in blood pressure, and subsequently applied metoprolol abolished the reflex (Figure 5b). Repeated daily s.c. injections of 6-hydroxydopamine (total dose of 0.6 mmol kg^{-1}), reduced the noradrenaline concentrations in peripheral tissues by over 80–95%, whereas the catecholamine levels in the adrenal glands and in the central nervous system were not affected (Table 2). In these animals, the electrical stimulation of the biliopancreatic duct caused shortlasting rises in mean arterial

pressure similar to untreated rats (Figure 5c). These rises were abolished by phentolamine. However, the α-blocker was unable to reveal any significant depressor responses. A further administration of metroprolol was without effect.

The elevation of intraductal pressure in adrenalectomized rats was followed by consistent reflex falls in blood pressure

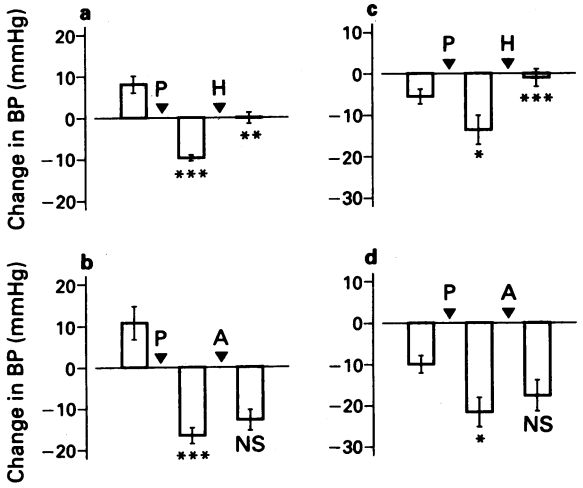

Figure 4 Effects of hexamethonium and atropine on reflex changes in mean arterial pressure (in mmHg) following electrical stimulation of the biliopancreatic duct (a and b) or elevation of intraductal pressure (c and d): Responses were measured before and after the i.p. administration of phentolamine (P, 7 μmol kg^{-1}). A third set of painful stimuli was performed after the i.p. administration of hexamethonium (H, 10 mg kg^{-1}) or atropine (A, 3 μmol kg^{-1}). Drug administrations are indicated by the arrows. Significance of difference from the effect before the previous drug administration: $*P<0.05$, $**P<0.01$; $***P<0.001$; NS, not significant. Means ± s.e. mean, $n = 5-6$.

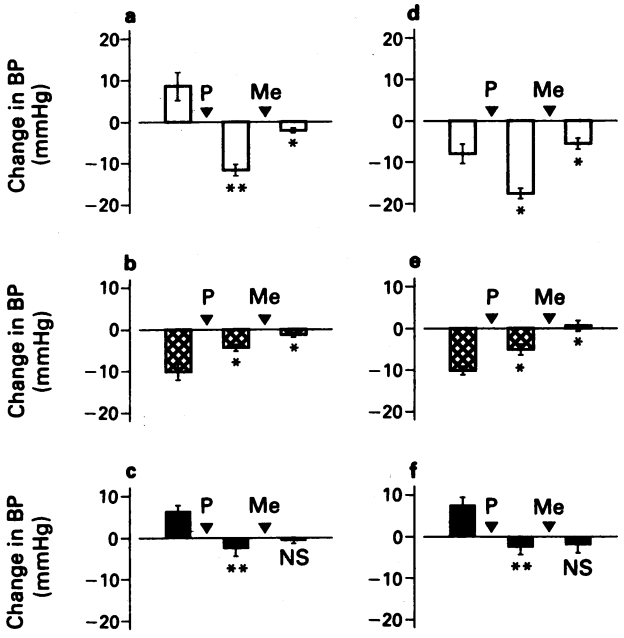

Figure 5 Effects of adrenalectomy and chemical sympathectomy on blood pressure reflexes (in mmHg) induced by electrical stimulation of the biliopancreatic duct (a–c) or by elevation of intraductal pressure (d–f): Adrenalectomy was performed at the beginning of the experiment (hatched columns, b and e), sham-operated controls are shown in panels (a) and (d). Chemical sympathectomy was accomplished with 6-hydroxydopamine (0.6 mmol kg^{-1} divided into 6 equal doses given s.c. on the 6 days before the experiment; solid columns, c and e). During the course of the experiment, phentolamine (P, 7 μmol kg^{-1}) and metoprolol (Me, 6 μmol kg^{-1}) were administered i.p. as indicated by the arrows. Significance of difference from the effect before the previous drug administration: $*P<0.05$, $**P<0.01$; $***P<0.001$; NS, not significant. Means ± s.e. mean; $n = 4-5$.

Table 1 Reflex changes in systemic blood pressure (in mmHg) in anaesthetized rats induced by electrical stimulation of the biliopancreatic duct or by elevation of intraductal pressure

Electrical stimulation			*Elevation of intraductal pressure*		
Before	Drug	After	Before	Drug	After
21 ± 2	(−)-Propranolol	21 ± 2	− 7 ± 1	(−)-Propranolol	3 ± 2**
16 ± 5	Hexamethonium	− 6 ± 9*	− 8 ± 2	Hexamethonium	− 1 ± 2**
9 ± 1	Atropine	7 ± 3	− 5 ± 1	Atropine	− 7 ± 2

Electrical stimulation (30 V, 3 ms, 50 Hz) was carried out for 20 s at intervals of 5 min. Intraductal pressure was elevated by about 10 mmHg for 35 s by retrograde injections of 300 μl of saline. Blood pressure reflexes were monitored before and 15–25 min after the i.p. administration of (−)-propranolol (3 μmol kg^{-1}), hexamethonium (10 μmol kg^{-1}), or atropine (3 μmol kg^{-1}). Means ± s.e.mean; $n = 4-6$. Significance of difference to values obtained before drug: $*P<0.05$, $**P<0.01$.

Table 2 Effect of 6-hydroxydopamine (6-OHDA) pretreatment on tissue concentrations of noradrenaline (NA) and adrenaline (Ad) in rats

Tissue	*Catecholamine*	*Control*	*6-OHDA*
Right atrium	NA (ng g^{-1} wet wt.)	1,952 ± 73	73 ± 9**
Left ventricle	NA (ng g^{-1} wet wt.)	644 ± 34	28 ± 2**
Spleen	NA (ng g^{-1} wet wt.)	741 ± 47	73 ± 9**
Parietal cortex	NA (ng g^{-1} wet wt.)	254 ± 19	293 ± 17
Adrenal gland	NA (μg g^{-1} wet wt.)	115 ± 20	99 ± 16
	Ad (μg g^{-1} wet wt.)	349 ± 47	396 ± 40

Rats were pretreated with 6-OHDA (0.6 mmol kg^{-1}, s.c., divided into 6 daily doses), control rats received injections of the solvent (1% w/v ascorbic acid in saline) instead. All rats were used in experiments for the measurement of the blood pressure reflexes following either electrical stimulation of the biliopancreatic duct or elevation of intraductal pressure. During the course of these experiments, phentolamine (7 μmol kg^{-1}, i.p.) and metoprolol (6 μmol kg^{-1}, i.p.) were administered. The tissues were taken at the end of the experiments. Means ± s.e.mean; $n = 6$ for both groups. Significance of difference from control group: $**P<0.01$.

(Figure 5e). Unlike in sham controls (compare Figure 5d), phentolamine did not augment these hypotensive responses, but significantly ($P<0.05$) reduced the response. The subsequent administration of metoprolol caused a further significant ($P<0.05$) reduction of the effect. Following chemical sympathectomy, the initial blood pressure reflexes in response to elevation in intraductal pressure consisted of shortlasting rises in systemic arterial pressure (Figure 5f) which is in contrast to the effects obtained in rats with intact peripheral sympathetic neurones. Similar to the responses to electrical stimulation of the biliopancreatic duct in sympathectomized rats, phentolamine abolished these pressor effects, but could not reveal any falls in blood pressure. Metoprolol also had no further effect.

In both experimental models, the basal blood pressure was the same in adrenalectomized rats as in sham-operated controls (120–140 mmHg), but was reduced in 6-hydroxydopamine-treated rats (100–115 mmHg, $P<0.05$). Phentolamine significantly ($P<0.05$) reduced blood pressure in sham controls and adrenalectomized rats (to 100–120 mmHg) as well as in rats that had undergone chemical sympathectomy (to 80–100 mmHg). The subsequent treatment with metoprolol caused a further reduction in blood pressure only in adrenalectomized rats (by about 20 mmHg) but had no effect in the two other groups.

Discussion

In anaesthetized rats and rabbits, painful stimuli such as distension of the small or large intestine (Lembeck & Skofitsch, 1982; Ness & Gebhart, 1988), distension of the renal pelvis (Brasch & Zetler, 1982), electrical stimulation of the saphenous nerve (Lembeck & Donnerer, 1983), intra-arterial injection of capsaicin (Donnerer & Lembeck, 1983), or visceral or somatic administration of algesic agents (Juan & Lembeck, 1974; Holzer-Petsche, 1992) elicit reflex falls in systemic arterial pressure.

In the present experiments, electrical stimulation of the biliopancreatic duct, however, caused increases, rather than decreases, in blood pressure. Since a pressor response mediated by α-adrenoceptors was observed as part of a triphasic blood pressure reflex following the distension of the small intestine (Lembeck & Skofitsch, 1982), phentolamine was used to block effects mediated by these receptors. This treatment transformed the pressor responses into consistent and reproducible depressor reflexes. Thus, the electrical stimulation of the biliopancreatic duct is followed by the activation of more than one single effector mechanism, one of which is α-adrenergic leading to a rise in blood pressure. Since the depressor responses observed after the administration of phentolamine are similar to cardiovascular reflexes in other rat models of visceral pain, phentolamine was routinely applied in the further experiments.

An increase in intraductal pressure was produced experimentally by retrograde injection of saline into the biliopancreatic duct. The ensuing increase in intraductal pressure of about 10 mmHg may seem to be only small. However, similarly small increases in intraductal pressure have been shown to elicit pain in man especially under pathological conditions (Gaensler, 1951). Since the elevation of intraductal pressure did not induce any rises in systemic arterial pressure the procedure seems to be more selective as far as the type of blood pressure response is concerned. However, the response still contains an α-adrenergic component, since phentolamine augmented the depressor effect.

Blockade by morphine of depressor reflexes elicited by distension of the small intestine (Lembeck & Skofitsch, 1982; Clark & Smith, 1985) or the renal pelvis (Brasch & Zetler, 1982) has been used to classify these responses as nociceptive reflexes. The mode of action of morphine in preventing the reflex presumably involves both peripheral and central sites of action (Clark & Smith, 1985). It has been shown that, in dogs and cats, narcotic analgesics can produce hypotension via a central action (Laubie *et al.*, 1974; Daskalopoulos *et al.*, 1975). This effect could interfere with blood pressure reflexes unspecifically. In the present investigation, however, morphine had only small, if any, hypotensive effects of its own which by itself do not seem to be sufficient to explain the inhibitory effects of morphine. Thus, it seems to be more likely that the morphine-induced inhibition is related to its analgesic activity and the depressor effects constitute pseudo-affective reflex responses accompanying nociceptive afferent information similar to those described in other models of visceral noxious stimulation (see Ness & Gebhart, 1990).

Indications that visceral nociceptive stimuli activate small unmyelinated fibres, i.e. C- and Aδ-fibres, have already been obtained by Gernandt & Zotterman (1946). High doses of capsaicin have profound actions on these afferent neurones, leading to defunctionalization (see Fitzgerald, 1983; Holzer, 1991): acute administration of such high doses will lead to a desensitization of the afferent neurones by depletion of the neurotransmitters and also by blockade of nerve conduction. The time needed for this desensitization to come into effect varies from as little as 10 min to several days, depending on the model used (Lembeck & Donnerer, 1981). Neonatal treatment with capsaicin causes a relatively selective degeneration of the C-fibre afferents (Jancsó *et al.*, 1977). Whereas this treatment causes an almost complete degeneration of unmyelinated fibres, small myelinated fibres are affected only to a minor extent (Nagy *et al.*, 1983). The depressor responses observed in both experimental models of the present investigation were blocked by capsaicin already 15 min after its s.c. application. The nociceptive reflexes were similarly inhibited when capsaicin was administered on the day before the experiment or when rats treated with capsaicin as neonates were used. Thus, the afferent part of the reflex arc leading to the depressor responses clearly consists of activation of capsaicin-sensitive neurones.

It is interesting to note that the initial responses, i.e. the blood pressure effects before the administration of phentolamine, were also diminished by capsaicin (compare Figure 2b–d and f–h). This implies that the pressor response following electrical stimulation, at least partly involves capsaicin-sensitive nerve fibres, which is in contrast to the pressor component of the blood pressure reflex following distension of the small intestine where a contribution of such fibres was excluded (Lembeck & Skofitsch, 1982). Acute administration of capsaicin completely blocked the basal depressor responses following elevation of intraductal pressure; pretreatment with capsaicin either in adult rats on the day before the experiment or already on the 2nd day of life only partly reduced the depressor response (Figure 2g and h) while completely preventing the depressor component otherwise revealed by phentolamine. Thus, elevation of intraductal pressure may also activate some other afferent fibres not sensitive to capsaicin, but also leading to a depressor response.

The initial finding that the electrical stimulation of the biliopancreatic duct was followed, in the majority of cases, by rises in systemic arterial pressure was unexpected since nociceptive cardiovascular responses in the rat commonly are described as hypotensive effects. Such hypotensive effects were, however, readily elicited when the animals were treated with the α-adrenoceptor blocker, phentolamine. Therefore, a separate reflex mechanism comprising the stimulation of vascular α-receptors must be in operation. The same mechanism can also be demonstrated in the cardiovascular reflexes following elevation of intraluminal pressure in the biliopancreatic duct since phentolamine potentiated the depressor responses in this model. Vascular α receptors can be stimulated via two mechanisms. Firstly, α-adrenoceptor vasoconstriction can be due to the release of noradrenaline from the sympathetic postganglionic nerve fibres supplying the vasculature; secondly, the release of catecholamines from the adrenal glands into the blood can lead to the same effect. Pressor responses to painful stimuli in cats have been shown to be largely depen-

dent upon the adrenal glands (Newman, 1953). Since in adrenalectomized rats both the pressor effects of electrical stimulation and the phentolamine-induced augmentation of depressor responses following elevation of intraductal pressure are completely absent, it can be concluded that catecholamine release from the adrenal medulla also occurs in both models used in the present investigation. This mechanism may also be responsible for the fact that distension of hollow organs in rats was found to elicit typical depressor reflexes only in about two thirds of the animals tested (Brasch & Zetler, 1982; Lembeck & Skofitsch, 1982).

The transformation by an α-adrenoceptor blocker of a pressor response into a depressor effect would be in agreement with catecholamines now producing vasodilatation via the activation of vascular β-adrenoceptors. The inhibitory effects of the unselective β-blocker, propranolol, would also support this possible explanation. However, there are three facts that are in conflict with this explanation. Firstly, certain differences in the time courses of the pressor and depressor responses suggest differences in the underlying mechanisms. Secondly, elevations of intraductal pressure cause hypotensive responses even before the administration of phentolamine also suggesting an additional mechanism. Thirdly, if this mechanism were the only one leading to the depressor effects then this response would be expected to be intact in sympathectomized animals. However, in animals which were pretreated with 6-hydroxydopamine leading to a degeneration of postganglionic sympathetic nerve endings (see Kostrzewa & Jacobowitz, 1974) only very small hypotensive effects could be observed (Figure 5c and f).

Since metoprolol, which is 50–100 times more active on β_1 than on β_2 receptors (Åblad *et al.*, 1973), greatly reduces the depressor reflexes (Figure 3b and e), the response seems to be dependent, at least partly, upon β_1-adrenoceptors. Although it was originally held that β_1 receptors were only present in the heart whereas β_2 receptors were contained only in other tissues, it is now believed that both β-adrenoceptor subtypes coexist in many tissues. Both subtypes often, but not always, mediate the same physiologic response. Thus, both β_1 and β_2 receptors in blood vessels of the rat can mediate vasodilatation (Cohen & Wiley, 1978; O'Donnell & Wanstall, 1981). On the other hand, only the β_1 receptors seem to be responsible for the positive chronotropic and inotropic effects of catecholamines in the rat heart although both subtypes are present (Juberg *et al.*, 1985). As a consequence, two possibilities exist for the explanation of depressor responses inhibited by metoprolol. Firstly, a reflex stimulation of such vascular β_1 receptors would decrease blood pressure via vasodilatation. Secondly, a fall in blood pressure could also be caused by a reflex reduction of the sympathetic nervous tone which supports blood pressure via the positive inotropic and chronotropic effects of the cardiac β_1 receptors. Both mechanisms would be inhibited by β_1-receptor blockade. Since the vascular β_1 receptors described were found in jugular veins (Cohen & Wiley, 1978) and pulmonary artery preparations (O'Donnell & Wanstall, 1981) rather than in resistance vessels, they are unlikely to account for the observed blood pressure changes. Thus, the second explanation for β_1-dependent depressor responses has to be favoured.

When inhibitory effects of drugs on blood pressure reflexes are to be interpreted, it might be argued that depressor reflexes would be diminished when basal blood pressure is lowered by the drug in question. However, (−)-propranolol and metoprolol abolished the depressor responses without having any effect on blood pressure by themselves whereas atropine significantly reduced blood pressure but left the depressor reflexes unaffected. This confirms that the inhibitory action of the β-blockers should be attributed to their receptor-blocking properties rather than to changes in the general level of blood pressure.

In adrenalectomized rats, the depressor responses are not augmented, but diminished by phentolamine. Thus, the nociceptive reflexes also seem to involve the reflex inhibition of the sympathetic α-adrenergic vasoconstrictor tone. Butoxamine, which exhibits some selectivity towards β_2 as compared to β_1 sites (Bieth *et al.*, 1980; Satoh *et al.*, 1993), did not have a significant effect on the depressor reflexes. Therefore, a contribution of β_2 receptors is unlikely. The crucial importance of the sympathetic nervous system for both the pressor and depressor reflexes is further confirmed by the inhibitory action of hexamethonium (Figure 4a and c, Table 2). Although hexamethonium certainly would also inhibit ganglionic transmission in the parasympathetic nervous system, a significant contribution of this part of the autonomic nervous system can be excluded since atropine was without effect (Figure 4b and d, Table 2).

The present results show that activation of capsaicin-sensitive afferent fibres in, or in the vicinity of, the biliopancreatic duct causes nociceptive cardiovascular reflex responses in anaesthetized rats and – in the absence of anaesthesia – would lead to the perception of pain. It is also demonstrated that increases in pressure in the biliopancreatic duct system cause pain involving capsaicin-sensitive afferent neurones. Increases in intraductal pressure frequently occur in obstructive diseases of the biliopancreatic duct system (Geenen *et al.*, 1989; Moody *et al.*, 1990; Prinz & Greenlee, 1990) and also occur in certain diagnostic or therapeutic procedures (Lasson *et al.*, 1988; Jaschke *et al.*, 1992). Capsaicin-sensitive afferent fibres can not only be activated by mechanical stimuli such as increases in pressure within the biliopancreatic duct system as demonstrated here, but can also be activated by bradykinin (Juan & Lembeck, 1974; Holzer-Petsche, 1992). Thus, the endogenous release of kinins in the pancreas during acute inflammation (Griesbacher & Lembeck, 1992; Griesbacher *et al.*, 1993), can also be expected to lead to activation of these fibres and consequently to symptoms of pain. A better understanding of the types of nerves leading to pain in these conditions will be important for future treatment if the transmitters of the afferent part of the reflex arcs are better defined and accessible by appropriate selective antagonists.

The work was supported by the Pain Research Commission of the Austrian Academy of Sciences and by the Franz-Lanyar-Stiftung.

References

ÅBLAD, B., CARLSSON, E. & EK, L. (1973). Pharmacological studies of two new cardioselective adrenergic beta-receptor antagonists. *Life Sci.*, **12**, 107–119.

BARRETT, A.M. & CULLUM, V.A. (1968). The biological properties of the optical isomers of propranolol and their effects on cardiac arrhythmias. *Br. J. Pharmacol.*, **34**, 43–55.

BIETH, N., ROUOT, B., SCHWARTZ, J. & VELLY, J. (1980). Comparison of pharmacological and binding assays for ten β-adrenoceptor blocking agents and two β-adrenoceptor agonists. *Br. J. Pharmacol.*, **68**, 563–569.

BRASCH, H. & ZETLER, G. (1982). Cerulein and morphine in a model of visceral pain: effects on the hypotensive response to renal pelvis distension in the rat. *Naunyn-Schmied. Arch. Pharmacol.*, **319**, 161–167.

CERVERO, F. (1982a). Noxious intensities of visceral stimulation are required to activate viscerosomatic multireceptive neurons in the thoracic spinal cord of the cat. *Brain Res.*, **240**, 350–352.

CERVERO, F. (1982b). Afferent activity evoked by natural stimulation of the biliary system in the ferret. *Pain*, **13**, 137–151.

CHAPMAN, W.P., HERRERA, R. & JONES, C.M. (1949). A comparison of pain produced experimentally in lower esophagus, common bile duct, and upper small intestine with pain experienced by patients with disease of biliary tract and pancreas. *Surg. Gynecol. Obstet.*, **89**, 573–582.

CLARK, S.J. & SMITH, T.W. (1985). Opiate-induced inhibition of the visceral distension reflex by peripheral and central mechanisms. *Naunyn-Schmied. Arch. Pharmacol.*, **330**, 179–183.

COHEN, M.L. & WILEY, K.S. (1978). Beta$_1$ and beta$_2$ receptor mechanisms in rat jugular veins: differences between norepinephrine and isoproterenol-induced relaxation. *Life Sci.*, **23**, 1997–2006.

CONOVER, W.J. (1980). *Practical Nonparametric Statistics*. 2nd ed. pp. 295–299. New York: Wiley.

COSTA, M., CUELLO, A.C., FURNESS, J.B. & FRANCO, R. (1980). Distribution of enteric neurons showing immunoreactivity for substance P in the guinea-pig ileum. *Neuroscience*, **5**, 323–331.

DASKALOPOULOS, N.T., LAUBIE, M. & SCHMITT, H. (1975). Localization of the central sympatho-inhibitory effect of a narcotic analgesic agent, fentanyl, in cats. *Eur. J. Pharmacol.*, **33**, 91–97.

DONNERER, J. (1988). Reflex activation of the adrenal medulla during hypoglycemia and circulatory dysregulations is regulated by capsaicin-sensitive afferents. *Naunyn-Schmied. Arch. Pharmacol.*, **338**, 282–286.

DONNERER, J. & LEMBECK, F. (1983). Capsaicin-induced reflex fall in blood pressure is mediated by afferent substance P-containing neurones via a reflex centre in the brain stem. *Naunyn-Schmied. Arch. Pharmacol.*, **324**, 293–295.

FITZGERALD, M. (1983). Capsaicin and sensory neurones – a review. *Pain*, **15**, 109–130.

FURNESS, J.B., PAPKA, R.E., DELLA, N.G., COSTA, M. & ESKAY, R.L. (1982). Substance P-like immunoreactivity in nerves associated with the vascular system in guinea-pigs. *Neuroscience*, **7**, 447–459.

GAENSLER, E.A. (1951). Quantitative determination of the visceral pain threshold in man: characteristics of visceral pain, effect of inflammation and analgesics on the threshold, and relationship of analgesia to visceral spasm. *J. Clin. Invest.*, **30**, 406–420.

GEENEN, J.E., HOGAN, W.J., DODDS, W.J., TOOULI, J. & VENU, R.P. (1989). The efficacy of endoscopic sphincterotomy after cholecystectomy in patients with sphincter-of-Oddi dysfunction. *New Engl. J. Med.*, **320**, 82–87.

GERNANDT, B. & ZOTTERMAN, Y. (1946). Intestinal pain: an electrophysiological investigation on mesenteric nerves. *Acta Physiol. Scand.*, **12**, 56–72.

GRIESBACHER, T. & LEMBECK, F. (1992). Effects of the bradykinin antagonist, HOE 140, in experimental acute pancreatitis. *Br. J. Pharmacol.*, **107**, 356–360.

GRIESBACHER, T. & LEMBECK, F. (1993). Increase in pressure in the biliopancreatic duct causes nociceptive blood pressure reflexes via capsaicin-sensitive afferents in the rat. *Vth Joint meeting between the British and Italian Societies of Pharmacology*, Rome, Italy. 13–16 September.

GRIESBACHER, T., TIRAN, B. & LEMBECK, F. (1993). Pathological events in experimental acute pancreatitis prevented by the bradykinin antagonist, Hoe 140. *Br. J. Pharmacol.*, **108**, 405–411.

HOLZER, P. (1991). Capsaicin: cellular targets, mechanisms of action, and selectivity for thin sensory neurons. *Pharmacol. Rev.*, **43**, 143–201.

HOLZER, P., GAMSE, R. & LEMBECK, F. (1980). Distribution of substance P in the rat gastrointestinal tract – lack of effect of capsaicin pretreatment. *Eur. J. Pharmacol.*, **61**, 303–307.

HOLZER, P., BUCSICS, A. & LEMBECK, F. (1982). Distribution of capsaicin-sensitive nerve fibres containing immunoreactive substance P in cutaneous and visceral tissues of the rat. *Neurosci. Lett.*, **31**, 253–257.

HOLZER-PETSCHE, U. (1992). Blood pressure and gastric motor responses to bradykinin and hydrochloric acid injected into somatic or visceral tissues. *Naunyn-Schmied. Arch. Pharmacol.*, **346**, 219–225.

INOUE, N., SAKAI, H,. MAGARI, S. & SANAKA, M. (1992). Distribution and possible origins of substance P-containing nerve fibres in the rat liver. *Anat. Anz.*, **174**, 557–560.

JANCSÓ, G., KIRÁLY, E. & JANCSÓ-GÁBOR, A. (1977). Pharmacologically induced selective degeneration of chemosensitive primary sensory neurons. *Nature*, **270**, 741–743.

JASCHKE, W., KLOSE, K.J. & STRECKER, E.P. (1992). A new balloon-expandable tantalum stent (Strecker-Stent) for the biliary system: preliminary experience. *Cardiovasc. Intervent. Radiol.*, **15**, 356–359.

JUAN, H. & LEMBECK, F. (1974). Action of peptides and other algesic agents on paravascular pain receptors of the isolated perfused rabbit ear. *Naunyn-Schmied. Arch. Pharmacol.*, **283**, 151–164.

JUBERG, E.N., MINNEMAN, K.P. & ABEL, P.W. (1985). β_1- and β_2-adrenoceptor binding and functional response in right and left atria of rat heart. *Naunyn-Schmied. Arch. Pharmacol.*, **330**, 193–202.

KOSTRZEWA, R.M. & JACOBOWITZ, D.M. (1974). Pharmacological actions of 6-hydroxydopamine. *Pharmacol. Rev.*, **26**, 199–288.

LASSON, Å., FORK, F.-T., TRÄGÅRDH, B. & ZEDERFELDT, B. (1988). The postcholecystectomy syndrome: bile ducts as pain trigger zone. *Scand. J. Gastroenterol.*, **23**, 265–271.

LAUBIE, M., SCHMITT, H., CANELLAS, J., ROQUEBERT, J. & DEMICHEL, P. (1974). Centrally mediated bradycardia and hypotension induced by narcotic analgesics: dextromoramide and fentanyl. *Eur. J. Pharmacol.*, **28**, 66–75.

LEMBECK, F. & DONNERER, J. (1981). Time course of capsaicin-induced functional impairments in comparison with changes in neuronal substance P content. *Naunyn-Schmied. Arch. Pharmacol.*, **316**, 240–243.

LEMBECK, F. & DONNERER, J. (1983). Reflex fall in blood pressure mediated by capsaicin-sensitive afferent fibres of the rat splanchnic nerve. *Naunyn-Schmied. Arch. Pharmacol.*, **322**, 286–289.

LEMBECK, F. & SKOFITSCH, G. (1982). Visceral pain reflex after treatment with capsaicin and morphine. *Naunyn-Schmied. Arch. Pharmacol.*, **321**, 116–122.

MCGOWAN, J.M., BUTSCH, W.L. & WALTERS, W. (1936). Pressure in the common bile duct of man: its relation to pain following cholecystectomy. *J. Am. Med. Assoc.*, **106**, 2227–2230.

MOODY, F.G., CALABUIG, R,. VECCHIO, R. & RUNKEL, N. (1990). Stenosis of the sphincter of Oddi. *Surg. Clin. North Am.*, **70**, 1341–1354.

NAGY, J.I., IVERSEN, L.L., GOEDERT, M., CHAPMAN, D. & HUNT, S.P. (1983). Dose-dependent effects of capsaicin on primary sensory neurons in the neonatal rat. *J. Neurosci.*, **3**, 399–406.

NESS, T.J. & GEBHART, G.F. (1988). Colorectal distension as a noxious visceral stimulus: physiologic and pharmacologic characterization of pseudoaffective reflexes in the rat. *Brain Res.*, **450**, 153–169.

NESS, T.J. & GEBHART, G.F. (1990). Visceral pain: a review of experimental studies. *Pain*, **41**, 167–234.

NEWMAN, P.P. (1953). Changes in arterial blood pressure following stimulation of the gall bladder. *J. Physiol.*, **119**, 46P–47P.

O'DONNELL, S.R. & WANSTALL, J.C. (1981). Demonstration of both β_1- and β_2-adrenoceptors mediating relaxation of isolated ring preparations of rat pulmonary artery. *Br. J. Pharmacol.*, **74**, 547–552.

ORDWAY, G.A., LONGHURST, J.C. & MITCHELL, J.H. (1983). Stimulation of pancreatic afferents reflexly activates the cardiovascular system in cats. *Am. J. Physiol.*, **245**, R820–R826.

PRINZ, R.A. GREENLEE, H.B. (1990). Pancreatic duct drainage in chronic pancreatitis. *Hepatogastroenterology*, **37**, 295–300.

SATOH, E., NARIMATSU, A., HOSOHATA, Y., TSUCHIHASHI, H. & NAGATOMO, T. (1993). The affinity of betaxolol, a β_1-adrenoceptor-selective blocking agent, for β-adrenoceptors in the bovine trachea and heart. *Br. J. Pharmacol.*, **108**, 484–489.

SHARKEY, K.A., WILLIAMS, R.G. & DOCKRAY, G.J. (1984). Sensory substance P innervation of the stomach and pancreas; demonstration of capsaicin-sensitive sensory neurons in the rat by combined immunohistochemistry and retrograde tracing. *Gastroenterology*, **87**, 914–921.

UENO, T., INUZUKA, S., TORIMURA, T., SAKATA, R., SAKAMOTO, M., GONDO, K., AOKI, T., TANIKAWA, K. & TSUTSUMI, V. (1991). Distribution of substance P and vasoactive intestinal peptide in the human liver: light and electron immunoperoxidase methods of observation. *Am. J. Gastroenterol.*, **86**, 1633–1637.

WOODSWORTH, R.S. & SHERRINGTON, C.S. (1904). A pseudoaffective reflex and its spinal path. *J. Physiol.*, **31**, 234–243.

(Received August 17, 1993
Revised October 25, 1993
Accepted October 28, 1993)

Br. J. Pharmacol. (1994), **111**, 555–560

Increased arterial distensibility induced by the angiotensin-converting enzyme inhibitor, lisinopril, in normotensive rats

Touria Makki, Rabelais Tatchum Talom, Nathalie Niederhoffer, Fatiha Amin, *Pierre Tankosic, **Paul-Michel Mertès & [1]Jeffrey Atkinson

Laboratoire de Pharmacologie Cardio-vasculaire, Faculté de Pharmacie, 5 rue Albert Lebrun, 54000 Nancy, France, *INSERM U308, 38 rue Lionnois, 54000 Nancy, France and **Service des Explorations Fonctionnelles Rénales et Métaboliques, Centre Hospitalier Régional et Universitaire de Nancy, Hôpitaux de Brabois, Allée de Morvan, 54511 Vandoeuvre Cedex, France

1 We investigated possible structural correlates of the beneficial effect of chronic angiotensin-converting enzyme inhibition (ACEI) with lisinopril on the aortic distensibility of normotensive rats.

2 Experiments were performed in young (4-month old), normotensive, Wistar rats which received lisinopril in their drinking water (0.9 or 9 mg kg^{-1} day^{-1}) for 9 months.

3 Following ACEI treatment, rats were pithed and aortic pulse wave velocity was measured during the progressive rise in mean arterial blood pressure produced by i.v. infusion of the α_1-adrenoceptor agonist, phenylephrine. The slope of the regression line relating aortic pulse wave velocity to mean arterial blood pressure was taken as an index of aortic distensibility. Following this, the aorta was fixed *in situ* at a normotensive pressure level and histomorphometry was performed. We also measured the calcium content of the aortic wall by atomic absorption.

4 The lower dose of lisinopril failed to lower systolic arterial blood pressure (unanaesthetized rat) or mean arterial blood pressure (pithed rat). Chronic ACEI with the higher dose of lisinopril lowered both systolic arterial blood pressure (104 ± 6 mmHg, controls 133 ± 4 mmHg, unanaesthetized), and mean arterial blood pressure (27 ± 1 mmHg, controls 34 ± 2 mmHg, pithed).

5 Although the lower dose of lisinopril did not lower blood pressure, it did improve aortic distensibility as revealed by a fall in the slope relating aortic pulse wave velocity (Y) to mean arterial blood pressure (X). Values were 5.7 ± 0.7, 3.8 ± 0.6 and 2.7 ± 0.3 in controls, and in low and high ACEI groups, respectively.

6 Lisinopril treatment did not modify the calcium content, the internal and external diameters or the medial thickness of the aorta. Chronic ACEI did, however, increase the thickness of the medial elastic fibres (controls 3.55 ± 0.05 μm, low dose ACEI 4.05 ± 0.15 μm ($P<0.05$), and high dose ACEI 4.18 ± 0.15 μm ($P<0.05$)).

7 In conclusion, we would suggest that ACEI treatment with a low dose of lisinopril can decrease aortic stiffness via a pressure-independent mechanism which possibly involves an effect of ACEI on elastic fibres.

Keywords: Aortic distensibility; ACEI; lisinopril; normotensive rat; pulse wave velocity

Introduction

Chronic angiotensin converting enzyme inhibition (ACEI) increases arterial compliance in normotensive rats (Levy *et al.*, 1992). Such an increase in compliance could result from the fall in blood pressure produced by ACEIs. Pressure-independent functional and/or structural effects on the arterial wall stiffness could also be involved (Safar *et al.*, 1986; Levy *et al.*, 1989a,b). We investigated the effect of chronic treatment with the ACEI, lisinopril, on arterial distensibility in normotensive rats, and the possible links between the latter effect and the effects of lisinopril on arterial structure. Improvement in vascular compliance could be important in the therapeutic use of ACEI. An increase in arterial distensibility has been reported to attenuate cardiac hypertrophy (Asmar *et al.*, 1988). We also evaluated, therefore, changes in ventricular mass compared to body weight.

As our main interest was in pressure-independent effects of ACEI, we used normotensive rats and a low dose of lisinopril which did not lower blood pressure. Aortic distensibility was estimated from carotid to femoral pulse wave velocity. Pulse wave velocity is directly related to blood pressure (Milnor, 1989). We measured pulse wave velocity, therefore, in the pithed rat which has the advantage that its blood pressure can be set at a given value, over the range of 20 to 100 mmHg, by infusion of vasoconstrictors such as the α_1-adrenoceptor agonist, phenylephrine (Vargas *et al.*, 1991). It is in the lower blood pressure range that transmural pressure is low and, presumably, transmural strain is borne mainly by elastic fibres (Milnor, 1989).

Two aspects of aortic structure were investigated. Following fixation *in situ* at a normotensive arterial blood pressure, the thoracic aorta was removed. After the preparation of transverse sections, inner and outer diameters, medial thickness, and the number and thickness of the elastic fibres were determined, using a computerized image analysis system. Finally the calcium content of the wall of the thoracic aorta was measured.

Methods

Animals and chronic ACEI treatment

Eighteen normotensive male, outbred Wistar rats (4 month-old, 360–380 g; Iffa-Credo SA, 69210 L'Arbresle, France), were housed under standard conditions with a light-dark

[1] Author for correspondence.

cycle of 07 h 00 min/19 h 00 min. They were given a standard rodent diet (UAR, 91360 Villemoisson sur Orge, France) and water. Animals were randomized on the basis of their systolic arterial blood pressures into three groups of six. The first two groups were given drinking water containing lisinopril ((1-N^2-((S)-1-carboxy-3-phenylpropyl) -L-lysyl)-L-proline dihydrate), the concentrations of which were adjusted every 2nd day in an attempt to maintain daily doses at 1 or 10 mg kg^{-1} day^{-1}. Average daily doses were calculated on the basis of the fluid intake and body weight of the rat and the concentration of lisinopril in the drinking water. In spite of weekly adjustment of the concentration of lisinopril, rats did not reach the daily predicted doses and doses over the treatment period were, in fact, 0.9 and 9 mg kg^{-1} day^{-1}. The treatment period lasted 9 months, during which time food intake, body weight and water consumption were measured at weekly intervals. A third control group ($n = 6$) received normal drinking water.

Doses of lisinopril were chosen on the basis of a preliminary experiment in which normotensive rats were given 1, 3, 10 or 30 mg kg^{-1} day^{-1} lisinopril orally (in drinking water, $n = 6$ per group). Systolic arterial blood pressures after 20 days' treatment were: controls, 129 ± 2; 1 mg kg^{-1}, 127 ± 4 (NS versus controls); 3 mg kg^{-1}, 116 ± 3 ($P < 0.05$ versus controls); 10 mg kg^{-1}, 113 ± 2 ($P < 0.05$ versus controls) and 30 mg kg^{-1}, 108 ± 3 mmHg ($P < 0.05$ versus controls). Thus in this preliminary experiment, a dose of 1 mg kg^{-1} day^{-1} did not lower blood pressure, whereas larger doses of lisinopril ($\geq$ 3 mg kg^{-1} day^{-1}) produced significant, sustained falls in blood pressure. The choice was made, therefore, to use doses of 1 and 10 mg kg^{-1} day^{-1}.

Systolic arterial blood pressure and heart rate in unanaesthetized animals

Systolic arterial blood pressures were measured in the afternoon. As feeding (and presumably drinking also) is limited to 3 to 5 equally spaced periods during the dark phase (Weihe, 1989), we can estimate that blood pressure was measured some 8 h following the last drug intake. Rats were placed in restraining cages in a specially constructed incubator for 15 min. A cuff was put around the base of the tail and a microphone was placed over the ventral tail artery, distal to the cuff. The cuff was inflated and systolic arterial blood pressure (mmHg) was taken as being equivalent to the cuff pressure at which the pressure pulse of the tail artery could no longer be detected. Heart rate (beats min^{-1}, b.p.m.) was obtained from a fast speed chart recording.

Measurements were repeated at least three times and an average was taken. Systolic arterial blood pressure and heart rate were recorded before the start of treatment, and at regular intervals throughout the 9 months' treatment period.

Arterial blood pressure and aortic pulse wave velocity in the pithed rat

A nylon cannula (1.02 mm o.d., 0.58 mm i.d.; Portex S.A., 62600 Berck sur Mer, France) was inserted, under halothane/oxygen anaesthesia, into the right common carotid artery for measurement of arterial blood pressure (systolic, diastolic, mean and pulse, mmHg) and heart rate (b.p.m.). The left common carotid artery was tied off. A second nylon cannula was placed in the left femoral artery for the determination of femoral arterial blood pressure, and the carotid to femoral, aortic pulse wave velocity (cm s^{-1}).

The nylon cannulae were connected to low volume, pressure transducers (World Precision Instruments Inc., Sarasota, FL, U.S.A.). The frequency response of the cannula plus pressure transducer was flat up to 30 Hz, i.e., the fifth harmonic of the basal signal in the pithed rat. The phase lag of the pressure signal was negligible up to 30 Hz. Pressure transducers were connected to a Maclab/Macbridge system (AD Instrument Ltd., Hampstead, London) for online recording of the two arterial pressure signals.

Aortic pulse wave velocity was determined by first calculating the foot of each systolic pressure wave, following digital conversion of the original analogue pulse signal. The foot was defined as the point obtained by extrapolating the wave front downward to the point of intersection with the exponential decay of the diastolic pressure. The exponential nature of the diastolic pressure decay was confirmed by an exponential best fit programme. The distance (12.0–12.5 cm) between the two cannula tips was determined by direct measurement following *post mortem* dissection. There were no differences in this distance amongst the three groups (results not shown). Pulse wave velocity, arterial blood pressures and heart rate were determined for ten heart beats, and averaged.

Rats were also fitted with a femoral venous catheter for the continuous infusion of the α_1-adrenoceptor agonist, phenylephrine. The infusion of phenylephrine was maintained up to the end of the experiment.

Animals were fitted with an endotracheal tube, pithed and ventilated with a rodent respirator (1 ml 100 g^{-1} body weight, 50 strokes min^{-1}; rodent respirator 601, Harvard Apparatus, South Natick, MA, U.S.A.). After surgery, each animal was allowed to stabilize for 30 min. Blood gas parameters were checked (pH/Blood gaz analyzer model 170, Corning Medical, Medfield, MA, U.S.A.) and found to be stable throughout the experimental protocol. Average values were: $PaCO_2$ 33 ± 5, PaO_2 90 ± 4 and pH 7.40 ± 0.03. There were no differences between the groups (results not shown).

A blood sample (0.5 ml) was removed for the determination of plasma renin activity (Peters-Haefeli, 1971) and plasma angiotensin I converting enzyme activity (Ryan *et al.*, 1977).

Thirty minutes following pithing, starting values for aortic pulse wave velocity and arterial blood pressure were recorded. Rats were then continuously infused with phenylephrine (40 to 80 nmol kg^{-1} min^{-1}, the dose was adjusted so as to restore blood pressure to normotensive levels). The gradual, step-wise increase in arterial blood pressure produced by phenylephrine lasted some 30 min. During this time, aortic pulse wave velocity and arterial blood pressure were recorded continuously.

Values for aortic pulse wave velocity, obtained during this initial period of phenylephrine infusion, are expressed as a function of the mean arterial blood pressure (carotid artery), measured simultaneously. Results were grouped over mean arterial blood pressure ranges, the upper and lower limits of which defined a 5 mmHg pressure rise, during which arterial blood pressure was stable. Regression analysis was performed to determine the relationship between the two parameters.

In a preliminary experiment using 12-month old Wistar rats ($n = 6$), subdiaphragmatic aortic blood velocity was measured (20 MHz flow probe, Crystal Biotech, Hopkinton, MA, U.S.A) in addition to the parameters given above. With both carotid arteries tied off, this can be taken as an approximation of cardiac output. I.v. infusion of phenyleprhine (according to the protocol described above) did not modify aortic blood velocity (starting value 4.1 ± 0.6 kHz, final value 5.1 ± 0.5 kHz). This absence of any significant change in velocity suggests (i) that the increase in mean arterial blood pressure produced by phenylephrine stems from an increase in total peripheral resistance, and (ii) changes in cardiac output are a neglible factor in changes in aortic pulse wave velocity.

Aortic structure and calcium content, and cardiac mass

At the end of the haemodynamic experiment, rats were perfused for 1 h at a normotensive arterial blood pressure level via the right carotid arterial cannula with 10% formol containing phosphate-buffered saline (NaCl 120 mmol l^{-1}, KCl 2.7 mmol l^{-1}, in a phosphate buffer 10 mmol l^{-1}, pH 7.4 at 25°C). At the end of the perfusion, the aorta was excised, and immersed in 10% formol. A 1-cm specimen of each thoracic

aorta was dehydrated in graded ethanol solutions and embedded in paraffin. Three 20 μm thick sections were cut and stained with hematoxylin plus eosin for the determination of outer and inner diameters, and medial thickness. A further three sections (10 μm) were stained with Weigert's solution (basic fuchsin plus resorcin) and the number and thickness of the medial elastic fibres was determined. Morphometric analysis was performed using the Optilab algorithm (Graphtek, 93510 Meudon-la-Forêt, France). Each section was examined three times in a blind fashion.

An autopsy was carried out and the ventricles were weighed. A sample of the thoracic aorta was removed for determination of tissue calcium content (μmol g^{-1} dry weight, Henrion *et al.*, 1991).

Drugs

Phenylephrine hydrochloride was purchased from Sigma Chemical Company, St. Louis, MO, U.S.A. Lisinopril was provided by ICI Laboratories, Paris, France.

Statistics

Values are given as means ± s.e.mean. Significant differences between means were calculated using the ANOVA and Scheffe test. Linear regression analysis was performed using standard techniques and results are expressed as intercept (*a*), slope (*b*) and correlation (*r*).

Results

Effect of chronic ACEI on food intake, body weight and water consumption, plasma renin activity and angiotensin-converting enzyme activity

There was no effect of lisinopril on growth rate, which increased by 40% over the 9 month period. Weights at the start and the end of the experiment in controls were 367 ± 9 and 514 ± 21 g, and in the group receiving the higher dose of lisinopril (9 mg kg^{-1} day^{-1}), 368 ± 9 and 549 ± 25 g. Thus any changes in cardiac mass or arterial structure cannot be explained on the basis of a difference in growth rate in rats treated with lisinopril. Food intake decreased progressively up to the 150th day, and remained stable thereafter; there was no effect of lisinopril on food intake. Values for the start and the end of the experiment were for controls 63 ± 1 and 39 ± 2 g kg^{-1} day^{-1}, and for lisinopril (9 mg kg^{-1} day^{-1}) 66 ± 2 and 39 ± 2 g kg^{-1} day^{-1}.

Water intake decreased progressively up to the 100th day. Chronic treatment with lisinopril produced an initial, dose-related increase in water consumption (Figure 1). Although the concentration of lisinopril in the drinking water was adjusted frequently in an attempt to maintain drug intakes at 1 and 10 mg kg^{-1} day^{-1}, with the relatively rapid changes in intake in the lisinopril groups the calculated average lisinopril intake was, in fact, 0.9 and 9 mg kg^{-1} day^{-1}.

Plasma renin activity was similar in all groups (controls 8 ± 1 ng AI ml^{-1} h^{-1}). Angiotensin I converting enzyme activity was inhibited in a dose-related fashion by lisinopril, 0.9 mg kg^{-1} day^{-1}, 10 ± 2 ($P<0.05$); 9 mg kg^{-1} day^{-1}, 2 ± 1 ($P<0.05$), controls, 28 ± 5 nmol ml^{-1} min^{-1}.

Effect of chronic ACEI on systolic arterial blood pressure and heart rate in unanaesthetized animals

Chronic treatment with lisinopril at a dose of 0.9 mg kg^{-1} day^{-1} did not significantly modify systolic arterial blood pressure (start and end of experiment; 116 ± 3 and 123 ± 3 mmHg, controls 123 ± 1 and 133 ± 4 mmHg, Figure 2). Lisinopril at a higher dose of 9 mg kg^{-1} day^{-1} did lower blood pressure (Figure 2).

Chronic treatment with the higher dose of lisinopril produced a slight fall in heart rate ($P<0.05$, start and end of experiment 412 ± 8 and 381 ± 10 b.p.m.; controls, 386 ± 23 and 422 ± 15 b.p.m.).

Effect of chronic ACEI on arterial blood pressure and aortic pulse wave velocity in the pithed rat during phenylephrine infusion

Baseline mean arterial blood pressure was significantly lower in rats previously treated with the higher dose of lisinopril (27 ± 1 mmHg, $P<0.05$ versus controls 34 ± 2 mmHg). The lower dose of lisinopril had no effect on baseline mean arterial blood pressure. Values given are those for the carotid artery cannula; similar results (not shown) were obtained in the femoral artery cannula.

The continuous infusion of phenylephrine produced increases in aortic pulse wave velocity and mean arterial blood pressure in all three groups (Figure 3). Over the arterial blood pressure range studied (20 to 100 mmHg), there was a significant linear relationship between aortic pulse wave velocity (dependent variable) and (carotid artery) mean arterial blood pressure (independent variable). Similar results were obtained when the mean arterial blood pressure recorded in the femoral artery was taken as the independent variable (results not shown). Intercepts for the linear regression within

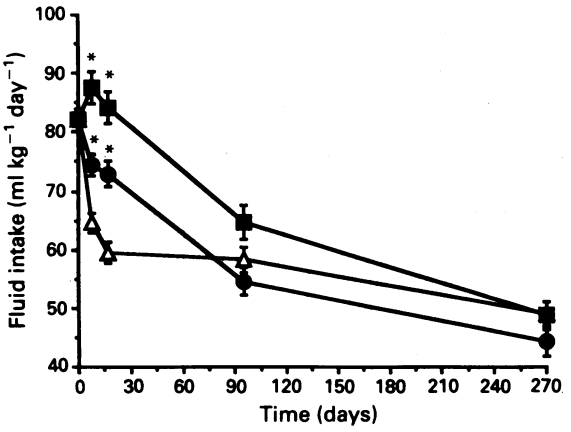

Figure 1 Effect of chronic ACEI with lisinopril on water intake in normotensive rats: controls (Δ), 0.9 mg kg^{-1} day^{-1} lisinopril (●), 9 mg kg^{-1} day^{-1} lisinopril (■). $n = 6$ per group. *$P<0.05$ ANOVA/Scheffe test compared to controls.

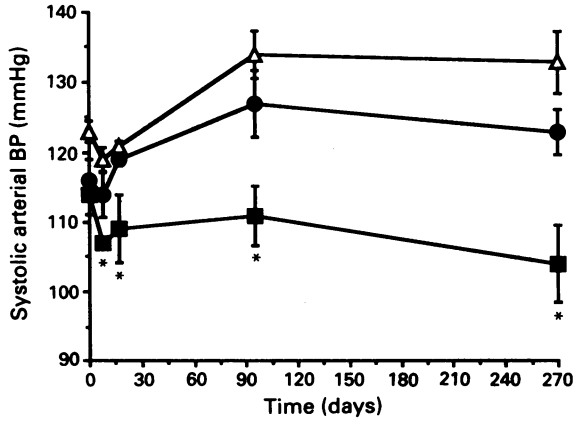

Figure 2 Effect of chronic ACEI with lisinopril on systolic arterial pressure of normotensive rats: controls (Δ), 0.9 mg kg^{-1} day^{-1} lisinopril (●), 9 mg kg^{-1} day^{-1} lisinopril (■). $n = 6$ per group. *$P<0.05$ ANOVA/Scheffe test compared to controls.

each group were not significantly different, whereas slopes were less steep in groups treated with lisinopril (Figure 3).

Chronic ACEI had no effect on heart rate in pithed rats. Values at baseline and at 90 mmHg were 288 ± 21 and 380 ± 38 b.p.m. for controls, 277 ± 5 and 419 ± 32 b.p.m. for lisinopril (0.9 mg kg^{-1} day^{-1}), and 251 ± 12 and 439 ± 26 b.p.m. for lisinopril (9 mg kg^{-1} day^{-1}).

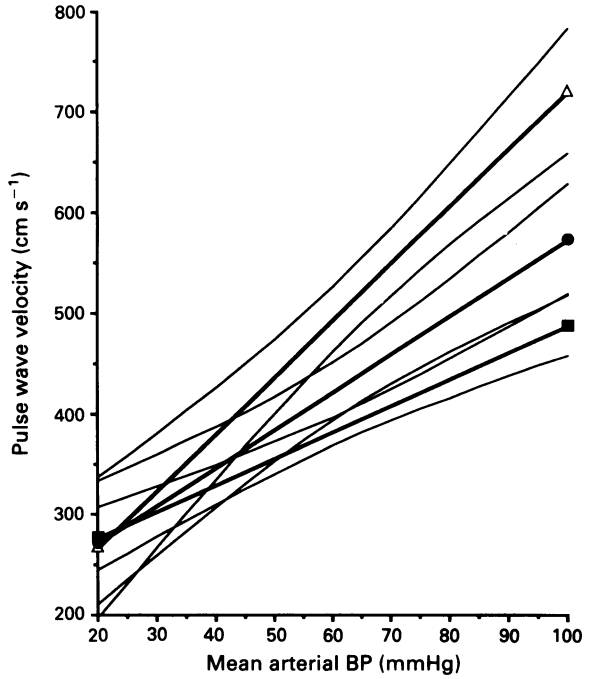

Figure 3 Effect of chronic ACEI with lisinopril on pulse wave velocity (cm s^{-1}), expressed as a function of mean arterial blood pressure (mmHg, carotid), in pithed normotensive rats, following a progressive rise in arterial blood pressure, produced by infusion of phenylephrine: controls (Δ), 0.9 mg kg^{-1} day^{-1} lisinopril (●) and 9 mg kg^{-1} day^{-1} lisinopril (■). For the sake of clarity regression lines and 95% confidence intervals only are shown. Linear regression analysis of pulse wave velocity (Y) on mean arterial blood pressure (X) ($n = 20$ points per group) revealed the following values:

Group	*Intercept (a)*	*Slope (b)*	*Correlation (r)*
Controls	154	5.7 ± 0.7	0.857 ($P<0.05$)
Lisinopril (0.9 mg kg^{-1} day^{-1})	197	3.8 ± 0.6*	0.824 ($P<0.05$)
Lisinopril (9 mg kg^{-1} day^{-1})	220	2.7 ± 0.3*	0.859 ($P<0.05$)

*$P<0.05$ versus controls.

Effect of chronic ACEI on aortic structure and calcium content, and cardiac mass

The only significant effect of lisinopril on aortic structure was an increase in the thickness of the elastic fibres (Table 1). Lisinopril had no effect on the calcium content of the aortic wall. Chronic treatment with lisinopril produced a fall in ventricular mass. Values were 2.4 ± 0.1 for controls, 2.0 ± 0.1 for 0.9 mg kg^{-1} day^{-1} lisinopril and 2.0 ± 0.1 (g kg^{-1} body weight) for 9 mg kg^{-1} day^{-1} lisinopril.

Discussion

The results of this experiment show that in normotensive rats, chronic ACEI with lisinopril improves arterial distensibility. This effect may be independent of pressure as low dose treatment, which has no chronic effect on blood pressure, will improve distensibility. Both low and high doses of lisinopril also lowered the cardiac mass to the same degree.

Although it did not lower blood pressure, the lower dose of lisinopril did have a significant effect on the renin-angiotensin system as shown by a decrease in ACE activity and a stimulation of water intake. The lack of effect of low dose lisinopril treatment on systolic arterial blood pressure is probably related to the lack of effect of this dose on peripheral resistance. This hypothesis is confirmed by the observation that mean arterial blood pressure in the pithed rat was no different from that of controls. Baseline mean arterial blood pressure in the pithed rat, recorded in the absence of any autonomic control, may be taken as indicative of the degree of structural adaptation of the resistance vessels. Folkow *et al.* (1970) have shown a close correlation between minimal perfusion at maximal dilatation and the ratio of wall thickness to internal radius in small resistance vessels. Although the pithed rat is probably not in a maximally dilated state, as a slight but significant decrease in blood pressure can be produced by perfusion with the vasodilators, nitroprusside and papaverine (Sano & Tarazi, 1987), blood pressure measured following pithing did indicate the degree of vascular hypertrophy in SHR following antihypertensive treatment (Sano & Tarazi, 1987).

Chronic ACEI with a higher dose of lisinopril lowered mean arterial blood pressure in the pithed rat. This suggests that such treatment modified the structure of the resistance vessels, leading to a fall in peripheral resistance, and hence to a fall in systolic arterial blood pressure recorded in the unanaesthetized rat.

Histomorphometric analysis of the aortic wall, however, revealed no effect of such treatment on medial hypertrophy or wall to lumen ratio. Two explanations for this apparent contradiction may be given. Firstly, resistance is inversely proportional to the fourth power of the internal radius of the vessel. This means that small changes in the diameter of the

Table 1 Effect of chronic ACEI with lisinopril on aortic calcium content, internal and external diameters and thickness of the media and the medial elastic fibres

	Controls	*Lisinopril*	
		0.9 mg kg^{-1} day^{-1}	9 mg kg^{-1} day^{-1}
Calcium (μmol g^{-1} dry wt.)	8.2 ± 0.9	9.0 ± 0.4	8.2 ± 1.2
Internal diameter (mm)	1.73 ± 0.09	1.65 ± 0.07	1.75 ± 0.06
External diameter (mm)	1.88 ± 0.09	1.80 ± 0.08	1.89 ± 0.06
Medial thickness (μm)	71 ± 1	71 ± 1	68 ± 1
Thickness of elastic fibres (μm)	3.55 ± 0.05	4.05 ± 0.15*	4.18 ± 0.15*

*$P<0.05$ versus controls.

resistance vessels may have a substantial effect on pressure. Our histological technique may not be able to detect such small changes, albeit that similar changes occur in resistance and compliance vessels. The second explanation is that the structural changes in small diameter, muscular, resistance vessels are not the same as those in large diameter, elastic compliance vessels.

Both low and high dose ACEI increased the thickness of the elastic fibres of the aorta. This effect is presumably independent of pressure as changes in elastic fibre thickness were similar with both doses, but only the higher dose of lisinopril lowered blood pressure. An age-related thinning of elastic fibres has been described in both man (Nejjar *et al.*, 1990; Nichols & O'Rourke, 1990) and animals (Fornieri *et al.*, 1992). In the latter study the structural changes, from birth to 2 years of age, in the thoracic aorta of outbred male Wistar rats, were reported. Although the ages of the animals studied do not exactly correspond to ours, the authors found a decrease in elastin cross-sectional area of 23% between the ages of 2 and 16 months. We can hypothesize that a similar change occurred in our control group between 4 and 13 months, and that chronic ACEI postponed this decrease.

At the present time we have no information on the mechanism by which chronic ACEI will protect elastic fibres. It has been proposed that calcium accumulation on the elastic fibres of the media modifies their structure, leading to an increase in arterial stiffness (Atkinson, 1992). Furthermore chronic ACEI lowers the calcium content of the arterial wall (Fleckenstein *et al.*, 1989), and protects elastic fibres (Michel *et al.*, 1990). Thus calcium accumulation in the aortic wall may constitute an initial step in this thinning of elastic fibres. In our experiment, however, chronic ACEI did not modify arterial wall calcium content. This lack of effect may be related to the relatively short treatment period, as the Fleckenstein group (1989) have shown that chronic ACEI of 20 months duration will slow down age-related calcium accumulation in the arterial wall. Thus calcium accumulation may be an amplifying but not an initiating factor in the loss of arterial wall elastin.

Another possibility is that the lack of change in the total calcium content of the arterial wall may mask more subtle changes, such as an ACEI-induced decrease in the amount of calcium bound to the elastic fibres. In a previous study (Henrion *et al.*, 1991) using a double-staining technique in which not only elastic fibres but also calcium deposits (with the von Kossa dye) were stained, we were able to demonstrate histologically that in the vitamin D_3-nicotine rat model, calcium is deposited on elastic fibres. In that model, however, calcium levels were 30 to 50 fold higher than in the normotensive, untreated rat and this double staining technique would appear to be unable to reveal an ACEI-induced fall in calcium bound to elastin in the latter model (unpublished results). We are currently investigating another method which involves isolation of the elastic fibre network by selective enzymatic degradation of the arterial wall followed by determination of elastin-bound calcium with atomic absorption. This methodology should have the sensitivity required to test our working hypothesis.

The link between the loss of elastin and the increase in wall stiffness has been discussed by several authors (Fleckenstein *et al.*, 1989; Nichols & O'Rourke, 1990; Atkinson, 1992). We would suggest that protection of elastic fibres by ACEI postpones the age-related increase in arterial stiffness, such that, in lisinopril-treated groups, arterial distensibility (as indicated by the ratio: pulse wave velocity/mean arterial blood pressure), is higher than in controls. Here again, as in the case with elastic fibre thickness, low and high dose ACEI had similar effects, and the effect of low dose ACEI was independent of pressure.

Another possibility is that the important determinant of arterial distensibility is not only the quantity and quality of elastin but also the relative amounts of elastin and collagen. Wolinsky (1972) has shown that the amount of collagen in the arterial wall increases with aging. As the elastic modulus of collagen is greater than that of elastin, such a change would produce a stiffer arterial wall. Lisinopril will reduce the amount of collagen in the left ventricular wall of the SHR (Brilla *et al.*, 1991). However, it should be noted that there was no effect in the WKY rat and similar studies on the arterial wall are lacking. At present the hypothesis of ACEI-induced inhibition of collagen synthesis in the arterial wall (possibly via aldosterone inhibition) leading to an improved elastin to collagen ratio and improved arterial distensibility is interesting but unproven.

Chronic ACEI lowered left ventricular wet weight and again both doses were equally effective. As the inhibition of plasma ACE was dose-related, but the structural effects of lisinopril (on both elastic fibre thickness and cardiac hypertrophy) were not related to dose, we would suggest that inhibition of plasma ACE is not the primary event in the structural effects of lisinopril. This observation raises the possibility that the structural effects of lisinopril are mediated via the inhibition of another system such as a local, tissue renin-angiotensin system.

Cardiac afterload has both a capacitance and a resistance component and the Safar group (Asmar *et al.*, 1988) have proposed that an increase in large artery compliance will attenuate cardiac hypertrophy, and *vice versa*. Our results would appear to agree with this, as a low dose of lisinopril, which did not lower peripheral resistance, did improve arterial distensibility. As arterial compliance is the product of wall distensibility and lumen volume and vascular dimensions did not change in the present experiment, we suggest that the improvement in arterial distensibility produced an improvement in compliance and so lowered left ventricular mass.

In conclusion, we suggest that our results raise the possibility of a new, pressure-independent effect of chronic ACEI, *viz*, a protection of elastic fibre structure, leading to an increase in arterial distensibility. One of the consequences of this on target organs of the cardiovascular system could be a decrease in cardiac afterload and subsequently, in left ventricular mass.

References

ASMAR, R.G., PANNIER, B., SANTONI, J.P., LAURENT, S., LONDON, G.M., LEVY, B.I. & SAFAR, M.E. (1988). Reversion of cardiac hypertrophy and reduced arterial compliance after converting enzyme inhibition in essential hypertension. *Circulation*, **78**, 941–950.

ATKINSON, J. (1992). Vascular calcium overload. Physiological and pharmacological consequences. *Drugs*, **44**, (suppl. 1), 710–714.

BRILLA, C.G., JANICKI, J.S. & WEBER, K.T. (1991). Cardioreparative effects of lisinopril in rats with genetic hypertension and left ventricular hypertrophy. *Circulation*, **83**, 1771–1779.

FLECKENSTEIN, A., FLECKENSTEIN-GRUN, G., FREY, N. & ZORN, J. (1989). Calcium antagonism and ACE inhibition. Two outstandingly effective means of interference with calcium overload, high blood pressure, and arteriosclerosis. *Am. J. Hypertens.*, **2**, 194–204.

FOLKOW, B., HALLBACK, M., LUNDGREN, Y. & WEISS, L. (1970). Background of increased flow resistance and vascular reactivity in spontaneously hypertensive rats. *Acta Physiol. Scand.*, **80**, 93–100.

FORNIERI, C., QUAGLINO, D. & MORI, G. (1992). Role of the extracellular matrix in age-related modifications of the rat aorta. *Arterioscl. Thromb.*, **12**, 1008–1016.

HENRION, D., CHILLON, J.M., GODEAU, G., MULLER, F., CAPDEVILLE-ATKINSON, C., HOFFMAN, M. & ATKINSON, J. (1991). The consequences of aortic calcium overload following vitamin D_3 plus nicotine treatment in young rats. *J. Hypertens.*, **9**, 919–926.

LEVY, B.I., BENESSIANO, J., POITEVIN, P. & SAFAR, M.E. (1989a). Angiotensin-converting enzyme inhibition and compliance of the carotid artery in normotensive and hypertensive rats. *J. Human Hypertens.*, **3**, 57–62.

LEVY, B.I., CURMI, P., POITEVIN, P. & SAFAR, M.E. (1989b). Modifications of the arterial mechanical properties of normotensive and hypertensive rats without arterial pressure changes. *J. Cardiovasc. Pharmacol.*, **14**, 253–259.

LEVY, B.I., STEFAS, L., BABALIS, D. & BENETOS, A. (1992). Vascular endothelium, mechanical properties of the arterial wall and local angiotensin converting enzyme inhibition. *J. Hypertens.*, **10** (suppl 5), S21–S27.

MICHEL, J.B., SALZMANN, J.L. & LEVY, B. (1990). Effect of hypertension and vasodilator treatment on arterial wall structure. In *Coronary and Cerebrovascular Effects of Antihypertensive Drugs*. ed. Atkinson, J., Capdeville, C. & Zannad, F. pp. 205–217. Tunbridge Wells: Transmedica.

MILNOR, W.R. (1989). *Hemodynamics*. Baltimore: Williams & Wilkins.

NEJJAR, I., PIERAGGI, M.T., THIERS, J.C. & BOUISSOU, H. (1990). Age-related changes in the elastic tissue of human thoracic aorta. *Atherosclerosis*, **90**, 199–208.

NICHOLS, W.W. & O'ROURKE, M.F. (1990). *McDonald's Blood Flow in Arteries*. pp. 398–420. London: Edward Arnold.

PETERS-HAEFELI, L. (1971). Rate of inactivation of endogenous and exogenous renin in normal and renin-depleted rats. *Am. J. Physiol.*, **221**, 1339–1345.

RYAN, J.W., CHUNG, A., AMMONS, C. & CARLTON, M.L. (1977). A simple radioassay for angiotensin-converting enzyme. *Biochem. J.*, **167**, 501–504.

SAFAR, M.E., LAURENT, S., BOUTHIER, J.A. & LONDON, G.M. (1986). Comparative effects of captopril and isosorbide dinitrate on the arterial wall of hypertensive human brachial arteries. *J. Cardiovasc. Pharmacol.*, **8**, 1257–1261.

SANO, T. & TARAZI, R.C. (1987). Differential structural responses of small resistance vessels to antihypertensive therapy. *Circulation*, **75**, 618–626.

VARGAS, H.M., CUEVAS, J.M., IGNARRO, L.J. & CHAUDHURI, G. (1991). Comparison of the inhibitory potencies of N^G-methyl-, N^G-nitro- and N^G-amino-l-arginine on EDRF function in the rat: evidence for continuous basal EDRF release. *J. Pharmacol. Exp. Ther.*, **257**, 1208–1215.

WEIHE, W.H. (1989). The laboratory rat. In *'The UFAW Handbook on the Care and Management of Laboratory Animals*. 6th ed. Poole, T.B. pp. 309–330. Harlow, Essex: Longman.

WOLINSKY, H. (1972). Long-term effects of hypertension on the rat aortic wall and their relation to concurrent aging changes. *Circ. Res.*, **30**, 301–309.

(Received May 6, 1993
Revised October 12, 1993
Accepted November 1, 1993)

Br. J. Pharmacol. (1994), **111**, 561–569

Inhibitory effects of nordihydroguaiaretic acid on ET_A-receptor-mediated contractions to endothelin-1 in rat trachea

Peter J. Henry

Department of Pharmacology, University of Western Australia, Nedlands, 6009, Australia

1 It has been shown previously that nordihydroguaiaretic acid (NDGA) inhibits endothelin-1 (ET-1)-induced contractions in rat isolated tracheal smooth muscle. To investigate the underlying mechanisms, this study examined the effects of NDGA on various aspects of the ET_A and ET_B receptor-effector systems which mediate ET-1-induced contractions in this preparation.

2 NDGA inhibited contractions induced by each of the isoforms of ET (ET-1, ET-2 and ET-3) but not those induced by the ET_B receptor-selective agonist, sarafotoxin S6c, the cholinoceptor agonist, carbachol or the depolarizing spasmogen, KCl.

3 Quantitative autoradiographic studies of [^{125}I]-ET-1 binding to rat tracheal smooth muscle indicated that NDGA was not an ET receptor antagonist.

4 NDGA inhibited the ET_A receptor-mediated, intracellular Ca^{2+}-dependent contractions induced by 100 nM ET-1 in Ca^{2+}-free solution (by 75%, $P<0.01$). Furthermore, NDGA markedly inhibited the contractions induced by ryanodine and cyclopiazonic acid; contractions purportedly due to Ca^{2+} release from intracellular stores.

5 Like NDGA, the sarcoplasmic reticulum Ca^{2+}-ATPase inhibitors cyclopiazonic acid and thapsigargin inhibited contractions to ET-1, but not carbachol or KCl. However, cyclopiazonic acid, but not NDGA, also (a) induced transient contractions in rat trachea, (b) potentiated contractions induced by KCl, and (c) potentiated the extracellular Ca^{2+}-dependent phase of ET-1-induced contractions, indicating that NDGA did not inhibit ET-1-induced contractions through Ca^{2+}-ATPase inhibition and depletion of sarcoplasmic reticular Ca^{2+}.

6 In control preparations, ET-1 induced a slowly developing, sustained contraction. However, in the presence of NDGA or the ET_A receptor antagonist, BQ123, ET-1-induced contractions resembled the transient contractions induced by sarafotoxin S6c. In nominally Ca^{2+}-free solution, ET_A receptor-mediated contractions induced by ET-1 developed very slowly and were inhibited by NDGA.

7 Additional studies indicated that the inhibitory effects of NDGA on endothelin-1-induced contractions were not the result of any significant actions of NDGA on lipoxygenase, cytochrome P_{450}, L- or T-type Ca^{2+}-channels, Na^+-channels or protein kinase C.

8 In summary, NDGA selectively inhibited ET-1-induced contractions in rat tracheal smooth muscle via a lipoxygenase-independent mechanism involving inhibition of the ET_A but not the ET_B, receptor-effector system. NDGA did not appear to inhibit the initial events in the ET_A signal transduction pathway, such as receptor binding and protein kinase C activation. However, NDGA inhibited the intracellular Ca^{2+}-dependent component of ET-1-induced contraction, possibly by inhibiting mobilisation of intracellular Ca^{2+}. As an apparent direct consequence of inhibiting the ET_A receptor-effector system, NDGA markedly changed the time course of ET-1-induced contractions; from a slowly developing and sustained contraction into a transient contraction resembling that induced by sarafotoxin S6c.

Keywords: Endothelin-1; sarafotoxin S6c; nordihydroguaiaretic acid; cyclopiazonic acid; staurosporine; ryanodine; rat trachea; endothelin receptors; airway smooth muscle

Introduction

Endothelin-1 (ET-1) is a potent spasmogen of airway smooth muscle in many animal species including man, and may contribute to the elevated bronchomotor tone of asthma (Uchida *et al.*, 1988; Advenier *et al.*, 1990; Henry *et al.*, 1990b; Springall *et al.*, 1991). ET-1 initiates contraction by stimulating high affinity receptors located on the surface membrane of the airway smooth muscle cells (Turner *et al.*, 1989; Henry *et al.*, 1990b; Mattoli *et al.*, 1991). At least two ET receptor subtypes have recently been identified, termed ET_A and ET_B, and both have been implicated in mediating ET-1-induced contraction of airway smooth muscle. For example, functional experiments using the ET_A receptor-selective antagonist, BQ123 and the ET_B receptor-selective agonist, sarafotoxin S6c, indicate that ET-1-induced contraction of airway smooth muscle is mediated primarily by ET_A receptors in some species, such as the sheep (Noguchi *et al.*, 1992) and by ET_B receptors in other species including the guinea-pig (Hay, 1992). In addition, recent autoradiographic, biochemical and functional studies indicate that ET-1-induced contractions in rat trachea appear to be mediated by both ET_A and ET_B receptor-effector systems (Henry, 1993). These latter studies showed that ET-1-induced contractions induced by the stimulation of ET_A receptors appear to have resulted from activation of the phosphoinositide pathway and the mobilisation of intracellular Ca^{2+}, whereas those induced by the stimulation of ET_B receptors seem to have resulted from the influx of extracellular Ca^{2+}.

Nordihydroguaiaretic acid (NDGA), a drug routinely used as a nonspecific inhibitor of lipoxygenase, has recently been

[1] Author for correspondence.

shown to inhibit ET-1-induced contractions in rat isolated tracheal smooth muscle (Henry *et al.*, 1992). However, it appears unlikely that products of arachidonic acid metabolism by 5-lipoxygenase, such as the leukotrienes, contributed significantly to ET-1-induced contractions in this preparation. Firstly, leukotrienes are poor spasmogens of rat isolated tracheal smooth muscle (Chand *et al.*, 1990). Secondly, the leukotriene receptor antagonist, SKF104353, did not inhibit ET-1-induced contractions (Henry *et al.*, 1992). Finally, in the current study, NDGA was the only lipoxygenase inhibitor tested that inhibited ET-1-induced contractions. Thus, NDGA appears to inhibit ET-1-induced contractions via a lipoxygenase-independent but as yet undefined, pathway. With respect to this pathway, NDGA has been reported to modulate the activity of other factors which may participate in smooth muscle contraction. For example, NDGA has been shown to inhibit enzymes such as protein kinase C, cyclo-oxygenase, guanylate cyclase and cytochrome P_{450} in various cell and tissue systems (Clark & Linden, 1986; Rondeau *et al.*, 1990; Force *et al.*, 1991). Furthermore, NDGA, inhibits Ca^{2+} currents in some cell systems (Korn & Horn, 1990) and has some structural similarities with the sarcoplasmic reticulum Ca^{2+}-ATPase inhibitor, cyclopiazonic acid.

Thus, the principle purpose of this study was to investigate the mechanisms through which NDGA inhibits ET-1-induced contractions in rat isolated tracheal smooth muscle. Functional and autoradiographic techniques were used to examine the effects of NDGA on various aspects of the recently elucidated ET_A and ET_B receptor-effector systems, which mediate ET-1-induced contractions in this preparation.

Methods

Preparation of tracheal segments

Male Wistar rats (10–12 weeks) and SR/C Tricolor guinea-pigs (6–8 weeks) were stunned and killed by cervical dislocation and exsanguination. The trachea was excised, placed in cold Krebs-bicarbonate solution (KBS) and cleaned of adhering connective tissue. The composition of KBS was (in mM): NaCl 117, KCl 5.36, $NaHCO_3$ 25.0, KH_2PO_4 1.03, $MgSO_4 \cdot 7H_2O$ 0.57, $CaCl_2 \cdot 2H_2O$ 2.5 and glucose 11.1. Eight tracheal ring segments (2 mm long) were obtained from each trachea and denuded of epithelium (Goldie *et al.*, 1986). Four preparations were used immediately and the remainder stored in KBS at 4°C and used within 3 h. Tracheal segments were suspended under a resting tension of 0.5 g and placed in organ baths containing 3 ml of KBS at 37°C, bubbled continuously with 5% CO_2 in O_2. Changes in isometric tension were measured with a Model 7D Polygraph via FTO3 force-displacement transducers (Grass Instruments). Tracheal segments were allowed to equilibrate for 45 min before exposure to the cumulative addition of 0.3 and 10 μM carbachol. Upon reaching contraction plateau the preparations were washed for 15 min with drug-free KBS.

Functional studies using tracheal segments

Concentration-effect curves to ET-1, carbachol, and KCl were constructed in the presence and absence of inhibitors of lipoxygenase (NDGA, phenidone, BW755C, eicosatetraynoic acid (ETYA)), cytochrome P_{450} (proadifen, metyrapone), Ca^{2+}- and Na^+-channels (verapamil, nicardipine, $NiCl_2$, amiloride), sarcoplasmic reticulum Ca^{2+}-ATPase (cyclopiazonic acid, thapsigargin) and protein kinase C (staurosporine). Unless otherwise stated, tracheal preparations were exposed for 20 min to an inhibitor or its solvent (paired control preparations) and then to cumulative additions of the spasmogens ET-1 (1–300 nM), carbachol (30 nM–100 μM) or KCl (15–90 mM). The Ca^{2+}-ATPase inhibitors induced transient contractions in these preparations (see below). Consequently, the pretreatment period of these drugs was extended to 30 min to allow the contraction to return to baseline levels of tone. In all experiments, only one concentration-effect curve was constructed on each preparation. Spasmogen-induced contractions were plotted as a percentage of the initial contraction produced by 10 μM carbachol (C_{max}) and the concentration of spasmogen producing 50%C_{max} was estimated by fitting the concentration-effect data to a logistic function using computer-assisted non-linear least squares regression analysis.

To determine the relative contribution of intracellular and extracellular Ca^{2+} to ET-1-induced contractions, contractile responses to 100 nM ET-1 were determined in nominally Ca^{2+}-free KBS (see Figure 3a for experimental protocol). In this series of experiments, preparations were washed four times during a 5 min period with Ca^{2+}-free KBS containing 10 μM EGTA and equilibrated for 20 min in Ca^{2+}-free KBS (without EGTA). Preparations were then exposed to 100 nM ET-1. When the ET-1-induced contraction had reached plateau, $CaCl_2$ was added to the bath at a final concentration of 2.5 mM and the subsequent contraction recorded until it had reached plateau. To establish the influence of NDGA and cyclopiazonic acid on these responses, preparations were incubated with 20 μM NDGA or 10 μM cyclopiazonic acid at the beginning of the 20 min equilibration period and for the remainder of the experiment (see Figure 3).

To determine the effect of NDGA on protein kinase C activity, concentration-effect curves to the protein kinase C activator, phorbol 12,13-dibutyrate were completed in the presence and absence of NDGA. Under conditions of basal tone, phorbol 12,13-dibutyrate-induced contractions were small (less than 15% C_{max} at 10 μM). It has been reported previously that phorbol ester-induced contractions can be markedly enhanced by pre-contracting the preparation with KCl (Menkes *et al.*, 1986; Huang *et al.*, 1987; Ozaki *et al.*, 1990). Thus, the effect of NDGA on phorbol 12,13-dibutyrate-induced contractions was determined in preparations pre-contracted with KCl to about 35% C_{max}. In all studies with phorbol 12,13-dibutyrate, concentration-effect curves to the inactive phorbol ester, 4α-phorbol 12,13-didecanoate (4α-Pdd), were concomitantly completed in paired preparations.

Autoradiography

The effects of NDGA on the binding of ET-1 to its receptor was investigated by use of quantitative autoradiography. Autoradiographs of [^{125}I]-ET-1 binding to rat tracheal sections were prepared as described previously (Henry *et al.*, 1990b). Each slide contained two tracheal sections (non-serial) from each of 4 rats. Slide-mounted tracheal sections were incubated with 0.5 nM [^{125}I]–ET-1 (specific activity; 674 Ci mmol^{-1}) in the presence of 10 μM NDGA or 1% ethanol (control). This concentration of [^{125}I]-ET-1 is close to the dissociation constant (K_d) of specific [^{125}I]-ET-1 binding determined previously in rat tracheal smooth muscle (0.43 nM; Henry *et al.*, 1990b). Non-specific binding was determined by use of 1 μM unlabelled ET-1 in the presence of 10 μM NDGA or vehicle (1% ethanol). Autoradiographic grain densities over the tracheal smooth muscle band were determined with an automated grain detection and counting system (Henry *et al.*, 1990a). Four separate fields (3 over smooth muscle and one background measurement over a non-tissue area) were viewed from each tracheal section and quadruplicate total and non-specific slides were analysed. Thus, a total of 512 fields were analysed [(4 fields per section) × (2 sections per rat trachea) × (4 rat tracheae per slide) × (4 slides per treatment) × (4 treatments)]. Autoradiographic grain densities were expressed as grains per 1000 μm^2 (grains 1000 μm^{-2}).

Drugs

Drugs used were; ET-1, ET-2, ET-3, [^{125}I]-ET-1, sarafotoxin S6c, BQ-123 (cyclo (D-Trp,D-Asp,L-Pro,D-Val,L-Leu); Auspep,

Melbourne, Australia), carbamylcholine chloride (carbachol), metyrapone, (±)-verapamil hydrochloride, nicardipine hydrochloride, amiloride hydrochloride, nordihydroguaiaretic acid (NDGA), phorbol 12,13-dibutyrate, 4α-phorbol 12,13 didecanoate (4α-Pdd), phenidone, cyclopiazonic acid, thapsigargin, ryanodine, TMB-8 (3,4,5-trimethoxybenzoic acid 8-(diethylamino)octyl ester), EGTA (Sigma Chemical Company, St. Louis, U.S.A.), eicosatetraynoic acid (ETYA, ICN Biomedicals, Sydney, Australia), staurosporine (Boehringer Mannheim), proadifen (SKF525A, SmithKline Beechams Laboratories), BW755C (3-amino-1-[*m*-(trifluoromethyl)-phenyl]-2-pyrazoline Wellcome Research Laboratories, UK). Staurosporine, phorbol esters, cyclopiazonic acid, thapsigargin and ETYA were dissolved in dimethylsulphoxide, and NDGA and metyrapone were dissolved in ethanol. All other drugs were made up in saline. Drugs were stored on ice and protected from light. In Ca^{2+}-free KBS, $CaCl_2$ was omitted.

Statistical analyses

In each preparation, contractile potency is expressed in terms of the concentration of drug required to produce 50% of the maximum response to 10 μM carbachol (50% C_{max}). Data are presented as mean [− log (concentration of drug producing 50% C_{max})] ± s.e.mean from n experiments (i.e. n different animals) and differences between treatment means assessed by analysis of variance followed by a modified t statistic (Wallenstein *et al.*, 1980). P values less than 0.05 were considered to be statistically significant.

Results

Functional studies

Selective inhibition of ET-1-induced contractions by NDGA As shown previously (Henry *et al.* 1990b; 1992), ET-1 was a potent spasmogen in rat isolated tracheal smooth muscle preparations (Figure 1a). The concentration of ET-1 required to induce a contraction of 50% C_{max} was 29 nM (95% confidence limits, 17–51 nM, $n = 6$). ET-1-induced contractions were concentration-dependently inhibited by NDGA (Figure 1a). For example, in the presence of 20 μM NDGA, the concentration of ET-1 required to induce a contraction of 50% C_{max} was 85 nM (95% confidence limits, 58–125 nM), 3 fold greater than in control preparations ($P < 0.01$). NDGA (20 μM) similarly inhibited contractions to ET-2 (concentration required to induce 50% C_{max} was 26 nM (13–52 nM) in the absence of NDGA versus 93 nM (36–240 nM) in the presence of NDGA; $n = 6$; $P < 0.05$) and to ET-3 (46 nM (34–62 nM) in the absence of NDGA versus 165 nM (105–265 nM) in the presence of NDGA; $n = 6$; $P < 0.05$). In contrast, 20 μM NDGA did not inhibit contractions to the ET_B receptor-selective agonist sarafotoxin S6c, the cholinoceptor agonist, carbachol or the depolarizing spasmogen, KCl (Figure 1).

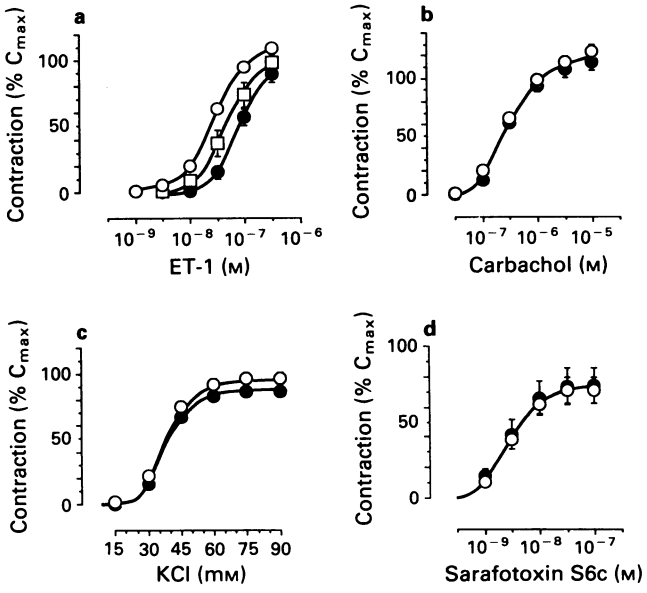

Figure 1 Mean concentration-effect curves to (a) ET-1, (b) carbachol, (c) KCl and (d) sarafotoxin S6c in the absence (○) or presence of NDGA (3 μM, □; 10 μM, △; 20 μM, ●) in rat isolated tracheal smooth muscle preparations. Note that the curve obtained to ET-1 in the presence of 10 μM NDGA is obscured by the curve obtained in the presence of 20 μM NDGA. Shown are the mean ± s.e.mean responses obtained from 5 or 6 separate experiments. For abbreviations, see text.

Despite the inhibitory effects of NDGA, ET-1-induced contractions were not inhibited by any of the other lipoxygenase inhibitors tested (phenidone, BW755C, ETYA) (Table 1). Furthermore, inhibitors of cytochrome P_{450} (proadifen, metyrapone), Ca^{2+}-channels ($NiCl_2$, verapamil, nicardipine) and Na^+ transport (amiloride) did not attenuate ET-1-induced contractions (Table 1).

Effects of NDGA on the time course of ET-1-induced contraction In addition to inhibiting the magnitude of the contractile response to ET-1, NDGA also changed the time course of contraction (Figure 2). In control preparations, contractile responses to 100 nM ET-1 were slow to develop (peak response of 91.3 ± 5.8% C_{max} after 20 min) and sustained (79.7 ± 5.1% C_{max} after 60 min). However, in the presence of NDGA, contractile responses to 100 nM ET-1 peaked earlier (53.3 ± 4.3% C_{max} after 10 min) and were not sustained (12.5 ± 4.1% C_{max} after 60 min) (Figure 2b). A similar effect was produced in the presence of the ET_A receptor antagonist, BQ-123 (peak response of 55.8 ± 5.0% C_{max} after 8 min reduced to 1.7 ± 2.2% C_{max} after 60 min) (Figure 2b). Indeed, in the presence of NDGA or BQ123, contractile responses to 100 nM ET-1 resembled the transient contractions induced by the ET_B receptor-selective agonist, sarafotoxin S6c (Figure 2c). In contrast, the ET_A receptor-mediated contractile responses to ET-1 in Ca^{2+}-free KBS were very slow to develop and sustained (Figure 2c).

Effect of NDGA on intracellular and extracellular Ca^{2+}-dependent contractions to ET-1 As shown previously (Henry, 1993), ET-1-induced contractions in rat isolated tracheal smooth muscle used both intracellular and extracellular Ca^{2+} (Figure 3). The intracellular Ca^{2+}-dependent contraction to 100 nM ET-1, produced in Ca^{2+}-free KBS, was significantly inhibited by 20 μM NDGA (53.5 ± 8.2% C_{max} versus 13.3 ± 3.5% C_{max} respectively, $n = 6$, $P < 0.01$). In contrast, the extracellular Ca^{2+}-dependent contraction to 100 nM ET-1, induced following the addition of 2.5 mM Ca^{2+}, was not inhibited by 20 μM NDGA (54.6 ± 5.8% C_{max} versus 56.0 ± 5.4% C_{max}, respectively). In additional experiments, the intracellular Ca^{2+}-dependent phase of contraction to 100 nM ET-1 (51.5 ± 3.9% C_{max}, $n = 6$) was significantly inhibited by TMB-8 (100 μM, 5.2 ± 0.9% C_{max}) and ryanodine (10 μM, 23.8 ± 3.7% C_{max}).

NDGA and modulators of intracellular Ca^{2+} Under conditions of basal tone, 10 μM ryanodine did not induce any contraction in rat tracheal smooth muscle preparations ($n = 5$). However, in preparations pre-contracted with KCl (concentration-range, 17.5–20 mM producing 10.6 ± 1.6% C_{max}, $n = 14$) 10 μM ryanodine induced an additional, slowly-developing contraction (36.7 ± 3.2% C_{max}, $n = 6$, Figure 4a). The ryanodine-induced contraction was markedly inhibited by both 10 μM and 20 μM NDGA (Figure 4).

The Ca^{2+}-ATPase inhibitor, cyclopiazonic acid, induced transient, concentration-dependent contractions of rat

Table 1 Effects of various drugs on the mean [− log (concentration of drug producing 50% C_{max})] for endothelin-1, carbachol and KCl in rat isolated trachea

Drug	*[Drug]* (μM)	*Endothelin-1*	*Endothelin-1 + drug*	*Carbachol*	*Carbachol + drug*	*KCl*	*KCl + drug*
Amiloride	10	7.50 ± 0.06	7.43 ± 0.07	6.63 ± 0.08	6.23 ± 0.10**	1.37 ± 0.07	1.22 ± 0.04*
Nickel chloride	330	7.63 ± 0.15	7.56 ± 0.14	6.48 ± 0.10	6.24 ± 0.10	1.35 ± 0.05	1.30 ± 0.08
Verapamil	10	7.61 ± 0.16	7.48 ± 0.12	6.60 ± 0.13	6.20 ± 0.12*	1.35 ± 0.05	NC[a]
Nicardipine	1	7.62 ± 0.15	7.38 ± 0.10	6.50 ± 0.10	6.24 ± 0.09	1.31 ± 0.03	NC[b]
NDGA	20	7.53 ± 0.09	7.07 ± 0.06**	6.64 ± 0.03	6.58 ± 0.03	1.57 ± 0.02	1.59 ± 0.02
Phenidone	100	7.67 ± 0.09	7.47 ± 0.08	6.89 ± 0.07	6.61 ± 0.10*	ND	ND
BW755C	50	7.71 ± 0.03	7.82 ± 0.19	6.47 ± 0.07	6.60 ± 0.10	ND	ND
ETYA	50	7.65 ± 0.17	7.59 ± 0.10	6.65 ± 0.07	6.66 ± 0.13	ND	ND
Proadifen	25	7.61 ± 0.15	7.67 ± 0.05	6.74 ± 0.04	5.70 ± 0.09***	ND	ND
Metyrapone	300	7.61 ± 0.15	7.52 ± 0.14	6.74 ± 0.04	6.47 ± 0.08**	ND	ND
Staurosporine	0.01	7.71 ± 0.03	7.32 ± 0.17*	6.47 ± 0.07	6.29 ± 0.08	ND	ND
	0.1	7.71 ± 0.03	7.10 ± 0.09***	6.47 ± 0.07	5.92 ± 0.14**	ND	ND

Each value is presented as the mean [− log (concentration of drug producing 50% C_{max})] ± s.e.mean and represents data obtained using preparations from each of 5 to 6 different animals.
*$P<0.05$, **$P<0.01$, ***$P<0.001$; indicate that in the presence of the drug, the mean [− log (concentration of drug producing 50% C_{max})] for the spasmogen were statistically different from than those values obtained in the absence of the drug.
ND; not determined. NC; not calculable because maximum response less than 50% C_{max}, NC[a]; maximum response to KCl was 19.5 ± 4.1% C_{max} in the presence of 10 μM verapamil, NC[b]; maximum response to KCl was 38.8 ± 5.5% C_{max} in the presence of 1 μM nicardipine.

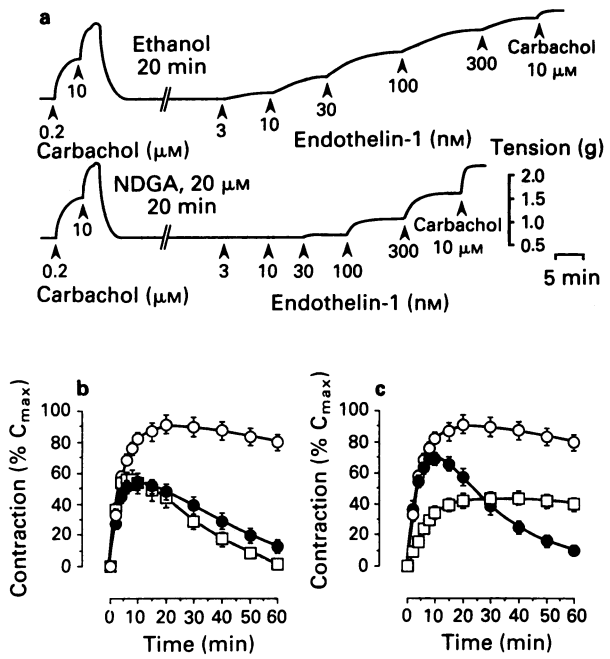

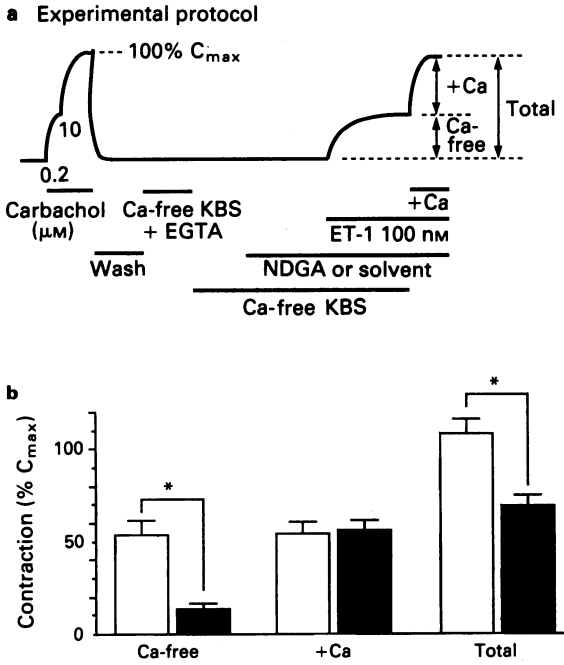

Figure 2 (a) Representative traces illustrating the effects of 20 μM NDGA on contractile responses of rat tracheal smooth muscle preparations to ET-1. In the presence of NDGA (lower trace) the contractile potency of ET-1 was reduced. Furthermore, the time required for each ET-1-induced contraction to reach plateau response was also reduced in the presence of NDGA. (b) Time course of contractions to 100 nM ET-1 in the absence (○) and presence of 20 μM NDGA (●) or the ET_A receptor-selective antagonist, BQ123 (10 μM, □). Shown are the mean ± s.e.mean of 6 experiments. (c) Time course of contractions to 100 nM ET-1 in normal (○) and Ca^{2+}-free (□) KBS and to the ET_B receptor-selective agonist, sarafotoxin S6c (●) in normal KBS. Shown are the mean ± s.e.mean responses of 6 experiments.

Figure 3 (a) Experimental protocol for experiments in Ca^{2+}-KBS (see Methods for details). (b) Contractile responses to 100 nM ET-1 produced in the absence (open columns) or presence of 20 μM NDGA (solid columns) in Ca^{2+}-free KBS ('Ca-free') and after the addition of 2.5 mM Ca^{2+} ('+ Ca'), according to the experimental protocol described in (a). The total contraction produced by 100 nM ET-1 (i.e. 'Ca-free' plus '+ Ca') is also presented ('Total'). Shown are the mean ± s.e.mean responses of 6 experiments.

isolated tracheal smooth muscle preparations (Figure 5a). Cyclopiazonic acid-induced contractions were not maintained and within 30 min of peak response, the contraction had usually returned to baseline levels of tone. The peak contractions induced by cyclopiazonic acid were markedly inhibited by 20 μM NDGA (Figure 5).

Contractions induced by ET-1 in preparations pretreated with 10 μM cyclopiazonic acid for 30 min were significantly attenuated compared to control contractions (Figure 6a). For example, in the presence of 10 μM cyclopiazonic acid, the concentration of ET-1 required to produce a 50% C_{max} contraction was 3.5 fold greater than in control preparations (1.2–10.4 fold, $n=6$, $P<0.05$). Experiments in Ca^{2+}-free KBS revealed that cyclopiazonic acid inhibited the intracellular Ca^{2+}-dependent phase of ET-1-induced contractions, but potentiated the extracellular Ca^{2+}-dependent phase of

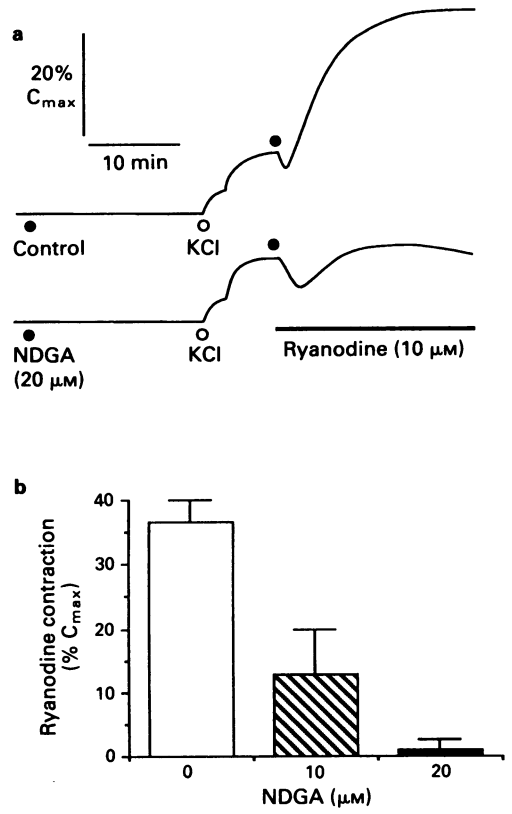

Figure 4 (a) Isometric tension recordings obtained simultaneously in paired rat tracheal smooth muscle preparations (precontracted with KCl) showing the contraction induced by ryanodine (control, upper trace) and its sensitivity to inhibition by 20 μM NDGA (lower trace). (b) Mean contractions induced by ryanodine in KCl-contracted preparations in the absence (open column, $n = 6$) and presence of 10 μM NDGA (hatched columns, $n = 4$) and 20 μM NDGA (solid columns, $n = 4$). Shown are the mean ± s.e.mean responses.

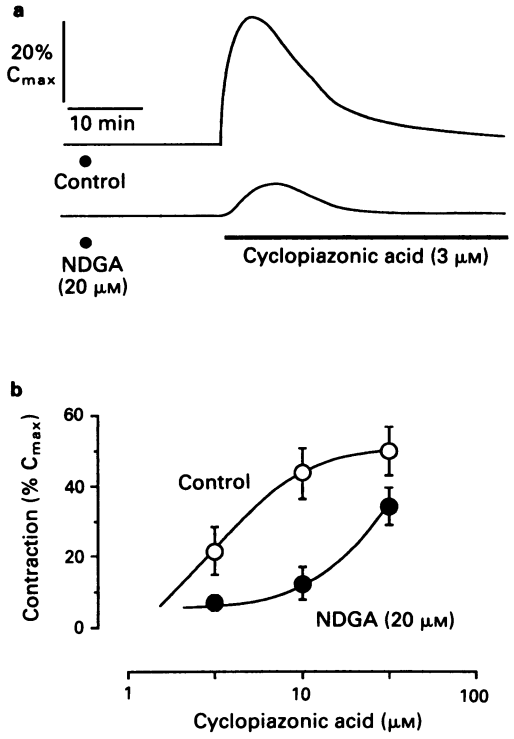

Figure 5 (a) Isometric tension recordings obtained simultaneously in paired rat tracheal smooth muscle preparations showing the transient contraction induced by cyclopiazonic acid (control, upper trace) and its sensitivity to inhibition by 20 μM NDGA (lower trace). (b) Mean concentration-effect curves to cyclopiazonic acid in the absence (○) and presence (●) of 20 μM NDGA. Contractions induced by cyclopiazonic acid were transient and hence cumulative concentration-effect curves were not performed. Each data point represents the mean (± s.e.mean) peak contractile response obtained to a single dose of cyclopiazonic acid (3, 10 or 30 μM) in 6–7 different preparations.

contraction (Figure 6b). Whereas cyclopiazonic acid inhibited contractile responses to ET-1, it was inclined to potentiate responses to carbachol (concentration required to produce 50% C_{max}; 165 nM (150–180 nM) in control preparations versus 90 nM (25–320 nM) in the presence of cyclopiazonic acid; $n = 3$, NS) and to KCl (39 mM (34–48 mM) in control preparations versus 31.5 mM (24–42 mM) in the presence of cyclopiazonic acid; $n = 3$, NS). Thapsigargin (3 μM), a structurally dissimilar inhibitor of Ca^{2+}-ATPase also inhibited contractions to ET-1 (3.1 (1.45–6.6) fold greater concentration of ET-1 required to produce 50% C_{max} in the presence of thapsigargin compared with control, $n = 7$, $P < 0.05$) but not those to carbachol ($n = 4$) or KCl ($n = 4$).

NDGA, ET-1 and protein kinase C ET-1-induced contractions were inhibited by the protein kinase C inhibitor staurosporine (Table 1). In the presence of 10 nM staurosporine, a 2.45 fold (1.1–5.6 fold, $n = 6$, $P < 0.05$) higher concentration of ET-1 was required to produce a 50% C_{max} contraction. This concentration of staurosporine had no significant inhibitory effect on contractile responses to carbachol (Table 1).

In rat isolated tracheal preparations precontracted with KCl (33.0 ± 2.1% C_{max}, $n = 10$), phorbol 12,13-dibutyrate induced concentration-dependent contractions (the concentration of phorbol 12,13-dibutyrate that induced a 50% C_{max} contraction, above the KCl-induced contraction, was 0.48 μM (0.062–3.7 μM) and the magnitude of contraction induced by 10 μM phorbol 12,13-dibutyrate was 66.0 ± 3.7% C_{max} above the KCl-induced contraction, $n = 5$). These phorbol 12,13-dibutyrate-induced contractions were not inhibited by 20 μM

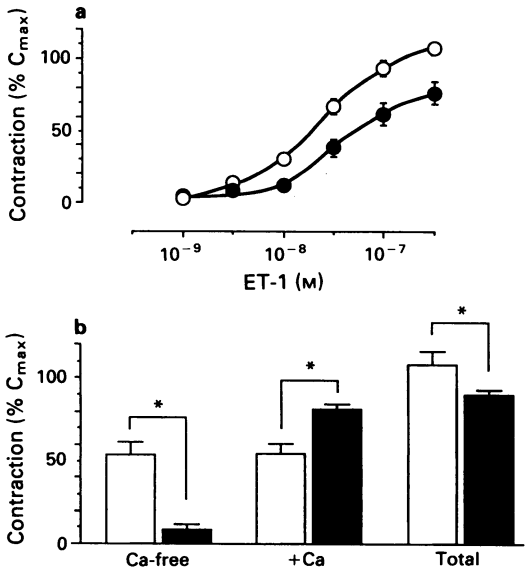

Figure 6 (a) Mean concentration-effect curves to ET-1 in the absence (○) or presence (●) of 10 μM cyclopiazonic acid. (b) Contractile responses to 100 nM ET-1 in the presence (solid columns) or absence (open columns) of 10 μM cyclopiazonic acid in Ca^{2+}-free KBS ('Ca-free') and after the addition of 2.5 mM Ca^{2+} ('+ Ca'), according to the experimental protocol described in Figure 3a (NDGA replaced by cyclopiazonic acid). The total contraction produced by 100 nM ET-1 (i.e. 'Ca-free' plus '+ Ca') is also presented ('Total'). The mean ± s.e.mean responses of 6 experiments is shown.

NDGA (in the presence of NDGA, the concentration of phorbol 12,13-dibutyrate that induced a 50% C_{max} contraction was 0.124 μM (0.021–0.75 μM) and the magnitude of contraction induced by 10 μM phorbol 12,13-dibutyrate was 71.2 ± 6.6% C_{max} above the KCl-induced contraction, $n = 5$). The inactive phorbol ester, 4α-phorbol didecanoate had no significant effect on KCl-induced tone in these preparations.

Effect of NDGA on guinea-pig isolated tracheal responses to ET-1 NDGA had no significant inhibitory effect on ET-1-induced contractions in epithelium-denuded, guinea-pig isolated tracheal preparations (concentration of ET-1 that produced 30% C_{max} was 14 nM (7.3–26 nM, $n = 5$) in control preparations and 16 nM (7.2–33 nM) in paired preparations exposed to 20 μM NDGA; the magnitude of contraction induced by 300 nM ET-1 was 56.1 ± 2.4% C_{max} in control preparations and 56.9 ± 2.3% C_{max} in preparations exposed to NDGA). Similarly, NDGA did not inhibit contractions induced by 10 μM ryanodine in KCl-contracted, guinea-pig isolated tracheal preparations (ryanodine-induced contractions; 60.7 ± 5.8% C_{max} and 59.3 ± 5.8% C_{max} in the absence and presence of 20 μM NDGA ($n = 7$), respectively). Furthermore, cyclopiazonic acid did not inhibit contractile responses to ET-1 in guinea-pig isolated tracheal preparations (concentration of ET-1 required to produce 30% C_{max}; 6.8 nM (1.8–25 nM, $n = 4$) in control preparations versus 6.1 nM (3.2–12 nM, $n = 4$) in the presence of 3.3 μM cyclopiazonic acid).

Quantitative autoradiography

In rat isolated tracheal sections incubated with 0.5 nM [^{125}I]-ET-1, light microscopic autoradiography revealed high densities of autoradiographic grains over the tracheal smooth muscle band. Over 90% of these autoradiographic grains were over specific [^{125}I]-ET-1 binding sites (total grain density, 331 ± 28 grains 1000 μm^{-2}; non-specific grain density, 26 ± 2 grains 1000 μm^{-2}; specific grain density, 305 ± 29 grains 1000 μm^{-2}, $n = 4$ rat trachea). NDGA (10 μM) had no significant effect on the density of autoradiographic grains over specific [^{125}I]-ET binding sites (312 ± 37 grains 1000 μm^{-2} in the presence of 10 μM NDGA versus 305 ± 29 grains 1000 μm^{-2} in the absence of NDGA, $n = 4$ rat trachea) or non-specific [^{125}I]-ET binding sites (32 ± 4 grains 1000 μm^{-2} in the presence of 10 μM NDGA versus 26 ± 2 grains 1000 μm^{-2} in the absence of NDGA, $n = 4$ rat trachea) in rat tracheal smooth muscle.

Discussion

NDGA and selective inhibition of the ET_A receptor-effector system

In rat tracheal smooth muscle, ET-1 can induce contractions by activating ET_A and/or ET_B receptor-effector systems (Henry, 1993). Thus, the findings in this study that NDGA inhibited the contractions induced by ET-1, but not those induced by the ET_B receptor selective agonist, sarafotoxin S6c, indicate that NDGA selectively attenuated the ET_A receptor-effector system. The marked similarities in the inhibitory effects of NDGA and the ET_A receptor-selective antagonist BQ-123 on the time-course of ET-1-induced contractions provides additional evidence that NDGA selectively inhibited the ET_A, but not the ET_B, receptor-effector system.

NDGA and BQ-123 inhibited ET-1-induced contractions in rat isolated tracheal smooth muscle. However, it is unlikely that NDGA acted as an ET_A-receptor antagonist because autoradiographic studies revealed that unlike BQ-123 (Henry, 1993), NDGA did not inhibit the binding of [^{125}I]-ET-1 to rat isolated tracheal smooth muscle in the current study. This is consistent with our previous studies showing that ET-1-induced accumulation of [^{3}H]-inositol phosphates in this tissue is inhibited by BQ-123 (Henry, 1993), but not by NDGA (Henry *et al.*, 1992). These latter findings agree with recent reports that NDGA (50–70 μM) did not inhibit phospholipase C activity in rat glomerular cells (Force *et al.*, 1991) or human T-lymphocytes (Mire-Sluis *et al.*, 1989). Thus, the site of action of NDGA in the ET_A receptor-effector system appears to be distal to ET_A receptor activation and the generation of inositol phosphates.

NDGA and modulators of intracellular Ca^{2+}

In rat tracheal smooth muscle, ET-1-induced contractions utilise intracellular and extracellular Ca^{2+} (Henry, 1993). The intracellular Ca^{2+}-dependent contractions induced by ET-1 in Ca^{2+}-free solution are mediated by ET_A receptors (Henry, 1993) and were inhibited in the current study by agents that deplete intracellular Ca^{2+} stores (ryanodine and cyclopiazonic acid) or that act as intracellular Ca^{2+} antagonists (TMB-8). Of particular interest was the finding that NDGA also selectively inhibited the intracellular Ca^{2+}-dependent component of ET-1-induced contraction.

One explanation for these findings is that NDGA inhibited the release of Ca^{2+} from intracellular stores such as the sarcoplasmic reticulum. Support for this explanation is provided by the findings that NDGA significantly inhibited contractions induced by both ryanodine and cyclopiazonic acid; contractions purportedly dependent upon Ca^{2+} release from the sarcoplasmic reticulum. Ryanodine is an agonist for the Ca^{2+}-release channel in the sarcoplasmic reticulum and thereby stimulates the release of Ca^{2+} from the sarcoplasmic reticulum, elevates cytosolic Ca^{2+} levels and may promote smooth muscle contraction (Low *et al.*, 1992; Missiaen *et al.*, 1992). The amount of Ca^{2+} in the sarcoplasmic reticulum is determined by a balance between the depletion of Ca^{2+} via passive outward leak or agonist-induced leak and the repletion of Ca^{2+} via the Ca^{2+}-ATPase pump (Low *et al.*, 1991). Thus, in the presence of a Ca^{2+}-ATPase inhibitor such as cyclopiazonic acid, the passive outward leak of sarcoplasmic reticular Ca^{2+} is not balanced by repletion of Ca^{2+} into the sarcoplasmic reticulum and the resultant rise in cytosolic Ca^{2+} levels initiates smooth muscle contraction (Groeger *et al.*, 1988; Seidler *et al.*, 1989; Shima & Blaustein, 1992). Hence, the inhibitory effects of NDGA on the contractions induced by ryanodine, cyclopiazonic acid and ET-1 may be explained by proposing that NDGA inhibited the release of Ca^{2+} from the sarcoplasmic reticulum and thereby prevented the rise in cytosolic Ca^{2+} levels that precedes contraction.

Little is presently known of the direct actions of NDGA on the release of Ca^{2+} from the sarcoplasmic reticulum, although NDGA has been shown to inhibit Ca^{2+}-channel activity in some cell systems. For example, in ArT-20 and GH_3 anterior pituitary cell lines, NDGA inhibited Ca^{2+}-channel activity by partitioning into the membrane and interacting either with the channel protein directly or with another membrane-bound Ca^{2+}-channel modulator, independently of actions on L-type Ca^{2+}-channels and of arachidonic acid metabolism (Korn & Horn, 1990). Thus, the findings in the current study that NDGA inhibited contractions to ryanodine and cyclopiazonic acid provides some evidence that NDGA may inhibit Ca^{2+} release from intracellular stores in rat isolated tracheal smooth muscle. Inhibition of agonist-induced Ca^{2+} mobilisation may likewise explain the attentuating actions of NDGA on ET-1-induced contractions.

An alternative, but less likely, explanation for the finding that NDGA inhibited the intracellular Ca^{2+}-dependent component of ET-1-induced contractions is that NDGA depleted the sarcoplasmic reticular stores of Ca^{2+}. With respect to this possibility, it is relevant to note that (a) NDGA has some structural resemblance to the sarcoplasmic reticulum Ca^{2+}-ATPase inhibitor, cyclopiazonic acid, an agent that depletes sarcoplasmic reticular stores of Ca^{2+} and (b) NDGA and

cyclopiazonic acid both inhibited ET-1-induced contractions. However, despite these similarities, many of the characteristic actions of Ca^{2+}-ATPase inhibitors were not exhibited by NDGA. For example, incubation with Ca^{2+}-ATPase inhibitors such as cyclopiazonic acid and the structurally unrelated agent thapsigargin, (a) induced marked transient contractions of tracheal smooth muscle preparations, (b) potentiated contractions induced by KCl and (c) potentiated the extracellular Ca^{2+}-dependent component of ET-1-induced contraction. Each of these effects is consistent with the actions of Ca^{2+}-ATPase inhibitors and have been previously explained on the basis that inhibition of Ca^{2+} uptake into the sarcoplasmic reticulum either reduces the buffering action that the sarcoplasmic reticulum normally exerts on rises in intracellular Ca^{2+} and/or enhances the plasma membrane permeability to Ca^{2+} (Mason *et al.*, 1991; Demaurex *et al.*, 1992; Shima & Blaustein, 1992; Shimamoto *et al.*, 1992). None of the actions was exhibited by NDGA and thus, on balance, it appears unlikely that NDGA inhibited ET-1-induced contractions by inhibiting sarcoplasmic reticulum Ca^{2+}-ATPase and depleting intracellular Ca^{2+} stores.

Recent studies report that ET-1-induced contractions in rat and guinea-pig tracheal smooth muscle involve, at least partly, stimulation of the phosphoinositide pathway and mobilisation of intracellular Ca^{2+} (Hay, 1990; Henry *et al.*, 1992). However, the findings in the current study that NDGA inhibited the contractile responses to ET-1 and ryanodine in the rat, but not the guinea-pig, indicate that significant differences exist between the species with respect to the mechanism of ET-1-induced contraction in airway smooth muscle. The reasons for these species differences are not yet clear. At present it is not known whether ET-1-induced contractions in human airway smooth muscle are affected by NDGA, although it is interesting to note that ET-1-induced contractions in human bronchial smooth muscle, like rat tracheal smooth muscle, appear to be dependent upon the mobilisation of intracellular Ca^{2+} stores (McKay *et al.*, 1991). Preliminary data from human vascular smooth muscle suggest that ET-1-induced contractions in some blood vessels (Resink *et al.*, 1989) although not all (Miyauchi *et al.*, 1990) may be susceptible to inhibition by NDGA.

Other possible mechanisms of NDGA action

Many other cellular processes involved in the regulation of smooth muscle tone can be modulated by NDGA and/or ET-1 including lipoxygenase, protein kinase C, guanylate cyclase, Na^+/H^+ exchange the L- and T-type Ca^{2+} channels. The possibility that NDGA may have inhibited ET-1-induced contraction via an action at one or other of these sites is addressed below.

The concentration-range for NDGA that selectively inhibited ET-1-induced contractions in the current study (3 to 20 μM) is similar to that routinely used to inhibit lipoxygenase activity. However, NDGA was the only lipoxygenase inhibitor tested that exerted any inhibitory effect on ET-1-induced contractions. Neither the acetylenic analogue of arachidonic acid, ETYA, nor lipoxygenase inhibitors having antioxidant activity (phenidone, BW755C) inhibited ET-1-induced contractions. Thus, it is unlikely that inhibition of lipoxygenase activity contributed significantly to the inhibitory effects of NDGA on ET-1-induced contractions.

The possibility that NDGA may have attenuated ET-1-induced contractions by inhibiting protein kinase C activity was examined in the light of a recent report that NDGA inhibited protein kinase C activity in cell cultures (Rondeau *et al.*, 1990) and that in airway smooth muscle cells ET-1 stimulates the generation of diacylglycerol, the proposed endogenous activator of protein kinase C (Mattoli *et al.*, 1991). Evidence supporting the involvement of protein kinase C in the spasmogenic actions of ET-1 in rat isolated tracheal smooth muscle is provided by the findings in this study that an inhibitor of protein kinase C, staurosporine, attenuated ET-1-induced contractions in this tissue. However, it should be noted that staurosporine is not a specific inhibitor of protein kinase C (Ruegg & Burgess, 1989) and that activation of protein kinase C by ET-1 remains to be shown using more direct methods. Nevertheless, it is unlikely that inhibition of protein kinase C activity contributed significantly to the inhibitory effects of NDGA on ET-1-induced contractions since NDGA had no inhibitory effects on contractions induced by a direct activator of protein kinase C such as phorbol 12, 13 dibutyrate in this preparation.

Activation of soluble guanylate cyclase, by agents such as nitric oxide, can inhibit the development of spasmogen-induced contraction in smooth muscle. Thus, although NDGA has previously been shown to attenuate guanylate cyclase activity (Clark & Linden, 1986) inhibition of guanylate cyclase by NDGA cannot explain the inhibitory effects of NDGA on the development of ET-1-induced contractions observed in rat tracheal smooth muscle.

Activation of the Na^+/H^+ exchanger has been implicated in ET-1-induced contractions in airway smooth muscle (Battistini *et al.*, 1991). At present the role of the Na^+/H^+ exchanger in ET-1-induced contractions and its susceptibility to inhibition by NDGA in rat tracheal smooth muscle is not known. However, it is unlikely that inhibition of the Na^+/H^+ exchanger can account for the inhibitory effects of NDGA on ET-1-induced contraction observed in the current study. For example, the findings that ET-1-induced contractions in guinea-pig tracheal smooth muscle are attenuated by inhibitors of the Na^+/H^+ exchanger (Battistini *et al.*, 1991), but not by NDGA (current study) suggest that NDGA does not inhibit the Na^+/H^+ exchanger in guinea-pig tracheal smooth muscle. These findings, together with those showing that ET-1-induced contractions in rat trachea were not inhibited by amiloride are not compatible with NDGA-induced inhibition of the Na^+/H^+ exchanger.

Finally, the findings that NDGA, but not inhibitors of L- and T-type Ca^{2+}-channels, inhibited ET-1-induced contractions is entirely consistent with the view that these Ca^{2+}-channels play no significant role in ET-1-induced contraction of rat tracheal smooth muscle (Turner *et al.*, 1989; Henry, 1993) and moreover that NDGA-induced inhibition of contractions to ET-1 in this preparation occur independently of plasmalemma Ca^{2+} channels.

NDGA and the time-course of ET-1-induced contractions

ET-1-induced contractions in vascular and airway smooth muscle are characteristically slow to develop, sustained and resistant to reversal by washout. Thus, it was of particular interest to find that NDGA significantly altered the time-course of ET-1-induced contractions; in the presence of NDGA, ET-1-induced contractions reached peak response more quickly and were not sustained. Subsequent experiments revealed that qualitatively similar effects on ET-1-induced contractions were produced by the ET_A receptor antagonist, BQ-123. Furthermore, the transient contractions induced by ET-1 in the presence of NDGA or BQ-123 closely resemble those induced by the ET_B receptor agonist, sarafotoxin S6c. The simplest interpretation of these findings is that stimulation of the ET_A and ET_B receptor-effector systems induce contractions with different temporal profiles. Stimulation of ET_A receptors induces a contraction that develops slowly and is sustained whereas stimulation of ET_B receptors induces a contraction that develops relatively quickly but is not sustained. Thus, by selectively inhibiting the slowly developing contraction induced by the ET_A receptor-effector system, NDGA and BQ-123 transformed the characteristically slow and sustained contraction of ET-1 into a transient contraction similar to that induced by the ET_B receptor-selective agonist, sarafotoxin S6c. At present it is not clear which events in the ET_A receptor effector system cause the slowly developing phase of contraction. However, it is of interest to note that ryanodine-induced contractions, which

were inhibited by NDGA, also developed very slowly in this preparation. Furthermore, the findings in the current study that NDGA inhibits ET-1-induced contractions via an action at the level of intracellular Ca^{2+}-mobilisation concur with the proposal of Marsault and coworkers (1991) that the rate limiting step for the contractile action of ET-1 is a post-receptor event distal to the early changes in intracellular Ca^{2+} levels.

Conclusions

In summary, the major finding of this study in rat isolated tracheal smooth muscle is that NDGA dose-dependently attenuates ET-1-induced contractions by selectively inhibiting the ET_A receptor-effector system, probably at the level of intracellular Ca^{2+} mobilisation. These effects do not involve an action of NDGA on arachidonic acid metabolism, ET receptors, inositol phosphate generation, protein kinase C, L- or T-type Ca^{2+}-channels or the ET_B receptor-effector pathway. As a further consequence of inhibiting the ET_A receptor-effector system, NDGA converts the ET-1-induced contraction from the characteristically slowly developing and sustained contraction into a transient contraction resembling that induced by the ET_B receptor agonist, sarafotoxin S6c.

This research was supported by grants from the National Health and Medical Research Council of Australia and the Child Health Research Foundation of Western Australia. The author would like to acknowledge Assoc. Prof. R.G. Goldie for helpful and constructive discussion during the preparation of this manuscript.

References

ADVENIER, C., SARRIA, B., NALINE, E., PUYBASSET, L. & LAGENTE, V. (1990). Contractile activity of three endothelins (ET-1, ET-2 and ET-3) on the human isolated bronchus. *Br. J. Pharmacol.*, **100**, 168–172.

BATTISTINI, B., FILEP, J.G., CRAGOE, E.J., FOURNIER, A. & SIROIS, P. (1991). A role for Na^+/H^+ exchange in contraction of guinea pig airways by endothelin-1 in vitro. *Biochem. Biophys. Res. Commun.*, **175**, 583–588.

CHAND, N., DIAMANTIS, W. & DUANE SOFIA, R. (1990). Pharmacologic modulation of endothelin-induced contraction in isolated rat tracheal segments. *Res. Commun. Chem. Pathol. Pharmacol.*, **70**, 173–181.

CLARK, D.L. & LINDEN, J. (1986). Modulation of guanylate cyclase by lipoxygenase inhibitors. *Hypertension*, **8**, 947–950.

DEMAUREX, N., LEW, D.P. & KRAUSE, K.-H. (1992). Cyclopiazonic acid depletes intracellular Ca^{2+} stores and activates an influx pathway for divalent cations in HL-60 cells. *J. Biol. Chem.*, **267**, 2318–2324.

FORCE, T., HYMAN, G., HAJJAR, R., SELLMAYER, A. & BONVENTRE, J.V. (1991). Noncyclooxygenase metabolites of arachidonic acid amplify the vasopressin-induced Ca^{2+} signal in glomerular mesangial cells by releasing Ca^{2+} from intracellular stores. *J. Biol. Chem.*, **266**, 4295–4302.

GOLDIE, R.G., PAPADIMITRIOU, J.M., PATERSON, J.W., RIGBY, P.J., SELF, H.M. & SPINA, D. (1986). Influence of the epithelium on responsiveness of guinea-pig isolated trachea to contractile and relaxant agonists. *Br. J. Pharmacol.*, **87**, 5–14.

GROEGER, D.E., RILEY, R.T., DORNER, J.W. & COLE, R.J. (1988). Cyclopiazonic acid inhibition of the Ca^{2+}-transport ATPase in rat skeletal muscle sarcoplasmic reticulum vesicles. *Biochem. Pharmacol.*, **37**, 978–981.

HAY, D.W.P. (1990). Mechanism of endothelin-induced contraction in guinea-pig trachea: comparison with rat aorta. *Br. J. Pharmacol.*, **100**, 383–392.

HAY, D.W.P. (1992). Pharmacological evidence for distinct endothelin receptors in guinea-pig bronchus and aorta. *Br. J. Pharmacol.*, **106**, 759–761.

HENRY, P.J. (1993). Endothelin-1 (ET-1) contractions in rat trachea: involvement of ET_A and ET_B receptors, and multiple signal transduction systems. *Br. J. Pharmacol.*, **110**, 435–441.

HENRY, P.J., RIGBY, P.J. & GOLDIE, R.G. (1990a). Distribution of β_1- and β_2-adrenoceptors in mouse trachea and lung: a quantitative autoradiographic study. *Br. J. Pharmacol.*, **99**, 136–144.

HENRY, P.J., RIGBY, P.J., SELF, G.J., PREUSS, J.M. & GOLDIE, R.G. (1990b). Relationship between endothelin-1 binding site densities and constrictor activities in human and animal airway smooth muscle. *Br. J. Pharmacol.*, **100**, 786–792.

HENRY, P.J., RIGBY, P.J., SELF, G.J., PREUSS, J.M. & GOLDIE, R.G. (1992). Endothelin-1-induced [^{3}H]-inositol phosphate accumulation in rat trachea. *Br. J. Pharmacol.*, **105**, 135–141.

HUANG, C.K., MUNAKATA, M., BARABAN, J.M. & MENKES, H. (1987). Protein kinase C and tracheal contraction at low temperature. *J. Pharmacol. Exp. Ther.*, **243**, 270–280.

KORN, S.J. & HORN, R. (1990). Nordihydroguaiaretic acid inhibits voltage-activated Ca^{2+} current independently of lipoxygenase inhibition. *Mol. Pharmacol.*, **38**, 524–530.

LOW, A.M., GASPAR, V., KWAN, C.Y., DARBY, P.J., BOURREAU, J.P. & DANIEL, E.E. (1991). Thapsigargin inhibits repletion of phenylephrine-sensitive intracellular Ca^{2+} pool in vascular smooth muscle. *J. Pharmacol. Exp. Ther.*, **258**, 1105–1113.

LOW, A.M., KWAN, C.Y. & DANIEL, E.E. (1992). Evidence for two types of internal Ca^{2+} stores in canine mesenteric artery with different refilling mechanisms. *Am. J. Physiol.*, **262**, H31–H37.

MARSAULT, R., VIGNE, P., BREITTMAYER, J.P. & FRELIN, C. (1991). Kinetics of vasoconstrictor action of endothelins. *Am. J. Physiol.*, **261**, C986–C993.

MASON, M.J., GARCIA-RODRIGUEZ, C. & GRINSTEIN, S. (1991). Coupling between intracellular Ca^{2+} stores and the Ca^{2+} permeability of the plasma membrane. *J. Biol. Chem.*, **266**, 20856–20862.

MATTOLI, S., SOLOPERTO, M., MEZZETTI, M. & FASOLI, A. (1991). Mechanisms of calcium mobilization and phosphoinositide hydrolysis in human bronchial smooth muscle cells by endothelin-1. *Am. J. Respir. Cell Mol. Biol.*, **5**, 424–430.

MCKAY, K.O., BLACK, J.L. & ARMOUR, C.L. (1991). The mechanism of action of endothelin in human lung. *Br. J. Pharmacol.*, **102**, 422–428.

MENKES, H., BARABAN, J.M. & SNYDER, S.H. (1986). Protein kinase C regulates smooth muscle tension in guinea-pig trachea and ileum. *Eur. J. Pharmacol.*, **122**, 19–27.

MIRE-SLUIS, A.R., COX, C.A., HOFFBRAND, A.V. & WICKREMASINGE, R.G. (1989). Inhibitors of arachidonic acid lipoxygenase inhibit the stimulation of inositol phospholipid hydrolysis by the T lymphocyte mitogen phytohaemagglutinin. *FEBS Lett.*, **258**, 84–88.

MISSIAEN, L., DE SMEDT, H., DROOGMANS, G., HIMPENS, B. & CASTEELS, R. (1992). Calcium ion homeostasis in smooth muscle. *Pharmacol. Ther.*, **56**, 191–231.

MIYAUCHI, T., TOMOBE, Y., SHIBA, R., ISHIKAWA, T., YANAGISAWA, M., KIMURA, S., SUGISHITA, Y., ITO, I., GOTO, K. & MASAKI, T. (1990). Involvement of endothelin in the regulation of human vascular tonus; potent vasoconstrictor effect and existence in endothelial cells. *Circulation*, **81**, 1874–1880.

NOGUCHI, K., ISHIKAWA, K., YANO, M., AHMED, A., CORTES, A., HALLMON, J. & ABRAHAM, W.M. (1992). An endothelin (ET_A) receptor antagonist, BQ123, blocks ET-1 induced bronchoconstriction and tracheal smooth muscle (TSM) contraction in allergic sheep. *Am. Rev. Respir. Dis.*, **145**, A858.

OZAKI, H., KWON, S.-C., TAJIMA, M. & KARAKI, H. (1900). Changes in cytosolic Ca^{2+} and contraction induced by various stimulants and relaxants in canine tracheal smooth muscle. *Pflügers Arch.*, **416**, 351–359.

RESINK, T.J., SCOTT-BURDEN, T. & BUHLER, F.R. (1989). Activation of phospholipaseA_2 by endothelin in cultured vascular smooth muscle cells. *Biochem. Biophys. Res. Commun.*, **158**, 279–286.

RONDEAU, E., GUIDET, B., LACAVE, R., BENS, M., SRAER, J., NAGAMINE, Y., ARDALLOU, R. & SRAER, J.D. (1990). Nordihydroguaiaretic acid inhibits urokinase synthesis by phorbol myristate acetate-stimulated LLC-PK1 cells. *Biochim. Biophys. Acta.*, **1055**, 165–172.

RUEGG, U.T. & BURGESS, G.M. (1989). Staurosporine, K-252 and UCN-01: potent but nonspecific inhibitors of protein kinases. *Trends Pharmacol. Sci.*, **10**, 218–220.

SEIDLER, N.W., JONA, I., VEGH, M. & MARTONOSI, A. (1989). Cyclopiazonic acid is a specific inhibitor of the Ca^{2+}-ATPase of sarcoplasmic reticulum. *J. Biol. Chem.*, **264**, 17816–17823.

SHIMA, H. & BLAUSTEIN, M.P. (1992). Modulation of evoked contractions in rat arteries by ryanodine, thapsigargin, and cyclopiazonic acid. *Circ. Res.*, **70**, 968–977.

SHIMAMOTO, H., KWAN, C.-Y. & DANIEL, E.E. (1992). Pharmacological assessment of Ca^{2+}-dependence of endothelin-induced response in rat aorta. *Eur. J. Pharmacol.*, **216**, 225–233.

SPRINGALL, D.R., HOWARTH, P.H., COUNIHAN, H., DJUKANOVIC, R., HOLGATE, S.T. & POLAK, J.M. (1991). Endothelin immunoreactivity of airway epithelium in asthmatic patients. *Lancet*, **337**, 697–701.

TURNER, N.C., POWER, R.F., POLAK, J.M., BLOOM, S.R. & DOLLERY, C.T. (1989). Endothelin-induced contractions of tracheal smooth muscle and identification of specific endothelin binding sites in the trachea of the rat. *Br. J. Pharmacol.*, **98**, 361–366.

UCHIDA, Y., NINOMIYA, H., SAOTOME, M., NOMURA, A., OHTSUKA, M., YANAGISAWA, A., GOTO, K., MASAKI, T. & HASEGAWA, S. (1988). Endothelin, a novel vasoconstrictor, as potent bronchoconstrictor. *Eur. J. Pharmacol.*, **154**, 227–228.

WALLENSTEIN, S., ZUCKER, C.L. & FLEISS, J.L. (1980). Some statistical methods useful in circulation research. *Circ. Res.*, **47**, 1–9.

(Received May 17, 1993
Revised September 29, 1993
Accepted October 7, 1993)

Br. J. Pharmacol. (1994), **111**, 570–574

Characterization of the tachykinin NK_2 receptor in the human bronchus: influence of amastatin-sensitive metabolic pathways

[1]Mara Astolfi, *Stefano Treggiari, †Antonio Giachetti, †Stefania Meini, †Carlo Alberto Maggi & Stefano Manzini

Pharmacology Departments, Menarini Ricerche Sud, Pomezia, Rome, Italy and †A. Menarini Pharmaceuticals, Florence, Italy, *Department of Thoracic Surgery, Forlanini Hospital, Rome, Italy

1 The aim of this study was to characterize the tachykinin NK_2 receptor subtype mediating the spasmogenic response in the human isolated bronchus. The motor response to neurokinin A (NKA) and the selective NK_2 agonist [βAla^8]NKA(4–10), as well as the antagonistic effects of cyclic (L659,877) and linear (MEN 10376) peptide NK_2 antagonists were assessed in the presence or absence of amastatin (an inhibitor of aminopeptidases A and M).

2 NKA was more potent than [βAla^8]NKA(4–10) in eliciting bronchoconstriction (pD_2 being 7,43 and 6,87 respectively). In the presence of amastatin (1 μM), the estimated affinity of [βAla^8]NKA(4–10), but not that of NKA, was significantly increased to yield a pD_2 of 7,44.

3 L659,877 and MEN 10376 inhibited [βAla^8]NKA(4–10)-induced contraction with similar affinities; pA_2 values were 5.7 ± 0.22 and 6.3 ± 0.32, respectively. Amastatin (1 μM) increased the potency of MEN 10376 to 7.28 ± 0.46, whereas that of L659,877 was unaffected.

4 In the presence of amastatin the pseudopeptide MDL 28,564 behaved as a partial agonist.

5 We conclude that the NK_2 receptor subtype present in the human bronchus has properties similar to those described for the circular muscle of the human colon and thus may be classified as a 'NK_{2A}' subtype. We show that the apparent potency of peptides, bearing N-terminal acidic residues, is influenced by an amastatin-sensitive peptidase, possibly aminopeptidase A.

Keywords: Human bronchus; amastatin; NK_2 receptor; tachykinins; aminopeptidases; tachykinin antagonists

Introduction

Tachykinin-containing sensory nerves are present in the human airways (Lundberg *et al.*, 1984; Martling *et al.*, 1987; Komatsu *et al.*, 1991). In human bronchial smooth muscle, natural tachykinins (TKs) (substance P, neurokinin A, neurokinin B) act as potent inducers of mucus secretion (Rogers *et al.*, 1989) and smooth muscle contraction (Advenier *et al.*, 1987; Honda *et al.*, 1991). Previous studies have clearly identified the NK_2 receptor as responsible for the TK-induced bronchoconstriction (Naline *et al.*, 1989; Dion *et al.*, 1990a; Rhoden & Barnes, 1990). The spasmogenic effects elicited by TKs in various human tissues such as urinary bladder (Dion *et al.*, 1990a), urethra (Parlani *et al.*, 1990) and circular muscle of colon (Giuliani *et al.*, 1991) and ileum (Maggi *et al.*, 1992) are also mediated by the NK_2 receptor. Recent findings have suggested that the NK_2 receptor might be heterogeneous and that at least two subtypes (termed NK_{2A} and NK_{2B}) may exist (Ireland *et al.*, 1991; Van Giersbergen *et al.*, 1991; Patacchini *et al.*, 1991). One of the criteria for such classification is the reverse order of potency between a cyclic peptide (L659,877) and a linear peptide (MEN 10376) in antagonizing the two receptor subtypes (Patacchini *et al.*, 1991). Results obtained so far on human isolated bronchus are contradictory as they do not clearly identify the NK_2 receptor subtype subserving contractility (Rhoden & Barnes, 1990; Dion *et al.*, 1990a; Ellis & Undem, 1992).

Since pharmacological receptor classification is mainly based on the rank order of potency of antagonists, it is important to control tissue enzymatic activities which may influence the response to these peptides (Devillier *et al.*, 1988; Patacchini *et al.*, 1989). Several TK degrading enzymes (namely neutral endopeptidase 24.11 and angiotensin converting enzyme (ACE)) have been described in human airways (Honda *et al.*, 1991; Cheung *et al.*, 1992). For this reason, ACE and endopeptidase 24.11 inhibitors have been commonly used in studies aiming to classify tachykinin receptors. Recently, however, we discovered that amastatin, a potent inhibitor of aminopeptidases (Rich *et al.*, 1984), can significantly affect the estimate of potency of linear peptide NK_2 receptor antagonists (Patacchini & Maggi, 1993; Giuliani *et al.*, 1993). In particular, experiments in the human isolated urinary bladder have shown that addition of amastatin enhances the antagonist potency of MEN 10376, providing a pattern indicative of the existence of NK_{2A} receptor at this level.

The aim of this study was to characterize the NK_2 receptor subtype mediating spasmogenic response to TKs in the human bronchus, by comparing the antagonistic properties of L659,877 and MEN 10376 in the presence or absence of amastatin. We show that, after blockade of the amastatin-sensitive enzymatic activity, this receptor can be pharmacologically classified as belonging to the NK_{2A} subtype.

Methods

Human bronchial tissues, obtained from 17 patients (14 men and 3 women) undergoing surgery for lung cancer, were immediately placed in cold oxygenated Krebs solution of the following composition (mM): NaCl 119, $NaHCO_3$ 25, glucose 11, KCl 4.7, $MgSO_4$ 1.5, KH_2PO_4 1.2 and $CaCl_2$ 2.5. From each specimen, several (4–8) bronchial rings of 3–5 mm internal diameter were cut as far as possible from the malignancy and kept at 4°C until the beginning of the experiments (within 1 h after the resection). The epithelium was gently removed by rubbing the luminal surface with a cotton swab. The preparations were allowed to equilibrate for 1 h in 5 ml organ baths containing Krebs solution maintained at 37°C

[1] Author for correspondence at: Pharmacology Department, Menarini Ricerche Sud, Via Tito Speri 10, 00040 Pomezia, Rome, Italy.

and replaced every 15 min. All the experiments were performed in the presence of indomethacin 5 μM and a mixture of peptidase inhibitors (thiorphan, captopril and bestatin, 1 μM each). In some experiments the effect of the aminopeptidase inhibitor amastatin (1 μM, contact time 1 h) was also investigated. Contractions were recorded isometrically under a resting tension of 1–2 g depending on the diameter. After the equilibration period, the rings were challenged with acetylcholine (1 mM) 2–3 times until reproducible responses were obtained. At this time atropine, diphenhydramine and propranolol (1 μM each) were added to the medium. Cumulative concentration-response curves to NKA, [βAla^8]NKA (4–10) and MDL 28,564 were constructed, the next concentration being added when the effect of the preceding one had reached a steady state. The antagonists (30 min contact time) were challenged with [βAla^8]NKA(4–10). Rings obtained from the same bronchial specimen were used to evaluate the motor effect of [βAla^8]NKA(4–10) in the absence or presence of various concentrations of the antagonist(s). Only one concentration-response curve was recorded for each ring. All values are expressed as mean ± s.e.mean. Statistical analysis was performed by Student's t test for unpaired data; P values lower than 0.05 were considered significant. pD_2 values for NKA and [βAla^8]NKA(4–10) were calculated as the negative log of the peptide concentration that caused 50% of the maximal effect. For each antagonist, at least three experiments at 3–4 different concentrations were performed on bronchial rings from four patients. The pA_2 values and slopes were determined by regression analysis of Schild plots by use of a computer programme for Apple II (Tallarida & Murray, 1981).

Drugs

Drugs used were: thiorphan, captopril, bestatin, amastatin, indomethacin, (±)-propranolol HCl, diphenhydramine HCl (Sigma), atropine sulphate monohydrate (Fluka), acetylcholine chloride (Serva), neurokinin A (Peninsula), L659,877 (Cambridge Research Biochemicals). [βAla^8]NKA(4–10) and MEN 10376 were synthetized in the Chemistry Department, A. Menarini Pharmaceuticals, Florence, Italy by conventional solid-phase method. MDL 28,564 was provided by Dr S.H. Buck, Marion Merrell Dow, Cincinnati, U.S.A.

Results

Effect of NK_2 receptor agonists and their blockade by L659,877 and MEN 10376, in the absence of amastatin

These experiments were carried out in the presence of indomethacin (5 μM), propranolol (1 μM), atropine (1 μM), diphenhydramine (1 μM) and inhibitors of aminopeptidases B and M (bestatin 1 μM), ACE (captopril, 1 μM) and neutral endopeptidase 24.11 (thiorphan 1 μM). Under these conditions human bronchial rings were quiescent; administration of neurokinin A (1 nM–3 μM) or of [βAla^8]NKA(4–10) (1 nM–30 μM) elicited a marked, concentration-dependent motor response (Figure 1). NKA had a pD_2 significantly ($P<0.05$) higher than that of [βAla^8]NKA(4–10) (Table 1). In addition, contractions induced by NKA were more prompt in their onset and the time to reach a steady-state averaged 6–7 min, while those elicited by [βAla^8]NKA(4–10) were slower (10–15 min). Both L659,877 (3, 10 and 20 μM) and MEN 10376 (1, 3 and 10 μM) exerted a rather weak competitive antagonism of [βAla^8]NKA(4–10); the concentration-response curves exhibited very similar pA_2 values (Table 2) and the slopes of the Schild plots were not significantly different from unity: −1.21 ± 0.49 for MEN 10376 and −1.32 ± 0.28 for L659,877.

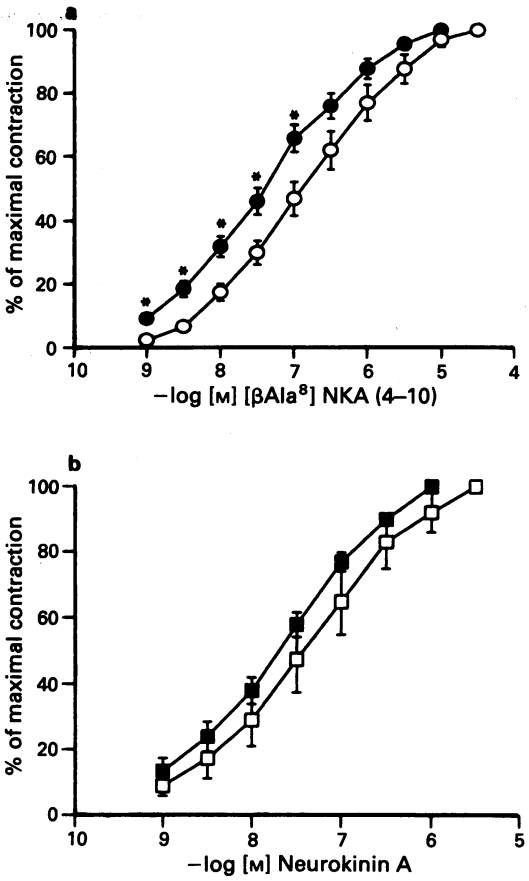

Figure 1 Concentration-response curves to (a) [βAla^8]NKA(4–10) (circles) and (b) neurokinin A (squares) in the presence (filled symbols) or absence (open symbols) of amastatin (1 μM, 1 h incubation time) in the human isolated bronchi. Each value is the mean ± s.e. mean of at least seven experiments. *$P<0.01$; Student's t test for unpaired data.

Table 1 Influence of amastatin on pD_2 values of neurokinin A and [βAla^8]NKA(4–10) in human isolated bronchi

	pD_2 values	
Agonist	*Without amastatin*	*With amastatin*
NKA	7.43 (7.38–7.48)	7.73 (7.58–7.87)
[βAla^8]NKA(4–10)	6.87 (6.83–6.91)*	7.44 (7.27–7.61)**

Each value is mean of at least six experiments. In parentheses are 95% confidence limits.
*$P<0.05$, significantly different from the value obtained with NKA (t test for unpaired data).
**$P<0.02$, significantly different from the value obtained in the absence of amastatin (t test for unpaired data).

Table 2 Influence of amastatin on pA_2 values of L659,877 and MEN 10376 in human isolated bronchi

	pA_2 values	
Antagonist	*Without amastatin*	*With amastatin*
L659,877	5.70 ± 0.22	5.69 ± 0.25
MEN 10376	6.30 ± 0.32	7.28 ± 0.46*

Each value is mean ± s.e.mean of at least nine experiments.
*$P<0.02$, significantly different from the value obtained in the absence of amastatin (t test for unpaired data).

Effect of NK_2 receptor agonists and their blockade by L659,877 and MEN 10376, in the presence of amastatin

These experiments were performed in the presence of the cocktail of antagonists and enzyme inhibitors described above, with the addition of the aminopeptidases inhibitor, amastatin (1 μM). The presence of amastatin did not modify the concentration-response curve to NKA, while that of [βAla^8]NKA(4–10) was shifted to the left (Figure 1). The pD_2 of the latter peptide increased significantly from 6.87 to 7.44 ($P<0.02$) (Table 1), and also the onset of contractions was more rapid, each concentration reaching a steady state within 8–9 min. Amastatin did not modify the antagonistic properties of the cyclic peptide L659,877 (Table 2). On the other hand, the affinity of the linear peptide MEN 10376 was enhanced significantly ($P<0.02$); its pA_2 increased from 6.3 ± 0.32 (slope − 1.21 ± 0.49) to 7.28 ± 0.46 (slope − 0.85 ± 0.28) in the absence or presence of amastatin, respectively (Figure 2 and Table 2). The nature of the antagonism exerted by both peptides was competitive as indicated by the slopes of the Schild plots (Figure 2).

In the presence of amastatin, the pseudopeptide MDL 28,564 (0.1 μM–30 μM) behaved as a partial agonist (Figure 3). Its maximal effect (measured as % of the maximal contraction elicited by acetylcholine 1 mM) was 63 ± 8% as compared to 166 ± 33% and 103 ± 8% obtained with NKA and [βAla^8]NKA(4–10), respectively.

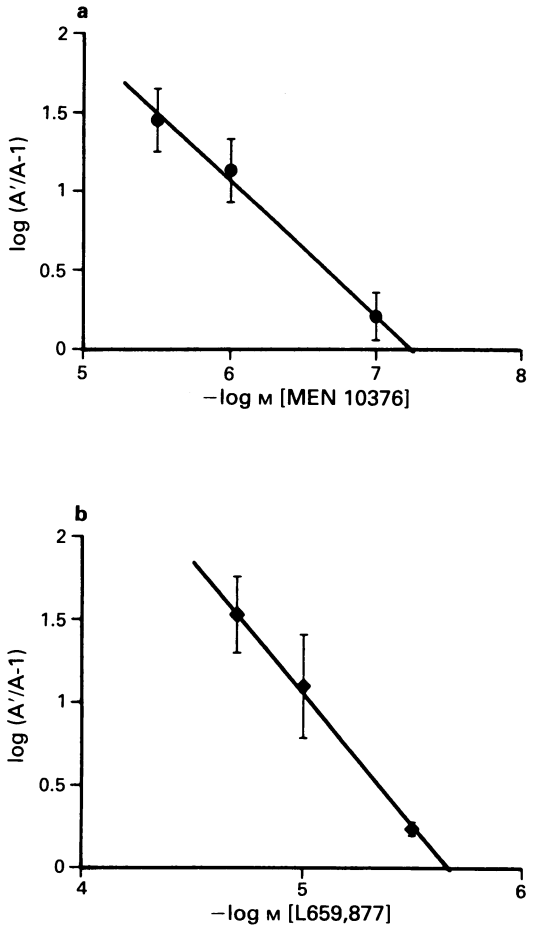

Figure 2 Schild plots relative to the antagonism of the contractile responses to [βAla^8]NKA(4–10) in the human isolated bronchi by MEN 10376 (a, $pA_2 = 7.28 \pm 0.46$; slope = − 0.85 ± 0.28) and L659,877 (b, $pA_2 = 5.69 \pm 0.25$; slope = − 1.59 ± 0.65) in the presence of amastatin (1 μM, 1 h incubation time). Each value is the mean ± s.e.mean of at least three experiments.

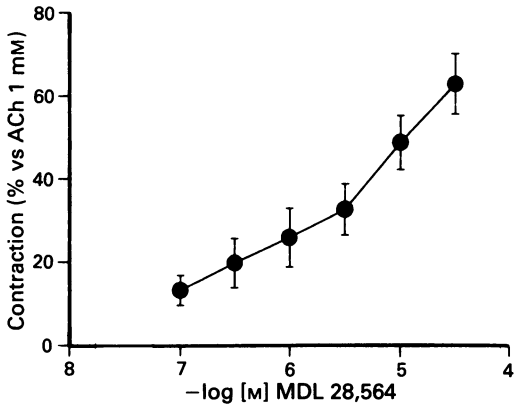

Figure 3 Concentration-dependent agonist effect of the pseudopeptide MDL 28,564 in the human isolated bronchi. Experiments were carried out in the presence of amastatin (1 μM, 1 h incubation time). Contraction is expressed as a percentage of the response to acetylcholine 1 mM. Each value is the mean ± s.e.mean of six experiments.

Discussion

Although it is well established that the contractions induced by TKs in human airways are mediated by stimulation of NK_2 receptors (Naline *et al.*, 1989), their identification as NK_{2A} or NK_{2B} has been hampered by conflicting reports. The subdivision of NK_2 receptors into NK_{2A} and NK_{2B} subtypes is based on two major pharmacological criteria: (1) the rank order of potency of some linear or cyclic peptide antagonists i.e. MEN 10376 > L659,877 for the NK_{2A} subtype and L659,877 > MEN 10376 for the NK_{2B} and (2) the pharmacological behaviour of the pseudopeptide, MDL 28,564, which shows agonist or antagonist features when interacting at the NK_{2A} or NK_{2B} subtype, respectively (Patacchini *et al.*, 1991). While most authors (Rhoden & Barnes, 1990; Advenier *et al.*, 1992; Ellis & Undem, 1992) have observed patterns of antagonist potency consistent with the NK_{2A} classification, Dion *et al.* (1990a,b) have provided evidence for the presence of NK_{2B} subtype in the human bronchus. In this study no differences in the antagonist potency between cyclic (L659,877) and linear (MEN 10376) peptides could be detected, when tested in the conventional medium (presence of captopril, bestatin and thiorphan); therefore no conclusion about the NK_2 subtype involved could be drawn. However, when the inhibitor of aminopeptidases, amastatin, was added to the medium, the affinity of MEN 10376 was definitely higher than that of L659,877. This finding indicates the prevalence of an NK_{2A} subtype population in the human bronchus. The conclusion is further substantiated by the observation that MDL 28,564 behaves as an agonist (although partial).

Synthetic tachykinin antagonists, bearing a linear peptide structure, may be degraded by amastatin-sensitive aminopeptidases (Patacchini & Maggi, 1993; Giuliani *et al.*, 1993). Therefore, amastatin, in addition to other peptidase inhibitors, provides a means for blocking peptide ligands metabolism; hence it allows adequate interaction of these molecules with their receptors. Amastatin beside inhibiting aminopeptidase M, which hydrolizes N-terminal neutral and basic aminoacids, inhibits aminopeptidase A, which cleaves N-terminal acidic residues (Ahmad & Ward, 1990; Wang *et al.*, 1991). The finding that the apparent potency of MEN 10376, a peptide antagonist containing an aspartic acid moiety at its N-terminal, increased in the presence of amastatin, strongly argues for the existence of aminopeptidase A in human bronchus (see Table 3). In accord with this, the apparent potency of [βAla^8]NKA(4–10), a compound containing an aspartic acid residue at its N-terminal, is also increased in the presence of amastatin. Derivatives of [βAla^8]NKA(4–10) and

Table 3 Amino acid sequences of peptides used in this study

NKA	H-His-Lys-Thr-Asp-Ser-Phe-Val-Gly-Leu-Met-NH2
[βAla^8]NKA(4–10)	H-Asp-Ser-Phe-Val-βAla-Leu-Met-NH2 (↑ after Ser)
MEN 10376	H-Asp-Tyr-D-Trp-Val-D-Trp-D-Trp-Lys-NH2 (↑ after Tyr)
L659,877	Cyclo(Leu-Met-Gln-Trp-Phe-Gly)

The arrow shows the possible site of cleavage by aminopeptidase A.

MEN 10376 lacking the N-terminal aspartic acid residue have been shown to exert remarkably lower biological effects in other tissues (data not shown). In agreement with our functional data, aminopeptidase A would not cleave the cyclic peptide L659,877 or the natural ligand neurokinin A. Recently Giuliani *et al.* (1993) confirmed in human urinary bladder that an amastatin-sensitive peptidase (possibly aminopeptidase A) could limit the biological activity of linear peptides bearing an N-terminal Asp residue such as MEN 10376 and MEN 10207 on smooth muscle. Our data that a NK_{2A} subtype mediates the motor effects of TKs in human bronchus is in keeping with the similar biological role of this NK_2 receptor subtype in other human tissues such as urinary bladder and circular muscle of ileum and colon (Giuliani *et al.*, 1991; 1993).

In conclusion, amastatin enables the characterization of the NK_2 receptor mediating TKs contractility in the human bronchus as a NK_{2A} subtype. The human bronchus contains an amastatin-sensitive metabolic pathway, possibly aminopeptidase A, which should be taken into account when assessing the biological activity of linear peptides bearing acidic residues at their N-terminal.

We wish to thank Prof. G. Storniello (Department of Histopathology, Ospedale Forlanini, Roma, Italy) for providing human lung specimens.

References

ADVENIER, C., NALINE, E., DRAPEAU, G. & REGOLI, D. (1987). Relative potencies of neurokinins in guinea pig trachea and human bronchus. *Eur. J. Pharmacol.*, **139**, 133–137.

ADVENIER, C., ROUISSI, N., NGUYEN, Q.T., EMONDS-ALT, X., BRELIERE, J.C., NELIAT, G., NALINE, E. & REGOLI, D. (1992). Neurokinin A (NK_2) receptor revisited with SR 48968, a potent non-peptide antagonist. *Biochem. Biophys. Res. Commun.*, **184**, 1418–1424.

AHMAD, S. & WARD, P.E. (1990). Role of aminopeptidase activity in the regulation of the pressor activity of circulating angiotensins. *J. Pharmacol. Exp. Ther.*, **252**, 643–649.

CHEUNG, D., BEL, E.H., DEN HARTIGH, J., DIJKMAN, J.H. & STERK, P.J. (1992). The effect of an inhaled neutral endopeptidase inhibitor, thiorphan, on airway responses to neurokinin A in normal humans in vivo. *Am. Rev. Respir. Dis.*, **145**, 1275–1280.

DEVILLIER, P., ADVENIER, C., DRAPEAU, G., MARSAC, J. & REGOLI, D. (1988). Comparison of the effects of epithelium removal and of an enkephalinase inhibitor on the neurokinin-induced contractions of guinea-pig isolated trachea. *Br. J. Pharmacol.*, **94**, 675–684.

DION, S., ROUISSI, N., NANTEL, F., DRAPEAU, G., REGOLI, D., NALINE, E. & ADVENIER, C. (1990a). Receptors for neurokinins in human bronchus and urinary bladder are of the NK_2 type. *Eur. J. Pharmacol.*, **178**, 215–219.

DION, S., ROUISSI, N., NANTEL, F., JUKIC, D., RHALEB, N.E., TOUSIGNANT, C., TELEMAQUE, S., DRAPEAU, G., REGOLI, D., NALINE, E., ADVENIER, C., ROVERO, P. & MAGGI, C.A. (1990b). Structure-activity study of neurokinins. Antagonists for the NK_2 receptor. *Pharmacology*, **41**, 184–194.

ELLIS, J.L. & UNDEM, B.J. (1992). Tachykinin receptor subtypes in human bronchi. *Am. Rev. Respir. Dis.*, **145**, A260.

GIULIANI, S., BARBANTI, G., TURINI, D., QUARTARA, L., ROVERO, P., GIACHETTI, A. & MAGGI, C.A. (1991). NK_2 tachykinin receptors and contraction of circular muscle of the human colon: characterization of the NK_2 receptor subtype. *Eur. J. Pharmacol.*, **203**, 365–370.

GIULIANI, S., PATACCHINI, R., BARBANTI, G., TURINI, D., ROVERO, P., QUARTARA, L., GIACHETTI, A. & MAGGI, C.A. (1993). Characterization of the tachykinin NK_2 receptor in the human urinary bladder by means of selective competitive receptor antagonists. *J. Pharmacol. Exp. Ther.* (in press).

HONDA, I., KOHROGI, H., YAMAGUCHI, T., ANDO, M. & ARAKI, S. (1991). Enkephalinase inhibitor potentiates substance P- and capsaicin-induced bronchial smooth muscle contractions in humans. *Am. Rev. Respir. Dis.*, **143**, 1416–1418.

IRELAND, S.J., BAILEY, F., COOK, A., HAGAN, R.M., JORDAN, C.C. & STEPHENS-SMITH, M.L. (1991). Receptors mediating tachykinin-induced contractile responses in guinea-pig trachea. *Br. J. Pharmacol.*, **103**, 1463–1469.

KOMATSU, T., YAMAMOTO, M., SHIMOKATA, K. & NAGURA, H. (1991). Distribution of substance P-immunoreactive and calcitonin gene-related peptide-immunoreactive nerves in normal human lungs. *Int. Arch. Allergy Appl. Immunol.*, **95**, 23–28.

LUNDBERG, J.M., HOKFELT, T., MARTLING, C.R., SARIA, A. & CUELLO, C. (1984). Substance P immunoreactive sensory nerves in the lower respiratory tract of various mammals including man. *Cell Tissue Res.*, **235**, 251–261.

MAGGI, C.A., GIULIANI, S., PATACCHINI, R., SANTICIOLI, P., THEODORSSON, E., BARBANTI, G., TURINI, D. & GIACHETTI, A. (1992). Tachykinin antagonists inhibit nerve-mediated contractions in the circular muscle of the human ileum: involvement of NK_2 receptors. *Gastroenterology*, **102**, 88–96.

MARTLING, C.R., THEODORSSON-NORHEIM, E. & LUNDBERG, J.M. (1987). Occurrence and effects of multiple tachykinins: Substance P, Neurokinin A and neuropeptide K in human lower airways. *Life Sci.*, **40**, 1633–1643.

NALINE, E., DEVILLIER, P., DRAPEAU, G., TOTY, L., BAKDACH, H., REGOLI, D. & ADVENIER, C. (1989). Characterization of neurokinin effects and receptor selectivity in human isolated bronchi. *Am. Rev. Resp. Dis.*, **140**, 679–686.

PARLANI, M., CONTE, B., MAIMONE, S., MAGGI, C.A., ROVERO, P. & GIACHETTI, A. (1990). The contractile effect of tachykinins on human prostatic urethra: involvement of NK_2 receptors. *J. Urology*, **144**, 1543–1545.

PATACCHINI, R., ASTOLFI, M., QUARTARA, L., ROVERO, P., GIACHETTI, A. & MAGGI, C.A. (1991). Further evidence for the existence of NK_2 tachykinin receptor subtypes. *Br. J. Pharmacol.*, **104**, 91–96.

PATACCHINI, R., MAGGI, C.A., ROVERO, P., REGOLI, D., DRAPEAU, G. & MELI, A. (1989). Effect of thiorphan on tachykinin-induced potentiation of nerve-mediated contractions of the rat isolated vas deferens. *J. Pharmacol. Exp. Ther.*, **250**, 678–681.

PATACCHINI, R. & MAGGI, C.A. (1993). Amastatin interferes with the antagonist properties of MEN 10208 in the rabbit pulmonary artery but not in the hamster trachea. *Eur. J. Pharmacol.*, **236**, 31–37.

RHODEN, K.J. & BARNES, P.J. (1990). Classification of tachykinin receptors on guinea-pig and human airway smooth muscle. *Am. Rev. Respir. Dis.*, **141**, A726.

RICH, D.H., MOON, B.J. & HARBESON, S. (1984). Inhibition of aminopeptidases by amastatin and bestatin derivatives. Effect of inhibitor structure on slow-binding processes. *J. Med. Chem.*, **27,** 417–422.

ROGERS, D.F., AURSUDKIJ, B. & BARNES, P.J. (1989). Effects of tachykinins on mucus secretion in human bronchi in vitro. *Eur. J. Pharmacol.*, **174,** 283–286.

TALLARIDA, R.J. & MURRAY, R.B. (1981). *Manual of Pharmacologic Calculation with Computer Programs.* New York: Springer Verlag.

VAN GIERSBERGEN, P.L.M., SHATZER, S.A., HARBESON, S.L., ROUISSI, N., NANTEL, F. & BUCK, S.H. (1991). Multiple NK_2 receptor subtypes are suggested by physiological and biochemical studies with neurokinin A (NKA) analogues and antagonists. *Ann. New York Acad. Sci.*, **632,** 483–484.

WANG, L., AHMAD, S., BENTER, I.F., CHOW, A., MIZUTANI, S. & WARD, P. (1991). Differential processing of substance P and neurokinin A by plasma dipeptidyl(amino)peptidase IV, aminopeptidase M and angiotensin converting enzyme. *Peptides*, **12,** 1357–1364.

(Received June 30, 1993
Revised September 23, 1993
Accepted October 11, 1993)

Br. J. Pharmacol. (1994), 111, 575–581

Inhibition of human monocyte adhesion to endothelial cells by the coumarin derivative, cloricromene

Salvatore Tranchina, Sergio Bernasconi, Elisabetta Dejana & [1]Aldo Del Maschio

Istituto di Ricerche Farmacologiche 'Mario Negri', Via Eritrea 62, 20157-Milano, Italy

1 The ability of the coumarin derivative cloricromene (8-monochloro-3-β-diethylaminoethyl-4-methyl-7-ethoxy-carbonylmethoxycoumarin) to inhibit monocyte adhesion to human cultured umbilical vein endothelial cells (HUVEC) was investigated.

2 Cloricromene (10–200 μM) inhibited, in a concentration-dependent manner, the adhesion of both resting and activated monocytes to HUVEC. Significant inhibition was reached with drug concentrations ranging between 15 to 30 μM.

3 The inhibitory activity was, at least in large part, directed to monocytes since no inhibition was observed after selective preincubation of HUVEC with cloricromene and the drug maintained its effect also on monocyte adhesion to paraformaldehyde-treated HUVEC.

4 Inhibition was maximal after 1 min of exposure of monocytes to cloricromene and persisted even in the absence of the drug.

5 Both basal and chemoattractant-mediated monocyte adhesion was inhibited by cloricromene as it was by TS1/18, a monoclonal antibody (mAb) directed to β2 integrins; however, cytofluorimetric analysis showed that cloricromene was unable to modulate the expression of β2 integrins on the monocyte surface.

6 When monocyte adhesion was mediated by a large set of adhesive receptors, as obtained after treatment of HUVEC with either interleukin 1β (IL-1; 50 ng ml^{-1}) or tumour necrosis factor-α (TNF; 100 u ml^{-1}), the inhibitory effect of cloricromene was considerably reduced.

7 The results of this study show that cloricromene may regulate monocyte adhesion to HUVEC, an event relevant *in vivo* in the pathogenesis of inflammatory and atherosclerotic processes.

Keywords: Monocyte adhesion; endothelial cells; adhesive molecules; cloricromene

Introduction

In pathological states, such as, hyperlipidaemia, hypertension and immune injury, the adhesion of circulating monocytes to the endothelial lining of arterial vessels is enhanced (Ross, 1986; Munro & Cotran, 1988). This is considered an early event in the pathogenesis of atherosclerosis (Gerrity *et al.*, 1979; Alderson *et al.*, 1986). Experimental evidence demonstrates that in hypercholesterolaemic animals, monocytes may adhere to an apparently intact endothelium, preferentially in the junctional areas between endothelial cells (Faggiotto *et al.*, 1984).

Transendothelial migration, leads to the accumulation of monocytes which subsequently undergo transformation into lipid-engorged foam cells (Gerrity, 1981). Concomitant release of oxygen metabolites and proteases (Babior, 1984; Nathan, 1987) promote cellular injury (Ross, 1986).

Monocyte extravasation is accompanied by secretion of growth factors, lipids and cytokines which participate in the progression of the atherosclerotic plaque (Munro & Cotran, 1988). Monocyte-derived growth factors, such as, platelet-derived growth factor (PDGF) induce migration and proliferation of fibroblasts and smooth muscle cells (Leibovich & Ross, 1976; Grotendorst *et al.*, 1981; Glenn & Ross, 1981; Martin *et al.*, 1981). Moreover, monocyte-derived lipids such as, platelet activating factor (PAF) and leukotriene B_4 (LTB_4) as well as cytokines, such as interleukin-1β (IL-1), tumour necrosis factor α (TNF) and monocyte chemoattractant protein-1 (MCP-1) participate in the growth of the atherosclerotic plaque by increasing leukocyte recruitment (Wang *et al.*, 1987; Verghese & Synderman, 1989; Yoshimura *et al.*, 1989), promoting endothelial expression of monocyte adhesive molecules (Bevilacqua *et al.*, 1985; Carlos *et al.*, 1991; Cybulsky & Gimbrone, 1991; Poston *et al.*, 1992) and secreting substances able to injure the connective tissue (Werb *et al.*, 1980; Nathan, 1987).

Thus, pharmacological inhibition of monocyte adhesion may be relevant for therapeutic intervention aimed to block the sequence of events leading to the chronic atherosclerotic process, a condition often associated with severe acute complications, such as, myocardial infarction and stroke (Schwartz *et al.*, 1978).

We tested the effect of cloricromene on monocyte adhesion, since this compound, which exerts antithrombotic and vasodilator activities *in vivo* (Aporti *et al.*, 1978; Prosdocimi *et al.*, 1985), reduce both monocyte chemotaxis (Bertocchi *et al.*, 1989) and TNF release (Squadrito *et al.*, 1992). Results described in this study show that cloricromene inhibits monocyte adhesion to resting endothelium. This effect is comparable to that of a blocking mAb directed to β2 integrins.

Methods

Monocytes

Monocytes were purified from peripheral blood of normal healthy volunteers as described by Colotta *et al.* (1984). Briefly, monocytes were obtained from Ficoll Hypaque-separated mononuclear cells by centrifugation on a discontinuous (46%) gradient of isosmotic (285 mOsmol) Percoll. Purified monocytes were radiolabeled for 1 h at room temperatue with $Na_2{}^{51}CrO_4$ (1 μCi/10^6 cells), washed twice and resuspended in Tyrode buffer (containing 1 mM $CaCl_2$).

[1] Author for correspondence.

Endothelial cells

Endothelial cells (HUVEC) were isolated from human umbilical vein, cultured in medium 199 supplemented with 20% FCS in the presence of endothelial cell growth supplement (50 $\mu g\ ml^{-1}$) and heparin (100 $\mu g\ ml^{-1}$) and maintained in a 37°C, 5% CO_2 humidified atmosphere. For the adhesion assay, the cells were detached by brief exposure to trypsin (0.25%)-EDTA (0.022%), plated and grown to confluence in 96-well plates, as previously described (Breviario *et al.*, 1988). In some experiments, endothelial cells from bovine thoracic aorta (BAEC) were used (Bazzoni *et al.*, 1991).

Adhesion of monocytes to endothelial cells

^{51}Cr-labelled monocytes ($3 \times 10^6\ ml^{-1}$) were preincubated with cloricromene at room temperature for 5 min, unless otherwise specified. Monocytes were then layered on 96-wells cultured HUVEC and subsequently stimulated with either fMLP or PMA (respectively, 10^{-7} and 10^{-8} M) for 20 min at 37°C. When fMLP was used as stimulus, monocytes were pretreated with 2.5 $\mu g\ ml^{-1}$ cytochalasin B. Adhesion was also induced when monocytes were layered for 20 min on HUVEC pretreated (for 4 and 24 h) with either TNF or IL-1 (100 u ml^{-1} and 50 ng ml^{-1}) respectively. Wells were washed three times to remove nonadherent cells, the remaining bound cells were lysed with 0.1% sodium dodecyl sulphate and individual lysates were counted in a Beckman Gamma 5500 counter (Fullerton, CA, U.S.A.). In some experiments, monocyte adhesion was tested on 3% paraformaldehyde-fixed HUVEC (15 min at room temperature), as well as on cloricromene (100 μM)-pretreated HUVEC. Both paraformaldehyde and cloricromene treated HUVEC's were carefully washed twice before monocyte addition.

Cytofluorimetric analysis

Phenotyping of monocytes was performed by indirect immunofluorescence. Monocytes were preincubated with 50 or 100 μM cloricromene (or control saline) for 5 min at room temperature, exposed to 10^{-8} M PMA (or control saline) and finally incubated with mAb TS1/18 (1:100 final dilution) for 30 min at 4°C. Monocytes were subsequently washed and incubated with fluoresceinated affinity-purified sheep anti-mouse IgG F(ab')2 for 30 min at 4°C. Cells were washed twice and fluorescence measured on a Becton Dickinson FACStar plus.

Materials

The suppliers for chemicals were Sigma Chemical Co. (St. Louis, MO, U.S.A.) for N-formyl-L-methionyl-L-leucyl-L-phenylalanine (fMLP), phorbol 12-myristate 13-acetate (PMA), heparin, cytochalasin B, endothelial cell growth supplement and HEPES; Genzyme (Boston, Mass, U.S.A.) for human recombinant TNF; Sclavo (Siena, Italy) for the recombinant human IL-1; Hyclone Lab (Logan, UT, U.S.A.) for aseptically collected foetal calf serum (FCS); Pharmacia Fine Chemicals (Uppsala, Sweden) for Percoll; Amersham (Buckinghamshire, UK) for $Na_2{}^{51}CrO_4$; Techno Genetics, New England Corp (Boston, MA, U.S.A.) for fluoresceinated affinity-purified sheep anti-mouse IgG $F(ab')_2$; Biochrom KG (Berlin, Germany) for RPMI 1640, $NaHCO_3$, L-glutamine and Ficoll separating solution; Gibco-Europe (Paisley, UK) for medium 199 and all other reagents for endothelial cell culture; gentamicin (Gentalyn) was a generous gift of Schering-Plough (Comazzo, Italy). Cloricromene and cloricromene acid were provided by Fidia (Albano Terme, Italy). Tyrode buffer (pH 7.4), contained (mM): NaCl 129, $NaHCO_3$ 9.9, KCl 2.8, KH_2PO_4 0.8, $MgCl_2.6H_2O$ 0.8, dextrose 5.6, $CaCl_2$ 1 and HEPES 10.

Antibodies

Monoclonal antibodies used in this study were: mAb anti β2 integrins, clone TS1/18 (ATCC; Rockville, MD, U.S.A.); mAb anti VLA-4, clone HP1/2, a generous gift from Dr F. Sanchez-Madrid, Univ. Madrid (Madrid, Spain); mAb anti E-selectin, clone BB11, a generous gift from Dr J. Harlan, Univ. Washington (Seattle, WA, U.S.A.). Antibodies were used at maximal blocking concentrations, as specified in the text.

Statistical analysis

Statistical analysis was performed by one-way analysis of variance (ANOVA) followed by Dunnett's test or by Student's unpaired *t* test.

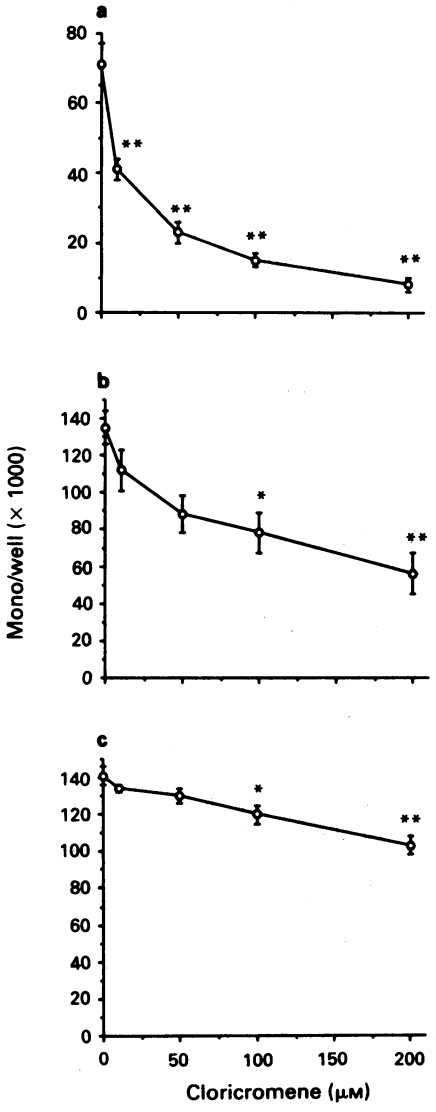

Figure 1 Effect of cloricromene on monocyte (Mono) adhesion to resting HUVEC, in basal conditions (a) and after activation with 10^{-8} M PMA (b), or to TNF (100 u ml^{-1} ml; 4 h)-activated HUVEC (c). ^{51}Cr-labelled monocytes ($3 \times 10^6\ ml^{-1}$) were preincubated for 5 min with cloricromene, layered on HUVEC and subsequently stimulated (b). After incubation (20 min at 37°C), nonadherent cells were removed and radioactivity associated with adherent cells was determined. Data (mean ± s.e.mean) are derived from eight different experiments and are expressed as the number of adherent monocytes/well ($\times 10^3$). Data were analysed by ANOVA and Dunnett's test. $^*P<0.05$ and $^{**}P<0.01$ as compared to control (in the absence of cloricromene). For abbreviations, see text.

Results

Effect of cloricromene on monocyte adhesion to endothelial cells

The effect of chloricromene on monocyte adhesion to resting HUVEC was evaluated. Basal monocyte adhesion was $71 \pm 6 \times 10^3$ mono/well and increased to $135 \pm 9 \times 10^3$ mono/well when monocytes were activated by PMA (10^{-8} M). As shown in Figure 1, cloricromene (10–200 μM) reduced both basal (a) and PMA-induced adhesion (b) in a concentration-dependent manner.

When monocytes were stimulated by fMLP (10^{-7} M), the adhesion to HUVEC was comparable to that induced by PMA (from $70 \pm 3 \times 10^3$ mono/well, in resting conditions, to 138 ± 7 mono/well after fMLP activation). Cloricromene (10–200 μM) significantly inhibited monocyte adhesion induced by fMLP. For instance, 10 and 200 μM of cloricromene reduced monocyte adhesion to 99 ± 13 and 25 ± 6 mono/well respectively (mean ± s.e.mean of three separate experiments; $P < 0.01$ by ANOVA).

We next evaluated adhesion of resting monocytes to HUVEC previously activated with TNF (100 u ml^{-1} for 4 h). Pretreatment of HUVEC with the inflammatory cytokine rendered the cellular surface hyperadhesive for monocytes. Cloricromene very weakly reduced adhesion of monocytes to TNF-activated HUVEC (Figure 1c). Similar results were obtained when we evaluated monocyte adhesion to IL-1-activated HUVEC (50 ng ml^{-1} for 4 h). The increase of monocyte adhesion on IL-1-treated HUVEC was comparable to that observed onto TNF-treated HUVEC (from $67 \pm 3 \times 10^3$ mono/well on resting HUVEC to 125 ± 6 mono/well on IL-1-treated HUVEC). Cloricromene reduced monocyte adhesion to IL-1-treated HUVEC to a significant extent only at 200 μM. At this concentration the adhesion was reduced to $90 \pm 6 \times 10^3$ mono/well (mean ± s.e.mean of six separate experiments; $P < 0.01$ by ANOVA). Analysis of dose-response curves by the ALLFIT programme (DeLean *et al.*, 1978), gave the estimates of drug concentration producing half-maximal inhibition of monocyte adhesion to HUVEC. These values were 16 ± 1 μM for basal adhesion and 37 ± 3 μM and 29 ± 2 μM respectively for PMA- and fMLP-

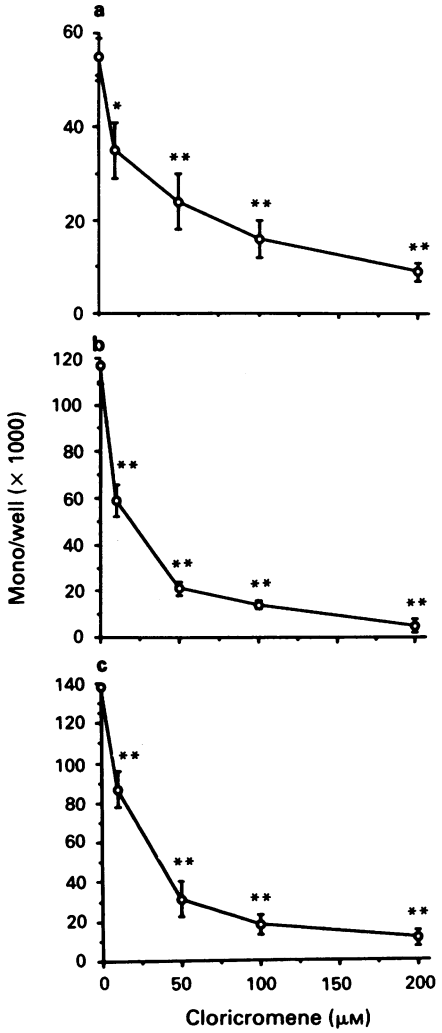

Figure 2 Effect of cloricromene on monocyte (Mono) adhesion to resting BAEC, in basal conditions (a) and after activation with 10^{-7} M fMLP (b) or 10^{-8} M PMA (c). ^{51}Cr-labelled monocytes (3×10^6 ml^{-1}) were preincubated for 5 min with cloricromene, layered on HUVEC and subsequently stimulated (b and c). After incubation (20 min at 37°C), nonadherent cells were removed and radioactivity associated with adherent cells was determined. Data (mean ± s.e.mean) are derived from three (a and b) and four (c) different experiments and are expressed as the number of adherent monocytes/well (× 10^3). Data were analysed by ANOVA and Dunnett's test. *$P < 0.05$ and **$P < 0.01$ as compared to control (in the absence of cloricromene). For abbreviations, see text.

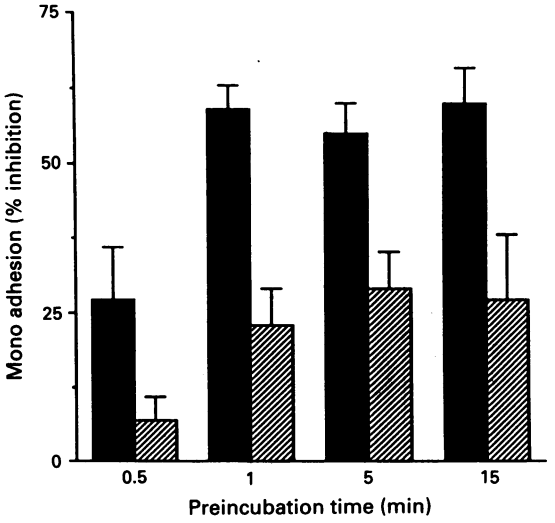

Figure 3 Effect of the time of preincubation of cloricromene with monocytes. ^{51}Cr-labelled monocytes (3×10^6 ml^{-1}) were preincubated with cloricromene for different times (0.5–15 min) and layered on HUVEC. Subsequent monocyte adhesion, either basal (solid columns) or 10^{-8} M PMA-stimulated (hatched columns) was performed as described in Methods. Data (mean ± s.e.mean) are derived from four different experiments and are expressed as the number of adherent monocytes/well (× 10^3). For abbreviations, see text.

Table 1 Effect of cloricromene acid (Cloricr ac) on monocyte adhesion to human umbilical vein endothelial cells (HUVEC)

	Basal	*PMA*	*TNF* (4)	*TNF* (24)
Control	68 ± 2	116 ± 3	155 ± 2	134 ± 5
Cloricr ac (100 μM)	73 ± 4	110 ± 1	158 ± 4	127 ± 3
Cloricr ac (200 μM)	76 ± 3	107 ± 2	159 ± 4	126 ± 2

Monocytes (3×10^6 ml^{-1}) were treated with cloricromene acid, layered on 96-wells cultured HUVEC and radioactivity associated to adherent monocytes was counted as described in Methods. Data are expressed as number of monocytes/well (× 10^3) and are mean ± s.e.mean of three different experiments.
PMA, phorbol 12-myristate 13-acetate; TNF, tumour necrosis factor.

induced adhesion, but for adhesion on cytokine-activated HUVEC the value was beyond 200 μM (mean ± s.e.mean of three to eight different experiments).

As shown in Figure 2, monocyte adhesion to BAEC, either basal (a) or induced by 10^{-7} M fMLP (b) or 10^{-8} M PMA (c), was reduced by cloricromene in a way more marked than to HUVEC. Indeed, both basal and chemoattractant-activated adhesion to BAEC were inhibited by cloricromene to a similar extent (Figure 2).

Monocyte adhesion was rapidly modulated by cloricromene. As shown in Figure 3, maximal inhibition of both basal and PMA-induced adhesion was observed after 1 min of preincubation with cloricromene (50 μM). No further inhibition was observed when monocytes were preincubated with the drug for longer times. Cloricromene acid, the active intracellular metabolite, was unable to reduce monocyte adhesion to HUVEC, thus indicating the specificity of the effect of the ester form (Table 1).

Figure 4 shows that basal (a), PMA- (b) and TNF-induced (c) monocyte adhesion to paraformaldehyde-fixed HUVEC was reduced in a concentration-dependent manner by cloricromene (10–200 μM). Monocyte adhesion to fixed HUVEC was always lower than that observed to the untreated HUVEC, indicating a modification of the adhesive properties of the cells exerted by paraformaldehyde treatment.

As shown in Figure 5, monocyte pretreatment with cloricromene (10-200 μM) followed by washing resulted in significant reduction of basal (a), PMA-(b) and TNF-induced (c) adhesion even if this effect was lower than when the drug was maintained during the adhesion assay. In contrast, the

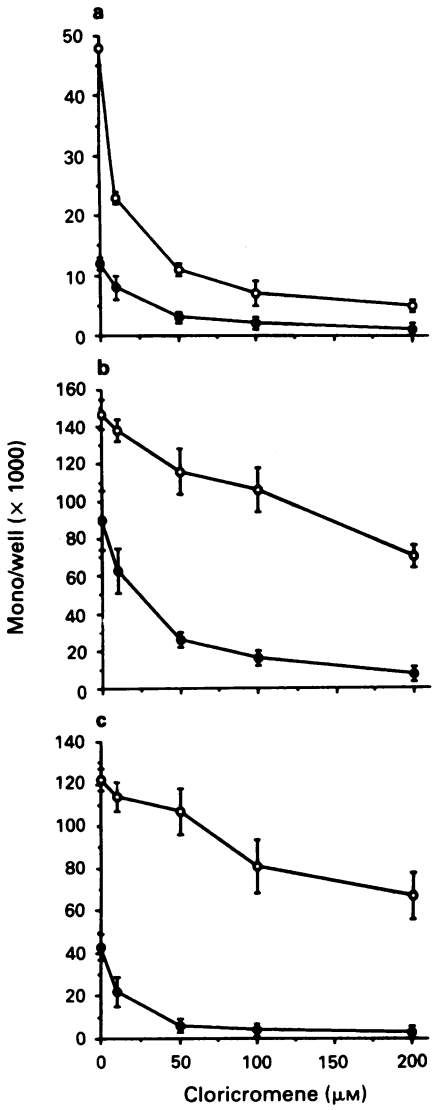

Figure 4 Effect of cloricromene on monocyte adhesion to paraformaldehyde-treated HUVEC. Resting (a and b) and TNF-activated (100 u ml^{-1} for 4 h; c) HUVEC were treated with 3% paraformaldehyde (●) or control buffer (○) as described in Methods. ^{51}Cr-labelled monocytes (3×10^6 ml^{-1}) were preincubated for 5 min with cloricromene, layered on HUVEC and exposed to 10^{-8} M PMA (b) or control buffer (a and c). After incubation (20 min at 37°C), nonadherent cells were removed and radioactivity associated with adherent cells was determined. Data (mean ± s.e.mean) are derived from three different experiments and are expressed as the number of adherent monocytes/well ($\times 10^3$). For abbreviations, see text.

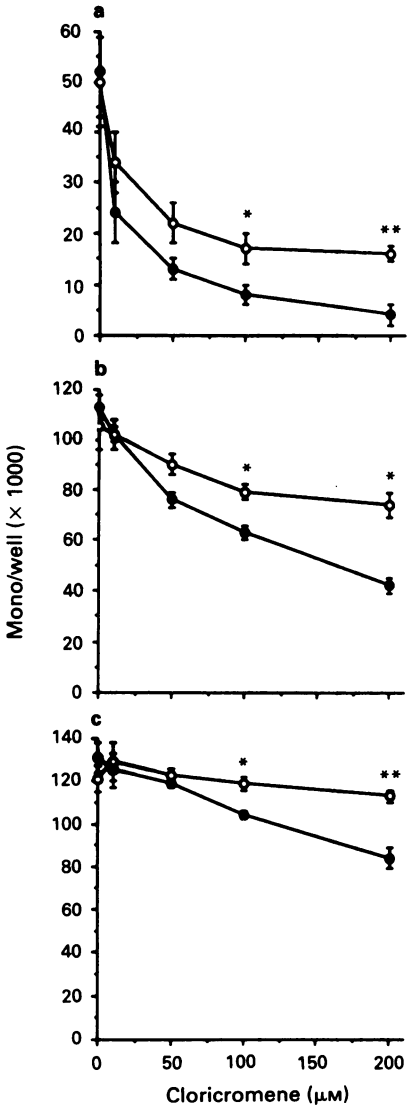

Figure 5 Effect of the presence of cloricromene during monocyte adhesion to HUVEC. ^{51}Cr-labelled monocytes (3×10^6 ml^{-1}) were preincubated for 5 min with cloricromene, washed and resuspended with cloricromene (●) or control buffer (○). Monocytes were layered on resting (a and b) and TNF-activated (100 u ml^{-1} for 4 h; c) HUVEC and subsequently exposed to 10^{-8} M PMA (b) or control buffer (a and c). After incubation (20 min at 37°C), nonadherent cells were removed and radioactivity associated with adherent cells was determined. Data (mean ± s.e.mean) are derived from six (a) and three (b and c) different experiments and are expressed as the number of adherent monocytes/well ($\times 10^3$). Data were analysed by Student's t test to assess differences between the presence and absence of cloricromene during the adhesion assay. $^*P < 0.05$ and $^{**}P < 0.01$. For abbreviations, see text.

drug (used in the same range of concentrations) did not show any significant inhibitory effect on basal, PMA- and TNF-induced adhesion when it was selectively preincubated with HUVEC and washed before the adhesion assay (not shown). Finally, preliminary results obtained by high performance liquid chromatography (h.p.l.c.) analysis of cloricromene (10–100 μM)-treated HUVEC extracts, indicate that drug uptake was below 5% after 5 and 160 min of incubation, in contrast to the efficient uptake performed by platelets and leukocytes (Travagli *et al.*, 1989; Betocchi *et al.*, 1989).

Overall these data indicate that a significant part of cloricromene activity is directed to monocytes.

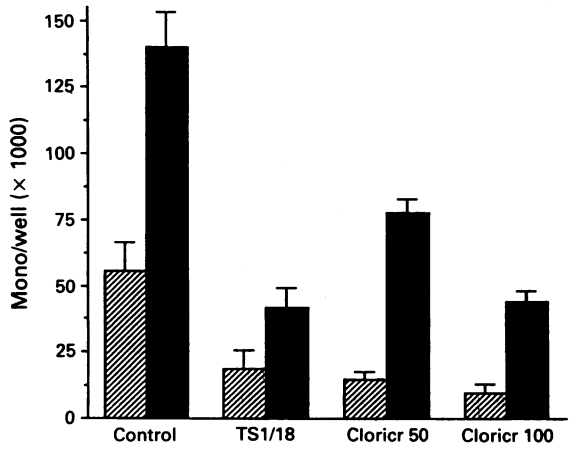

Figure 6 Comparison of the effect of cloricromene with the anti β2 integrin mAb (TS1/18) on monocyte adhesion to resting HUVEC. ^{51}Cr-labelled monocytes (3×10^6 ml^{-1}) were preincubated with cloricromene (50 and 100 μM) or with TS1/18 (1:100 final dilution) and layered on HUVEC. Subsequent monocyte adhesion, either basal (hatched columns) or 10^{-8} M PMA-stimulated (solid columns), was performed as described in Methods. Data (mean ± s.e.mean) are derived from five different experiments and are expressed as the number of adherent monocytes/well ($\times 10^3$). For abbreviations, see text.

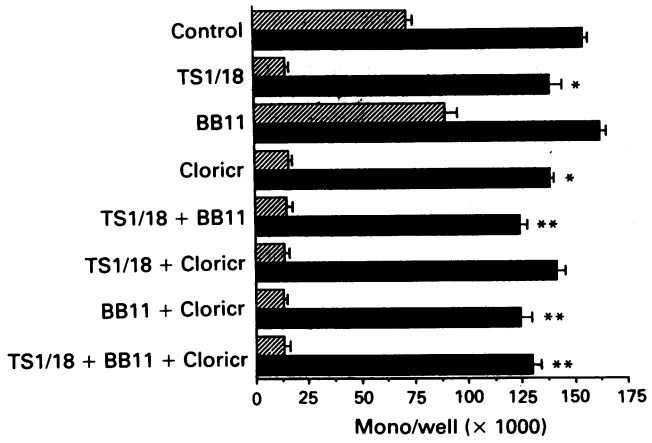

Figure 7 Comparison of the effect of cloricromene (Cloricr) with the anti β2 integrin mAb (TS1/18) and anti E-selectin mAb (BB11) on moncyte (mono) adhesion to TNF-activated HUVEC for 4 h. ^{51}Cr-labelled monocytes (3×10^6 ml^{-1}) were preincubated for 5 and 15 min respectively with cloricromene (100 μM) or TS1/18 (1:100 final dilution) and then layered on untreated (hatched columns) or TNF (100 u ml^{-1})-activated (solid columns) HUVEC. When indicated, HUVEC were pretreated with BB11 (10 μg ml^{-1}) for 20 min. Monocyte adhesion was measured as described in Methods. Data (mean ± s.e.mean) are derived from three different experiments and are expressed as the number of adherent monocytes/well ($\times 10^3$). Data were analysed by ANOVA and Dunnett's test. *$P<0.05$ and **$P<0.01$ as compared to control. For abbreviations, see text.

Effect of cloricromene on the different pathways of monocyte adhesion

We have investigated the influence of cloricromene on the different pathways of monocyte adhesion to HUVEC.

As indicated in Figure 6, cloricromene (50 and 100 μM) reduced both basal and PMA-induced monocyte adhesion, similarly to mAb TS1/18 (1:100 final dilution). These data suggest that cloricromene could modulate β2 integrin expression on monocyte surface. However, flow cytometry analyses showed that cloricromene was unable to modify substantially the expression of β2 integrins on either resting or PMA-activated monocytes. Mean fluorescence intensity of control monocytes was 572 ± 24 and 735 ± 51 (respectively resting and activated by 10^{-8} M PMA), and 529 ± 33 and 742 ± 27 of cloricromene (100 μM)-treated monocytes.

We then evaluated whether cloricromene could have an additive or synergistic effect with antibodies blocking the leukocyte/endothelial cells adhesive molecules. We studied the effect of cloricromene on monocyte adhesion to HUVEC preexposed to TNF (100 u ml^{-1}) for 4 and 24 h. Under these conditions, adhesive molecules on endothelial surface were differently upregulated (Pober & Cortan, 1990; Butcher, 1991).

As shown in Figure 7, and in Figure 1, cloricromene (100 μM) inhibited monocyte adhesion to resting HUVEC. The drug was able to induce a weak, but significant ($P<0.05$ by ANOVA), reduction of monocyte adhesion to TNF (100 u ml^{-1})-treated HUVEC (4 h), similarly to mAb TS1/18. Anti E-selectin mAb BB11 (10 μg ml^{-1}), was inactive by itself and increased inhibition only slightly when added in combination with mAb TS 1/18 or cloricromene ($P<0.01$ by ANOVA). The combination of TS 1/18, BB11 and cloricromene did not show any further inhibitory effect. As shown in Figure 8, monocyte adhesion to TNF (100 u ml^{-1})-treated HUVEC (24 h), was reduced by mAb TS1/18 ($P<0.01$ by ANOVA), while anti VLA-4 mAb HP1/2 (10 μg ml^{-1}) and cloricromene (100 μM) were inactive. Cloricromene did not increase the inhibitory activity of TS1/18, but did so when added to HP1/2. The combination of the three (TS1/18, HP1/2 and cloricromene) produced the highest inhibitory effect (Figure 8).

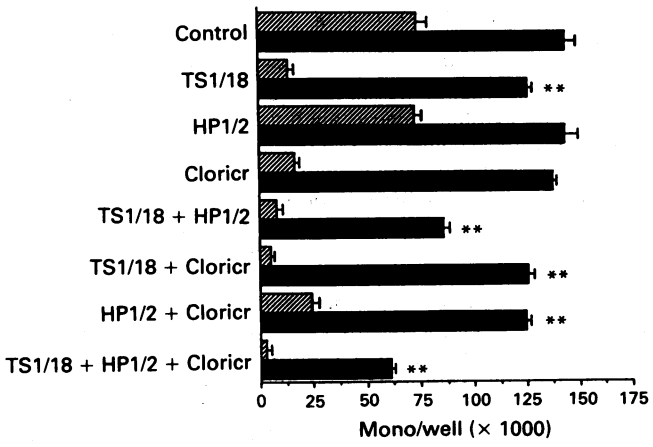

Figure 8 Comparison of the effect of cloricromene (Cloricr) with the anti β2 integrin mAb (TS1/18) and anti VLA-4 mAb (HP1/2) on monocyte adhesion to TNF-activated HUVEC for 24 h. ^{51}Cr-labelled monocytes (3×10^6 ml^{-1}) were preincubated with cloricromene (100 μM) for 5 min, or with TS1/18 (1:100 final dilution) and HP1/2 (10 μg ml^{-1}) for 15 min and then layered on untreated (hatched columns) or TNF (100 u ml^{-1})-activated (solid columns) HUVEC. Monocyte (Mono) adhesion was measured as described in Methods. Data (mean ± s.e.mean) are derived from three different experiments and are expressed as the number of adherent monocytes/well ($\times 10^3$). Data were analysed by ANOVA and Dunnett's test. *$P<0.05$ and **$P<0.01$ as compared to control. For abbreviations, see text.

Discussion

The central finding of this work is that cloricromene, a coumarin derivative, reduced monocyte adhesion to HUVEC. Both basal and chemoattractant-mediated monocyte adhesion were significantly inhibited by cloricromene (Figures 1 and 6). The inhibitory activity found *in vitro* is exerted by cloricromene at concentrations (15–30 μM) which are in the range of those that can be found in dog plasma after administration of 0.5 mg kg^{-1} of the drug, a dose that can effectively reduce thrombus formation after coronary occlusion (Prosdocimi *et al.*, 1985).

As shown in Figure 3, a short preincubation of monocytes with chloricromene (1 min) was sufficient to reach maximal inhibition, suggesting that the drug is rapidly taken up by monocytes and then converted to its active metabolite, cloricromene acid, as previously described for platelets (Travagli *et al.*, 1989) and polymorphonuclear leukocytes (Bertocchi *et al.*, 1989). The acid metabolite cannot enter the cells when given as such and essentially is inactive in other biological tests performed (Squadrito *et al.*, 1991).

The effect of cloricromene was, at least to a large extent, maintained when monocytes were preincubated with the drug followed by washing (Figure 5). In contrast, when HUVEC were selectively treated with cloricromene (and the drug washed out before the adhesion assay) the inhibitory activity was lost. In addition, the compound retained its effect even when HUVEC were fixed by paraformaldehyde (Figure 4).

Overall these data emphasize that a significant part of cloricromene effect is directed to monocytes and not to the endothelium. This is in agreement with the low uptake of the drug by HUVEC, as measured by h.p.l.c. analysis.

Monocyte-endothelial cell recognition is a complex mechanism regulated by several adhesive molecules (Carlos *et al.*, 1990; 1991; Springer, 1990; Hakkert *et al.*, 1991; Jonjic *et al.*, 1992). To clarify better the inhibitory mechanism of cloricromene, we compared the effect of the compound with that of mAbs directed to both monocyte and endothelial adhesion molecules.

Monocyte adhesion to resting HUVEC is essentially medicated by ICAM-1 (intercellular adhesion molecule-1) and ICAM-2 adhesive molecules on the endothelium and by β2 integrins on monocytes. Data shown in Figure 6, suggest that cloricromene could counteract this type of binding, since monocyte adhesion to resting HUVEC was reduced by cloricromene to the same extent than using mAb directed to β2 integrins. This effect was, however, not accounted for by a reduction in the expression of surface β2 integrins, as assessed by cytofluorimetric analysis.

The picture becomes more complex when HUVEC were activated by inflammatory cytokines such as TNF or IL-1. In this condition, the adhesion of monocytes to HUVEC is mediated by several adhesive molecules (Springer, 1990; Pober & Cotran, 1990; Butcher, 1991). After 4 h of TNF pretreatment, HUVEC express ICAM-1 and ICAM-2 and *ex novo* expose E-selectin on their surface. At 24 h HUVEC express high levels of ICAM-1 and VCAM-1 (vascular cell adhesion molecule-1). ICAM-1 and ICAM-2 are bound by β2 integrin counterreceptors (LFA-1 and MAC-1) on leukocytes while VCAM-1 is recognized by the α4β1 integrin, VLA-4 (very late antigen-4). Monocytes express VLA-4 and β2 integrins and are able to bind all the endothelial adhesive molecules indicated above. As previously reported, monocyte adhesion could be significantly reduced only by the combined inhibition of the different adhesive receptors on monocytes and/or endothelial cells (Jonjic *et al.*, 1992).

When HUVEC were activated by TNF (100 u ml^{-1}) for 4 h, cloricromene *per se* exerted a weak inhibitory activity similar to that of the anti β2 mAb. This effect was slightly increased by the combination with the anti E-selectin mAb (Figure 7). As reported in Figure 8, monocyte adhesion to HUVEC activated for 24 h with TNF (100 u ml^{-1}), was strongly reduced by the combined treatment of monocytes with anti β2 integrins and anti VLA-4 mAbs (40% of inhibition as compared to the control).

Cloricromene, which was inactive *per se*, increased the inhibition of these two mAbs (60% of inhibition) possibly by an additive effect.

Overall, these observations indicate that the effect of cloricromene is considerably decreased when monocyte adhesion is mediated by a large set of receptors, such as after activation of HUVEC with inflammatory cytokines. The drug however could increase the inhibitory activity of both anti β2 integrin and E-selectin mAbs.

Cloricromene, besides reducing monocyte adhesion, is effective against monocyte chemotaxis (Bertocchi *et al.*, 1989) and TNF release (Squadrito *et al.*, 1992), by a mechanism of action which remains still obscure. This compound may induce a general inhibitory activity on platelets and polymorphonuclear leukocytes (Squadrito *et al.*, 1991) possibly through its ability to modulate the levels of biochemical messengers which regulate cellular response. Cloricromene is able to reduce platelet response by reducing cytoplasmic Ca^{2+} mobilization and increasing guanosine 3′:5′-cyclic monophosphate (cyclic GMP) levels through the inhibition of the cyclic GMP phosphodiesterase (Hakim *et al.*, 1988; Del Maschio *et al.*, 1990). Moreover, cloricromene inhibits the release of arachidonic acid and diglycerides from membrane phospholipids, suggesting a possible interference with the activity of phospholipase A_2 and/or phospholipase C (Porcellati *et al.*, 1990).

Although several compounds such as corticosteroids, antibiotics, methylxanthines and nonsteroidal anti-inflammatory drugs, were tested for their ability to regulate monocyte chemotaxis (Panerai *et al.*, 1992) and production of cytokines (Waage & Bakke, 1988; Schandené *et al.*, 1992; Breban *et al.*, 1992), oxygen radicals (French *et al.*, 1987) and proteolytic enzymes (Wahl & Winter, 1984), little is known of the pharmacological modulation of monocyte adhesion to endothelial cells.

This study reports that cloricromene is a compound able to reduce monocyte adhesion to HUVEC. This finding may be useful in defining new substances pharmacologically active in pathologies where monocyte recruitment and activation should be limited.

We are indebted with Drs M. Prosdocimi, E.J. Hornby and A. Zatta for very useful comments. This work was supported by the Italian National Research Council (Special projects Biotecnologie e Biostrumentazione). S.T. is a fellow of the Istituto Biochimico Italiano Giovanni Lorenzini (IBI).

References

ALDERSON, L.M., ENDEMANN, G., LINDSEY, S., PRONCZUK, A., HOOVER, R.L. & HAYES, K.C. (1986). LDL enhances monocyte adhesion to endothelial cells in vitro. *Am. J. Pathol.*, **123**, 334–342.

APORTI, F., FINESSO, M. & GRANATA, L. (1978). Effects of 8-monochloro-3-beta-diethylaminoethyl-4-methyl-7-ethoxycarbonylmethoxy coumarin (AD6) on the coronary circulation in the dog. *Pharmacol. Res. Commun.*, **10**, 469–477.

BABIOR, B.M. (1984). Oxidants from phagocytes: agents of defense and destruction. *Blood*, **64**, 959–966.

BAZZONI, G., DEJANA, E. & DEL MASCHIO, A. (1991). Adrenergic modulation of human polymorphonuclear leukocyte activation. Potentiating effect of adenosine. *Blood*, **77**, 2042–2048.

BERTOCCHI, F., BREVIARIO, F., PROSERPIO, P., WANG, J.M., GHEZZI, P., TRAVAGLI, R.A., PROSDOCIMI, M. & DEJANA, E. (1989). In vitro inhibition of human polymorphonuclear cell function by cloricromene. *Naunyn-Schmied. Arch. Pharmacol.*, **339**, 697–703.

BEVILACQUA, M.P., POBER, J.S., WHEELER, M.E., COTRAN, R.S. & GIMBRONE, M.A. Jr. (1985). Interleukin 1 acts on cultured human vascular endothelium to increase the adhesion of polymophonuclear leukocytes, monocytes and related leukocyte cell lines. *J. Clin. Invest.*, **76**, 2003–2011.

BREBAN, M., FOURNIER, C., GOUGEROT-POCIDALO, M.A., MUFFAT-JOLY, M. & POCIDALO, J.J. (1992). Protective effects of ciprofloxacin against type II collagen induced arthritis in rats. *J. Rheumatol.*, **19**, 216–222.

BREVIARIO, F., BERTOCCHI, F., DEJANA, E. & BUSSOLINO, F. (1988). IL-1-induced adhesion of polymorphonuclear leukocytes to cultured human endothelial cells. Role of platelet-activating factor. *J. Immunol.*, **141**, 3391–3397.

BUTCHER, E.C. (1991). Leukocyte-endothelial cell recognition: three (or more) steps to specificity and diversity. *Cell*, **67**, 1033–1036.

CARLOS, T.M., DOBRINA, A., ROSS, R. & HARLAN, J.M. (1990). Multiple receptors on human monocytes are involved in adhesion to cultured human endothelial cells. *J. Leukoc. Biol.*, **48**, 451–456.

CARLOS, T., KOVACH, N., SCHWARTZ, B., ROSA, M., NEWMAN, B., WAYNER, E., BENJAMIN, C., OSBORN, L., LOBB, R. & HARLAN, A. (1991). Human monocytes bind to two cytokine-induced adhesive ligands on cultured endothelial cells: endothelial leukocyte adhesion molecule-1 and vascular cell adhesion molecule-1. *Blood*, **77**, 2266–2271.

COLOTTA, F., PERI, G., VILLA, A. & MANTOVANI, A. (1984). Rapid killing of actinomycin D-treated tumor cells by human mononuclear cells. Effectors belong to the monocyte-macrophage lineage. *J. Immunol.*, **132**, 936–944.

CYBULSKY, M.I. & GIMBRONE, M.A. Jr. (1991). Endothelial expression of a mononuclear leukocyte adhesion molecule during atherogenesis. *Science*, **251**, 788–791.

DELEAN, A., MUNSON, P.J. & RODBARD, D. (1978). Simultaneous analysis of families of sigmoidal curves: application to bioassay, radioligand assay, and physiological dose-response curves. *Am. J. Physiol.*, **235**, E97–E102.

DEL MASCHIO, A., BAZZONI, G., ZATTA, A., CHEN, Z.M., DEJANA, E. & PROSDOCIMI, M. (1990). Cloricromene inhibits the activation of human platelets by ADP alone or in combination with adrenaline. *Eur. J. Pharmacol.*, **187**, 541–545.

FAGGIOTTO, A., ROSS, R. & HARKER, L. (1984). Studies of hypercholesterolemia in the nonhuman primate. I. Changes that lead to fatty streak formation. *Arteriosclerosis*, **4**, 323–340.

FRENCH, J.K., HURST, N.P., MCCOLL, S.R. & CLELAND, L. (1987). Effects of piroxicam on superoxide generation, phospholipid methylation and leukotriene production by human blood mononuclear cells. *J. Rheumatol.*, **14**, 1018–1021.

GERRITY, R.G. (1981). The role of the monocyte in atherogenesis. I: Transition of blood-borne monocytes into foam cells in fatty lesions. *Am. J. Pathol.*, **103**, 181–190.

GERRITY, R.G., NAITO, H.K., RICHARDSON, M. & SCHWARTZ, C.J. (1979). Dietary induced atherogenesis in swine: Morphology of the intima in prelesion stages. *Am. J. Pathol.*, **95**, 775–792.

GLENN, K.C. & ROSS, R. (1981). Human monocyte-derived growth factor(s) for mesenchymal cells: Activation of secretion by endotoxin and concanavalin A. *Cell*, **25**, 603–615.

GROTENDORST, G.R., SEPPÄ, H.E.J., KLEINMAN, H.K. & MARTIN, G.R. (1981). Attachment of smooth muscle cells to collagen and their migration toward platelet-derived growth factor. *Proc. Natl. Acad. Sci. U.S.A.*, **78**, 3669–3672.

HAKIM, G., FIORENTINI, D., FALASCA, A., PROSDOCIMI, M. & ROSSI, C.A. (1988). Effect of AD6 (8-monochloro-3-beta-diethylamino-ethyl-4-methyl-7-ethoxycarbonyl-methoxy coumarin) on cyclic nucleotide phosphodiesterases in human platelets. *Experientia*, **44**, 226–228.

HAKKERT, B.C., KUIJPERS, T.W., LEEUWENBERG, J.F., VAN MOURIK, J.A. & ROOS, D. (1991). Neutrophil and monocyte adherence to and migration across monolayers of cytokine-activated endothelial cells: the contribution of CD18, ELAM-1 and VLA-4. *Blood*, **78**, 2721–2726.

JONJIC, N., JILEK, P., BERNASCONI, S., PERI, G., MARTIN-PADURA, I., CENZUALES, S., DEJANA, E. & MANTOVANI, A. (1992). Molecules involved in the adhesion and cytotoxicity of activated monocytes on endothelial cells. *J. Immunol.*, **148**, 2080–2083.

LIEBOVICH, S.J. & ROSS, R. (1976). A macrophage-dependent factor that stimulates the proliferation of fibroblasts in vitro. *Am. J. Pathol.*, **84**, 501–514.

MARTIN, B.M., GIMBRONE, M.A. Jr., UNANUE, E.R. & COTRAN, R.S. (1981). Stimulation of nonlymphoid mesenchymal cell proliferation by a macrophage-derived growth factor. *J. Immunol.*, **126**, 1510–1515.

MUNRO, J.M. & COTRAN, R.S. (1988). The pathogenesis of atherosclerosis: atherogenesis and inflammation. *Lab. Invest.*, **58**, 249–261.

NATHAN, C.F. (1987). Secretory products of macrophages. *Blood*, **79**, 319–326.

PANERAI, A.E., LOCATELLI, L. & SACERDOTE, P. (1992). Effects of piroxicam and ibuprofen on substance P induced chemotaxis of human monocytes and polymorphonuclear cells. *Pharmacol. Res.*, **26** (Suppl. 2), 30–31.

POBER, J.S. & COTRAN, R.S. (1990). The role of endothelial cells in inflammation. *Transplantation*, **50**, 537–544.

PORCELLATI, S., COSTANTINI, V., PROSDOCIMI, M., STASI, M., PISTOLESI, R., NENCI, G.G. & GORACCI, G. (1990). The coumarin derivative AD6 inhibits the release of arachidonic acid by interfering with phospholipase A2 activity in human platelets stimulated with thrombin. *Agents Actions*, **29**, 364–373.

POSTON, R.N., HASKARD, D.O., COUCHER, J.R., GALL, N.P. & JOHNSON-TIDEY, R.R. (1992). Expression of intercellular adhesion molecule-1 in atherosclerotic plaques. *Am. J. Pathol.*, **140**, 665–673.

PROSDOCIMI, M., FINESSO, M., TESSARI, F., GORIO, A., LANGUINO, L.R., DE GAETANO, G. & DEJANA, E. (1985). Inhibition by AD6 (8-monochloro-3-beta-diethylaminoethyl-4-methyl-7-ethoxycarbonylmethoxycoumarin) of platelet aggregation in dog stenosed coronary artery. *Thromb. Res.*, **39**, 399–409.

ROSS, R. (1986). The pathogenesis of atherosclerosis: an update. *N. Engl. J. Med.*, **341**, 488–500.

SCHANDENE, L., VANDENBUSSCHE, P., CRUSIAUX, A., ALEGRE, M.L., ABRAMOWICZ, D., DUPONT, E., CONTENT, J. & GOLDMAN, M. (1992). Differential effects of pentoxifylline on the production of tumor necrosis factor-alpha (TNF-α) and interleukin-6 (IL-6) by monocytes and T cells. *Immunology*, **76**, 30–34.

SCHWARTZ, C.J., CHANDLER, A.B., GERRITY, R.G. & NAITO, H.K. (1978). Clinical and pathological aspects of arterial thrombosis and thromboembolism. In *The Thrombotic Process in Atherogenesis* ed. Chandler, A.B., Eurenius, K., McMillan, G.C., Nelson, C.B., Schwartz, C.J. & Wessler, S. pp. 111–126. New York: Plenum Press.

SPRINGER, T.A. (1990). Adhesion receptors of the immune system. *Nature*, **346**, 425–434.

SQUADRITO, F., ALTAVILLA, D., CAMPO, G.M., CALAPAI, G., IOCULANO, M., ZINGARELLI, B., SAITTA, A., PROSDOCIMI, M. & CAPUTI, A.P. (1992). Cloricromene, a coumarine derivative, protects against lethal endotoxin shock in rats. *Eur. J. Pharmacol.*, **210**, 107–113.

SQUADRITO, F., PROSDOCIMI, M., ALTAVILLA, D., ZINGARELLI, B. & CAPUTI, A.P. (1991). Cloricromene. *Cardiovasc. Drug Rev.*, **9**, 357–371.

TRAVAGLI, R.A., ZATTA, A., BANZATTO, N., FINESSO, M., MARIOT, R., TESSARI, F. & PROSDOCIMI, M. (1989). Molecular aspects of cloricromene (AD6) distribution in human platelets and its pharmacological effects. *Thromb. Res.*, **54**, 327–338.

VERGHESE, M.W. & SNYDERMAN, R. (1989). Chemotaxis and chemotactic factors. In *Human Monocytes*. ed. Zembala, M. & Asherton, G.L. pp. 167–175. San Diego: Academic Press.

WAAGE, A. & BAKKE, O. (1988). Glucocorticoids suppress the production of tumor necrosis factor by lipopolysaccharide-stimulated human monocytes. *Immunology*, **63**, 299–302.

WAHL, L.M. & WINTER, C.C. (1984). Regulation of guinea pig macrophage collagenase production by dexamethasone and colchicine. *Arch. Biochem. Biophys.*, **230**, 661–667.

WANG, J.M., BERSANI, L. & MANTOVANI, A. (1987). Tumor necrosis factor is chemotactic for monocytes and polymorphonuclear leukocytes. *J. Immunol.*, **138**, 1469–1474.

WERB, Z., BANDA, M.J. & JONES, P.A. (1980). Degradation of connective tissue matrices by macrophages. I. Proteolysis of elastine, glycoproteins and collagen by proteinases isolated from macrophages. *J. Exp. Med.*, **152**, 1340–1357.

YOSHIMURA, T., ROBINSON, E.A., TANAKA, S., APPELLA, E. & LEONARD, E.J. (1989). Purification and amino acid analysis of two human monocyte chemotractants produced by phytohemaglutinin-stimulated human blood mononuclear leukocytes. *J. Immunol.*, **142**, 1956–1962.

(Received July 21, 1993
Revised September 21, 1993
Accepted October 13, 1993)

Br. J. Pharmacol. (1994), **111**, 582–588

Potentiation by tonic A_{2a}-adenosine receptor activation of CGRP-facilitated [^{3}H]-ACh release from rat motor nerve endings

P. Correia-de-Sá & *[1]J.A. Ribeiro

Laboratory of Pharmacology, ICBAS, University of Oporto, 4000 Oporto, and *Laboratory of Pharmacology, Gulbenkian Institute of Science, 2781 Oeiras, Portugal

1 The effect of calcitonin gene-related peptide (CGRP) on [^{3}H]-acetylcholine ([^{3}H]-ACh) release from motor nerve endings and its interaction with presynaptic facilitatory A_{2a}-adenosine and nicotinic acetylcholine receptors was studied on rat phrenic nerve-hemidiaphragm preparations loaded with [^{3}H]-choline.

2 CGRP (100–400 nM) increased electrically evoked [^{3}H]-ACh release from phrenic nerve endings in a concentration-dependent manner.

3 The magnitude of CGRP excitation increased with the increase of the stimulation pulse duration from 40 μs to 1 ms, keeping the frequency, the amplitude and the train length constants. With 1 ms pulses, the evoked [^{3}H]-ACh release was more intense than with 40 μs pulse duration.

4 Both the nicotinic acetylcholine receptor agonist, 1,1-dimethyl-4-phenylpiperazinium, and the A_{2a} adenosine receptor agonist, CGS 21680C, increased evoked [^{3}H]-ACh release, but only CGS 21680C potentiated the facilitatory effect of CGRP. This potentiation was prevented by the A_{2a} adenosine receptor antagonist, PD 115,199.

5 Adenosine deaminase prevented the excitatory effect of CGRP (400 nM) on [^{3}H]-ACh release. This effect was reversed by the non-hydrolysable A_{2a}-adenosine receptor agonist, CGS 21680C.

6 The nicotinic antagonist, tubocurarine, did not significantly change, whereas the A_2-adenosine receptor antagonist, PD 115,199, blocked the CGRP facilitation. The A_1-adenosine receptor antagonist, 1,3-dipropyl-8-cyclopentylxanthine, potentiated the CGRP excitatory effect.

7 The results suggest that the facilitatory effect of CGRP on evoked [^{3}H]-ACh release from rat phrenic motor nerve endings depends on the presence of endogenous adenosine which tonically activates A_{2a}-adenosine receptors. Since both CGRP and A_{2a}-adenosine receptors are positively coupled to the adenylate cyclase/cyclic AMP system, cooperation between these receptors might occur at the second messenger transduction system level.

Keywords: Calcitonin gene-related peptide; A_{2a}-adenosine receptor; nicotinic acetylcholine receptor; adenosine deaminase; [^{3}H]-acetylcholine release; motor nerve terminals; rat diaphragm

Introduction

A_{2a}-adenosine receptors are present at rat phrenic motor nerve terminals enhancing the evoked release of acetylcholine (ACh) (Correia-de-Sá *et al.*, 1991). In a recent report, Correia-de-Sá & Ribeiro (1993) showed that facilitation of evoked [^{3}H]-ACh release from the phrenic-diaphragm preparation by an activator of the catalytic subunit of adenylate cyclase, forskolin, depends on A_{2a}-adenosine receptor activation by endogenous adenosine.

Calcitonin gene-related peptide (CGRP) is co-secreted with ACh at the motor endplates of mammals (Rodrigo *et al.*, 1985; Takami *et al.*, 1985), and increases ACh release apparently through stimulation of adenylate cyclase activity (Kobayashi *et al.*, 1987; Mullholland & Jaffer, 1990) increasing intracellular accumulation of cyclic AMP (Takami *et al.*, 1986). It therefore seemed of interest to investigate whether activation of A_{2a}-adenosine receptors by endogenous adenosine and selective A_{2a} receptor agonists affects the enhancement of [^{3}H]-ACh release caused by CGRP at phrenic motor nerve endings. Interactions between CGRP and nicotinic presynaptic receptors which also mediate facilitation of [^{3}H]-ACh release (Wessler *et al.*, 1986) were also examined.

[1] Author for correspondence.

Methods

[^{3}H]-acetylcholine release

The experiments were carried out on rat phrenic nerve-hemidiaphragm preparations (8 mm width) from Wistar rats of either sex of about 200 g in weight. The procedures used for labelling the preparations and measuring evoked [^{3}H]-ACh release were described previously by Correia-de-Sá *et al.* (1991) with minor modifications. Briefly, the preparations were superfused (3 ml min^{-1}) in 3 ml organ baths at 37°C with Krebs solution continuously gassed with 95% O_2 and 5% CO_2, containing (mM): NaCl 137, KCl 2.7, $CaCl_2$ 1.8, $MgCl_2$ 1, NaH_2PO_4 0.4, $NaHCO_3$ 11.9, glucose 11.2 and choline 0.001. After a 30 min equilibration period the perfusion was stopped and the nerve endings were labelled during 40 min with 1 μM [^{3}H]-choline (specific activity 2.5 μCi nmol^{-1}) under electrical stimulation at 1 Hz with supramaximal rectangular pulses of 15 V and 40 μs duration. After the end of the labelling period, the preparations were again superfused (15 ml min^{-1}) and the nerve stimulation stopped. From this time onwards hemicholinium-3 (10 μM) was present to prevent uptake of choline. After a 60 min period of washout, the perfusion was stopped, and 3 ml bath samples were collected every 3 min by emptying and refilling again the organ bath with the solution in use. Aliquots (1 ml) of the incubation medium were added to 6 ml of Packard Insta Gel II scintillator. Radioactivity was measured in a Beckman

model LS 3801 scintillation spectrometer. [^{3}H]-ACh release was evoked by electrical nerve stimulation at 5 Hz frequency with trains of 750 supramaximal rectangular pulses of 15 V and 40 μs or 1 ms duration, which were monitored with a Meguro model MO-1251A oscilloscope. Two stimulation periods were used: at 12 min (S_1) and at 39 min (S_2) after the end of washout (zero time). It was shown (see Wessler & Kilbinger, 1986) that [^{3}H]-ACh release evoked by electrical stimulation of the phrenic nerve with pulses of up to 500 μs duration is abolished in the absence of calcium ions or by tetrodotoxin (TTX). In the present work we confirmed that TTX (1 μM) abolished the evoked [^{3}H]-ACh release elicited by electrical stimulation pulses with durations between 40 and 500 μs; with pulses of 1 ms duration, the evoked [^{3}H]-ACh release in the presence of TTX (1 μM) persisted as 40 ± 7% ($n = 4$) of the control values. Moreover, electrical stimulation of the phrenic nerve increased only the release of [^{3}H]-ACh while the output of [^{3}H]-choline remained unchanged (Wessler & Kilbinger, 1986). Therefore, evoked [^{3}H]-ACh release was calculated by subtracting the basal tritium outflow from the total tritium outflow during the stimulation period (cf. Correia-de-Sá *et al.*, 1991). Test drugs were added 15 min before S_2 and were present up to the end of the experiments. Their effects were expressed by the ratios S_2/S_1, i.e. the ratio between the evoked [^{3}H]-ACh release during the second stimulation period (in the presence of the test drug) and the evoked [^{3}H]-ACh release during the first stimulation period (without the test drug).

Drug interactions

When testing the ability of the nicotinic acetylcholine antagonist, (+)-tubocurarine (TC), the A_2-adenosine agonist, CGS 21680C, the A_2-adenosine antagonist, PD 115,199, the A_1-adenosine antagonist, 1,3-dipropyl-8-cyclopentylxanthine (DPCPX) and adenosine deaminase (ADA) (which deaminates adenosine into the inactive derivative inosine) to modify the effect of CGRP, the preparations were pretreated with those drugs 15 min before each stimulation period and were washed out immediately after each stimulation period, i.e. they were present in both S_1 and S_2, whereas CGRP was present only in S_2. In the experiments where the nicotinic agonist, 1,1-dimethyl-4-phenylpiperazinium (DMPP), was used, shorter, but efficient, pretreatment periods of 3 min were carried out before S_1 and S_2, to avoid presynaptic nicotinic acetylcholine receptor desensitization (Wessler *et al.*, 1986); in these experiments CGRP was also present only in S_2. When the same drugs were present in both S_1 and S_2, the S_2/S_1 ratios were not appreciably different from those obtained in control conditions, i.e., without addition of drugs (S_2/S_1 values were 0.81 ± 0.03, $n = 8$, and 0.81 ± 0.02, $n = 3$, for trains of 40 μs and 1 ms pulse width, respectively, see Table 1). Averaged evoked [^{3}H]-ACh release during S_1 (S_1 average) in control conditions were 30.3 ± 1.7 × 10^3 d.p.m. g^{-1} (n = 19) and 37.8 ± 3.5 × 10^3 d.p.m. g^{-1} ($n = 21$) of wet weight of preparation, which corresponds to about 25% increase in [^{3}H]-ACh release when the stimulation pulse was enlarged from 40 μs to 1 ms, keeping the frequency and the train length constants (cf. Ohhashi & Jacobowitz, 1988). The concentrations of CGS 21680C (1 nM–3 μM), PD 115,199 (25–100 nM) and DPCPX (2.5–5 nM) used, when present only in S_2, have been tested previously, and their effects on evoked [^{3}H]-ACh release from rat phrenic motor nerve terminals described (see Correia-de-Sá *et al.*, 1991; 1992). The effects of DMPP (1–30 μM) and TC (1–10 μM) on [^{3}H]-ACh release were previously investigated (Wessler *et al.*, 1986), and their effects were also studied in the presently described experimental conditions; similar results were obtained (see Results). None of the compounds used to interact with CGRP modified in a measurable way the basal tritium outflow.

Drugs

Adenosine deaminase (ADA) (type II), rat cyclic calcitonin gene-related peptide (CGRP), choline chloride, 1,1-dimethyl-4-phenylpiperazinium iodide (DMPP), hemicholinium-3, Sigmacote, tetrodotoxin (TTX), (+)-tubocurarine chloride USP grade (TC) (Sigma); CGS 21680C (2-[*p*-(2-carboxyethylphenethylamino]-5′-N-ethylcarboxamide adenosine), 1,3-dipropyl-8-cyclopentylxanthine (DPCPX) (Res. Biochem. Inc.); [methyl-^{3}H]-choline chloride (ethanol solution, 80 Ci $mmol^{-1}$) (Amersham); PD 115,199 (N-(2-(dimethylamino)-ethyl)-N-methyl-4-(2,3,6,7-tetrahydro-2,6-dioxo-1,3-dipropyl-1H-purine-8-yl)-benzene sulphonamide) was a gift from Dr R.F. Bruns of Park-Davis (U.S.A.). DPCPX was made up in a 5 mM stock solution in 99% dimethylsuphoxide (DMSO)/1% NaOH 1 M (v/v); PD 115,199 was made up in a 1 mM stock solution in 80% methanol/20% NaOH 1 M (v/v). All stock solutions were stored as frozen aliquots at − 20°C. Dilutions of these stock solutions and appropriate solvent controls were made.

Handling of calcitonin gene-related peptide (CGRP): CGRP is readily adsorbed onto plastic. To minimize losses, all plastiware used in handling CGRP (i.e. pipette tips, Eppendorf tubes, automatic pumps) were pretreated with Sigmacote,

Table 1 The influence of stimulation pulse width on the facilitation induced by calcitonin gene-related peptide (CGRP), adenosine deaminase (ADA), CGS 21680C, (+)tubocurarine (TC) and 1,1-dimethyl-4-piperazinium iodide (DMPP) on evoked [^{3}H]-acetylcholine ([^{3}H]-ACh) release

		40 μs	*1 ms*
		S_1 average (× 10^3 d.p.m. g^{-1})	
		30.3 ± 1.7 (19)	37.8 ± 3.5 (21)***
		S_2/S_1	
Control		0.81 ± 0.03 (8)	0.81 ± 0.02 (3)
CGRP	200 nM	0.86 ± 0.06 (3)	1.13 ± 0.01 (4)*,**
ADA	0.5 u ml^{-1}	1.00 ± 0.05 (5)*	0.72 ± 0.06 (3)**
	2.5 u ml^{-1}	1.03 ± 0.04 (2)*	1.11 ± 0.10 (3)*
CGS	2 nM	1.00 ± 0.02 (4)*	1.09 ± 0.09 (4)*
TC	0.1 μM	0.75 ± 0.03 (3)	0.82 ± 0.07 (4)
	1 μM	0.43 ± 0.10 (3)*	0.88 ± 0.05 (3)**
DMPP	1 μM	1.13 ± 0.05 (3)*	1.15 ± 0.08 (2)*

CGRP, ADA, CGS 21680C and TC were added 15 min before S_2 and remained in the bath solution until the end of the experiments. DMPP was added 3 min before and was washed out immediately after S_2. 750 supramaximal intensity, 5 Hz frequency and 40 μs or 1 ms duration were used.

*$P < 0.05$ (Student's t test) when compared to S_2/S_1 ratio obtained in control conditions; **$P < 0.05$ (Student's t test) when compared to S_2/S_1 ratio obtained with the same drug when 40 μs stimulation pulses were applied; ***$P < 0.01$ (Student's t test) as compared to S_1 evoked release when 40 μs pulses were applied.

which is a silicone solution water repellent that easily forms a tight, microscopically thin film on glass and plastic. Control experiments in which Sigmacote was used were not significantly different from those in its absence.

Statistics

The data are expressed as mean ± s.e.mean from n number of experiments. The significance of the differences was evaluated by Student's t test. $P<0.05$ were considered to represent a significant difference.

Results

Effects of CGRP

A typical effect of CGRP (200 nM) applied 15 min before S_2 is illustrated in Figure 1, where it is shown that the effect of CGRP was dependent upon the width of pulse stimulation. When pulse width was 40 μs, CGRP caused little or no effect on [^{3}H]-ACh release, but with a pulse width of 1 ms, CGRP markedly increased [^{3}H]-ACh release. Similar results on evoked [^{3}H]-ACh release with CGRP (100–800 nM) were obtained in fourteen other experiments where pulses of 1 ms duration were used (Figure 2). The effect of CGRP (100–400 nM) was concentration-dependent, and a concentration of 800 nM did not cause a greater increase in [^{3}H]-ACh release than that of 400 nM (see Figure 2). In three out of seven experiments, CGRP (200 nM) increased basal tritium outflow by 20.3 ± 1.9 × 10^3 d.p.m. g^{-1}. This facilitatory effect on spontaneous tritium outflow was observed immediately after CGRP (200 nM) application and lasted 6–9 min.

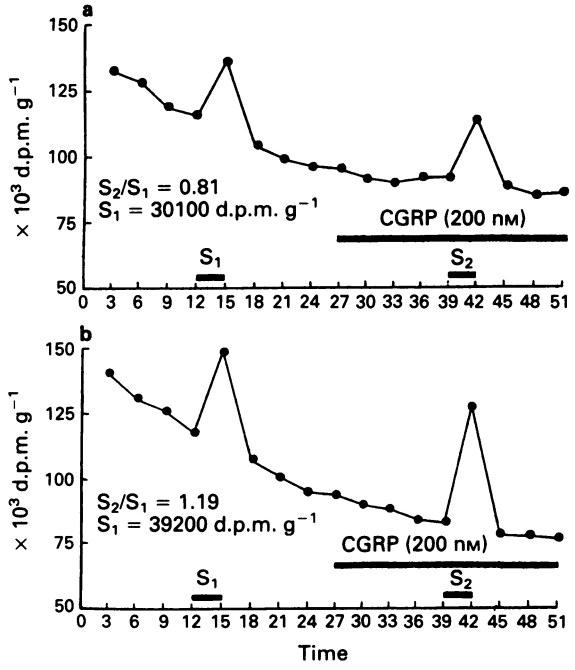

Figure 1 Effect of calcitonin gene-related peptide (CGRP, 200 nM) on tritium outflow from rat phrenic nerve terminals labelled with [^{3}H]-choline: influence of stimulation pulse width (40 μs and 1 ms). After the labelling and washout periods, [^{3}H]-acetylcholine ([^{3}H]-ACh) release was elicited by two electrical nerve stimulations with 750 pulses, 5 Hz frequency and (a) 40 μs and (b) 1 ms pulse width applied at the indicated times (S_1 and S_2). Tritium outflow was measured in samples collected every 3 min. CGRP was applied 15 min before S_2 and remained in the bath until the end of the experiments, as represented by the horizontal bar. S_1 averages and S_2/S_1 ratios were also given for comparison.

CGRP and A_{2a}-adenosine receptor activation

It is well established that adenosine is formed and accumulated extracellularly at neuromuscular junctions and that this accumulation of adenosine depends on the intensity of electrical stimulation (Cunha & Sebastião, 1993). As adenosine, through A_{2a}-adenosine receptor activation, can increase [^{3}H]-ACh release from phrenic nerve terminals (Correia-de-Sá *et al.*, 1991), we decided to investigate how inactivation of adenosine by adenosine deaminase (ADA) modifies the response to CGRP, as well as how the A_{2a} adenosine receptor agonist (CGS 21680C) interacts with CGRP.

ADA, the enzyme that hydrolyses adenosine into inosine, was applied 15 min before S_2 using stimulation pulse trains with 40 μs duration. In these conditions ADA increased the S_2/S_1 ratio to 1.00 ± 0.05 ($n = 5$) for ADA (0.5 u ml^{-1}) and to 1.03 ± 0.04 ($n = 2$) for ADA (2.5 u ml^{-1}) as compared with a control S_2/S_1 ratio of 0.81 ± 0.03 ($n = 8$) (Table 1). This effect of ADA is probably the consequence of removing the tonic inhibitory influence of adenosine as previously suggested (Ribeiro & Sebastião, 1987). When increasing the intensity of stimulation by increasing the duration of the pulse to 1 ms, ADA (0.5 u ml^{-1}) did not change or slightly decreased the ratio S_2/S_1 (0.72 ± 0.06, $n = 3$), as compared with the control (0.81 ± 0.02, $n = 3$), but in a higher amount ADA (2.5 u ml^{-1}) significantly increased [^{3}H]-ACh release up to 1.11 ± 0.10 ($n = 3$) (equivalent to 37% increase in [^{3}H]-ACh release when compared to control) (Table 1). The need to increase the ADA concentration to observe its excitatory effect on [^{3}H]-ACh release induced by wider stimulation pulses, probably resulted from greater extracellular adenine nucleotides/adenosine accumulation, in consequence of increasing stimulus intensity (Silinsky, 1975; Cunha & Sebastião, 1993).

To investigate the role of adenosine in the excitatory effect of CGRP on evoked [^{3}H]-ACh release, experiments were carried out in which the effect of this peptide, applied 15 min

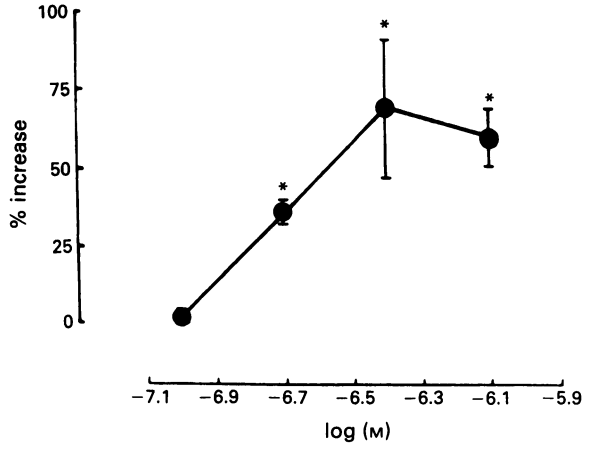

Figure 2 Concentration-response curve for the facilitatory effect of calcitonin gene-related peptide (CGRP) on electrically-evoked tritium outflow from phrenic-diaphragm preparations loaded with [^{3}H]-choline. Evoked [^{3}H]-acetylcholine ([^{3}H]-ACh) release was elicited by nerve stimulation with 5 Hz frequency and supramaximal intensity (15 V) 750 pulses of 1 ms width. The ordinates are percentage increases in the S_2/S_1 ratios as compared with the S_2/S_1 ratios in control experiments. Zero percent represents identity between the two ratios. Average S_2/S_1 ratio in control experiments: 0.81 ± 0.02 ($n = 3$). Average of evoked tritium outflow during S_1: 37.8 ± 3.8 × 10^3 d.p.m. g^{-1} of wet weight of preparation ($n = 15$). CGRP was applied 15 min before the end of S_2 and remained in the bath up to the end of the experiments. Each point is the mean of 3–4 experiments. The vertical bars represent ± s.e.mean, and are shown when they exceed the symbols in size. *$P<0.05$ (Student's t test) when compared with zero percent.

before S_2 in a supramaximal concentration of 400 nM, was studied in the presence of ADA, applied in both S_1 and S_2 with a pulse duration of 1 ms. It was observed that ADA (2.5 u ml^{-1}) (S_1 average: $50.4 \pm 3.3 \times 10^3$ d.p.m. g^{-1}, $n = 4$) prevented the excitatory effect of CGRP (400 nM) (see Figure 3). This blockade seems to depend on the intensity of adenosine deamination, since a submaximal concentration of ADA (0.5 u ml^{-1}) (S_1 average: $35.9 \pm 4.0 \times 10^3$ d.p.m. g^{-1}, $n = 2$), applied in the same conditions, decreased the excitatory effect of CGRP (400 nM) by only 50% ($n = 2$, data not shown). Using the stable A_{2a}-selective adenosine analogue, CGS 21680C, in a concentration (2 nM) near its EC_{50} value for the increase in evoked [^{3}H]-ACh release (see Correia-de-Sá *et al.*, 1991), together with ADA (2.5 u ml^{-1}), in both S_1 and S_2 (S_1 average: $63.4 \pm 5.3 \times 10^3$ d.p.m. g^{-1}, $n = 4$), the facilitation induced by CGRP (400 nM), applied only in S_2, recovered to almost its value obtained in the absence of ADA (2.5 u ml^{-1}) + CGS 21680C (2 nM). The effect of CGRP (400 nM) was blocked by the A_2 adenosine antagonist, PD 115,199 (25 nM) (S_1 average: $37.0 \pm 2.1 \times 10^3$ d.p.m. g^{-1}, $n = 4$), and was greatly enhanced by the A_1 antagonist, DPCPX (2.5 nM) (S_1 average: $39.1 \pm 2.0 \times 10^3$ d.p.m. g^{-1}, $n = 4$). ADA (0.5–2.5 u ml^{-1}), CGS 21680C (2 nM), PD 115,199 (25 nM) and DPCPX (2.5 nM) applied in both S_1 and S_2 were virtually devoid of effects on the S_2/S_1 ratio.

CGRP (200 nM) applied in S_2 was tested during stimulation (40 μs pulse duration), in which on its own it was virtually devoid of effect on [^{3}H]-ACh release (see Figure 4). However, when using the A_{2a} agonist, CGS 21680C (2 nM, a concentration near its EC_{50} value), in both S_1 and S_2, the excitatory effect of CGRP (200 nM) became apparent. In these conditions, this peptide increased [^{3}H]-ACh release by $49 \pm 4\%$ ($n = 4$), which is a significantly ($P < 0.05$) higher effect than that obtained by increasing stimulus intensity (pulse width change from 40 μs to 1 ms) ($36 \pm 4\%$, $n = 4$). In both conditions, pretreatment with CGS 21680C (2 nM, 40 μs) (S_1 average: $36.6 \pm 1.9 \times 10^3$ d.p.m. g^{-1}, $n = 7$) and increase in pulse duration to 1 ms (S_1 average: $37.8 \pm 3.5 \times 10^3$ d.p.m. g^{-1}, $n = 21$), resulted in similar increase in evoked [^{3}H]-ACh release in both stimulation periods, when compared to control conditions with 40 μs pulse duration (S_1 average: $30.3 \pm 1.7 \times 10^3$ d.p.m. g^{-1}, $n = 19$). The potentiation of the effect of CGRP by CGS 21680C was prevented by applying the A_2 antagonist, PD 115,199 (25 nM), together with CGS 21680C (2 nM) (S_1 average: $28.0 \pm 1.8 \times 10^3$ d.p.m. g^{-1}, $n = 6$).

CGRP and nicotinic receptor activation

Increase in the intensity of electrical stimulation of the rat phrenic nerve enhances ACh release from the motor nerve terminals. This increase in ACh release could mediate a positive feed-back mechanism by activating nicotinic autoreceptors (Wessler *et al.*, 1986). The increase in pulse width from 40 μs to 1 ms increased evoked [^{3}H]-ACh release by about 25% (Table 1). To examine the role of presynaptic nicotinic receptor activation in the facilitatory effect of CGRP on the release of evoked [^{3}H]-ACh, we performed experiments with the nicotinic agonist, DMPP, to stimulate, and with the nicotinic antagonist, TC, to block these receptors. DMPP (0.3–1 μM) increased in a concentration-dependent manner [^{3}H]-ACh release when applied 3 min before S_2 and washed out immediately after S_2. A maximal increase in evoked [^{3}H]-ACh release of $40 \pm 3\%$ ($n = 4$) occurred with a

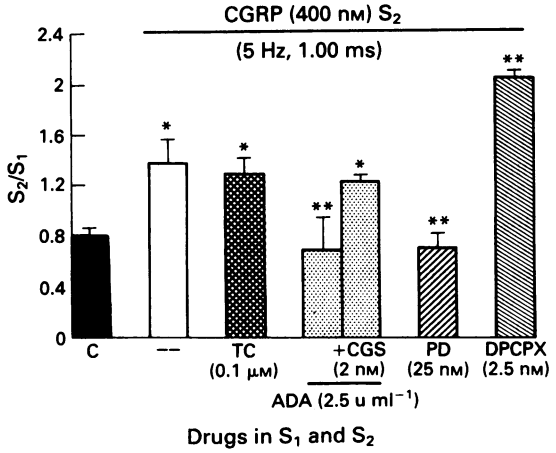

Figure 3 Effects of (+)-tubocurarine (TC), adenosine deaminase (ADA), CGS 21680C, PD 115,199 (PD) and 1,3-dipropyl-8-cyclopentylxanthine (DPCPX) on the excitatory effect of calcitonin gene-related peptide (CGRP) on electrically-evoked [^{3}H]-acetylcholine ([^{3}H]-ACh) release from rat phrenic nerve endings loaded with 1 μM [^{3}H]-choline (specific activity 2.5 μCi $nmol^{-1}$). After labelling the preparations, hemicholinium-3 (10 μM) was present to prevent re-uptake of choline. TC (0.1 μM), ADA (2.5 u ml^{-1}), ADA (2.5 u ml^{-1}) + CGS 21680C (2 nM), PD 115,199 (25 nM) and DPCPX (2.5 nM) were added to the bath solution 15 min before and were immediately washed out after each stimulation period (S_1 and S_2) (5 Hz, 750 pulses, 1 ms pulse width); the S_2/S_1 ratios obtained under these conditions were not statistically different from the ratios obtained in control experiments (C, without any drug during S_1 and S_2) (S_2/S_1 ratio = 0.81 ± 0.02, $n = 3$). CGRP (400 nM) was applied 15 min before S_2. The ordinates represent evoked tritium outflow expressed by S_2/S_1 ratios. Each column represents pooled data from 3–4 experiments. The vertical bars represent ± s.e.mean. *$P < 0.05$ (Student's t test) when compared to S_2/S_1 ratio in control conditions; **$P < 0.05$ (Student's t test) when compared with the effect of CGRP in the absence of drugs, respectively.

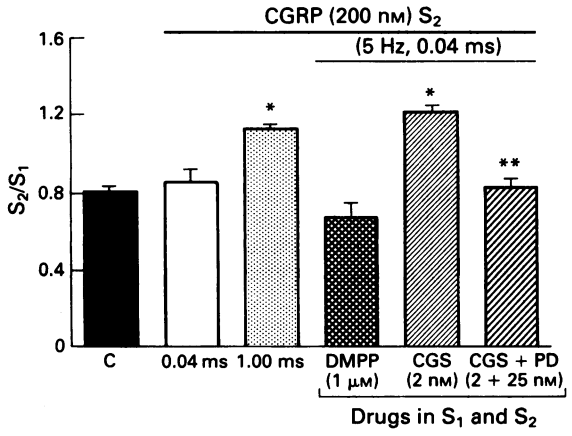

Figure 4 Stimulation pulse enlargement and activation of presynaptic A_{2a}-adenosine receptors, but not nicotinic cholinoceptors, potentiate the excitatory effects of calcitonin gene-related peptide (CGRP, 200 nM) on electrically evoked [^{3}H]-acetylcholine ([^{3}H]-ACh) release from rat phrenic nerve endings loaded with 1 μM [^{3}H]-choline (specific activity 2.5 μCi $nmol^{-1}$). After labelling the preparations, hemicholinium-3 (10 μM) was present to prevent re-uptake of choline. CGS 21680C (2 nM) with or without PD 115,199 (25 nM) were added 15 min before, whereas 1,1-dimethyl-4-piperazinium iodide (DMPP, 1 μM) was added 3 min before, and both were immediately washed out from the bath after each stimulation period (drugs in S_1 and S_2) (5 Hz, 750 pulses, 40 μs); in another set of experiments, evoked [^{3}H]-ACh release was induced by supramaximal intensity electrical stimulation (5 Hz, 750 pulses) with 1 ms pulse width, in both S_1 and S_2. The S_2/S_1 ratios obtained under those conditions were not statistically different from the ratio obtained in control experiments (C, without any drug during S_1 and S_2, 750 pulses, 40 μs) (S_2/S_1 ratio = 0.81 ± 0.03, $n = 8$). CGRP (200 nM) was applied 15 min before S_2. The ordinates represent evoked tritium outflow expressed by S_2/S_1 ratios. Each column represents pooled data from 3–8 experiments. The vertical bars represent ± s.e.mean. *$P < 0.05$ (Student's t test) when compared to S_2/S_1 ratio in control conditions; **$P < 0.05$ (Student's t test) when compared with the effect of CGRP in the presence of CGS 21680C.

concentration of DMPP of 1 μM, whilst a concentration of 10 μM was less effective (increase in [^{3}H]-ACh release of 20 ± 4%, $n = 2$). The facilitatory effects of DMPP on [^{3}H]-ACh release were not statistically different ($P > 0.05$) (Table 1), during electrical stimulations with pulses of 40 μs or 1 ms duration. DMPP (1 μM), applied 15 min before S_2, as we did with other compounds, did not facilitate [^{3}H]-ACh release, and in a concentration of 10 μM even decreased evoked [^{3}H]-ACh release by 20 ± 6% ($n = 2$), as previously described (see Wessler *et al.*, 1986). These authors suggested that this effect of DMPP results from desensitization of presynaptic nicotinic receptors by high agonist concentration and/or longer exposure time.

The nicotinic antagonist TC (0.1–10 μM) decreased electrically evoked [^{3}H]-ACh release in a concentration-dependent manner, when added to the bathing solution 15 min before S_2. The [^{3}H]-ACh released by electrical trains with pulses of 1 ms duration were less affected by TC than by trains with pulses with shorter duration (40 μs), i.e., S_2/S_1 ratios of 0.43 ± 0.10 ($n = 3$) and 0.88 ± 0.05 ($n = 3$) were found after applying TC (1 μM) 15 min before S_2 in 40 μs and 1 ms pulse width stimulating conditions, respectively (Table 1). Since a similar potency for DMPP (1 μM) was observed in both stimulation conditions, this difference could reflect competitive antagonism between TC and the increased levels of ACh released by longer pulses. TC (0.1 μM), in a concentration virtually devoid of effect on [^{3}H]-ACh release, applied in both S_1 and S_2, blocked the excitatory effect of DMPP (1 μM, applied 3 min before S_2) and prevented the desensitization by DMPP (10 μM, applied 15 min before S_2) in relation to its ability to increase evoked tritium outflow.

TC (0.1 μM), applied in both S_1 and S_2 (S_1 average: 35.0 ± 3.1 × 10^3 d.p.m. g^{-1}) did not significantly modify the excitatory effect of CGRP used in a supramaximal concentration (400 nM, 1 ms pulse duration, $n = 4$) (see Figure 3). The effect of CGRP (200 nM, 40 μs pulse duration) on evoked [^{3}H]-ACh release, when applied in S_2 in the presence of DMPP (1 μM, added to the bathing solution 3 min before both S_1 and S_2) remained about the same (see Figure 4); DMPP (1 μM, 40 μs pulse duration) alone increased [^{3}H]-ACh release (S_1 average: 42.6 ± 3.7 × 10^3 d.p.m. g^{-1}, $n = 4$). In contrast, when the intensity of stimulation was increased by increasing pulse duration to 1 ms (S_1 average: 37.8 ± 3.5 × 10^3 d.p.m. g^{-1}, $n = 21$), the excitatory effect of CGRP (200 nM) on [^{3}H]-ACh release was greatly enhanced (Figure 4).

Discussion

The results show that the facilitatory effect of CGRP on evoked [^{3}H]-ACh release from the phrenic motor nerve endings depends on the presence of endogenous adenosine, which is tonically activating A_{2a}-adenosine receptors. Presynaptic activation of nicotinic receptors did not contribute to the excitatory effect of CGRP on ACh release.

CGRP markedly facilitated electrically evoked [^{3}H]-ACh release from rat phrenic nerve endings. It has been shown that CGRP receptor-mediated effects are positively coupled to the adenylate cyclase adenosine 3':5'-cyclic monophosphate (cyclic AMP) transducing system (Takami *et al.*, 1986; Kobayashi *et al.*, 1987), and additionally, it was demonstrated that substances that increase intracellular cyclic AMP levels also increase evoked [^{3}H]-ACh release (Correia-de-Sá *et al.*, 1992). Cyclic AMP is involved in regulating metabolic activity associated with synthesis, mobilization and storage of ACh (Wilson, 1974). It appears unlikely that the effect of CGRP is primarily mediated by an action on the synthesis of the transmitter, but rather by other mechanisms involved in transmitter release (i.e. increase release probability, mobilization, recruitment of active release zones), because after the labelling with [^{3}H]-choline and its washing out, hemicholinium-3 was added to prevent further re-uptake of [^{3}H]-choline, particularly that originating from hydrolysis of released [^{3}H]-ACh. In this condition, the synthesis of [^{3}H]-ACh was prevented (Takagi *et al.*, 1970).

CGRP can increase the frequency of miniature endplate potentials (Jinnai *et al.*, 1989). This effect is thought to reflect presynaptic events facilitating spontaneous ACh release from motor nerve endings. The increase in spontaneous tritium outflow, observed in a few experiments, immediately after exogenously applied CGRP is consistent with the above studies, and suggests that CGRP is also able to enhance spontaneous ACh release.

In the present experimental conditions, where using electrical stimulation with pulses of 1 ms duration, but not 40 μs duration, it is likely that local depolarization (TTX-insensitive) of the motor nerve endings occurs, causing increase in the probability of quantal release (see e.g. Katz, 1969; Dudel, 1989). This could explain why CGRP did not increase [^{3}H]-ACh release with pulses of 40 μs duration, but did increase the release of [^{3}H]-ACh evoked by pulses of 1 ms duration. Thus, the effect of CGRP may depend (a) on the amount of ACh, itself, being released and regulating its own release through the presynaptic nicotonic receptors (Wessler *et al.*, 1986), or (b) on the release of a factor that occurs concomitantly with the release of ACh. Substances released together with ACh upon electrical stimulation from motor nerve terminals are adenine nucleotides (Silinsky, 1975; Ribeiro & Sebastião, 1987; Smith, 1991; Cunha & Sebastião, 1993) and adenosine (Ribeiro & Sebastião, 1987; Smith, 1991; Cunha & Sebastião, 1993).

The increase in release of [^{3}H]-ACh evoked by nerve stimulation (5 Hz, 750 pulses) is, in part, regulated through activation of nicotinic receptors. The nicotinic agonist, DMPP, enhanced, and the antagonist, TC, decreased electrically evoked [^{3}H]-ACh release. The inhibitory effect of TC and its dependency on the duration of the stimulation pulse, taken together with the fact that no change was found in the sensitivity of the nicotinic receptors to agonists, namely to DMPP, when comparing the effect of DMPP in both (40 μs and 1 ms pulse duration) stimulation conditions, indicate that these nicotinic autoreceptors mediate a positive feedback and, therefore, ACh may enhance its own release during repetitive nerve stimulation. The facilitatory action of DMPP declined when the incubation time was increased from 3 min to 15 min before stimulation. Moreover, a concentration of 10 μM DMPP was less effective than a concentration of 1 μM, suggesting that the presynaptic nicotinic receptor like other nicotinic receptors present in muscle, ganglia, sympathetic neurones and central neurones can be desensitized by increasing the concentration of the agonist, or by prolonging incubation time with the agonist (for a review see Wessler, 1989). Pretreatment with the nicotinic antagonist, TC, prevented the desensitization induced by a high concentration of DMPP (10 μM) incubated for 15 min.

The increase in the evoked [^{3}H]-ACh release caused by ADA is in agreement with previous findings (Ribeiro & Sebastião, 1987), suggesting that endogenous adenosine is tonically inhibiting ACh release. However, when the width of the stimulation pulse was increased from 40 μs to 1 ms, ADA (0.5 u ml^{-1}) had virtually no effect on [^{3}H]-ACh release, whereas when the amount of ADA (2.5 u ml^{-1}) was increased a consistent excitatory effect was obtained. This probably results from greater increase in extracellular adenosine accumulation, by release as such and/or formed from ATP degradation (Cunha & Sebastião, 1993), requiring higher amounts of ADA to be inactivated. In both stimulation conditions (40 μs and 1 ms pulse duration), no significant change was observed in the dose-response curves obtained for the excitatory effect of the A_{2a} stable adenosine agonist, CGS 21680C. This suggests that the sensitivity for the A_{2a}-adenosine receptor agonist was not markedly modified by increasing stimulus intensity and by the increase in endogenous adenosine levels.

It was demonstrated in the present work that the excitatory effect of CGRP on evoked [^{3}H]-ACh release depends on

the presence of endogenous adenosine, since ADA, an enzyme that inactivates adenosine to the inactive compound inosine (Arch & Newsholme, 1978), prevented this effect. Furthermore, we concluded that facilitation by CGRP cannot be evident without A_{2a} receptor activation from the findings that CGRP maximal excitation was blocked by pretreatment with the A_{2a}-adenosine antagonist, PD 115,199, and, that the ADA prevention of the CGRP effect on [^{3}H]-ACh release was almost completely reversed by applying the non-hydrolysable A_{2a}-adenosine agonist, CGS 21680C, together with ADA. The potentiating effect of CGS 21680C on the excitatory action of CGRP was indeed mediated through A_{2a} receptors, since this effect was completely antagonized by PD 115,199. The facilitation of evoked [^{3}H]-ACh release by CGRP was greatly potentiated when the A_1-inhibitory adenosine receptors were antagonized by the A_1 receptor antagonist, DPCPX, which indicates that tonic A_1-adenosine receptor activation is in part counteracting the A_{2a}-adenosine receptor-mediated potentiation. In the experimental conditions used in the present work, no interaction was found between CGRP and nicotinic receptor activation, because pretreatment with the nicotinic antagonist, TC, applied in a concentration sufficient to block the excitatory effect of DMPP, did not significantly modify the facilitatory action of CGRP, contrasting with the effects caused by ADA, CGS 21680C, PD 115,199 and DPCPX when applied in the same conditions.

The A_{2a} receptor agonist, CGS 21680C, but not the nicotinic receptor agonist, DMPP, (1) potentiated the effect of CGRP, when applied in conditions where no facilitation by CGRP on evoked [^{3}H]-ACh release was observed (5 Hz frequency, 40 μs), and (2) reversed the blockade of the effect of CGRP induced by ADA. The peptide facilitatory action on neurotransmission, observed when ACh release was induced by pulses of 1 ms duration, was reproduced in preparations stimulated with 40 μs pulses pretreated with CGS 21680C. These results suggest that the increase in extracellular endogenous adenosine, rather than the increase in ACh release, plays a critical role in the CGRP facilitation of ACh release depending on the presynaptic A_{2a}-adenosine receptor activation. The fact that both the receptor for CGRP (Takami *et al.*, 1986; Kobayashi *et al.*, 1987) and the A_{2a}-adenosine receptor (Correia-de-Sá *et al.*, 1992), are positively coupled to the adenylate cyclase/cyclic AMP transducing system, could indicate that cooperation between CGRP and CGS 21680C occurs at the level of the second messenger transducing system.

We recently showed (Correia-de-Sá & Riberior, 1993), that the excitatory effect of the catalytic subunit adenylate cyclase activator, forskolin, on evoked [^{3}H]-ACh release from rat phrenic nerve endings depends on tonic A_{2a}-adenosine receptor activation. The increase in evoked [^{3}H]-ACh release from rat phrenic motor nerve endings in consequence of adenylate cyclase stimulation via receptor activation, by the A_{2a}-adenosine agonist (CGS 21680C), or by CGRP, is about twice as effective as direct activation induced by forskolin. Since it has been reported that forskolin preferentially binds and activates adenylate cyclase when this enzyme is bound to the stimulatory G-protein G_s (Battaglia *et al.*, 1986), and, consequently, interacts synergistically with agents that activate adenylate cyclase through G_s-proteins (Seamon & Daly, 1983), our observations might suggest that signal transduction amplification occurs at the receptor/G_s-protein level. Whether the activation of A_{2a}-adenosine receptors, facilitate interaction of forskolin or CGRP with adenylate cyclase by recruiting G_s proteins and increasing the availability of the catalytic subunit (Alousi *et al.*, 1991), remains to be investigated. Besides suggestions that CGRP increases ACh release via a cyclic AMP-dependent pathway (Mullholland & Jaffer, 1990), this neuropeptide can also, in part, increase ACh release through activation of neuronal calcium channels (Wiley *et al.*, 1992).

In conclusion, the present results support a physiological role for the A_{2a}-adenosine receptors present at the motor nerve terminals. It appears that substances that facilitate neurotransmitter release through activation of adenylate cyclase increasing cyclic AMP accumulation, need the presence of endogenous adenosine tonically activating A_{2a}-adenosine receptors.

We gratefully acknowledge the skilful technical assistance of Dr M.A. Timóteo, and thank Dr A.M. Sebastião for critically reading the manuscript. We thank Warner-Lambert/Park-Davis for the gift of PD 115,199. The work performed in ICBAS is supported by JNICT (PMCT/C/SAU/792-90). P.C.S. is in receipt of a JNICT Ph.D. studentship (BD/721-90-ID).

References

ALOUSI, A.A., JASPER, J.R., INSEL, P.A. & MOTULSKY, H.J. (1991). Stoichiometry of receptor-G_s-adenylate cyclase interactions. *FASEB J.*, **5**, 2300–2303.

ARCH, J.R.S. & NEWSHOLME, E.A. (1978). The control of metabolism and the hormonal role of adenosine. In *Essays in Biochemistry*, Vol. 14, ed. Campbell, P.N. & Aldridge, W.N. pp. 82–123. New York: Academic Press.

BATTAGLIA, G., NORMAN, A.B., HESS, E.J. & CREESE, I. (1986). Forskolin potentiates the stimulation of striatal adenylate cyclase mediated by D-1 dopamine receptors, guanine nucleotides and sodium fluoride. *J. Neurochem.*, **46**, 1180–1185.

CORREIA-DE-SÁ, P. & RIBEIRO, J.A. (1993). Facilitation of [^{3}H]-ACh release by forskolin depends on A_2-adenosine receptor activation. *Neurosci. Lett.*, **151**, 21–24.

CORREIA-DE-SÁ, P., SEBASTIÃO, A.M. & RIBEIRO, J.A. (1991). Inhibitory and excitatory effects of adenosine receptor agonists on evoked transmitter release from phrenic nerve endings of the rat. *Br. J. Pharmacol.*, **103**, 1614–1620.

CORREIA-DE-SÁ, P., TIMÓTEO, M.A. & RIBEIRO, J.A. (1992). Presynaptic A_2 adenosine receptors of the motor nerve endings of the rat are coupled to adenylate cyclase/cyclic AMP transducing system. *Br. J. Pharmacol.*, **105** (Suppl.), 312P.

CUNHA, R.A. & SEBASTIÃO, A.M. (1993). Adenosine and adenine nucleotides are independently released from both the nerve terminals and the muscle fibers upon electrical stimulation of the innervated skeletal muscle of the frog. *Pflügers Arch.*, **424**, 503–510.

DUDEL, J. (1989). Nerve terminal depolarization, calcium inflow and transmitter release. In *Neuromuscular Junction*, ed. Sellin, L.C., Libelius, R. & Thesleff, S. pp. 149–159. Amsterdam: Elsevier.

JINNAI, K., CHIHARA, K., KANDA, F., TADA, K. & FUJITA, T. (1989). Calcitonin gene-related peptide enhances spontaneous release from the rat motor nerve terminal. *Neurosci. Lett.*, **103**, 64–68.

KATZ, B. (1969). *The Release of Neural Transmitter Substances.* pp. 31–39. Liverpool: Liverpool University Press.

KOBAYASHI, H., HASHIMOTO, K., UCHIDA, S., SAKUMA, J., TAKAMI, K., TOHYAMA, M., IZUMI, F. & YOSHIDA, H. (1987). Calcitonin gene-related peptide stimulates adenylate cyclase activity in rat striated muscle. *Experientia*, **43**, 314–316.

MULLHOLLAND, M.W. & JAFFER, S. (1990). Stimulation of acetylcholine release in myenteric plexus by calcitonin gene-related peptide. *Am. J. Physiol.*, **259**, G934–G939.

OHHASHI, T. & JACOBOWITZ, D.M. (1988). Effects of calcitonin gene-related peptide on neuromuscular transmission in the isolated rat diaphragm. *Peptides*, **9**, 613–617.

RIBEIRO, J.A. & SEBASTIÃO, A.M. (1987). On the role, inactivation and origin of endogenous adenosine at the frog neuromuscular junction. *J. Physiol.*, **384**, 571–585.

RODRIGO, J., POLAK, J.M., FERNANDEZ, L. GHATEI, M.A., MULDERRY, P. & BLOOM, S.R. (1985). Calcitonin gene-related peptide immunoreactive sensory and motor nerves of the rat, cat, and monkey esophagus. *Gastroenterology*, **88**, 129–135.

SEAMON, K.B. & DALY, J.W. (1983). Forskolin, cyclic AMP and cellular physiology. *Trends Pharmacol. Sci.*, **9**, 120–123.

SILINSKY, E.M. (1975). On the association between transmitter secretion and the release of adenine nucleotides from mammalian motor nerve terminals. *J. Physiol.*, **247**, 145–162.

SMITH, D.O. (1991). Sources of adenosine released during neuromuscular transmission in the rat. *J. Physiol.*, **432**, 343–354.

TAKAGI, H., KOJIMA, M., NAGATA, M. & KUROMI, H. (1970). On the site of action of hemicholinium-3 at the rat phrenic nerve-diaphragm preparation with special references to its multiple presynaptic actions. *Neuropharmacology*, **9**, 359–367.

TAKAMI, K., HASHIMOTO, K., UCHIDA, S., TOHYAMA, M. & YOSHIDA, H. (1986). Effect of calcitonin gene-related peptide on the cyclic AMP level of isolated mouse diaphragm. *Jpn. J. Pharmacol.*, **42**, 345–350.

TAKAMI, K., KAWAI, Y., UCHIDA, S., TOHYAMA, M., SHIOTANI, Y., YOSHIDA, H., EMSON, P.C., GIRGIS, S., HILLYARD, C.J. & MACINTYRE, I. (1985). Effect of calcitonin gene-related peptide on contraction of striated muscle in the mouse. *Neurosci. Lett.*, **60**, 227–230.

WESSLER, I. (1989). Control of transmitter release from the rat motor nerve by presynaptic nicotinic and muscarinic autoreceptors. *Trends Pharmacol. Sci.*, **10**, 110–114.

WESSLER, I., HALANK, M., RASBACH, J. & KILBINGER, H. (1986). Presynaptic nicotinic receptors mediating a positive feed-back on transmitter release from the rat phrenic nerve. *Naunyn-Schmied. Arch. Pharmacol.*, **334**, 365–372.

WESSLER, I. & KILBINGER, H. (1986). Release of [^{3}H]-acetylcholine from a modified rat phrenic nerve-hemidiaphragm preparation. *Naunyn-Schmied. Arch. Pharmacol.*, **334**, 357–364.

WILEY, J.W., GROSS, R.A. & MACDONALD, R.L. (1992). The peptide CGRP increases a high-threshold Ca^{2+} current in rat nodose neurons via a pertussis toxin-sensitive pathway. *J. Physiol.*, **455**, 367–381.

WILSON, D.F. (1974). The effects of dibutyryl cyclic adenosine 3',5'-monophosphate, theophylline and aminophylline on neuromuscular transmission in the rat. *J. Pharmacol. Exp. Ther.*, **188**, 447–452.

(Received June 14, 1993
Revised October 11, 1993
Accepted October 13, 1993)

Br. J. Pharmacol. (1994), **111**, 589–597

Regional haemodynamic responses to pituitary adenylate cyclase-activating polypeptide and vasoactive intestinal polypeptide in conscious rats

[1]S.M. Gardiner, T. Rakhit, P.A. Kemp, J.E. March & T. Bennett

Department of Physiology & Pharmacology, University of Nottingham Medical School, Queen's Medical Centre, Nottingham NG7 2UH

1 Regional haemodynamic responses to the homologous peptides, pituitary adenylate cyclase-activating peptide (1-27) (PACAP27) and vasoactive intestinal polypeptide (VIP) were assessed by giving 20 min infusions (1.5–15 nmol kg^{-1} h^{-1}) in conscious, chronically-instrumented, Long Evans rats.

2 PACAP27 caused dose-dependent depressor and tachycardic effects associated with renal, mesenteric and hindquarters vasodilatations, although only in the latter vascular bed was there a sustained increase in flow.

3 VIP caused dose-dependent depressor and tachycardic effects that were not significantly different from those caused by equimolar doses of PACAP27. However, the hindquarters vasodilator effects of VIP (at 7.5 and 15 nmol kg^{-1} h^{-1}) were greater than those of PACAP27 (at the same doses), and accompanied by reductions in renal and mesenteric flows and conductances.

4 In the presence of the nitric oxide (NO) synthase inhibitor, N^G-nitro-L-arginine methyl ester (L-NAME; 11 μmol kg^{-1} h^{-1}), there was significant inhibition of the hindquarters vasodilator effects of PACAP27 and VIP (at 7.5 and 15 nmol kg^{-1} h^{-1}). Under these circumstances the renal and mesenteric vasoconstrictor effects of VIP were abolished.

5 The β_2-adrenoceptor antagonist, ICI 118551 (670 nmol kg^{-1} bolus, 335 nmol kg^{-1} h^{-1} infusion), reduced the matched hindquarters vasodilator responses to PACAP27 (15 nmol kg^{-1} h^{-1}) and VIP (7.5 nmol kg^{-1} h^{-1}), and also abolished the renal vasoconstrictor effects of VIP.

6 The AT_1-receptor antagonist, losartan potassium (20 μmol kg^{-1}), had no significant effect on the haemodynamic response to PACAP27 (15 nmol kg^{-1} h^{-1}), but augmented the hypotensive action of VIP (7.5 nmol kg^{-1} h^{-1}). This influence of losartan was associated with conversion of the renal and mesenteric vasoconstrictor effect of VIP to vasodilatation.

7 Our findings show that similar changes in mean systemic arterial blood pressure in response to PACAP27 and VIP conceal substantial differences in their regional haemodynamic actions. Although the hindquarters vasodilator effects of both peptides involve NO- and β_2-adrenoceptor-mediated mechanisms, it appears that activation of the renin-angiotensin system contributes significantly to the haemodynamic effects of VIP, but not to those of PACAP27.

Keywords: Pituitary adenylate cyclase-activating polypeptide (1-27) (PACAP27); vasoactive intestinal polypeptide (VIP); NO; N^G-nitro-L-arginine methyl ester (L-NAME); ICI 118551; losartan potassium; haemodynamics

Introduction

Pituitary adenylate cyclase-activating polypeptide (PACAP) was originally isolated from the sheep hypothalamus as a 38 amino acid peptide (Miyata *et al.*, 1989). Subsequently, the existence of a peptide corresponding to the N terminal 27 residues of PACAP (PACAP27) was demonstrated (Miyata *et al.*, 1990); PACAP27 shows 68% sequence homology with vasoactive intestinal polypeptide (VIP; Miyata *et al.*, 1990). PACAP27, like VIP, causes hypotension in anaesthetized rats (Miyata *et al.*, 1990; Nandha *et al.*, 1991; Absood *et al.*, 1992) and cats (Minkes *et al.*, 1992). Nandha *et al.* (1991) concluded that the hypotensive effects of PACAP27 and VIP were through interaction with the same receptor type, whereas Minkes *et al.* (1992) provided evidence that distinct receptors were involved in the cardiovascular responses to PACAP27 and VIP. Since the study of Nandha *et al.* (1991) quantitated the cardiovascular effects of PACAP27 and VIP only on the basis of changes in mean arterial blood pressure, they would not have detected any putative differences in the regional haemodynamic effects of the peptides. Moreover, in the studies cited above, only responses to bolus injections of PACAP27 and VIP were assessed and hence effects under steady state conditions were not observed. Therefore, the first objective of the present study was to determine regional haemodynamic changes during 20 min infusions of 3 doses (1.5, 7.5 and 15 nmol kg^{-1} h^{-1}) of PACAP27 or VIP, in conscious, unrestrained rats.

The *in vitro* vasorelaxant effects of PACAP27 and VIP on the rabbit aorta have been described by Warren *et al.* (1991) as endothelium-independent, although they did not formally compare responses to the peptides in the presence and absence of the endothelium. Nonetheless, the finding of Minkes *et al.* (1992), that responses to PACAP27 and VIP were unaffected by the nitric oxide (NO) synthase inhibitor, N^G-nitro-L-arginine methyl ester (L-NAME), is consistent with the cardiovascular responses to the peptides *in vivo* being endothelium-independent. However, these observations were made in anaesthetized cats and there is evidence that the L-arginine/NO system is less important in the control of haemodynamics in cats than in rats (van Gelderen *et al.*, 1991). Moreover, prior to the publication of the paper by Minkes *et al.* (1992), we had preliminary unpublished data showing a marked effect of L-NAME on some haemodynamic responses to PACAP27 and VIP in conscious rats. Therefore, the second objective of the present work was to assess haemodynamic responses to infusions of PACAP27 or VIP, in the absence and presence of L-NAME, in the same conscious rats.

[1] Author for correspondence.

Since there is evidence that PACAP27 and VIP can stimulate release of catecholamines from the adrenal gland of the rat (Malhotra & Wakade, 1987; Wakade *et al.*, 1991a,b), and since adrenaline causes marked β_2-adrenoceptor-mediated hindquarters vasodilatation in the conscious rat (Gardiner *et al.*, 1991a,b), our third objective was to determine the possible involvement of this mechanism in the hindquarters vasodilator effects of PACAP27 and VIP, by recording responses in the absence and in the presence of the β_2-adrenoceptor antagonist, ICI 118551 (erythro-(±)-1-[7-methylidan-4-yloxy]-3-isopropyl-aminobutan-2-ol)hydrochloride) (Bilski *et al.*, 1983).

In dogs (Porter *et al.*, 1982), and rabbits (Dimaline *et al.*, 1983), VIP stimulates renin release, possibly through direct and indirect mechanisms. However, there are no data available relating to the involvement of the renin-angiotensin system in the regional haemodynamic responses to VIP and so, our fourth objective was to determine the effects of the AT_1-receptor antagonist, losartan potassium (DuP 753; Wong *et al.*, 1990; Batin *et al.*, 1991) on regional haemodynamic responses to PACAP27 or VIP in conscious rats.

Methods

Male, Long Evans rats (350–450 g) bred in the Biomedical Services Unit in Nottingham were used for all experiments. Under sodium methohexitone (Brietal, Lilly) anaesthesia (40–60 mg kg^{-1}, i.p. supplemented as necessary), pulsed Doppler flow probes (Haywood *et al.*, 1981) were implanted around the left renal and superior mesenteric arteries, and the distal abdominal aorta, below the level of the ileocaecal artery (to monitor flow to the hindquarters). After surgery, animals were given ampicillin (Penbritin, Beechams; 7 mg kg^{-1}, i.m.) and returned to individual home cages with free access to food and water. At least 1 week later, animals were anaesthetized (sodium methohexitone, 40 mg kg^{-1}, i.p.) and had an intra-arterial (distal abdominal aorta via the ventral caudal artery) and 3 intravenous (right jugular vein) catheters inserted. The catheters were led subcutaneously to emerge at the back of the neck with the wires from the Doppler probes. The probe wires were soldered into a microconnector (Microtech Inc., Boothwyn, U.S.A.) that was clamped into a harness fitted to the rat. A flexible spring was connected to the harness, and the catheters ran through the spring to prevent the rat interfering with them. The spring was supported by a counterbalanced lever system that allowed the rat unrestrained movement. The animals were allowed at least 1 day to recover from anaesthesia and catheterisation before experiments were begun. The following experimental protocols were employed.

Regional haemodynamic effects of repeated infusions of PACAP27 or VIP

In order to ensure that responses to PACAP27 or VIP were reproducible, rats ($n = 2$) were given 20 min infusions of PACAP27 (15 nmol kg^{-1} h^{-1}, see below) or VIP (7.5 nmol kg^{-1} h^{-1}, see below) on separate experimental days. The renal and mesenteric vascular responses to both peptides were not consistently different on the separate experimental days. The tachycardia, hypotension and hindquarters vasodilatation were numerically less on the second day for both peptides in both animals, but in each case the reduction (area under or over curve for 0–20 min) was less than 10%.

Regional haemodynamic effects of PACAP27 in the absence and presence of L-NAME

One group of 9 rats was given 20 min infusions of PACAP27 at doses of 1.5, 7.5 and 15 nmol kg^{-1} h^{-1} (these doses were chosen on the basis of preliminary experiments). The infusions were all given on the same experimental day, in random order, but separated by at least 1 h to allow all variables to return to baseline before the next infusion was started. On the first experimental day, an infusion of saline (154 mmol l^{-1} NaCl, 0.3 ml h^{-1}) was started, 90 min before the first infusion of PACAP27 was begun. The saline infusion was continued throughout the experiment to control for L-NAME infusion (see below).

Animals were left undisturbed for the day after PACAP27 infusion, with the second arm of the experiment starting the day after. L-NAME (11 μmol kg^{-1} h^{-1}, 0.3 ml h^{-1}) was infused throughout this experiment with the first infusion of PACAP27 beginning 90 min after the L-NAME infusion was started, and the subsequent two infusions of PACAP27 being given at least 1 h apart. The order of administration of the 3 doses of PACAP27 was the same as in the absence of L-NAME.

Regional haemodynamic effects of VIP in the absence and presence of L-NAME

A separate group of 9 rats was used in this protocol, which was identical to that above except the animals received 20 min infusions of VIP (1.5, 7.5 and 15 nmol kg^{-1} h^{-1}) in the presence of saline or L-NAME.

Regional haemodynamic effects of PACAP27 and VIP in the absence and presence of ICI 118551

Since the hindquarters vasodilator effects of PACAP27 at a dose of 15 nmol kg^{-1} h^{-1} and VIP at a dose of 7.5 nmol kg^{-1} h^{-1} were not significantly different (see Results), we assessed responses to randomized 20 min infusions of these doses of the peptides (separated by at least 24 h) before, and at least 60 min after the onset of a primed infusion of ICI 118551 (670 nmol kg^{-1} bolus, 335 nmol kg^{-1} h^{-1} infusion) (Gardiner *et al.*, 1992) in 7 Long Evans rats.

Regional haemodynamic effects of PACAP27 and VIP in the absence and presence of losartan potassium

In 9 Long Evans rats, randomized 20 min infusions of PACAP27 (15 nmol kg^{-1} h^{-1}) and VIP (7.5 nmol kg^{-1} h^{-1}) were given before and 30 min after losartan potassium (20 μmol kg^{-1}). Elsewhere (Batin *et al.*, 1991), we have shown this dose of losartan potassium blocks the haemodynamic effects of exogenous angiotensin II (AII, 125 pmol kg^{-1}) for at least 9 h.

Drugs and peptides

PACAP27 and VIP were obtained from Bachem (U.K.) and L-NAME hydrochloride from Sigma. ICI 118551 hydrochloride was a gift from ICI Pharmaceuticals plc, and losartan potassium was a gift from Dr R. Smith (DuPont, U.S.A.). The peptides were dissolved in sterile isotonic saline containing 1% bovine serum albumin (Sigma); L-NAME and losartan potassium were dissolved in saline, as was ICI 118551, but the latter required gentle warming.

Data analysis

Before and throughout the infusions of PACAP27 or VIP, continuous recordings were made of instantaneous heart rate, phasic and mean arterial blood pressures and phasic and mean Doppler shift signals from the renal, mesenteric and hindquarters probes. Values for heart rate, mean arterial blood pressure, and mean renal, mesenteric and hindquarters Doppler shift signals were averaged over 1 min epochs immediately before infusion of PACAP27 or VIP, and at 5, 10, 15 and 20 min during infusion of the peptides. Vascular conductances were calculated by dividing the mean Doppler shift signal by the corresponding mean arterial blood pressure signal (Gardiner *et al.*, 1991a,b; 1992). Responses to PACAP27 or VIP were assessed by Friedman's test; res-

ponses to each peptide in the absence and presence of L-NAME were compared by Wilcoxon's test applied to the integrated responses (i.e. areas under or over curves calculated from the values measured at the times above). Responses to PACAP27 and VIP in the absence or presence of L-NAME were compared by the Mann-Whitney U test applied to integrated responses. Effects of ICI 118551 or losartan on responses to PACAP27 or VIP were assessed by applying Wilcoxon's test to the integrated responses in the absence and presence of these drugs. A P value <0.05 was taken as significant.

Results

Regional haemodynamic responses to PACAP27 in the presence of saline

Infusion of PACAP27 at 1.5 nmol kg^{-1} h^{-1} caused a slight hypotension and modest tachycardia but no significant changes in renal, mesenteric or hindquarters flows, or vascular conductances (Figures 1 and 2, Table 1).

Infusion of PACAP27 at 7.5 and 15 nmol kg^{-1} h^{-1} caused marked, dose-dependent, depressor effects and tachycardia (Figures 1 and 3, Table 1). There were slight, and variable increases in renal and mesenteric flows, but substantial increases in hindquarters flow (Figures 1 and 3). There were increases in vascular conductances in renal, mesenteric and, particularly, hindquarter vascular beds (Figure 2, Table 1).

Regional haemodynamic responses to PACAP27 in the presence of L-NAME

In the presence of L-NAME, mean arterial blood pressure was increased significantly, in association with bradycardia and reductions in renal, mesenteric, and hindquarters flows and conductances (Figures 1 and 2).

Under these conditions, infusion of PACAP27 at a dose of 1.5 nmol kg^{-1} h^{-1} caused a significantly greater hypotension than in the presence of saline, although the tachycardia was

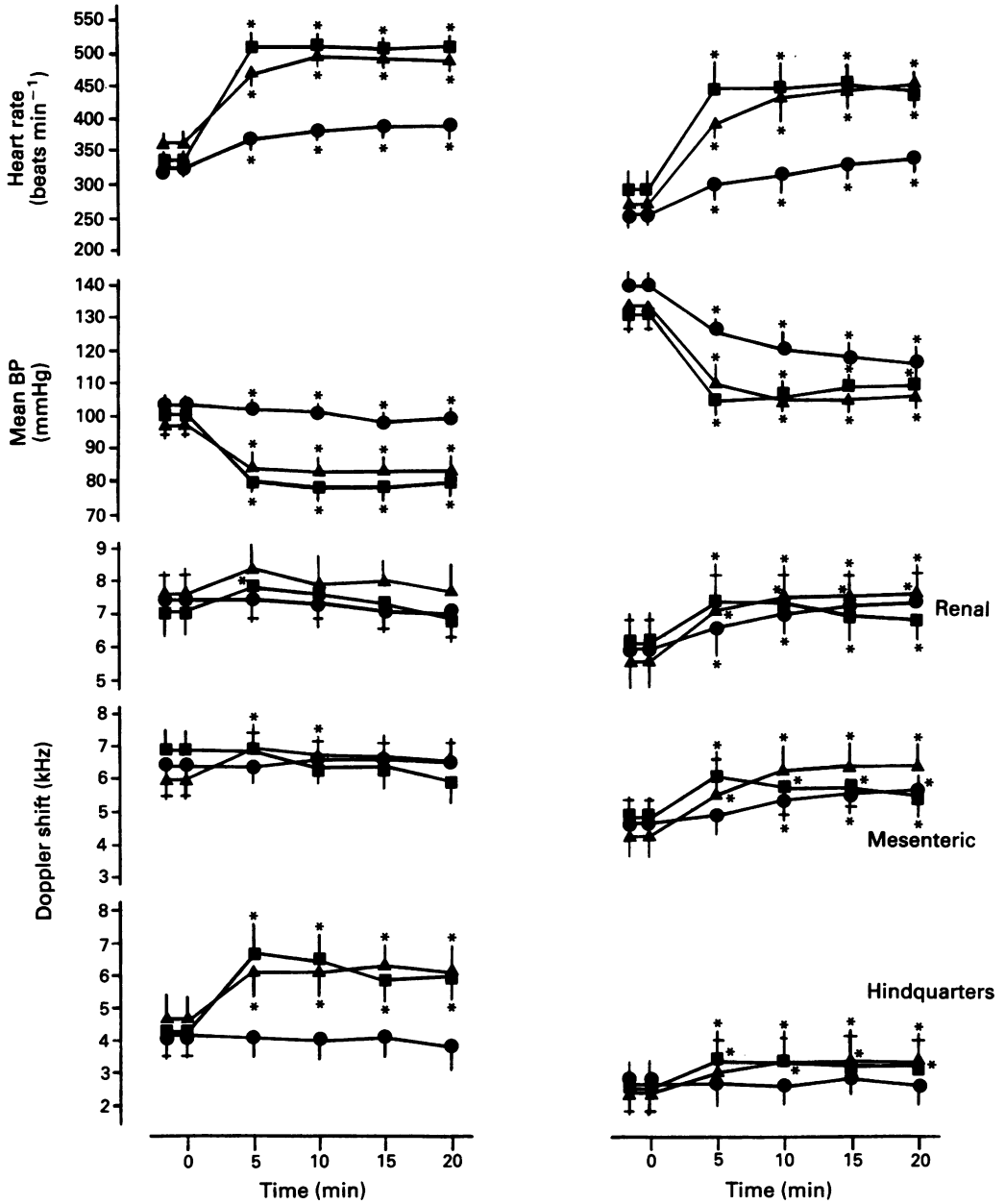

Figure 1 Cardiovascular changes during 20 min infusions of PACAP27 at 1.5 nmol kg^{-1} h^{-1} (●), 7.5 nmol kg^{-1} h^{-1} (▲), or 15 nmol kg^{-1} h^{-1} (■) in the absence (left-hand panels) or presence (right-hand panels) of N^G-nitro-L-arginine methyl ester (L-NAME, 11 μmol kg^{-1} h^{-1}) in the same conscious, Long Evans rats ($n = 9$). Values are mean with s.e.mean; $*P<0.05$ versus preinfusion baseline (Friedman's test).

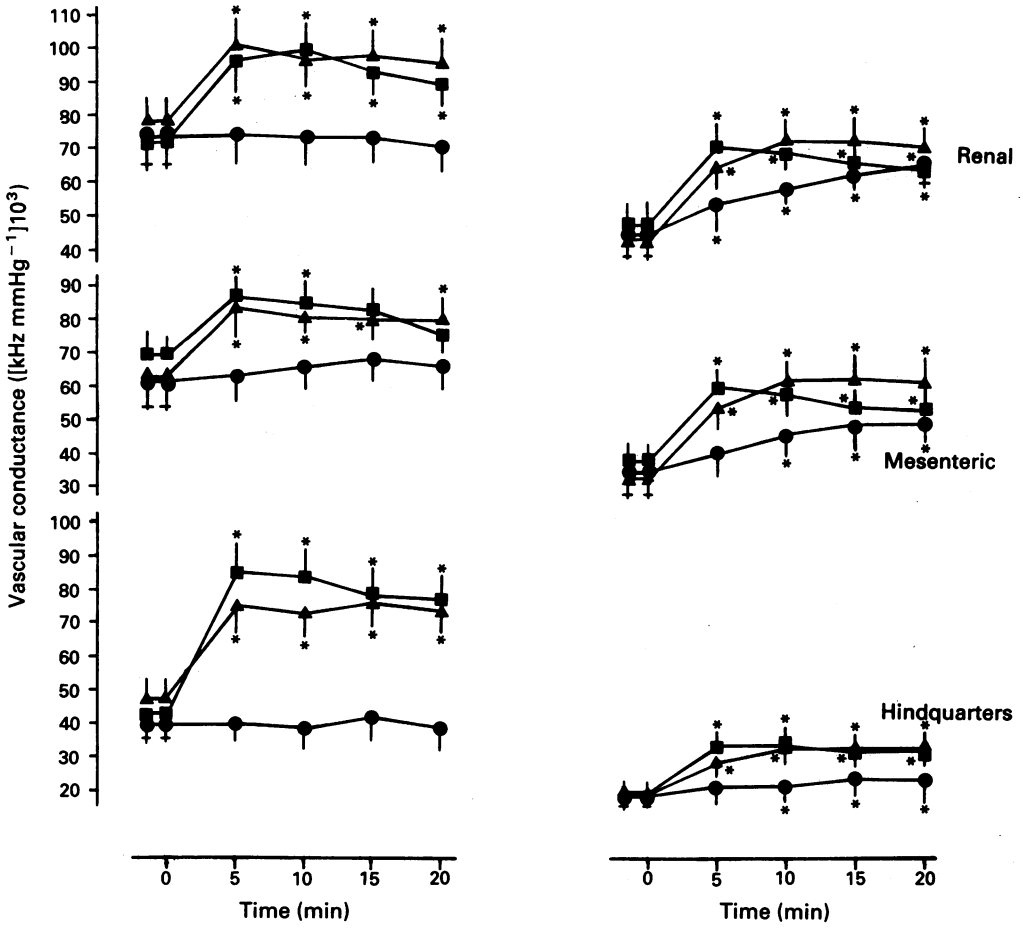

Figure 2 Cardiovascular changes during 20 min infusions of PACAP27 at 1.5 nmol kg^{-1} h^{-1} (●), 7.5 nmol kg^{-1} h^{-1} (▲), or 15 nmol kg^{-1} h^{-1} (■) in the absence (left-hand panels) or presence (right-hand panels) of N^{G}-nitro-L-arginine methyl ester (L-NAME, 11 μmol kg^{-1} h^{-1}) in the same conscious, Long Evans rats ($n = 9$). Values are mean with s.e.mean; *$P < 0.05$ versus preinfusion baseline (Friedman's test).

Table 1 Integrated cardiovascular responses (areas under or over curves; AUC, AOC) during 20 min infusions of PACAP27 in the absence and presence of N^{G}-nitro-L-arginine methyl ester (L-NAME, $n = 9$), or vasoactive intestinal polypeptide (VIP) in the absence and presence of L-NAME ($n = 9$) in conscious, Long Evans rats

	PACAP27 (1.5 nmol kg^{-1} h^{-1})	*+L-NAME*	*PACAP27* (7.5 nmol kg^{-1} h^{-1})	*+L-NAME*	*PACAP27* (15 nmol kg^{-1} h^{-1})	*+L-NAME*
Heart rate (AUC; beats)	917 ± 223	1078 ± 106	2122 ± 199	2640 ± 349	2957 ± 216	2543 ± 265
Mean arterial blood pressure (AOC; mmHg min)	−91 ± 19	−371 ± 66*	−270 ± 33	−513 ± 87*	−428 ± 34	−496 ± 96
Renal conductance (AUC; [kHz mmHg^{-1}]10^3 min)	54 ± 19	241 ± 27*	343 ± 88	457 ± 56	414 ± 98	345 ± 60
Mesenteric conductance (AUC; [kHz mmHg^{-1}]10^3 min)	89 ± 32	188 ± 60	322 ± 41	460 ± 73	276 ± 85	321 ± 68
Hindquarters conductance (AUC; [kHz mmHg^{-1}]10^3 min)	36 ± 14	64 ± 12	363 ± 65	223 ± 46*	663 ± 41	253 ± 53*
	VIP (1.5 nmol kg^{-1} h^{-1})	*+L-NAME*	*VIP* (7.5 nmol kg^{-1} h^{-1})	*+L-NAME*	*VIP* (15 nmol kg^{-1} h^{-1})	*+L-NAME*
Heart rate (AUC; beats)	432 ± 100	410 ± 104	2476 ± 166	2171 ± 282	3201 ± 136	2228 ± 342*
Mean arterial blood pressure (AOC; mmHg min)	−85 ± 24	−134 ± 21†	−389 ± 59	−392 ± 36	−518 ± 31	−653 ± 53*
Renal conductance (AUC or AOC; [kHz mmHg^{-1}]10^3 min)	67 ± 34	69 ± 16†	−105 ± 29†	117 ± 31*†	−208 ± 48†	60 ± 25*†
Mesenteric conductance (AUC or AOC; [kHz mmHg^{-1}]10^3 min)	82 ± 24	114 ± 27	−240 ± 60†	117 ± 32*†	−298 ± 59†	−57 ± 19*†
Hindquarters conductance (AUC; [kHz mmHg^{-1}]10^3 min)	49 ± 13	26 ± 9	822 ± 135†	227 ± 36*	996 ± 108†	426 ± 73*

*$P < 0.05$ versus corresponding response in the absence of L-NAME (Wilcoxon's test);
†$P < 0.05$ versus corresponding response to PACAP27 (Mann-Whitney U test).

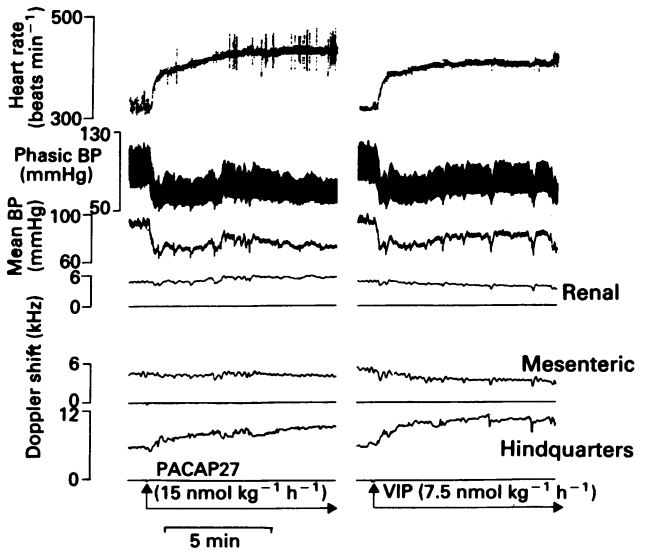

Figure 3 Contrasting cardiovascular changes at the onset of infusion of PACAP27 or vasoactive intestinal polypeptide (VIP) in different conscious, Long Evans rats. Note that although the fall in mean arterial blood pressure (BP) was very similar, VIP caused reductions in renal and mesenteric Doppler shift signals, whereas PACAP27 did not.

similar (Figure 1, Table 1). There were significant increases in renal and mesenteric flows but only the renal vasodilator response to PACAP27 was significantly greater than that seen during infusion of PACAP27 in the presence of saline (Figures 1 and 2, Table 1).

In L-NAME-treated animals, an infusion of PACAP27 at 7.5 and 15 nmol kg^{-1} caused similar falls in blood pressure, and rises in heart rate and in renal, mesenteric and hindquarters flows and vascular conductances (Figures 1 and 2). Although the hypotensive responses to PACAP27 at a dose of 7.5 nmol kg^{-1} h^{-1} were enhanced relative to those in the presence of saline (Figure 1, Table 1), there was a significant reduction in its hindquarters hyperaemic vasodilator action, whereas its vasodilator effects in renal and mesenteric vascular beds were not changed significantly (Figures 1 and 2, Table 1). There was also a significant inhibition of the hindquarters haemodynamic effects of the highest dose of PACAP27 in the presence of L-NAME, but in this instance the hypotensive response was not different from that seen in the presence of saline (Figures 1 and 2, Table 1).

Regional haemodynamic responses to VIP in the presence of saline

VIP at a dose of 1.5 nmol kg^{-1} h^{-1} caused slight hypotension and tachycardia, but no significant regional haemodynamic changes (Figures 4 and 5, Table 1).

VIP at 7.5 and 15 nmol kg^{-1} h^{-1} caused dose-dependent hypotension and tachycardia accompanied by reductions in renal and mesenteric flows and vascular conductances, but increases in hindquarters flow and vascular conductance (Figures 3–5, Table 1).

Regional haemodynamic responses to VIP in the presence of L-NAME

As above, L-NAME caused hypertension, bradycardia and reductions in renal, mesenteric and hindquarters flows and vascular conductances (Figures 4 and 5). The cardiovascular effects of VIP at 1.5 nmol kg^{-1} h^{-1} in the presence of L-NAME were not significantly different from those in the presence of saline (Figures 4 and 5, Table 1). The slight hypotensive response to VIP at 7.5 nmol kg^{-1} h^{-1} was not enhanced by L-NAME, relative to that in the presence of saline, but the renal and mesenteric vasoconstrictions were abolished and the hindquarters vasodilatation substantially reduced (Figures 4 and 5, Table 1).

A similar pattern of effects was seen with VIP at 15 nmol kg^{-1} h^{-1}, but in this instance the hypotensive response was enhanced in the presence of L-NAME relative to that seen in the presence of saline (Figures 4 and 5, Table 1).

Comparison of the regional haemodynamic effects of PACAP27 and VIP

In the presence of saline, each of the equimolar doses of PACAP27 and VIP induced hypotensive effects which were not significantly different (Table 1). At the lowest dose (1.5 nmol kg^{-1} h^{-1}) the hypotension caused by PACAP27 or VIP was accompanied by trivial regional haemodynamic effects that were not different between the two peptides (Table 1). However, at doses of 7.5 and 15 nmol kg^{-1} h^{-1}, although the depressor effects of PACAP27 and VIP were similar, the former caused renal, mesenteric and hindquarters vasodilatation whereas VIP caused a significantly greater hindquarters vasodilatation, accompanied by renal and mesenteric vasoconstrictions (Table 1).

Effect of ICI 118551 on regional haemodynamic responses to PACAP27 and VIP

In the absence of ICI 118551, the patterns of haemodynamic response to PACAP27 (15 nmol kg^{-1} h^{-1}; Table 2) and VIP (7.5 nmol kg^{-1} h^{-1}; Table 2) were similar to those in the previous experiment (Table 1). In the presence of ICI 118551, the hindquarters vasodilator effect of PACAP27 was attenuated (Table 2), but there were no other significant changes (Table 2). ICI 118551 also diminished the hindquarters vasodilator response to VIP and abolished its renal vasoconstrictor action (Table 2).

Effect of losartan on regional haemodynamic responses to PACAP27 and VIP

In the absence of losartan, the patterns of haemodynamic response to PACAP27 (15 nmol kg^{-1} h^{-1}; Table 3) and VIP (7.5 nmol kg^{-1} h^{-1}; Table 3) were similar to those in the previous experiments (Tables 1 and 2).

In the presence of losartan, there were no significant changes in the haemodynamic effects of PACAP27 (Table 3). In contrast, losartan enhanced the hypotensive action of VIP, and this effect was associated with renal and mesenteric vasodilatation, rather than vasoconstriction.

Discussion

In the present work, 20 min infusions of equimolar doses of PACAP27 and VIP caused similar, dose-dependent, hypotensive responses. However, this similarity of effect on mean systemic arterial blood pressure was accompanied by different regional haemodynamic changes. Thus, at doses of 7.5 and 15 nmol kg^{-1} h^{-1}, the hindquarters hyperaemic vasodilator effects of VIP were greater than those of PACAP27, and were accompanied by renal and mesenteric vasoconstrictions rather than vasodilatations, as seen with PACAP27. Previous work in anaesthetized dogs has shown that VIP can cause reductions in renal and superior mesenteric flows and vascular conductances (Blitz & Charbon, 1983; Naruse *et al.*, 1986). However, in those studies, VIP also caused no change, or a reduction, in femoral arterial flow. Our finding of a marked vasodilator effect of VIP in the hindquarters of the conscious rat is thus more in line with the recent observations of Minkes *et al.* (1992) in the anaesthetized cat. How-

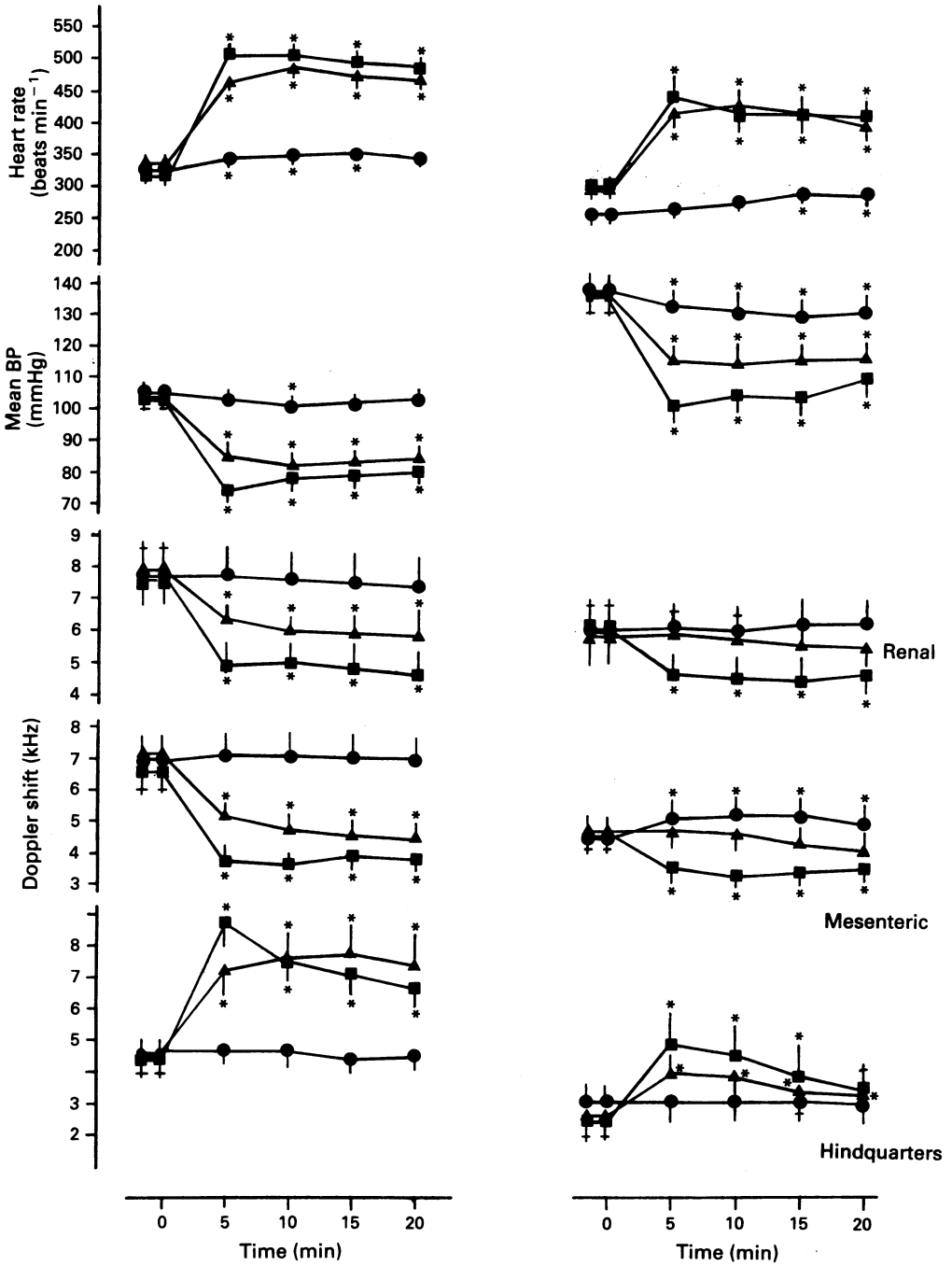

Figure 4 Cardiovascular changes during 20 min infusions of vasoactive intestinal polypeptide (VIP) at 1.5 nmol kg^{-1} h^{-1} (●), 7.5 nmol kg^{-1} h^{-1} (▲), or 15 nmol kg^{-1} h^{-1} (■) in the absence (left-hand panels) or presence (right-hand panels) of N^G-nitro-L-arginine methyl ester (L-NAME, 11 μmol kg^{-1} h^{-1}) in the same conscious, Long Evans rats ($n = 9$). Values are mean with s.e.mean; *$P < 0.05$ versus preinfusion baseline (Friedman's test).

ever, the latter workers found that PACAP27 caused biphasic changes (increase followed by decrease) in hindquarters vascular conductance and systemic arterial blood pressure. The delayed pressor and vasoconstrictor effects of PACAP27 were abolished by phentolamine or adrenalectomy, but these interventions did not influence the hindquarters dilator or depressor responses to VIP. Moreover, L-NAME and propranolol were without effect on the haemodynamic actions of PACAP27 or VIP (Minkes *et al.*, 1992). It is clear, therefore, that there are fundamental differences between the haemodynamic effects of PACAP27 and of VIP, in conscious rats compared to anaesthetized cats.

Our results indicate that the hindquarters vasodilator effects of PACAP27 and VIP involved an L-NAME-sensitive component, and that the latter was larger in the case of VIP. It is feasible that both endothelium-dependent and endothelium-independent mechanisms (Gaw *et al.*, 1991; Warren *et al.*, 1991) were involved, because in the presence of L-NAME there was a significant residual hindquarters vasodilator response to PACAP27 and VIP.

Since the β_2-adrenoceptor antagonist, ICI 118551, caused significant inhibition of the hindquarters vasodilator effect of VIP and of PACAP27, and since both peptides have been shown to stimulate adrenal medullary catecholamine release in the rat (Malhotra & Wakade, 1987; Wakade *et al.*, 1991a,b), it is likely that a proportion of the hindquarters vasodilator action of PACAP27 and VIP involved adrenal medullary adrenaline release causing activation of hind-

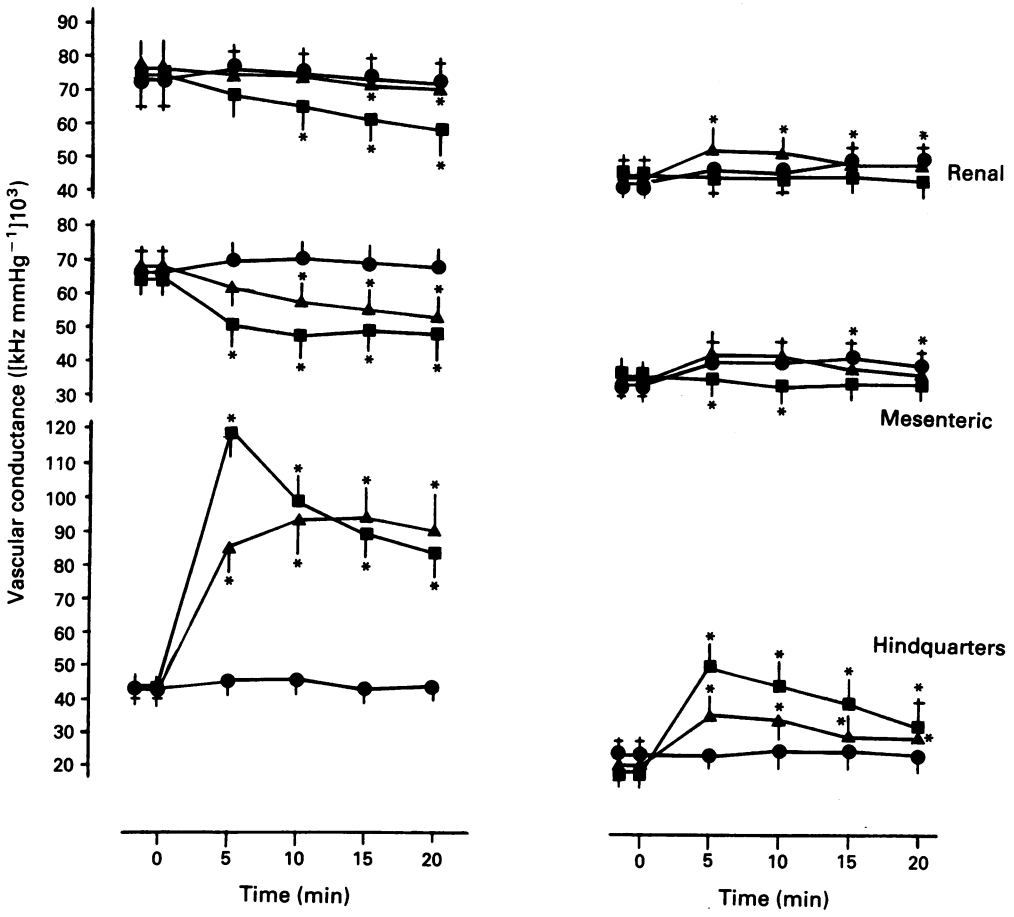

Figure 5 Cardiovascular changes during 20 min infusions of vasoactive intestinal polypeptide (VIP) at 1.5 nmol $kg^{-1} h^{-1}$ (●), 7.5 nmol $kg^{-1} h^{-1}$ (▲), or 15 nmol $kg^{-1} h^{-1}$ (■) in the absence (left-hand panels) or presence (right-hand panels) of N^G-nitro-L-arginine methyl ester (L-NAME, 11 μmol $kg^{-1} h^{-1}$) in the same conscious, Long Evans rats ($n = 9$). Values are mean with s.e.mean; $^*P < 0.05$ versus preinfusion baseline (Friedman's test).

Table 2 Integrated (area under or over curve, AUC or $AOC_{0-20\,min}$, respectively) cardiovascular responses during infusion of PACAP27 (15 nmol $kg^{-1} h^{-1}$) or vasoactive intestinal polypeptide (VIP) (7.5 nmol $kg^{-1} h^{-1}$) in the same conscious Long Evans rats ($n = 7$) in the absence (control) or presence of ICI 118551 (670 nmol kg^{-1} bolus; 335 nmol $kg^{-1} h^{-1}$ infusion)

		PACAP27	*VIP*
Heart rate	Control	2581 ± 222	2071 ± 89
(AUC; beats)	+ICI 118551	2581 ± 249	1970 ± 238
Mean blood pressure	Control	−396 ± 27	−364 ± 32
(AOC; mmHg min)	+ICI 118551	−312 ± 40	−319 ± 36
Renal conductance	Control	260 ± 50	−121 ± 48
(AUC or AOC; [kHz $mmHg^{-1}$]10^3 min)	+ICI 118551	248 ± 55	63 ± 21†
Mesenteric conductance	Control	306 ± 36	−309 ± 42
(AUC or AOC; [kHz $mmHg^{-1}$]10^3 min)	+ICI 118551	262 ± 48	−235 ± 54
Hindquarters conductance	Control	638 ± 109	744 ± 108
(AUC; [kHz $mmHg^{-1}$]10^3 min)	+ICI 118551	396 ± 67†	540 ± 107†

Values are mean ± s.e.mean.
†$P < 0.05$ versus control (Wilcoxon's test).

quarters, β_2-adrenoceptor-mediated vasodilatation (Gardiner *et al.*, 1991a,b). It is possible that a component of this response contributed to the L-NAME-sensitive hindquarters vasodilator effect of PACAP27 and VIP, since elsewhere (Gardiner *et al.*, 1991a,b) we have shown the hindquarters vasodilator effects of exogenous β_2-adrenoceptor agonists are reduced in the presence of L-NAME.

Although the hypotensive effects of PACAP27 and VIP were matched, the former caused renal and mesenteric vasodilatations whereas VIP caused vasoconstriction in these vascular beds. Since there was little change in renal or mesenteric blood flows in the presence of PACAP27, it is possible that the increases in renal and mesenteric vascular conductances were a manifestation of autoregulation. However, it then remains to explain why such a phenomenon was not apparent during infusion of VIP. It could be that activation of indirect vasoconstrictor mechanisms during infusion of VIP had a predominant influence in the renal and mesenteric vascular beds. But, in the presence of L-NAME, the highest dose of VIP had an enhanced hypotensive effect,

Table 3 Integrated (area under or over curve, AUC or $AOC_{0-20\,min}$, respectively) cardiovascular responses during infusion of PACAP27 (15 nmol kg^{-1} h^{-1}) or vasoactive intestinal polypeptide (VIP) (7.5 nmol kg^{-1} h^{-1}) in the same conscious Long Evans rats ($n = 9$) in the absence (control) or presence of losartan (20 μmol kg^{-1})

		PACAP27	*VIP*
Heart rate	Control	3001 ± 159*	2229 ± 293*
(AUC; beats)	+losartan	2421 ± 90*	2163 ± 144*
Mean blood pressure	Control	−418 ± 32*	−406 ± 51*
(AOC; mmHg min)	+losartan	−428 ± 38*	−589 ± 43*†
Renal conductance	Control	406 ± 74*	−75 ± 32*
(AUC or AOC; [kHz $mmHg^{-1}$]10^3 min)	+losartan	340 ± 42*	184 ± 40*†
Mesenteric conductance	Control	389 ± 43*	−151 ± 33*
(AUC or AOC; [kHz $mmHg^{-1}$]10^3 min)	+losartan	543 ± 102*	138 ± 41*†
Hindquarters conductance	Control	613 ± 95*	582 ± 96*
(AUC; [kHz $mmHg^{-1}$]10^3 min)	+losartan	585 ± 80*	826 ± 81*

Values are mean ± s.e.mean.
*$P > 0.05$ versus baseline;
†$P < 0.05$ versus control (Wilcoxon's test).

yet there was no renal or mesenteric vasoconstriction. Thus, it would have to be proposed that, in the presence of L-NAME-induced hypertension, activation of vasoconstrictor mechanisms, consequent upon VIP-induced hypotension, did not occur in the way it did in the absence of L-NAME because, in the presence of L-NAME, VIP did not cause blood pressure to fall below baseline levels. Since losartan augmented the hypotensive effects of VIP, and suppressed its renal and mesenteric vasoconstrictor actions it is likely that the latter effects were normally due to VIP-induced activation of the renin-angiotensin system. However, if this was a direct effect of VIP (Porter *et al.*, 1982) it should occur in the presence of L-NAME, unless VIP-induced stimulation of renin release involved NO.

An indirect action of VIP to stimulate renin release through β_2-adrenoceptors is consistent with the finding that ICI 118551 abolished the renal vasoconstrictor response to VIP. However, in conscious rabbits, the non-selective β-adrenoceptor antagonist, propranolol, had no effect on renin release in response to VIP (Calam *et al.*, 1982). Moreover, if VIP-induced renin release was secondary to its hypotensive effect, it is unclear why PACAP27 should not have a similar effect, but it did not appear to do so because losartan had no influence on the haemodynamic actions of PACAP27. It is feasible that the latter peptide interfered with renin release, or had such potent renal and mesenteric dilator actions that any constrictor effect of angiotensin II on the renal or mesenteric vascular bed was not expressed in its presence.

It is clear from the above that the regional haemodynamic effects of PACAP27 and VIP probably involved a number of different mechanisms, both direct and indirect, the contributions from which varied according to the peptide, and the dose. Thus, the differential effects of L-NAME on the hypotensive actions of PACAP27 and VIP probably reflected the changing relations between vasoconstriction and vasodilatation in the different vascular beds. For example, in one situation in the presence of L-NAME the hypotension was augmented in association with enhancement of renal vasodilatation (e.g. PACAP27 at 1.5 nmol kg^{-1} h^{-1}), whereas in another situation there was no augmentation of the hypotension since, although in renal and mesenteric vascular beds, vasoconstrictions had been converted to vasodilatations, there was marked attenuation of the large hindquarters vasodilatation (e.g. VIP at 7.5 nmol kg^{-1} h^{-1}). We have already discussed possible mechanisms underlying the inhibitory effects of L-NAME on vasodilator responses (see above). Since L-NAME inhibits NO production, and thereby decreases activation of cytosolic guanylate cyclase (see Ignarro, 1991, for review), then any augmented vasodilator responses to PACAP27 or VIP, in the presence of L-NAME, may have been due to enhanced effects of adenosine 3':5'-cyclic monophosphate (cyclic AMP), contingent upon decreased cyclic GMP-mediated stimulation of phosphodiesterase (see Lincoln & Cornwell, 1993, for review). However, additional experiments would be needed to demonstrate such putative interactions *in vivo*.

Whatever the details underlying the differences between the haemodynamic actions of PACAP27 and VIP, our findings are consistent with these peptides acting on different receptors (Minkes *et al.*, 1992) rather than on the same receptors (Nandha *et al.*, 1991) to exert their haemodynamic effects.

References

ABSOOD, A., CHEN, D., WANG, Z.-Y. & HÅKANSON, R. (1992). Vascular effects of pituitary adenylate cyclase activating peptide: a comparison with vasoactive intestinal peptide. *Regul. Pept.*, **40**, 323–329.

BATIN, P., GARDINER, S.M., COMPTON, A.M. & BENNETT, T. (1991). Differential regional haemodynamic effects of the non-peptide angiotensin II antagonist, DuP 753, in water-replete and water-deprived Brattleboro rats. *Life Sci.*, **48**, 733–739.

BILSKI, A.J., HALLIDAY, S.E., FITZGERALD, J.D. & WALE, J.L. (1983). The pharmacology of a β_2-selective adrenoceptor antagonist (ICI 118551). *J. Cardiovasc. Pharmacol.*, **5**, 430–437.

BLITZ, W. & CHARBON, G.A. (1983). Regional vascular influences of vasoactive intestinal polypeptide. *Scand. J. Gastroenterol.*, **18**, 755–763.

CALAM, J., DIMALINE, R., PEART, W.S. & UNWIN, R.J. (1982). Vasoactive intestinal polypeptide (VIP) and renin release in the conscious rabbit. *J. Physiol.*, **329**, 66P.

DIMALINE, R., PEART, W.S. & UNWIN, R.J. (1983). Effects of vasoactive intestinal polypeptide (VIP) on renal function and plasma renin activity in the conscious rabbit. *J. Physiol.*, **344**, 379–388.

GARDINER, S.M., KEMP, P.A. & BENNETT, T. (1991a). Effects of N^G-nitro-L-arginine methyl ester on vasodilator responses to acetylcholine, 5'-N-ethylcarboxamidoadenosine or salbutamol in conscious rats. *Br. J. Pharmacol.*, **103**, 1725–1732.

GARDINER, S.M., KEMP, P.A. & BENNETT, T. (1991b). Effects of N^G-nitro-L-arginine methyl ester on vasodilator responses to adrenaline or BRL 38227 in conscious rats. *Br. J. Pharmacol.*, **104**, 731–737.

GARDINER, S.M., KEMP, P.A., BENNETT, T., BOSE, C., FOULKES, R. & HUGHES, B. (1992). Involvement of β_2-adrenoceptors in the regional haemodynamic responses to bradykinin in conscious rats. *Br. J. Pharmacol.*, **105**, 839–848.

GAW, A.J., ABERDEEN, J., HUMPHREY, P.P.A., WADSWORTH, R.M. & BURNSTOCK, G. (1991). Relaxation of sheep cerebral arteries by vasoactive intestinal polypeptide and neurogenic stimulation: inhibition by L-N^G-monomethyl arginine in endothelium-denuded vessels. *Br. J. Pharmacol.*, **102,** 567–572.

HAYWOOD, J.R., SHAFFER, R.A., FASTENOW, C., FINK, G.D. & BRODY, M.J. (1981). Regional blood flow measurement with pulsed Doppler flowmeter in conscious rat. *Am. J. Physiol.*, **241,** H273–H278.

IGNARRO, L.J. (1991). Signal transduction mechanisms involving nitric oxide. *Biochem. Pharmacol.*, **41,** 485–490.

LINCOLN, T.M. & CORNWELL, T.L. (1993). Intracellular cyclic GMP receptor proteins. *FASEB J.*, **7,** 328–338.

MALHOTRA, R.K. & WAKADE, A.R. (1987). Vasoactive intestinal polypeptide stimulates the secretion of catecholamines from the rat adrenal gland. *J. Physiol.*, **388,** 285–294.

MINKES, R.K., MCMAHON, T.J., HIGUERA, T.R., MURPHY, W.A., COY, D.H. & KADOWITZ, P.J. (1992). Analysis of systemic and pulmonary vascular responses to PACAP and VIP: role of adrenal catecholamines. *Am. J. Physiol.*, **263,** H1659–1669.

MIYATA, A., ARIMURA, A., DAHL, R.R., MINAMINO, N., UEHARA, A., JIANG, L., CULLER, M.D. & COY, D.H. (1989). Isolation of a novel 38 residue-hypothalamic polypeptide which stimulates adenylate cyclase in pituitary cells. *Biochem. Biophys. Res. Commun.*, **164,** 567–574.

MIYATA, A., JIANG, L., DAHL, R.D., KITADA, C., KUBO, K., FUJINO, M., MINAMINO, N. & ARIMURA, A. (1990). Isolation of a neuropeptide corresponding to the N-terminal 27 residues of the pituitary adenylate cyclase activating polypeptide with 38 residues (PACAP38). *Biochem. Biophys. Res. Commun.*, **170,** 643–648.

NANDHA, K.A., BENITO-ORFILA, M.A., SMITH, D.M., GHATEI, M.A. & BLOOM, S.R. (1991). Action of pituitary adenylate cyclase-activating polypeptide and vasoactive intestinal polypeptide on the rat vascular system: effects on blood pressure and receptor binding. *J. Endocrinol.*, **129,** 69–73.

NARUSE, S., YASUI, A., KISHIDA, S., KADOWAKI, M., HOSHINO, M., OZAKI, T., ROBBERECHT, P., CHRISTOPHE, J., YANAIHARA, C. & YANAIHARA, N. (1986). Helodermin has a VIP-like effect upon canine blood flow. *Peptides*, **7** (Suppl 1), 237–240.

PORTER, J.P., REID, I.A., SAID, S.I. & GANONG, W.F. (1982). Stimulation of renin secretion by vasoactive intestinal peptide. *Am. J. Physiol.*, **234,** F306-F310.

VAN GELDEREN, E.M., HEILIGERS, J.P.C. & SAXENA, P.R. (1991). Haemodynamic changes and acetylcholine-induced hypotensive responses after N^G-nitro-L-arginine methyl ester in rats and cats. *Br. J. Pharmacol.*, **103,** 1899–1904.

WAKADA, T.D., BLANK, M.A., MALHOTRA, R.K., POURCHOSE, R. & WAKADE, A.R. (1991a). The peptide VIP is a neurotransmitter in rat adrenal medulla: physiological role in controlling catecholamine secretion. *J. Physiol.*, **444,** 349–362.

WAKADA, A.R., GUO, X., STRONG, R., ARIMURA, A. & HAYCOCK, J. (1991b). Pituitary adenylate cyclase-activating polypeptide (PACAP) as a neurotransmitter in rat adrenal medulla. *Regul. Pept.*, **37,** 331.

WARREN, J.B., DONNELLY, L.E., CULLEN, S., ROBERTSON, B.E., GHATEI, M.A., BLOOM, S.R. & MACDERMOT, J. (1991). Pituitary adenylate cyclase-activating polypeptide: a novel, long-lasting endothelium-independent vasorelaxant. *Eur. J. Pharmacol.*, **197,** 131–134.

WONG, P.C., PRICE, W.A., CHIU, A.T., DUNCIA, J.V., CARINI, D.J., WEXLER, R.R., JOHNSON, A.L. & TIMMERMANS, P.B.M.W.M. (1990). Hypotensive action of DuP 753, an angiotensin II antagonist, in spontaneously hypertensive rats. *Hypertension*, **15,** 459–468.

(Received May 25, 1993
Revised October 12, 1993
Accepted October 18, 1993)

Br. J. Pharmacol. (1994), **111**, 598–608

Calcium-dependence of histamine- and carbachol-induced inositol phosphate formation in human U373 MG astrocytoma cells: comparison with HeLa cells and brain slices

J.A. Arias-Montaño, V. Berger & [1]J.M. Young

Department of Pharmacology, University of Cambridge, Tennis Court Road, Cambridge CB2 1QJ

1 Histamine (1 mM) induced an accumulation of inositol monophosphate ([^{3}H]-IP_1) in the U373 MG human astrocytoma cell line which increased with time in the presence of 30 mM Li^+. After a 30 min incubation period with 1 mM histamine [^{3}H]-IP_1 was the major product detected (84 ± 1% of total [^{3}H]-IP_x) and was present at a level 11 (± 1) fold of basal accumulation.

2 Concentration-response curves for histamine-induced [^{3}H]-IP_1 accumulation in U373 MG cells (EC_{50} 5.4 ± 0.5 μM) were shifted to the right in a parallel fashion by mepyramine (slope of a Schild plot 0.99 ± 0.08), yielding a K_d for mepyramine of 3.5 ± 0.3 nM, consistent with the involvement of histamine H_1-receptors.

3 The temelastine-sensitive binding of [^{3}H]-mepyramine to a membrane fraction from U373 MG cells was hyperbolic and had a mean K_d of 2.5 ± 1.0 nM. The maximum amount of temelastine-sensitive binding was 86 ± 19 pmol g^{-1} membrane protein.

4 Carbachol also induced [^{3}H]-IP_1 accumulation in U373 MG cells, 2.8 (± 0.1) fold of basal with 1 mM carbachol, with an EC_{50} of 48 ± 8 μM. Pirenzepine shifted carbachol concentration-response curves to the right (slope of Schild plot 0.89 ± 0.07) giving a K_d for pirenzepine of 0.10 ± 0.01 μM, suggesting that phosphoinositide hydrolysis in U373 MG cells is mediated by the M_3-, rather than the M_1-, muscarinic receptor subtype.

5 [^{3}H]-IP_1 accumulation induced by both 1 mM histamine and by 1 mM carbachol increased when the Ca^{2+} concentration of the medium was increased from 'zero' (no added Ca^{2+}) to 0.3 mM. Histamine-stimulated [^{3}H]-IP_1 accumulation was further increased, although not so markedly, as the Ca^{2+} was raised to 4 mM. The same pattern was apparent with histamine-induced accumulations of [^{3}H]-IP_2 and [^{3}H]-IP_3. In contrast, [^{3}H]-IP_x accumulation in response to carbachol increased between 0.3 and 1.3 mM, but thereafter remained unchanged ([^{3}H]-IP_1) or declined ([^{3}H]-IP_2 and [^{3}H]-IP_3).

6 In HeLa cells, [^{3}H]-IP_1 accumulations induced by 1 mM histamine and 1 mM carbachol showed the same pattern of Ca^{2+} dependence and were independent of extracellular Ca^{2+} above 0.3 mM (histamine) or 1.3 mM (carbachol). The response to carbachol appeared to be mediated by an M_3-muscarinic receptor (apparent K_d for pirenzepine 0.09 μM).

7 In cross-chopped slices of guinea-pig cerebral cortex and guinea-pig cerebellum, [^{3}H]-IP_1 accumulation induced by 1 mM histamine in the presence of 10 mM Li^+ increased as the extracellular Ca^{2+} was increased from 0.3 to 2.5 mM, but a further increase to 4 mM had no further effect. In contrast the response to histamine in rat cerebral cortex increased markedly between 1.3 and 4 mM Ca^{2+}. Accumulations of [^{3}H]-IP_1 induced by carbachol in guinea-pig or rat cerebral cortical slices were not increased as extracellular Ca^{2+} was raised from 0.3 to 4 mM.

8 Nimodipine (100 nM) and ω-conotoxin (3 μM) had no significant effect on histamine-induced [^{3}H]-IP_1 accumulation in rat cerebral cortical slices or in U373 MG cells.

9 We conclude that histamine-induced [^{3}H]-IP_1 accumulation in U373 MG cells does appear to have a component dependent on the extracellular Ca^{2+} concentration. The degree of Ca^{2+}-dependence approaches that observed in guinea-pig cerebral cortex but is much less than in rat cerebral cortex. Whether U373 MG cells will be of use as a model system for the apparent Ca^{2+}-entry component observed in guinea-pig or rat brain slices remains to be established.

Keywords: Histamine H_1-receptors; muscarinic M_3-receptors; calcium; inositol phosphates; U373 MG astrocytoma cells; HeLa cells; guinea-pig-brain; rat cerebral cortex

Introduction

There is now a body of evidence that histamine H_1-receptors in brain are associated with the 'arousal' response to histamine (Schwartz *et al.*, 1991), but the locus and cellular mechanisms involved remain uncertain. The primary cellular response to H_1-receptor activation appears to be G protein-mediated activation of phosphoinositidase C (PIC) (Hill, 1990) and in guinea-pig brain there is a good correlation between H_1-receptor density in different regions and histamine-stimulated inositol phosphate ([^{3}H]-IP) formation (Daum *et al.*, 1983). However, there are indications that there may be an additional pathway of phosphoinositide hydrolysis in brain. The most direct evidence is that in mouse and rat cerebral cortical slices, histamine-stimulated [^{3}H]-IP accumulation is almost linearly dependent on the Ca^{2+} content of the medium in the millimolar concentration range (Alexander *et al.*, 1990a), strongly suggesting the involvement of a Ca^{2+} entry step and Ca^{2+} activation of one or more PIC isoenzymes (Eberhard & Holz, 1988; Baird & Nahorski, 1990). Noradrenaline appears to be the only other monoamine to show this degree of Ca^{2+}-dependence of phosphoinositide breakdown in brain slices (Knepper & Rutledge, 1987; Alex-

[1] Author for correspondence.

ander *et al.*, 1990a) and in this case there is evidence for distinct α_1-adrenoceptor subtypes coupling with PIC and Ca^{2+} entry (Summers & McMartin, 1993), although the subtypes involved in [^{3}H]-IP formation in rat cerebral cortex remain uncertain (Michel *et al.*, 1990; Minneman & Atkinson, 1991). In contrast, carbachol-stimulated [^{3}H]-IP accumulation in mouse and rat cerebral cortex is essentially independent of extracellular Ca^{2+} above 0.3 mM (Alexander *et al.*, 1990a).

Histamine-activated Ca^{2+} channels or non-selective cation channels are well established in peripheral tissues such as intestinal smooth muscle cells (Komori *et al.*, 1992), endothelial cells (Yamamoto *et al.*, 1992) and adrenal medullary chromaffin cells (Goh & Kurosawa, 1991), and in the guinea-pig smooth muscle cells there is evidence that the non-selective cation channel is activated via a pertussis toxin-sensitive G protein (Komori *et al.*, 1992). However, there is no direct evidence for the presence of such channels in brain. A detailed investigation of the pathways of histamine-induced phosphoinositide metabolism in brain is hampered by the inherent complexity of brain slices and in particular by the presence of multiple cell types. There is thus a need for a simple model system. Ideally, two model systems are required: one which has only the direct H_1-receptor/G protein activation of PIC and a second with as large a contribution as possible from the presumed Ca^{2+} entry component. We have presented preliminary evidence that the human HeLa cell line may be a suitable model for the direct pathway (Arias-Montaño & Young, 1992), but finding a cell line of central origin as a model for the Ca^{2+}-dependent pathway has proved to be difficult. We describe here the characterization of histamine- and carbachol-induced inositol phosphate formation in human U373 MG astrocytoma cells and a comparison of the patterns of Ca^{2+}-dependence with those observed in HeLa cells and brain slices. To test for possible species differences in the latter we have compared the Ca^{2+}-dependence of histamine-induced [^{3}H]-IP_1 accumulation in slices from rat and guinea-pig cerebral cortex. In addition, since in rat cerebral cortex there is indirect evidence that H_1-receptors coupled to phosphoinositide hydrolysis are located, at least in part, on glial cells (Arbonés *et al.*, 1988), we have also made a comparison with guinea-pig cerebellum, where H_1-receptors are apparently predominantly neuronal (Palacios *et al.*, 1981).

Methods

Accumulation of [^{3}H]-inositol phosphates in U373 MG cells

U373 MG cells (National Culture Collection, Porton Down) were grown to near confluence in Dulbecco's modified Eagle medium (DMEM)/nutrient mixture F-12 (1:1 v/v; Gibco), containing 10% (v/v) bovine foetal calf serum and 2 mM glutamine (Gibco) and supplemented with penicillin (50 u ml^{-1}) and streptomycin (50 mg ml^{-1}) (Flow Laboratories), in flasks at 37°C in a CO_2-incubator (5% CO_2). The culture medium was removed and the cells washed in approximately 14 ml inositol-free DMEM before addition of inositol-free DMEM containing 10% dialysed calf serum, 10 μM *myo*-inositol and 2.5 μCi ml^{-1} [^{3}H]-inositol (0.16 μM). The cells were then incubated for 24 h. The [^{3}H]-inositol-labelled cells were washed once with approximately 15 ml phosphate buffered saline (PBS) (in mM: NaCl 137, KCl 2.7, Na_2HPO_4 8.1 and KH_2PO_4 1.5) containing 0.6 mM EDTA before dissociation with 10 ml trypsin/EDTA (500–750 BAEE units ml^{-1}/0.6 mM, Sigma). After centrifugation at 220 *g* for 5 min the cells were resuspended in Krebs-Henseleit medium (in mM: NaCl 116, KCl 4.7, $MgSO_4$ 1.2, KH_2PO_4 1.2, $NaHCO_3$ 25, $CaCl_2$ 2.5 and D-glucose 11). Cells (50 μl, approximately 8×10^5 cells) were added to 190 μl Krebs-Henseleit solution containing LiCl (final concentration 30 mM), gassed with O_2:CO_2 (95:5%), v/v, and incubated for 15 min at 37°C, before addition of 10 μl histamine or carbachol (final concentration 0.1–1000 μM). After each addition the tubes were gassed with O_2:CO_2 (95:5%, v/v) and the incubation continued at 37°C in a shaking water bath, usually for 30 min. Mepyramine or pirenzepine, where present, was added 15 min before the agonist. Incubations were terminated by addition of 250 μl of an ice-cold solution of 10% perchloric acid, containing 1 mM ethylenediaminetetraacetic acid (EDTA) and 1 mg ml^{-1} phytic acid, and allowed to stand on ice for 15 min. Inositol phosphates were extracted by the trioctylamine-freon method (Sharpes & McCarl, 1982; Downes *et al.*, 1986). Trioctylamine/1,1,2-trichlorotrifluoroethane (1:1, v/v) (0.4 ml) was added to the sample, the solution mixed thoroughly and then centrifuged at 950 *g* for 5 min to separate the phases. A sample (0.38 ml) of the upper phase was transferred to an insert vial, 4 ml 50 mM 2-amino-2-hydroxymethyl-propan-1,3-diol (Tris) buffer, pH 7.5, added and the mixture applied to an AG 1-X8 (formate form, 100–200 mesh; Biorad) anion-exchange column.

[^{3}H]-inositol and [^{3}H]-glycerophosphoinositol were eluted with 10 ml water and 10 ml 60 mM ammonium formate/5 mM sodium tetraborate, respectively, and [^{3}H]-inositol monophosphates ([^{3}H]-IP_1) then eluted with 10 ml 200 mM ammonium formate/100 mM formic acid. Higher phosphates were eluted by sequential addition of 10 ml 400 mM ammonium formate/100 mM formic acid (for [^{3}H]-inositol bisphosphates, [^{3}H]-IP_2) and 10 ml 800 mM ammonium formate/100 mM formic acid (for [^{3}H]-inositol trisphosphates, [^{3}H]-IP_3). This procedure does not separate individual mono-, bis-, and trisphosphate isomers. Thus the trisphosphate fraction will contain both 1,4,5- and 1,3,4-IP_3. Quicksafe A (10 ml, Zinnser) was added to each fraction and tritium determined by liquid scintillation counting. Within an experiment 3–4 replicate determinations were made of each incubation condition.

Accumulation of [^{3}H]-inositol phosphates in HeLa cells

HeLa cells (S3 clone) were grown to near confluence in DMEM (Gibco), containing 5% (v/v) bovine foetal calf serum and 5% (v/v) bovine neonate calf serum (Gibco) and supplemented with penicillin (50 u ml^{-1}) and streptomycin (50 mg ml^{-1}), in flasks at 37°C in a CO_2-incubator (5% CO_2). The culture medium was removed and the cells washed in approximately 14 ml inositol-free DMEM before addition of inositol-free DMEM containing 10% dialysed calf serum, 10 μM *myo*-inositol and 2.5 μCi ml^{-1} [^{3}H]-inositol (0.16 μM). Labelling of the cells, incubation with histamine and carbachol and extraction of [^{3}H]-inositol phosphates was carried out as described above. Antagonists were added 15 min before histamine or carbachol.

Accumulation of [^{3}H]-inositol phosphates in brain slices

Cross-chopped slices (350 × 350 μm, McIlwain tissue chopper) of guinea-pig (Dunkin-Hartley strain, males, 350–500 g; Tucks, Battlebridge, Essex) cerebellum and cerebral cortex and rat (Wistar strain, males, 200–350 g; Tucks, Battlebridge, Essex) cerebral cortex were washed three times and then incubated at 37°C for 60 min in Krebs-Henseleit medium with three further changes of medium. The medium was bubbled throughout with O_2/CO_2 (95:5, v/v). The slices were washed once more and then transferred to a flat-bottom vial (Hughes & Hughes, scintillation vial insert) and allowed to settle under gravity. Portions of the slices (30 μl) were added to 210 μl Krebs-Henseleit medium, containing 0.33 μM *myo*-[2-^{3}H]-inositol (1 μCi per incubation) and 10 mM LiCl, in insert vials. The mixture was incubated for 30 min in a shaking water bath before addition of 10 μl histamine or carbachol solution and further incubation for 60 min. Incubations were terminated and [^{3}H]-inositol phosphates determined as described under U373 MG cells above.

Ca^{2+}-dependence of [^{3}H]-inositol phosphate accumulation

In experiments on the Ca^{2+}-dependence of histamine- or carbachol-induced [^{3}H]-inositol phosphate accumulation, brain slices were preincubated in normal Krebs-Henseleit and then labelled with [^{3}H]-inositol and exposed to agonist in medium containing the concentration of Ca^{2+} under test. U373 MG and HeLa cells were labelled with [^{3}H]-inositol and dissociated following the standard protocol (see above). The dissociated cells were washed twice in Krebs-Henseleit solution from which Ca^{2+} had been omitted and then equilibrated for 15 min in Krebs-Henseleit solution containing the Ca^{2+} concentration under test. Further incubation with or without 1 mM histamine or 1 mM carbachol was for 30 min. For '0 Ca^{2+}', Ca^{2+} was omitted from the medium.

Measurement of [^{3}H]-mepyramine binding to U373 MG cell membranes

U373 MG cells were lysed in 50 mM Na-K phosphate buffer (37.8 mM Na_2HPO_4, 12.2 mM KH_2PO_4), pH 7.5, and centrifuged at *circa* 15,000 *g* for 10 min. The pellet was resuspended in buffer and recentrifuged at *circa* 15,000 *g* for 10 min. The final pellet was resuspended in buffer and stored at − 20°C. When required, pellets were thawed and homogenized in a teflon-glass homogenizer with a motor-driven pestle (300 r.p.m., 10 up and down strokes) and resuspended in buffer. Protein was measured essentially as described by Lowry *et al.* (1951).

Incubations in 50 mM Na-K phosphate buffer, pH 7.5, contained [^{3}H]-mepyramine (0.3–20 nM) and U373 MG cell membrane homogenate (0.19–0.23 mg protein) in a final volume of 1.0 ml (3–4 replicates at each concentration). A parallel set of incubations contained in addition 1 μM temelastine to define non-H_1-receptor binding. Incubation was for 60 min at 30°C and was terminated by filtration through Whatman GF/B glass fibre paper, pre-soaked in 0.3% (w/v) polyethylenimine for 3–5 h, using a Brandel (Gaithersburg, Md, U.S.A.) cell harvester. The filters were washed with ice-cold buffer and then transferred to scintillation insert vials and 4.0 ml Emulsifier-Safe scintillator (Packard) added. The vials were allowed to stand at room temperature for at least 2 h before counting.

Analysis of data

Concentration-response data for agonist-induced [^{3}H]-IP_1 accumulation (after subtraction of basal accumulation) were fitted to a Hill equation (logistic equation) using the Harwell Library non-linear regression programme VB01A. The actual equation fitted was:

$$[^3H]\text{-}IP_1 \text{ accumulated} = Resp_{max}.C^n/(C^n + EC_{50}^n)$$

where C is the agonist concentration, EC_{50} is the concentration giving the half-maximal response, n is the Hill coefficient and $Resp_{max}$ is the maximum response. Each point was weighted according to the reciprocal of the variance associated with it. Curves of the temelastine-sensitive binding of [^{3}H]-mepyramine *versus* the concentration of [^{3}H]-mepyramine were analysed similarly to obtain best-fit values of the Hill coefficient. Since the Hill coefficient was not significantly different from unity in any of the three experiments, the data were fitted to a hyperbola (n = 1 in the equation above) to obtain the EC_{50} (= K_d) and B_{max}.

Statistical comparison of parameters characterizing two concentration-response curves was made by fitting the curves simultaneously (using the NAG library routine E04FDF) and assessing the increase in the residual sum of squares when

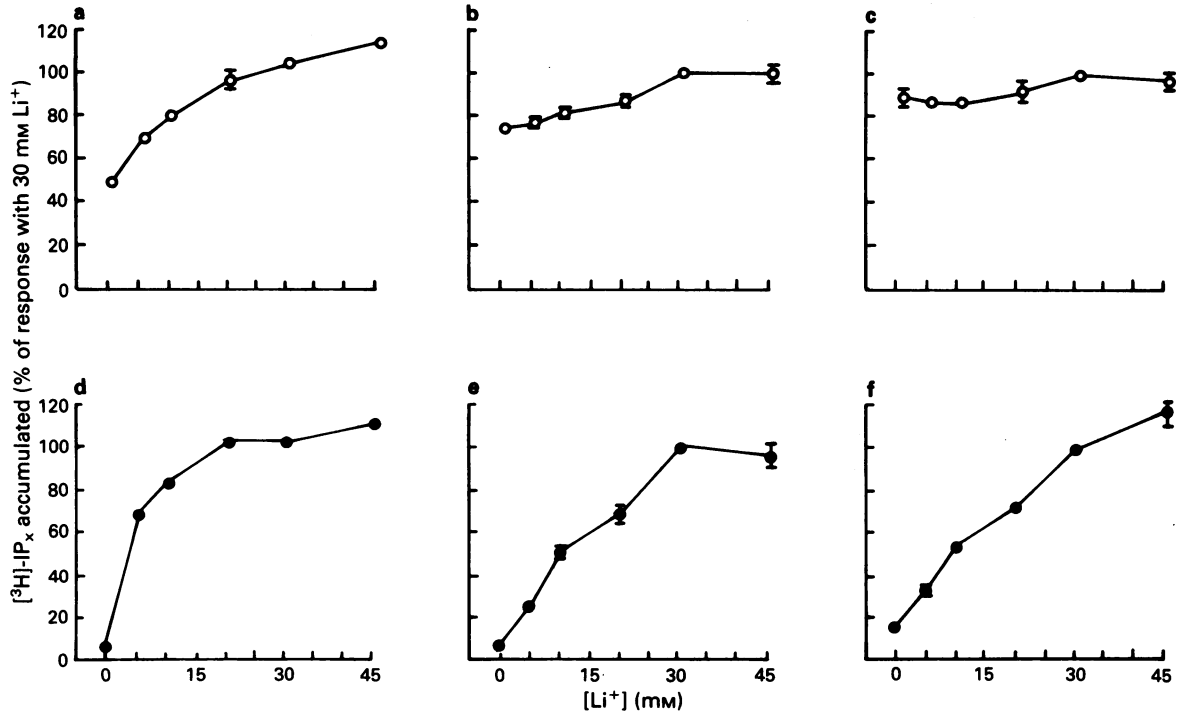

Figure 1 Sensitivity of basal and histamine-induced [^{3}H]-IP_1, [^{3}H]-IP_2 and [^{3}H]-IP_3 accumulation to Li^+. U373 MG cells were incubated with the test concentration of Li^+ for 15 min before incubation for 30 min in the presence or absence (basal) of 1 nM histamine. Values are the weighted means ± s.e.mean from three experiments. To allow for variation in the absolute magnitude of the response between experiments, accumulations in the presence of 30 mM Li^+ were set at 100%. Where no error bars are shown the error was within the size of the symbol. Mean basal accumulations (○) in the presence of 30 mM Li^+ were: [^{3}H]-IP_1 (a) 1,305 ± 16 d.p.m., [^{3}H]-IP_2 (b) 880 ± 9 d.p.m., and [^{3}H]-IP_3 (c) 320 ± 13 d.p.m. Corresponding accumulations induced by 1 mM histamine (basal accumulation subtracted) (●) were: [^{3}H]-IP_1 (d) 18,642 ± 131 d.p.m., [^{3}H]-IP_2 (e) 3,353 ± 89 d.p.m., and [^{3}H]-IP_3 (f) 938 ± 20 d.p.m.

parameters were constrained to be the same for both curves, by calculating the *F*-statistic (Rodbard, 1974):

$$F = \{(SS_2 - SS_1)/(df_2 - df_1)\}/(SS_1/df_1)$$

where SS_2 is the sum of squares when a parameter is shared (df_2 degrees of freedom) and SS_1 the sum of squares when all parameters are allowed to float freely for each curve (df_1 degrees of freedom).

The dissociation constants for mepyramine and pirenzepine in U373 MG cells were determined from shifts of the concentration-response curve for histamine- or carbachol-induced [^{3}H]-IP$_1$ accumulation using the relationship: log (concentration-ratio − 1) = log([A]) − log(K_d), where the concentration-ratio is the ratio of the EC_{50} values in the presence and absence of antagonist, [A] is the concentration of the antagonist and K_d its dissociation constant. Unbiased estimates of the concentration-ratio were obtained from best-fit EC_{50} values by fitting simultaneously (using the E04FDF routine as above) curves in the presence and absence of a single concentration of mepyramine or pirenzepine, measured in the same experiment, with the Hill slope and the maximum response constrained to be the same for both curves. This obviates difficulties with shifted curves where the maximum response is poorly defined. Where individual curves could be fitted satisfactorily without constraints, constraining Hill coefficients and maximum responses did not significantly worsen the fit.

Multiple comparisons of values at different times or under different incubation conditions within a single experiment were made using the Student-Newman-Keuls multiple range test.

Drugs

Myo-[2-^{3}H]-inositol, 20–24 Ci mmol^{-1}, was obtained from New England Nuclear and [*pyridinyl*-5-^{3}H]-mepyramine, 21 Ci mmol^{-1}, from Amersham International. Adenosine, carbachol (carbamylcholine chloride), histamine dihydrochloride, mepyramine maleate, N-methylatropine bromide, phytic acid, pirenzepine hydrochloride, prazosin hydrochloride and ω-conotoxin GVIA were purchased from Sigma; 1,1,2-trichlorotrifluoroethane (freon) and tri-n-octylamine from Aldrich. Temelastine was kindly provided by Smith, Kline & French Research Ltd and nimodipine by Dr K. Byron, University of Cambridge.

Results

Lithium-sensitivity of histamine-induced [^{3}H]-IP$_x$ accumulation in U373 MG cells

Basal accumulation of [^{3}H]-IP$_1$ in U373 MG cells, measured 45 min after addition of Li^+, increased as the concentration of Li^+ present was increased from 0 to 45 mM (Figure 1a). The accumulations of [^{3}H]-IP$_2$ and [^{3}H]-IP$_3$ were much less affected (Figure 1b,c). However, accumulations of all three fractions induced by incubation with 1 mM histamine for 30 min were much more sensitive to Li^+ than the corresponding basal accumulations. Histamine-induced accumulation of [^{3}H]-IP$_1$ appeared to reach a plateau level at approximately 20 mM Li^+ (Figure 1d), whereas the accumulation of [^{3}H]-IP$_3$ increased throughout the range 0 to 45 mM Li^+ (Figure 1f) and that of [^{3}H]-IP$_2$ only appeared to have reached a maximum level at 45 mM Li^+ (Figure 1e). Since [^{3}H]-IP$_1$ is present in the greatest amounts (see below), all subsequent incubations were carried out with 30 mM Li^+ present.

Characterization of histamine-induced [^{3}H]-IP$_x$ accumulation in U373 MG cells

In the presence of 1 mM histamine and 30 mM Li^+ the accumulation of [^{3}H]-IP$_1$ increased with time over the period studied (Figure 2a), whereas the accumulations of [^{3}H]-IP$_2$ and [^{3}H]-IP$_3$ initially increased rapidly, but had reached a maximum by 10 and 5 min, respectively (Figure 2b and 2c). Basal levels of [^{3}H]-IP$_1$, but not [^{3}H]-IP$_2$ and [^{3}H]-IP$_3$, increased slightly, but significantly, over the 60 min. In all subsequent experiments the period of incubation with histamine was 30 min. Under these conditions [^{3}H]-IP$_1$ accounts for 84 ± 1% of total [^{3}H]-IP$_1$ + [^{3}H]-IP$_2$ + [^{3}H]-IP$_3$ (nine determinations). The mean accumulation of [^{3}H]-IP$_1$ in the presence of 1 mM histamine was 11 (± 1) fold of basal accumulation ($n = 31$). There was no indication of any change in the extent of the response to histamine with passage number (up to 40). The EC_{50} for histamine-induced accumulation was 5.4 ± 0.5 μM (best-fit value to the combined data from 15 determinations; best-fit value of the Hill coefficient 0.89 ± 0.06).

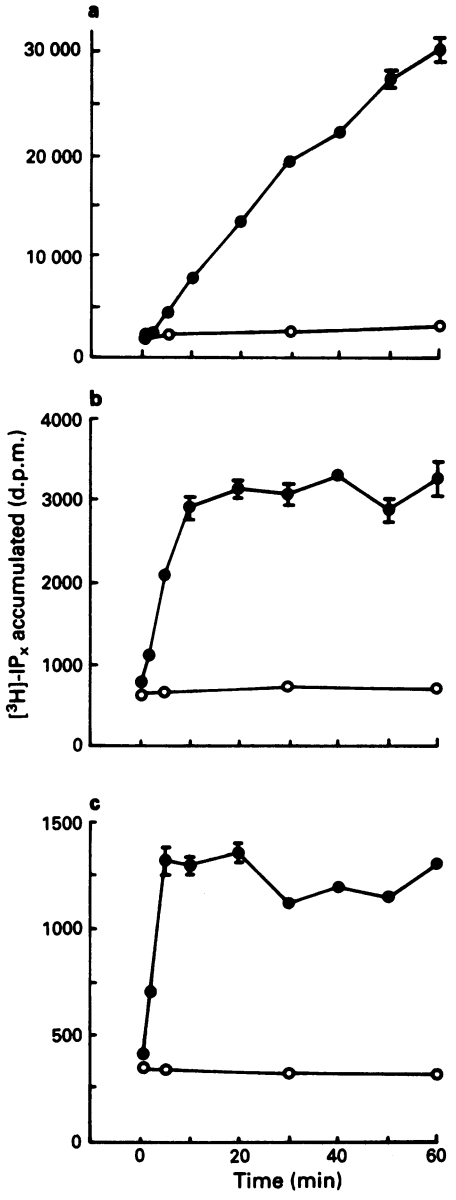

Figure 2 Time course of [^{3}H]-IP$_x$ accumulation in the presence and absence of 1 mM histamine. Incubation with 1 mM histamine was for 30 min. Values are the means ± s.e.mean from triplicate determinations from a single experiment. Where no error bars are shown the error was within the size of the symbol. The whole experiment was repeated three times with similar results. (a) [^{3}H]-IP$_1$, (b) [^{3}H]-IP$_2$, (c) [^{3}H]-IP$_3$. (○) No addition (basal); (●) + 1 mM histamine.

Concentration-response curves for histamine-induced [^{3}H]-IP_1 accumulation were displaced to the right in a parallel fashion by increasing concentrations of mepyramine (Figure 3a). A Schild plot of the data from 11 experiments with 10–100 nM mepyramine was linear with a slope of 0.99 ± 0.08 (Figure 3b). Log K_d derived from this plot was 8.46 ± 0.03 (K_d 3.5 ± 0.3 nM, approximate s.e.mean).

[^{3}H]-mepyramine binding to U373 MG cell membranes

The binding of [^{3}H]-mepyramine insensitive to inhibition by 1 μM temelastine (non-H_1-receptor binding) increased linearly with the concentration of [^{3}H]-mepyramine between 0.4 and 20 nM. The non-specific binding accounted for 30–45% of the total binding at 2 nM and 70–77% of the total binding at 20 nM [^{3}H]-mepyramine (three experiments). The Hill coefficients of the curves of the temelastine-sensitive binding of [^{3}H]-mepyramine did not differ significantly from unity. The maximum H_1-receptor binding was 78 ± 12, 122 ± 5 and 59 ± 4 pmol g^{-1} protein in the three experiments, with corresponding EC_{50} (K_d) values of 2.1 ± 0.5, 4.3 ± 0.5 and 1.0 ± 0.2 nM, respectively (mean 2.5 ± 1.0 nM). The error on the mean K_d is appreciable, but the value is in reasonable accord with the value of 3.5 ± 0.3 nM obtained from inhibition of histamine-induced [^{3}H]-IP_1 accumulation.

Characteristics of carbachol-induced [^{3}H]-IP_x accumulation in U373 MG cells

Carbachol also stimulated [^{3}H]-IP_1 accumulation in U373 MG cells, with a time-course similar to that observed for histamine, although the extent of the accumulation was less, 2.8 (± 0.1) fold of basal in the presence of 1 mM carbachol (n = 17). [^{3}H]-IP_1 was again much the major labelled product under these conditions (88 ± 1% of total [^{3}H]-IP_1 + [^{3}H]-IP_2 + [^{3}H]-IP_3, seven determinations).

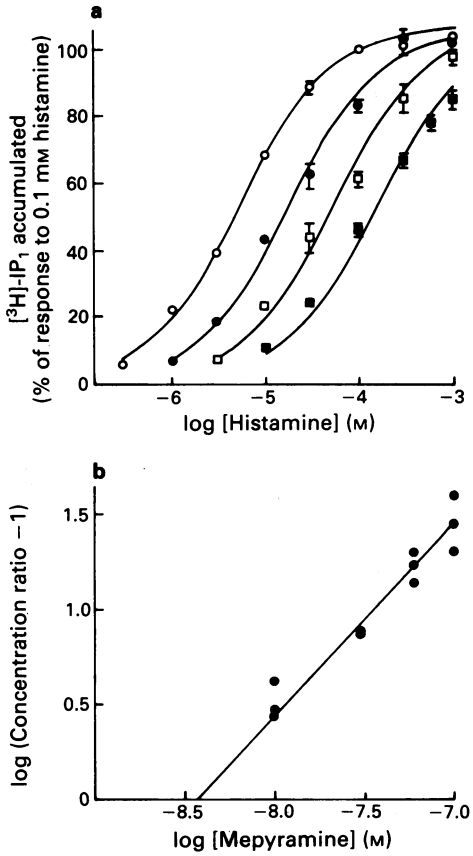

Figure 3 Inhibition of histamine-induced [^{3}H]-IP_1 accumulation by mepyramine. (a) Values are the weighted means ± s.e.mean from the combined data from 11 curves for histamine, two curves with 3 nM mepyramine and three curves with 10 and 100 nM mepyramine. To allow for variations in the absolute magnitude of the accumulation of [^{3}H]-IP_1 between experiments, the data have been normalised by setting the response in the presence of 100 μM histamine to 100%. Where no error bars are shown the error was within the size of the symbol. The lines drawn are the best-fit curves with maximum values and Hill coefficients constrained to a common value (see Methods). (○) Histamine alone; (●) + 10 nM mepyramine; (□) + 30 nM mepyramine; (■) + 100 nM mepyramine. (b) Schild plot of the data for mepyramine. Each point is an unbiased estimate of the concentration-ratio obtained from the ratio of the EC_{50} values obtained by fitting simultaneously concentration-response curves for histamine and histamine + 10, 30, 60 or 100 nM mepyramine measured in the same experiment, with the Hill coefficient and the maximum response constrained to be the same for both curves (see Methods). For clarity the error bars (estimated error) have been omitted. The line drawn was calculated by linear regression analysis. Best-fit values: slope 0.99 ± 0.08, intercept (log affinity constant) 8.46 ± 0.03.

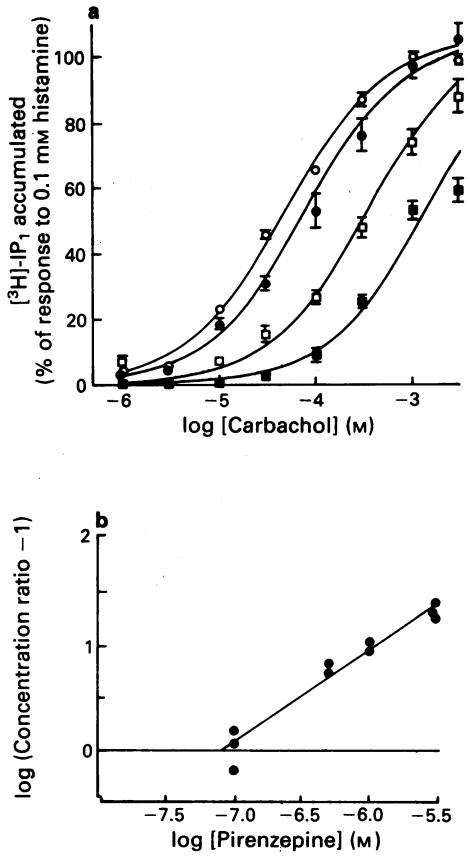

Figure 4 Inhibition of carbachol-induced [^{3}H]-IP_1 accumulation by pirenzepine. (a) Values are the weighted means ± s.e.mean from the combined data from 10 curves for carbachol, three curves with 100 nM and 3 μM pirenzepine and two curves with 1 μM pirenzepine. To allow for variations in the absolute magnitude of the accumulation of [^{3}H]-IP_1 between experiments, the data have been normalised by setting the response in the presence of 1 mM carbachol to 100%. Where no error bars are shown the error was within the size of the symbol. The lines drawn are the best-fit curves with maximum values and Hill coefficients constrained to a common value (see Methods). (○) Carbachol alone; (●) + 100 nM pirenzepine; (□) + 1 μM pirenzepine; (■) + 3 μM pirenzepine. (b) Schild plot of the data for pirenzepine. Each point is an unbiased estimate of the concentration-ratio obtained from the ratio of the EC_{50} values obtained by fitting simultaneously concentration-response curves for carbachol and carbachol + 100 nM, 500 nM, 1 μM and 3 μM pirenzepine measured in the same experiment, with the Hill coefficient and the maximum response constrained to be the same for both curves (see Methods). The error bars have been omitted for clarity. The line drawn was calculated by linear regression analysis. Best-fit value of the slope 0.89 ± 0.07.

Concentration-response curves for carbachol-induced [^{3}H]-IP_1 accumulation, EC_{50} 48 ± 8 μM and Hill coefficient of 0.85 ± 0.07 (best-fit values ± approximate s.e. to the combined data from 12 determinations), were displaced to the right by pirenzepine (Figure 4a). A Schild plot of the data (Figure 4b) had a slope, 0.89 ± 0.07, not significantly different from unity. Constraining the slope to be unity yielded a log K_d of 7.0 ± 0.01 (K_d 1.01 ± 0.04 × 10^{-7} M, approximate s.e.), a value in the range expected for binding to the M_3-muscarinic receptor subtype (Hulme *et al.*, 1990).

Ca^{2+}-dependence of histamine- and carbachol-induced [^{3}H]-IP_x accumulation in U373 MG cells

[^{3}H]-IP_1, [^{3}H]-IP_2 and [^{3}H]-IP_3 accumulations in the presence of 1 mM histamine increased markedly as the Ca^{2+} concentration in the medium was increased from nominally zero (no added Ca^{2+}) to 0.3 mM, followed by less pronounced, but statistically significant ($P<0.05$, Student-Newman-Keuls multiple range test), increases as extracellular Ca^{2+} was increased to 1.3 mM and from 1.3 to 4.0 mM (Figure 5). The pattern of the Ca^{2+}-dependence was similar for all three fractions. There was a small, statistically significant, increase in basal [^{3}H]-IP_1 and [^{3}H]-IP_2 accumulation between no added Ca^{2+} and 0.3 mM Ca^{2+}, but a further increase in the concentration of Ca^{2+} in the medium had no added effect (Figure 5). The relative amount of [^{3}H]-IP_1 induced by 1 mM histamine, expressed as a percentage of [^{3}H]-IP_1 + [^{3}H]-IP_2 + [^{3}H]-IP_3 accumulated, did not differ significantly at 2.5 mM Ca^{2+}, 84 ± 1% (9), and 4.0 mM Ca^{2+}, 85 ± 1% (4).

Carbachol-induced accumulation of [^{3}H]-IP_1, [^{3}H]-IP_2 and [^{3}H]-IP_3 also increased between 'zero' and 0.3 mM Ca^{2+} (Figure 6). There was an additional increase in [^{3}H]-IP_1 and [^{3}H]-IP_2 accumulation as the Ca^{2+} was increased to 1.3 mM, but further increase to 4 mM had no significant effect on the amount of [^{3}H]-IP_1 and caused a decrease in [^{3}H]-IP_2. Amounts of [^{3}H]-IP_3 accumulated were very small (Figure 6c), but there was no indication of the stimulatory effect of increasing the extracellular Ca^{2+} from 0.3 to 4 mM seen with the response to histamine (Figure 5).

Ca^{2+}-dependence of histamine- and carbachol-induced [^{3}H]-IP_x accumulation in HeLa cells

Histamine (1 mM) induced an accumulation of [^{3}H]-IP_1 8.03 (± 0.08) fold (17) of basal level in the HeLa S3 clone. This is approximately 4 fold greater than the magnitude of the response to histamine in the unspecified clone used in our earlier study with HeLa cells (Bristow *et al.*, 1991). In

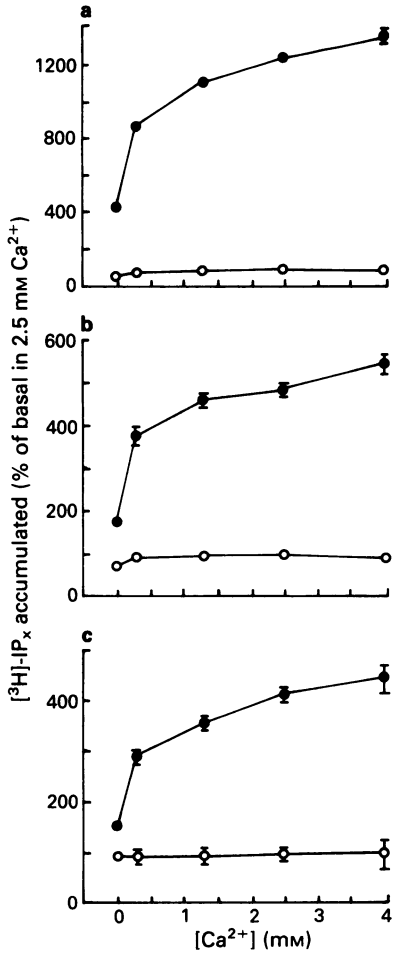

Figure 5 Ca^{2+}-dependence of histamine-induced [^{3}H]-IP_x accumulation. Values are the weighted means ± s.e.mean from 3 experiments. To allow for differences in the absolute magnitude of the accumulation between experiments, values have been expressed as a percentage of basal acccumulation of each isomer in the presence of 2.5 mM Ca^{2+}. (a) [^{3}H]-IP_1; (b) [^{3}H]-IP_2; (c) [^{3}H]-IP_3 (mean basal accumulations at 2.5 mM Ca^{2+} 1187 ± 11, 465 ± 9 and 260 ± 9 d.p.m., respectively). Where no error bar is shown the error was within the size of the symbol. (○) No addition (basal); (●) + 1 mM histamine.

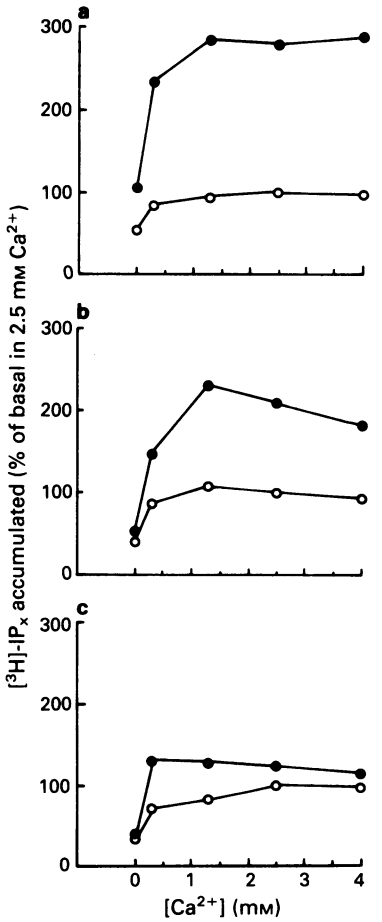

Figure 6 Ca^{2+}-dependence of carbachol-induced [^{3}H]-IP_x accumulation. Values are the weighted means ± s.e.mean from 4 experiments. To allow for differences in the absolute magnitude of the accumulation between experiments, values have been expressed as a percentage of basal acccumulation of each isomer in the presence of 2.5 mM Ca^{2+}. (a) [^{3}H]-IP_1; (b) [^{3}H]-IP_2; (c) [^{3}H]-IP_3 (mean basal accumulations at 2.5 mM Ca^{2+} 808 ± 7, 357 ± 5 and 264 ± 5 d.p.m., respectively). Where no error bar is shown the error was within the size of the symbol. (○) No addition (basal); (●) + 1 mM carbachol.

occasional experiments the response to 1 mM histamine was as much as 14–20 fold of basal, without there being any appreciable change in the basal accumulation. In one experiment in which the response to 1 mM histamine was 19 fold of basal, the concentration-response curve to histamine (EC_{50} 11.3 ± 1.1 μM, Hill coefficient 0.93 ± 0.04) appeared to be shifted somewhat to higher concentrations compared with curves in cells showing the normal, approximately 8 fold, stimulation (EC_{50} 3.9 ± 0.7 μM, Hill coefficient 0.68 ± 0.08; best-fit values to the combined data from a total of 18 experiments). The properties of the histamine response in the S3 clone, where tested, appeared to be the same as in the unspecified clone used earlier and in particular showed the same lower sensitivity of [^{3}H]-IP_1 accumulation to Li^+ (Bristow *et al.*, 1991) than in brain slices or U373 MG cells. The proportion of [^{3}H]-IP_1 as a percentage of [^{3}H]-IP_1 + [^{3}H]-IP_2 + [^{3}H]-IP_3 after a 30 min incubation with 1 mM histamine in the presence of 30 mM Li^+ was 92 ± 1% (16).

Carbachol also stimulated [^{3}H]-IP_1 accumulation in the S3 clone and the extent of the stimulation, 3.9 (± 0.1) fold of basal (6), was again greater than in the unspecified clone used earlier, 1.8 (± 0.1) fold of basal (10). The concentration-response curve for carbachol-induced [^{3}H]-IP_1 formation (EC_{50} 21 ± 4 μM, Hill coefficient 1.22 ± 0.31; best-fit values to the combined data from a total of 11 experiments) was shifted to the right by 100 nM and 1 μM pirenzepine, but in this series of experiments the fit to the combined data was significantly worsened when the Hill coefficient and the maximum attainable response were constrained to be the same in the presence and absence of pirenzepine (see Analysis of data under Methods). However, the apparent K_d values derived for pirenzepine, 1.0×10^{-7} M and 0.84 ± 10^{-7} M, indicate the probable presence of the M_3-muscarinic receptor subtype (Hulme *et al.*, 1990).

The pattern of Ca^{2+}-dependence of [^{3}H]-IP_1 accumulation induced by 1 mM histamine in HeLa cells was closely similar to that for the response to 1 mM carbachol (Figure 7). After the initial increase between 'zero' and 0.3 mM Ca^{2+} the response to histamine was not significantly altered as the Ca^{2+} in the medium was increased to 4.0 mM. The response to carbachol did increase significantly between 0.3 and 1.3 mM Ca^{2+}, but there was no further increase at higher Ca^{2+} concentrations. Basal [^{3}H]-IP_1 accumulation also increased between 0 (nominal) and 0.3 mM Ca^{2+}, but remained unchanged thereafter (Figure 7). The same pattern of Ca^{2+}-dependence of basal and histamine-stimulated [^{3}H]-IP_1 accumulation as in the S3 clone was observed in 4 experiments with the clone of HeLa cells showing the lower stimulation with histamine (data not shown).

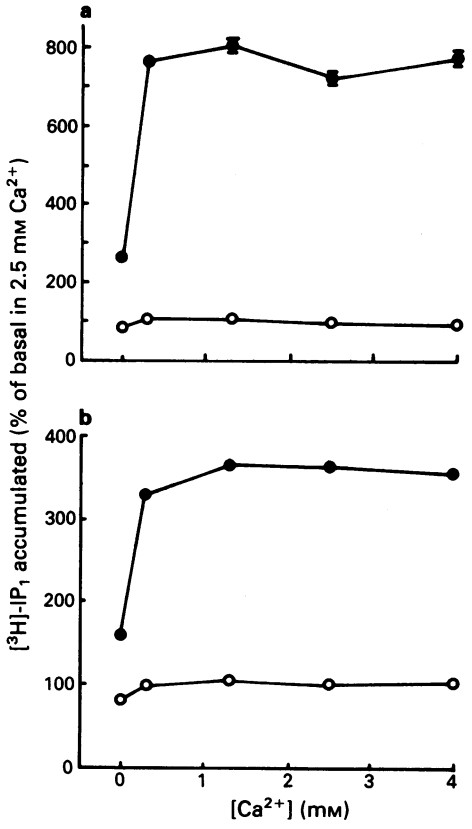

Figure 7 Ca^{2+}-dependence of histamine- and carbachol-induced [^{3}H]-IP_1 accumulation in HeLa cells (S3 clone). Cells were labelled with [^{3}H]-inositol and dissociated following the standard protocol (see Methods). The dissociated cells were equilibrated for 15 min and incubated with or without 1 mM histamine (a) or 1 mM carbachol (b) for 30 min in Krebs-Henseleit solution containing the Ca^{2+} concentration under test. For '0 Ca^{2+}', Ca^{2+} was omitted from the medium. Points are the combined values from 4 experiments with histamine and three experiments with carbachol and are expressed as a percentage of the 30 min basal value in 2.5 mM Ca^{2+} (3276 ± 49 and 2339 ± 75 d.p.m. in the two sets of experiments, respectively) to allow for differences in the absolute magnitude of the response between experiments. (○) Basal; (●) 1 mM histamine (a) or 1 mM carbachol (b).

Ca^{2+}-dependence of [^{3}H]-IP_1 accumulation in rat and guinea-pig brain slices

Basal accumulation of [^{3}H]-IP_1 in rat and guinea-pig cerebral cortical slices and in guinea-pig cerebellar slices was not significantly altered, except at 4.0 mM Ca^{2+} in rat cerebral cortex, when slices were labelled with [^{3}H]-inositol and incubated in Krebs-Henseleit solutions with no added Ca^{2+} or with Ca^{2+} concentrations from 0.3 to 4.0 mM (Figure 8a). In contrast, [^{3}H]-IP_1 accumulation induced by 1 mM histamine in rat cerebral cortical slices increased markedly with the Ca^{2+} concentration, in agreement with the previously reported Ca^{2+}-dependence of histamine-induced [^{3}H]-IP accumulation in mouse cerebral cortex (Alexander *et al.*, 1990a,b). Amounts of [^{3}H]-IP_2 and [^{3}H]-IP_3 were much less than those of [^{3}H]-IP_1, but the pattern of Ca^{2+}-dependence was essentially the same as that for [^{3}H]-IP_1 (data not shown).

Histamine-induced [^{3}H]-IP_1 accumulation in guinea-pig cerebellar slices, a tissue relatively rich in H_1-receptors (Hill *et al.*, 1978), was also Ca^{2+}-dependent, but the pattern of the Ca^{2+}-dependence differed from that in rat cerebral cortex, in that there was a marked increase in the response between no added Ca^{2+} and 0.3 mM Ca^{2+}, followed by a less steep increase to 2.5 mM Ca^{2+} (Figure 8c). There was no further increase between 2.5 and 4.0 mM. The pattern of histamine-induced [^{3}H]-IP_2 accumulation was similar, whereas amounts of [^{3}H]-IP_3 appeared to decrease between 2.5 and 4.0 mM (data not shown). The Ca^{2+}-dependence of the histamine response in guinea-pig cerebral cortical slices was intermediate between that of rat cerebral cortex and that of guinea-pig cerebellum (Figure 8b).

The Ca^{2+}-dependence of carbachol-induced [^{3}H]-IP_1 accumulation was similar in rat cerebral cortex and in guinea-pig cerebral cortex and in both tissues differed from that for histamine (Figure 8d,e). The pattern observed, an initial increase between 0 (nominal) and 0.3 mM Ca^{2+} but no further increase (up to 4.0 mM Ca^{2+}), is similar to that reported for carbachol-induced [^{3}H]-IP accumulation in mouse cerebral cortex (Alexander *et al.*, 1990a). The Ca^{2+}-dependence of carbachol-induced [^{3}H]-IP_2 and [^{3}H]-IP_3 accumulation in rat cerebral cortex was similar to that for [^{3}H]-IP_1, except that 1.3 mM Ca^{2+} was required to obtain the maximum amount of [^{3}H]-IP_3.

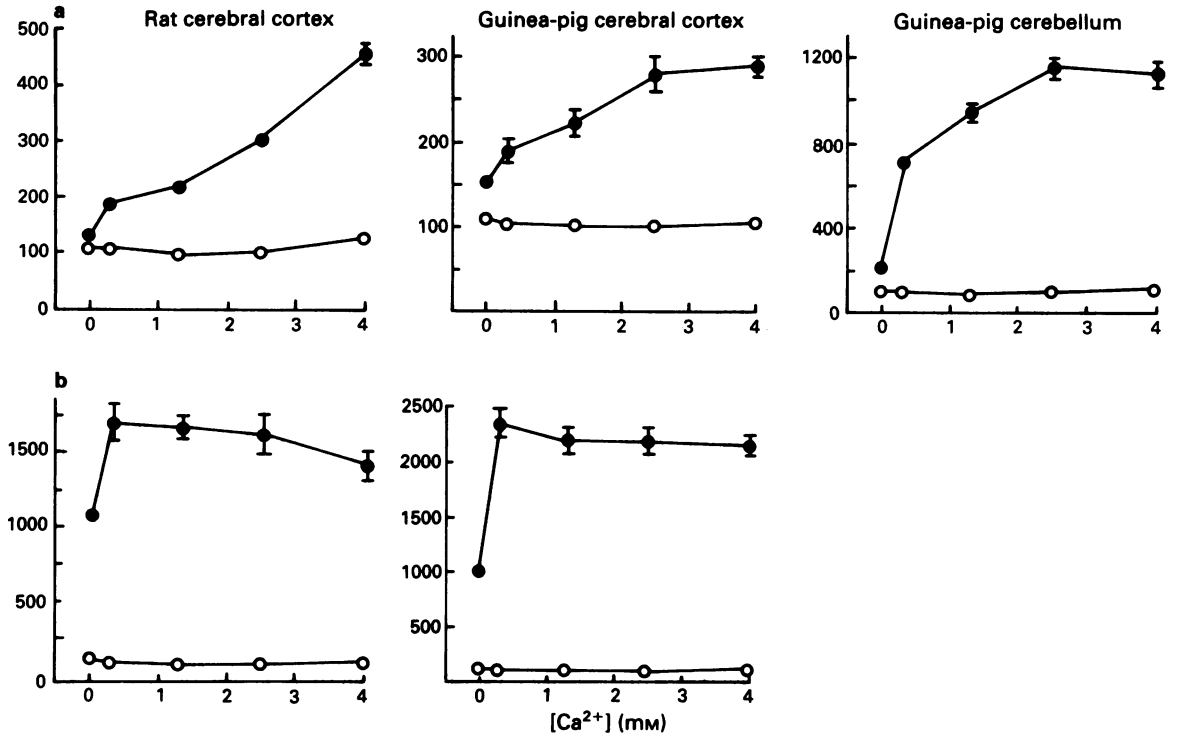

Figure 8 Ca^{2+}-dependence of histamine- and carbachol-induced [^{3}H]-IP_1 accumulation in rat and guinea-pig brain slices; (a) histamine, (b) carbachol. Slices were preincubated in normal Krebs-Henseleit and then labelled with [^{3}H]-inositol and incubated with or without (basal) agonist in Krebs-Henseleit solution containing the Ca^{2+} concentration indicated. Incubations with 1 mM histamine or 1 mM carbachol were for 60 min. Points are weighted means ± approximate s.e.mean from 3 or 4 independent determinations and are expressed as a percentage of the 30 min basal value with 2.5 mM Ca^{2+} to allow for differences in the absolute magnitude of the responses between experiments. Mean basal accumulation in 2.5 mM Ca^{2+} were 1583 ± 12 (37) in rat cerebral cortex, 926 ± 7 (11) in guinea-pig cerebral cortex and 3479 ± 71 (8) in guinea-pig cerebellum. (○) Basal; (●) 1 mM histamine (a) or 1 mM carbachol (b).

Effect of nimodipine and ω-conotoxin on histamine-induced [^{3}H]-IP_1 accumulation

Blockade of L-type Ca^{2+} channels with 100 nM nimodipine did not inhibit [^{3}H]-IP_1 accumulation induced by 1 mM histamine in the presence of 2.5 mM Ca^{2+} in rat cerebral cortical slices (104 ± 9% of the response in the absence of antagonist, $n = 3$) or in U373 MG cells (102 ± 2%, $n = 4$), the two preparations showing a calcium-dependence of the histamine response. Nimodipine was similarly ineffective against histamine in slices of guinea-pig cerebral cortex and cerebellum (94 ± 4% and 98 ± 6% of control, respectively; $n = 3$). Blockade of N-type Ca^{2+} channels by ω-conotoxin (0.1–3 μM) also failed to have any significant effect on [^{3}H]-IP_1 accumulation induced by 1 mM histamine in rat cerebral cortical slices (103 ± 8% of control with 3 μM ω-conotoxin, $n = 3$) or in U373 MG cells (104 ± 2%, $n = 4$).

The lack of effect of blockade of N-type Ca^{2+} channels suggests that the Ca^{2+}-dependence of the response to histamine in rat cerebral cortical slices is not likely to be due to H_1-receptor-mediated release of a secondary stimulator of phosphoinositidase C. Acetylcholine and noradrenaline are apparently not involved, since N-methylatropine (1 μM) and prazosin (1 μM) had no significant effect on [^{3}H]-IP_1 accumulation induced by 1 mM histamine in the slices (105 ± 7% and 96 ± 5%, respectively, of the response to histamine alone, $n = 3$).

Discussion

The relatively large magnitude of histamine H_1-receptor-induced phosphoinositide hydrolysis in U373 MG human astrocytoma cells, 11 fold of basal levels, compared with the response to histamine in most other cell types makes them attractive as a model system on which to study H_1-receptor function. However, how good a model the U373 MG cells are of the apparent Ca^{2+}-dependent component of the response to histamine apparent in slices of mouse and rat cerebral cortex (Alexander *et al.*, 1990a) is less clear. One particular problem in making a judgement is that in most brain regions there is little indication which cell type or types are responding to histamine. In the molecular layer of guinea-pig cerebellum autoradiographic studies of the effect of kainic acid lesions on the binding of [^{3}H]-mepyramine suggest that H_1-receptors have a neuronal location, presumably on the dendrites of Purkinje cells (Palacios *et al.*, 1981). A neuronal location of some H_1-receptors is also indicated by the observation of histamine-induced [^{3}H]-IP accumulation in primary cultures of striatal neurones, although the magnitude of the response was modest (Weiss *et al.*, 1988). However, neither kainic acid nor lesioning of the medial forebrain bundle in rats caused any persistent decrease in the binding of [^{3}H]-mepyramine to hippocampal membranes and the conclusion was drawn that the majority of hippocampal H_1-receptors were on glial cells (Chang *et al.*, 1980). Cerebral microvessels also possess histamine H_1-receptors (Peroutka *et al.*, 1980), but it has been estimated that they account for less than 1% of total cerebral H_1-receptors (Culvenor & Jarrott, 1981).

More direct evidence for a glial cell location is provided by the presence of histamine H_1-receptors on primary cultures of astrocytes from neonate rat brain, as evidenced both by [^{3}H]-mepyramine binding (Inagaki *et al.*, 1989) and by histamine-stimulated [^{3}H]-IP accumulation (Arbonés *et al.*, 1988). More specifically, Wada and his collaborators have

demonstrated that phosphoinositide hydrolysis in response to histamine is localized to type-2 astrocytes (Kondou *et al.*, 1991) and that Ca^{2+} signals induced by H_1-receptor activation can first be detected on the process of these cells (Inagaki *et al.*, 1991). Functionally, astrocytes are a major site of glycogen storage in the CNS (Murphy & Pearce, 1987) and H_1-receptor-mediated stimulation of glycogenolysis has been demonstrated in primary cultures of astrocytes (Arbonés *et al.*, 1990). It therefore seems probable that the glycogen breakdown induced by H_1-receptor activation in slices of mouse cerebral cortex (Quach *et al.*, 1980) reflects the presence of functional H_1-receptors on astrocytes in cerebral cortex *in vivo*. A strong argument can thus be made for astrocyte-derived cell lines as model systems for the study of H_1-receptor mechanisms in mammalian CNS.

Functional responses to H_1-receptor activation have been reported in the 1321N1 and UC11 MG human astrocytoma cell lines (Nakahata *et al.*, 1986; Medrano *et al.*, 1992; Lucherini & Gruenstein, 1992) and Johnson & Johnson (1992) noted, without presenting any experimental detail, that histamine-induced formation of [^{3}H]-IP_1 could be detected in UC11 MG cells, but that it was less than that in U373 MG cells. The data presented in the present study provide evidence that histamine does induce a large accumulation of [^{3}H]-IP_1 in U373 MG cells and that the effect is mediated by an H_1-receptor. Moreover, there is a clear dependence of the magnitude of the response to histamine on the extracellular Ca^{2+} concentration, even after the initial step to 0.3 mM Ca^{2+} (Figure 5). The marked inhibition of histamine-induced [^{3}H]-IP formation if Ca^{2+} is omitted from the medium is well established, both in brain slices (Kendall & Nahorski, 1984) and in primary cultures of astrocytes (Arbonés *et al.*, 1988) and is not confined to the H_1-receptor, as is evident with the response to carbachol in brain slices (Alexander *et al.*, 1990a; Figure 8d), HeLa cells (Figure 7) and U373 MG cells (Figure 6). However, it is the marked effect of increasing the Ca^{2+} concentration in the millimolar range which is the striking feature of the response to histamine in rat cerebral cortex (Figure 8d) and the same characteristic is shown, although to a lesser degree, by the U373 MG cells (Figure 5). The possibility that the effect of Ca^{2+} reflects an action on histamine binding to the H_1-receptor, rather than some aspect of the mechanism of phosphoinositide hydrolysis, is made unlikely by comparison with the Ca^{2+}-dependence of [^{3}H]-IP_1 formation induced by histamine in HeLa cells (Figure 7).

Histamine-stimulated phosphoinositide hydrolysis in HeLa cells is well characterised (Tilly *et al.*, 1990b; Bristow *et al.*, 1991) and we have provided evidence that the binding properties of the H_1-receptor mediating the response are similar to those of H_1-receptors in mammalian brain (Arias-Montaño & Young, 1993a). The dependence of phosphoinositidase C (PIC) on low levels of intracellular Ca^{2+} has also been demonstrated in these cells (Tilly *et al.*, 1990a). However, it has been suggested that in non-excitable cells, such as epithelia, Ca^{2+} entry mechanisms may be confined to that associated with the refilling of 1,4,5-IP_3-sensitive intracellular stores (Putney, 1990). The lack in HeLa cells, a line derived from human uterine cervical epithelium, of any effect on histamine-induced [^{3}H]-IP_1 formation of increasing the extracellular Ca^{2+} above 0.3 mM would be consistent with this proposition. It also suggests that HeLa cells may be valuable as a model system on which to study H_1-receptor/G protein activation of PIC without the complication of an additional component in the mechanism dependent on extracellular Ca^{2+}. The presence of a response to carbachol in HeLa cells gives the added advantage of a second receptor system coupled to PIC, which can in principle be used as a control for H_1-receptor-specific effects of agents or treatments. It is probable that the muscarinic receptor mediating the response to carbachol is of the M_3-subtype, as in U373 MG cells, but the lack of strict parallelism in the concentration-response curves in the presence and absence of pirenzepine indicates the need for a more detailed study. In U373 MG cells the evidence from the K_d for pirenzepine for the involvement of M_3-muscarinic receptors in carbachol-stimulated [^{3}H]-IP_1 accumulation is given some indirect support by the report of M_3-receptor mediation of [^{3}H]-IP_1 formation in 1321N human astrocytoma cells (Kunysz *et al.*, 1989). In rat cerebral cortex the response to muscarinic agonists appears to be mediated predominantly by M_1-receptors (Forray & El-Fakahany, 1990).

The pattern of the Ca^{2+}-dependence of carbachol stimulated [^{3}H]-IP_1 accumulation is similar in HeLa cells, U373 MG cells, and guinea-pig and rat brain slices. This is not the case with histamine-induced [^{3}H]-IP_1 accumulation. Not only does the pattern differ between U373 MG and HeLa cells, there is also a clear species difference between rat and guinea-pig cerebral cortex, which is also evident in the data of Alexander *et al.* (1990b) over a more limited range of Ca^{2+} concentrations. The difference between guinea-pig cerebral cortex and cerebellum lies largely in the magnitude of the initial increase between no added Ca^{2+} and 0.3 mM Ca^{2+}, which could reflect the difference in H_1-receptor density between the two tissues (Hill *et al.*, 1978). Whether any of the difference in the pattern between rat cerebral cortex (Figure 8a), in which there is indirect evidence for location of at least some H_1-receptors on astrocytes (Arbonés *et al.*, 1990), and guinea-pig cerebellum (Figure 8c), where the receptors may be neuronal (Palacios *et al.*, 1981), reflects a differing cellular locus is unknown. However, it is clear that not all brain tissues show the same very marked dependence on extracellular Ca^{2+} as mouse and rat cerebral cortex and the Ca^{2+}-dependence observed in the U373 MG cells is much closer to that in the guinea-pig tissues. There is as yet no indication whether this is also the pattern in human cerebral cortex, a tissue in which histamine is known to stimulate phosphoinositide hydrolysis (Kendall & Firth, 1990) and it would be unwise to make predictions on the basis of the response in a transformed cell line.

The difference between histamine and carbachol in the pattern of Ca^{2+}-dependence of [^{3}H]-IP_1 accumulation in U373 MG cells is lessened by the increase in the response to carbachol between 0.3 and 1.3 mM Ca^{2+} (Figure 6a). However, the difference is clearer in the comparisons of the Ca^{2+}-dependence of [^{3}H]-IP_2 and [^{3}H]-IP_3 formation (Figure 5b,c; Figure 6b,c), although the amount of material in the trisphosphate fraction in the presence of carbachol is small. The modest decline in the [^{3}H]-IP_1 response to carbachol between 1.3 and 4 mM Ca^{2+} in U373 MG cells could conceivably reflect the reported inhibition of the response to carbachol by Ca^{2+} (Baird *et al.*, 1989), although this effect is not otherwise apparent in our measurements.

A better understanding of the significance of the modest Ca^{2+}-dependence of the histamine-response in U373 MG cells will become clearer when selective blockade of the Ca^{2+}-dependent component in brain tissue becomes possible. Neither L-type nor N-type Ca^{2+} channels appear to be involved and the use of divalent cations such as Ni^{2+} as non-selective blockers of Ca^{2+} entry is complicated by a possible additional action at the level of the H_1-receptor, evident in the inhibition by Cd^{2+}, Zn^{2+}, Ni^{2+} and Co^{2+} of [^{3}H]-mepyramine binding to guinea-pig cerebellar membranes (Treherne *et al.*, 1991). The secondary action of Ni^{2+} on histamine-induced [^{3}H]-IP_1 formation, without affecting the response to carbachol, has been demonstrated directly in HeLa cells, illustrating their utility as a model system (Arias-Montaño & Young, 1993b). The availability of a selective blocker for the presumed Ca^{2+}-entry component in brain slices would provide a much simpler and more satisfactory assay than the measurement of Ca^{2+}-dependence for screening cell lines as possible model systems. It would also enable an approach to be made to the central question of the functional significance of the Ca^{2+}-dependent component at the normal Ca^{2+} concentration, *circa* 1.3 mM, of the cerebrospinal fluid.

We are grateful to the Wellcome Trust for financial support and to Martin Bootman for kindly providing the S3 HeLa cell clone.

References

ALEXANDER, S.P.H., HILL, S.J. & KENDALL, D.A. (1990a). Differential effects of elevated calcium ion concentrations on inositol phospholipid responses in mouse and rat cerebral cortical slices. *Biochem. Pharmacol.*, **40**, 1793–1799.

ALEXANDER, S.P.H., HILL, S.J. & KENDALL, D.A. (1990b). Is the adenosine receptor modulation of histamine-induced accumulation of inositol phosphates in cerebral cortical slices mediated by effects on calcium ion fluxes? *J. Neurochem.*, **55**, 1138–1141.

ARBONÉS, L., PICATOSTE, F. & GARCIA, A. (1988). Histamine H_1-receptors mediate phosphoinositide hydrolysis in astrocyte-enriched primary cultures. *Brain Res.*, **450**, 144–152.

ARBONÉS, L., PICATOSTE, F. & GARCIA, A. (1990). Histamine stimulates glycogen breakdown and increases $^{45}Ca^{2+}$ permeability in rat astrocytes in primary culture. *Mol. Pharmacol.*, **37**, 921–927.

ARIAS-MONTAÑO, J.A. & YOUNG, J.M. (1992). Different patterns of Ca^{2+}-dependence of histamine-induced inositol phosphate formation in HeLa cells and rat brain. *Br. J. Pharmacol.*, **105**, 23P.

ARIAS-MONTAÑO, J.A. & YOUNG, J.M. (1993a). Characteristics of histamine H_1 receptors on HeLa cells. *Eur. J. Pharmacol.*, **245**, 291–295.

ARIAS-MONTAÑO, J.A. & YOUNG, J.M. (1993b). Locus of action of Ni^{2+} on histamine-induced inositol phosphate formation in brain slices and in HeLa cells. *Eur. J. Pharmacol.*, **245**, 221–228.

BAIRD, J.G., CHILVERS, E.R., KENNEDY, E.D. & NAHORSKI, S.R. (1989). Changes in extracellular calcium within the physiological range influence receptor-mediated inositol phosphate responses in brain and tracheal smooth muscle slices. *Naunyn-Schmied Arch. Pharmacol.*, **339**, 247–251.

BAIRD, J.G. & NAHORSKI, S.R. (1990). Increased intracellular calcium stimulates ^{3}H-inositol polyphosphate accumulation in rat cerebral cortical slices. *J. Neurochem.*, **54**, 555–561.

BRISTOW, D.R., ARIAS-MONTAÑO, J.A. & YOUNG, J.M. (1991). Histamine-induced inositol phosphate accumulation in HeLa cells: lithium sensitivity. *Br. J. Pharmacol.*, **104**, 677–684.

CHANG, R.S.L., TRAN, V.T. & SNYDER, S.H. (1980). Neurotransmitter receptor localizations: brain lesion induced alterations in benzodiazepine, GABA, β-adrenergic and histamine H_1-receptor binding. *Brain Res.*, **190**, 95–110.

CULVENOR, A.J. & JARROTT, B. (1981). Comparison of histamine H_1-receptors in bovine intracerebral microvessels with cerebral grey matter by [^{3}H]mepyramine binding. *Neurochem. Int.*, **3**, 365–369.

DAUM, P.R., DOWNES, C.P. & YOUNG, J.M. (1983). Histamine-induced inositol phospholipid breakdown mirrors H_1-receptor density in brain. *Eur. J. Pharmacol.*, **87**, 497–498.

DOWNES, C.P., HAWKINS, P.T. & IRVINE, R.F. (1986). Inositol 1,3,4,5-tetrakisphosphate and not phosphatidylinositol 3,4-bisphosphate is the probable precursor of inositol 1,3,4-trisphosphate in agonist-stimulated parotid gland. *Biochem. J.*, **238**, 501–506.

EBERHARD, D.A. & HOLZ, R.W. (1988). Intracellular Ca^{2+} activates phospholipase C. *Trends Neurosci.*, **11**, 517–520.

FORRAY, C. & EL-FAKAHANY, E.E. (1990). On the involvement of multiple muscarinic receptor subtypes in the activation of phosphoinositide metabolism in rat cerebral cortex. *Mol. Pharmacol.*, **37**, 893–902.

GOH, Y. & KUROSAWA, A. (1991). Characterization and Ca^{2+} requirement of histamine-induced catecholamine secretion in cultured bovine chromaffin cells. *J. Neurochem.*, **57**, 1249–1257.

HILL, S.J. (1990). Distribution, properties and functional characteristics of three classes of histamine receptor. *Pharmacol. Rev.*, **42**, 45–82.

HILL, S.J., EMSON, P.C. & YOUNG, J.M. (1978). The binding of [^{3}H]mepyramine to histamine H_1 receptors in guinea-pig brain. *J. Neurochem.*, **31**, 997–1004.

HULME, E.C., BIRDSALL, N.J.M. & BUCKLEY, N.J. (1990). Muscarinic receptor subtypes. *Annu. Rev. Pharmacol. Toxicol.*, **30**, 633–673.

INAGAKI, N., FUKUI, H,. TAGUCHI, Y., WANG, N.P., YAMOTADANI, A. & WADA, H. (1989). Characterization of histamine H_1-receptors on astrocytes in primary culture: [^{3}H]-mepyramine binding studies. *Eur. J. Pharmacol.*, **173**, 43–51.

INAGAKI, N., FUKUI, H., ITO, S., YAMOTADANI, A. & WADA, H. (1991). Single type-2 astrocytes show multiple independent sites of Ca^{2+} signaling in response to histamine. *Proc. Natl. Acad. Sci. U.S.A.*, **88**, 4215–4219.

JOHNSON, C.L. & JOHNSON, C.G. (1992). Characterization of receptors for substance P in human astrocytoma cells: radioligand binding and inositol phosphate formation. *J. Neurochem.*, **58**, 471–477.

KENDALL, D.A. & FIRTH, J.L. (1990). Inositol phospholipid hydrolysis in human brain; adenosine inhibition of the response to histamine. *Br. J. Pharmacol.*, **100**, 37–40.

KENDALL, D.A. & NAHORSKI, S.R. (1984). Inositol phospholipid hydrolysis in rat cerebral cortical slices: II. Calcium requirement. *J. Neurochem.*, **42**, 1388–1394.

KNEPPER, S.M. & RUTLEDGE, C.O. (1987). Effects of calcium depletion on norepinephrine- and A23187-induced stimulation of inositol phosphate formation. *Biochem. Pharmacol.*, **36**, 3043–3050.

KOMORI, S., KAWAI, M., TAKEWAKI, T. & OHASHI, H. (1992). GTP-binding protein involvement in membrane currents evoked by carbachol and histamine in guinea-pig ileal muscle. *J. Physiol.*, **450**, 105–126.

KONDOU, H., INAGAKI, N., FUKUI, H., KOYAMA, Y., KANAMURA, A. & WADA, H. (1991). Histamine-induced inositol phosphate accumulation in type-2 astrocytes. *Biochem. Biophys. Res. Commun.*, **177**, 734–738.

KUNYSZ, E.A., MICHEL, A.D., WHITING, R.L. & WOODS, K. (1989). The human astrocytoma cell line 1321N1 contains M_2-glandular type muscarinic receptors linked to phosphoinositide turnover. *Br. J. Pharmacol.*, **96**, 271–278.

LOWRY, O.H., ROSEBROUGH, N.J., FARR, A.L. & RANDALL, R.J. (1951). Protein measurements with the Folin phenol reagent. *J. Biol. Chem.*, **193**, 265–275.

LUCHERINI, M.J. & GRUENSTEIN, E. (1992). Histamine H_1 receptors in UC-11MG astrocytes and their regulation of cytoplasmic Ca^{2+}. *Brain Res.*, **592**, 193–201.

MEDRANO, S., GRUENSTEIN, E. & DIMLICH, R.V.W. (1992). Histamine stimulates glycogenolysis in human astrocytoma cells by increasing intracellular free calcium. *Brain Res.*, **592**, 202–207.

MICHEL, M.C., HANFT, G. & GROSS, G. (1990). α_{1B}- but not α_{1A}-adrenoceptors mediate inositol phosphate generation. *Naunyn-Schmied. Arch. Pharmacol.*, **341**, 385–387.

MINNEMAN, K.P. & ATKINSON, B. (1991). Interaction of subtype-selective antagonists with α_1-adrenergic receptor-mediated second messenger responses in rat brain. *Mol. Pharmacol.*, **40**, 523–530.

MURPHY, S. & PEARCE, B. (1987). Functional receptors for neurotransmitters on astroglial cells. *Neurosci.*, **22**, 381–394.

NAKAHATA, N., MARTIN, M.W., HUGHES, A.R., HEPLER, J.R. & HARDEN, T.K. (1986). H_1-Histamine receptors on human astrocytoma cells. *Mol. Pharmacol.*, **29**, 188–195.

PALACIOS, J.M., WAMSLEY, J.K. & KUHAR, M.J. (1981). GABA, benzodiazepine and histamine-H_1 receptors in the guinea pig cerebellum: effects of kainic acid injections studied by autoradiographic methods. *Brain Res.*, **214**, 155–162.

PEROUTKA, S.J., MOSKOWITZ, M.A., RIENHARD, Jr, J.F. & SNYDER, S.H. (1980). Neurotransmitter receptor binding in bovine cerebral microvessels. *Science*, **208**, 610–612.

PUTNEY, Jr, J.W. (1990). Capacitative calcium reentry revisited. *Cell Calcium*, **11**, 611–624.

QUACH, T.T., DUCHEMIN, A.-M., ROSE, C. & SCHWARTZ, J.-C. (1980). ^{3}H-Glycogen hydrolysis elicited by histamine in mouse brain slices: selective involvement of H_1 receptors. *Mol. Pharmacol.*, **17**, 301–308.

RODBARD, D. (1974). Statistical quality control and routine data processing for radioimmunoassays and immunoradiometric assays. *Clin. Chem.*, **20**, 1255–1270.

SCHWARTZ, J.-C., ARRANG, J.-M., GARBARG, M., POLLARD, H. & RUAT, M. (1991). Histaminergic transmission in mammalian brain. *Physiol. Rev.*, **71**, 1–51.

SHARPES, E.S. & MCCARL, R.L. (1982). A high-performance liquid chromatographic method to measure ^{32}P incorporation into phosphorylated metabolites in cultured cells. *Anal. Biochem.*, **124**, 421–424.

SUMMERS, R.J. & MCMARTIN, L.R. (1993). Adrenoceptors and their second messenger systems. *J. Neurochem.*, **60**, 10–23.

TILLY, B.C., LAMBRECHTS, A.C., TERTOOLEN, L.G.J., DE LAAT, S.W. & MOOLENAAR, W.H. (1990a). Regulation of phosphoinositide hydrolysis induced by histamine and guanine nucleotides in human HeLa carcinoma cells. *FEBS Lett*, **265**, 80–84.

TILLY, B.C., TERTOOLEN, L.G.J., LAMBRECHTS, A.C., REMORIE, R., DE LAAT, S.W. & MOOLENAAR, W.H. (1990b). Histamine-H_1-receptor-mediated phosphoinositide hydrolysis, Ca^{2+} signalling and membrane-potential oscillations in human HeLa carcinoma cells. *Biochem. J.*, **266**, 235–243.

TREHERNE, J.M., STERN, J.S., FLACK, W.J. & YOUNG, J.M. (1991). Inhibition by cations of antagonist binding to histamine H_1-receptors: differential effect of sodium ions on the binding of two radioligands. *Br. J. Pharmacol.*, **103**, 1745–1751.

WEISS, S., SCHMIDT, B.H., SEBBEN, M., KEMP, D., BOCKAERT, J. & SLADECZEK, F. (1988). Neurotransmitter-induced inositol phosphate formation in neurons in primary culture. *J. Neurochem.*, **50**, 1425–1433.

YAMAMOTO, Y., CHEN, G., MIWA, K. & SUZUKI, H. (1992). Permeability and Mg^{2+}-blockade of histamine-operated cation channel in endothelial cells of rat intrapulmonary artery. *J. Physiol.*, **450**, 395–408.

(Received September 1, 1993
Revised October 15, 1993
Accepted October 18, 1993)

Br. J. Pharmacol. (1994), **111**, 609–615

Endothelin receptors mediating functional responses in human small arteries and veins

[1]Jan Riezebos, *Ian S. Watts & Patrick J.T. Vallance

Dept. of Pharmacology and Clinical Pharmacology, St. George's Hospital Medical School, Cranmer Terrace, Tooting, London SW17 0RE and *Department of Gastrointestinal Pharmacology, Glaxo Group Research, Park Road, Ware, Herts SG12 0DP

1 In the present study, responses of human omental small arteries and veins to endothelin-1 and endothelin-3 were characterized by use of the ET_B receptor selective agonist, sarafotoxin S6c, the ET_A receptor antagonist, BQ123, the ET_B receptor antagonist, IRL1038, the NO-synthase inhibitor N^G-monomethyl-L-arginine (L-NMMA, 300 μM) and indomethacin (10 μM).

2 Small arteries (internal diameter 413 ± 22 μm) and parallel running veins (646 ± 35 μm) were mounted in a myograph under a normalized tension equivalent to 90% of a transmural pressure of 100 mmHg and 19 mmHg *in vivo*, respectively.

3 In small arteries and veins, endothelin-1 caused a concentration-dependent increase in wall tension (E_{max} = 3.90 ± 0.56 mN mm^{-1} and 1.90 m ± 0.32 mN mm^{-1} respectively, $P<0.05$) and was equipotent (arteries: pD_2 = 8.91 ± 0.11; veins: pD_2 = 8.63 ± 0.08, NS). In endothelium intact arteries, L-NMMA significantly enhanced the sensitivity to endothelin-1 (pD_2 control: 8.92 ± 0.16; pD_2 L-NMMA: 9.37 ± 0.11; $P<0.05$). L-NMMA did not affect the sensitivity of veins to endothelin-1. Indomethacin was without effect in arteries and veins. In veins, endothelin-3 was about a hundred times less potent than endothelin-1 and showed a biphasic response curve. Small arteries did not contract to endothelin-3. Neither small arteries nor veins contracted to sarafotoxin S6c. Furthermore, no relaxation to endothelin-1 or sarafotoxin S6c was seen in any precontracted vessels.

4 BQ123 (0.03–3 μM) produced a concentration-dependent rightward parallel displacement of the endothelin-1 concentration-response curve in small arteries and veins yielding pA_2 values of 7.09 and 7.48 respectively. The slope of the Schild plot in arteries and veins was 1.26 ± 0.24 (NS from unity) and 0.61 ± 0.13 ($P<0.05$ compared to unity) respectively. IRL1038 (3 μM) did not affect the potency of endothelin-1 in arteries and veins. In veins, the low sensitivity component (pD_2 = 7.16 ± 0.08) of the biphasic response curve to endothelin-3 was completely blocked by BQ123 (3 μM), whereas the high sensitivity component (pD_2 = 8.66 ± 0.08) was resistant to BQ123 (3 μM) and IRL1038 (3 μM).

5 These results indicate that contractions of human small vessels to endothelin-1 are predominantly mediated by ET_A receptors and that nitric oxide modulates the response to endothelin-1 in small arteries but not in veins. The different antagonistic potency of BQ123 against endothelin-1 and the differential endothelin-1/endothelin-3 potency ratios in arteries and veins provide evidence for the hypothesis that ET_A receptors in human small arteries are different from ET_A receptors in human small veins. There is no evidence of contractions mediated by 'classical' ET_B receptors in these vessels, but small veins appear to contain a functional non ET_A/non ET_B receptor with a high affinity for endothelin-3.

Keywords: Endothelin-1; endothelin-3; sarafotoxin S6c; ET_A receptor, ET_B receptor; N^G-monomethyl-L-arginine (L-NMMA); human small vessels

Introduction

Endothelin-1 (Yanagisawa *et al.*, 1988), its isoforms endothelin-2 and endothelin-3 (Inoue *et al.*, 1989), and the snake venoms known as sarafotoxins (Kloog *et al.*, 1988) constitute a family of structurally homologous peptides composed of 21 amino acids. Endothelin-1 is the most potent endogenous vasoconstrictor substance yet described and has been implicated in the control of vascular tone in animals and man. Furthermore, circulating levels of endothelins are increased in a variety of disease states although the precise physiological and pathophysiological roles of the endothelins remain to be determined (Miller *et al.*, 1993).

In the cardiovascular system current evidence suggests that endothelins act on two receptor subtypes. One receptor, termed ET_A, has a high affinity for endothelin-1 compared with other members of the endothelin family (Arai *et al.*, 1990) whereas the other receptor, ET_B, has similar affinity for endothelin-1, endothelin-2 and endothelin-3 and the sarafotoxins (Sakurai *et al.*, 1990). Specific agonists and antagonists for endothelin receptor subtypes are now available; sarafotoxin S6c is a selective agonist for the ET_B receptor (Williams *et al.*, 1991), the cyclic peptide BQ123 (D-Asp-L-Pro-D-Val-L-Leu-D-Trp) is a highly selective ET_A receptor antagonist (Ihara *et al.*, 1992) and IRL1038 ([Cys^{11}-Cys^{15}]-endothelin-1(11-21)) is an ET_B-selective antagonist (Urade *et al.*, 1992; Karaki *et al.*, 1993).

By use of these agonists and antagonists it has been demonstrated in arteries from several species that the contractile response to endothelin-1 is mediated via ET_A receptors (Moreland *et al.*, 1992; Sumner *et al.*, 1992; Cardell *et al.*, 1993). In contrast, in certain veins, contractions to endothelin-1 appear to be mediated by the ET_B receptor (Moreland *et al.*, 1992; Sumner *et al.*, 1992). ET_B receptors have also been found on endothelial cells (Sakurai *et al.*, 1990; Sakamoto *et al.*, 1991), and evidence is emerging to suggest that activation of ET_B receptors is responsible for the transient endothelin-1 induced vasodilatation in animal vessels *in vitro* (Clozel *et al.*, 1992) and *in vivo* (Bigaud & Pelton, 1992). This ET_B-mediated vasodilatation may be due to a stimulated release of nitric oxide (NO) and/or prostacyclin (PGI_2) (Fozard & Part, 1992). Furthermore, the contractile response to endothelin-1 *in vivo* is modulated by NO and prostaglandins (Rogerson *et al.*, 1993).

Endothelins also alter the tone of human blood vessels.

[1] Author for correspondence.

Endothelin-1 causes potent contractions of human isolated arteries, veins (Lüscher et al., 1990; McNamara et al., 1992; MacLean et al., 1992) and small resistance vessels (Watt et al., 1989; Schiffrin et al., 1992), constricts dorsal hand veins in vivo (Haynes & Webb, 1993), reduces forearm blood flow when infused directly into the brachial artery (Kiowski et al., 1991) and increases arterial pressure when infused systemically (Vierhapper et al., 1990). A small vasodilator effect of endothelin has been reported in one study in which endothelin was infused in the forearm (Kiowski et al., 1991) and the cyclo-oxygenase inhibitor, aspirin, enhanced the constrictor effect of endothelin in human hand veins in vivo (Haynes & Webb, 1993). However, the receptor subtypes mediating the responses to endothelins in the human cardiovascular system are not yet known, and the precise role of prostaglandins and nitric oxide in modifying contractions remain to be determined.

Studies in animals suggest that the microcirculation may be particularly sensitive to the effects of endothelins (Brain et al., 1988; Boric et al., 1990; Lamping et al., 1992) and that veins are more sensitive than arteries (Cocks et al., 1989; Miller et al., 1989). However, there appear to be differences between species and between vascular beds in the response to endothelins. In the present study, we have examined the effects of endothelins in human isolated small arteries and veins, characterized the receptors mediating the responses seen and determined the effects of inhibitors of NO and prostaglandin synthesis. Some of the data have been presented to the British Pharmacological Society (Riezebos et al., 1993).

Methods

Tissue preparation

The study had the approval of the St. George's Hospital District Ethical Committee. Vessels were obtained from omentum removed during surgery; small pieces (2 × 2 × 1 cm) of omentum were isolated and placed in ice-cold Krebs buffer (composition, mM: NaCl 118, KCl 4.69, $CaCl_2$ 1.25, KH_2PO_4 1.18, $MgSO_4$ 1.18, $NaHCO_3$ 25 and glucose 11) oxygenated with 95% O_2 and 5% CO_2 (pH = 7.4). Small parallel running arteries and veins were identified under the microscope (Zeiss, Citoval 2), dissected free from fat tissue and mounted as ring preparations on a myograph (JP Trading, Aarhus, Denmark) for measurement of isometric tension (Mulvany & Halpern, 1977). The vessels were bathed in Krebs buffer at 37°C and bubbled with 95% O_2 and 5% CO_2. After 30 min equilibration, vessels were stretched to determine their passive tension-internal circumference relation using Laplace's equation, and internal diameter was calculated (Mulvany & Halpern, 1977). Arteries were stretched to an internal circumference equivalent to 90% of that which they would have had when relaxed in vivo under a transmural pressure of 100 mmHg (13.3 kPa) (Mulvany & Halpern, 1977). Veins were stretched to an internal circumference equivalent to 90% of that which they would have had in vivo under a transmural pressure of 19 mmHg (2.5 kPa). To assess contractile response, vessels were then maximally contracted for a 4 min period with 50 mM KCl, on three separate occasions with a 10 min wash-out period between each contraction. These responses served as standardized control responses. Any artery failing to produce a maximum active tension equivalent to a pressure of 100 mmHg on the third contraction was rejected. Veins were rejected if developed tension on the third KCl contraction did not equal a 20 mmHg increase in pressure.

Experimental protocol

Arteries and veins were submaximally precontracted with the thromboxane A_2-mimetic 9α-11α-methanoepoxy-prostaglandin $F_{2\alpha}$ (U46619; 0.01–0.1 μM). After contractions had stabilized, vessels were exposed to acetylcholine (ACh, 1 μM) followed by bradykinin (BK, 1 μM) to determine endothelial integrity. In arteries and veins, the endothelium was considered intact if relaxation to BK was >80% of their U46619-induced tone.

Contractions to endothelin-1, endothelin-3 (0.01–1000 nM) and sarafotoxin S6c (0.01–30 nM) were studied by increasing the concentration cumulatively by half-log increments. Concentration-response curves to endothelin-1 were constructed in the presence or absence of BQ123 (0.03, 0.3 and 3 μM), IRL1038 (3 μM), the NO-synthase inhibitor N^G-monomethyl-L-arginine (L-NMMA; 300 μM) or indomethacin (10 μM). Concentration-response curves to endothelin-3 were constructed in the presence or absence of BQ123 (3 μM) or IRL1038 (3 μM). Vessels were preincubated for 30 min with either BQ123, IRL1038 or L-NMMA and for 60 min with indomethacin prior to exposure to the agonist. In a separate set of experiments, the ability of BQ123 to reverse endothelin-1-induced contractions in arteries and veins was studied. After maximum contraction to endothelin-1 was reached and had stabilized (usually at 100 nM endothelin-1), a single concentration of BQ123 (3 μM) was added, and tension was recorded for at least 15 min. All experiments studying the effects of BQ123, IRL1038, L-NMMA and indomethacin on agonist-induced contractions were performed in paired rings of arteries and veins taken from the same vessel segment. To study relaxations to endothelin-1 and sarafotoxin S6c, arteries and veins were submaximally precontracted with U46619 (0.01–0.1 μM). After tension had stabilized, cumulative concentrations of endothelin-1 and sarafotoxin S6c (0.01–30 nM) were added to the bath.

Chemicals

The following drugs were used: acetylcholine hydrochloride, indomethacin, bradykinin acetate (Sigma, Poole, UK), N^G-monomethyl-L-arginine acetate (L-NMMA; Wellcome Research Laboratories, Kent), U46619 (9α,11α-methanoepoxy-prostaglandin $F_{2\alpha}$) (Upjohn company, Kalamazoo, U.S.A), endothelin-1, endothelin-3, sarafotoxin S6c (Peptide Institute, Japan), BQ123 (cyclo(-D-Val-Leu-D-Trp-D-Asp-Pro); Neosystem Laboratoires, France) and IRL1038 ([Cys^{11}-Cys^{15}]-endothelin-1(11-21); Cambridge Research Biochemicals, Cambridge). U46619 was dissolved in absolute ethanol and diluted with Krebs buffer (final bath concentration <0.001%). Endothelin-1, endothelin-3 and sarafotoxin S6c were dissolved in ammonium acetate (0.1 M). IRL1038 was dissolved in 1 part NaOH (1 M) and 9 parts ammonium acetate (0.1 M). Indomethacin was dissolved in saturated $NaHCO_3$ solution. Unless otherwise stated, drugs were dissolved in Krebs buffer. Solutions were prepared freshly every day and kept on ice.

Data analysis

Contractions were expressed either as active wall tension or as a percentage of the maximum tension produced by 50 mM KCl. Active wall tension is the increase in wall force upon stimulation divided by twice the length of the vessel segment. Concentration-response curves based on a Hill-relationship were fitted to individual concentration-response data by a computer programme (Inplot, Graphpad Inc, San Diego, U.S.A). Agonist potencies were calculated on the basis of data from individual vessels and are expressed as $pD_2 = -\log EC_{50}$ where EC_{50} is the concentration of the agonist needed to produce 50% of the maximal response. The concentration-ratio is the ratio of the EC_{50} values in the presence and absence of an antagonist. Antagonist pA_2-values were determined by Schild analysis (Arunlakshana & Schild, 1959). The relaxation responses are expressed as percentage decrease in tension of the contraction induced by U46619 (0.01–0.1 μM) or endothelin-1 (100 nM).

Statistics

Data are given as mean ± s.e.mean. In all experiments, n equals the number of patients from whom the blood vessels were obtained. Statistical differences between two means were determined by Student's two-tailed, paired or unpaired t test or by analysis of variance as appropriate. Differences were accepted as significant at $P<0.05$.

Results

Relaxations to endothelium-dependent dilators

In arteries (internal diameter: 413.6 ± 22.1 μm, 43 rings), maximal relaxations to ACh (1 μM) and BK (1 μM) were 43 ± 6% and 91 ± 2% respectively. Veins (internal diameter: 646.7 ± 34.6 μm, 43 rings) relaxed minimally to ACh (maximum: 9 ± 3%) but showed virtually complete relaxation to BK (82 ± 3%).

Responses to endothelin-1, endothelin-3 and sarafotoxin S6c

Endothelin-1 (0.01–100 nM) produced sustained concentration-dependent increases in wall tension in human arteries and veins. Endothelin-1 was equipotent in arteries and veins with mean pD_2 values of 8.91 ± 0.11 and 8.63 ± 0.08 respectively. However, the maximum tension developed in response to endothelin-1 was greater in arteries (E_{max} = 3.90 ± 0.56 mN mm^{-1}, n = 13) compared with veins (E_{max} = 1.90 ± 0.32 mN mm^{-1}, n = 14, $P<0.05$; Figure 1). However, E_{max} values of veins are significantly higher than those of arteries when expressed as a percentage of the KCl induced contraction (Tables 1 and 2). In small veins, the concentration-response curve to endothelin-3 was biphasic and consisted of a high sensitivity component (pD_2 = 8.66 ± 0.08; E_{max} = 0.20 ± 0.07 mN mm^{-1}; n = 5) and a low sensitivity component (pD_2 = 7.16 ± 0.08; E_{max} = 1.50 ± 0.32 mN mm^{-1}; n = 5). In contrast, small arteries did not contract to endothelin-3 in concentrations up to 1000 nM (Figure 1), even after blockade of nitric oxide production with L-NMMA (300 μM; data not shown). Neither arteries nor veins contracted to sarafotoxin S6c (0.01–30 nM; n = 3; Figure 1) but showed maximal contraction to endothelin-1 (1 μM). No relaxation to endothelin-1 or sarafotoxin S6c was seen in any endothelium-intact vessel (data not shown).

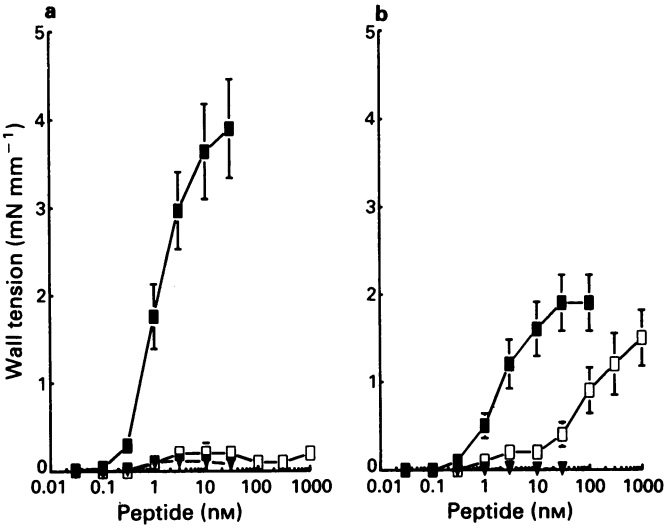

Figure 1 Increase in active wall tension (mN mm^{-1}) to endothelin-1 (ET-1; n = 13/14; ■), endothelin-3 (ET-3; n = 5; □) and sarafotoxin S6c (S6c; n = 3; ▼) in human small arteries (a) and small veins (b). Responses are expressed as the mean ± s.e.mean.

Effects of BQ123

In human arteries and veins, BQ123 (0.03–3 μM) produced parallel, concentration-dependent rightward shifts in the ago-

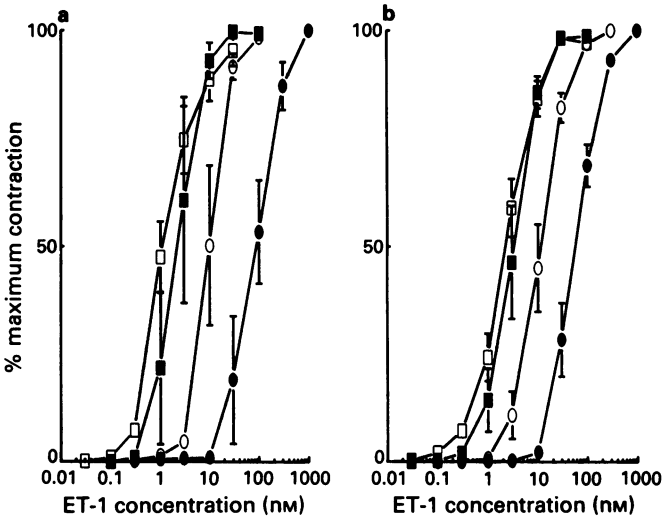

Figure 2 Effect of the ET_A antagonist, BQ123 on the endothelin-1 (ET-1) concentration-response curve in human small arteries (a) and small veins (b). Vessels were incubated for 30 min with either vehicle or BQ123: control (□, n = 13–14); 0.03 μM BQ123 (■, n = 3); 0.3 μM BQ123 (○, n = 5) and 3 μM BQ123 (●, n = 5–6). Values are means ± s.e.mean normalized to the maximum response of the agonist.

Table 1 Effects of different concentrations of BQ123 on endothelin-1 (ET-1) induced responses in human small arteries and veins

	n	K^+ (mN mm^{-1})†	E_{max} (%)‡	pD_2§
Arteries				
ET-1 (control)	13	2.85 ± 0.45	148 ± 12	8.91 ± 0.11
+ BQ123 (0.03 μM)	3	2.10 ± 0.79	119 ± 14	8.65 ± 0.23
+ BQ123 (0.3 μM)	5	3.30 ± 0.98	152 ± 30	7.99 ± 0.12*
+ BQ123 (3 μM)	5	3.50 ± 0.82	101 ± 15	7.05 ± 0.17*
Veins				
ET-1 (control)	14	0.80 ± 0.18	275 ± 34	8.63 ± 0.08
+ BQ123 (0.03 μM)	3	1.50 ± 0.40	218 ± 70	8.49 ± 0.11
+ BQ123 (0.3 μM)	5	0.90 ± 0.21	255 ± 63	7.96 ± 0.10*
+ BQ123 (3 μM)	6	0.80 ± 0.17	232 ± 48	7.25 ± 0.09*

*$P<0.05$ vs. control (analysis of variance). Values are expressed as mean ± s.e.mean.
†Absolute maximal increase in wall tension per mm vessel length to 50 mM KCl.
‡Maximal responses to endothelin-1 expressed as a percentage of the contraction induced by 50 nM KCl.
§Potency of endothelin-1 is expressed as the negative logarithm of the concentration producing half the maximum response.

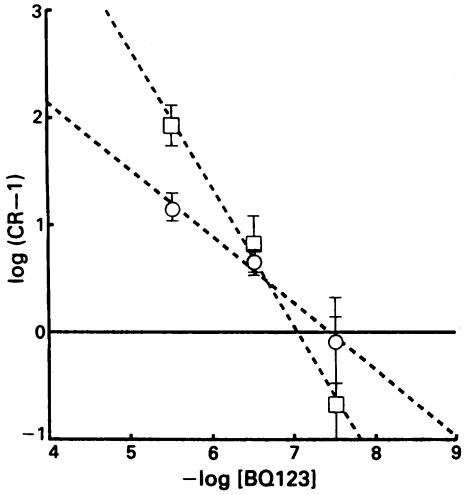

Figure 3 Schild plot for BQ123 at concentrations of 0.03 μM (n = 3), 0.3 μM (n = 5) and 3 μM (n = 5–6) on contractions induced by endothelin-1 in human small arteries (□) and small veins (○) with endothelium. Results are expressed as mean ± s.e.mean. CR is the concentration-ratio.

nist response curves to endothelin-1 but did not cause any reduction in the maximal response (Table 1 and Figure 2). Interestingly, BQ123 (3 μM) caused a rightward shift with a mean concentration-ratio of some 19.8 ± 5.5 for endothelin-1 in veins (n = 6) compared with 118.1 ± 39.4 in arteries (n = 5; $P<0.05$). The rightward displacements of the endothelin-1-induced concentration-response curves caused by BQ123 were used to construct Schild plots (Figure 3). In arteries and veins, the concentration-ratios for BQ123 yielded pA_2 values of 7.09 and 7.48 respectively, while the slopes of the lines were 1.26 ± 0.24 for arteries (not significantly different from unity) and 0.61 ± 0.13 for veins ($P<0.05$ compared to unity).

In small veins, BQ123 (3 μM) did not alter the high sensitivity component of the biphasic endothelin-3 response curve (pD_2 = 8.80 ± 0.20; E_{max} = 0.46 ± 0.22 mN/mm^{-1}; n = 4) but completely blocked the low sensitivity component (Figure 4a).

The ability of BQ123 to reverse a maximum contraction to endothelin-1 was studied in arteries and veins. In small arteries and veins, the maximum increase in wall tension by endothelin-1 was 4.23 ± 0.70 mN mm^{-1} (8 rings) and 2.75 ± 0.94 mN mm^{-1} (6 rings) respectively. In the arteries, BQ123 (3 μM) reversed this contraction by 94.3 ± 1.1% after 15 min, compared to a decline in tension of 35.3 ± 18.7% in the control vessel ($P<0.05$, n = 4) over the same period. A

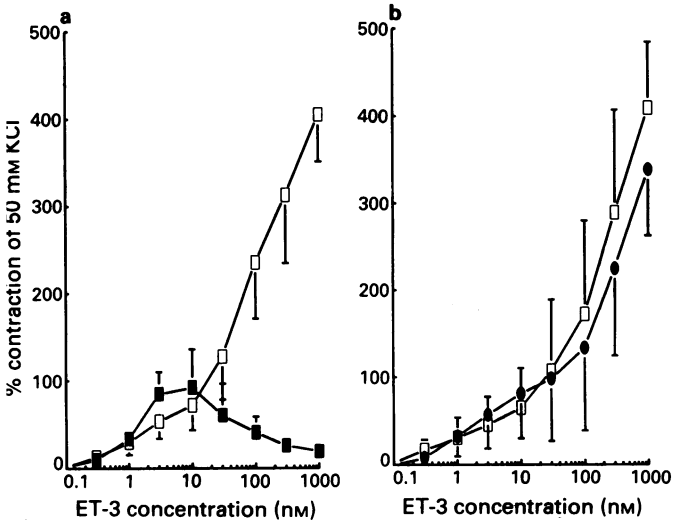

Figure 4 (a) Effect of the ET_A antagonist, BQ123, on the endothelin-3 (ET-3) concentration-response curve in human small veins. Vessels were incubated for 30 min with either vehicle (□; n = 4) or 3 μM BQ123 (■; n = 4). (b) Effect of the ET_B antagonist, IRL1038, on the endothelin-3 (ET-3) concentration-response curve in human small veins. Vessels were incubated for 30 min with either vehicle (□; n = 4) or 3 μM IRL1038 (●; n = 4). Values are mean ± s.e.mean normalized to the maximum response of 50 mM KCl.

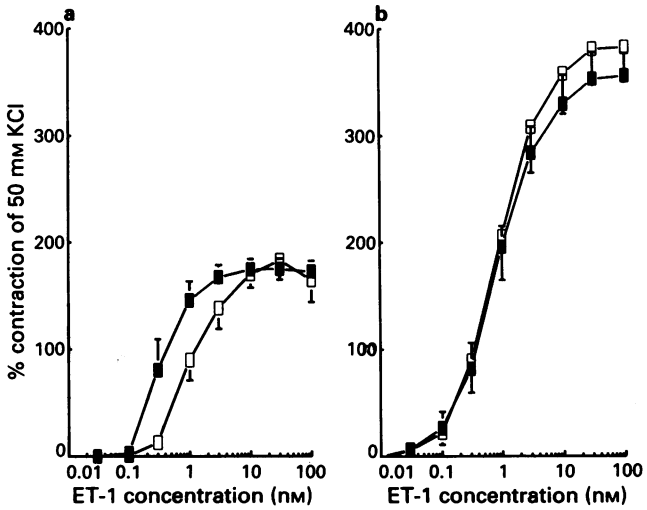

Figure 5 Effect of the NO-synthase inhibitor N^G-monomethyl-L-arginine (L-NMMA) on the endothelin-1 (ET-1) concentration-response curve in human small arteries (a) and veins (b). Vessels were incubated for 30 min with vehicle (□, n = 4–5) or 300 μM L-NMMA (■, n = 4–5). Responses are expressed as mean ± s.e.mean.

Table 2 Effects of N^G-monomethyl-L-arginine (L-NMMA, 300 μM) and indomethacin (10 μM) on endothelin-1 induced responses in human small arteries and veins

	n	K^+ (mN mm^{-1})†	E_{max} (%)‡	pD_2§
Arteries				
ET-1 (control)	5	2.00 ± 0.28	185 ± 21	8.92 ± 0.16
+ L-NMMA	5	1.60 ± 0.23	175 ± 10	9.37 ± 0.11*
ET-1 (control)	3	3.03 ± 1.13	153 ± 16	9.57 ± 0.01
+ indomethacin	3	2.63 ± 1.09	169 ± 18	9.40 ± 0.19
Veins				
ET-1 (control)	4	0.40 ± 0.08	383 ± 30	9.04 ± 0.15
+ L-NMMA	4	0.55 ± 0.08	356 ± 21	9.07 ± 0.10
ET-1 (control)	4	1.05 ± 0.28	315 ± 56	8.96 ± 0.13
+ indomethacin	4	0.97 ± 0.20	340 ± 60	8.93 ± 0.15

*$P<0.05$, ET-1 control vs. ET-1 + L-NMMA (Student's paired t test). Values are expressed as mean ± s.e.mean.
†Absolute maximal increase in wall tension per mm vessel length to 50 mM KCl.
‡Maximal responses to endothelin-1 expressed as a percentage of the contraction induced by 50 mM KCl.
§Potency of endothelin-1 is expressed as the negative logarithm of the concentration producing half the maximum response.

similar effect of BQ123 was observed in maximally contracted veins (BQ123: 84.7 ± 3.3% reversal vs. control 40.7 ± 6.6%; $P<0.05$, $n=3$).

Effects of IRL1038

The ET_B antagonist IRL1038 (3 μM) did not signficantly alter pD_2 values or E_{max} values of the endothelin-1 response curve in small arteries or veins (data not shown). In the presence of IRL1038 (3 μM), the concentration-response curve to endothelin-3 was biphasic and not significantly different from the control curves (Figure 4b).

Effects of L-NMMA and indomethacin

Incubation with L-NMMA (300 μM) for 30 min significantly enhanced the sensitivity of arteries to endothelin-induced contraction (pD_2 control: 8.92 ± 0.16; pD_2 L-NMMA: 9.37 ± 0.11; concentration shift, 3 fold; $P<0.05$), but did not enhance maximum responses to endothelin-1 (Table 2 and Figure 5a). In contrast, L-NMMA did not alter maximum responses or pD_2 values of endothelin-1 in veins with endothelium (Table 2 and Figure 5b). Indomethacin (10 μM) did not alter responses to endothelin-1 in arteries or veins (Table 2).

Discussion

The results of this study demonstrate that endothelin-1 is a potent constrictor of human small arteries and veins and that the peptide is equipotent on the two vessel types. The ET_A receptor antagonist, BQ123, caused a parallel and concentration-dependent rightward shift of the concentration-response curve to endothelin-1 in both arteries and veins indicating that the ET_A receptor mediates contractile responses to endothelin-1 in human small vessels. This is supported by the observation in arteries and veins that endothelin-1 is more potent than endothelin-3 and that sarafotoxin S6c is without effect. Furthermore, the use of a specific inhibitor of nitric oxide synthesis indicates differential modulation of the response to endothelin in arteries and veins.

Arteries and their anatomically adjacent veins which drain the capillary bed supplied by the arteries were equally sensitive to endothelin-1. These data contrast with findings in large arteries and veins from animals and man which indicate that endothelin is a venoselective constrictor (Cocks *et al.*, 1989; Miller *et al.*, 1989; Lüscher *et al.*, 1990; McNamara *et al.*, 1992; MacLean *et al.*, 1992). However, in the microcirculation of animals it has also been shown that endothelin-1 is equipotent in arterioles and venules (Boric *et al.*, 1990; Brain *et al.*, 1988). This suggests that there is a general difference between large and small veins with respect to their response to endothelin-1. In the present study, the normalized maximal response to endothelin-1 (expressed as a percentage of the response to 50 mM KCl) was greater in the veins than in the arteries although the absolute tension developed was 2 fold greater in the arteries. The smaller absolute tension developed in the veins probably reflects the relative lack of media in these vessels compared with arteries.

In arteries and veins, the ET_A antagonist, BQ123 but not the ET_B antagonist, IRL1038, caused a parallel rightward shift of the concentration-response curve to endothelin-1 while the ET_B receptor-selective agonist, sarafotoxin S6c, had no contractile effect. Together, these data demonstrate that the receptor mediating contractions to endothelin-1 in human omental arteries and veins has the profile of an ET_A subtype. Studies in animal tissues have identified ET_A-mediated contractions in large arteries (Sumner *et al.*, 1992; Cardell *et al.*, 1993), and predominantly ET_B-mediated contractions in large veins (Moreland *et al.*, 1992; Sumner *et al.*, 1992). Human large veins (saphenous) also appear to possess contractile ET_B receptors (Bax *et al.*, 1993) and contract to sarafotoxin S6c (our unpublished observations) but the present study suggests that, at least in the omentum, neither human small arteries nor small veins possess functionally significant contractile 'classical' ET_B receptors.

Endothelin-3 had a much higher potency in small veins than in small arteries. Indeed, even after inhibition of basal nitric oxide production, endothelin-3 (1 μM) did not contract arteries. This finding suggests a heterogeneity of ET_A receptors in these small vessels which is also supported by the observation that BQ123 (3 μM) is a more potent antagonist against endothelin-1 in arteries than it is in veins. The existence of ET_A receptor subtypes has been suggested in rat thoracic aorta (Sumner *et al.*, 1992) and goat cerebral artery (Salom *et al.*, 1993).

In the human vessels the pA_2 value for BQ123 (arteries: 7.1; veins: 7.5) was of the same order as that found in animal tissues (Ihara *et al.*, 1992; Sumner *et al.*, 1992; Taddei *et al.*, 1993). In the arteries the slope of the Schild plot for BQ123 was not significantly different from unity indicating that this compound behaves as a competitive antagonist of endothelin-1 in these vessels. However, in human small veins the slope of the Schild plot was significantly less than unity, possibly indicating non-competitive antagonism. BQ123 has been reported to be a non-competitive antagonist of endothelin-1-induced increases in intracellular Ca^{2+} concentration in SK-NMC cells derived from human neuroblastoma (Hiley *et al.*, 1992).

However, another explanation for a Schild slope different from unity is the presence of a BQ123-resistant receptor subtype in the veins. The concentration-response curve to endothelin-3 was biphasic, with a low sensitivity component which was blocked by BQ123 (3 μM) but not by IRL1038 (3 μM) and a high sensitivity component, accounting for approximatly 25% of the total endothelin-3 contraction, which was resistant to both the ET_A antagonist, BQ123 (3 μM) and the ET_B antagonist, IRL1038 (3 μM). This, taken together with the lack of activity of the ET_B agonist, sarafotoxin S6c, suggests that endothelin-3 might activate an ET_A receptor (low potency) and a non ET_A/non ET_B receptor (high potency). This would be in line with other studies showing the existence of a non ET_A/non ET_B receptor in pig coronary artery (Harrison *et al.*, 1992), guinea-pig pulmonary artery (Cardell *et al.*, 1992) and rat vas deferens (Eglezos *et al.*, 1993). Only very recently, a novel, BQ123-insensitive, IRL 1038 insensitive contractile ET_B receptor very similar to the one described in this study, has been demonstrated in swine pulmonary vein (Sudjarwo *et al.*, 1993). Although the magnitude of the BQ123-resistant contraction to endothelin-3 in the human veins is relatively small compared to the overall response, it is nevertheless as large as the response to 50 mM KCl and could therefore be functionally significant.

BQ123 fully reversed established contractions produced by endothelin-1 in human small vessels, indicating that this antagonist can displace endothelin-1 from the ET_A receptor in resistance arteries. This finding suggests that BQ123 may provide a useful tool to assess the physiological and pathophysiological roles of ET_A receptors on vascular tone in man.

No relaxant effect of endothelin-1 or sarafotoxin S6c was seen in submaximally precontracted human arteries or veins. These data are consistent with the observation that endothelin-1 induces a very small (Kiowski *et al.*, 1991) or no vasodilatation (Clarke *et al.*, 1989) in the human forearm and does not dilate human dorsal hand veins (Haynes & Webb, 1993). The nitric oxide synthesis inhibitor L-NMMA significantly increased the pD_2 value of endothelin-1 in arteries without affecting the maximum response. In contrast, L-NMMA did not alter the efficacy or potency of endothelin in veins. Together these findings suggest that endothelin does not stimulate the release of nitric oxide in human small vessels but that basal release of nitric oxide, which is present in arteries and not veins, modulates the contractile responses

to endothelin-1. It is unlikely that the failure to demonstrate a relaxation to endothelin-1 was due to endothelial damage since the response to endothelium-dependent vasodilators was intact. Indomethacin did not alter the responses to endothelin-1 in human arteries or veins indicating that prostanoids generated within the vessel wall do not modify the response to endothelin-1 in these vessels *in vitro*.

Endothelin-1 is a very potent contractor of human small arteries and veins and our results suggest that these vessels are an order of magnitude more sensitive to the constrictor effects of endothelin-1 than are human large vessels such as the saphenous vein, in which the pD_2 for endothelin-1 is approximately 8 (Bax *et al.*, 1993). These responses to endothelin-1 are mediated by ET_A receptors in both vessel types, although our studies suggest that the ET_A receptor may differ between arteries and veins. The small veins, but not the small arteries, are also very sensitive to endothelin-3 and the high potency contractions to this peptide appear to be mediated by a non ET_A/non ET_B receptor subtype similar to that reported in certain animal tissues (Sudjarwo *et al.*, 1993). In the presence of tissue hypoxia, endothelin production appears to be increased (Yasuda *et al.*, 1990) and the observations that small arteries supplying and veins draining the tissues contract to these peptides suggest a possible role for endothelin in the response of the microcirculation to ischaemia. Furthermore, our results demonstrate that if endothelial cell function is impaired, the arteries are exquisitely sensitive to endothelin-1 with nanomolar concentrations of endothelin-1 producing near maximal contraction. The presence of multiple endothelin receptor subtypes in the human microcirculation opens the possibility of developing endothelin receptor antagonists with different haemodynamic profiles.

References

ARAI, H., HORI, S., ARAMORI, I., OHKUBO, H. & NAKANISHI, S. (1990). Cloning and expression of cDNA encoding an endothelin receptor. *Nature*, **348**, 730–732.

ARUNLAKSHANA, O. & SCHILD, H.O. (1959). Some quantitative uses of drug antagonists. *Br. J. Pharmacol. Chemother.*, **14**, 48–58.

BAX, W.A., BOS, E. & SAXENA, P.R. (1993). Heterogeneity of endothelin/sarafotoxin receptors mediating contraction of the human isolated saphenous vein. *Eur. J. Pharmacol.*, **239**, 267–268.

BIGAUD, M. & PELTON, J.T. (1992). Discrimination between ET_A- and ET_B-receptor-mediated effects of endothelin-1 and [Ala1,3,11, 15]endothelin-1 by BQ123 in the anaesthetized rat. *Br. J. Pharmacol.*, **107**, 912–918.

BORIC, M.P., DONOSO, V., FOURNIER, A., ST PIERRE, S. & HUIDOBRO-TORO, J.P. (1990). Endothelin reduces microvascular blood flow by acting on arterioles and venules of the hamster cheek pouch. *Eur. J. Pharmacol.*, **190**, 123–133.

BRAIN, S.D., TIPPINS, J.R. & WILLIAMS, T.J. (1988). Endothelin induces potent microvascular constriction. *Br. J. Pharmacol.*, **95**, 1005–1007.

CARDELL, L.O., UDDMAN, R. & EDVINSSON, L. (1992). Evidence for multiple endothelin receptors in the guinea-pig pulmonary artery and trachea. *Br. J. Pharmacol.*, **105**, 376–380.

CARDELL, L.O., UDDMAN, R. & EDVINSSON, L. (1993). A novel ET_A-receptor antagonist, FR 139317, inhibits endothelin-induced contractions of guinea-pig pulmonary arteries, but not trachea. *Br. J. Pharmacol.*, **108**, 448–452.

CLARKE, J.G., BENJAMIN, N., LARKIN, S.W., WEBB, D.J., DAVIES, G.J. & MASERI, A. (1989). Endothelin is a potent long-lasting vasoconstrictor in men. *Am. J. Physiol.*, **257**, H2033–H2035.

CLOZEL, M., GRAY, G.A., BREU, V., LOFFLER, B.M. & OSTERWALDER, R. (1992). The endothelin ET_B receptor mediates both vasodilation and vasoconstriction in vivo. *Biochem. Biophys. Res. Commun.*, **186**, 867–873.

COCKS, T.M., FAULKNER, N.L., SUDHIR, K. & ANGUS, J. (1989). Reactivity of endothelin-1 on human and canine large veins compared with large arteries in vitro. *Eur. J. Pharmacol.*, **171**, 17–24.

EGLEZOS, A., CUCCHI, P., PATACCHINI, R., QUARTARA, L., MAGGI, C.A. & MIZRAHI, J. (1993). Differential effects of BQ123 against endothelin-1 and endothelin-3 on the rat vas deferens: evidence for atypical endothelin receptor. *Br. J. Pharmacol.*, **109**, 736–738.

FOZARD, J.R. & PART, M.L. (1992). The role of nitric oxide in the regional vasodilator effects of endothelin-1 in the rat. *Br. J. Pharmacol.*, **105**, 744–750.

HARRISON, V.J., RANDRIANTSOA, A. & SCHOEFFTER, P. (1992). Heterogeneity of endothelin-sarafotoxin receptors mediating contraction of pig coronary artery. *Br. J. Pharmacol.*, **105**, 511–513.

HAYNES, W.G. & WEBB, D.J. (1993). Endothelium-dependent modulation of responses to endothelin-1 in human veins. *Clin. Sci.*, **84**, 427–433.

HILEY, C.R., COWLEY, D.J., PELTON, J.T. & HARGREAVES, A.C. (1992). BQ123, cyclo(-D-Trp-D-Asp-Pro-D-Val-Leu), is a non-competitive antagonist on the actions of endothelin-1 in SK-N-MC human neuroblastoma cells. *Biochem. Biophys. Res. Commun.*, **184**, 504–510.

IHARA, M., NOGUCHI, K., SAEKI, T., FUKURODA, T., TSUCHIDA, S., KIMURA, S., FUKAMI, T., ISHIKAWA, K., NISHIKIBE, M. & YANO, M. (1992). Biological profiles of highly potent novel endothelin antagonists selective for the ET_A receptor. *Life Sci.*, **50**, 247–255.

INOUE, A., YANAGISAWA, M., KIMURA, S., KASUYA, Y., MIYAUCHI, T., GOTO, K. & MASAKI, T. (1989). The human endothelin family: three structurally and pharmacologically distinct isopeptides predicted by three separate genes. *Proc. Natl. Acad. Sci. U.S.A.*, **86**, 2863–2867.

KARAKI, H., SUDJARWO, S.A., HORI, M., SAKATA, K., URADE, Y., TAKAI, M. & OKADA, T. (1993). ET_B receptor antagonist, IRL 1038, selectively inhibits the endothelin-induced endothelium-dependent vascular relaxation. *Eur. J. Pharmacol.*, **231**, 371–374.

KIOWSKI, W., LÜSCHER, T.F., LINDER, L. & BUHLER, F.R. (1991). Endothelin-1-induced vasoconstriction in humans. Reversal by calcium channel blockade but not by nitrovasodilators or endothelium-derived relaxing factor. *Circulation*, **83**, 469–475.

KLOOG, Y., AMBAR, I., SOKOLOVSKY, M., KOCHVA, E., WOLLBERG, Z. & BDOLAH, A. (1988). Sarafotoxin, a novel vasoconstrictor peptide: phosphoinositide hydrolysis in rat heart and brain. *Science*, **242**, 268–270.

LAMPING, K.G., CLOTHIER, J.L., EASTHAM, C.L. & MARCUS, M.L. (1992). Coronary microvascular response to endothelin is dependent on vessel diameter and route of administration. *Am. J. Physiol.*, **263**, H703–H709.

LÜSCHER, T.F., YANG, Z., TSCHUDI, M., VON SEGESSER, L., STULTZ, P., BOULANGER, C., SIEBENMANN, R., TURINA, M. & BUHLER, F. (1990). Interaction between endothelin-1 and endothelium-derived relaxing factor in human arteries and veins. *Circ. Res.*, **66**, 1088–1094.

MACLEAN, M.R., TEMPLETON, A.G.B. & MCGRATH, J.C. (1992). The influence of endothelin-1 on human foeto-placental blood vessels: a comparison with 5-hydroxytryptamine. *Br. J. Pharmacol.*, **106**, 937–941.

MCNAMARA, D.B., LIGHT, J.T., MINKES, R.K., SAROYAN, R.M., KVAMME, P., ROWE, N., WEBB, W.R., FOX, L., KERSTEIN, M.D., MILLES, N.L. & KADOWITZ, P.J. (1992). Comparative effects of endothelin (ET-1) and U46619 on human saphenous vein and gastroepiploic artery, sources of human autologous graft. *Mol. Cell. Biochem.*, **117**, 81–85.

MILLER, R.C., PELTON, J.T. & HUGGINS, J.P. (1993). Endothelins – from receptors to medicine. *TIPS*, **14**, 54–60.

MILLER, V.M., KOMORI, K., BURNETT, J.C. & VANHOUTTE, P.M. (1989). Differential sensitivity to endothelin in canine arteries and veins. *Am. J. Physiol.*, **257**, H1127–H1131.

MORELAND, S., MCMULLEN, D.M., DELANEY, C.L., LEE, V.G. & HUNT, J.T. (1992). Venous smooth muscle contains vasoconstrictor ET_B-like receptors. *Biochem. Biophys. Res Commun.*, **184**, 100–106.

MULVANY, M.J. & HALPERN, W. (1977). Contractile properties of small arterial resistance vessels in spontaneously hypertensive and normotensive rats. *Circ. Res.*, **41**, 19–25.

RIEZEBOS, J., WATTS, I.S. & VALLANCE, P.J.T. (1993). Preliminary evidence for a novel endothelin receptor subtype in human small blood vessels. *Br. J. Pharmacol.*, in press.

ROGERSON, M.E., CAIRNS, H.S., FAIRBANKS, L.D., WESTWICK, J. & NEILD, G.H. (1993). Endothelin-1 in the rabbit: interactions with cyclo-oxygenase and NO-synthase products. *Br. J. Pharmacol.*, **108,** 838–843.

SAKAMOTO, A., YANAGISAWA, M., SAKURAI, T., TAKUWA, Y., YANAGISAWA, H. & MASAKI, T. (1991). Cloning and functional expression of human cDNA for the ET_B endothelin receptor. *Biochem. Biophys. Res. Commun.*, **178,** 286–292.

SAKURAI, T., YANGISAWA, M., TAKUWA, Y., MIYAZAKI, K., KIMURA, S., GOTO, K. & MASAKI, T. (1990). Cloning of a cDNA encoding non-isopeptide-selective subtype of the endothelin-receptor. *Nature*, **348,** 732–735.

SALOM, J.B., TORREGROSA, G., BARBERA, M.D., JOVER, T. & ALBORCH, E. (1993). Endothelin receptors mediating contraction in goat cerebral arteries. *Br. J. Pharmacol.*, **109,** 826–830.

SCHIFFRIN, E.L., DENG, L.Y. & LAROCHELLE, P. (1992). Blunted effects of endothelin upon small subcutaneous resistance arteries of mild essential hypertensive patients. *J. Hypertension*, **10,** 437–444.

SUDJARWO, S.A., HORI, M., TAKAI, M., URADE, Y., OKADA, T. & KARAKI, H. (1993). A novel subtype of endothelin B receptor mediating contraction in swine pulmonary vein. *Life Sci.*, **53,** 431–437.

SUMNER, M.J., CANNON, T.R., MUNDIN, J.W., WHITE, D.G. & WATTS, I.S. (1992). Endothelin ET_A and ET_B receptors mediate vascular smooth muscle contraction. *Br. J. Pharmacol.*, **107,** 858–860.

TADDEI, S. & VANHOUTTE, P.M. (1993). Role of endothelium in endothelin-evoked contractions in the rat aorta. *Hypertension*, **21,** 9–15.

URADE, Y., FUJITANI, Y., ODA, K., WATAKABE, T., UMEMURA, I., TAKAI, M., OKADA, T., SAKATA, K. & KARAKI, H. (1992). An endothelin B receptor-selective antagonist: IRL1038, [Cys–Cys]-endothelin-1 (11–21).*FEBS lett.*, **311,** 12–16.

VIERHAPPER, H., WAGNER, O., NOWOTNY, P. & WALDHAUSL, W. (1990). Effect of endothelin-1 in man. *Circulation*, **81,** 1415–1418.

WATT, P.A.C., BAKER, A.R. & THURSTON, H. (1989). Vasoconstrictor actions of endothelin-1 in human resistance vessels. *J. Hypertension*, **7** (suppl. 6), S134–S135.

WILLIAMS, D.L., JONES, K.L., PETTIBONE, D.J., LIS, E.V. & CLINE-SCHMIDT, B.V. (1991). Sarafotoxin S6c: an agonist which distinguishes between endothelin receptor subtypes. *Biochem. Biophys. Res. Commun.*, **175,** 556–561.

YANAGISAWA, M, KURIHARA, H., KIMURA, S., TOMOBE, Y., KOBAYASHI, M., MITSUI, Y., YAZAKI, Y., GOTO, K. & MASAKI, T. (1988). A novel potent vasoconstrictor peptide produced by vascular endothelial cells. *Nature*, **332,** 411–415.

YASUDA, M., KOHNO, M., TAHARA, A., ITAGANE, H., TODA, I., AKIOKA, K. *et al.* (1990). Circulating immunoreactive endothelin in ischaemic heart disease. *Am. Heart J.*, **118,** 801–806.

(Received July 23, 1993
Revised September 29, 1993
Accepted October 20, 1993)

Br. J. Pharmacol. (1994), **111**, 616–624

Comparison of the effects of IVth ventricular administration of some tryptamine analogues with those of 8-OH-DPAT on autonomic outflow in the anaesthetized cat

[1]Sara L. Shepheard, *David Jordan & [2]Andrew G. Ramage

Academic Department of Pharmacology and *Physiology, Royal Free Hospital School of Medicine, Rowland Hill St, Hampstead, London NW3 2PF

1 The present study compares the effects on representative autonomic outflows of IVth ventricular application of tryptamine analogues which act at 5-HT_1 receptors with 8-hydroxy-2-(di-n-propylamino)tetralin (8-OH-DPAT).

2 Cumulative doses of 8-OH-DPAT, N,N-di-n-propyl-5-carboxamidotryptamine (DP-5-CT) and 5-carboxamidotryptamine (5-CT, 2.5–40 nmol kg^{-1}), sumatriptan (10–160 nmol kg^{-1}), indorenate (100–800 nmol kg^{-1}), 5-hydroxytryptamine (5-HT, 20–640 nmol kg^{-1}) both alone and in the presence of cinanserin (0.1 mg kg^{-1}) were given into the IVth ventricle of cats which were anaesthetized with a mixture of α-chloralose and pentobarbitone sodium, neuromuscularly blocked and artificially ventilated. Recordings were made of arterial blood pressure, heart rate, renal, cardiac, splanchnic and phrenic nerve activities, femoral arterial flow, tracheal and intragastric pressures.

3 Central application of each of the agonists evoked significant falls in arterial blood pressure. In addition 8-OH-DPAT, DP-5-CT, 5-CT and 5-HT all evoked a differential inhibition of sympathetic nerve activities, with renal nerve activity being the most sensitive and cardiac nerve activity the least sensitive. In the dose-ranges used, administration of sumatriptan evoked reductions only in renal and splanchnic nerve activities whilst indorenate reduced activity in all three sympathetic nerves to a similar extent.

4 The effect of the agonists on heart rate was more inconsistent than the effects on sympathetic outflow. IVth ventricular application of 5-CT and sumatriptan were without effect on heart rate whilst 8-OH-DPAT, DP-5-CT, indorenate and 5-HT alone and in the presence of cinanserin all evoked significant bradycardias. However, whilst atropine partially reversed the bradycardias evoked by 8-OH-DPAT and only slightly reversed those caused by indorenate, atropine was without effect on those evoked by DP-5-CT or 5-HT.

5 None of the analogues tested had significant effects on gut motility, phrenic nerve discharge or tracheal pressure. 8-OH-DPAT, DP-5-CT, indorenate and 5-HT were without effect on femoral arterial conductance. However, following pretreatment with cinanserin, 5-HT evoked a significant reduction in femoral arterial conductance. At its highest dose, sumatriptan evoked a significant increase in femoral arterial conductance as did 5-CT at the 20 nmol kg^{-1} dose.

6 It is concluded that the present data support the view that 5-HT_{1A} receptors at the level of the brainstem are involved in the central sympathoinhibitory effects caused by intravenous administration of 5-HT_{1A} agonists. Further, brainstem 5-HT_{1A} receptors play an important role in the control of renal sympathetic outflow while brainstem 5-HT_2 receptors are involved in the control of skeletal muscle and/or skin blood flow. Selective tryptamine agonists for 5-HT_{1A} receptors differ from non-tryptamine agonists in that they do not cause an increase in central cardiac vagal tone.

Keywords: 5-HT_{1A} receptors; 8-hydroxy-2-(di-n-propylamino)tetralin (8-OH-DPAT); N,N,-di-n-propyl-5-carboxamidotryptamine (DP-5-CT); 5-carboxamidotryptamine (5-CT); sumatriptan; indorenate; 5-hydroxytryptamine (5-HT); cinanserin; sympathetic nerve activity; blood pressure

Introduction

Determination of the *in vivo* function of particular receptors is often made by studying the deficit produced by application of selective antagonists for the receptor. However, such determination of the functions of the many subtypes of the 5-HT_1 receptor has been particularly difficult due to the lack of selective antagonists (see Hamon *et al.*, 1990). Another method for investigating the specific role of different receptor subtypes *in vivo* is the use of agonists for that particular subtype. Although in the case of the 5-HT_{1A} receptor subtype these agonists are more selective than the available antagonists, they may still not be totally selective and therefore *in vivo* it is sometimes difficult to assign all the observed induced changes to activation of a particular receptor subtype. However, if other structurally different agonists also produce the same range of effects, it is then much more likely that these effects are mediated through activation of one particular receptor subtype. In investigating the function of 5-HT_{1A} receptors in cardiovascular regulation the most commonly used agonist is the aminotetralin 8-hydroxy-2-(di-n-propylamino)tetralin HBr (8-OH-DPAT) a simplified ergot congener (Hjorth *et al.*, 1982). In addition, a small amount of data exists on other agonists, such as flesinoxan, an N-substituted phenylpiperazine analogue (Wouters *et al.*, 1988). Using such information it has been concluded that the sympathoinhibition, increase in vagal drive to the heart and fall in blood pressure observed with these compounds is due to activation of 5-HT_{1A} receptors (see Ramage, 1990). It has recently been suggested that if agonists must be used alone to

[1] Present address: Merck Sharp & Dohme Research Laboratories, Neuroscience Research Centre, Terlings Park, Eastwick Road, Harlow CM20 2QR.
[2] Author for correspondence.

determine the function of a particular receptor then it may be preferable to use agonists which are structurally-related to the natural transmitter (Leff & Martin, 1988). Analogues of 5-HT which are selective for 5-HT$_1$ receptors such as N,N-di-n-propyl-5-carboxamidotryptamine maleate (DP-5-CT; highly selective for the 1_A subtype), 5-carboxamidotryptamine maleate (5-CT; highly potent at the 1_A, 1_B and 1_D receptor subtypes) and sumatriptan (with 30 times higher affinity for 1_D than 1_A; see Hoyer & Fozard, 1991) do exist. However, little is known of their central effects on autonomic regulation, although it has been suggested that indorenate, a tryptamine analogue, causes its central hypotensive action by activation of 5-HT$_1$ receptors (Safdy *et al.*, 1982). One probable reason for this lack of information is that these substances do not cross the blood-brain barrier well (Mir *et al.*, 1987; Humphrey *et al.*, 1990). In addition, the wide distribution of 5-HT$_{1A}$ receptors within the central nervous system (Pazos & Palacios, 1985) forestalls the use of local injection of these compounds into the central nervous system, since this may not produce the complete range of autonomic effects as observed for intravenous 8-OH-DPAT.

The present experiments were carried out to compare the action of tryptamine analogues DP-5-CT, 5-CT, sumatriptan and indorenate with that of 8-OH-DPAT on sympathetic nerve activity, blood pressure and heart rate by administering these compounds into the IVth ventricle. This method of administration will allow substances to reach the ventral surface of the brainstem, an area which has recently been identified as a site for the central cardiovascular effects of 8-OH-DPAT (Gillis *et al.*, 1989; Laubie *et al.*, 1989; King & Holtman, 1990). In addition, the effects of 5-HT alone and in the presence of the 5-HT$_2$ antagonist cinanserin were also investigated, since it has previously been reported that 5-HT applied to the ventral surface of the brain stem failed to affect sympathetic nerve activity and blood pressure (Coote *et al.*, 1987), though effects could be observed if the 5-HT were applied in the presence of a 5-HT$_2$ receptor antagonist (Gillis *et al.*, 1989).

Preliminary accounts of some of these observations have been given (Shepheard *et al.*, 1989; 1990).

Methods

Experiments were performed on male adult cats anaesthetized with a mixture of α-chloralose (70 mg kg^{-1}) and pentobarbitone sodium (6 mg kg^{-1}) i.v.; supplementary doses of α-chloralose (10–15 mg kg^{-1}) were given as required. Following a tracheotomy low in the neck, the animals were intubated and artificially ventilated (rate 30 per min, tidal volume 17–20 ml) with oxygen-enriched room air using a positive pressure ventilator (Harvard 665A) after neuromuscular blockade with vecuronium bromide (200 μg kg^{-1}). Arterial blood pressure, heart rate, body temperature and arterial blood gases and pH were monitored as previously described (Shepheard *et al.*, 1991b). A constant infusion of a solution comprising 500 ml plasma substitute (Gelofusine), 500 ml H_2O, 8.4 g $NaHCO_3$ and 2 g of glucose was given at a rate of 6 ml kg^{-1} h^{-1} into the brachial vein to maintain blood volume and to counteract the development of non-respiratory acidosis. During the experiments, pH and arterial blood gases were kept within the following ranges, pH 7.24–7.35; $PaCO_2$ 41–48 mmHg and PaO_2 112–130 by varying the rate and tidal volume of the ventilator or by a slow infusion i.v. of 1M sodium bicarbonate.

Simultaneous recordings were made of right inferior cardiac, splanchnic and renal nerve activities and left phrenic nerve activity. The right inferior cardiac nerve was exposed retropleurally by deflecting the scapula and removing the second rib. The splanchnic and renal nerves were exposed by a retroperitoneal approach through the right flank. The left phrenic nerve was exposed low down in the neck at the level of the 4th and 5th spinal nerves. Whole nerve activity was recorded from the intact nerves by use of bipolar silver hook electrodes as previously described (Shepheard *et al.*, 1991b). In all experiments sympathetic nerve activity was tested to see if it was under baroreceptor modulation by checking that activity in the nerves increased during a fall in blood pressure induced by sodium nitroprusside (2 μg kg^{-1}, i.v.) or decreased during a rise in blood pressure induced by noradrenaline (0.5 μg per animals, i.v.). In addition, femoral arterial flow, from which conductance was calculated, was measured with an electromagnetic flow probe placed on the right femoral artery. Tracheal pressure was monitored by a pressure transducer connected to a side arm of the tracheal cannula. Gastric motility was measured by inserting a rubber balloon into the stomach via the oesophagus. This balloon was then filled with 30 ml of saline and connected to a pressure transducer.

To give microinjections into the IVth ventricle the animal's head was placed in a stereotaxic frame and a cannula placed so that its tip lay in the IVth ventricle as described previously (Shepheard *et al.*, 1991b). The position was confirmed at the end of the experiment by injecting pontamine sky blue dye (20 μl over 1 min). When the cannula was correctly placed it was found that the dye was distributed over the floor of the IVth ventricle from its anterior end to the level of the lateral recesses and from there through the lateral recesses, down on to the ventral surface of the medulla.

All variables were recorded for a 20 min stabilization period. In each animal a microinjection of vehicle ('initial' vehicle) was then given into the IVth ventricle (i.c.v.) followed 10 min later by cumulative doses of either a test drug or vehicle, only one drug or vehicle being tested per animal.

Table 1 Baseline values of heart rate (HR), mean arterial blood pressure, (BP), femoral arterial conductance (FAC), gastric motility (GM), tracheal pressure (TP) and inspiratory rate (Insp rate)

	n	*HR* (beats min^{-1})	*BP* (mmHg)	*FAC* (ml min^{-1} mmHg^{-1} × 10^{-3})	*GM* (line length mm min^{-1})	*TP* (cmH_2O)	*Insp rate* (burst min^{-1})
Control CSF	5	205 ± 12	150 ± 7	48 ± 4	58 ± 11	7.4 ± 0.4	8.6 ± 0.9
Control saline	5	197 ± 8	117 ± 10	67 ± 9	49 ± 4	6.9 ± 0.3	9.7 ± 0.8 (n = 4)
8-OH-DPAT	5	211 ± 10	120 ± 12	96 ± 18	47 ± 7	9.1 ± 1.1	10.0 ± 1.1 (n = 3)
DP-5-CT	5	218 ± 11	137 ± 10	53 ± 12	36 ± 7	7.6 ± 0.5	9.5 ± 0.5 (n = 4)
5-CT	5	221 ± 15	116 ± 11	63 ± 11	42 ± 8	8.2 ± 0.6	7.6 ± 1.0
Indorenate	5	197 ± 12	117 ± 8	77 ± 14	60 ± 6	7.4 ± 0.4	7.2 ± 1.6
Sumatriptan	5	224 ± 11	103 ± 4	77 ± 19	43 ± 6	8.2 ± 0.3	6.8 ± 0.2
5-HT	5	215 ± 7	126 ± 5	65 ± 22	30 ± 7	9.0 ± 0.4	8.0 ± 1.0 (n = 2)
Cinanserin	5	202 ± 8	107 ± 11	74 ± 4	57 ± 14	8.1 ± 0.4	5.2 ± 0.8 (n = 4)
Cinanserin/5-HT	5	200 ± 8	104 ± 11	88 ± 7	55 ± 6	8.1 ± 0.4	5.5 ± 0.9 (n = 4)

8-OH-DPAT, 8-hydroxy-2-(di-n-propylaminotetralin); DP-5-CT, N,N-di-n-propyl-5-carboxamidotryptamine; 5-CT, 5-carboxamidotryptamine; 5-HT, 5-hydroxytryptamine.

Test drugs were administered cumulatively at 10 min intervals except for 5-HT alone, 5-HT in the presence of cinanserin and sumatriptan which were given at 15 min intervals. In all experiments atropine methylnitrate (0.1 mg kg^{-1}, i.v.) was administered at least 10 min after the last dose of the test drug. The times between injections represent the time taken for the changes in blood pressure and nerve activities to stabilize. All i.c.v. injections were given in a volume of 20 µl over a period of 1 min.

Two sets of control experiments were performed. The first set were controls for drugs dissolved in CSF. Test i.c.v. injections of CSF were given at 10 min intervals which corresponded in time to the i.c.v. injections of 8-OH-DPAT and 5-CT. However, after the time of the final 5-CT injection, the CSF injections were continued at 10 min intervals so that they could be used as controls for the 5-HT, 5-HT in the presence of cinanserin and sumatriptan experiments in which the drugs were administered at 15 min intervals. In these latter controls, values were taken at time intervals which corresponded to the application of the drugs, though this did not necessarily match an injection of CSF. The second set of controls were for drugs dissolved in saline. Test i.c.v. injections of saline were given at 10 min intervals to correspond to the time of i.c.v. injections of DP-5-CT and indorenate.

Analysis of data

All sympathetic nerve activities were quantified by rectifying and integrating the signals above background noise over 5 s periods using solid state electronic integrators. The outputs were then displayed on a Grass polygraph recorder and were calibrated in arbitrary units. Phrenic nerve activity was quantified by integrating the amplitude and frequency of the action potentials in each inspiratory burst or, if continuous, by integrating the amount of activity in a 5 s period, again using a solid state electronic integrator, the output of which was displayed on the Grass polygraph in arbitrary units (see Shepheard *et al.*, 1991b). The first method of quantifying phrenic nerve activity gives an indication of both the amount of activity in each inspiratory burst and the frequency of inspiratory bursts. The validity of the threshold setting used to quantify the nerve activities was verified at the end of each experiment after administration of pentobarbitone sodium (60 mg per animal) or by crushing the nerves centrally to block all activity. All nerve activity was measured as the mean level over 1 min in arbitrary units.

Intragastric pressure was quantified by displaying the output from the pressure transducer on the Grass polygraph recorder. The total line length of the ink trace was measured with an IBAS IPS image analyser (Kontron U.K.) and converted to give mean line length in mm min^{-1}. Total line length gives an indication of changes in both frequency and amplitude of gastric contractions (see Shepheard *et al.*, 1991b). Tracheal pressure was continually monitored throughout each experiment but as no obvious changes were observed no further analysis was carried out.

Except for gastric motility, measurements of all variables were made in the minute before each injection of test substance. Because of its slow periodicity, measurements of gastric motility were made in the 3 min period before each injection of test substance. In all experiments baseline values were those values measured just before the first injection of test drug or vehicle. This was usually 10 min after the 'initial' vehicle. However, in the cinanserin pretreatment experiments, cinanserin was administered 10 min after 'initial' vehicle followed 10 min later by 5-HT. Baseline values for these experiments were taken as those values prior to the first injection of 5-HT. All results are expressed as changes from baseline values. In order to normalize the data, changes in integrated nerve activity are given as percentage changes from baseline. The changes in all other variables are presented as actual changes.

The changes in response to test drugs were compared with the responses to the appropriate vehicle injections at matched time intervals by two way analysis of variance and the least significant difference for comparisons between the means (Sokal & Rohlf, 1969). Changes from baseline values caused by cinanserin were statistically analysed by Student's paired *t* test. Differences were considered significant when $P<0.05$.

Drugs and solutions

The following drugs were used:- 8-hydroxy-2-(di-n-propylamino)tetralin HBr (8-OH-DPAT), N,N-di-n-propyl-5-carboxamidotryptamine maleate (DP-5-CT), 5-carboxamidotryptamine maleate (5-CT, Research Biochemicals Inc., Semat Technical Ltd, St. Albans, Herts); sumatriptan HCl (a gift from the Wellcome Research Laboratories, Kent);

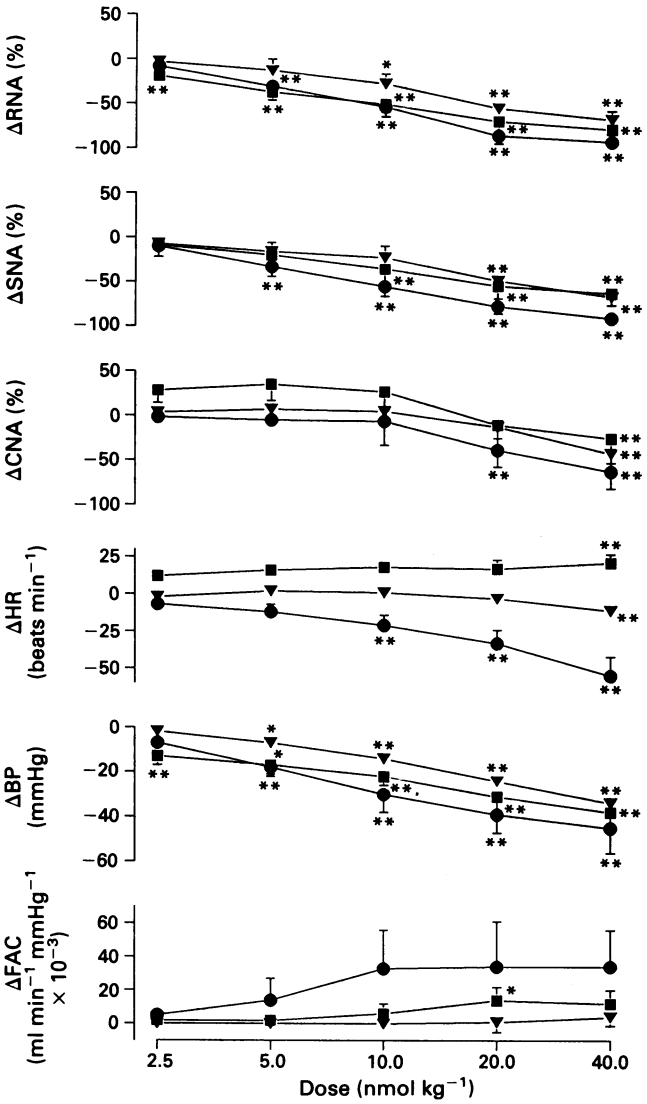

Figure 1 Anaesthetized cats: the effect of cumulative doses (2.5–40 nmol kg^{-1}) of 8-hydroxy-2-(di-n-propylamino)tetralin (8-OH-DPAT, ●), N,N-di-n-propyl-5-carboxamidotryptamine (DP-5-CT, ▼) and 5-carboxamidotryptamine (5-CT, ■) administered into the IVth ventricle on changes (Δ) from baseline values in renal (RNA), splanchnic (SNA) and cardiac (CNA) nerve activities, heart rate (HR), mean arterial blood pressure (BP) and femoral arterial conductance (FAC). Each point represents the mean value ($n = 5$) with s.e.mean. The above changes were compared to changes caused by the appropriate vehicle administration using two way analysis of variance and the least significant difference test to compare the means, $*P<0.05$; $**P<0.01$. The data for the appropriate vehicle control has been omitted for the sake of clarity.

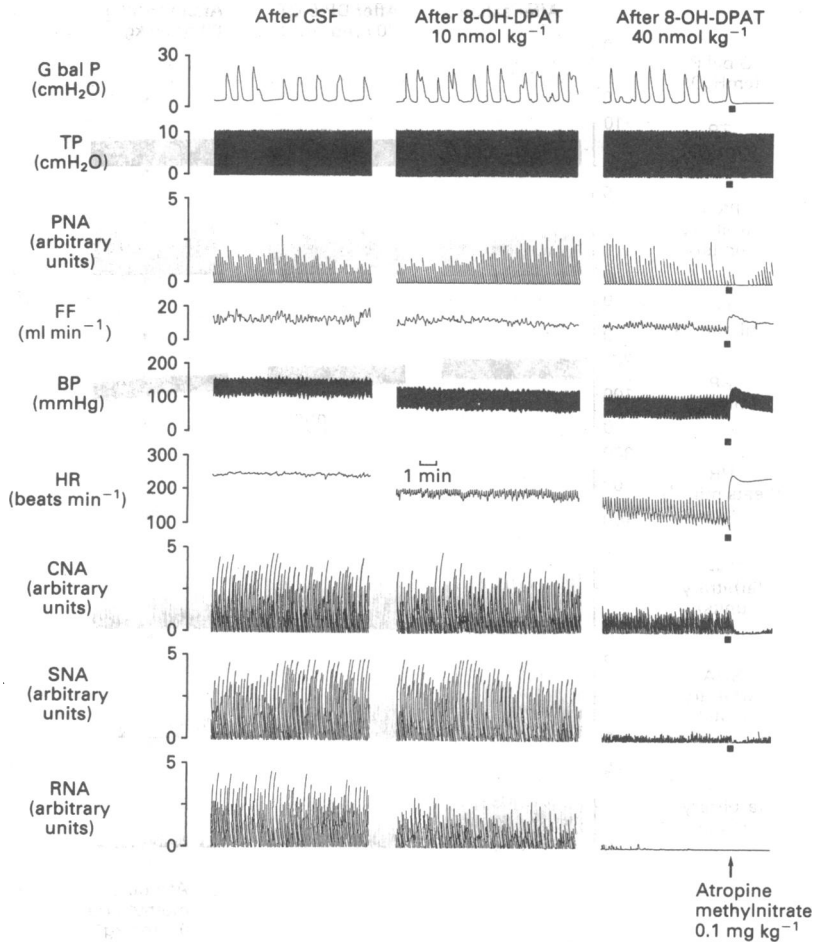

Figure 2 Traces showing recordings of gastric balloon pressure (G bal P), tracheal pressure (TP), integrated phrenic nerve activity (PNA), femoral arterial flow (FF), arterial blood pressure (BP), heart rate (HR), integrated cardiac (CNA), splanchnic (SNA) and renal (RNA) nerve activities in an anaesthetized cat. The three panels show the effects of CSF and then the cumulative doses of 10 and 40 mmol kg^{-1} of 8-hydroxy-2-(di-n-propylamino) tetralin (8-OH-DPAT) administered into the IVth ventricle. In the third panel the effect of an i.v. bolus injection of atropine methylnitrate (0.1 mg kg^{-1}) is illustrated.

indorenate HCl, (a gift from Miles Laboratories, Inc., Elkhart, Indiana, U.S.A.); Gelofusine (Consolidated Chem., Wrexham, Clwyd); 5-hydroxytryptamine creatinine sulphate (5-HT, BDH, Poole, Dorset); noradrenaline acid tartrate (Winter, Guildford, Surrey); cinanserin HCl (a gift from Squibb & Sons, Inc., Princeton, N.J., U.S.A.); α-chloralose, sodium nitroprusside and atropine methylnitrate (Sigma Chemical Co., Poole, Dorset). Drugs given i.c.v. were dissolved in artificial CSF (8-OH-DPAT, 5-CT, 5-HT, sumatriptan) or 0.9% w/v saline (DP-5-CT, indorenate, cinanserin). The composition of the artificial CSF used was (mM): KH_2PO_4 2.2, $MgSO_4.7H_2O$ 1.2, KCl 2.0, glucose 10, $NaHCO_3$ 25, NaCl 115 and $CaCl_2.2H_2O$ 2.5. All doses except noradrenaline refer to the salts of the drug.

Results

The baseline values for all experimental groups are shown in Table 1.

Controls: effects of i.c.v. injections of CSF and saline

Injection of CSF ($n = 5$) every 10 min over a 90 min period caused only small changes from baseline in mean blood pressure (-6 ± 4 mmHg), heart rate ($+6 \pm 5$ beats min^{-1}), femoral arterial conductance ($+2 \pm 3$ ml min^{-1} mmHg^{-1} $\times$ 10^{-3}), renal ($+12 \pm 13\%$) and splanchnic ($+17 \pm 15\%$) nerve activity whereas cardiac nerve activity increased from baseline by $+55 \pm 19\%$. Data for 75 min of this control are shown in Figure 5. The rate of bursting and magnitude of each phrenic burst showed no significant change ($+1.0 \pm 0.5$ burst min^{-1} and $+22 \pm 11\%$ respectively) from baseline values). Tracheal pressure and gastric motility ($+16 \pm 6$ mm min^{-1}) changes little over this period.

Injections of saline ($n = 5$) at 10 min intervals over 60 min caused only small changes from baseline values in blood pressure (-3 ± 1 mmHg), heart rate ($+4 \pm 3$ beats min^{-1}), femoral arterial conductance ($+7 \pm 3$ ml min^{-1} mmHg^{-1} $\times$ 10^{-3}), in splanchnic ($+3 \pm 10\%$) and renal ($-6 \pm 4\%$) nerve activity. Cardiac nerve activity showed a small increase from baseline of $15 \pm 2\%$. The rate of bursting and magnitude of each phrenic burst showed no significant change ($+1.3 \pm 0.5$ burst min^{-1} and $+3 \pm 36\%$, respectively) from baseline values. Again tracheal pressure and gastric motility ($+2 \pm 6$ mm min^{-1}) changes little over this period. Data for 40 min of this control are shown in Figure 4.

Effects of cumulative doses (2.5–40 nmol kg^{-1}) of 8-OH-DPAT, DP-5-CT and 5-CT injected into the IVth ventricle

All three compounds caused dose-related decreases in sympathetic nerve activity and blood pressure (Figure 1). Blood pressure fell from baseline values by 45 ± 11, 34 ± 4 and 38 ± 6 mmHg for 8-OH-DPAT, DP-5-CT and 5-CT respec-

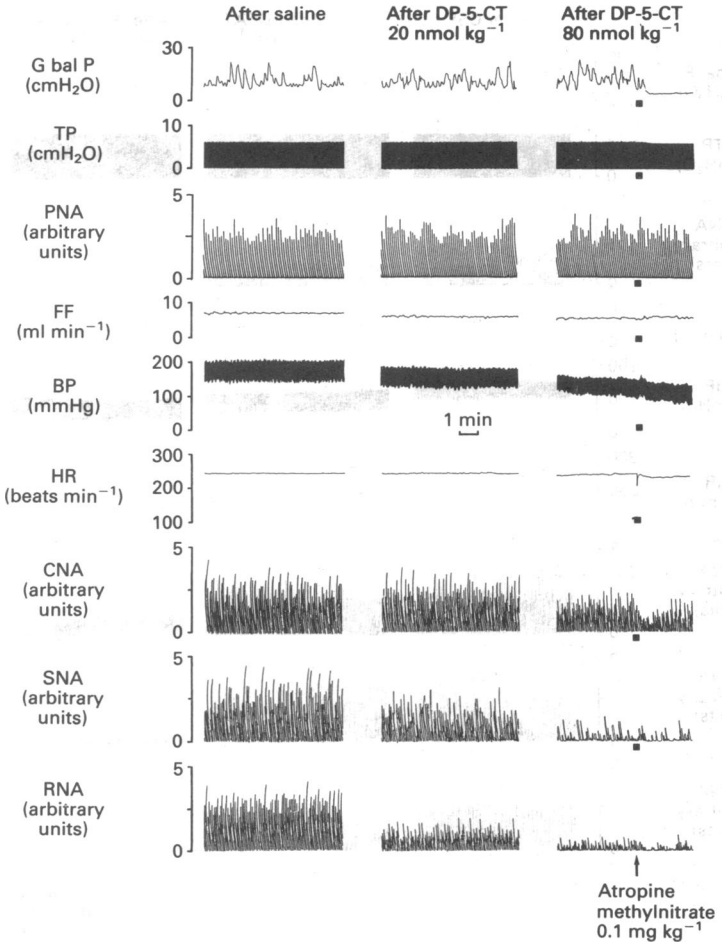

Figure 3 Traces showing recordings of gastric balloon pressure (G bal P), tracheal pressure (TP), integrated phrenic nerve activity (PNA), femoral arterial flow (FF), arterial blood pressure (BP), heart rate (HR), integrated cardiac (CNA), splanchnic (SNA) and renal (RNA) nerve activities in an anaesthetized cat. The three panels show the effects of CSF and then the cumulative doses of 20 and 80 nmol kg^{-1} of N,N-di-n-propyl-5-carboxamidotryptamine (DP-5-CT) administered into the IVth ventricle. In the third panel the effect of an i.v. bolus injection of atropine methylnitrate (0.1 mg kg^{-1}) is illustrated.

tively by the highest dose. The decrease in sympathetic nerve activity in the sympathetic outflows was not uniform. For 8-OH-DPAT ($n = 5$) the reductions in renal and splanchnic nerve activity became significant ($P < 0.05$), compared with control, at the 5 nmol kg^{-1} dose (Figure 1) reaching $-92 \pm 4\%$ and $-90 \pm 3\%$ respectively by the highest dose. The reduction in cardiac nerve activity was not significant until the 20 nmol kg^{-1} dose and only reached $-62 \pm 9\%$ at the highest dose. Representative traces from a typical experiment are shown in Figure 2.

In the DP-5-CT experiments ($n = 5$) the decrease in renal nerve activity became significant by the 10 nmol kg^{-1} dose reaching $-67 \pm 10\%$ by the highest dose while the reduction in splanchnic nerve activity became significant by the 20 nmol kg^{-1} dose, reaching $-66 \pm 2\%$ by the highest dose. Again the reduction in cardiac nerve activity was smaller, only becoming significant at 40 nmol kg^{-1} reaching $-42 \pm 16\%$. Representative traces from one of these experiments is shown in Figure 3.

5-CT ($n = 5$) caused a similar profile of sympathoinhibition to that observed for 8-OH-DPAT and DP-5-CT, renal nerve activity being most sensitive to the sympathoinhibitory actions of 5-CT. A significant reduction in renal nerve activity was observed by the lowest dose and reached $-78 \pm 15\%$ by the highest dose of 5-CT. The reduction in splanchnic nerve activity became significant at the 10 nmol kg^{-1} dose and reached $-62 \pm 13\%$ while the reduction in cardiac nerve activity was not significantly different from control values until the highest dose reaching $-25 \pm 27\%$.

Surprisingly, the reductions in sympathetic outflow and blood pressure caused by all three drugs were not associated with changes in femoral arterial conductance. Only 5-CT, at the dose of 20 nmol kg^{-1}, caused a small but significant increase in femoral arterial conductance of 14 ± 8 ml min^{-1} $mmHg^{-1} \times 10^{-3}$ (Figure 1).

The reductions in sympathetic outflow and blood pressure evoked by the two tryptamine analogues were associated with only small changes in heart rate (Figure 1). For DP-5-CT there was a significant reduction in heart rate of -11 ± 4 at 40 nmol kg^{-1} and for 5-CT there was an increase in heart rate of 22 ± 11 beats min^{-1} at the highest dose. 8-OH-DPAT caused dose-related decreases in heart rate reaching -55 ± 13 beats min^{-1} at the highest dose. In some cats (Figure 2) a profound sinus arrhythmia was also observed by the highest dose. Injection of atropine methylnitrate (0.1 mg kg^{-1}, i.v.) after the highest dose of 8-OH-DPAT caused the heart rate to return towards baseline levels (see Figure 2) producing a mean increase of 46 ± 14 beats min^{-1}. In contrast, intravenous injection of atropine methylnitrate did not affect the changes in heart rate caused either by DP-5-CT or by 5-CT.

Effects of cumulative doses of indorenate (100–800 nmol kg^{-1}) injected into the IVth ventricle

Indorenate ($n = 5$) caused dose related decreases in blood pressure, heart rate and activity in all three sympathetic nerves (Figure 4). The reduction in all the sympathetic nerve

activities was significant at all four doses. Although the decrease in cardiac nerve activity at the 100 nmol kg^{-1} dose ($-25 \pm 11\%$) was slightly less than that observed in renal ($-46 \pm 17\%$) and splanchnic ($-45 \pm 17\%$) nerve activity, by the highest dose the reduction in cardiac nerve activity ($-80 \pm 8\%$) was similar to that observed in splanchnic ($-87 \pm 11\%$) and renal ($-90 \pm 7\%$) nerve activities. This sympathoinhibition was associated with a decrease in blood pressure of -23 ± 8 mmHg at the highest dose but there was no significant change in femoral arterial conductance. There was however, a significant fall in heart rate which reached a maximum of -33 ± 10 beats min^{-1} by the highest dose. Subsequent administration of atropine methylnitrate caused a small increase in heart rate in 3 out of the 5 experiments of between 10–15 beats min^{-1}.

Effects of cumulative doses of sumatriptan (10–160 nmol kg^{-1}) injected into the IVth ventricle

Sumatriptan ($n = 5$, Figure 5), like 8-OH-DPAT, DP-5-CT and 5-CT caused sympathoinhibition and a fall in blood pressure. As with the other agonists, the renal nerve activity was the most sensitive to administration of sumatriptan, sympathoinhibition being observed at a dose of 10 nmol kg^{-1} whereas sympathoinhibition in the splanchnic nerve became apparent only at the 20 nmol kg^{-1} dose. These reached near maxima at 20 min and were $-45 \pm 8\%$ and $-34 \pm 17\%$, respectively at the highest doses. Sumatriptan was without significant effect on both cardiac nerve activity and heart rate. The sympathoinhibitory action of sumatriptan was associated with a maximum fall in blood pressure of 24 ± 5 mmHg at the highest dose, becoming significant at the 20 nmol kg^{-1} doses. The maximum fall in blood pressure was associated with a significant increase in femoral conductance of 13 ± 9 ml min^{-1} mmHg^{-1} $\times 10^{-3}$.

Effects of cumulative doses of 5-hydroxytryptamine (20–640 nmol kg^{-1}) injected into the IVth ventricle alone and in the presence of cinanserin (0.1 mg kg^{-1})

Pretreatment with cinanserin (0.1 mg kg^{-1}, $n = 5$) had little effect on the parameters being recorded except femoral arterial conductance in which there was a significant increase of 14 ± 4 ml min^{-1} mmHg^{-1} $\times 10^{-3}$ (Table 1). Cumulative doses of either 5-HT alone or in the presence of cinanserin caused significant falls in blood pressure by the highest dose of 19 ± 5 and 22 ± 3 mmHg respectively. Again, this was associated with a non-uniform sympathoinhibition (Figure 6). For 5-HT alone ($n = 5$) splanchnic nerve activity had declined significantly compared to control values at the dose of 80 nmol kg^{-1} while significant sympathoinhibition was not observed in the renal nerve until the dose of 320 nmol kg^{-1} both reaching a maximum of $-47 \pm 15\%$ and $-47 \pm 21\%$ respectively by the highest dose. Cardiac nerve activity was unaffected by cumulative doses of 5-HT alone. In the presence of cinanserin, 5-HT ($n = 5$) caused significant sympathoinhibition initially in the renal nerve at the dose of 80 nmol kg^{-1} whereas significant sympathoinhibition was not observed in the splanchnic nerve until the following dose of 160 nmol kg^{-1} declining to a maximum of $-43 \pm 24\%$ while renal declined by $-60 \pm 21\%$ in both cases by the highest dose. Furthermore, cardiac nerve activity also fell by $-9 \pm 24\%$. Although this was a small fall, it was significant compared to control data because in the control CSF alone experiments, cardiac nerve activity increased quite markedly over this time period (see above). In fact, cardiac nerve activity was significantly different from control values by the dose of 160 nmol kg^{-1}. In addition 5-HT in the presence of cinanserin caused a significant decrease in femoral arterial conductance at a dose of 160 nmol kg^{-1} reaching a maximum fall of -13 ± 9 ml min^{-1} mmHg^{-1} $\times 10^{-3}$ by the highest dose, whereas 5-HT alone caused no significant change.

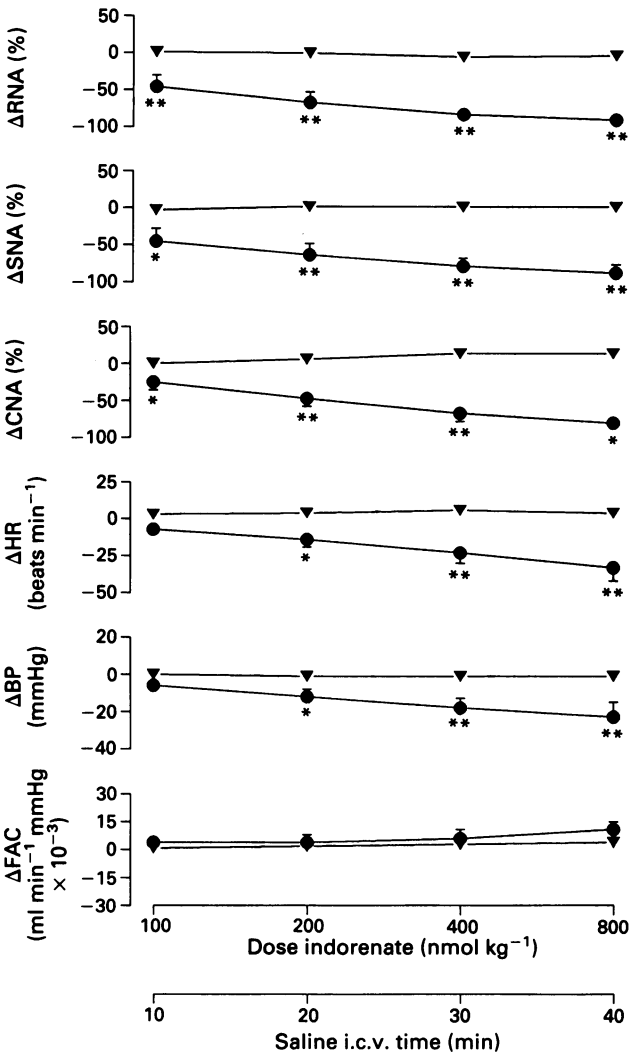

Figure 4 Anaesthetized cats: comparison of the effect of cumulative doses (100–800 nmol kg^{-1}) of indorenate (●), with time matched saline control values (▼) administered into the IVth ventricle on changes (Δ) from baseline values in renal (RNA), splanchnic (SNA) and cardiac (CNA) nerve activities, heart rate (HR), mean arterial blood pressure (BP) and femoral arterial conductance (FAC). Each point represents the mean value ($n = 5$) with s.e.mean. Comparisons of the changes evoked by indorenate with those produced by saline were made by two way analysis of variance and the least significant difference test to compare the means; $^*P < 0.05$; $^{**}P < 0.01$.

Finally, 5-HT both alone and in the presence of cinanserin caused a significant decline in heart rate reaching, by the highest dose, -18 ± 8 and -9 ± 5 beats min^{-1} respectively. These falls in heart rate were unaffected by atropine methylnitrate.

Effect of all drugs on the magnitude or rate of phrenic nerve activity, tracheal pressure and gastric motility

None of the drugs had significant effects on the above variables. Data are illustrated only for single experiments with 8-OH-DPAT and DP-5-CT, (Figures 2 and 3) and the mean changes on gastric motility were $+16 \pm 6$ mm min^{-1} and $+2 \pm 4$ mm min^{-1}, respectively.

Discussion

IVth ventricular application of the tryptamine analogues DP-5-CT, 5-CT, indorenate and sumatriptan and the simplified

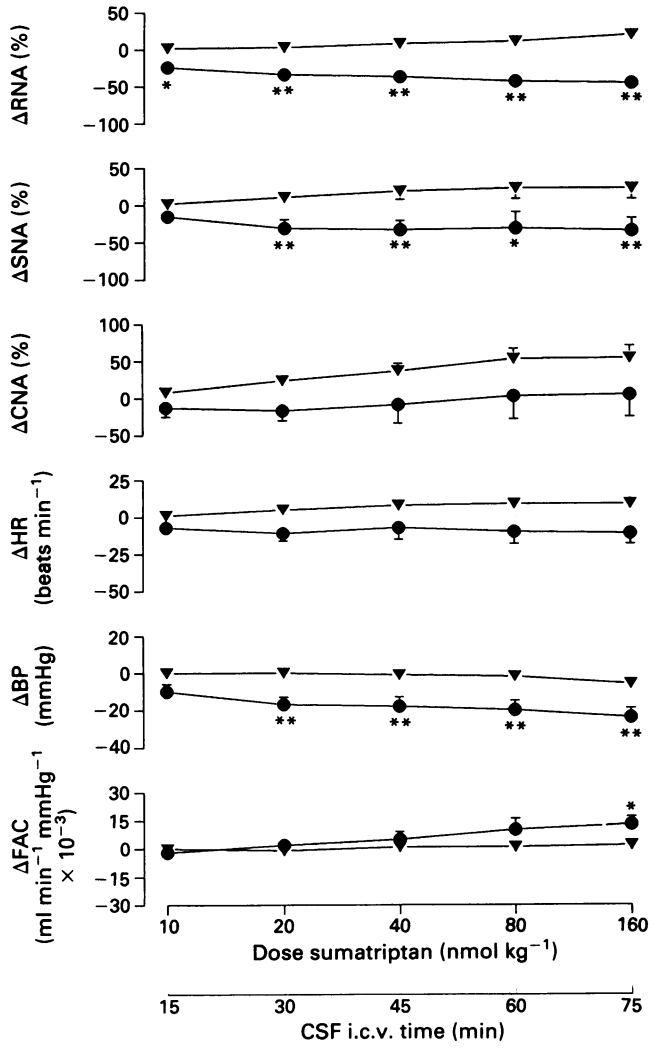

Figure 5 Anaesthetized cats: comparison of the effect of cumulative doses (10–160 nmol kg^{-1}) of sumatriptan (●), with time matched CSF control values (▼) administered into the IVth ventricle on changes (Δ) from baseline values in renal (RNA), splanchnic (SNA) and cardiac (CNA) nerve activities, heart rate (HR), mean arterial blood pressure (BP) and femoral arterial conductance (FAC). Each point represents the mean value ($n = 5$) with s.e.mean. Comparison of the changes evoked by sumatriptan with those produced by CSF were made by two way analysis of variance and the least significant difference test to compare the means; $*P<0.05$; $**P<0.01$.

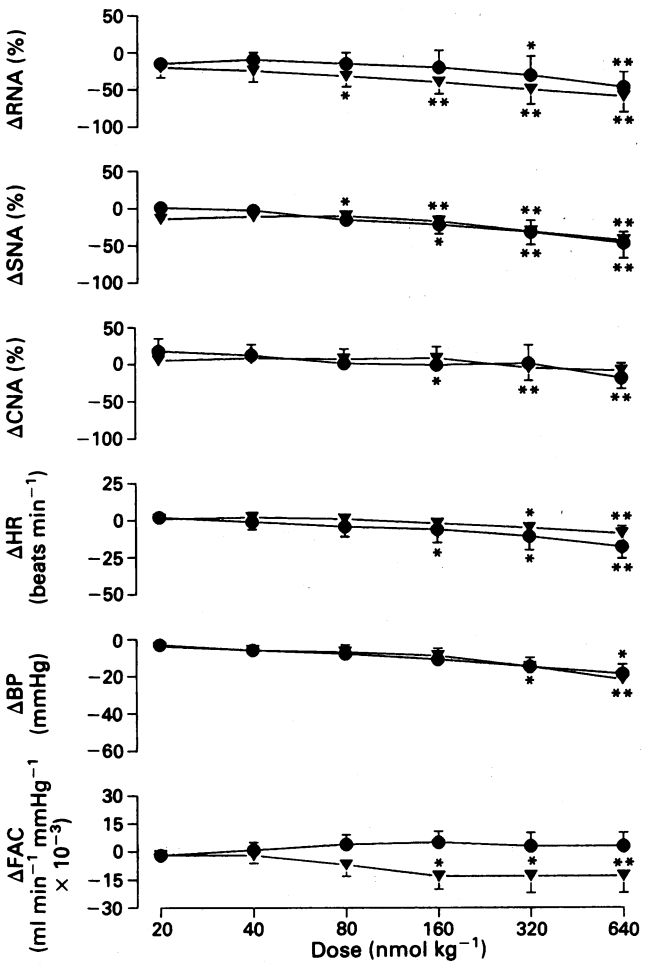

Figure 6 Anaesthetized cats: the effect of cumulative doses (20–640 nmol kg^{-1}) of 5-hydroxytryptamine alone (●), and in the presence of 0.1 mg kg^{-1} cinanserin (▼) administered into the IVth ventricle on changes (Δ) from baseline values in renal (RNA), splanchnic (SNA) and cardiac (CNA) nerve activities, heart rate (HR), mean arterial blood pressure (BP) and femoral arterial conductance (FAC). Each point represents the mean value ($n = 5$) with s.e.mean. The above changes were compared with changes caused by the CSF vehicle alone by two way analysis of variance and the least significant difference test to compare the means; $*P<0.05$; $**P<0.01$. The data for the CSF vehicle control has been omitted for the sake of clarity.

ergot congener, 8-OH-DPAT, all caused significant falls in sympathetic nerve activity and blood pressure. These falls were associated with little change in femoral arterial conductance. The sympathoinhibition was not uniform in the three different sympathetic outflows that were monitored, renal nerve activity was much more sensitive to the sympathoinhibitory actions of these compounds than cardiac nerve activity. Such a profile of action has been previously observed in anaesthetized cats with i.v. administration of 8-OH-DPAT, ipsapirone and flesinoxan (Ramage & Fozard, 1987; Ramage *et al.*, 1988; Ramage & Wilkinson, 1989). It has also been demonstrated that the sympathoinhibitory action of i.v. 8-OH-DPAT and the hypotensive action of DP-5-CT, administered via the vertebral artery of anaesthetized cats, can be reversed by spiperone (McCall *et al.*, 1987) or is blocked by pretreatment with (−)-pindolol (Doods *et al.*, 1988), respectively. As both drugs act as antagonists at 5-HT$_{1A}$ receptors, and since all the above compounds bind to 5-HT$_{1A}$ receptors (see Hoyer & Fozard, 1991) it can be concluded that the central hypotensive action of all the above compounds can be explained, at least in part, by activation of 5-HT$_{1A}$ receptors at the level of the brainstem.

Both DP-5-CT and 5-CT showed a similar potency in their sympathoinhibitory actions when compared to the potency of 8-OH-DPAT. The potency of these compounds in causing sympathoinhibition is in line with their comparative affinities for 5-HT$_{1A}$ receptors (DP-5-CT and 5-CT pK_D 9.5 c.f. 8-OH-DPAT pK_D 8.7, see Hoyer & Fozard, 1991). Further, as all agonists tested caused a decrease in renal nerve activity it may be suggested that reduction in this variable is related to the affinity of these compounds for 5-HT$_{1A}$ receptors. Sumatriptan, which, depending on the species, is also considered to be an agonist at 5-HT$_{1D}$ or 5-HT$_{1B}$ receptors (Peroutka & McCarthy, 1989) was found to cause a decrease in renal nerve activity. However the selectivity of sumatriptan for 5-HT$_{1D}$ compared to 5-HT$_{1A}$ receptors is not particularly large since it has about a 30 times higher affinity for the former compared with the latter (see Hoyer & Fozard, 1991). Thus, an agonist action at 5-HT$_{1A}$ receptor could explain the

ability of sumatriptan to cause renal sympathoinhibition. As the sumatriptan dose-response curve for renal sympathoinhibition is very shallow it may be that there is an interaction between 5-HT$_{1A}$ and 5-HT$_{1D}$ receptors at this level. In this respect, addition of 8-OH-DPAT after sumatriptan failed to have any further sympathoinhibitory action (unpublished observation). 5-CT however, has no greater selectivity between 5-HT$_{1A}$ and 5-HT$_{1D}$ receptors than sumatriptan but has a much higher affinity for both subtypes (see Hoyer & Fozard, 1991) but causes a fairly steep dose-related reduction in renal nerve activity. Therefore attributing any effects observed in the present study to activation of 5-HT$_{1D}$ is impossible due to the lack of a selective agonist for this receptor type. The failure of indorenate to cause an overt differential sympathoinhibition may be related to the large dose chosen as at high doses of all 5-HT$_{1A}$ agonists there is a large reduction in cardiac as well as renal nerve activity. Interestingly enough, even at the dose chosen, there was no increase in femoral arterial conductance. However little is known of the binding profile of indorenate to 5-HT receptor subtypes and the failure to cause differential sympathoinhibition may be related to indorenate interacting with other 5-HT receptors. In this respect indorenate, when given i.v. to anaesthetized cats, can cause an increase in tracheal pressure which is indicative of an agonist at 5-HT$_2$ receptors (see Ramage, 1990).

The finding that 8-OH-DPAT applied to the IVth ventricle caused an increase in cardiac vagal drive in the present study confirms previous observations with i.v. administration of 8-OH-DPAT, flesinoxan and ipsapirone (Ramage & Fozard, 1987; Ramage *et al.*, 1988) in anaesthetized cats and is consistent with the large amount of evidence for a role of 5-HT$_{1A}$ receptors in the control of cardiac vagal motoneurone excitability (Bogle *et al.*, 1990; Sporton *et al.*, 1991; Chitravanshi & Calaresu, 1992). However, the tryptamine analogues, except indorenate which caused only a small increase in cardiac vagal tone, failed to increase cardiac vagal tone in the present study. Even a very high dose of DP-5-CT (80 nmol kg^{-1}, see Figure 3) failed to cause an increase in vagal tone to the heart. This is somewhat surprising since the tryptamine analogues DP-5-CT and 5-CT have comparable effects to 8-OH-DPAT on central sympathetic drive, especially renal nerve activity, which it is possible (see above) to attribute to activation of 5-HT$_{1A}$ receptors. Further it is interesting that none of the agonists used in the present study, even 8-OH-DPAT, increased the excitability of other central parasympathetic motoneurones, such as those that control the airways and gastric motility, although central 5-HT pathways have been implicated in the control of gastric motility (Hornby *et al.*, 1990). This suggests that the properties of cardiac vagal motoneurones may differ from those of other vagal motoneurones.

The effects of IVth ventricular administration of 5-HT in the present study confirm those of Coote *et al.* (1987), in that administration of 5-HT caused a decrease in renal nerve activity. However, in the present experiments, administration of cinanserin into the IVth ventricle, to block 5-HT$_2$ receptors, which have been demonstrated to have a sympathoexcitatory action (Gillis *et al.*, 1989; Shepheard *et al.*, 1991b), did not unmask a greater sympathoinhibitory action and hypotensive effect of 5-HT as might be expected from the suggested opposing action of 5-HT$_{1A}$ and 5-HT$_2$ receptors on sympathetic tone (Gillis *et al.*, 1989). The present data only demonstrated that the fall in blood pressure was of a similar magnitude but the changes in the various variables which were causing the fall in blood pressure differed, suggesting that the relationship between 5-HT$_{1A}$ and 5-HT$_2$ receptors in control of sympathetic outflow is not simply opposing at the level of the brainstem.

The fact that IVth ventricular application of cinanserin caused femoral arterial vasodilatation with little effect on blood pressure and central sympathetic outflow supports previous reports that this is a characteristic effect of 5-HT$_2$ antagonists in anaesthetized cats (Ramage, 1988). Furthermore, activation of 5-HT$_2$ receptors at the level of the brainstem also causes femoral arterial vasoconstriction (Shepheard *et al.*, 1991b). It is therefore surprising that 5-HT in the presence of cinanserin also causes femoral arterial vasoconstriction, since this is not a characteristic effect of activation of 5-HT$_{1A}$ receptors and suggests that another type of 5-HT receptor is involved in the control of the femoral bed as well as the 5-HT$_2$ receptor. This could be a 5-HT$_3$ receptor, as the 5-HT$_3$ receptor agonist, phenylbiguanide, given i.c.v., causes a decrease, while the 5-HT$_3$ receptor antagonist, granisetron causes an increase in femoral arterial conductance (Shepheard *et al.*, 1991a).

The present results also confirm that the braimstem is the major site of action for the sympathoinhibitory effect of 5-HT$_{1A}$ agonists administered i.v. The rostral ventrolateral medulla (RVLM) has been suggested as the main site within the brainstem at which 5-HT$_{1A}$ agonists act to cause sympathoinhibition (Gillis *et al.*, 1989; King & Holtman, 1990; Laubie *et al.*, 1990). Neurones in this area are known to project to preganglionic sympathetic neurones in the intermediolateral cell column and many 5-HT-containing neurones are also found in this area (see Ciriello *et al.*, 1986). In addition, stimualtion of neurones in the RVLM is known to cause differential effects on symapthetic nerve outflow to the kidney compared with outflow to skeletal muscle (McAllen & Dampney, 1992). Whether the differential effects on sympathetic outflow seen in the present study by administering 5-HT$_{1A}$ agonists into the IVth ventricle can be explained by an action at the RVLM alone or by an interaction of the RVLM with other brain areas remains to be determined.

It is concluded that at present, tryptamine analogues do not confer any advantages over non-tryptamine analogues in investigating the function of brainstem 5-HT$_{1A}$ receptors in the control of central autonomic function. However, the present data support the view that 5-HT$_{1A}$ receptors do play an important role in brainstem control of renal and splanchnic sympathetic outflow while 5-HT$_2$ receptors play a role in the control of skeletal muscle and/or skin blood flow. Further, selective tryptamine agonists for 5-HT$_{1A}$ receptors differ from non-tryptamine agonists in that they do not cause an increase in central cardiac vagal tones.

We would like to thank Mr S. Wilkinson for technical assistance. This work is supported by the Wellcome Trust. We wish to thank Drs P.L.R. Andrews and T. Cowen for help with analysis of gut motility.

References

BOGLE, R.G., PIRES, J.G.P. & RAMAGE, A.G. (1990). Evidence that central 5-HT$_{1A}$-receptors play a role in the von Bezold-Jarisch reflex in the rat. *Br. J. Pharmacol.*, **100**, 757–760.

CHITRAVANSHI, V.C. & CALARESU, F.R. (1992). Additive effects of dopamine and 8-OH-DPAT microinjected into the nucleus ambiguus in eliciting vagal bradycardia in rats. *J. Auton. Nerv. Syst.*, **41**, 121–128.

CIRIELLO, J., CAVERSON, M.M. & POLOSA, C. (1986). Function of the ventrolateral medulla in the control of the circulation. *Brain Res. Rev.*, **11**, 359–391.

COOTE, J.H., DALTON, D.W., FENIUK, W. & HUMPHREY, P.P.A. (1987). The central site of the sympatho-inhibitory action of 5-hydroxytryptamine in the cat. *Neuropharmacol.*, **26**, 147–154.

DOODS, H.N., BODDEKE, H.W.G.M., KALKMAN, H.O., HOYER, D., MATHY, M.J. & ZWIETEN, P.A. (1988). Central 5-HT_{1A} receptors and the mechanism of the central hypotensive effect of (+)8-OH-DPAT, DP-5-CT, R28935, and urapidil. *J. Cardiovasc. Pharmacol.*, **11**, 432–437.

GILLIS, R.A., HILL, K., KIRBY, J.S., QUEST, J.A., HAMOSH, P., NORMAN, W.P. & KELLAR, K.J. (1989). Effect of activation of central nervous system serotonin 1A receptors on cardiorespiratory function. *J. Pharmacol Exp. Ther.*, **248**, 851–857.

HAMON, M., GOZLAN, H., EL MESTIKAWAY, S., EMERIT, M.B., BALANOS, F. & SCHECHTER, L. (1990). The central 5-HT_{1A} receptors: pharmacology, biochemistry, functional and regulatory properties. In *The Neuropharmacology of Serotonin*. ed. Whitaker-Azimitia, P.M. & Peroutka, S.J. *Ann. N.Y. Acad.*, Vol 600, pp. 114–131.

HJORTH, S., CARLSSON, A., LINDBERG, P., SANCHEZ, D., WIKSTROM, H., ARVIDSSON, L.E., HACKSELL, U. & NILSSON, J.L.G. (1982). 8-Hydroxy-2-(Di-n-Propylamino)Tetralin, 8-OH-DPAT, a potent and selective amplified ergot congener with central 5-HT-receptor stimulating activity. *J. Neural. Transm.*, **55**, 169–188.

HORNBY, P.J., ROSSITER, C.D., WHITE, R.L., NORMAN, W.P., KUHN, D.H. & GILLIS, R.A. (1990). Medullary raphe: a new site for vagally mediated stimulation of gastric motility in cats. *Am. J. Physiol.*, **258**, G637–G647.

HOYER, D. & FOZARD, J.R. (1991). 5-Hydroxytryptamine receptors. In *Receptor Data for Biological Experiments: A Guide to Drug Selectivity*, ed. Doods, H.N. & Van Meel, J.C.A. pp. 35–41. New York: Ellis Horwood.

HUMPHREY, P.P.A., FENIUK, W., PERREN, M.J., BERESFORD, I.J.M. SKINGLE, M. & WHALLEY, E.T. (1990). Serotonin and migraine. In *The Neuropharmacology of Serotonin*, ed. Whitaker-Azimitia, P.M. & Peroutka, S.J. *Ann. N.Y. Acad.*, Vol 600, pp. 587–600.

KING, K.A. & HOLTMAN, J.R. (1990). Characterization of the effects of activation of ventral medullary serotonin receptor subtypes on cardiovascular activity and respiratory motor outflow to the diaphragm and larnyx. *J. Pharmacol. Exp. Ther.*, **252**, 665–674.

LAUBIE, M., DROUILLAT, M., DABIRE, H., CHERQUI, C. & SCHMITT, H. (1989). Ventrolateral medullary pressor area: site of hypotensive and sympatho-inhibitory effects of (+)(−)8-OH-DPAT in anaesthetised dogs. *Eur. J. Pharmacol.*, **160**, 385–394.

LEFF, P. & MARTIN, G.R. (1988). The classification of 5-hydroxytryptamine receptors. *Med. Res. Rev.*, **8**, 187–202.

MCALLEN, R.M. & DAMPNEY, R.A.L. (1992). Vasomotor neurons in the rostral ventral lateral medulla are organized topographically with respect to type of vascular bed but not body region. *Neurosci. Lett.*, **110**, 91–96.

MCCALL, R.B., PATEL, B.N. & HARRIS, L.T. (1987). Effects of $serotonin_1$ and $serotonin_2$ receptor agonists and antagonists on blood pressure, heart rate and sympathetic nerve activity. *J. Pharmacol. Exp. Ther.*, **242**, 1152–1158.

MIR, A.K., HIBERT, M. & FOZARD, J.R. (1987). Cardiovascular effects of N,N-dipropyl-5-carboxamidotryptamine, a potent and selective 5-HT_{1A} receptor ligand. In *Neuronal Messengers in Vascular Function*, ed. Nobin, A., Owman, C. & Arneklo-Noblin, B. pp. 21–29. Netherlands: Elsevier Science Publishers (Biomedical Division).

PAZOS, A. & PALACIOS, J.M. (1985). Quantitative autoradiographic mapping of serotonin receptors in the rat brain. I. Serotonin-1 receptors. *Brain Res.*, **346**, 205–230.

PEROUTKA, S.J. & MCCARTHY, B.G. (1989). Sumatriptan (GR43175) interacts selectively with 5-HT_{1B} and 5-HT_{1D} binding sites. *Eur. J. Pharmacol.*, **163**, 133–136.

RAMAGE, A.G. (1988). Examination of the effects of some 5-HT_2 receptor antagonists on central sympathetic outflow and blood pressure in anaesthetised cats. *Naunyn-Schmied. Arch. Pharmacol.*, **338**, 601–607.

RAMAGE, A.G. (1990). Influence of 5-HT_{1A} receptor agonists on sympathetic and parasympathetic nerve activity. *J. Cardiovasc. Pharmacol.*, **15** (Suppl 7), S75–S85.

RAMAGE, A.G. & FOZARD, J.R. (1987). Evidence that the putative 5-HT_{1A} receptor agonists, 8-OH-DPAT and ipsapirone, have a central hypotensive action that differs from that of clonidine in anaesthetised cats. *Eur. J. Pharmacol.*, **138**, 179–191.

RAMAGE, A.G. & WILKINSON, S.J. (1989). Evidence that different regional sympathetic outflows vary in their sensitivity to the sympathoinhibitory actions of putative 5-HT_{1A} and α_2-adrenoceptor agonists in anaesthetised cats. *Br. J. Pharmacol.*, **98**, 1157–1164.

RAMAGE, A.G., WOUTERS, W. & BEVAN, P. (1988). Evidence that the novel antihypertensive agent, flesinoxan, causes differential sympathoinhibition and also increases vagal tone by a central action. *Eur. J. Pharmacol.*, **151**, 373–379.

SAFDY, M.E., KURCHACOVA, E., SCHUT, R.N., VIDRIO, H. & HONG, E. (1982). Tryptophan analogues. 1. synthesis and antihypertensive activity of positional isomers. *J. Med. Chem.*, **25**, 723–730.

SHEPHEARD, S.L., JORDAN, D. & RAMAGE, A.G. (1989). The effects of central administration of 8-OH-DPAT and GR43175 on autonomic outflow in the anaesthetised cat. *Br. J. Pharmacol.*, **98**, 641P.

SHEPHEARD, S.L., JORDAN, D. & RAMAGE, A.G. (1990). Action of some tryptamine analogues that are agonists at 5-HT_1 receptors on central autonomic outflow in anaesthetized cats. *Br. J. Pharmacol.*, **101**, 520P.

SHEPHEARD, S.L., JORDAN, D. & RAMAGE, A.G. (1991a). The role of brainstem 5-HT_3 and putative 5-HT_4 receptors on sympathetic outflow in anaesthetized cats. *Fund. Clin. Pharmacol.*, **5**, 418.

SHEPHEARD, S.L., JORDAN, D. & RAMAGE, A.G. (1991b). Investigation of the effects of IVth ventricular administration of the 5-HT_2 agonist, 1-(2,5-dimethoxy-4-iodophenyl)-2-aminopropane (DOI), on autonomic outflow in the anaesthetized cat. *Br. J. Pharmacol.*, **104**, 367–372.

SOKAL, R.R. & ROHLF, F.J. (1969). *Biometry: The Principles and Practice of Statistics in Biological Research.*, New York: Freeman, W.H. & Company.

SPORTON, S.C.E., SHEPHEARD, S.L., JORDAN, D. & RAMAGE, A.G. (1991). Microinjections of 5-HT_{1A} agonists into the dosal motor vagal nucleus produce a bradycardia in the atenolol-pretreated anaesthetized rat. *Br. J. Pharmacol.*, **104**, 466–470.

WOUTERS, W., HARTOG, J. & BEVAN, P. (1988). Flesinoxan. *Cardiovas. Drug Rev.*, **6**, 71–83.

(Received September 10, 1993
Revised October 18, 1993
Accepted October 21, 1993)

Br. J. Pharmacol. (1994), **111**, 625–631

Effects of cyclic AMP and analogues on neurogenic transmission in the rat tail artery

Sylvin Ouedraogo, Jean-Claude Stoclet & [1]Bernard Bucher

Laboratoire de Pharmacologie Cellulaire et Moléculaire, C.N.R.S. URA 600, Université Louis Pasteur Strasbourg, B.P. 24, 67401 Illkirch, France

1 The effects of two 8-substituted analogues of adenosine 3':5'-cyclic monophosphate (cyclic AMP) were compared with those of forskolin and isoprenaline on [^{3}H]-noradrenaline release and vasoconstriction induced by electrical field stimulation (24 pulses at 0.4 Hz, 200 mA, 0.3 ms duration) in the rat tail artery, in the absence and in the presence of protein kinase inhibitors.

2 8-Bromo-adenosine 3':5'-cyclic monophosphate (8-bromo-cyclic AMP, 10–300 μM), 8-(4-chlorophenylthio)-adenosine 3':5' cyclic monophosphate (8-pCPT-cyclic AMP, 3–300 μM), forskolin (0.3–10 μM) and isoprenaline (1 nM–1 μM) all concentration-dependently enhanced stimulation-induced [^{3}H]-noradrenaline release. The effect of cyclic AMP analogues was larger (2.5 fold at 300 μM) than those of cyclic AMP elevating drugs (1.6 fold at 10 μM for forskolin and 1.5 fold at 30 nM for isoprenaline).

3 At concentrations active at the prejunctional level, the four drugs had differential effects on stimulation-induced vasoconstriction, which was enhanced by the two cyclic AMP analogues, decreased by forskolin and not significantly altered by isoprenaline.

4 The [^{3}H]-noradrenaline release-enhancing effects of 8-bromo-cyclic AMP, forskolin and isoprenaline were significantly decreased by the cyclic AMP-dependent protein kinase (PKA) inhibitor {N-[2-((3-(4-bromophenyl)-2-propenyl)-amino)-ethyl]-5-isoquinolinesulphonamide, di-hydrochloride} (H-89; 100 nM). By contrast they were unaffected by the cyclic GMP-dependent protein kinase (PKG) inhibitor, 8-bromo-guanosine 3':5'-cyclic monophosphorothioate, Rp-isomer (Rp-8-bromo-cyclic GMPS; 10 μM). At the same concentrations the PKA inhibitor attenuated only the nerve-induced vasoconstrictor responses obtained in the presence of 8-bromo-cyclic AMP, whereas the PKG inhibitor did not modify that obtained in the presence of 8-bromo-cyclic AMP or forskolin.

5 Exposure to the protein kinase C (PKC) activator, phorbol 12-myristate 13-acetate (1 μM) enhanced nerve-evoked [^{3}H]-noradrenaline release, and this effect was decreased by the PKC inhibitor, 2-[1-(3-dimethylaminopropyl)-indol-3-yl]-3-(-indol-3-yl)-maleimide (GF 109203X; 100 nM). However, the latter drug did not modify the enhancing effect of 8-bromo-cyclic AMP on [^{3}H]-noradrenaline release.

6 It is concluded that activation of cyclic AMP-dependent protein kinase is involved in the enhancing effect of cyclic AMP-elevating compounds on prejunctional release of noradrenaline. In addition the results provide no clear-cut evidence for a vasodilator role of PKA.

Keywords: Neurogenic vasoconstriction; noradrenaline release; cyclic AMP; forskolin; isoprenaline; cyclic AMP-dependent protein kinase; rat tail artery

Introduction

Adenosine 3':5'-cyclic monophosphate (cyclic AMP) is an ubiquitous second messenger which is involved in the mediation of functional responses to a variety of hormones and neurotransmitters (reviewed by Beebe & Corbin, 1986). In vascular smooth muscle cells, β-adrenoceptor stimulation or forskolin-induced activation by adenylyl cyclase are associated with an increase in the intracellular level of cyclic AMP (Kramer & Hardman, 1980) and with relaxation, but the precise mechanism by which the cyclic nucleotide causes relaxation is not clear. Cyclic AMP is also operative in perivascular sympathetic nerve endings where it modulates neurotransmitter release. In support of this, we and others have reported that drugs which increase intracellular level of cyclic AMP facilitate electrically-induced noradrenaline release (Göthert & Hentrich, 1984; Hentrich *et al.*, 1985; Johnston & Majewski, 1986; Costa & Majewski, 1988; Bucher *et al.*, 1990). However, although cyclic AMP is able to modulate noradrenaline release, it does not appear to play a role in the initiation of the release process itself (Bucher *et al.*, 1990).

Until recently, all known actions of cyclic AMP or its derivatives were assumed to operate via activation of cyclic AMP-dependent protein kinase (PKA) (reviewed by Beebe & Corbin, 1986). However, several recent studies addressed the question whether cyclic AMP activation of PKA is the sole mechanism of cyclic AMP-dependent relaxation in smooth muscle. It has been shown by use of dibutyryl cyclic AMP and 8-bromo-cyclic AMP that a dissociation is observed between PKA activation and inhibition of contractions of rat vas deferens, suggesting that PKA is not responsible for the relaxant effects of these cyclic nucleotide analogues in this tissue (Hei *et al.*, 1991). Other investigators reported that activation of the cyclic GMP-dependent protein kinase (PKG) rather than PKA was responsible for smooth muscle relaxation elicited by cyclic nucleotide analogues (Francis *et al.*, 1988). In addition, recent data support the view that activation of PKG by endogenously formed cyclic AMP may lead to a reduction of intracellular calcium and subsequent relaxation (Lincoln *et al.*, 1990; Lincoln & Cornwell, 1991). Interestingly, there is also evidence for the existence of other mechanisms involving a non-ATP-sensitive K^+ channel and possibly PKG in the mediation of smooth muscle relaxation elicited by cyclic AMP (Haynes *et al.*, 1992).

The possible role for activation of either cyclic AMP-dependent protein or cyclic GMP-dependent protein kinases in the regulation of both adrenergic neurotransmitter release and pressor responses has not been documented as yet in a vascular preparation. Therefore, the present study was designed to examine further the effects of cyclic AMP on vasoconstriction and noradrenaline release evoked by electrical field

[1] Author for correspondence.

stimulation of the rat tail artery. Specifically, we investigated the influence of selective cyclic AMP- and cyclic GMP-dependent protein kinase inhibitors on cyclic AMP-mediated effects.

Methods

Measurement of [^{3}H]-noradrenaline release and vasoconstriction

Male Wistar rats (12 weeks old) were killed by cervical dislocation and exsanguinated. A segment of about 2–2.5 cm of the proximal part of the ventral tail artery was dissected out as previously described (Illes *et al.*, 1987; Bucher *et al.*, 1992) and kept in oxygenated (95% O_2; 5% CO_2) physiological saline solution which contained (mM): NaCl 118, KCl 4.8, $CaCl_2$ 2.5, KH_2PO_4 0.9, $NaHCO_3$ 25, glucose 11, ascorbic acid 0.3 and disodium EDTA 0.03. The two latter compounds were added to prevent the spontaneous oxidation of catecholamines. The arteries were cannulated at one end and preincubated for 1 h at 37°C in 1.5 ml of medium of the same composition as above containing in addition 2.2 μM (−)-[^{3}H]-noradrenaline (specific activity 4.4 Ci mmol^{-1}). The vessels were then washed three times with 20 ml of [^{3}H]-noradrenaline-free medium, and suspended vertically, distal end uppermost, between two platinum wire electrodes. The gaps between the arteries and the electrodes were wide enough to allow undisturbed contraction or relaxation, yet sufficiently narrow to stimulate intramural nerve terminals effectively. The arteries were perfused via their proximal ends with medium by means of a roller pump with physiological saline solution containing 10 μM cocaine in order to block the re-uptake of released [^{3}H]-noradrenaline. The perfusion rate was gradually increased from 0 to 2.2 ml min^{-1} during the first 10 min after suspension of the arterial segment between the two electrodes, and kept constant thereafter. The intraluminal perfusion pressure was determined with a pressure transducer and recorded on a pen recorder. Changes in perfusion pressure reflected changes in the resistance to flow, i.e. the degree of vasoconstriction. After having passed through the lumen, the perfusate was allowed to superfuse the advential surface of the vessel.

Experiments were done with arteries with functional endothelium unless otherwise stated. We have previously shown that electrical field stimlation did not produce endothelial damage (Bucher *et al.*, 1992). In some arteries the endothelium was removed by passing a stream of 95% O_2:5% CO_2 through the lumen of the arterial segment at a pressure of 40–50 mmHg. The presence or absence of functional endothelium was verified by the presence or absence of relaxant responses to 10 μM acetylcholine in noradrenaline (1 μM) precontracted arteries (Bucher *et al.*, 1992).

Each artery was subjected to six stimulation periods (24 pulses at 0.4 Hz; 0.3 ms; 200 mA). The first stimulation period was applied after 96 min of perfusion and others followed at intervals of 16 min. Collection of the perfusate/superfusate started after 124 min of perfusion in 1, 2 or 6 min fractions. The stimulation period beginning at 128 min was termed S_1 and subsequent ones S_2–S_n. S_2 served as a control of stimulation-evoked tritium overflow (since the response was stable thereafter). The compounds were infused with a syringe pump into the perfusion stream at a rate of 17 μl min^{-1} for 8 min before either S_1 or S_3 and this was maintained until the end of the experiment when the arteries were solubilized in 1 ml Soluene 100 (Packard Instrument, Paris, France). Tritium in the superfusate samples and arteries was measured by liquid scintillation spectrometry.

Tritium overflow was calculated as a fraction of the amount of tritium present in the tissue at the start of the respective collection period (fractional rate of outflow). For evaluation of stimulation-evoked tritium overflow, the difference between the overall tritium outflow during stimulation plus the following 4 min and the estimated basal outflow was calculated. The latter was assumed to change linearly from the 1 min collection period before the beginning of stimulation to that 5 to 6 min after the start of stimulation. The evoked tritium overflow was calculated as a percentage of the amount of tissue tritium at the beginning of the respective stimulation period.

Data and statistical analysis

In order to quantify drug effects on the evoked overflow or vasoconstriction, the ratio of the overflow or vasoconstriction evoked by the stimulation period in the presence of the drug at the fourth stimulation period (S_4) over the last evoked overflow or vasoconstriction preceding application of the drug (S_2) was determined. S_4 was chosen because in preliminary experiments the maximal effect of each drug concentration was reached in these conditions. Drug effects on basal outflow were quantified in the following way: ratios of the fractional rate of outflow (b_n) in the fraction collected immediately before the onset of the stimulation periods in the presence of drugs (S_3–S_4) over the fractional rate of outflow in the fraction immediately before the onset of the last stimulation period preceding the application of any drug (S_2) were calculated (b_n/b_2).

Results are given as mean ± s.e.mean where n is the number of experiments. Comparisons were made by the Mann-Whitney test if the Kruskall-Wallis analysis indicated a significant difference between multiple groups. A probability level of 0.05 or less was considered significant. For multiple comparisons with the same control group, the limit of significance was divided by the number of comparisons according to Bonferroni (Wallenstein *et al.*, 1980).

Drugs

The following compounds were used: (−)-noradrenaline hydrochloride, 8-bromo-adenosine 3′:5′-cyclic monophosphate (sodium salt; 8-bromo-cyclic AMP), 8-(4-chlorophenylthio)-adenosine 3′:5′-cyclic monophosphate (sodium salt; 8-pCPT-cyclic AMP), (±) -isoprenaline hydrochloride, forskolin, phorbol 12-myristate 13-acetate (PMA) (Sigma, L'Isle d'Abeau Chesnes, France); 8-bromo-guanosine 3′:5′-cyclic monophosphorothioate, Rp-isomer (sodium salt; Rp-8-bromo-cyclic GMPS; Biolog, Bremen, Germany); {N-[2-((3-(4-bromophenyl) -2-propenyl)-amino)-ethyl] -5-isoquinolinesulphonamide, di-hydrochloride} (H-89), (Calbiochem, Meudon, France); 2-[1-(3-dimethylaminopropyl)-indol-3-yl]-3-(-indol-3-yl)maleimide (GF 109203X; kindly donated by Glaxo, France). Stock solutions of all other substances were prepared with Milli-Q water (Millipore) and diluted as required with the exception of forskolin which was dissolved in 5% ethanol and of PMA and GF109203X which were dissolved in 10% dimethylsulphoxide (DMSO). Preliminary experiments showed that at the concentration used, ethanol and DMSO did not alter basal or electrically-evoked overflow of tritium or vasosconstriction (see also control values in the figures and table). (−)-[Ring-2,5,6-^{3}H]-noradrenaline, specific activity 43.7–56.9 Ci mmol^{-1} (New England Nuclear, Dreieich, Germany) was diluted with unlabelled (−)-noradrenaline hydrochloride in order to obtain a specific activity of 4.4 Ci mmol^{-1}.

Results

Effects of 8-substituted analogues of cyclic AMP, forskolin and isoprenaline

In control as well as in treated arteries, tritium overflow and peak vasoconstriction evoked by the stimulation period S_2 amounted respectively to 0.191 ± 0.005% of tissue tritium and 100.7 ± 2.4 mmHg (n = 158; all appropriate experiments

pooled). Under control conditions, stimulation-evoked overflow of tritium and vasoconstriction did not change upon subsequent stimulations, resulting thus in S_n/S_2 ratio which were not different from the unity but the fractional rate of basal tritium outflow declined with time (not shown). 8-Bromo-cyclic AMP (300 μM), increased the basal rate of tritium outflow compared to control experiments (b_4/b_2: 1.07 ± 0.02; $n = 15$ and 0.98 ± 0.02; $n = 18$, respectively; $P <$ 0.01). Infusion of the solvent or of the drugs did not cause any change in basal perfusion pressure (not shown).

8-Bromo-cyclic AMP (10–300 μM), 8-pCTP-cyclic AMP (3–300 μM), isoprenaline (0.001–1 μM) and forskolin (0.3–10 μM) produced concentration-dependent increases in electrically-evoked tritium overflow (Figures 1 and 2). However, although forskolin and isoprenaline were more potent than the 8-substituted cyclic AMP analogues, the maximal effect obtained with either 10 μM forskolin (S_4/S_2: 1.62 ± 0.06; $n = 8$; $P < 0.01$ vs control) or isoprenaline (S_4/S_2: 1.54 ± 0.03; $n = 6$; $P < 0.05$ vs control) was significantly lower ($P < 0.01$) than the maximal effect obtained with either 300 μM 8-bromo-cyclic AMP (S_4/S_2: 2.31 ± 0.07; $n = 15$; $P < 0.01$ vs control) or 300 μM 8-pCPT-cyclic AMP (S_4/S_2: 2.38 ± 0.17; $n = 5$; $P < 0.05$ vs control). In addition, when isoprenaline (30 nM) was added in combination with propranolol (30 nM), the facilitatory effect of the β-adrenoceptor agonist on the electrically-evoked release of tritium was significantly reduced ($P < 0.01$), the respective S_4/S_2 ratios in the absence and presence of the β-antagonist being 1.54 ± 0.03; $n = 6$ and 1.17 ± 0.03; $n = 6$, respectively.

The stimulation-induced vasoconstriction was slightly increased by 8-bromo-cyclic AMP (Figure 1). However, the maximal effect of 8-bromo-cyclic AMP was less pronounced than that observed with 8-pCPT-cyclic AMP which reached its maximum at 30 μM (S_4/S_2: 1.66 ± 0.05; $n = 7$; $P < 0.05$ vs control) and decreased thereafter. In contrast, forskolin (3 μM) induced a significant decrease in the stimulation-induced vasoconstriction (Figure 4) whereas isoprenaline had no effect. The S_4/S_2 ratio for 30 nM isoprenaline was not significantly different from the corresponding control values (1.18 ± 0.07; $n = 6$ and 1.07 ± 0.05; $n = 6$; respectively; $P >$ 0.05).

In arteries without functional endothelium, forskolin (1 μM), produced the same relative enhancement of the tritium overflow (S_4/S_2: 1.20 ± 0.05; $n = 5$) as it did in the presence of functional endothelium (S_4/S_2: 1.25 ± 0.03; $n = 7$). The forskolin-mediated vasodilatation was slightly decreased in arteries without endothelium compared to the response observed in the presence of endothelium (S_4/S_2: 0.62 ± 0.08; $n = 5$ and 0.47 ± 0.05; $n = 7$; respectively; $P > 0.05$).

Influence of H-89

The enhancing effect of 8-bromo-cyclic AMP (100 μM) on both electrically-induced vasoconstriction and tritium overflow (S_4/S_2: 1.42 ± 0.07 and 1.63 ± 0.06; $n = 6$; respectively) was not significantly inhibited by H-89 10 nM (S_4/S_2: 1.39 ± 0.07 and 1.56 ± 0.03; $n = 6$; respectively) and 30 nM (S_4/S_2: 1.38 ± 0.12 and 1.50 ± 0.06; $n = 6$; respectively). However, a concentration of 100 nM of the protein kinase A inhibitor maximally inhibited the 8-bromo-cyclic AMP-mediated effects on both electrically-evoked noradrenaline overflow and vasoconstriction (Figure 3). A concentration of 300 nM of

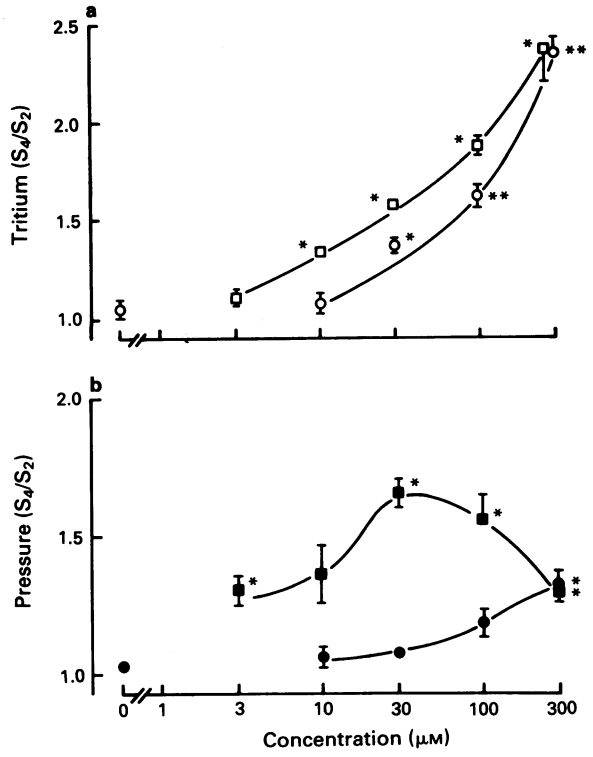

Figure 1 Effects of 8-bromo-cyclic AMP (○, ●) and of 8-pCPT-cyclic AMP (□, ■) on electrically-evoked overflow of tritium (open symbols; a) and change in perfusion pressure (solid symbols; b) in rat tail arteries with functional endothelium preincubated with [^{3}H]-noradrenaline. Four periods (S_1–S_4) of field stimulation were delivered at intervals of 16 min (24 pulses at 0.4 Hz, 200 mA, 0.3 ms duration). Each concentration of 8-bromo-cyclic AMP and of 8-pCPT-cyclic AMP or the solvent (control group) was added 8 min before S_3 and maintained in the medium for the duration of the experiment. The effect of the drug is presented as the ratio of tritium overflow or change in perfusion pressure evoked by S_4 over that evoked by S_2. Each point represents the means ± s.e.mean from 5–15 arteries. Significant difference from control: $*P < 0{,}05$, $**P < 0.01$.

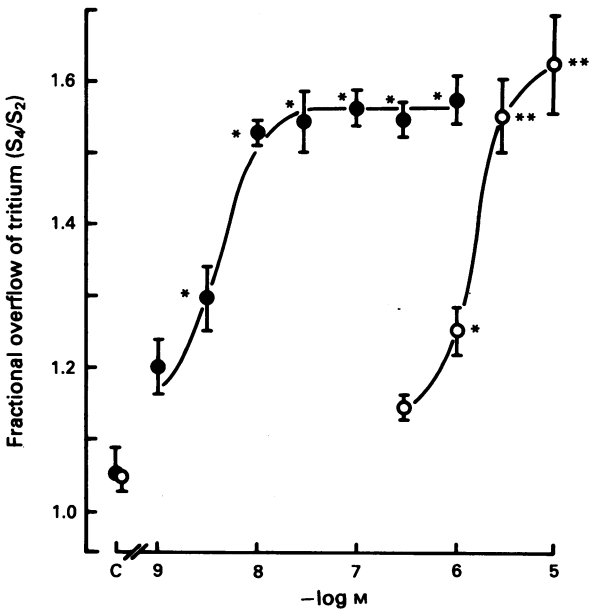

Figure 2 Concentration-dependent effects of isoprenaline (●) and forskolin (○) on electrically-evoked overflow of tritium in rat tail arteries preincubated with [^{3}H]-noradrenaline. Four periods (S_1–S_4) of field stimulation were delivered at intervals of 16 min (24 pulses at 0.4 Hz, 200 mA, 0.3 ms duration). Each concentration of isoprenaline or its solvent and forskolin or its solvent was added 8 min before S_3 and maintained in the medium for the duration of the experiment. The effects of the drugs are presented as the ratio of tritium overflow evoked by S_4 over that evoked by S_2. Each point represents the means ± s.e.mean from six arteries. Significant difference from control: $*P < 0.05$, $**P < 0.01$.

H-89 produced a non-specific increase of the basal outflow of tritiated noradrenaline and the stimulation-induced overflow could not be satisfactorily estimated.

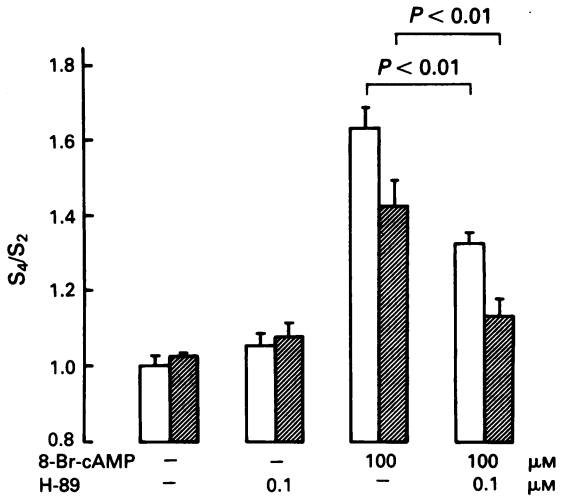

Figure 3 Effects of H-89 and 8-bromo-cyclic AMP alone or in combination on electrically-evoked tritium overflow (open columns) and change in perfusion pressure (hatched columns) in rat tail arteries preincubated with [^{3}H]-noradrenaline. Four periods (S_1–S_4) of field stimulation were delivered at intervals of 16 min (24 pulses at 0.4 Hz, 200 mA, 0.3 ms duration). H-89, 8-bromo-cyclic AMP or their solvents (control group) were added 8 min before S_3. All compounds were maintained in the medium for the duration of the experiment. The effect of the drugs are presented as the ratio of tritium overflow or change in perfusion pressure evoked by S_4 over that evoked by S_2. Each column represents the mean with s.e.mean from 6–7 arteries. The statistically significant differences between some values are indicated.

By itself, 100 nM of the cyclic AMP-dependent protein kinase inhibitor, H-89, added to the perfusion/superfusion medium before S_1 or S_3 did not induce any modification in tritium overflow and vasoconstrictor response to periarterial nerve stimulation (Figures 3, 4 and 5). As shown in Figure 4, the enhancing effect of 3 μM forskolin on electrical field-elicited tritium overflow was significantly decreased in the presence of 0.1 μM H-89 whereas stimulation-induced vasoconstriction was unchanged. Also, H-89 (100 nM) significantly attenuated the facilitatory effect of isoprenaline (30 nM) on tritium overflow without effecting the stimulation-induced vasoconstriction (Figure 5).

Influence of Rp-8-bromo-cyclic GMPS

A stable membrane permeant competitive inhibitor of cyclic GMP-dependent protein kinase, Rp-8-bromo-cyclic GMPS, was used in order to determine whether a PKG is involved in the effects of the cell permeant analogue 8-bromo-cyclic AMP or the adenylyl cyclase activator forskolin. Rp-8-bromo-cyclic GMPS (10 μM) added before S_1 or S_3 had no significant effect by itself or on the electrically-evoked tritium overflow and vasoconstriction (Figures 6 and 7). Furthermore, it did not modify the effects of 8-bromo-cyclic AMP (100 μM) (Figure 6) and forskolin (1 μM) (Figure 7) on the electrically-evoked tritium overflow and vasoconstriction.

Influence of protein kinase C activators and inhibitors

The addition of PMA (1 μM) before S_3 resulted in an increase in both the stimulation-induced overflow of tritium and resulting vasoconstriction (Table 1). A potent protein kinase C inhibitor, GF 109203X (100 nM), produced no significant effect by itself but it significantly attenuated the enhancing effects of PMA (1 μM) on the stimulation-evoked noradrenaline release (Table 1). By contrast, the solvent of both GF 109203X and PMA (10% DMSO) was without effect by

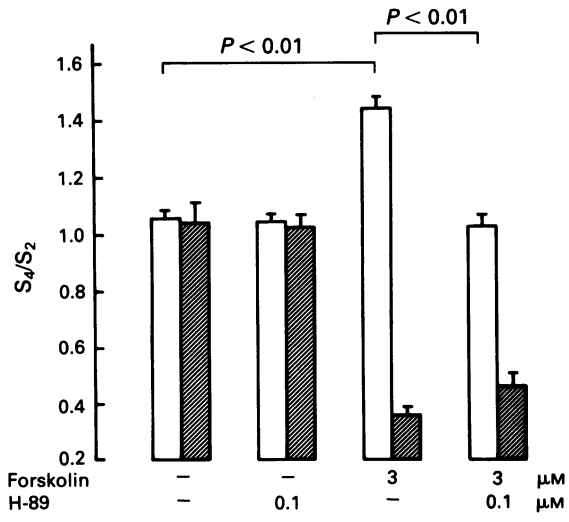

Figure 4 Effects of H-89 and forskolin alone or in combination on electrically-evoked tritium overflow (open columns) and change in perfusion pressure (hatched columns) in rat tail arteries preincubated with [^{3}H]-noradrenaline. Four periods (S_1–S_4) of field stimulation were delivered at intervals of 16 min (24 pulses at 0.4 Hz, 200 mA, 0.3 ms duration). H-89 or its solvent (control group) was added 8 min before S_1. Forskolin or its solvent was added 8 min before S_3. All compounds were maintained in the medium for the duration of the experiment. The effects of the drugs are presented as the ratio of tritium overflow or change in perfusion pressure evoked by S_4 over that evoked by S_2. Each column represents the mean with s.e.mean from 6–8 arteries. The statistically significant differences between some values are indicated.

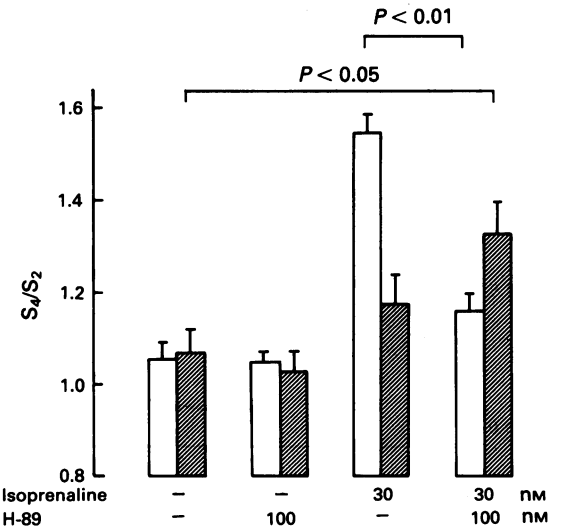

Figure 5 Effects of H-89 and isoprenaline alone or in combination on electrically-evoked tritium overflow (open columns) and change in perfusion pressure (hatched columns) in rat tail arteries preincubated with [^{3}H]-noradrenaline. Four periods (S_1–S_4) of field stimulation were delivered at intervals of 16 min (24 pulses at 0.4 Hz, 200 mA, 0.3 ms duration). H-89 or its solvent (control group) was added 8 min before S_1. Isoprenaline or its solvent was added 8 min before S_3. All compounds were maintained in the medium for the duration of the experiment. The effects of the drugs are presented as the ratio of tritium overflow or change in perfusion pressure evoked by S_4 over that evoked by S_2. Each column represents the mean with s.e.mean from 6 arteries. The statistically significant differences between some values are indicated.

itself. GF 109203X (100 nM) had no effect on the facilitatory effect of 8-bromo-cyclic AMP (100 μM) on electrical field-evoked tritium overflow and vasoconstriction (Table 1), showing no evidence for the involvement of PKC in the effects of cyclic AMP.

Discussion

The results of the present investigation provide additional evidence supporting the view that cyclic AMP increases the electrically-evoked overflow of [^{3}H]-noradrenaline from the rat tail artery. In addition, they clearly show that the prejunctional enhancing effects of cyclic AMP-elevating drugs and cyclic AMP analogue on electrical-field induced [^{3}H]-noradrenaline release were reduced by a PKA inhibitor, but were unaffected by either a PKG or a PKC inhibitor.

The cyclic AMP-mediated enhancement of electrically-stimulated neurotransmitter release observed here is in good agreement with previous results obtained in the same vessel (Bucher *et al.*, 1990) and in other vascular preparations (Göthert & Hentrich, 1984; Hentrich *et al.*, 1985; Johnston & Majewski, 1986; Costa & Majewski, 1988). The two adenylyl cyclase stimulating drugs, isoprenaline and forskolin, acted with the potency that could be expected from their effects on cyclic AMP production (Seamon & Daly, 1986). Their maximal effects (1.6 fold stimulation) were not different from each other, but were lower than the effects of high concentra-

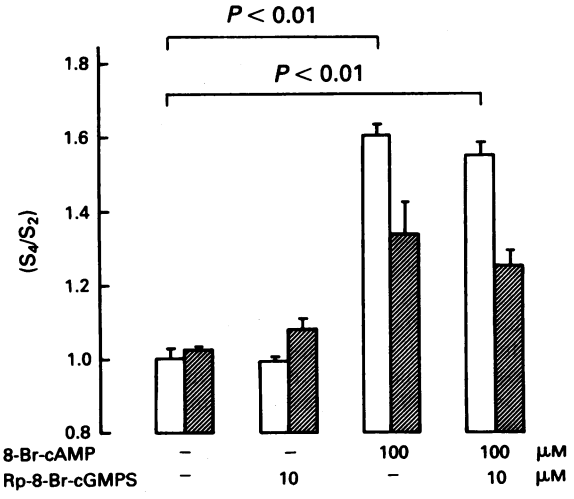

Figure 6 Effects of Rp-8-bromo-cyclic GMPS and 8-bromo-cyclic AMP alone or in combination on electrically-evoked tritium overflow (open columns) and change in perfusion pressure (hatched columns) in rat tail arteries preincubated with [^{3}H]-noradrenaline. Four periods (S_1-S_4) of field stimulation were delivered at intervals of 16 min (24 pulses at 0.4 Hz, 200 mA, 0.3 ms duration). Rp-8-bromo-cyclic GMPS, 8-bromo-cyclic AMP or their solvents (control group) were added 8 min before S_3. All compounds were maintained in the medium for the duration of the experiment. The effect of the drugs are presented as the ratio of tritium overflow or change in perfusion pressure evoked by S_4 over that evoked by S_2. Each column represents the mean with s.e.mean from 4–7 arteries. The statistically significant differences between some values are indicated.

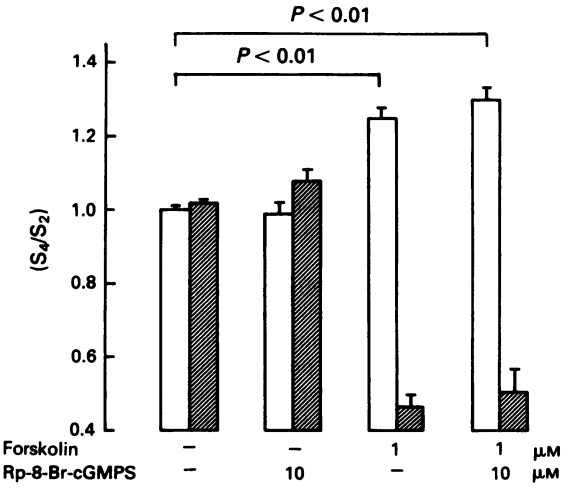

Figure 7 Effects of Rp-8-bromo-cyclic GMPS and forskolin alone or in combination on electrically-evoked tritium overflow (open columns) and change in perfusion pressure (hatched columns) in rat tail arteries preincubated with [^{3}H]-noradrenaline. Four periods (S_1-S_4) of field stimulation were delivered at intervals of 16 min (24 pulses at 0.4 Hz, 200 mA, 0.3 ms duration). Rp-8-bromo-cyclic GMPS, or its solvent (control group) was added 8 min before S_1. Forskolin or its solvent was added 8 min before S_3. All compounds were maintained in the medium for the duration of the experiment. The effects of the drugs are presented as the ratio of tritium overflow or change in perfusion pressure evoked by S_4 over that evoked by S_2. Each column represents the mean with s.e.mean from 4–7 arteries. The statistically significant differences between some values are indicated.

Table 1 Effects of phorbol 12-myristate 13-acetate (PMA) and 8-bromo-cyclic AMP alone or in combination with GF 109203X on electrically-evoked tritium overflow and change in perfusion pressure in rat tail arteries

		S_4/S_2 ratio	
Treatment	n	*Tritium overflow*	*Vasoconstriction*
H_2O	6	1.01 ± 0.03	1.03 ± 0.01
DMSO 10%	9	1.02 ± 0.02	1.06 ± 0.02
GF 109203X 100 nM	6	1.06 ± 0.04	1.05 ± 0.04
PMA 1 μM	7	1.67 ± 0.09[b]	1.23 ± 0.08[a]
PMA 1 μM + GF 109203X 100 nM	6	1.28 ± 0.02[b,c]	1.17 ± 0.07[a]
8-bromo-cyclic AMP 100 μM	4	1.57 ± 0.04[b]	1.31 ± 0.05[b]
8-bromo-cyclic AMP 100 μM + GF 109203X 100 nM	4	1.44 ± 0.09[b]	1.15 ± 0.02[a]

Rat tail arteries were preincubated with [^{3}H]-noradrenaline. Four periods (S_1-S_4) of field stimulation were delivered at intervals of 16 min (24 pulses at 0.4 Hz, 200 mA, 0.3 ms duration). PMA, 8-bromo-cyclic AMP and GF 109203X or their solvents (control group) were added 8 min before S_3. All compounds were maintained in the medium for the duration of the experiment. The effects of the drugs are presented as the ratio of tritium overflow or change in perfusion pressure evoked by S_4 over that evoked by S_2. Mean ± s.e.mean from *n* arteries.

[a] $P<0.05$; significant differences from drug-free control experiments.

[b] $P<0.01$; significant differences from drug-free control experiments.

[c] $P<0.01$; significant differences from experiments in the absence of GF 109203X.

tions (300 μM) of the two cyclic AMP analogues (2.5 fold stimulation), suggesting that maximal stimulation of adenylyl cyclase by either isoprenaline or forskolin could not produce maximal enhancement of noradrenaline release. As expected from its higher lipophilicity resulting in good membrane permeability (Sandberg *et al.*, 1991), 8-pCPT-cyclic AMP acted at lower concentrations than 8-bromo-cyclic AMP.

In the current study, H-89, a selective PKA inhibitor (Chijiwa *et al.*, 1990) by itself did not alter spontaneous and electrical stimulation-induced release of neurotransmitter. However, it reduced the enhancement of [^{3}H]-noradrenaline release by forskolin, isoprenaline and 8-bromo-cyclic AMP. Taken together these results indicate that following stimulation by exogenous agents, PKA enhances noradrenaline release, but this pathway appears not to be endogenously active in the absence of such agents. Furthermore, neither Rp-8-bromo-cyclic GMPS, an 8-bromo derivative of Rp-cyclic GMPS, which is a membrane permeant and metabolically stable selective inhibitor of PKG (Butt *et al.*, 1990), nor GF 109203X, a potent and selective inhibitor of PKC (Toullec *et al.*, 1991), had any effect on stimulation-induced noradrenaline release or vasoconstriction. Neither poor membrane permeability nor the use of inadequate concentrations of these drugs could explain their lack of effects: in the same experimental conditions GF 109203X was able to antagonize PMA (this study) and Rp-8-bromo-cyclic GMPS was able to attenuate significantly the 8-bromo-cyclic GMP-induced relaxation (data not shown).

As previously discussed (Bucher *et al.*, 1990), the effects of drugs on vasoconstriction elicited by periarterial nerve stimulation are more difficult to interpret, since they may represent the net result of pre- and post-junctional actions. Although the rat tail artery is endowed with postjunctional β-adrenoceptors (Bao *et al.*, 1990; Rajanayagam *et al.*, 1990), isoprenaline had no significant effect on neurogenic vasoconstriction. Although there was a prejunctional β-adrenoceptor-mediated increase in noradrenaline release from nerve terminals, any postjunctional α-adrenoceptor-mediated response was probably inhibited via the postjunctional β-adrenoceptor-mediated relaxant effect of isoprenaline. In spite of increasing neurotransmitter release, forskolin produced a concentration-dependent vasodilatation, whereas both of the cyclic AMP analogues potentiated nerve-induced vasoconstriction. These differences may reflect differences in the sensitivity of the pre- and postjunctional target systems and/or differences in the ability of the drugs to diffuse into the respective cellular compartments. Additionally, 8-pCPT-cyclic AMP, although increasing stimulation-induced vasoconstriction at concentrations up to 30 μM, decreased it at higher concentrations. It has been shown recently that 8-pCPT-cyclic AMP shows little selectivity for the activation of PKA over PKG (Sandberg *et al.*, 1991) and that it is also a potent inhibitor of the cyclic GMP-specific phosphodiesterase (PDE V_A) (Connolly *et al.*, 1992). This provides further reasons to interpret with caution the biphasic effect on stimulation-induced vasoconstriction observed in the present experiments. It is therefore possible that the observed effects with higher concentrations of this cyclic AMP derivative might be secondary to PDE V_A inhibition which in turn increases the intracellular level of cyclic GMP and induces vasorelaxation. In these conditions, due to the complex pharmacological effects of this derivative and its poor selectivity for PKA the effects of protein kinase inhibitors were only investigated with the 8-bromo-analogue.

The attenuation by H-89 of the enhancing effect of 8-bromo-cyclic AMP on stimulation-induced vasoconstriction could result from the above discussed inhibition of the prejunctional effect of the cyclic AMP analogue on noradrenaline release. The findings that, in spite of antagonizing the cyclic AMP-induced increase in neurotransmitter release, H-89 did not modify vasoconstrictor responses obtained in the presence of isoprenaline and forskolin, would imply that both pre- and postjunctional effects of these drugs were decreased by the PKA inhibitor. However, the persistence of a marked depressor effect of forskolin on vasoconstriction, in the presence of H-89, suggests that a mechanism other than PKA activation may be involved. It has previously been shown that a non-cyclic AMP-mediated relaxant effect of forskolin due to a direct effect on K^+ channels (Hoshi *et al.*, 1988; Ertl & Nawrath, 1989) is not likely since 1,9-dideoxy-forskolin was unable to decrease the stimulation-elicited vasoconstriction (Bucher *et al.*, 1990). Other mechanisms, perhaps involving adenylyl cyclase activation or not, cannot be excluded. The results obtained here with forskolin are consistent with recent observations showing that Rp-cyclic AMPS (Rp diastereoisomer of adenosine 3':5'-cyclic monophosphorothioate), a PKA inhibitor had no effect on forskolin-mediated vasodilatation (Haynes *et al.*, 1992). In addition, the present finding showing that the PKG inhibitor, Rp-8-bromo-cyclic GMPS, did not alter forskolin-induced inhibition of the vessel contraction and had no effect on vasoconstriction elicited in the presence of 8-bromo-cyclic AMP do not support a role of PKG in these drugs actions.

It is clear from our previous research that neither the endothelium nor the L-arginine-NO pathway is implicated in the modulation of stimulation-induced noradrenaline release from postganglionic nerve endings in the rat tail artery (Bucher *et al.*, 1992). However, an important question that arises from the present study relates to the possible influence of the endothelium on the cyclic AMP-dependent effects on vasoconstriction. In the present study and in previous work (Bucher *et al.*, 1990) only forskolin produced a clear-cut concentration-dependent decrease in the stimulation-induced vasoconstriction. This inhibitory effect is considered to occur via an increase in cyclic AMP within the smooth muscle cells (Kukovetz *et al.*, 1981). The fact that in the present study endothelium removal failed to alter significantly forskolin-induced relaxation suggests that the vascular effects of the adenylyl cyclase activator occurred independently of the endothelium. A similar conclusion has been reached by others (Kamata *et al.*, 1989; Graves & Poston, 1993).

Reciprocal interactions between the cyclic AMP/PKA pathway and PKC had been suggested in a variety of tissues (Rozengurt *et al.*, 1987; Naghshineh *et al.*, 1989; Gorin *et al.*, 1990; Anderson *et al.*, 1991; Mazancourt *et al.*, 1991). In the rat tail artery, a role for PKC in the prejunctional release of noradrenaline has recently been suggested (Bucher *et al.*, 1991). Consistent with this suggestion, it was found here that PMA enhanced electrical field-induced noradrenaline release. However, inhibition of PKC did not modify the effect of 8-bromo-cyclic AMP at this level, providing no evidence for a role of PKC in cyclic AMP-mediated modulation of neurotransmitter release.

Altogether, the current study shows that, in the rat tail artery, the prejunctional cyclic AMP-mediated facilitation of stimulated noradrenaline release involves the activation of cyclic AMP-dependent protein kinase but provides no substantial evidence for a postjunctional vasodilator role of the kinase.

References

ANDERSON, R.J., BRECKON, R. & COLSTON, D. (1991). Regulation by forskolin of cyclic AMP phosphodiesterase and protein kinase C activity in LLC-PK$_1$ cells. *Biochem. J.*, **279**, 23–27.

BAO, J.X., ERIKSSON, I.E. & STJÄRNE, I. (1990). Neurotransmitter and pre- and post-junctional receptors involved in the vasoconstrictor response to sympathetic nerve stimulation in the rat tail artery. *Acta Physiol. Scand.*, **140**, 467–479.

BEEBE, S.J. & CORBIN, J.D. (1986). Cyclic nucleotide-dependent protein kinases. In *The Enzymes*, vol. XVII. ed. Boyer, P.D. & Krebs, E.G., pp. 43–111. New York: Academic Press.

BUCHER, B., NEUBURGER, J. & ILLES, P. (1991). Protein kinase C and α_2-adrenoceptor-mediated inhibition of noradrenaline release from the rat tail artery. *J. Cardiovasc. Pharmacol.*, **17**, 913–915.

BUCHER, B., OUEDRAOGO, S., TSCHÖPL, M., PAYA, D. & STOCLET, J.-C. (1992). Role of the L-arginine-NO pathway and of cyclic GMP in electrical field-induced noradrenaline release and vasoconstriction in the rat tail artery. *Br. J. Pharmacol.*, **107**, 976–982.

BUCHER, B., PAIN, L., STOCLET, J.-C. & ILLES, P. (1990). Role of cyclic AMP in the prejunctional α_2-adrenoceptor modulation of noradrenaline release from the rat tail artery. *Naunyn-Schmied. Arch. Pharmacol.*, **342**, 640–649.

BUTT, E., VAN BEMMELEN, M., FISCHER, L., WALTER, U. & JASTORFF, B. (1990). Inhibition of cGMP-dependent protein kinase by (Rp)-guanosine 3',5'-monophosphorothioates. *FEBS Lett.*, **263**, 47–50.

CHIJIWA, T., MISHIMA, A., HAGIWARA, M., SANO, M., HAYASHI, K., INOUE, T., NAITO, K., TOSHIOKA, T. & HIDAKI, H. (1990). Inhibition of forskolin-induced neurite outgrowth and protein phosphorylation by a newly synthesized selective inhibitor of cyclic AMP-dependent protein kinase, N-[2-(*p*-bromocinnamylamino)ethyl]-5-isoquinolinesulfonamide (H-89), of PC12D pheochromocytoma cells. *J. Biol. Chem.*, **265**, 5267–5272.

CONNOLLY, B.J., WILLITS, P.B., WARRINGTON, B.H. & MURRAY, K.J. (1992). 8-(4-Chlorophenyl)thio-cyclic AMP is a potent inhibitor of the cyclic GMP-specific phosphodiesterase (PDE V_A). *Biochem. Pharmacol.*, **44**, 2303–2306.

COSTA, M. & MAJEWSKI, H. (1988). Facilitation of noradrenaline release from sympathetic nerves through activation of ACTH receptors, β-adrenoceptors and angiotensin II receptors. *Br. J. Pharmacol.*, **95**, 993–1001.

ERTL, R. & NAWRATH, H. (1989). Cyclic AMP-independent membrane effects of forskolin in atrial and ventricular heart and aortic smooth muscle preparations from guinea pigs. *Naunyn-Schmied. Arch. Pharmacol.*, **339**, R52.

FRANCIS, S.H., NOBLETT, B.D., TODD, B.W., WELLS, J.N. & CORBIN, J.D. (1988). Relaxation of vascular and tracheal smooth muscle by cyclic nucleotide analogs that preferentially activate purified cGMP-dependent protein kinase. *Mol. Pharmacol.*, **34**, 506–517.

GORIN, E., TAI, L.R., HONEYMAN, T.W. & GOODMAN, H.M. (1990). Evidence for a role of protein kinase C in the stimulation of lipolysis by growth hormone and isoproterenol. *Endocrinology*, **126**, 2973–2982.

GÖTHERT, M. & HENTRICH, F. (1984). Role of cAMP for regulation of impulse-evoked noradrenaline release from the rabbit pulmonary artery and its possible relationship to presynaptic ACTH receptors. *Naunyn-Schmied. Arch. Pharmacol.*, **328**, 127–137.

GRAVES, J. & POSTON, L. (1993). β-Adrenoceptor agonist mediated relaxation of rat isolated resistance arteries: a role for the endothelium and nitric oxide. *Br. J. Pharmacol.*, **108**, 631–637.

HAYNES Jr, J., ROBINSON, J., SAUNDERS, L., TAYLOR, A.E. & STRADA, S.J. (1992). Role of cAMP-dependent protein kinase in cAMP-mediated vasodilation. *Am. J. Physiol.*, **262**, H511– H516.

HEI, Y.-J., MACDONELL, K.L., MCNEILL, J.H. & DIAMOND, J. (1991). Lack of correlation between activation of cyclic AMP-dependent protein kinase and inhibition of vas deferens by cyclic AMP analogs. *Mol. Pharmacol.*, **39**, 233–238.

HENTRICH, F., GÖTHERT, M. & GRESCHUCHNA, D. (1985). Involvement of cAMP in modulation of noradrenaline release in the human pulmonary artery. *Naunyn-Schmied Arch. Pharmacol.*, **330**, 245–247.

HOSHI, T., GARBER, S.S. & ALDRICH, R.W. (1988). Effect of forskolin on voltage-gated K^+ channels is independent of adenylate cyclase activation. *Science*, **240**, 1652–1655.

ILLES, P., BETTERMANN, R., BROD, I. & BUCHER, B. (1987). β-Endorphin-sensitive opioid receptors in the rat tail artery. *Naunyn-Schmied. Arch. Pharmacol.*, **335**, 420–427.

JOHNSTON, H. & MAJEWSKI, H. (1986). Prejunctional β-adrenoceptors in rabbit pulmonary artery and mouse atria; the effect of α-adrenoceptor blockade and phosphodiesterase inhibition. *Br. J. Pharmacol.*, **87**, 553–562.

KAMATA, K., MIYATA, N. & KASUYA, Y. (1989). Involvement of endothelial cells in relaxation and contraction responses to isoproterenol in naive and streptozotocin-induced diabetic rats. *J. Pharmacol. Exp. Ther.*, **249**, 890–894.

KRAMER, G.L. & HARDMAN, J.G. (1980). Cyclic nucleotides and blood vessel contraction. In *Handbook of Physiology: The Cardiovascular System.* II.– *Vascular Smooth Muscle.* ed. Bohr, D.F., Somlyo, A.P. & Sparks, H.P. pp. 179–199. Bethesda: American Physiological Society.

KUKOVETZ, W.R., POCH, G. & HOLZMANN, S. (1981). Cyclic nucleotides and relaxation of vascular smooth muscle. In *Vasodilatation.* ed. Vanhoutte, P.M. & Leusen, I. pp. 339–353. New York: Raven Press.

LINCOLN, T.M. & CORNWELL, T.L. (1991). Towards an understanding of the mechanism of action of cyclic AMP and cyclic GMP in smooth muscle relaxation. *Blood Vessels*, **28**, 129–137.

LINCOLN, T.M., CORNWELL, T.L. & TAYLOR, A.E. (1990). cGMP-dependent protein kinase mediates the reduction of Ca^{2+} by cAMP in vascular smooth muscle cells. *Am. J. Physiol.*, **258**, C399–C407.

DE MAZANCOURT, P., DARIMONT, C., GIOT, J. & GIUDICELLI, Y. (1991). Differential modulation of the adenylate cyclase/cyclic AMP stimulatory pathway by protein kinase C activation in rat adipose tissue and isolated fat cells. *Biochem. Pharmacol.*, **42**, 1791–1797.

NAGHSHINEH, S., NOGUCHI, M., HUANG, K.P. & LONDOS, C. (1989). Activation of adipocyte adenylate cyclase by protein kinase C. *J. Biol. Chem.*, **261**, 14534–14538.

RAJANAYAGAM, M.A.S., MEDGETT, I.C. & RAND, M.J. (1990). Vasoconstrictor responses of rat tail artery to sympathetic nerve stimulation contain a component due to activation of postjunctional β- or α_2-adrenoceptors. *Eur. J. Pharmacol.*, **177**, 35–41.

ROZENGURT, E., MURAY, M, ZACHARI, I. & COLLINS, M. (1987). Protein kinase C activation enhances cAMP accumulation in Swiss 3T3 cells: inhibition by pertussis toxin. *Proc. Natl. Acad. Sci. U.S.A.*, **84**, 2282–2286.

SANDBERG, M., BUTT, E., NOLTE, C., FISCHER, L., HALBRÜGGE, M., BELTMAN, J., JAHNSEN, T., GENIESER, H.-G., JARSTORFF, B. & WALTER, U. (1991). Characterization of Sp-5,6-dichloro-1-β-D-ribofuranosyl-benzimidazole-3', 5'-monophosphorothioate (Sp-5,6-DCl-cBiMPS) as a potent and specific activator of cyclic-AMP-dependent protein kinase in cell extracts and intact cells. *Biochem. J.*, **279**, 521–527.

SEAMON, K.B. & DALY, J.W. (1986). Forskolin: its biological and chemical properties. *Adv. Cyclic Nucleotide Protein Phosphorylation Res.*, **20**, 1–150.

TOULLEC, D., PIANETTI, P., COSTE, H., BELLEVERGUE, P., GRANDPERRET, T., AJAKANE, M., BAUDET, V., BOISSIN, P., BOURSIER, E., LORIOLLE, F., DUHAMEL, L., CHARON, D. & KIRILOVSKY, J. (1991). The bisindolylmaleimide GF 109203X is a potent and selective inhibitor of protein kinase C. *J. Biol. Chem.*, **266**, 15771–15781.

WALLENSTEIN, S., ZUCKER, C.L. & FLEISS, J.L. (1980). Some statistical methods used in circulation research. *Circ. Res.*, **47**, 1–9.

(Received July 12, 1993
Revised October 11, 1993
Accepted October 22, 1993)

Br. J. Pharmacol. (1994), **111**, 632–640

Mg^{2+}-dependent inhibition of K_{ATP} by sulphonylureas in CRI-G1 insulin-secreting cells

K. Lee, *S.E. Ozanne, *C.N. Hales & [1]M.L.J. Ashford

Department of Pharmacology, University of Cambridge, Tennis Court Road, Cambridge, CB2 1QJ and *Department of Clinical Biochemistry, University of Cambridge, Addenbrooke's Hospital, Hills Road, Cambridge CB2 2QR

1 Patch-clamp recording techniques were used to examine the effects of tolbutamide, glibenclamide, meglitinide and thiopentone on K_{ATP} in CRI-GI insulin-secreting cells in the presence and absence of Mg^{2+}.

2 In the absence of Mg^{2+} in the intracellular bathing solution, tolbutamide was significantly less effective when applied either to the intracellular or to the extracellular surfaces of cell-free patches. Removal of extracellular Mg^{2+} did not alter the effectiveness of tolbutamide provided that Mg^{2+} was present at the intracellular surface of the patch.

3 Tolbutamide was also significantly less effective when applied to the intracellular surface of cell-free patches when Mn^{2+} was used as a replacement for Mg^{2+}.

4 Both the sulphonylurea, glibenclamide and the non-sulphonylurea derivative, meglitinide also showed Mg^{2+} dependent inhibitory effects in cell-free patches. In contrast, the barbiturate thiopentone inhibited K_{ATP} in a Mg^{2+}-independent manner.

5 Whole-cell $I_{K(ATP)}$ were used to quantify the effects of tolbutamide and glibenclamide in the presence and absence of intracellular Mg^{2+}. Concentration-inhibition curves, in the presence of intracellular Mg^{2+}, resulted in IC_{50} values of 12.1 μM and 2.1 nM for tolbutamide and glibenclamide, respectively. In the absence of intracellular Mg^{2+}, the corresponding IC_{50} values were 25.3 mM and 3.6 μM, respectively. The values of IC_{50} for thiopentone in the presence and absence of intracellular Mg^{2+} were 69.4 μM and 69.2 μM, respectively.

6 With respect to the high affinity binding sites for [^{3}H]-glibenclamide in CRI-G1 membranes, no significant differences were found between the dissociation constants for, or the maximal binding capacities of, [^{3}H]-glibenclamide in the presence or absence of Mg^{2+}.

7 In the CRI-G1 insulin-secreting cell line, it is concluded that intracellular Mg^{2+} does not influence the affinity of the sulphonylureas for the sulphonylurea receptor but that this ion is critically important for the interaction between the sulphonylurea receptor and K_{ATP}.

Keywords: Sulphonylureas; K_{ATP}; magnesium; β-cells; sulphonylurea receptors

Introduction

The ATP-sensitive potassium channel (K_{ATP}) has been identified in a variety of tissues including cardiac muscle, pancreatic β cells, skeletal muscle and mammalian central neurones (for review, see Ashcroft & Ashcroft, 1990). In the pancreatic β cell, intracellular Mg^{2+} has a number of important effects upon K_{ATP}. For example, this divalent cation is at least partially responsible for the inward rectification displayed by this ion channel (Findlay, 1987; Ciani & Ribalet, 1988). In addition, Mg^{2+} has a direct inhibitory effect upon the open state probability of the channel (Findlay, 1987; Ashcroft & Kakei, 1989) and is critically involved in the process of rundown (Kozlowski & Ashford, 1990), since complete removal of this cation from the intracellular compartment drastically reduces the rate of loss of channel activity with respect to time. The presence of intracellular Mg^{2+} also influences many of the interactions between nucleotides and K_{ATP}. For example, Mg^{2+} reduces the inhibitory effect of ATP on channel activity (Ashcroft & Kakei, 1989) but is required in order for ATP to refresh run-down channels (Findlay & Dunne, 1986; Ohno-Shosaku *et al.*, 1987). Further, nucleotide diphosphates such as ADP and GDP inhibit K_{ATP} in the absence of Mg^{2+}, but enhance channel activity in its presence (Findlay, 1987; Hopkins *et al.*, 1992).

Similarly, many of the reported interactions between nucleotides, K_{ATP} and pharmacological agents are also dependent on the presence of intracellular Mg^{2+}. For example, diazoxide-induced K_{ATP} activation in the presence of ATP requires internal Mg^{2+} whereas in the absence of Mg^{2+}, diazoxide is an inhibitor of the channel (Kozlowski *et al.*, 1989). Recently, it has been suggested that MgADP is more potent than MgATP at enhancing the ability of diazoxide to increase channel activity in isolated patches (Schwanstecher *et al.*, 1992a), although the same does not appear to be true of the whole-cell configuration (Kozlowski & Ashford, 1992). In the presence of intracellular Mg^{2+}, certain nucleotides (e.g. ADP) also enhance the sensitivity of K_{ATP} to the sulphonylureas (Schwanstecher *et al.*, 1992b) and a model for K_{ATP} involving the presence of stimulatory and inhibitory nucleotide binding sites, in addition to receptors for diazoxide and the sulphonylureas has been proposed (Schwanstecher *et al.*, 1992a).

However, despite the undenied importance of Mg^{2+} in the production of all these effects, little attention has been focused on the direct effect of this cation on the interaction between the sulphonylureas and K_{ATP} itself. We now show that the inhibitory effects of the sulphonylureas on K_{ATP} in an insulin-secreting cell line are dependent upon the presence of intracellular Mg^{2+}. In contrast, the barbiturate thiopentone, which is also an inhibitor of K_{ATP} (Kozlowski & Ashford, 1991), does not exhibit Mg^{2+}-dependent inhibitory properties. Some of these results have been communicated to the British Pharmacological Society (Lee & Ashford, 1993).

[1] Author for correspondence.

Methods

Cell culture

Cells of the rat pancreatic islet cell line CRI-G1 were cultured and passaged at 2–5 day intervals as previously described (Carrington *et al.*, 1986). Cells used for patch-clamp experiments were plated onto 3.5 cm Petri dishes (Falcon 3001) at a density of approximately 1.5×10^5 cells per dish. The cells were used 2–4 days (inclusive) after plating.

Preparation of CRI-G1 membranes and measurement of ^{3}H-ligand binding

CRI-G1 cells were grown to 70–80% confluence in Falcon 3027, 805 cm^2 roller bottles (approximately 2.5×10^7 cells per bottle), harvested by scraping with a rubber policeman into Hank's physiological saline which consisted of (mM); NaCl 137, KCl 5.4, $MgSO_4$ 1.67, $CaCl_2$ 4, Na_2HPO_4 0.34, $NaHCO_3$ 4.2, pH 7.4. This and all subsequent steps were carried out in the presence of either 0.65 mM $MgCl_2$ or 10 mM EDTA. The cell suspension was centrifuged for 10 min at 220 *g* (MSE, Crawley, UK), the resulting supernatant removed by aspiration and cells were resuspended in ice-cold 10 mM HEPES containing 200 mM (+)-mannitol and 65 mM sucrose (pH 7.4). All subsequent procedures were performed at 4°C. The cell suspension was homogenized in a 40 ml capacity glass tube homogenizer using 10 strokes of a Teflon pestle driven at 600 r.p.m., then sonicated for 10 seconds at 30W (MSE Sonifier). The homogenate was centrifuged for 15 min at 500 *g* to remove unbroken cells and nuclei and the resulting supernatant was centrifuged for 30 min at 70,000 *g* to produce a crude membrane fraction. The resulting pellet was resuspended in 50 mM Tris/HCl buffer (pH 7.4) and the latter centrifugation step was repeated. Finally this pellet was suspended in 50 mM Tris/HCl containing phenylmethylsulphonyl fluoride 100 μM, pepstatin A 10 μM and *trans*-epoxysuccinyl-L-leucylamido(4-guanido)-butane (E64) 20 μM and stored in liquid nitrogen prior to use. Protein concentration was determined by the method of Bradford (1976) with bovine serum albumin (BSA) used as a standard.

CRI-G1 membranes (50 μg protein) were incubated for 2 h at room temperature in 0.5 ml assay buffer (50 ml Tris/HCl, pH 7.4) containing 0.04–10 nM [^{3}H]-glibenclamide (50.9 Ci $mmol^{-1}$, Dupont (U.K.) Ltd) and either 0.65 mM $MgCl_2$ or 10 mM EDTA. Incubations were terminated by addition of 2 ml ice-cold buffer and bound ligand was collected by rapid vacuum filtration onto 2.5 cm diameter Whatman GF/B glass fibre filters by use of a 10-place filtration block. Filters were washed with 4×2 ml of buffer and the bound radioactivity determined by liquid scintillation counting using Optiphase HiSafe II (LKB Scintillation Products, Loughborough) and a Packard liquid-scintillation spectrophotometer (Canberra Packard, Berks). Non-specific binding was determined in the presence of 1 μM glibenclamide. Curves for the amount of [^{3}H]-glibenclamide bound versus its concentration were fitted to the equation:

$$[^3\text{H}]\text{-glibenclamide bound} = B_{max} \times A^n/A^n + EC_{50}{}^n$$

where B_{max} is the maximum amount of [^{3}H]-glibenclamide bound, A is the concentration of [^{3}H]-glibenclamide, EC_{50} is the concentration of [^{3}H]-glibenclamide giving half-maximal binding and n is the Hill coefficient. The best fit values of B_{max} and EC_{50} were determined by non-linear regression using GraphPad InPlot (GraphPAD Software, San Diego, U.S.A.). Values quoted in the text are the mean ± s.e.mean of three experiments each performed in triplicate.

Electrical recording and analysis

This study employed both the cell-free and whole-cell configurations of the patch-clamp recording technique,. as described by Hamill *et al.* (1981). Recording electrodes were pulled from borosilicate glass capillaries and when filled with electrolyte had resistances of 8–12 MΩ for isolated patch experiments, and 2–5Ω for whole-cell recording. Single channel events were detected with a List EPC-7 patch clamp amplifier and were stored on digital audio tape. Records used for illustrative purposes were replayed into a chart recorder (Gould 2200) which filtered the data at 140 Hz. The potential across the membrane is described following the usual sign convention for membrane potential (i.e. inside negative). Outward current (defined as the current flowing from the intra- to the extracellular side of the membrane) is shown as upward deflections on all traces. The single channel current analysis was determined off-line using a programme that incorporated a 50% threshold crossing parameter to detect events (Dempster, 1988) and run on an Apricot XEN-i286/45 microcomputer. Data segments between 30 and 90 s duration were replayed at the recorded speed and filtered at 1.0 kHz using an 8-pole Bessel filter and digitised at 5.0 kHz using a Data Translation 2801A interface. The average channel activity ($N_f.P_o$) where N_f is the number of functional channels in the patch and P_o is the open state probability, was determined by measuring the total time spent at each unitary current level and expressed as a proportion of the total time recorded (Kozlowski *et al.*, 1989; Kozlowski & Ashford, 1990). Changes in $N_f.P_o$ as a result of drug effects are expressed as a percentage of control. In order to determine whether modification of intracellular Mg^{2+} modified the inhibitory effects of the various agents, the percentage inhibition produced in the presence and absence of Mg^{2+} was assessed for significant differences by one-way analysis of variance (ANOVA). To obtain whole-cell currents, cells were clamped at a holding potential of −70 mV, and 10 mV pulses each of 200 ms duration and of alternating polarity were applied at 2 s intervals as described previously (Sturgess *et al.*, 1988; Kozlowski *et al.*, 1989). Drug effects were quantified by measuring the amplitude of the current responses (I) during drug exposure and comparing them with those observed under control conditions (I_c). Values for the controls were obtained by calculating the mean amplitude before and after the application of drug. This allowed compensation for the slow process of 'run-down' which occurred when Mg^{2+} was present in the electrode solution. The concentration-inhibition curves were fitted by non-linear regression to the following equation:

$$I/I_c = 1/1 + (a/b)^n$$

where a = drug concentration, b = half maximal inhibitory concentration and n = Hill coefficient. All electrophysiological experiments were conducted at room temperature (22–25°C).

Solutions

Before use the cells were washed thoroughly with solution A which consisted of (mM): NaCl 135.0, KCl 5.0, $CaCl_2$ 1.0, $MgCl_2$ 1.0, HEPES 10.0, pH adjusted to 7.4 with NaOH. For whole-cell voltage-clamp studies, the cells were bathed in solution A. When cells were dialysed with a Mg^{2+}-containing solution, the pipette contained (mM): KCl 140.0, $MgCl_2$ 1.0, $CaCl_2$ 2.0, K_2EGTA 10.0, HEPES 10.0, pH adjusted to 7.2 with KOH which resulted in free Ca^{2+} and Mg^{2+} concentration of 20 nM and 0.65 mM respectively (solution B). In experiments conducted in the absence of intracellular Mg^{2+}, solution B in the pipette was replaced by solution C which contained (mM): KCl 140.0, $CaCl_2$ 4.6, K-EDTA 10.0, HEPES 10.0; pH adjusted to 7.2 with KOH. This resulted in free Ca^{2+} and Mg^{2+} concentrations of 20 nM and <3.0 nM, respectively. In order to calculate these values it was necessary to assume that the salts used to prepare this solution were contaminated with the trace levels of Mg^{2+} indicated by the manufacturers.

In experiments using the inside-out configuration, the pipette contained (mM): KCl 140.0, $MgCl_2$ 1.0, $CaCl_2$ 1.0, HEP-

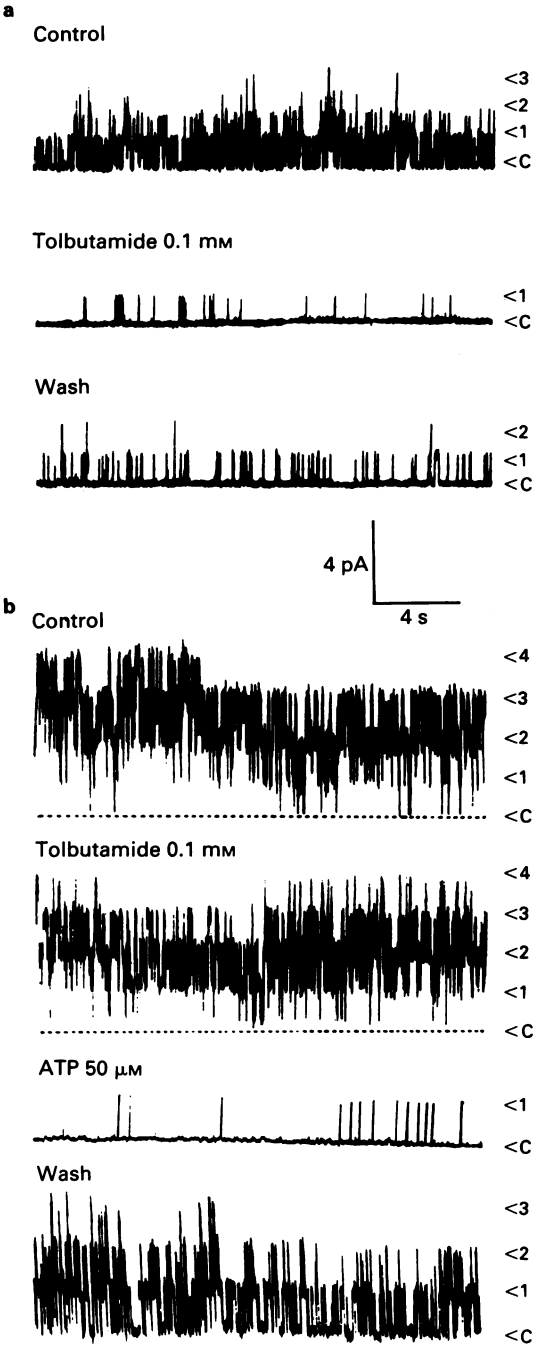

Figure 1 Single channel currents recorded from inside-out membrane patches exposed to symmetrical 140 mM KCl held at a membrane potential of: (a) 30 mV or (b) + 40 mV. Single channel openings are denoted by upward deflections (outward currents). (a) Tolbutamide (100 μM), in the presence of Mg^{2+} (0.65 mM) inhibited the activity of K_{ATP} in a reversible manner. The values of $N_f.P_o$ were as follows: control 0.867; tolbutamide 0.045; wash 0.118. (b) Tolbutamide (100 μM), in the absence of Mg^{2+} produced a much weaker inhibition of K_{ATP} activity. However ATP (50 μM) retained its inhibitory effectiveness. The values of $N_f.P_o$ were as follows: control 2.434; tolbutamide 1.819; ATP 0.031; wash 0.897. Note the much greater level of channel activity in the absence of Mg^{2+} before drug application.

ES 10.0, pH adjusted to 7.2 with KOH (solution D) whilst the bath solution was either solution B (Mg^{2+} present) or solution C (Mg^{2+} absent). In experiments designed to examine the ability of Mn^{2+} to mimic Mg^{2+}, the bath solution contained (mM): KCl 140.0, $MnCl_2$ 1.0, $CaCl_2$ 2.0, K_2EGTA 10.0, HEPES 10.0, pH adjusted to 7.2 with KOH. This resulted in free Ca^{2+} and Mn^{2+} concentrations of 20 nM and

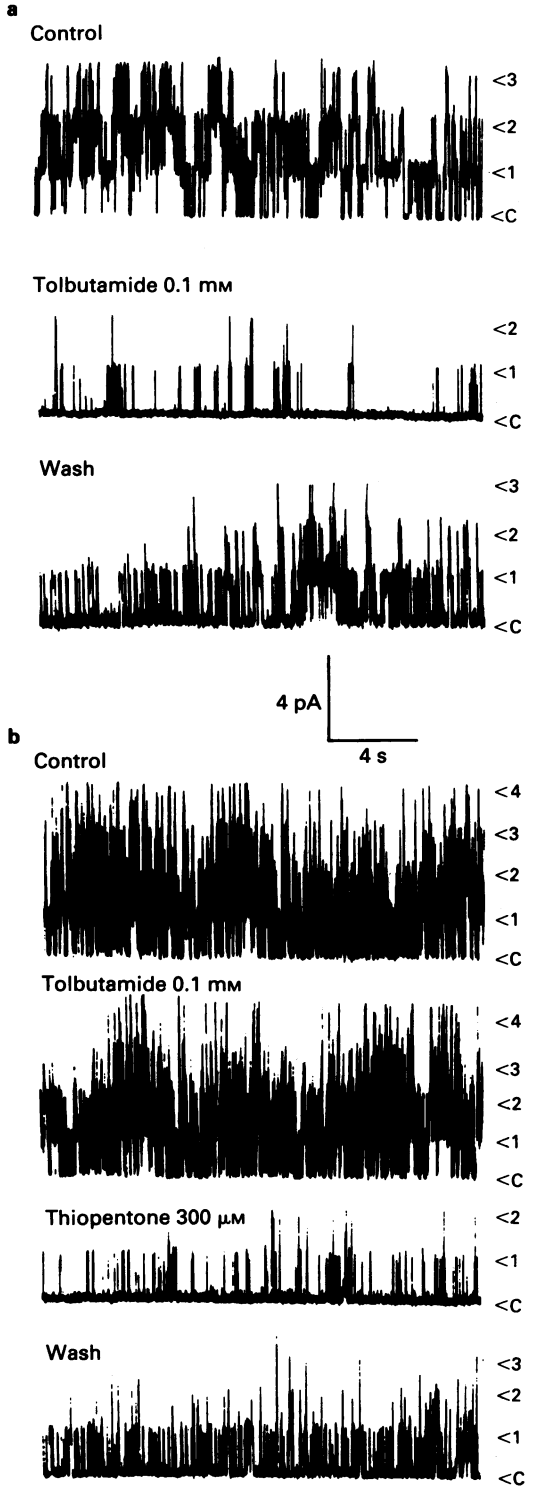

Figure 2 Single channel currents recorded from outside-out membrane patches exposed to symmetrical 140 mM KCl held at a membrane potential of + 40 mV. Single channel openings are denoted by upward deflections (outward currents). (a) Tolbutamide (100 μM), in the presence of Mg^{2+} (0.65 mM) inhibited the activity of K_{ATP} in a reversible manner. The values of $N_f.P_o$ were as follows: control 2.142; tolbutamide 0.110; wash 0.820. (b) Tolbutamide (100 μM), in the absence of Mg^{2+} produced a much weaker inhibition of K_{ATP} activity. However thiopentone (300 μM) retained its inhibitory effectiveness. The values of $N_f.P_o$ were as follows: control 2.610; tolbutamide 1.862; thiopentone 0.151; wash 0.456.

0.65 mM respectively (solution E). In experiments on outside-out patches, the bath solution was solution D whilst the pipette solution was either solution B (Mg^{2+} present) or solution C (Mg^{2+} absent). In control experiments designed to

assess the ability of tolbutamide to inhibit whole-cell currents in the presence of 0.65 mM free Mg^{2+} and 10 mM EDTA, the pipette solution contained (mM): KCl 140.0, $MgCl_2$ 10.57, $CaCl_2$ 0.035, K-EDTA 10.0, HEPES 10.0, pH adjusted to 7.2 with KOH (solution F). The concentrations of free divalent cations were determined by using a programme for calculating metal ion/ligand binding 'METLIG' (P. England & R. Denton, University of Bristol).

Membrane patches or whole-cells were continuously perfused throughout the course of the experiment by a gravity feed system at a rate of approximately 0.5 ml s^{-1}, which allowed complete solution exchange within 45 s. Tolbutamide and thiopentone were each made up as 500 mM stock solutions in either 1 M KOH or 1 M NaOH. Meglitinide (HB699) was made up as a 100 mM stock solution in dimethylsulphoxide (DMSO) whilst glibenclamide stock solutions (5 mM) were made up in methanol. Meglitinide was provided by Hoechst Aktiengesellshaft, Frankfurt, Germany. K_2ATP and all other drugs were obtained from Sigma (Poole, Dorset).

All data in the text, tables and figures are presented as mean values ± s.e.mean unless otherwise stated.

Results

Single channel studies

Recordings of single K_{ATP} currents from inside-out membrane patches isolated from the CRI-G1 cell-line were made in symmetrical (140 mM KCl in pipette and bath) K^+-containing solution both in the presence and absence of 0.65 mM Mg^{2+} in the internal bath solution (Figure 1a,b). Under these recording conditions, K_{ATP} activity was observed to be consistently higher in the absence, compared to the presence ($P<0.05$) of internal Mg^{2+} (Figure 1a,b) as previously reported (Findlay, 1987; Kolzlowski & Ashford, 1990). In order to examine the relative effectiveness of K_{ATP} inhibitors under the two conditions, drug concentrations were chosen which were capable of producing near maximal inhibition in the presence of 0.65 mM Mg^{2+}. In the presence of intracellular Mg^{2+}, the sulphonylurea tolbutamide (100 μM) produced a large inhibition of channel activity (Figure 1a) irrespective of whether the membrane patch was depolarized or hyperpolarized (Table 1). However, when tolbutamide was tested in the absence of Mg^{2+} (Figure 1b), there was a statistically significant reduction in its effectiveness at both depolarized and hyperpolarized potentials ($P<0.05$; see Table 1).

Since tolbutamide normally accesses its site of action from the external surface, a similar study was performed using the outside-out patch configuration (Figure 2). Tolbutamide (100 μM) produced a substantial inhibition of K_{ATP} activity in the presence of 0.65 mM internal Mg^{2+} (Figure 2a) but was significantly less effective as an inhibitor in the absence of Mg^{2+} (Figure 2b). These actions of tolbutamide were also independent of membrane potential (Table 1). In contrast, when the Mg^{2+} present in the solution bathing the external surface was removed in either patch configuration, tolbutamide (100 μM) retained its effectiveness with an inhibition of 94.3 ± 2.3% ($n = 4$) and 92.3 ± 1.6% ($n = 4$) for inside-out and outside-out membrane patches respectively (data not shown) provided that Mg^{2+} (0.65 mM) was present in the intracellular solution.

These findings are at variance with a previous report which suggested that tolbutamide inhibition of K_{ATP} activity was Mg^{2+}-independent (Dunne *et al.*, 1987). However, on close inspection of the protocols used by these authors it appears that in the experiments conducted in 'Mg^{2+}-free' conditions, 3 μM Mg^{2+} remained in the internal solution. In the present study it was found essential to remove as much internal Mg^{2+} as possible. This was achieved by 'washing' the internal face of the inside-out patch surface with approximately 50 ml of solution D (which contained 10 mM EDTA) following excision of the patch into this solution. In preliminary experiments where such a procedure was not employed, the reduction in sulphonylurea sensitivity was not nearly so marked (data not shown). A similar washing procedure was not found to be necessary for outside-out and whole-cell recording configurations. This is probably because in these configurations the internal surface of the patch is in direct contact with the extremely large pool of Mg^{2+}-free solution and the accessibility problems associated with the inside-out configuration are avoided.

In several experiments using inside-out patches, the internal bath solution contained Mn^{2+} in the place of Mg^{2+} (solution E) in an attempt to elucidate the specificity of this process for Mg^{2+}. In the presence of 0.65 mM Mn^{2+}, tolbutamide (100 μM) produced a 48.5 ± 4.4% ($n = 5$) and a 52.5 ± 6.6% ($n = 5$) inhibition of channel activity at depolarized and hyperpolarized potentials respectively. These values are significantly different ($P<0.05$) from the inhibition produced both in the presence and absence of Mg^{2+} (Table 1).

Tolbutamide is a first generation sulphonylurea. It has been suggested that the more potent second generation sulphonylureas, such as glibenclamide which contain a benzoic acid moiety in addition to the sulphonylurea component,

Table 1 Inhibition of K_{ATP} activity by tolbutamide, glibenclamide, meglitinide and thiopentone on isolated membrane patches in the presence and absence of Mg^{2+} (0.65 mM) in the internal bath solution

Compound		*% Inhibition* + Mg^{2+}	− Mg^{2+}
Tolbutamide 100 μM			
(i/o)	+ 40 mV	96.1 ± 2.9% ($n = 7$)	29.2 ± 3.9% ($n = 5$)*
	− 40 mV	95.1 ± 4.2% ($n = 7$)	34.5 ± 3.3% ($n = 5$)*
Tolbutamide 100 μM			
(o/o)	+ 40 mV	96.0 ± 4.1% ($n = 4$)	24.0 ± 8.7% ($n = 4$)*
	− 40 mV	95.5 ± 4.5% ($n = 4$)	22.6 ± 6.7% ($n = 4$)*
Glibenclamide 1 μM			
(i/o)	+ 30/+ 40 mV	90.7 ± 4.2% ($n = 7$)	33.7 ± 8.9% ($n = 6$)*
	− 30/− 40 mV	99.1 ± 0.8% ($n = 7$)	42.0 ± 5.3% ($n = 5$)*
Meglitinide 10 μM			
(i/o)	+ 40 mV	91.1 ± 1.9% ($n = 6$)	29.6 ± 6.5% ($n = 6$)*
	− 40 mV	93.4 ± 4.5% ($n = 7$)	36.2 ± 7.3% ($n = 5$)*
Thiopentone 300 μM			
(i/o)	+ 40 mV	97.1 ± 1.6% ($n = 4$)	97.0 ± 3.1% ($n = 5$)
	− 40 mV	97.3 ± 1.4% ($n = 4$)	95.3 ± 4.3% ($n = 4$)

The results are expressed as % inhibition ± s.e.mean. The number of patches used are shown in parentheses. *$P<0.01$ relative to inhibition observed in the presence of Mg^{2+}.

have two sites of interaction with the sulphonylurea receptor (Ashford, 1990). Therefore studies were performed to determine whether glibenclamide also exhibited Mg^{2+}-dependent K_{ATP} inhibition. As shown in Figure 3a, glibenclamide (1 μM) applied to the intracellular aspect of inside-out membrane patches produced a substantial inhibition of the channel in the presence of 0.65 mM Mg^{2+} irrespective of membrane voltage (Table 1). In contrast, in the absence of intracellular Mg^{2+}, significantly less inhibition ($P<0.05$) of channel activity was produced by the same concentration of glibenclamide (Figure 3b) and this was also independent of membrane potential (Table 1). Meglitinide, which can be regarded as the non-sulphonylurea structural component of glibenclamide, also has hypoglycaemic properties and is a potent inhibitor of K_{ATP} activity (Sturgess *et al.*, 1988). As this compound does not contain the sulphonylurea nucleus the Mg^{2+}-dependence of its K_{ATP} inhibitory effects was also examined. Figure 4a shows that application of 10 μM meglitinide in the presence of 0.65 mM Mg^{2+} markedly reduced channel activity independent of membrane holding potential (Table 1). However in the absence of Mg^{2+}, 10 μM meglitinide (Figure 4b) produced significantly ($P<0.05$) less inhibition of K_{ATP} activity (see also Table 1).

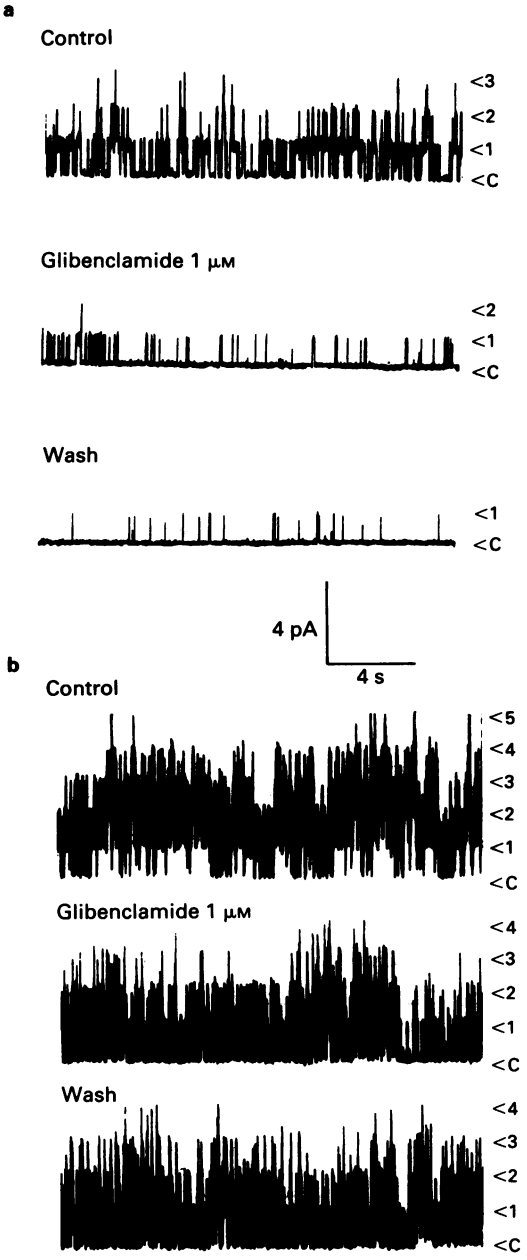

Figure 3 Single channel currents recorded from inside-out membrane patches exposed to symmetrical 140 mM KCl held at a membrane potential of +40 mV. Single channel openings are denoted by upward deflections (outward currents). (a) Glibenclamide (1 μM) in the presence of Mg^{2+} (0.65 mM) inhibited the activity of K_{ATP} in a irreversible manner. The values of $N_f.P_o$ were as follows: control 0.804; glibenclamide 0.061; wash 0.021. (b) Glibenclamide (1 μM) in the absence of Mg^{2+} produced a much weaker inhibition of K_{ATP} activity. The values of $N_f.P_o$ were as follows: control 3.550; glibenclamide 2.541; wash 2.765.

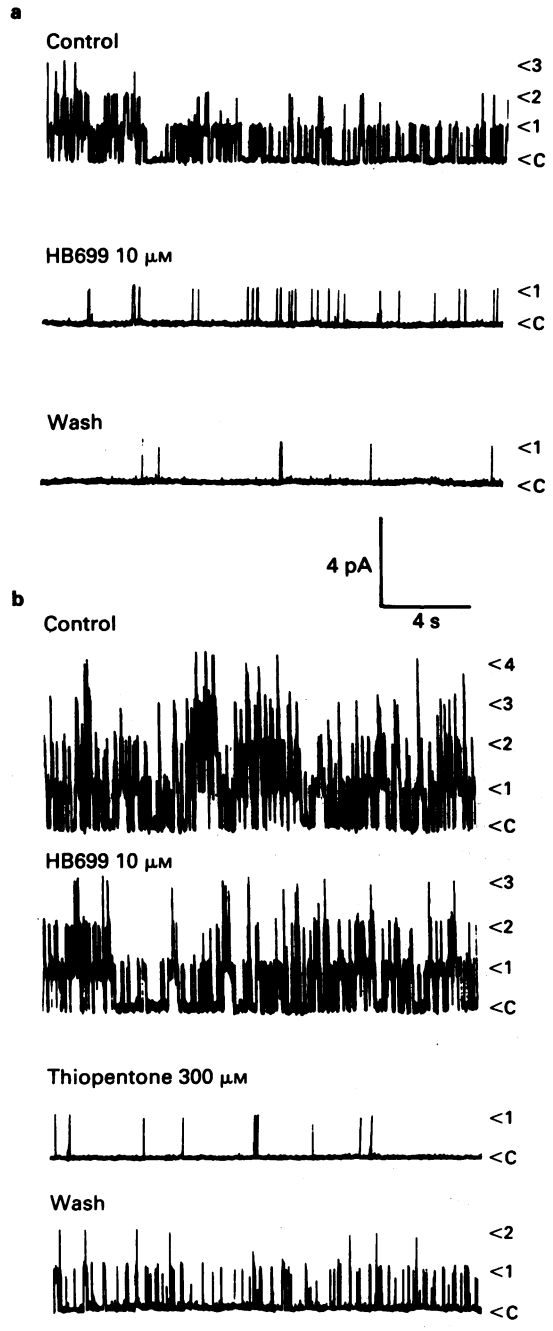

Figure 4 Single channel currents recorded from inside-out membrane patches exposed to symmetrical 140 mM KCl held at a membrane potential of +40 mV. Single channel openings are denoted by upward deflections (outward currents). (a) Meglitinide (10 μM) (HB 699) in the presence of Mg^{2+} (0.65 mM) inhibited the activity of K_{ATP} in an irreversible manner. The values of $N_f.P_o$ were as follows: control 0.861; HB699 0.032; wash 0.023. (b) Meglitinide (HB699) (10 μM) in the absence of Mg^{2+} produced a much weaker inhibition of K_{ATP} activity. However thiopentone (300 μM) retained its inhibitory effectiveness. The values of $N_f.P_o$ were as follows: control 1.508; HB699 0.978; thiopentone 0.001; wash 0.190.

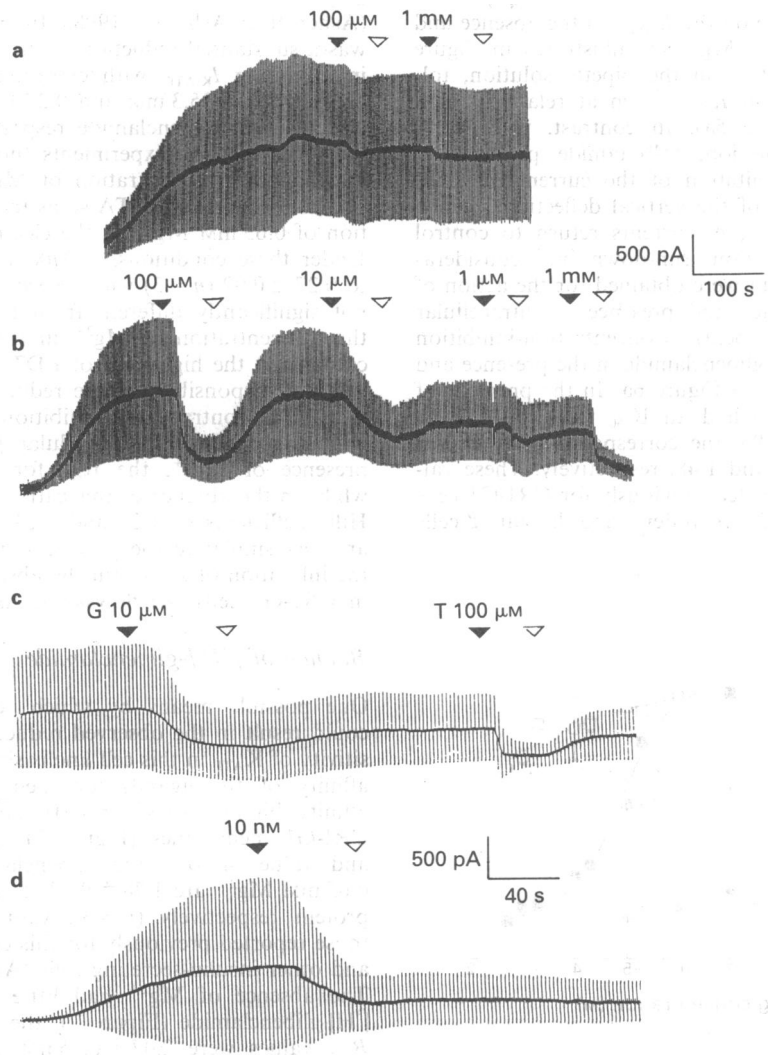

Figure 5 Recordings of whole-cell voltage-clamped $I_{K(ATP)}$ from single CRI-G1 cells. The extracellular solution was A and the pipette solution was either C (a,c) or B (b,d). The cell membrane was clamped at -70 mV and alternate voltage pulses of ± 10 mV, 200 ms in duration were applied at 2 s intervals. The current responses are denoted by the vertical lines. Drug additions are denoted by (▼) and washouts by (▽). (a) In the absence of Mg^{2+} in the pipette solution, tolbutamide (100 μM and 1 mM) produced a very small inhibition of the whole-cell $I_{K(ATP)}$, indicated by a decrease in the size of the current responses and a concomitant shift in the holding current (indicated by the horizontal line). (b) In the presence of Mg^{2+} (0.65 mM) in the pipette solution, tolbutamide induced a clear concentration-dependent inhibition of whole-cell $I_{K(ATP)}$ indicated by the reversible decrease in the size of the current responses. Note the reversible nature of the inhibition elicited by tolbutamide at concentrations below 500 μM. (c) In the absence of Mg^{2+} in the electrode, only high concentrations of glibenclamide, for example 10 μM (denoted in the figure by G 10 μM) produced a significant reduction in the magnitude of the whole-cell $I_{K(ATP}$. Although this inhibition was not reversed on washout of the drug, the current remaining was still sensitive to inhibition by thiopentone (100 μM). (d) In the presence of Mg^{2+} (0.65 mM) in the electrode, $I_{K(ATP)}$ were much more susceptible to inhibition by glibenclamide, 10 nM producing a marked reduction in the magnitude of the current which was also not reversed on wash. Note the slower time-scale for (a) and (b).

In order to determine whether such Mg^{2+}-dependence was typical for all compounds capable of inhibiting K_{ATP} activity, the effects of the barbiturate, thiopentone were also examined in the presence and absence of Mg^{2+}. As shown in Table 1, the inhibitory effects of this compound were not dependent upon the presence of Mg^{2+}. Examples of the inhibitory action of thiopentone in the absence of internal Mg^{2+} are shown for outside-out (Figure 2b) and inside-out (Figure 4b) configurations.

Whole-cell studies

Detailed studies of the concentration-dependence of K_{ATP} inhibitors cannot easily be performed on isolated membrane patches. The principle reasons for this are the wide variations in the channel activity between patches and the phenomenon of channel run-down which occurs in the presence of Mg^{2+} (Kozlowski & Ashford, 1990). In order to obtain reliable data therefore, it is necessary to use relatively high drug concentrations as exemplified by the present study. A more accurate means by which to assess the concentration-dependence of the above compounds is to use the whole-cell configuration (Trube *et al.*, 1986; Sturgess *et al.*, 1988). By allowing dialysis of the cell interior with the pipette solution (and washout of ATP), the overall potassium conductance observed under voltage clamp is due to the increased activation of K_{ATP} (Rorsman & Trube, 1985). As rundown of channel activity occurs (in the presence of Mg^{2+} ions), there is a gradual decline in the observed potassium conductance. Hence by employing this patch clamp configuration, the phenomenon of rundown is now continuous and can be quantified (Sturgess *et al.*, 1988) allowing drugs to be tested over a wide range of concentrations.

The effects of tolbutamide on the $I_{K(ATP)}$ in the absence and presence of 0.65 mM internal Mg^{2+} are illustrated in Figure 5a,b. In the absence of Mg^{2+} in the pipette solution, tolbutamide had little effect on $I_{K(ATP)}$ even at relatively high (mM) concentrations (Figure 5a). In contrast, with Mg^{2+} present in the pipette solution, tolbutamide produced a concentration-dependent inhibition of the current (denoted by the decrease in the size of the vertical deflections) which was reversible on washout. (i.e. currents return to control values taking, by extrapolation, run-down into consideration). Essentially similar data were obtained for the action of glibenclamide in the absence and presence of intracellular Mg^{2+} respectively (Figure 5c,d). Concentration-inhibition curves for tolbutamide and glibenclamide in the presence and absence of Mg^{2+} are shown in Figure 6a. In the presence of 0.65 mM Mg^{2+}, tolbutamide had an IC_{50} value of 12.1 μM and a Hill coefficient of 0.95: the corresponding values for glibenclamide were 2.1 nM and 1.48, respectively. These values are similar to those reported previously for CRI-G1 cells (Sturgess et al., 1988) and for rodent and human β-cells

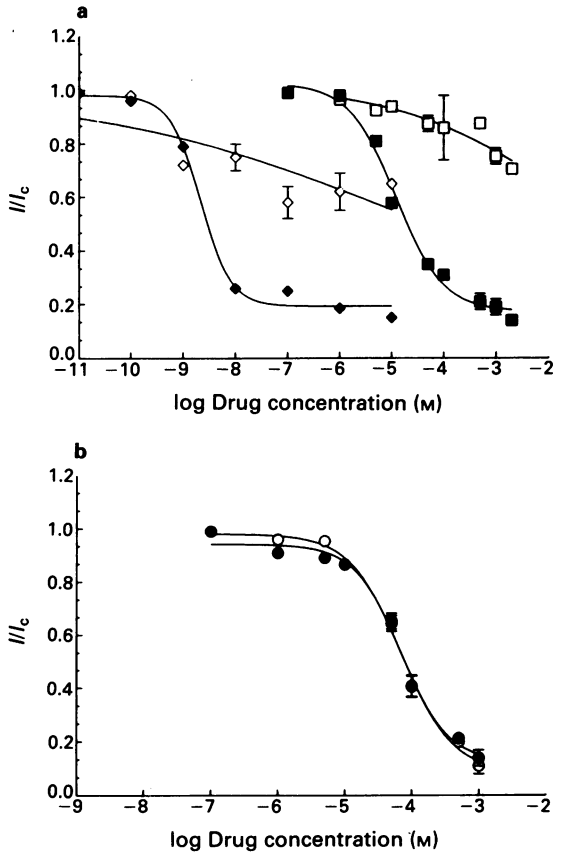

Figure 6 Concentration-inhibition curves for (a) the sulphonylureas, tolbutamide (■, □) and glibenclamide (◆, ◇) and (b) thiopentone (●, ○) upon $I_{K(ATP)}$ recorded using the whole-cell configuration. Solid symbols indicate that the pipette solution contained 0.65 mM free Mg^{2+}; open symbols indicate that the pipette solution was essentially Mg^{2+}-free. In all recordings the bath contained solution A. The cell membrane was clamped at −70 mV and alternate voltage pulses of ± 10 mV were applied. Data are presented as fractions of control currents (I_c), taking run-down into consideration in the experiments where Mg^{2+} was present in the pipette solution. All points are the means of between three and eight separate experiments; vertical lines show s.e.mean and where no vertical lines are shown the s.e.mean was smaller than the symbol. The values for IC_{50} (half maximal inhibitory concentration) were obtained by fitting the data by non linear regression to a modified Hill equation using GraphPAD Inplot (GraphPAD Software, San Diego, U.S.A.). In order to fit curves for tolbutamide and glibenclamide in the absence of Mg^{2+}, the data were fitted assuming the same maximal response as obtained in the presence of Mg^{2+}.

(Ashcroft & Ashcroft, 1990). In the absence of Mg^{2+}, there was a substantial reduction in the effectiveness of both drugs in inhibiting $I_{K(ATP)}$ with extrapolated IC_{50} values and Hill coefficients of 25.3 mM and 0.27 for tolbutamide and 3.6 μM and 0.17 for glibenclamide respectively.

Further control experiments (not shown) were performed in which the concentration of $MgCl_2$ was increased in the presence of 10 mM EDTA so as to give a final free concentration of 0.65 mM Mg^{2+} in the electrode solution (solution F). Under these conditions, 100 μM tolbutamide reduced $I_{K(ATP)}$ to 0.27 ± 0.02 ($n = 3$) with respect to control. This value was not significantly different from the inhibition obtained for this concentration of Mg^{2+} in the absence of EDTA indicating that the high level of EDTA in the electrode solution was not responsible for the reduction in sulphonylurea sensitivity. In contrast, the inhibition of $I_{K(ATP)}$ by thiopentone was independent of intracellular Mg^{2+} (Figure 6b). In the presence of Mg^{2+}, the IC_{50} for thiopentone was 69.4 μM whilst in the absence of this cation the IC_{50} was 69.2 μM with Hill coefficients of 1.25 and 1.13, respectively. These values are very similar to the previously-reported IC_{50} of 62 μM for the inhibition of $I_{K(ATP)}$ (in the absence of intracellular Mg^{2+}) in CRI-G1 cells (Kozlowski & Ashford, 1991).

Binding of [^{3}H]-glibenclamide to CRI-G1 membranes

One possible means by which removal of internal Mg^{2+} could result in the observed reduction of sulphonylurea sensitivity of K_{ATP} in this cell line is simply via a reduction in the affinity of the ligands for their receptor. Saturable high affinity binding sites for [^{3}H]-glibenclamide are present in CRI-G1 membranes (Figure 7). The dissociation constant and value of B_{max} for glibenclamide in the presence of 0.65 mM Mg^{2+} are 1.78 ± 0.27 nM and 1911 ± 202 fmol mg^{-1} protein respectively ($n = 3$); values essentially identical to those reported previously for this cell line (Khan et al., 1993) and other insulin-secreting cells (Ashcroft & Ashcroft, 1992). The absence of Mg^{2+} had little effect on the binding of [^{3}H]-glibenclamide (Figure 7); the dissociation constant and B_{max} values were 2.07 ± 0.15 nM and 1960 ± 318 fmol mg^{-1} protein, respectively ($n = 3$). Thus a reduction of the affinity of the sulphonylureas for their receptor is not the mechanism by which removal of Mg^{2+} induces such a marked reduction in the sensitivity of K_{ATP} to glibenclamide.

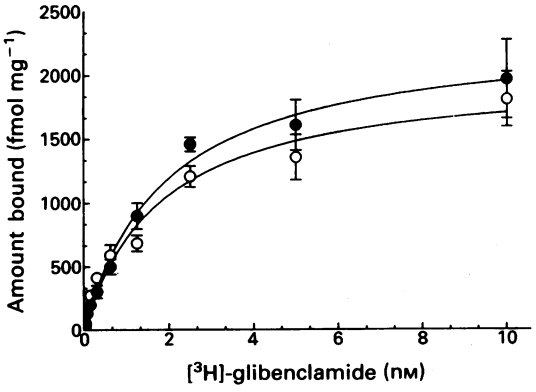

Figure 7 Binding of [^{3}H]-glibenclamide to CRI-G1 membranes. Membranes were incubated with the indicated concentrations of [^{3}H]-glibenclamide in the presence of (0.65 mM; ●) and absence (<3 nM; ○) of Mg^{2+}. Non-specific binding (NSB) was determined in the presence of glibenclamide (1 μM). Results are expressed as fmol [^{3}H]-glibenclamide bound mg^{-1} protein, after subtraction of NSB and are the mean ± s.d. of triplicate determinations. The result of a typical experiment is shown and the best-fit values for K_d and B_{max} are as follows: 2356 ± 139 fmol mg^{-1} protein and 1.74 ± 0.18 nM in the presence of Mg^{2+} and 1900 ± 215 fmol mg^{-1} protein and 1.83 ± 0.41 nM in the absence of Mg^{2+}.

Discussion

In the CRI-G1 insulin-secreting cell line, the present study has clearly shown that the presence of the divalent cation Mg^{2+} is critically important for the hypoglycaemic sulphonylureas to interact with, and therefore inhibit K_{ATP}. This study also suggests that the Mg^{2+} ion must be available at the internal surface of the membrane since removal of this cation from the external solution did not alter K_{ATP} sensitivity to the sulphonylureas. Upon patch formation, K_{ATP} undergoes a time-dependent fall in activity termed run-down which can be prevented by removal of intracellular Mg^{2+} (Kozlowski & Ashford, 1990). However, the difference in the inhibition produced by the sulphonylureas in the presence and absence of intracellular Mg^{2+} cannot be accounted for solely in terms of run-down since under whole-cell recording conditions (where run-down can be quantified), removal of intracellular Mg^{2+} leads to an equally significant loss of sulphonylurea potency.

The fact that a prolonged 'wash' period with EDTA-containing solution was required to achieve these results for inside-out patches might suggest that only very small amounts of Mg^{2+} are necessary for the activity of the sulphonylureas to be retained. This may explain the reason for the different results reported previously (Dunne *et al.*, 1987), as in these studies up to 3 μM Mg^{2+} was available at the intracellular surface. The inability to remove completely K_{ATP} sensitivity to the sulphonylureas may be due to our inability to remove all the Mg^{2+} bound to the membrane. Alternatively, it is possible that a proportion of the inhibitory effect of the sulphonylureas is Mg^{2+}-independent. It may thus simply be related to non-specific inhibition of channel activity as it has been shown that concentrations of glibenclamide in the μM range inhibit certain voltage-dependent potassium currents (Reeve *et al.*, 1992; Crépel *et al.*, 1992).

It has recently been shown (Ripoll *et al.*, 1993) that K_{ATP} of rat ventricular myocytes are inhibited by application of glibenclamide to the internal surface with a half-maximal inhibitory concentration of 6 μM and a Hill coefficient of 0.35. This contrasts with the corresponding values of 6 nM and 1.26 reported by Findlay (1992) in guinea-pig ventricular myocytes. Although the protocols employed in these two studies are not directly comparable, it is interesting to note that no Mg^{2+} was present in the intracellular solution in the experiments of Ripoll *et al.* (1993) whereas Findlay (1992) used a Mg^{2+}-containing (1.4 mM) solution. The differences between these two sets of data in ventricular myocytes are thus remarkably similar to those observed in the present study in insulin-secreting cells both with respect to the magnitude of the shift in the half-maximal inhibitory concentration for glibenclamide and in the reduction of the value of the Hill coefficient. Consequently we suggest that it is the absence of intracellular Mg^{2+} that has induced such a dramatic alteration in glibenclamide sensitivity of the cardiac K_{ATP} as reported by Ripoll *et al.* (1993).

In the present study the reduction in effectiveness of the sulphonylureas upon removal of Mg^{2+} was evident at both depolarizing and hyperpolarizing potentials and thus the site at which Mg^{2+} interacts with the sulphonylurea receptor/K_{ATP} does not appear to sense the membrane field. The inability of Mn^{2+} to substitute for Mg^{2+} in this process is evidence for a specific interaction involving Mg^{2+}. The need for a prolonged washout period led to difficulties in assessing the ability of Mn^{2+} to substitute for Mg^{2+} since Mn^{2+} can itself induce channel rundown (Kozlowksi & Ashford, 1990). Because of this a prolonged wash period (using Mn^{2+}-containing saline) to remove bound Mg^{2+} could not be performed. Thus the greater inhibition achieved by tolbutamide in these experiments, as opposed to the Mg^{2+}-free experiments, may have arisen as a result of the failure to remove completely all the intracellular Mg^{2+}. Alternatively, it may be that Mn^{2+} can only partially mimic the effects of Mg^{2+}, which is in contrast to the ability of Mn^{2+} to mimic Mg^{2+} in inducing K_{ATP} run-down (Kozlowksi & Ashford, 1990). It is interesting to note that Mn^{2+} was also unable to mimic Mg^{2+} in its interaction with diazoxide, regardless of the species of nucleotide present (Kozlowski & Ashford, 1992).

In order to account for these observations, it may be necessary to assume that at least two binding sites for Mg^{2+} are associated with the K_{ATP}/sulphonylurea receptor complex. One of these, at which Mn^{2+} can act to replace Mg^{2+} is linked to processes such as channel rundown. The other site, which is more specific for Mg^{2+}, is involved in the stimulatory and inhibitory effects of diazoxide and of the sulphonylureas, respectively. It has recently been suggested that certain nucleotides in the presence of Mg^{2+} can enhance the effectiveness of both sulphonylureas and diazoxide on K_{ATP} in pancreatic β-cells. (Schwanstecher *et al.*, 1992a). However, in view of the data obtained in the present study, we feel that the models proposed by these authors do not indicate the full importance of Mg^{2+} in the interaction between the sulphonylurea receptor and K_{ATP}.

Meglitinide (a non-sulphonylurea) also exhibits dependence on Mg^{2+} for its inhibitory effects upon K_{ATP} which suggests that the mechanism by which this agent acts is similar to that of the sulphonylureas. The structural differences between tolbutamide and meglitinide (which is a benzoic derivative) may lead one to infer that these agents are unlikely to interact with the same binding site. Thus from the data of the present study it would follow that both putative sites require the presence of Mg^{2+} ions for the functional coupling of inhibitory receptor and K_{ATP}. However, in the two-site model for the interaction of sulphonylureas with their recognition site, it was suggested (Brown & Foubister, 1984) that the carboxyl group of meglitinide is able to interact with the same site as the SO_2 NHCONH group of the sulphonylureas. Thus in this model, only a single Mg^{2+}-dependent site is required to allow functional coupling. Our data do not allow us to discriminate between these models.

It is clear from our [^{3}H]-glibenclamide binding studies that removal of Mg^{2+} had no significant effect on the number or affinity of sulphonylurea receptors in CRI-G1 membranes. Previous studies have also indicated that Mg^{2+} does not influence the radioligand binding characteristics of glibenclamide to high affinity sites (compare values in Panten *et al.*, 1989 (no Mg^{2+} added) with Schwanstecher *et al.*, 1991 (1 mM Mg^{2+} present)). Following these observations and given the large reduction in the Hill coefficients for tolbutamide and glibenclamide in the absence of Mg^{2+} to values substantially less than one, we suggest that the absence of intracellular Mg^{2+} functionally uncouples the sulphonylurea receptor from the K_{ATP}. The residual inhibition induced by high concentrations of these agents may simply reflect a non-specific, much more general interaction with K^+ channels. Consequently we suggest that removal of intracellular Mg^{2+} does not alter the affinity of ligands for the sulphonylurea receptor. Instead it induces a loss or substantial reduction in the inhibitory efficacy of the ligand-receptor interaction. The ability of both thiopentone and ATP to inhibit K_{ATP} in the absence of Mg^{2+} suggests that the Mg^{2+}-dependence of K_{ATP} inhibition by ligands at the sulphonylurea receptor is specific for such agents and may eventually provide important clues regarding structural interactions between the sulphonylurea receptor and the channel protein.

K.L. is a Wellcome Prize Student. This work was supported by the Wellcome Trust and the MRC.

References

ASHCROFT, F.M. & KAKEI, M. (1989). ATP sensitive K^+ channels in rat pancreatic β cells: Modulation by ATP and Mg^{2+} ions. *J. Physiol.*, **416**, 349–367.

ASHCROFT, S.J.H. & ASHCROFT, F.M. (1990). Properties and functions of ATP sensitive K^+ channels. *Cell. Signal.*, **2**, 197–214.

ASHCROFT, S.J.H. & ASHCROFT, F.M. (1992). The sulphonylurea receptor. *Biochem. Biophys. Acta*, **1175**, 45–59.

ASHFORD, M.L.J. (1990). Potassium channels and modulation of insulin secretion. In *Potassium Channels: Structure, Classification, Function and Therapeutic Potential.* ed. Cook, N.S. pp. 300–325. Chichester: Ellis Horwood Limited.

BRADFORD, M.M. (1976). A rapid and sensitive method for the quantitation of microgram quantities of protein utilizing the principle of protein-dye binding. *Anal. Biochem.*, **72**, 248–254.

BROWN, G.R. & FOUBISTER, A.J. (1984). Receptor binding sites of hypoglycaemic sulphonylureas and related [(acylamino) alkyl] benzoic acids. *J. Med. Chem.*, **27**, 79–81.

CARRINGTON, C.A., RUBERY, E.D., PEARSON, E.C. & HALES, C.N. (1986). Five new insulin-producing cell lines with differing secretory properties. *J. Endocrinol.*, **109**, 193–200.

CIANI, S. & RIBALET, B. (1988). Ion permeation and rectification in ATP sensitive channels from insulin secreting cells (RIN m5F): effects of K^+, Na^+ and Mg^{2+}. *J. Membr. Biol.*, **103**, 171–180.

CREPEL, V., KRNJEVIC, K. & BEN ARI, Y. (1992). Glibenclamide depresses the slowly inactivating outward current (I_D) in hippocampal neurons. *Can J. Physiol. Pharmacol.*, **70**, 306–307.

DEMPSTER, J. (1988). Computer analysis of electrophysiological signals. In *Microcomputers in Physiology: A Practical Approach.* ed. Fraser, P.J. pp. 51–95. Oxford: IRL Press.

DUNNE, M.J., ILLOT, M.C. & PETERSON, O.H. (1987). Interaction of diazoxide, tolbutamide and ATP^{4-} on nucleotide dependent K^+ channels in an insulin secreting cell line. *J. Membr. Biol.*, **99**, 215–224.

FINDLAY, I. (1987). The effects of magnesium upon adenosine triphosphate sensitive potassium channels in a rat insulin secreting cell line. *J. Physiol.*, **391**, 611–629.

FINDLAY, I. & DUNNE, M.J. (1986). ATP maintains ATP inhibited K^+ channels in an operational state. *Pflügers Arch.*, **407**, 238–240.

FINDLAY, I. (1992). Inhibition of ATP-sensitive K^+ channels in cardiac muscle by the sulphonylurea drug glibenclamide. *J. Pharmacol. Exp. Ther.*, **261**, 540–545.

HAMILL, O.P., MARTY, A., NEHER, E., SAKMANN, B. & SIGWORTH, F.J. (1981). Improved patch clamp techniques for high resolution current recording from cells and cell free membrane patches. *Pflügers Arch.*, **391**, 85–100.

HOPKINS, W.F,. FATHERAZI, S., PETER-RIESCH, B., CORKEY, B.E. & COOK, D.L. (1992). Two sites for adenine-nucleotide regulation of ATP-sensitive potassium channels in mouse pancreatic β-cells and HIT cells. *J. Membr. Biol.*, **129**, 287–295.

KHAN, R.N., HALES, C.N., OZANNE, S.E., ADOGU, A.A. & ASHFORD, M.L.J. (1993). Dissociation of K_{ATP} channel and sulphonylurea receptor in the rat clonal insulin secreting cell line, CRI-D11. *Proc. R. Soc. B.*, **253**, 225–231.

KOZLOWSKI, R.Z. & ASHFORD, M.L.J. (1990). ATP-sensitive K^+-channel run-down is Mg^{2+} dependent. *Proc. Soc. B.*, **240**, 397–410.

KOZLOWSKI, R.Z. & ASHFORD, M.L.J. (1991). Barbiturates inhibit ATP-K^+ channels and voltage-activated currents in CRI-G1 insulin secreting cells. *Br. J. Pharmacol.*, **103**, 2021–2029.

KOZLOWSKI, R.Z. & ASHFORD, M.L.J. (1992). Nucleotide-dependent activation of K_{ATP} channels by diazoxide in CRI-G1-insulin secreting cells. *Br. J. Pharmacol.*, **107**, 34–43.

KOZLOWSKI, R.Z., HALES, C.N. & ASHFORD, M.L.J. (1989). Dual effects of diazoxide on ATP-K^+ currents recorded from an insulin-secreting cell line. *Br. J. Pharmacol,.* **97**, 1039–1050.

LEE, K. & ASHFORD, M.L.J. (1993). Mg^{2+} dependent inhibition of K_{ATP} channels by sulphonylureas in CRI-G1 insulin-secreting cells. *Br. J. Pharmacol.*, **108**, 35P.

OHNO-SHOSAKU, T., ZUNKLER, B.J. & TRUBE, G. (1987). Dual effects of ATP on K^+ currents of mouse pancreatic β-cells. *Pflügers Arch.*, **408**, 133–138.

PANTEN, U., BURGFIELD, J., GOERKE, F., RENNICKE, M., SCHWANSTECHER, M., WALLASCH, A., ZUNKLER, B.J. & LENZEN, S. (1989). Control of insulin secretion by sulfonylureas, meglitinide and diazoxide in relation to their binding to the sulfonylurea receptor in pancreatic islets. *Biochem. Pharmacol.*, **38**, 1217–1229.

REEVE, H.L., VAUGHAN, P.F.T. & PEERS, C. (1992). Glibenclamide inhibits a voltage gated K^+ current in the human neuroblastoma cell line SH-SY5Y. *Neurosci. Lett.*, **135**, 37–40.

RIPOLL, C., LEDERER, W.J. & NICHOLS, C.G. (1993). On the mechanism of inhibition of K_{ATP} channels by glibenclamide in rat ventricular myocytes. *J. Cardiovasc. Electrophysiol.*, **4**, 38–47.

RORSMAN, P. & TRUBE, G. (1985). Glucose dependent K^+-channels in pancreatic β cells are regulated by intracellular ATP. *Pflügers Arch.*, **405**, 305–309.

SCHWANSTECHER, C., DICKEL, C., EBERS, I., LINS, S., ZUNKLER, B.J. & PANTEN, U. (1992a). Diazoxide-sensitivity of the adenosine 5'-triphosphate-dependent K^+ channel in mouse pancreatic β-cells. *Br. J. Pharmacol.*, **107**, 87–94.

SCHWANSTECHER, C., DICKEL, C. & PANTEN, U. (1992b). Cytosolic nucleotides enhance the tolbutamide sensitivity of the ATP-dependent K^+ channel in mouse pancreatic β cells by their combined actions at inhibitory and stimulatory receptors. *Mol. Pharmacol.*, **41**, 480–486.

SCHWANSTECHER, M., LÖSER, S., RIETZE, I. & PANTEN, U. (1991). Phosphate and thiophosphate group denoting adenine and guanine nucleotides inhibit glibenclamide binding to membranes from pancreatic islets. *Naunyn Schmied. Arch. Pharmacol.*, **343**, 83–89.

STURGESS, N.C., KOZLOWSKI, R.Z., CARRINGTON, C.A., HALES, C.N. & ASHFORD, M.L.J. (1988). Effects of sulphonylureas and diazoxide on insulin secretion and nucleotide-sensitive channels in an insulin-secreting cell line. *Br. J. Pharmacol.*, **95**, 83–94.

TRUBE, G., RORSMAN, P. & OHNO SHOSAKU, T. (1986). Opposite effects of tolbutamide and diazoxide on the ATP dependent K^+ channel in mouse pancreatic β-cells. *Pflügers Arch.*, **407**, 493–499.

(Received July 13, 1993
Revised October 15, 1993
Accepted October 25, 1993)

Br. J. Pharmacol. (1994), **111**, 641–647

Inhibition by salbutamol of the proliferation of human airway smooth muscle cells grown in culture

[1]Paul R. Tomlinson, *John W. Wilson & Alastair G. Stewart

Microsurgery Research Centre, St. Vincent's Hospital, Fitzroy 3065, Victoria, Australia and *Department of Respiratory Medicine, Alfred Hospital, Prahran 3181, Victoria, Australia.

1 β_2-Adrenoceptor agonists may exacerbate asthma by reducing the release of the anti-proliferative and anti-inflammatory molecule, heparin from mast cells in the airway. In this study, the direct effects of the clinically used bronchodilator, salbutamol, on the proliferation of airway smooth muscle cells grown in culture and stimulated with a range of mitogens have been examined.

2 In mitogen-stimulated cells, salbutamol (0.1–100 nM) inhibited [^{3}H]-thymidine incorporation in a concentration-dependent manner. Salbutamol (100 nM) pretreatment reduced the mitogenic responses to thrombin (0.3 u ml^{-1}), epidermal growth factor (EGF) (300 pM) and U46619 (100 nM) by 61.7 ± 6.1%, 46.9 ± 13.9% and 57.6 ± 12.7%, respectively. However, salbutamol pretreatment did not appear to reduce the small mitogenic response to endothelin-1.

3 Increases in [^{3}H]-leucine incorporation in thrombin (0.3 u ml^{-1})-stimulated cells were reduced by salbutamol (100 nM) by 27.7 ± 2.8%. Similarly, thrombin (0.3 u ml^{-1})-stimulated increases in cell number were also inhibited by salbutamol (100 nM) pretreatment. Thus, the effect of salbutamol in decreasing thrombin-induced [^{3}H]-leucine incorporation may, at least in part, be explained by inhibition of cell proliferation.

4 The inhibition of cell proliferation by salbutamol was prevented by pretreatment with either the non-selective β-adrenoceptor antagonist, propranolol (0.3 μM) or the selective β_2-adrenoceptor antagonist, ICI 118551 (50 nM).

5 These results indicate that salbutamol, through activation of a β_2-adrenoceptor, has a direct inhibitory effect on proliferation elicited by the mitogens thrombin, EGF, and U46619. Thus, it seems likely that this direct inhibitory action of β_2-adrenoceptor agonists would override any indirect action to accelerate airway smooth muscle proliferation. These observations lead us to suggest that β_2-adrenoceptor agonists exacerbate asthma by mechanisms unrelated to airway smooth muscle proliferation.

Keywords: Asthma; β_2-adrenoceptor agonists; salbutamol; propranolol; ICI 118551; thrombin; epidermal growth factor; endothelin-1; U46619; airway smooth muscle cell proliferation

Introduction

Asthma is regarded as a disease characterized by reversible airway obstruction and nonspecific bronchial hyperresponsiveness. Evidence gained from studies of submucosal biopsy tissue from mild asthmatics has shown the presence of eosinophils and mast cells with morphological features of activation in the submucosa and epithelium, which suggests the presence of underlying chronic inflammation (Beasley *et al.*, 1989; Jeffery *et al.*, 1989). Pathological findings in *post mortem* tissues from patients that have died in *status asthmaticus* have shown: occlusion of bronchial lumen with mucus; loss of ciliated epithelium; eosinophil infiltration of the submucosa; hyperplasia of mucous glands; thickening of the airway wall as a result of increased collagen deposition in the basement membrane; and hypertrophy and hyperplasia of bronchial smooth muscle (Dunnill *et al.*, 1969; Hossain, 1973). It has been proposed that the thickened airway wall could be as important as smooth muscle shortening in determing airway responsiveness in asthmatics (James *et al.*, 1989; Wiggs *et al.*, 1992).

Until recently, treatment of asthma has relied on the reduction of bronchospasm by the use of β_2-adrenoceptor agonists to increase airway wall calibre by smooth muscle relaxation. However, concern over an increase in asthma morbidity and mortality linked to β_2-adrenoceptor agonist usage has focussed research on the inflammatory aspect of asthma (Anderson, 1989; Sears *et al.*, 1990; Ernst *et al.*, 1993). It has been suggested that the inhibition of mast cell degranulation by β_2-adrenoceptor agonists may deprive airway tissue of the potentially anti-inflammatory effects of the heparin released from mast cell granules (Page, 1991). In addition, heparin may act as an antiproliferative agent, since it inhibits the growth of vascular smooth cells (Clowes & Karnowsky, 1977) and also appears to reduce proliferation of canine airway smooth muscle cells (Panettieri *et al.*, 1990). Therefore, prevention of the release of heparin may exacerbate the proliferation of airway smooth muscle in response to mitogens released by damaged epithelial cells, infiltrating eosinophils, and activated macrophages, thus leading to airway wall thickening. However, the direct effects of clinically used β-adrenoceptor agonists on airway smooth muscle proliferation have not been described.

Recent reviews on airway wall remodelling have commented on the paucity of data concerning the factors that influence airway smooth muscle proliferation (Hirst & Twort, 1992; Stewart *et al.*, 1993). In this study, the direct effects of the β_2-adrenoceptor agonist, salbutamol, on smooth muscle cell proliferation have been examined. Human airway smooth muscle derived from non-asthmatic patients was used to establish primary cell cultures. We found that the proliferative effects of thrombin, epidermal growth factor (EGF), and the thromboxane A_2-mimetic, U46619 were inhibited by salbutamol, whereas that induced by endothelin-1 appeared to be resistant to the inhibitory action of salbutamol.

[1] Author for correspondence.

Methods

Cell culture

Human airway smooth muscle cells were harvested from bronchi obtained from lung resections. For each cell culture, 0.1 g of smooth muscle tissue was stripped from the wall of the bronchus. The tissue was initially immersed in Dulbecco's Modified Eagle's Medium (DMEM) (supplemented with 2 mM L-glutamine, 0.25% w/v bovine serum albumin (BSA), 100 u ml^{-1} penicillin-G, 100 $\mu g\ ml^{-1}$ streptomycin and 2 $\mu g\ ml^{-1}$ amphotericin B) containing 3 mg ml^{-1} collagenase for 25 min at 37°C in a humidified incubator containing 5% CO_2 in air. Following the partial digestion, the tissue was rinsed in phosphate buffered saline to remove the epithelium and was cut into small pieces, approximately 2 mm^3. The chopped tissue was digested further by incubation in DMEM (supplemented with 2 mM L-glutamine, 0.25% w/v BSA, 100 u ml^{-1} penicillin-G, 100 $\mu g\ ml^{-1}$ streptomycin and 2 $\mu g\ ml^{-1}$ amphotericin B) containing elastase (0.5 mg ml^{-1}) for 2 h, followed by a 12 h incubation in collagenase (1 mg ml^{-1}), at 37°C. Examination of the tissue upon completion of the digestion revealed a high proportion of single cells. The cells were centrifuged (5 min, 100 g, room temperature) and washed three times in DMEM (supplemented with 2 mM L-glutamine, 0.25% w/v BSA, 100 u ml^{-1} penicillin-G, 100 $\mu g\ ml^{-1}$ streptomycin and 2 $\mu g\ ml^{-1}$ amphotericin B). The final cell resuspension was made in 25 ml of DMEM (supplemented with 10% v/v heat-inactivated foetal calf serum, 2 mM L-glutamine, 100 u ml^{-1} penicillin-G, 100 $\mu g\ ml^{-1}$ streptomycin and 2 $\mu g\ ml^{-1}$ amphotericin B) and the cells were seeded in one 25 cm^2 culture flask. The primary isolates were incubated for 7 days to reach confluency. Thereafter, cells were harvested weekly by 10 min exposure to 0.5% trypsin, 1 mM EDTA and passaged at a 1:3 ratio in 75 cm^2 culture flasks. Cells at passage numbers 3 to 18 were used for experiments.

Immunocytochemistry

The expression of smooth muscle specific α-actin was used to determine the identity of the cultures (Skalli *et al.*, 1986). Cells were subcultured into 8-well glass tissue culture chamber slides. They were allowed to grow to 100% monolayer confluency, in the presence of DMEM (supplemented with 10% v/v heat-inactivated foetal calf serum, 2 mM L-glutamine, 100 u ml^{-1} penicillin-G, 100 $\mu g\ ml^{-1}$ streptomycin and 2 $\mu g\ ml^{-1}$ amphotericin B). The cells were then washed three times in phosphate buffered saline before being fixed in acetone for 7 min at 4°C. Fixed cells were then stored at 4°C for up to 4 weeks before staining. Prior to staining, the fixed cells were rehydrated in phosphate buffered saline containing 1% w/v BSA for 20 min and then exposed to the primary antibody, anti smooth muscle α-actin (mouse monoclonal), for 1 h at room temperature. This was followed by exposure to the secondary antibody, anti-mouse Ig F(ab')2 fragment FITC-conjugate, for 1 h at room temperature. Background staining controls were provided by reversal of the order of antibody exposure. In addition, cells were stained with a monoclonal antibody for the endothelial cell marker, CD31. The staining of the fixed cells was then observed by fluorescence microscopy. Each of the cell lines used in these studies showed uniform staining for smooth muscle specific α-actin, but did not express CD31. Moreover, there did not appear to be any relationship between passage number and the intensity of staining for smooth muscle α-actin.

Proliferation assay

Cells were subcultured into 24 well plates at a 1:3 split ratio and allowed to grow to confluency over a 72 h period. Twenty-four hours before stimulation the medium was re-

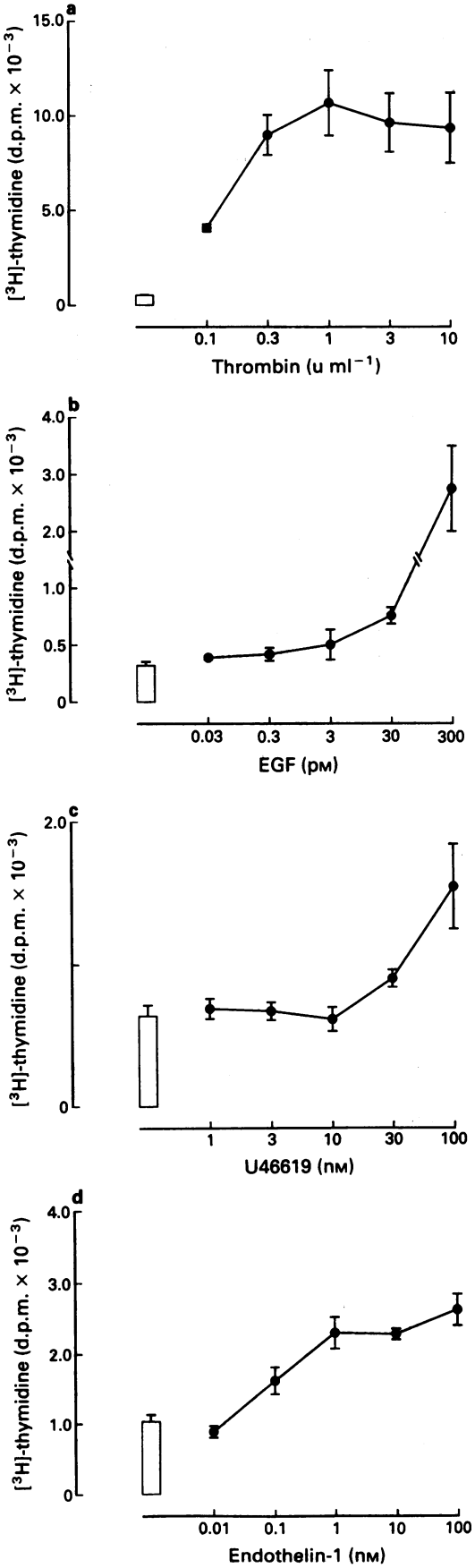

Figure 1 Increase in [^{3}H]-thymidine incorporation in cells stimulated with thrombin (a); epidermal growth factor (EGF) (b); U46619 (c); and endothelin-1 (d). Histograms represent [^{3}H]-thymidine incorporation in unstimulated cells. Data are presented as the mean ± s.e. of quadruplicate incubations conducted in one cell line and are representative of experiments carried out in three cell lines.

placed with DMEM (supplemented with 2 mM L-glutamine, 0.25% w/v BSA, 100 u ml^{-1} penicillin-G, 100 $\mu g\ ml^{-1}$ streptomycin and 2 $\mu g\ ml^{-1}$ amphotericin B). This incubation was designed to deprive the cells of serum mitogens and produce growth arrest to synchronize cells proliferation upon subsequent stimulation. Prior to stimulation, a 30 min preincubation with salbutamol or a 30 min preincubation with a β-adrenoceptor antagonist followed by a salbutamol preincubation was conducted where indicated. Upon stimulation, the putative mitogen and a supplement containing insulin, transferrin and selenium (Monomed A, 1% v/v) were added to the allotted wells. The duration of stimulation with growth factors and growth-promoting substances was 24 h for [^{3}H]-thymidine incorporation assays and 48 h for [^{3}H]-leucine incorporation assays. Cells were incubated for 4 h in the presence of either [^{3}H]-thymidine or [^{3}H]-leucine at a final concentration of 1 $\mu Ci\ ml^{-1}$ to allow their incorporation into DNA and protein, respectively. Harvesting procedures followed the method described by Dicker & Rozengurt (1980), in which the cultures were washed twice in phosphate buffered saline to rinse loosely associated radioactive tracer from the wells. Acid-soluble radioactivity was removed by 20 min treatment with 5% trichloroacetic acid (TCA) at 4°C, followed by washing the cultures twice in 95% ethanol. The remaining material, which represented the acid-insoluble pools, was solubilized by a 30 min incubation with 2% Na_2CO_3 in 0.1 M NaOH. The radioactivity was determined by liquid scintillation counting. Cell counting was conducted on cells that were subcultured into six well plates at a low seeding density and allowed to grow to 30–40% monolayer confluency in the presence of DMEM (supplemented with 10% v/v heat-inactivated foetal calf serum, 2 mM L-glutamine, 100 u ml^{-1} penicillin-G, 100 $\mu g\ ml^{-1}$ streptomycin and 2 $\mu g\ ml^{-1}$ amphotericin B). A 24 h serum deprivation period preceded mitogen stimulation, which was conducted in the manner described above. However, a 5 day incubation period was used before the cells were harvested with 0.1% trypsin for 1 h at 37°C and counted in a haemocytomer. The initial low seeding density and prolonged incubation were required to obtain increases in the number of thrombin-stimulated cells of a sufficient magnitude to detect statistically inhibitory effects of salbutamol.

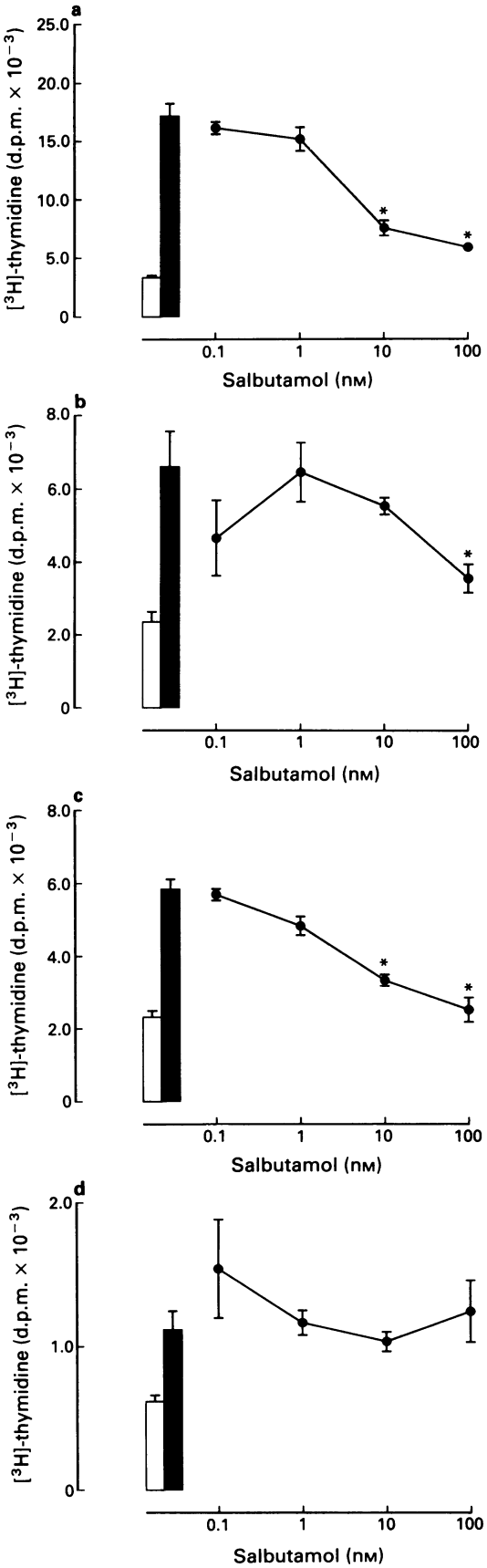

Materials

All chemicals used were of analytical grade or higher. The compounds used and their sources were as follows: L-glutamine, essentially fatty acid free bovine serum albumin fraction V (BSA), thrombin (bovine plasma), human recombinant [Leu^{21}]-epidermal growth factor (EGF), U46619 (9,11-dideoxy-11α,9α-epoxymethano-prostaglandin $F_{2\alpha}$), salbutamol (α-[(*t*-butylamino) methyl]-4-hydroxy-*m*-xylene-α,α′-diol), (±)-propranolol (1-[isopropylamino]-3-[1-naphthyloxy]-2-propanol), Sigma, U.S.A.; ICI 118551 (erythro-(±)-1-(7-methylindan-4-yloxy)-3-isopropylaminobutan-2-ol), Research Biochemicals International, U.S.A.; amphotericin B (Fungizone), Gibco Laboratories, U.S.A.; collagenase type CLS 1, elastase, Worthington Biochemical, U.S.A.; Dulbecco 'A' phosphate buffer saline (PBS), Oxoid, England; trypsin, versene, penicillin-G, streptomycin, Monomed A, CSL, Australia; foetal calf serum (FCS), Flow Laboratories, Australia; Dulbecco's Modified Eagle's Medium (DMEM). Flow Laboratories, Scotland; endothelin-1 (human, porcine), Auspep, Australia; [6-^{3}H]-thymidine (185 GBq $mmol^{-1}$, 5 Ci $mmol^{-1}$), Amersham, UK; L-[4,5-^{3}H(N)]-leucine (2.0 TBq $mmol^{-1}$, 54

Figure 2 Inhibition by salbutamol (●) of [^{3}H]-thymidine incorporation in cells stimulated with thrombin (0.3 u ml^{-1}) (a); epidermal growth factor (EGF, 300 pM) (b); and U46619 (100 nM) (c). Salbutamol fails to inhibit [^{3}H]-thymidine incorporation in endothelin-1 (100 nM)-stimulated cells (d). Histograms represent [^{3}H]-thymidine incorporation in unstimulated cells (open columns) and cells stimulated with mitogen (solid column). Data are presented as the mean ± s.e. of quadruplicate incubations conducted in one cell line and are representative of experiments carried out in three cell lines. *$P <$ 0.05, Student's unpaired *t* test, compared to mitogen-stimulated cells.

Ci mmol^{-1}) ICN Radiochemicals, U.S.A.; emulsifier-safe scintillant, Canberra-Packard, Australia. The antibodies used for immunocytochemistry were anti-smooth muscle α-actin (mouse monoclonal) (Dako M851), monoclonal mouse anti-human endothelial cell, CD31 (DAKO-CD31, JC/70A) (Dako M823), Dako Corporation, U.S.A.; and anti-mouse Ig F(ab')2 fragment FITC-conjugate (host sheep) (Silenus DD-AF), Silenus, Australia.

Statistics

Incubations in [^{3}H]-thymidine and [^{3}H]-leucine incorporation assays were carried out in quadruplicate and in three cell lines derived from lung resection specimens obtained from three individuals. Incubations for cell counting experiments were done in duplicate in three cell lines. Results are expressed as mean values ± s.e.means for n cell lines ($n = 3$). Student's t test was used for comparisons between incubations within a cell line. Differences were considered to be statistically significant between quadruplicate incubations when $P < 0.05$. Fold increases were calculated from a baseline of the unstimulated mean of quadruplicate incubations within a cell line. Percentage decreases were calculated from the mean of the [^{3}H]-thymidine incorporation in agonist-stimulated cells (100%) of individual experiments for each of the three cell lines used. The existence of concentration-response relationships for the inhibitory effects of salbutamol were established by regression analyses, testing whether: (1) there was a linear relationship between log concentration and response using the F test; (2) the slope of the regression line differed significantly from 0 by Student's t test.

Results

Mitogen stimulation of [^{3}H]-thymidine incorporation

Thrombin (0.3 u ml^{-1}) elicited the greatest mitogenic response in each of the cell lines examined, causing a 15.3 ± 5.6 fold increase in [^{3}H]-thymidine incorporation ($n = 3$) (Figure 1a). EGF (300 pM) elicited a 6.6 ± 1.7 fold increase in [^{3}H]-thymidine incorporation ($n = 3$) (Figure 1b). Both endothelin-1 and the thromboxane A_2 mimetic, U46619, had similar efficacy in eliciting increases in [^{3}H]-thymidine incorporation. U46619 (100 nM) elicited a 2.4 ± 0.1 fold increase ($n = 3$) (Figure 1c) and endothelin-1 (100 nM) elicited a 2.3 ± 0.1 fold increase in [^{3}H]-thymidine incorporation ($n = 3$) (Figure 1d).

Inhibition of mitogen-stimulated [^{3}H]-thymidine incorporation by salbutamol

Preincubation with the β_2-adrenoceptor agonist, salbutamol (0.1–100 nM), for 30 min prior to mitogen addition, reduced the proliferative response to thrombin, EGF or U46619. Regression analyses indicated that there was a significant concentration-response relationship ($P < 0.05$, Student's t test) for the effect of salbutamol against thrombin, EGF and U46619, but not for endothelin-1 ($P > 0.05$, Student's t test). Pretreatment with salbutamol (100 nM) inhibited the incorporation of [^{3}H]-thymidine in cells stimulated with thrombin (0.3 u ml^{-1}) by 61.7 ± 6.1% ($n = 3$) (Figure 2a); with EGF (300 pM) by 46.9 ± 13.9% ($n = 3$) (Figure 2b); and with U46619 (100 nM) by 57.6 ± 12.7% ($n = 3$) (Figure 2c). Salbutamol had no inhibitory effect on the [^{3}H]-thymidine incorporation in the three cell lines stimulated with endothelin-1 (100 nM) (Figure 2d). A fixed concentration of salbutamol (100 nM) suppressed the incorporation of [^{3}H]-thymidine in cells stimulated with a range of thrombin concentrations (0.1–10 u ml^{-1}), with complete suppression of the mitogenic response being observed at the lower concentrations of thrombin (0.1–1 u ml^{-1}). In addition, salbutamol (100 nM) significantly reduced the [^{3}H]-thymidine incorporation in unstimulated cells ($P < 0.05$, paired Student's t test, $n = 3$) (Figure 3).

Inhibition of thrombin-stimulated [^{3}H]-leucine incorporation and increases in cell number by salbutamol pretreatment

Thrombin (0.3 u ml^{-1}) elicited a 2.0 ± 0.2 fold increase in [^{3}H]-leucine incorporation ($n = 3$). In cells pretreated with salbutamol (100 nM), the thrombin-stimulated [^{3}H]-leucine incorporation was inhibited by 27.7 ± 2.8% ($P < 0.05$, paired Student's t test, $n = 3$). Salbutamol (100 nM) did not significantly reduce [^{3}H]-leucine incorporation in unstimulated cells ($P > 0.05$, Student's paired t test, $n = 3$) (Figure 4).

Cell counting was used to confirm the apparent inhibitory effect that salbutamol had on mitogen-induced proliferation.

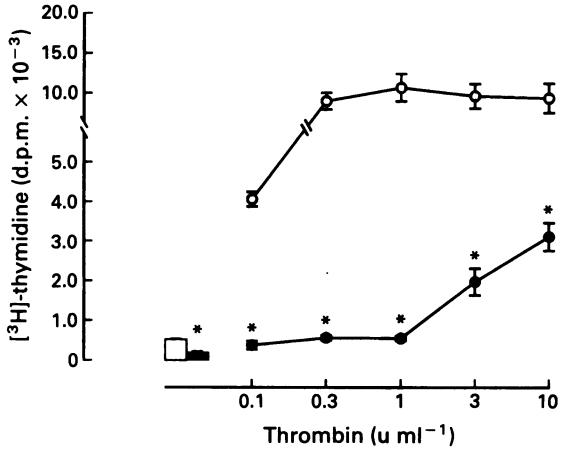

Figure 3 The inhibitory effect of salbutamol (100 nM) (●) on thrombin (0.1–10 u ml^{-1})-induced [^{3}H]-thymidine incorporation (○). Histograms represent [^{3}H]-thymidine incorporation in unstimulated cells in the absence (open columns) or presence (solid column) of salbutamol. Data are presented as the mean ± s.e. of quadruplicate incubations conducted in one cell line and are representative of experiments carried out in three cell lines. *$P < 0.05$, Student's unpaired t test, compared with unstimulated cells in the absence of salbutamol.

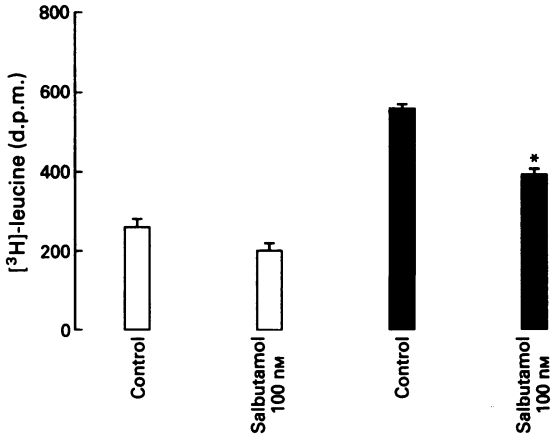

Figure 4 Inhibition by salbutamol (100 nM) of [^{3}H]-leucine incorporation in unstimulated cells (open columns) and thrombin (0.3 u ml^{-1})-stimulated cells (solid columns). Data are presented as the mean ± s.e. of quadruplicate incubations conducted in one cell line and are representative of experiments carried out in three cell lines. *$P < 0.05$, Student's unpaired t test, compared to thrombin-stimulated cells.

Thrombin (0.3 u ml^{-1}) elicited a 2.6 ± 0.5 fold increase in cell number in the three cell lines; salbutamol (100 nM) prevented the increase in cell number ($P<0.05$, Student's paired t test, $n=3$) (Table 1).

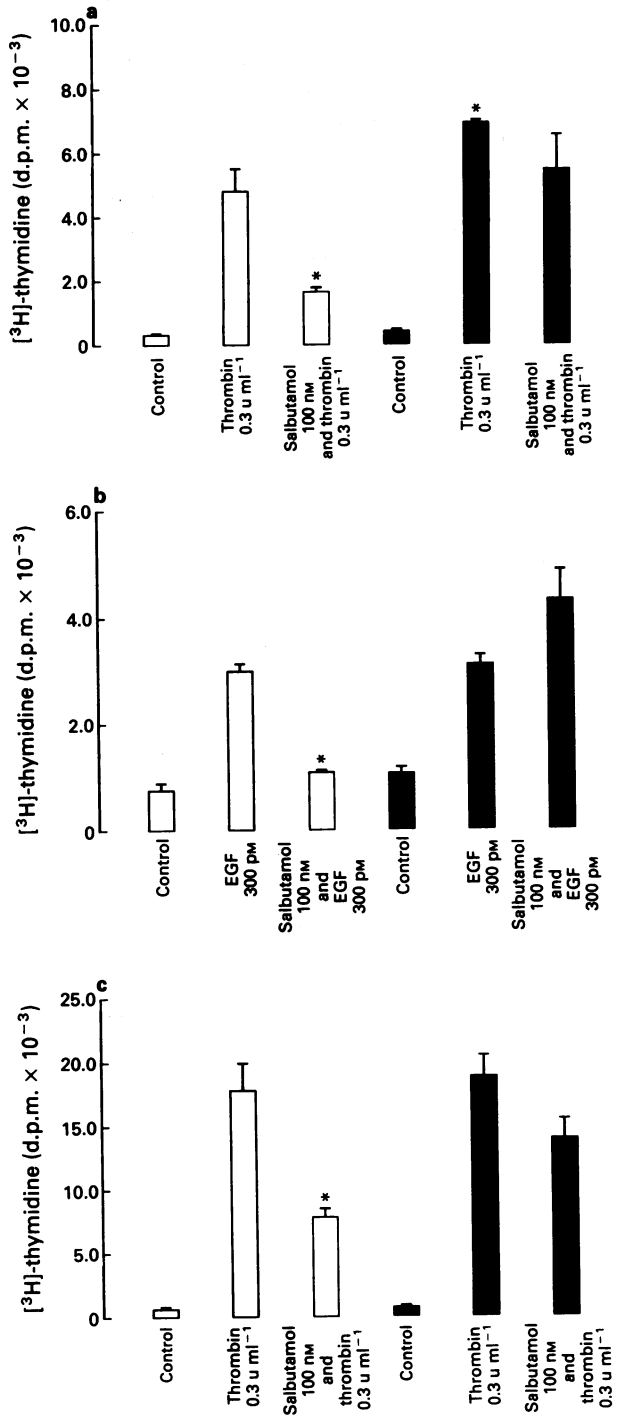

Effects of β-adrenoceptor antagonists on inhibition of mitogen-stimulated [^{3}H]-thymidine incorporation by salbutamol pretreatment

Incubation with either the non-selective β-adrenoceptor antagonist, propranolol or the selective β_2-adrenoceptor antagonist, ICI 118551 was used to determine whether the inhibitory effects of salbutamol were receptor-dependent. Cells were preincubated with either antagonist for 30 min before the addition of salbutamol. Pretreatment with propranolol (0.3 μM) prevented the inhibitory effect of salbutamol (100 nM) on [^{3}H]-thymidine incorporation in cells that had been stimulated with either thrombin (0.3 u ml^{-1}) (Figure 5a) or EGF (300 pM) (Figure 5b). The propranolol (0.3 μM) pretreatment also significantly augmented the stimulant effect of thrombin (0.3 u ml^{-1}) ($P<0.05$, Student's paired t test; $n=3$). Pretreatment with ICI 118551 (50 nM) prevented the inhibitory effect of salbutamol (100 nM) on [^{3}H]-thymidine incorporation in thrombin (0.3 u ml^{-1})-stimulated cells (Figure 5c).

Discussion

We have demonstrated that the widely used bronchodilator, salbutamol has a direct inhibitory effect on mitogen-induced proliferation of airway smooth muscle cells. This effect is mediated via a β_2-adrenoceptor. However, salbutamol appeared to lack an inhibitory effect on the small degree of cell proliferation elicited by endothelin-1.

Airway epithelial cells produce endothelin-1 in culture (Black *et al.*, 1989), and bronchial epithelial cells from asthmatics express preproendothelin-1 mRNA and release the mature and biologically active peptide when incubated over a 48 h period (Vittori *et al.*, 1992). Thus, endothelin may have a role in acute and chronic asthma (Hay *et al.*, 1993). Endothelin-1 elicits the proliferation of rabbit (Noveral *et al.*, 1992), guinea-pig (Stewart *et al.*, 1993) and ovine (Glassberg *et al.*, 1992) airway smooth muscle cells grown in culture. In this study we have shown that endothelin-1 also has a small proliferative effect in human airway smooth muscle, which is prevented by the selective endothelin$_A$ (ET_A) receptor antagonist, BQ123 (Stewart, Harris & Tomlinson, unpublished

Figure 5 Prevention by propranolol (0.3 μM) of salbutamol-induced inhibition of [^{3}H]-thymidine incorporation in cells stimulated with thrombin (a) and epidermal growth factor (EGF) (b). Histograms represent incubations without propranolol pretreatment (open columns) and incubations with propranolol pretreatment (solid columns). Prevention by ICI 118551 (50 nM) of salbutamol-induced inhibition of [^{3}H]-thymidine incorporation in cells stimulated with thrombin (c). Histograms represent incubations without (open columns) and incubations with ICI 118551 pretreatment (solid columns). Data are presented as the mean ± s.e. of quadruplicate incubations conducted in one cell line and are representative of experiments carried out in three cell lines. *$P<0.05$, Student's unpaired t test, compared to cells treated with mitogen alone (column 2) or compared to cells treated with mitogen and propranolol (column 5).

Table 1 The effect of salbutamol (100 nM) on thrombin (0.3 u ml^{-1})-induced increases in cell number

Cell number (× 10^{-4}/cm^2)		
Control	Thrombin (0.3 u ml^{-1})	Thrombin (0.3 u ml^{-1}) + salbutamol (100 nM)
2.3 ± 0.38	6.0 ± 1.5*	2.6 ± 0.57 NS

Data represent the means and s.e.mean of three experiments using three cell lines, each experiment being carried out in duplicate.
*$P<0.05$, paired Student's t test, compared to control.
NS not significant.

observations). A possible explanation for the lack of an inhibitory effect of salbutamol on endothelin-1-stimulated incorporation of [^{3}H]-thymidine is suggested by the observation that in rat aortic smooth muscle cell, adenosine 3':5'-cyclic monophosphate (cyclic AMP) increases the number of ET_A receptors. The resulting effect was an increased intracellular calcium rise in response to endothelin-1 stimulation (Nishimura *et al.*, 1992). Alternatively, it has been reported that ET_A receptors are themselves linked to elevation of cyclic AMP (Aramori & Nakanishi, 1992). Thus, endothelin-1 may maximally stimulate increases in cyclic AMP levels and therefore further stimulation by pretreatment with salbutamol may be of no consequence. This possibility may also explain why the effects of endothelin-1 are modest, for the endothelin-1 induced increases in cyclic AMP may lead to a self-limiting effect on cell proliferation.

The proliferation responses to optimal concentrations of EGF, U44619 and thrombin stimulated cells were partially inhibited by salbutamol pretreatment. It is important to note that the proliferative effects of submaximal concentrations of thrombin were completely blocked by 100 nM salbutamol. Further experiments are required to establish whether there is a receptor reserve for this β-adrenoceptor-mediated action. In addition, it will be of considerable relevance to the current debate regarding the prophylactic versus the symptomatic use of β-adrenoceptor agonists (Barnes & Chung, 1992) to determine whether salbutamol inhibits proliferation responses that have already been initiated by growth factors or bronchoconstrictors and to examine interactions between salbutamol and other anti-asthma agents. These experiments would mimic the so-called symptomatic use of β-adrenoceptor agonists.

Our findings are consistent with the report that a very high concentration of isoprenaline (100 μM) reduced proliferation of human airway smooth muscle cells (Panettieri *et al.*, 1991). The concentration range of salbutamol used in this study is about half a log unit lower than that which has been reported previously to relax isolated human airway smooth muscle (Raffestin *et al.*, 1985; Goldie *et al.*, 1986). Therefore, the therapeutic dose may be supramaximal for the direct inhibitory effect of salbutamol on proliferation of airway smooth muscle. The inhibitory effects of salbutamol were blocked by concentrations of ICI 118551 and propranolol that are regraded as specific (Hall *et al.*, 1992). However, there was a significant increase in [^{3}H]-thymidine incorporation by cells incubated with propranolol and thrombin, compared to thrombin stimulation alone, which merits further investigation. The complete block of the response to the β_2-selective adrenoceptor agonist, salbutamol by the β_2-selective antagonist, ICI 118551 constitutes strong evidence of a β_2-adrenoceptor-mediated effect. We cannot completely exclude the possibility that β_1-adrenoceptor stimulation plays a role, since the effects of β_1-adrenoceptor selective antagonist were not examined in this study.

Isoprenaline stimulates an increase in cyclic AMP levels in human cultured tracheal smooth muscle cells via activation of β_2-adrenoceptors (Hall *et al.*, 1992). Elevation of cyclic AMP has been linked to increases in proliferation of rat parotid cells *in vivo* and *in vitro* (Tsang *et al.*, 1980) and of dog thyroid cells (Roger *et al.*, 1983). However, in rat arterial smooth muscle cells, increases in intracellular concentrations of cyclic AMP elicited by prostaglandin E_1 (Nilsson & Olsson, 1984) or adenosine (Jonzon *et al.*, 1985) have been shown to inhibit proliferation. In addition, activation of adenylyl cyclase activity inhibits thrombin-stimulated mitogenesis in human vascular smooth muscle (Kanthou *et al.*, 1992). Thus, the component of the mitogen-stimulated increases in proliferation induced by thrombin, EGF or U46619, that are partially inhibited by β_2-adrenoceptor stimulation, may represent the cyclic AMP-sensitive component of the signal transduction mechanism stimulated by these agents. A recent study indicates that injection of the catalytic subunit of cyclic AMP-dependent protein kinase inhibits proliferation induced by EGF, and to a much greater extent, that induced by the protein kinase C stimulant, phorbol myristate acetate (Panettieri *et al.*, 1993). The relationship between these differential inhibitory effects and the apparent lack of effect of salbutamol on the mitogenic response to endothelin-1 requires further elucidation.

Airway wall remodelling, and in particular, smooth muscle proliferation is regarded as an important component of bronchial hyperresponsiveness (James *et al.*, 1989; Wiggs *et al.*, 1992). Chronic, regular β_2-adrenoceptor agonist usage has been linked to an exacerbation of asthma and of airway hyperresponsiveness (Anderson, 1989; Sears *et al.*, 1990; Ernst *et al.*, 1993). One suggested explanation relates to the possibility that β_2-adrenoceptor agonists suppress the release of heparin from mast cells (Green *et al.*, 1993).This heparin normally inhibits the toxic actions of cationic proteins such as major basic protein and reduces the proliferation of smooth muscle (Page, 1991). Our findings indicate that the exacerbatory influence of β_2-adrenoceptor agonists on hyperresponsiveness is unlikely to be due to the loss of the antiproliferative effect of mast-cell derived heparin, since salbutamol has pronounced direct inhibitory effects on a range of mitogenic stimuli. However, we cannot exclude the possibility that the major stimulus to airway smooth muscle proliferation in asthma is resistant to the inhibitory effect of salbutamol.

In summary, we have demonstrated that salbutamol has a direct inhibitory effect on mitogen-induced proliferation of airway smooth muscle cells and that this effect is mediated via a β_2-adrenoceptor. However, salbutamol appeared to lack an inhibitory effect on the small degree of cell proliferation elicited by endothelin-1. In addition, the therapeutic dose of salbutamol may be supramaximal for its direct effect on the inhibition of proliferation of airway smooth muscle. Further work needs to be carried out to determine whether salbutamol has a similar inhibitory effect after mitogen-induced stimulation of proliferation has occurred.

We thank Mr Michael Mullerworth and Dr Tim MacKenzie at the Royal Melbourne Hospital for providing us with lung tissue resections for cell culture and Ms Trudi Harris for technical assistance. This study was supported by the National Health and Medical Research Council of Australia.

References

ANDERSON, H.R. (1989). Increase in hospital admissions for childhood asthma: trends in referral, severity, and readmissions from 1970 to 1985 in a health region of the United Kingdom. *Thorax*, **44**, 614–619.

ARAMORI, I. & NAKANISHI, S. (1992). Coupling of two endothelin receptor subtypes to differing signal transduction in transfected chinese hamster ovary cells. *J. Biol. Chem.*, **267**, 12468–12474.

BARNES, P.N. & CHUNG, K.F. (1992). Questions about inhaled β_2-adrenoceptor agonists in asthma. *Trends Pharmacol. Sci.*, **13**, 20–23.

BEASLEY, R., ROCHE, W.R., ROBERTS, J.A. & HOLGATE, S.T. (1989). Cellular events in the bronchi in mild asthma and after bronchial provocation. *Am. Rev. Respir. Dis.*, **139**, 806–817.

BLACK, P.N., GHATEI, M.A., TAKAHASHI, K., BRETHERTON-WATT, D., DOLLERY, C.T. & BLOOM, S.R. (1989). Formation of endothelin by cultured airway epithelial cells. *FEBS Lett.*, **255**, 129–132.

CLOWES, A.W. & KARNOWSKY, M.J. (1977). Suppression by heparin of smooth muscle cell proliferation in injured arteries. *Nature*, **265**, 625–626.

DICKER, P. & ROZENGURT, E. (1980). Phorbol esters and vasopressin stimulate DNA synthesis by a common mechanism. *Nature*, **287**, 607–612.

DUNNILL, M.S., MASSARELLA, G.R. & ANDERSON, J.A. (1969). A comparison of the quantitative anatomy of the bronchi in normal subjects, in status asthmaticus, in chronic bronchitus, and in emphysema. *Thorax*, **24**, 176–179.

ERNST, P., HABBICK, B., SUISSA, S,. HEMMELGRAN, B., COCKROFT, D., BUIST, A.S., HORWITZ, R.I., MCNUTT, M. & SPITZER, W.O. (1993). Is the association between inhaled beta-agonist use and life-threatening asthma because of confounding by severity? *Am. Rev. Respir. Dis.*, **148**, 75–79.

GLASSBERG, M.K., ERGUL, A., WANNER, A. & PUETT, D. (1992). Endothelin binding and stimulation of mitogenesis in ovine airway smooth muscle cells. *Am. Rev. Respir. Dis.*, **145**, A124.

GOLDIE, R.G., SPINA, D., HENRY, P.J., LULICH, K.M. & PATERSON, J.W. (1986). *In vitro* responsiveness of human asthmatic bronchus to carbachol, histamine, β-adrenoceptor agonists and theophylline. *Br. J. Clin. Pharmacol.*, **22**, 669–676.

GREEN, W.F., KONNARIS, K. & WOOLCOCK, A.J. (1993). Effect of salbutamol, fenoterol, and sodium cromoglycate on the release of heparin from sensitized human lung fragments challenged with *Dermatophagoides pteronyssinus* Allergen. *Am. J. Respir. Cell Mol. Biol.*, **8**, 518–521.

HALL, I.P., WIDDOP, S., TOWNSEND, P. & DAYKIN, K. (1992). Control of cyclic AMP levels in primary cultures of human tracheal smooth muscle cells. *Br. J. Pharmacol.*, **107**, 422–428.

HALL, D.W.P., HENRY, P.J. & GOLDIE, R.G. (1993). Endothelin and the respiratory system. *Trends Pharmacol. Sci.*, **14**, 29–32.

HIRST, S.J. & TWORT, C.H.C. (1992). The proliferative response of airway smooth muscle. *Clin. Exp. Allergy*, **22**, 907–915.

HOSSAIN, S. (1973). Quantitative measurement of bronchial muscle in men with asthma. *Am. Rev. Respir. Dis.*, **107**, 99–109.

JAMES, A.L., PARE, P.D. & HOGG, J.C. (1989). The mechanics of airway narrowing in asthma. *Am. Rev. Respir. Dis.*, **139**, 242–246.

JEFFERY, P.K., WARDLAW, A.J., NELSON, F.C., COLLINS, J.V. & KAY, A.B. (1989). Bronchial biopsies in asthma: an ultrastructural, quantitative study and correlation with hyperreactivity. *Am. Rev. Respir. Dis.*, **140**, 1745–1753.

JONZON, B., NILSSON, J. & FREDHOLM, B.B. (1985). Adenosine receptor-mediated changes in cyclic AMP production and DNA synthesis in cultured arterial smooth muscle cells. *J. Cell. Physiol.*, **124**, 451–456.

KANTHOU, C., PARRY, G., WIJELATH, E., KAKKAR, V.V. & DEMOLIOU-MASON, C. (1992). Thrombin-induced proliferation and expression of platelet-derived growth factor-A chain gene in human vascular smooth muscle cells. *FEBS Lett.*, **314**, 143–148.

NILSSON, J. & OLSSON, A.G. (1984). Prostaglandin E_1 inhibits DNA synthesis in arterial smooth muscle cells stimulated with platelet-derived growth factor. *Atherosclerosis*, **53**, 77–82.

NISHIMURA, J., CHEN, X., JAHAN, H., SHIKASHO, T., KOBAYASHI, S. & KANAIDE, H. (1992). cAMP induces up-regulation of ET_A receptor mRNA and increases responsiveness to endothelin-1 of rat aortic smooth muscle cells in primary culture. *Biochem. Biophys. Res. Commun.*, **188**, 719–726.

NOVERAL, J.P., ROSENBERG, S.M., ANBAR, R.A., PAWLOWSKI, N.A. & GRUNSTEIN, M.M. (1992). Role of endothelin-1 in regulating proliferation of cultured rabbit airway smooth muscle cells. *Am. J. Physiol,*. **263**, L317–L324.

PAGE, C.P. (1991). One explanation of the asthma paradox: inhibition of natural anti-inflammatory mechanism by β_2-agonists. *Lancet*, **337**, 717–720.

PANETTIERI, R.A., COHEN, M.D. & BILGEN, G. (1993). Airway smooth muscle cell proliferation is inhibited by microinjection of the catalytic subunit of cAMP dependent protein kinase. *Am. Rev. Respir. Dis.*, **147**, A252.

PANETTIERI, R.A., RUBINSTEIN, N.A., FEUERSTEIN, B. & KOTLIKOFF, M.I. (1991). Beta-adrenergic inhibition of airway smooth muscle cell proliferation. *Am. Rev. Respir. Dis.*, **143**, A608.

PANETTIERI, R.A., YADVISH, P.A., KELLY, A.M., RUBINSTEIN, N.A. & KOTLIKOFF, M.I. (1990). Histamine stimulates proliferation of airway smooth muscle and induces c-*fos* expression. *Am. J. Physiol.*, **259**, L365–L371.

RAFFESTIN, B., CERRINA, J., BOULLET, C,. LABAT, C., BENVENISTE, J. & BRINK, C. (1985). Response and sensitivity of isolated human pulmonary muscle preparations to pharmacological agents. *J. Pharmacol. Exp. Ther.*, **233**, 186–194.

ROGER, P.P., SERVAIS, P. & DUMONT, J.E. (1983). Stimulation by thyrotropin and cyclic AMP of the proliferation of quiescent canine thyroid cells cultured in a defined medium containing insulin. *FEBS Lett.*, **157**, 323–329.

SEARS, M.R., TAYLOR, D.R., PRINT, C.G., LAKE, D.C., LI, Q., FLANNERY, E.M., YATES, D.M., LUCAS, M.K. & HERBISON, G.P. (1990). Regular inhaled beta-agonist treatment in bronchial asthma. *Lancet*, **336**, 1391–1396.

SKALLI, O., ROPRAZ, P., TRZECIAK, A., BENZONANA, G., GILLESSEN, D. & GABBIANI, G. (1986). A monoclonal antibody against α-smooth muscle actin: a new probe for smooth muscle differentiation. *J. Cell Biol.*, **103**, 2787–2796.

STEWART, A.G., GRIGORIADIS, G. & HARRIS, T. (1993). Dissociation of epidermal growth factor induced mitogenesis and increases in intracellular calcium in cultured airway smooth muscle. *Am. Rev. Respir. Dis.*, **147**, A253.

STEWART, A.G., TOMLINSON, P.R. & WILSON, J. (1993). Airway wall remodelling in asthma: a novel target for the development of anti-asthma drugs. *Trends Pharmacol. Sci.*, **14**, 275–279.

TSANG, B.K., RIXON, R.H. & WHITFIELD, J.F. (1980). A possible role for cyclic AMP in the initiation of DNA synthesis by Isoproterenol-activated parotid gland cells. *J. Cell. Physiol.*, **102**, 19–26.

VITTORI, E., MAURIZIO, M., FASOLI, A., DE FRANCHIS, R. & MATTOLI, S. (1992). Increased expression of endothelin in bronchial epithelial cells of asthmatic patients and effect of corticosteroids. *Am. Rev. Respir. Dis.*, **146**, 1320–1325.

WIGGS, B.R., BOSKEN, C., PARE, P.D. & HOGG, J.C. (1992). A model of airway narrowing in asthma and in chronic obstructive pulmonary disease. *Am. Rev. Respir. Dis.*, **145**, 1251–1258.

(Received August 17, 1993
Revised October 14, 1993
Accepted October 25, 1993)

Erratum

Br. J. Pharmacol. (1993) **110**, 1291–1296

M. Facklam & N.G. Bowery. Solubilization and characterization of $GABA_B$ receptor binding sites from porcine brain synaptic membranes

In the above article, an error appeared in Figure 2 as it was published in the December issue of the journal due to a transposition of axes labels in Figure 2a.

The figure is reproduced in its correct form below.

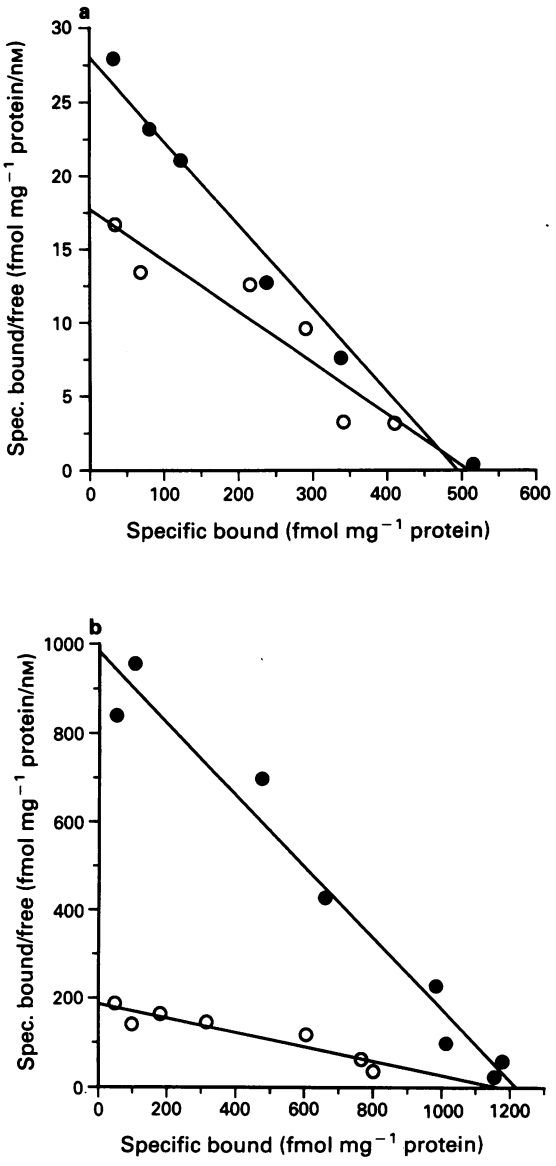

Figure 2 Saturation experiments shown as Scatchard plots of a representative of 3–6 experiments performed in triplicate of the agonist [^{3}H]-GABA (a) and the antagonist [^{3}H]-CGP 54626 (b) to membrane bound (●) and solubilized (○) $GABA_B$ receptors.

British Journal of Pharmacology

VOLUME 111 (2) FEBRUARY 1994

BRITISH JOURNAL OF PHARMACOLOGY

The *British Journal of Pharmacology* welcomes contributions in all fields of experimental pharmacology including neuroscience, biochemical, cellular and molecular pharmacology. The Board of Editors represents a wide range of expertise and ensures that well-presented work is published as promptly as possible, consistent with maintaining the overall quality of the journal.

Edited for the British Pharmacological Society by

A.T. Birmingham
(Chairman)

R.W. Horton **W.A. Large**
(Secretaries)

Submission of manuscripts: Manuscripts (two copies) should be sent to The Editorial Office, British Journal of Pharmacology, St. George's Hospital Medical School, Cranmer Terrace, London SW17 0RE.

Authors should consult the Instructions to Authors and the Nomenclature Guidelines for Authors in Vol. **111,** 378–387. These Instructions and Guidelines also appear with the journal Index for Volumes **108–110**, 1993. A checklist of the essential requirements is summarised in each issue of the journal, or as the last page of the issue.

The *British Journal of Pharmacology* is published monthly by the Scientific & Medical Division, Macmillan Press Ltd.

The journal is covered by *Current Contents*, *Excerpta Medica* and *Index Medicus*.

All business correspondence and reprint requests should be addressed to the Scientific & Medical Division, Macmillan Press Ltd., Houndmills, Basingstoke, Hampshire RG21 2XS, UK. Telephone: (0256) 29242; Fax: (0256) 810526.

Enquiries concerning advertising space or rates should be addressed to: Michael Rowley, Advertisement Manager, Macmillan Press Ltd., 4 Little Essex Street, London WC2R 3LF. Telephone: 071 836 6633; Fax: 071 379 0820.

Annual subscription prices for 1993 EC £540, elsewhere £595/US$950 (sterling rate is definitive). Orders must be accompanied by remittance. Cheques should be made payable to Macmillan Press, and sent to: Macmillan Press Ltd., Subscription Department, Brunel Road, Houndmills, Basingstoke, Hampshire RG21 2XS, UK.
Overseas subscribers may make payments into UK Post Office Giro Account No. 5192455. Full details must accompany the payment.

British Journal of Pharmacology (ISSN 0007–1188) is published monthly by Macmillan Publishers Ltd, c/o Mercury Airfreight International Ltd, 2323 Randolph Avenue, Avenel, NJ 07001, USA. Subscription price is $950.00 per annum. 2nd class postage is paid at Rahway NJ. *Postmaster*: send address corrections to Macmillan Publishers, c/o Mercury Airfreight International Ltd, 2323 Randolph Avenue, Avenel NJ 07001.

ISSN 0007–1188
0007–1188/94 $9.00 + $0.00

PREPARATION OF MANUSCRIPTS

Authors are strongly recommended to read the full *Instructions to Authors* and *Nomenclature Guidelines for Authors* (*Br. J. Pharmacol.* 1993, **108,** 275–284) before submitting a manuscript for publication in the *British Journal of Pharmacology*. The manuscript and cover letter should be checked against the following list before mailing.

The original and one copy of the manuscript must be supplied. Manuscripts must be typed in double-line spacing on one side of A4 paper, in type not smaller than 12 characters per inch or 10 point. Both copies to include Tables and a set of labelled Figures. One set of Figures without numbers or letters is also to be included. The text to be arranged in the following subsections:

1. **Title**—To have no more than 150 characters on a separate page, which should also include a Short Title (50 characters maximum) and the name and address of the author for correspondence.
2. **Summary**—To be arranged in numbered paragraphs (Full Papers) or a single paragraph (Special Reports).
   —to include aims, principal results and conclusions.
   —to include Key words (10 maximum) at end of summary.
3. **Introduction**—To contain concise statements of the problem and the aims of the investigation.
4. **Methods**—To have brief but adequate account of the procedures; *full names of drugs* (*including those referred to by manufacturer's code*), sources of drugs and statistical tests to be stated.
5. **Results**—To have no repetition of data in Figures, Tables and text.
6. **Discussion**—Findings and conclusions to be placed in context of other relevant work.
   NB Simple repetition of results and unwarranted speculation are not acceptable.
7. **Acknowledgments**—Sources of support. Sources of drugs not widely available commercially.
8. **References**—All references in the text to be included in the Reference List and *vice versa*. References in alphabetical order with complete citations; Journals publishing 'in press' papers identified.
   References to manuscripts submitted to other journals but not yet accepted are not allowed.
9. **Tables**—Each on a separate page and prepared in accordance with current requirements of the Journal.
10. **Figures**—Both labelled and non-labelled Figures to be prepared in accordance with current requirements of the Journal (see *Instructions to Authors*, 1993, **108,** 275–281) and provided with Figure Number and Authors' names on back (*in pencil*).
    —each legend to be typed on a separate page and carrying keys to symbols.
    —keys to symbols and histograms must not appear on the figures themselves, but in the respective legends.
    —'box style' figures are not in keeping with the Journal style; line drawings etc must have only left-hand and bottom axes.
11. **Manuscripts**—To be accompanied by a declaration signed by each author that
    (a) results are original
    (b) approval of all persons concerned has been given to submit manuscripts for consideration (see also 12b)
    (c) the same material is neither 'in press' (i.e. is in proof or has definitely been accepted for publication) nor under consideration elsewhere. Furthermore it will not be submitted or published elsewhere before a decision has been reached by the Editorial Board of the *British Journal of Pharmacology* and will not be submitted elsewhere if accepted by the *British Journal of Pharmacology*.
    (d) Copyright assignment is included.
12. **Cover letter**—To state clearly
    (a) Corresponding author's full postal address, telephone, telex or Fax number
    (b) where appropriate, that *either* ethical approval has been given for investigation *or* Company or Institutional permission to publish work has been received.
13. **Reminder**—Packaging to be sufficiently robust to protect Figures and to withstand mailing.

Failure to comply with *Instructions to Authors* may lead to substantial delays in processing, review and publication and may even jeopardize acceptance of the manuscript.

NOMENCLATURE

Authors are reminded that accepted receptor and associated terminology is laid out in *Nomenclature Guidelines for Authors*, as published in the *British Journal of Pharmacology, Br. J. Pharmacol.*, 1994, **111,** 385–387.

SPECIAL REPORTS

The purpose of *Special Reports* is to provide rapid publication for **new** and **important** results which the Editorial Board considers are likely to be of special pharmacological significance. *Special Reports* will have publication priority over all other material and so authors are asked to consider carefully the status of their work before submission.

In order to speed publication there is normally no revision allowed beyond very minor typographical or grammatical corrections. If significant revision is required, the Board may either invite rapid re-submission or, more probably, propose that it be re-written as a Full Paper and be re-submitted for consideration. In order to reduce delays, proofs of *Special Reports* will be sent to authors but **essential corrections must reach the Production Office within 48 hours of receipt.** Authors should ensure that their submitted material conforms exactly to the following requirements.

Special Reports should normally occupy no more than two printed pages of the Journal; two illustrations (Figures or Tables, with legends) are permitted. As a guideline, with type face of 12 pitch and double-line spacing, a page of A4 paper could contain about 400 words. The absolute maximum length of the *Special Report* is 1700 words. For each Figure or Table, please deduct 200 words. The manuscript should comprise a Title page with key words (maximum of 10), a Summary consisting of a single short paragraph, followed by Introduction, Methods, Results, Discussion and References (maximum of 10). In all other respects, the requirements are the same as for Full Papers (see current 'Instructions to Authors').

BRITISH JOURNAL OF PHARMACOLOGY VOLUME 111 (2) 1994

SPECIAL REPORTS

PAPERS

ERRATUM 648

Br. J. Pharmacol. (1993), **110**, 1291–1296

M. Facklam & N.G. Bowery. Solubilization and characterization of $GABA_B$ receptor binding sites from porcine brain synaptic membranes

Typeset by Elite Typesetting Techniques, Southampton, Hampshire
and printed in Great Britain by Unwin Brothers Ltd., The Gresham Press, Old Woking, Surrey